
THE UNIVERSITY OF ADELAIDE

School of Earth & Environmental Sciences
Geology & Geophysics

# DEVELOPING A TECTONIC FRAMEWORK FOR THE SOUTHERN CURNAMONA CU-AU PROVINCE: GEOCHEMICAL AND RADIOGENIC ISOTOPE APPLICATIONS

Lachlan Rutherford, BSc (Hons)

April, 2006

Thesis submitted for the degree of Doctor of Philosophy
in the University of Adelaide, Faculty of Science

# TABLE OF CONTENTS

# LIST OF FIGURES

# LIST OF TABLES

# ABSTRACT

The late Palaeoproterozoic to early Mesoproterozoic (1720 – 1550 Ma) tectonic history of the southern Curnamona Province is characterised by multiple episodes of transient lithospheric thinning and thickening. Such a complicated lithospheric evolution is matched only by the diversity of studies conducted in the region, and the number of different models proposed for the tectonic evolution of the southern Curnamona Province. Although the timing of maximum deposition of the Willyama Supergroup is now well constrained (~1720 – 1645 Ma), and closely correlated with the depositional history of metasediments of the Mt. Isa Inlier, uncertainty still surrounds the timing of high-grade metamorphism and deformation, the petrogenesis of mafic and alkaline magmatism, and the source of Fe-oxide Cu-Au mineralisation in the southern Curnamona Province.

The timing of Proterozoic high-grade metamorphism in the southern Curnamona Province as indicated by *in situ* chemical U-Th-Pb ages of metamorphic monazite occluded by prograde metamorphic minerals (garnet-andalusite-sillimanite) shows no evidence of high-grade metamorphism prior to the Olarian Orogeny at ca. 1610 Ma). Models that propose that high-grade metamorphism occurred contemporaneously with deposition of the upper Willyama Supergroup (~1690 – ≤1640 Ma) are unsubstantiated. Furthermore, extensional tectonic models proposed to have occurred during this time interval have no metamorphic expression as proposed, and consequently have no bearing on the metamorphic evolution of the southern Curnamona Province. In addition, tectonic reconstruction models that are based on the correlation of high-T metamorphism in the southern Curnamona Province with high-T metamorphism in southwest Laurentia (AUSWUS) are unsubstantiated. Monazite chemical ages record a punctuated metamorphic history in the southern Curnmona Province spanning ~60 million years (~1610 – 1550 Ma), contrary to previous models of a single, long-lived metamorphic event. At least two episodes of high-grade metamorphism (~1600 and 1575 Ma) and multiple episodes of fluid-driven retrograde metamorphism (~1585 and 1550 Ma) occurred during this time interval.

Central to models of the tectonothermal evolution of the southern Curnamona Province at ~1690 Ma is the intrusion of high-Fe tholeiitic mafic magmas into metasedimentary rocks of the Curnamona Group and Broken Hill Group. Geochemical and Nd isotopic constraints on metabasites from across the southern Curnamona Province are interpreted to reflect near closed-system fractionation of mantle-derived melts, sourced from a compositionally and isotopically heterogeneous subcontinental lithospheric mantle. High-degree partial melts of an isotopically depleted ($\varepsilon Nd_i$ = 2.6) to slightly enriched ($\varepsilon Nd_i$ = –1.5) mantle intruded the deepest part of the Willyama basin in the Broken Hill Domain. Lower-degree partial melts of an enriched and predominantly isotopically evolved ($\varepsilon Nd_i$ = –3.8 to 1.5) subcontinental lithospheric mantle took place on the flank of the Willyama basin in the Olary Domain. Different degrees of lithospheric thinning across the Willyama basin are interpreted to have accentuated the compositional and isotopic heterogeneity in the subcontinental lithospheric mantle during partial melting. It is speculated that this is a result of differences in lithospheric strength across the southern Curnamona Province, associated with contrasting ages and histories of the subcontinental lithospheric mantle beneath the Broken Hill and Olary Domains.

High-T, low-P metamorphism associated with the Olarian Orogeny culminated with bimodal magmatism and crustal anatexis at ~1585 Ma. The intrusion of silica-undersaturated, nepheline-normative alkaline magmatism during this time occurred in the northwestern Olary Domain. Feldspathic ijolite (feldspar-feldspathoid-pyroxene rocks), syenitic porphyries, and lamprophyric dyke phases were generated from near closed-system fractionation of mantle-derived melts. Low-degree partial melting of over a large region initially produced Na-rich melts, as represented by the ijolite and lamprophyric phases ($\varepsilon Nd_i$ = 0.6 – 1.0). Fractionation of the Na-rich melt generated progressively K-rich, Na-poor melt fractions that culminated in the generation of the porphyritic K-feldspar-rich syenite phases ($\varepsilon Nd_i$ = 1.3 – 2.8). Partial melting is interpreted to have occurred as a response to convective thinning of the lithosphere. Lithospheric thinning is a necessary compensation for the previous episode of crustal thickening associated with nappe emplacement during the early Olarian Orogeny. The generation of bimodal magmatism, alkaline magmatism, crustal anatexis and low-P, high-T metamorphism are all a manifestation of the high geothermal gradient that accompanied lithospheric thinning during the early Mesoproterozoic. Emplacement of the mantle-derived melts was facilitated by mid- to upper-crustal extension and hydrothermal brecciation of the country rock at ~1585 Ma.

The source of Fe-oxide Cu-Au (IOCG) mineralisation in the southern Curnamona Province is constrained by trace element geochemistry and Nd isotopic compositions to be derived solely from fluids extracted from calc-silicate, meta-evaporitic and exhalative horizons of the lower Willyama Supergroup. Chlorine-and saline-rich fluids circulating through the metasedimentary sequence are interpreted to have leached metals from the anomalously metalliferous, oxidised lower Willyama Supergroup metasediments. On contact with the anoxic metasediments of the Strathearn Group, or through mixing with reducing fluids at the contact between the upper and lower Willyama Supergroup, precipitation of Fe-oxide Cu-Au mineralisation occurred. The Nd isotopic

composition of ore samples are interpreted to reflect two periods of IOCG mineralisation, both of which were derived from the Willyama Supergroup. Initial IOCG mineralisation occurred synchronous with prograde metamorphism associated with the Olarian Orogeny. A second mineralisation event, or remobilisation of initial mineralisation, occurred ~1100 million years later during the *c.* 500 Ma Delamerian Orogeny, that reached amphibolite-grade metamorphic conditions in the southern Curnamona Province.

Pervasive reworking of the southern Curnamona Province occurred during the Delamerian Orogeny, and was not only restricted to shear zone reactivation as previously thought. Monazite electron microprobe Th-U-Pb and garnet Sm-Nd isotopic data from metapelitic assemblages in the Willyama Supergroup in the southern Curnamona Province indicate the terrain underwent regional greenschist to amphibolite-grade metamorphism during the Delamerian Orogeny. The Delamerian-aged mineral assemblages include the development of prograde garnet-staurolite and kyanite-bearing associations that overprint andalusite and sillimanite bearing assemblages that developed during the c. 1600 Ma Olarian Orogeny. Importantly, the development of secondary kyanite-bearing assemblages in the southern Curnamona Province has been used previously to suggest that the Olarian Orogeny followed an anticlockwise *P-T* evolution. As such assemblages are the product of *c.* 500 Ma metamorphism, the thermobarometric evolution of the Olarian Orogeny needs to be re-evaluated. This study highlights the utility of linking in situ geochronological approaches and petrologically important phases. Such an approach will provide a robust framework for establishing *P-T-t* evolutions within complexly deformed and polytectonic terrains.

# DISCLAIMER

This thesis contains no material which has been accepted for the award of any other degree or diploma in any university or other tertiary institution and, to the best of my knowledge and belief, contains no material previously published or written by another person, except where due reference has been made in the text. I give my consent to this copy of my thesis, when deposited in the University Library, being available for loan and photocopying.

.....

Lachlan Rutherford

# ACKNOWLEDGMENTS

Associate Professor Martin Hand, Dr Karin Barovich and Professor John Foden for the opportunity, their enthusiasm and patience.

Wolfgang Preiss, Colin Conor, Andy Burtt, Alistair Crooks, Michael Szpunar and Stuart Robertson, Geological Survey Branch, Primary Industries & Resources of South Australia, for assistance with field work and insightful discussions on the geology of the southern Curnamona Province.

Garry Davidson for his insightful comments on the Fe-oxide Cu-Au mineralisation section.

Angus Netting, John Terlet and Dr Peter Self, Adelaide Microscopy, for their assistance with microanalysis.

David Bruce, University of Adelaide, for assistance with TIMS.

Colleagues of the Continental Evolution Research Group for countless good times and memories.

This study was supported by ARC Linkage Grant LP0347342 awarded to Hand, Barovich & Foden.

# Chapter 1
# INTRODUCTION

## 1.1 Overview and aims

The southern Curnamona Province (SCP) is located in northeastern South Australia and western New South Wales in southern Australia (Fig. 1.1). It is a near oval-shaped inlier of late Palaeoproterozoic (~1715 – 1645 Ma) metasedimentary and metaigneous rocks (Willyama Supergroup; Stevens et al., 1980; Willis et al., 1983; Page et al., 1998, 2000, 2003) intruded by early Mesoproterozoic granitic intrusives and felsic volcanics (~1590 – 1580 Ma; Ludwig & Cooper, 1984; Page et al., 2003). Extensive Neoproterozoic and early Phanerozoic cover sequences unconformably overlie and obscure the basement rocks of the Willyama Supergroup. Notable geophysical, stratigraphic, metallogenic and tectonothermal differences in the Willyama Supergroup across the SCP in the Mingary 1:100 000 map sheet region resulted in the subdivision of the southern Curnamona Province into the Broken Hill and Olary Domains (Stevens, 1986; Robertson et al., 1998; Crooks, 2000; Fig. 1.1).

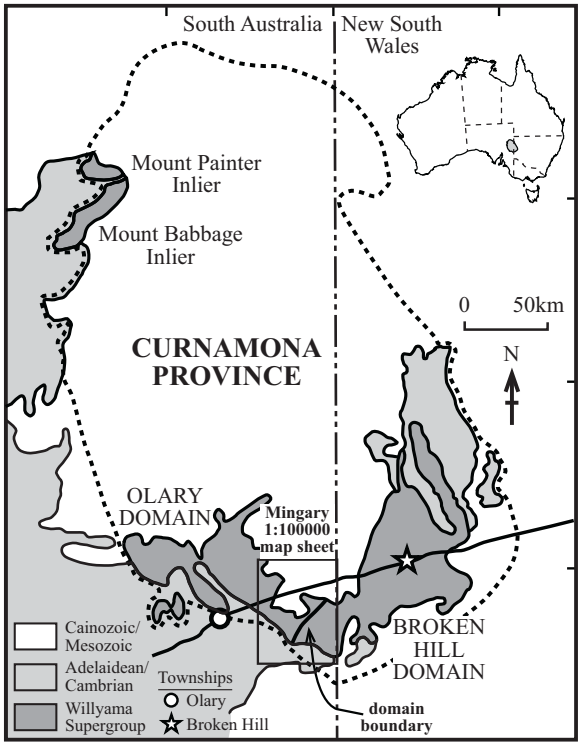


**Figure 1.1.** Location of the Curnamona Province in southern Australia. Outcropping region of Willyama Supergroup in southern Curnamona Province subdivided into Olary Domain and Broken Hill Domain.

The SCP is best known for the world-class Broken Hill Pb-Zn-Ag deposit. Since the first major discovery in the 1890's, the Broken Hill deposit and its surrounding regions has been the focus of intense national and international research. To date, research on the tectonothermal history of the SCP has been mainly based on the geology of the Broken Hill region, focussing on the stratigraphy of the Willyama Supergroup, and the magmatic and metamorphic evolution of the terrain (e.g. Stevens et al., 1980; Corbett & Phillips, 1981; Phillips & Wall, 1981; Willis et al., 1983; Phillips et al., 1985; Stüwe & Ehlers, 1997; Nutman & Ehlers, 1998; Ashley et al., 1996; Page et al., 1998, 2000, 2003). Fewer studies have been conducted within the Olary Domain, although considerable efforts have been made in understanding the: lithostratigraphy and provenance of the Willyama Supergroup (Clarke et al., 1986; Laing, 1996a; Conor, 2000a, 2000b; Page et al., 2000, 2003; Barovich et al., 2002, Barovich, 2003; Conor & Page, 2003; Barovich & Hand, 2004); correlation of the Willyama Supergroup between the Olary Domain and Broken Hill Domain (Page et al., 1998, 2000, 2003; Conor & Page, 2003); metamorphic history of the Olary region (Clarke et al., 1987, 1995); timing and genesis of syn-Willyama and post-tectonic magmatic events (Ashley et al., 1996; Page et al., 2000, 2003; Barovich & Foden, 2002);

and genesis of stratabound and epigenetic base metal mineralisation (Bierlein et al., 1995, 1996a, 1996b; Lottermoser & Ashley, 1996; Williams & Skirrow, 2000). Despite considerable effort expanded in developing a comprehensive tectonic framework for the evolution of the SCP, there are still major unknowns and controversies regarding:

1. The timing of high-grade metamorphism (Donaghy et al., 1998; Nutman & Ehlers, 1998, 1999; Stevens, 1999, 2000; Gibson 2000; Page et al., 2000, 2003; Gibson & Nutman, 2004; Conor et al., 2005).
2. The structural character of regional deformation events (Laing et al., 1978; Laing, 1996b; Donaghy et al., 1998; Gibson, 2000; Stevens, 2000; Gibson & Nutman, 2004; Conor et al., 2005);
3. The significance and genesis of mafic magmatism and alkaline magmatism (Gibson & Nutman, 2004; Conor, 2004; Conor et al., 2005);
4. The source and timing of iron-oxide copper-gold (IOCG) mineralisation (Skirrow et al., 1999, 2000; Williams & Skirrow et al., 2000);
5. The relationship of the SCP with similar aged basement rocks and tectonic histories in northern, southern and central Australia (Laing, 1996c; Myers et al., 1996; Betts et al., 2002; Giles et al., 2002, 2004);
6. The significance of the tectonometamorphic evolution of the SCP in relation to the Palaeo- and early Mesoproterozoic history of the Columbia supercontinent (Karlstrom et al., 1999, 2001; Burrett & Berry, 2000, 2002).

Uncertainties surrounding interpretations made about these issues are primarily due to the intense deformation and high-grade metamorphism of the Palaeo- and Mesoproterozoic rocks during the Olarian Orogeny (~1600 ± 8 Ma; Page & Laing, 1992), and low- to medium-grade metamorphism during the Delamerian Orogeny (~500 Ma; Dutch & Hand, 2003; Dutch et al., 2005). These events have increased the complexity of the rocks in the SCP, especially in the high metamorphic grade region in the Broken Hill Domain and southern Olary Domain. For this reason, this study primarily focuses on understanding the tectonothermal history, timing of metamorphism, and genesis of IOCG mineralisation of the SCP within the Olary Domain. The effects of the Olarian Orogeny are not as pervasive as in the Broken Hill Domain, and therefore the pre-Olarian tectonic and metallogenic history of the SCP should be better preserved. Following is a summary outlining the questions investigated in this thesis.

## 1.2 Outline and organisation of thesis

The aim of this study is to provide geochemical and isotopic constraints on:

1. The timing of tectonism in the SCP, and its relationship to the Proterozoic *P-T* evolution proposed for the terrain and continental reconstruction models based on the timing of metamorphism in the SCP.
2. The genesis and tectonic significance of syn-Willyama mafic magmatism in the Olary Domain and western Broken Hill Domain;
3. The genesis and tectonic significance of

syn-orogenic silica-undersaturated alkaline magmatism in the northwestern Olary Domain;
4. The source of hydrothermal fluids in iron-oxide copper-gold (IOCG) systems in the SCP;
5. Impact of the Delamerian Orogeny on the basement rocks of the SCP.

*Chapter 2* summarises the regional geological and metallogenic framework for the SCP. Due to the extraordinary amount of literature pertaining to the southern Curnamona Province (>1000 abstracts, reports, theses, journal articles), this chapter is divided into two sections. *Section 2.1* discusses studies related to the deposition and provenance of the Willyama Supergroup, timing and genesis of major magmatic events, timing of metamorphism, and tectonic reconstruction models for the late Palaeo- and Mesoproterozoic involving the SCP. *Section 2.2* discusses previous work on the different styles of mineralisation and alteration, with emphasis placed on Fe-oxide Cu-Au (IOCG) systems. Models for the timing and sources of mineralisation and alteration are discussed.

*Chapter 3* addresses what is arguably the most controversial scientific topic within the SCP, that is, the timing and duration of metamorphism (Page & Laing, 1992; Nutman & Ehlers, 1998, 1999; Donaghy et al., 1998; Stevens, 1999; Page et al., 1998; 2000; Gibson & Nutman, 2004; Conor et al., 2005). In this chapter, the age of regional deformation and metamorphism across the terrain is constrained by *in situ* chemical U-Th-Pb monazite ages derived by electron microprobe analysis (EPMA). Previous geochronological studies have been predominantly based on U-Pb age constraints on magmatic events that are interpreted to bracket deformation (e.g. Nutman & Ehlers, 1998; Donaghy et al., 1998; Page et al., 1998, 2000; Gibson & Nutman, 2004). The *in situ* EPMA ages directly constrain the timing of monazite growth and can be directly related to metamorphic textures and therefore the tectonic evolution of the terrain. A study of this type has not yet been undertaken in the SCP. The importance of constraining the timing of metamorphism in the SCP is highlighted by Proterozoic tectonic reconstruction models that relate the timing of metamorphism in the SCP and in southwest Laurentia that propose a Australia – southwest Laurentia connection at ~1690 Ma (AUSWUS; Karlstrom et al., 1999; Burrett & Berry, 2000, 2002). Based on EPMA age constraints generated in this study, the possible position of Proterozoic Australia within a continental reconstruction framework is addressed.

*Chapter 4* summarises the geochemical and radiogenic isotopic composition (Nd-Sr) of rift-related tholeiitic mafic magmatism that accompanied deposition of the lower Willyama Supergroup at ~1700 Ma and ~1685 Ma (Page et al., 2000; Conor, 2004). Detailed studies on this suite of mafic magmatic rocks in the Olary Domain have not yet been undertaken. The aim is to determine the petrogenesis of mafic magmatism by characterising the magmatic processes that were operating. Furthermore, geochemical and isotopic characteristics of the subcontinental lithospheric mantle (SCLM) beneath the SCP are evaluated. These characteristics form the basis for proposing models on the lithospheric evolution of the SCP, and provide information

about mantle-crust interactions in this part of Proterozoic Australia. Previous studies of this magmatic event in the Broken Hill Domain identified a suite of high-Fe tholeiitic mafic magmatic rocks derived from partial melting of a depleted mantle source within a propagating rift system (Phillips et al., 1985; James et al., 1987). Fractional crystallisation of a high-level magma chamber generated high-Fe tholeiitic melts. In the Broken Hill region, the high geothermal gradient associated with mafic magmatism generated a contemporaneous suite of felsic magmatic rocks. Magmatism was concomitant with an increase in accommodation space within the Willyama basin (Broken Hill Group; Willis et al., 1983; Page et al., 2000, 2003). These conditions may have been critical for the genesis of the Broken Hill deposit (James et al., 1987).

*Chapter 5* describes the geochemistry and Nd isotopic characteristics of a suite of silica-undersaturated, alkaline magmatic rocks in the northern Olary Domain. This study provides the first detailed geochemical, isotopic and petrological analysis of this magmatic event. Silica-undersaturated, alkaline magmatism is often associated with carbonatitic magmatism, and is unequivocally of mantle origin (e.g. Sørensen, 1974; Woolley, 2001). Therefore, geochemical and isotopic studies on these rocks provide a window into the source region (SCLM) and magmatic processes that operated during the genesis of this suite of rocks.

*Chapter 6* presents the trace element geochemistry and neodymium isotopic composition of mineralised volumes from IOCG prospects in the SCP. Fluid and metal sources are assessed with respect to potential reservoirs, such as the Willyama Supergroup metasedimentary sequences and magmatic rock systems. The geochemical and isotopic characterisation of the different reservoirs are compared with that of IOCG mineralisation in order to assess potential source regions. By determining which reservoirs were the most likely sources to mineralisation, genetic models are explored for the generation of IOCG mineralisation in the SCP, and implications for exploration models.

*Chapter 7* investigates the effects of the Delamerian Orogeny on the SCP. Reactivation of shear zones during the Delamerian Orogeny has been shown to be an important response to Cambrian tectonism (e.g. Dutch et al., 2005), but its pervasive effects on the basement rocks have yet to be determined. The recognition that the metamorphic grade in the shear zones attained staurolite-kyanite grade (Dutch et al., 2005), may have important implications for the Olarian Orogeny, as the *P-T* path proposed for the Olarian Orogeny is based on the development of late-stage staurolite-kyanite assemblages that post-date andalusite-sillimanite grade assemblages (e.g. Clarke et al., 1987, 1995).

# Chapter 2
# GEOLOGICAL FRAMEWORK

## 2.1 Tectonothermal history of the Willyama Inliers

This section outlines previous work on the Willyama Basin and the tectonothermal history of the southern Curnamona Province (SCP). The depositional age and provenance of the Willyama Supergroup is summarised, along with the different tectonic settings that have been proposed for the Willyama Basin (*section 2.1.1*). The SCP has undergone several major magmatic events, some of which were coincident with deposition of the Willyama Supergroup. A brief description of each of these magmatic events follows, with emphasis placed on the timing and genesis of these different events (*section 2.1.2*). Interpretations made about the timing of tectonism in the SCP are detailed from geochronological studies that have been conducted in the terrain (*section 2.1.3*). Emphasis is placed on the contrasting interpretations that have been made about the tectonic evolution of the SCP. Tectonometamorphic models proposed for the SCP are summarised (*section 2.1.4*). The significance of tectonic interpretations made from these different studies is emphasised in the context of the role that the SCP played in Palaeo- and Mesoproterozoic tectonic reconstruction models (*section 2.1.5*). Contrasting interpretations about the timing of tectonism in the SCP has led to different models, that are both related to, and have no implications for the eastern margin of Proterozoic Australia with Laurentia.

### *2.1.1 Willyama Supergroup: deposition, provenance & tectonic setting*

The Willyama Supergroup was deposited between 1715 – 1645 Ma (Fig. 2.1, 2.2, 2.3; Page et al., 1998, 2000, 2003). Neither the basal unconformity nor the stratigraphic top of the Willyama Supergroup has been observed. Estimates of the preserved stratigraphic thickness range between 4 and 13 km (Willis et al., 1983). There is an apparent increase in stratigraphic thickness from west to east (Olary Domain to Broken Hill Domain), with a greater thickness of metapelitic sediments in the Broken Hill Domain and a greater thickness of calc-silicates and calc-albitites in the Olary Domain (Willis et al., 1983; Conor & Page, 2003; Fig. 2.1). To explain the differences in the stratigraphy between the two Domains, a number of workers (e.g. Laing, 1996b; Conor & Page, 2003) have suggested that the Broken Hill Domain lay proximal to the depocentre of the Willyama basin, with the Olary Domain occupying a position on its flank.

An extensive U-Pb detrital and magmatic zircon dataset constrains much of the stratigraphic age of the Willyama Supergroup, and the timing of major magmatic events (Page & Laing, 1992; Ashley et al., 1996; Page et al., 1998, 2000, 2003; Fig. 2.2, 2.3). Data considered to be unsubstantiated or highly contentious (e.g. Stevens, 1999; Page et al., 2000) relating to the timing of deposition of the lower Willyama Supergroup in the Broken Hill Domain have been excluded for clarity (e.g. Nutman & Ehlers, 1998). The lower sequences of the Willyama Supergroup include psammo-pelitic metasediments, migmatised quartzofeldspathic rocks, and calc albitites,

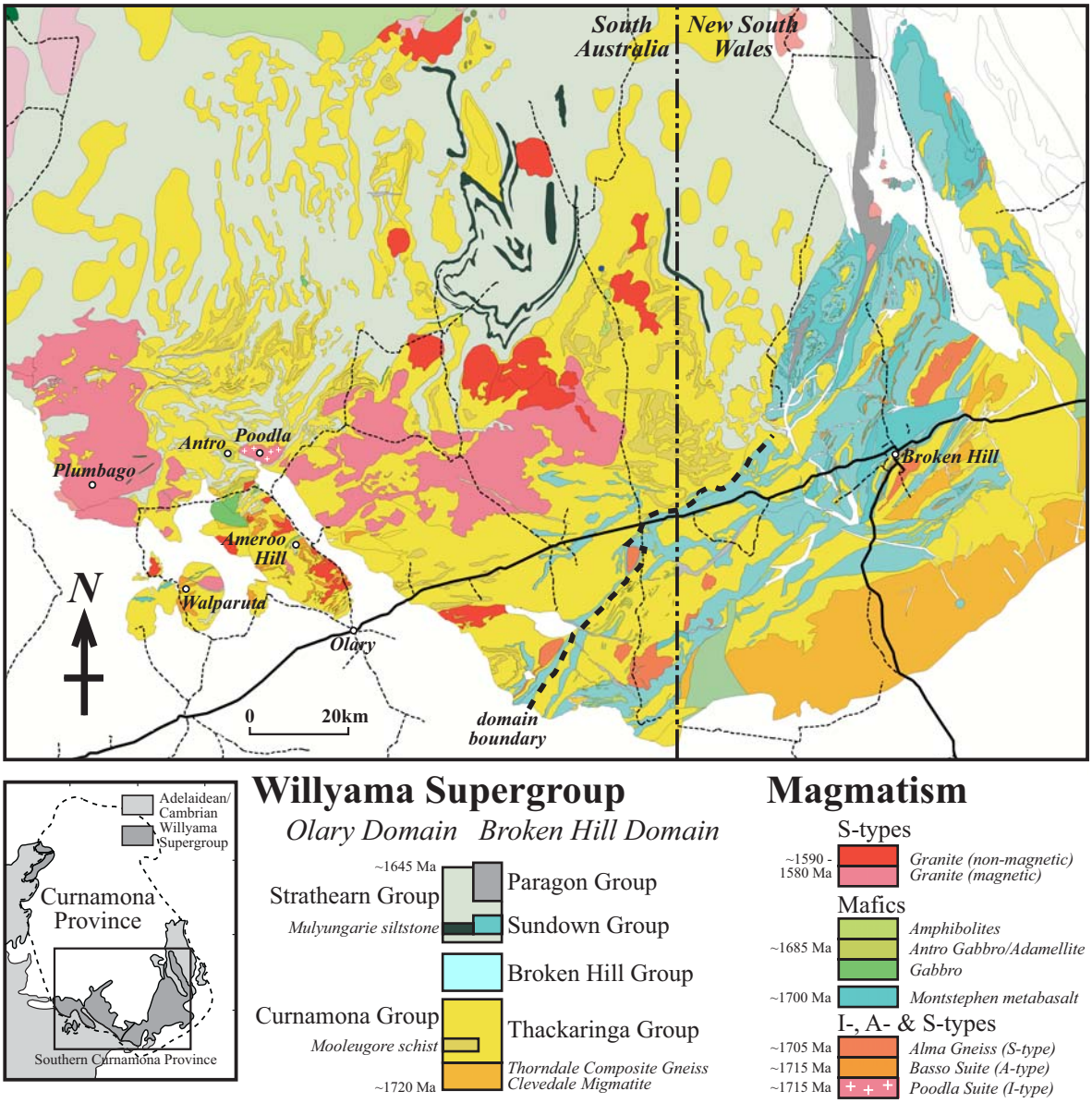


**Figure 2.1.** Interpreted solid geology of the southern Curnamona Province highlighting the distribution of stratigraphic units of the Willyama Supergroup (Jenkins & Burtt, 2003). Note the greater proportion of pelitic metasediments in the Broken Hill Domain relative to the Olary Domain (Broken Hill Group and Upper Willyama Supergroup [Paragon Group and Sundown Group]).

albite-quartz rocks (Thackaringa Group: ~1720 – 1705 Ma, and Wiperaminga Subgroup: 1720 – 1715 Ma), and interbedded A- and S-type felsic volcanic to subvolcanic rocks (*section 2.1.2*; Fig. 2.1, 2.2, 2.3). These sequences are no younger than ~1715 Ma based on zircon U-Pb isotopic studies (e.g. Page et al., 1998, 2000, 2003; Fig. 2.2). In the Olary Domain, the Wiperaminga Subgroup is overlain by the Ethiudna Subgroup (1715 – 1705 Ma; Page et al., 2003). The Ethiudna Subgroup is composed of quartzites, volcanoclastics, exhalatives, calc-silicates and calc-albitites (Conor, 2000a). Magmatic zircon from volcanoclastics and tuffaceous metasediments within the lower Ethiudna Subgroup constrain the maximum depositional age of this unit to be ~1715 Ma (Page et al., 2003; Fig. 2.2, 2.3). Together, the Wiperaminga and Ethiudna Subgroups in the Olary Domain are termed the Curnamona Group (1720 – 1705 Ma), which is directly correlated with the Thackaringa Group in the Broken Hill Domain (Conor, 2000a; Conor & Page, 2003).

A deepening of the depositional

**Figure 2.2.** Detrital, magmatic, tuffaceous and metamorphic zircon ages from the Willyama Supergroup metasediments and intrusives in the Broken Hill and Olary Domains determined by SHRIMP U-Pb studies by Page et al., (1998, 2000, 2003).

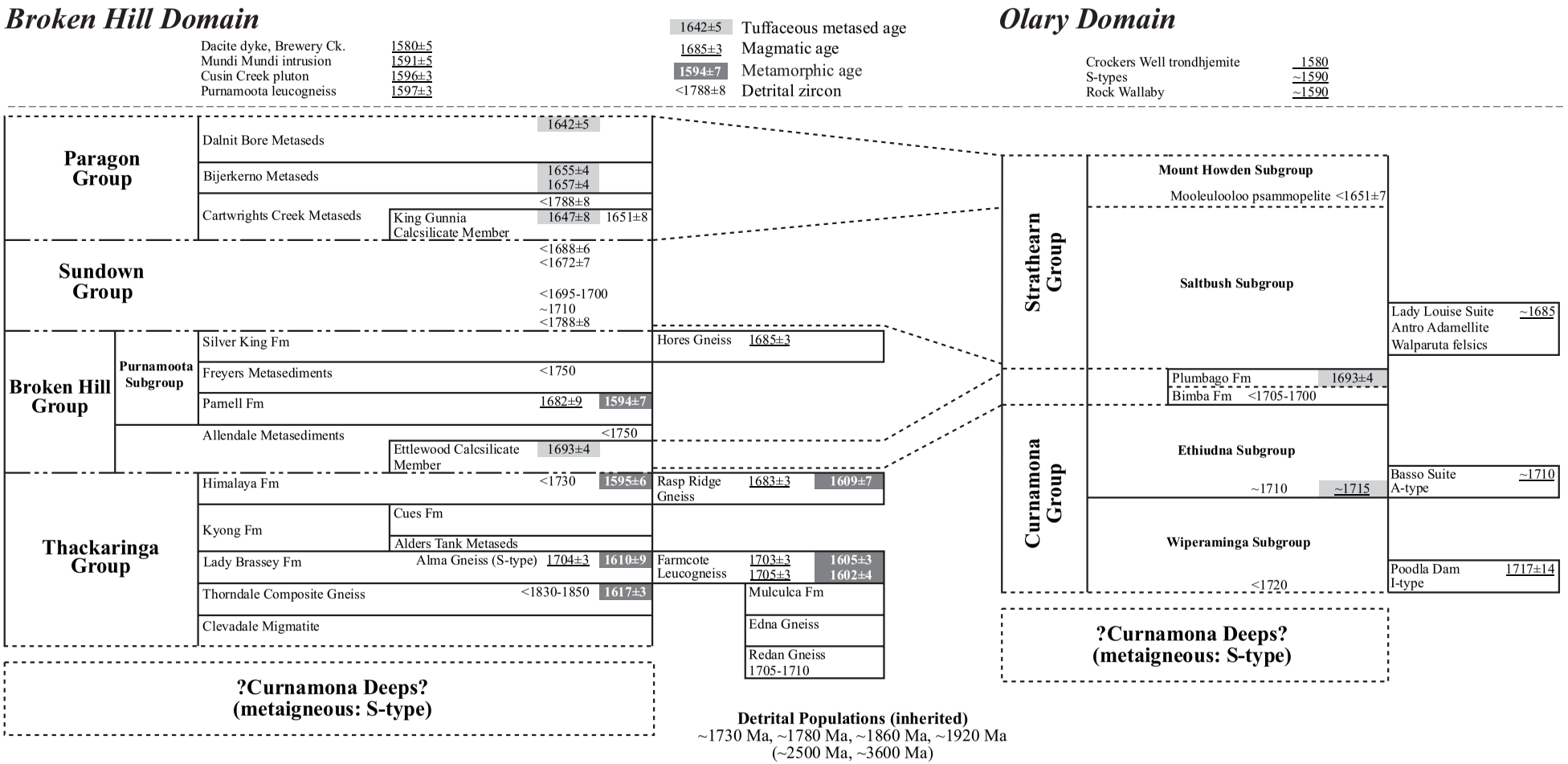

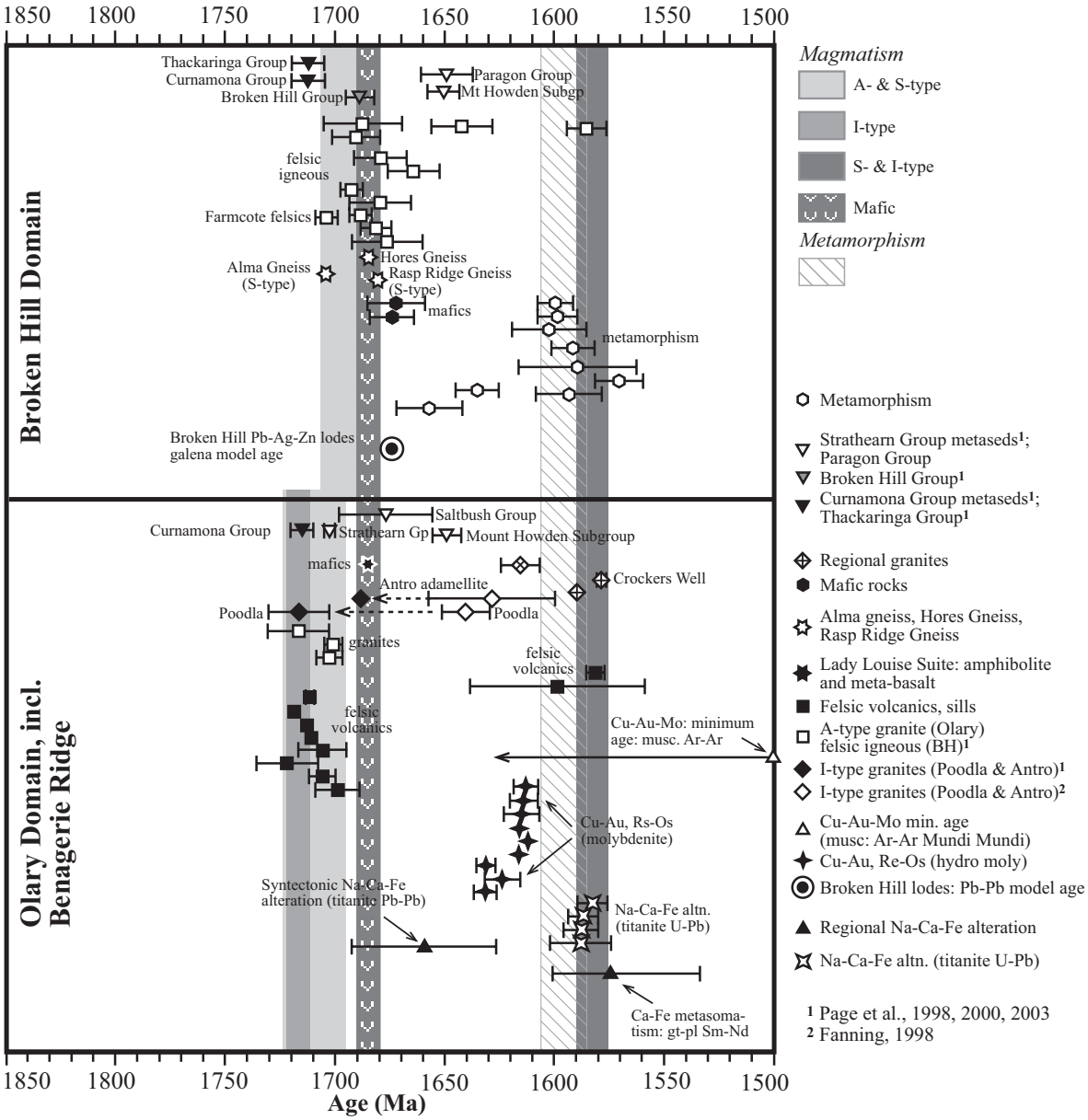


**Figure 2.3.** Summary of the southern Curnamona Province magmatic and metamorphic events after Skirrow et al. (1999) and Skirrow & Ashley (2000). Based on SHRIMP geochronology (Page & Laing, 1992; Ashley et al., 1996; Fanning et al., 1998; Donaghy et al., 1998; Nutman & Ehlers, 1998; Page et al., 1998, 2000). Titanite U-Pb (Skirrow et al., 2000). Ar-Ar (muscovite), Pb-Pb step-leach (titanite), Re-Os (molybdenite; Skirrow et al., 2000) and Sm-Nd (garnet-plag; Kent et al., 2000) constraints on hydrothermal events.

environment of the Willyama Basin resulted in the deposition of well-bedded, pelitic sediments and calc-silicates with exhalatives and basaltic magmatism (Broken Hill Group; Fig. 2.1, 2.2, 2.3). The Broken Hill Group (~1695 – 1685 Ma) is absent in the Olary Domain, but the tuffaceous Ettlewood Calsilicate Member (1693 ± 4 Ma; Page et al., 2003) of the lower Broken Hill Group has been correlated with the tuffaceous Plumbago Formation in the Olary Domain (1693 ± 3 Ma). The Plumbago Formation occupies a position either at the uppermost Ethiudna Subgroup or lowest Strathearn Group (e.g. Conor, 2000a; Page et al., 2003; Fig. 2.2, 2.3).

An upward transition to a basin wide deep-water environment is marked by the deposition of pelitic and minor psammitic sediments. Pelitic metasediments (Sundown and Strathearn Groups; Fig. 2.1, 2.2) overlie the Curnamona and Broken Hill Groups, and mafic and quartzofeldspathic lithologies are absent (Willis et al., 1983; Conor, 2000a). The

base of the Strathearn Group in the Olary Domain is constrained to be no older than ~1690 Ma based on the age of the Plumbago Formation (Page et al., 2000, 2003). A continued deepening of the Willyama Basin was accompanied by the deposition of the upper Paragon Group and Mount Howden Subgroup. Deposition occurred no earlier than 1657 ± 4 Ma, 1655 ± 4 Ma and 1642 ± 5 Ma for the Broken Hill Domain (upper Paragon Group), and 1651 ± 7 Ma in the Olary Domain (Mount Howden Subgroup) based on detrital zircon populations (Page et al., 2003; Fig. 2.2, 2.3). Much of the youngest Willyama metasedimentary sequences have age and lithostratigraphic similarities to sequences that host the Mount Isa and McArthur River orebodies in northern Australia (Page et al., 2000, 2003).

Metasediments of the Willyama Supergroup have detrital zircon U-Pb populations at ~1730 Ma, ~1780 Ma, ~1860 Ma, ~1920 Ma, with minor input of material from a ~2500 Ma and ~3600 Ma source (Page et al., 1998, 2000). Potential sources for detritus of this age could come from the Gawler Craton and/or Arunta crust (Collins & Shaw, 1995), however the latter region is favoured on the basis of geochemical composition and Nd isotopic studies on the Willyama Supergroup metasediments (Appendix 1; Barovich et al., 2002; Barovich, 2003; Barovich & Hand, 2004). The felsic, highly enriched rocks of the Arunta crust are consistent with the relatively enriched geochemical character of the Willyama Supergroup (Barovich, 2003; Fig. 2.4a). However, the Nd isotope compositions of the lower Willyama Supergroup are too evolved to be solely derived from an Arunta source, and may require an additional source that is likely to be Archaean age (Barovich, 2003). The Sleaford and Mulgathing Complexes from the Gawler Craton could potentially provide this component (Swain et al., 2005), as could either Archaean or Proterozoic crust from northern Australia or western Laurentia (e.g. Barovich, 2003; Fig. 2.4a).

Tectonic environments proposed for the deposition of the Willyama Supergroup include a shallow marine shelf or platform, intracratonic and back-arc rift basins (e.g. Willis et al., 1983; Giles et al., 2002, 2004). Willis et al. (1983) proposed that the Curnamona, Thackaringa and Broken Hill Groups represent a more advanced stage of rifting, as these units may represent a period of deepening shelf sedimentation during which time there was widespread bimodal volcanism (James et al., 1987). The most favoured tectonic setting for the deposition of the Willyama Supergroup is a volcanically active failed intracontinental rift, with initial intercalated terrestrial, lacustrine/sabhka and marine sequences being succeeded by deeper marine/lacustrine sequences (Willis et al., 1983; Page et al., 2000, 2003; Conor & Page, 2003). An ensialic rift environment is supported by the presence of felsic volcanics and high-Fe tholeiites (Phillips et al., 1985; James et al., 1987; *Chapter 4*). However, coarse-grained clastics and alkaline basic magmatism commonly seen in the early stages of continental rifting are not exposed (Willis et al., 1983; *and references therein*).

Rift-related models for the deposition of the Willyama Supergroup were thought to be

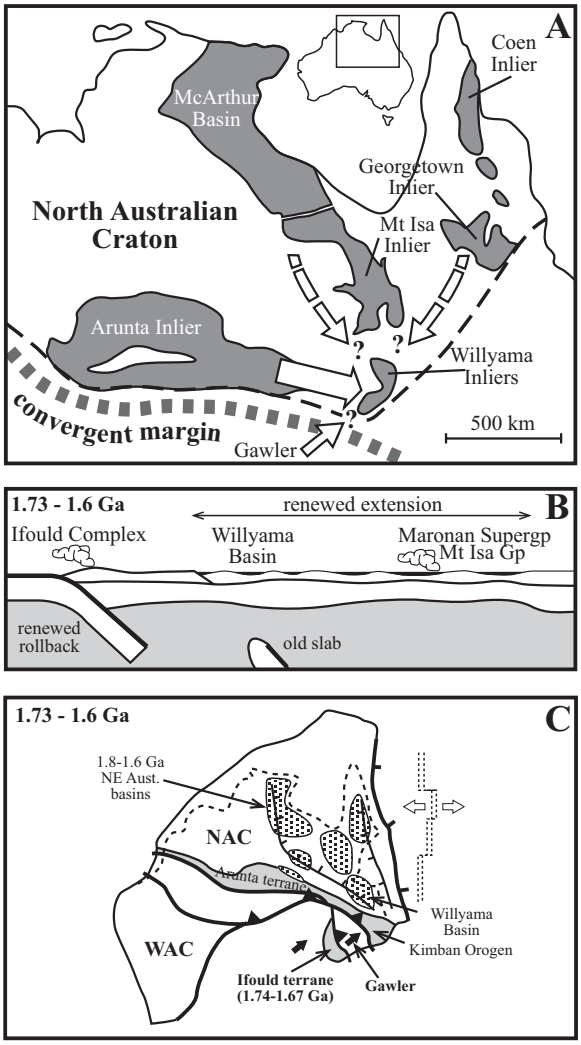


**Figure 2.4. (a)** Late Palaeoproterozoic tectonic reconstruction highlighting the close spatial proximity of the Willyama Basin to the Maronoan Basin in northern Australia. Both basins are situated in the back-arc to a convergent margin along the southern margin of the North Australian Craton (after Giles et al., 2002). Willyama Supergroup provenance studies favour a dominant detrital component from Arunta crust (Barovich, 2003). The lower Willyama Supergroup requires a more evolved crustal component, possibly from North Australia or the Gawler Craton (Barovich, 2003). **(b)** Convergent margin - back-arc basin model for tectonic setting of Willyama Basin (Giles et al., 2002). **(c)** Position of Willyama Basin relative to convergent margin south of Gawler Craton between 1.74 - 1.67 Ga as outlined in Fig. 9 of Betts et al. (2002).

analogous to the development of the Mount Isa Rift system in northern Australia, primarily because of their exhalative base metal association (Willis et al., 1983; Phillips et al., 1985). Evidence supporting an episodic rift-sag regime in the Mount Isa Inlier is well established, in the form of an extensive blanket of carbonaceous shale, dolostone and minor sandstone (e.g. Betts & Lister, 2001; Giles et al., 2002). However, such supporting evidence is not found in the Willyama Supergroup. On the basis of lithostratigraphic and depositional ages, the youngest basin development in the Willyama Supergroup has similarities with sequences in northern Australia (Page et al., 2003). These similarities have been used to directly correlate these regions of Proterozoic Australia within the same tectonic and depositional regime (e.g. Page et al., 2000, 2003; Giles et al., 2002).

Recently, a back-arc basin tectonic environment was suggested as a tectonic setting for the deposition of the Willyama Supergroup (Giles et al., 2002, 2004; Betts et al., 2002; Fig. 2.4b). This is based on reconstructions during the Palaeo- and Mesoproterozoic involving the North Australian Craton (NAC) and South Australia Craton (SAC; Myers et al., 1996). Giles et al. (2002, 2004) and Betts et al. (2002) propose that the Willyama Basin occupied a position in the back-arc to a convergent margin situated to the south of the Gawler Craton at ~1730 Ma (Fig. 2.4c). The occurrence of subduction-related calcalkaline magmatism in the southwestern Gawler Craton (Teasdale, 1997), was used as the basis for the convergent margin – back-arc model (Giles et al., 2002, 2004). The location of the Willyama Basin proximal to a convergent margin is supported in part by the rare earth element (REE) geochemistry of volcanogenic metasediments associated with sulphide mineralisation in the Olary Domain. These are interpreted to be derived from an andesitic source, which are often associated with convergent margin settings (Pearce & Cann, 1973; Pearce & Norry, 1979; Bierlein, 1995).

### *2.1.2 Magmatism in the southern Curnamona Province*

Several episodes of magmatism and volcanism occurred in the SCP during the Palaeo- and Meso-proterozoic. Syn-sedimentary A-type (Basso Suite) and S-type felsic magmatism (Alma Gneiss) intruded the Willyama Basin contemporaneously with deposition of the lower Willyama Supergroup (Curnamona Group and Thackaringa Group) with magmatic ages between *ca.* 1710-1705 Ma (Fanning, 1995; Ashley et al., 1996; Page et al., 1998, 2000, 2003; Barovich, 2003; Barovich & Hand, 2004; Fig. 2.1, 2.2, 2.3). Isolated occurrences of subvolcanic mafic magmatism also occurred at this time within Ethiudna Subgroup in the northern Weekeroo Inliers (Olary Domain; *ca.* 1700 Ma), and as irregular pods and plugs within the A-type felsic intrusives (e.g. Walparuta Inlier (*Chapter 4*) and Ameroo Hill; Ashley et al., 1996; Conor, 2000).

A widely distributed and volumetrically significant intrusive and subvolcanic basaltic magmatic event occurred at *ca.* 1685 Ma (*Chapter 4*; Page & Laing, 1992; Nutman & Ehlers, 1998, Conor & Fanning, 2001; Gibson & Nutman, 2004; Fig. 2.2, 2.3). These rocks intruded the lower Willyama Supergroup (Ethiudna Subgroup in the Olary Domain, and the Broken Hill Group (BHG) and Thackaringa Group in the Broken Hill Domain; Phillips et al., 1985; James et al., 1987; Conor, 2000a; Fig. 2.3; *Chapter 4*). Within the Olary Domain, this suite of magmatic rocks has been informally referred to as the Lady Louise Suite, and dated at 1685 ± 6 Ma (Conor & Fanning, 2001). This magmatic event occurred in conjunction with an increase in accommodation space within the Willyama basin (syn-Broken Hill Group deposition; Page et al., 2003), and was most likely the result of lithospheric thinning of the subcontinental lithospheric mantle (SCLM) beneath the Willyama basin. The effects of lithospheric thinning are most evident in the Broken Hill Domain with the deposition of the Broken Hill Group and bimodal magmatism (Parnell Formation, Rasp Ridge Gneiss, Hores Gneiss; Fig. 2.2, 2.3). Regional subsidence of the SCP occurred after deposition of the BHG, and was followed by deposition of deeper water sediments (Strathearn, Sundown and Paragon Groups; Fig. 2.2, 2.3; Stevens et al., 1980; Willis et al., 1983; Page et al., 2003; Conor & Page, 2003).

Mafic I-type tonalite and/or adamellite and granodiorite rocks have been interpreted to intrude the metasediments in the Olary Domain between 1660 – 1640 Ma, at Antro and Poodla respectively (Fanning et al., 1998; Fig. 2.1). These intrusives were interpreted to have magmatic crystallisation zircon ages of 1641 ± 11 Ma and 1629 ± 29 Ma, respectively (Cook et al., 1994; Fanning, 1995; Fanning et al., 1998). However, zircon from the Poodla Hill granodiorite is now considered to have a U-Pb SHRIMP magmatic age of 1717 ± 14 Ma, making this I-type magmatic suite the same age as A- and S-type magmatism across the southern Curnamona Province (Page et al., 2003). Additionally the Antro adamellite and felsic intrusives in the southeastern Walparuta Inlier in the Olary Domain (Fig. 2.1) are now interpreted to have the same magmatic age as the Lady Louise Suite, and are therefore an expression of the same

regionally extensive tectonothermal event (Fig. 2.1, 2.2; Page et al., 2003).

Widespread syn- to post-deformational granitoid magmatism occurred during the early Mesoproterozoic, mostly in the Olary Domain and Benagerie Ridge region (*ca.* 1590 – 1580 Ma; Ludwig & Cooper, 1984; Fanning et al., 1998; Page et al., 2003; Fig. 2.1, 2.2, 2.3). These include S-type granite, monzogranite, trondhjemite and more mafic I-type granodiorite to diorite (Appendix 1). A source dominated by anatexis of the metasediments is proposed for the S-type granites, while the trondhjemites and granodiorites require a more primitive source component based on their Nd isotopic compositions (Appendix 1; Barovich & Foden, 2002). Syn- to post-tectonic volcanism and bimodal magmatism occurred in the Plumbago region in the western Olary Domain and under cover in the Benagerie Ridge region, north of the Olary Domain (Fig. 2.1). This bimodal volcanic event includes porphyritic rhyolite-rhyodacite and amygdaloidal basalt (Teale & Flint, 1993). A U-Pb SHRIMP ages of 1582 ± 4 Ma has been obtained for the porphyritic rhyolite (Fanning et al., 1998; Fig. 2.3).

### *2.1.3 Timing of tectonism in the southern Curnamona Province*

The construction of a polymetamorphic history for the SCP was initially based on conventional U-Pb isotopic studies. Gulson (1984) proposed that metamorphism occurred at ~1660 – 1640 Ma and ~1600 – 1565 Ma (Olarian Orogeny). SHRIMP U-Pb zircon studies in the late-1990's resulted in two contrasting models on the timing of metamorphism in the SCP. Donaghy et al. (1998), Nutman & Ehlers (1998), Gibson (2000) and Gibson & Nutman (2004) proposed that metamorphism and extension occurred between ~1690 – 1670 Ma. Evidence of this event is interpreted by Gibson and Nutman (2004) to be reflected by different *P-T* histories in the lower Willyama Supergroup (lower plate) and upper Willyama Supergroup (upper plate). In the model of Gibson and Nutman (2004), the two plates were juxtaposed against one another during the Olarian Orogeny, in the same style as the exhumation of a metamorphic core complex.

In contrast, other detailed SHRIMP U-Pb zircon studies found no evidence of metamorphism between ~1690 – 1640 Ma (Page et al., 1998, 2000, 2003). These results led Stevens (2000) and Conor et al. (2005) to emphatically deny that metamorphism occurred prior to the Olarian Orogeny. Conor et al. (2005) refuted the Gibson & Nutman (2004) model on the basis that it was 'model-driven' and founded on misinterpretations about the lithostratigraphy, regional geology and geochronological interpretations. Resolving the timing of metamorphism in the SCP is one of the primary objectives of this study (*Chapter 3*).

Thermochronological (Ar-Ar, K-Ar, Rb-Sr) techniques have recorded discrete tectonothermal events associated with the Neoproterozoic Musgravian Event (~1200 – 1000 Ma) and Cambro-Ordovician Delamerian Orogeny (~500 – 480 Ma) as recorded by $^{40}Ar/^{39}Ar$ mica, hornblende and K-feldspar thermochronology and apatite fission track dating (Hartley et al., 1998). Local reactivation

of pre-existing shear zones in the SCP occurred during the ~500 Ma Delamerian Orogeny (Dutch et al., 2005).

### *2.1.4 Metamorphic expression of tectonism in the southern Curnamona Province*

The regional metamorphic pattern of the SCP was initially detailed by Binns (1964), Phillips (1980), Corbett & Phillips (1981), Phillips & Wall (1981) and Hobbs et al. (1984) in the Broken Hill Domain, and by Clarke et al. (1987) in the Olary Domain. These studies were built on further and refined by Clarke et al (1995), Stüwe & Ehlers (1997) and Wilson & Powell (2001). On the regional scale, the metamorphic grade increases from the NW to the SE in the entire Curnamona Province, with the highest grade attained in the Broken Hill region (e.g. Phillips & Wall, 1981; Clarke et al., 1987; Laing, 1996b).

In earlier studies the metamorphic pattern across the SCP was considered to have developed during a single event associated with the Olarian Orogeny. Three phases of metamorphism (M1, M2/M3) were identified within this single metamorphic event. Laing (1996b) provided the first regional synthesis of the earlier studies, and further refined the interpreted regional metamorphic isograd pattern across the SCP for M1 and M2/M3 (Fig. 2.5). In the earlier models, compression during cooling was inferred from the superposition of low-T, high-P assemblages (M2/M3) onto high-T, low-P assemblages (M1; Fig. 2.5; Phillips & Wall, 1981; Clarke et al., 1987). This model was reinforced further by Clarke et al. (1995), based on the post-deformational growth of staurolite – chloritoid ± kyanite that overgrew all earlier fabric elements. Clarke et al. (1995) interpreted that the low-T, high-P (kyanite-staurolite) assemblages formed during retrograde metamorphism associated with the Olarian Orogeny, and used this as supporting evidence of an anticlockwise *P-T* path. More recently, Stüwe & Ehlers (1997) focused more on the thermobarometric differences between the high-T, low-P and low-T, high-P assemblages. They concluded that the development of the low-T, high-P (480°C, 5 kbar) assemblages (staurolite – chloritoid) was unrelated to the earlier high-T, low-P event (650°C, 4-5 kbar), but were the result of a distinct metamorphic event, probably of Grenvillian (~1200 Ma) or Delamerian (~500 Ma) age (Fig. 2.6). Apart from the earlier geochronological studies (e.g. Gulson, 1984), this was the first independent interpretation that the SCP preserved a polymetamorphic history. Recently, thermobarometric studies by Swapp and Frost (2003) in the Broken Hill region concluded that peak M1 metamorphism conditions were as high as ~750 – 850°C and 8 – 9 kbar (Fig. 2.6).

Thermobarometric studies by Stüwe & Ehlers (1997), Clarke et al. (1995) or Swapp and Frost (2003) did not infer the existence of a high-grade metamorphic event prior to the Olarian Orogeny. This is contrary to interpretations of a tectonothermal event between 1690 – 1670 Ma (Donaghy et al., 1998; Nutman & Ehlers, 1998; Gibson, 2000; Gibson & Nutman, 2004). However, Stüwe & Ehlers (1997) correlate high-T, low-P assemblages with the second of two melting events. Gibson (2000) and Gibson & Nutman (2004) capitalised on this interpretation, and

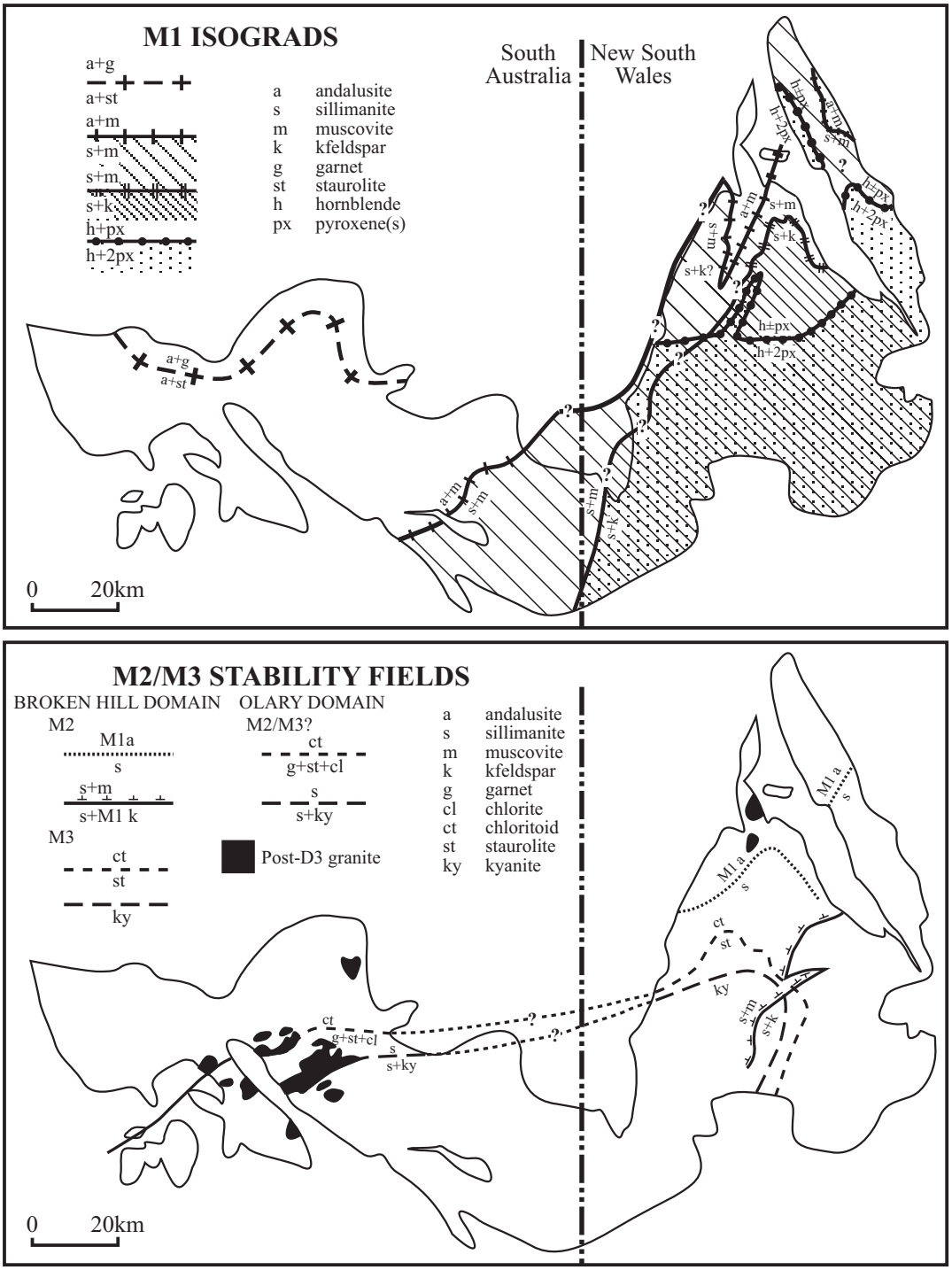


**Figure 2.5.** Map of the southern Curnamona Province outlining metamorphic isograds associated with: **(a)** M1 metamorphism, associated with D1 nappe deformation; **(b)** M2 and M3 metamorphism, associated with D2 and D3 folding and retrograde shear zone deformations (after Laing, 1996b). Data from Phillips (1980), Corbett & Phillips (1981), Phillips & Wall (1981), Clarke et al. (1987), Stevens et al. (1986), Stüwe & Ehlers (1997) and Webb & Crooks (2003).

proposed that ~1690 Ma tectonism is expressed by the presence of bimodal magmatism and metasomatism in the lower sequences of the Willyama Supergroup (Curnamona – Thackaringa Groups) versus absence in the upper Willyama Supergroup (Strathearn – Sundown – Paragon Groups). Gibson & Nutman (2004) also interpret that the lower and upper Willyama Supergroup sequences preserve different metamorphic mineral assemblages. Clearly the timing of development of the different metamorphic mineral assemblages in the SCP is crucial to understanding the metamorphic history of the

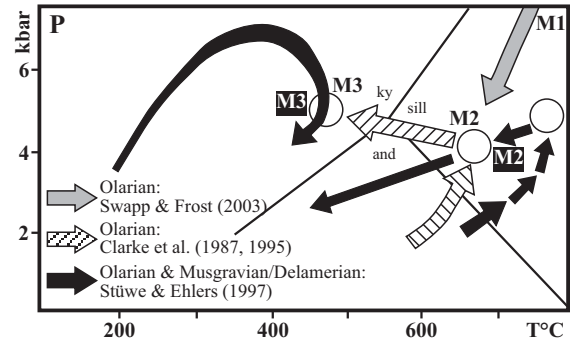


**Figure 2.6.** Simplified P-T paths for contrasting models relating to the metamorphic history in the SCP. Black arrowed path shows polymetamorphic history identified by Stüwe & Ehlers (1997). Patterned arrows shows single metamorphic path identified by Clarke et al. (1987, 1995). Modified from Stüwe & Ehlers (1997). Grey arrowed path of Swapp & Frost (2003).

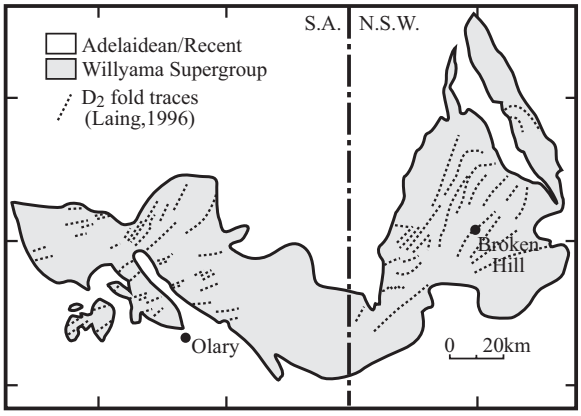


**Figure 2.7.** Regional geological map of the southern Curnamona Province showing distribution of Willyama Supergroup, and $D_2$ fold traces from the regional structural synthesis of Laing (1996b).

terrain (e.g. Clarke et al., 1995; Stüwe & Ehlers, 1997; Gibson & Nutman, 2004). This is one of the main objectives of this study, and will be explored further in the *Chapter 3*.

The structural evolution of the SCP is as complex as the metamorphic history. At least five deformational events have affected rocks of the SCP, and have been interpreted to have formed anywhere between the Palaeoproterozoic and Cambrian (Campana & King, 1958; Webster, 1996; Wilson & Powell, 2001; Gibson & Nutman, 2004). The development of migmatites, gneissic layering and partial melting often accompanied by a layer parallel foliation ($S_1$), has been interpreted differently. Initially these features were interpreted to have developed during nappe emplacement associated with $D_1$ at ~1600 Ma (Laing et al., 1978; Clarke et al., 1986). More recently, $D_1$ was attributed to crustal extension during lithospheric thinning associated with bimodal magmatism at ~1690 Ma (Donaghy et al., 1998; Nutman & Ehlers, 1998; Gibson, 2000; Gibson & Nutman, 2004; Gibson et al., 2004). The uncertainty surrounding the character and timing of $D_1$ is accentuated by the absence of mappable $F_1$ folds across the SCP (Gibson & Nutman, 2004).

Within most regions of the SCP, the dominant penetrative fabric observed in outcrop has been interpreted to develop during the Olarian Orogeny. At most localities, this has been referred to as $S_2$ and has developed most strikingly in $F_2$ folds that are responsible for many of the map-scale fold patterns (Laing, 1996b; Laing et al., 1978; Clarke et al., 1986; Fig. 2.7). $D_3$ and possibly $D_4$ are interpreted to have formed during retrograde metamorphism and retrograde shearing during the waning stages of the Olarian Orogeny (Corbett & Phillips, 1981; Phillips & Wall, 1981; Clarke et al. 1987). However, recent investigations on the 'retrograde' shear zones have found that reactivation and fabric development on some of these shear zones occurred during the Delamerian Orogeny (Dutch et al., 2005).

At least two fabrics are interpreted to have developed during the ~500 Ma Delamerian Orogeny. Macroscopic refolding of $D_2$ structures, crenulation of pre-existing fabrics, and shear zone reactivation has been interpreted to develop during this time ($D_4$ and $D_5$; Campana & King, 1958; Berry et al., 1984; Webster, 1996; Dutch et al., 2005).

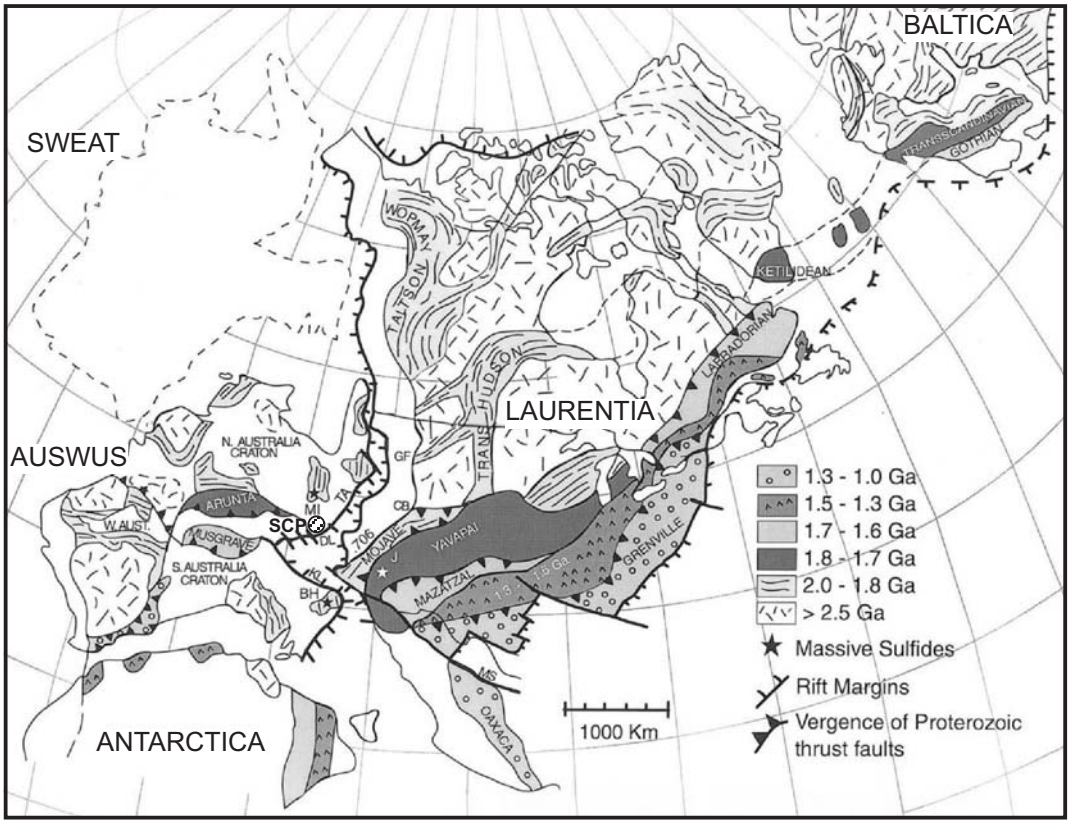


**Figure 2.8.** AUSWUS reconstruction for the Proterozoic (Karlstrom et al., 2001). The position of Australia in the SWEAT reconstruction is shown for comparison (Moores, 1991). Crustal provinces inferred from U/Pb data; 0.706=Sr 0.706 line; CB=Cheyenne Belt; DL=Diamantina lineament; GF=Great Falls tectonic zone; KL=Koonenberry fault zone; MS=Mojave–Sonora megashear; TA=Tasman Line. Centralian Superbasin includes the Officer basin (O), Amadeus basin (AM), Georgina basin (G), and Adelaidian basin (AD); Neoproterozoic rocks in Laurentia outcrop in Caborca (C), Death Valley (DV), and Uinta Mountains (U).

### *2.1.5 The southern Curnamona Province within a plate tectonic framework*

Studies focussing on tectonic reconstructions have suggested that a pre-Rodinian supercontinent existed (e.g. Windley, 1995; Rogers, 1996). Rogers and Santosh (2002) named this "Columbia". This entity contained all of the world's continental blocks which amalgamated during global 2.1 – 1.8 Ga collisional orogens (see Zhao et al., 2004 for detailed summary). Following its assembly, Columbia underwent subduction-related outgrowth between ~1.8 – 1.3 Ga (Zhao et al., 2004). Breakup of Columbia is interpreted to have began at ~1.6 Ga, and was followed by amalgamation of the Rodinia supercontinent by ~1.0 Ga (Dalziel, 1995).

The exact role Proterozoic Australia played in the Columbia supercontinent remains uncertain (e.g. Zhao et al., 2004). Continental outgrowth along accretionary magmatic arcs is supported along the southern and eastern margins of the North Australian Craton (NAC) (Myers et al., 1996; Giles et al., 2002). This outgrowth coincided with major tectonic events, producing a complex continental margin along the southern and eastern margins of the NAC (Giles et al., 2002; Fig. 2.4).

The earliest model correlated the Proterozoic of eastern Australia with northwest Laurentia (SWEAT model; Moores, 1991; Fig. 2.8, 2.9a). This relationship was supported by the correlation of numerous breccia zones within both the Yukon (Wernecke breccias) and the Olympic Dam region in the eastern

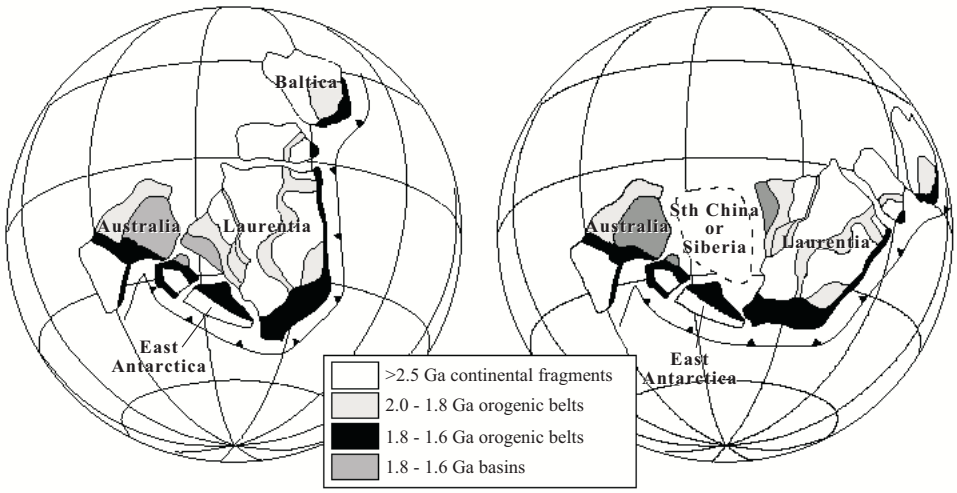


**Figure 2.9.** Two possible configurations of Australia, East Antarctica, Laurentia and Baltica at ca. 1.7 Ga based on modification of Karlstrom et al. (1999) reconstruction to account for rotation of the South Australia Craton and its proposed continuations in East Antarctica (Giles et al., 2004). (a) Australia occupies a SWEAT position with respect to North America; (b) Australia occupies a more westerly position allowing space for another continental fragment between Australia and North America.

Gawler Craton (Thorkelson et al., 2001a; 2001b). Widespread brecciation in the Olary Domain is nearly contemporaneous with the Wernecke and Olympic Dam breccias, although the breccias in the Wernecke and Olympic Dam regions are related to sub-volcanic activity, whereas the Olary Domain breccias are metamorphic in origin (e.g. Clark & James, 2003).

The SCP occupies an important place in the tectonic history of eastern Proterozoic Australia, as the tectonothermal history interpreted for the SCP has been crucial to linkages made between eastern Australia and Laurentia during Palaeoproterozoic and early Mesoproterozoic times (~1715 – 1550 Ma; Kalstrom et al., 1999; Burrett & Berry, 2000, 2002; Zhao et al., 2004; Fig. 2.8). The proposal of tectonism as early as ~1690 Ma in the SCP has led to its prominence in plate tectonic reconstruction models supporting a connection between Australia and southwest Laurentia (AUSWUS; Kalstrom et al., 1999; Burrett & Berry, 2000, 2002; Fig. 2.8). If tectonism occurred no earlier than the ~1600 Ma Olarian Orogeny, then these interpretations involving the SCP are incorrect, and require that models regarding the relationship between the late-Palaeoproterozoic of eastern Australia and western Laurentia be re-evaluated.

As an alternative to SWEAT and AUSWUS models, Wingate et al. (2002) proposed a northern Australia – southernmost Laurentia connection (AUSMEX) on the basis of palaeomagnetic data. Subsequently, palaeomagnetic data has been shown to be at odds to any Australia – Laurentia connection, as Australia was positioned at high latitudes at ~1.2 Ga, whereas Laurentia occupied low latitudes at this time (Pisarevsky et al., 2003). Recently, it has been proposed that Australia and Laurentia were in no way connected during the Proterozoic, and either Siberia or Australia occupied a position to the east of Proterozoic Australia and west of Laurentia (Fig. 2.9b; Li et al., 1995; Sears & Price, 2000; Giles et al., 2004).

## 2.2 Mineralisation and alteration systems of the southern Curnamona Province

This section reviews studies on the different styles and genesis of alteration and mineralisation in the Olary Domain, excluding the well known Pb-Zn-Ag systems. Particular emphasis is placed on Fe-oxide Cu-Au (IOCG) mineralisation, as occurrences of this style of mineralisation are becoming of increasing economic importance in the Olary Domain. All mineralisation styles occur predominantly in albitic and calc-albitic metasedimentary rocks near the top of the lower Willyama Supergroup (Thackaringa, Broken Hill and Curnamona Groups). *Section 2.2.1* summarises the different styles of syngenetic mineralisation. *Section 2.2.2* summarises the different epigenetic mineralisation styles that have been reported. The different alteration styles and relative timing of alteration and IOCG mineralisation is summarised in *section 2.2.3*. Potential sources of the different mineralisation styles are summarised in *section 2.2.4*. Finally, a re-evaluation of geochronological constraints on IOCG mineralisation is made, as recent advances in the Re-Os techniques used to acquire these constraints casts doubts on the accuracy of these ages (*section 2.2.5*).

### *2.2.1 Syngenetic mineralisation*

An abundance of barite-rich horizons, quartz-magnetite ± hematite and magnetite-hematite rich iron-formations in the Curnamona Group have been interpreted to represent original facies variations within a hydrothermally active depositional environment (e.g. Lottermoser & Ashley, 1996). Competing volcanogenic and chemical sedimentation with multiple hydrothermal events resulted in a variety of depositional products. These include quartz – Fe-oxide ± barite iron formations in the Wiperaminga Subgroup, and stratabound hematitic iron formations with Ca-Fe-Na silicates and oxidic Mn-bearing rocks in the Ethiudna Subgroup (Conor, 2004). These likely represent evaporitic and exhalative chemical sediments (Cook & Ashley, 1992). Unlike chemical sediments in the Broken Hill Domain, barite-rich rocks, ironstones and iron formations in the Curnamona Group have low Pb and Zn values. However, scattered elevated Cu and Au concentrations point to a potential for stratabound Cu-Au mineralisation (Lottermoser & Ashley, 1996).

Localised manganiferous iron formations with elevated concentrations of As, Au, Mn, P, U and Zn have previously been interpreted to represent pure high-temperature chemical precipitates (Lottermoser & Ashley, 1996). These have similar mineralogical and geochemical characteristics to banded iron formations associated with stratiform Pb-Zn-Ag sulphides in the Broken Hill region (Lottermoser & Ashley, 1996). The abundance and diversity of such chemical sediment accumulations in the Olary Domain relative to the Broken Hill Domain led to them being correlated with palaeoenvironments including hot spring, evaporitic sabkha and/or playa settings, similar to those of the modern East Africa Rift, Dead Sea, Red sea or the Salton Sea in the Gulf of California (Ashley et al., 1994).

Compared to the extremely homogeneous lead isotopic signature of the Broken Hill stratiform Pb-Zn-Ag mineralisation (e.g. Parr et al., 2004), stratiform and stratabound mineralisation in the Olary Domain has a heterogeneous distribution of lead isotope ratios (Bierlein et al., 1996b). Bierlein et al. (1996b) interpreted that syngenetic and diagenetic mineralisation in the Olary Domain was the product of a single-pass fluid, or restricted fluid circulation in relatively confined convective cells. These concentrated hydrothermal cells were thought to be responsible for hot spring activity and the localised accumulation of anomalous metals in the metasediments. The oxidised nature of the fluids that produced the iron-formations and barite-rich rocks makes the formation of massive sulphide accumulations improbable due to the absence of reduced sulphur (e.g. Lottermoser & Ashley, 1996).

### *2.2.2 Epigenetic mineralisation*

Ashley et al. (1994) and Lottermoser & Ashley (1996) recognised that iron formations were locally reworked and/or replaced during or after peak metamorphism forming stratabound, epigenetic veins, massive to brecciated iron oxide-rich bodies and calcsilicate matrix breccias, some of which have elevated Cu and Au contents. Oxidised and saline hydrothermal fluids were interpreted to be responsible for this (Lottermoser & Ashley, 1996; Bierlein et al., 1996a). Fe, Cu and Au were mobilised and subsequently precipitated in suitable sites such as shear zones, dilatancy zones and pre-existing iron formations and feldspar-rich rocks. Epigenetic mineralisation has been noted to overprint or replace earlier stratiform or stratabound Pb-Zn mineralisation (Lottermoser & Ashley, 1996; Bierlein et al., 1996a; Ashley, 2000; Skirrow et al., 2000; Teale & Fanning, 2000a).

Vein-style, breccia and replacement style mineralisation often occur as stratabound zones in albitic and calcalbitic metasedimentary units of the Curnamona Group and metapelitic units of the lower Strathearn Group (e.g. Kalkaroo, North Portia, Waukaloo, Polygonum; Skirrow et al., 2000). Often this mineralisation is associated with K±Na alteration that extends stratigraphically upwards into the Strathearn Group (Skirrow et al., 2000). An elemental association of Fe-Cu-Au-Mo-REE-F-Ba-Co with highly oxidised, Fe-rich host rocks are characteristic of Proterozoic IOCG systems (e.g. Hitzman, 2000), and led to the recognition of such styles of mineralisation in the SCP (e.g. Skirrow et al., 2000; Teale & Fanning, 2000a).

Although the majority of significant mineralisation is stratabound, located at the redox interface between the Curnamona and Strathearn Groups (e.g. Robertson et al., 1988; Ashley, 2000; Leyh & Conor, 2000), structurally controlled mineralisation styles are also recognised in the lower Willyama Supergroup. Massive iron-oxide Cu-Au(-Mo) (e.g. North Portia) and structurally controlled, fault bounded Cu-Mo(-Cu) breccia pipes are present (e.g. White Dam, Kalkaroo and Portia prospects; Skirrow et al., 2000; Teale & Fanning, 2000a). The diversity of mineralisation styles that characterise IOCG systems elsewhere in the world (e.g. Hitzman et al., 1992; Haynes, 2000; Hitzman, 2000) is exemplified by IOCG systems across the SCP.

IOCG systems in the SCP vary from iron-oxide-poor, Au-rich, Cu-poor (e.g. White Dam prospect) to iron-oxide-rich, Cu-rich, Au-poor (e.g. Copper Blow prospect). The full spectrum of IOCG systems in the SCP is summarised by the regional syntheses of Skirrow et al. (2000) and Williams & Skirrow (2000).

### *2.2.3 Alteration styles and timing of IOCG mineralisation*

The relationship between alteration and mineralisation that is characteristic of IOCG systems elsewhere in Australia and the world (e.g. Partington & Williams, 2000; Barton & Johnson, 2004), is also evident in IOCG systems of the SCP. Regional- to local-scale alteration affects much of the SCP. Textural evidence in the low-grade Benagerie Ridge region bracket the timing of regional Na-Fe alteration between diagenetic formation of carbonate evaporites and metamorphic recrystallisation to albite and/or magnetite during $D_1$ and $D_2$ (Skirrow et al., 2000). Other styles of alteration include pre- or early-tectonic stratabound Na-Fe metasomatism, and syntectonic stratabound Na-Ca-Fe metasomatism (Kent et al., 2000; Teale & Fanning, 2000a; Skirrow et al., 2000). SHRIMP U-Pb (titanite) dating of Na-Ca-Fe metasomatism yielded ages of ~1588-1583 Ma, which is contemporaneous with the latter stages of the Olarian Orogeny ($D_3$; Skirrow & Ashley, 2000; Skirrow et al., 2000). Syntectonic alteration systems include calcsilicate matrix breccias and vein networks, brecciated ironstones, albitisation and massive garnet-epidote replacement zones (Yang & Ashley, 1994; Skirrow et al., 2000; Kent et al., 2000). The timing of garnet-epidote alteration is comparable with that of the Na-Ca-Fe alteration event at 1575 ± 26 Ma (garnet Sm-Nd errorchron; Kent et al., 2000).

The timing of IOCG mineralisation has been interpreted to be syn- to post-peak metamorphic, during the late-Palaeoproterozoic to early- Mesoproterozoic Olarian Orogeny. This is based on both the textural relationships between mineralisation, alteration, deformation, and geochronological constraints (e.g. Skirrow et al., 2000; Williams & Skirrow, 2000). The earliest and highest temperature alteration event after regional syn-diagenetic albitisation, that included mineralisation (chalcopyrite – pyrite molybdenite), is characterised by iron-calcic assemblages (Skirrow et al., 2000). Mineralisation styles associated with this alteration event include veins and replacements, containing assemblages such as magnetite – actinolite – K-feldspar – quartz – albite – titanite – allanite (e.g. Kalkaroo, Waukaloo; Skirrow et al., 2000). Rhenium – osmium (Re-Os) isotope dating of molybdenite from this mineralisation event at North Portia, Kalkaroo, White Dam and Waukaloo yield pre-peak metamorphic ages ranging from ~1632 – 1612 Ma (Skirrow et al., 1999). A critical re-evaluation of the Re-Os ages will be addressed in *section 2.2.4*.

In addition, hydrothermal monazite associated with the invasive albitisation has been interpreted to record the timing of this event to be ~1630 Ma (SHRIMP U-Pb; Teale & Fanning, 2000a). SHRIMP U-Pb studies on hydrothermal monazite from a number of areas in the SCP also record discordant $^{207}Pb/^{206}Pb$ ages at ~2300 Ma, ~1810 Ma,

~1705 Ma, ~1640 Ma and ~1550 Ma (Teale & Fanning, 2000b). Consequently, the interpreted albitisation age of ~1630 Ma is questionable given the complicated age spectra, and potential for mixing of age populations.

Major deposition of chalcopyrite, gold and molybdenite mineralisation occurred in association with invasive potassic and sodic alteration (biotite, quartz, K-feldspar, albite; Skirrow et al., 2000; Teale & Fanning, 2000a). Hydrothermal monazite associated with this event at North Portia record the timing of this event to be ~1605 Ma (SHRIMP U-Pb; Teale & Fanning, 2000a). In the Benagerie Ridge region, this alteration event is dominated by albite – quartz – calcite ± ankerite (Teale & Fanning, 2000a). The pervasive potassic-sodic alteration overprints and/or forms in zones above or lateral to the earlier iron-calcic alteration assemblages (amphibole, Fe-oxides, carbonate; Skirrow & Ashley, 1998; Skirrow et al., 2000). Pervasive 'red-rock' potassic alteration characterised by K-feldspar containing hematite inclusions are common (Skirrow et al., 2000). Hydrothermal and/or metamorphic magnetite may also accompany the pervasive alteration and mineralisation event in veins or disseminations (e.g. Polygonum), as massive replacements (e.g. Copper Blow), and within breccia matrix (e.g. Walparuta; Skirrow et al., 2000). Syntectonic alteration in the northern Olary Domain that is similar to alteration associated with mineralisation in the Benagerie Ridge region includes calcsilicate-matrix breccias, vein networks and intense albitisation (Skirrow et al., 2000). Assemblages include albite, clinopyroxene, quartz, magnetite, hematite, garnet and titanite.

Late-stage, low-temperature carbonate – chlorite assemblages form replacements and vein networks (Skirrow et al., 2000; Teale & Fanning, 2000a). This was accompanied by minor chalcopyrite – pyrite mineralisation, chloritisation, quartz, fluorite, hematite and rutile crystallisation, and minor remobilisation and upgrading of pre-existing mineralisation (Skirrow et al., 2000; Teale & Fanning, 2000a). It is possible this alteration and mineralisation event developed during the Delamerian Orogeny, as *P-T* estimates for the Delamerian Orogeny would be conducive to the re-equilibration of these assemblages (*Chapter 3*; Dutch et al., 2005). Additionally, $^{40}Ar/^{39}Ar$ age spectra of micas associated with sulphide-bearing epigenetic veins are interpreted to represent emplacement ages of 450 – 480 Ma (Bierlein et al., 1996c). Chalcopyrite mineralisation associated with metamorphic recrystallisation of actinolite – magnetite – garnet ± pyrrhotite ± pyrite (e.g. Lawson and Wilkins prospects), and magnetite – actinolite – biotite – garnet – staurolite ± arsenopyrite (Green & Gold prospect; Skirrow et al., 2000) may also be associated with the Delamerian reworking.

### *2.2.4 Potential sources of mineralisation*

A direct genetic link between the earlier stratiform or stratabound mineralisation with epigenetic mineralisation has not been established (e.g. Ashley et al., 2000). Fluid inclusion, sulphur isotope and lead isotope studies on the different mineralisation styles showed that dense and moderately saline $CO_2$–$CH_4$-rich fluid prevailed early in the Olarian Orogeny, and became increasingly denser and more saline during rehydration

and retrogression in the later stages of the Olarian Orogeny (Bierlein et al., 1996a; 1996b). Relatively uniform $\delta^{34}S$ values (+5 – +10‰) in both stratabound and epigenetic mineralisation are interpreted to have developed by large-scale leaching of volcaniclastic and sedimentary source rocks, or alternatively convective homogenisation of a mixed evaporitic or seawater sulphate and igneous sulphide source (Bierlein et al., 1996a). It is suggested this fluid mixed with sedimentary sulphur in stratabound occurrences to produce lighter sulphur isotope compositions ($\delta^{34}S \geq -15.6$‰) in sulphides associated with carbonaceous pelites (Bierlein et al., 1996a). Stable isotope and fluid inclusion studies of IOCG systems in the Benagerie Ridge region support that mineralising fluids had temperatures ranging between ~250 – 450°C and were hypersaline Na-Ca-K fluids (Skirrow et al., 2000; Williams & Skirrow, 2000).

The epigenetic styles of mineralisation are characterised by a narrow range in sulphur isotopic composition ($\delta^{34}S \geq +5.8 – +7.6$‰), relative to that of stratabound mineralisation, which excludes simple remobilisation of earlier stratabound mineralisation (Bierlein et al., 1996a). Bierlein et al. (1996a) alternatively suggested that periodic extraction of the same source region to that of stratabound mineralisation occurred during post-peak Olarian tectonothermal events. Lead isotope studies on mineralisation further corroborated this interpretation, which indicated periodic extraction of lead occurred from a relatively homogenous source (Bierlein et al., 1996b). It was concluded from these studies that post-peak metamorphic fluids were sourced from a deep-seated hydrothermal reservoir, which remobilised metals as it circulated to the upper crust during tectonically induced circulation. The ascending hydrothermal system interacted with infiltrating surface waters, resulting in dilution, cooling and precipitation of metals (Bierlein et al., 1996a).

$\delta^{18}O$ compositions of syntectonic regional alteration fluids are in the range of 8 – 11‰ calculated at ~450 – 500°C, and are consistent with derivation from post-peak metamorphic fluids being sourced from the Willyama Supergroup metasediments (Skirrow et al., 2000). Fluids involved in regional epigenetic mineralisation have a wider range in $\delta^{18}O$ values (4.4 – 13.4‰), and are consistent with either a metamorphic or hydrothermal origin, or combination of both (Bierlein et al., 1996a). The lower $\delta^{18}O$ values are consistent with a dominant meteoric component, which is further corroborated by oxygen isotopes from mineralisation in the Benagerie Ridge (4.2 – 8.5‰ at ~300 – 450°C; Skirrow et al., 2000). However, Skirrow et al. (2000) interpreted that this isotopically lighter composition was potentially related to magmatically-derived fluids.

The apparent coincidence of the timing of alteration and IOCG mineralisation in the SCP with syn- to post-tectonic felsic magmatism (~1590 – 1580 Ma; Page et al., 2003), has encouraged connections to be made between the mineralising fluid source and magmatic fluids similar to the Olympic Dam system (e.g. Robertson et al., 1998; Skirrow et al., 2000). However, unlike other regions where the connection has been well established (e.g. Mt Isa Inlier: Pollard, 2001; Tennant Creek:

Compston & McDougall, 1994; Olympic Dam: Johnson & McCulloch, 1995), such a link has not been unequivocally proven in the SCP. Furthermore, the syn- to post-tectonic granitoids in the Olary Domain are chemically reduced, and do not contain significant IOCG mineralisation, or show evidence of significant fluid evolution (Ashley et al., 2000).

### *2.2.5 Re-evaluation of timing of IOCG mineralisation*

Re-Os isotopic studies on the timing of molybdenite growth associated with IOCG mineralisation in the SCP showed that mineralisation at North Portia, Kalkaroo, White Dam and Waukaloo prospects occurred between ~1632 – 1612 Ma, with 66% of the analyses ranging in age from 1616 – 1612 Ma (Skirrow et al., 2000). Skirrow et al. (2000) indicated that these analyses not only have very high precision (± 1.1 – 6.5 Ma) and consistent reducibility (0.1 – 0.4%), but also have uncertainties surrounding the $^{187}$Re decay constant (Smoliar et al., 1996) which equates to age errors of between 0.5 – 1%. This equates to absolute errors of ~8 – 16 million years on the calculated ages, resilting in a range in Re-Os ages that overlap with pre-peak to syn-peak Olarian metamorphism (*Chapter 3*; Page et al., 1998, 2000, 2003).

Since the Re-Os molybdenite studies were conducted on IOCG mineralisation in the SCP, it has also been documented that additional sources of potential error in Re-Os ages may stem from spatial decoupling of $^{187}$Re parent and $^{187}$Os daughter within individual coarse-grained molybdenite grains (e.g. Stein et al., 2001). Stein et al. (2001) experimentally deduced that fine-grained molybdenite samples, which are completely homogenised during sample preparation and digestion, gave accurate ages compared to coarse-grained molybdenite, or pieces of a coarse grain that gave a variation in isotopic ages. This equated to a variation in ages of up to ~50 – 200 m.y. on the Archaean-aged molybdenite sample used in the study of Stein et al. (2001).

As the uncertainties surrounding the variation in the $^{187}$Re decay constant and Re-Os parent-daughter spatial decoupling were not as clearly understood when the Re-Os isotopic study was conducted on IOCG mineralisation in the SCP, the estimated timing of mineralisation in the SCP is more likely to be syn-Olarian. Textural relationships between fabric development, mineralisation and alteration suggest that the mineralisation took place subsequent to the fabric development, and even up to the formation of crenulation cleavage development at Polygonum prospect (Leyh, 1995). This equates to pre-peak to post-peak Olarian age for mineralisation, based on the timing of Olarian metamorphism across the SCP (~1610 – 1560 Ma; *Chapter 3*; Page et al., 1998, 2000, 2003).

# Chapter 3
# TIMING OF PROTEROZOIC METAMORPHISM

**This chapter is a version of a manuscript in press with the Australian Journal of Earth Sciences under the title: "Timing of Proterozoic metamorphism in the southern Curnamona Province: Implications for tectonic models and continental reconstructions". Authors: Rutherford, Hand, Barovich & Clark. Aspects relating to the regional geological framework in the submitted version have been removed from this chapter to avoid repetition.**

***SUMMARY***
*Chemical U-Th-Pb monazite ages from metasedimentary and meta-igneous units of the Willyama Supergroup have confirmed initial SHRIMP U-Pb metamorphic zircon ages constraining the onset of the earliest tectonometamorphic event (the Olarian Orogeny) at ca. 1610 Ma in the southern Curnamona Province. An additional episode of high-grade metamorphism and heterogeneously distributed retrograde metamorphism and monazite recrystallisation occurred between ~1570 – 1550 Ma. The specific chemical age groupings between ~1610 – 1550 Ma indicates that Proterozoic metamorphism in the SCP was episodic, likely occurring as a series of punctuated events. This is contrary to previous interpretations of the structural and metamorphic history of the SCP in terms of a continuous single-cycle tectonothermal event. Furthermore, tectonometamorphic models based on ~1690 Ma low-P, high-T metamorphism in the southern Curnamona Province are not supported. Therefore, tectonic reconstructions that rely on the correlation of ~1690 Ma deformation and metamorphism in the Broken Hill region with a similar aged event in the Mojave tarrane of southwestern Laurentia (AUSWUS) are not supported.*

## 3.1 Introduction

The single most debated and most controversial issue in the Palaeoproterozoic – Mesoproterozoic southern Curnamona Province (SCP) is the timing and duration of metamorphism and deformation (Harrison & McDougall, 1981; Gulson, 1984; Page & Laing, 1992; Donaghy et al., 1998; Hartley et al., 1998; Nutman & Ehlers, 1998; Page et al., 1998, 2000, 2003; Gibson, 2000; Stevens, 1999, 2000; Gibson & Nutman, 2004; Gibson et al., 2004a; Conor et al., 2005). From these studies, tectonothermal events within the SCP have been proposed to have occurred at ~1690 Ma, ~1660 Ma, ~1640 Ma, ~1600 Ma, ~1500 Ma, ~1200 Ma and ~500 Ma. Despite the arguments surrounding the tectonothermal history of the SCP, it has only recently been realised that the region has undergone polymetamorphism (e.g. Stüwe & Ehlers, 1997; Nutman & Ehlers, 1998; Gibson & Nutman, 2004). In general, two contrasting models have been proposed for the timing of Proterozoic tectonism in the SCP – tectonism at ~1690 Ma and ~1600 Ma (e.g. Nutman & Gibson 2004), and tectonism only at ~1600 Ma (e.g. Page & Laing, 1992; Page et al., 1998, 2000, 2003).

The SCP occupies an important place in the tectonic history of eastern Proterozoic Australia, because of its apparently close relationship with the tectonothermal history of the Georgetown and Mt Isa Inliers that culminated in the Olarian, Isan and Ewamin Orogens (collectively termed the Diamantina Orogen; ~1600 – 1500 Ma; Page & Laing, 1992; Laing, 1996a; Myers et al., 1996). Tectonothermal events at ~1600 Ma in the Gawler Craton (Hiltaba Event; Creaser & Cooper, 1993) and Arunta Inlier (Chewings Orogeny; Collins & Shaw, 1995; Collins et al., 1995) indicate that the entire southeastern and eastern margins of Proterozoic Australia underwent periodic compressional tectonics between ~1600 – 1500 Ma (Betts et al. 2002).

In a broader context, the timing of tectonism in the SCP has been an important issue in regard to potential links between Australia and Laurentia during the late-Palaeoproterozoic (e.g. Kalstrom et al., 1999; Burret & Berry, 2000, 2002; Thorkelson et

al., 2001a, 2001b). The proposal that metamorphism in the SCP occurred at ~1660 – 1690 Ma (Gulson, 1984; Donaghy et al., 1998; Nutman & Ehlers, 1998; Gibson & Nutman, 2004), is used as supporting evidence in plate tectonic reconstruction models featuring an Australia – southwest U.S. connection at ~1690 Ma (AUSWUS; Kalstrom et al., 1999; Burrett & Berry, 2000, 2002). However, this connection is based on geochronological data that is widely disputed (e.g. Stevens, 1999), and has not been supported by recent metamorphic zircon U-Pb studies (e.g. Page et al., 2000, 2003), Pb-Pb stepwise leaching of silicates (Tonelli et al., 2003), and Sm-Nd garnet geochronology (Hand et al., 2003). These recent studies documented only Olarian Orogeny age events (~1600 Ma), and Delamerian reworking (Hand et al., 2003; Dutch et al., 2005). If high-grade metamorphism occurred no earlier than the Olarian Orogeny, then the AUSWUS model connecting Australia and the southwest U.S. at ~1690 Ma is unsubstantiated.

Palaeomagnetic data is also at odds with an Australia – Laurentia connection (Pisarevsky et al., 2003). Palaeomagnetic data places Australia at high latitudes at ~1.2 Ga, whereas Laurentia occupied low latitudes at this time (Pisarevsky et al., 2003). If Australia and Laurentia were joined during the late-Palaeoproterozoic or early Mesoproterozoic, then a major episode of continental rifting must be accounted for in tectonic reconstruction model between ~1.5 – 1.2 Ga.

Clearly the only unequivocal technique that will constrain the timing of metamorphism in the Willyama Supergroup is one in which a dateable mineral is analysed *in situ*, and is constrained both texturally and within the metamorphic paragenesis of the sample being analysed. The aim of this study is to evaluate the timing, style and duration of tectonism across the entire SCP by integrating geochronological data with textural and mineralogical observations from meta-sedimentary and meta-igneous rocks of the Willyama Supergroup. The two contrasting tectonometamorphic models proposed for the SCP should be resolvable since the early event in the two event model is >50 million years older than the Olarian Orogeny (Nutman & Ehlers, 1998; Gibson & Nutman, 2004).

To constrain the timing of metamorphic mineral growth, *in situ* chemical Th-U-Pb dating of monazite is utilised with the electron microprobe (EMPA). Samples analysed are from metapelitic and metaigneous lithologies belonging to the upper and lower Willyama Supergroup. The EMPA technique capitalises on the ability of monazite to preserve multiple episodes of growth and regrowth, as very small areas (<10 μm) can be accurately analysed (e.g. Copeland et al., 1988; Montel et al., 1996; Braun et al., 1998; Cocherie et al., 1998; Crowley & Ghent, 1999; Williams et al., 1999; Williams & Jercinovic, 2002; Bell & Welch, 2002; Jercinovic & Williams, 2005; Pyle et al., 2005). Importantly, a number of experimental studies, and studies of natural rock systems, have shown that monazite lacks significant lead diffusion within a closed-system to in excess of 650 – 750°C, and possibly even as high as ~900°C (Copeland et al., 1988; Parrish, 1990; Cocherie et al., 1998; Crowley & Ghent, 1999; Montel et al., 1996; Braun et al., 1998; Rubatto et al., 2001;

Cherniak et al., 2004). Furthermore, since monazite commonly occurs as inclusions in common metamorphic minerals, it offers the opportunity to constrain the timing of metamorphic mineral growth, and therefore constrain the timing of metamorphism. In complex, multiply deformed terrains such as the SCP where there is a liklihood that the terrain underwent polymetamorphism, EMPA chemical monazite analysis is an ideal geochronological tool for investigating the timing of metamorphism.

## 3.2 Previous interpretations on tectonometamorphism in the SCP

Following is a detailed outline of the different tectonic models proposed for the tectonometamorphic evolution of the SCP. A lengthy description of the models proposed is necessary due to the diversity of models proposed, and the far reaching implications these models have for Proterozoic tectonic reconstruction models involving the SCP.

At least five deformational events have affected rocks of the SCP, which have been interpreted to form between the Palaeoproterozoic and Cambro-Ordovician (Campana & King, 1958; Webster, 1996; Wilson & Powell, 2001; Gibson & Nutman, 2004). Early models based on U-Pb isotopic dating of zircon from meta-igneous lithologies (Gulson, 1984), proposed that granulite facies metamorphism occurred at ~1660 – 1640 Ma and ~1600 – 1565 Ma in the Broken Hill region. Contrary to the polymetamorphic history proposed by Gulson (1984), SHRIMP U-Pb metamorphic zircon studies (Page & Laing, 1992; Page et al., 1998, 2000, 2003), and interpretation of metamorphic patterns of the region, identified a single, high-grade metamorphic event (~1600 Ma Olarian Orogeny; e.g. Binns, 1964; Phillips & Wall, 1981; Hobbs et al., 1984; Clarke et al., 1987; Page & Laing, 1992). The ubiquitous development of a pervasive layer parallel fabric was interpreted to be related to compression and associated with nappe emplacement during the initial stages of the Olarian Orogeny (Laing et al., 1978; Clarke et al., 1986; Laing, 1996b).

The metamorphic expression of the Olarian Orogeny was interpreted to be indicative of an anti-clockwise *P-T-t* path, due to the superposition of low-T, high-P assemblages onto high-T, low-P assemblages (e.g. Corbett & Phillips, 1981; Hobbs et al., 1984; Clarke et al., 1987, 1995). In contrast to these studies, Stüwe and Ehlers (1997) recognised that the superposition of the different assemblages was most likely the result of two unrelated metamorphic events. Pinpointing precisely which of the different mineral parageneses correlates with which tectonometamorphic event has been difficult due to the large number of thermal events proposed for the SCP.

Other recent SHRIMP U-Pb magmatic zircon studies in conjunction with field relations between the magmatic rocks and the lithostratigraphy indicate that in addition to the Olarian Orogeny, high-T metamorphism of the lower Willyama Supergroup occurred between ~1690 – 1670 Ma (Donaghy et al., 1998; Nutman & Ehlers, 1998; Gibson & Nutman, 2004). Within this model, the development of migmatites and partial melting, commonly accompanied by a layer parallel

gneissic foliation, was attributed to crustal extension during lithospheric thinning and bimodal magmatism at ~1690 – 1670 Ma (Donaghy et al., 1998; Nutman & Ehlers, 1998; Gibson & Nutman, 2004; Gibson et al., 2004). In this model the lower Willyama Supergroup (Curnamona Group and Thackaringa Group: lower plate) was exhumed and juxtaposed against the upper Willyama Supergroup (Strathearn Group and Paragon/Sundown Groups: upper plate) along a low-angle detachment surface as a metamorphic core complex (Gibson & Nutman, 2004; Gibson et al., 2004a). Consequently within this model, the lower Willyama Supergroup (lower plate) and upper Willyama Supergroup (upper plate) are interpreted to preserve different tectonometamorphic histories.

Across the SCP, the layer parallel fabric has been overprinted and folded, forming map-scale fold patterns and a pervasive axial planar cleavage that is the dominant penetrative fabric observed in outcrop. All tectonometamorphic models proposed for the SCP agree that this occurred during the Olarian Orogeny (e.g. Laing et al., 1978; Gibson & Nutman, 2004). At least two other deformational events are interpreted to have formed during retrograde Olarian metamorphism. These events are characterised by the static growth of low-T, high-P assemblages, and retrograde shearing interpreted to have occurred during the waning stages of the Olarian Orogeny (~1585 Ma; Corbett & Phillips, 1981; Phillips & Wall, 1981; Clarke et al., 1987, 1995). However, recent garnet Sm-Nd studies and chemical monazite ages from major retrograde shear zones have recognised that these shear zones, and the retrograde assemblages preserved within them, developed during the Delamerian Orogeny (Dutch et al., 2005).

## 3.3 Analytical techniques

The monazite Th-U-Pb chemical age technique was first implemented by Suzuki and Adachi (1991) and Suzuki et al. (1994), with the theoretical basis detailed by Montel et al. (1996) and Rhede et al. (1996). Monazite compositions and garnet elemental maps were acquired using a Cameca SX51 electron microprobe at Adelaide Microscopy, University of Adelaide. Operating conditions were 15kv and 100 nA for garnet imaging, and 20kV and 60nA for monazite analysis. In addition to U, Th and Pb, an additional suite of elements (Ca, P, Y, La, Ce, Pr, Nd, Sm, Gd, Dy, Er, Si, Al) were analysed as a monitor for monazite composition, unintentional probing of inclusions, and/or grain boundary mixing. A PAP correction program was used to correct matrix effects (Pouchou & Pichoir, 1985). Total counting times were 320 s for Pb, 160 s for U and 80 s for Th. X-ray lines used were Pb$M\beta$, Th$M\beta$ and U$M\beta$ lines. Huttonite ($ThSiO_4$), $UO_2$ and NBS824 standards were used for calibrating Th, U and Pb respectively. Background measurement positions were selected so as to minimise overlaps with other elements. The spectral interference of the second order Ce escape peak on Pb$M\beta$ was corrected off-line, reducing Pb concentrations by ~100 ppm (c.f. Kelsey et al., 2003; Pyle et al., 2002). The concordant 514 Ma Malagasy monazite (MAD; Kinny, 1997) is used as our in-house standard. Repeat analyses of MAD during the course of this study yielded an age

of 512 ± 10 Ma (2σ). Prior to analysis, monazites were imaged with a backscatter electron detector on a Philips XL30 FEGSEM at Adelaide Microscopy, University of Adelaide, to determine compositional zonation patterns.

## 3.4 Monazite systematics and age determination

Isotopic U-Pb dating of monazite indicates that common lead content is generally very low (<1 ppm; Parrish, 1990), and analyses are commonly concordant, suggesting that the U-Pb system does not suffer lead loss during subsequent events (e.g. Montel et al., 1996). One of the reasons for the generation of discordant U-Pb isotopic ages that is sometimes reported from SHRIMP monazite is related to the mixing of different age domains, due to the relatively large width of the ion probe beam (e.g. Crowley & Ghent, 1999). Due to the much smaller beam width of the microprobe (~3 μm), chemical ages in monazite can potentially record detrital relics, the initial timing of crystallisation (from an igneous protolith), and all subsequent tectonothermal events (e.g. Copeland et al., 1988; Dobmeier & Simmat, 2002; Cocherie et al., 2005; Pyle et al., 2005). This makes the chemical U-Th-Pb monazite chemical dating technique ideal for determining the metamorphic history of the SCP due to the relatively old age of metamorphism in the region, and therefore the large amount of time for radiogenic lead to accumulate.

Another advantage of monazite EPMA chemical dating is that the *in situ* nature of the technique allows linkages to be made between mean ages and the monazite textural position. Metamorphic monazite typically grows with xenotime in chlorite and biotite zone metapelites that have sufficient Ca to stabilise allanite (Franz et al., 1996; Pyle et al., 2001; Spear & Pyle, 2002). Another pulse of metamorphic monazite growth in metapelites occurs under amphibolite facies conditions at approximately *P-T* conditions near that of the staurolite isograd (Smith & Barreiro, 1990; Kingsbury et al., 1993; Pyle & Spear, 1999; Pyle et al., 2001; Kohn & Malloy, 2004). This monazite growth event has been directly linked to the breakdown of garnet to produce staurolite (Spear & Pyle, 2002; Kohn & Malloy, 2004). Therefore, chemical ages can potentially be linked to the timing of metamorphic mineral growth, and a *P-T-t* path can be interpreted for the host rock (e.g. Foster & Parrish, 2003; Fitzsimons et al., 2005; Foster et al., 2000, 2002, 2004; Gibson et al., 2004b).

### *3.4.1 Age determination*

Age derivation was made using the technique of Montel et al. (1996). Assuming common lead and lead diffusion is negligible for most monazites (e.g. Parrish, 1990; Montel et al., 1996; Cocherie et al., 2005), an age can be calculated for each analysis based on the equation:

$$Pb = \left(\frac{Th}{232}\right)\left[e^{\lambda^{232}\tau}\text{-}1\right]208 + \left(\frac{U}{238.04}\right)0.9928\ \text{x}\left[e^{\lambda^{238}\tau}\text{-}1\right]206 + \left(\frac{U}{238.04}\right)0.0072\ \text{x}\left[e^{\lambda^{235}\tau}\text{-}1\right]207 \quad (1)$$

where Pb, Th and U are in ppm and $\lambda^{232}$, $\lambda^{238}$ and $\lambda^{235}$ are the radioactive decay constants of $Th^{232}$, $U^{238}$ and $U^{235}$ respectively. Individual ages are calculated by entering age estimates

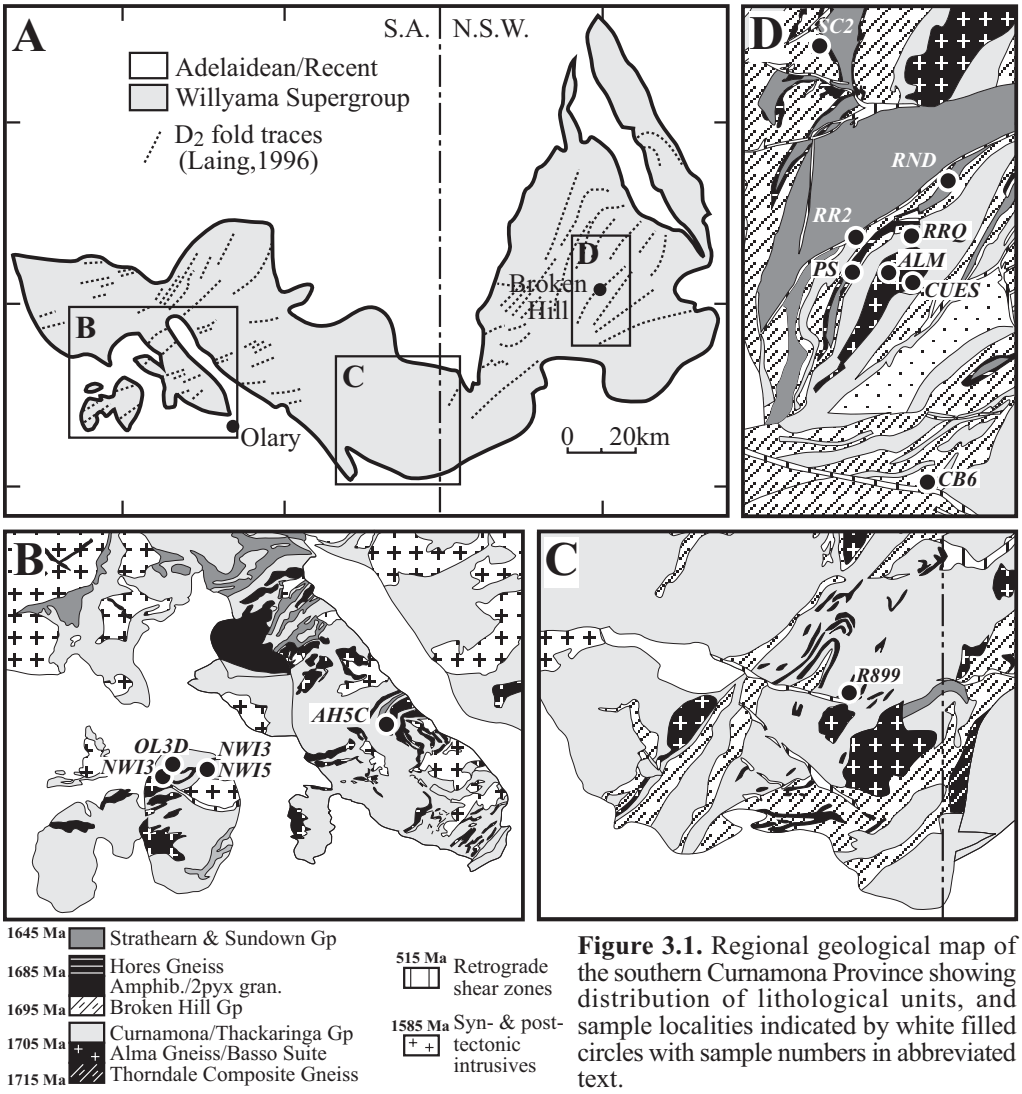


**Figure 3.1.** Regional geological map of the southern Curnamona Province showing distribution of lithological units, and sample localities indicated by white filled circles with sample numbers in abbreviated text.

into the equation (1) with the known concentrations of Th, U and calculating the expected value of Pb. The age is then calculated iteratively by varying the calculated Pb until it matches the measured Pb (Williams & Jercinovic, 2002). Uncertainties for individual spot ages are calculated by propagating counting errors through the age equation. Counting errors ($1\sigma$) are approximately equal to one over the square root of the number of counts (Poisson statistics). Where possible, monazite grains occluded by non-fractured silicate phases were analysed, as included monazite is less likely to have been reset during later events (e.g. DeWolf et al., 1993; Hawkins & Bowring, 1997; Zhu et al., 1997; Braun et al., 1998; Crowley & Ghent, 1999; Montel et al., 2000). Assuming common Pb is negligible, and there has been no modification in the U-Th-Pb ratios except by radioactive decay, a reliable age can be calculated for each analysis. Once individual ages and errors have been calculated for each analysis spot, monazite mean ages are calculated using the weighed average function in Isoplot v 3.0 (Ludwig, 2003). The mean population ages quoted in this study are at 95% confidence interval.

## 3.5 Monazite chemical age constraints

In order to resolve the timing of Proterozoic metamorphism in the SCP as described in

**Table 3.1.** Summary of monazite chemical age data from samples analysed in this study. Distinction made between different occluding phases and the mean chemical ages of monazite included in these phases. Th-U-Pb data Appendix 2. Full monazite compositions Appendix 3.

| Sample | Lithology[1] | Locality | Grid reference (WDS84) | Stratigraphic position | Occluding phase | Wt% Pb Avg. | Wt% Pb S.D.[2] | Wt% Th Avg. | Wt% Th S.D. | Wt% U Avg. | Wt% U S.D. | Early/Peak Meta. Age and error (Ma)[3] | n | Post-peak Meta. Age and error (Ma) | n | |
|---|---|---|---|---|---|---|---|---|---|---|---|---|---|---|---|---|
| ***BROKEN HILL DOMAIN*** | | | | | | | | | | | | | | | | |
| *SC2* | gt-sill-bt schist | Southern Cross | 539561, 6476859 | Broken Hill Gp | matrix (micas) | 0.540 | 0.105 | 5.516 | 0.966 | 0.612 | 0.363 | 1594 ± 17 | 82 | | | |
| *RND* | gt-sil-(mu) gneiss | Round Hill, NE of Broken Hill | 549046, 6467095 | Sundown Gp | sillimanite | 0.479 | 0.123 | 4.356 | 0.968 | 0.582 | 0.237 | 1612 ± 18 | 47 | **1610 ± 16 (60)** | | |
| | | | | | matrix (micas) | 0.461 | 0.025 | 4.397 | 0.284 | 0.513 | 0.030 | 1601 ± 42 | 13 | | | |
| | | | | | garnet | 0.483 | 0.059 | 4.774 | 0.625 | 0.526 | 0.137 | | | 1570 ± 18 | 41 | |
| *RRQ* | gt-sill-pl-bt gneiss | Rasp Ridge Gneiss quarry | 546400, 6463100 | Thackaringa Gp | garnet | 0.451 | 0.049 | 4.536 | 0.391 | 0.450 | 0.240 | 1591 ± 17 | 101 | | | |
| *RR2* | Kfsp-pl-q-bt gneiss | Rasp Ridge Gneiss Block 10 | 542607, 6463043 | Thackaringa Gp | plagioclase | 0.502 | 0.096 | 5.078 | 0.937 | 0.517 | 0.161 | | | 1571 ± 29 | 34 | **1557 ± 18 (78)** |
| | | | | | K-feldspar | 0.490 | 0.036 | 4.834 | 0.334 | 0.568 | 0.093 | | | 1547 ± 24 | 44 | |
| *ALM* | Kfsp-pl-qtz-sill-gt gneis | Airport entrance, Broken Hill | 544781, 6460324 | Alma Gneiss | plagioclase | 0.714 | 0.050 | 7.213 | 0.577 | 0.689 | 0.254 | 1596 ± 22 | 31 | | | |
| | | | | | sillimanite | 0.683 | 0.064 | 6.710 | 1.277 | 0.766 | 0.371 | | | 1565 ± 22 | 33 | |
| *CUES* | gt-crd-sill-plag gneiss | Airport runway, Broken Hill | 546513, 6459686 | Thackaringa Gp | plagioclase | 0.482 | 0.037 | 5.035 | 0.474 | 0.423 | 0.148 | 1591 ± 50 | 15 | | | |
| | | | | | cordierite | 0.604 | 0.079 | 6.055 | 1.328 | 0.612 | 0.114 | 1587 ± 23 | 34 | **1587 ± 13 (134)** | | |
| | | | | | garnet | 0.510 | 0.040 | 5.113 | 0.570 | 0.514 | 0.134 | 1586 ± 20 | 73 | | | |
| | | | | | sillimanite | 0.543 | 0.037 | 5.312 | 0.517 | 0.591 | 0.146 | 1585 ± 31 | 12 | | | |
| *PS* | gt-sill-bt-(mu) gneiss | Reservoir: Broken Hill | 542148, 6460392 | Hores Gneiss | mica | 0.579 | 0.180 | 4.130 | 1.543 | 1.043 | 0.560 | 1601 ± 18 | 90 | | | |
| *CB6* | mu-bt-pl-q-(ser) schist | Copper Blow Cu-Au prospect | 547736, 6445055 | Thackaringa Gp | quartz | 0.723 | 0.165 | 7.119 | 2.074 | 0.849 | 0.269 | | | 1554 ± 18 | 41 | |
| *R899* | gt-pl-(bt-mu) schist | Mingary, western BHD | 490580, 6427130 | Thackaringa Gp | plagioclase | 0.559 | 0.056 | 5.897 | 0.786 | 0.525 | 0.112 | | | 1560 ± 38 | 12 | |
| | | | | | matrix | 0.542 | 0.042 | 5.388 | 0.473 | 0.608 | 0.195 | | | 1554 ± 17 | 62 | **1551 ± 13 (103)** |
| | | | | | garnet | 0.516 | 0.042 | 5.306 | 0.446 | 0.545 | 0.139 | | | 1542 ± 27 | 29 | |
| ***OLARY DOMAIN*** | | | | | | | | | | | | | | | | |
| *AH5C* | gt-sill-(bt) schist | Ameroo Hill | 425230, 6444277 | Saltbush SG | garnet | 0.429 | 0.234 | 2.169 | 1.854 | 1.027 | 0.485 | 1605 ± 30 | 49 | | | |
| *NWI3* | and-gt-st schist | Northern Walparuta Inlier | 408070, 6439907 | Wiperaminga SG | anda (retro) | 0.327 | 0.149 | 3.213 | 2.164 | 0.357 | 0.209 | 1589 ± 26 | 63 | | | |
| *NWI5* | and-gt-st schist | Northern Walparuta Inlier | 408070, 6439907 | Wiperaminga SG | andalusite | 0.286 | 0.102 | 2.904 | 1.458 | 0.269 | 0.112 | 1607 ± 17 | 172 | | | |
| *OL3D* | gt-(mu-chl-bt) schist | Northern Walparuta Inlier | 404535, 6440075 | Wiperaminga SG | matrix (micas) | 0.538 | 0.153 | 5.194 | 1.813 | 0.647 | 0.481 | | | 1559 ± 16 | 101 | |
| *WW18* | gt-(mu-bt-ser) schist | Northern Walparuta Inlier | 403986, 6439213 | Wiperaminga SG | mica (retro) | 0.439 | 0.150 | 4.877 | 2.131 | 0.342 | 0.206 | | | 1573 ± 29 | 55 | |

[1] Retrograde phases in brackets
[2] Avg. & S.D.: average & standard deviation
[3] Error: 95% confidence interval

section 2.1.3, samples were selected such that they are representative of the upper and lower Willyama Supergroup, from lithologies as defined in the upper and lower plates of extensional model of Gibson & Nutman, 2004), and from mid-amphibolite to granulite facies rocks. In the course of this study a comprehensive data set of over 1200 analyses was generated from 14 samples. U-Th-Pb concentration summaries, and monazite chemical age summaries are listed in Table 3.1, and sample localities shown in Fig. 3.1. *Appendix 2* lists all the Th, U, Pb concentrations, peak and background counts, counting errors, individual spot age and error (1σ), and sample weighted mean age and error (95% confidence interval) of the samples listed in Table 3.1, which records Mesoproterozoic monazite chemical ages. *Appendix 3* lists the full compositional data (weight %) of all monazite analyses. *Appendix 4* describes the petrography and monazite textural setting of all samples analysed. The cause and effects of Delamerian reworking are discussed in *Chapter 7*.

Summarising the dataset (Table 3.1, *Appendix 2*), most monazite grains analysed are largely chemically homogeneous. Minor zoning was detected in a few monazite grains that had appreciable differences in Th and/or Y contents. When appreciable zoning was detected, analysis spot locations were chosen within each of zone. Zoning was only detectable when compositional domains varied by greater than >3 wt% Th, or ~2 wt% Y.

At the thin section scale, U, Th and Pb concentrations are variable, but predominantly range between 3-8 wt% Th, <1 wt% U and <0.7 wt% Pb (Table 3.1; *Appendix 2*). Average 1σ errors on U, Th and Pb EPMA measurements are approximately 87 ppm, 443 ppm and 94 ppm, respectively. Individual spot ages have 1σ errors typically between 40–60 Ma. Errors on mean ages range between 15-40 Ma (95% confidence interval). As individual spot ages in a single thin section or occluding phase tightly cluster, all monazites within the same sample, or same occluding phase within the one sample, are considered as a single distribution.

From a combination of monazite textural position, composition and mean age, two major monazite age groups can be identified (*see below*). These are early- to peak-Olarian metamorphic monazite (~1610 – 1585 Ma), and post-peak Olarian metamorphic monazite (<1585 Ma). Following is a description of the textural position and mean chemical ages of monazite grains from the two groups.

### *3.5.1 Early- to peak-metamorphic monazite*

The oldest calculated mean ages come from monazite inclusions within the earliest formed, major metamorphic minerals from metapelitic lithologies from both the upper and lower Willyama Supergroup across the SCP (Table 3.1; Fig. 3.1). Occluding phases include andalusite from a metapelite (*NWI5*; Fig. 3.2a) in the Curnamona Group (1607 ± 17 Ma; n=172; Table 3.1), and garnet from a metapelite (*AH5C*; Fig. 3.2b) in the Strathearn Group (1605 ± 30 Ma; n=49; Table 3.1), both located within the Olary Domain (Fig. 3.1). Monazite inclusions from the garnet-bearing metapelite at Ameroo Hill (*AH5C*; Fig. 3.1, 3.2c) are situated in the core of a two-stage garnet.

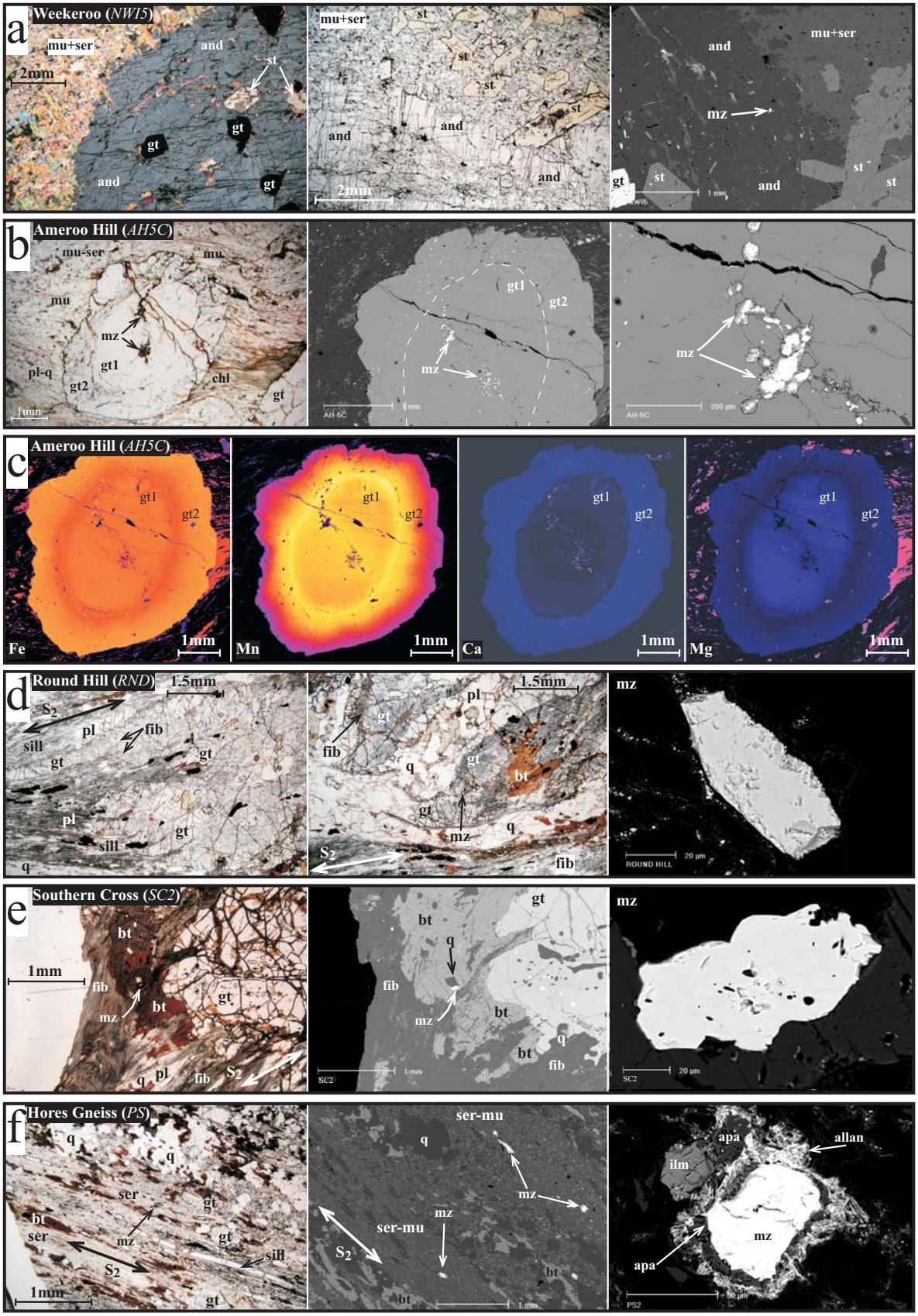


**Figure 3.2.** Pre-peak to syn-peak metamorphic monazite hosting lithologies. (a) Andalusite-garnet-staurolite-mica metapelitic schist (*NWI5*). Monazite occluded by synkinematic andalusite porphyroblasts; (b) Garnet-fibrolite-biotite-muscovite-chloritoid metapeltic schist (*AH5C*). Monazites occur as clusters within fracture dissecting the core of a two-stage garnet; (c) Qualitative elemental maps (Ca, Mn, Fe, Mg) of polymetamorphic garnets from Ameroo Hill (*AH5C*); (d) Garnet-sillimanite-cordierite-mica metapelitic gneiss (*RND*). Monazite occluded within fractured and flattened garnet porphyroblasts and sillimanite; (e) Garnet-sillimanite-fibrolite-mica metapelitic schist (*SC2*). Monazite occluded within matrix micas defining post-kinematic fabric; (f) Garnet-sillimanite-biotite-muscovite metapelitic gneiss (*PS*). Monazite in the mica dominated matrix. Monazite rims replaced by apatite-allanite coronas, suggesting reaction kinetics were diffusion controlled and relatively slow

**Figure 3.2.** *Continued.*

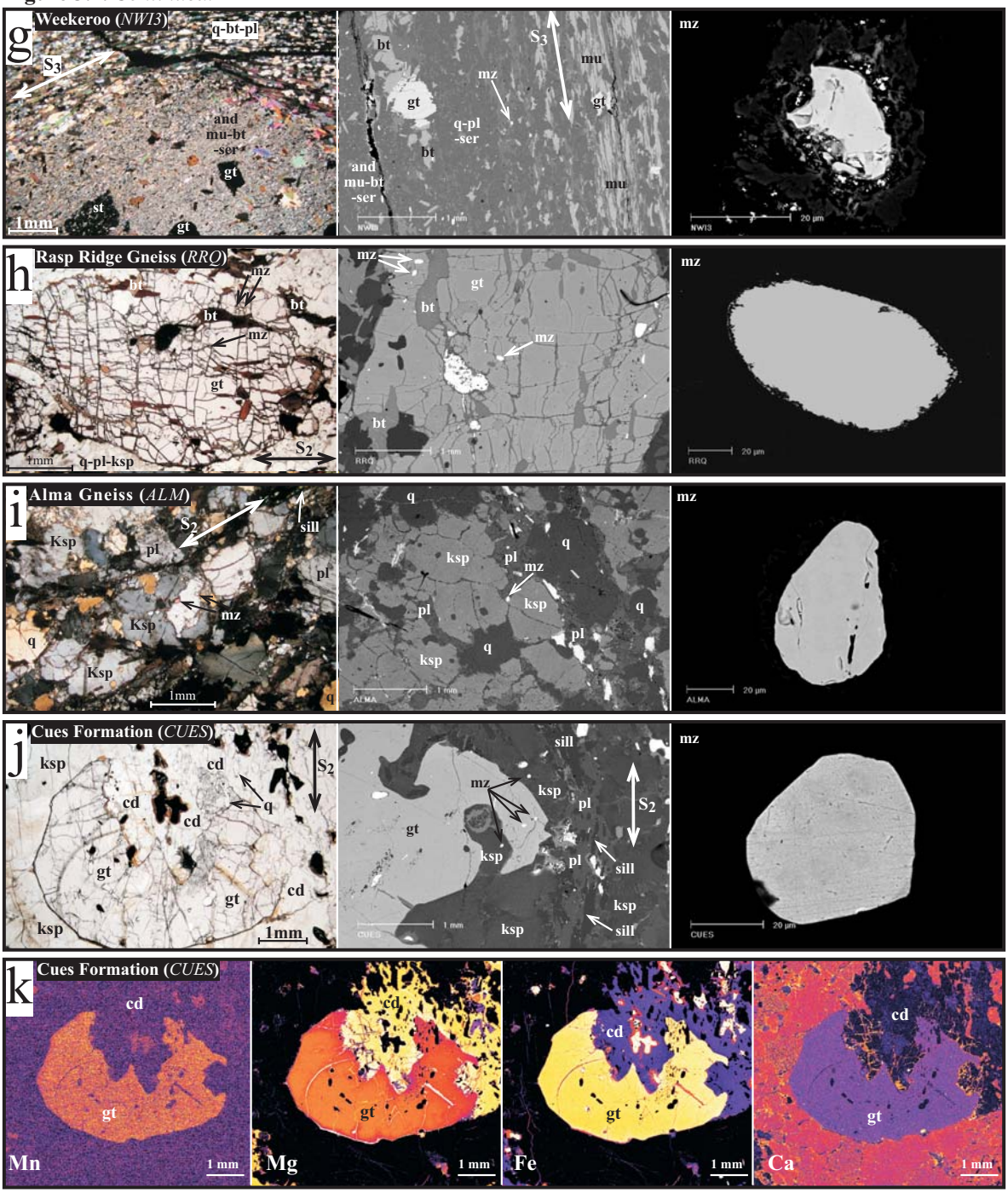


(Finger et al., 1998); (g) Andalusite-garnet-staurolite-mica metapelitic unit (*NWI3*). Monazite occluded within the partly retrogressed andalusite porphyroblasts; (h) Plagioclase-quartz-biotite-garnet granitic gneiss (*RRQ*). Monazite occluded within the fractured garnet porphyroblasts; (i) Sillimanite-quartz-feldspar-garnet-biotite gneiss (*ALM*). Monazite occluded by plagioclase and sillimanite; (j) Garnet-cordierite-sillimanite-feldspar-biotite gneissic metapelitic gneiss (*CUES*). Monazite occluded within all major silicate phases; (k) Qualitative elemental maps (Ca, Mn, Fe, Mg) of garnet-cordierite decompression texture from sample *CUES*. *Mineral abbreviations: allan: allanite; and: andalusite; apa: apatite; bt: biotite; cd: cordierite; chl: chlorite; fib: fibrolite; gt: garnet; ilm: ilmenite; Ksp: K-feldspar; mu: muscovite; mz: monazite; pl: plagioclase; q: quartz; ser: sericite; sill: sillimanite; st: staurolite.*

Garnets within this lithology have a distinctive core and rim as evidenced by compositional mapping (Fig. 3.2c). Previous studies utilising Sm-Nd garnet geochronology on similar polymetamorphic garnets have constrained the timing of garnet core and rim growth to be ~1585 Ma and ~510 Ma, respectively (Hand et al., 2003).

Monazite occluded by sillimanite in a

metapelitic gneiss (*RND*; Fig. 3.1, 3.2d) from the Sundown Group in the Broken Hill region (Round Hill; Fig. 3.1) has a mean age of 1612 ± 18 Ma (n=47; Table 3.1). Monazite within matrix biotite from the same sample has a mean age of 1601 ± 42 Ma (n=13; Table 3.1). Averaged together, monazite in sample *RND* has a mean age of 1610 ± 16 Ma (n=60). Pre-peak to syn-peak matrix minerals (biotite) that occlude monazite from metapelitic lithologies of the Broken Hill Group and Sundown Group in the Broken Hill region have monazite with a mean age of 1594 ± 17 Ma (n=82; *SC2*; Fig. 3.1, 3.2e; Table 3.1) and 1601 ± 18 Ma (n=90; *PS*; Fig. 3.1, 3.2f; Table 3.1), respectively. Monazite grains situated in partly retrogressed andalusite porphyroblasts (partly pseudomorphed by muscovite) in a metapelitic unit (Curnamona Group) from the western Olary Domain have a mean age of 1589 ± 26 Ma (n=63; *NWI3*; Fig. 3.1, 3.2g; Table 3.1).

Monazite within granitic gneisses from the Broken Hill Domain (Rasp Ridge Gneiss and Alma Gneiss) record the timing of recrystallisation of these lithologies, as they have igneous crystallisation ages of 1683 ± 3 Ma and 1704 ± 3 Ma, respectively (Page et al., 2000). Monazite occluded by fractured and elongated garnet porphyroblasts from the Rasp Ridge Gneiss has a mean age of 1591 ± 17 Ma (n=101; *RRQ*; Fig. 3.1, 3.2h; Table 3.1). The Alma Gneiss has monazite occluded by plagioclase with a mean age of 1596 ± 22 Ma (n=31; *ALM*; Fig. 3.1, 3.2i; Table 3.1).

A gneissic metapelitic lithology from the Cues Formation (*CUES*; Fig. 3.1, 3.2j), lower Thackaringa Group in the Broken Hill region, records the timing of peak pressure metamorphism (Swapp & Frost, 2003). Cordierite replaces and/or forms embayments into pervasively fractured garnet porphyroblasts (Fig. 3.2j, k). This relationship has previously been interpreted to represent a decompression texture (Swapp & Frost, 2003). Such an interpretation may be supported by the resorption of Mg from the garnet into the cordierite as evident in garnet elemental composition maps (Fig. 3.2k). Monazite occluded by garnet, cordierite, sillimanite and plagioclase gives mean ages of 1586 ± 20 Ma (n=73), 1587 ± 23 Ma (n=34), 1585 ± 31 Ma (n=12) and 1591 ± 50 Ma (n=15; Table 3.1), respectively. Averaged together, all monazite from sample *CUES* has a mean age of 1587 ± 13 Ma (n=134; Table 3.1).

### *3.5.2 Post-peak Olarian metamorphic monazite*

Several samples have monazite chemical ages that record ages that post-date previous age constraints on peak metamorphism associated with the Olarian Orogeny (1600 ± 8 Ma; Page & Laing, 1992). Alternatively, these ages record an as yet unrecognised high-grade metamorphic and/or pervasive hydrothermal event. Monazite occluded by different silicate minerals in the same sample can have different mean ages, as observed in samples *RND* and *ALM*. However, all ages from these samples are within error of each other (Table 3.1). Monazite occluded by garnet in sample *RND* has a mean age of 1570 ± 18 Ma (n=41; Table 3.1), compared with sillimanite (~1612 Ma) and biotite (~1601 Ma) from the same sample. Likewise, monazite occluded by coarse-grained sillimanite in the felsic Alma Gneiss sample (*ALM*; Fig. 3.2i)

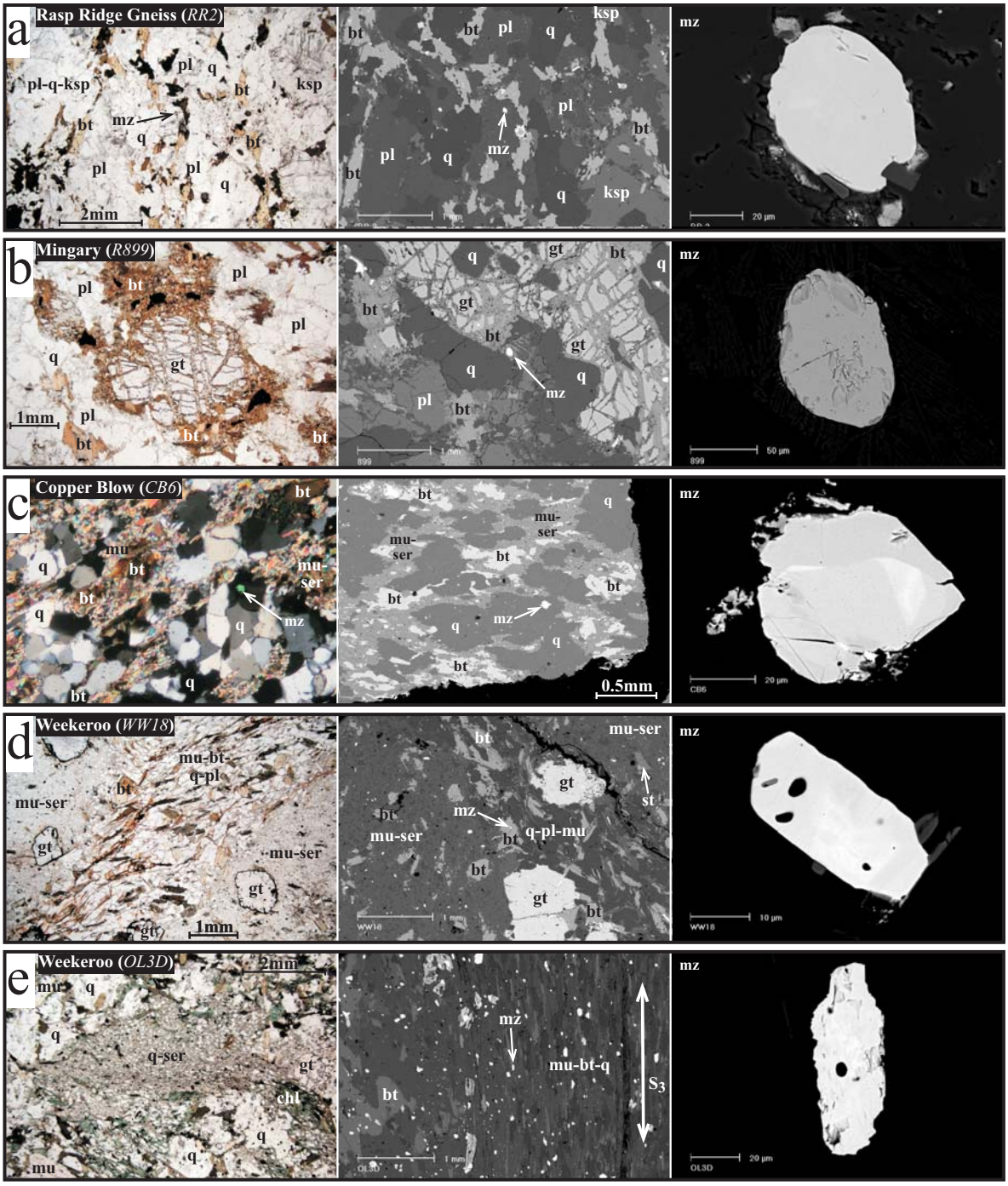


**Figure 3.3.** Lithologies containing monazite that post-dates previous constraints on the timing of Olarian metamorphic (1600 ± 8 Ma; Page & Laing, 1992). (a) Quartz-feldspar-biotite granitic gneiss (Rasp Ridge Gneiss). Monazite occluded by plagioclase and K-feldspar; (b) Garnet-sillimanite-biotite-feldspar-quartz metapelitic granulite (*R899*). Monazite occluded within matrix biotite and plagioclase; (c) Mica-magnetite-quartz lithology (*CB6*). Monazite located at quartz triple point; (d) Retrograde muscovite-sericite schist (*NWI3*). Monazite analysed from within the retrograde matrix; (e) Retrograde chlorite-sericite-muscovite-biotite schist (*OL3D*). Monazite within strongly foliated matrix. Mineral abbreviations listed in Figure 3.2.

also has a younger mean age of 1565 ± 22 Ma (n=33; Table 3.1), relative to plagioclase from the same sample (~1596 Ma).

Another sample of the Rasp Ridge Gneiss (*RR2*; Fig. 3.3a) from within the Broken Hill region has monazite occluded by plagioclase and K-feldspar that have mean ages of 1571 ± 29 Ma (n=34) and 1547 ± 24 Ma (n=44; Table 3.1), respectively. All monazite analysed in sample *RR2* has a mean age of 1557 ± 18 (n=78; Table 3.1). A retrogressed garnet-bearing metapelitic gneiss (*R899*; Fig. 3.3b) adjacent to a metabasite that intruded the

Curnamona Group in the far western Broken Hill Domain has monazite grains occluded by biotite that have a mean age of 1554 ± 17 Ma (n=62; Table 3.1). Monazite occluded by plagioclase and garnet within the same sample have mean ages of 1560 ± 38 Ma (n=12) and 1542 ± 27 Ma (n=29; Table 3.1), respectively.

A single monazite grain located at a quartz triple-point from an altered and strongly foliated and mineralised mica-magnetite-quartz lithology (*CB6*; Fig. 3.3c) from the Thackaringa Group (Fig. 3.1) adjacent to the Copper Blow Cu-Au prospect has a mean age of 1554 ± 18 Ma (n=41; Table 3.1). Finally, two foliated and pervasively retrogressed metapelitic schists from the Curnamona Group in the western Olary Domain (*WW18* and *OL3D*; Fig. 3.1, 3.3d, e) with monazite associated with retrograde phases (muscovite and sericite) have mean ages of 1573 ± 29 Ma (n=55) and 1559 ± 16 Ma (n=101; Table 3.1), respectively.

## 3.6 Discussion

The acquisition of monazite chemical ages, and the relevance of these apparent ages within the tectonothermal history of a terrain, needs to be critically evaluated with respect to several factors, including: (1) the potential incorporation of common Pb; (2) the robustness of the U-Th-Pb system to open-system behaviour; (3) the potential for recrystallisation or replacement by hydrothermal monazite; (4) the bulk chemical control on monazite growth; (5) incorporating independently established, preexisting geochronological datasets (e.g. Parrish, 1990; Montel et al., 1996; Braun et al., 1998; Cocherie et al., 1998; Crowley & Ghent, 1999; Catlos et al., 2002; Fitzsimons et al., 2005). Following is a brief documentation of recent studies that have addressed these issues, as they need consideration prior to evaluating the monazite mean age data in this study.

### *3.6.1 Assessing the contribution of common lead*

Although there is a general recognition that monazite incorporates little common Pb relative to radiogenic Pb accumulation (e.g. Parrish, 1990), the amount of common Pb that has been measured in isotopic studies is highly variable (e.g. 0.006 – 1.1 ppm; Parrish, 1990). Despite this, TIMS isotope dilution studies of monazite indicate that common lead content in monazite is usually very low (<1 ppm; Parrish, 1990). If common Pb is a factor, an increase in Pb/(Th+U) will result in older apparent chemical ages. The oldest mean chemical ages obtained in this study are in close agreement with existing isotopic U-Pb zircon geochronology (e.g. Page et al., 2000, 2003). Therefore the quantity of common Pb in monazites of the SCP is likely to be negligible relative to accumulated radiogenic lead. This is despite the fact that three samples used in this study (*PS*, *RR2* and *RND*) come from within ten's of metres of the Line of Lode at Broken Hill, which is renowned for its vast Pb accumulation. Viewed in this context, this study provides additional evidence that incorporation of common Pb in monazite is generally insignificant.

### *3.6.2 Closure temperature/conditions*

The closure temperature of the U-Th-Pb chemical system is important when assessing monazite chemical ages. Inheritance in monazite in high-grade metamorphic rocks is uncommon (e.g. Spear & Parrish, 1996; Bingen & vanBreeman, 1998), but can be a factor that needs consideration (Pyle et al., 2005). However, ultimately factors including monazite grainsize, composition, rate of cooling, fluid/melt availability and bulk composition will ultimately determine the close temperature of a particular sample and whether inherited components are preserved (e.g. Parrish, 1990; Bingen & vanBreeman, 1998; Ayers et al., 1999; Zhu & O'Nions, 1999; Cherniak et al., 2004; Rubatto et al., 2001).

It has been experimentally shown that the monazite U-Th-Pb system has a relatively high closure temperature (~900°C at a cooling rate of 10°C/My in a 10μm grain; Cherniak et al., 2004). Additionally, studies on natural systems have shown that significant lead diffusion is negligible at temperatures below 650 – 750°C, and to even as high as 850°C (Montel et al., 1996; Braun et al., 1998; Cocherie et al., 1998; Crowley & Ghent, 1999; Cocherie & Albarede, 2001). Peak metamorphic temperatures estimated for the SCP during the Olarian Orogeny range between ~650 – 750°C for the Broken Hill Domain, and ~600°C for the Olary Domain (Stüwe & Ehlers, 1997; Swapp & Frost, 2003; Clarke et al., 1995). The maximum temperature the SCP attained during the Olarian Orogeny did not exceed the Pb closure temperature for monazite. Therefore, the mean chemical ages can be interpreted as either growth ages, or recrystallisation ages when fluid/rocks ratios are interpreted to be high. Furthermore, chemical ages recorded by monazite occluded by silicate phases constrain the maximum growth age of those silicates, as pristine monazite often persists when occluded by silicate phases so that monazite is armoured from fluids even under relatively high fluid/rock ratios (DeWolf et al., 1993; Hawkins & Bowring, 1997; Braun et al., 1998; Crowley & Ghent, 1999; Montel et al., 2000).

Within the context of this study, the lack of lead diffusion is exemplified by sample *PS*. Monazite within this sample preserves coronas surrounding the monazite grains that are composed of an inner ring of apatite (<8 μm) and an outer ring of allanite (<10 μm; Fig. 3.2f). Similar reaction textures elsewhere have been described as showing that only the outer most rim of monazite was affected by reaction kinetics that are slow and diffusion controlled, and that the preserved monazite cores are unaffected by the diffusion. Therefore, the development of such reaction textures indicates that the monazite cores preserve their radiogenic lead composition (Finger et al., 1998).

### *3.6.3 Monazite recrystallisation and hydrothermal monazite*

Fluid-induced recrystallisation of monazite has been documented extensively (e.g. DeWolf et al., 1993; Poitrasson et al., 2000; Braun et al., 1998; Crowley & Ghent, 1999; Schandl & Gorton, 2004). Total replacement of pre-existing monazite during recrystallisation has been documented to preferentially occur along grain boundaries, within fractures, in inclusion-rich zones, and within fine-grained matrices

(Ayers et al., 1999; Crowley & Ghent, 1999; Carson et al., 2004). Seriticised feldspar, interstitial carbonates, greisenisation, and chloritised biotite have been used as supporting evidence for fluid-related recrystallisation (e.g. Poitrasson et al., 1996; Crowley & Ghent, 1999; Poitrasson et al., 2000).

Field and textural observations indicate that relatively high degrees of fluid flow occurred in some regions during retrograde metamorphism (e.g. Clarke et al., 1987, 1995; Clark & James, 2003), and likely would have resulted in monazite recrystallisation. This is exemplified by samples *OL3D* and *WW18* in the western Olary Domain (Fig. 3.1), in which prograde metamorphic andalusite is ubiquitously replaced by hydrous phases such as muscovite, enveloped by a fine-grained matrix of biotite-muscovite-quartz±(plagioclase-chlorite; Fig. 3.3d, e). Monazite associated with these retrograde phases preserves post-peak Olarian chemical ages (~1560 – 1575 Ma). In addition to these samples, sample *R899* also preserves post-peak Olarian retrograde reactions, whereby garnet porphyroblasts are fractured and infilled and replaced by biotite (Fig. 3.3b). Monazite occluded by biotite coronas and mica matrix record the maximum timing of replacement to be 1540 – 1560 Ma.

### *3.6.4 Timing of metamorphism in the SCP*

Based on the extensive monazite EPMA data set collected in this study (>1600 analyses), at least two monazite growth events during the early Mesoproterozoic. The first metamorphic monazite growth event at ~1610 – 1600 Ma (Table 3.1), is nearly identical to SHRIMP U-Pb metamorphic zircon studies that constrain the Olarian Orogeny (1600 ± 8 Ma; Page & Laing, 1992; Page et al., 2003). By pooling all the lithologies together that contain textural pre-peak to syn-peak metamorphic Olarian assemblages and monazite ages, the maximum mean age of high-grade metamorphism within the SCP is constrained to be 1597 ± 6 Ma (M1, Fig. 3.4; n=782). This age for the earliest tectonometamorphic event in the SCP is independently supported by Pb-Pb stepwise leaching geochronology of major silicate phases (Tonelli et al., 2003), and Sm-Nd garnet geochronological constraints (Hand et al., 2003). Peak pressure metamorphism was attained prior to ~1585 Ma based on the development of retrograde textures in the Broken Hill region (Swapp & Frost, 2003; White et al., 2005). Peak temperatures as indicated by bimodal magmatism in the western Olary Domain, and crustal anatexis throughout the SCP, was attained at *ca.* 1585 Ma (Ludwig & Cooper, 1984; Page et al., 2003).

On the basis of this study, no evidence was found for high-T metamorphism as early as ~1690 – 1660 Ma (c.f. Donaghy et al., 1998; Nutman & Ehlers, 1998; Gibson & Nutman, 2004). Importantly, samples *SC2*, *RRQ*, *RR2*, *CUES*, *CB6*, *R899*, *NWI3* and *NWI5* are all from the lower Willyama Supergroup, or the lower plate of the extensional model of Gibson & Nutman (2004), and none preserve monazite growth prior to the Olarian Orogeny. Most significantly, samples *NWI3* and *NWI5* from the relatively low metamorphic grade region in the western Olary Domain (andalusite-grade: *c.* 600°C, 4 kbars; Clarke et al., 1987)

are both from the lower Willyama Supergroup (Wiperaminga Subgroup). Therefore, these assemblages at no stage reached temperatures sufficient to reset monazite. Monazite occluded by andalusite in these samples record the maximum age of metamorphism in the SCP to be no earlier that ~1610 Ma. As reinforced by Conor et al. (2005), high-grade metamorphism postulated to have occurred in the SCP at ~1690 – 1660 Ma (Gibson & Nutman, 2004, Gibson et al., 2004a), is unsubstantiated and based on erroneous geological and geochronological criteria.

On the basis of previous interpretations constraining the timing of the Olarian Orogeny (~1600 – 1585 Ma; Page & Laing, 1992; Page et al., 2000, 2003), several post-Olarian tectonometamorphic events are identified by monazite U-Th-Pb chemical dating in this study. Monazite growth and/or recrystallisation is recorded at ~1570 Ma, ~1560 Ma and ~1550 Ma (Table 3.1). Evidence of high-grade metamorphism at ~1570 Ma is supported by non-retrogressed samples in the Broken Hill region (monazite occluded by garnet in sample *RND*; monazite occluded by plagioclase in sample *RR2*; monazite occluded by sillimanite in sample *ALM*; monazite at quartz triple junction in sample *CB6*). Independent evidence of a high-grade metamorphic event at 1574 ± 6 Ma is provided by metamorphic zircon U-Pb SHRIMP ages from the Redan calcalbitite, south of Broken Hill (R. Page *pers. comm.*, 2005). By pooling all the lithologies together that contain post-peak metamorphic Olarian assemblages and monazite ages, the mean age of the second high-grade and retrograde metamorphic event (M2) within the SCP is 1560 ± 7 Ma (Fig. 3.4; n=452; 95% confidence interval).

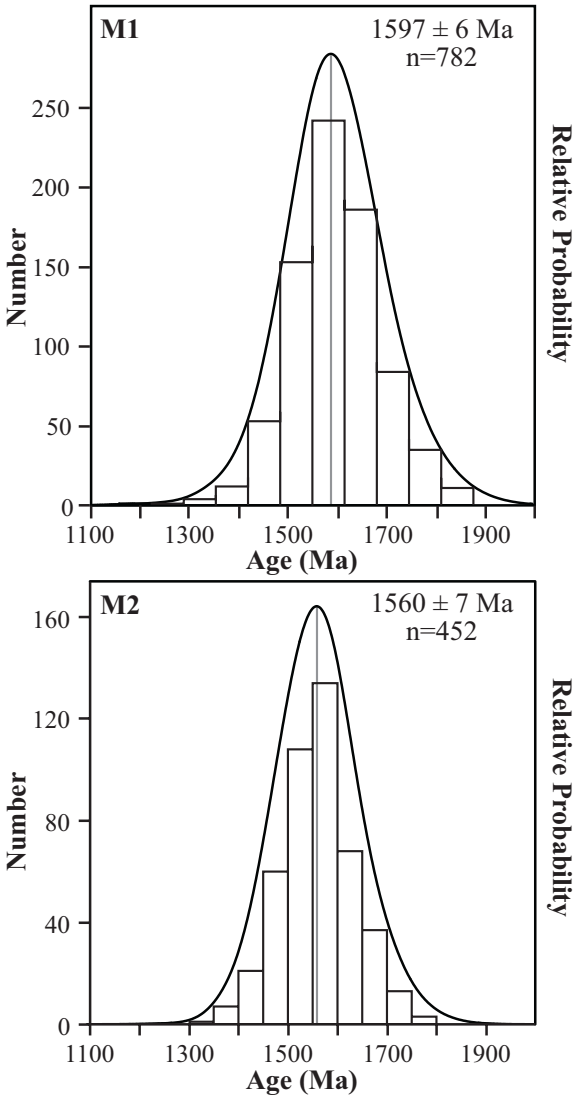


**Figure 3.4.** Probability density plots of all monazite chemical ages pooled together with regard to the two metamorphic events identified in this study.

In addition to the as yet unrecognised high-grade metamorphic event post-dating the Olarian Orogeny, evidence for fluid-induced hydrothermal recrystallisation structurally higher in the orogen is recorded by retrograde metamorphism in the western Olary Domain and western Broken Hill Domain (samples *OL3D, WW18, R899*). The source of the fluids responsible for retrograde metamorphism structurally higher in the orogen may be related to high-grade metamorphism at mid-crustal levels as preserved by rocks in the Broken Hill region. Alternatively, it is possible that

fluids released from crystallisation of magmatic rocks generated during crustal anatexis at ~1585 Ma were responsible for retrogression.

Another important outcome of the identification of retrograde metamorphism between ~1570 – 1550 Ma is that monazite grains that records this age are texturally related to the pervasive NE-trending fabric in the western Olary Domain ($S_3$; Grady et al., 1989). $D_3$ has previously been interpreted to have developed between 1596 ± 3 Ma and 1591 ± 5 Ma, based on the presence and absence of this fabric in the Cusin Creek and Mundi Mundi granitoids, respectively (Page et al., 2000). However, interpretations such as this rely crucially on the notion that strains are pervasive in the terrain, rather that partitioned. As monazite growth associated with the $S_3$ fabric in this study developed between ~1570 – 1550 Ma, then structural and tectonic models for the Olarian Orogeny need re-evaluating as they are based on the assumption that deformation and metamorphism ceased by 1585 Ma (Page et al., 2000). Furthermore, the retrograde samples in the western Olary Domain have post-kinematic staurolite and garnet (post-$D_3$) that has previously been interpreted to represent high-P, low-T assemblages that overprint earlier formed low-P, high-T assemblages, and thereby constrain the anticlockwise *P-T* path of the Olarian Orogeny (Clarke et al., 1995). The observation by Stüwe & Ehlers (1997) that these high-P, low-T assemblages are unrelated to the Olarian Orogeny, and related to a younger Grenvillian or Delamerian tectonometamorphic event seem warranted on the basis that these high-P, low-T assemblages overprint the $D_3$ fabric (~1570 – 1550 Ma; *this study*).

It is clear that Olarian metamorphism in the SCP was episodic, contrary to previous interpretations of the structural and metamorphic history of the SCP in terms of a continuous single-cycle tectonothermal event (e.g. Hobbs et al., 1984; Clarke et al., 1987; 1995). Metamorphic processes likely occurred as a series of punctuated events, whose causes are conceivably related to both external (plate-margin) and internal processes (dehydration, rehydration, recycling) within a developing orogen.

### *3.6.5 Implications for continental reconstructions*

This study found no evidence to support metamorphism in the SCP at ~1690 Ma. Therefore, tectonic reconstructions such as the AUSWUS connection (Karlstrom et al., 1999; Burrett & Berry, 2000, 2002), that rely on matching metamorphic belts of this age at Broken Hill and the Mojave terrain of California and Nevada, southwest Laurentia (Ivanpah Orogeny; Wooden & Miller, 1990) do not appear to be substantiated. It is suggested that the Olarian Orogeny at ~1610 – 1585 Ma was a response to convergence along the eastern margin of the NAC. The Isan and Ewamin Orogenies also record evidence of intermittent shortening along the eastern margin of the NAC in the Mt Isa and Georgetown Inliers between ~1600 – 1580 Ma (Page & Sun, 1998; Betts et al., 2000; Giles & Nutman, 2002; Black et al., 1979; Blewett et al., 1998). Clearly, such widespread compressional tectonics and high-grade metamorphism along the eastern margin of

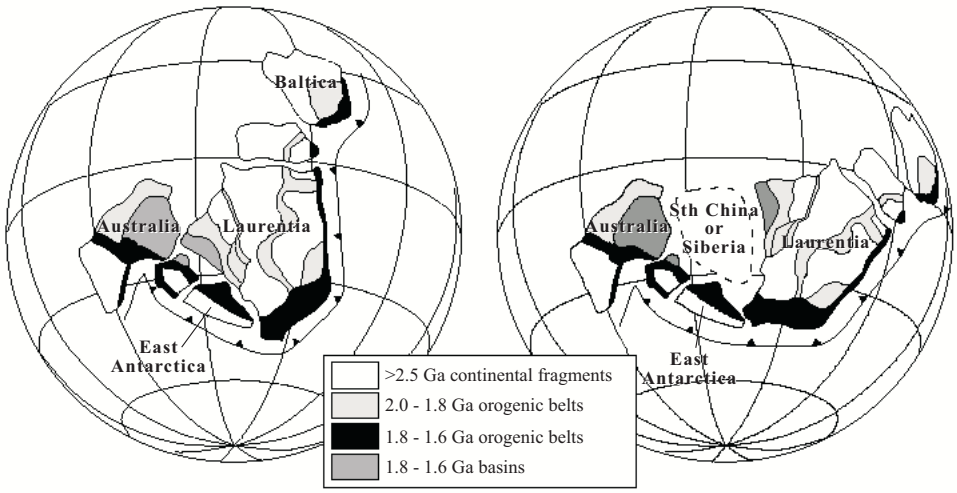


**Figure 3.5.** Two possible configurations of Australia, East Antarctica, Laurentia and Baltica at ca. 1.7 Ga based on modification of Karlstrom et al. (1999) reconstruction to account for rotation of the South Australia Craton and its proposed continuations in East Antarctica (Giles et al., 2004). (a) Australia occupies a SWEAT position with respect to North America; (b) Australia occupies a more westerly position allowing space for another continental fragment between Australia and North America.

the NAC during this time interval was a response to a major tectonic driver.

Previous tectonic reconstruction models interpret that tectonism at ~1550 Ma recorded in the Mt Isa Inlier and Georgetown Inlier was a response either to accretion of the Georgetown crustal block with the eastern margin of the NAC at ~1550 Ma (Boger & Hansen, 2004), and/or Laurentia with the eastern margin of the NAC (Betts et al., 2002). On the basis of palaeomagnetic data, the Laurentia-Australia amalgamation at ~1550 Ma is unlikely. If such a collisional event did occur at this time, then the two lithospheric regions must have rifted apart well before ~1200 Ma to satisfy the palaeomagnetic data. Evidence of major continental rifting between ~1550 – 1200 Ma along the eastern margin of the NAC is not recorded. As an alternative to the Australia – Laurantia connection during the Palaeo- Mesoproterozoic, it has been proposed that South China or Siberia occupied a position to the east of Australia (Fig. 3.5; Li et al., 1995; Sears & Price, 2000; Giles et al., 2004). It is possible that contractional phases recorded along the eastern margin of Proterozoic Australia were related to the accretion of South China or Siberia crustal fragments.

The recognition of orogenesis and high-grade metamorphism along the eastern margin of the NAC between ~1610 – 1550 Ma is interpreted to be predominantly related to contractional phases in a long-lived accretionary orogen. Whereas tectonic reconstructions of Giles et al. (2004) related contractional phases to accretionary tectonics along the southern margin of Proterozoic Australia, it is also possible that the 1610 – 1550 Ma contractional phases were related to an accretionary margin along the eastern margin of Proterozoic Australia. Changes in plate vectors, differences in age of the subducting plate and the angle of subduction, and reorganisation of the plate margin, could all potentially cause contractional phases in the over-riding plate (e.g. Cawood et al., 2005).

Evidence of major compressional tectonics along the southern margin of the NAC at

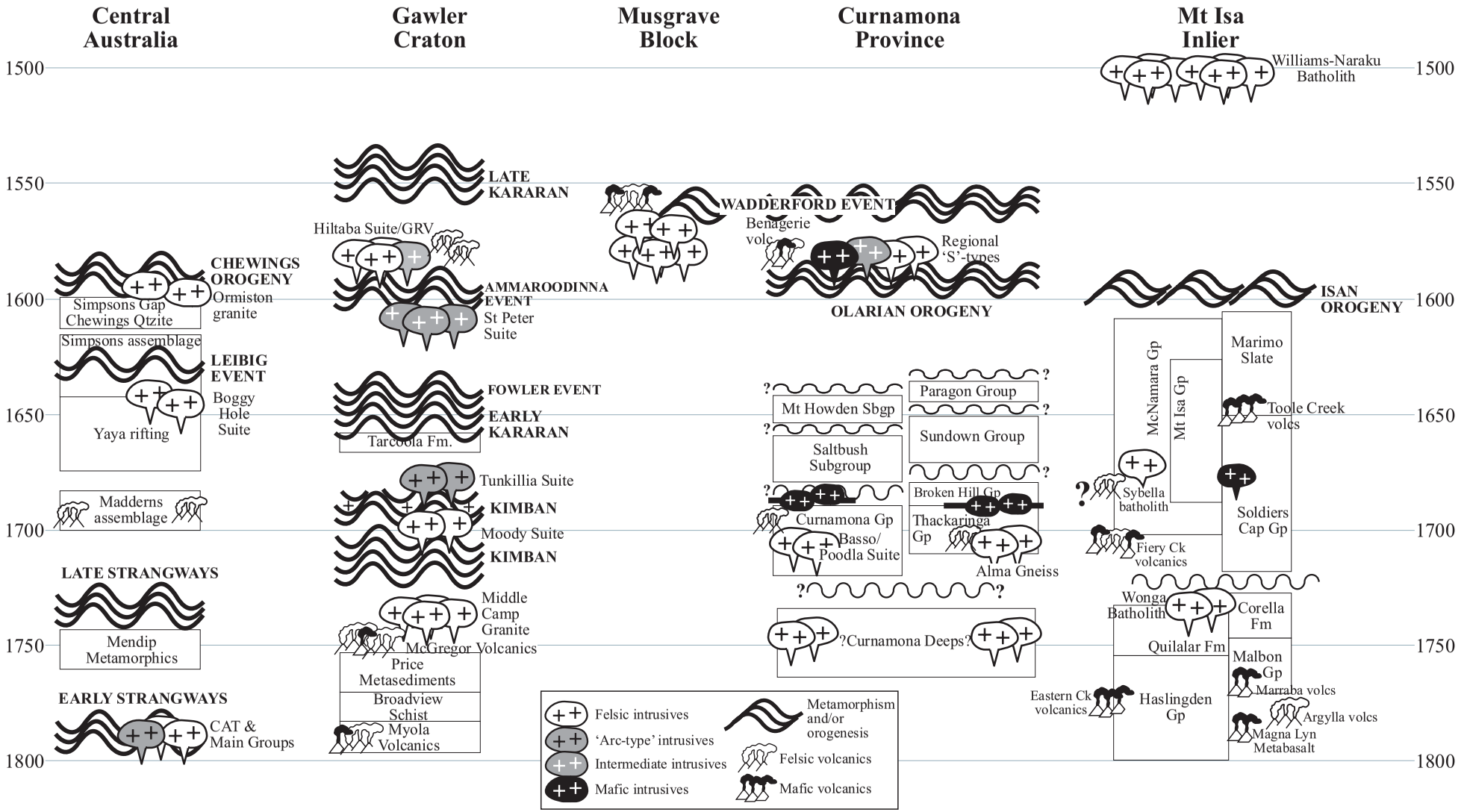


**Figure 3.6.** Time-space plot for eastern Proteozoic Australia between 1.8 and 1.6 Ga (modified from Giles et al., 2004). Compiled from Collins & Shaw (1995), Zhao & McCulloch (1995), Daly et al. (1998), Teasdale (1997), O'Dea et al. (1997), Page & Sun (1998), Page & Laing (1992), Nutman & Gibson (1998), Page et al. (2000), Black et al. (1998), Rawlings (1999), Vassallo & Wilson (2002), Wade *pers. comm.* (2005) and Dutch *pers. comm.* (2005).

~1600 Ma is also recorded by the Chewings Orogeny in the Arunta Inlier (Fig. 3.6; Collins & Shaw, 1995; Collins et al., 1995). It has been proposed that this event was a response to the amalgamation of the Mawson Continent with the southern margin of the NAC (Wade et al., 2005). Recent *in situ* monazite chemical dating has identified that a major tectonometamorphic event at ~1600 Ma was recorded across the Gawler Craton, as the Ammaroodinna Event in the northern Gawler (Fig. 3.6; B. Wade pers. comm., 2005), the late-Kararan and Fowler Event in the southern and western Gawler (Fig. 3.6; R. Dutch pers. comm., 2005), and the Hiltaba Event in the central Gawler (Fig. 3.6; Creaser & Cooper, 1993).

Near simultaneous contractional events along the eastern and southern margin of the NAC at ~1600 Ma is in contrast to many other parts of the Columbia supercontinent, that were undergoing rifting and anorogenic magmatism at this time, both along its margins and within its interior (Rogers & Santosh, 2002; Zhao et al., 2004). Rifting within other parts of Columbia potentially may have driven accretionary processes at the southern and eastern margins of the NAC between ~1600 – 1550 Ma. The amalgamation of crustal fragments with Proterozoic Australia may also have occurred during this time interval (e.g. Betts et al., 2002; Boger & Hanson, 2004), and in doing so laterally built onto Proterozoic Australia crust. However, palaeomagnetic data is required for the different crustal fragments to test such a hypothesis.

*In situ* chemical U-Th-Pb monazite dating presented in this study provides evidence of two episodes of high-grade metamorphism in the early Mesoproterozoic of the SCP. The first of these high-grade events occurred between ~1610 – 1585 Ma, and culminated in widespread bimodal magmatism and crustal anatexis at ~1585 Ma (Ludwig & Cooper, 1984). This age for the earliest metamorphic event is in agreement with SHRIMP U-Pb metamorphic zircon results (Page & Laing, 1992; Page et al., 2003). Evidence of a ~1690 Ma high-grade metamorphic event as proposed by Nutman & Ehlers (1998) and reinforced by Gibson & Nutman (2004) is not supported by this study. An additional episode of high-grade metamorphism, now preserved in the Broken Hill region, and retrograde metamorphism preserved in the Olary Domain and western Broken Hill Domain occurred between ~1570 – 1550 Ma. This event has been previously unidentified in the SCP, but has correlatives in the Mt Isa Inlier and Georgetown Inlier.

## 3.7 Conclusions

# Chapter 4
# PALAEOPROTEROZOIC MAFIC MAGMATISM

**This chapter is a version of a manuscript in press with the Australian Journal of Earth Sciences (V53, p501-519, 2006) under the title: "Continental *ca* 1.7 – 1.69 Ga Fe-rich metatholeiites in the Curnamona Province, Australia: a record of melting of a heterogeneous, subduction-modified lithospheric mantle". Authors: Rutherford, Barovich, Hand & Foden. Aspects relating to the regional geological framework in the submitted version have been removed from this chapter to avoid repetition.**

***SUMMARY***

*Iron enriched metatholeiites intruded the Willyama Supergroup of the southern Australian Curnamona Province in the late Paleoproterozoic (~1685 Ma) during a period of punctuated extension. Major element concentrations are variable ($SiO_2$ = 45.4 – 56.5 wt%; $Fe_2O_3$* = 8.5 – 20.7; $TiO_2$ = 0.46 – 2.52 wt%; Mg# = 70.5 – 29.1), and in conjunction with trace element data support near closed-system fractionation of a mantle-derived melt with little or no replenishment. Fractionation produced progressively Fe-rich derivative melts. Crystallising phases were dominated by clinopyroxene and olivine, whereas Fe-(Ti) oxide crystallisation was hindered. Primitive-mantle normalised immobile trace elements are characterised by variable Th, Nb, Sr, P and Ti anomalies. Chondrite-normalised rare earth element patterns for the most primitive, Mg-rich samples have $La_N/Sm_N<1$, whereas the most evolved Fe-rich samples have ratios of $La_N/Sm_N>1$. Initial εNd values range between -2.2 and +2.7 for the majority of the samples, with the isotopic compositions showing no correlation with differentiation or assimilation. The combined geochemical and isotopic data suggests that the southern Curnamona Province metatholeiites were extracted from a depleted mantle, and a variably enriched, heterogeneous subcontinental lithospheric mantle. Magmatism most likely occurred in a back-arc basin or intracontinental setting. It is suggested that the geochemically enriched mantle component was conceivably derived from subduction-related processes.*

## 4.1 Introduction

The geochemical and isotopic nature of mafic magmatism can provide vital information when trying to evaluate the tectonothermal evolution of the lithosphere (Christie & Sinton, 1981; Sinton et al., 1983; Pearce et al., 1994; Ziegler & Cloetingh, 2004). Deciphering the tectonic evolution of Proterozoic terrains is often made difficult due to the likelihood of multiple episodes of deformation, metamorphism and alteration. Syn- and post-magmatic processes can potentially alter major element, trace element and isotopic compositions and thereby obscure primary magmatic characteristics that may be pertinent to a particular source region(s) and geodynamic setting (e.g. Floyd & Winchester, 1978; Pearce & Norry, 1979; Myers & Breitkopf, 1989; Borsi et al., 1995; Lindh et al., 2001; Kryza & Pin, 2002). Nevertheless, interpretations about the genesis of mafic magmatism can be made by using immobile trace elements and radiogenic isotope geochemistry, and integrating them with the broader established lithotectonic framework.

Interpreting source regions and the tectonic environments of mafic magmatic rocks remains a topic of great debate (e.g. Winchester & Floyd, 1977; Floyd & Winchester, 1978; Pearce & Norry, 1979; Meschede, 1986; Hergt, 1989; Antonini et al., 1999; Hergt, 2000; Antonini et al., 2000). Key issues include whether the immobile trace element signatures which are associated with a geodynamic setting have been constant throughout Earth history, and whether tectonic settings can be determined from complex, often multi-sourced magmatic systems (e.g. Zhao & McCulloch, 1993; Downes et al., 2001; Goodenough et al., 2002; Piercey et al., 2002; Kryza & Pin, 2002; Gómez-Pugnaire et al., 2003). Additional processes that influence the geochemical signature of mafic magmatism include the degree of partial melting, the crustal level at which assimilation and fractionation took place, and whether the primary melt was sourced from the asthenosphere or lower lithosphere (e.g. Thompson & Gibson, 1994;

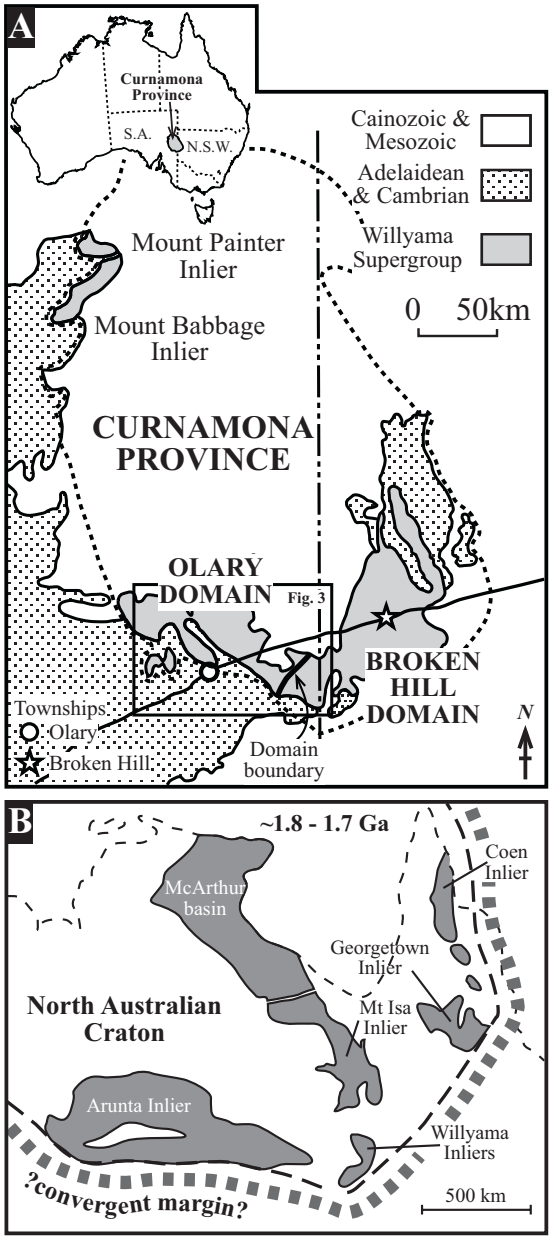


**Figure 4.1. (a)** Location of the Curnamona Province in south-central Australia. Southern Curnamona Province subdivided into the Olary Domain and Broken Hill Domain. Boxed area (Fig. 4.3) shows sample localities. **(b)** Palaeoproterozoic tectonic reconstruction model (~1.7 Ga) of the North Australian Craton highlighting the close spatial proximity of the Willyama basin to the Mt Isa region and central Australia (modified from Giles et al., 2002).

Borsi et al., 1995; Downes et al., 2001; Lindh et al., 2001; Goodenough et al., 2002; Halama et al., 2004; Lassen et al., 2004).

This study focuses on a suite of metabasites in the South Australian portion of the southern Curnamona Province (SCP; Fig. 4.1). A widespread and voluminous episode of mafic magmatism (Lady Louise Suite) intruded the SCP in the form of sills and dykes at ~1685 Ma (Conor & Fanning, 2001). A slightly older extrusive to subvolcanic mafic magmatic event (Montstephen Metabasalts) occurred between ~1715 – 1700 Ma (Conor, 2005). The petrogenesis of the metabasites is discussed, and compared with other documented Proterozoic mafic magmatic events in the Broken Hill region, in northern and central Proterozoic Australia, and the western Namaqua province of South Africa (Wilson et al., 1985; James et al., 1987; Reid et al., 1987; Williams, 1998; Zhao & McCulloch, 1993; Zhao, 1994). These comparisons highlight the similarities in mafic magmatism between these regions, including their common association within an intra-crustal setting, the magmatic processes that operated, and the requirement for enriched and depleted lithospheric source regions. Geochemical associations and similarities between the different regions add weight to tectonic reconstruction models that propose accretionary margins bordered the North Australian Craton (NAC) during the Palaeoproterozoic (Fig. 4.1b; Zhao & McCulloch, 1993; Myers et al., 1996; Giles et al., 2002).

## 4.2 Previous work

The absolute timing of the mafic magmatism in the SCP is well known in relation to deposition of the Willyama Supergroup metasedimentary sequence (ca. 1685 Ma; Page & Laing, 1992; Conor & Fanning, 2001). Geochemical studies of this magmatic event in the Broken Hill region, were conducted in the mid-1980's (Phillips et al., 1985; James

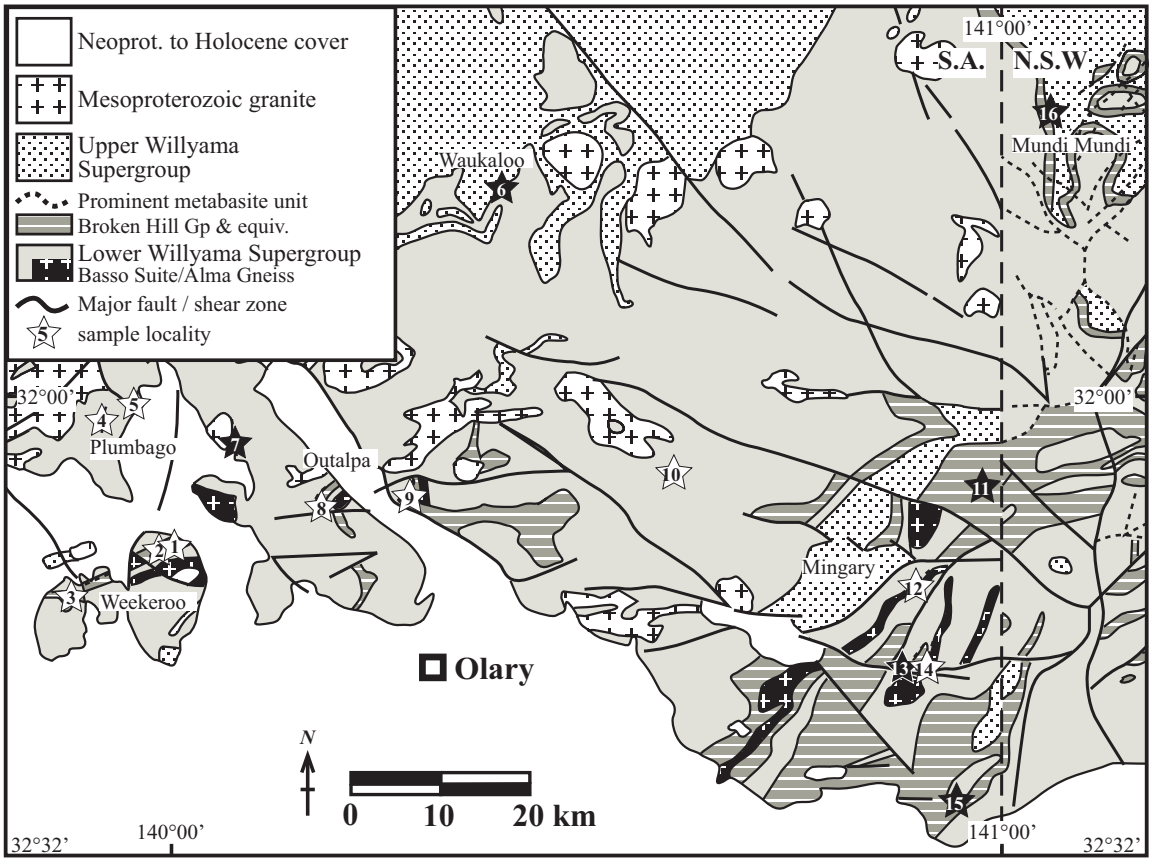


**Figure 4.2.** Sample locality map. Stars and corresponding number indicate sample localities. Weekeroo region: (1) M01, M02; (2) M03, M04; (3) M06. Plumbago region: (4) M07; (5) M08. Waukaloo region: (6) M13, M14. Outalpa region: (7) M11, M12; (8) M15, M16, M17, M18, M19; (9) M20, M21. Mingary region: (10) M33; (11) M22; (12) M23, M24, M25, M26; (13) M27; (14) M28; (15) M29. Mundi Mundi region: (16) M31, M32.

et al., 1987). These studies identified a suite of high-Fe continental tholeiites, some of which are associated with Pb-Zn-Ag mineralisation. In the Broken Hill Domain, subvolcanic magmatism occurred contemporaneously with deposition of fine-grained clastic sediments of the Broken Hill Group (Willis et al, 1983), and intrude only the Broken Hill Group and Thackaringa Group (Willis et al., 1983). Within the Olary Domain, the metabasites intrude the Ethiudna Subgroup of the lower Willyama Supergroup, and are known as the Lady Louise Suite (Conor & Fanning, 2001).

## 4.3 Field relations and petrography of metabasites

### *4.3.1 Field relations*

All the samples in this study come from mafic rocks that either have extrusive or intrusive relationships with the lower sequences of the Willyama Supergroup (Curnamona Group and Broken Hill Group; Fig. 4.2). Samples were obtained from across the southwestern Curnamona Province in order to characterise similarities or differences in mafic magmatism on the scale of the whole province. Samples M01 – M06 are from the Weekeroo region (Fig. 4.2). These metamorphosed mafic sills and/or flows are termed the Montstephen Metabasalt (Conor, 2004), and are intercalated with the Ethiudna Subgroup (1.72 – 1.7 Ga; Page et al., 2003) and hence are 15-20 million years older than the Lady Louise Suite. Therefore, the Montstephen Metabasalts are more likely to be mafic phases of the Basso Suite (1.7 Ga; Ashley et al., 1996). The Montstephen

Metabasalts preserve pillow structures and amygdaloidal textures, supporting an extrusive or subvolcanic origin (Conor, 2000, 2004).

Samples M07 – M32 are interpreted to be representative of the Lady Louise Suite (~1685 Ma; Conor & Fanning, 2001), and all intrude the Ethiudna Subgroup or equivalents. Samples M15 – M21 from the Outalpa region form part of large-scale differentiated mafic-granitic sills, however, only the mafic components have been sampled (Fig. 4.2). Samples M22 – M29 intrude the Broken Hill Group in the Mingary region of the western Broken Hill Domain (Fig. 4.2), and are interpreted to be sills, as they have concordant relationships with bedding and layer parallel structural fabrics.

Samples M31 and M32 are from diamond drill core from the Polygonum Fe-oxide Cu-Au prospect in the Mundi Mundi Plain (Fig. 4.2). They intrude what is interpreted to be an upper Thackaringa Group equivalent (Himalaya Formation; Leyh & Conor, 2000). Sample M31 is a coarse-grained variety, whereas M32 possibly represents a chilled margin. Sample M33 comes from a mafic body within the White Dam Fe-oxide Au(-Cu) prospect that intrudes a quartzofeldspathic lithology within the lower Willyama Supergroup (Wiperaminga Subgroup; Fig. 4.2).

### *4.3.2 Petrography of metabasites in the SCP*

All the samples in this study have been metamorphosed and deformed under amphibolite to granulite facies conditions associated with the Olarian Orogeny (Clarke et al., 1987; Page & Laing, 1992). Consequently, relict igneous textures are rare, except in samples M01, M02 and M06 from the Montstephen Metabasalt, which preserve orthocumulate textures (not shown). All samples contain metamorphic mineral assemblages dominated by actinolite, hornblende, orthopyroxene, clinopyroxene, ilmenite and magnetite. In some samples, plagioclase aggregates potentially represent pseudomorphs of large primary magmatic cumulate plagioclase. Mineral compositions were not investigated as primary igneous minerals were replaced during metamorphism.

## 4.4 Geochemistry

### *4.4.1 Analytical methods*

Samples were analysed for major and trace elements and Sm-Nd isotopic compositions (Table 4.1, 4.2). Samples for elemental and isotopic analysis were crushed, and splits powdered in a tungsten-carbide mill. For analysis of major elements a 0.1 g sub-sample of the analytical pulp was fused with lithium metaborate followed by dissolution in nitric acid solution to give a “total solution” ready for ICPMS analysis. Analysis of trace and rare earth elements was achieved by digestion of up to 0.5 g of analytical pulp in a HF/multi-acid solution and presented to an ICPMS for the quantification of elements of interest. All dissolution and element analysis were carried out at Amdel Laboratories, Adelaide. Amdel adopts the ISO 9000 Quality Management Systems. All Amdel laboratory work to documented procedures in accordance with this standard.

**Table 4.1.** Whole rock major and trace element data

| **Sample** | M01 | M02 | M03 | M04 | M06 | M07 | M08 | M11 | M12 | M13 |
|---|---|---|---|---|---|---|---|---|---|---|
| **Region** | Weekeroo | Weekeroo | Weekeroo | Weekeroo | Weekeroo | Plumbago | Plumbago | Outalpa | Outalpa | Waukaloo |
| **Northing**[1] | 6439902 | 6439902 | 6439751 | 6439658 | 6435000 | 6454208 | 6456607 | 6453030 | 6452376 | 6478287 |
| **Easting** | 406977 | 406977 | 405687 | 405674 | 396757 | 399275 | 404058 | 415022 | 414475 | 442538 |
| **$SiO_2$** | 47.30 | 45.40 | 46.90 | 46.70 | 49.40 | 49.50 | 49.60 | 53.00 | 48.00 | 48.40 |
| **$TiO_2$** | 1.42 | 1.54 | 2.17 | 1.45 | 1.66 | 2.03 | 0.70 | 1.64 | 1.37 | 1.21 |
| **$Al_2O_3$** | 14.70 | 13.70 | 12.10 | 14.10 | 3.50 | 13.30 | 17.40 | 13.40 | 14.20 | 13.70 |
| **$Fe_2O_3$** | 13.90 | 16.00 | 20.70 | 16.30 | 19.20 | 15.00 | 9.99 | 13.30 | 14.60 | 14.20 |
| **MnO** | 0.13 | 0.17 | 0.18 | 0.17 | 0.10 | 0.13 | 0.18 | 0.08 | 0.05 | 0.21 |
| **MgO** | 9.34 | 10.80 | 4.06 | 5.25 | 12.70 | 6.10 | 6.50 | 5.06 | 8.44 | 6.48 |
| **CaO** | 4.11 | 4.73 | 7.61 | 9.42 | 10.80 | 6.07 | 12.50 | 6.71 | 4.73 | 8.65 |
| **Na2O** | 3.97 | 4.12 | 4.85 | 4.49 | 1.57 | 5.34 | 2.04 | 5.67 | 5.36 | 3.85 |
| **$K_2O$** | 3.60 | 0.19 | 0.28 | 0.71 | 0.08 | 0.31 | 0.27 | 0.32 | 0.26 | 1.22 |
| **$P_2O_5$** | 0.07 | 0.07 | 0.30 | 0.14 | 0.26 | 0.17 | 0.03 | 0.21 | 0.05 | 0.08 |
| **LOI** | 1.03 | 2.96 | 0.32 | 0.78 | 0.95 | 0.70 | 1.03 | 0.45 | 2.98 | 1.96 |
| **Total** | 99.57 | 99.68 | 99.47 | 99.51 | 100.22 | 98.65 | 100.24 | 99.84 | 100.04 | 99.96 |
| | | | | | | | | | | |
| **Mg#** | 58.5 | 58.6 | 29.1 | 40.3 | 58.1 | 46.0 | 57.7 | 44.4 | 54.8 | 48.9 |
| **Sc** | 44.0 | 56.0 | 28.0 | 36.0 | 48.0 | 40.0 | 34.0 | 40.0 | 38.0 | 40.0 |
| **V** | 360.0 | 360.0 | 350.0 | 330.0 | 460.0 | 370.0 | 210.0 | 330.0 | 350.0 | 330.0 |
| **Cr** | 40.0 | 54.0 | 3.0 | 43.0 | 58.0 | 37.0 | 29.0 | 38.0 | 78.0 | 70.0 |
| **Co** | 50.0 | 48.0 | 54.0 | 50.0 | 52.0 | 66.0 | 42.0 | 50.0 | 42.0 | 45.0 |
| **Ni** | 72.0 | 84.0 | 17.0 | 40.0 | 110.0 | 45.0 | 70.0 | 25.0 | 58.0 | 68.0 |
| **Cu** | bd | 11.0 | bd | 78.0 | bd | 1650.0 | 195.0 | 115.0 | bd | 155.0 |
| **Zn** | 33.0 | 47.0 | 17.0 | 23.0 | 17.0 | 18.0 | 56.0 | bd | bd | 15.0 |
| **Pb** | 12.0 | 10.0 | 24.0 | 24.0 | 38.0 | 10.0 | 12.0 | 18.0 | 12.0 | 20.0 |
| **Ga** | 19.5 | 16.0 | 21.5 | 18.5 | 9.0 | 20.0 | 17.0 | 18.0 | 18.5 | 17.0 |
| **Cs** | 7.5 | 0.5 | bd | 0.1 | bd | 0.5 | 0.3 | bd | 0.6 | 0.5 |
| **Rb** | 260.0 | 11.5 | 4.5 | 8.0 | 1.5 | 13.5 | 9.5 | 3.0 | 16.0 | 32.0 |
| **Ba** | 270.0 | 75.0 | 45.0 | 125.0 | 10.0 | 75.0 | 190.0 | 55.0 | 70.0 | 1300.0 |
| **Sr** | 92.0 | 76.0 | 170.0 | 175.0 | 10.0 | 160.0 | 140.0 | 56.0 | 46.0 | 210.0 |
| **Y** | 17.5 | 22.5 | 46.5 | 27.0 | 37.5 | 29.5 | 12.5 | 26.0 | 17.5 | 21.0 |
| **Zr** | 50.0 | 60.0 | 170.0 | 80.0 | 90.0 | 130.0 | 30.0 | 130.0 | 60.0 | 50.0 |
| **Th** | 0.7 | 0.9 | 3.5 | 1.7 | 1.6 | 3.6 | 0.4 | 6.5 | 0.9 | 0.6 |
| **U** | 0.9 | 0.5 | 0.8 | 0.5 | 2.5 | 6.0 | 0.1 | 1.5 | 1.3 | 0.9 |
| **Nb** | 3.5 | 2.0 | 13.0 | 6.0 | 9.5 | 10.0 | 2.0 | 8.0 | 1.5 | 3.5 |
| **La** | 8.0 | 36.0 | 11.5 | 6.5 | 10.5 | 14.5 | 2.5 | 12.0 | 14.5 | 5.0 |
| **Ce** | 13.5 | 54.0 | 27.0 | 15.5 | 27.0 | 31.5 | 5.5 | 22.5 | 22.0 | 11.5 |
| **Pr** | 2.1 | 6.5 | 4.8 | 2.7 | 5.5 | 5.0 | 1.1 | 3.1 | 2.9 | 1.9 |
| **Nd** | 9.5 | 22.5 | 23.0 | 13.0 | 27.5 | 23.0 | 5.0 | 12.5 | 12.5 | 9.0 |
| **Sm** | 2.9 | 4.0 | 7.0 | 3.9 | 8.0 | 6.0 | 1.5 | 2.8 | 3.5 | 2.6 |
| **Eu** | 1.3 | 1.1 | 2.1 | 1.5 | 2.0 | 1.6 | 0.7 | 1.4 | 1.4 | 1.3 |
| **Gd** | 3.2 | 4.0 | 8.0 | 4.5 | 7.5 | 6.0 | 2.0 | 3.1 | 3.7 | 3.4 |
| **Tb** | 0.6 | 0.7 | 1.3 | 0.7 | 1.1 | 0.9 | 0.3 | 0.5 | 0.5 | 0.6 |
| **Dy** | 3.5 | 4.3 | 9.0 | 5.0 | 7.0 | 6.0 | 2.3 | 4.2 | 3.3 | 3.9 |
| **Ho** | 0.7 | 0.9 | 2.0 | 1.1 | 1.4 | 1.2 | 0.5 | 1.1 | 0.7 | 0.9 |
| **Er** | 2.0 | 2.6 | 5.5 | 3.2 | 4.0 | 3.5 | 1.5 | 3.2 | 2.0 | 2.4 |
| **Tm** | 0.3 | 0.4 | 0.9 | 0.5 | 0.6 | 0.5 | 0.2 | 0.5 | 0.3 | 0.4 |
| **Yb** | 2.1 | 2.5 | 6.0 | 3.4 | 3.9 | 3.5 | 1.5 | 3.6 | 1.9 | 2.5 |
| **Lu** | 0.3 | 0.3 | 0.8 | 0.5 | 0.6 | 0.5 | 0.2 | 0.5 | 0.3 | 0.4 |
| **Eu/Eu*** | 1.25 | 0.84 | 0.86 | 1.06 | 0.79 | 0.79 | 1.20 | 1.45 | 1.19 | 1.29 |
| **Sum REE** | 49.92 | 139.74 | 108.77 | 61.88 | 106.51 | 103.62 | 24.61 | 70.99 | 69.46 | 45.60 |

[1]**Datum GDA94**

Samples for Sm-Nd isotopic analysis were spiked with a $^{150}Nd$-$^{149}Sm$ solution, digested in $HF/HNO_3$ in sealed high pressure Teflon bombs for 4 days, evaporated, and digested in HCl and sealed again in bombs overnight. Sm-Nd isotopic ratios were measured by thermal ionisation mass spectrometry on Finnigan Mat 261 and 262 mass spectrometers. The $^{143}Nd/^{144}Nd$ ratio is normalised to $^{146}Nd/^{144}Nd = 0.721903$. Total blanks for Sm-Nd were 50-100 pg. The $^{143}Nd/^{144}Nd$ ratio of the in-house standard (Johnson Matthey) at the University of Adelaide laboratory during the coarse of the analysis was 0.511601 ± 0.000008 (1σ; n=7). Running average for La Jolla over the year is 0.511838 ± 0.000008

**Table 4.1.** *Continued.*

| **Sample** | M14 | M15 | M16 | M17 | M18 | M19 | M20 | M21 | M22 | M23 |
|---|---|---|---|---|---|---|---|---|---|---|
| **Region** | Waukaloo | Outalpa | Outalpa | Outalpa | Outalpa | Outalpa | Outalpa | Outalpa | Mingary | Mingary |
| **Northing** | 6478288 | 6444796 | 6445051 | 6445226 | 6445617 | 6445109 | 6446121 | 6446121 | 6447843 | 6436714 |
| **Easting** | 442547 | 423120 | 423451 | 423596 | 423754 | 423316 | 432966 | 432966 | 497914 | 491423 |
| **$SiO_2$** | 48.70 | 50.40 | 50.00 | 49.00 | 48.70 | 48.60 | 47.80 | 50.00 | 49.40 | 49.40 |
| **$TiO_2$** | 1.21 | 1.60 | 1.31 | 1.34 | 1.71 | 1.31 | 1.41 | 1.72 | 1.04 | 0.87 |
| **$Al_2O_3$** | 13.50 | 12.70 | 13.60 | 13.50 | 13.30 | 13.80 | 14.10 | 15.30 | 12.80 | 13.70 |
| **$Fe_2O_3$** | 13.60 | 16.50 | 12.30 | 13.90 | 17.70 | 14.00 | 14.80 | 16.30 | 13.10 | 12.10 |
| **MnO** | 0.20 | 0.14 | 0.27 | 0.22 | 0.27 | 0.22 | 0.20 | 0.21 | 0.22 | 0.19 |
| **MgO** | 6.63 | 5.60 | 6.68 | 6.17 | 4.59 | 7.65 | 5.73 | 3.46 | 7.97 | 7.72 |
| **CaO** | 8.46 | 8.51 | 9.35 | 9.98 | 8.80 | 8.90 | 6.78 | 7.49 | 12.10 | 11.70 |
| **Na2O** | 3.45 | 3.53 | 4.24 | 3.76 | 3.09 | 3.45 | 3.63 | 3.84 | 1.78 | 1.69 |
| **$K_2O$** | 1.82 | 0.56 | 0.41 | 0.45 | 0.80 | 1.21 | 2.31 | 0.86 | 0.21 | 0.55 |
| **$P_2O_5$** | 0.09 | 0.14 | 0.10 | 0.11 | 0.12 | 0.09 | 0.11 | 0.12 | 0.07 | 0.06 |
| **LOI** | 1.49 | 0.47 | 0.89 | 1.00 | 0.83 | 1.24 | 2.08 | 0.56 | 0.79 | 0.90 |
| **Total** | 99.15 | 100.15 | 99.15 | 99.43 | 99.91 | 100.47 | 98.95 | 99.86 | 99.48 | 98.88 |
| | | | | | | | | | | |
| **Mg#** | 50.5 | 41.6 | 53.2 | 48.2 | 35.2 | 53.4 | 44.8 | 30.8 | 56.0 | 57.2 |
| **Sc** | 38.0 | 42.0 | 46.0 | 42.0 | 44.0 | 36.0 | 38.0 | 34.0 | 46.0 | 46.0 |
| **V** | 310.0 | 380.0 | 340.0 | 350.0 | 550.0 | 310.0 | 340.0 | 470.0 | 310.0 | 270.0 |
| **Cr** | 78.0 | 11.0 | 39.0 | 35.0 | 4.0 | 24.0 | 15.0 | 20.0 | 120.0 | 160.0 |
| **Co** | 47.0 | 47.0 | 62.0 | 50.0 | 62.0 | 52.0 | 50.0 | 58.0 | 52.0 | 48.0 |
| **Ni** | 62.0 | 56.0 | 64.0 | 58.0 | 38.0 | 100.0 | 39.0 | 31.0 | 86.0 | 88.0 |
| **Cu** | 380.0 | 45.0 | 180.0 | 90.0 | 49.0 | 62.0 | 155.0 | 100.0 | 72.0 | 130.0 |
| **Zn** | 13.0 | 6.0 | 29.0 | 58.0 | 115.0 | 68.0 | 45.0 | 50.0 | 94.0 | 80.0 |
| **Pb** | 18.0 | 16.0 | 24.0 | 14.0 | 16.0 | 30.0 | 10.0 | 20.0 | 22.0 | 18.0 |
| **Ga** | 17.0 | 19.5 | 18.5 | 18.5 | 21.0 | 18.0 | 19.5 | 23.0 | 16.0 | 15.5 |
| **Cs** | 0.8 | 0.1 | bd | bd | 0.3 | 0.5 | 6.0 | 0.8 | 0.3 | 0.3 |
| **Rb** | 54.0 | 10.0 | 5.5 | 10.0 | 19.5 | 52.0 | 135.0 | 35.0 | 9.0 | 21.5 |
| **Ba** | 1700.0 | 70.0 | 100.0 | 125.0 | 120.0 | 185.0 | 115.0 | 230.0 | 200.0 | 290.0 |
| **Sr** | 195.0 | 125.0 | 210.0 | 140.0 | 140.0 | 120.0 | 105.0 | 155.0 | 105.0 | 130.0 |
| **Y** | 24.0 | 30.5 | 24.5 | 24.0 | 28.0 | 22.0 | 25.0 | 27.5 | 27.0 | 21.5 |
| **Zr** | 60.0 | 80.0 | 60.0 | 60.0 | 70.0 | 80.0 | 60.0 | 90.0 | 50.0 | 40.0 |
| **Th** | 0.6 | 2.2 | 0.7 | 0.6 | 2.3 | 0.6 | 1.3 | 3.2 | 0.5 | 0.8 |
| **U** | 1.6 | 1.0 | 1.1 | 0.2 | 2.1 | 0.5 | 0.4 | 0.6 | 0.1 | 0.2 |
| **Nb** | 3.5 | 5.0 | 4.0 | 3.5 | 4.5 | 3.5 | 4.0 | 5.5 | 2.5 | 2.0 |
| **La** | 8.5 | 11.0 | 14.5 | 5.5 | 10.0 | 6.5 | 6.0 | 9.0 | 8.0 | 4.5 |
| **Ce** | 17.0 | 19.0 | 28.0 | 13.0 | 19.0 | 14.0 | 13.5 | 18.5 | 11.5 | 8.0 |
| **Pr** | 2.7 | 3.5 | 3.8 | 2.4 | 3.2 | 2.3 | 2.3 | 3.0 | 2.3 | 1.5 |
| **Nd** | 11.5 | 16.5 | 15.0 | 11.5 | 15.5 | 10.0 | 10.5 | 14.5 | 11.5 | 7.5 |
| **Sm** | 2.9 | 4.9 | 4.0 | 3.6 | 4.4 | 3.0 | 3.5 | 4.0 | 3.5 | 2.2 |
| **Eu** | 1.6 | 1.4 | 1.4 | 1.1 | 1.4 | 0.9 | 1.3 | 1.3 | 1.1 | 0.9 |
| **Gd** | 3.9 | 5.5 | 4.4 | 4.3 | 4.7 | 3.7 | 4.1 | 4.9 | 4.4 | 3.2 |
| **Tb** | 0.7 | 0.9 | 0.7 | 0.7 | 0.8 | 0.6 | 0.7 | 0.8 | 0.7 | 0.5 |
| **Dy** | 4.5 | 5.5 | 4.5 | 4.7 | 5.0 | 3.9 | 4.6 | 5.0 | 4.5 | 3.6 |
| **Ho** | 1.0 | 1.3 | 1.0 | 1.0 | 1.1 | 0.8 | 1.0 | 1.2 | 1.0 | 0.8 |
| **Er** | 2.7 | 3.5 | 2.7 | 2.9 | 3.2 | 2.4 | 2.9 | 3.3 | 2.8 | 2.4 |
| **Tm** | 0.5 | 0.6 | 0.4 | 0.5 | 0.5 | 0.4 | 0.4 | 0.5 | 0.4 | 0.4 |
| **Yb** | 3.0 | 3.6 | 2.9 | 3.1 | 3.2 | 2.4 | 2.9 | 3.4 | 2.8 | 2.5 |
| **Lu** | 0.4 | 0.5 | 0.4 | 0.4 | 0.4 | 0.3 | 0.4 | 0.5 | 0.4 | 0.3 |
| **Eu/Eu*** | 1.41 | 0.82 | 0.98 | 0.85 | 0.91 | 0.78 | 1.05 | 0.90 | 0.86 | 0.98 |
| **Sum REE** | 60.78 | 77.55 | 83.65 | 54.64 | 72.31 | 51.15 | 54.11 | 69.76 | 54.89 | 38.20 |

(1σ; n=6).

### *4.4.2 Major element variation*

$SiO_2$ contents in all samples are restricted to between 45 and 53 wt% (Table 4.1). MgO contents are also highly variable (3.5 – 12.7 wt%), as is $Fe_2O_3$* which range from 8.5 to 12.7 wt%. Major elements are plotted against the fractionation index Mg# (Mg# = $100Mg^{2+}/[Mg^{2+}+Fe^{2+}]$) in Fig. 4.3 to assess whether any magmatic differentiation trends are evident, and if so, which phases crystallised from the magma. An assumption regarding the $FeO/Fe_2O_3$* ratio (= 0.85; $Fe_2O_3$* = total Fe) is made based on observed in fresh

**Table 4.1.** *Continued.*

| **Sample** | M24 | M25 | M26 | M27 | M28 | M29 | M31 | M32 | M33 |
|---|---|---|---|---|---|---|---|---|---|
| **Region** | Mingary | Mingary | Mingary | Mingary | Mingary | Mingary | Mundi | Mundi | Mingary |
| **Northing** | 6436935 | 6436545 | 6436504 | 6426989 | 6427029 | 6411001 | 6494500 | 6494500 | 6449051 |
| **Easting** | 491058 | 490647 | 490723 | 490335 | 491769 | 495730 | 503100 | 503100 | 460175 |
| **$SiO_2$** | 49.50 | 50.30 | 50.00 | 50.30 | 49.10 | 49.10 | 49.40 | 47.30 | 49.00 |
| **$TiO_2$** | 0.46 | 0.66 | 0.49 | 1.14 | 1.16 | 1.33 | 1.55 | 2.52 | 1.25 |
| **$Al_2O_3$** | 14.30 | 11.90 | 14.20 | 15.40 | 14.80 | 13.60 | 12.80 | 14.40 | 13.80 |
| **$Fe_2O_3$** | 8.47 | 11.40 | 9.12 | 13.10 | 14.90 | 15.00 | 15.60 | 15.40 | 14.50 |
| **MnO** | 0.16 | 0.20 | 0.16 | 0.20 | 0.24 | 0.23 | 0.41 | 0.40 | 0.17 |
| **MgO** | 9.64 | 10.50 | 9.24 | 5.70 | 6.96 | 7.11 | 5.62 | 4.56 | 6.14 |
| **CaO** | 14.60 | 12.90 | 14.20 | 10.60 | 10.00 | 9.56 | 7.75 | 10.70 | 9.58 |
| **Na2O** | 1.36 | 1.37 | 1.87 | 1.05 | 2.05 | 1.95 | 3.07 | 3.12 | 3.69 |
| **$K_2O$** | 0.25 | 0.21 | 0.40 | 0.49 | 0.31 | 0.64 | 0.97 | 0.63 | 0.80 |
| **$P_2O_5$** | 0.02 | 0.04 | 0.03 | 0.09 | 0.05 | 0.11 | 0.10 | 0.18 | 0.10 |
| **LOI** | 0.93 | 0.74 | 0.97 | 0.78 | 0.95 | 1.23 | 3.13 | 1.00 | 1.21 |
| **Total** | 99.69 | 100.22 | 100.68 | 98.85 | 100.52 | 99.86 | 100.40 | 100.21 | 100.24 |
| | | | | | | | | | |
| **Mg#** | 70.5 | 65.9 | 68.0 | 47.7 | 49.5 | 49.8 | 43.0 | 38.3 | 47.0 |
| **Sc** | 50.0 | 50.0 | 50.0 | 38.0 | 36.0 | 42.0 | 42.0 | 50.0 | 42.0 |
| **V** | 210.0 | 250.0 | 220.0 | 290.0 | 360.0 | 350.0 | 400.0 | 550.0 | 340.0 |
| **Cr** | 260.0 | 210.0 | 260.0 | 50.0 | 45.0 | 105.0 | 17.0 | bd | 74.0 |
| **Co** | 41.0 | 50.0 | 40.0 | 48.0 | 56.0 | 56.0 | 45.0 | 34.0 | 74.0 |
| **Ni** | 115.0 | 130.0 | 120.0 | 56.0 | 70.0 | 82.0 | 46.0 | 32.0 | 88.0 |
| **Cu** | 58.0 | 66.0 | 56.0 | 100.0 | 270.0 | 125.0 | 60.0 | bd | 410.0 |
| **Zn** | 39.0 | 72.0 | 41.0 | 175.0 | 92.0 | 190.0 | 200.0 | 185.0 | 74.0 |
| **Pb** | 6.0 | 10.0 | 14.0 | 38.0 | 20.0 | 22.0 | 18.0 | 24.0 | 12.0 |
| **Ga** | 13.5 | 13.0 | 13.0 | 19.5 | 18.0 | 19.0 | 18.0 | 25.0 | 18.5 |
| **Cs** | 0.6 | 0.2 | 0.3 | 0.3 | 0.1 | 0.8 | 13.5 | 2.5 | bd |
| **Rb** | 9.0 | 5.0 | 15.0 | 10.5 | 7.0 | 21.5 | 62.0 | 29.0 | 9.0 |
| **Ba** | 40.0 | 20.0 | 50.0 | 195.0 | 135.0 | 165.0 | 135.0 | 130.0 | 70.0 |
| **Sr** | 105.0 | 78.0 | 105.0 | 110.0 | 110.0 | 130.0 | 190.0 | 250.0 | 120.0 |
| **Y** | 10.5 | 12.5 | 11.0 | 21.0 | 14.5 | 24.5 | 26.5 | 52.0 | 23.0 |
| **Zr** | 20.0 | 30.0 | 20.0 | 50.0 | 30.0 | 70.0 | 80.0 | 130.0 | 60.0 |
| **Th** | 0.2 | 0.3 | 0.2 | 0.8 | 0.6 | 0.4 | 1.6 | 2.6 | 0.7 |
| **U** | 0.1 | 0.2 | 0.1 | 1.5 | 0.1 | 0.6 | 0.5 | 0.9 | 1.4 |
| **Nb** | 1.0 | 1.5 | 1.0 | 3.5 | 2.0 | 3.5 | 6.0 | 8.5 | 3.5 |
| **La** | 1.0 | 2.0 | 1.5 | 4.5 | 2.5 | 4.5 | 5.0 | 8.0 | 7.5 |
| **Ce** | 3.5 | 5.5 | 4.0 | 11.0 | 6.5 | 9.5 | 12.0 | 20.5 | 14.0 |
| **Pr** | 0.6 | 0.9 | 0.7 | 1.9 | 1.1 | 2.0 | 2.1 | 3.9 | 2.2 |
| **Nd** | 3.1 | 4.4 | 3.1 | 9.5 | 5.5 | 10.5 | 10.0 | 20.0 | 10.0 |
| **Sm** | 1.1 | 1.6 | 1.3 | 2.9 | 1.8 | 3.4 | 3.6 | 7.0 | 3.1 |
| **Eu** | 0.4 | 0.6 | 0.5 | 1.1 | 0.8 | 1.2 | 1.2 | 2.8 | 1.1 |
| **Gd** | 1.5 | 2.0 | 1.6 | 3.5 | 2.3 | 3.8 | 4.5 | 8.5 | 3.6 |
| **Tb** | 0.3 | 0.4 | 0.3 | 0.6 | 0.4 | 0.7 | 0.7 | 1.4 | 0.6 |
| **Dy** | 1.9 | 2.3 | 2.0 | 3.8 | 2.6 | 4.3 | 5.0 | 9.5 | 4.0 |
| **Ho** | 0.4 | 0.5 | 0.4 | 0.8 | 0.6 | 1.0 | 1.1 | 2.0 | 0.9 |
| **Er** | 1.2 | 1.5 | 1.3 | 2.4 | 1.6 | 2.8 | 3.0 | 6.0 | 2.6 |
| **Tm** | 0.2 | 0.2 | 0.2 | 0.4 | 0.3 | 0.5 | 0.5 | 0.8 | 0.4 |
| **Yb** | 1.2 | 1.4 | 1.3 | 2.6 | 1.8 | 3.0 | 3.1 | 6.0 | 2.6 |
| **Lu** | 0.2 | 0.2 | 0.2 | 0.4 | 0.2 | 0.4 | 0.4 | 0.8 | 0.4 |
| **Eu/Eu*** | 0.98 | 0.99 | 1.10 | 1.06 | 1.14 | 0.98 | 0.87 | 1.11 | 0.96 |
| **Sum REE** | 16.40 | 23.33 | 18.17 | 45.26 | 27.89 | 47.43 | 52.10 | 97.18 | 52.91 |

unaltered basaltic rocks (Ragland, 1989). Mg# ranges between 29 and 70. The samples with the highest Mg# from the Mingary Group (MgO ~10 wt%), are interpreted to have the compositions closest to that of the parental melt. $SiO_2$ contents in all samples are relatively restricted between, and show no correlation with Mg# fractionation index ($r$ = 0.12). Excluding the Montstephen Metabasalt samples, $Fe_2O_3$*, $TiO_2$ and $P_2O_5$ show a negative correlation with increasing Mg# ($r$ = -0.89, -0.85, -0.75, respectively), while CaO and MgO have a positive trend ($r$ = 0.67, 0.94, respectively). The Montstephen Metabasalt samples are excluded from discussion relating to magmatic differentiation given their

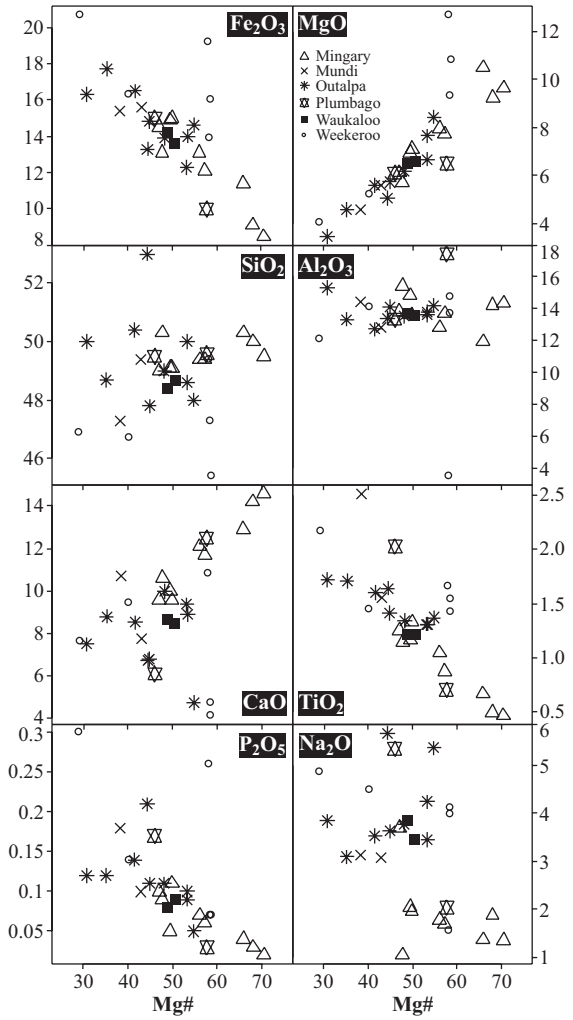


**Figure 4.3.** Major-elements vs. fractionation index Mg# (Mg# = 100 $Mg^{2+}/[Fe^{2+}+Mg^{2+}]$; $FeO/Fe_2O_3$* = 0.85, calculated on basis of that for unaltered basalts; Ragland, 1989).

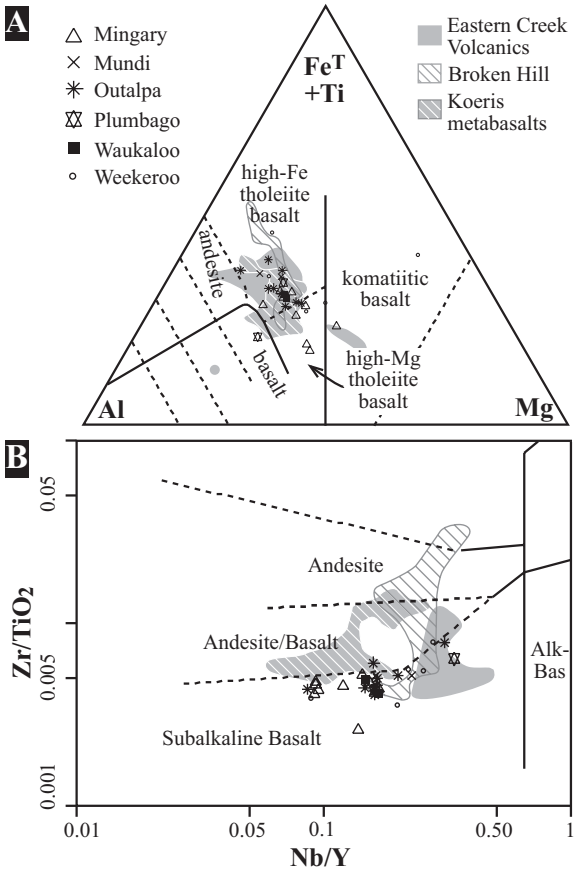


**Figure 4.4. (a)** AFM ternary classification diagram (Irvine & Baragar, 1971); **(b)** Al – $Fe^T$+Ti – Mg ternary cation classification plot (Jensen, 1976); **(c)** $Zr/TiO_2$ vs. Nb/Y ratio plot classification scheme (Winchester & Floyd, 1977). Fields for Eastern Creek Volcanics, Broken Hill and Koeris metabasalts taken from data of Williams (1998), James et al. (1987) and Reid et al. (1987), respectively.

cumulate origin and comparatively older age relative to the Lady Louise Suite.

The Al – $Fe_2O_3$*+Ti – Mg ternary cation classification plot (Jensen, 1976), classifies the samples as predominantly high-Fe tholeiites, with the most silica-depleted samples from the Mingary region plotting in the high-Mg tholeiite field or basalt field (Fig. 4.4a).

### *4.4.3 Trace element variation*

The incompatible HFSE, REE, and the compatible transition metals are particularly useful in interpreting the petrogenesis and tectonic setting of metabasites, as they are generally less mobile during alteration and metamorphism (e.g. Pearce & Cann, 1973; Winchester & Floyd, 1977; MacLean & Barrett, 1993). The immobile element $Zr/TiO_2$ vs. Nb/Y ratio plot (Winchester & Floyd, 1977; Fig. 4.4b) supports a subalkaline basaltic composition for the metabasites. The Montstephen Metabasalts trend towards the alkaline basalt field on the $Zr/TiO_2$ vs Nb/Y plot.

Compatible ferromagnesian elements (Ni, Co, Cr, V, Sc) are plotted against the fractionation index in Fig. 4.5. Ni and Cr decrease with differentiation, whereas V shows a positive trend early with differentiation. Sc and Co have no clear relationship with the

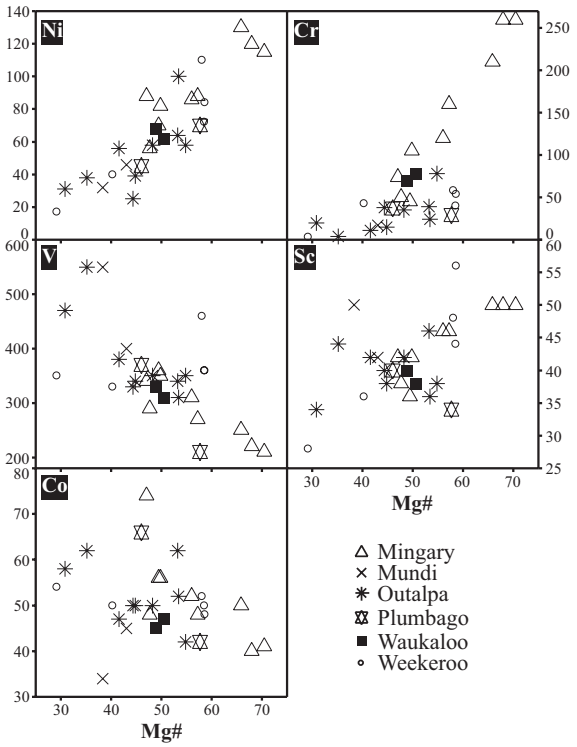


**Figure 4.5.** Compatible ferromagnesian elements Ni, Cr, V, Sc and Co vs. Mg#. Trends in Ni, Cr and Sc indicative of crystallisation of olivine and clinopyroxene.

fractionation index. The large ion lithophile elements (LILE) Rb, Sr, Ba, Cs show no obvious trends with increasing differentiation (not shown), but are likely to be susceptible to the effects of alteration and metamorphism (e.g. Ludden et al., 1982). The base metals Pb, Zn and Cu show considerable variation and no systematic relationship to Mg# (not shown).

Primitive mantle-normalised incompatible trace element diagrams are shown in Fig. 4.6. For clarity, samples have been grouped together in relation to their geographic locality (see Fig. 4.2). The normalised patterns are variable within and between localities, but are weakly to strongly enriched relative to primitive mantle values (up to 1000 times primitive mantle values). The majority of samples are relatively enriched in the LILE relative to the HFSE, although given the susceptibility for LILE mobility under metasomatic conditions (e.g. Winter, 2001), no interpretations are made regarding the significance of these enrichments. With the exception of the Mingary Group, patterns reproduce well for the incompatible elements, and are comparable to N-MORB compositions (Sun & McDonough, 1989). The Mingary Group are depleted in the HFSE relative to N-MORB.

The metabasite suite as a whole is comparatively enriched in Th (0.18 – 3.6 ppm) relative to N-MORB (0.12 ppm; Fig. 4.6), being comparable to that of E-MORB (0.6 ppm; Sun & McDonough, 1989). With the exception of the metabasites from Mingary, the remainder of the metabasites are relatively enriched in Nb and have similar or enriched concentrations of Ti relative to N-MORB (Fig. 4.6). The Mingary, Weekeroo and Outalpa groups have consistent Nb depletions. All the primitive mantle-normalised plots are characterised by extreme Pb enrichment (>100 times primitive mantle and N-MORB values). Lead concentrations range between 10 and 38 ppm (Table 4.1), which are considerable higher than those of average basalts (~6 ppm; Condie, 1993).

### *4.4.4 Rare earth elements*

Chondrite-normalised REE diagrams are presented in Fig. 4.6. Total REE abundances increase with progressive fractionation (ΣREE 27.1 – 162.3 ppm, excluding the cumulate samples) and are typical of those documented for continental tholeiites (e.g. Weaver & Tarney, 1981; Turner & Hawkesworth, 1995; Condie, 1997). The majority of the samples are slightly enriched in the LREE ($La_N/Sm_N$

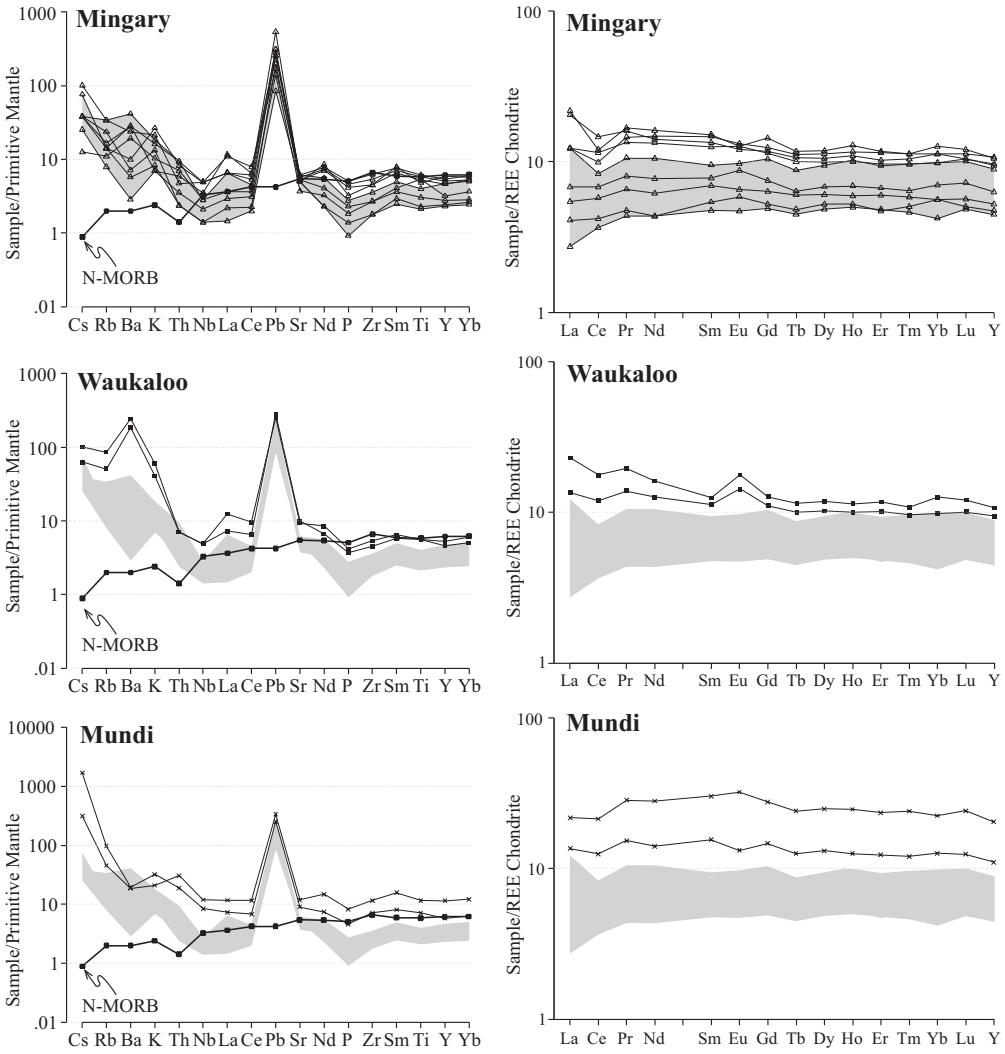


**Figure 4.6.** Primitive mantle and chondrite normalised compositions. Normalisation values are from Sun & McDonough (1989) and Taylor & McLennan (1985), respectively. Samples are grouped together based on geographical region (see Fig. 4.2). Shaded area represents the most primitive samples from the Mingary region for inter-location comparison. NMORB (Sun & McDonough, 1989) plotted for comparison.

= 1.03 – 5.66), while the remainder of the samples, predominantly from Mingary Group, have slightly depleted to flat LREE ($La_N/Sm_N$ = 0.57 – 0.98). All the samples have relatively flat HREE profiles ($Gd_N/Yb_N$ = 0.7 – 1.58). Eu anomalies are variable (Eu/Eu* = 0.79 – 1.45). The Waukaloo samples have positive Eu anomalies (Eu/Eu* = 0.28 – 1.41), as do samples M11 and M12 of the Outalpa Group (Antro Gabbro; Eu/Eu* = 1.45 and 1.19, respectively). The remainder of the Outalpa sample have variably negative Eu anomalies (Eu/Eu* = 0.82 – 1.05).

### *4.4.5 Radiogenic isotopic composition*

Initial εNd values for the Montstephen Metabasalt samples were calculated at 1700 Ma, and the Lady Louise Suite samples at 1685 Ma (Conor 2000, 2004; Conor & Fanning, 2001). Sm/Nd ratios for the Monstephen Metabasalt samples are variable, ranging between 0.1051 – 0.1721 (Table 4.2). The variability in Sm/Nd ratios are also reflected by initial εNd values for the Montstephen Metabasalt samples, that range between -3.8 and 2.1 (Table 4.2).

Sm/Nd ratios of the Lady Louise Suite can broadly be divided into two groups. The majority of samples from the Mingary Group have Sm/Nd ratios ranging between 0.1858 –

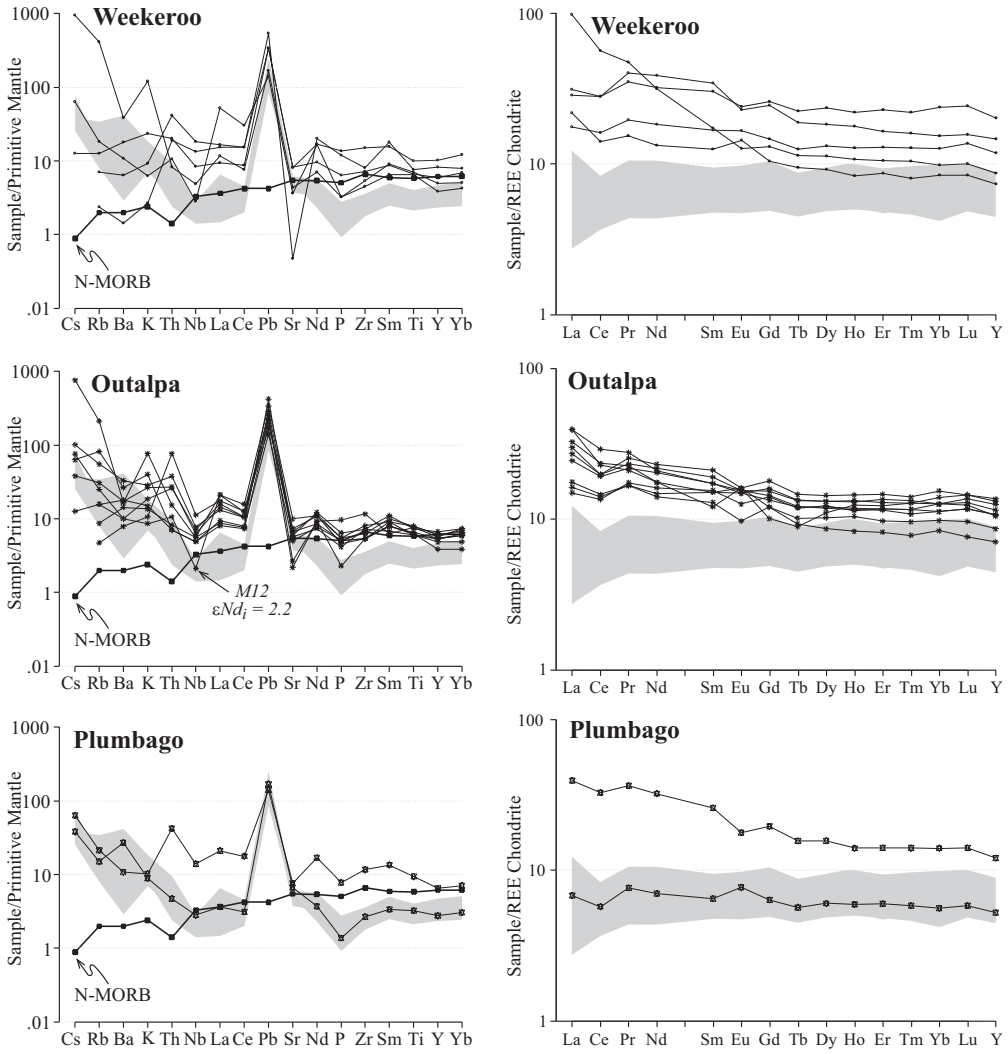


**Figure 4.6.** *Continued.*

0.2119, while the majority of the remainder of the Lady Louise Suite has Sm/Nd ratios between 0.1339 and 0.1852 (Table 4.2). The Mingary samples also generally have the higher $^{143}Nd/^{144}Nd$ values that the remainder of samples, ranging between 0.512545 to 0.512932 (Table 4.2). Initial εNd values for the Lady Louise Suite samples range between –2.2 and 2.7 (Table 4.2). Nd isotopic signatures of the Lady Louise Suite metabasites do not vary with differing degrees of fractionation (Fig. 4.7; $r$ = -0.005).

## 4.5 Source region characterisation and tectonic setting

Trace elements used for tectonic discrimination are the immobile HFSE and REE, as these have distinctively different concentrations in different tectonic settings (e.g. Floyd & Winchester, 1978; Meschede, 1986; Cabanis & Lécolle, 1989). The Nbx2 – Zr/4 – Y ternary diagram (Fig. 4.8a) distinguishes between normal MORB (N-MORB) and enriched MORB (E-MORB) sources (Meschede, 1986). With the exception of samples M06 (E-MORB field), M07 and M11 (combined intraplate tholeiite and volcanic arc basalt fields), the remainder of the samples plot in the combined N-MORB and volcanic arc basalt field (Fig. 4.8a). To more accurately discriminate between arc basalts and MORB series basalts, the Y/15 – La/10 – Nb/8 ternary discrimination diagram

**Table 4.2.** Radiogenic isotope data.

| Sample | Region | Age | Nd (ppm) | Sm (ppm) | $^{147}Sm/^{144}Nd$ | $^{143}Nd/^{144}Nd$ | $2\sigma^1$ | $\varepsilon Nd_0$ | $\varepsilon Nd_i$ |
|---|---|---|---|---|---|---|---|---|---|
| M01 | Weekeroo | 1700 | 10.0 | 2.8 | 0.1674 | 0.512420 | 11 | -4.2 | 2.1 |
| M02 | Weekeroo | 1700 | 21.5 | 3.7 | 0.1051 | 0.511492 | 9 | -22.4 | -2.4 |
| M03 | Weekeroo | 1700 | 21.9 | 6.2 | 0.1725 | 0.512429 | 10 | -4.1 | 1.2 |
| M04 | Weekeroo | 1700 | 12.4 | 3.5 | 0.1721 | 0.512457 | 10 | -3.5 | 1.8 |
| M06 | Weekeroo | 1700 | 25.2 | 7.0 | 0.1686 | 0.512134 | 9 | -9.8 | -3.8 |
| M07 | Plumbago | 1685 | 21.2 | 5.2 | 0.1488 | 0.511998 | 8 | -12.5 | -2.2 |
| M08 | Plumbago | 1685 | 4.9 | 1.5 | 0.1886 | 0.512679 | 10 | 0.8 | 2.6 |
| M11 | Outalpa | 1685 | 11.4 | 2.5 | 0.1339 | 0.511888 | 10 | -14.6 | -1.1 |
| M12 | Outalpa | 1685 | 12.0 | 3.1 | 0.1584 | 0.512326 | 9 | -6.1 | 2.2 |
| M13 | Waukaloo | 1685 | 8.7 | 2.7 | 0.1852 | 0.512652 | 10 | 0.3 | 2.7 |
| M14 | Waukaloo | 1685 | 11.1 | 3.1 | 0.1679 | 0.512366 | 9 | -5.3 | 0.9 |
| M15 | Outalpa | 1685 | 15.5 | 4.3 | 0.1680 | 0.512397 | 9 | -4.7 | 1.5 |
| M16 | Outalpa | 1685 | 15.3 | 3.7 | 0.1446 | 0.512046 | 10 | -11.5 | -0.3 |
| M17 | Outalpa | 1685 | 10.7 | 3.2 | 0.1817 | 0.512542 | 9 | -1.9 | 1.4 |
| M18 | Outalpa | 1685 | 14.0 | 3.8 | 0.1663 | 0.512372 | 9 | -5.2 | 1.4 |
| M19 | Outalpa | 1685 | 10.0 | 2.9 | 0.1754 | 0.512404 | 13 | -4.6 | 0.0 |
| M20 | Outalpa | 1685 | 10.2 | 3.1 | 0.1847 | 0.512569 | 9 | -1.3 | 1.2 |
| M21 | Outalpa | 1685 | 12.9 | 3.7 | 0.1726 | 0.512400 | 11 | -4.7 | 0.6 |
| M22 | Mingary | 1685 | 11.1 | 3.2 | 0.1743 | 0.512316 | 10 | -6.3 | -1.5 |
| M23 | Mingary | 1685 | 7.0 | 2.2 | 0.1866 | 0.512557 | 10 | -1.6 | 0.6 |
| M24 | Mingary | 1685 | 3.0 | 1.1 | 0.2119 | 0.512932 | 9 | 5.7 | 2.4 |
| M25 | Mingary | 1685 | 4.4 | 1.5 | 0.2020 | 0.512796 | 9 | 3.1 | 1.9 |
| M26 | Mingary | 1685 | 3.4 | 1.2 | 0.2103 | 0.512895 | 10 | 5.0 | 2.1 |
| M27 | Mingary | 1685 | 9.2 | 2.8 | 0.1858 | 0.512597 | 10 | -0.8 | 1.5 |
| M28 | Mingary | 1685 | 3.3 | 1.0 | 0.1884 | 0.512650 | 10 | 0.2 | 2.0 |
| M29 | Mingary | 1685 | 9.5 | 3.0 | 0.1890 | 0.512675 | 10 | 0.7 | 2.4 |
| M31 | Mundi | 1685 | 10.1 | 3.3 | 0.2005 | 0.512716 | 11 | 1.5 | 0.7 |
| M32 | Mundi | 1685 | 18.8 | 6.3 | 0.2040 | 0.512777 | 10 | 2.7 | 1.1 |
| M33 | Mingary | 1685 | 9.1 | 2.7 | 0.1764 | 0.512545 | 8 | -1.8 | 2.6 |

[1] Isotope error measurements are 2 S.E. $^{143}Nd/^{144}NdCHUR(0)=0.512638$, $^{147}Sm/^{144}NdCHUR=0.1967$.

of Cabanis & Lécolle (1989) is utilised (Fig. 4.8b). An additional advantage of this system is that it highlights potential contaminants from the continental crust, as contaminated samples plot closer to the La – Nb join on the ternary diagram. Of the southern Curnamona metabasites, the primitive samples from the Mingary Group ($\varepsilon Nd_i > 1.5$) in the western Broken Hill Domain are predominantly classified as back-arc basalts (BAB; Cabanis & Lécolle, 1989), with one sample plotting in the N-MORB field (sample M24), one sample in the arc tholeiite field (sample M23), and two samples in the transitional field between arc tholeiite and calc-alkaline (samples M22 and M33; Fig. 4.8b). The remainder of the samples from throughout the Olary Domain are slightly more enriched in the LREE and Nb relative to the primitive samples, and consequently plot almost entirely in the BAB field. Three samples also plot between the N-MORB and E-MORB fields (samples M03, M31, M32), with the remainder of the samples trending towards the transitional field (samples M14, M15, M18) to calc-alkaline field (samples M01, M02, M12, M16). Displacement towards the La – Nb join on the ternary diagram occurs for some of the Olary Domain samples (samples M07 and M11), whereas samples M01, M12 and M17 trend towards more La-rich, Y-depleted compositions.

As an additional assessment of the potential

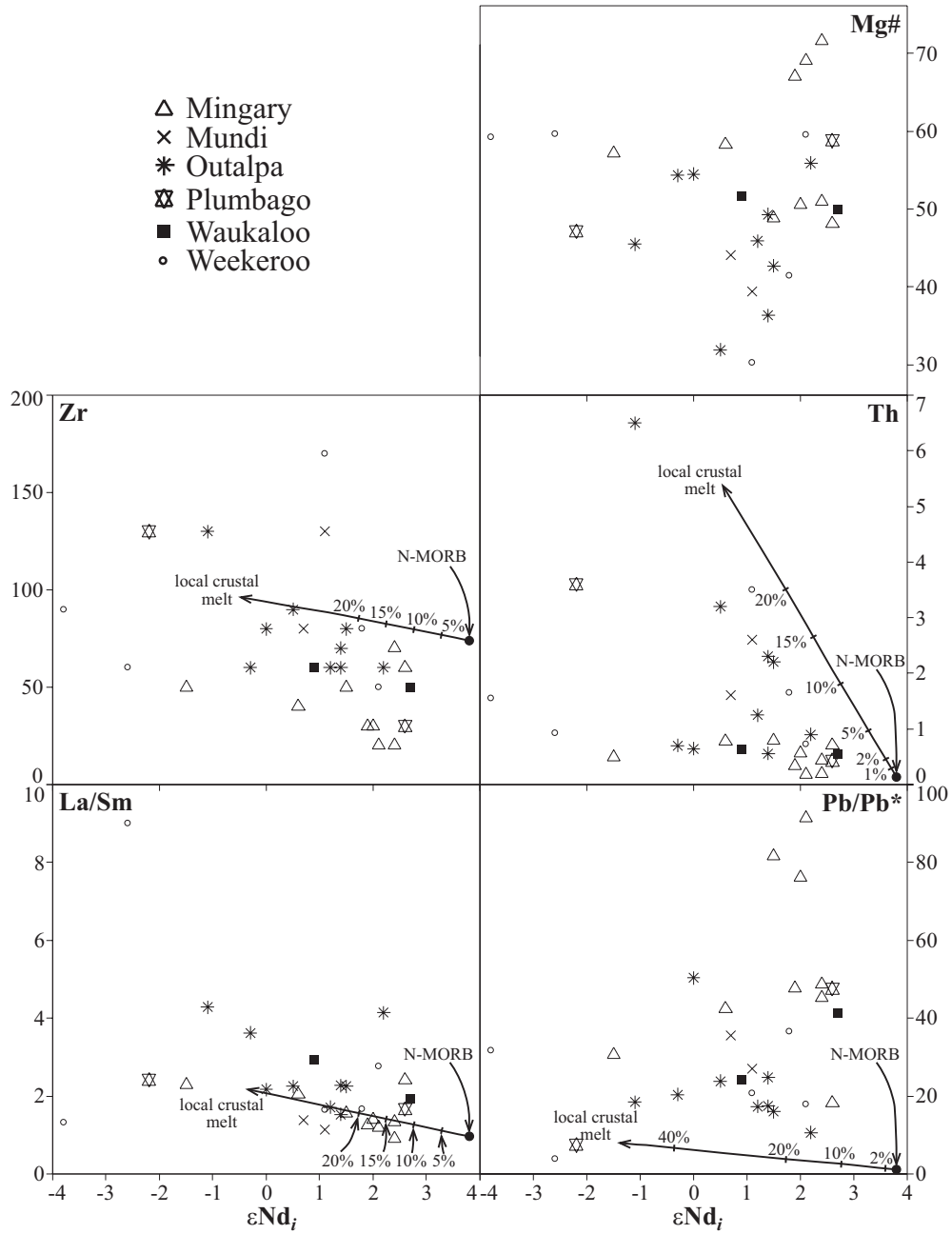


**Figure 4.7.** Zr, Mg#, $SiO_2$, Th, La/Sm and Pb/Pb* vs. initial εNd plot. There is no correlation between those elements partitioned into the crust with more negative εNd values, as expected with crustal contamination. Vectors show percentage assimilation of typical crustal melt to a NMORB source.

effects of crustal contamination, the Nb/Y – Zr/Y plot of Fitton et al. (1997) is utilised. Samples M07 and M11 plot between the lower crust and mid crust values, and are potentially contaminated. M01, M04, M12, M19, M21 and M31 plot between the E-MORB/N-MORB and lower crust points, with the remainder of the samples plotting in and around primitive mantle values.

## 4.6 Discussion

### *4.6.1 Generation of high-Fe tholeiitic melt*

High-Fe (>15 wt% $Fe_2O_3$) basalts are rare and apparently restricted to extensional tectonic settings (Sinton et al., 1983; James et al., 1987; Brooks et al., 1991). Factors that have been postulated to promote extreme Fe-enrichment during fractionation include the geochemical character of the source region, low $fO_2$ and

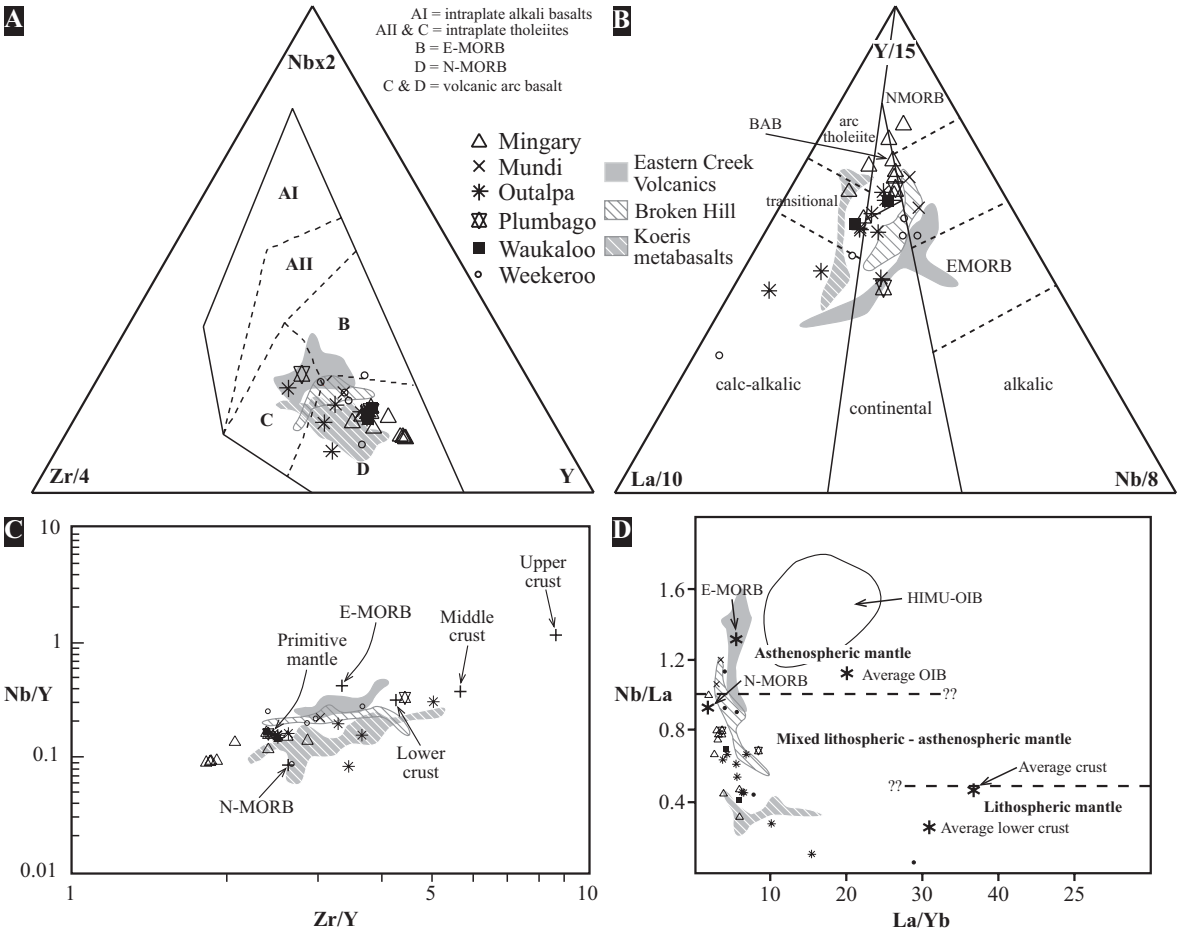


**Figure 4.8.** Tectonic discrimination diagrams. **(a)** Nbx2 – Zr/4 – Y ternary (Meschede, 1986); **(b)** Y/15 – La/10 – Nb/8 ternary (Cabanis & Lécolle, 1989); **(c)** Nb/Y – Zr/Y plot (Fitton et al., 1997); **(d)** Nb/La vs La/Yb plot (Abdel-Rahman, 2002). Fields for Eastern Creek Volcanics (Mt Isa), Broken Hill and Koeris metabasalts (Namaqualand) listed in Fig. 4.4.

the relatively high density of Fe-rich liquids (James et al., 1987; Brooks et al., 1991; Williams, 1998). Low $fO_2$ results in basaltic magmas being undersaturated with respect to magnetite and Fe-Ti oxides, therefore allowing Fe-enrichment in the most evolved fractionates (Osborn, 1959). Possible causes of low $fO_2$ is either a function of the source region of the magma, or the ambient conditions within the crustal magma chamber where differentiation takes place (Brooks et al., 1991).

Studies by Brooks & Nielsen (1978) on the Skaergaard intrusions show that Fe-rich liquids evolve from common MORB-type basalts that have undergone simple crystal fractionation in a closed or near-closed system that maintained a low $fO_2$. Sinton et al. (1983) reached a similar conclusion for Fe-rich mid-ocean ridge basalts, where the Fe-enrichment could only form when conditions of magma supply and cooling rates are favourable for closed system differentiation. Fractionation processes are further enhanced by the high density of high-Fe magmas, which suppress their ability to erupt (Brooks et al., 1991).

In the context of the metabasites of the SCP, the trend towards progressively Fe-rich fractionates in the Lady Louise suite was likely a function of low $fO_2$ in the source region or magma chamber, such that crystallisation and fractionation of Fe(-Ti) oxides was suppressed. Another requirement for the generation of high-Fe tholeiitic magmas is that fractionation must occur in a near closed system (Brooks

et al., 1991). As a further test that Fe-enrichment is due to magmatic processes, and not incorporation of Fe-rich contaminants into the evolving magma, the potential effects of crustal contamination are investigated below.

### *4.6.2 Assessing crustal contamination*

The requirement for near closed-system fractionation to achieve relatively Fe-rich magma compositions (e.g. Brooks & Nielsen, 1978; Sinton et al., 1983), excludes high degrees of crustal assimilation in the evolving magma. However basaltic melt en route to upper crustal levels may be crustally contaminated to some degree. This makes the task of discriminating an enriched versus depleted lithospheric mantle source region from a melt with even small degrees of crustal contamination difficult, as both will show similar geochemical characteristics, and evolved Nd isotopic signatures (e.g. Hergt, 2000, Hergt et al., 1989; Gallagher & Hawkesworth, 1994; Turner & Hawkesworth, 1995).

Depletion in HFSE relative to the LILE, and a trend towards lower Nd isotopic ratios are characteristics that often are linked to crustal contamination (e.g. Antonini et al., 1999; Antonini et al., 2000; Halama et al., 2004; Kryza & Pin, 2002). Due to the likelihood of LILE enrichment during alteration, this simple relationship cannot be used for the SCP metabasites. On the basis of immobile trace elements, significant crustal contamination of the evolving basaltic melt in the SCP is at odds with their predominantly low Zr (20 – 130 ppm) and Nb (1 – 10 ppm) concentrations, excluding the Montstephen Metabasalts, relative to average crust (210 ppm and 13 ppm, respectively). This is further supported by Zr/Y values of the majority of the SCP metabasites, which plot below mid to lower crustal values (with the exception of samples M07 and M11; Fig. 4.8c). Samples that have Nb/Y and Zr/Y values approaching that of lower crustal values have relatively primitive $\varepsilon Nd_i$ values (M01 = 2.1, M03 = 1.1, M04 = 1.8, M12 = 2.2, M19 = 0, M21 = 0.5, M29 = 2.4), discounting large degrees of crustal contamination. Consequently, relatively high HFSE concentrations in the SCP metabasites are more likely to reflect those of the source region.

The most likely composition of a contaminant to the evolving basaltic magma in the SCP is locally derived felsic melt (Stewart & Foden, 2001; Barovich & Foden, 2002). The effects of simple end-member mixing between a local felsic melt with a N-MORB source had been modelled in Fig. 4.7. Initial $\varepsilon Nd_i$ values for the SCP metabasites are plotted against several elements and ratios that are indicative of crustal contamination ($\varepsilon Nd_i$ value for N-MORB taken to be represented by depleted mantle at 1685 Ma = 3.8). Clearly, simple mixing between N-MORB and a felsic melt cannot account for the differentiating trends of the southern Curnamona metabasites, particularly with respect to Zr and Th, which require a much less differentiated contaminant to account for the mixing trend. Of the elements that are preferentially concentrated into the crust, such as Pb, $SiO_2$, LREE and Th, there is no obvious correlation between these elements and more evolved $\varepsilon Nd_i$ values (Fig. 4.7). This is highlighted by how $Pb_N/Pb_N$* values of the

most evolved metabasites approach those of the felsic melt values and Willyama Supergroup metasediments ($Pb_N/Pb_N^*$ = 0 – 20; Pb* = interpolated concentration of Pb with respect to La and Nd in primitive mantle normalised pattern). Greater than 40% mixing of felsic melt is required to achieve the lead enrichment observed in the SCP metabasite suite, which can not have occurred given the concentrations of $SiO_2$ and Th that would be expected at similar levels of contamination (Fig. 4.7). This strongly implies that the geochemical character of the southern Curnamona metabasites was inherited from the source region. Potential sources that could account for these characteristics are discussed below.

### *4.6.3 Magmatic differentiation*

Within the Lady Louise Suite, general trends in $TiO_2$, CaO, $Fe_2O_3$*, and to a lesser degree $P_2O_5$, against Mg# (Fig. 4.3) and Zr (not shown), display a near-continuous series typical of that generated by fractional crystallisation processes, with olivine and pyroxene being the dominant crystallising phases. These interpretations are in part supported by trace element patterns (Ni, Cr, V; Fig. 4.5). Apatite, Fe-Ti oxides and plagioclase were not significant crystallising phases, as indicated by an increase in $P_2O_5$ and $TiO_2$ with fractionation, and no variation in $Al_2O_3$. Only the more evolved samples at Outalpa have consistent negative Eu anomalies, and may be suggestive of late-stage plagioclase fractionation.

Despite the overall scatter, major element and trace element trends between and within groups in the Olary Domain likely represent differentiation trends that reflect converging magmatic histories between the regions with respect to similar source region, extraction and crystallisation paths. Progressive crystallisation of clinopyroxene and olivine resulted in the generation of more Fe-rich differentiates (up to ~18 wt% $Fe_2O_3$), as exemplified in the Outalpa group (Fig. 4.3).

The most Mg-rich, relatively undifferentiated, generally isotopically primitive and geochemically depleted samples are predominantly from the western Broken Hill Domain (Mingary Group). The Mingary Group consistently plots separately from the other groups from the Olary Domain in all figures, and likely underwent a distinct magmatic evolution to that of the Olary Domain groups. Consequently, the unevolved and primitive metabasites of the Mingary Group are interpreted to have formed by higher degrees of partial melting of a depleted mantle source, relative to the more evolved and enriched metabasites of the Olary Domain.

### *4.6.4 Constraints on source region composition*

Since crustal contamination does not appear to be a major factor in the magmatic evolution of the SCP metabasites, the generation of geochemically enriched basaltic magmatism elsewhere has been interpreted to develop by: 1) infiltration of small partial melt fractions from underlying asthenosphere; 2) incorporating small amounts of sediment into the source region through subduction processes; 3) mantle metasomatism by relatively LILE- and HFSE-enriched fluids,

potentially slab-derived; or 4) melts being derived from a fossil or active subducting slab (e.g. Hergt et al., 1989; McKenzie, 1989; Zhao & McCulloch, 1993; Zhao, 1994; Turner & Hawkesworth, 1995).

Within the Australian Proterozoic context, Zhao & McCulloch (1993) and Zhao (1994) argued that the geochemical signature of continental tholeiites in central Australia were formed by partial melting of the continental lithospheric mantle, which was modified by subduction processes during major crust-formation events in the region. An implication of the studies of Zhao & McCulloch (1993) and Zhao (1994) is that a Palaeoproterozoic convergent margin existed south of the NAC, and subduction-related processes re-fertilised the continental lithospheric mantle in the over-riding plate, which subsequently produced geochemically-enriched, and relatively isotopically depleted melts during partial melting.

A similar scenario as proposed by Zhao & McCulloch (1993) and Zhao (1994) is favoured to explain the geochemical characteristics of the metabasites from the Olary Domain in the SCP. This is because the geochemical and Nd isotopic differences between the Broken Hill Domain metabasites (N-MORB: depleted mantle) and the Olary Domain metabasites (N-MORB – E-MORB – BAB: depleted to enriched mantle; Fig. 4.8) cannot be entirely attributed to be the result of only magmatic processes or crustal contamination. They therefore must reflect geochemical and isotopic heterogeneity in the source region. Heterogeneity in the continental lithospheric mantle from which the Olary Domain mafic magmas were derived is exemplified by the La/Sm vs $\varepsilon Nd_i$ plot (Fig. 4.7). Variations in La/Sm (1.7 – 4.1) for the relatively isotopically primitive samples from the Olary Domain ($\varepsilon Nd_i > 2$; M01, M08, M12, M13) can not be explained by differing degrees of crustal contamination, and therefore is interpreted to reflect source region compositions.

A mixed asthenospheric – lithospheric source region across the SCP is further supported by the Nb/La vs La/Yb plot (Fig. 4.8d). As an asthenospheric source seems unlikely to explain the geochemical enrichment of the Olary Domain samples, and the depleted mantle-like geochemical signature of the Mingary Group, it is proposed that the geochemically anomalous source region to the Olary Domain metabasites was caused by re-fertilisation of the continental lithospheric mantle by a subduction related component. Supporting evidence of this interpretation is indicated by the Outalpa samples, which have Nb depletions and relatively isotopically primitive compositions (e.g. sample M12: $\varepsilon Nd_i = 2.2$; Fig. 4.6). It can only be speculated whether the subduction component added to the continental lithospheric mantle was subducted sediment or fluids derived from the subducting slab. The relatively high Th contents of the metabasites may signify enriched sediments were incorporated into the source region, although this is speculative.

### *4.6.5 Proterozoic tectonic implications*

It is proposed that a subduction-related component was added to the continental lithospheric mantle prior to deposition of the Willyama Supergroup. This interpretation is

in part supported by tectonic reconstruction models of eastern Proterozoic Australia that propose a convergent margin existed along the southern margin of the NAC during mid-Palaeoproterozoic (Fig. 4.1b; Zhao, 1994; Giles et al., 2002; Betts et al., 2002). Giles et al. (2002, 2004) proposed that a convergent margin was active between ~1.8 and 1.6 Ga along the southern margin of Proterozoic eastern Australia, during which time it migrated southward. Potentially, any subduction-related, geochemically enriched component detected in the Curnamona metabasites could have been incorporated into the lithospheric mantle anytime during this time interval.

Differences observed between the trace element geochemistry of metabasites of the Broken Hill Domain relative to those in the Olary Domain are interpreted to reflect source region heterogeneities (Fig. 4.8). This may signify a fundamental difference in the lithosphere between the two regions, which had a first order-control on the composition of magma derived from the two regions upon partial melting. It is speculated that the two geochemically and isotopically distinct lithospheric fragments amalgamated during the early to mid Palaeoproterozoic. Amalgamation of the two fragments was likely facilitated by accretionary processes, which caused re-fertilisation of the Olary Domain continental lithospheric mantle. The currently accepted position of the SCP domain boundary (Fig. 4.1a) may represent an upper expression of the suture between the two lithospheric fragments, and consequently the suture had fundamental controls on the Willyama basin evolution during the late-Palaeoproterozoic and early-Mesoproterozoic.

### *4.6.6 Proterozoic comparisons*

Fe-rich tholeiitic magmatism during the Palaeoproterozoic was not only confined to the Olary Domain. Basic gneisses in the Broken Hill region (James et al., 1987), the Eastern Creek Volcanics in the Mt Isa Inlier (~1780 Ma; Wilson et al., 1985; Williams, 1998; Scott et al., 2000), and the Koeris metabasalts from Namaqualand (~1650 ± 100 Ma; Reid et al., 1987), are a similar occurrence of strongly differentiated high-Mg and high-Fe tholeiitic magmatism (Fig. 4.4a). However, the Eastern Creek Volcanics are slightly more alkaline-rich relative to the SCP metabasites, whereas the Broken Hill basic gneiss and Koeris metabasites have slightly more intermediate compositions (Fig. 4.4b). All these regions have $Fe_2O_3$* contents in excess of ~17 wt%.

Source characterisation and tectonic discrimination diagrams also highlight some similarities between tholeiitic magmatism in the aforementioned regions and those in this study (Fig. 4.8). The Eastern Creek Volcanics have compositions more representative of E-MORB to volcanic-arc basalts, whereas the Koeris metabasalts have compositions that are suggestive of re-enriched lithospheric mantle (Fig. 4.8; Reid et al., 1987).

Although the Eastern Creek Volcanics are ~80 – 100 million years older than the metabasites of this study, and the Koeris metabasalts ~30 million years younger, it is apparent that similar magmatic processes were likely operating in the two regions, resulting in the formation of the high-Fe tholeiites. Furthermore, with the exception of the Eastern

Creek Volcanics that are apparently derived from the asthenosphere (Fig. 4.8), the Koeris metabasalts can also be interpreted to be derived from a re-fertilised lithospheric mantle (Fig. 4.8; Reid et al., 1987). Similar to interpretations of a subduction-related component affecting the lithospheric mantle of the Olary Domain, Reid et al. (1987) suggests the source region to the Koeris metabasalts also experienced geochemical modification, potentially through subduction-related metasomatism.

## 4.7 Conclusions

Mafic magmatism at ~1685 Ma in the SCP is interpreted to be sourced from a heterogeneous lithospheric mantle, with both isotopically depleted, LREE depleted and isotopically enriched, LREE enriched components. Near-closed system fractionation generated high-Fe tholeiitic. Low $fO_2$ hindered Fe(-Ti) oxide crystallisation such that progressively Fe-rich fractionates were generated. The low degree of crustal contamination implied by the generation of Fe-rich tholeiites indicates that geochemical and isotopic heterogeneities observed in the SCP metabasites reflect source region heterogeneities.

The favoured explanation for regional differences in the lithospheric mantle in the SCP is through the incorporation of subduction-related components into the source region. Similar explanations have been suggested for geochemically enriched and isotopically depleted tholeiites elsewhere where crustal contamination does not adequately explain the geochemical characteristics of the mafic magmatism (e.g. Reid et al., 1987; Hergt et al., 1989; Zhao, 1994; Zhao & McCulloch, 1993; Hergt, 2000; Iacumin, et al. 2003). Greater degrees of lithospheric thinning in the Broken Hill Domain relative to the Broken Hill Domain resulted in more depleted and primitive melts being generated within the Broken Hill Domain. Lesser degrees of lithospheric thinning in the Olary Domain allowed a greater proportion of enriched lithospheric to be incorporated into the partial melt.

# Chapter 5
# MESOPROTEROZOIC ALKALINE MAGMATISM

***SUMMARY***

*The Billeroo alkaline magmatic complex is comprised of a series of feldspathic ijolite (feldspathoid-pyroxene-feldspar rocks), syenite and lamprophyric dyke phases. Field relations imply the ijolite phases intruded first, followed by the syenite phases, and then the cross-cutting lamprophyric dykes. Intrusion of the syenite phases occurred in association with hydraulic fracturing and brecciation of the surrounding metasediments. Deformational fabrics preserved within brecciated metasedimentary clasts, and the $D_3$ fabric developed in the different magmatic phases and surrounding country rock, constrain the ages of alkaline magmatism to between ~1610 – 1550 Ma (Olarian Orogeny). The alkaline magmatic phases are high in alkalis ($K_2O+Na_2O$=9-13 wt.%), $Al_2O_3$ (15-22 wt.%) and $TiO_2$ (1.2-2.4 wt.%), have moderately high MgO (0.2-3.4 wt.%), $P_2O_5$ (0.1-1.2 wt.%) and $Fe_2O_3$* (8.1-11.6 wt.%), with variable CaO (1.6-7.3 wt.%), and low $SiO_2$ (44-59 wt.%). The ijolite and lamprophyric dyke phases display a fractionation trend defined by decreasing $Na_2O$, CaO, MgO and $P_2O_5$ with increasing $SiO_2$, reflecting crystallisation of feldspathoids, pyroxene, plagioclase and phlogopite. Syenite phases show highly variable $Na_2O$, $K_2O$, CaO and MnO with little variation in $SiO_2$, defining a distinct differentiation trend to that of the ijolites and lamprophyres. Differentiation of the syenite phases was primarily controlled by K-feldspar crystallisation. All phases are light REE and LILE enriched. The ijolite phases are also enriched in Pb, Ti and P. The syenite phases are most enriched in LILE (Rb, Ba, K) and HFSE (Nb, Zr, Th, Pb), have variable REE abundances and positive Eu anomalies, and are enriched in the HREE with respect to MREE. Late-stage cross-cutting lamprophyric dykes have lesser abundances of LILE, variable HFSE and REE abundances, positive Eu anomalies and variable enrichment in HREE relative to MREE. Initial εNd values of the different phases range between –0.3 and 2.8, with the syenite phases having the most primitive isotopic signatures. The feldspathic ijolites and lamprophyre dykes preserve the most primitive Sr isotopic compositions ($^{87}Sr/^{86}Sr$ = 0.7089 – 0.7101). Major-element, trace-element and Nd isotope characteristics of the Billeroo magmatic complex are interpreted to reflect the fractionation of a low-degree partial melt derived from the SCLM. The partial melt inherited the heterogeneous character of the SCLM, producing varying degrees of LREE- and HFSE-enriched melt fractions. It is speculated that the SCLM source region inherited its geochemical enrichment through regional-scale mantle metasomatism. The intrusion of the Billeroo alkaline magmatic phases was contemporaneous with bimodal magmatism and crustal anatexis in the western Olary Domain. This demonstrates that lithospheric thinning occurred after a period of crustal thickening associated with the Olarian Orogeny, and may have been a major factor in generating high-T, low-P metamorphism that characterises the Olarian Orogeny.*

## 5.1 Introduction

Occurrences of alkaline magmatism are important in that they can potentially record lithospheric evolution through time, as they are often closely associated with carbonatitic melts that are indisputably sourced from the mantle (e.g. Bell, 1998; Harmer, 1999; Sørenson, 1974; Woolley, 2001; Zhang et al., 2005). Lithospheric thinning and associated intracontinental rift systems have been highlighted as favourable tectonic settings for the generation of carbonatites and alkaline magmatism (e.g. East Africa rift system: Woolley et al., 1995; Kabeto et al., 2001; Clement et al., 2003). Carbonatites and alkaline magmatic occurrences are also found in oceanic settings and collision-type tectonic settings, although the occurrence in these setting are far fewer than in rift systems (Bell, 1998).

Deciphering exactly what alkaline magmatism tells us about the mantle has been a topic of much controversy due to uncertainty surrounding whether alkaline magmatic rocks were sourced entirely from the mantle, or represent the mixing of a mantle-derived melt with altered lower crustal rocks (e.g. Kramm, 1994; Simonetti & Bell, 1994; Bell, 1998; Harmer, 1999). Geochemical and isotopic studies are important when trying to assess the relative contributions of mantle and lower crustal components (Bell, 1998). Radiogenic isotopic studies are crucial in any interpretation, given that they have the ability to provide information on proportions of source input.

A key question in relation to the generation of alkaline magmas is how they can become enriched in alkalis, high field strength elements (HFSE) and trace elements from a mantle

source that is otherwise generally regarded to be depleted in such elements. Some processes that have been proposed to produce such enrichment include large-scale, regional mantle metasomatism (Morris & Pasteris, 1987; Woolley, 1987); assimilation of enriched lower crustal material (Sørenson, 1974); and continent-continent convergence that potentially could push pre-existing alkaline magmatic complexes to the base of the crust and become the source region of subsequent alkaline magmatic systems (Burke et al., 2003). The incorporation of juvenile and enriched material into the subcontinental lithospheric mantle (SCLM) along a convergent margin could also produce such anomalous enrichment of the SCLM (Zhao et al., 1994; Zhao & McCulloch, 1995; Wade et al., 2006; Zhang et al., 2005).

Although occurrences of alkaline magmatism are dominantly found within continental rift environments (e.g. Gardar Province, Pearce & Leng, 1996), they are documented to occur in nearly all tectonic settings with the exception of mid-ocean ridges. Alkaline magmatism has been associated with extension after compressional tectonics and amphibolite-facies metamorphism (e.g. Southern Victoria Land, Worley et al., 1995); within apparently stable continental regions (e,g, Kola Peninsula, Verhulst et al., 2000); during basin development on a stable platform (e.g. Paraná Basin, Morbidelli et al., 1995); and during reactivation of crustal-scale lineaments (e.g. Turiy Peninsula, Ivanikov et al., 1998).

Occurrences of Proterozoic alkaline magmatism are apparently less common than during the Phanerozoic (Blichert-Toft et al., 1996). The paucity of alkaline magmatic rocks in the Proterozoic relative to the Phanerozoic is thought to be due to several factors, including: (1) the vulnerability of alkaline rocks to chemical effects of secondary processes; (2) the preferential destruction of terrains conducive to hosting alkaline magmatism (e.g. rift-systems); and (3) possibly secular changes in the conditions of the mantle such that it was not conducive to alkaline magma generation in the Proterozoic (Blichert-Toft et al., 1996). Occurrences of alkaline magmatism provinces within the Australian Proterozoic are rare. Late Mesoproterozoic (1150 Ma) alkaline magmatic rocks have been reported from the Mordor Complex, central Australia (Langworthy & Black, 1978; Nelson et al., 1989). Isolated occurrences of carbonatite include the Neoproterozoic (730 Ma) Mud Tank Carbonatite in the Strangways Range, central Australia (Crohn & Moore, 1984); the Mount Weld Carbonatite in the Archaean Yilgarn Craton of Western Australia (Duncan & Willettt, 1990); and Cummins Range Carbonatite of the Archaean Pilbara Craton, Western Australia (Andrew, 1990).

In Proterozoic Australia, the southern Curnamona Province (SCP) is one of the few regions that contain alkaline magmatic rocks. Bell et al. (1979) identified nepheline syenites, ijolites, metasomatised volcanics and breccias in the Billeroo region in the northern Olary Domain (Fig. 5.1). The Billeroo alkaline magmatic complex typifies the great variability in petrology and geochemistry that characterises silica-undersaturated alkaline magmatism (e.g. Morbidelli et al., 1995; Woolley et al., 1995; Bell, 1998; Harmer,

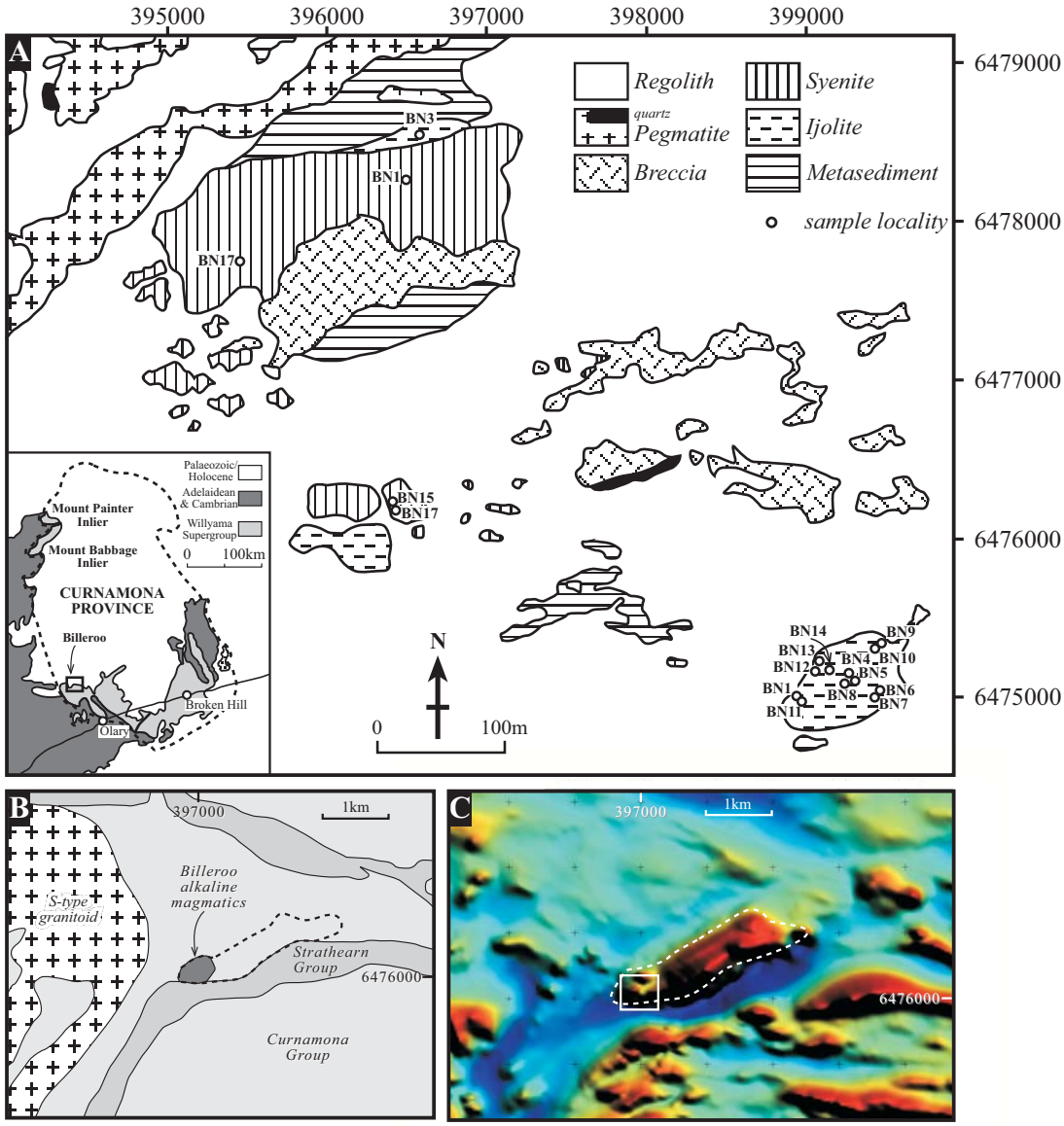


**Figure 5.1.** (a) Distribution of different magmatic phases, surrounding country rock, and sample localities of the Billeroo alkaline magmatic complex (Datum: GDA94); (b) Interpreted solid geology of Billeroo alkaline magmatic complex region (Jenkins & Burtt, 2003). Dashed line represents interpreted under cover extension of the intrusive body; (c) TMI image of Billeroo alkaline magmatic complex region (Jenkins & Burtt, 2003). Dashed line represents interpreted under cover extension of the intrusive body. Boxed area represents outcrop region.

1999).

In this chapter, the petrology, mineral chemistry, whole-rock geochemistry and Nd-Sr isotopic characteristics of the Billeroo alkaline magmatic complex are documented. The information will be used to evaluate the petrogenesis of this event in order to constrain possible source component in the SCLM at the time of intrusion. The timing of magmatism is constrained by field and petrological observations. The significance of this alkaline magmatic complex within the Proterozoic tectonothermal evolution of SCP is evaluated.

## 5.2 Intrusive relationships between magmatic phases and country rock

The Billeroo alkaline magmatic complex is located ~60km northwest of Olary, South Australia (Fig. 5.1a). Alkaline magmatic phases intrude the Ethiudna Subgroup near the contact between the Curnamona Group and Strathearn

Group (Fig. 5.1b). The complex consists of a series of layered feldspathic ijolites (true "ijolites" are nepheline-pyroxene rocks without modal feldspar; Harmer, 1999), massive syenite bodies (K-feldspar phenocrysts and porphyries), and alkali lamprophyre dykes. An extensive brecciated metasedimentary rock mass and minor occurrences of pegmatite and quartz are also associated with the alkaline magmatic rocks (Fig. 5.1a). The complex occupies limited outcrop (~1km$^2$), but geophysical data suggests that the complex may have a two dimensional extent of more than 5 km$^2$ (Fig. 5.1c).

The main feldspathic ijolite body occurs in the southeast of the complex (Fig. 5.1a). It has a dark-grey blotchy layered appearance with a well-formed NE-trending tectonic fabric (Fig. 5.2a). This fabric is oriented parallel to the regional $D_3$ fabric that is interpreted to have developed during the waning stages of the Olarian Orogeny (~1585 – 1550 Ma; *Chapter 3*; Berry et al., 1984). Fine- and medium-grained aggregates of felsic and mafic minerals define the fabric. At least three alkali lamprophyre dyke sets crosscut the feldspathic ijolites. The majority of dykes are dark in appearance, ranging in width between ~2 and 10 cm (Fig. 5.2b). One of the dyke sets has a similar appearance to the massive syenite body to the northwest (Fig. 5.1a), and contains weakly aligned K-feldspar phenocrysts within a fine-grained matrix (Fig. 5.2c).

The syenite phases outcrop as several discrete bodies, and constitute the dominant lithology of the complex (Fig. 5.1a). Syenite phases are varied in appearance, occurring as coarse-grained, medium-grained and porphyritic varieties. The main syenite body is less deformed than the feldspathic ijolites, likely a function of strain partitioning around the massive syenite bodies. K-feldspar phenocrysts are randomly oriented in the majority of the syenite bodies (Fig. 5.2d), but are weakly aligned at the margins of the bodies. Consequently the syenite bodies appear to have acted as mega-boudins, resulting in the strain being partitioned into the surrounding rocks.

Relationships between the feldspathic ijolites and syenites are ambiguous, as the two are never observed in direct contact. However, interpretations can be made about the intrusive history based on other observations of the different phases. The syenitic dyke that crosscuts the main ijolite body implies that the syenite was emplaced after the ijolite. Other lamprophyric dykes that crosscut the ijolites indicate that other alkaline magmatic phases intruded contemporaneously with the syenite. The syenite is brecciated in parts, and intermingled with clasts of foliated Willyama Supergroup metasediments. Syenitic dykes locally crosscut the breccia, and have been further reworked and brecciated (Fig. 5.2e). In places, the breccia is supported by a felsic matrix of syenitic affinity. Elsewhere, the breccia is annealed by patchy carbonate-rich zones that contain coarse-grained crystals (<5 cm) of calcite. The observed relationship between the syenite and breccia implies emplacement of the syenite was facilitated by brecciation of the metasedimentary sequence.

The breccia body also has a weak NE-rending fabric of the same generation and parallel to that observed in the feldspathic

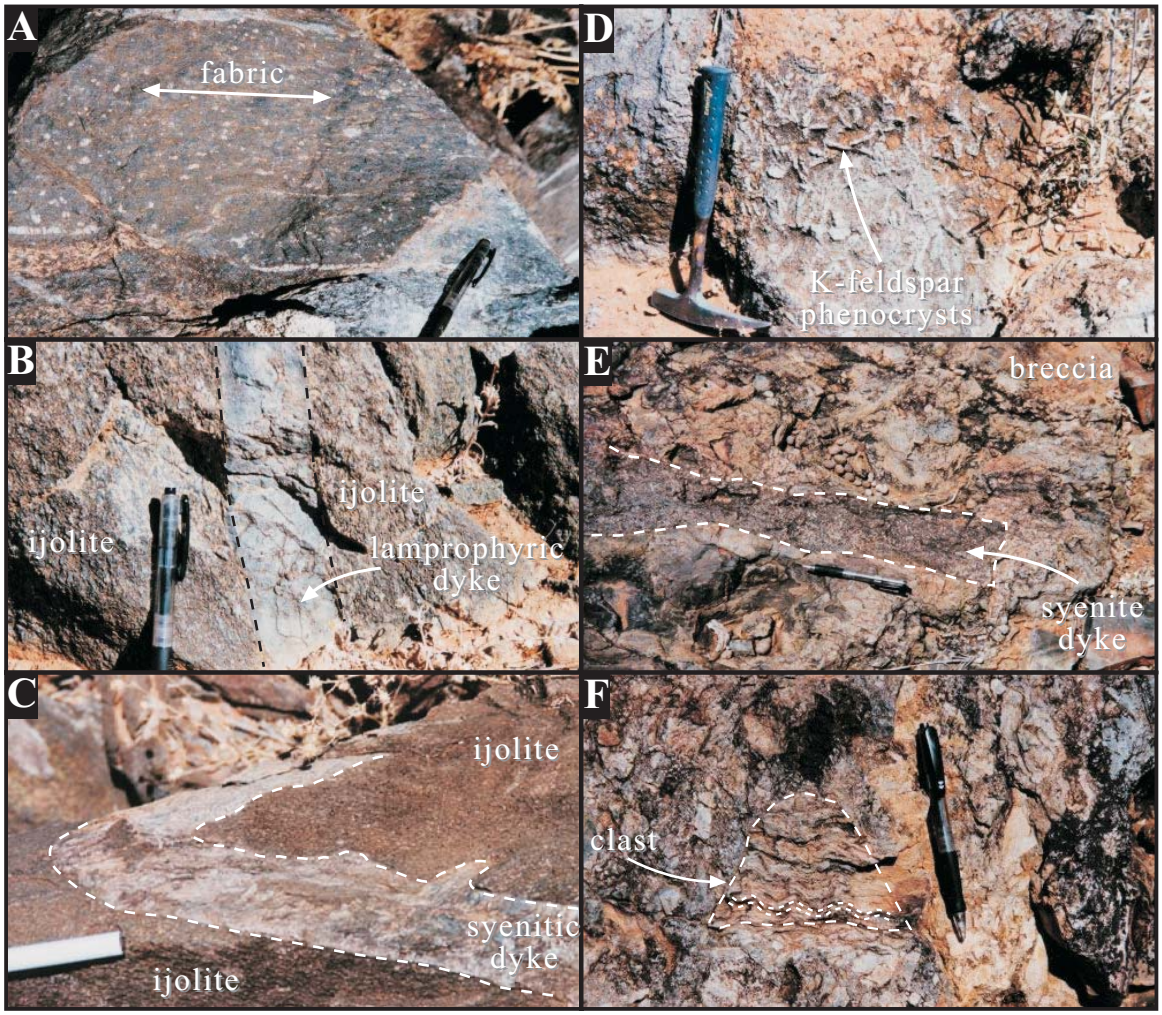


**Figure 5.2.** (a) Ijolite outcrop with pervasive northeast trending fabric. Light coloured patches and streaks are aggregates of plagioclase, nepheline and cancrinite. Darker areas are pyroxene, phlogopite, titanite and oxides; (b) Lamprophyric dyke (outlined) crosscutting main ijolite outcrop; (c) Syenitic dyke (outlined) crosscutting ijolite, (d) Syenite outcrop with randomly orientated K-feldspar phenocrysts; (d) Outcrop of brecciated syenite dyke (outlined) within massive breccia; (f) Outcrop of massive breccia with crenulated Willyama Supergroup metasedimentary clast (outlined).

ijolites ($D_3$). Crenulated clasts of Willyama Supergroup metasediments (<10 cm) are entrained in the brecciated mass (Fig. 5.2f). The regional fabric has crenulated the layer parallel fabric within the breccia clasts, and therefore is a key constraint on the timing of emplacement of the magmatic complex. Based on the development of the regional $D_3$ fabric in parts of the magmatic complex, the Billeroo alkaline magmatic event could not have occurred later than ~1585 – 1550 Ma (*Chapter 3*). The maximum age of intrusion is constrained by the timing of development of the layer parallel fabric in the Willyama Supergroup metasedimentary clasts within the breccia. Metamorphism and the earliest formed fabrics in the SCP occurred no earlier than ~1610 Ma (*Chapter 3*; Page et al., 2000, 2003). Therefore the maximum intrusive age of the Billeroo alkaline magmatic complex is ~1610 Ma. This implies that alkaline magmatism in the Olary Domain occurred between ~1610 – 1550 Ma, and is therefore coincident with the Olarian Orogeny.

## 5.3 Analytical methods

Twenty-two samples were analysed for major and trace elements. Representative samples

of the different alkaline magmatic phases were also analysed for Sm-Nd isotopic compositions. The sample preparation technique and analytical procedure are the same as those outlined in the mafic magmatic study (*Chapter 4*). Mineral compositions were obtained using the same instrumentation as in *Chapter 3*, however the operating conditions were 15kV, 20nA. Standards used in microprobe analysis were a combination of natural and synthetic materials.

## 5.4 Petrography and mineralogy

For the purpose of this study, only the alkaline variants of the Billeroo magmatic complex were analysed. These include feldspathic ijolite phases, potassic syenite phases and lamprophyric dykes. Locations and detailed sample descriptions are listed in *Appendix 5*. The degree of metamorphism and alteration known to have occurred in this part of the Olary Domain (sillimanite-grade; Webb & Crooks, 2003) is taken into account when evaluating the petrogenesis of the complex.

### *5.4.1 Feldspathic ijolite series*

The feldspathic ijolites have great textural and mineralogical variation. Heterogeneity in these types of rocks is not uncommon (e.g. Woolley et al., 1995; Harmer, 1999). These magmatic phases have been recrystallised to have a schistose to mylonitic fabric, with fine- to medium-grained mineral bands defining a prominent tectonic layering (Fig 5.3a). Mineralogical variations in the feldspathic ijolites are primarily related to differing proportions of nepheline in a matrix of cancrinite and albite. Bands of biotite and muscovite define the foliation. K-feldspar, epidote, clinopyroxene, garnet, titanite and magnetite are all common (Fig. 5.3b). Magnetite often encloses the titanite in stringer-like clots. Minor phases include apatite, ilmenite, sodalite, analcite and calcite. Small veins of calcite crosscut the tectonic fabric and are interpreted to be of metamorphic origin. Cancrinite appears to be primary, although some of it likely formed through magmatic reaction between nepheline and K-feldspar (Deer et al., 1992). Such a reaction is indicative of an evolving alkaline magma series in which cancrinite forms by the reaction between nepheline and $CO_2$-rich residual liquids (Henderson & Gibb, 1983).

Most of the primary pyroxene is pseudomorphed by a garnet-phlogopite-epidote assemblage (Fig. 5.3c). However, primary magmatic zoning is still evident in some of the pyroxenes, and in the arrangement of the pseudomorphs. Highly altered ijolite contains abundant epidote, and fine-grained albite that is enclosed by prismatic albite. These mineral aggregates likely represent pseudomorphs after primary sodic pyroxene. Coarse-grained albite is also present, and encloses fine-grained albite forming pseudomorphs after pyroxene. Other metasomatised ijolites consist essentially of albite and cancrinite. Na-metasomatism has been intense, with late-stage development of albite that completely replaces and envelops pyroxene. Textures suggest albite areas in the bands of cancrinite were originally occupied by nepheline. The mobility of Si and Al at subsolidus temperatures can result in the conversion of nepheline to albite (e.g. Dollase & Thomas, 1978).

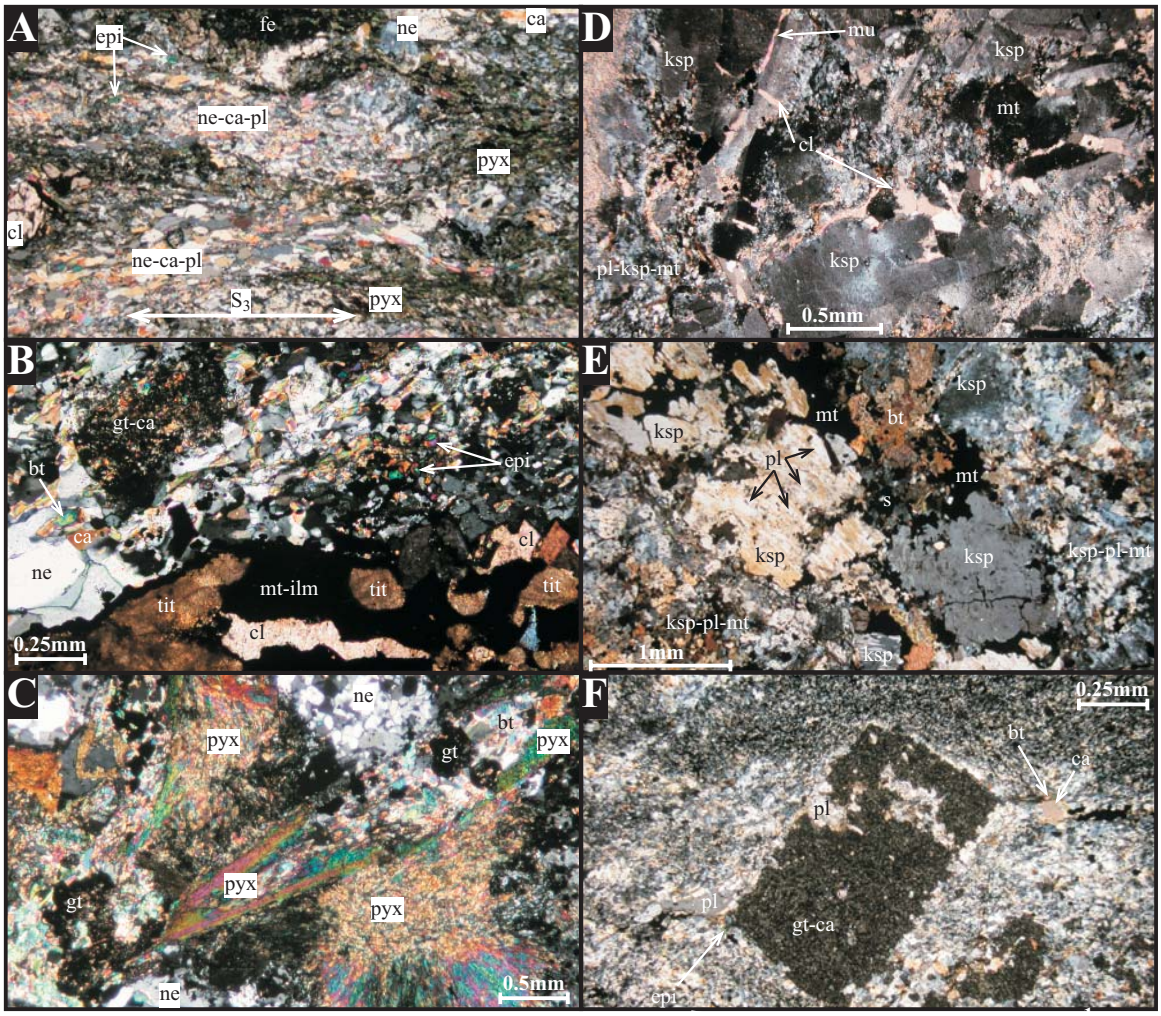


**Figure 5.3.** Photomicrographs of alkaline magmatic varieties. All images taken under cross-polarised light. (a) Layered feldspathic ijolite with felsic bands of nepheline-cancrinite-albite-muscovite and mafic bands of pyroxene-phlogopite-Fe-oxide. Fabric correlated with $D_3$ of Berry et al. (1984); (b) Both primary magmatic minerals (nepheline-cancrinite-pyroxene) and metamorphic minerals (epidote-titanite-ilmenite-magnetite-garnet) exemplify the mineralogical diversity of the ijolite phases; (c) Primary magmatic pyroxene partially replaced by garnet-phlogopite-epidote assemblage during metamorphism; (d) Porphyritic syenite with K-feldspar phenocrysts and matrix composed of albite-K-feldspar-biotite-muscovite-magnetite-calcite. Late-stage calcite veins also croscut the syenite; (e) Porphyritic syenite with interstitial magnetite and sulphides; (f) Primary magmatic pyroxene partially replaced by garnet-phlogopite-epidote assemblage during metamorphism. *Mineral abbreviations: ne: nepheline; ca: cancrinite; pl: albitic plagioclase; ksp: K-feldspar; pyx: aegerine-augite pyroxene; epi: epidote; gt: andradite-grossular garnet; bt: phlogopitic biotite; mu: muscovite; tit: titanite; cl: calcite; mt: magnetite; ilm: ilmenite; s: sulphide.*

### *5.4.2 Syenite phases*

The Billeroo syenites are dominantly porphyritic, composed of euhedral perthitic sanidine phenocrysts (up to ~5 cm) with carlsbad twinning within a matrix of K-feldspar, biotite, muscovite, albite, magnetite and calcite (Fig. 5.3d). Perthites show a blotchy replacement of sanidine by albite and are commonly fractured and veined by carbonate with inclusions of magnetite and biotite common (Fig. 5.3e). Micas are dominantly biotite but lesser amounts of metamorphic muscovite also exist. Some carbonate is stained by limonite, suggesting it is iron-rich. Abundant titanite occurs in blotchy patches associated with magnetite. Some biotite is altered to chlorite. Larger masses of sericite occur between the phenocrysts in some syenites, defining a weak schistosity. Prismatic areas of fine-grained albite may represent pseudomorphed sodic amphiboles. Some syenites have visible sulphides including pyrite and chalcopyrite.

### 5.4.3 Lamprophyre dykes

The three alkaline lamprophyre dykes located in this study, like the ijolite phases, are very heterogeneous. Two of the dykes are relatively enriched in silica, composed of very fine-grained albite, cancrinite, magnetite, garnet, epidote, biotite, phlogopite and K-feldspar. Minor phases include titanite, sodalite, fluorite, calcite and apatite. Fluorite occurs as a late-crystallising product, and therefore may be of hydrothermal origin, as is common in alkaline magmatic rocks (Deer et al., 1992). Fine-grained magnetite within the matrix appears to be a primary magmatic product. Metamorphic replacement textures are also numerous in the dyke phases. Large crystals of garnet up to ~5 mm have pseudomorphed cancrinite producing a poikiloblastic texture (Fig. 5.3f). The cancrinite may also have replaced euhedral primary magmatic nepheline. Large aggregates of slightly coarser cancrinite, albite, garnet and sodalite appear to have pseudomorphed sodic pyroxene or amphibole. The other lamprophyric dyke has less silica relative to the other two samples due to a greater proportion of cancrinite and relict primary nepheline. This suggests it may have evolved from a more undifferentiated magma relative to the other two lamprophyric dykes.

### 5.4.4 Mineral compositions

*Appendix 6* lists all of the minerals that were analysed. Following is a summary of the mineral chemistry of the different phases, with representative analyses presented in Tables 5.1 – 5.7. Feldspathoid compositions are variable, with nepheline compositions being particularly variable, some of which are outside the Morozewicz-Buerger convergence field for plutonic nephelines (Fig. 5.4; Table 5.1; Tilley, 1954). Isotherms for the limits of solid solution as defined by Hamilton (1961) indicate nephelines have equilibrated over a temperature range between 500 – 800°C. The higher temperatures probably do not represent magmatic conditions, but temperatures at which they underwent re-equilibration. Cancrinite compositions are typical of other reported compositions, except for slightly less $SiO_2$ and $Al_2O_3$ (Deer et al., 1992; Table 5.2). Clinopyroxenes are dominantly sodic and include aegirine-augite, aegirine-hedenbergite and aegirine (Fig. 5.5; Table 5.3). Relic zoning in some aegirine-augite suggests a range of pyroxene compositions existed within single crystals. Such zoning is typical of crystal fractionation processes (Woolley et al., 1995).

Plagioclase compositions in all the magmatic phases are dominated by albite ($Ab_{97-99}$; Fig. 5.6; Table 5.4). The near pure albite composition of plagioclase in the feldspathic ijolite phases is interpreted to be the result of the high $Na_2O$ content of the primary magma and later enrichment during Na-alteration. The transformation of nepheline to albite from the movement of Si and Al during metamorphism may have been coincident with the Na-alteration. In the syenites, K-feldspar (sanidine) compositions range between $Or_{96-99}$ and commonly have blotchy exsolution of near pure albite ($Ab_{98-99}$). Near pure albite compositions are also preserved in the matrix of the syenites and lamprophyres.

Garnet compositions are typically of the

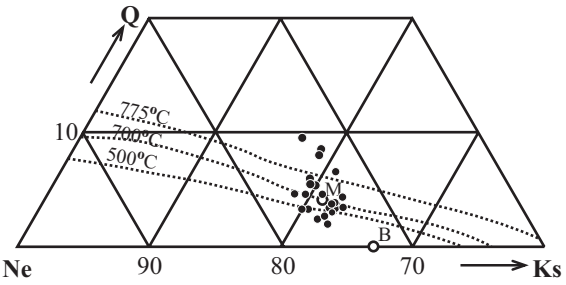


**Figure 5.4.** Nepheline compositions from ijolites in the system Ne-Ks-Qtz. Endmember calculations following procedure of Peterson (1989). M and B define the Morozewicz-Buerger convergence field for nephelines (Tilley, 1954). Isotherms after Hamilton (1961). N=20.

**Table 5.1.** Representative compositions of nepheline.

| Sample | BN3 | BN3 | BN4 | BN3 | BN1 |
|---|---|---|---|---|---|
| Phase | ijolite | ijolite | ijolite | ijolite | ijolite |
| Point No. | 1 | 2 | 3 | 4 | 5 |
| $SiO_2$ | 42.82 | 43.18 | 42.19 | 43.43 | 42.15 |
| $Al_2O_3$ | 34.22 | 35.43 | 34.47 | 34.75 | 33.49 |
| $TiO_2$ | 0.01 | 0.01 | 0.00 | 0.02 | 0.00 |
| FeO | 0.03 | 0.00 | 0.11 | 0.04 | 0.16 |
| CaO | 0.22 | 0.09 | 0.04 | 0.26 | 0.17 |
| $Na_2O$ | 15.92 | 15.73 | 16.13 | 15.69 | 15.63 |
| $K_2O$ | 6.14 | 6.17 | 7.12 | 6.18 | 6.60 |
| BaO | 0.02 | 0.01 | 0.04 | 0.00 | 0.12 |
| SrO | 0.00 | 0.00 | n/a | 0.00 | 0.00 |
| Sum | 99.42 | 100.62 | 100.10 | 100.37 | 98.33 |
| | | | | | |
| Si | 8.267 | 8.211 | 8.148 | 8.283 | 8.26 |
| Al | 7.785 | 7.939 | 7.847 | 7.809 | 7.733 |
| Ti | 0.002 | 0.002 | 0 | 0.003 | 0 |
| $Fe^{3+}$ | 0.001 | 0 | 0.017 | 0.006 | 0.027 |
| Ca | 0.047 | 0.018 | 0.008 | 0.053 | 0.036 |
| Na | 5.958 | 5.799 | 6.038 | 5.803 | 5.938 |
| K | 1.514 | 1.498 | 1.755 | 1.505 | 1.651 |
| Ba | 0.002 | 0.001 | 0.003 | 0 | 0.009 |
| Sr | 0 | 0 | - | 0 | 0 |
| Total | 23.575 | 23.466 | 23.816 | 23.461 | 23.655 |
| | | | | | |
| Ne | 74.91 | 72.64 | 75.55 | 73.02 | 74.57 |
| Ks | 19.04 | 18.76 | 21.95 | 18.94 | 20.73 |
| Q | 6.05 | 8.59 | 2.49 | 8.04 | 4.71 |

Nepheline cations calculated on 32O
n/a : not analysed
- : not calculated

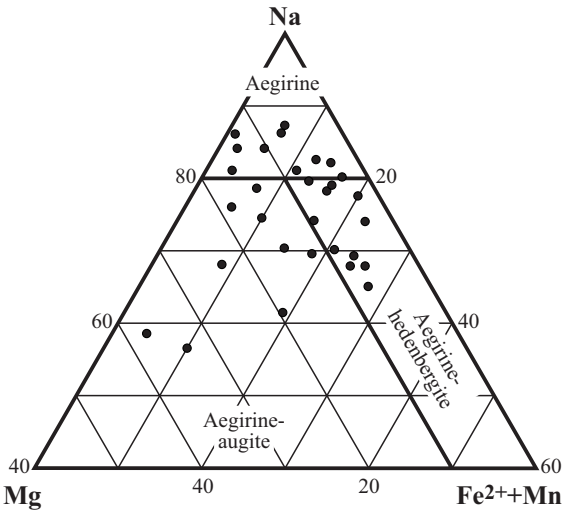


**Figure 5.5.** Plot of clinopyroxene compositions from ijolites. Classification fields after Jones (1984). Endmember proportions calculated following procedures outlined in Deer et al. (1992). N=30.

**Table 5.2.** Representative compositions of cancrinite.

| Sample | BN8 | BN8 | BN6 | BN6 | BN6 |
|---|---|---|---|---|---|
| Phase | ijolite | ijolite | lampro | lampro | lampro |
| Point no. | 1 | 2 | 3 | 4 | 5 |
| $SiO_2$ | 37.91 | 39.72 | 41.52 | 42.95 | 40.36 |
| $Al_2O_3$ | 32.34 | 32.13 | 34.30 | 35.27 | 33.81 |
| FeO | 0.14 | 0.10 | 0.07 | 0.01 | 0.12 |
| CaO | 6.03 | 5.93 | 5.81 | 5.93 | 4.97 |
| MnO | 0.02 | 0.00 | 0.04 | 0.00 | 0.07 |
| MgO | 0.003 | 0.01 | 0.00 | 0.00 | 0.01 |
| $Na_2O$ | 15.44 | 15.21 | 11.11 | 10.87 | 12.27 |
| $K_2O$ | 0.56 | 0.63 | 0.76 | 0.42 | 1.33 |
| BaO | 0.00 | 0.05 | 0.00 | 0.00 | 0.04 |
| SrO | n/a | n/a | n/a | 0.00 | n/a |
| $SO_3$ | 4.4875 | 3.97 | 3.94 | 2.31 | 4.66 |
| Cl | 0.0053 | 0.00 | 0.00 | 0.02 | 0.01 |
| F | 0.0006 | 0.05 | 0.00 | 0.00 | 0.16 |
| Sum | 96.938 | 97.80 | 97.56 | 97.78 | 97.81 |
| | | | | | |
| Si | 5.984 | 6.143 | 6.08 | 6.098 | 6.039 |
| Al | 6.016 | 5.857 | 5.92 | 5.902 | 5.961 |
| $Fe^{2+}$ | 0.019 | 0.013 | 0.009 | 0.001 | 0.015 |
| Ca | 1.02 | 0.982 | 0.912 | 0.902 | 0.796 |
| Mn | 0.003 | 0 | 0.005 | 0 | 0.009 |
| Mg | 0 | 0.002 | 0 | 0 | 0.001 |
| Na | 4.725 | 4.56 | 3.154 | 2.992 | 3.559 |
| K | 0.113 | 0.124 | 0.143 | 0.077 | 0.253 |
| Ba | 0 | 0.003 | 0 | 0 | 0.002 |
| Sr | - | - | - | 0 | - |
| S | 1.327 | 1.152 | 1.08 | 0.614 | 1.306 |
| Cl | 0.001 | 0 | 0 | 0.005 | 0.003 |
| F | 0 | 0.023 | 0 | 0 | 0.077 |
| Total | 19.209 | 18.859 | 17.302 | 16.59 | 18.022 |

Cancrinite ions calculated on basis of (Si+Al)=12
n/a : not analysed
- : not calculated

andradite-grossular solid-solution series ($and_{86}gro_{11}spe_3$; Table 5.5). Similar andradite-grossular compositions are found in alkaline igneous rocks (Deer et al., 1992). The predominant replacement of pyroxene by garnet favours either late-stage magmatic replacement of pyroxene by garnet, or garnet growth due to contact or regional metamorphism. Epidote compositions are fairly constant with $XFe^{3+}$ varying between 0.26 – 0.32 (Table 5.6). Overprinting textures in the matrix support a metamorphic origin for epidote growth. Mica compositions range between phlogopite and biotite, which coexist with muscovite (Table 5.7). Phases not chemically analysed include those from the stronalsite-banalsite (Sr-Ba) solid-solution series, Sr-Na silicates (up to 12wt% SrO), and Na-Ca-Ti silicates. Microprobe analysis of calcite identified a manganese component (~5 wt% Mn).

**Table 5.3.** Representative compositions of pyroxene.

| Sample | BN1 | BN1 | BN1 | BN4 | BN4 |
|---|---|---|---|---|---|
| Phase | ijolite | ijolite | ijolite | ijolite | ijolite |
| Point no. | 1 | 2 | 3 | 4 | 5 |
| $SiO_2$ | 52.12 | 47.03 | 51.28 | 52.39 | 52.40 |
| $TiO_2$ | 0.66 | 2.21 | 4.23 | 0.08 | 0.82 |
| $Al_2O_3$ | 1.73 | 1.59 | 0.79 | 1.01 | 1.48 |
| FeO | 22.99 | 18.75 | 24.35 | 25.78 | 24.04 |
| CaO | 5.31 | 16.44 | 3.50 | 3.97 | 5.22 |
| MnO | 0.39 | 0.81 | 0.27 | 0.39 | 0.30 |
| MgO | 3.334 | 4.46 | 1.46 | 2.05 | 2.83 |
| $Na_2O$ | 10.44 | 5.79 | 10.71 | 11.11 | 10.44 |
| $K_2O$ | 0.03 | 0.00 | 0.00 | 0.01 | 0.00 |
| Sum | 96.99 | 97.06 | 96.58 | 96.79 | 97.53 |
| | | | | | |
| Si | 1.983 | 1.837 | 1.998 | 2.008 | 1.993 |
| Ti | 0.019 | 0.065 | 0.124 | 0.002 | 0.023 |
| $Al^{iv}$ | 0.017 | 0.073 | 0.002 | 0 | 0.007 |
| $Al^{vi}$ | 0.061 | 0 | 0.034 | 0.046 | 0.06 |
| $Fe^{3+}$ | 0.69 | 0.561 | 0.529 | 0.76 | 0.67 |
| $Fe^{2+}$ | 0.041 | 0.051 | 0.265 | 0.066 | 0.094 |
| Ca | 0.216 | 0.688 | 0.146 | 0.163 | 0.213 |
| Mn | 0.013 | 0.027 | 0.009 | 0.013 | 0.01 |
| Mg | 0.189 | 0.26 | 0.085 | 0.117 | 0.16 |
| Na | 0.77 | 0.438 | 0.809 | 0.825 | 0.77 |
| K | 0.001 | 0 | 0 | 0 | 0 |
| Total | 4 | 4 | 4 | 4 | 4 |
| | | | | | |
| Na | 0.76 | 0.565 | 0.693 | 0.808 | 0.745 |
| Mg | 0.186 | 0.335 | 0.073 | 0.115 | 0.155 |
| $Fe^{2+}$+Mn | 0.053 | 0.1 | 0.234 | 0.077 | 0.1 |

Pyroxene ions calculated on basis of 6O

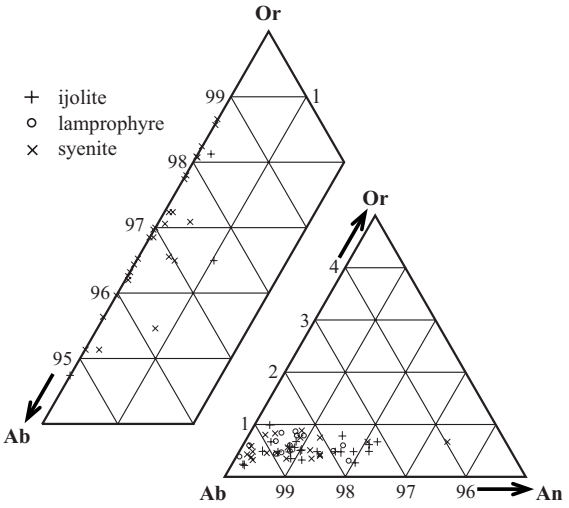


**Figure 5.6.** Feldspar compositions plot in the system Or-Ab-An. Endmember proportions calculated following procedures outlined in Deer et al. (1992).

## 5.5 Whole-rock geochemistry and Nd-Sr isotopes

Samples selected for whole-rock geochemistry were chosen on the basis of demonstrating the greatest textural and mineralogical compositions (Table 5.8). The Billeroo alkaline magmatic rocks are typical of most alkaline suites in that they are critically undersaturated in silica, and all but two samples yield normative nepheline (*Appendix 7*).

**Table 5.4.** Representative composition of feldspars.

| Sample | BN17 | BN17 | BN2 | BN1 | BN7 |
|---|---|---|---|---|---|
| Phase | syenite | syenite | syenite | ijolite | lampro |
| Feldspar | perthite | albite | K-spar | albite | albite |
| Point no. | 1 | 2 | 3 | 4 | 5 |
| $SiO_2$ | 65.59 | 69.21 | 63.51 | 68.72 | 69.15 |
| $Al_2O_3$ | 19.10 | 19.88 | 20.38 | 19.31 | 19.34 |
| FeO | 0.06 | 0.16 | 0.13 | 0.08 | 0.12 |
| CaO | 0.00 | 0.03 | 0.08 | 0.18 | 0.16 |
| MnO | 0.00 | 0.00 | 0.07 | 0.06 | 0.03 |
| MgO | 0.00 | 0.01 | 0.06 | 0.00 | 0.02 |
| $Na_2O$ | 0.25 | 11.19 | 0.27 | 11.44 | 11.58 |
| $K_2O$ | 14.64 | 0.10 | 15.74 | 0.12 | 0.15 |
| BaO | 0.07 | 0.00 | 0.41 | 0.01 | 0.02 |
| Sum | 99.72 | 100.58 | 100.65 | 99.91 | 100.56 |
| | | | | | |
| Si | 12.021 | 11.993 | 11.69 | 12.013 | 12.018 |
| Al | 4.125 | 4.06 | 4.421 | 3.977 | 3.96 |
| $Fe^{2+}$ | 0.009 | 0.023 | 0.02 | 0.012 | 0.017 |
| Ca | 0 | 0.006 | 0.016 | 0.033 | 0.03 |
| Mn | 0 | 0 | 0.01 | 0.009 | 0.004 |
| Mg | 0 | 0.004 | 0.017 | 0 | 0.004 |
| Na | 3.423 | 3.759 | 0.096 | 3.878 | 3.901 |
| K | 0.005 | 0.022 | 3.695 | 0.026 | 0.033 |
| Ba | 0.005 | 0 | 0.029 | 0 | 0.001 |
| Total | 19.672 | 19.867 | 19.995 | 19.95 | 19.97 |
| | | | | | |
| Or | 97.5 | 0.6 | 97.05 | 0.67 | 0.84 |
| Ab | 2.5 | 99.3 | 2.52 | 98.48 | 98.4 |
| An | 0 | 0.2 | 0.42 | 0.85 | 0.76 |

Feldspar compositions calculated on basis of 32O
1,3: phenocrysts; 2: overgrowth; 4,5: albite grains

**Table 5.5.** Representative compositions of garnet.

| Sample | BN1 | BN4 | BN3 | BN6 | BN6 |
|---|---|---|---|---|---|
| Phase | ijolite | ijolite | lampro | lampro | lampro |
| Point no. | 1 | 2 | 3 | 4 | 5 |
| $SiO_2$ | 34.91 | 37.95 | 34.35 | 34.75 | 35.01 |
| $TiO_2$ | 0.60 | 1.09 | 1.50 | 1.84 | 1.39 |
| $Al_2O_3$ | 2.51 | 2.91 | 2.48 | 4.68 | 5.43 |
| $Cr_2O_3$ | 0.00 | 0.00 | 0.00 | 0.00 | 0.01 |
| FeO | 24.23 | 23.54 | 23.04 | 19.68 | 18.53 |
| CaO | 31.75 | 28.83 | 31.83 | 32.34 | 32.62 |
| MnO | 1.46 | 0.57 | 1.27 | 1.57 | 1.30 |
| MgO | 0.00 | 0.69 | 0.00 | 0.00 | 0.00 |
| $Na_2O$ | 0.04 | 1.62 | 0.09 | 0.02 | 0.02 |
| $K_2O$ | 0.01 | 0.01 | 0.01 | 0.00 | 0.02 |
| Sum | 95.52 | 97.22 | 94.56 | 94.89 | 94.31 |
| | | | | | |
| Si | 5.951 | 6.419 | 5.9159 | 5.908 | 5.958 |
| Al | 0.505 | 0.58 | 0.504 | 0.939 | 1.088 |
| Cr | 0 | 0 | 0 | 0 | 0 |
| $Fe^{3+}$ | 3.435 | 2.127 | 3.267 | 2.772 | 2.637 |
| Ti | 0.077 | 0.139 | 0.194 | 0.236 | 0.178 |
| Mg | 0 | 0.174 | 0.001 | 0.001 | 0 |
| $Fe^{2+}$ | 0.02 | 1.076 | 0.05 | 0.026 | 0 |
| Mn | 0.211 | 0.082 | 0.186 | 0.226 | 0.187 |
| Ca | 5.797 | 5.225 | 5.873 | 5.89 | 5.948 |
| Na | 0.014 | 0.532 | 0.029 | 0.008 | 0.006 |
| K | 0.003 | 0.003 | 0.001 | 0 | 0.001 |
| Total | 16.013 | 16.357 | 16.021 | 16.006 | 16.003 |
| | | | | | |
| pyr | 0.001 | 2.657 | 0.011 | 0.012 | 0.001 |
| alm | 0.331 | 16.413 | 0.825 | 0.417 | 0 |
| spe | 3.496 | 1.254 | 3.037 | 3.678 | 3.055 |
| and | 85.524 | 74.748 | 82.403 | 70.247 | 67.56 |
| uv | 0 | 0 | 0 | 0 | 0 |
| gro | 10.647 | 4.928 | 13.723 | 25.647 | 29.384 |

Garnet ions calculated on basis of 24O

### *5.5.1 Chemical classification*

Remobilisation of major elements, typically Si, Na, and Al, altered the final mineralogy of the Billeroo alkaline magmatic phases. This is recorded by the replacement of nepheline by cancrinite and albite, pyroxene by garnet

**Table 5.6.** Representative compositions of epidote.

| Phase | ijolite | ijolite | ijolite | lampro | lampro |
|---|---|---|---|---|---|
| Sample | BN1 | BN1 | BN4 | BN6 | BN7 |
| Point no. | 1 | 2 | 3 | 4 | 5 |
| $SiO_2$ | 37.15 | 36.85 | 37.08 | 36.31 | 37.37 |
| $TiO_2$ | 0.09 | 0.04 | 0.07 | 0.65 | 0.01 |
| $Al_2O_3$ | 22.28 | 22.96 | 21.57 | 21.35 | 22.55 |
| FeO | 12.23 | 11.65 | 14.11 | 13.57 | 13.46 |
| CaO | 22.39 | 21.02 | 21.59 | 22.11 | 21.45 |
| MnO | 0.16 | 0.13 | 0.13 | 1.47 | 0.35 |
| MgO | 0.02 | 0.00 | 0.00 | 0.00 | 0.02 |
| $Na_2O$ | 0.02 | 1.22 | 0.03 | 0.02 | 0.04 |
| $K_2O$ | 0.02 | 0.04 | 0.04 | 0.02 | 0.01 |
| Sum | 94.36 | 93.91 | 94.62 | 97.01 | 95.24 |
| | | | | | |
| Si | 3.028 | 3.014 | 3.021 | 3.101 | 3.016 |
| Ti | 0.006 | 0.002 | 0.004 | 0.042 | 0 |
| Al | 2.141 | 2.213 | 2.072 | 2.051 | 2.146 |
| $Fe^{3+}$ | 0.834 | 0.797 | 0.962 | 0.969 | 0.909 |
| Ca | 1.955 | 1.843 | 1.885 | 1.931 | 1.856 |
| Mn | 0.011 | 0.009 | 0.009 | 0.106 | 0.024 |
| Mg | 0.002 | 0 | 0 | 0 | 0.002 |
| Na | 0.002 | 0.193 | 0.005 | 0.003 | 0.006 |
| K | 0.002 | 0.005 | 0.004 | 0.003 | 0.001 |
| Total | 7.981 | 8.076 | 7.962 | 8.206 | 9.96 |

Epidote ions calculated on basis of 12.5O

**Table 5.7.** Representative compositions of mica.

| Phase | ijolite | ijolite | lampro | syenite | syenite |
|---|---|---|---|---|---|
| Sample | BN1 | BN4 | BN7 | BN16 | BN16 |
| Point no. | 1 | 2 | 3 | 4 | 5 |
| $SiO_2$ | 45.51 | 37.67 | 36.52 | 45.84 | 36.68 |
| $TiO_2$ | 0.00 | 0.54 | 0.63 | 0.05 | 2.49 |
| $Al_2O_3$ | 37.88 | 18.29 | 19.18 | 34.51 | 18.63 |
| FeO | 0.25 | 8.56 | 10.47 | 4.60 | 17.09 |
| CaO | 0.02 | 0.04 | 0.01 | 0.02 | 0.03 |
| MnO | 0.06 | 1.13 | 2.24 | 0.00 | 0.46 |
| MgO | 0.74 | 19.24 | 15.55 | 1.43 | 11.30 |
| $Na_2O$ | 0.23 | 0.13 | 0.21 | 0.29 | 0.09 |
| $K_2O$ | 10.40 | 10.05 | 9.51 | 10.21 | 9.25 |
| Sum | 95.08 | 95.64 | 94.31 | 96.95 | 96.03 |
| | | | | | |
| Si | 6.024 | 5.458 | 5.429 | 6.092 | 5.468 |
| $Al^{iv}$ | 1.976 | 2.542 | 2.571 | 1.908 | 2.532 |
| $Al^{vi}$ | 3.932 | 0.58 | 0.788 | 3.497 | 0.74 |
| Ti | 0 | 0.058 | 0.07 | 0.005 | 0.279 |
| $Fe^{2+}$ | 0.027 | 1.037 | 1.301 | 0.511 | 2.13 |
| Mn | 0.007 | 0.138 | 0.282 | 0 | 0.058 |
| Mg | 0.145 | 4.156 | 3.446 | 0.283 | 2.511 |
| Ca | 0.003 | 0.006 | 0.001 | 0.003 | 0.005 |
| Na | 0.059 | 0.036 | 0.059 | 0.074 | 0.027 |
| K | 1.755 | 1.857 | 1.804 | 1.731 | 1.76 |
| Total | 13.929 | 15.869 | 15.751 | 14.103 | 15.51 |

Mica ions calculated on basis of 22O
1,4: muscovite; 2: phlogopite; 3,5: biotite

and albite, and K-feldspar by albite. When the different alkaline magmatic phases are evaluated using nomenclature or classification schemes such as total alkali versus silica diagrams (TAS; Cox et al., 1979; Middlemost, 1994), they all have relatively enriched alkali contents (Fig. 5.7). Although the mobility of Si, K and Na occurred, comparatively narrow ranges of Si and K+Na compositions suggest that primary rock compositions may still be representative.

In the TAS classification scheme for plutonic rocks of Cox et al. (1979), the feldspathic ijolites plot in unnamed fields between those designated for 'ijolites' and 'nepheline syenites' (Fig. 5.7a). Two of the syenites plot in the given field for 'syenites', while the other four plot in the 'nepheline syenite' field. On the more recent classification scheme of Middlemost (1994), the ijolites classify as foidolite, foid monzosyenite and foid monzogabbro, and the syenites classify as foid syenite and foid monzosyenite (Fig. 5.7b). One of the lamprophyric dykes is more silica-undersaturated (phonotephrite) relative to the other two lamprophyres (trachyandesites; Middlemost, 1994; Fig. 5.7b). Using the $K_2O$ vs. $Na_2O$ subdivision for alkaline magmatic rocks (McBirney, 1993), the ijolite phases and the dykes have high $Na_2O/K_2O$ ratios and therefore belong to the Na-series of alkaline magmatism (Fig. 5.8). This reflects the high albite and feldspathoidal content of these samples. The syenites plot in the K-series and the high-K series, which is related to their high sanidine contents.

### *5.5.2 Major elements*

Harker variation diagrams define two broad trends in the majority of major elements (Fig. 5.9). The feldspathic ijolites and lamprophyres define one trend, and the other trend is defined by the syenites. Na, Ca, Mg and P behave, to varying degrees, as compatible elements in the ijolite series. The compatible behaviour of these elements in the ijolite series is consistent with crystallisation of pyroxene, nepheline (cancrinite), plagioclase, apatite and phlogopite early in the magmatic history. The trend defined by the syenite phases is steeper that the other phases. However, Na, K, Ca, Mg and Mn record large variations. The trends

**Table 5.8.** Whole-rock geochemical data of selected phases from the Billeroo alkaline magmatic complex.

| Sample | BN12 | 887 | BN5 | BN13 | BN4 | BN8 | BN3 | 884 | BN14 | BN1 | BN9 | BN10 |
|---|---|---|---|---|---|---|---|---|---|---|---|---|
| R no.[a] | 493982 | 474887 | 493978 | 493983 | 493977 | 493979 | 493976 | 474884 | 493984 | 493975 | 493980 | 493981 |
| Phase | ijo | ijo | ijo | ijo | ijo | ijo | ijo | ijo | ijo | ijo | ijo | ijo |
| $SiO_2$ | 44.0 | 44.8 | 44.9 | 44.9 | 45.1 | 46.2 | 46.2 | 47.0 | 48.1 | 49.2 | 49.9 | 50.4 |
| $TiO_2$ | 1.89 | 2.12 | 1.73 | 1.87 | 1.78 | 2.39 | 1.61 | 1.45 | 2.0 | 1.92 | 1.91 | 1.99 |
| $Al_2O_3$ | 17.8 | 17.5 | 18.9 | 18.0 | 18.7 | 22.0 | 20.7 | 19.0 | 18.5 | 18.9 | 17.8 | 17.3 |
| $Fe_2O_3$*[b] | 9.89 | 10.7 | 9.74 | 10.2 | 9.42 | 8.7 | 8.76 | 8.4 | 10.7 | 9.7 | 11.1 | 11.2 |
| MnO | 0.22 | 0.29 | 0.19 | 0.23 | 0.2 | 0.16 | 0.21 | 0.2 | 0.26 | 0.22 | 0.2 | 0.21 |
| MgO | 3.37 | 2.86 | 3.31 | 2.97 | 3.36 | 1.99 | 2.6 | 2.79 | 1.98 | 2.0 | 2.17 | 1.92 |
| CaO | 7.01 | 6.57 | 7.27 | 6.26 | 7.24 | 4.07 | 5.37 | 5.92 | 3.96 | 3.89 | 4.18 | 4.02 |
| $Na_2O$ | 8.78 | 9.37 | 7.62 | 9.41 | 7.49 | 7.19 | 9.11 | 10.1 | 7.64 | 7.66 | 7.04 | 7.3 |
| $K_2O$ | 2.95 | 2.75 | 3.29 | 2.85 | 3.15 | 3.51 | 2.99 | 2.34 | 2.96 | 4.03 | 2.35 | 2.51 |
| $P_2O_5$ | 1.02 | 0.83 | 1.24 | 0.91 | 1.1 | 0.37 | 0.75 | 0.72 | 0.53 | 0.49 | 0.74 | 0.59 |
| LOI | 2.35 | 1.89 | 1.83 | 2.12 | 1.94 | 3.01 | 2.06 | 2.92 | 3.16 | 2.36 | 2.14 | 1.96 |
| Total | 99.28 | 99.68 | 100.02 | 99.72 | 99.48 | 98.89 | 100.36 | 100.84 | 99.79 | 100.37 | 99.53 | 99.4 |
| V | 360 | 390 | 340 | 340 | 320 | 190 | 280 | 200 | 260 | 250 | 270 | 240 |
| Co | 53 | 36 | 43 | 49 | 43 | 42 | 48 | 26 | 48 | 54 | 46 | 47 |
| Ni | 8 | - | 3 | - | 4 | - | 8 | - | - | 56 | - | - |
| Cu | 78 | 43 | 30 | 86 | 26 | 17 | 35 | 21 | 175 | 135 | 55 | 41 |
| Zn | 99 | 105 | 73 | 88 | 84 | 44 | 88 | 99 | 94 | 79 | 96 | 83 |
| Rb | 93 | 82 | 91 | 87 | 91 | 110 | 100 | 68 | 95 | 100 | 96 | 93 |
| Sr | 850 | 850 | 1050 | 1050 | 900 | 1200 | 950 | 800 | 800 | 950 | 1150 | 1150 |
| Ba | 360 | 370 | 350 | 460 | 430 | 1100 | 550 | 550 | 900 | 1300 | 370 | 450 |
| Th | 9 | 4.3 | 4.3 | 8.5 | 7 | 1.6 | 6 | 9 | 6 | 4.5 | 2.1 | 2.6 |
| U | 2.8 | 1.55 | 1.05 | 1.8 | 1.7 | 0.25 | 0.75 | 1.65 | 1.5 | 0.79 | 0.55 | 0.51 |
| Zr | 80 | 110 | 80 | 80 | 80 | 90 | 70 | 110 | 90 | 80 | 130 | 140 |
| Hf | 2 | 3 | 2 | 2 | 2 | 3 | 2 | 3 | 2 | 2 | 3 | 3 |
| Pb | 10 | 15 | 10 | 15 | - | 20 | 10 | 10 | 15 | 5 | 5 | 10 |
| Nb | 45 | 47 | 35 | 50 | 45 | 75 | 45 | 62 | 55 | 40 | 85 | 85 |
| Y | 25 | 19.5 | 20 | 24.5 | 22 | 10.5 | 16.5 | 23.5 | 14.5 | 12.5 | 17 | 15 |
| La | 34 | 37 | 37.5 | 32.5 | 34 | 19.5 | 25 | 35.5 | 21.5 | 21 | 34.5 | 25.5 |
| Ce | 54 | 62 | 60 | 49.5 | 53 | 33 | 37.5 | 56 | 33.5 | 32 | 57 | 42 |
| Nd | 21.5 | 24 | 24 | 20.5 | 21.5 | 12.5 | 15 | 21.5 | 12.5 | 12.5 | 22.5 | 18 |
| Sm | 5 | 5 | 5.5 | 5 | 5 | 3.4 | 3.6 | 4.3 | 3.3 | 3.3 | 5.5 | 4.5 |
| Eu | 1.35 | 1.75 | 1.4 | 1.35 | 1.3 | 0.99 | 1 | 1.55 | 0.93 | 1 | 1.45 | 1.2 |
| Gd | 3.7 | 3 | 3.8 | 3.6 | 3.7 | 2.2 | 2.6 | 2.2 | 2.2 | 2.1 | 3.8 | 3.2 |
| Dy | 4.3 | 3.8 | 3.8 | 4.3 | 4 | 2.6 | 3.1 | 4.1 | 2.7 | 2.5 | 4 | 3.6 |
| Er | 2.4 | 2.2 | 1.9 | 2.4 | 2.1 | 1.15 | 1.75 | 2.6 | 1.65 | 1.4 | 1.8 | 1.65 |
| Yb | 2.4 | 1.55 | 1.9 | 2.4 | 2.2 | 1.12 | 1.9 | 1.65 | 1.9 | 1.6 | 1.8 | 1.75 |
| Lu | 0.31 | 0.26 | 0.27 | 0.32 | 0.3 | 0.16 | 0.26 | 0.36 | 0.26 | 0.23 | 0.24 | 0.23 |
| Tb | 0.62 | 0.53 | 0.59 | 0.61 | 0.58 | 0.37 | 0.43 | 0.42 | 0.4 | 0.36 | 0.63 | 0.54 |
| Ho | 0.84 | 0.67 | 0.68 | 0.83 | 0.74 | 0.45 | 0.59 | 0.75 | 0.55 | 0.47 | 0.69 | 0.62 |
| Tm | 0.35 | 0.3 | 0.25 | 0.36 | 0.3 | 0.15 | 0.25 | 0.35 | 0.25 | 0.2 | 0.25 | 0.25 |
| Ga | 23 | 20.5 | 20 | 23.5 | 20.5 | 24.5 | 22.5 | 20.5 | 29.5 | 27.5 | 28 | 27 |
| Pr | 6.5 | 7 | 7 | 6.5 | 6.5 | 3.9 | 4.7 | 6.5 | 3.9 | 3.7 | 7 | 5.5 |
| S | 1050 | 950 | 1200 | 1050 | 1150 | 1500 | 1100 | 300 | 1750 | 2700 | 1100 | 250 |

[a] R no. : R number in PIRSA database
[b] $Fe_2O_3$* : refers to total Fe as $Fe_2O_3$
- : below detection level

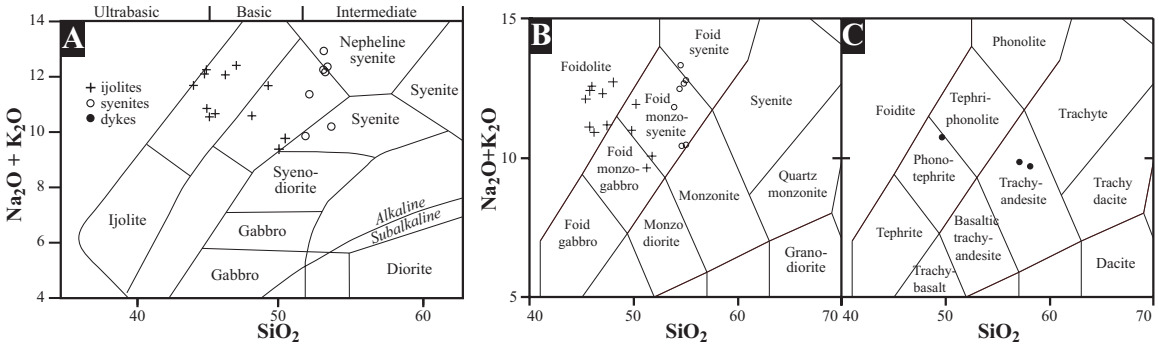


**Figure 5.7.** Different nomenclature schemes of magmatic rocks using total alkali versus silica classification for plutonic rocks (a) Cox et al. (1979); (b) Middlemost (1994); and volcanic rocks (c) Middlemost (1994).

observed in K, Na and Ca are consistent with K-feldspar and plagioclase being the dominant crystallising phases in the syenite series. No clear trends are observed in $Fe_2O_3$*, MnO and $TiO_2$ for any of the series.

### *5.5.3 Trace elements*

Trace elements are plotted against $SiO_2$ in Fig. 5.10 and normalised to chondrite and primitive mantle in Fig. 5.11. All samples are LREE and LILE enriched. The ijolites are enriched in LREE (ΣREE = 92 – 169 ppm; $[La/Yb]_N$ = 7.7 – 16.1; $[Tb/Yb]_N$ = 0.9 – 1.5), and LILE, with positive Pb, P and Ti anomalies and variably negative Th anomalies. The

**Table 5.8.** *Continued.*

| Sample | BN15 | 888 | 886 | BN2 | 885 | BN17 | BN16 | BN11 | BN6 | BN7 |
|---|---|---|---|---|---|---|---|---|---|---|
| R No. | 493988 | 474888 | 493886 | 493991 | 474885 | 493990 | 493989 | 493987 | 493985 | 493986 |
| Phase | sye | sye | sye | sye | sye | sye | sye | lamp | lamp | lamp |
| $SiO_2$ | 51.8 | 52.1 | 53.1 | 53.1 | 53.2 | 53.3 | 53.6 | 48.4 | 56.3 | 57.7 |
| $TiO_2$ | 1.24 | 1.47 | 1.2 | 1.43 | 1.29 | 1.35 | 1.62 | 1.37 | 1.28 | 1.91 |
| $Al_2O_3$ | 15.9 | 15.2 | 15.9 | 16.0 | 15.9 | 15.6 | 16.1 | 18.1 | 17.3 | 17.4 |
| $Fe_2O_3$* | 8.12 | 10.5 | 9.7 | 10.1 | 11.6 | 8.95 | 10.8 | 10.8 | 10.2 | 10.3 |
| MnO | 0.38 | 0.37 | 0.28 | 0.19 | 0.42 | 0.46 | 0.35 | 0.22 | 0.16 | 0.13 |
| MgO | 1.23 | 0.22 | 1.2 | 0.31 | 1.39 | 1.68 | 0.86 | 2.12 | 0.97 | 0.7 |
| CaO | 6.01 | 5.01 | 2.98 | 3.21 | 1.61 | 3.05 | 3.45 | 4.63 | 2.29 | 2.0 |
| $Na_2O$ | 5.99 | 3.76 | 1.55 | 0.63 | 1.38 | 1.26 | 6.05 | 9.13 | 9.02 | 9.1 |
| $K_2O$ | 3.86 | 7.61 | 10.7 | 12.3 | 10.8 | 11.1 | 4.12 | 1.32 | 0.66 | 0.5 |
| $P_2O_5$ | 0.29 | 0.27 | 0.15 | 0.06 | 0.11 | 0.1 | 0.32 | 0.82 | 0.18 | 0.1 |
| LOI | 4.96 | 4.09 | 2.86 | 3.03 | 1.66 | 2.62 | 2.65 | 2.31 | 0.92 | 0.57 |
| Total | 99.78 | 100.6 | 99.62 | 100.36 | 99.36 | 99.47 | 99.92 | 99.76 | 99.37 | 99.78 |
| | | | | | | | | | | |
| V | 120 | 90 | 80 | 105 | 90 | 90 | 140 | 200 | 150 | 170 |
| Co | 23 | 5 | 17 | 36 | 18 | 30 | 27 | 44 | 34 | 29 |
| Ni | - | - | 3 | 3 | 3 | 3 | - | - | - | - |
| Cu | 500 | - | 15 | 19 | 105 | 57 | 1350 | 11 | 8 | 7 |
| Zn | 53 | 22 | 41 | 30 | 800 | 650 | 140 | 89 | 69 | 39 |
| Rb | 150 | 145 | 280 | 320 | 280 | 470 | 125 | 79 | 34.5 | 28 |
| Sr | 320 | 130 | 155 | 185 | 190 | 130 | 270 | 1350 | 340 | 380 |
| Ba | 1150 | 1000 | 3200 | 3700 | 1850 | 1300 | 1150 | 200 | 90 | 80 |
| Th | 14.5 | 15 | 10.5 | 9.5 | 59 | 10 | 14 | 3.2 | 8 | 9 |
| U | 6 | 3.1 | 4.5 | 3.3 | 4.6 | 3.1 | 5.5 | 0.46 | 1.2 | 1.4 |
| Zr | 140 | 160 | 190 | 170 | 240 | 180 | 170 | 150 | 200 | 220 |
| Hf | 3 | 5 | 4 | 3 | 5 | 3 | 3 | 3 | 4 | 4 |
| Pb | 35 | 15 | 25 | 25 | 290 | 430 | 35 | 15 | - | - |
| Nb | 115 | 37 | 77 | 80 | 95 | 105 | 130 | 75 | 70 | 70 |
| Y | 26 | 23.5 | 20 | 18 | 58 | 20.5 | 24.5 | 13.5 | 12.5 | 12.5 |
| La | 40 | 44.5 | 25 | 29.5 | 71 | 49 | 32 | 32.5 | 17 | 8.5 |
| Ce | 55 | 63 | 37 | 38 | 100 | 70 | 43 | 52 | 23.5 | 12.5 |
| Nd | 13.5 | 17.5 | 11 | 9.5 | 30.5 | 17.5 | 12 | 21.5 | 7.5 | 4 |
| Sm | 3.4 | 3.6 | 2.3 | 3.3 | 7 | 3.8 | 3.1 | 5 | 1.65 | 1.1 |
| Eu | 1 | 2.1 | 3 | 1.4 | 3.5 | 1.1 | 0.92 | 1.25 | 0.46 | 0.34 |
| Gd | 2.6 | 2.4 | 1.9 | 1.65 | 4.2 | 2.4 | 2.4 | 3.4 | 1.3 | 1.05 |
| Dy | 4.2 | 4 | 2.8 | 2.6 | 9.5 | 3.3 | 4 | 3.3 | 2.1 | 2 |
| Er | 2.7 | 2.8 | 2.1 | 1.8 | 6.5 | 2.1 | 2.6 | 1.4 | 1.4 | 1.55 |
| Yb | 3.1 | 2.3 | 1.75 | 2.4 | 4.3 | 2.8 | 2.9 | 1.55 | 2 | 2.1 |
| Lu | 0.42 | 0.49 | 0.43 | 0.38 | 0.78 | 0.43 | 0.41 | 0.23 | 0.28 | 0.3 |
| Tb | 0.54 | 0.44 | 0.3 | 0.33 | 0.87 | 0.44 | 0.5 | 0.53 | 0.26 | 0.23 |
| Ho | 0.9 | 0.8 | 0.61 | 0.57 | 1.85 | 0.68 | 0.84 | 0.55 | 0.44 | 0.46 |
| Tm | 0.45 | 0.45 | 0.35 | 0.3 | 1.05 | 0.35 | 0.4 | 0.2 | 0.25 | 0.3 |
| Ga | 28.5 | 20.5 | 24.5 | 22.5 | 22 | 29.5 | 26.5 | 27 | 29.5 | 28.5 |
| Pr | 5 | 6 | 3.5 | 3.2 | 9.5 | 6.5 | 4.2 | 6.5 | 2.5 | 1.3 |
| S | - | - | - | - | 50 | 150 | 100 | 1950 | 400 | 100 |

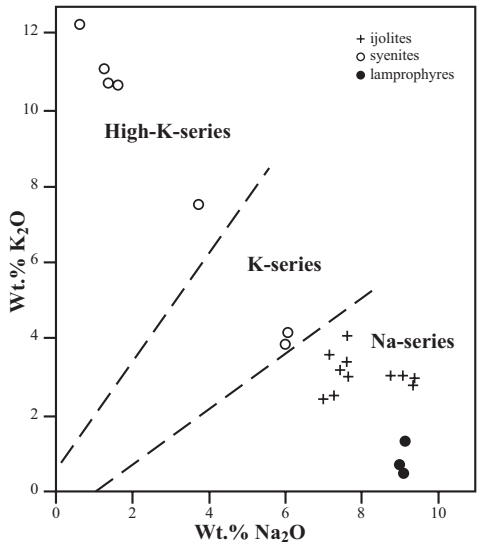


**Figure 5.8.** $K_2O$ vs. $Na_2O$ diagram subdividing the alkaline magma series into High-K-, K-, and Na-subseries (McBirney, 1993).

syenites are mostly enriched in LILE (Rb, Ba, K) and HFSE (Nb, Zr, Th, Pb), have variable REE abundances and positive Eu anomalies, and are enriched in the HREE with respect to MREE (ΣREE = 112 – 309 ppm; $[La/Yb]_N$ = 7.5 – 13.1; $[Tb/Yb]_N$ = 0.6 – 0.9). Nb abundances are relatively enriched in the syenite (~100 ppm). Ba and Rb are preferentially enriched in the syenites (~1500 ppm and ~300 ppm, respectively), due to the substitution of these elements in K-feldspar (Deer, 1992). The positive Eu anomaly that characterises the syenite phases is likely due to the preferential substitution of $Eu^{2+}$ into plagioclase. The cross-cutting lamprophyric dykes have lesser abundances of LILE, variable HFSE and REE abundances, and positive Eu anomalies with variable enrichment in HREE relative to MREE (ΣREE = 48 – 143 ppm; $[La/Yb]_N$ = 8.3 – 13.1; $[Tb/Yb]_N$ = 0.6 – 0.9; $[Tb/Yb]_N$ = 0.5 – 1.5).

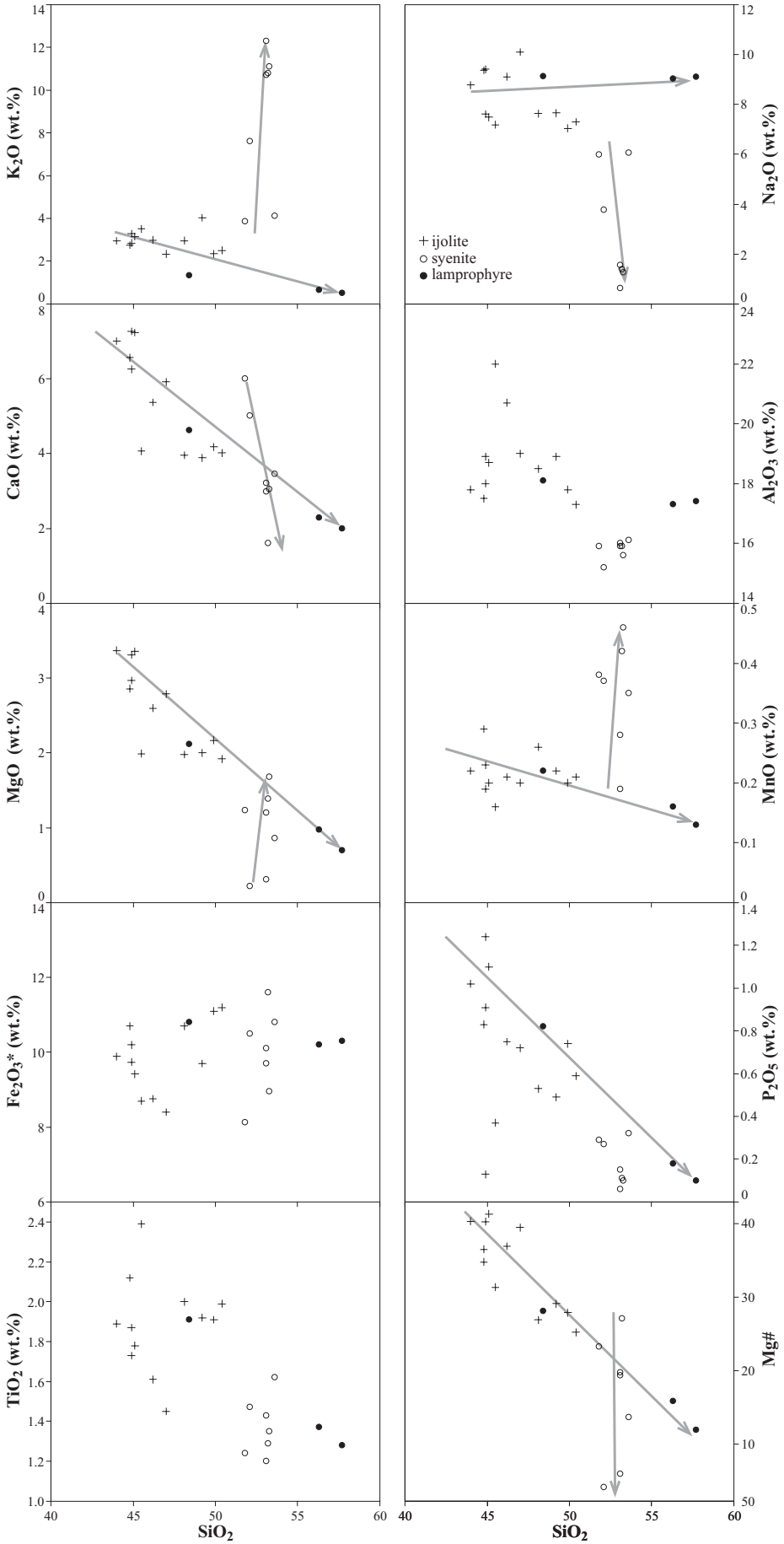


**Figure 5.9.** Harker variation diagram showing plots of a range of oxides (wt%) for ijolites (crosses), syenites (open circles) and lamprophyric dykes (filled circles). Although some scatter is evident, two trends are evident: a continuous series is defined by the ijolite phases and the lamrophyres, and a second trend is defined by the syenite phases.

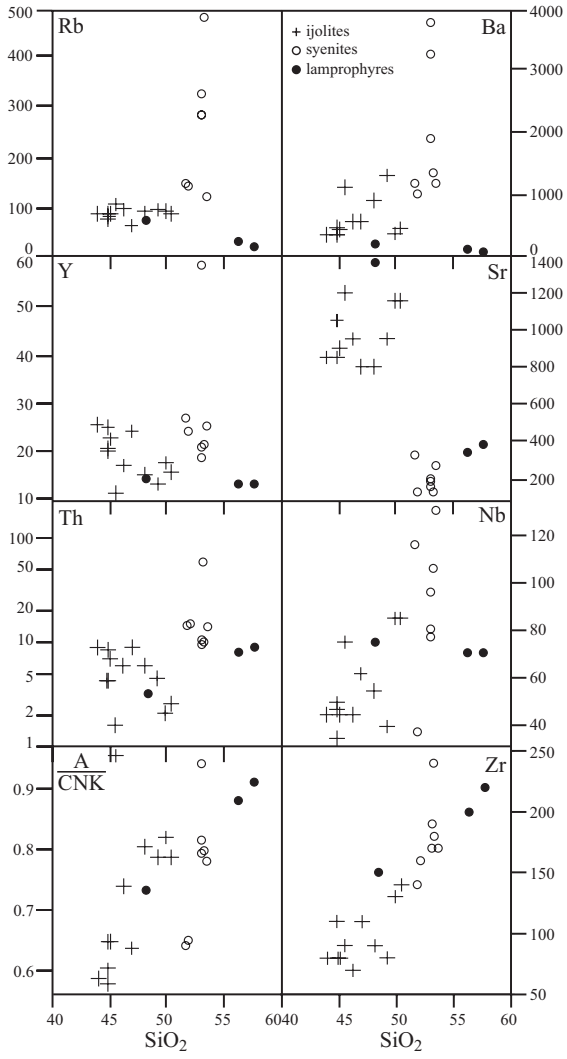


**Figure 5.10.** Selected trace elements (ppm) and major element (A/CNK) vs. $SiO_2$ for the different magmatic phases of the Billeroo alkaline magmatic complex.

### *5.5.4 Nd-Sr isotopic analysis*

Sm-Nd isotope ratios were analysed for five samples from the Billeroo alkaline magmatic complex. All of these samples produced primitive initial $\varepsilon Nd_{(1590)}$ values range between -0.3 and 2.8 (Table 5.9). Relative to other magmatic events in the Olary Domain, such as the ~1700 Ma A-types (Ashley et al. 1996), and the ~1690 Ma mafics (*Chapter 4*), the Billeroo alkaline magmatic phases have more primitive $\varepsilon Nd_i$ values (Fig. 5.12). However, the initial εNd values of the Billeroo alkaline magmatics are similar to the most primitive mafic rocks (*Chapter 4*), but more primitive than the rift-related 1700 Ma A-type granitoids ($\varepsilon Nd_i$ = 0.3 and 1.4; Ashley et al. 1996). $T_{DM}$ model ages for the Billeroo alkaline magmatics (1800 – 2200 Ma) are systematically younger relative to the mafics (>2210 Ma).

Initial Sr isotopic values at 1590 Ma for the Billeroo alkaline magmatics are 0.569273 and 0.653995 for the syenites, and are relatively consistent for the ijolite and lamprophyre samples, ranging between 0.702242 – 0.705238. $^{87}Rb/^{86}Sr$ values for the syenites are 5.04 and 10.57, whereas the ijolites ratios are lower, ranging between 0.21 – 0.29. All initial Sr isotopic values are more radiogenic than the mantle growth curve, and are likely to be a result of variable post-magmatic disturbance of the Rb/Sr ratio.

## 5.6 Discussion

Following is a summary of some of the constraints that can be imposed on the petrogenesis of the Billeroo alkaline magmatic complex.

### *5.6.1 Magmatic differentiation and emplacement*

Near contemporaneous intrusion of the two differentiating magmas is supported by field evidence, with the feldspathic ijolites being the first intruding phase, followed by the syenites and lamprophyre dykes. Emplacement of the syenites was facilitated by brecciation of the surrounding country rock. Such a relationship has been documented elsewhere, whereby an increase in $H_2O$ activity has been associated with high-K magmas (Bailey &

**Table 5.9.** Sm-Nd isotopic data of selected samples from Billeroo alkaline magmatic complex.

| Sample | R no. | Phase | Age (Ma) | Nd (ppm) | Sm (ppm) | $^{147}Sm/^{144}Nd$ | $^{143}Nd/^{144}Nd$ | 2 S.E.[a] | $\varepsilon Nd_{(0)}$ | $\varepsilon Nd_{(1590)}$ | $T_{DM}$ (Ma) |
|---|---|---|---|---|---|---|---|---|---|---|---|
| BN4 | 493977 | Ijolite | 1590 | 26.4 | 4.9 | 0.1132 | 0.511819 | 0.00001 | -16.0 | 1.0 | 1997 |
| BN10 | 493981 | Ijolite | 1590 | 24.9 | 4.8 | 0.1173 | 0.511841 | 0.00001 | -15.5 | 0.6 | 2047 |
| BN7 | 493986 | Lampro | 1590 | 8.4 | 1.8 | 0.1267 | 0.511893 | 0.00001 | -14.5 | -0.3 | 2175 |
| BN17 | 493990 | Syenite | 1590 | 17.6 | 2.9 | 0.1007 | 0.511777 | 0.00001 | -16.8 | 2.8 | 1835 |
| BN2 | 493991 | Syenite | 1590 | 10.7 | 2.0 | 0.1112 | 0.511811 | 0.00001 | -16.1 | 1.3 | 1971 |

| Sample | R no. | Phase | Age (Ma) | Sr (ppm) | Rb (ppm) | Rb/Sr | $^{87}Sr/^{86}Sr$ | $^{87}Rb/^{86}Sr$ | $^{87}Sr/^{86}Sr_{(T)}$ |
|---|---|---|---|---|---|---|---|---|---|
| BN4 | 493977 | Ijolite | 1590 | 900 | 91 | 0.1 | 0.71011 | 0.29 | 0.7034 |
| BN10 | 493981 | Ijolite | 1590 | 1150 | 93 | 0.08 | 0.70893 | 0.23 | 0.7036 |
| BN7 | 493986 | Lampro | 1590 | 380 | 28 | 0.21 | 0.71011 | 0.21 | 0.7052 |
| BN17 | 493990 | Syenite | 1590 | 130 | 470 | 10.57 | 0.81053 | 10.57 | 0.5693 |
| BN2 | 493991 | Syenite | 1590 | 185 | 320 | 5.03 | 0.76896 | 5.03 | 0.6540 |

[a] Isotope error measurements are 2 standard errors.
$^{143}Nd/^{144}Nd_{CHUR(0)} = 0.512638$, $^{147}Sm/^{144}Nd_{CHUR} = 0.1967$
blank: 266 pg Nd

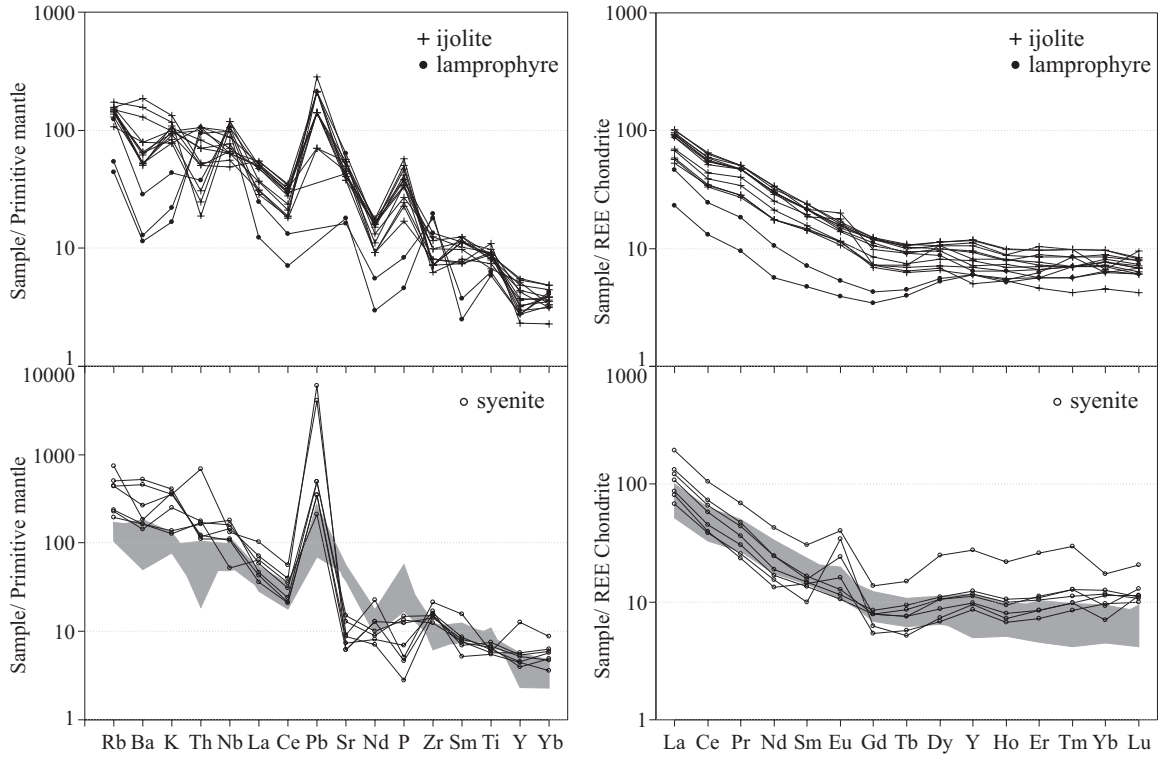


**Figure 5.11.** Chondrite and primitve mantle normalised diagrams of Billeroo alkaline magmatic phases. Shaded area represents range of ijolites for comparison with syenites. Normalisation values of Taylor & McLennan (1985) and Sun & McDonough (1989) for chondrite and primitive mantle, respectively.

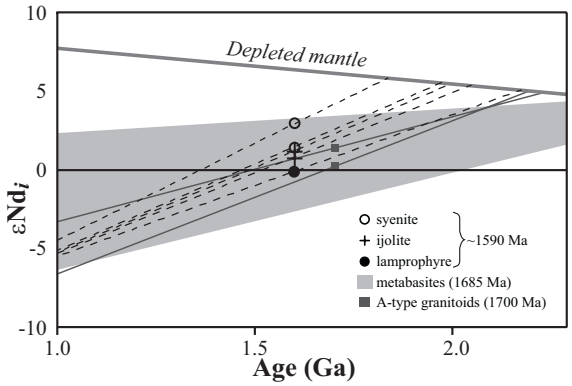


**Figure 5.12.** Plot of eNd versus time (Ga) for selected phases from the Billeroo alkaline magmatic complex. Shaded area represents field for SCP metabasites (*Chapter 4*).

Hampton, 1990). Fluids may have also been derived from the surrounding metasediments during contact metamorphism as the alkaline magmatic phases intruded into the upper crust. The pervasive effects of late-stage Ca-rich fluids are also evident by abundant crosscutting calcite veins in the feldspathic ijolite and syenite phases.

Major element and trace element patterns of the different phases of the Billeroo alkaline magmatic complex support differentiation of a silica-undersaturated, alkali-rich primary

melt in which two distinct differentiation trends are evident (Fig. 5.9, 5.10). The feldspathic ijolites and lamprophyres define a trend in which Na, Ca, Mg and P behave as compatible elements consistent with crystallisation of pyroxene, feldspathoids, plagioclase, apatite and phlogopite. Rare primary magmatic zoning preserved in some pyroxenes is typical of crystal fractionation processes (e.g. Woolley et al., 1995). The differentiation trend of the syenite is defined primarily by enrichment in $K_2O$, resulting in high modal K-feldspar. The general trend towards more K-rich differentiation products is not unusual in continental alkaline magmatic rocks (e.g. McBirney, 1993), and signifies that although two differentiation trends are evident, both melts were likely sourced from the same parental melt evolving at depth. Further supporting evidence of this is recorded by chondrite normalised REE patterns that are relatively similar for the ijolite and syenite phases (Fig. 5.11), and reflect enrichment by fractionation of a silica-undersaturated, LREE-enriched alkaline source. Nepheline syenites reported by Bell et al. (1979) were not identified in sampling. However, given the sodic alteration and metamorphism recorded in surrounding Curnamona Group metasediments and within the alkaline magmatic complex, it is likely that nepheline was pervasively replaced by albite in the syenites.

### *5.6.2 Alkaline magmatic comparisons*

The Billeroo alkaline magmatic complex has similarities to other silica-undersaturated rocks, some of which are associated with carbonatites. Feldspathic ijolites and syenites at Billeroo are comparable in composition to silicate rocks from the Bingo alkaline magmatic complex, Zaire (Woolley et al., 1995), the Spitskop Complex, South Africa (Harmer, 1999), the Pipecleaner Glacier region of Southern Victoria Land, Antarctica (Worley et al., 1995), the Fortaleza alkaline district, Brazil (Morbidelli et al., 1995), and the Igaliko Complex, South Greenland (Jones & Larsen, 1985; Pearce & Leng, 1996). The main difference between the Billeroo alkaline magmatic complex and other alkaline magmatic rocks is the relatively high $TiO_2$ content of the Billeroo rocks. Alkaline phases at the Billeroo complex have $TiO_2$ concentrations between 1.2 and 2.4 wt%, whereas the majority of other alkaline magmatic occurrences have <1 wt% $TiO_2$. Given the accepted immobility of Ti, it is interpreted that the $TiO_2$ concentrations of the Billeroo Complex of primary magmatic origin, and therefore related to the source region. This is in part supported by the $TiO_2$ concentrations of the Lady Louise metatholleites (*Chapter 4*), which are also relatively high in $TiO_2$.

Another key distinguishing feature of the Billeroo Complex magmas is that they have relatively undifferentiated compositions, recorded by low $(Ce/Yb)_N$ ratios <10, and Zr<240 ppm. Only ijolites and nepheline syenites from the Spitskop Complex in the Kaapvaal Craton, South Africa (1341 Ma), have similar unevolved compositions (<250 ppm Zr and $(Ce/Yb)_N$ <15; Harmer, 1999). However, unlike the alkaline intrusives of the Spitskop Complex that are interpreted to have developed through mixing of a mantle-derived melt and a lower crustal melt ($\varepsilon Nd_{1341}$ = –8.4 to –12.7; Harmer, 1999), the Billeroo alkaline

magmatic phases have primitive Nd isotopic values reflecting a mantle dominated source. Further characterisation of the source region is discussed below.

### *5.6.3 Source region characteristics*

The occurrence of alkaline magmatism in the SCP has important implications for understanding the geochemical and isotopic character of the SCLM beneath the Olary Domain during the mid Proterozoic. Geochemical and isotopic heterogeneities that are characteristic of alkaline magmatism rocks have been used elsewhere as evidence for a heterogeneous SCLM (e.g. Bell, 1998; Bühn & Trumbull, 2003; Zhang et al., 2005). With respect to the Billeroo alkaline magmatism, the variability exhibited by the HREE and the HFSE between the different phases reflects the heterogeneous character of the lithosphere beneath the Olary Domain. This interpretation is in part supported by the initial εNd values of the Billeroo alkaline magmatic phases being comparable to the most primitive of the ~1690 Ma Lady Louise Suite mafics in the Mingary region of the western Broken Hill Domain which are indisputably of primary mantle origin (*Chapter 4*). Further to this, the relatively evolved initial εNd values for the Willyama Supergroup metasediments (-2.8 to –5.4; Barovich, 2003; Barovich et al., 2002; *Appendix 1*), and the high $SiO_2$ content of the metasediments discount derivation of the ijolite and syenite phases through rheomorphism of fenites, as has been shown to be the case elsewhere (e.g. Woolley, 1987; Kramm, 1994; Harmer, 1999). However, the possibility exists that a mantle-derived melt interacted with lower crustal granulites or lower crustal melt, however such a crustal component would need to be isotopically primitive and have a relatively low silica content (e.g. mafic granulites) so as not to greatly effect the primary mantle melt composition.

Given the primitive isotopic composition of the alkaline magmatic phases, the effects of crustal contamination are interpreted to be minimal. Consequently, a isotopically heterogeneous source region is considered to be reflected by the differences in initial εNd values between the ijolites and syenites (0.6 – 1.0 and 1.3 – 2.8, respectively; Table 5.9). Differences in trace element and Nd isotopic composition of the Billeroo alkaline magmatic phases from that of depleted mantle requires the existence of a modified mantle source region. This interpretation is supported by the most isotopically primitive ($\varepsilon Nd_i$ = 1.3 and 2.8) and most differentiated alkaline magmatic phases at Billeroo being the syenite phases. As theses phases were the final products of differentiation, and were minimally effected by crustal protoliths, the LREE- and HFSE-enriched composition of the syenites reflects that of the source region.

The Billeroo alkaline magmatic complex provides further proof, in addition to mafic magmatic rocks in the Olary Domain (*Chapter 4*), that the SCLM within the Olary Domain is unusually enriched in HFSE and LREE. A relatively high proportion of elements that are otherwise preferentially partitioned into the crust indicates the SCLM in the Olary Domain has been modified to some degree. Such modification can potentially be achieved through either the incorporation of juvenile subducted sediments into the source region

during convergence along the southern or eastern margins of the NAC between ~1.8 – 1.7 Ga (Betts et al., 2002; Giles et al., 2002), or more likely through metasomatism of the source region. Metasomatic fluids may have been derived from the accretionary margin proposed by Giles et al. (2002) that may have been situated along the southern margin of the NAC. The timing of metasomatism is unclear, however Nd model ages ($T_{DM}$) between ~1830 and 2200 Ma may record this event. This approximate time of crustal extraction is younger than the minimum $T_{DM}$ ages for the Lady Louise Suite (>2230 Ma). A low degree partial melt from a substantial area of modified SCLM could generate alkaline magmatism with appreciable concentrations of incompatible elements, that are further enriched during magmatic differentiation (Woolley, 2001). HFSE and REE abundances of the Billeroo complex are not as enriched as alkaline igneous – carbonatite associations elsewhere (Blichert-Toft et al., 1996; Harmer, 1999; Woolley, 2001), but still imply that a isotopically primitive but relatively HFSE- and REE-enriched mantle reservoir exist in the SCLM at the time of melt generation.

### *5.6.4 Mid-Proterozoic tectonic implications*

On the basis of the development of the regional NE-trending $D_3$ fabric in the alkaline magmatic phases and the surrounding country rock, and the effects of metasomatism and metamorphism on the mineralogy of the alkaline magmatic rocks, the minimum age of intrusion is constrained to be ~1550 Ma (*Chapter 3*). The preservation of Willyama Supergroup metasedimentary clasts within the breccia body that have a bedding parallel foliation that have been crenulated by the $D_3$ fabric constrains the maximum magmatic age to be no earlier than ~1610 Ma, based on the known timing of development of the earliest formed fabrics in the SCP (*Chapter 3*). Therefore the age of the Billeroo complex is constrained to be between ~1610 – 1550 Ma, and coincident with the Olarian Orogeny. Consequently, the Billeroo alkaline magmatic complex represents a member of the rare orogenic or collision-type alkaline magmatic occurrence (Blichert-Toft et al., 1996).

Although the Billeroo alkaline magmatic complex shares compositional similarities with other alkaline magmatic districts (Morbidelli et al., 1995), they are predominantly from very different tectonic settings. Only the nepheline syenites of Southern Victoria Land in Antarctica share a common association of compression followed by extension and the intrusion of alkaline magmas (Worley et al., 1995). With the exception of the Fortaleza alkaline district that is related to predominantly transtensional tectonics (Morbidelli et al., 1995), the majority of alkaline magmatic occurrences are associated with continental rifting (Blichert-Toft et al., 1996; Burke et al., 2003).

As the intrusion of the Billeroo alkaline magmatism was near contemporaneous with bimodal magmatism, crustal anatexis and intrusion of primitive TTG phases in the western Olary Domain (~1585 Ma; Ludwig & Cooper, 1984; Fanning et al., 1998; Barovich & Foden, 2002), then alkaline magmatism occurred during a time when the upper crust was experiencing highly elevated geothermal

gradients, potentially as a response to lithospheric thinning. It is suggested that lithospheric thinning was most likely a response to convective instability (Sandiford & Powell, 1990) in the asthenosphere bought on by an earlier episode of crustal thickening in the Olarian Orogeny (~1610 – 1590 Ma).

### *5.6.5 Carbonatite association*

Although no evidence of carbonatitic melt fractions were found in this study, carbonatitic phases have been reported in company open-file reports (Conor, 2004). The occurrence of coarse-grained calcite crystals in the Billeroo breccia complex may have led to the inference of carbonatitic melts. Additionally, the common occurrence of late-stage calcite veining across the Billeroo complex does indicate that at $CaCO_3$-rich fluids were prevalent. However, interstitial calcite within the different alkaline magmatic phases indicates that a carbonate-rich melt fraction did not separate during differentiation of the silica-undersaturated magma, as has been proposed for the generation of carbonatitic melt (e.g. Lee & Wyllie, 1994; Harmer, 1999). The possibility still exists that carbonatitic immiscible melt intruded contemporaneously with the alkaline magmatic phases, and may be concealed by regolith or broken up during brecciation.

## 5.7 Conclusion

Alkaline magmatism at Billeroo in the northern Olary Domain, South Australia, contains feldspathic ijolite, syenite and lamprophyric phases that intruded the Willyama Supergroup. The alkaline magmatic phases at Billeroo are silica-undersaturated and predominantly nepheline normative, and are characterised by a high alkali content ($K_2O + Na_2O$ = 9-13 wt.%). Unlike many other silica-undersaturated alkaline magmatic occurrences, the Billeroo alkaline complex preserves isotopically primitive initial εNd values (-0.3 to +2.8 at 1590 Ma), consistent with limited degrees of crustal contamination. It is suggested that the SCLM may have attained an unusually alkali- and HFSE-enriched composition through metasomatism of the mantle, possibly during convergence along accretionary margins either at the southern or eastern margin of the NAC between ~1.8 – 1.7 Ga (Fig. 2.4). Fluids derived from a convergent margin, either active during intrusion of the Billeroo alkaline magmas, or prior to the development of the Willyama basin, could have altered the SCLM to the appropriated composition. Low-degree partial melting of the source region generated the primary melt that subsequently underwent differentiation, forming two melt components, one represented by the ijolite and lamprophyric phases, and the other by the syenite phases. It is suggested that partial melting was a response to lithospheric thinning caused by convective instability in the asthenosphere brought about by a prior period of crustal thickening associated with the early Olarian Orogeny. Emplacement of the Billeroo alkaline magmatism was facilitated by upper- to mid-crustal extension and brecciation.

# Chapter 6
# GEOCHEMICAL & ISOTOPIC COMPOSITION OF FE-OXIDE CU-AU MINERALISATION

***SUMMARY***

*ICPMS trace element data of ore separates (sulphides and Fe-oxide), and in situ LA-ICPMS analyses of ore phases, indicate that REE abundances are related to hydrothermal accessory phases associated with the ore phases, and inclusions hosted by ore phases, and not detrital rock fragments incorporated within the mineralised volumes. REE compositions and Nd isotopic compositions of Fe-oxide Cu-Au mineralisation in the southern Curnamona Province are interpreted to have developed during two distinctly different mineralisation events. The first of these events occurred during prograde metamorphism associated with the Olarian Orogeny (~1610 Ma), and formed the stratabound systems at North Portia, Kalkaroo, Waukaloo and Polygonum. The majority of ore samples from the stratabound systems are preferentially enriched in LREEs relative to the HREEs. Nd isotopic compositions of the stratabound ore samples are identical to the Willyama Supergroup metasedimentary sequence ($\varepsilon Nd_{1600}$ = –4.6 to –7.4). Other ore samples within the stratabound systems have highly evolved Nd isotopic compositions at 1600 Ma ($\varepsilon Nd_i$ = –9.4 to –17.2), and are not comparable to any known reservoir in the southern Curnamona Province at Mesoproterozoic times. These ore samples have lower REE abundances, and are less enriched in LREEs. Consequently the latter ore samples with highly evolved Nd isotopic compositions are interpreted to be associated with a second Cu-Au mineralisation event in the southern Curnamona Province, that was most likely associated with the Delamerian Orogeny (~500 Ma). Shear-hosted or shear-related Cu-Au mineralisation have comparable Nd isotopic compositions to the most evolved samples from the stratabound prospects ($\varepsilon Nd_{500}$ = –13.5 to –18.6). These $\varepsilon Nd_i$ values are also comparable to that of the Willyama Supergroup $\varepsilon Nd$ values at 500 Ma. On the basis of ore sample trace element and Nd isotopic compositions, it is proposed that IOCG mineralisation in the southern Curnamona Province was derived from abundant carbonate, evaporitic and exhalative/inhalative horizons in the lower Willyama Supergroup metasedimentary sequence (Ethiudna Subgroup). Highly saline, chlorine-rich fluids migrated through the metasedimentary pile, leaching metals from the metalliferous lower Willyama Supergroup. Deposition of the metals took place predominantly along the redox boundary interface between the lower and upper Willyama Supergroup. Mineralisation was contemporaneous with iron, potassic and sodic alteration. A second mineralisation event, or local remobilisation and reworking of pre-existing mineralisation took place during the Delamerian Orogeny (~500 Ma). This event is associated with propylitic-phyllitic alteration in the stratabound systems, and iron-potassic alteration in the shear-related system. Both mineralisation events share a common metasedimentary source component to the hydrothermal fluid.*

## 6.1 Introduction

The iron-oxide copper-gold (IOCG) styles of mineralisation have attracted great interest from researchers and explorationists, especially within Palaeo- and Mesoproterozoic terranes of Australia. These periods were marked by widespread development of IOCG mineralisation in Australia (e.g., Hitzman et al., 1992; Davidson & Large, 1994; 1998; Williams, 1998b; Partington & Williams, 2000). IOCG mineralisation occurred in three periods spanning 1.9 – 1.5 Ga (Williams & Skirrow, 2000). IOCG mineralisation in the Tennant Creek district occurred at ~1.85 Ga (Compston, 1995; Davidson & Large, 1998), at ~1.6 Ga in the Olympic Dam Cu-Au province and southern Curnamona Province (Haynes et al., 1995; Johnson & McCulloch, 1995; Johnson & Cross, 1995; Skirrow et al., 2000) and at ~1.55 – 1.5 Ga in the Cloncurry district (Pollard & Perkins, 1997; Williams & Skirrow, 2000; Fig. 6.1).

Understanding the genesis of each of the IOCG provinces in Proterozoic Australia is critical not only for expanding our knowledge of the formation of IOCG systems, but also in assisting exploration models in Proterozoic Australia. As yet, there has only been limited work done on the IOCG systems in the southern Curnamona Province (SCP) (e.g. Teale & Fanning, 2000a; Skirrow et al., 2000; Williams & Skirrow, 2000; summarised in *Chapter 2*). This is in contrast to numerous studies completed on the Cloncurry District (e.g., Williams, 1998b; Pollard, 2001; Mark et al., 2004; Oliver et al., 2004; Mark et al., 2005; *and references therein*), and on the Olympic Dam Cu-Au province (e.g., Haynes et al., 1995; Johnson & Cross, 1995; Johnson & McCulloch, 1995; Reynolds, 2000; Skirrow

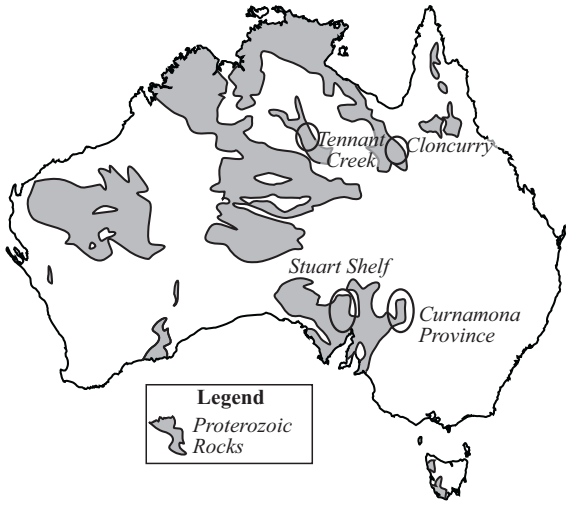


**Figure 6.1.** Map highlighting location of major iron-oxide copper-gold districts within Proterozoic rocks of Australia. Distribution of Proterozoic rocks highlighted by shading.

et al., 2002; Ferris et al., 2002; *and references therein*). Given the similarities between the lithostratigraphy and mineralisation styles of the Willyama Supergroup with the Mt Isa region (Yates, 1992; Laing, 1996c), further studies on IOCG systems in the Curnamona Province are warranted.

Due to the diversity of IOCG-type deposits, there has been much discussion over the source of the fluids responsible for alteration and mineralisation, and the role of magmatism in their generation (e.g., Johnson & McCulloch, 1995; Hitzman et al., 1992; Gleason et al., 2000; Hitzman, 2000). Models proposed include sedimentary-exhalative types (e.g., Parak, 1988), intrusion of immiscible Fe-oxide sulphide melts (Frietsch, 1989), or other types of magmatically dominated systems (e.g., Perring et al., 2000; Pollard, 2000; Pollard, 2001); and hydrothermal replacement and wall rock controlled systems (Hitzman et al., 1992; Haynes et al., 1995; Barton & Johnson, 1996; 2000). Although the sedimentary-exhalative and Fe-oxide melt models have more recently been discounted by geological and experimental criteria, the genesis of IOCG systems is still poorly understood (*see review by* Partington & Williams, 2000).

Conventional stable isotope (S and O) and fluid inclusion studies are typically applied to mineralised systems to understand potential fluid and/or metal sources. These techniques can be equivocal in identifying sources when multiple hydrothermal fluids may be involved, and are better indices of the processes operating. If the different mineralising and alteration fluids have different compositions, then upon ore deposition they can reflect a mixed isotopic signature (e.g., Haynes et al., 1995). Alternatively, convective homogenisation of a mixed fluid source can lead to a relatively uniform isotopic composition in the hydrothermal fluid, and subsequently relinquish information on the end-member fluid components (e.g. evaporitic or seawater sulphate, igneous sulphides; Bierlein et al., 1996a, b).

In addition to stable isotopes and fluid inclusion studies, other techniques that have been useful in understanding hydrothermal systems include trace element and radiogenic isotope studies (e.g. Campbell et al., 1998). The different radiogenic isotopic systems (e.g. Pb-Pb, Re-Os, Ar-Ar, Sm-Nd), can not only provide geochronological constraints, but can also be useful as ore fluid tracers (e.g., Campbell et al., 1998), although they too are to some degree open to water/rock effects along fluid pathways (Farmer & DePaolo, 1997). Furthermore, the use of immobile trace elements, particularly the high field strength elements (HFSE; e.g. Th, U, Zr, Hf, Ti, Nb, Ta) and rare earth elements (REE), as petrogenetic tracers has long been recognised

(e.g. Pearce & Cann, 1973; Winchester & Floyd, 1977; Pearce & Norry, 1979; Wood, 1980; Meschede, 1986). However, typically the immobility or mobility of the REE, Th and U depends on the specific hydrothermal environment in question, and the geochemical characteristics of the hydrothermal fluid (e.g. Wood, 1990; Bau, 1991; Lottermoser, 1992; Ward et al., 1992; Poitrasson et al., 1995; Lewis et al., 1997; de Jong et al., 1998; Gimeno-Serrano et al., 2000; Smith et al., 2000; Rolland et al., 2003). A proliferation of studies on REE behaviour associated with different hydrothermal environments provides some insights into the relative immobility or mobility of the REE elements at varying fluid temperatures and compositions (*see below*; e.g. Graf, 1977; Taylor & Fryer, 1982; Michard & Albaréde, 1986; Michard, 1989; Wood, 1990; Haas et al., 1995; Douville et al., 1999).

The Nd isotopic character of host rocks and potential source rocks also needs to be constrained to accurately assess the potential influences of these reservoirs on the evolving hydrothermal system. Nd isotopic constraints on the supracrustal rocks of the SCP are well established. Potential source components to mineralisation include the Willyama Supergroup metasediments (Barovich, 2003; Barovich et al., 2002; *Appendix 1*); ~1700 Ma A-type, I-type and S-type granitoids (Ashley et al., 1996; Barovich & Hand, 2004; *Appendix 1*); ~1685 Ma tholeiitic mafic magmatism (*Chapter 4*); syn-tectonic alkaline magmatism (*Chapter 5*); and syn- to post-tectonic bimodal (predominantly felsic) magmatism (Barovich, 2003; Barovich & Foden, 2002; *Appendix 1*).

This chapter summarises the trace element geochemistry and Nd isotopic composition of mineralised volumes (sulphides and Fe-oxides) from seven IOCG prospects in the SCP (Fig. 6.2). Limited stable isotope and fluid inclusion data exists for some of the IOCG prospects in the SCP (Skirrow et al., 2000; Williams & Skirrow, 2000; Chapter 2). This information provides useful constraints that can potentially aid in interpreting the REE and Nd isotopic compositions of ore samples from IOCG systems in the SCP. The siting of REE in the ore samples is assessed using ICPMS trace element data, and *in situ* laser ablation inductively coupled plasma mass spectrometry (LA-ICPMS) analyses of the mineralised volumes. The Nd isotopic composition of the mineralised volumes are described, and in conjunction with the trace element data, used to assess potential sources of IOCG mineralisation in the SCP (e.g. Willyama metasediments or magmatic phases).

## 6.2 IOCG mineralisation in the SCP

Brief descriptions of some of the prospects and mineralisation styles are outlined elsewhere (e.g. Williams & Skirrow, 2000; Skirrow et al., 2000; Teale & Fanning, 2000a; 2000b). The major outcomes of these studies are detailed in *Chapter 2.2*. Detailed summaries of the seven IOCG mineral systems analysed in this study are given in *Appendix 8*. In summary, the four prospects North Portia, Kalkaroo, Waukaloo and Polygonum are located in the relatively low metamorphic grade (greenschist facies) region of the northern SCP (Fig. 6.2). Primary mineralisation at these prospects is stratabound and locally stratiform. Mineralisation is disseminated, and also occurs as replacements and vein networks

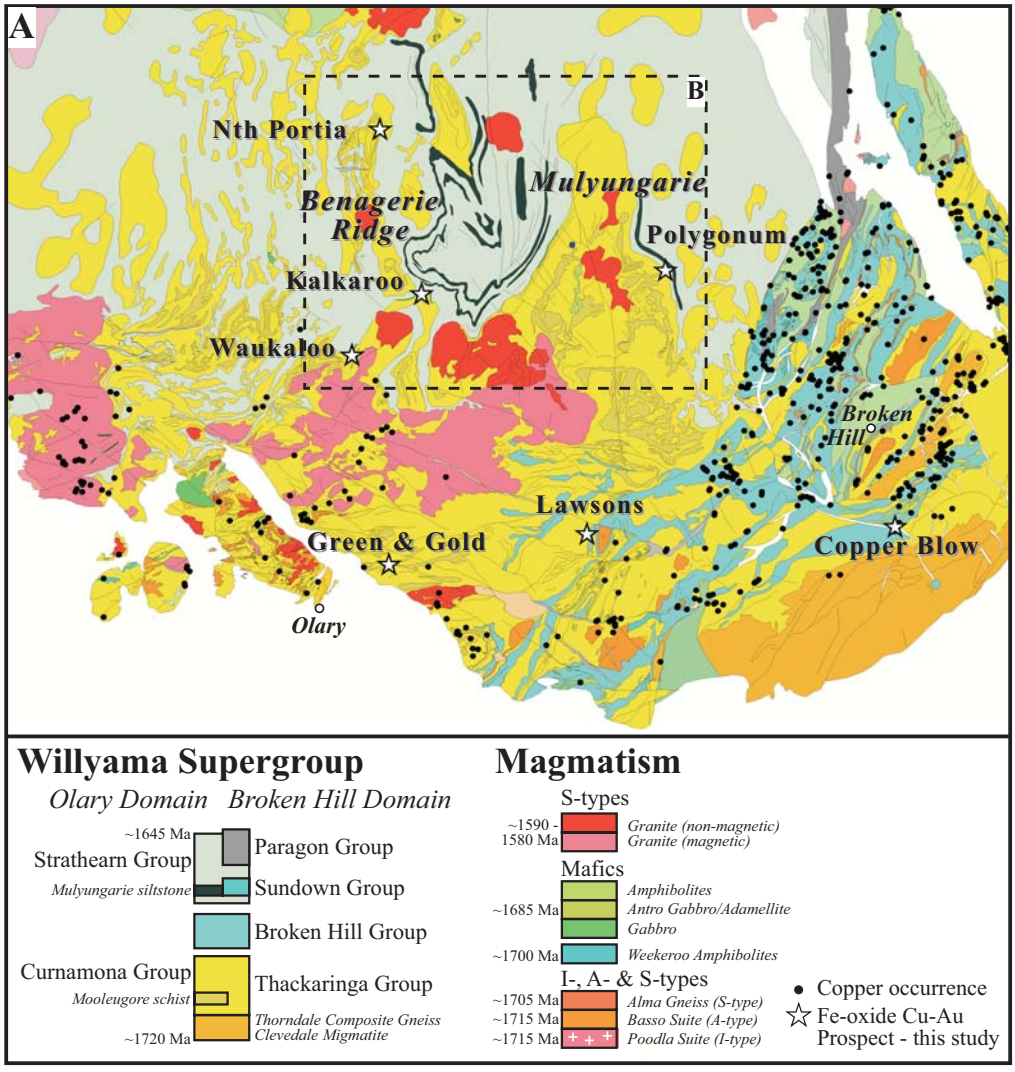


**Figure 6.2.** (a) Interpreted solid geology of southern Curnamona Province showing localities of iron-oxide copper-gold (IOCG) prospects in this study (*stars*) and anomalous copper occurrences (*dots*; Jenkins & Burtt, 2003).(b) Total magnetic intensity image of the Benagerie Ridge and Mulyungarie regions showing locations of known prospects (italics represents those included in this study; *North Portia*, Shylock, *Kalkaroo*, *Waukaloo*, Hunters Dam, Crabb Dam, *Polygonum*; Jenkins & Burtt, 2003). Position of the Bimba Formation and/or redox boundary highlighted.

(Williams & Skirrow, 2000; Teale & Fanning, 2000a; Leyh, 1995). Prospects of the Benagerie Ridge region (e.g. North Portia, Kalkaroo, Waukaloo) and Mulyungarie region (Polygonum; Fig. 6.2) are the largest known IOCG systems in the SCP. They are commonly associated with gravity and/or magnetic anomalies related to large zones of magnetite alteration or ironstones (Fig. 6.2b). Aeromagnetic data also displays what has been interpreted as fold interference patterns in the Benagerie Ridge and Mulyungarie regions, which was attributed to complex folding of the stratigraphy (Hayward, 1998). The North Portia, Kalkaroo and Polygonum prospects are concealed below cover sequences of up to ~150m in thickness.

The Lawsons, Green & Gold and Copper

Blow prospects, occur within the higher metamorphic grade region (amphibolite – granulite facies) of the SCP (Fig. 6.2). These prospects are shear zone-hosted, or located proximal to major shear zones. Mineralisation typically occurs as replacements and vein networks in the shear related prospects (e.g. Burton, 1994; Williams & Skirrow, 2000). Mineralisation in these prospects occur in the form of ferruginous gossan and secondary copper mineralisation (e.g. ironstone and malachite). Several studies have shown that much of the shear zone development occurred during the Delamerian Orogeny, some of which contain known Cu-Au association (e.g. Walparuta, Kings Dam, Mutooroo and Billeroo shear zones; Dutch et al., 2005).

## 6.3 Rare earth element systematics and Nd isotopes in hydrothermal systems

Studies utilising REE as tracers in mineralised systems have mainly focussed on using the REE as a tool for identifying highly altered protoliths, which may assist in identifying metal bearing or barren horizons. The use of REE in this way as an exploration tool has been applied in the vicinity of Pb-Zn-Ag or Cu-Zn stratabound massive sulphide deposits (e.g. Campbell et al., 1982; Lesher et al., 1985; Lambert & Simmons, 1988; Schandl et al., 1995; Bjerkgård & Bjørlykke, 1995; Gale et al., 1997). Similar applications have also been found in other mineralisation styles such as lode gold deposits (Fleet et al., 1997). Using REE directly as ore fluid tracers on mineralised volumes (i.e. ore samples and/or sulphide separates) is not a technique that has been widely used, but has been applied to a variety of mineralisation styles (e.g. VHMS deposits: Campbell et al., 1982; Gale et al., 1997; Davidson et al., 2001; MVT deposits: Graf, 1990; and gold deposits: Siva Siddaiah et al., 1994; Fleet et al., 1997; Giritharan & Rajamani, 2001). Such studies typically focus on hydrothermal accessory phases associated with mineralisation (e.g. fluorite, scheelite, apatite, titanite, tourmaline; Slack, 1999; Bau et al., 2003; Rolland et al., 2003), and not directly on ore minerals. This study focuses directly on the mineralised volumes. Consequently, REE systematics and behaviour in a variety of different hydrothermal fluids are assessed, as some are similar environments to those in IOCG ore systems. In addition, the application of Nd isotopic studies to ore fluid systems in general will be discussed.

### *6.3.1 REE systematics and behaviour*

The REE readily form complexes across the stability conditions of aqueous solutions, with only very low temperatures being the exception, where they can exist as unassociated ions (e.g. Haas et al., 1995; Fig. 6.3). Behaviour of REE complexes in hydrothermal systems is governed by factors including temperature, pH, oxygen fugacity ($fO_2$), and the concentration of potential REE ligands and their individual activities (e.g. chloride-, sulphate-, carbonate-, hydroxide-, bi-carbonate-, fluoride-, and phosphate-complexes). Variations in these parameters affects not only which REE-complexes will be dominant in a hydrothermal fluid, but also the stability of REE-bearing mineral phases (e.g. Haas et al., 1995; Rolland et al., 2003). Therefore, if the REE geochemistry of phases

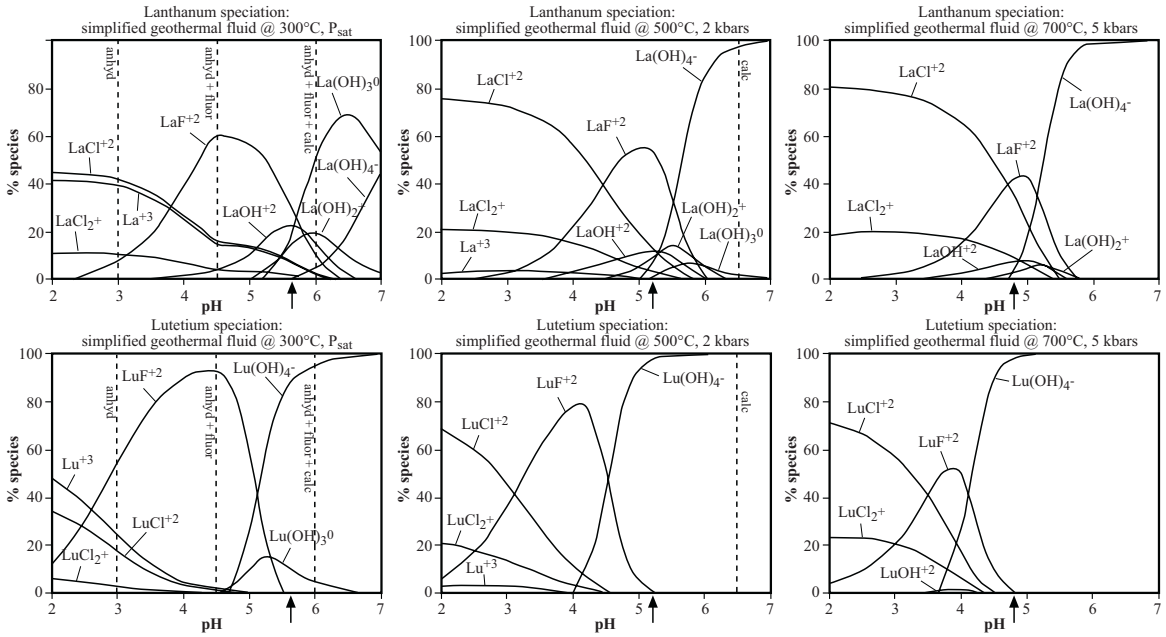


**Figure 6.3.** Results of speciation calculation for a simulated geothermal fluid at 300°C, $P_{sat}$; 500°C, 2 kbars; 700°C, 5 kbars (Haas et al., 1995). The percentage of each species is plotted against fluid pH. Vertical dashed lines represent minimum pH of fluid saturation with noted mineral assemblages. Vertical arrow along abscissa shows point of neutral pH at given temperature and pressure. Modelled fluid composition is $Na^+$ = charge bal., 0.1 M $K^+$, ≤0.1 M $Ca^{2+}$, 1 M $Cl^-$, ≤0.001 M $F^-$, ≤0.001 M $C_{tot}$, ≤0.01 M $S_{tot}$, $La^{+3}$ = 1 ppb, $Lu^{+3}$ = 1 ppb, $I_{tot}$ ~ 1.

precipitated from a hydrothermal fluid are a proxy for the REE geochemistry of the hydrothermal fluid, they can be useful in assessing where the fluids came from, and what the most likely source of metals were.

Studies on REE behaviour in a variety of hydrothermal systems, both in non-mineralising environments (e.g. mid-ocean ridges: Michard & Albaréde, 1986; Douville et al., 1999; Klinkhammer et al., 1994; back-arc basins: Klinkhammer et al., 1994; continental geothermal fields: Michard, 1989; Lewis et al., 1997), and in mineralised environments (e.g. VHMS deposits: Schandl et al., 1995; porphyry copper: Taylor & Fryer, 1982; Fleet et al., 1997; hydrothermal uranium: Taylor & Fryer, 1982; mesothermal gold: Giritharan & Rajamani, 2001), provide information about the behaviour of REE in different hydrothermal solutions. The dominant complexing agent in a hydrothermal solution is primarily a function of pH and the relative abundance of anions present (Haas et al., 1995). At relatively high temperatures and pressures (>300°C, >3 kbars; Fig. 6.3), REE-chloride complexes are dominant under acidic conditions, REE-fluorides are the dominant species at near neutral conditions, and REE-hydroxide and carbonate complexes are the dominant species under basic conditions (Haas et al., 1995). However, at lower temperatures and pressures, sulphate and carbonate complexes can account for a larger fraction of REE complexes in solution, and in some cases can be the predominant species (Haas et al., 1995). The formation of carbonate complexes is inhibited at low pH, but can control the mobility of REE at higher pH (Michard & Albarede, 1986; Wood, 1990).

Within the context of IOCG mineralisation, chloride complexes are the dominant ligand in IOCG systems worldwide (e.g. Huston & Large, 1989; Davidson & Large, 1994; Fig. 6.4). This is a function of the relatively high

salinity of Cu-Au bearing solutions (15 – 35 equiv. wt% NaCl), relatively high temperatures (300 – 450°C), and low pH fluid environments (Davidson & Large, 1994; Fig. 6.4). Consequently, chloride-complexes have the potential to influence the REE behaviour more than any other ligand. Although chloride-complexes are the dominant ligand, accessory phases identified by petrographic observations (*Appendix 8*) indicate that carbonate-, phosphate-, sulphate- and fluoride-complexes were also present in minor quantities. Carbonate, bicarbonate and fluoride complexes are particularly relevant in the mobility of the HREE in IOCG systems, whereas on the basis of pH, hydroxide complexes are unlikely.

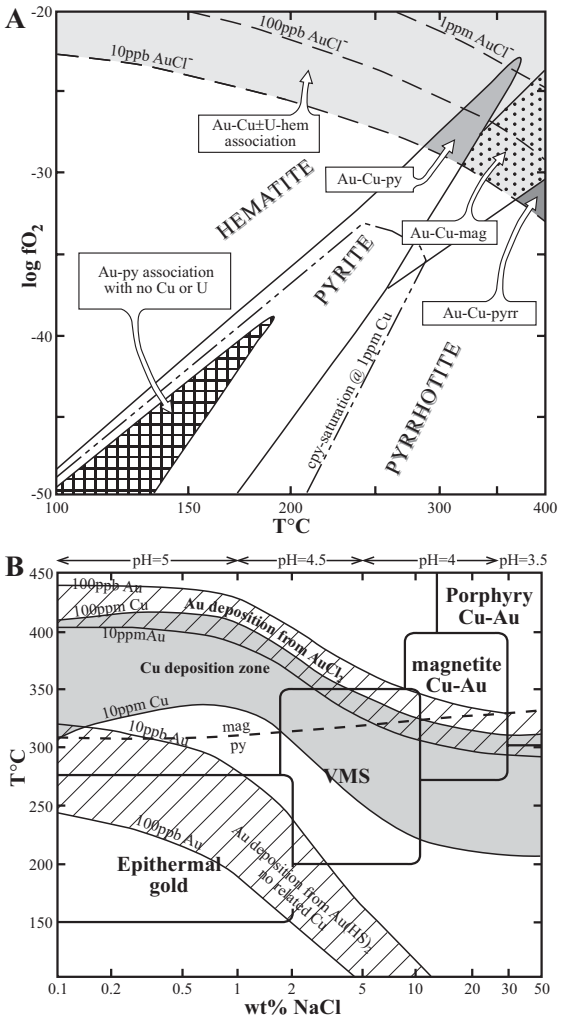


**Figure 6.4.** (a) Fields of gold transport and deposition in $fO_2$-temperature space. The Cu-Au association is controlled by the stability of $AuCl_2^-$ complexes (high T and $fO_2$. Fluid conditions: $a_{\Sigma S} = 10^{-3}$, $a_{Cl^-} = 10^{0.5}$, pH = 4 (Davidson & Large, 1994); (b) Temperature-salinity diagram modelling relationship between fluid chemistry and deposit type. IOCG styles occur at the overlap zone for both Cu and Au deposition from chloride complexes (Davidson & Large, 1994).

### *6.3.2 Nd isotope applications to mineralisation*

Studies utilising radiogenic isotopes (Pb, Nd, Sr) on mineralised systems are numerous (*reviewed by* Campbell et al., 1998). Of particular interest to this study is the use of the Nd isotopic system on mineralised volumes. Pb and Sr isotopic compositions of the different IOCG systems were not analysed, as insufficient data exists for these isotopic systems on the different rock reservoirs in the SCP that may have contributed to mineralisation. This information is particularly critical in Pb isotopic studies on ore systems in order to gain insight into which particular rock reservoir a hydrothermal fluid may have flowed through (e.g. Tosdal et al., 1999).

Nd isotopic analyses of mineralisation and host rocks have been utilised on several mineralisation styles, including massive sulphide deposits (e.g. Childe, 1996; Kumpulainen et al., 1996; Watanabe et al., 1998; Jiang et al., 2000; Relvas et al., 2001); Ni-Cu mineralisation (Ripley et al., 1999; Prevec et al., 2000); U mineralisation (Maas et al., 1987); gold deposits (Campbell et al., 1998; Frei et al., 1998; Stendal et al., 2001; Yang & Zhou, 2001); skarn and porphyry copper systems (Dupont et al., 2002); and iron-oxide copper-gold (IOCG) systems (Johnson & McCulloch, 1995; Campbell et al., 1998; Gleason et al., 2000). These studies have shown that radiogenic isotopes are useful for unravelling fluid characteristics, fluid

sources and metal sources of mineralised systems. The Nd isotopic system is therefore crucial to this study, given the extensive Nd isotope dataset that exists for protoliths within the SCP that can be compared to the Nd isotopic signature of IOCG mineralisation (e.g. Ashley et al., 1996; Barovich, 2003; Barovich & Foden, 2002; Barovich et al., 2002).

## 6.4 Analytical procedures

Ore samples taken from the seven IOCG prospects (*Appendix 8*) were separated from host rock lithologies. Mineralisation occurs as predominantly replacement styles, although vein-styles also occur (e.g., samples *BN1*, *BN5*, *K7*, *K9*, *GG19*; *Appendix 8*). Different sulphide phases were separated by hand picking, such that each sample is composed of pure sulphide. Silicates associated with mineralisation were physically removed, as were host rocks fragments. Samples finer than <125 μm that were too fine for handpicking, were magnetically separated on the Franz isodynamic separator. Individual ore samples were homogenised by milling with an agate mortar and pestle. Although all care was taken, some micro-inclusions of accessory and/or gangue phases would have been homogenised with the milled samples.

### *6.4.1 LA-ICPMS*

In order to investigate the siting of REEs within the different samples, LA-ICPMS data was acquired at the Centre for Ore Deposit Research (CODES), School of Earth Sciences, University of Tasmania. Off-cuts of the same mineralised volumes used for chemical and isotopic analysis were mounted in epoxy resin blocks and polished. Reflected light microscopy and SEM analysis of the polished blocks identified primary phases (*Appendix 8*), and assisted in locating specific sites where *in situ* analysis was required. Analyses were conducted on an Agilent HP 4500 ICP-MS with a Merchantek 213nm laser by Sarah Gilbert. LA-ICPMS analyses were obtained using a 60-80 μm diameter spot size, a laser repetition rate of 5-10 Hz, and a power density setting of ~ 6 J/cm$^2$. This produced steady signals and count rates sufficient for analysis. Elements analysed for were $^{27}$Al, $^{43}$Ca, $^{49}$Ti, $^{65}$Cu, $^{90}$Zr, $^{137}$Ba, $^{139}$La, $^{140}$Ce, $^{146}$Nd, $^{147}$Sm, $^{153}$Eu, $^{157}$Gd, $^{163}$Dy, $^{166}$Er, $^{172}$Yb, $^{232}$Th and $^{238}$U (isotope of element analysed in superscript; Table 6.1). Data were collected in time-resolved mode using 20 ms dwell time per mass. For each analysis, data were collected for ~100 s, including ~30 s of instrumental background. After ablation initiation, ~5-10s were required for signal stabilisation, which was excluded on visual inspection of each spectrum during the data collection process. Concentration and detection limits were calculated using modified data-reduction software (Longerich et al., 1996). Each set of analytical results were normalised to the Fe content of the sample as an internal standard. Four analyses of the calibration standard (STDGL-1) were made for every 16-20 unknowns. STDGL-1 is an in-house calibration standard at the School of Earth Sciences, University of Tasmania, designed specifically for the analysis of sulphides (Norman et al., 2003; Danyushevsky et al., 2003). Drift corrections were applied using a weighted mean of the standards composition.

### *6.4.2 Trace elements*

Trace elements were analysed in solution using ICP-MS (Table 6.2, 6.3). Analysis of trace and REE was achieved by digestion of up to 0.5 g of analytical pulp in HF/multi-acid solution and presented to an ICPMS for quantification of elements of interest. All dissolution and element analyses were carried out at Amdel Laboratories, Adelaide. The following elements were analysed: Fe, Cu, Co, Cr, Ag, As, Mo, Zn, Pb, Ni, Ca, K, Mg, Mn, Na, P, Ti, V, Bi, Cd, Cs, Ga, In, Nb, Tb, Sb, Se, Sr, Te, Th, Tl, U, W, Y and REE. Detection limits range from 100 ppm for Fe, to between 10 – 0.1 ppm for the remainder of the elements, with the majority of elements having a detection limit better than 0.5 ppm. Detection limits for REE range between 0.5 – 0.02 ppm.

### *6.4.3 Sm-Nd isotopes*

The dissolution technique for sulphides was based on that of Jiang et al (2000). Milled samples were spiked with a $^{150}Nd$-$^{149}Sm$ solution, and digested in Teflon vials at 130°C in 4mL of 7N $HNO_3$ for ~24 hours until completely evaporated. Another 4mL of 7N $HNO_3$ was added, and vials capped and heated for 48 hours at 130°C. Samples were evaporated to dryness at 130°C. 6mL of 6N HCL was added and evaporated to dryness at 130°C. Another 6mL of HCL was added, and vials capped and heated at 130C for 12 hours. Samples were then evaporated to dryness before adding 1.5mL of 2N HCL and performing column chemistry. Nd and Sm concentrations were calculated by isotope dilution, with Nd isotope ratios measured by thermal ionisation mass spectrometry (TIMS) on a Finnigan MAT 262 mass spectrometer, and Sm isotope ratios measured on a Finnigan MAT 261 mass spectrometer. Nd blanks carried out during the course of the analyses range from 101 to 108 pg. The $^{143}Nd/^{144}Nd$ ratio is normalised to $^{146}Nd/^{144}Nd = 0.721903$. The $^{143}Nd/^{144}Nd$ ratio of the in-house standard (Johnson-Matthey) during the course of the analyses was $0.511594 \pm 0.000006$ ($1\sigma$, n=5). Running average for La Jolla over the year is quoted in Chapter 4. Sm-Nd isotopic compositions of all samples are listed in Table 6.4.

## 6.5 *In situ* analyses and the siting of REE within ore minerals

The absolute abundances of REE within pyrite, chalcopyrite and Fe-oxides were analysed using LA-ICPMS (Table 6.1). This was done to precisely determine the quantities of REE within the primary ore phases, i.e. other than the proportion derived from accessory REE-bearing phases (e.g. monazite and/or zircon). Also of interest is how the REE are situated within the sulphides and Fe-oxides. The greatest benefit of the LA-ICPMS technique is that it is possible to visually monitor the ablation profile to assess how the quantity of an element varies within a specific phase during a single ablation (Fig. 6.5). This makes it possible to determine whether the calculated abundances are due to constant counts/second rates, or punctuated counts/second rates. Consequently it is possible to assess whether a given element or group of elements is housed within the crystallographic structure of the analysed phase, or hosted within an inclusion,

since coarse inclusions will result in transiently elevated elemental contributions as the laser ablates them. A more difficult situation is the separation of inclusion micro-clusters that are uniformly distributed within crystals, and for this, a method such as Mossbauer spectroscopy or SIMS is required (but was not undertaken).

Samples analysed by LA-ICPMS are the same polished blocks that are petrographically described in *Appendix 8*. All results are listed in Table 6.1 at ppm level, with each element from each analysis having a unique analytical precision (%; shaded number in Table 6.1). Detection limits are also unique for each element in each analysis, and are individually listed.

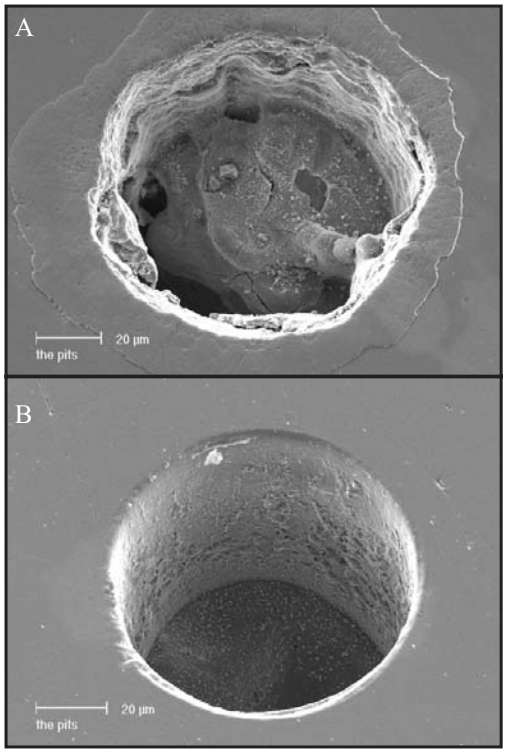


**Figure 6.5.** Secondary electron images of LA-ICPMS analysis points in (a) chalcopyrite; (b) pyrite.

### *6.5.1 Total REE abundance determined by LA-ICPMS analyses*

The majority of LA-ICPMS analyses on different phases from the IOCG prospects have REE concentrations below that of detection limits (~<10 ppb). Those analyses that are above detection limit have concentrations as high as 50 ppb, however most are in the range of <20 ppb (Table 6.1). There is no relationship between which phase was analysed and total REE concentration. Additionally, there is no preference towards any specific REE group being any more abundant than another group. Both LREE enriched analyses (e.g. analytical points *BN5 01*, *BN5 06*, *K705*, *K708*, *WA1 06*, *GG19 01*, *GG19 02*, *GG19 06*, *GG19 11*) and HREE enriched analyses (e.g. analytical points *K703*, *WA1 04*, *WA1 09*, *GG19 08*) are observed (Table 6.1). Some samples are enriched in all of the REE (e.g. analytical points *WA1 02*, *CB602*, *CB604*, *CB607*, *CB608*, *CB609*; Table 6.1).

### *6.5.2 Siting of REE in sulphides and iron oxides*

Two types of patterns are observed for the REE in the counts/second versus ablation time plots (Fig. 6.6). In the most common type, the count/second rates for the REE are simultaneously punctuated (i.e. counts/second spike), as would be expected if ablation of a REE-bearing inclusion, or a REE-bearing phase adsorbed onto a phase surface occurred (herein referred to as 'inclusion-type'). Analyses of the inclusion-types are most spectacularly observed in ablations of chalcopyrite grains from the Waukaloo prospect (Fig. 6.6a, b). Analytical points *WA1 02* and *WA1 04* show that the HREE (Dy, Er, Yb: 282 – 537 ppb) are the most abundant within the REE-bearing inclusions, with lesser quantities of MREE (Sm, Eu, Gd: 29 – 198

**Table 6.1.** Laser ablation ICP-MS data of individual points analysed for rare earth element content (ppm). Analytical precision (%; shaded) and detection limit of each element from each analytical point shown.

| Sample | Prospect | Phase | Point no. | $Al^{27}$ | $Ca^{43}$ | $Ti^{49}$ | $Fe^{57}$ | $Cu^{65}$ | $Zr^{90}$ | $Ba^{137}$ | $La^{139}$ | $Ce^{140}$ | $Nd^{146}$ | $Sm^{147}$ | $Eu^{153}$ | $Gd^{157}$ | $Dy^{163}$ | $Er^{166}$ | $Yb^{172}$ | $Th^{232}$ | $U^{238}$ |
|---|---|---|---|---|---|---|---|---|---|---|---|---|---|---|---|---|---|---|---|---|---|
| BN1 | Nth. Portia | py | BN102 py | 0.802 | 35.223 | 14.218 | 465500 | 4320.706 | <0.005 | <0.02 | <0.002 | 0.008 | <0.01 | <0.013 | <0.004 | 0.008 | <0.008 | <0.004 | <0.007 | <0.003 | <0.003 |
| | | | | 60 | 16 | 5 | 6 | 19 | | | | 76 | | | | 48 | | | | | |
| BN1 | Nth. Portia | py | BN103 py | 0.277 | 57.511 | 15.328 | 465500 | 5760.049 | <0.004 | <0.023 | <0.003 | <0.002 | <0.011 | <0.012 | <0.004 | <0.01 | <0.007 | <0.007 | <0.008 | <0.003 | 0.020 |
| | | | | 12 | 9 | 4 | 5 | 9 | | | | | | | | | | | | | 61 |
| BN1 | Nth. Portia | py | BN106 py | 0.123 | 44.669 | 15.893 | 465500 | 941.122 | <0.002 | 0.019 | <0.002 | 0.003 | <0.005 | <0.007 | <0.001 | <0.006 | <0.005 | <0.004 | <0.005 | 0.024 | 0.007 |
| | | | | 9 | 11 | 4 | 5 | 16 | | 35 | | 53 | | | | | | | | 34 | 83 |
| BN1 | Nth. Portia | py | BN107 py | 0.211 | 39.525 | 15.295 | 465500 | 0.889 | <0.004 | <0.018 | <0.002 | <0.002 | <0.008 | <0.01 | <0.002 | <0.009 | <0.006 | <0.003 | <0.007 | 0.040 | <0.002 |
| | | | | 15 | 14 | 5 | 6 | 28 | | | | | | | | | | | | 40 | |
| BN1 | Nth. Portia | cpy | BN101 cpy | 0.164 | 122.702 | 14.372 | 304300 | 367387 | <0.007 | 0.179 | <0.005 | <0.004 | <0.017 | <0.02 | <0.004 | <0.024 | <0.011 | <0.009 | <0.015 | <0.004 | <0.004 |
| | | | | 14 | 8 | 4 | 3 | 3 | | 13 | | | | | | | | | | | |
| BN1 | Nth. Portia | cpy | BN104 cpy | 0.147 | 159.934 | 14.366 | 304300 | 351540 | <0.01 | 0.170 | <0.005 | <0.005 | <0.02 | <0.035 | <0.008 | <0.021 | <0.018 | <0.012 | 0.018 | <0.007 | <0.005 |
| | | | | 20 | 7 | 4 | 3 | 3 | | 17 | | | | | | | | | 22 | | |
| BN1 | Nth. Portia | cpy | BN105 cpy | 0.117 | 146.136 | 14.087 | 304300 | 353735 | <0.007 | <0.05 | <0.006 | <0.006 | <0.02 | <0.022 | <0.009 | 0.016 | <0.015 | <0.012 | 0.014 | <0.005 | <0.005 |
| | | | | 21 | 7 | 4 | 3 | 3 | | | | | | | | 43 | | | 39 | | |
| BN5 | Nth. Portia | py | BN5 01 py | 0.090 | 10.868 | 11.879 | 465500 | 0.208 | <0.005 | <0.02 | <0.002 | 0.007 | <0.007 | 0.010 | 0.003 | <0.01 | 0.041 | <0.005 | <0.008 | 0.013 | 0.020 |
| | | | | 24 | 36 | 5 | 6 | 28 | | | | 53 | | 38 | 98 | | 94 | | | 33 | 67 |
| BN5 | Nth. Portia | py | BN5 03 py | 0.637 | 25.284 | 16.655 | 465500 | 851.879 | 0.005 | 0.478 | <0.002 | 0.004 | <0.009 | <0.012 | <0.003 | <0.012 | <0.007 | <0.004 | <0.007 | 0.123 | 0.007 |
| | | | | 17 | 18 | 4 | 4 | 22 | 43 | 43 | | 59 | | | | | | | | 28 | 89 |
| BN5 | Nth. Portia | py | BN5 06 py | 1.306 | 31.960 | 13.349 | 465500 | 41.121 | 0.005 | <0.016 | 0.004 | 0.009 | <0.009 | 0.027 | 0.004 | <0.008 | <0.007 | <0.005 | <0.005 | 0.005 | 0.029 |
| | | | | 9 | 13 | 4 | 5 | 100 | 33 | | 24 | 41 | | 38 | 86 | | | | | 27 | 53 |
| BN5 | Nth. Portia | py | BN5 08 py | 3.836 | 34.895 | 12.285 | 465500 | 0.195 | <0.004 | 0.032 | 0.002 | <0.001 | <0.009 | <0.012 | <0.003 | <0.008 | <0.006 | <0.004 | 0.009 | 0.004 | 0.006 |
| | | | | 28 | 14 | 4 | 5 | 36 | | 43 | 74 | | | | | | | | 71 | 43 | 103 |
| BN5 | Nth. Portia | cpy | BN5 02 cpy | 0.614 | 157.644 | 14.656 | 304300 | 363861 | 0.030 | 0.224 | <0.005 | <0.004 | <0.016 | <0.026 | <0.006 | <0.028 | <0.014 | <0.01 | <0.016 | 0.114 | 0.009 |
| | | | | 16 | 7 | 4 | 3 | 3 | 30 | 25 | | | | | | | | | | 22 | 88 |
| BN5 | Nth. Portia | cpy | BN5 04 cpy | 1.352 | 202.481 | 13.206 | 304300 | 361233 | <0.013 | <0.038 | <0.004 | <0.005 | <0.025 | <0.02 | <0.007 | <0.022 | <0.013 | <0.01 | <0.016 | 0.022 | <0.006 |
| | | | | 15 | 8 | 4 | 4 | 3 | | | | | | | | | | | | 29 | |
| BN5 | Nth. Portia | cpy | BN5 05 cpy | 0.313 | 148.874 | 13.287 | 304300 | 365248 | <0.01 | <0.042 | 0.006 | <0.006 | <0.017 | <0.021 | <0.008 | <0.027 | <0.016 | <0.009 | <0.019 | 0.012 | <0.005 |
| | | | | 12 | 9 | 4 | 4 | 4 | | | 37 | | | | | | | | | 35 | |
| BN5 | Nth. Portia | cpy | BN5 07 cpy | 0.298 | 126.585 | 10.542 | 304300 | 369427 | <0.012 | <0.042 | <0.005 | <0.005 | <0.025 | <0.028 | <0.007 | <0.016 | <0.013 | <0.011 | <0.014 | <0.006 | <0.004 |
| | | | | 12 | 10 | 5 | 4 | 3 | | | | | | | | | | | | | |
| BN600 | Nth. Portia | cpy | BN600 04 cpy | 0.123 | 119.620 | 14.457 | 304300 | 331773 | <0.008 | 0.460 | <0.004 | <0.004 | <0.018 | <0.022 | <0.005 | <0.018 | <0.016 | <0.014 | <0.017 | <0.007 | <0.006 |
| | | | | 18 | 9 | 4 | 4 | 3 | | 11 | | | | | | | | | | | |
| BN600 | Nth. Portia | cpy | BN600 05 cpy | 0.267 | 118.958 | 15.179 | 304300 | 367947 | <0.009 | <0.047 | <0.005 | <0.006 | <0.021 | <0.022 | <0.007 | <0.023 | <0.017 | <0.007 | <0.012 | <0.005 | <0.004 |
| | | | | 19 | 10 | 4 | 3 | 4 | | | | | | | | | | | | | |
| K7 | Kalkaroo | py | K703 py | 522.845 | 37.031 | 38.618 | 465500 | 66.902 | 4.936 | 13.401 | <0.005 | 0.022 | <0.02 | <0.026 | 0.008 | 0.030 | 0.079 | 0.059 | 0.070 | 0.097 | 0.127 |
| | | | | 9 | 25 | 7 | 5 | 15 | 27 | 13 | | 32 | | | 40 | 40 | 27 | 35 | 29 | 21 | 18 |
| K7 | Kalkaroo | py | K705 py | 452.914 | 36.990 | 18.324 | 465500 | 105.694 | 0.189 | 4.301 | 0.129 | 0.179 | 0.038 | <0.016 | <0.005 | 0.018 | <0.009 | <0.007 | <0.009 | 0.033 | 0.036 |
| | | | | 11 | 15 | 6 | 7 | 25 | 15 | 19 | 10 | 13 | 24 | | | 34 | | | | 20 | 32 |
| K7 | Kalkaroo | py | K706 py | 143.978 | 25.774 | 22.345 | 465500 | 0.289 | 1.093 | <0.034 | <0.006 | 0.008 | <0.022 | <0.027 | <0.006 | <0.019 | <0.011 | <0.011 | <0.014 | 0.008 | 0.057 |
| | | | | 22 | 23 | 6 | 5 | 35 | 44 | | | 103 | | | | | | | | 38 | 44 |
| K7 | Kalkaroo | cpy | K701 cpy | <0.068 | 40.041 | 16.340 | 304300 | 372475 | <0.01 | <0.053 | <0.006 | <0.005 | <0.025 | <0.022 | <0.009 | <0.024 | <0.019 | <0.011 | <0.014 | <0.005 | <0.016 |
| | | | | | 16 | 4 | 3 | 3 | | | | | | | | | | | | | |

**Table 6.1.** *Continued.*

| Sample | Prospect | Phase | Point no. | $Al^{27}$ | $Ca^{43}$ | $Ti^{49}$ | $Fe^{57}$ | $Cu^{65}$ | $Zr^{90}$ | $Ba^{137}$ | $La^{139}$ | $Ce^{140}$ | $Nd^{146}$ | $Sm^{147}$ | $Eu^{153}$ | $Gd^{157}$ | $Dy^{163}$ | $Er^{166}$ | $Yb^{172}$ | $Th^{232}$ | $U^{238}$ |
|---|---|---|---|---|---|---|---|---|---|---|---|---|---|---|---|---|---|---|---|---|---|
| K7 | Kalkaroo | cpy | K702 cpy | 0.130 | 112.182 | 17.212 | 304300 | 362777 | <0.016 | <0.035 | <0.005 | <0.005 | <0.022 | <0.027 | <0.005 | <0.026 | <0.011 | <0.014 | 0.021 | 0.007 | <0.006 |
| | | | | 19 | 7 | 4 | 3 | 3 | | | | | | | | | | | 26 | 37 | |
| K7 | Kalkaroo | cpy | K707 cpy | 3.698 | 161.656 | 15.575 | 304300 | 379226 | <0.011 | <0.046 | <0.006 | <0.004 | <0.025 | <0.028 | <0.007 | <0.025 | <0.018 | <0.011 | <0.016 | 0.008 | <0.004 |
| | | | | 23 | 6 | 4 | 3 | 4 | | | | | | | | | | | | 32 | |
| K7 | Kalkaroo | cpy | K708 cpy | 0.525 | 143.442 | 18.741 | 304300 | 353044 | 0.054 | <0.035 | 0.029 | 0.048 | <0.018 | <0.021 | <0.007 | <0.021 | <0.011 | <0.012 | <0.016 | 0.126 | <0.005 |
| | | | | 12 | 7 | 4 | 3 | 3 | 17 | | 12 | 10 | | | | | | | | 32 | |
| K7 | Kalkaroo | cpy | K709 cpy | 1.502 | 149.831 | 14.500 | 304300 | 344293 | <0.01 | <0.035 | <0.005 | <0.006 | <0.023 | <0.022 | <0.009 | <0.023 | <0.012 | <0.009 | <0.014 | 0.042 | <0.007 |
| | | | | 22 | 7 | 4 | 4 | 4 | | | | | | | | | | | | 61 | |
| K8 | Kalkaroo | py | K8 02 py | 0.177 | 33.766 | 14.770 | 465500 | 0.594 | <0.004 | <0.017 | <0.002 | <0.002 | <0.013 | 0.011 | <0.003 | <0.017 | <0.006 | <0.005 | <0.007 | 0.012 | 0.002 |
| | | | | 10 | 13 | 4 | 5 | 21 | | | | | | 41 | | | | | | 27 | 102 |
| K8 | Kalkaroo | py | K8 03 py | 506.650 | 34.630 | 15.321 | 465500 | 1.369 | 0.066 | 0.201 | 0.003 | <0.001 | 0.010 | <0.009 | <0.002 | <0.007 | <0.003 | <0.004 | <0.006 | 0.013 | 0.002 |
| | | | | 10 | 10 | 4 | 4 | 8 | 23 | 10 | 70 | | 25 | | | | | | | 14 | 29 |
| K8 | Kalkaroo | py | K8 04 py | 0.128 | 30.134 | 15.564 | 465500 | 0.554 | <0.003 | <0.014 | <0.002 | 0.002 | <0.005 | <0.008 | <0.003 | <0.008 | <0.005 | <0.004 | <0.004 | 0.011 | <0.002 |
| | | | | 10 | 10 | 4 | 5 | 14 | | | | 39 | | | | | | | | 27 | |
| K8 | Kalkaroo | py | K8 05 py | 0.132 | 39.968 | 16.630 | 465500 | 0.347 | <0.005 | <0.03 | <0.003 | <0.002 | <0.008 | <0.013 | <0.004 | <0.01 | <0.006 | <0.007 | <0.007 | <0.003 | 0.005 |
| | | | | 12 | 14 | 4 | 4 | 24 | | | | | | | | | | | | | 98 |
| K8 | Kalkaroo | py | K8 06 py | 0.121 | 42.207 | 16.294 | 465500 | 0.459 | 0.003 | <0.023 | <0.003 | <0.002 | <0.01 | <0.011 | <0.002 | <0.01 | <0.007 | <0.004 | <0.006 | <0.002 | <0.002 |
| | | | | 11 | 11 | 4 | 5 | 21 | 32 | | | | | | | | | | | | |
| WA1 | Waukaloo | py | WA1 06 py | 0.114 | 55.133 | 15.364 | 465500 | 0.493 | <0.006 | 0.046 | 0.007 | 0.012 | <0.011 | <0.011 | <0.003 | <0.011 | <0.007 | <0.006 | <0.007 | <0.003 | 0.027 |
| | | | | 12 | 13 | 4 | 4 | 16 | | 33 | 55 | 47 | | | | | | | | | 10 |
| WA1 | Waukaloo | py | WA1 07 py | 0.174 | 34.678 | 14.483 | 465500 | 0.287 | <0.005 | <0.03 | <0.002 | <0.002 | <0.011 | <0.011 | <0.003 | <0.012 | <0.008 | <0.006 | <0.005 | 0.010 | <0.003 |
| | | | | 13 | 18 | 5 | 6 | 26 | | | | | | | | | | | | 44 | |
| WA1 | Waukaloo | cpy | WA1 02 cpy | 97.955 | 170.937 | 14.752 | 304300 | 367750 | 0.056 | <0.045 | 0.004 | 0.021 | 0.041 | 0.059 | 0.029 | 0.198 | 0.537 | 0.437 | 0.282 | 1.265 | 30.974 |
| | | | | 18 | 8 | 4 | 4 | 3 | 23 | | 42 | 23 | 39 | 28 | 22 | 24 | 23 | 22 | 24 | 18 | 21 |
| WA1 | Waukaloo | cpy | WA1 03 cpy | 2.187 | 148.743 | 14.675 | 304300 | 350774 | <0.009 | <0.039 | <0.003 | <0.005 | <0.024 | <0.023 | <0.005 | <0.021 | 0.052 | 0.031 | 0.020 | 0.710 | 2.440 |
| | | | | 15 | 8 | 4 | 4 | 4 | | | | | | | | | 34 | 34 | 51 | 12 | 32 |
| WA1 | Waukaloo | cpy | WA1 04 cpy | 119.554 | 163.439 | 14.001 | 304300 | 355434 | 0.142 | <0.035 | <0.004 | 0.040 | <0.021 | 0.032 | 0.010 | 0.091 | 0.230 | 0.204 | 0.164 | 5.324 | 16.040 |
| | | | | 18 | 8 | 4 | 3 | 3 | 37 | | | 80 | | 31 | 35 | 27 | 24 | 22 | 23 | 41 | 26 |
| WA1 | Waukaloo | cpy | WA1 08 cpy | 0.147 | 136.121 | 14.074 | 304300 | 350550 | <0.005 | <0.042 | <0.004 | <0.005 | <0.029 | <0.041 | <0.004 | <0.015 | <0.015 | <0.009 | <0.019 | 0.005 | <0 .007 |
| | | | | 15 | 10 | 4 | 3 | 3 | | | | | | | | | | | | 117 | |
| WA1 | Waukaloo | cpy | WA1 09 cpy | 0.139 | 144.665 | 15.227 | 304300 | 356430 | 0.008 | <0.047 | <0.005 | <0.004 | <0.022 | <0.021 | <0.008 | <0.022 | 0.038 | 0.033 | <0.018 | 0.104 | 2.355 |
| | | | | 18 | 9 | 4 | 3 | 3 | 37 | | | | | | | | 65 | 61 | | 53 | 55 |
| WA1 | Waukaloo | mt | WA1 01 mt | 88.482 | 63.129 | 133.820 | 723600 | <0.29 | <0.01 | <0.031 | <0.005 | 0.011 | <0.019 | <0.029 | <0.006 | <0.021 | <0.016 | <0.011 | <0.013 | 0.020 | 0.006 |
| | | | | 3 | 14 | 4 | 3 | | | | | 32 | | | | | | | | 33 | 29 |
| SR1A | Polygonum | cpy | SR1A 03 cpy | 0.103 | 137.563 | 14.215 | 304300 | 358888 | 0.011 | <0.053 | <0.005 | <0.005 | <0.014 | <0.021 | <0.006 | <0.016 | <0.014 | <0.008 | <0.015 | 0.006 | <0.006 |
| | | | | 23 | 8 | 4 | 3 | 3 | 32 | | | | | | | | | | | 33 | |
| SR1A | Polygonum | cpy | SR1A 04 cpy | 1.341 | 1510.751 | 15.246 | 304300 | 354058 | <0.009 | 9.790 | <0.004 | 0.004 | <0.02 | <0.025 | <0.007 | <0.019 | <0.01 | <0.016 | <0.016 | 0.076 | <0.006 |
| | | | | 81 | 34 | 4 | 4 | 3 | | 40 | | 43 | | | | | | | | 44 | |
| SR1A | Polygonum | mt | SR1A 01 mt | 311.599 | 20.153 | 542.876 | 723600 | <0.27 | <0.009 | 0.191 | <0.004 | <0.003 | <0.026 | <0.021 | <0.006 | <0.026 | <0.01 | <0.007 | <0.013 | <0.004 | <0.004 |
| | | | | 3 | 38 | 4 | 3 | | | 14 | | | | | | | | | | | |
| SR1A | Polygonum | mt | SR1A 02 mt | 555.240 | 57.327 | 556.342 | 723600 | <0.33 | <0.009 | <0.032 | <0.004 | <0.006 | <0.02 | <0.024 | <0.006 | <0.02 | <0.014 | <0.007 | <0.012 | <0.006 | <0.004 |
| | | | | 3 | 17 | 3 | 3 | | | | | | | | | | | | | | |
| GG19 | Green & Gold | py | GG19 01 py | 0.388 | 18.039 | 13.105 | 465500 | <0.15 | <0.004 | 0.023 | 0.041 | 0.131 | 0.085 | 0.030 | 0.011 | 0.019 | 0.011 | <0.004 | <0.007 | 0.088 | 0.046 |
| | | | | 5 | 15 | 3 | 3 | | | 40 | 6 | 5 | 9 | 21 | 15 | 26 | 26 | | | 4 | 6 |
| GG19 | Green & Gold | py | GG19 02 py | 0.470 | 20.513 | 14.262 | 465500 | 0.218 | <0.003 | <0.013 | 0.015 | 0.035 | 0.023 | 0.013 | 0.003 | <0.007 | <0.006 | <0.004 | <0.005 | 0.061 | 0.013 |
| | | | | 5 | 14 | 4 | 4 | 23 | | | 9 | 7 | 16 | 34 | 31 | | | | | 9 | 13 |

**Table 6.1.** *Continued.*

| Sample | Prospect | Phase | Point no. | $Al^{27}$ | $Ca^{43}$ | $Ti^{49}$ | $Fe^{57}$ | $Cu^{65}$ | $Zr^{90}$ | $Ba^{137}$ | $La^{139}$ | $Ce^{140}$ | $Nd^{146}$ | $Sm^{147}$ | $Eu^{153}$ | $Gd^{157}$ | $Dy^{163}$ | $Er^{166}$ | $Yb^{172}$ | $Th^{232}$ | $U^{238}$ |
|---|---|---|---|---|---|---|---|---|---|---|---|---|---|---|---|---|---|---|---|---|---|
| GG19 | Green & Gold | py | GG19 03 py | 0.541 | 27.290 | 14.743 | 465500 | 0.459 | <0.003 | <0.016 | 0.011 | 0.027 | 0.016 | <0.01 | <0.003 | <0.011 | <0.007 | <0.005 | <0.006 | 0.045 | 0.028 |
| | | | | 5 | 11 | 4 | 4 | 19 | | | 12 | 7 | 28 | | | | | | | 9 | 9 |
| GG19 | Green & Gold | py | GG19 05 py | 0.396 | 27.175 | 15.552 | 465500 | 0.597 | <0.004 | <0.015 | 0.013 | 0.026 | 0.017 | <0.008 | <0.003 | <0.008 | <0.007 | <0.003 | <0.007 | 0.020 | 0.072 |
| | | | | 5 | 12 | 4 | 4 | 20 | | | 13 | 13 | 28 | | | | | | | 9 | 5 |
| GG19 | Green & Gold | py | GG19 06 py | 1.284 | 30.160 | 15.922 | 465500 | 0.383 | <0.004 | 0.043 | 0.012 | 0.030 | 0.016 | <0.012 | <0.003 | <0.013 | <0.008 | <0.004 | <0.008 | 0.022 | 0.110 |
| | | | | 4 | 11 | 3 | 3 | 15 | | 22 | 12 | 6 | 29 | | | | | | | 11 | 4 |
| GG19 | Green & Gold | cpy | GG19 09 cpy | 243.011 | 126.558 | 15.261 | 304300 | 257459 | <0.013 | <0.06 | 0.036 | 0.049 | 0.050 | <0.037 | <0.01 | 0.036 | <0.024 | <0.013 | <0.02 | 0.074 | 0.049 |
| | | | | 10 | 11 | 7 | 7 | 6 | | | 21 | 15 | 25 | | | 31 | | | | 16 | 13 |
| GG19 | Green & Gold | cpy | GG19 11 cpy | 0.243 | 183.725 | 14.799 | 304300 | 360218 | <0.01 | <0.045 | 0.036 | 0.094 | 0.061 | <0.034 | <0.007 | <0.021 | <0.014 | <0.009 | <0.017 | <0.006 | 0.001 |
| | | | | 13 | 7 | 4 | 3 | 3 | | | 19 | 21 | 26 | | | | | | | | 171 |
| GG19 | Green & Gold | mt | GG19 07 mt | 2674.489 | 53.293 | 1893.195 | 723600 | <0.26 | <0.007 | <0.026 | <0.004 | 0.003 | <0.02 | <0.022 | <0.007 | <0.027 | <0.013 | <0.011 | <0.011 | <0.004 | 0.002 |
| | | | | 3 | 14 | 3 | 3 | | | | | 47 | | | | | | | | | 74 |
| GG19 | Green & Gold | mt | GG19 08 mt | 2293.318 | 53.289 | 1594.639 | 723600 | 0.493 | 18.862 | 0.040 | 0.005 | 0.063 | <0.017 | 0.028 | 0.021 | 0.174 | 0.455 | 0.233 | 0.184 | 0.034 | 0.078 |
| | | | | 3 | 12 | 3 | 3 | 26 | 35 | 40 | 40 | 96 | | 45 | 40 | 35 | 36 | 36 | 34 | 34 | 31 |
| DD96 | Lawsons | py | DD96 02 py | 0.189 | 31.618 | 11.282 | 465500 | 0.257 | <0.004 | <0.018 | 0.005 | <0.002 | <0.006 | <0.008 | <0.002 | <0.007 | <0.005 | <0.003 | <0.004 | 0.005 | 0.021 |
| | | | | 8 | 11 | 4 | 4 | 22 | | | 88 | | | | | | | | | 20 | 73 |
| DD96 | Lawsons | py | DD96 03 py | 0.326 | 46.083 | 10.895 | 465500 | 0.291 | <0.006 | <0.025 | 0.004 | 0.004 | <0.012 | <0.014 | <0.003 | <0.007 | <0.006 | <0.004 | <0.007 | 0.021 | <0.002 |
| | | | | 9 | 10 | 5 | 5 | 23 | | | 122 | 101 | | | | | | | | 22 | |
| DD96 | Lawsons | py | DD96 04 py | 0.526 | 36.291 | 11.310 | 465500 | 0.234 | <0.004 | <0.018 | 0.002 | 0.013 | <0.009 | <0.007 | <0.003 | <0.009 | <0.006 | <0.004 | <0.007 | 0.032 | <0.002 |
| | | | | 12 | 14 | 5 | 6 | 26 | | | 60 | 58 | | | | | | | | 23 | |
| DD96 | Lawsons | py | DD96 08 py | 0.204 | 42.836 | 10.469 | 465500 | 0.212 | <0.005 | 0.023 | 0.006 | <0.002 | <0.01 | <0.009 | <0.003 | <0.01 | <0.006 | <0.005 | <0.008 | 0.043 | 0.017 |
| | | | | 11 | 11 | 5 | 5 | 35 | | 42 | 126 | | | | | | | | | 27 | 69 |
| DD96 | Lawsons | py | DD96 09 py | 0.134 | 39.907 | 9.597 | 465500 | 0.421 | <0.004 | <0.015 | 0.003 | 0.009 | <0.006 | <0.007 | <0.003 | <0.006 | <0.005 | <0.003 | <0.004 | <0.001 | 0.011 |
| | | | | 10 | 9 | 5 | 6 | 15 | | | 98 | 95 | | | | | | | | | 75 |
| DD96 | Lawsons | cpy | DD96 05 cpy | 1.444 | 87.250 | 8.861 | 304300 | 348335 | <0.008 | <0.035 | <0.004 | <0.005 | <0.023 | <0.018 | <0.006 | <0.022 | <0.015 | <0.009 | <0.015 | 0.730 | <0.004 |
| | | | | 10 | 11 | 6 | 5 | 4 | | | | | | | | | | | | 17 | |
| DD96 | Lawsons | cpy | DD96 06 cpy | 0.232 | 107.360 | 9.704 | 304300 | 359472 | <0.008 | <0.039 | <0.004 | <0.004 | <0.019 | 0.020 | <0.006 | <0.02 | <0.009 | <0.007 | <0.009 | <0.006 | <0.003 |
| | | | | 16 | 10 | 5 | 3 | 3 | | | | | | 36 | | | | | | | |
| DD96 | Lawsons | cpy | DD96 07 cpy | 0.215 | 112.874 | 9.297 | 304300 | 363398 | <0.014 | <0.035 | <0.004 | <0.005 | <0.019 | <0.026 | <0.006 | <0.018 | <0.012 | <0.01 | <0.014 | <0.005 | <0.005 |
| | | | | 17 | 9 | 5 | 4 | 3 | | | | | | | | | | | | | |
| CB6 | Copper Blow | cpy | CB605 cpy | 1.067 | 150.172 | 12.881 | 304300 | 365590 | <0.008 | <0.042 | <0.007 | <0.004 | <0.024 | <0.023 | <0.006 | <0.024 | <0.017 | <0.013 | <0.019 | 0.036 | <0.004 |
| | | | | 15 | 7 | 4 | 3 | 3 | | | | | | | | | | | | 44 | |
| CB6 | Copper Blow | cpy | CB606 cpy | 9.275 | 118.533 | 13.510 | 304300 | 361273 | <0.009 | 0.181 | <0.006 | <0.005 | <0.023 | <0.026 | <0.007 | <0.016 | <0.012 | <0.011 | <0.018 | <0.005 | <0.005 |
| | | | | 38 | 9 | 4 | 3 | 3 | | 37 | | | | | | | | | | | |
| CB6 | Copper Blow | mt | CB602 mt | 2500.528 | 569.439 | 1076.231 | 723600 | 28.947 | <0.011 | 11.312 | 0.257 | 0.732 | 0.246 | 0.111 | 0.037 | 0.214 | 0.497 | 0.439 | 0.541 | 0.007 | 1.841 |
| | | | | 4 | 11 | 3 | 3 | 21 | | 7 | 21 | 27 | 22 | 21 | 20 | 18 | 19 | 20 | 20 | 37 | 19 |
| CB6 | Copper Blow | mt | CB603 mt | 2048.673 | 67.216 | 988.742 | 723600 | 162.942 | <0.008 | 2.167 | <0.005 | 0.297 | <0.02 | <0.024 | <0.005 | <0.019 | 0.014 | 0.016 | 0.044 | 0.008 | 0.024 |
| | | | | 3 | 11 | 3 | 3 | 9 | | 10 | | 98 | | | | | 47 | 41 | 19 | 36 | 19 |
| CB6 | Copper Blow | mt | CB604 mt | 4563.973 | 609.455 | 1145.493 | 723600 | 275.773 | 0.070 | 43.928 | 0.044 | 0.146 | 0.217 | 0.164 | 0.061 | 0.409 | 0.784 | 0.426 | 1.057 | <0.006 | 0.098 |
| | | | | 3 | 5 | 3 | 3 | 11 | 9 | 18 | 9 | 8 | 8 | 10 | 8 | 6 | 4 | 4 | 4 | | 6 |
| CB6 | Copper Blow | mt | CB607 mt | 4283.105 | 672.681 | 1122.414 | 723600 | 1191.095 | 0.092 | 15.406 | 0.124 | 0.520 | 0.569 | 0.365 | 0.078 | 0.653 | 0.932 | 1.024 | 2.963 | <0.005 | 0.206 |
| | | | | 3 | 5 | 3 | 4 | 8 | 9 | 4 | 14 | 14 | 12 | 8 | 9 | 7 | 5 | 4 | 4 | | 6 |
| CB6 | Copper Blow | mt | CB608 mt | 2376.608 | 207.603 | 888.121 | 723600 | 12861.058 | 0.020 | 9.326 | 0.015 | 0.056 | 0.054 | 0.052 | 0.014 | 0.126 | 0.210 | 0.247 | 0.627 | 0.442 | 0.151 |
| | | | | 3 | 7 | 3 | 3 | 9 | 23 | 6 | 24 | 14 | 25 | 25 | 24 | 12 | 7 | 6 | 5 | 71 | 5 |
| CB6 | Copper Blow | mt | CB609 mt | 3917.881 | 472.620 | 590.620 | 723600 | <0.29 | 0.050 | 12.100 | 0.030 | 0.135 | 0.199 | 0.162 | 0.048 | 0.362 | 0.529 | 0.309 | 0.814 | <0.004 | 0.096 |
| | | | | 3 | 5 | 3 | 3 | | 11 | 4 | 10 | 6 | 8 | 9 | 9 | 6 | 5 | 5 | 4 | | 16 |

ppb) and even lesser quantities of LREE (La, Ce, Nd: 4 – 41 ppb; Table 6.1; Fig. 6.6a, b). The increase in REE abundances is also accompanied by increases in U (16.04 – 30.97 ppm) and Th (1.27 – 5.32 ppm) during the same ablation interval. Additionally, increases in Al and Zr counts/second rates are also observed, although the increase in Al does not always precisely coincide with the increase in REE at the same ablation interval (e.g. WA1 02; Fig. 6.6a). Other inclusion-type REE-bearing phases are only enriched in the LREE (e.g. analytical points *WA1 06* and *GG19 09*; Fig. 6.6c and 6.6d, respectively). In these analyses, La and Ce ± Nd are the only REE above background levels (La: 9 – 36 ppb; Ce: 12 – 49 ppb; Nd: 50 ppb; Table 6.1). In analytical point *GG19 09*, the increase in La and Ce is broadly associated with an increase in count rate for Al.

The second type of ablation pattern observed for the REE has counts/second rates for selected REE that are constantly above that of background levels (Fig. 6.6e, f). This analysis type only occurred in sulphides and magnetite associated within the shear-related prospects at Green & Gold and Copper Blow. Analytical point *GG19 01* ablated in a pyrite grain from Green & Gold prospect is mildly enriched in the LREE and MREE (La: 41 ppb; Ce: 131 ppb; Nd: 85 ppb; Sm: 30 ppb; Eu: 11 ppb; Gd: 19 ppb; Dy: 11 ppb; Table 6.1). The counts/second rates of these elements are approximately constant, which would appear to rule out the siting of the REE as inclusions (Fig. 6.6e). Similarly, analytical point *CB6 07* from a magnetite grain in the Copper Blow prospect has near constant counts/second rates for the HREE (Yb: 2.96 ppm; Er: 1.02 ppm; Dy: 932 ppb; Table 6.1). However, LREE and MREE spikes are also observed, suggesting that (La, Ce, Nd ± Sm ± Eu)-bearing inclusions also exist in this sample (Fig. 6.6f).

## 6.6 Trace element geochemistry of ore separates and host rocks

Rare earth element and selected trace element abundances for sulphide separates and two whole-rock samples are summarised in Table 6.2 and 6.3. REE abundance and selected chondrite normalised element ratios are listed in Table 6.3. Chondrite normalised REE patterns of sulphide separates are presented in Fig. 6.7. Chondrite normalisation values are those of Taylor and McLennan (1985). A feature common to nearly all the REE patterns of the sulphide samples from the SCP is that they are all LREE-enriched relative to the HREE, have negative Eu anomalies, and nearly all have enrichment in Gd relative to the heavier LREE (Nd and Sm; Fig. 6.7). Although the Gd anomaly is accentuated by the ubiquitously present negative Eu anomaly, it is still evident in samples that have very little Eu depletion. Following is a description of the trace element geochemistry, including detailed documentation of the REE systematics of each of the samples.

### *6.6.1 Stratabound prospects*

Trace element abundances of the sulphide separates from the stratabound prospects (North Portia, Kalkaroo, Waukaloo and Polygonum) are variable, a feature that is likely to be directly related to minor amounts of inclusions and/or accessory gangue phases

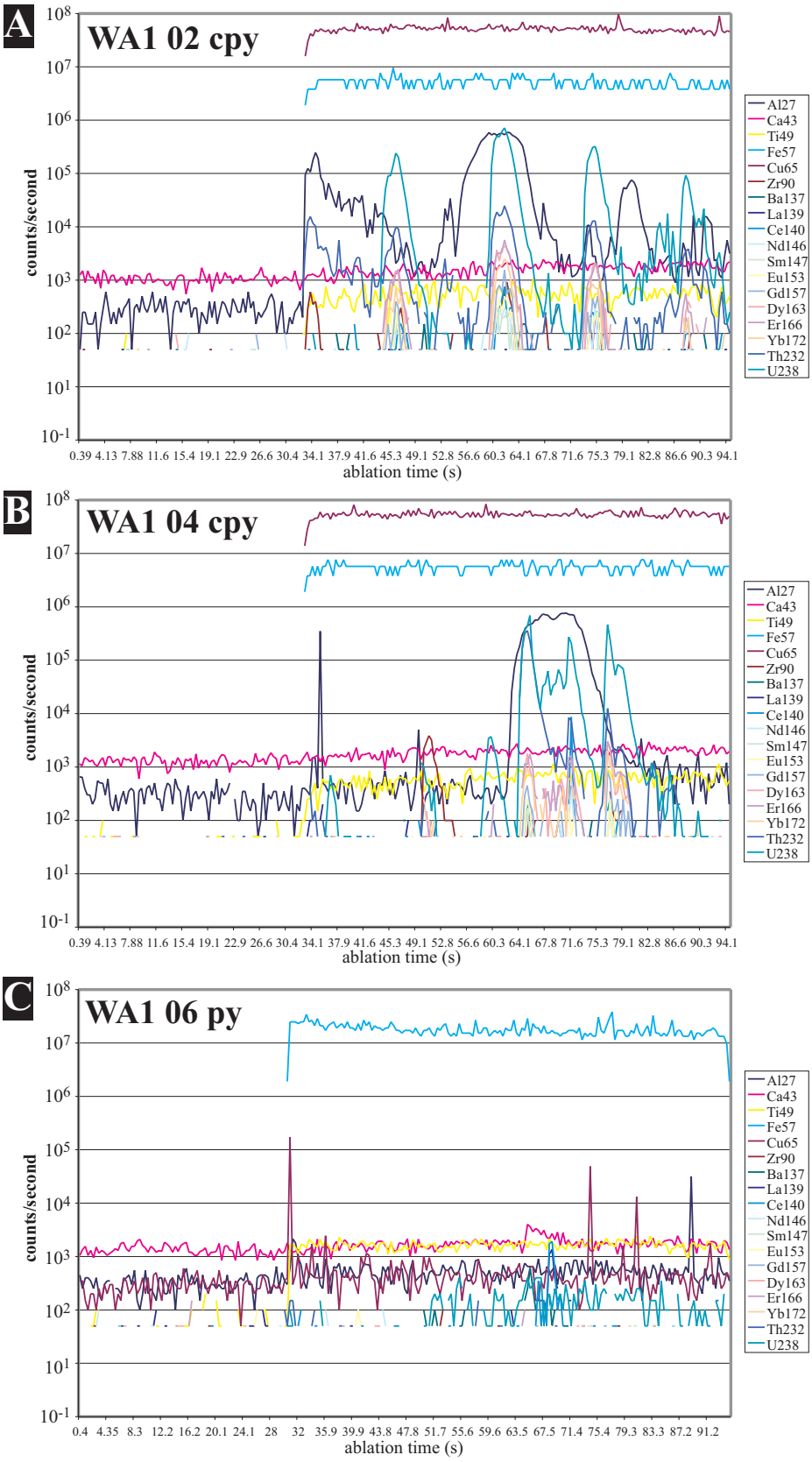


**Figure 6.6.** LA-ICPMS elemental profiles (counts/second vs ablation time). (a) and (b) from Waukaloo prospect - chalcopyrite: analytical points WA1 02 and WA1 04, respectively. HREE- and MREE-enriched inclusions; (c) WA1 06: Waukaloo prospect - pyrite, LREE-enriched inclusion; (d) GG19 09: Green & Gold prospect - chalcopyrite: LREE-enriched inclusions; (e) GG19 01: Green & Gold prospect - pyrite, constant counts/second rate for HREE and heaviest MREE; (f) CB6 07: Copper Blow prospect - magnetite, constant counts/second rate for HREE, LREE incorporated within inclusions.

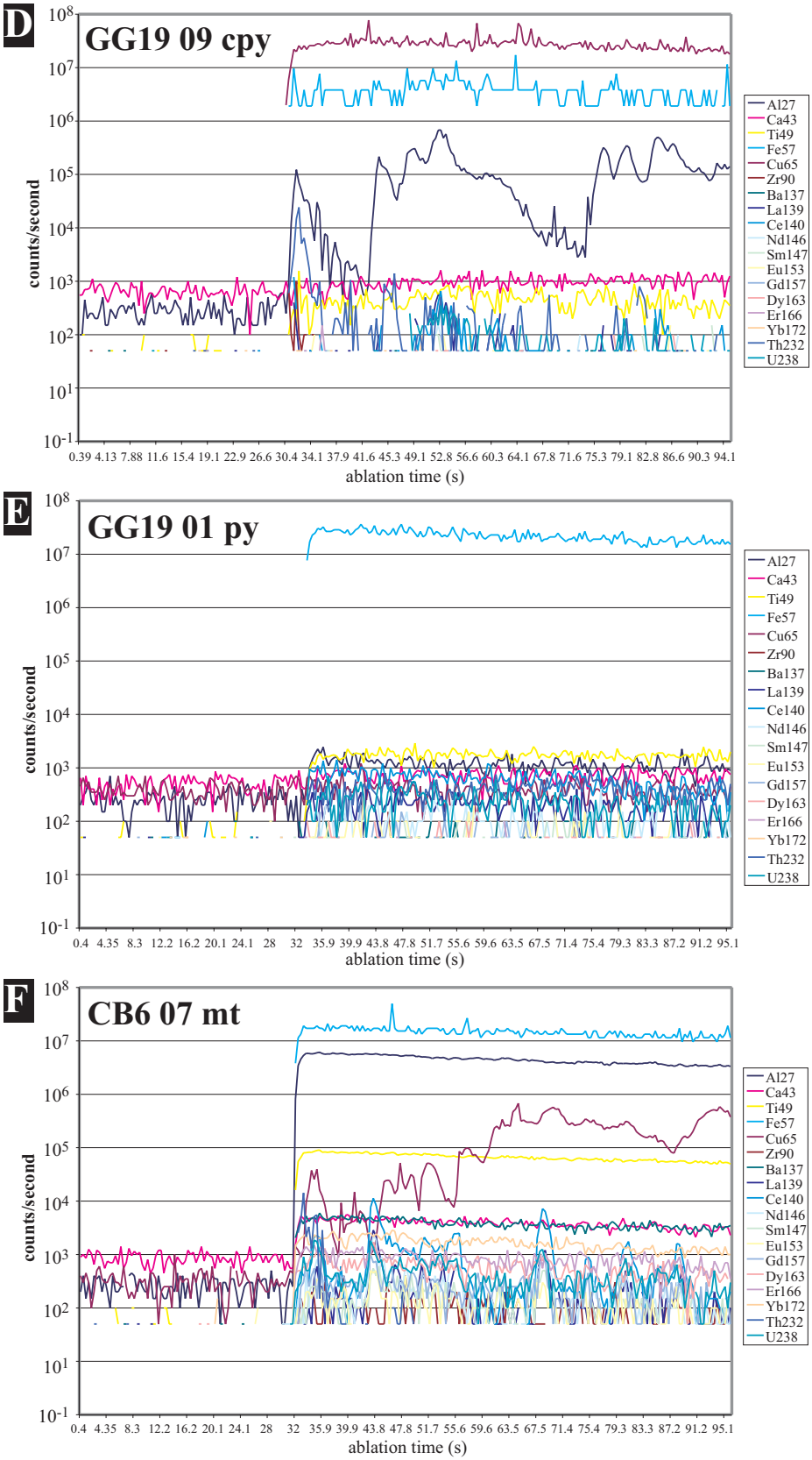


**Figure 6.6.** *Continued.*

being incorporated with the sample. Elevated concentrations of Ca (27600 ppm), Mg (<13300 ppm) and Mn (<2350 ppm) can be attributed to the presence of carbonates, such as ankerite (*BN4*, *BN5*), calcite (*BN1*, *BN3*, *BN600*, *WA15*) and K-feldspar (*K7*; Table 6.2; *Appendix 8*). At Kalkaroo prospect, relatively high concentrations of Ca (5900 ppm), Na (1150 ppm) and K (5550ppm) are likely to be due to the presence of inclusions of feldspar

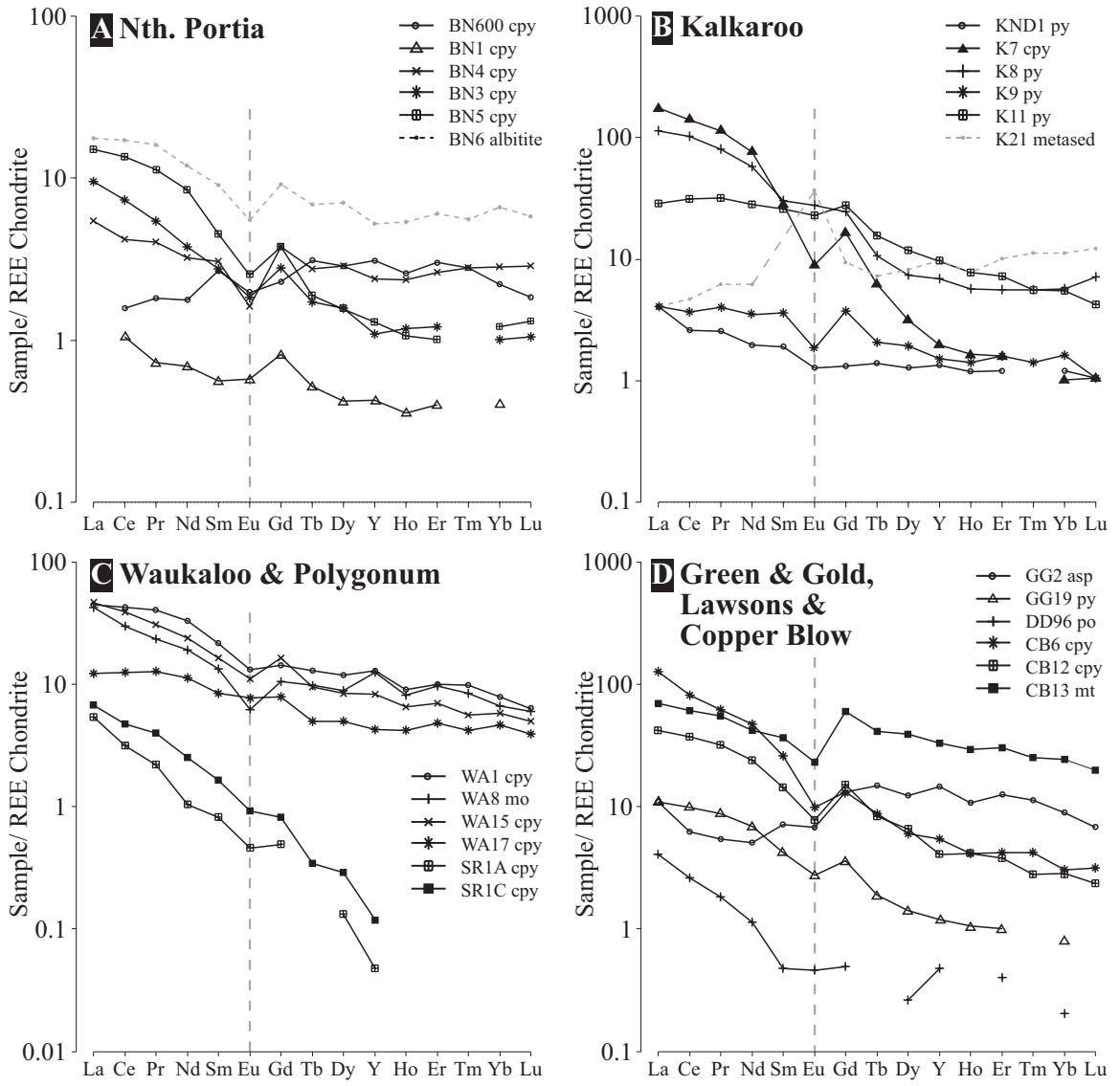


**Figure 6.7.** Chondrite normalised REE patterns of ore samples from IOCG mineralisation in the southern Curnamona Province. Stratabound prospects: (a) North Portia; (b) Kalkaroo; (c) Waukaloo & Polygonum; (d) Shear related prospects: Green & Gold, Lawsons and Copper Blow.

± chlorite ± calcite (Table 6.2; *Appendix 8*).

Elevated concentrations of other trace elements such as P (1950 – 3900 ppm), Ca (8400 ppm) and Na (750 – 1650 ppm) can be related to apatite and/or monazite (*BN600*, *WA1*, *SR1A*, *SR1C*) and albite inclusions (*BN5*), respectively (Table 6.2; *Appendix 8*). Relatively high concentrations of Cu in pyrite samples (e.g. 350 ppm: *KND1*) can be related to chalcopyrite micro-inclusions. Alternatively, relatively high Co (2000 ppm), Ni (260 ppm) and Bi (40.5 ppm) concentrations in chalcopyrite separates can be correlated with minor pyrite (*WA15*, *SR1A*; Table 6.2; *Appendix 8*). Elevated Ti (1800 ppm) and Mo (2600 – 7550 ppm) concentrations can be related to the presence of Fe-Ti oxides and molybdenite, respectively (Table 6.2).

The majority of samples from the stratabound prospects have LREE-enriched chondrite normalised patterns ($Ce_N/Yb_N$ = 1.5 – 139.90), with the exception of *BN600* ($Ce_N/Yb_N$ = 0.71; Table 6.3; Fig. 6.7). REE concentrations are generally low (ΣREE = 3.3 – 287.3; average 79 ppm), with LREE concentrations ($La_N$ – $Pr_N$) range from 64 ppm

**Table 6.2.** ICP-MS and ICP-OES trace element data (ppm) of ore samples from IOCG prospects in the southern Curnamona Province.

| Sample no. | Prospect | Hole I.D. | Depth (m) | Phase | Fe | Cu | Ca | Na | K | Mn | Mg | P | Ti | Mo | As | Co | Zn | Pb | Ni | Cr | V | Ag | Bi | Te | U | Th |
|---|---|---|---|---|---|---|---|---|---|---|---|---|---|---|---|---|---|---|---|---|---|---|---|---|---|---|
| BN600 | Nth. Portia | BN600 | 320.8 | cpy | 282000 | 331000 | 16600 | 750 | 330 | 800 | 1100 | 1950 | 45 | <50 | 100 | <0.2 | 72 | 200 | 3 | 4 | 3 | 49 | 10.5 | 23.5 | 100 | 7.5 |
| BN1 | Nth. Portia | BN599 | 365.65 | cpy | 293000 | 339000 | 8100 | 110 | 40 | 150 | 155 | <5 | 55 | 11.5 | 12 | 12.5 | 76 | 50 | 6 | 11 | 3 | 1.8 | 37 | 15 | 0.51 | 0.07 |
| BN3 | Nth. Portia | BN596 | 263.65 | cpy | 267000 | 331000 | 14900 | 50 | 60 | 280 | 290 | 24 | <10 | 8 | 11 | 3.8 | 40 | 48.5 | 5 | 5 | <2 | 1.7 | 2.5 | 18.5 | 0.48 | 0.52 |
| BN4 | Nth. Portia | BN592 | 348 | cpy | 261000 | 240000 | 27600 | 150 | 550 | 2350 | 13300 | 650 | 120 | 10.5 | 52 | 340 | 60 | 44 | 84 | 5 | 20 | 10.5 | 32.5 | 9.5 | 2.6 | 0.61 |
| BN5 | Nth. Portia | BN592 | 243.8 | cpy | 252000 | 320000 | 12600 | 270 | 175 | 400 | 4500 | <5 | 30 | 14.5 | 6 | 38 | 34.5 | 24 | 11 | 5 | 4 | 2 | 10 | 3.2 | 0.13 | 0.72 |
| BN6 | Nth. Portia | BN592 | 243.8 | albitite | 8250 | 850 | 12100 | 67700 | 3600 | 250 | 6950 | 330 | 2000 | 12 | 3 | 4.5 | 7.5 | 4.5 | 11 | 13 | 47 | 0.2 | 0.2 | <0.2 | 2.9 | 11.5 |
| KND1 | Kalkaroo | KND1 | 312 | py | 489000 | 350 | 2450 | 95 | 250 | 56 | 600 | 48 | 440 | 2600 | 250 | 800 | 33 | 100 | 1000 | 7 | 11 | 2.2 | 15.5 | 10 | 10.5 | 0.63 |
| K7 | Kalkaroo | KND1 | 298.16 | cpy | 291000 | 315000 | 5900 | 1150 | 5550 | 130 | 1950 | 86 | 460 | 16.5 | 72 | 52 | 170 | 7 | 33 | 8 | 17 | 0.5 | 8 | 1.4 | 0.78 | 4.9 |
| K8 | Kalkaroo | KND3 | 239.4 | py | 434000 | 600 | 1000 | 950 | 1050 | 66 | 2800 | 38 | 100 | 2.3 | 28.5 | 1800 | 20.5 | 7.5 | 195 | 4 | 2 | 0.3 | 38 | 9.5 | 4.1 | 0.52 |
| K9 | Kalkaroo | KND8 | 246 | py | 445000 | 3950 | 3700 | 310 | 2200 | 40 | 900 | 70 | 210 | 1.5 | 3450 | 13000 | 35 | 68 | 900 | 7 | 3 | 0.4 | 7 | 2.8 | 0.36 | 0.26 |
| K11 | Kalkaroo | KND9 | 258.6 | py | 428000 | 29700 | 2800 | 320 | 340 | 34 | 430 | 210 | 1650 | 9.5 | 210 | 5850 | 30 | 54 | 650 | 14 | 6 | 0.7 | 25.5 | 5.5 | 5.5 | 1.6 |
| K21 | Kalkaroo | KND8 | 246 | metased. | 27800 | 300 | 7650 | 28300 | 74600 | 430 | 21400 | 290 | 4150 | 0.2 | 3 | 68 | 16 | 5.5 | 14 | 43 | 185 | <0.1 | 0.2 | <0.2 | 9 | 22.5 |
| WA1 | Waukaloo | WA1 | 101.2 | cpy | 297000 | 327000 | 8400 | 1650 | 50 | 100 | 1050 | 1950 | 1800 | 50 | <50 | 260 | 84 | 100 | 3 | 6 | 3 | 2.6 | 2.2 | 3.4 | 11 | 4 |
| WA8 | Waukaloo | WA8 | 143.7 | mo | 271000 | 550 | 6150 | 900 | 700 | 34 | 1200 | 3900 | 290 | 225000 | 400 | 5950 | 34 | <0.005 | 110 | 40 | 110 | 16.5 | 68 | 185 | 2.1 | 1.25 |
| WA15 | Waukaloo | WA8 | 101.9 | cpy | 316000 | 226000 | 2200 | 30 | 35 | 18 | 400 | 300 | 85 | 16.5 | 185 | 2000 | 49.5 | 21.5 | 260 | 4 | <2 | 3.4 | 40.5 | 17.5 | 6.5 | 1.25 |
| WA17 | Waukaloo | WA8 | 143.7 | cpy | 282000 | 335000 | 1650 | 500 | 190 | 22 | 1300 | 8 | 1750 | 7550 | 3 | 13.5 | 52 | 13 | <2 | 8 | 3 | 3.5 | 7 | 3.1 | 17 | 6.5 |
| SR1A | Polygonum | SR1 | 338 | cpy | 320000 | 347000 | 220 | 30 | 370 | 36 | 250 | 2250 | 20 | <0.1 | 70 | 430 | 74 | 8.5 | 115 | 4 | <2 | 18 | 110 | 60 | <0.02 | 0.06 |
| SR1C | Polygonum | SR1 | 504.8 | cpy | 305000 | 476000 | 190 | 45 | 135 | 16 | 220 | 3300 | 25 | <0.1 | 5.5 | 4.4 | 165 | 34.5 | 2 | 3 | <2 | 12.5 | 16.5 | 1.6 | 0.04 | 0.47 |
| GG2 | Green & Gold | GG2 | 85.25 | asp | 328000 | 100 | 1300 | 190 | 360 | 410 | 800 | 180 | 90 | 650 | 454000 | 13300 | 25.5 | <0.005 | 1000 | 21 | <2 | 21.5 | 8.5 | 19.5 | 0.74 | 0.3 |
| GG19 | Green & Gold | GG2 | 87.2 | py | 435000 | 16300 | 380 | 145 | 75 | <5 | 330 | 74 | 20 | 11 | 13500 | 1350 | 33 | 10 | 600 | 7 | <2 | 0.6 | 23 | 1 | 0.45 | 0.65 |
| DD96 | Lawsons | DD96 | 108.5 | po | 470000 | 2300 | 1800 | 170 | 250 | 26 | 410 | 52 | 40 | 50 | 750 | 11900 | 110 | 50 | 21 | 14 | <2 | 2 | 2.6 | 9 | 0.42 | 0.29 |
| CB6 | Copper Blow | CB6 | 118.2 | cpy | 304000 | 342000 | 240 | 65 | 180 | 30 | 95 | 2300 | <10 | 100 | 250 | 78 | 5400 | 200 | 120 | 4 | <2 | 48.5 | 5.5 | 18.5 | 9 | 0.1 |
| CB12 | Copper Blow | CB6 | 144.3 | cpy | 296000 | 302000 | 1200 | 85 | 350 | 14 | 410 | 550 | 25 | 23 | 25 | 500 | 1350 | 27.5 | 360 | 5 | <2 | 12.5 | 1.1 | 6 | 68 | 1.4 |
| CB13 | Copper Blow | CB6 | 144.3 | mt | 573000 | 15400 | 1300 | 145 | 3600 | 250 | 4950 | 270 | 550 | 48.5 | 1.5 | 74 | 290 | 15.5 | 98 | 26 | 240 | 1.3 | 0.2 | 0.4 | 230 | 4.5 |

to below detection levels (average 14 ppm). Chalcopyrite samples from Polygonum have the lowest REE concentration abundances (ΣREE = 6.6 and 10.4 ppm), with HREEs below detection limits. The majority of samples have relatively flat HREE patterns ($Y_N/Yb_N$ = 0.9 – 1.9; Table 6.3; Fig. 6.7). In contrast to the North Portia and Kalkaroo samples, the Waukaloo samples have a greater proportion of HREE. The majority of samples have negative europium anomalies (Eu/Eu* = 0.22 – 1.05; Eu* = $Eu_N/[(Nd_N+Tb_N)/2]$). Eu anomalies are calculated with respect to Nd and Tb, instead of Sm and Gd, as all samples have elevated Gd concentrations. It is unclear whether the Gd enrichment is due to analytical procedures, or a primary compositional characteristic.

Samples *BN600* and *BN1* from North Portia prospect, and samples *KND1* and *K9* from Kalkaroo have very low REE abundances relative to the other samples (ΣREE = 3.3 – 15.2 ppm), and REE patterns that are not as LREE-enriched ($Ce_N/Yb_N$ = 0.7 – 2.6), as the other stratabound samples with higher REE abundances. Sample *K11* from Kalkaroo shows some evidence of LREE depletion, particularly in La and Ce relative to the other REE enriched samples from Kalkaroo (*K7* and *K8*; Fig. 6.7b). Samples *SR1A* and *SR1C* have very low total REE abundances (ΣREE = 6.6 and 10.4 ppm, respectively), with the HREE (Ho to Lu) being below detection limit (<0.05 ppm). Both sample have extremely fractionated REE patterns ($Gd_N/Y_N$ = 9.8 and 6.8), with moderate europium anomalies (Eu/Eu* = 0.7 and

**Table 6.3.** REE concentrations (ppm) and selected chondrite normalised REE ratios from IOCG ores (normalisation values of Taylor & McLennon, 1985).

| Sample no. | Prospect | Hole I.D. | Depth (m) | Phase | La | Ce | Pr | Nd | Sm | Eu | Gd | Tb | Dy | Y | Ho | Er | Tm | Yb | Lu | REE | Eu/Eu*[1] | $Ce_N/Yb_N$ | $Ce_N/Sm_N$ | $Gd_N/Y_N$ | $Y_N/Yb_N$ |
|---|---|---|---|---|---|---|---|---|---|---|---|---|---|---|---|---|---|---|---|---|---|---|---|---|---|
| BN600 | Nth. Portia | BN600 | 320.8 | cpy | <0.5 | 1.5 | 0.25 | 1.25 | 0.62 | 0.17 | 0.7 | 0.18 | 1.1 | 6.5 | 0.22 | 0.75 | 0.1 | 0.55 | 0.07 | 13.96 | 0.80 | 0.71 | 0.58 | 0.74 | 1.40 |
| BN1 | Nth. Portia | BN599 | 365.65 | cpy | <0.5 | 1 | 0.1 | 0.49 | 0.13 | 0.05 | 0.25 | 0.03 | 0.16 | 0.9 | 0.03 | 0.1 | <0.05 | 0.1 | <0.02 | 3.34 | 0.94 | 2.59 | 1.86 | 1.91 | 1.08 |
| BN3 | Nth. Portia | BN596 | 263.65 | cpy | 3.5 | 7 | 0.75 | 2.7 | 0.64 | 0.16 | 0.85 | 0.1 | 0.6 | 2.3 | 0.1 | 0.3 | <0.05 | 0.25 | 0.04 | 19.29 | 0.67 | 7.26 | 2.64 | 2.53 | 1.09 |
| BN4 | Nth. Portia | BN592 | 348 | cpy | 2 | 4 | 0.55 | 2.3 | 0.71 | 0.14 | 1.15 | 0.16 | 1.1 | 5 | 0.2 | 0.65 | 0.1 | 0.7 | 0.11 | 18.87 | 0.54 | 1.48 | 1.36 | 1.58 | 0.84 |
| BN5 | Nth. Portia | BN592 | 243.8 | cpy | 5.5 | 13 | 1.55 | 6 | 1.05 | 0.22 | 1.15 | 0.11 | 0.59 | 2.7 | 0.09 | 0.25 | <0.05 | 0.3 | 0.05 | 32.56 | 0.49 | 11.23 | 2.99 | 2.91 | 1.07 |
| BN6 | Nth. Portia | BN592 | 243.8 | albitite | 6.5 | 16.5 | 2.2 | 8.5 | 2.1 | 0.48 | 2.8 | 0.4 | 2.7 | 11 | 0.46 | 1.5 | 0.2 | 1.65 | 0.22 | 57.21 | 0.59 | 2.59 | 1.9 | 1.75 | 0.79 |
| KND1 | Kalkaroo | KND1 | 312 | py | 1.5 | 2.5 | 0.35 | 1.4 | 0.44 | 0.11 | 0.4 | 0.08 | 0.48 | 2.8 | 0.1 | 0.3 | <0.05 | 0.3 | 0.04 | 10.8 | 0.75 | 2.16 | 1.37 | 0.98 | 1.10 |
| K7 | Kalkaroo | KND1 | 298.16 | cpy | 64 | 135 | 15.5 | 54 | 6.5 | 0.78 | 5 | 0.36 | 1.2 | 4.1 | 0.14 | 0.4 | <0.05 | 0.25 | 0.04 | 287.27 | 0.22 | 139.94 | 5.01 | 8.38 | 1.93 |
| K8 | Kalkaroo | KND3 | 239.4 | py | 42 | 98 | 11 | 41 | 7 | 2.4 | 7.5 | 0.62 | 2.8 | 14.5 | 0.48 | 1.4 | 0.2 | 1.4 | 0.27 | 230.57 | 0.81 | 18.14 | 3.38 | 3.55 | 1.22 |
| K9 | Kalkaroo | KND8 | 246 | py | 1.5 | 3.5 | 0.55 | 2.5 | 0.83 | 0.16 | 1.15 | 0.12 | 0.73 | 3.2 | 0.12 | 0.4 | 0.05 | 0.4 | 0.04 | 15.25 | 0.66 | 2.27 | 1.02 | 2.47 | 0.94 |
| K11 | Kalkaroo | KND9 | 258.6 | py | 10.5 | 30 | 4.4 | 20 | 6 | 2 | 8.5 | 0.9 | 4.5 | 20 | 0.66 | 1.8 | 0.2 | 1.35 | 0.16 | 110.97 | 1.05 | 5.76 | 1.21 | 2.92 | 1.75 |
| K21 | Kalkaroo | KND8 | 246 | metased. | 1.5 | 4.5 | 0.85 | 4.4 | <0.02 | 3.2 | 2.9 | 0.42 | 3.1 | 20.5 | 0.66 | 2.5 | 0.4 | 2.8 | 0.47 | 48.2 | 5.48 | 0.42 | - | 0.97 | 0.86 |
| WA1 | Waukaloo | WA1 | 101.2 | cpy | 16.5 | 41 | 5.5 | 23.5 | 5 | 1.15 | 4.4 | 0.75 | 4.5 | 27 | 0.77 | 2.5 | 0.35 | 1.95 | 0.24 | 135.11 | 0.58 | 5.45 | 1.98 | 1.12 | 1.64 |
| WA8 | Waukaloo | WA8 | 143.7 | mo | 15.5 | 28.5 | 3.2 | 13.5 | 3.1 | 0.54 | 3.2 | 0.57 | 3.4 | 26 | 0.69 | 2.4 | 0.3 | 1.65 | 0.23 | 102.78 | 0.43 | 4.48 | 2.22 | 0.84 | 1.86 |
| WA15 | Waukaloo | WA8 | 101.9 | cpy | 17 | 37.5 | 4.2 | 17 | 3.8 | 0.96 | 5 | 0.55 | 3.2 | 17.5 | 0.56 | 1.75 | 0.2 | 1.45 | 0.19 | 110.86 | 0.66 | 6.7 | 2.38 | 1.96 | 1.42 |
| WA17 | Waukaloo | WA8 | 143.7 | cpy | 4.5 | 12 | 1.75 | 8 | 1.95 | 0.67 | 2.4 | 0.29 | 1.9 | 9 | 0.36 | 1.2 | 0.15 | 1.15 | 0.15 | 45.47 | 0.95 | 2.7 | 1.49 | 1.83 | 0.92 |
| SR1A | Polygonum | SR1 | 338 | cpy | 2 | 3 | 0.3 | 0.74 | 0.19 | 0.04 | 0.15 | <0.02 | 0.05 | 0.1 | <0.02 | <0.05 | <0.05 | <0.05 | <0.02 | 6.57 | - | - | 3.81 | 9.80 | - |
| SR1C | Polygonum | SR1 | 504.8 | cpy | 2.5 | 4.5 | 0.55 | 1.8 | 0.38 | 0.08 | 0.25 | 0.02 | 0.11 | 0.25 | <0.02 | <0.05 | <0.05 | <0.05 | <0.02 | 10.44 | 0.64 | - | 2.86 | 6.83 | - |
| GG2 | Green & Gold | GG2 | 85.25 | asp | 4 | 6 | 0.75 | 3.6 | 1.65 | 0.59 | 4 | 0.86 | 4.7 | 30.5 | 0.92 | 3.1 | 0.4 | 2.2 | 0.26 | 63.53 | 0.68 | 0.71 | 0.88 | 0.90 | 1.64 |
| GG19 | Green & Gold | GG2 | 87.2 | py | 4 | 9.5 | 1.2 | 4.9 | 0.98 | 0.24 | 1.1 | 0.11 | 0.54 | 2.5 | 0.09 | 0.25 | <0.05 | 0.2 | <0.02 | 25.61 | 0.63 | 12.31 | 2.34 | 3.02 | 1.47 |
| DD96 | Lawsons | DD96 | 108.5 | po | 1.5 | 2.5 | 0.25 | 0.81 | 0.11 | 0.04 | 0.15 | <0.02 | 0.1 | 1 | <0.02 | 0.1 | <0.05 | 0.05 | <0.02 | 6.61 | - | 12.96 | 5.49 | 1.02 | 2.40 |
| CB6 | Copper Blow | CB6 | 118.2 | cpy | 46.5 | 78 | 8.5 | 33.5 | 6 | 0.86 | 4 | 0.51 | 2.3 | 11.5 | 0.35 | 1.05 | 0.15 | 0.75 | 0.12 | 194.09 | 0.35 | 26.95 | 3.14 | 2.39 | 1.81 |
| CB12 | Copper Blow | CB6 | 144.3 | cpy | 15.5 | 35.5 | 4.4 | 17 | 3.3 | 0.68 | 4.6 | 0.48 | 2.5 | 8.5 | 0.35 | 0.95 | 0.1 | 0.7 | 0.09 | 94.65 | 0.49 | 13.14 | 2.6 | 3.71 | 1.44 |
| CB13 | Copper Blow | CB6 | 144.3 | mt | 25.5 | 58 | 7.5 | 30 | 8.5 | 2 | 18.5 | 2.4 | 15 | 70 | 2.5 | 7.5 | 0.9 | 6 | 0.76 | 255.06 | 0.55 | 2.51 | 1.65 | 1.81 | 1.38 |

[1] $Eu^* = Eu_N/[(Nd_N+Tb_N)/2]$

0.8; Table 6.3; Fig. 6.7c).

### *6.6.2 Shear zone related prospects*

Similar to trace element concentrations of sulphide separates from the stratabound prospects, variations in trace elements can be related to different proportions of accessory phases. Relatively high Co (11900 – 13300 ppm) and Ni (1000 ppm) in arsenopyrite (*GG2*) from Green & Gold and pyrrhotite (*DD96*) from Lawsons is likely due to the presence of pyrite in the ore separate (Table 6.2; *Appendix 8*). High As contents (13500 ppm) in pyrite sample *GG19* are due to arsenopyrite inclusions. High Zn contents in sample *CB6* from Copper Blow is due to sphalerite (Table 6.2; *Appendix 8*). Chalcopyrite sample (*CB12*) and magnetite (*CB13*) has very high U contents (68 ppm and 230 ppm, respectively; Table 6.2).

Chondrite normalised REE patterns of sulphide separates from the shear zone related prospects are also highly variable, but predominantly LREE enriched ($Ce_N/Yb_N$ = 2.5 – 26.9; Table 6.3; Fig. 6.7d). The only exception is arsenopyrite sample (*GG2*), which has an unusual sinusoidal REE pattern (Fig. 6.7d). REE concentration are relatively enriched at Copper blow (ΣREE = 94.5 – 254.2 ppm), but relatively low at Green & Gold and Lawsons prospects (ΣREE = 6.6 – 63.1 ppm). HREE concentrations approach that of detection limit for samples from Lawsons (*DD96*) and Green & Gold (*GG19*). Eu anomalies are also variable, but consistently negative (Eu/Eu* = 0.35

– 0.68). Magnetite sample *CB13* from Copper Blow prospect not only has anomalous U contents (230 ppm), but also has the highest concentration of REE of all shear related prospects (ΣREE = 255 ppm; Table 6.3). Given the high U and REE concentrations in the samples from Copper Blow, it is likely that these samples contained (U-REE)-bearing inclusions that strongly affected the bulk sulphide sample geochemistry.

An altered albitite sample from Portia (*BN6*) has the highest REE contents of all samples analysed from Nth. Portia (ΣREE = 57.21 ppm). Sodic alteration is characteristic of mineralisation stratigraphically higher in the Portia system (*Appendix 8*). The Na-altered lithology has similar REE fractionation trends and total REE abundances to samples *BN5* and *BN3* from Portia, with a LREE-enriched composition ($Ce_N/Yb_N$ = 2.59; $Ce_N/Sm_N$ = 1.9; Table 6.3).

### *6.6.3 Host rock compositions*

A sample of metapelitic host rock from Kalkaroo (*K21*) adjacent to vein-style mineralisation (*K9*) was also analysed (Table 6.2, 6.3; *Appendix 8*). Although this sample is adjacent to vein mineralisation and K-Na alteration, the metasedimentary host sample had minimal alteration upon visual inspection (*Appendix 8*). This sample was analysed to create a reference point for the composition of the host metasedimentary sequence in the vicinity of Kalkaroo mineralisation. The metapelitic sample has a different trace element composition to the lower Willyama Supergroup metasediments (Barovich et al., 2002; Barovich, 2003). Relative to the Willyama metasediments elsewhere, it has high concentrations of Cu (300 ppm), and low concentrations of Zn (16 ppm) and Pb (5.5 ppm) (*Appendix 1*). The REE concentrations and chondrite normalised pattern are strikingly different to that of the Willyama Supergroup elsewhere (Barovich et al., 2002; Barovich, 2003), being LREE depleted ($La_N/Nd_N$ = 0.7;Fig. 6.7b; Table 6.3), has Sm below detection limit, and has a positive Eu anomaly (Eu/Eu* = 5.5), and an enrichment in HREE ($Y_N/Yb_N$ = 0.86).

## 6.7 Hydrothermal origin for REE and Cu mineralisation

As the majority of LA-ICPMS analyses of sulphides and Fe-oxides have REE concentrations below that of the detection limit, it is interpreted that REE concentrations detected by whole-rock analyses, and the few that were detected by LA-ICPMS, are from accessory REE-bearing phases or REE-bearing inclusions. The majority of these phases are not sulphide and Fe-oxide hosted, as petrographic and SEM investigations did not identify any REE-bearing phases hosted within sulphides or Fe-oxides. Accessory phases that were identified that contain REE in their crystallographic structure include apatite (La, Ce: samples *BN3*, *K9*, *WA1*, *WA8*, *SR1C*, *GG19*), monazite (La, Ce, Pr, Nd, Sm: sample *BN5*), titanite (Ce, Nd: sample *WA8*), ankerite (La, Ce, Pr, Nd, Sm: sample *BN4*), fluorite (La, Ce, Pr, Nd, Sm), garnet (HREE: sample *GG19*), epidote (LREE), fluocarbonates (LREE: Portia) (Fig. 6.8; *Appendix 8*). REE-bearing phases that can be identified in the LA-ICPMS ablation profiles include zircon (Zr[HREE]$SiO_4$; Fig. 6.6a, b), and potentially

monazite [(Ce,La,Nd)$PO_4$] or bastnäsite [(Ce,La,Nd)$CO_3$]. Some analyses that contain elevated REE concentrations could not be matched with elevated concentrations of Al, Ca, Ti, Zr, Th or U, as would be expected if the REE were derived from accessory zircon, apatite or monazite.

LA-ICPMS analyses also identified that sulphides and magnetite in the shear-related IOCG systems at Green & Gold and Copper Blow prospects potentially contain REE that are accommodated as impurities in the crystallographic structure of these phases. A relatively constant counts/second rate for the entire ablation interval is recorded by analytical point *GG19 01* (pyrite; Fig. 6.6e) for La, Ce and Nd, and by analytical point *CB6 07* (magnetite; Fig. 6.6f) for Yb, Er and Dy. Alternatively, the relatively constant counts/second rate may be recording REE-bearing inclusion micro-clusters.

It is interpreted that REEs recorded by whole-rock trace element and LA-ICPMS analyses are hydrothermal in origin. This is supported by the identification of accessory hydrothermal REE-bearing phases, and the few LA-ICPMS analyses that detected REE. Furthermore, REE concentrations recorded by whole-rock analyses are not derived from Willyama metasediment detrital rock fragments, as no rock fragments were observed to be hosted by the sulphide phases or Fe-oxide phases during rigorous petrographic observations, and care was taken during mineral separation to exclude silicate phases and host rock fragments. This interpretation is also supported by the majority of LREE concentrations of the ore samples, which are unlike that of the extreme LREE-enriched Willyama metasediments (Table 6.2, *Appendix 1*). With the exception of the extremely LREE-enriched and HREE-depleted sample *K7* (Fig. 6.7), average $La_N/Yb_N$ for the ore samples is 9.7 ($\sigma$ = 10.5), whereas the Willyama metasediments have an average $La_N/Yb_N$ of 15.1 ($\sigma$ = 7.4; Barovich et al., 2002; Barovich, 2003).

As the REE abundances are correlated with REE-bearing accessory phases and inclusions, it is inferred that the REE-bearing phases and the ore phases precipitated from the same hydrothermal fluid. Consequently, the total REE concentrations of the ore samples are considered to be representative of the composition of the hydrothermal fluid from which the ore phases precipitated, as available data on the uptake of REE from ore solutions suggest that sulphides do not fractionate REE to any significant extent (Graf, 1977; Siva Siddaiah et al., 1994). Therefore, the Nd isotopic composition of the fluid is also representative of the mineralising fluid, and therefore reflects the isotopic composition of the source(s).

## 6.8 Neodymium isotopic compositions of ore separates

Sm-Nd isotopic compositions of the majority of the samples analysed for trace element concentrations are listed in Table 6.3. Initial $^{143}Nd/^{144}Nd$ ratios were calculated at 1600 Ma for the stratabound prospects (North Portia, Kalkaroo, Waukaloo, Polygonum) and at 500 Ma for the shear-related prospects (Green & Gold, Lawsons, Copper Blow). It is reasonable to assume that sulphide remobilisation

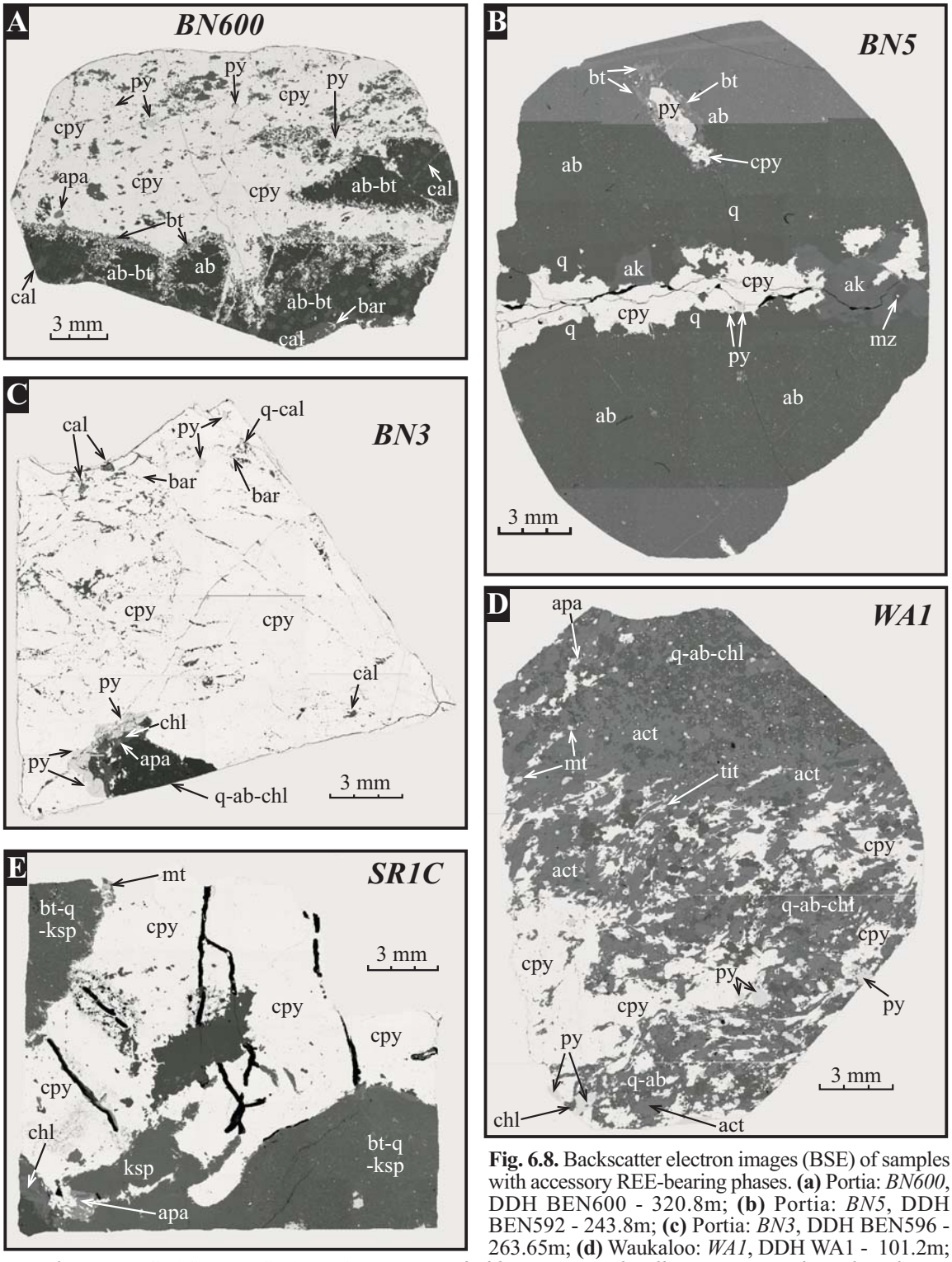


**Fig. 6.8.** Backscatter electron images (BSE) of samples with accessory REE-bearing phases. **(a)** Portia: *BN600*, DDH BEN600 - 320.8m; **(b)** Portia: *BN5*, DDH BEN592 - 243.8m; **(c)** Portia: *BN3*, DDH BEN596 - 263.65m; **(d)** Waukaloo: *WA1*, DDH WA1 - 101.2m; **(e)** Polygonum: *SR1C*, DDH SR1 - 504.8m. *Mineral abbreviations: ab: albite, act: actinolite, ak: ankerite, apa: apatite, bar: barite, bt: biotite, cal: calcite, chl: chlorite, cpy: chalcopyrite, ksp: K-feldspar, mt: magnetite, mz: monazite, py: pyrite, tit: titanite, q: quartz.*

occurred in the shear-related systems during the Delamerian Orogeny, considering that *P-T* estimates for Delamerian shear zone reactivation are in the order of 5 kbars and 530 – 600°C (Dutch et al., 2005).

### *6.8.1 Stratabound prospects*

The isotopic dataset as a whole shows a large variation in $^{147}Sm/^{144}Nd$ for the stratabound prospects, ranging between 0.0756 and 0.2801, however, the majority of samples

range between 0.1005 and 0.1935, reflecting the LREE enriched compositions (Table 6.4; Fig. 6.9). $^{143}Nd/^{144}Nd$ ratios are also variable, ranging between 0.511157 and 0.512953 (Table 6.4). $\varepsilon Nd_{1600}$ values range between –4.1 and –17.2 (Table 6.4; Fig. 6.9). The evolved $\varepsilon Nd_{1600}$ values of samples *K9*, *KND1*, *BN600*, *BN4* and *WA17* ($\varepsilon Nd_{1600}$ = –17. 2 to –9.4) are too evolved relative to any other initial εNd values of any protolith in the SCP (Barovich et al., 2002; Barovich, 2003; *Appendix 1*), and are therefore thought to be related to a younger event. The most likely event that this would be is the Delamerian Orogeny (~500 Ma; Dutch et al., 2005). Potential implications of these extremely evolved initial εNd values are discussed below.

### *6.8.2 Shear-related prospects*

Due to the occurrence of the shear related prospects being adjacent to, or within shear zones reactivated during the Delamerian Orogeny, or within parts of the SCP that have been pervasively reworked during the Delamerian Orogeny (Dutch et al., 2005; *Chapter 7*), the initial $^{143}Nd/^{144}Nd$ ratios are calculated at 500 Ma. Temperature within shear zones reactivated during the Delamerian Orogeny have been calculated to be ~550°C (Dutch et al., 2005), and it is therefore likely that sulphides were remobilised, and the Nd isotopic compositions re-equilibrated during the Delamerian Orogeny. $^{147}Sm/^{144}Nd$ ratios are variable, ranging between 0.0620 and 0.3021 (Fig. 6.9), thus reflecting the LREE enriched compositions of the sulphides. $^{143}Nd/^{144}Nd$ ratios range between 0.511247 and 0.512953. Initial εNd values range between –0.6 and –18.6 (Table 6.4; Fig. 6.9).

## 6.9 Discussion

### *6.9.1 Mineralising fluid composition and effects on REE mobility*

With the exception of the arsenopyrite sample (*GG2*), all samples of sulphide mineralisation in this study show a relative enrichment of LREE relative to HREE, regardless of total REE abundance. The majority of samples also have variably negative Eu anomalies. As chloride complexes are the dominant species in acidic (pH = 3.5 – 4), relatively high temperature (~300 – 400°C), and Cu-Au-bearing hydrothermal fluids (Davidson & Large, 1994; Fig. 6.4), then the LREE will be relatively enriched relative to the HREE in the hydrothermal fluid given species calculations for REE-complexation (Haas, 1995; Fig. 6.3). This is reflected by the REE patterns of the ore samples that are consistently LREE-enriched (Fig. 6.7). Available data on the uptake of REE from ore solutions suggest that sulphides do not fractionate REE to any significant extent (Siva Siddaiah et al., 1994; Graf, 1977). Therefore, the LREE-enriched composition of the ore precipitates are interpreted to be representative of the mineralising fluid.

REE abundances and LREE-enriched compositions of the ore samples suggest that the fluid were most likely $H_2O$-dominated crustally derived fluids, as mantle derived $H_2O$-$CO_2$ fluids are reported to have very high REE abundances (Hansen, 1981). The hypersaline composition of the ore fluids reported for the North Portia, Kalkaroo and Waukaloo and IOCG systems prospects (e.g. Skirrow et al., 2000), and indicative of IOCG

**Table 6.4.** Sm-Nd isotope data of ores from IOCG prospects in southern Curnamona Province.

| Sample | Prospect | Phase | Nd (ppm) | Sm (ppm) | Age (Ma) | $^{147}Sm/^{144}Nd$ | 2σ | $^{143}Nd/^{144}Nd$ | 2σ | εNd | $^{143}Nd/^{144}Nd_{(i)}$ | $\varepsilon Nd_{(i)}$ | $T_{DM}$ | $T_{CHUR}$ |
|---|---|---|---|---|---|---|---|---|---|---|---|---|---|---|
| BN600 | Nth. Portia | cpy | 1.31 | 0.61 | 1600 | 0.2801 | 0.00170 | 0.512935 | 0.00005 | 5.8 | 0.50999 | -11.4 | -503 | 543 |
| BN3 | Nth. Portia | cpy | 1.67 | 0.51 | 1600 | 0.1861 | 0.00002 | 0.512180 | 0.00001 | -8.9 | 0.51022 | -6.8 | 5140 | 6545 |
| BN4 | Nth. Portia | cpy | 1.88 | 0.59 | 1600 | 0.1886 | 0.00005 | 0.512075 | 0.00001 | -11.0 | 0.51009 | -9.4 | 6223 | 10429 |
| BN5 | Nth. Portia | cpy | 6.44 | 1.12 | 1600 | 0.1047 | 0.00063 | 0.511411 | 0.00001 | -23.9 | 0.51031 | -5.1 | 2402 | 2027 |
| KND1 | Kalkaroo | py | 1.16 | 0.34 | 1600 | 0.1766 | 0.00026 | 0.511829 | 0.00001 | -15.8 | 0.50997 | -11.7 | 5243 | 6071 |
| K7 | Kalkaroo | cpy | 49.01 | 6.13 | 1600 | 0.0756 | 0.00001 | 0.511157 | 0.00001 | -28.9 | 0.51036 | -4.1 | 2178 | 1860 |
| K8 | Kalkaroo | py | 34.46 | 5.73 | 1600 | 0.1005 | 0.00001 | 0.511300 | 0.00001 | -26.1 | 0.51024 | -6.4 | 2462 | 2115 |
| K9 | Kalkaroo | py | 2.01 | 0.64 | 1600 | 0.1935 | 0.00007 | 0.511729 | 0.00001 | -17.7 | 0.50969 | -17.2 | 9989 | 38802 |
| K11 | Kalkaroo | py | 18.55 | 5.07 | 1600 | 0.1651 | 0.00001 | 0.511936 | 0.00002 | -13.7 | 0.51020 | -7.2 | 3709 | 3366 |
| WA1 | Waukaloo | cpy | 29.39 | 6.55 | 1600 | 0.1348 | 0.00001 | 0.511610 | 0.00001 | -20.0 | 0.51019 | -7.4 | 2924 | 2520 |
| WA8 | Waukaloo | moly | 12.41 | 3.04 | 1600 | 0.1482 | 0.00001 | 0.511833 | 0.00001 | -15.7 | 0.51027 | -5.8 | 3010 | 2526 |
| WA15 | Waukaloo | cpy | 14.91 | 3.32 | 1600 | 0.1345 | 0.00002 | 0.511674 | 0.00001 | -18.8 | 0.51026 | -6.1 | 2796 | 2356 |
| WA17 | Waukaloo | cpy | 6.80 | 1.69 | 1600 | 0.1506 | 0.00001 | 0.511677 | 0.00001 | -18.8 | 0.51009 | -9.4 | 3487 | 3164 |
| SR1A | Polygonum | cpy | 0.45 | 0.10 | 1600 | 0.1287 | 0.00342 | 0.511691 | 0.00001 | -18.5 | 0.51034 | -4.6 | 2578 | 2117 |
| SR1C | Polygonum | cpy | 1.71 | 0.28 | 1600 | 0.0974 | 0.00017 | 0.511299 | 0.00001 | -26.1 | 0.51027 | -5.8 | 2398 | 2050 |
| GG2 | Green & Gold | asp | 2.79 | 1.40 | 500 | 0.3021 | 0.00001 | 0.512953 | 0.00002 | 6.1 | 0.51196 | -0.6 | -345 | 456 |
| GG19 | Green & Gold | py | 2.93 | 0.78 | 500 | 0.1600 | 0.00003 | 0.511777 | 0.00001 | -16.8 | 0.51125 | -14.5 | 3808 | 3560 |
| DD96 | Lawsons | po | 1.55 | 0.16 | 500 | 0.0620 | 0.00301 | 0.511247 | 0.00001 | -27.1 | 0.51104 | -18.6 | 1896 | 1572 |
| CB6 | Copper Blow | cpy | 35.76 | 6.44 | 500 | 0.1089 | 0.00001 | 0.511515 | 0.00001 | -21.9 | 0.51116 | -16.3 | 2349 | 1946 |
| CB12 | Copper Blow | cpy | 18.25 | 3.38 | 500 | 0.1118 | 0.00001 | 0.511667 | 0.00001 | -18.9 | 0.51130 | -13.5 | 2193 | 1742 |
| CB13 | Copper Blow | mt | 24.53 | 6.62 | 500 | 0.1630 | 0.00001 | 0.511699 | 0.00001 | -18.3 | 0.51116 | -16.2 | 4249 | 4215 |

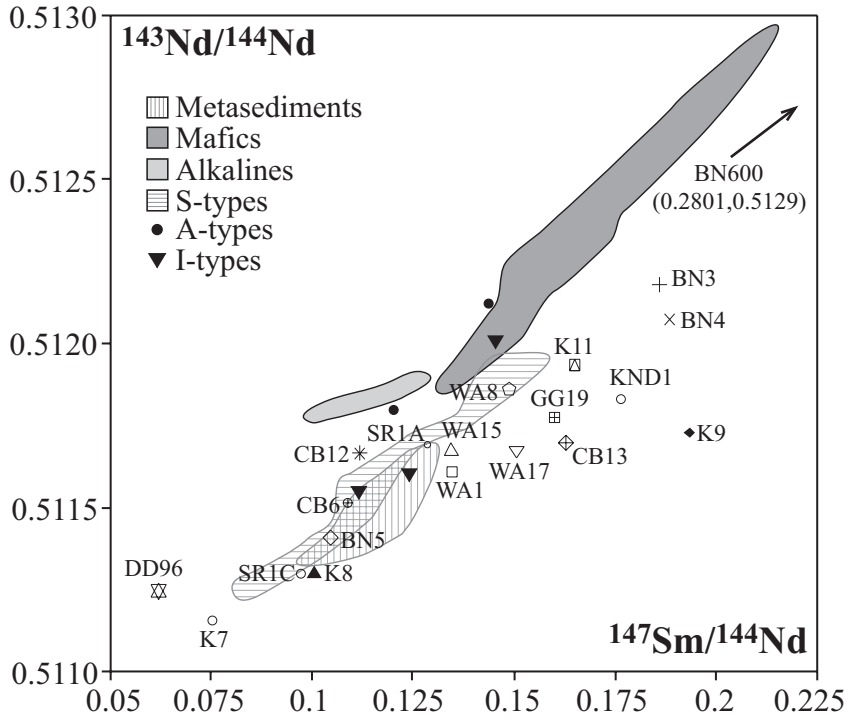


**Figure 6.9.** $^{143}Nd/^{144}Nd$ versus $^{147}Sm/^{143}Nd$ plot of individual ore samples from IOCG prospects. Fields of major protoliths in the Olary Domain highlighted. Data sources: metasediments - Barovich et al., 2002; S-types - Barovich & Foden, 2002; A-types - Ashley et al., 1996; I-types - Freeman, 1995; Mafics - *Chapter 4*; Alkalines - *Chapter 5*.

mineralising fluids (10 – 30 wt% NaCl; Davidson & Large, 1995), require that the source of the mineralising fluids be enriched in $H_2O$ and NaCl.

Possible sources of $H_2O$ and NaCl enriched fluids include: prograde metamorphic fluids, retrograde metamorphic fluids; and granitic fluids. Given that IOCG mineralisation in the SCP occurred during prograde Olarian metamorphism (~1610 – 1600 Ma; *section 2.2.5*), the $H_2O$-NaCl enriched fluids could only be derived during prograde metamorphism, as magmatism and retrograde metamorphism occurred at least 15 million years after mineralisation (Skirrow et al., 2000; Page et al., 2003). Consequently, the most likely source for deriving such $H_2O$-NaCl enriched fluids is interpreted to be the lower Willyama Supergroup metasediments (Ethiudna Subgroup; Conor, 2000a, b). Lithologies in this part of the Willyama Supergroup sequence are oxidised and enriched in meta-evaporitic and exhalative lithologies (Conor, 2000a).

Relatively saline- and chlorine-rich fluids could potentially be generated through leaching of the Ethiudna Subgroup sequences, which are the dominant host rocks to many of the IOCG prospects in this study (e.g. North Portia, Kalkaroo, Polygonum, Green & Gold; *Appendix 8*). The timing of development of these brines remains unclear, but could have started to develop as early as diagenesis (~1715 Ma), through to the onset of prograde metamorphism (~1610 Ma; *Chapter 3*). Absolute variations in total REE abundances and LREE enrichment is likely due to several factors, including variations in fluid temperature and composition (Fig. 6.3), differences in abundance of REE-bearing inclusions within the ore samples, and/or subsequent remobilisation of the REE during

leaching. Additionally, the proximity of the site of mineralisation to the main fluid conduit has also been shown to effect REE abundances, which elsewhere have been shown to decrease with increasing distance from the main conduit (Baker & Hellingwerf, 1988).

Evidence for leaching of the metasedimentary sequence in the vicinity of mineralisation is in part suggested by the LREE depletion of the metasedimentary host lithology at Kalkaroo prospect (sample *K9*; Fig. 6.7b). Although few interpretations can be made with confidence on the basis of one sample, given that the stratigraphic level of mineralisation at Kalkaroo is the Ethiudna Subgroup, then the host sequence at Kalkaroo has been depleted in LREE relative to Willyama Supergroup metasediments elsewhere (Barovich et al., 2002; Barovich, 2003). As the Ethiudna Subgroup has abundant evaporite and exhalative horizons (Conor, 2000a, b; 2004), the potential exists that saline, chlorine-rich, and metalliferous fluids responsible for IOCG mineralisation were derived from the Ethiudna Subgroup.

The cause of the consistent enrichment of Gd relative to Eu and Tb is not clear. It may be a sample dissolution or analytical quirk, however its consistency among all phases (chalcopyrite, pyrite, magnetite), and at all prospects may indicate it is a primary signature of the samples. It has been documented that fluorite deposited from hydrothermal fluids derived from pure sedimentary carbonates have anomalously high Gd concentrations (Bau et al., 2003). Given that the Ethiudna Subgroup has a high proportion of calc-silicate and carbonate lithologies (Conor, 2000a, b), then one consistent notion is that the enriched Gd concentrations of the ore samples may be inherited from sedimentary fluorite contained within carbonate lithologies of the Ethiudna Subgroup.

The leaching of REE from the metasedimentary sequence by saline, chlorine-rich fluids also has implications for the mobility of metals in the SCP. The composition of the fluids suggests Cu and S would also have been leached from the host rocks (e.g. De Jong et al., 1998; Oliver et al., 2004). It is highly likely that the metasedimentary sequences could be a significant source component to nearby mineralisation, given that the Ethiudna Subgroup is anomalous in base metal content (Conor, 2004). Broad-scale leaching of the metasedimentary sequence could potentially mobilise metals that could accumulate to appreciable quantities. A similar process for the generation of Cu-Au deposits from deep underlying host rocks by saline, chlorine-rich fluids has been proposed in the Cloncurry district and Olympic Dam region, which caused the generation of several economic Cu-Au deposits (De Jong et al., 1998; Haynes et al., 1995; Johnson & McCulloch, 1995). Furthermore, the derivation of complexing agents from evaporitic sources and the ultimate generation of IOCG deposits from hydrothermal fluids have also been recorded in both Phanerozoic and Proterozoic extensional continental and continent-margin settings (Barton & Johnson, 1996).

### *6.9.2 Comparison of Nd isotopic compositions of ores with known reservoirs*

As the REE concentrations of the sulphides

and Fe-oxides are derived from hydrothermal accessory phases or inclusions hosted by the ore phases (*section 6.7*), the Nd isotope compositions of the mineralised volumes are interpreted to be representative of the mineralising fluid, and not detrital rock fragments or host rocks. Consequently, the Sm-Nd isotopic systematics provides information about the most likely hydrothermal reservoir components (source regions). Fig. 6.10 shows initial εNd values versus age (Ga) for the different IOCG ore samples. These values are superimposed on the Nd isotopic arrays for major protolith reservoirs in the southern Curnamona Province. A clear correlation between the IOCG ore samples and the Nd isotopic composition of the Willyama Supergroup metasediments exist (Barovich, 2003; Barovich et al., 2002; *Appendix 1*). This correlation is also corroborated by cumulative histograms plots of $\varepsilon Nd_i$ values for the ore samples and the potential reservoirs, calculated at 1600 Ma and 500 Ma for stratabound and shear-related mineralisation, respectively (Fig. 6.11).

For the stratabound mineralised systems, four samples plot outside the field of Willyama metasediments at 1600 Ma (samples *BN4*, *BN600*, *KND1*, *K9*, *WA17*). These samples have far too evolved $\varepsilon Nd_i$ values at 1600 Ma to be derived from any known protolith in the SCP at this time. Consequently, these samples are interpreted to have had their Nd isotopic systematics altered from their initial compositions, or they potentially are related to an entirely different mineralisation event to the majority of other stratabound mineralisation. The only other substantial tectonothermal event shown to have affected the SCP, and when epigenetic mineralisation occurred elsewhere, is the Delamerian Orogeny (~500 Ma; Bierlein et al., 1996c; Dutch et al., 2005). Therefore, the Nd isotopic compositions of these samples are interpreted to be related to a ~500 Ma event. When the Nd isotopic compositions of these samples are re-calculated at 500 Ma, they have $\varepsilon Nd_i$ values that are similar, and overlap with those of the Willyama Supergroup metasediments at ~500 Ma (Fig. 6.10, 6.11).

Samples *BN600* and *BN4* from the North Portia prospect, which have relatively low REE concentrations and show evidence for LREE depletion (Fig. 6.7), are interpreted to reflect hydrothermal activity related to the Delamerian Orogeny. The Delamerian Orogeny may have introduced a distinctly new mineralised hydrothermal fluid into these prospects, or simply remobilised pre-existing mineralisation. Widespread propylitic-phyllitic alteration (carbonate – chlorite – talc) and local chalcopyrite-pyrite mineralisation that post-dates all other alteration and mineralisation events has been recorded at North Portia and Kalkaroo prospects (e.g. Teale & Fanning, 2000a; Skirrow et al., 2000). This alteration and mineralisation event is interpreted to be associated with the Delamerian Orogeny, and responsible for altering the REE systematics of the samples mentioned from North Portia, Kalkaroo and Waukaloo.

Similar to the Nd isotopic composition of stratabound IOCG in the SCP, the shear-related IOCG systems also have Nd isotopic compositions that overlap with the Willyama Supergroup metasedimentary sequence at 500

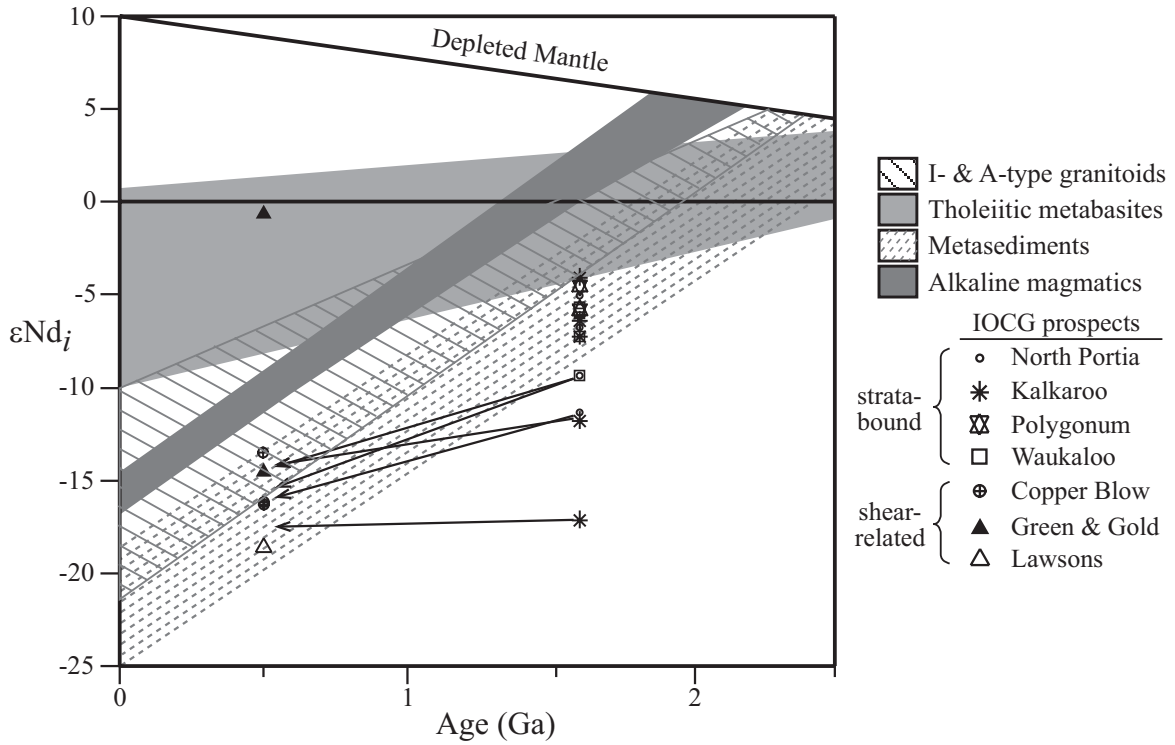


**Figure 6.10.** εNd$_i$ versus age (Ga) for IOCG ore samples and major reservoirs that could potentially contribute to mineralised hydrothermal fluid. Initial Nd isotopic composition for stratabound/stratiform mineralisation calculated at 1600 Ma. Shear-related prospects calculated at 500 Ma (Data for A-types from Ashley et al., 1996; I-types from Freeman, 1995).

Ma. The only exception to this is the arsenopyrite sample (*GG2*) from the Green & Gold prospect, which has a distinctly more primitive εNd$_i$. This sample also displays unusual fractionation in its chondrite-normalised pattern for the entire range of REE (Fig. 6.7d). It is unclear what the cause of this REE fractionation pattern and Nd isotopic composition.

On the basis of data presented in this study, it is not possible to determine whether Delamerian aged mineralisation involved a newly generated mineralised hydrothermal fluid, or merely remobilised pre-existing mineralisation. However, on the basis of the sulphur isotopic signatures from epigenetic mineralisation elsewhere in the SCP, Bierlein et al (1996a) interpreted that epigenetic mineralisation was formed from its own distinct hydrothermal fluid generated during the Delamerian Orogeny, and not through simple remobilisation of pre-existing mineralisation.

### *6.9.3 Genesis of IOCG mineralisation in the SCP*

The combination of trace element and Nd isotopic compositions of ore samples from IOCG mineralisation in the SCP provide initial constraints on the establishing a genetic model for the generation of IOCG in the SCP. Fig. 6.12 shows a schematic representation of the critical elements from this study that need to be taken into account in any model. Following is a summary of key components viewed to be crucial for the genesis of IOCG mineralisation in the SCP:

- Dewatering of lower Willyama Supergroup (Ethiudna Subgroup) during prograde metamorphism associated with the Olarian Orogeny (~1610 Ma) generated highly

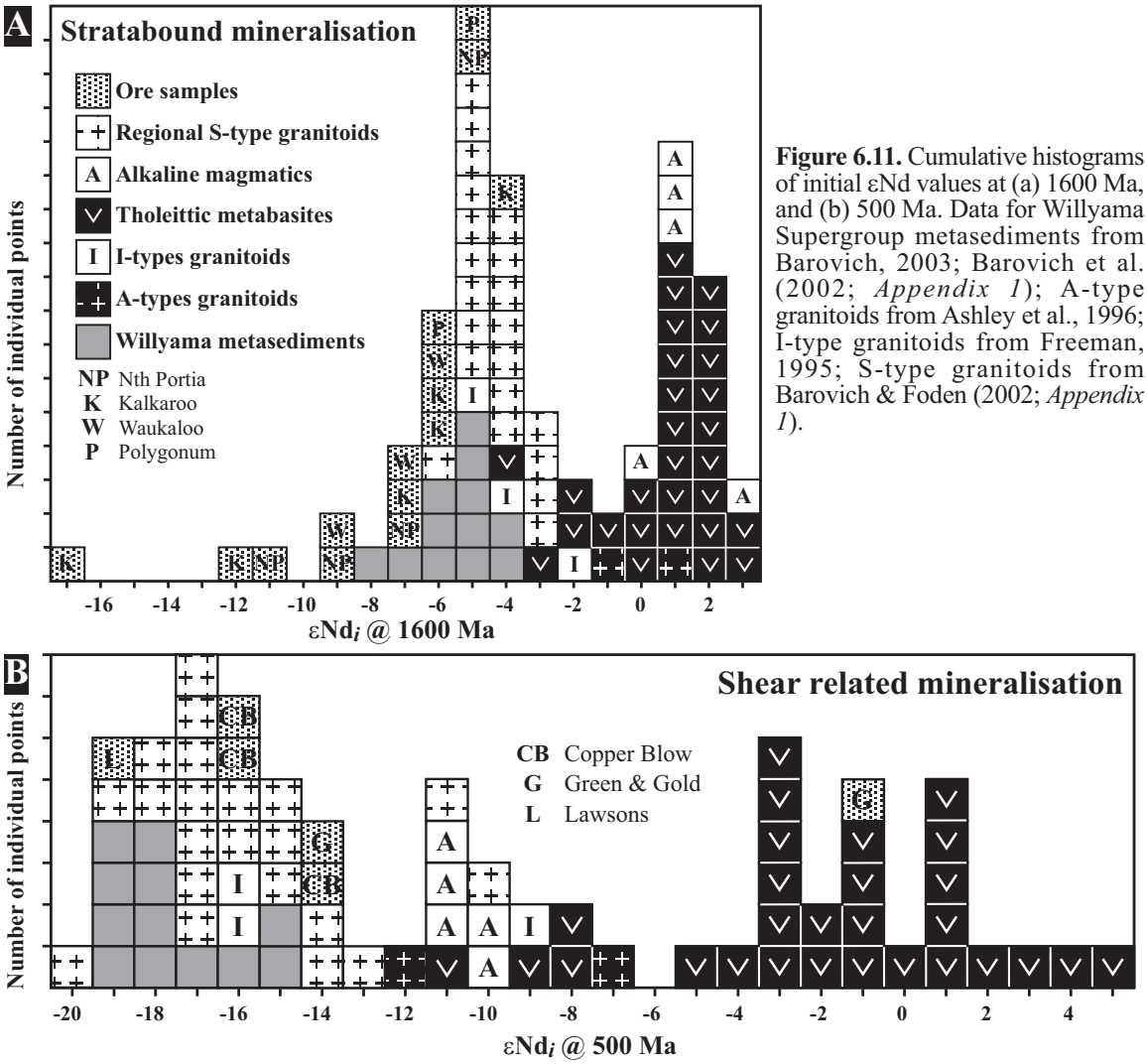


**Figure 6.11.** Cumulative histograms of initial εNd values at (a) 1600 Ma, and (b) 500 Ma. Data for Willyama Supergroup metasediments from Barovich, 2003; Barovich et al. (2002; *Appendix 1*); A-type granitoids from Ashley et al., 1996; I-type granitoids from Freeman, 1995; S-type granitoids from Barovich & Foden (2002; *Appendix 1*).

saline, chlorine-rich and metalliferous fluids;

- Mineralising fluid migrated through metasedimentary sequence by tectonic pumping mechanisms (e.g. Bierlein et al., 1995), and accumulated in favourable structural and/or chemical settings where metals could precipitate from solution. Redox boundary between Curnamona Group (oxidised) and Strathearn Group (reduced) critical horizon at which fluids began precipitating metals (e.g. Leyh & Conor, 2000). Sodic and potassic alteration of surrounding metasediments associated with mineralisation (e.g. Teale & Fanning, 2000a; Skirrow et al., 2000; *Appendix 8*);

- Overprinting of syn-Olarian mineralisation by a new hydrothermal system, or remobilisation and upgrading of pre-existing mineralisation (e.g. Teale & Fanning, 2000a), occurred during the Delamerian Orogeny (~500 Ma) and was associated with propylitic-phyllitic alteration (e.g. Teale & Fanning, 2000a).

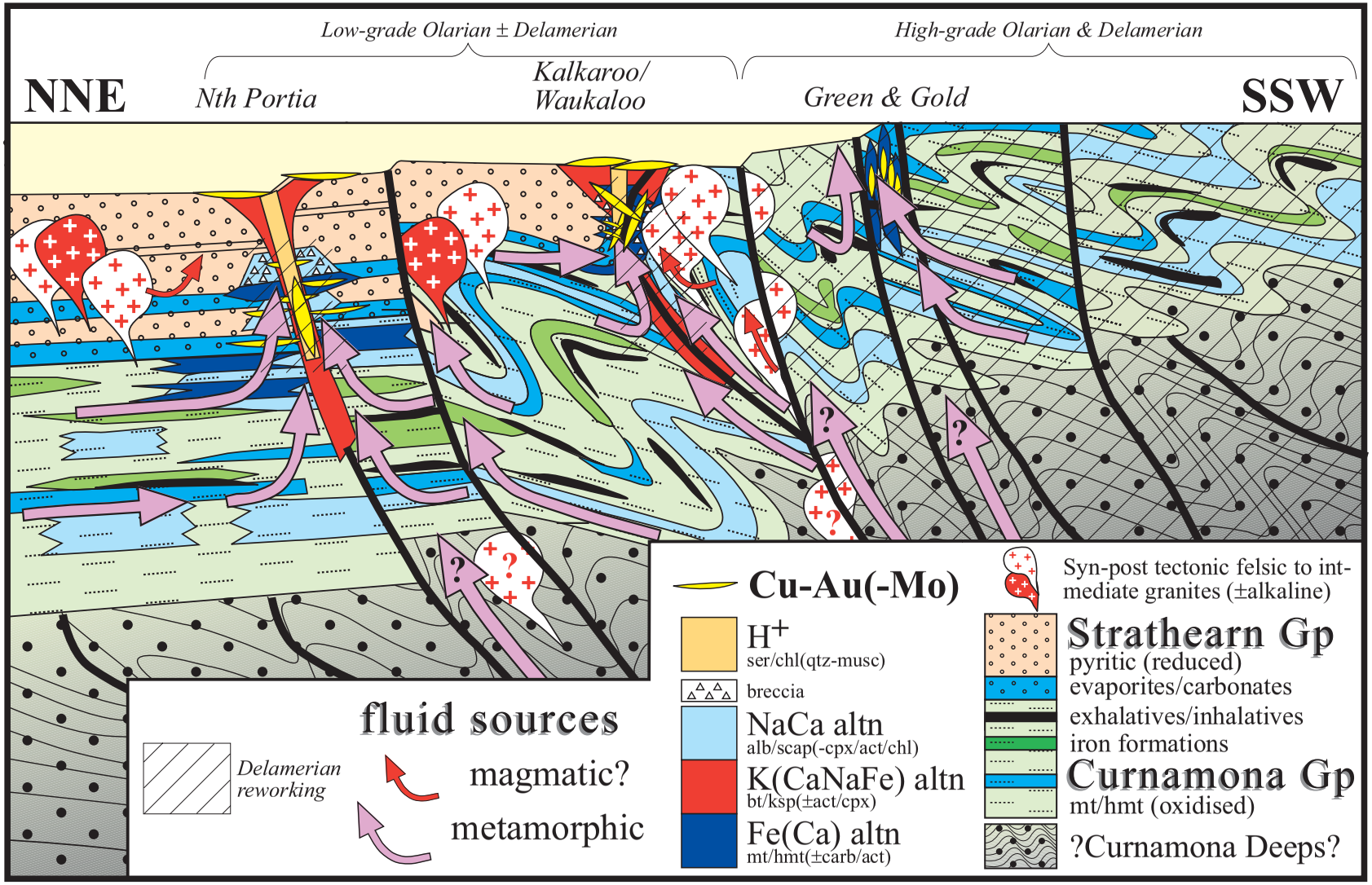


**Figure 6.12.** Schematic representation of iron-oxide copper-gold mineral systems in the southern Curnamona Province. Cross-section incorporates mineralisation from the Benagerie Ridge region in the northeast (e.g. North Portia) to the shear-related systems in the southwest (e.g. Green & Gold).

# Chapter 7

# DELAMERIAN-AGED METAMORPHISM: IMPLICATIONS FOR THE EVOLUTION OF THE OLARIAN OROGENY

**This chapter is a version of a manuscript published in Terra Nova (V18, p138-146, 2006) under the title: "Delamerian-aged metamorphism in the southern Curnamona Province, Australia: implications for the evolution of the Mesoproterozoic Olarian Orogeny". Authors: Rutherford, Hand & Mawby. Aspects relating to the regional geological framework and analytical procedures have been removed from this chapter to avoid repetition of previous chapters.**

***SUMMARY***

*Monazite electron microprobe Th-U-Pb and garnet Sm-Nd isotopic data from metapelitic assemblages in the Willyama Supergroup in the southern Curnamona Province indicate that terrain underwent regional greenschist to amphibolite-grade metamorphism during the c. 500 Ma Delamerian Orogeny. The Delamerian-aged mineral assemblages include the development of prograde garnet-staurolite and kyanite-bearing associations that overprint andalusite and sillimanite bearing assemblages that developed during the c. 1600 Ma Olarian Orogeny. Importantly, the development of secondary kyanite-bearing assemblages in the southern Curnamona Province has been used previously to suggest that the Olarian Orogeny followed an anticlockwise P-T evolution. If such assemblages are the product of c. 500 Ma metamorphism, the thermobarometric evolution of the Olarian Orogeny needs to be re-evaluated. This study highlights the utility of linking in situ geochronological approaches and petrologically important phases. Such an approach will provide a robust framework for establishing P-T-t evolutions within complexly deformed and polytectonic terrains.*

## 7.1 Introduction

The metamorphic evolution of basement terrains holds important clues regarding the mechanisms that lead to metamorphism and associated deformations (Wickham & Oxburgh, 1987; Sandiford & Powell, 1990). One of the key steps in constraining the thermobarometric evolution of the terrain is the identification of mineral parageneses that reflect the progress of a single tectonic event (Clarke et al., 1987; 1995; Stüwe & Ehlers, 1997). If the products of several events are casually linked, there is a danger of producing apparent metamorphic histories that provide little constraint on the evolution of any of the events that have affected the terrains (e.g. Kelsey et al., 2003; Carson et al., 2004).

In this study, geochemical and isotopic data from retrograde metapelitic assemblages in the southern Curnamona Province (SCP) is presented. The SCP has been the focus of a large number of studies on the structural and metamorphic evolution of the c. 1600 Ma Olarian Orogeny, which shaped much of the geological character of the SCP (Stevens et al., 1980; Clarke et al., 1986; 1987; Robertson et al., 1998). A key outcome of this body of work is that the Olarian Orogeny followed an anticlockwise *P-T* evolution (Phillips & Wall, 1981; Corbett & Phillips, 1981; Clarke et al., 1987; 1995). This conclusion was based on the observed sequence of mineral growth that was interpreted to be characterised by staurolite- and kyanite-bearing mineral assemblages that overprinted the regional high-grade andalusite- and sillimanite-bearing assemblages (Phillips & Wall, 1981; Corbett & Phillips, 1981; Clarke et al., 1987). The growth of late-stage kyanite staurolite-bearing assemblages at the expense of andalusite and sillimanite provided control points for the model *P-T* path. The interpretation that the SCP had undergone an anticlockwise *P-T* evolution has implications for the nature of the thermal processes responsible for high-T metamorphism, namely advective heating. However, the SCP is one of the problem regions in Proterozoic Australia where the thermal drivers that could generate anticlockwise *P-T* paths are hard to find (e.g.

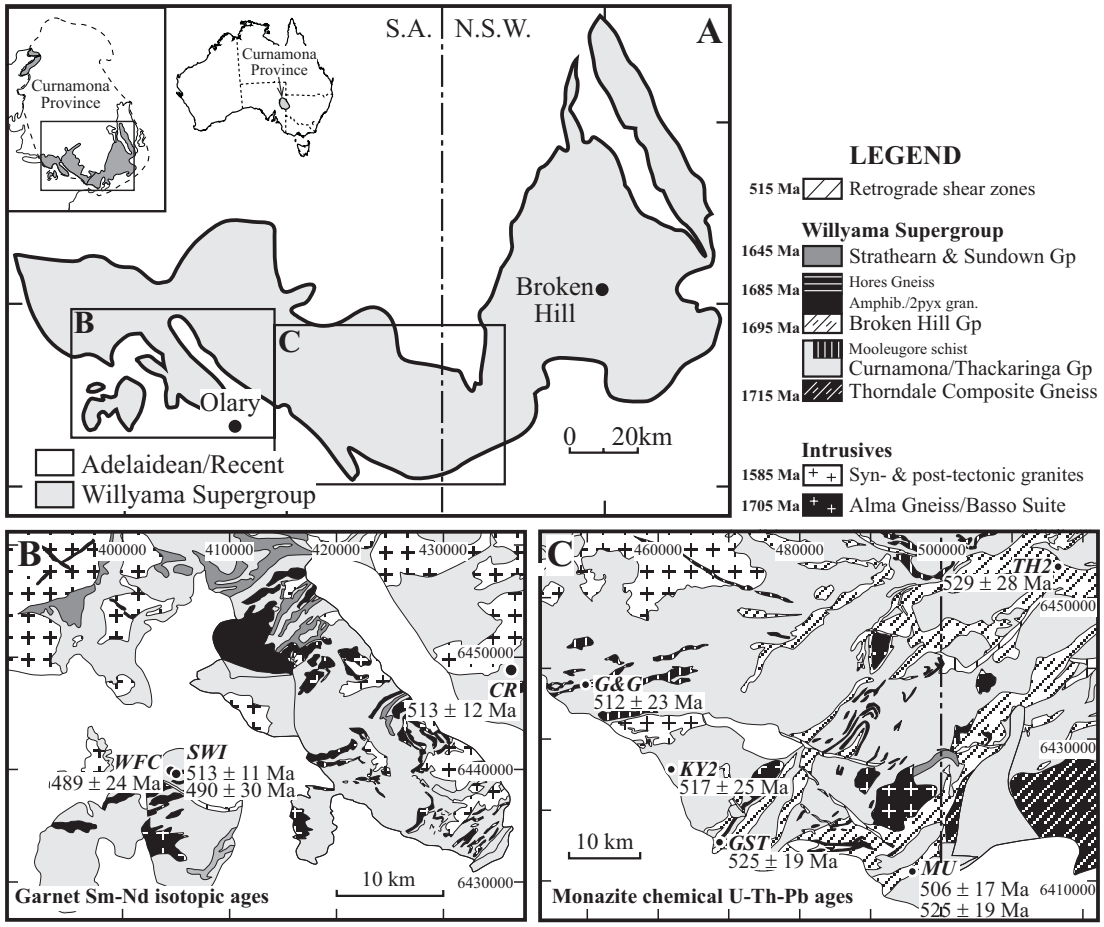


**Figure 7.1.** Regional interpreted solid geological maps of the southern Curnamona Province (Jenkins & Burtt, 2003; Datum: GDA94), showing sample localities and corresponding ages.

Sandiford & Hand, 1998).

The data presented in this study suggests that the development of secondary mineral assemblages formed during the Delamerian Orogeny (c. 500 Ma), rather than the Olarian Orogeny. This means that the interpreted *P-T* evolution for the Olarian Orogeny requires revision, and highlights the importance of obtaining age constraints for the growth of key minerals used in the establishment of *P-T* paths.

## 7.2 Analytical techniques

Sample localities and summary of all age data is provided in Fig. 7.1. A summary of the petrography and age data is listed in Table 7.1. The analytical procedure and age calculation technique for chemical U-Th-Pb monazite dating using the electron microprobe (EPMA) is outlined in *Chapter 3*. A summary of the chemical age data is listed in Table 7.2. Appendix 10 lists the entire chemical U-Th-Pb monazite age data set. Table 7.3 lists the garnet Sm-Nd data. A detailed description of the garnet Sm-Nd technique is supplied in Gray et al. (2004). For the garnet overgrowth sample (*CR*), a large garnet (>2 cm) with a thick overgrowth rim was shaved off. Overgrowths have a distinct colouration difference relative to the core making separation relatively easy. For the other two samples (*WFC and SWI*), the garnets were separated from the whole rock and were crushed, milled and sieved. Mineral fractions were extracted using a magnetic separator and

**Table 7.1.** Metapelitic lithologies used in this study that preserve Delamerian mineral assemblages.

| Sample name | Location (Grid ref: GDA94) | Lithology | Stratigraphic unit | Description / petrography | Analytical technique | Age (Ma) |
|---|---|---|---|---|---|---|
| *GST* | Radium Hill (6415381, 468784) | gt-st-bt metapelitic schist | Wiperaminga Subgroup | Foliated metapelite with post-kinematic garnet porphyroblasts (<2 mm). Syn- and post-kinematic staurolite porphyroblasts (<5 mm). Monazite occluded by staurolite. | Chemical U-Th-Pb monazite | 525 ± 19 (n=40; 95% c.i.)<br>1511 ± 42 (n=26; 95% c.i.) |
| *KY2* | Radium Hill (6425540, 461845) | ky-bt metapelitic schist | Wiperaminga Subgroup | Coarse-grained ky and bt. Large ky porphyroblasts randomly oriented | Chemical U-Th-Pb monazite | 517 ± 25 (n=86; 95% c.i.) |
| *MU* | Mutooroo (6444277, 425230) | gt-chl-bt-mu-fsp-qtz retrograde metapelitic schist | Thackaringa Group | Lithology pervasively retrogressed, with very fine-grained matrix of mu-seri. Pervasively fractured gt porphyroblasts have fractured infilled with bt-mu-seri | Chemical U-Th-Pb monazite | 506 ± 17 (n=86; 95% c.i.) |
| *TH* | Thackaringa (6454117, 516246) | gt-bt-mu-fsp-qtz metapelitic schist | Thackaringa Group | Fabric defined by bt-mu and qtz-fsp layers. Pervasively fractured gt porphyroblasts have bt coronas. Other less fractured gt porphyroblasts postdate fabric development. | Chemical U-Th-Pb monazite | 529 ± 28 (n=29; 95% c.i.) |
| *G&G* | Green & Gold (6437528, 449522) | hb-q-gt-bt-mt-st metapelitic schist | Curnamona Group | Strongly folitated hb-bt-gt-mt-chl metapelitic schist within shear zone (altered). | Chemical U-Th-Pb monazite | 512 ± 23 (n=69; 95% c.i.) |
| *CR* | Cathedral Rock (6446728, 433985) | two-stage gt-bt-mu-q-fsp metapelitic schist | Wiperaminga Subgroup | Two-stage gt-bt-mu-q-fsp metapelitic schist. Garnet overgrowths post-date fabric. | Garnet Sm-Nd isotopes | 513 ± 12 Ma (2σ) |
| *WFC* | Weekeroo (6440017, 404671) | mu-bt-q-chl-gt retrograde metapelitic schist | Wiperaminga Subgroup | Pervasively retrogressed metapelitic schist. Former andalusite porphyroblasts pseudomorphed by mu-bt-chl-q-gt aggregates. | Garnet Sm-Nd isotopes | 476 ± 29 Ma (2σ) |
| *SWI* | Weekeroo (6439419, 405039) | mu-bt-q-chl-gt retrograde metapelitic schist | Wiperaminga Subgroup | Pervasively retrogressed metapelitic schist. Former andalusite porphyroblasts pseudomorphed by mu-bt-chl-q-gt aggregates. | Garnet Sm-Nd isotopes | 513 ± 11 Ma (2σ);<br>490 ± 30 Ma (2σ) |

**Table 7.2.** Summary of monazite chemical age data.

| Sample | Lithology | Locality | Stratigraphic position | Occluding phase | Wt% Pb Avg., S.D.a | Wt% Th Avg., SD. | Wt% U Avg., SD. | Age and error (Ma) | N= |
|---|---|---|---|---|---|---|---|---|---|
| *MU* | gt-chl-mica-fsp schist | Mutooroo | Broken Hill Gp | mu, bt | 0.110, 0.046 | 4.025, 1.99 | 0.267, 0.048 | 506 ± 17 | 86 |
| *TH* | gt-mica-fsp-q schist | Thackaringa | Broken Hill Gp | bt, fsp | 0.155, 0.036 | 4.710, 0.931 | 0.582, 0.103 | 523 ± 12 | 122 |
| *KY2* | ky-bt schist | Radium Hill | Curnamona Gp | ky | 0.082, 0.036 | 2.428, 1.236 | 0.341, 0.103 | 517 ± 25 | 86 |
| *GST* | gt-st-bt schist | Radium Hill | Curnamona Gp | st | 0.192, 0.081 | 6.858,3.341 | 0.408, 0.164 | 525 ± 19 | 40 |
| | | | | st | 0.506, 0.052 | 5.376, 0.186 | 0.534, 0.085 | 1511 ± 42 | 26 |
| G&G | hb-bt-gt-st schist | Green&Gold | Curnamona Gp | hb | 0.082, 0.036 | 2.715, 1.669 | 0.279, 0.078 | 512 ± 23 | 69 |

heavy liquids. To minimise the effects of heavy rare earth element inclusions, samples were leached in hot HF for ~1 hour. Isotopic ratios were analysed on a Finnagan MAT262 Mass Spectrometer at Geology & Geophysics, University of Adelaide.

## 7.3 Textural relationships and geochronology

### *7.3.1 Monazite-bearing metapelites*

Metapelitic samples from across the SCP record monazite EMPA ages that relate to the Delamerian aged metamorphism (Fig. 7.1; Table 7.1, 7.2). Monazite occluded by post-kinematic staurolite within garnet-biotite metapelites (*GST*; Fig. 7.2a), and monazite occluded by post-kinematic kyanite (*KY2*; Fig. 7.2b) have monazite U-Th-Pb chemical ages of 525 ± 19 Ma (n=40) and 517 ± 25 Ma (n=86), respectively (Table 7.2). Sample *GST* also preserves an older monazite growth event related to a Proterozoic tectonothermal event (1511 ± 42 Ma; n=26). Monazite grains in sample *GST* have complex compositional zoning as reflected in BSE images (Fig. 7.2b). This is due to variations in Th concentrations (4-10 wt%; Fig. 7.2b). Complex zoning in sample *KY2* is due to variations in Th concentration between 1 – 4 wt%.

Strongly retrogressed and foliated garnet-mica-feldspar-bearing metapelites (*MU* and *TH*) have fractured garnet porphyroblasts within a fine-grained mica matrix (Fig. 7.2c, d). Fine-grained muscovite and sericite infill the fractures within the garnet porphyroblasts. Garnet is also partially replaced by biotite. Anhedral monazite grains within the retrogressed matrix are compositionally zoned, with some showing evidence of partial breakdown/resorption (Fig. 7.2c). Monazite chemical U-Th-Pb age data record crystallisation of monazite at 529 ± 28 Ma (n=29; *TH*) and 506 ± 17 Ma (n=86; *MU*; Table 7.2). Another foliated and retrogressed garnet-staurolite-hornblende-biotite metapelite associated with Fe(-Au-Cu) mineralisation at Green and Gold prospect contains monazite occluded by hornblende (Fig. 7.2e). Monazite chemical U-Th-Pb age data record crystallisation of monazite at 512 ± 23 Ma (n=69; *G&G*; Table 7.2). The hornblende is locally overprinted by garnet-magnetite aggregates.

### *7.3.2 Garnet-bearing metapelites*

At least three garnet growth events have been identified in metapelitic lithologies within the SCP, and analysed using the Sm-Nd technique. Two garnet growth events are recorded in sample *CR*, evident in compositional mapping as low-Ca cores that are partially reabsorbed during growth of high-Ca rims (Fig. 7.3). The earliest garnet growth was associated with the Olarian Orogeny (Hand et al., 2003), whereas Sm-Nd isotopic data of the overgrowths record crystallisation during the Delamerian Orogeny (513 ± 12 Ma; Table 7.3).

The timing of garnet growth associated with the breakdown of andalusite was also investigated with Sm-Nd isotopic analysis. Garnet occurs in association with muscovite-quartz pseudomorphs after andalusite, and post-dates the retrogression of the andalusite

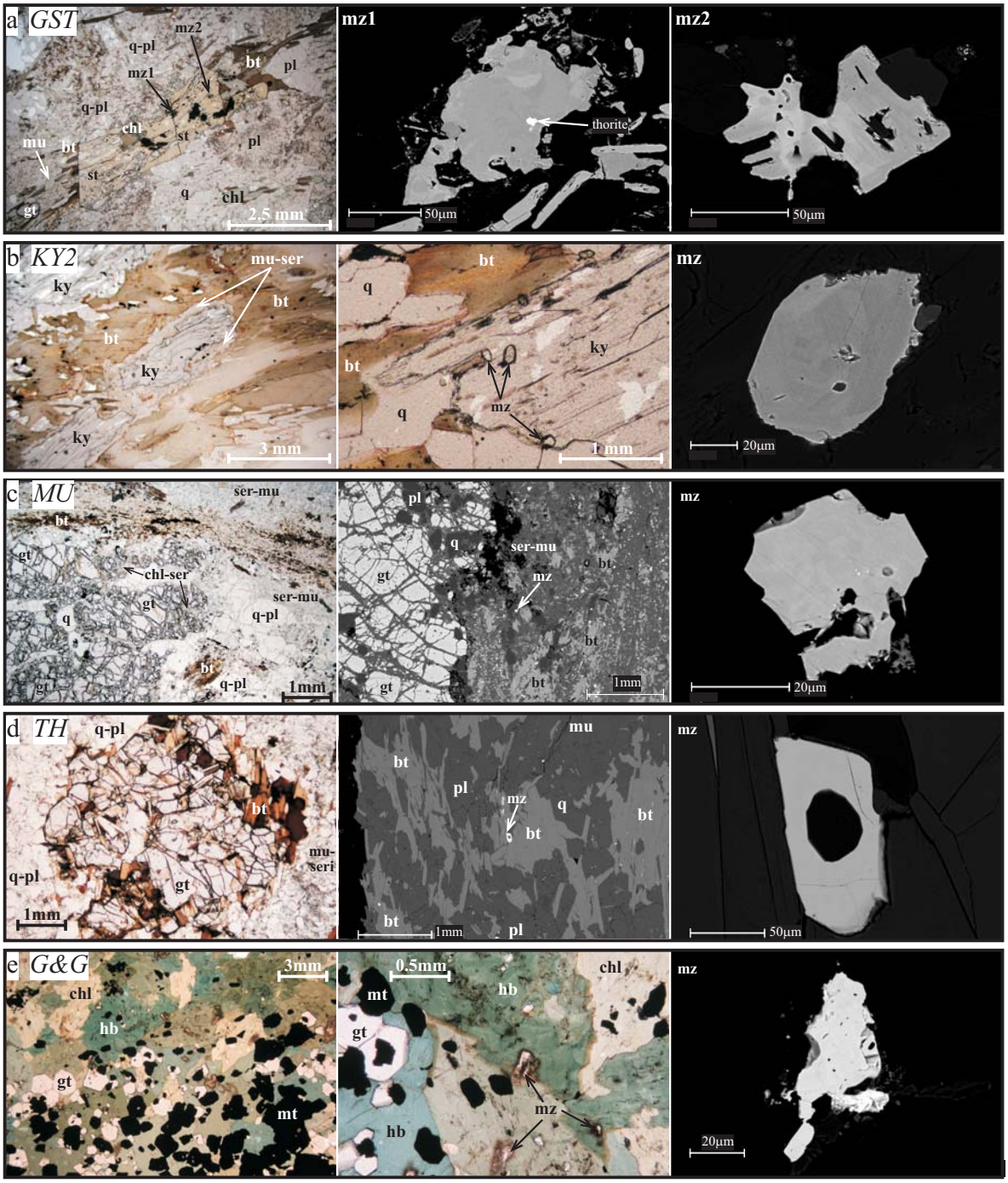


**Figure 7.2.** Samples used in chemical U-Th-Pb monazite analysis. (a) Foliated garnet–staurolite–biotite metapelitic schist (*GST*). Analysed monazite occuluded by staurolite; (b) Coarse-grained kyanite-biotite metapelitic schist (*KY2*). Analysed monazite occuluded by kyanite; (c) Garnet-chlorite-biotite-muscovite-feldspar-quartz metapelitic schist (*MU*). Analysed monazite within mica matrix; (d) Foliated garnet-biotite-muscovite-feldspar-quartz metapelitic schist (*TH*). Analysed monazite within retrograde biotite; (e) Biotite-hornblende-garnet-chlorite-magnetite metapelitic schist. Analysed monazite within hornblende.

**Table 7.3.** Garnet Sm-Nd data

| Sample | | Sm (ppm) | Nd (ppm) | $^{147}Sm/^{144}Nd$ | 2σ | $^{143}Nd/^{144}Nd$ | 2σ | Age |
|---|---|---|---|---|---|---|---|---|
| *CR* | garnet | 0.15 | 0.19 | 0.5007 | 0.0017 | 0.512762 | 0.000044 | |
| | garnet leachate | 0.80 | 1.75 | 0.2909 | 0.0010 | 0.512036 | 0.000012 | |
| | whole-rock | 4.807 | 26.229 | 0.1108 | 0.0004 | 0.511435 | 0.000012 | 513 ± 12 Ma |
| *SWI* | garnet | 1.21 | 3.52 | 0.2075 | 0.0007 | 0.511712 | 0.000011 | |
| | whole-rock | 5.94 | 31.73 | 0.1128 | 0.0004 | 0.511408 | 0.000016 | 490 ± 30 Ma |
| | garnet | 0.23 | 0.43 | 0.3226 | 0.0011 | 0.512206 | 0.00001 | |
| | whole-rock | 5.94 | 33.24 | 0.1080 | 0.0004 | 0.511486 | 0.000011 | 513 ± 11 Ma |
| *WFC* | garnet | 1.21 | 3.52 | 0.2075 | 0.0007 | 0.511712 | 0.000011 | |
| | whole-rock | 5.66 | 30.35 | 0.1123 | 0.0004 | 0.511415 | 0.000015 | 476 ± 29 Ma |

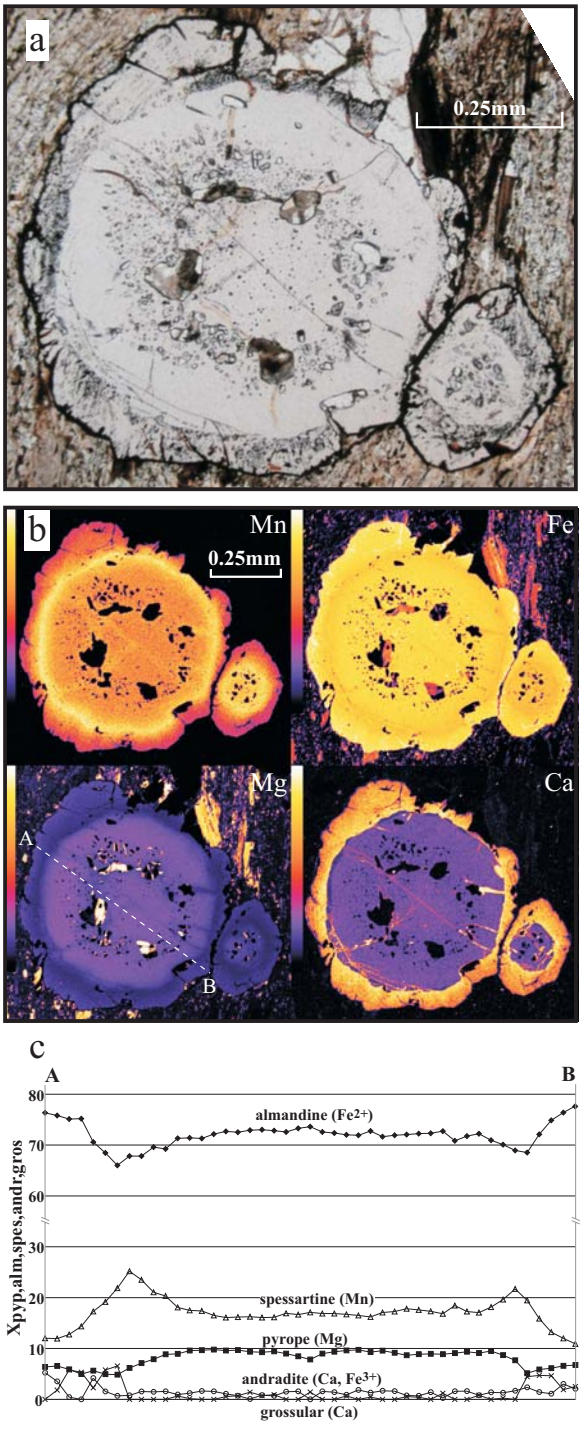


**Figure 7.3.** Two-stage garnet growth in biotite-muscovite-quartz-feldspar metapelitic of the Wiperaminga Subgroup, Cathedral Rock region. (a) Photomicrograph; (b) Compositional image of garnet; (c) Garnet composition transect (A-B) across two-stage garnet.

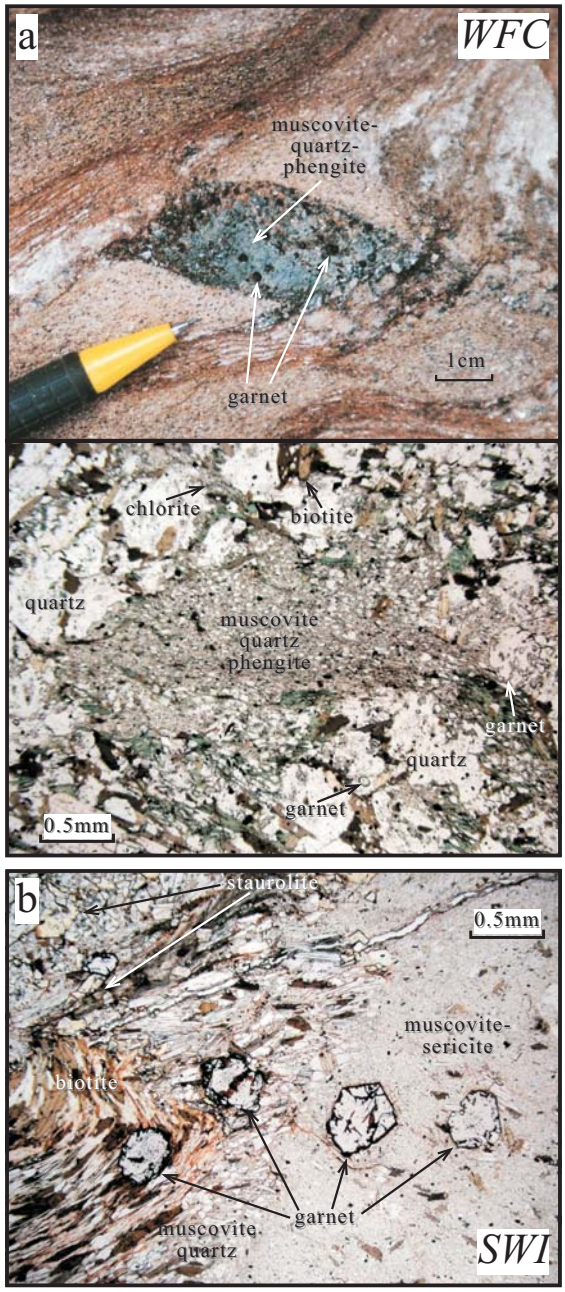


**Figure 7.4.** (a) Sample *WFC*: garnet development during breakdwon of pre-existing andalusite, forming pseudomorphs composed of chlorite, phengite, quartz, muscovite and garnet; (b) Sample *SWI*: Muscovite-sericite-garnet pseudomorph after andalusite within a biotite-quartz-staurolite matrix. Garnet produced durting breakdown of andalusite to mica. Note static staurolite growth upper left corner.

## 7.4 Discussion

(Fig. 7.4). Locally the post-andalusite assemblages also include staurolite (Fig. 7.4b). Sm-Nd isotopic analysis of two separate garnet-bearing retrograde metapelites assemblages yielded ages of 490 ± 30 Ma and 513 ± 11 Ma for sample *SWI*, and 476 ± 29 Ma for sample *WFC* (Table 7.3).

The age data collected are from assemblages that are pervasively developed throughout the SCP, and therefore have important implications for the tectonometamorphic evolution of the region. Previous interpretations of an anticlockwise *P-T* path for the Olarian Orogeny are predominantly based on the widespread

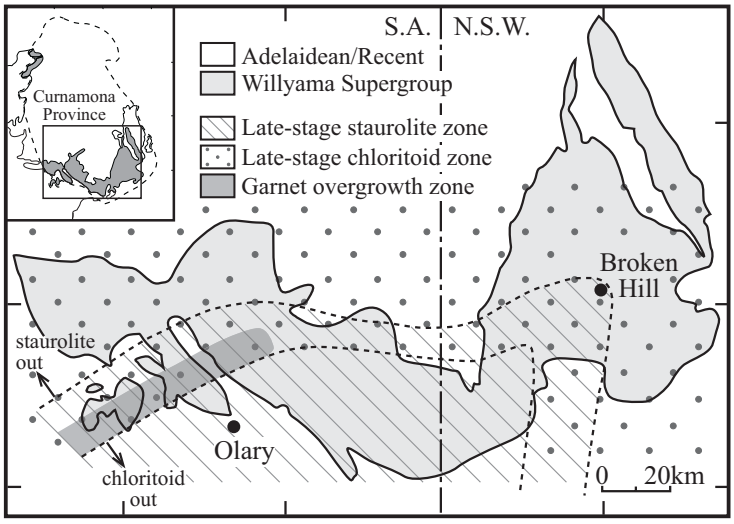


**Figure 5.** Interpreted regional isograds for metamorphic minerals as a result of the Delamerian Orogeny. Modified after Laing (1996).

occurrence of late-stage or post-kinematic kyanite and staurolite (Phillips & Wall, 1981; Clarke et al., 1987). The development of retrograde shear zones and retrogression of prograde Olarian-aged assemblages was also previously attributed to have occurred during retrograde Olarian metamorphism (~1585 Ma; Corbett & Phillips, 1981; Phillips & Wall, 1981; Gulson, 1984; Clarke et al., 1987). This study has recognised that this is not the case, and that all these features developed during prograde metamorphism associated with the *c.* 500 Ma Delamerian Orogeny.

The occurrence of garnet overgrowths, and late-stage staurolite and chloritoid kyanite in the SCP is widespread, signifying that their growth is a pervasive feature in the region (Fig. 7.5; e.g. Clarke et al., 1987; Laing, 1996; Stüwe & Ehlers, 1997). Based on this spatial observation, Delamerian-aged metamorphism was apparently more intense along the southern margin of the SCP, possibly as a result of greater depositional thickening of the overlying Adelaidean sedimentary package (Dutch et al., 2005). This study highlights that Delamerian metamorphism was not just confined to shear zone reactivation (e.g Dutch et al., 2005), but was pervasive throughout the SCP. Furthermore, growth of garnet within retrogressed andalusite porphyroblasts (Fig. 7.4), development of garnet-magnetite aggregates (Fig. 7.2e) and potentially replacement of Olarian-aged garnet by biotite (Fig. 7.2d), occurred during the Delamerian Orogeny.

## 7.5 Conclusion

Two independent geochronological techniques specifically targeting post-kinematic or late-stage growth of kyanite, staurolite and late-stage garnet in the southern Curnamona Province has found that these minerals grew during the Delamerian Orogeny (~530 – 500 Ma). Prograde metamorphism during the Delamerian Orogeny attained kyanite-staurolite-garnet grade (amphibolite-facies). Previous interpretations of an anticlockwise *P-T* path for the Olarian Orogeny need revising, as these interpretations have been shown in this study to be based on textural relationships spanning ~1100 million years. This highlights the importance of *in situ* geochronological techniques in defining robust *P-T-t* paths for a region.

# REFERENCES


Andrew, R.L., 1990. Cummins Range carbonatite. In: F.E. Hughes (Editor), Geology of the mineral deposits of Australia and Papua New Guinea. Monograph Series - Australasian Institute of Mining and Metallurgy, Melbourne, pp. 711-713.

Antonini, P., Piccirillo, E.M., Petrini, R., Civetta, L., D'Antonio, M. and Orsi, G., 1999. Enriched mantle - Dupal signature in the genesis of the Jurassic Ferrar tholeiites from Prince Albert Mountains (Victoria Land, Antartica). Contributions to Mineralogy and Petrology, 136: 1-19.

Antonini, P., Piccirillo, E.M., Petrini, R., Civetta, L., D'Antonio, M. and Orsi, G., 2000. Reply to the comment by J. Hergt on the paper "Enriched mantle - Dupal signature in the genesis of the Jurassic Ferrar tholeiites from Prince Albert Mountains (Victoria Land, Antartica)" by Antonini et al. Contributions to Mineralogy and Petrology, 139: 245-249.

Ashley, P.M., 2000. Review of the geology and metallogenesis of the Olary Domain, South Australia. AGSO Record, 2000/10: 4-7.

Ashley, P.M., Cook, N.D.J. and Plimer, I.R., 1994. Diversity of metallogenesis in the Willyama Supergroup, Olary Block, South Australia, Australian Research on Ore Genesis Symposium. Australian Mineral Foundation, pp. 18.1-18.5.

Ashley, P.M., Cook, N.D.F. and Fanning, C.M., 1996. Geochemistry and age of metamorphosed felsic igneous rocks with A-type affinities in the Willyama Supergroup, Olary Block, South Australia. Lithos, 38: 167-184.

Ayers, J.C., Miller, C., Gorisch, B. and Milleman, J., 1999. Textural development of monazite during high-grade metamorphism: Hydrothermal growth kinetics, with implications for U, Th-Pb geochronology. American Mineralogist, 84(11-12): 1766-1780.

Bailey, D.K. and Hampton, C.M., 1990. Volatiles in alkaline magmatism. Lithos, 26: 157-165.

Baker, J.H. and Hellingwerf, R.H., 1988. Rare earth element geochemistry of W-Mo-(Au) skarns and granites from western Bergslagen, central Sweden. Mineralogy and Petrology, 39(3-4): 231-244.

Barovich, K., 2003. Geochemical and Nd isotopic evidence for sedimentary source changes in the Willyama Basin, Curnamona Province. AGSO Record, 2003/13: 3.

Barovich, K.M. and Foden, J., 2002. Nd isotopic constraints on the origin of 1580 Ma Curnamona Province granitoid magmatism. In: W.V. Preiss (Editor), Geoscience 2002: Expanding Horizons. Geological Society of Australia, Abstracts of the 16th Australian Geological Convention, Adelaide Convention Centre, Adelaide, pp. 156.

Barovich, K. and Hand, M., 2004. A geochemical and isotopic perspective on the early development of the Willyama Supergroup, Curnamona Province. In: J. McPhie and P. McGoldrick (Editors), Dynamic Earth: Past, Present and Future. Abstracts of the 17th Australian Geological Convention, Hobart, Tasmania, Australia, Hobart, Tasmania, pp. 144.

Barovich, K.M., Conor, C. and Foden, J., 2002. Geochemical and Nd isotopic constraints on provenance of the Willyama Supergroup, South Australia, and comparisons to the Mt Isa Inlier. In: W.V. Preiss (Editor), Geoscience 2002: Expanding Horizons. Geological Society of Australia, Abstracts of the 16th Australian Geological Convention, Adelaide Convention Centre, Adelaide, pp. 457.

Barton, M.D. and Johnson, D.A., 1996. Evaporitic-source model for igneous-related Fe oxide-(REE-Cu-Au-U) mineralization. Geology, 24(3): 259-262.

Barton, M.D. and Johnson, D.A., 2000. Alternative brine sources for Fe-Oxide(-Cu-Au) systems: Implications for hydrothermal alteration and metals. In: T.M. Porter (Editor), Hydrothermal Iron Oxide Copper-Gold and Related Deposits: A Global Perspective. Australian Mineral Foundation, Adelaide, pp. 43-60.

Barton, M.D. and Johnson, D.A., 2004. Footprints of Fe-oxide(-Cu-Au) systems. SEG 2004: Predictive Mineral Discovery Under Cover. Centre for Global Metallogeny, Spec. Pub. 33, The University of Western Australia, 112-116.

Bau, M., 1991. Rare-earth element mobility during hydrothermal and metamorphic fluid-rock interaction and the significance of the oxidation state of europium. Chemical Geology, 93: 219-230.

Bau, M., Romer, R.L., Luders, V. and Dulski, P., 2003. Tracing element sources of hydrothermal mineral deposits: REE and Y distribution and Sr-Nd-Pb isotopes in fluorite from MVT deposits in the Pennine Orefield, England. Mineralium Deposita, 38: 992-1008.

Bell, A.J., Croxford, N.J.W. and Flemming, G.R., 1979. Alkaline igneous rocks at North Billeroo, Olary Province, South Australia. South Australia Geological Survey. Quarterly Geological Notes, 69: 4-9.

Bell, K., 1998. Radiogenic isotope constraints on relationships between carbonitites and associated silicate rocks - a brief review. Journal of Petrology, 39(11-12): 1987-1996.

Bell, T.H. and Welch, P.W., 2002. Prolonged Acadian orogenesis; revelations from foliation intersection axis (FIA) controlled monazite dating of foliations in porphyroblasts and matrix. American Journal of Science, 302(7): 549-581.

Bennett, V.C. and DePaolo, D.J., 1987. Proterozoic crustal histroy of the western United States as determined by Neodymium isotopic mapping. Geological Society of America Bulletin, 99(5): 674-685.

Berry, R.F., Flint, R.B. and Grady, A.E., 1984. Deformation history of the Outalpa area and its application to the Olary Province, South Australia. Transactions of the Royal Society of South Australia, 102: 43-53.

Betts, P.G. and Lister, G.S., 2001. Comparison of the 'strike-slip' versus the 'episodic rift-sag' models for the origin of the Isa Superbasin. Australian Journal of Earth Sciences, 48: 265-280.

Betts, P.G., Ailleres, L., Giles, D. and Hough, M., 2000. Deformation history of the Hampton Synform in the Eastern Fold Belt of the Mt Isa terrane. Australian Journal of Earth Sciences, 47(6): 1113-1125.

Betts, P.G., Giles, D., Lister, G.S. and Frick, L.R., 2002. Evolution of the Australian lithosphere. Australian Journal of Earth Sciences, 49(4): 661-695.

Bierlein, F.P., 1995. Rare-earth element geochemistry of clastic and chemical metasedimentary rocks associated with hydrothermal sulphide mineralisation in the Olary Block, South Australia. Chemical Geology, 122: 77-98.

Bierlein, F.P., Ashley, P.M. and Plimer, I.R., 1995. Sulphide mineralisation in the Olary Block, South Australia: evidence for syn-tectonic to late stage mobilisation. Mineralium Deposita, 30: 424-438.

Bierlein, F.P., Ashley, P.M. and Seccombe, P.K., 1996a. Origin of hydrothermal Cu-Zn-Pb mineralisation in the Olary Block, South Australia: evidence from fluid inclusions and sulphur isotopes. Precambrian Research, 79: 281-305.

Bierlein, F.P., Haack, U., Forster, B. and Plimer, I.R., 1996b. Lead isotope study on hydrothermal sulfide mineralisation in the Willyama Supergroup, Olary Block, South Australia. Australian Journal of Earth Sciences, 43: 177-187.

Bierlein, F.P., Foster, D.A. and Plimer, I.R., 1996c. Tectonothermal implications of laser 40Ar/39Ar ages of sulphide-bearing veins and their hosts in the Willyama Supergroup, South Australia. Mineralogy and Petrology, 58: 1-22.

Bingen, B. and vanBreemen, O., 1998. U-Pb monazite ages in amphibolite- to granulite-facies orthogneiss reflect hydrous mineral breakdown reactions: Sveconorwegian Province of SW Norway. Contributions to Mineralogy and Petrology, 132: 336-353.

Binns, R.A., 1964. Zones of progressive regional metamorphism in the Willyama Complex, Broken Hill district, New South Wales. Journal of the Geological Society of Australia, 11: 283-330.

Bjerkgard, T. and Bjorlykke, A., 1996. Sulfide deposits in Folldal, southern Trondheim region Caledonides, Norway: Sources of metals and wall-rock alterations related to host rocks. Economic Geology, 91: 676-696.

Black, L.P., Bell, T.H., Rubenach, M.J. and Withnall, I.W., 1979. Geochronology of discrete structural-metamorphic events in a multiply deformed Precambrian terrain. Tectonophysics, 54: 103-137.

Black, L.P., Gregory, P., Withnall, I.W. and Bain, J.H.C., 1998. U-Pb zircon age for the Etheridge Group, Georgetown Inlier, North Queensland: Implications for relationship with the Broken Hill and Mount Isa sequences. Australian Journal of Earth Sciences, 45: 925-935.

Blewett, R.S., Black, L.P., Sun, S.S., Hutton, L.J. and Bain, J.C., 1998. U-Pb zircon and Sm-Nd geochronology of the Mesoproterozoic of north Queensland: implications for Rodinia and connection with the Belt supergroup of North America. Precambrian Research, 89: 101-127.

Blichert-Toft, J., Arndt, N.T. and Ludden, J.N., 1996. Precambrian alkaline magmatism. Lithos, 37: 97-111.

Blissett, A.H., 1986. Subdivision of the Gawler Range Volcanics in the Gawler Carton. Quarterly Geological Notes - Geological Survey of South Australia, 97: 2-11.

Boger, S.D. and Hansen, D., 2004. Metamorphic evolution of the Georgetown Inlier, northeast Queensland, Australia; evidence for an accreted Palaeoproterozoic terrane? Journal of Metamorphic Geology, 22(6): 511-527.

Borsi, L., Petrini, R., Talarico, F. and Palmeri, R., 1995. Geochemistry and Sr-Nd isotopes of amphibolite dykes of northern Victoria Land, Antartica. Lithos, 35: 245-259.

Bradley, G.M. and Brown, R.E., 1988. Rockwell 1:25 000 Geological Sheet, 7233-1V-N. Geological Survey of New South Wales, Sydney.

Braun, I., Montel, J.M. and Nicollet, C., 1998. Electron microprobe dating of monazites from high-grade gneisses and pegmatites of the Kerala khondalite belt, southern India. Chemical Geology, 146(1-2): 65-85.

Brookfield, M.E., 1993. Neoproterozoic Laurentia-Australia fit. Geology, 21: 683-686.

Brooks, C.K. and Nielsen, T.F.D., 1978. Early stages in the differentiation of the Skaergaard magma as revealed by a closely related suite of dike rocks. Lithos, 11(1): 1-14.

Brooks, C.K., Larsen, L.M. and Nielsen, T.F.D., 1991. Importance of iron-rich tholeiitic magmas at divergent plate margins: A reappraisal. Geology, 19: 269-272.

Bühn, B. and Trumbull, R.B., 2003. Comparisons of petrogenetic signatures between mantle-derived alkali silicate intrusives with and without associated carbonatite, Namibia. Lithos, 66: 201-221.

Burke, K., Ashwal, L.D. and Webb, S.J., 2003. New ways to map old sutures using deformed alkaline rocks and carbonatites. Geology, 31(5): 391-394.

Burrett, C. and Berry, R., 2000. Proterozoic Australia-Western United States (AUSWUS) fit between Laurentia and Australia. Geology, 28(2): 103-106.

Burrett, C. and Berry, R., 2002. A statistical approach to defining Proterozoic crustal provinces and testing continental reconstructions of Australia and Laurentia - SWEAT or AUSWUS. Gondwana Research, 5(1): 109-122.

Burton, G.R., 1994. Metallogenic studies of the Broken Hill and Euriowie Blocks, New South Wales. Mineral deposits of the southeastern Broken Hill Block. Geological Survey of New South Wales, Bulletin, 32(3): 100-104.

Cabanis, B. and Lecolle, M., 1989. The La/ 10-Y/ 15-Nb/ 8 diagram; a tool for distinguishing volcanic series and discovering crustal mixing and/ or contamination. Comptes Rendus de l'Academie des Sciences, Serie 2, Mecanique, Physique, Chimie, Sciences de l'Univers, Sciences de la Terre., 309(20): 2023-2029.

Campana, B. and King, D., 1958. Regional geology and mineral resources of the Olary province. South Australia Geological Survey, Bulletin, 34.

Campbell, I.H., Coad, P., Franklin, J.M., Gorton, M.P., Scott, S.D., Sowa, J. and Thurston, P.C., 1982. Rare earth elements in volcanic rocks associated with Cu-Zn massive sulphide mineralization: a preliminary report. Canadian Journal of Earth Sciences, 19(1-4): 619-623.

Campbell, I.H., Compston, D.M., Richards, J.P., Johnson, J.P. and Kent, A.J.R., 1998. Review of the application of isotopic studies to the genesis of Cu-Au mineralisation at Olympic Dam and Au mineralisation at Porgera, the Tennant Creek district and Yilgarn Craton. Australian Journal of Earth Sciences, 45: 201-218.

Carson, C.J., Berman, R.G., Stern, R.A., Sanborn-Barrie, M., Skulski, T. and Sandeman, H.A.I., 2004. Age constraints on the Paleoproterozoic tectonometamorphic history of the Committee Bay region, western Churchill Province, Canada: evidence from zircon and in situ monazite SHRIMP geochronology. Canadian Journal of Earth Sciences, 41: 1049-1076.

Catlos, E.J., Gilley, L.D. and Harrison, T.M., 2002. Interpretation of monazite ages obtained via in situ analysis. Chemical Geology, 188(3-4): 193-215.

Cherniak, D.J., Watson, E.B., Grove, M. and Harrison, T.M., 2004. Pb diffusion in monazite: a combined RBS/SIMS study. Geochimica et Cosmochimica Acta, 68(4): 829-840.

Childe, F., 1996. U-Pb geochronology and Nd and Pb isotopic characteristics of the Au-Ag-rich Eskay Creek volcanogenic massive sulfide deposit, British Columbia. Economic Geology, 91: 1209-1224.

Christie, D.M. and Sinton, J.M., 1981. Evolution of abyssal lavas along propagating segments of the Galapogas spreading centre. Earth and Planetary Science Letters, 56: 321-335.

Clark, C. and James, P., 2003. Hydrothermal brecciation due to fluid pressure fluctuations: examples from the Olary Domain, South Australia. Tectonophysics, 366: 187-206.

Clarke, G.L., Burg, J.P. and Wilson, C.J.L., 1986. Stratigraphic and structural constraints of the Proterozoic tectonic history of the Olary Block, South Australia. Precambrian Research, 34: 107-137.

Clarke, G.L., Guiraud, M., Powell, R. and Burg, J.P., 1987. Metamorphism in the Olary Block, South Australia: compression with cooling in a Proterozoic fold belt. Journal of Metamorphic Geology, 5: 291-306.

Clarke, G.L., Powell, R. and Vernon, R.H., 1995. Reaction relationships during retrograde metamorphism at Olary, South Australia. Journal of Metamorphic Geology, 13: 715-726.

Clement, J.-P., Caroff, M., Hemond, C., Tiercelin, J-J., Bollinger, C., Guillou, H. and Cotten, J., 2003. Pleistocene magmatism in a lithospheric transition area: petrogenesis of alkaline and peralkaline lavas from the Baringo-Bogoria Basin, central Kenya Rift. Canadian Journal of Earth Sciences, 40: 1239-1257.

Cocherie, A. and Albarede, F., 2001. An improved U-Th-Pb age calculation for electron microprobe dating of monazite. Geochimica et Cosmochimica Acta, 65(24): 4509-4522.

Cocherie, A., Legendre, O., Peucat, J.J. and Kouamelan, A.N., 1998. Geochronology of polygenetic monazites constrained by in situ electron microprobe Th-U-total lead determination; implications for lead behaviour in monazite. Geochimica et Cosmochimica Acta, 62(14): 2475-2497.

Cocherie, A., Mezeme, E.B., Legendre, O., Fanning, C.M., Faure, M. and Rossi, P., 2005. Electron-microprobe dating as a tool for determining the closure of Th-U-Pb systems in migmatitic monazites. American Mineralogist, 90: 607-618.

Collins, W.J. and Shaw, R.D., 1995. Geochronological constraints on orogenic events in the Arunta Inlier: a review. Precambrian Research, 71: 315-346.

Compston, D.M., 1995. Time constraints on the evolution of the Tennant Creek block, northern Australia. Precambrian Research, 71(107-129).

Compston, D.M. and McDougall, I., 1994. 40Ar-39Ar and K-Ar age constraints on the early Proterozoic Tennant Creek Block, northern Australia, and the age of its gold deposits. Australian Journal of Earth Sciences, 41(6): 609-616.

Condie, K.C., 1993. Chemical composition and evolution of the upper continental crust: contrasting results from surface samples and shales. Chemical Geology, 104: 1-37.

Condie, K.C., 1997. Sources of Proterozoic mafic dyke swarms: constraints from Th/Ta and La/Yb ratios. Precambrian Research, 81: 3-14.

Conor, C. and Page, R., 2003. Depositional architecture of the upper Willyama Supergroup, Curnamona Province. AGSO Record, 2003/13: 30-32.

Conor, C.H.H., 2000a. Definition of major sedimentary and igneous units of the Olary Domain, Curnamona Province. MESA Journal, 19: 51-55.

Conor, C.H.H., 2000b. Towards a formal lithostratigraphy for the Olary Domain, Curnamona Province, South Australia. AGSO Record, 2000/10: 23-26.

Conor, C.H.H., 2004. Geology of the Olary Domain, Curnamona Province, South Australia, Primary Industries and Resources, South Australia, Report Book 2004/8.

Conor, C.H.H. and Fanning, C.M., 2001. Geochronology of the Woman-in-White Amphibolite, Olary Domain. MESA Journal, 20: 41-43.

Conor, C.H.H., Preiss, W.V., Page, R.W., Stevens, B.P.J., Plimer, I.R. and Ashley, P.M., 2005. Discussion on

detachment faulting and bimodal magmatism in the Palaeoproterozoic Willyama Supergroup, south-central Australia: keys to recognition of a multiply deformed Precambrian metamorphic core complex. Journal of the Geological Society of Australia, 162: 409-416.
Cook, N.D.F. and Ashley, P.M., 1992. Meta-evaporite sequence, exhalative chemical sediments and associated rocks in the Proterozoic Willyama Supergroup, South Australia: implications for metallogenesis. Precambrian Research, 56: 211-226.
Cook, N.D.F., Ashley, P.M. and Fanning, C.M., 1994. New geochronological results from the Willyama Supergroup, Olary Block, South Australia, Australian Research on Ore Genesis Symposium. Australian Mineral Foundation, Adelaide. (19.1-19.5).
Copeland, P., Parrish, R.R. and Harrison, T.M., 1988. Identification of inherited radiogenic Pb in monazite and its implication for U-Pb systematics. Nature, 333: 760-763.
Corbett, G.J. and Phillips, G.N., 1981. Regional retrograde metamorphism of a high grade terrain: the Willyama Complex, Broken Hill, Australia. Lithos, 14: 59-73.
Corbett, G.J. and Willis, I.L., 1989. Redan 1:25 000 Geological Sheet, 7233-1V-S. Geological Survey of New South Wales, Sydney.
Cox, K.G., 1983. The Karoo Province of Southern Africa; origin of trace element enrichment pattern. In: C.J. Hawkesworth and M.J. Norry (Editors), Continental basalts and mantle xenoliths; papers prepared for a UK Volcanic Studies Group meeting at the University of Leicester. Shiva Publ., Nantwich, United Kingdom, pp. 139-157.
Cox, K.G., Bell, J.D. and Pankhurst, R.J., 1979. The interpretation of igneous rocks. George Allen & Unwin. London, United Kingdom, 445 pp.
Creaser, R.A. and Cooper, J.A., 1993. U-Pb geochronology of middle Proterozoic felsic magmatism surrounding the Olympic Dam Cu-U-Au-Ag and Moonta Cu-Au-Ag deposits, South Australia. Economic Geology, 88: 186-197.
Crohn, P.W. and Moore, D.H., 1984. The Mud Tank Carbonatite, Strangways Range, central Australia. BMR Journal of Australian Geology and Geophysics, 9: 13-18.
Crooks, A.F., 2000. Olary - Broken Hill Domain boundary. MESA Journal, 20: 44-45.
Crowley, J.L. and Ghent, E.D., 1998. An electron microprobe study of the U-Th-Pb systematics of metamorphosed monazite; the role of diffusive Pb loss versus overgrowth and recrystallization. In: Anonymous (Editor), Geological Society of America, 1998 annual meeting. Abstracts with Programs - Geological Society of America, pp. 214.
Crowley, J.L. and Ghent, E.D., 1999. An electron microprobe study of the U-Th-Pb systematics of metamorphosed monazite; the role of Pb diffusion versus overgrowth and recrystallization. Chemical Geology, 157(3-4): 285-302.
Daly, S.J., Fanning, C.M. and Fairclough, M.C., 1998. Tectonic evolution and exploration potential of the Gawler Craton, South Australia. AGSO Journal of Australian Geology and Geophysics, 17: 145-168.
Dalziel, I.W.D., 1991. Pacific margins of Laurentia and East Antarctica-Australia as a conjugate rift pair: Evidence and implications for an Eocambrian supercontinent. Geology, 19: 598-601.
Dalziel, I.W.D., 1995. Earth before Pangea. Scientific American, 272: 58-63.
Danyushevsky, L., Robinson, P., McGoldrick, P., Large, R. and Gilbert, S., 2003. LA-ICPMS of sulphides: Evaluation of an XRF glass disc standard for analysis of different sulphide matrixes. 2003 Goldschmidt Conference, Japan. Geochimica et Cosmochimica Acta, 67(18): A73 Suppl.
Dashlooty, S.A. and Elliott, P.J., 1985. Progress Report on Els 1376, 1990, 2072 and Pls and PLAs covering areas of old ELs 1094, 1097, 1127 and 1161, Broken Hill, New South Wales, for the six months ending 30th June 1985, Billiton Australia, Broken Hill J.V. Geological Survey of New South Wales, Files GS 1985/184 (unpubl.).
Dashlooty, S.A. and Elliott, P.J., 1986. Progress Report on Els 1376, 1990 and Pls and PLAs covering areas of old ELs 1094, 1096, 1161 and 2072, Broken Hill, New South Wales, for the six months ending 30th June 1986, Billiton Australia, Broken Hill J.V. Geological Survey of New South Wales, Files GS 1986/177 (unpubl.).
Davidson, G.J. and Large, R.R., 1994. Gold metallogeny and the copper-gold association of the Australian Proterozoic. Mineralium Deposita, 29: 208-223.
Davidson, G.J. and Large, R.R., 1998. Proterozoic copper-gold deposits. AGSO Journal of Australian Geology and Geophysics, 17(4): 105-113.
Davidson, G.J., Stolz, A.J. and Eggins, S.M., 2001. Geochemical anatomy of silica iron exhalites: evidence for hydrothermal oxyanion cycling in response to vent fluid redox and thermal evolution (Mt. Windsor Subprovince, Australia). Economic Geology, 96: 1201-1226.
De Jong, G., Rotherham, J., Phillips, G.N. and Williams, P., 1998. Mobility of rare-earth elements and copper- during shear-zone-related retrograde metamorphism. Geologie en Mijnbouw, 76: 311-319.
Deer, W.A., Howie, R.A. and Zussman, J., 1992. An introduction to the rock-forming minerals - 2nd ed. Longman, Harlow, 696 pp.
DeWolf, C.P., Belshaw, N. and O'Nions, R.K., 1993. A metamorphic history from micron-scale 207Pb/206Pb chronometry of Archaean monazite. Earth and Planetary Science Letters, 120: 207-220.
Dobmeier, C. and Simmat, R., 2002. Post-Grenvillean transpression in the Chilka Lake area, Eastern Ghats Belt; implications for the geological evolution of Peninsular India. Precambrian Research, 113(3-4): 243-268.
Dollase, W.A. and Thomas, W.M., 1978. The crystal chemistry of silica-rich, alkali-deficient nephelines. Contributions to Mineralogy and Petrology, 66: 311-318.
Donaghy, A., Hall, M. and Gibson, G., 1998. The Palaeoproterozoic Thackaringa Group: deposition, deformation and stratigraphy. AGSO Record, 1998/25: 17-20.
Douville, E., Bienvenu, P., Charlou, J.L., Donval, J.P., Fouquet, Y., Appriou, P. and Gamo, T., 1999. Yttrium and rare earth elements in fluids from various deep-sea hydrothermal systems. Geochimica et Cosmochimica Acta, 63(5): 627-643.
Downes, H., Thirlwall, M.F. and Trayhorn, S.C., 2001. Miocene subduction-related magmatism in southern Sardinia: Sr-Nd- and oxygen isotopic evidence for mantle source enrichment. Journal of Volcanology and Geothermal Research, 106: 1-21.
Duncan, R.K. and Willett, G.C., 1990. Mount Weld Carbonatite. In: F.E. Hughes (Editor), Geology of the mineral deposits of Australia and Papua New Guinea. Monograph Series - Australasian Institute of Mining and Metallurgy, Melbourne, pp. 591-597.
Dupont, A., Vander, A.J., Pin, C., Marincea, S. and Berza, T., 2002. Trace element and isotope (Sr, Nd) geochemistry of porphyry- and skarn-mineralising Late Cretaceous intrusions from Banat, western South Carpathians, Romania. Mineralium Deposita, 37(6-7): 568-586.
Dutch, R. and Hand, M., 2003. Delamerian metamorphism in the Curnamona Province: Constraints from the prograde "retrograde" shear zones. AGSO Record, 2003/13: 36-41.
Dutch, R.A., Hand, M. and Clark, C., 2005. Tectonic reactivation pf the Proterozoic Curnamona Province, Australia; age constraints and implications for the tectonothermal evolution. Journal of the Geological Society of London, in press.
Fanning, C.M., 1995. Geological synthesis of southern Australia, Part 1. The Curnamona Province. PRISE report for the Dept of Mines & Energy, S.A, 18 pp.
Fanning, C.M., Ashley, P.M., Cook, N.D.F., Teale, G.S. and Conor, C.H.H., 1998. A geochronological perspective of crustal evolution in the Curnamona Province. AGSO Record, 1998/25: 30-35.
Farmer, G.L. and DePaolo, D.J., 1997. Sources of hydrothermal components; heavy isotopes. In: H.L. Barnes (Editor), Geochemistry of hydrothermal ore deposits. John Wiley & Sons, New York, pp. 31-61.
Ferris, G.M., Schwartz, M.P. and Heithersay, P., 2002. The geological framework, distribution and controls of Fe-oxide related alteration, and Cu-Au mineralisation in the Gawler Craton, South Australia: Part 1: Geological and tectonic framework. In: T.M. Porter (Editor), Hydrothermal Iron Oxide Copper-Gold and Related Deposits: A Global

Perspective, Volume 2. PGC Publishing, Adelaide.
Finger, F., Broska, I., Robertson, M.P. and Schermaier, A., 1998. Replacement of primary monazite by apatite-allanite-epidote coronas in an amphibolite facies granite gneiss from the eastern Alps. American Mineralogist, 83: 248-258.
Fitzsimons, I.C.W., Kinny, P.D., Wetherley, S. and Hollingsworth, D.A., 2005. Bulk chemical control on metamorphic monazite growth in pelitic schists and implications for U-Pb age data. Journal of Metamorphic Geology.
Fleet, M.E., Seller, M.H. and Pan, Y., 1997. Rare earth elements. protoliths, and alteration at the Hemlo gold deposit, Ontario, Canada, and comparisons with argillic and sericitic alteration in the Highland Valley Porphyry District, British Columbia, Canada. Economic Geology, 92: 551-568.
Floyd, P.A. and Winchester, J.A., 1978. Identification and discrimination of altered and metamorphosed volcanic rocks using immobile elements. Chemical Geology, 21: 291-306.
Foster, G.L. and Parrish, R.R., 2003. Metamorphic monazite and the generation of P-T-t paths. In: D. Vance, W. Muller and I.M. Villa (Editors), Geochronology: Linking the Isotopic Record with Petrology and Textures. Geological Society of London, Special Publication, pp. 25-47.
Foster, G., Kinny, P., Vance, D., Prince, C. and Harris, N., 2000. The significance of monazite U-Th-Pb age data in metamorphic assemblages; a combined study of monazite and garnet chronometry. Earth and Planetary Science Letters, 181(3): 327-340.
Foster, G., Gibson, H.D., Parrish, R., Horstwood, M., Fraser, J. and Tindle, A., 2002. Textural, chemical and isotopic insights into the nature and behaviour of metamorphic monazite. Chemical Geology, 191: 183-207.
Foster, G., Parrish, R.R., Horstwood, M.S.A., Chenery, S., Pyle, J. and Gibson, H.D., 2004. The generation of prograde P-T-t points and paths; a textural, compositional, and chronological study of metamorphic monazite. Earth and Planetary Science Letters, 228: 125-142.
Frei, R., Nagler, T.F., Schonberg, R. and Kramers, J.D., 1998. Re-Os, Sm-Nd, U-Pb and stepwise lead leaching isotopic systematics in shear-zone hosted gold mineralization: Genetic tracing and age constraints of crustal hydrothermal activity. Geochimica et Cosmochimica Acta, 62(11): 1925-1936.
Frietsch, R., 1989. The Kiruna iron ores. Abstracts with Programs - Geological Society of America, 21(6): A33.
Gale, G.H., Fedikow, M.A.F. and Dabek, L.B., 1997. The application of rare earth element analyses in the exploration for volcanogenic massive sulfide type deposits. Exploration and Mining Geology, 6(3): 233-252.
Gibson, G., 2000. Tectonic evolution of the Palaeoproterozoic Willyama Supergroup, Broken Hill: the early years. AGSO Record, 2000/10: 45-47.
Gibson, G.M. and Nutman, A.P., 2004. Detachment faulting and bimodal magmatism in the Palaeoproterozoic Willyama Supergroup, south-central Australia: Keys to recognition of a multiply deformed Precambrian metamorphic core complex. Journal of the Geological Society of London, 161: 55-66.
Gibson, G.M., Peljo, M. and Chamberlain, T., 2004a. Evidence and timing of crustal extension versus shortening in the early tectonothermal evolution of a Proterozoic continental rift sequence at Broken Hill, Australia. Tectonics, 23(5): TC5012, doi:10.1029/2003TC001552.
Gibson, H.D., Carr, S.D., Brown, R.L. and Hamilton, M.A., 2004b. Correlations between chemical and age domains in monazite, and metamorphic reactions involving major pelitic phases; an integration of ID-TIMS and SHRIMP geochronology with Y-Th-U X-ray mapping. Chemical Geology, 211(3-4): 237-260.
Giles, D. and Betts, P.G., 2001. Proterozoic interactions between Australia and North America. Abstracts with Programs - Geological Society of America, 33(6): 434.
Giles, D. and Nutman, A.P., 2002. SHRIMP U-Pb monazite dating of 1600-1580 Ma amphibolite facies metamorphism in the southeastern Mt Isa Block, Australia. Australian Journal of Earth Sciences, 49: 455-465.
Giles, D., Betts, P. and Lister, G., 2002. Far-field continental backarc setting for the 1.80-1.67 Ga basins of northeastern Australia. Geology, 30(9): 823-826.
Giles, D., Betts, P.G. and Lister, G.S., 2004. 1.8-1.5-Ga links between the North and South Australian Cratons and the Early-Middle Proterozoic configuration of Australia. Tectonophysics, 380: 27-41.
Gimeno-Serrano, M.J., Sanz, L.F.A. and Nordstrom, D.K., 2000. REE speciation in low-temperature acidic waters and the competitive effects of aluminium. Chemical Geology, 165: 167-180.
Giritharan, T.S. and Rajamani, V., 2001. REE geochemistry of ore zones in the Archean auriferous schist belts of the eastern Dharwar Craton, south India. Proceedings of the Indian Academy of Sciences: Earth and Planetary Sciences, 110(2): 143-159.
Gleason, J.D., Marikos, M.A., Barton, M.D. and Johnson, D.A., 2000. Neodymium isotopic study of rare earth element sources and mobility in hydrothermal Fe oxide (Fe-P-REE) systems. Geochimica et Cosmochimica Acta, 64(6): 1059-1068.
Gómez-Pugnaire, M.T., Azor, A., Fernández-Soler, J.M. and López Sánchez-Vizcaíno, V., 2003. The amphibolites from the Ossa-orena / Central Iberian Variscan suture (Southwestern Iberian Massif): geochemistry and tectonic implications. Lithos, 68: 23-42.
Goodenough, K.M., Upton, B.G.J. and Ellam, R.M., 2002. Long-term memory of subduction processes in the lithospheric mantle: evidence from the geochemistry of basic dykes in the Gardar Province of South Greenland. Journal of the Geological Society, London, 159: 705-714.
Grady, A.E., Flint, D.J. and Wiltshire, R., 1989. Excursion guide for Willyama Supergroup and related rocks, Olary district, SA, South Australia Department of Mines and Energy, Report Book, 89/23.
Graf, J.L., 1977. Rare earth elements as hydrothermal tracers during the formation of massive sulphide deposits in volcanic rocks. Economic Geology, 72(4): 527-548.
Graf, J.L., 1990. Rare earth element studies of Mississippi Valey-type (MVT) Pb-Zn-Cu deposits in Kansas, Oklahoma, and Missouri, USA. Documents - B.R.G.M., 183: 75-88.
Gulson, B.L., 1984. Uranium-lead and lead-lead inverstigations of minerals from the Broken Hill lodes and mine sequence rocks. Economic Geology, 79: 476-490.
Haas, J.R., Shock, E.L. and Sassani, D.C., 1995. Rare earth elements in hydrothermal systems: Estimates of standard partial molal thermodynamic properties of aqueous complexes of the rare earth elements at high pressures and temperatures. Geochimica et Cosmochimica Acta, 59(21): 4329-4350.
Halama, R., Marks, M., Brugmann, G., Siebel, W., Wenzel, T. and Markl, G., 2004. Crustal contamination of mafic magmas: evidence from a petrological, geochemical and Sr-Nd-Os-O isotopic study of the Proterozoic Isortoq dike swarm, South Greenland. Lithos, 74(3-4): 199-232.
Hamilton, D.L., 1961. Nephelines as crystallisation temperature indicators. Journal of Geology, 69: 321-329.
Hand, M., Rutherford, L. and Barovich, K., 2003. Garnet Sm-Nd age constraints on the timing of tectonism in the southwestern Curnamona Province: Implications for existing models and correlations. AGSO Record, 2003/13: 65-68.
Hansen, K., 1981. Systematic Sr-isotopic variation in alkaline rocks from West Greenland. Lithos, 14(3): 183-188.
Harmer, R.E., 1999. The Petrogenetic Association of Carbonatite and Alkaline Magmatism: Constraints from the Spitskop Complex, South Africa. Journal of Petrology, 40(4): 525-548.
Harrison, T.M. and McDougall, I., 1981. Excess 40Ar in metamorphic rocks from Broken Hill, New South Wales: implications for 40Ar/39Ar age spectra and the thermal history of the region. Earth and Planetary Science Letters, 55: 123-149.
Hartley, M.J., Foster, D.A., Gray, D.R. and Kohn, B.P., 1998. 40Ar-39Argon and apatite fission track thermochronology of the Broken Hill Inlier: implications for the Mesoproterozoic to Recent tectonics. AGSO Record, 1998/25: 46-49.
Hawkins, D.P. and Bowring, S.A., 1997. U-Pb systematics of monazite and xenotime: case studies from the

Palaeoproterozoic of the Grand Canyon, Arizona. Contributions to Mineralogy and Petrology, 127: 87-103.
Haynes, D.W., 2000. Iron oxide copper (-gold) deposits: Their position in the ore deposit spectrum and modes of origin. In: T.M. Porter (Editor), Hydrothermal Iron Oxide Copper-Gold and Related Deposits: A Global Perspective. Australian Mineral Foundation, Adelaide, pp. 71-90.
Haynes, D.W., Cross, K.C., Bills, R.T. and Reed, M.H., 1995. Olympic Dam ore genesis: A fluid mixing model. Economic Geology, 90: 281-307.
Hayward, S., 1998. Kalkaroo copper-gold project. AGSO Record, 1998/25: 50-51.
Henderson, C.M.B. and Gibb, F.G.F., 1983. Felsic mineral crystallization trends in differentiating alkaline basic magmas. Contributions to Mineralogy and Petrology, 84: 355-364.
Hergt, J., 2000. Comment on: "Enriched mantle - Dupal signature in the genesis of the Jurassic Ferrar tholeiites from Prince Albert Mountains (Victoria Land, Antarctica)" by Antonini P. et al. Contributions to Mineralogy and Petrology, 139: 240-244.
Hergt, J.M., Chappell, B.W., McCulloch, M.T., McDougall, I. and Chivas, A.R., 1989. Geochemical and isotopic constraints on the Jurassic dolerites of Tasmania. Journal of Petrology, 30: 841-883.
Hitzman, M.W., 2000. Iron oxide-Cu-Au deposits: What, where, when, and why. In: T.M. Porter (Editor), Hydrothermal Iron Oxide Copper-Gold and Related Deposits: A Global Perspective. Australian Mineral Foundation, Adelaide, pp. 9-25.
Hitzman, M.W., Oreskes, N. and Einaudi, M.T., 1992. Geological characteristics and tectonic setting of Proterozoic iron oxide (Cu-Au-Au-REE) deposits. Precambrian Research, 58: 241-287.
Hobbs, B.E., Archibald, N.J., Etheridge, M.A. and Wall, V.J., 1984. Tectonic history of the Broken Hill Block, Australia. In: A. Kroner and R. Greiling (Editors), Precambrian Tectonics Illustrated. E. Schweizerbartsche Verlagsbuchhandlung, Stuttgart, pp. 353-368.
Hobbs, B.E., Ord, A., Walshe, J., Zhang, Y. and Zhao, C., 2000. Geodynamic modelling of the Broken Hill Type mineralisation in the Broken Hill Block, NSW. AGSO Record, 2000/10: 61-62.
Hoffman, P.F., 1991. Did the breakout of Laurentia turn Gondwanaland inside-out? Science, 252: 1409-1411.
Huston, D.L. and Large, R.R., 1989. A chemical model for the concentration of gold in volcanogenic massive sulphide deposits. Ore Geology Reviews, 4: 171-200.
Irvine, T.N. and Baragar, W.R.A., 1971. A guide to the chemical classification of the common volcanic rocks. Canadian Journal of Earth Sciences, 8(5): 523-548.
Ivanikov, V.V., Rukhlov, A.S. and Bell, K., 1998. Magmatic evolution of the melilitite-carbonatite-nephelinite dyke series of the Turiy Peninsula (Kandalaksha Bay, White Sea, Russia). Journal of Petrology, 39(11-12): 2043-2059.
James, S.D., Pearce, J.A. and Oliver, R.A., 1987. The geochemistry pf the Lower Proterozoic Willyama Complex volcanics, Broken Hill Block, New South Wales. In: T.C. Pharaoh, R.D. Beckinsale and D.T. Rickard (Editors), Geochemistry and mineralization of Proterozoic volcanic suites. Geological Society of London Special Publications, pp. 395-408.
Jefferson, C.W., 1978. Correlation of middle and upper Proterozoic strata between northwestern Canada and central Australia. Abstracts with Programs - Geological Society of America, 7: A429.
Jenkins, G.W. and Burtt, A.C., 2003. Curnamona Province MGA GIS DVD, Version 2.0. South Australia. Department of Primary Industries and Resources, Mineral Exploration Data Package, 014.
Jensen, L.S., 1976. A new cation plot for classifying subalkalic volcanic rocks. Ontario Geological Survey Miscellaneous Paper, 66: 22.
Jercinovic, M.J. and Williams, M.L., 2005. Analytical perils (and progress) in electron microprobe trace element analysis applied to geochronology: Background acquisition, interferences, and beam irradiation effects. American Mineralogist, 90: 526-546.
Jiang, S.-Y., Slack, J.F. and Palmer, M.R., 2000. Sm-Nd dating of the giant Sullivan Pb-Zn-Ag deposit, British Columbia. Geology, 28(8): 751-754.
Johnson, J.P. and Cross, K.C., 1995. U-Pb geochronological constraints on the genesis of the Olympic Dam Cu-U-Au-Ag Deposit, South Australia. Economic Geology, 90: 1046-1063.
Johnson, J.P. and McCulloch, M.T., 1995. Source of minerlising fluids for the Olympic Dam deposit (South Australia): Sm-Nd isotopic constraints. Chemical Geology, 121: 177-199.
Jones, A.P. and Larsen, L.M., 1985. Geochemistry and REE minerals of nepheline syenites from the Motzfeldt Centre, South Greenland. American Mineralogist, 70: 1087-1100.
Kabeto, K., Sawada, Y., Iizumi, S. and Wakatsuki, T., 2001. Mantle sources and magma-crust interactions in volcanic rocks from the northern Kenya rift: geochemical evidence. Lithos, 56: 111-139.
Karlstrom, K.E., Harlan, S.S., Williams, M.L., McLelland, J., Geissman, J.W. and Ahall, K-I., 1999. Refining Rodinia: Geologic evidence for the Australia-Western U.S. connection in the Proterozoic. GSA Today, 9(10): 1-7.
Karlstrom, K.E., Ahall, K-I., Harlan, S.S., Williams, M.L., McLelland, J. and Geissman, J.W., 2001. Long-lived (1.8–1.0 Ga) convergent orogen in southern Laurentia, its extensions to Australia and Baltica, and implications for refining Rodinia. Precambrian Research, 111: 5-30.
Kelsey, D.E., Powell, R., Wilson, C.J.L. and Steele, D.A., 2003. (Th+U)-Pb monazite ages from Al-Mg-rich metapelites, Rauer Group, East Antarctica. Contributions to Mineralogy and Petrology, 146(3): 326-340.
Kent, A.J.R., Ashley, P.M. and Fanning, C.M., 2000. Metasomatic alteration associated with regional metamorphism: an example from the Willyama Supergroup, South Australia. Lithos, 54: 33-62.
Kinny, P.D., 1997. Users guide to U-Th-Pb dating of titanite, perovskite, monazite and baddeleyite using the W.A. SHRIMP. School of Physical Sciences Report No. SPS693/1997/AP72, Curtin University of Technology (unpublished), 21 pp.
Klinkhammer, G.P., Elderfield, H., Edmond, J.M. and Mitra, A., 1994. Geochemical implications of rare earth element patterns in hydrothermal fluids from mid-ocean ridges. Geochimica et Cosmochimica Acta, 58(23): 5105-5113.
Kramm, U., 1994. Isotope evidence for ijolite formation by fenitization: Sr-Nd data of ijolites from the type locality Iivaara, Finland. Contributions to Mineralogy and Petrology, 115: 279-286.
Kryza, R. and Pin, C., 2002. Mafic rocks in a deep-crustal segment of the Variscides (the Gory Sowie, SW Poland): evidence for crustal contamination in an extensional setting. International Journal of Earth Sciences, 91: 1017-1029.
Kumpulainen, R.A., Mansfield, J., Sundblad, K., Neymark, L. and Bergman, T., 1996. Stratigraphy, age, and Sm-Nd isotopic systematics of the country rocks to Zn-Pb sulfide deposits, Ammeberg District, Sweden. Economic Geology, 91: 1009-1021.
Laing, W.P., 1996a. Stratigraphic subdivision of the Willyama Supergroup - Olary Domain, South Australia. MESA Journal, 2: 39-48.
Laing, W.P., 1996b. Nappe interpretation, palaeogeography and metallogenic synthesis of the Broken Hill-Olary Block. In: J. Pongratz and G.J. Davidson (Editors), New Developments in Broken Hill Deposits. CODES Special Publication 1, Hobart, pp. 21-51.
Laing, W.P., 1996c. The Diamantina orogen linking the Willyama and Cloncurry Terrains, eastern Australia. In: J. Pongratz and G.J. Davidson (Editors), New developments in Broken Hill Type deposits. Centre for Ore Deposit and Exploration Studies. CODES Special Publications 1, pp. 67-72.
Laing, W.P., Marjoribanks, R.W. and Rutland, R.W.R., 1978. Structure of the Broken Hill mine area and its significance for the genesis of the orebodies. Economic Geology, 73: 1112-1136.
Lambert, D.D. and Simmons, E.C., 1988. Magma evolution in the Stillwater Complex, Montana: II. Rare Earth Element Evidence for the Formation of the J-M Reef. Economic Geology, 83(6): 1109-1126.
Langworthy, A.P. and Black, L.P., 1978. The Mordor Complex; a highly differentiated potassic intrusion with kimberlitic affinities in central Australia. Contributions to Mineralogy

and Petrology, 67(1): 51-62.
Lassen, B., Bridgwater, D., Bernstein, S. and Rosing, M., 2004. Assimilation and high-pressure fractional crystallization (AFC) recorded by Paleo-proterozoic mafic dykes, Southeast Greenland. Lithos, 72: 1-18.
Lee, W.J. and Wyllie, P.J., 1994. Experimental data bearing on liquid immiscibility, crystal fractionation, and the origin of calciocarbonatites and natrocarbonatites. International Geology Review, 36(797-819).
Lesher, C.M., Goodwin, A.M., Campbell, I.H. and Gorton, M.P., 1986. Trace-element geochemistry of ore-associated and barren, felsic metavolcanic rocks in the Superior Province, Canada. Canadian Journal of Earth Sciences, 23: 222-237.
Lewis, A.J., Palmer, M.R., Sturchio, N.C. and Kemp, A.J., 1997. The rare earth element geochemistry of acid-sulphate and acid-sulphate-chloride geothermal systems from Yellowstone National Park, Wyoming, USA. Geochimica et Cosmochimica Acta, 61(4): 695-706.
Leyh, W.R., 1995. Geological review and assessment of base metal and gold prospects, Savage Resources, Mundi Mundi project, Broken Hill, NSW. Report Book for Savage Resources. 1/2.
Leyh, W.R. and Conor, C.H.H., 2000. Stratigraphically controlled metallogenic zonation associated with the regional redox boundary of the Willyama Supergroup - economic implications for the southern Curnamona Province. MESA Journal, 16: 39-47.
Li, Z.-X., Zhang, L. and Powell, C.M., 1995. South China in Rodinia; part of the missing link between Australia - East Antarctica and Laurentia? Geology, 23: 407-410.
Lindh, A., Andersson, U.B., Lundqvist, T. and Claesson, S., 2001. Evidence of crustal contamination of mafic rocks associated with rapakivi rocks: an example from the Nordingra complex, Central Sweden. Geological Magazine, 138(4): 371-386.
Longerich, H.P., Jackson, S.E. and Gunther, D., 1996. Laser ablation inductively coupled plasma mass spectrometric transient signal data acquisition and analyte concentration calculation. Journal of Analytical and Atomic Spectroscopy, 11: 899-904.
Lottermoser, B.G., 1992. Rare earth elements and hydrothermal ore formation processes. Ore Geology Reviews, 7: 25-41.
Lottermoser, B.G. and Ashley, P.M., 1996. Geochemistry and exploration significance of ironstones and barite-rich rocks in the Proterozoic Willyama Supergroup, Olary Block, South Australia. Journal of Geochemical Exploration, 57: 57-73.
Ludden, J., Gelinas, L. and Trudel, P., 1982. Archean metavolcanics from the Rouyn-Noranda District, Abitibi greenstone belt, Quebec; 2, Mobility of trace elements and petrogenetic constraints. Canadian Journal of Earth Sciences, 19(12): 2276-2287.
Ludwig, K.R., 2003. Users Manual for Isoplot/Ex, Version 3.00, A Geochronological Toolkit for Microsoft Excel. Berkeley Geochronology Centre, Berkeley, CA, 2003. Special Publication No.4.
Ludwig, K.R. and Cooper, J.A., 1984. Geochronology of Precambrian granites and associated U-Ti-Th mineralization, northern Olary Province, South Australia. Contributions to Mineralogy and Petrology, 86(3): 298-308.
MacLean, W.H. and Barrett, T.J., 1993. Lithogeochemical techniques using immobile elements. Journal of Geochemical Exploration, 48: 109-133.
Mark, G., Foster, D.R.W., Pollard, P.J., Williams, P.J., Tolman, J., Darvall, M. and Blake, K.L., 2004. Stable isotope evidence for magmatic fluid input during large-scale NaCa alteration in the Cloncurry Fe oxide CuAu district, NW Queensland, Australia. Terra Nova, 16(2): 54-61.
Mark, G., Wilde, A., Oliver, N.H.S., Williams, P.J. and Ryan, C.G., 2005. Modeling outflow from the Ernest Henry Fe oxide Cu-Au deposit: implications for ore genesis and exploration. Journal of Geochemical Exploration, 85(1): 31-46.
Mass, R., McCulloch, M.T., Campbell, I.H. and Page, R., 1987. Sm-Nd isotopic systematics in uranium-rare earth element mineralization at the Mary Kathleen uranium mine, Queensland. Economic Geology, 82: 1805-1826.
McBirney, A.R., 1993. Igneous Petrology - 2nd ed. Jones & Bartlett Publishers, London, 508 pp.
Meert, J.G., 2002. Paleomagnetic evidence for a Paleo-Mesoproterozoic Supercontinent Columbia. Gondwana Research, 5(1): 207-215.
Meschede, M., 1986. A method of discriminating between different types of mid-ocean ridge basalts and continental tholeiites with the Nb-Zr-Y diagram. Chemical Geology, 56(3-4): 207-218.
Michard, A., 1989. Rare earth element systematics in hydrothermal fluids. Geochimica et Cosmochimica Acta, 53: 745-750.
Michard, A. and Albarede, F., 1986. The REE content of some hydrothermal fluids. Chemical Geology, 55: 51-60.
Middlemost, E.A.K., 1994. Naming materials in the magma/igneous rock system. Earth Science Reviews, 37: 215-224.
Miller, D.M., Goldstein, S.L. and Langmuir, C.H., 1994. Cerium/lead and lead isotope ratios in arc magmas and the enrichment of lead in the continents. Nature, 368: 514-520.
Montel, J.M., Foret, S., Veschambre, M., Nicollet, C. and Provost, A., 1996. Electron microprobe dating of monazite. Chemical Geology, 131: 37-53.
Montel, J.M., Kornprobst, J. and Vielzeuf, D., 2000. Preservation of old U-Th-Pb ages in shielded monazite; example from the Benmi Bousera Hercynian kinzigites (Morocco). Journal of Metamorphic Geology, 18(3): 335-342.
Moores, E.M., 1991. Southwest U.S.-East Antarctic (SWEAT) connection: A hypothesis. Geology, 19: 425-428.
Morbidelli, L., Gomes, C.B., Beccaluva, L., Brotzu, P., Conte, A.M., Ruberti, E. and Traversa, G., 1995. Mineralogical, petrological and geochemical aspects of alkaline and alkaline-carbonatite from Brazil. Earth Science Reviews, 39: 135-168.
Morris, E.M. and Pasteris, J.D., 1987. Mantle metasomatism and alkaline magmatism. Boulder, Colorado, 383 pp.
Myers, J.S., Shaw, R.D. and Tyler, I.M., 1996. Tectonic evolution of Proterozoic Australia. Tectonics, 15(6): 1431-1446.
Myers, R.E. and Breitkopf, J.H., 1989. Basalt geochemistry and tectonic settings: a new approach to relate tectonic and magmatic processes. Lithos, 23: 53-62.
Nelson, D.R., Black, L.P. and McCulloch, M.T., 1989. Nd-Pb isotopic characteristics of the Mordor Complex, North Territory; mid-Proterozoic potassic magmatism from an enriched mantle source. Australian Journal of Earth Sciences, 36(4): 541-551.
Nelson, R., 1992. Kalabity Project. CRA Exploration P/L, Unpublished Company Report.
Norman, M., Robinson, P. and Clark, D., 2003. Major- and trace-element analysis of sulphide ores by laser-ablation ICP-MS, solution ICP-MS, and XRF: New data on international reference materials. The Canadian Mineralogist, 41: 293-305.
Nutman, A.P. and Ehlers, K., 1998. Evidence for multiple Palaeoproterozoic thermal events and magmatism adjacent to the Broken Hill Pb-Zn-Ag orebody, Australia. Precambrian Research, 90: 203-238.
Nutman, A.P. and Ehlers, K., 1999. Evidence for multiple Palaeoproterozoic thermal events and magmatism adjacent to the Broken Hill Pb-Zn-Ag orebody, Australia: Correspondance. Precambrian Research, 98(1-2): 7-10.
Nutman, A.P. and Gibson, G., 1998. Zircon ages from metasediments, granites and mafic intrusions: reappraisal of the Willyama Supergroup. AGSO Record, 1998/25: 86-88.
O'Dea, M.G., Lister, G.S., MacCready, T., Betts, P.G., Oliver, N.H.S., Pound, K.S., Huang, W. and Valenta, R.K., 1997. Geodynamic evolution of the Proterozoic Mount Isa terrain. In: J.P. Burg and M. Ford (Editors), Orogeny Through Time. Geological Society Special Publication, pp. 99-122.
Oliver, N.H.S., Cleverley, J.S., Mark, G., Pollard, P.J., Fu, B., Marshall, L.J., Rubenach, M.J., Williams, P.J. and Baker, T., 2004. Modeling the Role of Sodic Alteration in the Genesis of Iron Oxide-Copper-Gold Deposits, Eastern Mount Isa Block, Australia. Economic Geology, 99(6): 1145-1176.
Page, R.W. and Laing, W.P., 1992. Felsic metavolcanic rocks related to the Broken Hill Pb-Zn-Ag orebody, Australia;

geology, depositional age, and timing of high grade metamorphism. Economic Geology, 87: 2138-2168.
Page, R.W. and Sun, S., 1998. Aspects of geochronology and crustal evolution in the Eastern Fold Belt, Mt. Isa Inlier. Australian Journal of Earth Sciences, 45: 343-362.
Page, R.W., Conor, C.H.H. and Sun, S.S., 1998. Geochronology of metasedimentary and metavolcanic successions in the Olary Domain and comparisons to Broken Hill. AGSO Record, 1998/25: 89-93.
Page, R.W., Stevens, B.P., Gibson, G.M. and Conor, C.H.H., 2000. Geochronology of Willyama Supergroup rocks between Olary and Broken Hill, and comparison to northern Australia. AGSO Record, 2000/10: 72-75.
Page, R., Stevens, B., Conor, C., Preiss, W., Crooks, A., Robertson, S., Gibson, G. and Foudoulis, C., 2003. SHRIMP U-Pb geochronology in the Curnamona Province: Improving the framework for mineral exploration. AGSO Record, 2003/13: 122-125.
Parak, T., 1988. How the classical intrusive-magmatic ores were reinterpreted (reexamined) and became exhalative-sedimentary; a process exemplified by the kiruna-type ores. Abstracts with Programs - Geological Society of America, 20(7): 20.
Parr, J.M., Stevens, B.P.J., Carr, G.R. and Page, R.W., 2004. Subseafloor origin for Broken Hill Pb-Zn-Ag mineralization, New South Wales, Australia. Geology, 32(7): 589-592.
Parrish, R.R., 1990. U-Pb dating of monazite and its application to geological problems. Canadian Journal of Earth Sciences, 27(11): 1431-1450.
Partington, G.A. and Williams, P.J., 2000. Proterozoic Lode Gold and (Iron)-Copper-Gold Deposits: A Comparison of Australian and Global Examples. In: S.G. Hagemann and P.E. Brown (Editors), Gold in 2000. Reviews in Economic Geology, pp. 69-101.
Payne, J.L., 2003. The Poodla granite in the Olary Domain, South Australia: Intrusive relationships, alteration and implications for Cu-Au mineralisation. University of Adelaide, unpublished Honours thesis.
Pearce, J.A. and Cann, J.R., 1973. Tectonic setting of basic volcanic rocks determined using trace element analyses. Earth and Planetary Science Letters, 19(2): 290-300.
Pearce, J.A. and Norry, M.J., 1979. Petrogenetic implications of Ti, Zr, Y, and Nb variations in volcanic rocks. Contributions to Mineralogy and Petrology, 69: 33-47.
Pearce, J.A., Ernewien, M., Bloomer, S.H., Parson, L.M., Murton, B.J., Johnson, L.E., 1994. Geochemistry of Lau Basin volcanic rocks: influence of ridge segmentation and arc proximity. In: J.L. Millie (Editor), Volcanism associated with extension at consuming plate margins. Geological Society of London, Special Publications, pp. 53-75.
Pearce, N.J.G. and Leng, M.J., 1996. The origin of carbonatites and related rocks from the Igaliko Dyke Swarm, Gardar Province, South Greenland: field, geochemical and C-O-Sr-Nd isotope evidence. Lithos, 39: 21-40.
Perring, C.S., Pollard, P.J., Dong, G., Nunn, A.J. and Blake, K.L., 2000. The Lightning Creek Sill Complex, Cloncurry District, Northwest Queensland: A source of fluids for Fe oxide Cu-Au mineralization and sodic-calcic alteration. Economic Geology, 95: 1067-1090.
Phillips, G.N., 1980. Water activity changes across an amphibolite-granulite facies transition, Broken Hill, Australia. Contributions to Mineralogy and Petrology, 75: 377-386.
Phillips, G.N. and Wall, V.J., 1981. Evaluation of prograde regional metamorphic conditions: their implications for the heat source and water activity during metamorphism in the Willyama Complex, Broken Hill, Australia. Bulletin de Mineralogie, 104: 801-810.
Phillips, G.N., Archibald, N.J. and Wall, V.J., 1985. Metamorphosed high-Fe tholeiites: their alteration and relationship to sulphide mineralization, Broken Hill, Australia. Transactions of the Geological Society of South Africa, 88: 49-59.
Piercey, S.J., Mortensen, J.K., Murphy, D.C., Paradis, S. and Creaser, R.A., 2002. Geochemistry and tectonic significance of alkalic mafic magmatism in the Yukon-Tanana Terrane, Finlayson Lake region, Yukon. Canadian Journal of Earth Sciences, 39: 1729-1744.
Plank, T. and Langmuir, C.H., 1998. The geochemical composition of subducting sediments and its consequences for the crust and mantle. Chemical Geology, 145: 325-394.
Poitrasson, F., Pin, C. and Duthou, J.L., 1995. Hydrothermal remobilization of rare earth elements and its efect on Nd isotopes in rhyolite and granite. Earth and Planetary Science Letters, 130: 1-11.
Poitrasson, F., Chenery, S. and Bland, D.J., 1996. Contrasted monazite hydrothermal alteration mechanisms and their geochemical implications. Earth and Planetary Science Letters, 145: 79-96.
Poitrasson, F., Chenery, S. and Shepherd, T.J., 2000. Electron microprobe and LA-ICP-MS study of monazite hydrothermal alteration: Implications for U-Th-Pb geochronology and nuclear ceramics. Geochimica et Cosmochimica Acta, 64(19): 3283-3297.
Pollard, P.J., 2000. Evidence of a magmatic fluid and metal source for Fe-Oxide Cu-Au mineralization. In: T.M. Porter (Editor), Hydrothermal Iron Oxide Copper-Gold and Related Deposits: A Global Perspective. Australian Mineral Foundation, Adelaide, pp. 27-41.
Pollard, P.J., 2001. Sodic(-calcic) alteration in the Fe-oxide-Cu-Au districts: an origin via unmixing of magmatic H2O-CO2-NaCl ± CaCl2-KCl fluids. Mineralium Deposita, 36: 93-100.
Pollard, P.J. and Perkins, C., 1997. 40Ar/39Ar geochronology of alteration and Cu-Au-Mo mineralization in the Cloncurry district, Mount Isa Inlier, Australia. AMIRA P438 Cloncurry Base Metals and Gold Final Report, Section 3, 40pp,.
Pouchou, J.L. and Pichoir, F., 1985. "PAP" phi-rho-Z procedure for improved quantitative microanalysis. In: J.L. Armstrong (Editor), Microbeam Analysis. San Francisco Press Inc., San Francisco, pp. 104-106.
Preiss, W.V. and Conor, C.H.H., 2001. Origin and nomenclature of the Willyama Inliers, Curnamona Province. MESA Journal, 21: 47-49.
Prevec, S.A., Lightfoot, P.C. and Keays, R.R., 2000. Evolution of the sublayer of the Sudbury Igneous Complex: geochemical, Sm-Nd isotopic and petrologic evidence. Lithos, 51: 271-292.
Pyle, J.M., Spear, F.S. and Wark, D.A., 2002. Electron microprobe analysis of REE in apatite, monazite and xenotime; protocols and pitfalls. Reviews in Mineralogy and Geochemistry, 48: 337-362.
Pyle, J.M., Spear, F.S., Wark, D.A., Daniel, C.G. and Storm, L.C., 2005. Contributions to precision and accuracy of monazite microprobe ages. American Mineralogist, 90: 547-577.
Rawlings, D.J., 1999. Stratigraphic resolution of a multiphase intercratonic basin system: The McArthur basin, northern Australia. Australian Journal of Earth Sciences, 46: 703-723.
Relvas, J.M.R.S., Tassinari, C.C.G., Munha, J. and Barriga, F.J.A.S., 2001. Multiple sources for ore-forming fluids in the Neves Corvo VHMS deposit of the Iberian Pyrite Belt (Portugal): strontium, neodymium and lead isotope evidence. Mineralium Deposita, 36: 416-427.
Reynolds, L.J., 2000. Geology of the Olympic Dam Cu-U-Au-Ag-REE deposit. In: T.M. Porter (Editor), Hydrothermal iron oxide copper-gold and related deposits; a global perspective; Vol. 1. AMF, Adelaide, pp. 93-104.
Rhede, D., Wendt, I. and Forster, H.J., 1996. A three-dimensional method for calculating independent chemical U/Pb-and Th/Pb-ages of accessory minerals. Chemical Geology, 130: 247-253.
Ripley, E.M., Lambert, D.D. and Frick, L.R., 1999. Re-Os, Sm-Nd, and Pb isotopic constraints on mantle and crustal contributions to magmatic sulfide mineralization in the Duluth Complex. Geochimica et Cosmochimica Acta, 62(19-20): 3349-3365.
Robertson, R.S., Preiss, W.V., Crooks, A.F., Hill, P.W. and Sheard, M.J., 1998. Review of the Proterozoic geology and mineral potential of the Curnamona Province in South Australia. AGSO Journal of Australian Geology and Geophysics, 17(3): 169-182.
Rogers, J.J.W., 1996. A history of continents in the past three billion years. Journal of Geology, 104: 91-107.
Rogers, J.J.W. and Santosh, M., 2002. Configuration of Columbia, a Mesoproterozoic Supercontinent. Gondwana Research, 5(1): 5-22.

Rolland, Y., Cox, S., Boullier, A.-M., Pennacchioni, G. and Mancktelow, N., 2003. Rare earth and trace element mobility in mid-crustal shear zones: insights from the Mont Blanc Massif (Western Alps). Earth and Planetary Science Letters, 214: 203-219.

Rubatto, D., Williams, I.S. and Buick, I.S., 2001. Zircon and monazite response to prograde metamorphism in the Reynolds Range, central Australia. Contributions to Mineralogy and Petrology, 140: 458-468.

Sandiford, M. and Hand, M., 1998. Australian Proterozoic high-temperature, low-pressure metamorphism in the conductive limit. Geological Society Special Publications, 138: 109-120.

Sandiford, M. and Powell, R., 1990. Some isostatic and thermal consequences of the vertical strain geometry in convergent orogens. Earth and Planetary Science Letters, 98(2): 154-165.

Schandl, E.S. and Gorton, M.P., 2004. A textural and geochemical guide to the identification of hydrothermal monazite: Criteria for selection of samples for dating epigenetic hydrothermal ore deposits. Economic Geology, 99: 1027-1035.

Schandl, E.S., Gorton, M.P. and Wasteneys, H.A., 1995. Rare earth element geochemistry of the metamorphosed volcanogenic massive sulphide deposits of the Manitouwadge Mining Camp, Superior Province, Canada: A potential exploration tool? Economic Geology, 90: 1217-1236.

Scott, D.L., Rawlings, D.J., Page, R.W., Tarlowski, C.Z., Idnurm, M., Jackson, M.J. and Southgate, P.N., 2000. Basement framework and geodynamic evolution of the Palaeoproterozoic Superbasins of north-central Australia: an integrated review of geochemical, geochronological and geophysical data. Australian Journal of Earth Sciences, 47: 341-380.

Sears, J.W. and Price, R.A., 2002. The hypothetical Mesoproterozoic Supercontinent Columbia: Implications of the Siberian-West Laurentian connection. Gondwana Research, 5(1): 35-39.

Simonetti, A. and Bell, K., 1994. Isotopic and geochemical investigation of the Chilwa Island carbonatite complex, Malawi: evidence for a depleted mantle source region, liquid immiscibility, and open-system behaviour. Journal of Petrology, 35(6): 1597-1621.

Sinton, J.M., Wilson, D.S., Christie, D.M., Hey, R.N. and Delaney, J.R., 1983. Petrologic consequences of rift propagation on oceanic spreading ridges. Earth and Planetary Science Letters, 62: 193-207.

Siva Siddaiah, N., Hanson, G.N. and Rajamani, V., 1994. Rare earth element evodence for syngeneitc origin of an Archean stratiform gold sulfide deposit, Kolar Schist Belt, south India. Economic Geology, 89: 1552-1566.

Skirrow, R.G. and Ashley, P.M., 1998. Cu-Au mineral systems and regional alteration, Curnamona Craton. AGSO Record, 1998/25: 104-108.

Skirrow, R.G. and Ashley, P.M., 2000. Proterozoic Cu-Au systems of the Curnamona Province. MESA Journal, 19: 48-49.

Skirrow, R.G., Mass, R. and Ashley, P.M., 1999. New age constraints for Cu-Au(-Mo) mineralisation and regional alteration in the Olary-Broken Hill region. AGSO Research Newsletter, 31: 22-25.

Skirrow, R.G., Ashley, P.M., McNaughton, N.J. and Suzuki, K., 2000. Time-space framework of Cu-Au(-Mo) and regional alteration systems in the Curnamona Province. AGSO Record, 2000/10: 83-86.

Skirrow, R.G., Bastrakov, E., Davidson, G.J., Raymond, O.L. and Heithersay, P., 2002. The geological framework, distribution and controls of Fe-oxide Cu-Au mineralisation in the Gawler Craton, South Australia; Part II, Alteration and mineralisation. In: T.M. Porter (Editor), Hydrothermal iron oxide copper-gold and related deposits; a global perspective; Vol. 2. AMF, Adelaide, pp. 33-47.

Slack, J.F., 1999. Sm-Nd geochronology of tourmalinites and sulfide ores from the Sullivan Ob-Zn-Ag deposit, southeastern British Columbia. Abstracts with Programs - Geological Society of America, 31(7): 31.

Smith, H.A. and Barreiro, B., 1990. Monazite U-Pb dating of staurolite grade metamorphism in pelitic schists. Contributions to Mineralogy and Petrology, 105: 602-615.

Smith, M.P., Henderson, P. and Campbell, L.S., 2000. Fractionation of the REE during hydrothermal processes: Constraints from the Bayan Obo Fe-REE-Nb deposit, Inner Mongolia, China. Geochimica et Cosmochimica Acta, 64(18): 3141-3160.

Smoliar, M.I., Walker, R.J. and Morgan, J.W., 1996. Re-Os isotopic constraints on the age of Group IIA, IIIA, IVA and IVB iron meterorites. Science, 271: 1099-1102.

Sørenson, H., 1974. The Alkaline Rocks. John Wiley & Sons Ltd, Letchworth, 622 pp.

Spear, F.S. and Parrish, R.R., 1996. Petrology and cooling rates of the Valhalla Complex, British Columbia. Journal of Petrology, 37: 733-765.

Stein, H.J., Markey, R.J., Morgan, J.W., Hannah, J.L. and Schersten, A., 2001. The remarkable Re-Os chronometer in molybdenite; how and why it works. Terra Nova, 13(6): 479-486.

Stendel, H., Frei, R., Hamilton, M.A. and Mueller, W.U., 2001. The Palaeoproterozoic Kangerluluk gold-copper mineralization (southeast Greenland): Pb and Nd isotopic constraints on its timing and genesis. Mineralium Deposita, 36: 177-188.

Stern, R.A. and Berman, R.G., 2000. Monazite U-Pb and Th-Pb geochronology by ion microprobe, with an application to in situ dating of an Archaean sedimentary rock. Chemical Geology, 172: 113-130.

Stevens, B.P., 1986. Post-deformational history of the Willyama Supergroup in the Broken Hill Block, N.S.W. Australian Journal of Earth Sciences, 33: 73-98.

Stevens, B.P., 1999. Evidence for multiple Palaeoproterozoic thermal events and magmatism adjacent to the Broken Hill Pb-Zn-Ag orebody, Australia: Discussion. Precambrian Research, 98(1-2): 1-5.

Stevens, B.P., 2000. Evaluating models for tectonic development of the Willyama Supergroup. AGSO Record, 2000/10: 87-90.

Stevens, B.P.J., Stroud, W.J., Willis, I.L., Bradley, G.M., Brown, R.E. and Barnes, R.G., 1980. A stratigraphic interpretation of the Broken Hill Block. In: B.P.J. Stevens (Editor), A guide to the stratigraphy and mineralization of the Broken Hill Block, New South Wales. Geological Survey of New South Wales, Sydney, pp. 9-32.

Stewart, K. and Foden, J., 2001. Mesoproterozoic Granites of South Australia. Mines Department of South Australia, unpublished report.

Stuwe, K. and Ehlers, K., 1997. Multiple metamorphic events at Broken Hill, Australia. Evidence from chloritoid-bearing parageneses in the Nine-Mile Mine region. Journal of Petrology, 38(9): 1167-1186.

Sun, S.S. and McDonough, W.F., 1989. Chemical and isotopic systematics of oceanic basalts; implications for mantle composition and processes. In: A.D. Saunders and M.J. Norry (Editors), Magmatism in the ocean basins. Geological Society of London, Special Publications, London, pp. 313-345.

Suzuki, K. and Adachi, M., 1991. Precambrian provenence and Silurian metamorphism of the subonosawa paragneiss in the South Kitakami terrane, Northeast Japan, revealed by the chemical Th-U-total lead isochron ages of monazite, zircon and xenotime. Geochemical Journal, 25: 357-376.

Suzuki, K., Adachi, M. and Kajizuka, I., 1994. Electron microprobe observations of Pb diffusion in metamorphosed detrital monazites. Earth and Planetary Science Letters, 128(3-4): 391-405.

Swain, G., Woodhouse, A., Hand, M., Barovich, K., Schwartz, M., Fanning, C.M., 2005. Provenance and tectonic development of the late Archaean Gawler Craton, Australia: U-Pb zircon, geochemical and Sm-Nd isotopic implications. Precambrian Research, *in press*.

Swapp, S.M. and Frost, B.R., 2003. Evidence of high-pressure metamorphism in the granulites of the Broken Hill area. AGSO Record, 2003/13: 174-175.

Taylor, R.P. and Fryer, B.J., 1982. Rare earth element geochemistry as an aid to interpreting hydrothermal ore deposits. In: A.M. Evans (Editor), Metallization Associated with Acid Magmatism. John Wiley & Sons Ltd, Chichester, United Kingdom, pp. 357-365.

Taylor, S.R. and McLennan, S.M., 1985. The Continental Crust: its composition and Evolution. Blackwell, Oxford., 312 pp.

Teale, G.S. and Fanning, C.M., 2000a. The Portia - North Portia Cu-Au(-Mo) Prospect, South Australia: Timing of Mineralisation, Albitisation and Origin of Ore Fluid. In: T.M. Porter (Editor), Hydrothermal Iron Oxide Copper-Gold and Related Deposits: A global Perspective. Australian Mineral Foundation, Adelaide, pp. 137-147.

Teale, G.S. and Fanning, C.M., 2000b. The timing of Cu-Au mineralisation in the Curnamona Province. AGSO Record, 2000/10: 98-100.

Teale, G.S. and Flint, R.B., 1993. Curnamona Craton and Mount Painter Province. In: J.F. Drexel, W.V. Preiss and A.J. Parker (Editors), The geology of South Australia. Volume 1 The Precambrian. Mines and Energy South Australia, pp. 147-167.

Teasdale, J., 1997. Methods for understanding poorly exposed terrains: The interpretive geology and tectonothermal evolution of the western Gawler craton. Ph.D. Thesis, University of Adelaide, Adelaide, 182 pp.

Thompson, R.N. and Gibson, S.A., 1994. Magmatic expression of lithospheric thinning across continentl rifts. Tectonophysics, 233(1-2): 41-68.

Thorkelson, D.J., Mortensen, J.K., Davidson, G.J., Creaser, R.A., Perez, W.A. and Abbott, J.G., 2001a. Early Mesoproterozoic intrusive breccias in Yukon, Canada: the role of hydrothermal systems in reconstructions of North America and Australia. Precambrian Research, 111: 31-55.

Thorkelson, D.J., Mortensen, J.K., Creaser, R.A., Davidson, G.J. and Abbott, J.G., 2001b. Early Proterozoic magmatism in Yukon, Canada: constraints on the evolution of northwestern Laurentia. Canadian Journal of Earth Sciences, 38: 1479-1494.

Tilley, C.E., 1954. Nepheline-alkali feldspar paragenesis. American Journal of Science, 252(65-75).

Tonelli, M., Woodhead, J. and Hergt, J., 2003. Pb-Pb dating of garnet, staurolite and tourmaline by stepwise dissolution technique. AGSO Record, 2003/13: 188-191.

Tosdal, R.M., Wooden, J.L. and Bouse, R.M., 1999. Pb isotopes, ore deposits, and metallogenic terranes. Reviews in Economic Geology, 12: 1-28.

Turner, S. and Hawkesworth, C., 1995. The nature of the sub-continental mantle: constraints from the major-element composition of continental flood basalts. Chemical Geology, 120: 295-314.

Valentine, J.W. and Moores, E.M., 1970. Plate-tectonic regulation of faunal diversiy and sea level: a model. Nature, 228: 657-659.

Vassallo, J.J. and Wilson, C.J.L., 2002. Palaeoproterozoic regional-scale non-coaxial deformation: An example from the Eyre Peninsula, South Australia. Journal of Structural Geology, 23(1-24).

Verhulst, A., Balaganskaya, E., Kirnarsky, Y. and Demaiffe, D., 2000. Petrological and geochemical (trace elements and Sr-Nd isotopes) characterisitics of the Palaeozoic Kovdor ultramafic, alkaline and carbonatite intrusion (Kola Peninsula, NW Russia). Lithos, 51: 1-25.

Wade, B.P., Barovich, K.M., Hand, M., Scrimgeour, I.R. and Close, D.F., 2006. Evidence for early-Mesoproterozoic arc magmatism in the Musgrave Block, central Australia: implications for Proterozoic crustal growth and tectonic reconstructions of Australia. Journal of Geology, 114: 43-63.

Ward, C.D., McArthur, J.M. and Walsh, J.N., 1992. Rare earth element behaviour during evolution and alteration of the Dartmoor Granite, SW England. Journal of Petrology, 33(4): 785-815.

Watanabe, M., Hoshino, K., Kagami, H., Nishido, H. and Sugiyama, M., 1998. Rb-Sr, Sm-Nd and K-Ar systematics of metamorphosed pillowed basalts and associated Besshi-type deposits in the Sanbagawa Belt, Japan. Mineralium Deposita, 34: 113-120.

Weaver, B.L. and Tarney, J., 1981. The Scourie dyke suite: petrogenesis and geochemical nature of the Proterozoic sub-continental mantle. Contributions to Mineralogy and Petrology, 78: 175-188.

Webb, G. and Crooks, A.F., 2003. A metamorphic investigation of the Palaeoproterozoic metasediments of the Willyama Inliers, southern Curnamona Province, South Australia, South Australia Department of Primary Industries and Resources. Report Book, 2003/11.

Webster, A.E., 1996. Delamerian refolding of the Palaeoproterozoic Broken Hill Block. Australian Journal of Earth Sciences, 43: 85-89.

White, R.W., Pomroy, N.E. and Powell, R., 2005. An in situ metatexite-diatexite transition in upper amphibolite facies rocks from Broken Hill, Australia. Journal of Metamorphic Geology, 23: 579-602.

Williams, M.L. and Jercinovic, M.J., 2002. Microprobe monazite geochronology; putting absolute time into microstructural analysis. Journal of Structural Geology, 24: 1013-1028.

Williams, M.L., Jercinovic, M.J., Terry, M.P. and Bosbyshell, H., 1999. Age mapping and dating of monazite on the electron microprobe; implications for multistage tectonic histories. In: Anonymous (Editor), Geological Society of America, 1999 annual meeting. Abstracts with Programs - Geological Society of America, pp. 428-429.

Williams, P.J., 1998a. Magmatic iron enrichment in high-iron metatholeiites associated with 'Broken Hill-type' Pb-Zn-Ag deposits, Mt Isa Eastern Succession. Australian Journal of Earth Sciences, 45: 389-396.

Williams, P.J., 1998b. Metalliferous economic geology of the Mt. Isa Eastern Succession, Queensland. Australian Journal of Earth Sciences, 45: 329-342.

Williams, P.J. and Skirrow, R.G., 2000. Overview of Iron Oxide-Copper-Gold Deposits in the Curnamona Province and Cloncurry District (Eastern Mount Isa Block), Australia. In: T.M. Porter (Editor), Hydrothermal Iron Oxide Copper-Gold and Related Deposits: A Global Perspective. Australian Mineral Foundation, Adelaide, pp. 105-122.

Willis, I.L., Brown, R.E., Stroud, W.J. and Stevens, B.P.J., 1983. The Early Proterozoic Willyama Supergroup: stratigraphic subdivision and interpretation of high to low-metamorphic rocks in the Broken Hill Block, New South Wales. Journal of the Geological Society of Australia, 30: 195-224.

Wilson, C.J.L. and Powell, R., 2001. Strain localisation and high-grade metamorphism at Broken Hill, Australia: A view from the Southern Cross area. Tectonophysics, 335: 193-210.

Wilson, I.H., Derrick, G.M. and Perkin, D.J., 1985. Eastern Creek Volcanics: their geochemistry and possible role in copper mineralisation at Mount Isa, Queensland. BMR Journal of Australian Geology and Geophysics, 9: 317-328.

Winchester, J.A. and Floyd, P.A., 1977. Geochemical discrimination of different magma series and their differentiation products using immobile elements. Chemical Geology, 20(4): 325-343.

Windley, B.F., 1995. The Evolving Continents, Third edition. Wiley, Chichester, 526 pp.

Wingate, M.T.D., Pisarevsky, S.A. and Evans, D.A.D., 2002. Rofinia connections between Australia and Laurentia: no SWEAT, no AUSWUS? Terra Nova, 14: 121-128.

Wood, D.A., 1980. The application of a Th-Hf-Ta diagram to problems of tectonomagmatic classification and to establishing the nature of crustal contamination of basaltic lavas of a British Tertiary volcanic province. Earth and Planetary Science Letters, 50: 11-30.

Wood, S.A., 1990. The aqueous geochemistry of the rare-earth elements and yttrium. 2. Theoretical predictions of speciation in hydrothermal solutions to 350ºC at saturation water vapor pressure. Chemical Geology, 88: 99-125.

Wooden, J.L. and Miller, D.M., 1990. Chronologic and isotopic framework for early Proterozoic crustal evolution in the eastern Mojave desert region, SE California. Journal of Geophysical Research, 95: 20133-20146.

Woolley, A.R., 1987. Lithosphere metasomatism and the petrogenesis of the Chilwa Province of alkaline igneous rocks and carbonitites, Malawi. Journal of African Earth Sciences, 6(6): 891-898.

Woolley, A.R., 2001. Alkaline rocks and carbonatites of the world; part 3, Africa. Geological Society of London, London, 372 pp.

Woolley, A.R., Williams, C.T., Wall, F., Garcia, D. and Moute, J., 1995. The Bingo carbonatite-ijolite-nepheline sysnite complex, Zaire: geology, petrography, mineralogy and petrochemistry. Journal of African Earth Sciences, 21(3): 1995.

Worley, B.A., Cooper, A.F. and Hall, C.E., 1995. Petrogenesis

of carbonate-bearing nepheline syenites and carbonatites from Southern Victoria Land, Antarctica: origin of carbon and the effects of calcite-graphite equilibrium. Lithos, 35: 183-199.

Yang, J.-H. and Zhao, X.-H., 2001. Rb-Sr, Sm-Nd, and Pb isotope systematics of pyrite: implications for the age and genesis of lode gold deposits. Geology, 29(8): 711-714.

Yang, K. and Ashley, P.M., 1994. Stratabound breccias in the Willyama Supergroup, Olary Block, South Australia, AMF, Proceedings, Australian Research on Ore Genesis Symposium, Adelaide, 16.1-16.5.

Yates, K.R., 1992. Review of company mineral exploration, Willyama Blocks and environs, OLARY 1:250 000 map sheet, South Australia. South Australia. Department of Mines and Energy. Report Book, 92/34.

Zhang, H.F., Sun, M., Zhou, X.H. and Ying, J.F., 2005. Geochemical constraints on the origin of Mesozoic alkaline intrusive complexes from the North China Craton and tectonic implications. Lithos, 81(1-4): 297-317.

Zhao, G., Sun, M., Wilde, S.A. and Li, S., 2004. A Paleo-Mesoproterozoic supercontinent: assembly, growth and breakup. Earth Science Reviews, 67: 91-123.

Zhao, J.-X., 1994. Geochemical and Sm-Nd isotopic study of amphibolites in the southern Arunta Inlier, central Australia: evidence for subduction at a Proterozoic continental margin. Precambrian Research, 65: 71-94.

Zhao, J.-X. and McCulloch, M.T., 1993. Melting of a subduction-modified continental lithospheric mantle: Evidence from Late Proterozoic mafic dike swarms in central Australia. Geology, 21: 463-466.

Zhao, J. and McCulloch, M.T., 1995. Geochemical and isotopic systematics of granites from the Arunta Inlier, central Australia: implications for Proterozoic crustal evolution. Precambrian Research, 71: 265-299.

Zhu, X.K. and O'Nions, R.K., 1999. Zonation of monazite in metamorphic rocks and its implications for high temperature thermochronology; a case study from the Lewisian terrain. Earth and Planetary Science Letters, 171(2): 209-220.

Zhu, X.K., O'Nions, R.K., Belshaw, N.S. and Gibb, A.J., 1997. Lewisian crustal history from insitu SIMS mineral chronometry and relatd metamorphic textures. Chemical Geology, 136: 205-218.

Ziegler, P.A. and Cloetingh, S., 2004. Dynamic processes controllong evolution of rifted basins. Earth Science Reviews, 64(1-2): 1-50.

# Appendix 1
# GEOCHEMISTRY & ISOTOPES

This appendix lists all major- and trace-element geochemistry, and Nd isotopic compositions of major protoliths in the SCP used for comparisons made in this study. Willyama Supergroup metasediments data of Barovich (2003), Barovich & Hand (2004) and Barovich et al. (2002); A-type granitoid data of Ashley et al. (1996); I-type granitoid data of Freeman (1995) and Payne (2003); S-type granitoid data of Stewart & Foden (2001); and intermediate granitoid data of Barovich & Foden (2002).

Table A1.1. Major- and trace-element and Nd isotopic compositions of major protoliths in the southern Curnamona Province

| **Sample** | 5018 | R350492 | R350483 | R350481 | R350485 | R350486 | R350491 | R350493 | R350494 | R350495 | R350480 | R350477 |
|---|---|---|---|---|---|---|---|---|---|---|---|---|
| **Lithology** | Metased | Metased | Metased | Metased | Metased | Metased | Metased | Metased | Metased | Metased | Metased | Metased |
| **Region** | Olary | Olary | Olary | Olary | Olary | Olary | Olary | Olary | Olary | Olary | Olary | Olary |
| **Group** | Mt. Howden SG | Saltbush SG | Saltbush SG | Plumbago Fm | Bimba Fm | Ethiudna SG | Ethiudna SG | Ethiudna SG | Wiperaminga SG | Wiperaminga SG | Wiperaminga SG | Wiperaminga SG |
| **Reference** | Barovich | Barovich | Barovich | Barovich | Barovich | Barovich | Barovich | Barovich | Barovich | Barovich | Barovich | Barovich |
| **$Al_2O_3$** | 14.08 | 17.48 | 32.20 | 13.16 | 14.64 | 8.17 | 17.00 | 15.87 | 17.84 | 6.76 | 15.66 | 4.58 | 4.89 |
| **CaO** | 0.47 | 0.44 | 0.39 | 0.95 | 0.08 | 21.08 | 0.19 | 0.81 | 0.58 | 0.07 | 0.46 | 0.05 | 0.06 |
| **$Fe_2O_3$** | 1.71 | 3.19 | 6.72 | 5.03 | 0.82 | 2.24 | 5.99 | 6.93 | 4.88 | 1.73 | 7.23 | 2.85 | 3.09 |
| **$K_2O$** | 1.96 | 2.92 | 8.27 | 2.57 | 4.63 | 2.30 | 5.17 | 7.53 | 5.39 | 3.91 | 5.78 | 0.21 | 0.24 |
| **MgO** | 0.77 | 0.74 | 2.62 | 1.52 | 0.84 | 3.07 | 2.07 | 2.23 | 2.32 | 0.19 | 2.81 | 0.06 | 0.06 |
| **MnO** | 0.02 | 0.01 | 0.11 | 0.16 | 0.01 | 0.13 | 0.08 | 0.18 | 0.10 | 0.02 | 0.13 | 0.00 | 0.00 |
| **$Na_2O$** | 4.17 | 2.90 | 0.75 | 1.69 | 0.33 | 0.56 | 1.15 | 2.01 | 1.59 | 0.99 | 1.47 | 2.42 | 2.61 |
| **$P_2O_5$** | 0.05 | 0.07 | 0.28 | 0.06 | 0.06 | 0.32 | 0.10 | 0.21 | 0.16 | 0.06 | 0.16 | 0.04 | 0.04 |
| **$SiO_2$** | 74.51 | 68.25 | 42.18 | 71.95 | 68.52 | 50.72 | 63.07 | 61.68 | 63.36 | 85.23 | 63.44 | 88.67 | 88.30 |
| **$TiO_2$** | 0.38 | 0.57 | 1.09 | 0.55 | 0.65 | 0.27 | 0.81 | 0.62 | 0.80 | 0.19 | 0.59 | 0.71 | 0.41 |
| **Sc** | 9.0 | 17.0 | 19.0 | 10.0 | 12.0 | 19.0 | 13.0 | 13.0 | 14.0 | 2.0 | 13.0 | 3.0 | 4.0 |
| **Ba** | 434.0 | 627.0 | 1672.0 | 370.0 | 1242.0 | 3573.0 | 721.0 | 2991.0 | 1098.0 | 1546.0 | 1361.0 | 22.0 | 40.0 |
| **Be** | 2.5 | 2.2 | 7.7 | 7.0 | 4.5 | 2.5 | 5.0 | 5.1 | 6.0 | 0.6 | 5.2 | 0.4 | 0.6 |
| **Hf** | na | na | na | na | na | na | na | na | na | na | na | na | na |
| **Rb** | 80.0 | 176.0 | 394.0 | 196.0 | 185.0 | 90.0 | 251.0 | 299.0 | 230.0 | 90.0 | 322.0 | 5.0 | 9.0 |
| **Sn** | 3.0 | 3.0 | 11.0 | 4.0 | 4.5 | 5.5 | 4.0 | 3.5 | 4.0 | 1.5 | 6.0 | 9.5 | 5.0 |
| **Sr** | 84.0 | 110.0 | 59.0 | 88.0 | 58.0 | 242.0 | 69.0 | 107.0 | 105.0 | 110.0 | 40.0 | 16.0 | 10.0 |
| **Ta** | 1.5 | 1.5 | 2.5 | 1.5 | 1.0 | 0.5 | 1.5 | 1.5 | 1.5 | 1.0 | 1.5 | 2.0 | 1.5 |
| **W** | na | na | na | na | na | na | na | na | na | na | na | na | na |
| **Zr** | 242.0 | 247.0 | 227.0 | 172.0 | 186.0 | 97.0 | 172.0 | 165.0 | 207.0 | 355.0 | 181.0 | 1978.0 | 1035.0 |
| **LOI** | 1.8 | 3.3 | 5.7 | 2.8 | 9.1 | 11.0 | 4.0 | 1.8 | 3.1 | 0.6 | 2.7 | 0.4 | 0.3 |
| **Ag** | na | na | na | na | na | na | na | na | na | na | na | na | na |
| **As** | 1.1 | 3.3 | 3.3 | 22.1 | 2.7 | 2.2 | 4.3 | 2.6 | 45.0 | 1.4 | 1.7 | 0.5 | 0.5 |
| **Co** | na | na | na | na | na | na | na | na | na | na | na | na | na |
| **Cr** | 23.0 | 25.0 | 151.7 | 58.6 | 61.8 | 29.6 | 77.9 | 71.0 | 80.7 | 16.8 | 68.0 | 21.1 | 16.7 |
| **Cu** | 4.0 | 32.0 | 12.0 | 96.0 | 15.0 | 54.0 | 75.0 | 14.0 | 93.0 | 14.0 | 31.0 | 94.0 | 10.0 |
| **Ni** | 19.0 | 8.0 | 25.0 | 13.0 | 0.0 | 16.0 | 8.0 | 28.0 | 15.0 | 0.0 | 21.0 | 0.0 | 0.0 |
| **Pb** | 11.0 | 39.0 | 67.5 | 47.5 | 99.5 | 22.5 | 75.5 | 15.0 | 89.0 | 18.0 | 6.5 | 13.0 | 5.5 |
| **S** | 60.0 | 100.0 | 30.0 | 90.0 | 610.0 | 40.0 | 2990.0 | 120.0 | 890.0 | 30.0 | 40.0 | 10.0 | na |
| **V** | 21.0 | 64.0 | 129.0 | 65.0 | 155.0 | 49.0 | 141.0 | 85.0 | 159.0 | 16.0 | 72.0 | 33.0 | 31.0 |
| **Zn** | 20.0 | 59.0 | 216.0 | 145.0 | 28.0 | 92.0 | 226.0 | 56.0 | 149.0 | 8.0 | 45.0 | 12.0 | na |
| **Bi** | 0.2 | 0.5 | 1.3 | 0.4 | 0.3 | 0.1 | 0.7 | 0.1 | 1.9 | na | na | na | na |
| **Cs** | 1.9 | 13.2 | 10.6 | 4.5 | 2.6 | 3.2 | 11.7 | 13.5 | 6.0 | 1.2 | 13.9 | 0.0 | 0.1 |
| **Ga** | 15.3 | 18.9 | 42.9 | 15.6 | 21.3 | 10.3 | 23.4 | 20.3 | 25.7 | 5.1 | 22.3 | 6.2 | 8.1 |
| **Mo** | 0.8 | 1.0 | 0.4 | 2.8 | 10.2 | 0.7 | 8.2 | 0.6 | 2.9 | 1.1 | 0.4 | 2.8 | 1.3 |
| **Sb** | -0.2 | -0.2 | -0.1 | 0.1 | 0.1 | 0.4 | 0.2 | 0.1 | 0.1 | 0.1 | 0.2 | 0.2 | |
| **Th** | 14.2 | 17.9 | 44.9 | 16.7 | 18.4 | 8.1 | 17.1 | 18.0 | 18.5 | 7.2 | 18.1 | 34.8 | 18.2 |
| **U** | 3.5 | 4.4 | 10.0 | 6.6 | 8.6 | 7.1 | 6.9 | 4.8 | 7.5 | 1.9 | 2.1 | 5.7 | 4.1 |
| **Y** | 39.0 | 42.4 | 40.1 | 31.1 | 22.0 | 19.0 | 23.8 | 31.7 | 28.0 | 12.9 | 33.1 | 35.6 | 45.2 |
| **Nb** | 15.6 | 16.8 | 25.7 | 14.2 | 16.1 | 7.7 | 15.1 | 13.6 | 16.4 | 2.9 | 13.4 | 13.2 | 15.5 |
| **Dy** | 5.9 | 7.2 | 8.9 | 5.3 | 3.0 | 3.0 | 4.3 | 6.2 | 5.2 | 2.1 | 5.9 | 5.4 | 6.6 |
| **Er** | 3.9 | 4.4 | 3.5 | 3.2 | 2.1 | 1.7 | 2.2 | 3.1 | 2.8 | 1.3 | 3.7 | 3.3 | 4.0 |
| **Eu** | 1.0 | 1.5 | 2.1 | 1.1 | 0.6 | 0.7 | 1.5 | 1.7 | 1.4 | 0.6 | 1.3 | 1.4 | 0.8 |
| **Gd** | 6.1 | 8.6 | 13.4 | 5.5 | 3.2 | 3.6 | 6.5 | 8.6 | 6.9 | 2.6 | 7.4 | 7.5 | 5.7 |
| **Ho** | 1.3 | 1.5 | 1.4 | 1.1 | 0.7 | 0.6 | 0.8 | 1.1 | 1.0 | 0.4 | 1.2 | 1.1 | 1.4 |
| **Lu** | 0.6 | 0.7 | 0.4 | 0.5 | 0.3 | 0.2 | 0.3 | 0.4 | 0.4 | 0.2 | 0.6 | 0.6 | 0.6 |
| **Nd** | 34.3 | 51.2 | 90.1 | 29.8 | 21.2 | 21.2 | 45.1 | 51.3 | 43.2 | 14.6 | 40.6 | 56.7 | 21.2 |
| **Pr** | 9.1 | 13.8 | 25.0 | 8.2 | 6.0 | 5.8 | 12.3 | 14.1 | 11.8 | 4.0 | 11.1 | 15.7 | 5.7 |
| **Sm** | 6.7 | 10.1 | 16.3 | 6.0 | 3.8 | 3.9 | 8.0 | 9.6 | 8.1 | 2.9 | 8.3 | 9.4 | 4.4 |

| Sample | 5018 | 5020 | R350492 | R350483 | R350481 | R350485 | R350486 | R350491 | R350493 | R350494 | R350495 | R350480 | R350477 |
|---|---|---|---|---|---|---|---|---|---|---|---|---|---|
| Lithology | Metased | Metased | Metased | Metased | Metased | Metased | Metased | Metased | Metased | Metased | Metased | Metased | Metased |
| Region | Olary | Olary | Olary | Olary | Olary | Olary | Olary | Olary | Olary | Olary | Olary | Olary | Olary |
| Group | Mt. Howden SG | Mt. Howden SG | Saltbush SG | Saltbush SG | Plumbago Fm | Bimba Fm | Ethiudna SG | Ethiudna SG | Ethiudna SG | Wiperaminga SG | Wiperaminga SG | Wiperaminga SG | Wiperaminga SG |
| Reference | Barovich | Barovich | Barovich | Barovich | Barovich | Barovich | Barovich | Barovich | Barovich | Barovich | Barovich | Barovich | Barovich |
| Tb | 1.1 | 1.4 | 2.0 | 1.0 | 0.5 | 0.6 | 0.9 | 1.3 | 1.1 | 0.4 | 1.2 | 1.1 | 1.1 |
| Yb | 4.0 | 4.4 | 2.6 | 3.2 | 2.3 | 1.6 | 2.0 | 2.7 | 2.6 | 1.2 | 4.0 | 3.5 | 3.7 |
| La | 36.8 | 58.1 | 109.7 | 35.0 | 31.2 | 25.6 | 56.9 | 62.3 | 49.1 | 17.8 | 44.2 | 72.7 | 23.7 |
| Ce | 76.6 | 121.4 | 218.6 | 71.2 | 54.9 | 52.2 | 108.4 | 124.3 | 103.3 | 38.9 | 96.8 | 140.4 | 48.7 |
| Age | 1650 | 1650 | 1690 | 1690 | 1695 | 1695 | 1700 | 1700 | 1700 | 1700 | 1700 | 1700 | 1700 |
| $^{143}Nd/^{144}Nd$ | na | na | 0.511428 | 0.511523 | 0.511422 | 0.511449 | 0.511349 | 0.511398 | 0.511401 | 0.511452 | 0.515500 | 0.511335 | 0.511668 |
| $^{147}Sm/^{144}Nd$ | na | na | 0.1083 | 0.1193 | 0.1057 | 0.1094 | 0.1050 | 0.1105 | 0.1097 | 0.1217 | 0.1236 | 0.0992 | 0.1294 |
| $^{143}Nd/^{144}Nd_{(T)}$ | na | na | na | na | na | na | 0.510175 | 0.510163 | 0.510175 | 0.510091 | na | 0.510226 | 0.510221 |
| $\varepsilon Nd_i$ | -0.2 | -1.4 | -4.4 | -4.9 | -3.9 | -4.2 | -5.2 | -5.4 | -5.2 | -6.8 | -5.3 | -4.2 | -4.3 |
| $T_{DM}$ | na | na | na | na | na | na | 2289 | 2335 | 2315 | 2513 | na | 2199 | 2369 |

| Sample | R350476 | R350474 | R68495 | R68592 | PD-1F | 1060-10 | 1060-12 | T1 | T4 | T9610/4 | T8 | T10 | T24 | T29 | 1027-109 | 1027-106 | T44 | T46 |
|---|---|---|---|---|---|---|---|---|---|---|---|---|---|---|---|---|---|---|
| Lithology | Metased | Metased | Granite | Granite | Granite | Granite | Granite | Granite | Granite | Granite | Granite | Granite | Granite | Granite | Granite | Granite | Granite | Granite |
| Region | Olary | Olary | Ameroo | Ameroo | Poodla | Poodla | Antro | Olary | Olary | Olary | Olary | Olary | Olary | Olary | Olary | Olary | Olary | Olary |
| Group | Wiperaminga SG | Wiperaminga SG | A-type | A-type | I-type | I-type | I-type | S-type | S-type | S-type | S-type | S-type | S-type | S-type | S-type | S-type | S-type | S-type |
| Reference | Barovich | Barovich | Ashley | Ashley | Payne | Freeman | Freeman | Stewart | Stewart | Stewart | Stewart | Stewart | Stewart | Stewart | Stewart | Stewart | Stewart | Stewart |
| $Al_2O_3$ | 12.38 | 15.30 | na | na | na | na | na | 14.59 | 14.80 | na | 15.46 | 14.86 | 14.07 | 14.84 | 14.74 | 14.20 | 14.54 | 15.19 |
| CaO | 0.05 | 0.03 | na | na | na | na | na | 0.32 | 0.32 | na | 0.45 | 0.41 | 0.41 | 0.38 | 0.46 | 0.33 | 0.58 | 0.99 |
| $Fe_2O_3$ | 15.21 | 13.62 | na | na | na | na | na | 1.37 | 1.86 | na | 1.15 | 1.34 | 1.46 | 1.24 | 1.49 | 1.36 | 1.49 | 2.32 |
| $K_2O$ | 1.75 | 3.10 | na | na | na | na | na | 4.94 | 5.10 | na | 4.28 | 4.62 | 4.43 | 4.43 | 5.02 | 4.97 | 5.71 | 5.61 |
| MgO | 0.07 | 0.08 | na | na | na | na | na | 0.38 | 0.43 | na | 0.34 | 0.37 | 0.34 | 0.34 | 0.43 | 0.42 | 0.43 | 0.64 |
| MnO | 0.01 | 0.01 | na | na | na | na | na | 0.05 | 0.01 | na | 0.01 | 0.01 | 0.02 | 0.02 | 0.01 | 0.01 | 0.02 | 0.02 |
| $Na_2O$ | 6.25 | 9.15 | na | na | na | na | na | 3.49 | 3.37 | na | 4.78 | 4.21 | 4.23 | 3.97 | 3.65 | 4.03 | 3.61 | 3.69 |
| $P_2O_5$ | 0.07 | 0.10 | na | na | na | na | na | 0.16 | 0.23 | na | 0.24 | 0.26 | 0.18 | 0.24 | 0.23 | 0.16 | 0.14 | 0.22 |
| $SiO_2$ | 63.20 | 57.31 | na | na | na | na | na | 73.26 | 72.25 | na | 72.34 | 72.06 | 73.39 | 73.96 | 72.93 | 73.41 | 72.33 | 70.61 |
| $TiO_2$ | 0.52 | 0.64 | na | na | na | na | na | 0.15 | 0.23 | na | 0.12 | 0.14 | 0.14 | 0.12 | 0.21 | 0.16 | 0.23 | 0.31 |
| Sc | 5.0 | 6.0 | na | na | na | na | na | 4.1 | 3.2 | na | 8.0 | 4.4 | 4.8 | 6.7 | 6.3 | 4.6 | 4.5 | 5.5 |
| Ba | 311.0 | 1338.0 | na | na | na | na | na | 418.0 | 329.0 | na | 93.0 | 150.0 | 273.0 | 160.0 | 222.0 | 167.0 | 294.0 | 370.0 |
| Be | 0.6 | 0.4 | na | na | na | na | na | na | na | na | na | na | na | na | na | na | na | na |
| Hf | na | na | na | na | na | na | na | 3.1 | 5.0 | na | 2.9 | 2.9 | 4.5 | 2.7 | 3.8 | 4.6 | 5.5 | 6.1 |
| Rb | 31.0 | 203.0 | na | na | na | na | na | 270.0 | 409.0 | 409.0 | 320.0 | 365.0 | 283.0 | 338.0 | 371.4 | 334.8 | 285.0 | 383.0 |
| Sn | 9.5 | 8.0 | na | na | na | na | na | na | na | na | na | na | na | na | na | na | na | na |
| Sr | 25.0 | 28.0 | na | na | na | na | na | 78.0 | 54.0 | 54.0 | 21.0 | 30.0 | 41.0 | 21.0 | 28.1 | 22.1 | 36.0 | 69.0 |
| Ta | 1.0 | 1.0 | na | na | na | na | na | na | na | na | na | na | na | na | na | na | na | na |
| W | na | na | na | na | na | na | na | 431.0 | 486.0 | na | 548.0 | 668.0 | 554.0 | 541.0 | 704.0 | 643.0 | 516.0 | 491.0 |
| Zr | 224.0 | 198.0 | na | na | na | na | na | 86.0 | 147.0 | na | 80.0 | 84.0 | 113.0 | 73.0 | 119.3 | 132.4 | 161.0 | 182.0 |
| LOI | 0.7 | 0.8 | na | na | na | na | na | 0.9 | 1.0 | na | 0.6 | 0.8 | 0.6 | 0.8 | 0.8 | 0.5 | na | na |
| Ag | na | na | na | na | na | na | na | na | na | na | na | na | na | na | na | na | na | na |
| As | 1.4 | 2.6 | na | na | na | na | na | na | na | na | na | na | na | na | na | na | na | 1.1 |
| Co | na | na | na | na | na | na | na | 45.8 | 51.7 | na | 55.9 | 68.6 | 59.3 | 55.4 | 78.7 | 72.8 | 69.2 | 69.9 |
| Cr | 49.3 | 70.7 | na | na | na | na | na | 0.0 | 0.0 | na | 4.0 | 0.0 | 0.0 | 8.0 | 0.0 | 0.0 | 5.0 | 3.0 |
| Cu | 7.0 | 21.0 | na | na | na | na | na | 12.0 | 8.0 | na | 7.0 | 5.0 | 6.0 | 3.0 | 3.0 | 4.0 | 4.0 | 6.0 |
| Ni | 10.0 | 10.0 | na | na | na | na | na | 3.0 | 2.0 | na | 4.0 | 0.0 | 2.0 | 2.0 | 0.0 | 0.0 | 3.0 | 5.0 |
| Pb | 4.0 | 6.0 | na | na | na | na | na | 26.0 | 34.0 | na | 13.0 | 16.0 | 14.0 | 16.0 | 36.9 | 8.1 | 26.1 | 29.2 |
| S | 620.0 | 1380.0 | na | na | na | na | na | na | na | na | na | na | na | na | na | na | na | na |
| V | 63.0 | 86.0 | na | na | na | na | na | 5.0 | 15.0 | na | 9.0 | 8.0 | 11.0 | 8.0 | 10.9 | 8.7 | 16.0 | 23.0 |
| Zn | 2.0 | 2.0 | na | na | na | na | na | 19.0 | 24.0 | na | 13.0 | 25.0 | 13.0 | 14.0 | 26.0 | 13.0 | 19.0 | 19.0 |
| Bi | na | 0.1 | na | na | na | na | na | na | na | na | na | na | na | na | na | na | na | na |
| Cs | 0.2 | 0.4 | na | na | na | na | na | 1.9 | 5.3 | na | 3.1 | 8.9 | 5.4 | 6.2 | 6.6 | 3.3 | 2.5 | 1.3 |
| Ga | 17.3 | 16.4 | na | na | na | na | na | 19.0 | 21.0 | na | 21.0 | 19.0 | 20.0 | 20.0 | 17.3 | 16.1 | 17.0 | 24.0 |

| Sample | R350476 | R350474 | R68495 | R68592 | PD-1F | 1060-10 | 1060-12 | T1 | T4 | T9610/4 | T8 | T10 | T24 | T29 | 1027-109 | 1027-106 | T44 | T46 |
|---|---|---|---|---|---|---|---|---|---|---|---|---|---|---|---|---|---|---|
| Lithology | Metased | Metased | Granite | Granite | Granite | Granite | Granite | Granite | Granite | Granite | Granite | Granite | Granite | Granite | Granite | Granite | Granite | Granite |
| Region | Olary | Olary | Ameroo | Ameroo | Poodla | Poodla | Antro | Olary | Olary | Olary | Olary | Olary | Olary | Olary | Olary | Olary | Olary | Olary |
| Group | Wiperaminga SG | Wiperaminga SG | A-type | A-type | I-type | I-type | I-type | S-type | S-type | S-type | S-type | S-type | S-type | S-type | S-type | S-type | S-type | S-type |
| Reference | Barovich | Barovich | Ashley | Ashley | Payne | Freeman | Freeman | Stewart | Stewart | Stewart | Stewart | Stewart | Stewart | Stewart | Stewart | Stewart | Stewart | Stewart |
| Mo | 6.5 | 0.5 | na | na | na | na | na | na | na | na | na | na | na | 5.3 | na | na | na | na |
| Sb | 0.2 | 0.3 | na | na | na | na | na | na | na | na | na | na | na | na | na | na | na | na |
| Th | 10.8 | 19.7 | na | na | na | na | na | 34.2 | 58.2 | na | 16.4 | 19.6 | 28.0 | 17.0 | 37.4 | 31.6 | 38.6 | 57.5 |
| U | 1.9 | 5.2 | na | na | na | na | na | 6.3 | 8.2 | na | 21.0 | 2.1 | 6.1 | 3.9 | 12.5 | 4.7 | 7.8 | 7.4 |
| Y | 30.8 | 49.7 | na | na | na | na | na | 29.0 | 31.0 | na | 34.0 | 24.0 | 51.0 | 29.0 | 32.6 | 63.8 | 55.0 | 34.0 |
| Nb | 13.2 | 10.9 | na | na | na | na | na | 21.0 | 27.0 | na | 32.0 | 25.0 | 25.0 | 33.0 | 26.1 | 20.4 | 12.4 | 23.8 |
| Dy | 4.7 | 7.3 | na | na | na | na | na | na | na | na | na | na | na | na | na | na | na | na |
| Er | 2.6 | 4.3 | na | na | na | na | na | na | na | na | na | na | na | na | na | na | na | na |
| Eu | 1.2 | 1.2 | na | na | na | na | na | 0.8 | 1.0 | na | na | 0.6 | 0.6 | 0.5 | na | na | 0.9 | 0.8 |
| Gd | 6.0 | 7.4 | na | na | na | na | na | na | na | na | na | na | na | na | na | na | na | na |
| Ho | 0.9 | 1.5 | na | na | na | na | na | na | na | na | na | na | na | na | na | na | na | na |
| Lu | 0.3 | 0.5 | na | na | na | na | na | 0.3 | 0.3 | na | 0.5 | 0.3 | 0.8 | 0.5 | 0.5 | 1.0 | 0.8 | 0.4 |
| Nd | 35.5 | 34.0 | 142.0 | 21.2 | 58.80 | 35.7 | 38.8 | 33.0 | 55.0 | 54.2 | 12.2 | 16.9 | 25.2 | 13.2 | 31.6 | 25.4 | 41.0 | 49.3 |
| Pr | 9.6 | 9.1 | na | na | na | na | na | na | na | na | na | na | na | na | na | na | na | na |
| Sm | 6.5 | 6.7 | 28.3 | 5.1 | 10.9 | 7.4 | 9.5 | 7.4 | 11.2 | 11.1 | 3.1 | 4.0 | 6.1 | 3.5 | 7.1 | 7.0 | 8.5 | 9.5 |
| Tb | 0.9 | 1.3 | na | na | na | na | na | na | na | na | na | na | na | na | na | na | na | na |
| Yb | 2.1 | 3.6 | na | na | na | na | na | 2.0 | 2.5 | na | 3.6 | 2.3 | 5.2 | 3.4 | 3.7 | 6.8 | 5.3 | 2.8 |
| La | 42.5 | 40.6 | na | na | na | na | na | 35.7 | 53.2 | na | 14.4 | 18.8 | 27.0 | 13.8 | 29.3 | 23.1 | 41.3 | 43.9 |
| Ce | 83.4 | 79.2 | na | na | na | na | na | 79.3 | 118.0 | na | 35.6 | 43.8 | 59.7 | 41.3 | 77.6 | 71.2 | 100.0 | 130.0 |
| Age | 1700 | 1700 | 1705 | 1700 | 1700 | 1715 | 1685 | 1600 | 1600 | 1600 | 1600 | 1600 | 1600 | 1600 | 1600 | 1600 | 1600 | 1600 |
| $^{143}Nd/^{144}Nd$ | 0.511523 | 0.511617 | 0.511796 | 0.512119 | 0.511550 | 0.510274 | 0.510414 | 0.511729 | 0.511632 | 0.511611 | 0.511939 | 0.511827 | 0.511925 | 0.511916 | 0.511738 | 0.51201 4 | 0.511677 | 0.511527 |
| $^{147}Sm/^{144}Nd$ | 0.1095 | 0.1209 | 0.1202 | 0.1439 | 0.1115 | 0.1245 | 0.1478 | 0.1359 | 0.1238 | 0.1242 | 0.1535 | 0.1447 | 0.1473 | 0.1600 | na | na | na | na |
| $^{143}Nd/^{144}Nd_{(T)}$ | 0.510299 | 0.510265 | na | na | na | na | na | 0.510345 | 0.510248 | 0.510227 | 0.510555 | 0.510443 | 0.510541 | 0.510532 | na | na | na | na |
| $\varepsilon Nd_i$ | -2.8 | -3.4 | -0.1 | 1.0 | -3.3 | -5.0 | -1.8 | -5.3 | -4.7 | -5.2 | -4.8 | -5.2 | -3.8 | -6.6 | -5.3 | -5.8 | -4.4 | -5.5 |
| $T_{DM}$ | 2147 | 2247 | 2227 | 2277 | 2136 | 2490 | 2440 | 2597 | 2773 | 2812 | 2216 | 2420 | 2242 | 2258 | na | na | na | na |

| Sample | T47 | T54 | T81 | T18 | T72 | T51(I) | R351038 | R351042 | R351044 | R351045 | R351058 | R351064 | kb01-2 | kb01-1 | kb01-3 |
|---|---|---|---|---|---|---|---|---|---|---|---|---|---|---|---|
| Lithology | Granite | Granite | Granite | Monzogranite | Monzogranite | Monzogranite | Monzogranite | Monzogranite | Monzogranite | Monzogranite | Monzogranite | Monzogranite | Syeno-diorites | Syeno-diorites | Syeno-diorites |
| Region | Olary | Olary | Olary | Olary | Olary | Olary | Olary | Olary | Olary | Olary | Olary | Olary | Olary | Olary | Olary |
| Group | S-type | S-type | S-type | Alkali granite | Alkali granite | Alkali granite | Alkali granite | Alkali granite | Alkali granite | Alkali granite | Alkali granite | Alkali granite | Intermediates | Intermediates | Intermediates |
| Reference | Stewart | Stewart | Stewart | Barovich | Barovich | Barovich | Barovich | Barovich | Barovich | Barovich | Barovich | Barovich | Barovich | Barovich | Barovich |
| $Al_2O_3$ | 15.52 | 14.36 | na | 15.02 | 15.24 | 15.09 | 14.39 | 15.24 | 14.08 | 14.93 | 14.99 | 15.75 | 15.10 | 14.63 | 14.76 |
| CaO | 0.63 | 1.09 | na | 0.87 | 1.40 | 2.27 | 0.71 | 0.75 | 0.91 | 1.57 | 1.39 | 0.63 | 6.04 | 6.25 | 5.01 |
| $Fe_2O_3$ | 2.35 | 0.74 | na | 1.71 | 3.41 | 4.60 | 2.11 | 3.25 | 1.11 | 4.32 | 3.57 | 2.36 | 11.22 | 11.52 | 10.35 |
| $K_2O$ | 6.03 | 1.13 | na | 5.27 | 4.50 | 3.91 | 5.08 | 5.54 | 4.69 | 4.39 | 4.35 | 5.33 | 1.49 | 1.11 | 1.43 |
| MgO | 0.61 | 0.24 | na | 0.59 | 0.78 | 1.01 | 0.47 | 0.74 | 0.39 | 1.09 | 0.71 | 0.66 | 3.18 | 3.76 | 2.58 |
| MnO | 0.02 | 0.00 | na | 0.01 | 0.01 | 0.03 | 0.01 | 0.01 | 0.01 | 0.03 | 0.01 | 0.02 | 0.09 | 0.09 | 0.09 |
| $Na_2O$ | 3.36 | 6.52 | na | 3.97 | 4.39 | 4.21 | 3.27 | 4.12 | 4.35 | 4.04 | 4.32 | 3.69 | 4.88 | 4.87 | 5.01 |
| $P_2O_5$ | 0.19 | 0.32 | na | 0.23 | 0.19 | 0.22 | 0.18 | 0.24 | 0.25 | 0.28 | 0.21 | 0.19 | 0.55 | 0.64 | 0.56 |
| $SiO_2$ | 70.18 | 74.91 | na | 71.15 | 69.17 | 66.94 | 72.45 | 68.40 | 73.39 | 68.04 | 69.43 | 69.67 | 55.20 | 55.09 | 57.92 |
| $TiO_2$ | 0.33 | 0.26 | na | 0.34 | 0.47 | 0.64 | 0.31 | 0.50 | 0.21 | 0.57 | 0.52 | 0.39 | 1.44 | 1.40 | 1.33 |
| Sc | 5.6 | 2.8 | na | 4.5 | 6.8 | 9.9 | 4.0 | 8.0 | 4.0 | 8.0 | 7.0 | 4.0 | 20.1 | 21.0 | 40.8 |
| Ba | 375.0 | 124.0 | na | 564.0 | 539.0 | 616.0 | 345.0 | 535.0 | 367.0 | 498.0 | 567.0 | 488.0 | 445.0 | 275.0 | 228.0 |
| Be | na | na | na | na | na | na | 1.5 | 2.2 | 2.4 | 3.9 | 1.7 | 6.1 | na | na | na |
| Hf | 7.5 | na | na | na | na | na | na | na | na | na | na | na | na | na | na |
| Rb | 381.0 | 44.0 | 352.0 | 264.0 | 240.0 | 203.0 | 280.0 | 264.0 | 188.0 | 235.0 | 261.0 | 248.0 | 47.2 | 24.6 | 80.4 |
| Sn | na | na | na | na | na | na | 8.0 | 7.5 | 4.0 | 5.0 | 6.0 | 4.0 | na | na | na |
| Sr | 54.0 | 118.0 | 68.0 | 76.0 | 83.0 | 125.0 | 48.0 | 109.0 | 68.0 | 85.0 | 71.0 | 59.0 | 224.8 | 256.1 | 184.0 |
| Ta | na | 8.3 | na | 4.4 | 7.0 | 2.4 | 1.0 | 1.0 | 1.0 | 1.0 | 1.5 | 2.0 | na | na | na |
| W | 418.0 | na | na | na | na | na | na | na | na | na | na | na | na | na | na |

| Sample | T47 | T54 | T81 | T18 | T72 | T51(I) | R351038 | R351042 | R351044 | R351045 | R351058 | R351064 | kb01-2 | kb01-1 | kb01-3 |
|---|---|---|---|---|---|---|---|---|---|---|---|---|---|---|---|
| **Lithology** | Granite | Granite | Granite | Monzogranite | Monzogranite | Monzogranite | Monzogranite | Monzogranite | Monzogranite | Monzogranite | Monzogranite | Monzogranite | Syeno-diorites | Syeno-diorites | Syeno-diorites |
| **Region** | Olary | Olary | Olary | Olary | Olary | Olary | Olary | Olary | Olary | Olary | Olary | Olary | Olary | Olary | Olary |
| **Group** | S-type | S-type | S-type | Alkali granite | Alkali granite | Alkali granite | Alkali granite | Alkali granite | Alkali granite | Alkali granite | Alkali granite | Alkali granite | Intermediates | Intermediates | Intermediates |
| **Reference** | Stewart | Stewart | Stewart | Barovich | Barovich | Barovich | Barovich | Barovich | Barovich | Barovich | Barovich | Barovich | Barovich | Barovich | Barovich |
| **Zr** | 234.0 | 151.0 | na | 225.0 | 303.0 | 360.0 | 197.0 | 313.0 | 151.0 | 314.0 | 355.0 | 229.0 | 516.9 | 371.2 | 525.7 |
| **LOI** | na | 0.0 | na | 0.6 | 0.0 | 0.0 | 1.1 | 1.0 | 0.7 | 1.0 | 0.8 | 1.3 | 0.4 | 0.3 | 0.2 |
| **Ag** | na | na | na | -5.0 | -5.0 | -5.0 | -0.5 | -0.5 | -0.5 | -0.5 | -0.5 | -0.5 | na | na | na |
| **As** | na | -1.0 | na | -1.0 | -1.0 | -1.0 | 0.6 | 1.1 | 0.5 | 0.7 | 0.8 | 1.5 | na | na | na |
| **Co** | 52.3 | na | na | na | na | na | na | na | na | na | na | na | na | na | na |
| **Cr** | 1.0 | 14.0 | na | 1.0 | 2.0 | 2.0 | 2.2 | 3.6 | 2.6 | 17.8 | 4.4 | 7.2 | 28.0 | 39.0 | 18.0 |
| **Cu** | 8.0 | 4.0 | na | 16.0 | 12.0 | 13.0 | 29.0 | 52.0 | 29.0 | 31.0 | 19.0 | 35.0 | 29.0 | 48.0 | 26.0 |
| **Ni** | 2.0 | 8.0 | na | 6.0 | 4.0 | 5.0 | -1.0 | 15.0 | -1.0 | 10.0 | 1.0 | 1.0 | 40.0 | 48.0 | 22.0 |
| **Pb** | 29.0 | 11.8 | na | 22.0 | 14.8 | 11.5 | 25.0 | 24.5 | 11.5 | 14.5 | 37.5 | 26.5 | 5.1 | 4.2 | 6.0 |
| **S** | na | na | na | na | na | na | 20.0 | 50.0 | 20.0 | 30.0 | 10.0 | 30.0 | na | na | na |
| **V** | 22.0 | 23.0 | na | 27.0 | 37.0 | 52.0 | 18.0 | 34.0 | 13.0 | 55.0 | 39.0 | 28.0 | 216.0 | 230.0 | 162.0 |
| **Zn** | 21.0 | 4.0 | na | 19.0 | 22.0 | 25.0 | 19.0 | 14.0 | 12.0 | 21.0 | 24.0 | 37.0 | 43.0 | 43.0 | 43.0 |
| **Bi** | na | na | na | na | na | na | -0.1 | -0.1 | -0.1 | -0.1 | -0.1 | 0.1 | na | na | na |
| **Cs** | 1.3 | 1.3 | na | na | na | 1.8 | 0.7 | 0.8 | 0.4 | 0.7 | 0.6 | 4.4 | na | na | na |
| **Ga** | 23.0 | 27.0 | na | 20.0 | 23.0 | 24.0 | 21.4 | 19.1 | 20.3 | 22.6 | 23.3 | 22.1 | 24.8 | 25.2 | 26.6 |
| **Mo** | na | na | na | -5.0 | -5.0 | -5.0 | 0.2 | 0.7 | 0.5 | 0.5 | 0.3 | 0.3 | na | na | na |
| **Sb** | na | na | na | na | na | na | -0.1 | -0.1 | -0.1 | -0.1 | -0.1 | -0.1 | na | na | na |
| **Th** | 84.6 | 59.9 | na | 85.0 | 92.2 | 43.9 | 78.3 | 121.8 | 36.3 | 73.6 | 126.6 | 58.7 | 43.7 | 40.2 | 25.2 |
| **U** | 16.2 | 8.7 | na | 2.8 | 3.5 | 8.8 | 7.7 | 5.6 | 3.4 | 2.6 | 6.6 | 6.1 | 3.7 | 5.9 | 6.2 |
| **Y** | 40.0 | 36.0 | na | 45.0 | 53.0 | 68.0 | 33.3 | 73.0 | 32.4 | 45.0 | 45.4 | 19.9 | 73.2 | 70.9 | 97.8 |
| **Nb** | 26.3 | 55.3 | na | 20.0 | 22.7 | 43.4 | 14.9 | 22.3 | 15.2 | 22.8 | 25.9 | 17.7 | 47.4 | 44.7 | 68.7 |
| **Dy** | na | na | na | na | na | na | 6.4 | 14.6 | 6.1 | 8.7 | 9.1 | 5.1 | na | na | na |
| **Er** | na | na | na | na | na | na | 3.1 | 6.3 | 2.9 | 4.1 | 3.9 | 2.2 | na | na | na |
| **Eu** | 1.0 | 0.7 | na | 0.9 | 3.0 | 1.2 | 0.9 | 1.7 | 1.0 | 1.7 | 1.7 | 1.3 | na | na | na |
| **Gd** | na | na | na | na | na | na | 10.0 | 23.1 | 8.6 | 14.0 | 16.3 | 9.4 | na | na | na |
| **Ho** | na | na | na | na | na | na | 1.1 | 2.5 | 1.1 | 1.5 | 1.6 | 0.9 | na | na | na |
| **Lu** | 0.4 | 0.4 | na | 0.5 | 2.3 | 0.4 | 0.4 | 0.6 | 0.3 | 0.4 | 0.4 | 0.3 | na | na | na |
| **Nd** | 97.7 | 17.0 | 50.2 | 126.0 | 92.0 | 76.0 | 76.2 | 150.6 | 59.3 | 99.3 | 154.7 | 81.6 | 77.0 | 90.0 | 63.0 |
| **Pr** | na | na | na | na | na | na | 21.1 | 41.5 | 16.5 | 27.1 | 40.9 | 21.4 | na | na | na |
| **Sm** | 17.1 | 4.9 | 9.6 | 23.1 | 16.8 | 16.4 | 14.4 | 29.2 | 10.6 | 17.8 | 25.7 | 16.0 | na | na | na |
| **Tb** | na | na | na | na | na | na | 1.4 | 3.3 | 1.3 | 1.9 | 2.1 | 1.2 | na | na | na |
| **Yb** | 3.4 | 3.1 | na | 3.4 | 4.1 | 7.0 | 2.5 | 4.2 | 2.1 | 3.1 | 2.8 | 2.0 | na | na | na |
| **La** | 86.4 | 12.0 | na | 113.0 | 92.0 | 92.0 | 74.4 | 148.8 | 67.3 | 107.0 | 138.2 | 69.2 | 85.0 | 54.0 | 93.0 |
| **Ce** | 207.0 | 32.0 | na | 268.0 | 246.0 | 215.0 | 175.4 | 339.3 | 143.4 | 214.6 | 323.4 | 207.0 | 173.0 | 123.0 | 190.0 |
| **Age** | 1600 | 1600 | 1600 | 1600 | 1600 | 1600 | 1600 | 1600 | 1600 | 1600 | 1600 | 1600 | 1600 | 1600 | 1600 |
| **$^{143}Nd/^{144}Nd$** | 0.511487 | 0.511967 | 0.511580 | 0.511409 | 0.511501 | 0.511525 | 0.511465 | 0.511574 | 0.511487 | 0.511470 | 0.511368 | 0.511460 | 0.511586 | 0.511715 | 0.511643 |
| **$^{147}Sm/^{144}Nd$** | na | na | na | 0.1047 | 0.1087 | 0.1104 | 0.1113 | 0.1167 | 0.1085 | 0.1087 | 0.0997 | 0.1119 | 0.1115 | 0.1263 | 0.1204 |
| **$^{143}Nd/^{144}Nd_{(T)}$** | na | na | na | na | na | na | na | na | na | na | na | na | na | na | na |
| **$\varepsilon Nd_i$** | -4.0 | -4.7 | -4.1 | -5.3 | -4.3 | -4.2 | -5.6 | -4.5 | -4.6 | -4.9 | -5.1 | -5.8 | -3.2 | -3.7 | -3.9 |
| **$T_{DM}$** | na | na | na | 2207 | 2163 | 2161 | 2262 | 2219 | 2177 | 2203 | 2167 | 2279 | 2100 | 2218 | 2198 |

| **Sample** | R351055 | R351078 | R351079 | T74 | R351041 | R351043 | R351048 | R351052 | R351077 |
|---|---|---|---|---|---|---|---|---|---|
| **Lithology** | Syeno-diorites | Syeno-diorites | Syeno-diorites | Trondhjemites | Trondhjemites | Trondhjemites | Trondhjemites | Trondhjemites | Trondhjemites |
| **Region** | Olary | Olary | Olary | Olary | Olary | Olary | Olary | Olary | Olary |
| **Group** | Intermediates | Intermediates | Intermediates | Trondhjemites | Trondhjemites | Trondhjemites | Trondhjemites | Trondhjemites | Trondhjemites |
| **Reference** | Barovich | Barovich | Barovich | Barovich | Barovich | Barovich | Barovich | Barovich | Barovich |
| **$Al_2O_3$** | 15.59 | 14.91 | 14.95 | 15.29 | 14.87 | 14.29 | 14.87 | 14.85 | 14.50 |
| **CaO** | 5.15 | 4.84 | 2.48 | 0.58 | 1.63 | 1.14 | 0.83 | 0.72 | 1.61 |
| **$Fe_2O_3$** | 8.53 | 10.14 | 6.73 | 1.11 | 3.50 | 0.85 | 0.20 | 1.12 | 1.38 |
| **$K_2O$** | 2.53 | 1.30 | 2.44 | 0.62 | 2.27 | 1.15 | 1.84 | 1.16 | 1.79 |
| **MgO** | 2.30 | 2.36 | 1.42 | 0.72 | 1.12 | 0.18 | 0.08 | 0.16 | 1.23 |
| **MnO** | 0.05 | 0.06 | 0.02 | 0.01 | 0.01 | 0.01 | 0.00 | 0.00 | 0.01 |
| **$Na_2O$** | 4.69 | 5.14 | 4.84 | 8.24 | 5.58 | 6.94 | 6.69 | 7.14 | 6.37 |
| **$P_2O_5$** | 0.50 | 0.58 | 0.40 | 0.22 | 0.33 | 0.51 | 0.10 | 0.05 | 0.65 |
| **$SiO_2$** | 58.71 | 58.77 | 65.04 | 72.12 | 69.54 | 74.09 | 74.87 | 74.05 | 71.72 |
| **$TiO_2$** | 1.23 | 1.23 | 0.86 | 0.43 | 0.58 | 0.16 | 0.08 | 0.33 | 0.25 |
| **Sc** | 16.0 | 26.0 | 5.0 | 9.4 | 9.0 | 3.0 | -1.0 | 3.0 | 3.0 |
| **Ba** | 617.0 | 179.0 | 584.0 | 77.0 | 198.0 | 120.0 | 114.0 | 153.0 | 66.0 |
| **Be** | 4.6 | 8.9 | 4.6 | na | 3.6 | 6.8 | 4.3 | 5.6 | 6.3 |
| **Hf** | na | na | na | na | na | na | na | na | na |
| **Rb** | 53.0 | 74.0 | 126.0 | 29.0 | 139.0 | 41.0 | 61.0 | 33.0 | 95.0 |
| **Sn** | 4.0 | 7.0 | 2.5 | na | 7.0 | 2.5 | 4.5 | 4.0 | 2.0 |
| **Sr** | 1357.0 | 189.0 | 134.0 | 40.0 | 121.0 | 77.0 | 44.0 | 96.0 | 42.0 |
| **Ta** | 2.0 | 8.5 | 2.0 | 3.0 | 2.0 | 10.5 | 5.5 | 4.5 | 4.0 |
| **W** | na | na | na | na | na | na | na | na | na |
| **Zr** | 520.0 | 633.0 | 605.0 | 311.0 | 340.0 | 99.0 | 27.0 | 226.0 | 179.0 |
| **LOI** | 1.1 | 1.2 | 0.9 | 0.0 | 0.9 | 0.7 | 0.4 | 0.5 | 0.8 |
| **Ag** | 0.5 | -0.5 | -0.5 | na | 0.5 | 1.5 | -0.5 | -0.5 | -0.5 |
| **As** | 1.3 | 1.5 | 0.7 | -1.0 | 0.5 | 0.3 | -0.2 | -0.2 | 0.5 |
| **Co** | na | na | na | na | na | na | na | na | na |
| **Cr** | 29.4 | 19.9 | 9.8 | 1.0 | 17.0 | 5.2 | 1.9 | 10.0 | 6.4 |
| **Cu** | 70.0 | 27.0 | 26.0 | 7.0 | 49.0 | 34.0 | 39.0 | 47.0 | 13.0 |
| **Ni** | 44.0 | 23.0 | 7.0 | 5.0 | 42.0 | 64.0 | -1.0 | -1.0 | 1.0 |
| **Pb** | 10.0 | 5.5 | 8.5 | 11.0 | 13.5 | 6.0 | 10.5 | 18.0 | 12.0 |
| **S** | 140.0 | 60.0 | 20.0 | na | 30.0 | 10.0 | -10.0 | -10.0 | 60.0 |
| **V** | 143.0 | 166.0 | 83.0 | 26.0 | 102.0 | 24.0 | 1.0 | 24.0 | 24.0 |
| **Zn** | 40.0 | 46.0 | 24.0 | 9.0 | 14.0 | 4.0 | 7.0 | 7.0 | 11.0 |
| **Bi** | -0.1 | -0.1 | -0.1 | na | -0.1 | -0.1 | -0.1 | -0.1 | -0.1 |
| **Cs** | 0.4 | 0.6 | 0.6 | na | 0.7 | 0.1 | 0.1 | 0.2 | 0.5 |
| **Ga** | 23.8 | 27.3 | 23.4 | 22.0 | 24.5 | 24.6 | 20.9 | 22.8 | 27.6 |
| **Mo** | 0.5 | 0.5 | 0.2 | na | 0.5 | 0.7 | 0.2 | 0.8 | 0.8 |
| **Sb** | -0.1 | -0.1 | -0.1 | na | -0.1 | -0.1 | -0.1 | -0.1 | -0.1 |
| **Th** | 40.7 | 24.7 | 42.6 | 115.6 | 30.1 | 28.0 | 12.6 | 109.0 | 33.5 |
| **U** | 4.3 | 6.3 | 4.4 | 9.9 | 5.0 | 30.8 | 1.0 | 3.7 | 26.0 |
| **Y** | 70.5 | 145.7 | 25.4 | 44.0 | 68.3 | 39.5 | 10.9 | 14.0 | 38.3 |
| **Nb** | 29.4 | 73.2 | 21.2 | 33.4 | 34.8 | 124.8 | 32.3 | 30.7 | 27.1 |
| **Dy** | 13.2 | 23.2 | 4.3 | na | 10.6 | 6.6 | 2.0 | 2.2 | 6.6 |
| **Er** | 6.9 | 14.0 | 2.5 | na | 6.6 | 3.8 | 1.0 | 1.6 | 3.8 |
| **Eu** | 3.4 | 3.6 | 1.9 | 1.0 | 1.2 | 0.8 | 0.5 | 0.5 | 0.7 |
| **Gd** | 17.8 | 25.4 | 6.8 | na | 10.6 | 7.2 | 3.3 | 2.2 | 8.4 |
| **Ho** | 2.5 | 4.8 | 0.8 | na | 2.2 | 1.3 | 0.3 | 0.5 | 1.4 |
| **Lu** | 0.7 | 1.7 | 0.4 | 0.6 | 0.7 | 0.5 | 0.1 | 0.3 | 0.4 |
| **Nd** | 108.6 | 138.1 | 62.5 | 61.0 | 41.4 | 30.2 | 23.0 | 12.3 | 32.5 |
| **Pr** | 29.8 | 35.3 | 18.6 | na | 10.6 | 7.5 | 6.3 | 3.4 | 7.0 |
| **Sm** | 19.6 | 27.3 | 8.7 | 11.4 | 10.2 | 6.8 | 4.3 | 2.3 | 8.3 |
| **Tb** | 2.7 | 4.3 | 0.9 | na | 1.9 | 1.2 | 0.4 | 0.4 | 1.3 |

| **Sample** | R351055 | R351078 | R351079 | T74 | R351041 | R351043 | R351048 | R351052 | R351077 |
|---|---|---|---|---|---|---|---|---|---|
| **Lithology** | Syeno-diorites | Syeno-diorites | Syeno-diorites | Trondhjemites | Trondhjemites | Trondhjemites | Trondhjemites | Trondhjemites | Trondhjemites |
| **Region** | Olary | Olary | Olary | Olary | Olary | Olary | Olary | Olary | Olary |
| **Group** | Intermediates | Intermediates | Intermediates | Trondhjemites | Trondhjemites | Trondhjemites | Trondhjemites | Trondhjemites | Trondhjemites |
| **Reference** | Barovich | Barovich | Barovich | Barovich | Barovich | Barovich | Barovich | Barovich | Barovich |
| **Yb** | 5.4 | 12.7 | 2.5 | 3.8 | 5.3 | 3.5 | 0.9 | 1.8 | 3.2 |
| **La** | 114.6 | 96.6 | 98.2 | 61.0 | 34.8 | 24.1 | 25.9 | 16.1 | 20.4 |
| **Ce** | 254.8 | 267.5 | 184.5 | 119.0 | 77.3 | 58.8 | 53.4 | 31.5 | 52.3 |
| **Age** | 1600 | 1600 | 1600 | 1600 | 1600 | 1600 | 1600 | 1600 | 1600 |
| $^{143}Nd/^{144}Nd$ | 0.511563 | 0.511650 | 0.511247 | 0.511467 | 0.511944 | 0.511749 | 0.511479 | 0.511510 | 0.511949 |
| $^{147}Sm/^{144}Nd$ | 0.1076 | 0.1191 | 0.0827 | 0.1099 | 0.1453 | 0.1360 | 0.1131 | 0.1130 | 0.1554 |
| $^{143}Nd/^{144}Nd_{(t)}$ | na | na | na | na | na | na | na | na | na |
| $\varepsilon Nd_i$ | -2.9 | -3.5 | -4.0 | -5.2 | -3.1 | -5.0 | -5.7 | -5.0 | -5.1 |
| $T_{DM}$ | 2058 | 2161 | 2036 | 2230 | 2313 | 2408 | 2279 | 2234 | 2651 |

**Table A4.1.** Monazite chemical EPMA age data of samples used in study on timing of Proterozoic metamorphism (*Chapter 3* ).

| Sample | Occluding phase | Label | Peak Counts Pk(Pb) | Pk(Th) | Pk(U ) | Background counts Bg(Pb) | Bg(Th) | Bg(U ) | W%(Pb) | W%(Pb) 1σ | W%(Th) | W%(Th) 1σ | W%(U) | W%(U) 1σ | Chemical age (Ma) | 1σ | Early/peak meta. age (Ma) & error (2σ) | n = | Post peak meta. age (Ma) & error (2σ) | n = |
|---|---|---|---|---|---|---|---|---|---|---|---|---|---|---|---|---|---|---|---|---|
| SC2 | bt | 1 | 36.5415 | 356.5811 | 148.1783 | 18.4569 | 30.8386 | 70.9166 | 0.6542 | 0.0122 | 5.5306 | 0.0485 | 0.8901 | 0.0113 | 1620 | 43 | | | | |
| SC2 | bt | 2 | 35.3600 | 327.7720 | 145.3509 | 19.1912 | 31.0350 | 69.1023 | 0.5861 | 0.0115 | 5.0527 | 0.0464 | 0.8785 | 0.0112 | 1550 | 43 | | | | |
| SC2 | bt | 3 | 34.1660 | 316.8008 | 136.5559 | 19.0417 | 28.6875 | 70.4491 | 0.5491 | 0.0112 | 4.9171 | 0.0458 | 0.7627 | 0.0105 | 1556 | 45 | | | | |
| SC2 | bt | 4 | 32.9032 | 268.0404 | 129.6504 | 17.7657 | 26.2429 | 70.2933 | 0.5538 | 0.0113 | 4.1546 | 0.0422 | 0.6868 | 0.0100 | 1787 | 52 | | | | |
| SC2 | bt | 5 | 34.9599 | 312.3424 | 136.0555 | 18.3942 | 28.0900 | 74.3781 | 0.6054 | 0.0118 | 4.8800 | 0.0458 | 0.7161 | 0.0102 | 1742 | 48 | | | | |
| SC2 | bt | 6 | 34.2535 | 329.6006 | 139.7210 | 18.4533 | 29.7527 | 68.4123 | 0.5787 | 0.0115 | 5.1587 | 0.0471 | 0.8305 | 0.0110 | 1543 | 43 | | | | |
| SC2 | bt | 7 | 33.7722 | 332.6566 | 145.3759 | 17.8798 | 29.9212 | 76.9939 | 0.5813 | 0.0115 | 5.2018 | 0.0473 | 0.7959 | 0.0108 | 1564 | 44 | | | | |
| SC2 | bt | 8 | 34.6849 | 314.8471 | 135.9304 | 18.9996 | 30.8510 | 68.7239 | 0.5753 | 0.0115 | 4.8935 | 0.0459 | 0.7829 | 0.0107 | 1614 | 46 | | | | |
| SC2 | bt | 9 | 35.0724 | 333.7087 | 144.4000 | 18.6338 | 29.0467 | 69.5698 | 0.6036 | 0.0118 | 5.2574 | 0.0476 | 0.8751 | 0.0113 | 1559 | 43 | | | | |
| SC2 | bt | 11 | 33.5846 | 312.1170 | 141.3224 | 18.6475 | 31.2339 | 69.8703 | 0.5498 | 0.0112 | 4.8576 | 0.0458 | 0.8351 | 0.0110 | 1522 | 44 | | | | |
| SC2 | bt | 12 | 30.8904 | 336.9904 | 108.6979 | 18.0592 | 30.6100 | 66.1863 | 0.4703 | 0.0104 | 5.2887 | 0.0478 | 0.4971 | 0.0085 | 1450 | 45 | | | | |
| SC2 | bt | 13 | 34.6911 | 316.8258 | 145.3258 | 18.4371 | 29.0976 | 66.0416 | 0.6029 | 0.0118 | 5.0092 | 0.0467 | 0.9336 | 0.0117 | 1563 | 43 | | | | |
| SC2 | bt | 14 | 38.1669 | 348.8647 | 179.1587 | 17.9475 | 29.2970 | 67.6554 | 0.7529 | 0.0132 | 5.5743 | 0.0493 | 1.3201 | 0.0140 | 1581 | 39 | | | | |
| SC2 | bt | 15 | 37.6418 | 347.5620 | 176.6436 | 18.1769 | 31.0289 | 67.6332 | 0.7247 | 0.0130 | 5.5207 | 0.0491 | 1.2898 | 0.0138 | 1549 | 39 | | | | |
| SC2 | bt | 16 | 32.4157 | 369.3839 | 94.5143 | 18.3440 | 29.8065 | 68.0339 | 0.5213 | 0.0110 | 5.9130 | 0.0507 | 0.3133 | 0.0068 | 1604 | 48 | | | | |
| SC2 | bt | 17 | 36.1664 | 476.6055 | 85.7471 | 18.0304 | 29.5662 | 64.9620 | 0.6721 | 0.0125 | 7.7966 | 0.0583 | 0.2495 | 0.0061 | 1670 | 44 | | | | |
| SC2 | bt | 18 | 35.1099 | 469.0842 | 91.8003 | 19.0094 | 31.1743 | 69.1914 | 0.5948 | 0.0117 | 7.6017 | 0.0574 | 0.2693 | 0.0063 | 1509 | 42 | | | | |
| SC2 | bt | 19 | 33.2596 | 370.8622 | 90.0743 | 18.6371 | 30.5647 | 68.3121 | 0.5404 | 0.0112 | 5.9095 | 0.0507 | 0.2568 | 0.0062 | 1706 | 51 | | | | |
| SC2 | bt | 20 | 36.0226 | 329.4252 | 171.3756 | 17.6090 | 30.9688 | 69.4474 | 0.6830 | 0.0126 | 5.1868 | 0.0475 | 1.1996 | 0.0133 | 1560 | 40 | | | | |
| SC2 | bt | 21 | 32.0906 | 387.3747 | 89.9243 | 18.0924 | 31.2445 | 69.1691 | 0.5196 | 0.0110 | 6.2178 | 0.0521 | 0.2467 | 0.0061 | 1585 | 48 | | | | |
| SC2 | bt | 22 | 36.9478 | 320.5329 | 170.1493 | 18.5818 | 28.5757 | 68.4902 | 0.6832 | 0.0126 | 5.0902 | 0.0471 | 1.1995 | 0.0133 | 1575 | 41 | | | | |
| SC2 | bt | 23 | 38.4419 | 331.5294 | 178.7833 | 18.3729 | 30.9116 | 67.4106 | 0.7489 | 0.0132 | 5.2520 | 0.0479 | 1.3181 | 0.0140 | 1619 | 40 | | | | |
| SC2 | bt | 24 | 32.7595 | 368.6322 | 105.4709 | 19.1390 | 29.7169 | 67.8780 | 0.5040 | 0.0108 | 5.8986 | 0.0507 | 0.4446 | 0.0081 | 1465 | 44 | | | | |
| SC2 | bt | 25 | 35.6663 | 322.0609 | 166.4205 | 18.7248 | 30.6338 | 67.7667 | 0.6293 | 0.0121 | 5.0775 | 0.0470 | 1.1632 | 0.0131 | 1483 | 40 | | | | |
| SC2 | bt | 26 | 35.7601 | 336.4142 | 151.5439 | 18.6659 | 28.7312 | 67.4662 | 0.6349 | 0.0121 | 5.3649 | 0.0484 | 0.9940 | 0.0121 | 1543 | 41 | | | | |
| SC2 | bt | 27 | 31.5155 | 360.2890 | 89.2239 | 18.7278 | 31.5771 | 68.4790 | 0.4734 | 0.0105 | 5.7298 | 0.0500 | 0.2455 | 0.0060 | 1554 | 49 | | | | |
| SC2 | bt | 28 | 33.3033 | 414.8156 | 93.4762 | 18.4534 | 30.0179 | 67.8112 | 0.5498 | 0.0113 | 6.7003 | 0.0540 | 0.3052 | 0.0067 | 1531 | 44 | | | | |
| SC2 | bt | 29 | 31.5592 | 334.5855 | 92.9384 | 18.8249 | 28.5594 | 68.1674 | 0.4715 | 0.0104 | 5.3344 | 0.0482 | 0.2925 | 0.0066 | 1599 | 51 | | | | |
| SC2 | bt | 30 | 31.5467 | 280.7863 | 100.0550 | 19.3305 | 29.5191 | 68.7017 | 0.4534 | 0.0103 | 4.3938 | 0.0438 | 0.3695 | 0.0074 | 1707 | 55 | | | | |
| SC2 | bt | 31 | 35.0537 | 435.0671 | 94.6644 | 17.8824 | 29.1627 | 67.4662 | 0.6349 | 0.0121 | 7.0476 | 0.0553 | 0.3232 | 0.0069 | 1670 | 46 | | | | |
| SC2 | bt | 32 | 36.2852 | 464.8474 | 96.8156 | 18.2286 | 27.9897 | 68.3789 | 0.6678 | 0.0124 | 7.5871 | 0.0574 | 0.3390 | 0.0071 | 1640 | 44 | | | | |
| SC2 | bt | 33 | 33.5659 | 385.4452 | 94.7144 | 18.7637 | 31.6578 | 69.0801 | 0.5445 | 0.0112 | 6.1174 | 0.0514 | 0.3017 | 0.0067 | 1635 | 48 | | | | |
| SC2 | bt | 34 | 29.4776 | 240.8239 | 98.0288 | 18.1454 | 28.2712 | 66.3977 | 0.4203 | 0.0099 | 3.7151 | 0.0403 | 0.3711 | 0.0074 | 1784 | 60 | | | | |
| SC2 | bt | 35 | 33.6159 | 394.2908 | 90.9373 | 17.8747 | 30.4540 | 65.7856 | 0.5824 | 0.0116 | 6.3240 | 0.0524 | 0.2979 | 0.0066 | 1699 | 48 | | | | |
| SC2 | bt | 36 | 35.2225 | 320.0570 | 141.4100 | 18.5961 | 30.0646 | 68.6794 | 0.6172 | 0.0120 | 5.0551 | 0.0469 | 0.8581 | 0.0112 | 1637 | 45 | | | | |
| SC2 | bt | 37 | 33.0470 | 320.7834 | 130.8138 | 19.2304 | 29.5550 | 65.8858 | 0.5145 | 0.0109 | 5.0995 | 0.0472 | 0.7693 | 0.0107 | 1431 | 43 | | | | |
| SC2 | bt | 38 | 33.3846 | 403.9138 | 88.7861 | 18.0370 | 29.8245 | 65.3960 | 0.5697 | 0.0115 | 6.5295 | 0.0534 | 0.2787 | 0.0064 | 1636 | 47 | | | | |
| SC2 | bt | 39 | 33.5784 | 411.8582 | 90.6747 | 18.6472 | 31.8760 | 68.9354 | 0.5535 | 0.0113 | 6.6239 | 0.0537 | 0.2587 | 0.0062 | 1588 | 46 | | | | |
| SC2 | bt | 40 | 33.4534 | 408.0740 | 88.7861 | 18.4001 | 30.5819 | 68.3232 | 0.5540 | 0.0113 | 6.5333 | 0.0532 | 0.2417 | 0.0060 | 1620 | 47 | | | | |
| SC2 | bt | 41 | 33.3846 | 341.4243 | 124.8467 | 18.1739 | 27.6768 | 69.0467 | 0.5649 | 0.0115 | 5.4702 | 0.0488 | 0.6597 | 0.0099 | 1563 | 45 | | | | |
| SC2 | bt | 42 | 29.2338 | 281.2120 | 92.8258 | 18.3036 | 31.6673 | 67.6888 | 0.4026 | 0.0096 | 4.3362 | 0.0434 | 0.2941 | 0.0066 | 1615 | 55 | | | | |
| SC2 | bt | 43 | 32.9970 | 360.2639 | 95.7900 | 18.4838 | 31.4196 | 68.1563 | 0.5364 | 0.0111 | 5.7119 | 0.0498 | 0.3259 | 0.0069 | 1682 | 50 | | | | |
| SC2 | bt | 44 | 32.2969 | 370.7870 | 97.3159 | 18.7288 | 30.7694 | 68.3789 | 0.4912 | 0.0105 | 5.7926 | 0.0497 | 0.3348 | 0.0070 | 1525 | 46 | | | | |
| SC2 | bt | 45 | 27.2272 | 212.8608 | 99.2420 | 18.0768 | 31.7882 | 70.0262 | 0.3316 | 0.0087 | 3.1052 | 0.0365 | 0.3348 | 0.0069 | 1661 | 62 | | | | |
| SC2 | bt | 46 | 33.8909 | 301.3722 | 130.7012 | 18.6747 | 31.7792 | 69.0022 | 0.5581 | 0.0113 | 4.6384 | 0.0447 | 0.7162 | 0.0102 | 1668 | 48 | | | | |
| SC2 | bt | 47 | 34.2348 | 387.3496 | 100.4553 | 18.9429 | 30.2824 | 69.3806 | 0.5584 | 0.0113 | 6.1236 | 0.0512 | 0.3626 | 0.0073 | 1626 | 47 | | | | |
| SC2 | bt | 49 | 35.2037 | 323.4135 | 147.8280 | 19.7446 | 29.6241 | 71.3061 | 0.5582 | 0.0112 | 4.9810 | 0.0459 | 0.8772 | 0.0112 | 1495 | 42 | | | | |
| SC2 | bt | 50 | 40.2736 | 318.0532 | 211.0836 | 19.1614 | 31.5650 | 71.2950 | 0.7523 | 0.0129 | 4.7739 | 0.0446 | 1.5731 | 0.0149 | 1565 | 37 | | | | |
| SC2 | bt | 51 | 38.3169 | 288.1489 | 200.9586 | 18.4845 | 30.8612 | 68.3566 | 0.7210 | 0.0128 | 4.3723 | 0.0431 | 1.5180 | 0.0147 | 1588 | 39 | | | | |
| SC2 | bt | 52 | 32.4719 | 321.1341 | 121.3442 | 18.3335 | 30.1742 | 67.3327 | 0.5135 | 0.0108 | 4.9637 | 0.0460 | 0.6227 | 0.0095 | 1548 | 46 | | | | |

| Sample | Occluding phase | Label | Peak Counts Pk(Pb) | Pk(Th) | Pk(U ) | Background counts Bg(Pb) | Bg(Th) | Bg(U ) | W%(Pb) | W%(Pb) 1σ | W%(Th) | W%(Th) 1σ | W%(U) | W%(U) 1σ | Chemica age (Ma) | 1σ | Early/peak meta. age (Ma) & error (2σ) | n = | Post peak meta. age (Ma) & error (2σ) | n = |
|---|---|---|---|---|---|---|---|---|---|---|---|---|---|---|---|---|---|---|---|---|
| SC2 | bt | 53 | 33.6596 | 311.0901 | 137.2440 | 19.0539 | 30.8072 | 67.9448 | 0.5342 | 0.0111 | 4.8101 | 0.0454 | 0.8029 | 0.0108 | 1511 | 44 | | | | |
| SC2 | bt | 54 | 35.1099 | 351.8210 | 145.5010 | 18.1684 | 30.8465 | 67.4217 | 0.6219 | 0.0119 | 5.5229 | 0.0487 | 0.9111 | 0.0115 | 1536 | 42 | | | | |
| SC2 | bt | 56 | 33.5471 | 301.9733 | 147.4402 | 17.9333 | 29.3266 | 67.2436 | 0.5777 | 0.0116 | 4.7287 | 0.0453 | 0.9388 | 0.0117 | 1548 | 43 | | | | |
| SC2 | bt | 57 | 33.7159 | 302.5995 | 136.4183 | 18.6368 | 29.3686 | 67.7779 | 0.5575 | 0.0114 | 4.7372 | 0.0453 | 0.8032 | 0.0108 | 1584 | 46 | | | | |
| SC2 | bt | 58 | 29.4338 | 288.3492 | 89.9618 | 18.3235 | 30.5531 | 66.1529 | 0.4078 | 0.0097 | 4.4613 | 0.0439 | 0.2776 | 0.0064 | 1617 | 55 | | | | |
| SC2 | bt | 59 | 26.6084 | 238.5957 | 83.0707 | 18.3401 | 29.4550 | 64.5168 | 0.3019 | 0.0083 | 3.6252 | 0.0396 | 0.2156 | 0.0056 | 1493 | 58 | | | | |
| SC2 | bt | 60 | 30.5090 | 335.4122 | 85.7846 | 18.6603 | 30.0464 | 65.4294 | 0.4338 | 0.0100 | 5.2733 | 0.0477 | 0.2381 | 0.0059 | 1537 | 50 | | | | |
| SC2 | bt | 61 | 30.4528 | 322.0108 | 85.3844 | 18.1442 | 30.5504 | 66.3087 | 0.4532 | 0.0102 | 5.0579 | 0.0468 | 0.2239 | 0.0057 | 1670 | 54 | | | | |
| SC2 | bt | 62 | 34.3410 | 309.4119 | 137.0063 | 18.3615 | 30.3603 | 69.5698 | 0.5919 | 0.0117 | 4.8442 | 0.0459 | 0.7907 | 0.0108 | 1660 | 47 | | | | |
| SC2 | bt | 63 | 32.9283 | 305.0789 | 134.9796 | 18.5631 | 28.1902 | 66.8986 | 0.5325 | 0.0111 | 4.8163 | 0.0458 | 0.7996 | 0.0108 | 1507 | 44 | | | | |
| SC2 | bt | 64 | 33.6159 | 308.5854 | 149.2418 | 18.9704 | 28.9436 | 65.6632 | 0.5395 | 0.0111 | 4.8533 | 0.0459 | 0.9816 | 0.0120 | 1411 | 41 | | | | |
| SC2 | bt | 65 | 34.0097 | 303.6514 | 134.7169 | 18.1732 | 29.4604 | 67.4217 | 0.5858 | 0.0116 | 4.7521 | 0.0454 | 0.7872 | 0.0107 | 1665 | 47 | | | | |
| SC2 | bt | 66 | 33.5159 | 322.3113 | 126.7732 | 18.7643 | 29.7622 | 65.8524 | 0.5467 | 0.0113 | 5.0884 | 0.0470 | 0.7166 | 0.0103 | 1549 | 45 | | | | |
| SC2 | bt | 67 | 27.6648 | 246.2568 | 85.9096 | 17.5855 | 29.7928 | 67.3215 | 0.3715 | 0.0093 | 3.7668 | 0.0405 | 0.2170 | 0.0056 | 1757 | 63 | | | | |
| SC2 | bt | 68 | 28.6212 | 269.0420 | 86.0347 | 18.3058 | 31.1033 | 66.8541 | 0.3789 | 0.0093 | 4.1252 | 0.0423 | 0.2235 | 0.0057 | 1661 | 59 | | | | |
| SC2 | bt | 71 | 32.5719 | 381.6114 | 93.0635 | 18.5328 | 31.9198 | 68.1006 | 0.4938 | 0.0104 | 5.7982 | 0.0490 | 0.2814 | 0.0063 | 1572 | 47 | | | | |
| SC2 | bt | 72 | 31.4092 | 304.9037 | 92.9634 | 20.1638 | 31.1394 | 71.7736 | 0.3860 | 0.0091 | 4.4347 | 0.0424 | 0.2311 | 0.0056 | 1588 | 53 | | | | |
| SC2 | bt | 73 | 34.4473 | 314.4213 | 130.8263 | 19.6306 | 31.9528 | 69.9371 | 0.5196 | 0.0107 | 4.6503 | 0.0437 | 0.6761 | 0.0097 | 1589 | 46 | | | | |
| SC2 | bt | 74 | 30.4903 | 320.3826 | 90.6872 | 19.3663 | 32.0698 | 70.2376 | 0.3918 | 0.0093 | 4.7955 | 0.0447 | 0.2296 | 0.0057 | 1515 | 51 | | | | |
| SC2 | bt | 76 | 29.1588 | 292.0306 | 88.4610 | 18.4307 | 30.0075 | 70.1263 | 0.3848 | 0.0093 | 4.4368 | 0.0433 | 0.2091 | 0.0055 | 1606 | 55 | | | | |
| SC2 | bt | 77 | 32.4969 | 248.8607 | 135.4926 | 18.4118 | 29.7888 | 67.3327 | 0.5107 | 0.0108 | 3.7294 | 0.0398 | 0.7787 | 0.0105 | 1683 | 50 | | | | |
| SC2 | bt | 78 | 31.9531 | 315.0976 | 118.9424 | 18.7975 | 31.6292 | 67.9893 | 0.4800 | 0.0105 | 4.8653 | 0.0457 | 0.5908 | 0.0093 | 1496 | 46 | | | | |
| SC2 | bt | 92 | 36.6728 | 326.8953 | 161.9536 | 18.7625 | 31.9487 | 69.6143 | 0.6467 | 0.0121 | 4.9944 | 0.0460 | 1.0576 | 0.0123 | 1592 | 42 | | | | |
| SC2 | bt | 93 | 28.1899 | 227.3049 | 104.4952 | 18.1190 | 29.3959 | 69.7145 | 0.3650 | 0.0091 | 3.3863 | 0.0381 | 0.3983 | 0.0076 | 1637 | 58 | | | | |
| SC2 | bt | 94 | 30.7653 | 305.1040 | 93.9140 | 18.3853 | 31.2984 | 69.0578 | 0.4481 | 0.0101 | 4.6667 | 0.0446 | 0.2858 | 0.0064 | 1697 | 55 | | | | |
| SC2 | bt | 95 | 30.2465 | 273.3490 | 94.8645 | 18.8324 | 28.9879 | 68.6794 | 0.4153 | 0.0097 | 4.1884 | 0.0424 | 0.3018 | 0.0066 | 1698 | 57 | | | | |
| SC2 | bt | 96 | 33.0158 | 333.8090 | 111.2997 | 18.4106 | 29.9164 | 69.2136 | 0.5318 | 0.0110 | 5.1972 | 0.0471 | 0.4871 | 0.0084 | 1653 | 49 | | | | |
| SC2 | bt | 97 | 35.5038 | 475.5274 | 91.8753 | 18.9055 | 30.7686 | 68.5013 | 0.6032 | 0.0117 | 7.5932 | 0.0569 | 0.2738 | 0.0063 | 1527 | 42 | | | | |
| SC2 | bt | 99 | 26.6646 | 223.0491 | 84.0712 | 18.2140 | 31.6578 | 68.1340 | 0.3072 | 0.0084 | 3.3011 | 0.0377 | 0.1839 | 0.0052 | 1674 | 65 | | | | |
| SC2 | bt | 100 | 36.9854 | 313.7951 | 159.5138 | 18.5832 | 29.5781 | 67.9893 | 0.6759 | 0.0125 | 4.8933 | 0.0459 | 1.0653 | 0.0124 | 1668 | 43 | | | | |
| SC2 | bt | 101 | 36.4165 | 306.5066 | 173.5528 | 18.4380 | 29.6982 | 67.4217 | 0.6621 | 0.0123 | 4.7770 | 0.0454 | 1.2373 | 0.0134 | 1558 | 40 | | | | |
| SC2 | bt | 102 | 27.9836 | 238.6457 | 95.8150 | 18.6246 | 29.1836 | 67.2214 | 0.3427 | 0.0089 | 3.6286 | 0.0396 | 0.3320 | 0.0069 | 1543 | 57 | 1594 ± 17 | 82 | | |
| RND | sill | 18 | 30.7966 | 308.5103 | 108.9481 | 17.9764 | 28.2334 | 66.1640 | 0.4670 | 0.0103 | 4.8485 | 0.0458 | 0.4963 | 0.0085 | 1530 | 48 | | | | |
| RND | sill | 19 | 31.9031 | 331.2539 | 94.0640 | 18.2980 | 30.1121 | 69.3917 | 0.4952 | 0.0106 | 5.1924 | 0.0473 | 0.2856 | 0.0064 | 1716 | 53 | | | | |
| RND | sill | 20 | 34.3285 | 300.4456 | 135.1423 | 18.6797 | 30.5849 | 67.7556 | 0.5786 | 0.0116 | 4.7062 | 0.0453 | 0.7862 | 0.0107 | 1656 | 47 | | | | |
| RND | sill | 23 | 24.0080 | 136.4308 | 90.2869 | 18.0836 | 29.5523 | 68.9020 | 0.2120 | 0.0069 | 1.8473 | 0.0283 | 0.2430 | 0.0059 | 1679 | 78 | | | | |
| RND | sill | 24 | 35.2537 | 316.7758 | 146.6270 | 18.1865 | 30.9793 | 67.7333 | 0.6246 | 0.0120 | 4.9312 | 0.0461 | 0.9121 | 0.0115 | 1642 | 44 | | | | |
| RND | sill | 26 | 33.6596 | 302.0485 | 141.4475 | 18.3120 | 29.7795 | 67.9003 | 0.5631 | 0.0114 | 4.7141 | 0.0452 | 0.8521 | 0.0111 | 1570 | 45 | | | | |
| RND | sill | 28 | 27.5898 | 220.3706 | 95.3398 | 18.9951 | 29.1814 | 66.9765 | 0.3114 | 0.0084 | 3.3080 | 0.0378 | 0.3256 | 0.0068 | 1512 | 59 | | | | |
| RND | sill | 30 | 36.0039 | 319.7815 | 150.0050 | 18.4166 | 30.5459 | 67.0210 | 0.6474 | 0.0122 | 5.0172 | 0.0466 | 0.9650 | 0.0118 | 1645 | 44 | | | | |
| RND | sill | 31 | 34.5473 | 312.1170 | 140.0088 | 18.3504 | 30.7338 | 69.0578 | 0.5918 | 0.0116 | 4.8503 | 0.0457 | 0.8190 | 0.0109 | 1639 | 46 | | | | |
| RND | sill | 32 | 35.8163 | 325.6428 | 156.4109 | 18.2966 | 30.6531 | 68.0561 | 0.6405 | 0.0121 | 5.0849 | 0.0468 | 1.0216 | 0.0122 | 1584 | 42 | | | | |
| RND | sill | 33 | 23.4454 | 116.2405 | 86.2723 | 18.5136 | 30.1323 | 67.7779 | 0.1750 | 0.0062 | 1.4894 | 0.0254 | 0.2098 | 0.0055 | 1680 | 87 | | | | |
| RND | sill | 35 | 34.8787 | 290.9287 | 145.2883 | 18.1853 | 28.5794 | 68.4679 | 0.6105 | 0.0118 | 4.5232 | 0.0442 | 0.8855 | 0.0113 | 1702 | 46 | | | | |
| RND | sill | 36 | 31.8968 | 266.4128 | 129.7505 | 17.8929 | 28.4629 | 69.6700 | 0.5137 | 0.0109 | 4.1234 | 0.0423 | 0.6942 | 0.0100 | 1671 | 50 | | | | |
| RND | sill | 37 | 30.4965 | 306.7069 | 100.8805 | 18.2367 | 31.3125 | 67.5330 | 0.4454 | 0.0101 | 4.7458 | 0.0452 | 0.3847 | 0.0074 | 1575 | 51 | | | | |
| RND | sill | 38 | 32.4282 | 279.7596 | 135.5676 | 17.9990 | 31.9126 | 67.3104 | 0.5266 | 0.0110 | 4.2742 | 0.0429 | 0.7859 | 0.0106 | 1605 | 47 | | | | |
| RND | sill | 39 | 32.7907 | 302.4492 | 126.0101 | 18.8076 | 30.4718 | 67.9782 | 0.5128 | 0.0108 | 4.7089 | 0.0451 | 0.6719 | 0.0099 | 1561 | 47 | | | | |
| RND | sill | 41 | 32.0093 | 307.9342 | 117.7416 | 18.7311 | 30.6647 | 67.4662 | 0.4871 | 0.0106 | 4.8104 | 0.0457 | 0.5838 | 0.0092 | 1532 | 48 | | | | |
| RND | sill | 42 | 31.8655 | 304.1022 | 117.9667 | 18.3814 | 29.2502 | 68.7239 | 0.4917 | 0.0106 | 4.7389 | 0.0452 | 0.5681 | 0.0091 | 1572 | 49 | | | | |
| RND | sill | 43 | 31.5217 | 304.9537 | 116.1530 | 18.2735 | 30.6716 | 67.7333 | 0.4842 | 0.0105 | 4.7411 | 0.0453 | 0.5601 | 0.0090 | 1555 | 48 | | | | |
| RND | sill | 44 | 32.9533 | 315.3481 | 117.1286 | 18.7243 | 31.6578 | 68.3455 | 0.5217 | 0.0109 | 4.9143 | 0.0461 | 0.5660 | 0.0091 | 1623 | 49 | | | | |
| RND | sill | 45 | 31.6718 | 302.0985 | 114.2266 | 18.4674 | 30.6751 | 67.8892 | 0.4800 | 0.0104 | 4.6676 | 0.0448 | 0.5330 | 0.0088 | 1580 | 49 | | | | |

| Sample | Occluding phase | Label | Peak Counts Pk(Pb) | Pk(Th) | Pk(U ) | Background counts Bg(Pb) | Bg(Th) | Bg(U ) | W%(Pb) | W%(Pb) 1σ | W%(Th) | W%(Th) 1σ | W%(U) | W%(U) 1σ | Chemical age (Ma) | 1σ | Early/peak meta. age (Ma) & error (2σ) | n = | Post peak meta. age (Ma) & error (2σ) | n = |
|---|---|---|---|---|---|---|---|---|---|---|---|---|---|---|---|---|---|---|---|---|
| RND | sill | 46 | 35.0662 | 323.2131 | 120.0307 | 20.2948 | 31.3717 | 73.4209 | 0.5408 | 0.0111 | 5.0490 | 0.0467 | 0.5406 | 0.0089 | 1668 | 50 | | | | |
| RND | sill | 47 | 31.8593 | 302.5995 | 112.9633 | 18.3541 | 30.3208 | 68.4679 | 0.4949 | 0.0106 | 4.7179 | 0.0452 | 0.5159 | 0.0086 | 1627 | 50 | | | | |
| RND | sill | 61 | 32.8220 | 295.3364 | 139.9462 | 18.4155 | 29.8094 | 67.1768 | 0.5289 | 0.0110 | 4.6009 | 0.0446 | 0.8429 | 0.0110 | 1509 | 44 | | | | |
| RND | sill | 62 | 33.4409 | 289.2257 | 139.6585 | 17.9557 | 30.2712 | 69.1691 | 0.5691 | 0.0114 | 4.4891 | 0.0441 | 0.8165 | 0.0109 | 1653 | 47 | | | | |
| RND | sill | 63 | 33.8347 | 304.5530 | 120.8938 | 18.8000 | 30.8008 | 66.3087 | 0.5530 | 0.0113 | 4.7565 | 0.0455 | 0.6349 | 0.0096 | 1691 | 50 | | | | |
| RND | sill | 64 | 33.1345 | 284.6929 | 143.1615 | 18.7609 | 30.8583 | 64.3276 | 0.5328 | 0.0111 | 4.4417 | 0.0441 | 0.9214 | 0.0116 | 1497 | 44 | | | | |
| RND | sill | 65 | 30.2840 | 279.1586 | 113.7888 | 17.8614 | 29.7662 | 66.7316 | 0.4611 | 0.0103 | 4.3761 | 0.0438 | 0.5510 | 0.0090 | 1572 | 51 | | | | |
| RND | sill | 66 | 30.8091 | 280.8615 | 113.9264 | 18.0101 | 28.0728 | 66.5313 | 0.4771 | 0.0105 | 4.4529 | 0.0443 | 0.5575 | 0.0091 | 1599 | 51 | | | | |
| RND | sill | 67 | 30.6278 | 287.8734 | 113.2259 | 17.9262 | 29.3083 | 66.4089 | 0.4724 | 0.0105 | 4.5457 | 0.0447 | 0.5499 | 0.0090 | 1570 | 50 | | | | |
| RND | sill | 68 | 22.9266 | 137.8320 | 75.8798 | 17.9688 | 27.6142 | 66.0193 | 0.1800 | 0.0064 | 1.9443 | 0.0293 | 0.1143 | 0.0041 | 1651 | 86 | | | | |
| RND | sill | 69 | 31.0279 | 250.3629 | 128.1117 | 17.3536 | 29.3160 | 65.2068 | 0.5100 | 0.0109 | 3.9078 | 0.0416 | 0.7417 | 0.0105 | 1670 | 51 | | | | |
| RND | sill | 70 | 25.6207 | 195.7399 | 77.5430 | 18.3170 | 29.7692 | 66.4422 | 0.2696 | 0.0079 | 2.9319 | 0.0360 | 0.1297 | 0.0044 | 1710 | 73 | | | | |
| RND | sill | 71 | 35.8851 | 345.1570 | 140.3966 | 18.0522 | 30.0215 | 66.1863 | 0.6657 | 0.0125 | 5.5466 | 0.0494 | 0.8784 | 0.0114 | 1650 | 44 | | | | |
| RND | sill | 72 | 32.4031 | 311.3906 | 123.0079 | 18.1382 | 29.1707 | 65.3404 | 0.5310 | 0.0111 | 4.9678 | 0.0468 | 0.6805 | 0.0100 | 1554 | 46 | | | | |
| RND | sill | 73 | 33.9034 | 308.8609 | 137.9821 | 17.8914 | 29.3637 | 65.6298 | 0.5994 | 0.0118 | 4.9351 | 0.0467 | 0.8560 | 0.0113 | 1617 | 45 | | | | |
| RND | sill | 74 | 25.6707 | 208.4803 | 81.9576 | 17.8650 | 30.0665 | 67.7445 | 0.2883 | 0.0082 | 3.1462 | 0.0372 | 0.1660 | 0.0049 | 1663 | 68 | | | | |
| RND | sill | 75 | 26.3333 | 194.2131 | 92.2380 | 18.2549 | 29.4202 | 65.3181 | 0.3003 | 0.0084 | 2.9239 | 0.0360 | 0.3160 | 0.0068 | 1601 | 64 | | | | |
| RND | sill | 76 | 23.4391 | 138.2573 | 79.5440 | 18.2044 | 28.0838 | 66.8207 | 0.1909 | 0.0066 | 1.9487 | 0.0294 | 0.1480 | 0.0046 | 1661 | 84 | | | | |
| RND | sill | 77 | 29.7714 | 247.5587 | 112.9508 | 18.3089 | 28.7320 | 66.7205 | 0.4285 | 0.0100 | 3.8747 | 0.0414 | 0.5448 | 0.0090 | 1591 | 53 | | | | |
| RND | sill | 78 | 31.8718 | 304.4278 | 108.4228 | 18.4734 | 29.3921 | 67.2436 | 0.4964 | 0.0107 | 4.8288 | 0.0460 | 0.4844 | 0.0084 | 1632 | 51 | | | | |
| RND | sill | 79 | 33.2846 | 312.8433 | 124.2588 | 18.4371 | 31.7218 | 66.9876 | 0.5478 | 0.0112 | 4.9021 | 0.0462 | 0.6692 | 0.0099 | 1621 | 47 | | | | |
| RND | sill | 81 | 33.5909 | 338.3431 | 118.5797 | 18.3814 | 31.6356 | 71.7513 | 0.5296 | 0.0107 | 5.0517 | 0.0456 | 0.5173 | 0.0085 | 1654 | 48 | | | | |
| RND | sill | 84 | 32.0656 | 318.5291 | 112.5005 | 18.5428 | 31.2249 | 68.1229 | 0.4871 | 0.0105 | 4.9027 | 0.0457 | 0.5075 | 0.0085 | 1570 | 49 | | | | |
| RND | sill | 85 | 32.1093 | 326.9203 | 113.9139 | 18.5096 | 30.5589 | 67.9225 | 0.4912 | 0.0105 | 5.0714 | 0.0466 | 0.5280 | 0.0087 | 1531 | 47 | | | | |
| RND | sill | 86 | 32.0406 | 324.0146 | 111.9751 | 18.6791 | 30.2639 | 68.7796 | 0.4838 | 0.0105 | 5.0407 | 0.0465 | 0.4972 | 0.0085 | 1538 | 48 | | | | |
| RND | sill | 88 | 33.3471 | 329.7258 | 111.2121 | 19.0669 | 31.9621 | 67.7111 | 0.5196 | 0.0109 | 5.1305 | 0.0470 | 0.5032 | 0.0085 | 1619 | 49 | 1612 ± 18 | 47 | | |
| RND | bt | 110 | 30.7966 | 281.3873 | 108.1351 | 18.9212 | 30.3429 | 67.2881 | 0.4353 | 0.0100 | 4.3693 | 0.0436 | 0.4751 | 0.0083 | 1554 | 51 | | | | |
| RND | bt | 111 | 31.6968 | 275.3272 | 110.6242 | 18.5269 | 30.5213 | 67.4440 | 0.4807 | 0.0105 | 4.2333 | 0.0428 | 0.4985 | 0.0085 | 1715 | 54 | | | | |
| RND | bt | 113 | 32.7845 | 288.8250 | 115.9903 | 19.3477 | 31.5399 | 70.4602 | 0.4658 | 0.0100 | 4.2268 | 0.0417 | 0.4992 | 0.0083 | 1668 | 52 | | | | |
| RND | bt | 114 | 32.4844 | 294.2846 | 115.5400 | 18.7492 | 31.6939 | 69.5142 | 0.4837 | 0.0103 | 4.3806 | 0.0427 | 0.5130 | 0.0085 | 1675 | 52 | | | | |
| RND | bt | 115 | 30.5903 | 267.9402 | 111.1496 | 18.3815 | 29.6204 | 67.9448 | 0.4338 | 0.0098 | 4.0170 | 0.0411 | 0.4855 | 0.0083 | 1627 | 53 | | | | |
| RND | bt | 116 | 32.0031 | 288.3743 | 115.8653 | 19.5793 | 30.6637 | 68.2231 | 0.4466 | 0.0100 | 4.3942 | 0.0433 | 0.5427 | 0.0088 | 1529 | 49 | | | | |
| RND | bt | 117 | 31.4155 | 289.5262 | 115.4900 | 18.5026 | 30.4217 | 68.6460 | 0.4605 | 0.0101 | 4.3811 | 0.0430 | 0.5293 | 0.0086 | 1587 | 50 | | | | |
| RND | bt | 118 | 30.6903 | 261.7303 | 110.4616 | 18.4343 | 29.9455 | 65.9525 | 0.4428 | 0.0100 | 3.9725 | 0.0413 | 0.5086 | 0.0085 | 1648 | 53 | | | | |
| RND | bt | 119 | 32.2469 | 300.2953 | 114.7895 | 18.8197 | 29.3101 | 68.4123 | 0.4872 | 0.0105 | 4.6577 | 0.0447 | 0.5335 | 0.0088 | 1603 | 50 | | | | |
| RND | bt | 120 | 31.8280 | 299.0931 | 115.1398 | 18.3185 | 30.6719 | 67.6220 | 0.4918 | 0.0106 | 4.6301 | 0.0447 | 0.5486 | 0.0089 | 1611 | 50 | | | | |
| RND | bt | 121 | 29.8027 | 273.1737 | 111.4998 | 18.4415 | 29.4189 | 67.6332 | 0.4107 | 0.0096 | 4.1863 | 0.0424 | 0.5029 | 0.0085 | 1492 | 50 | | | | |
| RND | bt | 122 | 31.3717 | 310.3136 | 105.9712 | 18.2067 | 29.4216 | 65.4739 | 0.4790 | 0.0104 | 4.8453 | 0.0457 | 0.4682 | 0.0082 | 1589 | 49 | | | | |
| RND | bt | 123 | 31.8093 | 310.6392 | 116.0654 | 18.7069 | 29.9508 | 67.0433 | 0.4793 | 0.0105 | 4.8675 | 0.0459 | 0.5698 | 0.0091 | 1508 | 47 | 1601 ± 42 | 13 | | |
| RND | gt | 1 | 31.4905 | 289.9520 | 113.7763 | 18.8086 | 30.7897 | 68.2676 | 0.4642 | 0.0103 | 4.4967 | 0.0442 | 0.5278 | 0.0087 | 1574 | 50 | | | | |
| RND | gt | 4 | 32.3281 | 295.0860 | 117.4414 | 18.9452 | 30.3411 | 70.8275 | 0.4872 | 0.0105 | 4.5656 | 0.0444 | 0.5376 | 0.0088 | 1621 | 50 | | | | |
| RND | gt | 5 | 30.3340 | 267.5646 | 113.7888 | 18.9742 | 28.2834 | 74.5006 | 0.4112 | 0.0096 | 4.1156 | 0.0421 | 0.4508 | 0.0080 | 1556 | 52 | | | | |
| RND | gt | 6 | 30.2090 | 272.9734 | 114.7270 | 18.7376 | 30.9351 | 68.5013 | 0.4152 | 0.0097 | 4.1608 | 0.0423 | 0.5302 | 0.0087 | 1491 | 49 | | | | |
| RND | gt | 7 | 32.0718 | 289.7266 | 115.4275 | 18.9416 | 31.8980 | 69.4696 | 0.4783 | 0.0104 | 4.4499 | 0.0438 | 0.5301 | 0.0087 | 1627 | 51 | | | | |
| RND | gt | 8 | 30.5903 | 278.2821 | 114.3517 | 17.9806 | 29.7871 | 69.1691 | 0.4587 | 0.0102 | 4.2838 | 0.0430 | 0.5200 | 0.0086 | 1613 | 51 | | | | |
| RND | gt | 9 | 31.1904 | 286.2206 | 114.0765 | 18.8548 | 30.6391 | 68.4011 | 0.4472 | 0.0101 | 4.3944 | 0.0435 | 0.5247 | 0.0087 | 1546 | 49 | | | | |
| RND | gt | 12 | 30.2340 | 286.4960 | 114.5268 | 18.5614 | 30.9014 | 68.4679 | 0.4242 | 0.0098 | 4.4104 | 0.0436 | 0.5311 | 0.0087 | 1464 | 48 | | | | |
| RND | gt | 14 | 30.9966 | 285.7948 | 113.2885 | 18.8761 | 31.0339 | 66.9208 | 0.4396 | 0.0100 | 4.3848 | 0.0434 | 0.5333 | 0.0088 | 1517 | 49 | | | | |
| RND | gt | 15 | 31.3467 | 297.4151 | 114.8145 | 18.9231 | 30.3441 | 68.2342 | 0.4523 | 0.0101 | 4.6130 | 0.0446 | 0.5383 | 0.0088 | 1503 | 48 | | | | |
| RND | gt | 48 | 30.9529 | 290.2525 | 112.7881 | 18.2173 | 30.7743 | 68.3232 | 0.4650 | 0.0103 | 4.4907 | 0.0441 | 0.5145 | 0.0086 | 1588 | 51 | | | | |
| RND | gt | 50 | 31.5655 | 317.3518 | 105.8461 | 18.8102 | 32.0007 | 67.9893 | 0.4605 | 0.0102 | 4.8866 | 0.0457 | 0.4345 | 0.0079 | 1550 | 49 | | | | |
| RND | gt | 51 | 31.6343 | 303.7265 | 117.9542 | 18.7892 | 28.8633 | 67.4440 | 0.4637 | 0.0102 | 4.7053 | 0.0449 | 0.5789 | 0.0091 | 1488 | 47 | | | | |
| RND | gt | 52 | 32.8157 | 322.1110 | 116.6283 | 18.4924 | 29.2958 | 69.6477 | 0.5189 | 0.0108 | 5.0224 | 0.0464 | 0.5406 | 0.0088 | 1611 | 48 | | | | |

| Sample | Occluding phase | Label | Peak Counts Pk(Pb) | Pk(Th) | Pk(U) | Background counts Bg(Pb) | Bg(Th) | Bg(U) | W%(Pb) | W%(Pb) 1σ | W%(Th) | W%(Th) 1σ | W%(U) | W%(U) 1σ | Chemical age (Ma) | 1σ | Early/peak meta. age (Ma) & error (2σ) | n = | Post peak meta. age (Ma) & error (2σ) | n = |
|---|---|---|---|---|---|---|---|---|---|---|---|---|---|---|---|---|---|---|---|---|
| RND | gt | 53 | 31.3592 | 308.7607 | 114.6769 | 18.7510 | 31.4268 | 69.5142 | 0.4551 | 0.0101 | 4.7492 | 0.0451 | 0.5180 | 0.0086 | 1498 | 48 | | | | |
| RND | gt | 54 | 32.1531 | 313.7450 | 115.0272 | 18.6293 | 29.0753 | 68.1674 | 0.4877 | 0.0105 | 4.8647 | 0.0456 | 0.5366 | 0.0088 | 1557 | 48 | | | | |
| RND | gt | 55 | 31.8405 | 288.1990 | 127.1110 | 18.2453 | 28.5376 | 68.0116 | 0.4975 | 0.0107 | 4.4912 | 0.0441 | 0.6830 | 0.0099 | 1554 | 48 | | | | |
| RND | gt | 56 | 34.9662 | 404.3148 | 99.1420 | 18.4356 | 30.9116 | 69.4251 | 0.6006 | 0.0117 | 6.4070 | 0.0524 | 0.3446 | 0.0071 | 1694 | 48 | | | | |
| RND | gt | 57 | 33.1470 | 278.0568 | 138.9704 | 18.7398 | 29.0883 | 68.5013 | 0.5251 | 0.0109 | 4.2848 | 0.0429 | 0.8094 | 0.0108 | 1582 | 46 | | | | |
| RND | gt | 58 | 31.9093 | 294.4098 | 124.0461 | 18.3031 | 30.3759 | 66.3643 | 0.4990 | 0.0107 | 4.5714 | 0.0445 | 0.6673 | 0.0098 | 1553 | 48 | | | | |
| RND | gt | 59 | 31.3842 | 306.2311 | 116.6283 | 18.0931 | 28.9658 | 67.2881 | 0.4802 | 0.0104 | 4.7492 | 0.0451 | 0.5660 | 0.0090 | 1537 | 48 | | | | |
| RND | gt | 60 | 31.6655 | 305.9556 | 111.8000 | 18.1062 | 30.7216 | 68.3010 | 0.4897 | 0.0105 | 4.7096 | 0.0449 | 0.4984 | 0.0084 | 1628 | 50 | | | | |
| RND | gt | 90 | 31.0967 | 326.7700 | 112.3629 | 18.1237 | 29.0293 | 68.0561 | 0.4559 | 0.0100 | 4.9652 | 0.0455 | 0.4957 | 0.0083 | 1472 | 46 | | | | |
| RND | gt | 91 | 33.5659 | 346.8105 | 116.8785 | 18.1650 | 31.6129 | 68.4790 | 0.5469 | 0.0110 | 5.2970 | 0.0472 | 0.5465 | 0.0088 | 1628 | 47 | | | | |
| RND | gt | 92 | 36.4290 | 344.6560 | 156.3358 | 18.1776 | 30.0927 | 67.5441 | 0.6597 | 0.0122 | 5.3602 | 0.0478 | 1.0165 | 0.0121 | 1585 | 42 | | | | |
| RND | gt | 93 | 32.5094 | 389.2290 | 83.6710 | 18.8500 | 31.1200 | 68.5347 | 0.4985 | 0.0107 | 6.1851 | 0.0517 | 0.1763 | 0.0051 | 1584 | 49 | | | | |
| RND | gt | 94 | 31.6468 | 323.3133 | 108.5979 | 17.9094 | 29.7523 | 70.2154 | 0.4991 | 0.0106 | 5.0561 | 0.0467 | 0.4437 | 0.0080 | 1622 | 50 | | | | |
| RND | gt | 95 | 26.4646 | 205.3765 | 99.3921 | 17.4665 | 28.3137 | 67.4328 | 0.3284 | 0.0087 | 3.0799 | 0.0366 | 0.3684 | 0.0073 | 1612 | 61 | | | | |
| RND | gt | 96 | 27.0522 | 248.2848 | 89.8367 | 17.3527 | 29.4455 | 65.8524 | 0.3554 | 0.0090 | 3.8155 | 0.0408 | 0.2783 | 0.0064 | 1598 | 59 | | | | |
| RND | gt | 97 | 31.7718 | 290.6282 | 119.0175 | 18.3083 | 27.6217 | 66.1195 | 0.4967 | 0.0107 | 4.5880 | 0.0447 | 0.6169 | 0.0095 | 1581 | 49 | | | | |
| RND | gt | 98 | 28.9213 | 283.9166 | 103.7573 | 17.3320 | 27.6586 | 64.5724 | 0.4274 | 0.0099 | 4.5019 | 0.0445 | 0.4612 | 0.0082 | 1509 | 50 | | | | |
| RND | gt | 99 | 31.9593 | 323.5137 | 120.0933 | 17.8548 | 29.8837 | 67.8001 | 0.5206 | 0.0110 | 5.1329 | 0.0474 | 0.6137 | 0.0095 | 1541 | 46 | | | | |
| RND | gt | 100 | 34.6724 | 386.0967 | 109.1482 | 18.4495 | 29.6193 | 67.3438 | 0.5892 | 0.0116 | 6.1297 | 0.0513 | 0.4855 | 0.0084 | 1618 | 46 | | | | |
| RND | gt | 101 | 32.2031 | 330.1767 | 107.1594 | 18.2368 | 29.2522 | 66.6760 | 0.5103 | 0.0108 | 5.2066 | 0.0475 | 0.4703 | 0.0083 | 1601 | 49 | | | | |
| RND | gt | 102 | 31.7530 | 306.0307 | 109.7111 | 18.2714 | 27.9882 | 67.1212 | 0.4953 | 0.0107 | 4.8332 | 0.0458 | 0.4958 | 0.0085 | 1619 | 50 | | | | |
| RND | gt | 103 | 30.9529 | 305.7552 | 110.5366 | 18.1243 | 31.0852 | 65.8078 | 0.4692 | 0.0104 | 4.7666 | 0.0455 | 0.5201 | 0.0087 | 1535 | 49 | | | | |
| RND | gt | 104 | 32.4844 | 330.0515 | 105.6460 | 18.2180 | 27.7408 | 66.8652 | 0.5226 | 0.0109 | 5.2467 | 0.0477 | 0.4521 | 0.0081 | 1643 | 50 | | | | |
| RND | gt | 105 | 30.6091 | 288.9753 | 113.9139 | 17.9502 | 28.1628 | 64.7282 | 0.4671 | 0.0104 | 4.5500 | 0.0445 | 0.5733 | 0.0091 | 1535 | 49 | | | | |
| RND | gt | 106 | 32.3781 | 357.2575 | 105.6210 | 17.9442 | 29.4526 | 65.9971 | 0.5276 | 0.0110 | 5.6799 | 0.0496 | 0.4626 | 0.0082 | 1558 | 47 | | | | |
| RND | gt | 108 | 31.8030 | 341.6749 | 101.7686 | 18.7861 | 29.6312 | 66.8207 | 0.4756 | 0.0104 | 5.4118 | 0.0484 | 0.4076 | 0.0077 | 1504 | 47 | | | | |
| RND | gt | 109 | 32.4469 | 265.4863 | 134.3041 | 18.0626 | 28.7049 | 66.9097 | 0.5292 | 0.0110 | 4.1146 | 0.0423 | 0.7811 | 0.0106 | 1649 | 49 | | | 1570 ± 18 | 41 |
| RRQ | gt | 1 | 29.2276 | 253.9183 | 115.2648 | 16.6406 | 25.9949 | 60.6325 | 0.5182 | 0.0115 | 4.4675 | 0.0468 | 0.7073 | 0.0107 | 1600 | 51 | | | | |
| RRQ | gt | 2 | 29.5651 | 262.8070 | 109.1607 | 16.8518 | 27.3683 | 61.6898 | 0.5248 | 0.0116 | 4.6269 | 0.0477 | 0.6168 | 0.0100 | 1654 | 52 | | | | |
| RRQ | gt | 3 | 24.9081 | 232.5121 | 71.1527 | 17.1890 | 27.4642 | 60.7104 | 0.3161 | 0.0090 | 4.0404 | 0.0446 | 0.1355 | 0.0047 | 1517 | 61 | | | | |
| RRQ | gt | 4 | 25.5020 | 248.4601 | 71.6529 | 16.4580 | 27.8547 | 61.3114 | 0.3722 | 0.0098 | 4.3510 | 0.0463 | 0.1346 | 0.0047 | 1664 | 63 | | | | |
| RRQ | gt | 5 | 26.5146 | 272.5477 | 78.6936 | 16.4340 | 27.2893 | 60.1094 | 0.4176 | 0.0104 | 4.8567 | 0.0490 | 0.2435 | 0.0063 | 1579 | 56 | | | | |
| RRQ | gt | 6 | 28.7525 | 251.0139 | 112.8382 | 17.2375 | 26.8853 | 61.3448 | 0.4778 | 0.0111 | 4.4329 | 0.0468 | 0.6724 | 0.0105 | 1517 | 50 | | | | |
| RRQ | gt | 7 | 29.5214 | 257.7241 | 106.6966 | 16.3697 | 26.0147 | 62.0348 | 0.5473 | 0.0119 | 4.5872 | 0.0476 | 0.5843 | 0.0098 | 1755 | 55 | | | | |
| RRQ | gt | 8 | 29.1963 | 267.2141 | 115.3024 | 16.3227 | 27.5921 | 60.8328 | 0.5361 | 0.0118 | 4.7489 | 0.0485 | 0.7141 | 0.0108 | 1587 | 50 | | | | |
| RRQ | gt | 9 | 30.1902 | 271.0703 | 123.4332 | 16.4035 | 26.1991 | 61.6564 | 0.5740 | 0.0122 | 4.8485 | 0.0490 | 0.8098 | 0.0115 | 1601 | 48 | | | | |
| RRQ | gt | 10 | 29.6839 | 257.8243 | 115.9528 | 16.5277 | 27.1603 | 61.5340 | 0.5500 | 0.0120 | 4.5862 | 0.0477 | 0.7151 | 0.0108 | 1657 | 51 | | | | |
| RRQ | gt | 11 | 30.8591 | 277.5810 | 124.4089 | 16.4370 | 24.3865 | 61.1222 | 0.6014 | 0.0125 | 5.0175 | 0.0499 | 0.8310 | 0.0117 | 1624 | 48 | | | | |
| RRQ | gt | 12 | 25.6207 | 281.0117 | 75.0919 | 16.2511 | 27.8762 | 61.7677 | 0.3875 | 0.0100 | 5.0106 | 0.0498 | 0.1747 | 0.0054 | 1494 | 55 | | | | |
| RRQ | gt | 13 | 24.6893 | 238.1450 | 71.2277 | 16.7443 | 26.2238 | 60.8551 | 0.3265 | 0.0092 | 4.1839 | 0.0454 | 0.1350 | 0.0047 | 1519 | 60 | | | | |
| RRQ | gt | 14 | 27.4148 | 274.2505 | 73.9289 | 16.2428 | 26.7220 | 61.1445 | 0.4645 | 0.0110 | 4.9045 | 0.0493 | 0.1676 | 0.0052 | 1813 | 62 | | | | |
| RRQ | gt | 15 | 25.2644 | 236.0671 | 71.5278 | 16.5237 | 27.3506 | 59.9647 | 0.3624 | 0.0097 | 4.1478 | 0.0454 | 0.1514 | 0.0050 | 1669 | 64 | | | | |
| RRQ | gt | 16 | 29.1275 | 276.2037 | 104.8455 | 15.8889 | 26.5849 | 60.7549 | 0.5529 | 0.0120 | 4.9587 | 0.0496 | 0.5800 | 0.0098 | 1691 | 53 | | | | |
| RRQ | gt | 17 | 28.7212 | 254.3690 | 110.3740 | 17.4107 | 25.7895 | 60.1317 | 0.4700 | 0.0110 | 4.5301 | 0.0474 | 0.6579 | 0.0104 | 1486 | 49 | | | | |
| RRQ | gt | 18 | 28.5962 | 257.3485 | 106.9093 | 16.4848 | 26.1165 | 60.9219 | 0.5053 | 0.0115 | 4.5936 | 0.0478 | 0.6037 | 0.0100 | 1616 | 52 | | | | |
| RRQ | gt | 19 | 27.4585 | 252.8416 | 106.6591 | 16.4159 | 26.8235 | 60.9664 | 0.4583 | 0.0109 | 4.4742 | 0.0471 | 0.5973 | 0.0099 | 1506 | 51 | | | | |
| RRQ | gt | 20 | 30.7903 | 273.5994 | 126.5480 | 16.2882 | 27.0093 | 60.9775 | 0.6042 | 0.0125 | 4.8860 | 0.0492 | 0.8606 | 0.0119 | 1635 | 48 | | | | |
| RRQ | gt | 21 | 29.9214 | 271.3457 | 126.6481 | 16.7075 | 26.1768 | 61.5785 | 0.5494 | 0.0119 | 4.8500 | 0.0490 | 0.8521 | 0.0118 | 1511 | 46 | | | | |
| RRQ | gt | 22 | 27.6961 | 272.9984 | 94.3642 | 16.5498 | 25.9665 | 60.4990 | 0.4617 | 0.0109 | 4.8823 | 0.0491 | 0.4431 | 0.0085 | 1548 | 52 | | | | |
| RRQ | gt | 23 | 25.1894 | 241.3747 | 72.0156 | 15.9891 | 27.1369 | 62.6692 | 0.3807 | 0.0099 | 4.2404 | 0.0458 | 0.1219 | 0.0045 | 1753 | 66 | | | | |
| RRQ | gt | 24 | 23.8830 | 222.7237 | 69.2269 | 16.4223 | 26.9968 | 60.1206 | 0.3071 | 0.0089 | 3.8785 | 0.0438 | 0.1187 | 0.0044 | 1548 | 64 | | | | |
| RRQ | gt | 25 | 23.5267 | 222.7988 | 71.3153 | 16.1248 | 28.0791 | 62.6915 | 0.3037 | 0.0088 | 3.8485 | 0.0436 | 0.1122 | 0.0043 | 1550 | 64 | | | | |
| RRQ | gt | 26 | 27.6585 | 318.0782 | 80.1693 | 17.3154 | 28.0020 | 61.9347 | 0.4263 | 0.0105 | 5.7132 | 0.0530 | 0.2388 | 0.0063 | 1415 | 49 | | | | |

| Sample | Occluding phase | Label | Peak Counts Pk(Pb) | Pk(Th) | Pk(U ) | Background counts Bg(Pb) | Bg(Th) | Bg(U ) | W%(Pb) | W%(Pb) 1σ | W%(Th) | W%(Th) 1σ | W%(U) | W%(U) 1σ | Chemical age (Ma) | 1σ | Early/peak meta. age (Ma) & error (2σ) | n = | Post peak meta. age (Ma) & error (2σ) | n = |
|---|---|---|---|---|---|---|---|---|---|---|---|---|---|---|---|---|---|---|---|---|
| RRQ | gt | 27 | 29.3838 | 277.7563 | 105.2832 | 16.8829 | 26.2216 | 61.9903 | 0.5179 | 0.0116 | 4.9647 | 0.0495 | 0.5661 | 0.0096 | 1602 | 51 | | | | |
| RRQ | gt | 28 | 28.6900 | 254.0184 | 108.3102 | 16.1454 | 25.9926 | 60.9664 | 0.5216 | 0.0116 | 4.5158 | 0.0473 | 0.6196 | 0.0101 | 1668 | 53 | | | | |
| RRQ | gt | 29 | 28.9838 | 261.6803 | 116.5407 | 16.5083 | 28.4134 | 60.3988 | 0.5186 | 0.0116 | 4.6168 | 0.0478 | 0.7346 | 0.0110 | 1551 | 49 | | | | |
| RRQ | gt | 30 | 28.3774 | 280.0851 | 117.9417 | 16.3410 | 26.0049 | 57.2269 | 0.4955 | 0.0113 | 5.0099 | 0.0497 | 0.7954 | 0.0114 | 1381 | 44 | | | | |
| RRQ | gt | 31 | 29.3776 | 258.9009 | 115.1398 | 16.6391 | 27.6666 | 59.6642 | 0.5294 | 0.0117 | 4.5743 | 0.0476 | 0.7253 | 0.0109 | 1596 | 50 | | | | |
| RRQ | gt | 32 | 27.8773 | 242.5263 | 104.7204 | 16.5919 | 28.0166 | 60.9330 | 0.4694 | 0.0110 | 4.2541 | 0.0459 | 0.5728 | 0.0097 | 1609 | 54 | | | | |
| RRQ | gt | 33 | 26.6334 | 283.5410 | 76.5176 | 16.6511 | 27.7333 | 61.6787 | 0.4120 | 0.0103 | 5.0477 | 0.0499 | 0.1940 | 0.0056 | 1556 | 55 | | | | |
| RRQ | gt | 34 | 24.3893 | 232.2868 | 70.8150 | 16.9409 | 26.8870 | 60.5991 | 0.3045 | 0.0088 | 4.0424 | 0.0446 | 0.1324 | 0.0046 | 1467 | 60 | | | | |
| RRQ | gt | 35 | 24.7706 | 224.6763 | 69.1393 | 15.8448 | 28.3484 | 60.5212 | 0.3673 | 0.0097 | 3.8712 | 0.0437 | 0.1118 | 0.0043 | 1846 | 71 | | | | |
| RRQ | gt | 36 | 24.2455 | 237.2688 | 71.2902 | 16.5476 | 28.3290 | 62.2129 | 0.3148 | 0.0090 | 4.1086 | 0.0449 | 0.1176 | 0.0044 | 1510 | 61 | | | | |
| RRQ | gt | 37 | 25.8458 | 258.8759 | 71.7029 | 16.7230 | 25.6553 | 61.3337 | 0.3749 | 0.0098 | 4.5898 | 0.0475 | 0.1348 | 0.0047 | 1600 | 60 | | | | |
| RRQ | gt | 38 | 28.4524 | 261.8305 | 105.8211 | 16.6235 | 26.3931 | 61.9903 | 0.4876 | 0.0112 | 4.6287 | 0.0477 | 0.5699 | 0.0096 | 1582 | 52 | | | | |
| RRQ | gt | 39 | 29.4464 | 276.5543 | 126.8608 | 16.4052 | 27.9332 | 60.8774 | 0.5415 | 0.0119 | 4.9120 | 0.0493 | 0.8632 | 0.0119 | 1474 | 45 | | | | |
| RRQ | gt | 41 | 27.5398 | 241.8754 | 106.5465 | 16.8544 | 26.7047 | 60.6882 | 0.4408 | 0.0107 | 4.2384 | 0.0457 | 0.5960 | 0.0098 | 1504 | 51 | | | | |
| RRQ | gt | 42 | 27.8586 | 241.8503 | 99.9299 | 16.7682 | 26.9364 | 61.4005 | 0.4573 | 0.0109 | 4.2266 | 0.0456 | 0.4998 | 0.0090 | 1640 | 56 | | | | |
| RRQ | gt | 1 | 28.1649 | 257.8743 | 105.9337 | 15.9580 | 27.1903 | 59.4862 | 0.5005 | 0.0113 | 4.5158 | 0.0470 | 0.6014 | 0.0099 | 1620 | 52 | | | | |
| RRQ | gt | 8 | 28.6900 | 262.9573 | 107.0093 | 16.4047 | 26.6559 | 61.6342 | 0.5051 | 0.0114 | 4.6303 | 0.0476 | 0.5879 | 0.0098 | 1620 | 52 | | | | |
| RRQ | gt | 9 | 28.5837 | 278.9583 | 100.9305 | 16.2252 | 27.3296 | 61.8011 | 0.5063 | 0.0114 | 4.9129 | 0.0490 | 0.5059 | 0.0090 | 1626 | 52 | | | | |
| RRQ | gt | 10 | 31.5717 | 277.2304 | 125.7599 | 16.5691 | 28.4893 | 63.3704 | 0.6178 | 0.0126 | 4.8675 | 0.0488 | 0.8083 | 0.0114 | 1708 | 50 | | | | |
| RRQ | gt | 12 | 28.9838 | 274.8264 | 101.9562 | 16.5178 | 27.6817 | 60.6770 | 0.5111 | 0.0114 | 4.8283 | 0.0486 | 0.5338 | 0.0093 | 1637 | 52 | | | | |
| RRQ | gt | 13 | 27.6398 | 277.0050 | 87.6480 | 16.6059 | 28.1923 | 61.7566 | 0.4534 | 0.0108 | 4.8804 | 0.0489 | 0.3361 | 0.0074 | 1612 | 55 | | | | |
| RRQ | gt | 14 | 27.3710 | 288.7249 | 88.1233 | 16.4624 | 27.3832 | 64.0938 | 0.4495 | 0.0108 | 5.1419 | 0.0503 | 0.3134 | 0.0071 | 1556 | 53 | | | | |
| RRQ | gt | 16 | 29.0150 | 292.6066 | 109.8612 | 16.3359 | 27.0204 | 61.6230 | 0.5225 | 0.0116 | 5.2177 | 0.0506 | 0.6289 | 0.0101 | 1519 | 48 | | | | |
| RRQ | gt | 17 | 24.5456 | 227.7054 | 72.4908 | 15.9241 | 26.6463 | 59.3192 | 0.3547 | 0.0096 | 3.9678 | 0.0442 | 0.1711 | 0.0053 | 1672 | 65 | | | | |
| RRQ | gt | 18 | 25.5020 | 243.5278 | 72.4282 | 16.5561 | 25.7387 | 61.3782 | 0.3678 | 0.0097 | 4.2886 | 0.0459 | 0.1435 | 0.0048 | 1655 | 63 | | | | |
| RRQ | gt | 19 | 24.6706 | 246.9829 | 72.8659 | 16.8957 | 29.0394 | 60.6659 | 0.3179 | 0.0090 | 4.2884 | 0.0459 | 0.1584 | 0.0051 | 1427 | 57 | | | | |
| RRQ | gt | 21 | 28.2336 | 295.3364 | 110.3365 | 16.7239 | 27.3063 | 62.5691 | 0.4749 | 0.0111 | 5.2834 | 0.0510 | 0.6252 | 0.0101 | 1382 | 45 | | | | |
| RRQ | gt | 22 | 24.1643 | 237.0685 | 69.9147 | 16.1199 | 26.5274 | 60.8551 | 0.3293 | 0.0092 | 4.1424 | 0.0451 | 0.1175 | 0.0044 | 1565 | 62 | | | | |
| RRQ | gt | 23 | 24.8206 | 253.3674 | 72.1906 | 16.2197 | 26.8391 | 60.0983 | 0.3546 | 0.0096 | 4.4748 | 0.0470 | 0.1576 | 0.0051 | 1528 | 58 | | | | |
| RRQ | gt | 26 | 26.8647 | 255.4706 | 88.8737 | 16.6559 | 26.9734 | 58.9965 | 0.4206 | 0.0104 | 4.5053 | 0.0471 | 0.3894 | 0.0080 | 1546 | 55 | | | | |
| RRQ | gt | 27 | 25.3519 | 257.3736 | 72.6033 | 16.5192 | 27.1611 | 61.2224 | 0.3650 | 0.0097 | 4.5562 | 0.0475 | 0.1487 | 0.0049 | 1556 | 59 | | | | |
| RRQ | gt | 28 | 26.5646 | 274.6511 | 86.7351 | 16.3687 | 26.4021 | 61.4895 | 0.4215 | 0.0104 | 4.9038 | 0.0492 | 0.3301 | 0.0073 | 1505 | 53 | | | | |
| RRQ | gt | 29 | 26.0895 | 247.3083 | 76.8927 | 16.6841 | 28.5876 | 59.8646 | 0.3881 | 0.0100 | 4.3203 | 0.0462 | 0.2219 | 0.0060 | 1640 | 61 | | | | |
| RRQ | gt | 31 | 27.7711 | 263.5081 | 110.4491 | 16.7230 | 27.9923 | 59.8980 | 0.4585 | 0.0109 | 4.6666 | 0.0481 | 0.6624 | 0.0104 | 1423 | 48 | | | | |
| RRQ | gt | 36 | 28.6837 | 245.6309 | 107.6598 | 16.4922 | 26.1305 | 57.9281 | 0.5051 | 0.0114 | 4.3433 | 0.0464 | 0.6506 | 0.0103 | 1633 | 53 | | | | |
| RRQ | gt | 37 | 27.1710 | 243.7531 | 103.9074 | 16.1892 | 25.6032 | 57.6610 | 0.4536 | 0.0108 | 4.3225 | 0.0463 | 0.6066 | 0.0100 | 1517 | 51 | | | | |
| RRQ | gt | 40 | 29.6214 | 273.5994 | 118.4546 | 16.5477 | 27.7880 | 61.5340 | 0.5434 | 0.0119 | 4.8657 | 0.0491 | 0.7463 | 0.0111 | 1562 | 48 | | | | |
| RRQ | gt | 41 | 27.7461 | 254.3940 | 110.9119 | 15.8681 | 27.3737 | 60.0315 | 0.4937 | 0.0113 | 4.4982 | 0.0472 | 0.6661 | 0.0104 | 1555 | 50 | | | | |
| RRQ | gt | 42 | 27.5398 | 242.0506 | 107.4721 | 16.9955 | 25.1593 | 59.2525 | 0.4372 | 0.0106 | 4.2963 | 0.0461 | 0.6304 | 0.0101 | 1455 | 50 | | | | |
| RRQ | gt | 43 | 27.1585 | 234.3647 | 96.2778 | 16.5189 | 26.1680 | 60.7772 | 0.4401 | 0.0107 | 4.1126 | 0.0451 | 0.4623 | 0.0087 | 1646 | 57 | | | | |
| RRQ | gt | 44 | 26.8647 | 237.4691 | 96.3904 | 16.6510 | 27.7105 | 60.9998 | 0.4225 | 0.0105 | 4.1465 | 0.0453 | 0.4612 | 0.0087 | 1578 | 56 | | | | |
| RRQ | gt | 45 | 28.3149 | 267.4394 | 101.2683 | 16.6683 | 26.8936 | 60.4656 | 0.4834 | 0.0112 | 4.7596 | 0.0485 | 0.5340 | 0.0093 | 1569 | 52 | | | | |
| RRQ | gt | 46 | 28.3524 | 244.9799 | 110.2615 | 16.3946 | 27.2498 | 61.3782 | 0.4959 | 0.0113 | 4.3022 | 0.0461 | 0.6374 | 0.0102 | 1625 | 53 | | | | |
| RRQ | gt | 47 | 27.7211 | 251.4646 | 109.3233 | 16.8952 | 26.8969 | 61.5006 | 0.4485 | 0.0108 | 4.4407 | 0.0469 | 0.6245 | 0.0101 | 1464 | 50 | | | | |
| RRQ | gt | 48 | 28.8713 | 258.7507 | 112.3629 | 16.0398 | 26.4644 | 61.0109 | 0.5310 | 0.0117 | 4.5770 | 0.0475 | 0.6689 | 0.0104 | 1642 | 52 | | | | |
| RRQ | gt | 49 | 28.7337 | 280.4858 | 110.0738 | 15.8813 | 26.5069 | 59.9981 | 0.5308 | 0.0117 | 5.0093 | 0.0497 | 0.6556 | 0.0104 | 1563 | 49 | | | | |
| RRQ | gt | 50 | 29.0900 | 267.0638 | 113.3886 | 16.1701 | 26.6259 | 60.2986 | 0.5359 | 0.0118 | 4.7467 | 0.0484 | 0.6933 | 0.0106 | 1602 | 50 | | | | |
| RRQ | gt | 51 | 28.2024 | 257.9745 | 102.5816 | 16.6680 | 28.3334 | 61.5674 | 0.4778 | 0.0111 | 4.5366 | 0.0473 | 0.5354 | 0.0093 | 1601 | 53 | | | | |
| RRQ | gt | 52 | 26.9459 | 248.9107 | 84.7716 | 16.2519 | 27.2652 | 61.2446 | 0.4425 | 0.0107 | 4.3783 | 0.0465 | 0.3067 | 0.0071 | 1737 | 61 | | | | |
| RRQ | gt | 53 | 26.5271 | 236.1672 | 89.5365 | 16.1822 | 26.7644 | 60.3543 | 0.4284 | 0.0105 | 4.1409 | 0.0452 | 0.3803 | 0.0079 | 1677 | 59 | | | | |
| RRQ | gt | 54 | 27.2522 | 244.2538 | 95.2272 | 15.9216 | 27.3553 | 60.9775 | 0.4697 | 0.0110 | 4.2875 | 0.0460 | 0.4466 | 0.0085 | 1715 | 58 | | | | |
| RRQ | gt | 55 | 27.0022 | 244.7296 | 97.7161 | 16.2130 | 27.0403 | 61.6342 | 0.4463 | 0.0107 | 4.2978 | 0.0461 | 0.4700 | 0.0087 | 1613 | 55 | | | | |
| RRQ | gt | 56 | 28.5774 | 251.4145 | 111.1370 | 16.6746 | 26.1494 | 62.4021 | 0.4915 | 0.0113 | 4.4320 | 0.0467 | 0.6331 | 0.0101 | 1587 | 52 | | | | |

| Sample | Occluding phase | Label | Peak Counts Pk(Pb) | Pk(Th) | Pk(U ) | Background counts Bg(Pb) | Bg(Th) | Bg(U ) | W%(Pb) | W%(Pb) 1σ | W%(Th) | W%(Th) 1σ | W%(U) | W%(U) 1σ | Chemica age (Ma) | 1σ | Early/peak meta. age (Ma) & error (2σ) | n = | Post peak meta. age (Ma) & error (2σ) | n = |
|---|---|---|---|---|---|---|---|---|---|---|---|---|---|---|---|---|---|---|---|---|
| RRQ | gt | 57 | 29.6964 | 261.3047 | 114.0140 | 16.4990 | 27.1503 | 59.9425 | 0.5459 | 0.0119 | 4.6086 | 0.0476 | 0.7036 | 0.0107 | 1650 | 51 | | | | |
| RRQ | gt | 58 | 28.2836 | 255.2954 | 109.8237 | 16.5313 | 26.6798 | 60.9441 | 0.4849 | 0.0112 | 4.4976 | 0.0470 | 0.6354 | 0.0102 | 1552 | 51 | | | | |
| RRQ | gt | 59 | 28.7337 | 273.5493 | 104.2576 | 16.3090 | 26.3600 | 59.6086 | 0.5157 | 0.0116 | 4.8842 | 0.0491 | 0.5840 | 0.0098 | 1599 | 51 | | | | |
| RRQ | gt | 60 | 24.7893 | 236.8181 | 72.3657 | 16.2016 | 26.2443 | 62.3465 | 0.3522 | 0.0095 | 4.1422 | 0.0451 | 0.1299 | 0.0046 | 1652 | 64 | | | | |
| RRQ | gt | 62 | 25.2144 | 227.6303 | 73.2536 | 16.9428 | 28.1155 | 62.5579 | 0.3285 | 0.0090 | 3.8083 | 0.0426 | 0.1343 | 0.0046 | 1655 | 65 | | | | |
| RRQ | gt | 63 | 28.2899 | 268.1155 | 100.3552 | 16.8918 | 27.0419 | 63.1701 | 0.4580 | 0.0107 | 4.6260 | 0.0471 | 0.4718 | 0.0087 | 1571 | 52 | | | | |
| RRQ | gt | 64 | 27.5585 | 291.7301 | 77.5430 | 16.8775 | 27.3261 | 62.1461 | 0.4344 | 0.0105 | 5.1322 | 0.0499 | 0.1980 | 0.0056 | 1610 | 55 | | | | |
| RRQ | gt | 65 | 29.1213 | 270.3691 | 101.4309 | 16.7001 | 27.5975 | 61.4784 | 0.5088 | 0.0114 | 4.7365 | 0.0481 | 0.5156 | 0.0091 | 1666 | 53 | | | | |
| RRQ | gt | 66 | 28.5712 | 253.9684 | 107.9850 | 16.3670 | 29.0058 | 61.4561 | 0.5008 | 0.0113 | 4.3971 | 0.0464 | 0.6004 | 0.0098 | 1649 | 53 | | | | |
| RRQ | gt | 67 | 28.1336 | 257.8243 | 112.8632 | 16.0751 | 28.1334 | 61.7677 | 0.4973 | 0.0113 | 4.5126 | 0.0471 | 0.6632 | 0.0104 | 1564 | 50 | | | | |
| RRQ | gt | 68 | 25.2582 | 240.6236 | 72.4908 | 15.9593 | 25.7712 | 62.1795 | 0.3820 | 0.0099 | 4.2230 | 0.0456 | 0.1336 | 0.0047 | 1750 | 65 | | | | |
| RRQ | gt | 69 | 22.6890 | 193.6875 | 68.1764 | 16.1511 | 25.8425 | 60.5212 | 0.2668 | 0.0082 | 3.3102 | 0.0404 | 0.0990 | 0.0040 | 1578 | 69 | | | | |
| RRQ | gt | 70 | 27.5460 | 303.1505 | 78.2058 | 16.8203 | 27.5118 | 60.5657 | 0.4424 | 0.0107 | 5.4238 | 0.0517 | 0.2303 | 0.0061 | 1537 | 53 | | | | |
| RRQ | gt | 71 | 25.0206 | 235.1157 | 71.7029 | 16.0453 | 26.7868 | 60.8996 | 0.3683 | 0.0097 | 4.0952 | 0.0449 | 0.1399 | 0.0048 | 1727 | 65 | | | | |
| RRQ | gt | 72 | 26.3208 | 267.3392 | 84.3839 | 16.5101 | 26.8964 | 62.5802 | 0.4041 | 0.0102 | 4.7394 | 0.0483 | 0.2843 | 0.0068 | 1524 | 55 | | | | |
| RRQ | gt | 73 | 26.7084 | 272.3223 | 73.3411 | 16.0914 | 27.5333 | 61.1667 | 0.4398 | 0.0107 | 4.8384 | 0.0489 | 0.1592 | 0.0051 | 1751 | 61 | | | | |
| RRQ | gt | 74 | 28.3712 | 248.1846 | 108.4353 | 16.2776 | 26.7378 | 59.5196 | 0.5005 | 0.0114 | 4.3654 | 0.0464 | 0.6365 | 0.0102 | 1626 | 53 | | | | |
| RRQ | gt | 75 | 27.3647 | 243.9784 | 101.6935 | 16.5044 | 27.1380 | 60.9553 | 0.4485 | 0.0108 | 4.2738 | 0.0459 | 0.5297 | 0.0093 | 1574 | 54 | | | | |
| RRQ | gt | 76 | 26.6834 | 274.1503 | 74.0790 | 16.8145 | 26.7041 | 61.3337 | 0.4091 | 0.0103 | 4.9026 | 0.0493 | 0.1671 | 0.0052 | 1610 | 58 | | | | |
| RRQ | gt | 77 | 23.1641 | 210.8583 | 69.6145 | 16.8548 | 26.3430 | 61.0666 | 0.2568 | 0.0081 | 3.6371 | 0.0423 | 0.1107 | 0.0042 | 1389 | 61 | | | | |
| RRQ | gt | 78 | 24.3643 | 243.8533 | 71.4028 | 16.0905 | 28.6572 | 60.4322 | 0.3396 | 0.0093 | 4.2420 | 0.0457 | 0.1426 | 0.0048 | 1550 | 60 | | | | |
| RRQ | gt | 79 | 29.3901 | 259.4768 | 111.8625 | 16.4302 | 25.8387 | 60.6214 | 0.5391 | 0.0118 | 4.6264 | 0.0479 | 0.6709 | 0.0105 | 1653 | 52 | 1591 ± 17 | 101 | | |
| RR2 | pl | 1 | 30.2652 | 302.1486 | 104.1200 | 18.2394 | 29.8902 | 67.1323 | 0.4405 | 0.0100 | 4.7025 | 0.0451 | 0.4266 | 0.0078 | 1535 | 50 | | | | |
| RR2 | pl | 2 | 31.4030 | 321.0589 | 108.7605 | 18.7224 | 30.2981 | 67.5664 | 0.4671 | 0.0104 | 5.0441 | 0.0468 | 0.4780 | 0.0083 | 1503 | 47 | | | | |
| RR2 | pl | 3 | 31.4030 | 317.7776 | 111.5873 | 18.4007 | 30.0027 | 67.0210 | 0.4782 | 0.0105 | 4.9835 | 0.0464 | 0.5161 | 0.0086 | 1520 | 47 | | | | |
| RR2 | pl | 4 | 33.2596 | 326.7951 | 120.8938 | 18.6372 | 29.7979 | 69.3695 | 0.5348 | 0.0111 | 5.1161 | 0.0469 | 0.5946 | 0.0093 | 1596 | 47 | | | | |
| RR2 | pl | 5 | 31.0154 | 299.3686 | 112.8882 | 17.6408 | 32.0233 | 68.0450 | 0.4932 | 0.0107 | 4.6426 | 0.0449 | 0.5200 | 0.0087 | 1636 | 50 | | | | |
| RR2 | pl | 6 | 29.7089 | 289.6014 | 101.0931 | 17.6078 | 28.5387 | 67.9559 | 0.4438 | 0.0101 | 4.5283 | 0.0443 | 0.3841 | 0.0075 | 1624 | 53 | | | | |
| RR2 | pl | 7 | 30.6591 | 300.2202 | 116.6033 | 18.2891 | 28.6487 | 67.3438 | 0.4562 | 0.0103 | 4.7175 | 0.0453 | 0.5713 | 0.0091 | 1469 | 47 | | | | |
| RR2 | pl | 8 | 26.9772 | 255.0450 | 83.4459 | 18.0329 | 30.7505 | 68.2898 | 0.3270 | 0.0086 | 3.8919 | 0.0411 | 0.1747 | 0.0050 | 1569 | 59 | | | | |
| RR2 | pl | 9 | 28.0586 | 269.2173 | 81.6575 | 17.9664 | 29.9122 | 68.2898 | 0.3704 | 0.0092 | 4.1528 | 0.0424 | 0.1543 | 0.0047 | 1698 | 61 | | | | |
| RR2 | pl | 10 | 31.6843 | 303.2757 | 111.3247 | 18.0419 | 29.8053 | 68.6126 | 0.5038 | 0.0108 | 4.7512 | 0.0454 | 0.4956 | 0.0085 | 1664 | 51 | | | | |
| RR2 | pl | 11 | 31.8468 | 324.8412 | 117.1161 | 18.8130 | 29.7955 | 67.7333 | 0.4816 | 0.0105 | 5.1302 | 0.0472 | 0.5746 | 0.0091 | 1460 | 45 | | | | |
| RR2 | pl | 12 | 32.2219 | 313.2191 | 117.6040 | 18.2940 | 30.1502 | 68.3344 | 0.5172 | 0.0110 | 4.9395 | 0.0464 | 0.5747 | 0.0092 | 1598 | 48 | | | | |
| RR2 | pl | 13 | 28.9213 | 277.8314 | 88.8237 | 17.6497 | 28.9556 | 68.5124 | 0.4155 | 0.0098 | 4.3289 | 0.0434 | 0.2353 | 0.0058 | 1729 | 59 | | | | |
| RR2 | pl | 14 | 30.2340 | 295.2112 | 107.2845 | 18.4352 | 29.9464 | 67.8335 | 0.4355 | 0.0100 | 4.6162 | 0.0448 | 0.4580 | 0.0082 | 1512 | 49 | | | | |
| RR2 | pl | 15 | 30.3278 | 295.8373 | 100.1176 | 17.6842 | 28.7166 | 68.3121 | 0.4704 | 0.0105 | 4.6730 | 0.0452 | 0.3712 | 0.0074 | 1688 | 54 | | | | |
| RR2 | pl | 16 | 31.0779 | 318.8547 | 106.5591 | 18.5852 | 30.0535 | 68.4790 | 0.4636 | 0.0104 | 5.0464 | 0.0470 | 0.4450 | 0.0081 | 1517 | 48 | | | | |
| RR2 | pl | 17 | 29.8027 | 303.3759 | 104.8955 | 18.2283 | 28.5598 | 67.7556 | 0.4291 | 0.0100 | 4.8053 | 0.0458 | 0.4337 | 0.0080 | 1469 | 48 | | | | |
| RR2 | pl | 18 | 36.5915 | 353.2740 | 139.8461 | 18.6301 | 29.9706 | 67.0433 | 0.6655 | 0.0124 | 5.6257 | 0.0495 | 0.8508 | 0.0111 | 1653 | 44 | | | | |
| RR2 | pl | 19 | 31.0904 | 319.3557 | 108.0100 | 19.1047 | 29.6652 | 65.9748 | 0.4449 | 0.0102 | 5.0707 | 0.0471 | 0.4923 | 0.0085 | 1421 | 46 | | | | |
| RR2 | pl | 20 | 32.6157 | 309.1615 | 122.1572 | 17.9247 | 29.8274 | 67.0099 | 0.5482 | 0.0113 | 4.8929 | 0.0463 | 0.6453 | 0.0097 | 1641 | 48 | | | | |
| RR2 | pl | 21 | 31.1092 | 313.5446 | 102.5190 | 18.0890 | 30.7115 | 67.5330 | 0.4844 | 0.0106 | 4.9497 | 0.0465 | 0.4092 | 0.0077 | 1631 | 51 | | | | |
| RR2 | pl | 22 | 30.4653 | 310.2635 | 111.2121 | 18.3025 | 30.4931 | 67.6666 | 0.4511 | 0.0102 | 4.8889 | 0.0462 | 0.5085 | 0.0086 | 1464 | 47 | | | | |
| RR2 | pl | 23 | 32.8595 | 312.2673 | 125.9351 | 18.2778 | 30.7982 | 66.7984 | 0.5380 | 0.0111 | 4.8919 | 0.0461 | 0.6876 | 0.0100 | 1583 | 46 | | | | |
| RR2 | pl | 24 | 33.6409 | 332.3059 | 129.6004 | 18.2877 | 31.9658 | 68.9910 | 0.5662 | 0.0114 | 5.2136 | 0.0476 | 0.7051 | 0.0101 | 1583 | 45 | | | | |
| RR2 | pl | 25 | 30.5028 | 304.5280 | 101.4184 | 18.3030 | 29.6090 | 69.4808 | 0.4522 | 0.0102 | 4.8018 | 0.0458 | 0.3726 | 0.0074 | 1595 | 51 | | | | |
| RR2 | pl | 26 | 29.8214 | 303.0252 | 102.1063 | 18.3654 | 30.2062 | 66.5869 | 0.4250 | 0.0099 | 4.7743 | 0.0457 | 0.4151 | 0.0078 | 1477 | 49 | | | | |
| RR2 | pl | 27 | 42.3054 | 603.7666 | 114.5769 | 18.4352 | 32.5248 | 69.7813 | 0.8730 | 0.0141 | 9.8474 | 0.0651 | 0.5322 | 0.0089 | 1607 | 37 | | | | |
| RR2 | pl | 28 | 33.8659 | 337.3661 | 123.9711 | 18.4722 | 30.7686 | 69.3249 | 0.5679 | 0.0114 | 5.3258 | 0.0481 | 0.6366 | 0.0096 | 1613 | 46 | | | | |
| RR2 | pl | 29 | 34.2160 | 334.4853 | 132.3275 | 17.6910 | 29.7744 | 68.5347 | 0.6114 | 0.0119 | 5.3041 | 0.0480 | 0.7450 | 0.0104 | 1653 | 46 | | | | |
| RR2 | pl | 30 | 30.8153 | 303.7014 | 108.5979 | 18.0493 | 30.5480 | 66.7539 | 0.4731 | 0.0105 | 4.7666 | 0.0456 | 0.4877 | 0.0084 | 1573 | 49 | | | | |
| RR2 | pl | 31 | 33.7284 | 341.6498 | 133.8662 | 18.4940 | 30.6031 | 68.4234 | 0.5617 | 0.0114 | 5.3998 | 0.0484 | 0.7623 | 0.0105 | 1502 | 43 | | | | |

| Sample | Occluding phase | Label | Peak Counts Pk(Pb) | Pk(Th) | Pk(U ) | Background counts Bg(Pb) | Bg(Th) | Bg(U ) | W%(Pb) | W%(Pb) 1σ | W%(Th) | W%(Th) 1σ | W%(U) | W%(U) 1σ | Chemical age (Ma) | 1σ | Early/peak meta. age (Ma) & error (2σ) | n = | Post peak meta. age (Ma) & error (2σ) | n = |
|---|---|---|---|---|---|---|---|---|---|---|---|---|---|---|---|---|---|---|---|---|
| RR2 | pl | 32 | 35.0287 | 345.9587 | 136.6685 | 18.6521 | 29.5344 | 67.6666 | 0.6056 | 0.0118 | 5.5057 | 0.0489 | 0.8062 | 0.0109 | 1563 | 43 | | | | |
| RR2 | pl | 33 | 31.8030 | 333.5084 | 117.8166 | 18.2760 | 29.1025 | 68.7573 | 0.5032 | 0.0108 | 5.3249 | 0.0483 | 0.5749 | 0.0092 | 1483 | 45 | | | | |
| RR2 | pl | 34 | 33.3908 | 374.1946 | 113.3761 | 17.7095 | 29.1451 | 67.7111 | 0.5818 | 0.0116 | 6.0119 | 0.0512 | 0.5351 | 0.0089 | 1588 | 45 | | | 1571 ± 29 | 34 |
| RR2 | K-fsp | 35 | 32.2469 | 296.9894 | 122.6451 | 18.8780 | 30.0028 | 66.8318 | 0.4964 | 0.0107 | 4.6643 | 0.0451 | 0.6509 | 0.0097 | 1540 | 47 | | | | |
| RR2 | K-fsp | 36 | 31.4092 | 269.3425 | 128.5496 | 17.8058 | 31.2511 | 69.0578 | 0.5057 | 0.0108 | 4.1644 | 0.0427 | 0.6928 | 0.0100 | 1640 | 50 | | | | |
| RR2 | K-fsp | 37 | 30.2652 | 298.3668 | 115.7652 | 17.9134 | 29.4436 | 66.6982 | 0.4597 | 0.0103 | 4.7131 | 0.0454 | 0.5741 | 0.0092 | 1479 | 47 | | | | |
| RR2 | K-fsp | 38 | 31.6718 | 301.0717 | 118.7798 | 17.8534 | 29.8450 | 66.7316 | 0.5149 | 0.0110 | 4.7514 | 0.0456 | 0.6090 | 0.0094 | 1605 | 48 | | | | |
| RR2 | K-fsp | 39 | 28.9963 | 298.3919 | 109.7486 | 17.9607 | 28.3517 | 67.3660 | 0.4073 | 0.0097 | 4.7103 | 0.0453 | 0.4938 | 0.0085 | 1376 | 46 | | | | |
| RR2 | K-fsp | 40 | 31.8093 | 266.5880 | 131.7270 | 18.1508 | 31.3934 | 67.3104 | 0.5068 | 0.0108 | 4.1055 | 0.0423 | 0.7484 | 0.0104 | 1613 | 49 | | | | |
| RR2 | K-fsp | 41 | 30.9216 | 304.7033 | 116.5157 | 18.2460 | 28.7553 | 66.1974 | 0.4703 | 0.0104 | 4.8201 | 0.0459 | 0.5872 | 0.0093 | 1479 | 46 | | | | |
| RR2 | K-fsp | 42 | 30.8904 | 300.9715 | 113.8264 | 18.4327 | 29.1159 | 68.4790 | 0.4608 | 0.0103 | 4.7380 | 0.0454 | 0.5278 | 0.0088 | 1511 | 48 | | | | |
| RR2 | K-fsp | 43 | 32.4719 | 266.9887 | 139.6960 | 17.8759 | 30.6298 | 68.9131 | 0.5409 | 0.0112 | 4.1178 | 0.0423 | 0.8210 | 0.0109 | 1650 | 48 | | | | |
| RR2 | K-fsp | 44 | 30.8404 | 260.3782 | 130.8263 | 18.5714 | 31.6898 | 68.1118 | 0.4533 | 0.0102 | 3.9820 | 0.0416 | 0.7262 | 0.0103 | 1498 | 47 | | | | |
| RR2 | K-fsp | 46 | 30.7653 | 306.4565 | 115.8778 | 18.3425 | 29.0739 | 66.1751 | 0.4683 | 0.0105 | 4.9237 | 0.0467 | 0.5897 | 0.0094 | 1451 | 46 | | | | |
| RR2 | K-fsp | 47 | 31.4717 | 301.7980 | 118.4796 | 18.3581 | 29.1098 | 68.6460 | 0.4892 | 0.0107 | 4.7897 | 0.0459 | 0.5848 | 0.0093 | 1542 | 48 | | | | |
| RR2 | K-fsp | 48 | 31.1342 | 294.0592 | 115.8277 | 18.2890 | 29.3503 | 67.7111 | 0.4812 | 0.0106 | 4.6664 | 0.0453 | 0.5661 | 0.0091 | 1558 | 49 | | | | |
| RR2 | K-fsp | 49 | 30.0902 | 275.4524 | 112.0752 | 17.8328 | 29.8384 | 67.4885 | 0.4597 | 0.0104 | 4.3391 | 0.0438 | 0.5248 | 0.0088 | 1599 | 51 | | | | |
| RR2 | K-fsp | 50 | 31.9343 | 331.9302 | 117.5289 | 17.2034 | 29.2741 | 67.5998 | 0.5552 | 0.0114 | 5.3588 | 0.0487 | 0.5924 | 0.0094 | 1605 | 47 | | | | |
| RR2 | K-fsp | 51 | 32.0156 | 330.8781 | 117.1161 | 17.8131 | 29.3591 | 66.8541 | 0.5354 | 0.0112 | 5.3424 | 0.0486 | 0.5967 | 0.0094 | 1552 | 46 | | | | |
| RR2 | K-fsp | 52 | 32.2969 | 323.9645 | 118.9549 | 17.9957 | 30.5652 | 66.0638 | 0.5404 | 0.0113 | 5.2088 | 0.0481 | 0.6287 | 0.0097 | 1569 | 47 | | | | |
| RR2 | K-fsp | 53 | 31.7718 | 310.0381 | 117.8041 | 18.3701 | 28.7288 | 68.2008 | 0.5062 | 0.0109 | 4.9979 | 0.0471 | 0.5894 | 0.0094 | 1545 | 47 | | | | |
| RR2 | K-fsp | 54 | 30.7903 | 321.7352 | 115.3399 | 18.1638 | 30.3810 | 66.9876 | 0.4764 | 0.0106 | 5.1752 | 0.0479 | 0.5748 | 0.0092 | 1437 | 45 | | | | |
| RR2 | K-fsp | 55 | 31.5280 | 316.0995 | 116.0654 | 17.7767 | 29.8845 | 65.7077 | 0.5200 | 0.0111 | 5.0873 | 0.0475 | 0.5988 | 0.0094 | 1558 | 47 | | | | |
| RR2 | K-fsp | 56 | 31.0841 | 320.2574 | 116.5282 | 18.2456 | 29.7745 | 67.4440 | 0.4842 | 0.0107 | 5.1553 | 0.0478 | 0.5830 | 0.0093 | 1457 | 45 | | | | |
| RR2 | K-fsp | 57 | 31.5905 | 308.2598 | 106.8217 | 18.0851 | 29.3522 | 66.2753 | 0.5102 | 0.0110 | 4.9539 | 0.0469 | 0.4814 | 0.0085 | 1648 | 51 | | | | |
| RR2 | K-fsp | 58 | 31.4467 | 302.9751 | 107.0093 | 18.2241 | 29.4743 | 65.9080 | 0.4989 | 0.0108 | 4.8527 | 0.0464 | 0.4872 | 0.0085 | 1633 | 51 | | | | |
| RR2 | K-fsp | 59 | 30.4965 | 303.1505 | 107.8474 | 17.7571 | 30.8886 | 68.8352 | 0.4803 | 0.0106 | 4.8286 | 0.0463 | 0.4621 | 0.0083 | 1602 | 51 | | | | |
| RR2 | K-fsp | 60 | 30.2465 | 307.3331 | 107.6097 | 18.2650 | 30.5268 | 66.0861 | 0.4502 | 0.0103 | 4.9033 | 0.0466 | 0.4916 | 0.0085 | 1471 | 47 | | | | |
| RR2 | K-fsp | 62 | 29.6089 | 301.2470 | 101.3933 | 17.8421 | 29.4317 | 65.7188 | 0.4419 | 0.0102 | 4.8122 | 0.0462 | 0.4219 | 0.0079 | 1518 | 50 | | | | |
| RR2 | K-fsp | 63 | 33.8847 | 335.4122 | 119.3177 | 18.6623 | 30.5710 | 68.0784 | 0.5664 | 0.0115 | 5.3428 | 0.0484 | 0.6026 | 0.0094 | 1630 | 47 | | | | |
| RR2 | K-fsp | 64 | 32.0968 | 323.7141 | 119.6304 | 19.0752 | 30.3551 | 67.7556 | 0.4836 | 0.0106 | 5.1439 | 0.0475 | 0.6097 | 0.0095 | 1440 | 44 | | | | |
| RR2 | K-fsp | 65 | 31.7968 | 310.8145 | 108.2101 | 18.6910 | 30.5509 | 67.4773 | 0.4900 | 0.0107 | 4.9342 | 0.0466 | 0.4796 | 0.0084 | 1594 | 50 | | | | |
| RR2 | K-fsp | 66 | 30.6466 | 305.3795 | 106.9968 | 17.9346 | 28.4155 | 66.8429 | 0.4771 | 0.0106 | 4.8941 | 0.0465 | 0.4742 | 0.0084 | 1568 | 49 | | | | |
| RR2 | K-fsp | 67 | 30.7341 | 292.3812 | 104.1575 | 17.7452 | 30.4002 | 67.8446 | 0.4899 | 0.0107 | 4.6493 | 0.0454 | 0.4301 | 0.0080 | 1703 | 54 | | | | |
| RR2 | K-fsp | 68 | 30.4153 | 298.3418 | 108.6729 | 17.7051 | 29.1560 | 69.4251 | 0.4797 | 0.0106 | 4.7822 | 0.0461 | 0.4657 | 0.0083 | 1608 | 51 | | | | |
| RR2 | K-fsp | 69 | 32.7970 | 354.3763 | 119.4303 | 17.9897 | 30.1508 | 68.5792 | 0.5522 | 0.0113 | 5.7007 | 0.0501 | 0.6013 | 0.0094 | 1527 | 44 | | | | |
| RR2 | K-fsp | 70 | 30.3590 | 301.5726 | 111.3247 | 18.1023 | 29.8209 | 67.2659 | 0.4618 | 0.0104 | 4.8212 | 0.0462 | 0.5221 | 0.0088 | 1501 | 48 | | | | |
| RR2 | K-fsp | 71 | 31.6468 | 302.4241 | 108.7480 | 18.0564 | 28.7976 | 67.6777 | 0.5128 | 0.0110 | 4.8508 | 0.0464 | 0.4863 | 0.0085 | 1676 | 51 | | | | |
| RR2 | K-fsp | 72 | 33.2783 | 306.3313 | 136.6310 | 18.5856 | 31.8356 | 66.1640 | 0.5494 | 0.0113 | 4.8347 | 0.0461 | 0.8302 | 0.0111 | 1528 | 44 | | | | |
| RR2 | K-fsp | 73 | 31.5030 | 303.1004 | 117.6415 | 18.6898 | 30.3608 | 66.8318 | 0.4820 | 0.0106 | 4.8324 | 0.0463 | 0.6016 | 0.0094 | 1500 | 47 | | | | |
| RR2 | K-fsp | 74 | 29.8527 | 300.5457 | 110.3740 | 18.0433 | 31.0624 | 67.1212 | 0.4441 | 0.0102 | 4.7786 | 0.0460 | 0.5124 | 0.0087 | 1463 | 48 | | | | |
| RR2 | K-fsp | 75 | 30.0527 | 303.4510 | 108.5478 | 17.7725 | 31.6316 | 67.0878 | 0.4658 | 0.0105 | 4.8531 | 0.0465 | 0.4945 | 0.0086 | 1527 | 49 | | | | |
| RR2 | K-fsp | 76 | 31.0779 | 298.9429 | 113.6888 | 18.2338 | 31.4399 | 65.5519 | 0.4810 | 0.0106 | 4.7252 | 0.0457 | 0.5683 | 0.0092 | 1543 | 48 | | | | |
| RR2 | K-fsp | 77 | 32.2781 | 294.6102 | 120.0307 | 17.9732 | 29.6622 | 67.5553 | 0.5392 | 0.0113 | 4.6970 | 0.0456 | 0.6214 | 0.0096 | 1676 | 50 | | | | |
| RR2 | K-fsp | 79 | 30.4715 | 303.1755 | 111.3622 | 17.8862 | 29.9241 | 66.1751 | 0.4739 | 0.0106 | 4.8447 | 0.0463 | 0.5354 | 0.0089 | 1522 | 48 | | | | |
| RR2 | K-fsp | 80 | 30.0652 | 308.2348 | 106.1463 | 18.2300 | 29.4563 | 67.0989 | 0.4421 | 0.0102 | 4.9096 | 0.0465 | 0.4596 | 0.0082 | 1469 | 48 | | | | |
| RR2 | K-fsp | 81 | 30.0652 | 312.2172 | 109.3484 | 17.9182 | 31.3526 | 66.3755 | 0.4543 | 0.0103 | 4.9487 | 0.0467 | 0.5062 | 0.0086 | 1464 | 47 | | | 1547 ± 24 | 44 |
| ALM | pl | 45 | 38.2731 | 421.7078 | 134.8796 | 18.5897 | 29.5312 | 65.9303 | 0.7155 | 0.0127 | 7.0248 | 0.0561 | 0.8467 | 0.0114 | 1543 | 39 | | | | |
| ALM | pl | 46 | 39.8235 | 414.7654 | 134.3041 | 19.1170 | 28.9701 | 64.7728 | 0.7532 | 0.0131 | 6.9113 | 0.0556 | 0.8533 | 0.0114 | 1631 | 41 | | | | |
| ALM | pl | 49 | 40.6925 | 401.7586 | 152.5072 | 19.1392 | 29.8089 | 64.7950 | 0.7870 | 0.0134 | 6.6828 | 0.0548 | 1.0780 | 0.0129 | 1612 | 39 | | | | |
| ALM | pl | 50 | 39.6422 | 396.1452 | 154.0462 | 18.6740 | 30.3347 | 66.1195 | 0.7652 | 0.0132 | 6.5699 | 0.0543 | 1.0797 | 0.0129 | 1586 | 39 | | | | |
| ALM | pl | 51 | 37.7855 | 393.0128 | 130.8889 | 18.6054 | 29.7619 | 66.0527 | 0.6990 | 0.0126 | 6.5234 | 0.0541 | 0.7961 | 0.0111 | 1611 | 42 | | | | |
| ALM | pl | 52 | 39.7235 | 372.1150 | 153.2329 | 18.6303 | 31.4801 | 65.4628 | 0.7715 | 0.0133 | 6.1294 | 0.0525 | 1.0773 | 0.0129 | 1662 | 41 | | | | |

| Sample | Occluding phase | Label | Peak Counts Pk(Pb) | Pk(Th) | Pk(U ) | Background counts Bg(Pb) | Bg(Th) | Bg(U ) | W%(Pb) | W%(Pb) 1σ | W%(Th) | W%(Th) 1σ | W%(U) | W%(U) 1σ | Chemical age (Ma) | 1σ | Early/peak meta. age (Ma) & error (2σ) | n = | Post peak meta. age (Ma) & error (2σ) | n = |
|---|---|---|---|---|---|---|---|---|---|---|---|---|---|---|---|---|---|---|---|---|
| ALM | pl | 53 | 40.0548 | 383.7413 | 154.9345 | 18.7353 | 30.8307 | 66.3866 | 0.7788 | 0.0133 | 6.3446 | 0.0534 | 1.0873 | 0.0129 | 1640 | 40 | | | | |
| ALM | pl | 54 | 40.4049 | 391.3840 | 159.5388 | 19.0998 | 29.9112 | 67.7556 | 0.7784 | 0.0133 | 6.4964 | 0.0540 | 1.1271 | 0.0132 | 1597 | 39 | | | | |
| ALM | pl | 56 | 39.6922 | 469.4352 | 120.5686 | 19.7975 | 31.2625 | 67.1434 | 0.7241 | 0.0128 | 7.8591 | 0.0594 | 0.6598 | 0.0101 | 1537 | 39 | | | | |
| ALM | pl | 57 | 39.6610 | 385.5956 | 149.9549 | 19.3434 | 29.5766 | 66.8207 | 0.7413 | 0.0130 | 6.3937 | 0.0536 | 1.0197 | 0.0125 | 1595 | 40 | | | | |
| ALM | pl | 58 | 41.2864 | 370.9373 | 166.4456 | 17.9601 | 29.9090 | 66.4868 | 0.8552 | 0.0140 | 6.1396 | 0.0526 | 1.2268 | 0.0137 | 1737 | 41 | | | | |
| ALM | pl | 59 | 36.9979 | 414.9659 | 115.3899 | 18.6431 | 30.3212 | 66.6537 | 0.6699 | 0.0124 | 6.9088 | 0.0557 | 0.5991 | 0.0096 | 1601 | 42 | | | | |
| ALM | pl | 60 | 37.3542 | 422.2342 | 113.7263 | 18.8228 | 29.5895 | 67.5330 | 0.6770 | 0.0124 | 7.0583 | 0.0563 | 0.5688 | 0.0094 | 1610 | 43 | | | | |
| ALM | pl | 61 | 36.9228 | 448.3773 | 106.9593 | 18.7120 | 29.1793 | 87.0787 | 0.6637 | 0.0123 | 7.5280 | 0.0581 | 0.2453 | 0.0062 | 1703 | 45 | | | | |
| ALM | pl | 62 | 37.7980 | 460.6858 | 105.4959 | 18.0566 | 32.5651 | 66.0193 | 0.7203 | 0.0128 | 7.6914 | 0.0588 | 0.4877 | 0.0087 | 1648 | 42 | | | | |
| ALM | pl | 63 | 37.6980 | 455.0453 | 107.6473 | 18.7547 | 29.5524 | 65.4851 | 0.6909 | 0.0125 | 7.6453 | 0.0586 | 0.5210 | 0.0090 | 1574 | 41 | | | | |
| ALM | pl | 64 | 37.0041 | 427.5477 | 106.4590 | 18.2166 | 28.7820 | 66.3866 | 0.6860 | 0.0125 | 7.1695 | 0.0568 | 0.4941 | 0.0087 | 1656 | 44 | | | | |
| ALM | pl | 65 | 38.8420 | 471.6163 | 113.8139 | 18.9777 | 31.2449 | 66.8986 | 0.7252 | 0.0129 | 7.9146 | 0.0596 | 0.5805 | 0.0095 | 1572 | 40 | | | | |
| ALM | pl | 66 | 37.6855 | 464.7471 | 112.3629 | 18.6247 | 30.3212 | 67.4217 | 0.6957 | 0.0126 | 7.8108 | 0.0593 | 0.5562 | 0.0093 | 1540 | 40 | | | | |
| ALM | pl | 67 | 35.0537 | 459.6580 | 100.8805 | 18.1883 | 28.4461 | 65.4739 | 0.6141 | 0.0118 | 7.7485 | 0.0590 | 0.4379 | 0.0082 | 1437 | 39 | | | | |
| ALM | pl | 68 | 37.3042 | 432.0593 | 110.2114 | 19.0722 | 31.4716 | 67.7890 | 0.6657 | 0.0123 | 7.2091 | 0.0570 | 0.5238 | 0.0090 | 1587 | 42 | | | | |
| ALM | pl | 69 | 38.5107 | 462.9170 | 112.7756 | 18.5934 | 29.7784 | 65.7633 | 0.7267 | 0.0129 | 7.7845 | 0.0591 | 0.5816 | 0.0095 | 1594 | 41 | | | | |
| ALM | pl | 70 | 36.8103 | 419.5524 | 109.2358 | 18.6993 | 30.8292 | 65.0733 | 0.6615 | 0.0123 | 6.9935 | 0.0561 | 0.5443 | 0.0092 | 1600 | 43 | | | | |
| ALM | pl | 71 | 36.5665 | 437.6990 | 107.4096 | 18.6801 | 31.1326 | 66.3977 | 0.6518 | 0.0122 | 7.2987 | 0.0572 | 0.5052 | 0.0088 | 1552 | 42 | | | | |
| ALM | pl | 73 | 37.0416 | 442.5869 | 109.4859 | 18.6146 | 30.2396 | 67.0321 | 0.6723 | 0.0124 | 7.4113 | 0.0577 | 0.5240 | 0.0090 | 1569 | 41 | | | | |
| ALM | pl | 74 | 36.9666 | 454.1178 | 111.9001 | 19.0153 | 29.0930 | 65.6298 | 0.6550 | 0.0122 | 7.6413 | 0.0586 | 0.5719 | 0.0094 | 1471 | 39 | | | | |
| ALM | pl | 75 | 38.3794 | 464.3961 | 112.3629 | 18.4101 | 30.0638 | 69.0912 | 0.7292 | 0.0129 | 7.8081 | 0.0592 | 0.5354 | 0.0091 | 1621 | 41 | | | | |
| ALM | pl | 76 | 37.7543 | 441.8850 | 105.5334 | 18.6919 | 30.7220 | 65.7411 | 0.6968 | 0.0126 | 7.4010 | 0.0577 | 0.4918 | 0.0087 | 1643 | 43 | | | | |
| ALM | pl | 77 | 37.9481 | 464.2708 | 110.7618 | 18.7684 | 30.6931 | 65.4628 | 0.7003 | 0.0126 | 7.7959 | 0.0592 | 0.5605 | 0.0093 | 1549 | 40 | | | | |
| ALM | pl | 78 | 37.9793 | 455.5216 | 108.4978 | 18.0210 | 29.6564 | 66.9097 | 0.7288 | 0.0129 | 7.6585 | 0.0587 | 0.5144 | 0.0089 | 1656 | 42 | | | | |
| ALM | pl | 79 | 38.6670 | 477.9594 | 119.2426 | 18.9394 | 30.6825 | 65.6298 | 0.7220 | 0.0129 | 8.0549 | 0.0602 | 0.6651 | 0.0102 | 1504 | 38 | 1596 ± 22 | 31 | | |
| ALM | sill | 6 | 36.4915 | 391.4091 | 127.2861 | 19.3198 | 30.3847 | 65.9080 | 0.6241 | 0.0119 | 6.4648 | 0.0538 | 0.7507 | 0.0107 | 1484 | 40 | | | | |
| ALM | sill | 7 | 36.9416 | 401.5081 | 120.3434 | 18.8127 | 29.8074 | 66.6203 | 0.6582 | 0.0122 | 6.6490 | 0.0545 | 0.6573 | 0.0100 | 1583 | 42 | | | | |
| ALM | sill | 8 | 36.4040 | 439.1528 | 108.7480 | 18.2349 | 30.7572 | 65.1623 | 0.6584 | 0.0122 | 7.2942 | 0.0571 | 0.5343 | 0.0090 | 1551 | 41 | | | | |
| ALM | sill | 9 | 36.7791 | 394.3911 | 110.4991 | 18.5068 | 30.7195 | 66.6092 | 0.6658 | 0.0123 | 6.5181 | 0.0540 | 0.5372 | 0.0091 | 1698 | 45 | | | | |
| ALM | sill | 10 | 37.9606 | 454.7947 | 114.7145 | 19.9664 | 30.1956 | 67.4106 | 0.6502 | 0.0121 | 7.5688 | 0.0581 | 0.5798 | 0.0094 | 1468 | 39 | | | | |
| ALM | sill | 11 | 37.6668 | 463.0423 | 113.2510 | 19.0458 | 31.2423 | 67.4996 | 0.6731 | 0.0123 | 7.6976 | 0.0586 | 0.5614 | 0.0093 | 1507 | 39 | | | | |
| ALM | sill | 12 | 39.2734 | 388.1264 | 150.9433 | 19.2697 | 30.4214 | 66.4311 | 0.7263 | 0.0128 | 6.3934 | 0.0534 | 1.0318 | 0.0125 | 1560 | 39 | | | | |
| ALM | sill | 13 | 37.8731 | 454.2933 | 110.6992 | 18.7114 | 30.5305 | 66.8763 | 0.6937 | 0.0125 | 7.5612 | 0.0581 | 0.5377 | 0.0091 | 1583 | 41 | | | | |
| ALM | sill | 16 | 34.0410 | 357.1072 | 111.6374 | 18.5210 | 29.9003 | 66.2642 | 0.5655 | 0.0113 | 5.8766 | 0.0514 | 0.5546 | 0.0092 | 1559 | 45 | | | | |
| ALM | sill | 17 | 37.9481 | 443.5895 | 115.6526 | 19.2346 | 31.4149 | 66.5202 | 0.6816 | 0.0125 | 7.3882 | 0.0575 | 0.6045 | 0.0096 | 1548 | 41 | | | | |
| ALM | sill | 18 | 37.0791 | 429.8286 | 115.6026 | 18.9843 | 31.0898 | 66.9097 | 0.6570 | 0.0122 | 7.1371 | 0.0565 | 0.5977 | 0.0096 | 1537 | 41 | | | | |
| ALM | sill | 21 | 37.2292 | 457.0759 | 115.4275 | 19.2502 | 30.8072 | 66.9876 | 0.6513 | 0.0121 | 7.6168 | 0.0583 | 0.5953 | 0.0096 | 1455 | 39 | | | | |
| ALM | sill | 22 | 36.5415 | 370.4863 | 129.3377 | 18.4270 | 30.6848 | 66.5536 | 0.6600 | 0.0123 | 6.0947 | 0.0523 | 0.7675 | 0.0108 | 1613 | 43 | | | | |
| ALM | sill | 23 | 36.2164 | 411.7329 | 120.4935 | 19.1671 | 30.5778 | 66.3643 | 0.6182 | 0.0118 | 6.8176 | 0.0552 | 0.6628 | 0.0101 | 1465 | 40 | | | | |
| ALM | sill | 25 | 37.7605 | 451.7614 | 112.8007 | 18.8695 | 30.5105 | 66.1417 | 0.6843 | 0.0124 | 7.5203 | 0.0579 | 0.5724 | 0.0094 | 1551 | 40 | | | | |
| ALM | sill | 26 | 38.0043 | 393.7395 | 129.8005 | 18.0217 | 30.2075 | 66.3532 | 0.7271 | 0.0129 | 6.5087 | 0.0540 | 0.7761 | 0.0109 | 1685 | 43 | | | | |
| ALM | sill | 27 | 40.0798 | 521.2137 | 106.5215 | 18.9470 | 31.0880 | 68.0450 | 0.7650 | 0.0132 | 8.7401 | 0.0624 | 0.4748 | 0.0086 | 1587 | 39 | | | | |
| ALM | sill | 28 | 41.9740 | 598.3723 | 112.4254 | 19.4995 | 31.0401 | 67.9559 | 0.8118 | 0.0135 | 10.1010 | 0.0671 | 0.5521 | 0.0093 | 1463 | 35 | | | | |
| ALM | sill | 29 | 40.2861 | 507.3962 | 114.0890 | 19.3882 | 30.5004 | 67.9893 | 0.7596 | 0.0131 | 8.5326 | 0.0618 | 0.5699 | 0.0094 | 1558 | 39 | | | | |
| ALM | sill | 30 | 38.6670 | 452.6639 | 112.7006 | 18.7506 | 30.1408 | 65.9525 | 0.7222 | 0.0128 | 7.5487 | 0.0581 | 0.5741 | 0.0094 | 1625 | 41 | | | | |
| ALM | sill | 31 | 37.5167 | 391.2086 | 124.7592 | 18.4711 | 29.5023 | 67.6332 | 0.6931 | 0.0126 | 6.4811 | 0.0539 | 0.6993 | 0.0103 | 1663 | 43 | | | | |
| ALM | sill | 32 | 38.2981 | 443.9906 | 118.9674 | 18.7127 | 31.6934 | 64.7839 | 0.7136 | 0.0127 | 7.3929 | 0.0576 | 0.6669 | 0.0101 | 1580 | 40 | | | | |
| ALM | sill | 33 | 37.5855 | 424.0387 | 121.7194 | 18.6698 | 29.3816 | 66.8318 | 0.6866 | 0.0125 | 7.0623 | 0.0562 | 0.6735 | 0.0102 | 1570 | 41 | | | | |
| ALM | sill | 34 | 36.4102 | 389.2540 | 124.8843 | 18.9664 | 29.2645 | 67.6999 | 0.6335 | 0.0120 | 6.4451 | 0.0537 | 0.6994 | 0.0103 | 1536 | 42 | | | | |
| ALM | sill | 35 | 35.6976 | 380.1330 | 119.8306 | 19.1019 | 31.0574 | 66.8318 | 0.6038 | 0.0117 | 6.2609 | 0.0530 | 0.6485 | 0.0100 | 1527 | 42 | | | | |
| ALM | sill | 36 | 36.2915 | 411.0813 | 119.1676 | 18.7476 | 30.6165 | 66.7873 | 0.6372 | 0.0120 | 6.8121 | 0.0552 | 0.6419 | 0.0099 | 1519 | 41 | | | | |
| ALM | sill | 37 | 35.5850 | 342.2260 | 129.9006 | 18.7857 | 28.9378 | 65.9637 | 0.6140 | 0.0118 | 5.6374 | 0.0504 | 0.7820 | 0.0109 | 1575 | 43 | | | | |
| ALM | sill | 38 | 38.0793 | 353.8001 | 151.6189 | 19.0609 | 31.6083 | 67.1657 | 0.6937 | 0.0126 | 5.7835 | 0.0509 | 1.0316 | 0.0126 | 1583 | 41 | | | | |

| Sample | Occluding phase | Label | Peak Counts Pk(Pb) | Pk(Th) | Pk(U ) | Background counts Bg(Pb) | Bg(Th) | Bg(U ) | W%(Pb) | W%(Pb) 1σ | W%(Th) | W%(Th) 1σ | W%(U) | W%(U) 1σ | Chemical age (Ma) | 1σ | Early/peak meta. age (Ma) & error (2σ) | n = | Post peak meta. age (Ma) & error (2σ) | n = |
|---|---|---|---|---|---|---|---|---|---|---|---|---|---|---|---|---|---|---|---|---|
| ALM | sill | 39 | 37.9043 | 327.6968 | 159.4262 | 18.7185 | 31.9650 | 67.3772 | 0.7013 | 0.0127 | 5.3153 | 0.0489 | 1.1226 | 0.0131 | 1621 | 41 | | | | |
| ALM | sill | 40 | 34.6286 | 334.7108 | 123.1330 | 18.4344 | 31.2691 | 66.3309 | 0.5916 | 0.0116 | 5.4584 | 0.0495 | 0.6936 | 0.0103 | 1610 | 45 | | | | |
| ALM | sill | 42 | 41.2051 | 231.4856 | 241.1118 | 18.5290 | 30.6719 | 67.5107 | 0.8402 | 0.0139 | 3.6392 | 0.0406 | 2.1121 | 0.0179 | 1615 | 36 | | | | |
| ALM | sill | 43 | 40.9925 | 237.9948 | 232.5997 | 18.8783 | 29.2510 | 65.6075 | 0.8183 | 0.0138 | 3.7804 | 0.0414 | 2.0322 | 0.0176 | 1597 | 37 | | | | |
| ALM | sill | 44 | 36.7040 | 326.9203 | 147.9281 | 18.9592 | 29.5639 | 68.3344 | 0.6471 | 0.0121 | 5.3374 | 0.0489 | 0.9695 | 0.0121 | 1589 | 42 | | | 1565 ± 22 | 33 |
| GTCD | gt | 1 | 31.9906 | 348.8146 | 104.0575 | 17.7096 | 29.2059 | 64.6058 | 0.5616 | 0.0117 | 5.9684 | 0.0528 | 0.4924 | 0.0088 | 1573 | 47 | | | | |
| GTCD | gt | 2 | 30.9279 | 336.0635 | 103.1444 | 17.7292 | 27.0603 | 66.5424 | 0.5179 | 0.0113 | 5.7669 | 0.0519 | 0.4562 | 0.0084 | 1520 | 47 | | | | |
| GTCD | gt | 3 | 31.3717 | 326.9955 | 104.4952 | 16.9894 | 30.9292 | 66.2864 | 0.5649 | 0.0118 | 5.5231 | 0.0508 | 0.4753 | 0.0086 | 1684 | 50 | | | | |
| GTCD | gt | 4 | 31.4342 | 344.5558 | 103.4071 | 17.0582 | 29.9979 | 64.3164 | 0.5648 | 0.0118 | 5.8712 | 0.0523 | 0.4876 | 0.0087 | 1604 | 48 | | | | |
| GTCD | gt | 5 | 31.5967 | 342.9274 | 107.2595 | 17.1791 | 30.4647 | 68.1563 | 0.5662 | 0.0118 | 5.8292 | 0.0521 | 0.4874 | 0.0087 | 1616 | 48 | | | | |
| GTCD | gt | 6 | 30.5653 | 334.3350 | 105.1707 | 17.9804 | 29.7200 | 63.4817 | 0.4938 | 0.0110 | 5.6890 | 0.0515 | 0.5197 | 0.0090 | 1427 | 45 | | | | |
| GTCD | gt | 7 | 31.6343 | 341.5246 | 106.3464 | 17.0899 | 31.2117 | 65.6965 | 0.5732 | 0.0119 | 5.8083 | 0.0521 | 0.5083 | 0.0089 | 1624 | 48 | | | | |
| GTCD | gt | 8 | 31.3529 | 322.1861 | 104.3076 | 17.6162 | 30.2527 | 65.8078 | 0.5391 | 0.0115 | 5.4427 | 0.0504 | 0.4784 | 0.0086 | 1627 | 50 | | | | |
| GTCD | gt | 9 | 31.4405 | 309.2867 | 107.8599 | 17.7447 | 26.7641 | 64.9397 | 0.5394 | 0.0115 | 5.2788 | 0.0497 | 0.5338 | 0.0091 | 1621 | 49 | | | | |
| GTCD | gt | 10 | 30.5403 | 310.5641 | 105.4083 | 16.7347 | 28.9579 | 64.3053 | 0.5481 | 0.0117 | 5.2981 | 0.0499 | 0.5146 | 0.0090 | 1655 | 50 | | | | |
| GTCD | gt | 11 | 30.2527 | 296.7389 | 110.5491 | 16.9722 | 28.6079 | 62.6025 | 0.5245 | 0.0114 | 5.0263 | 0.0485 | 0.5975 | 0.0096 | 1584 | 49 | | | | |
| GTCD | gt | 12 | 30.9091 | 330.0515 | 102.5440 | 17.8864 | 28.9239 | 65.5185 | 0.5125 | 0.0112 | 5.6365 | 0.0514 | 0.4625 | 0.0085 | 1526 | 47 | | | | |
| GTCD | gt | 13 | 30.4090 | 319.3557 | 102.0813 | 17.3504 | 29.1571 | 66.9542 | 0.5138 | 0.0112 | 5.4285 | 0.0504 | 0.4379 | 0.0083 | 1590 | 50 | | | | |
| GTCD | gt | 14 | 31.2154 | 322.1360 | 104.8079 | 17.9783 | 30.6430 | 64.0716 | 0.5202 | 0.0113 | 5.4480 | 0.0505 | 0.5076 | 0.0089 | 1552 | 48 | | | | |
| GTCD | gt | 15 | 30.9404 | 333.6086 | 105.3958 | 17.4287 | 29.1787 | 62.0794 | 0.5336 | 0.0115 | 5.7283 | 0.0519 | 0.5451 | 0.0093 | 1510 | 46 | | | | |
| GTCD | gt | 16 | 28.8838 | 308.4101 | 100.8680 | 17.0453 | 28.1460 | 63.3036 | 0.4664 | 0.0107 | 5.2654 | 0.0497 | 0.4703 | 0.0086 | 1462 | 48 | | | | |
| GTCD | gt | 17 | 30.1277 | 275.0768 | 113.0884 | 16.8272 | 27.4024 | 63.1812 | 0.5274 | 0.0114 | 4.6627 | 0.0468 | 0.6234 | 0.0099 | 1649 | 51 | | | | |
| GTCD | gt | 29 | 29.6401 | 303.9268 | 96.1027 | 17.7691 | 29.1451 | 66.3755 | 0.4597 | 0.0105 | 5.0705 | 0.0484 | 0.3650 | 0.0075 | 1562 | 51 | | | | |
| GTCD | gt | 30 | 29.0838 | 272.7230 | 112.9633 | 17.6413 | 27.3459 | 64.0382 | 0.4491 | 0.0105 | 4.5801 | 0.0462 | 0.6055 | 0.0097 | 1451 | 48 | | | | |
| GTCD | gt | 31 | 28.1899 | 294.1844 | 93.7013 | 17.4545 | 29.1836 | 64.7616 | 0.4177 | 0.0101 | 4.9265 | 0.0479 | 0.3578 | 0.0074 | 1465 | 50 | | | | |
| GTCD | gt | 33 | 27.7398 | 288.4243 | 94.1391 | 17.5092 | 27.9789 | 65.9191 | 0.3966 | 0.0098 | 4.8253 | 0.0473 | 0.3474 | 0.0073 | 1425 | 50 | | | | |
| GTCD | gt | 34 | 29.4839 | 286.0953 | 113.7513 | 17.6056 | 28.5212 | 64.9397 | 0.4672 | 0.0107 | 4.8170 | 0.0475 | 0.6062 | 0.0097 | 1457 | 47 | | | | |
| GTCD | gt | 35 | 30.3965 | 334.5354 | 100.7930 | 17.6035 | 28.8207 | 65.0176 | 0.4981 | 0.0110 | 5.6681 | 0.0513 | 0.4430 | 0.0083 | 1493 | 47 | | | | |
| GTCD | gt | 36 | 28.5774 | 294.9357 | 93.9640 | 17.6101 | 29.7776 | 67.0989 | 0.4249 | 0.0101 | 4.9043 | 0.0476 | 0.3304 | 0.0071 | 1516 | 51 | | | | |
| GTCD | gt | 39 | 30.6278 | 316.0494 | 96.7406 | 17.3187 | 27.6768 | 65.6743 | 0.5207 | 0.0113 | 5.3671 | 0.0500 | 0.3854 | 0.0077 | 1665 | 52 | | | | |
| GTCD | gt | 40 | 30.7028 | 318.7796 | 97.8287 | 17.7136 | 28.0659 | 64.8729 | 0.5094 | 0.0112 | 5.4251 | 0.0503 | 0.4101 | 0.0080 | 1599 | 50 | | | | |
| GTCD | gt | 41 | 29.9902 | 317.5522 | 94.9771 | 17.8682 | 29.2506 | 64.4945 | 0.4743 | 0.0108 | 5.3752 | 0.0501 | 0.3789 | 0.0077 | 1529 | 49 | | | | |
| GTCD | gt | 42 | 29.9964 | 304.3777 | 95.2022 | 17.3007 | 29.1394 | 64.2942 | 0.5009 | 0.0111 | 5.1694 | 0.0493 | 0.3866 | 0.0078 | 1650 | 52 | | | | |
| GTCD | gt | 43 | 29.8339 | 318.3287 | 95.8901 | 17.4904 | 27.6795 | 63.3704 | 0.4846 | 0.0109 | 5.4347 | 0.0504 | 0.4055 | 0.0080 | 1528 | 49 | | | | |
| GTCD | gt | 44 | 29.8589 | 312.9686 | 96.1527 | 17.3819 | 29.4348 | 64.8395 | 0.4840 | 0.0108 | 5.2387 | 0.0492 | 0.3854 | 0.0077 | 1583 | 51 | | | | |
| GTCD | gt | 45 | 30.2652 | 321.8855 | 95.2772 | 17.4067 | 27.5288 | 64.1829 | 0.5051 | 0.0111 | 5.5044 | 0.0507 | 0.3879 | 0.0078 | 1586 | 50 | | | | |
| GTCD | gt | 46 | 30.2152 | 327.0456 | 95.3898 | 18.1692 | 27.6309 | 63.7377 | 0.4703 | 0.0107 | 5.5723 | 0.0509 | 0.3932 | 0.0078 | 1467 | 47 | | | | |
| GTCD | gt | 47 | 28.2524 | 298.4420 | 93.7138 | 17.3105 | 29.5360 | 63.3927 | 0.4265 | 0.0102 | 5.0098 | 0.0483 | 0.3761 | 0.0076 | 1461 | 49 | | | | |
| GTCD | gt | 48 | 28.8525 | 325.4174 | 94.6519 | 17.8026 | 28.5300 | 64.8952 | 0.4333 | 0.0103 | 5.5572 | 0.0510 | 0.3717 | 0.0076 | 1375 | 46 | | | | |
| GTCD | gt | 49 | 30.8654 | 327.4213 | 98.5291 | 17.7863 | 29.5800 | 65.9080 | 0.5105 | 0.0112 | 5.5340 | 0.0507 | 0.4045 | 0.0079 | 1583 | 49 | | | | |
| GTCD | gt | 50 | 30.3090 | 315.1727 | 95.6900 | 17.6346 | 27.3021 | 63.0810 | 0.4971 | 0.0110 | 5.3752 | 0.0501 | 0.4059 | 0.0079 | 1577 | 50 | | | | |
| GTCD | gt | 51 | 30.7903 | 325.0667 | 96.0152 | 17.8361 | 28.4903 | 65.8635 | 0.5085 | 0.0112 | 5.5403 | 0.0509 | 0.3758 | 0.0077 | 1598 | 50 | | | | |
| GTCD | gt | 52 | 30.2652 | 325.0667 | 96.7906 | 17.8896 | 28.5650 | 63.9825 | 0.4824 | 0.0108 | 5.5049 | 0.0505 | 0.4063 | 0.0079 | 1506 | 48 | | | | |
| GTCD | gt | 53 | 30.5215 | 306.0307 | 96.0152 | 17.4923 | 28.6774 | 64.6169 | 0.5096 | 0.0112 | 5.1618 | 0.0490 | 0.3891 | 0.0078 | 1676 | 53 | | | | |
| GTCD | gt | 54 | 29.9902 | 327.5966 | 97.5285 | 17.7638 | 29.1441 | 64.8062 | 0.4766 | 0.0108 | 5.5443 | 0.0507 | 0.4056 | 0.0079 | 1482 | 47 | | | | |
| GTCD | gt | gt_94 | 33.3033 | 323.4636 | 102.3189 | 19.0154 | 31.0212 | 68.1340 | 0.5159 | 0.0108 | 5.1757 | 0.0479 | 0.4135 | 0.0079 | 1671 | 50 | | | | |
| GTCD | gt | gt_95 | 32.5282 | 264.6099 | 122.6451 | 18.2905 | 29.9577 | 66.7316 | 0.5176 | 0.0108 | 4.1762 | 0.0431 | 0.6761 | 0.0101 | 1686 | 51 | | | | |
| GTCD | gt | gt_96 | 33.6471 | 284.0418 | 122.9453 | 18.5287 | 30.6799 | 67.9782 | 0.5500 | 0.0112 | 4.5081 | 0.0448 | 0.6657 | 0.0100 | 1713 | 50 | | | | |
| GTCD | gt | gt_97 | 33.6096 | 323.8143 | 110.3615 | 18.4887 | 30.3539 | 67.2214 | 0.5477 | 0.0111 | 5.2029 | 0.0480 | 0.5226 | 0.0089 | 1668 | 49 | | | | |
| GTCD | gt | gt_98 | 33.0158 | 335.3370 | 104.9205 | 19.9355 | 30.0121 | 67.1212 | 0.4718 | 0.0103 | 5.4066 | 0.0489 | 0.4580 | 0.0083 | 1458 | 45 | | | | |
| GTCD | gt | gt_99 | 32.5219 | 251.1641 | 127.5863 | 18.4747 | 29.8925 | 67.4328 | 0.5105 | 0.0108 | 3.9388 | 0.0419 | 0.7267 | 0.0105 | 1678 | 50 | | | | |
| GTCD | gt | gt_100 | 31.9906 | 251.8401 | 128.0992 | 18.8263 | 29.6455 | 65.9414 | 0.4782 | 0.0104 | 3.9569 | 0.0420 | 0.7512 | 0.0107 | 1559 | 48 | | | | |
| GTCD | gt | gt_101 | 31.8593 | 270.0436 | 121.2816 | 18.7730 | 29.6640 | 64.4500 | 0.4769 | 0.0104 | 4.2906 | 0.0438 | 0.6894 | 0.0102 | 1531 | 48 | | | | |

| Sample | Occluding phase | Label | Peak Counts Pk(Pb) | Pk(Th) | Pk(U ) | Background counts Bg(Pb) | Bg(Th) | Bg(U ) | W%(Pb) | W%(Pb) 1σ | W%(Th) | W%(Th) 1σ | W%(U) | W%(U) 1σ | Chemical age (Ma) | 1σ | Early/peak meta. age (Ma) & error (2σ) | n = | Post peak meta. age (Ma) & error (2σ) | n = |
|---|---|---|---|---|---|---|---|---|---|---|---|---|---|---|---|---|---|---|---|---|
| GTCD | gt | gt_102 | 33.6096 | 340.6979 | 105.0706 | 18.7618 | 29.5023 | 67.8558 | 0.5367 | 0.0110 | 5.5093 | 0.0494 | 0.4510 | 0.0083 | 1628 | 48 | | | | |
| GTCD | gt | gt_103 | 32.4907 | 261.1294 | 127.2986 | 18.4134 | 28.9593 | 66.6871 | 0.5126 | 0.0108 | 4.1388 | 0.0429 | 0.7339 | 0.0105 | 1633 | 49 | | | | |
| GTCD | gt | gt_104 | 33.5721 | 257.3736 | 131.2517 | 17.9522 | 30.1113 | 64.8284 | 0.5673 | 0.0113 | 4.0376 | 0.0423 | 0.8015 | 0.0110 | 1755 | 50 | | | | |
| GTCD | gt | gt_105 | 34.0785 | 288.0487 | 125.9976 | 18.3564 | 30.9116 | 66.6760 | 0.5710 | 0.0114 | 4.5673 | 0.0450 | 0.7176 | 0.0104 | 1716 | 49 | | | | |
| GTCD | gt | gt_106 | 33.3471 | 328.4984 | 104.0700 | 19.1473 | 30.9886 | 70.1708 | 0.5127 | 0.0108 | 5.2639 | 0.0483 | 0.4101 | 0.0079 | 1644 | 50 | | | | |
| GTCD | gt | gt_107 | 32.4532 | 275.7529 | 124.9593 | 18.7149 | 29.9027 | 66.6203 | 0.4992 | 0.0106 | 4.3748 | 0.0441 | 0.7061 | 0.0103 | 1566 | 48 | | | | |
| GTCD | gt | gt_108 | 32.7032 | 288.8250 | 122.3449 | 19.0824 | 29.7801 | 67.9225 | 0.4943 | 0.0106 | 4.6039 | 0.0452 | 0.6586 | 0.0100 | 1540 | 47 | | | | |
| GTCD | gt | gt_109 | 34.6599 | 341.1488 | 108.5228 | 19.1708 | 30.6397 | 67.5219 | 0.5591 | 0.0112 | 5.4889 | 0.0493 | 0.4963 | 0.0087 | 1659 | 48 | | | | |
| GTCD | gt | gt_110 | 33.8222 | 345.4827 | 108.2351 | 19.4604 | 30.3457 | 67.7333 | 0.5180 | 0.0108 | 5.5711 | 0.0496 | 0.4904 | 0.0086 | 1534 | 46 | | | | |
| GTCD | gt | gt_112 | 32.5282 | 329.7509 | 107.4346 | 18.7402 | 31.8697 | 68.0561 | 0.4972 | 0.0106 | 5.2689 | 0.0483 | 0.4763 | 0.0085 | 1546 | 47 | | | | |
| GTCD | gt | gt_113 | 33.7222 | 329.7509 | 104.4577 | 19.0891 | 30.7591 | 67.9559 | 0.5291 | 0.0109 | 5.2948 | 0.0484 | 0.4419 | 0.0082 | 1660 | 49 | | | | |
| GTCD | gt | gt_114 | 35.0724 | 352.8231 | 109.3734 | 19.0083 | 30.3164 | 67.9893 | 0.5805 | 0.0115 | 5.7020 | 0.0502 | 0.5014 | 0.0087 | 1669 | 47 | | | | |
| GTCD | gt | gt_116 | 34.4598 | 339.0194 | 106.5716 | 19.8155 | 29.9464 | 68.9354 | 0.5288 | 0.0109 | 5.4681 | 0.0492 | 0.4557 | 0.0083 | 1610 | 48 | | | | |
| GTCD | gt | gt_117 | 33.9722 | 332.4062 | 107.3471 | 19.1299 | 31.7306 | 66.3755 | 0.5363 | 0.0110 | 5.3223 | 0.0485 | 0.4961 | 0.0087 | 1632 | 48 | | | | |
| GTCD | gt | gt_118 | 33.6659 | 330.1016 | 108.3852 | 18.9938 | 31.9767 | 68.7350 | 0.5304 | 0.0109 | 5.2795 | 0.0483 | 0.4801 | 0.0085 | 1636 | 49 | | | | |
| GTCD | gt | gt_119 | 34.0160 | 338.6187 | 106.0462 | 19.3744 | 30.2903 | 68.3789 | 0.5302 | 0.0110 | 5.4673 | 0.0492 | 0.4571 | 0.0083 | 1614 | 48 | | | | |
| GTCD | gt | gt_120 | 33.0845 | 305.1791 | 109.9863 | 18.4749 | 30.8079 | 66.0527 | 0.5305 | 0.0110 | 4.8756 | 0.0465 | 0.5324 | 0.0090 | 1684 | 50 | | | | |
| GTCD | gt | gt_121 | 33.5534 | 330.0765 | 109.3108 | 19.3145 | 30.7243 | 67.9448 | 0.5152 | 0.0108 | 5.3060 | 0.0485 | 0.5013 | 0.0087 | 1572 | 47 | | | | |
| GTCD | gt | gt_122 | 32.0406 | 251.8902 | 129.5879 | 18.7476 | 31.1910 | 65.9191 | 0.4814 | 0.0104 | 3.9201 | 0.0417 | 0.7674 | 0.0108 | 1564 | 48 | | | | |
| GTCD | gt | gt_124 | 32.6282 | 323.3884 | 107.6347 | 18.8527 | 30.3561 | 67.1434 | 0.4983 | 0.0106 | 5.1945 | 0.0480 | 0.4904 | 0.0086 | 1554 | 47 | | | | |
| GTCD | gt | gt_125 | 35.0412 | 250.3879 | 149.9299 | 19.2794 | 29.3799 | 67.2436 | 0.5709 | 0.0114 | 3.9190 | 0.0417 | 0.9955 | 0.0122 | 1642 | 46 | | | | |
| GTCD | gt | gt_126 | 31.7280 | 250.0374 | 123.3206 | 19.1046 | 30.0984 | 65.4294 | 0.4581 | 0.0102 | 3.9161 | 0.0418 | 0.6993 | 0.0103 | 1547 | 49 | | | | |
| GTCD | gt | gt_127 | 33.5971 | 335.9633 | 107.8849 | 18.2143 | 30.3500 | 66.2530 | 0.5598 | 0.0113 | 5.4359 | 0.0492 | 0.5064 | 0.0088 | 1665 | 48 | | | | |
| GTCD | gt | gt_128 | 32.7157 | 254.7946 | 125.9601 | 18.1011 | 30.6052 | 65.3626 | 0.5316 | 0.0110 | 3.9903 | 0.0421 | 0.7320 | 0.0105 | 1723 | 51 | | | | |
| GTCD | gt | gt_129 | 32.2594 | 251.4145 | 124.4339 | 18.3533 | 30.6278 | 64.8507 | 0.5060 | 0.0107 | 3.9331 | 0.0419 | 0.7200 | 0.0104 | 1671 | 51 | 1586 ± 20 | 73 | | |
| GTCD | crd | 67 | 29.7277 | 247.5838 | 116.8034 | 16.8676 | 26.5254 | 63.7822 | 0.5094 | 0.0112 | 4.1621 | 0.0443 | 0.6609 | 0.0101 | 1678 | 53 | | | | |
| GTCD | crd | 68 | 30.0090 | 258.1247 | 121.1190 | 16.9632 | 28.1927 | 63.6487 | 0.5140 | 0.0113 | 4.3067 | 0.0449 | 0.7133 | 0.0105 | 1617 | 50 | | | | |
| GTCD | crd | crd_67 | 41.0426 | 522.2169 | 102.8442 | 19.3927 | 30.4028 | 69.4251 | 0.7807 | 0.0133 | 8.6735 | 0.0618 | 0.4108 | 0.0079 | 1662 | 41 | | | | |
| GTCD | crd | crd_68 | 40.0986 | 487.1359 | 112.1627 | 20.1779 | 32.3984 | 69.3695 | 0.7162 | 0.0127 | 8.0026 | 0.0593 | 0.5231 | 0.0089 | 1571 | 40 | | | | |
| GTCD | crd | crd_69 | 39.1296 | 459.7583 | 129.5879 | 19.2597 | 33.7493 | 66.9431 | 0.7175 | 0.0127 | 7.5221 | 0.0576 | 0.7661 | 0.0108 | 1518 | 38 | | | | |
| GTCD | crd | crd_71 | 40.2174 | 478.8118 | 128.7872 | 20.2686 | 31.8292 | 68.3900 | 0.7178 | 0.0127 | 7.8714 | 0.0589 | 0.7384 | 0.0106 | 1485 | 37 | | | | |
| GTCD | crd | crd_72 | 35.4725 | 346.5599 | 128.2243 | 18.9883 | 29.5573 | 67.4328 | 0.5981 | 0.0116 | 5.6273 | 0.0500 | 0.7395 | 0.0106 | 1566 | 44 | | | | |
| GTCD | crd | crd_73 | 32.3906 | 288.6998 | 123.6584 | 18.8100 | 28.8242 | 66.0861 | 0.4936 | 0.0106 | 4.6309 | 0.0454 | 0.6990 | 0.0103 | 1504 | 46 | | | | |
| GTCD | crd | crd_74 | 33.3346 | 285.6696 | 124.1462 | 18.7376 | 29.4173 | 67.0878 | 0.5317 | 0.0110 | 4.5699 | 0.0451 | 0.6930 | 0.0103 | 1627 | 48 | | | | |
| GTCD | crd | crd_75 | 37.4855 | 416.1188 | 115.0522 | 19.8111 | 32.6008 | 68.8909 | 0.6361 | 0.0120 | 6.7631 | 0.0546 | 0.5617 | 0.0092 | 1571 | 42 | | | | |
| GTCD | crd | crd_76 | 37.3667 | 452.0121 | 105.1206 | 20.0373 | 32.3246 | 68.8575 | 0.6239 | 0.0118 | 7.4025 | 0.0571 | 0.4428 | 0.0082 | 1508 | 41 | | | | |
| GTCD | crd | crd_77 | 39.9673 | 459.1065 | 115.3899 | 19.6287 | 30.3778 | 68.3232 | 0.7311 | 0.0128 | 7.5436 | 0.0576 | 0.5739 | 0.0094 | 1644 | 42 | | | | |
| GTCD | crd | crd_78 | 37.5042 | 440.0050 | 112.7006 | 19.0235 | 32.3087 | 67.0099 | 0.6645 | 0.0122 | 7.1815 | 0.0562 | 0.5567 | 0.0092 | 1569 | 41 | | | | |
| GTCD | crd | crd_79 | 37.6605 | 428.8260 | 114.4518 | 19.3212 | 31.3958 | 69.6589 | 0.6593 | 0.0122 | 6.9985 | 0.0555 | 0.5450 | 0.0091 | 1594 | 42 | | | | |
| GTCD | crd | crd_80 | 32.7907 | 266.3627 | 125.8975 | 18.8543 | 29.1978 | 65.2736 | 0.5062 | 0.0107 | 4.2214 | 0.0433 | 0.7335 | 0.0105 | 1598 | 48 | | | | |
| GTCD | crd | crd_81 | 32.5594 | 260.3532 | 125.2971 | 18.6405 | 31.5816 | 68.3455 | 0.5050 | 0.0107 | 4.0680 | 0.0425 | 0.6879 | 0.0102 | 1664 | 50 | | | | |
| GTCD | crd | crd_82 | 37.5167 | 434.0896 | 117.7541 | 19.3420 | 29.4336 | 73.7882 | 0.6561 | 0.0122 | 7.1544 | 0.0562 | 0.5375 | 0.0091 | 1566 | 42 | | | | |
| GTCD | crd | crd_84 | 33.3221 | 333.2578 | 101.3808 | 19.0164 | 30.2029 | 66.8541 | 0.5174 | 0.0108 | 5.3687 | 0.0488 | 0.4183 | 0.0080 | 1628 | 49 | | | | |
| GTCD | crd | crd_85 | 37.2417 | 396.9221 | 121.7570 | 19.4100 | 29.7184 | 66.2308 | 0.6464 | 0.0121 | 6.5056 | 0.0537 | 0.6772 | 0.0102 | 1568 | 42 | | | | |
| GTCD | crd | crd_86 | 33.8659 | 260.8540 | 132.1399 | 19.1964 | 29.4451 | 66.4200 | 0.5320 | 0.0110 | 4.1126 | 0.0427 | 0.7938 | 0.0109 | 1647 | 48 | | | | |
| GTCD | crd | crd_87 | 33.2783 | 263.5081 | 125.1345 | 18.8438 | 30.7396 | 65.8301 | 0.5245 | 0.0109 | 4.1423 | 0.0429 | 0.7171 | 0.0104 | 1680 | 50 | | | | |
| GTCD | crd | crd_88 | 37.1416 | 361.0907 | 115.7527 | 19.3602 | 30.3481 | 68.1563 | 0.6421 | 0.0120 | 5.8474 | 0.0508 | 0.5776 | 0.0094 | 1741 | 47 | | | | |
| GTCD | crd | crd_89 | 37.0916 | 423.5876 | 116.2780 | 20.1164 | 31.5649 | 71.0279 | 0.6095 | 0.0117 | 6.8998 | 0.0551 | 0.5500 | 0.0091 | 1494 | 41 | | | | |
| GTCD | crd | crd_90 | 32.7470 | 293.4331 | 124.5715 | 18.7065 | 30.2388 | 66.1306 | 0.5092 | 0.0107 | 4.6768 | 0.0456 | 0.7076 | 0.0103 | 1533 | 46 | | | | |
| GTCD | crd | crd_91 | 34.8661 | 335.4122 | 117.3663 | 19.2547 | 29.9210 | 66.6203 | 0.5668 | 0.0113 | 5.4296 | 0.0491 | 0.6172 | 0.0097 | 1604 | 46 | | | | |
| GTCD | crd | crd_92 | 32.9908 | 280.9616 | 128.9123 | 18.7177 | 30.3509 | 66.2864 | 0.5182 | 0.0108 | 4.4569 | 0.0445 | 0.7582 | 0.0107 | 1565 | 47 | | | | |
| GTCD | crd | crd_93 | 38.3419 | 427.8484 | 119.7305 | 19.2736 | 31.7129 | 69.3806 | 0.6879 | 0.0125 | 6.9891 | 0.0555 | 0.6135 | 0.0097 | 1618 | 42 | | | | |
| GTCD | crd | crd_95 | 33.9285 | 368.3817 | 108.6604 | 19.3203 | 30.9073 | 68.6794 | 0.5266 | 0.0109 | 5.9638 | 0.0513 | 0.4849 | 0.0086 | 1488 | 44 | | | | |

| Sample | Occluding phase | Label | Peak Counts Pk(Pb) | Pk(Th) | Pk(U ) | Background counts Bg(Pb) | Bg(Th) | Bg(U ) | W%(Pb) | W%(Pb) 1σ | W%(Th) | W%(Th) 1σ | W%(U) | W%(U) 1σ | Chemical age (Ma) | 1σ | Early/peak meta. age (Ma) & error (2σ) | n = | Post peak meta. age (Ma) & error (2σ) | n = |
|---|---|---|---|---|---|---|---|---|---|---|---|---|---|---|---|---|---|---|---|---|
| GTCD | crd | crd_96 | 37.3167 | 411.9334 | 121.7319 | 19.2181 | 32.9294 | 67.6666 | 0.6526 | 0.0121 | 6.6861 | 0.0543 | 0.6575 | 0.0100 | 1564 | 42 | | | | |
| GTCD | crd | crd_97 | 35.9789 | 407.6229 | 96.7030 | 18.9692 | 32.1720 | 68.3455 | 0.6147 | 0.0118 | 6.6402 | 0.0542 | 0.3455 | 0.0073 | 1683 | 47 | | | | |
| GTCD | crd | crd_98 | 35.8976 | 404.0642 | 110.3115 | 19.4886 | 31.2904 | 67.8335 | 0.5922 | 0.0116 | 6.5870 | 0.0539 | 0.5170 | 0.0089 | 1524 | 43 | | | | |
| GTCD | crd | crd_99 | 35.2662 | 380.4086 | 110.5366 | 19.0724 | 31.9487 | 66.8429 | 0.5848 | 0.0115 | 6.1596 | 0.0522 | 0.5307 | 0.0090 | 1572 | 44 | | | | |
| GTCD | crd | crd_100 | 36.7728 | 397.5987 | 121.9696 | 18.8886 | 31.7132 | 67.0767 | 0.6462 | 0.0121 | 6.4653 | 0.0534 | 0.6677 | 0.0101 | 1580 | 42 | | | | |
| GTCD | crd | crd_101 | 36.3540 | 385.9714 | 115.7402 | 19.6202 | 33.0438 | 67.6777 | 0.6035 | 0.0117 | 6.2317 | 0.0524 | 0.5835 | 0.0094 | 1571 | 44 | 1587 ± 23 | 13 | | |
| GTCD | sill | als_1 | 33.6659 | 348.9900 | 99.3921 | 19.3551 | 31.6935 | 66.3198 | 0.5160 | 0.0108 | 5.6110 | 0.0498 | 0.4007 | 0.0078 | 1586 | 48 | | | | |
| GTCD | sill | als_2 | 33.9785 | 351.3700 | 109.6486 | 18.9030 | 29.7998 | 68.2231 | 0.5443 | 0.0111 | 5.6885 | 0.0502 | 0.5022 | 0.0087 | 1575 | 46 | | | | |
| GTCD | sill | als_3 | 32.9345 | 295.8624 | 115.6151 | 19.1540 | 28.8815 | 66.3421 | 0.5042 | 0.0107 | 4.7784 | 0.0462 | 0.6007 | 0.0096 | 1575 | 48 | | | | |
| GTCD | sill | als_4 | 33.3471 | 279.5342 | 127.8490 | 18.9256 | 29.7669 | 67.0544 | 0.5246 | 0.0109 | 4.4476 | 0.0445 | 0.7366 | 0.0106 | 1600 | 47 | | | | |
| GTCD | sill | als_5 | 32.2469 | 328.0976 | 112.0627 | 18.9711 | 28.9519 | 67.0433 | 0.4840 | 0.0105 | 5.3366 | 0.0488 | 0.5486 | 0.0091 | 1445 | 45 | | | | |
| GTCD | sill | als_6 | 35.2725 | 293.9840 | 133.4659 | 18.9375 | 30.9743 | 66.5536 | 0.5961 | 0.0117 | 4.6918 | 0.0457 | 0.8134 | 0.0111 | 1685 | 47 | | | | |
| GTCD | sill | als_7 | 35.0474 | 367.5047 | 106.6341 | 19.8615 | 31.7585 | 66.2976 | 0.5486 | 0.0111 | 5.9408 | 0.0513 | 0.4897 | 0.0086 | 1547 | 45 | | | | |
| GTCD | sill | als_8 | 33.1470 | 319.2805 | 113.3385 | 18.8888 | 31.9513 | 67.1880 | 0.5209 | 0.0109 | 5.1301 | 0.0479 | 0.5623 | 0.0093 | 1579 | 47 | | | | |
| GTCD | sill | als_9 | 35.6913 | 306.7821 | 137.7194 | 19.1625 | 30.5648 | 65.5296 | 0.6044 | 0.0118 | 4.9292 | 0.0469 | 0.8784 | 0.0116 | 1616 | 45 | | | | |
| GTCD | sill | als_10 | 34.9724 | 370.1356 | 111.6874 | 18.9669 | 30.6982 | 68.4902 | 0.5804 | 0.0115 | 6.0203 | 0.0517 | 0.5258 | 0.0089 | 1590 | 45 | | | | |
| GTCD | sill | als_11 | 34.1973 | 334.4102 | 115.5525 | 19.4136 | 30.9880 | 67.4551 | 0.5381 | 0.0111 | 5.3996 | 0.0490 | 0.5850 | 0.0094 | 1556 | 46 | | | | |
| GTCD | sill | als_13 | 34.2348 | 358.0341 | 103.6197 | 18.7488 | 31.3436 | 66.3866 | 0.5585 | 0.0112 | 5.7708 | 0.0505 | 0.4509 | 0.0083 | 1633 | 47 | 1585 ± 31 | 21 | | |
| GTCD | pl | 57 | 30.4028 | 250.7635 | 115.2273 | 16.8596 | 30.6528 | 64.8395 | 0.5299 | 0.0114 | 4.0909 | 0.0436 | 0.6196 | 0.0098 | 1793 | 55 | | | | |
| GTCD | pl | 58 | 29.9964 | 286.4960 | 110.5241 | 17.5407 | 28.1143 | 65.1067 | 0.4849 | 0.0109 | 4.7885 | 0.0471 | 0.5591 | 0.0093 | 1549 | 49 | | | | |
| GTCD | pl | 59 | 29.1525 | 300.9715 | 85.5720 | 17.6941 | 28.6021 | 64.1050 | 0.4479 | 0.0105 | 5.0749 | 0.0486 | 0.2661 | 0.0064 | 1608 | 54 | | | | |
| GTCD | pl | 60 | 29.8464 | 311.9417 | 97.0658 | 17.5394 | 29.5507 | 64.0827 | 0.4805 | 0.0108 | 5.2507 | 0.0494 | 0.4085 | 0.0080 | 1552 | 50 | | | | |
| GTCD | pl | 60 | 30.2027 | 298.2667 | 106.3839 | 17.2916 | 27.0451 | 63.7711 | 0.5110 | 0.0112 | 5.1067 | 0.0490 | 0.5340 | 0.0091 | 1577 | 49 | | | | |
| GTCD | pl | 61 | 29.8589 | 317.6274 | 95.2272 | 17.5206 | 29.1875 | 64.6392 | 0.4819 | 0.0108 | 5.3637 | 0.0499 | 0.3791 | 0.0077 | 1555 | 50 | | | | |
| GTCD | pl | 61 | 27.8836 | 242.2509 | 111.0120 | 16.8753 | 28.6113 | 62.3353 | 0.4443 | 0.0106 | 4.1098 | 0.0445 | 0.6196 | 0.0099 | 1525 | 51 | | | | |
| GTCD | pl | 62 | 29.2651 | 274.9266 | 98.6042 | 17.2803 | 28.3771 | 71.6178 | 0.4698 | 0.0107 | 4.6041 | 0.0464 | 0.3345 | 0.0072 | 1740 | 57 | | | | |
| GTCD | pl | 63 | 28.6087 | 318.9799 | 87.0102 | 16.5887 | 25.7554 | 59.9536 | 0.5087 | 0.0116 | 5.9044 | 0.0545 | 0.3642 | 0.0078 | 1532 | 50 | | | | |
| GTCD | pl | 64 | 30.4465 | 317.4270 | 95.7150 | 17.4369 | 29.2264 | 66.3755 | 0.5063 | 0.0111 | 5.3371 | 0.0497 | 0.3621 | 0.0075 | 1648 | 52 | | | | |
| GTCD | pl | 64 | 26.3896 | 277.3305 | 75.1419 | 15.3896 | 26.5101 | 59.7978 | 0.4715 | 0.0112 | 5.1146 | 0.0511 | 0.2081 | 0.0059 | 1733 | 59 | | | | |
| GTCD | pl | 65 | 29.3151 | 309.4370 | 96.1902 | 17.6580 | 28.2400 | 64.1050 | 0.4554 | 0.0105 | 5.2370 | 0.0494 | 0.3980 | 0.0079 | 1487 | 49 | | | | |
| GTCD | pl | 65 | 25.7520 | 271.6712 | 75.8673 | 16.2151 | 26.7399 | 59.4862 | 0.4111 | 0.0105 | 5.0369 | 0.0509 | 0.2240 | 0.0062 | 1528 | 56 | | | | |
| GTCD | pl | 66 | 30.0840 | 310.4388 | 94.9395 | 18.0052 | 29.4121 | 64.5279 | 0.4725 | 0.0107 | 5.2379 | 0.0494 | 0.3775 | 0.0077 | 1555 | 50 | | | | |
| GTCD | pl | 66 | 27.9711 | 278.7830 | 109.1482 | 15.2030 | 25.4326 | 59.4862 | 0.5583 | 0.0124 | 5.2628 | 0.0523 | 0.6873 | 0.0109 | 1566 | 49 | 1591 ± 50 | 15 | | |
| PS | bt | 1 | 37.8043 | 247.1832 | 228.9071 | 17.0528 | 30.3069 | 64.9174 | 0.8170 | 0.0142 | 4.0220 | 0.0432 | 2.0642 | 0.0180 | 1551 | 37 | | | | |
| PS | bt | 2 | 37.2354 | 245.9563 | 216.0149 | 17.0448 | 27.3118 | 64.2274 | 0.7977 | 0.0140 | 4.0698 | 0.0435 | 1.9184 | 0.0174 | 1576 | 38 | | | | |
| PS | bt | 3 | 36.4790 | 244.1537 | 181.7991 | 18.1968 | 28.5786 | 63.3148 | 0.7219 | 0.0133 | 4.0112 | 0.0432 | 1.4956 | 0.0154 | 1655 | 42 | | | | |
| PS | bt | 4 | 28.9775 | 200.8459 | 140.9221 | 17.0031 | 27.0151 | 62.0682 | 0.4787 | 0.0109 | 3.2773 | 0.0393 | 1.0024 | 0.0126 | 1515 | 48 | | | | |
| PS | bt | 5 | 23.6392 | 110.1864 | 110.3365 | 16.7812 | 28.3654 | 64.2942 | 0.2697 | 0.0081 | 1.5377 | 0.0269 | 0.5773 | 0.0095 | 1613 | 67 | | | | |
| PS | bt | 6 | 28.5837 | 258.5504 | 100.8430 | 16.6097 | 27.5094 | 62.5579 | 0.4759 | 0.0109 | 4.3384 | 0.0451 | 0.4879 | 0.0088 | 1683 | 55 | | | | |
| PS | bt | 7 | 24.3893 | 107.2345 | 116.9160 | 17.2105 | 28.4522 | 65.1178 | 0.2852 | 0.0084 | 1.4931 | 0.0266 | 0.6549 | 0.0102 | 1603 | 65 | | | | |
| PS | bt | 8 | 27.2835 | 203.0236 | 108.4478 | 16.9935 | 27.4921 | 64.3387 | 0.4093 | 0.0101 | 3.3044 | 0.0394 | 0.5599 | 0.0094 | 1660 | 58 | | | | |
| PS | bt | 10 | 26.7897 | 180.1223 | 108.4228 | 17.0502 | 28.0447 | 60.6436 | 0.3872 | 0.0098 | 2.8640 | 0.0367 | 0.6053 | 0.0098 | 1656 | 59 | | | | |
| PS | bt | 11 | 24.4268 | 119.3427 | 120.6687 | 17.3304 | 27.7214 | 61.7121 | 0.2812 | 0.0083 | 1.7331 | 0.0286 | 0.7451 | 0.0108 | 1402 | 57 | | | | |
| PS | bt | 12 | 23.8142 | 56.7597 | 132.7028 | 16.5480 | 27.3898 | 63.6709 | 0.2876 | 0.0084 | 0.5539 | 0.0162 | 0.8636 | 0.0116 | 1683 | 64 | | | | |
| PS | bt | 13 | 34.1973 | 243.8282 | 185.8410 | 17.3350 | 28.2047 | 63.1367 | 0.6678 | 0.0129 | 4.0263 | 0.0434 | 1.5547 | 0.0157 | 1513 | 40 | | | | |
| PS | bt | 14 | 37.9168 | 238.5957 | 228.2437 | 16.8308 | 28.7978 | 65.8524 | 0.8354 | 0.0144 | 3.9158 | 0.0427 | 2.0566 | 0.0180 | 1598 | 37 | | | | |
| PS | bt | 15 | 38.0668 | 240.3983 | 219.1690 | 17.1160 | 27.5976 | 62.2240 | 0.8341 | 0.0144 | 3.9902 | 0.0432 | 1.9973 | 0.0178 | 1613 | 38 | | | | |
| PS | bt | 16 | 35.4850 | 251.1891 | 197.3167 | 16.9558 | 28.1586 | 65.8078 | 0.7356 | 0.0135 | 4.1740 | 0.0442 | 1.6718 | 0.0163 | 1567 | 40 | | | | |
| PS | bt | 17 | 34.2285 | 241.6000 | 186.5919 | 16.9086 | 26.7064 | 65.9859 | 0.6888 | 0.0131 | 4.0286 | 0.0435 | 1.5342 | 0.0156 | 1566 | 41 | | | | |
| PS | bt | 18 | 32.1031 | 216.6908 | 155.9729 | 17.4917 | 28.1762 | 64.8062 | 0.5846 | 0.0121 | 3.5534 | 0.0409 | 1.1615 | 0.0136 | 1632 | 47 | | | | |
| PS | bt | 19 | 27.1522 | 194.6636 | 112.5505 | 16.9313 | 27.0104 | 62.7137 | 0.4070 | 0.0101 | 3.1583 | 0.0386 | 0.6326 | 0.0100 | 1619 | 57 | | | | |
| PS | bt | 20 | 28.1836 | 216.4905 | 120.2934 | 17.2897 | 28.3194 | 61.7566 | 0.4350 | 0.0104 | 3.5530 | 0.0410 | 0.7467 | 0.0109 | 1518 | 51 | | | | |
| PS | bt | 21 | 28.3837 | 199.3191 | 124.4214 | 16.6128 | 26.5630 | 62.8918 | 0.4700 | 0.0108 | 3.2554 | 0.0392 | 0.7818 | 0.0111 | 1668 | 54 | | | | |

| Sample | Occluding phase | Label | Peak Counts Pk(Pb) | Pk(Th) | Pk(U ) | Background counts Bg(Pb) | Bg(Th) | Bg(U ) | W%(Pb) | W%(Pb) 1σ | W%(Th) | W%(Th) 1σ | W%(U) | W%(U) 1σ | Chemical age (Ma) | 1σ | Early/peak meta. age (Ma) & error (2σ) | n = | Post peak meta. age (Ma) & error (2σ) | n = |
|---|---|---|---|---|---|---|---|---|---|---|---|---|---|---|---|---|---|---|---|---|
| PS | bt | 22 | 28.6900 | 219.7197 | 133.1782 | 16.8515 | 27.6518 | 62.9586 | 0.4721 | 0.0108 | 3.6165 | 0.0413 | 0.8936 | 0.0119 | 1506 | 48 | | | | |
| PS | bt | 23 | 36.5540 | 242.1508 | 189.7705 | 17.7886 | 27.8762 | 64.3610 | 0.7495 | 0.0137 | 4.0349 | 0.0436 | 1.6032 | 0.0160 | 1648 | 41 | | | | |
| PS | bt | 24 | 34.7911 | 230.1087 | 167.7969 | 18.3890 | 27.4906 | 65.6965 | 0.6564 | 0.0128 | 3.8319 | 0.0426 | 1.3099 | 0.0145 | 1655 | 45 | | | | |
| PS | bt | 25 | 32.3219 | 234.0392 | 162.5292 | 17.2355 | 26.4283 | 62.7137 | 0.5993 | 0.0122 | 3.8925 | 0.0427 | 1.2687 | 0.0142 | 1541 | 43 | | | | |
| PS | bt | 26 | 32.2531 | 239.0213 | 162.7669 | 16.5123 | 29.2243 | 64.2274 | 0.6260 | 0.0125 | 3.9335 | 0.0429 | 1.2524 | 0.0141 | 1605 | 44 | | | | |
| PS | bt | 27 | 33.2721 | 238.2452 | 163.9556 | 17.4422 | 27.2427 | 65.2291 | 0.6307 | 0.0125 | 3.9647 | 0.0432 | 1.2578 | 0.0142 | 1607 | 44 | | | | |
| PS | bt | 29 | 32.8282 | 235.7666 | 170.6999 | 17.7711 | 28.0452 | 63.8490 | 0.5996 | 0.0122 | 3.9045 | 0.0428 | 1.3617 | 0.0147 | 1488 | 42 | | | | |
| PS | bt | 30 | 36.1727 | 234.1143 | 204.9509 | 17.0307 | 28.5764 | 63.5374 | 0.7635 | 0.0138 | 3.8619 | 0.0426 | 1.8019 | 0.0169 | 1597 | 39 | | | | |
| PS | bt | 31 | 32.3406 | 230.7346 | 154.6968 | 17.4222 | 27.4332 | 62.3799 | 0.5944 | 0.0122 | 3.8201 | 0.0424 | 1.1750 | 0.0137 | 1599 | 45 | | | | |
| PS | bt | 32 | 28.7587 | 183.3758 | 131.6520 | 16.7937 | 27.8087 | 65.2736 | 0.4764 | 0.0109 | 2.9248 | 0.0371 | 0.8403 | 0.0115 | 1717 | 55 | | | | |
| PS | bt | 33 | 22.7953 | 127.4487 | 82.8831 | 17.1201 | 27.6142 | 64.1161 | 0.2220 | 0.0074 | 1.8816 | 0.0298 | 0.2365 | 0.0061 | 1744 | 84 | | | | |
| PS | bt | 34 | 35.4600 | 316.2999 | 159.0383 | 17.8383 | 28.7095 | 62.5579 | 0.7005 | 0.0132 | 5.3883 | 0.0502 | 1.2357 | 0.0141 | 1548 | 41 | | | | |
| PS | bt | 35 | 26.2396 | 197.1415 | 87.6605 | 17.9515 | 28.9055 | 66.1417 | 0.3269 | 0.0090 | 3.1733 | 0.0387 | 0.2742 | 0.0066 | 1694 | 67 | | | | |
| PS | bt | 36 | 22.9453 | 125.1720 | 87.8606 | 17.0223 | 28.7620 | 62.9363 | 0.2310 | 0.0075 | 1.8085 | 0.0291 | 0.3125 | 0.0070 | 1695 | 79 | | | | |
| PS | bt | 37 | 22.2327 | 103.1319 | 93.1135 | 17.1324 | 27.9023 | 64.7839 | 0.1993 | 0.0070 | 1.4223 | 0.0259 | 0.3572 | 0.0075 | 1594 | 79 | | | | |
| PS | bt | 38 | 28.1649 | 233.3382 | 104.5328 | 17.0798 | 27.6613 | 64.2274 | 0.4412 | 0.0105 | 3.8725 | 0.0427 | 0.5137 | 0.0090 | 1664 | 56 | | | | |
| PS | bt | 39 | 24.2830 | 163.5302 | 83.2833 | 16.9484 | 26.7021 | 65.5852 | 0.2885 | 0.0084 | 2.5713 | 0.0348 | 0.2234 | 0.0059 | 1830 | 78 | | | | |
| PS | bt | 41 | 37.5980 | 252.8416 | 190.5839 | 18.1517 | 29.2121 | 66.5424 | 0.7728 | 0.0139 | 4.1926 | 0.0443 | 1.5808 | 0.0159 | 1681 | 42 | | | | |
| PS | bt | 42 | 34.6286 | 244.3540 | 190.3211 | 17.1496 | 29.0859 | 62.4244 | 0.6952 | 0.0131 | 4.0391 | 0.0435 | 1.6293 | 0.0161 | 1529 | 40 | | | | |
| PS | bt | 44 | 39.8048 | 245.8562 | 216.2527 | 18.2021 | 26.1193 | 65.9859 | 0.8543 | 0.0145 | 4.0948 | 0.0437 | 1.9022 | 0.0173 | 1678 | 39 | | | | |
| PS | bt | 45 | 35.5288 | 247.5838 | 196.8161 | 17.2222 | 27.4248 | 63.2035 | 0.7203 | 0.0133 | 4.0853 | 0.0435 | 1.6840 | 0.0163 | 1544 | 39 | | | | |
| PS | bt | 46 | 34.6348 | 243.0271 | 181.4237 | 17.7372 | 29.3758 | 64.7171 | 0.6677 | 0.0128 | 3.9830 | 0.0431 | 1.4765 | 0.0153 | 1560 | 41 | | | | |
| PS | bt | 47 | 32.7845 | 239.8725 | 157.9623 | 16.5470 | 28.3840 | 67.8558 | 0.6474 | 0.0127 | 3.9709 | 0.0432 | 1.1470 | 0.0135 | 1715 | 47 | | | | |
| PS | bt | 48 | 32.9533 | 238.0699 | 157.6620 | 17.4437 | 27.4739 | 64.7616 | 0.6207 | 0.0125 | 3.9698 | 0.0433 | 1.1869 | 0.0138 | 1627 | 45 | | | | |
| PS | bt | 49 | 33.9785 | 239.7974 | 159.6264 | 17.9802 | 27.2398 | 63.8045 | 0.6368 | 0.0126 | 3.9875 | 0.0432 | 1.2189 | 0.0139 | 1641 | 45 | | | | |
| PS | bt | 50 | 31.5655 | 233.1630 | 160.9652 | 17.0251 | 27.2693 | 63.6264 | 0.5822 | 0.0121 | 3.8819 | 0.0428 | 1.2428 | 0.0141 | 1518 | 44 | | | | |
| PS | bt | 51 | 32.5282 | 229.3327 | 158.6880 | 17.9467 | 28.3141 | 64.4723 | 0.5841 | 0.0121 | 3.7904 | 0.0423 | 1.2022 | 0.0138 | 1562 | 45 | | | | |
| PS | bt | 53 | 30.4028 | 222.8739 | 152.8075 | 16.5118 | 25.9417 | 63.2925 | 0.5576 | 0.0118 | 3.7197 | 0.0419 | 1.1433 | 0.0135 | 1547 | 46 | | | | |
| PS | bt | 54 | 30.6403 | 223.0491 | 148.0282 | 16.7206 | 29.0430 | 62.7805 | 0.5590 | 0.0118 | 3.6687 | 0.0416 | 1.0899 | 0.0132 | 1595 | 47 | | | | |
| PS | bt | 56 | 25.1707 | 147.7905 | 106.4465 | 16.8829 | 25.8126 | 64.9174 | 0.3284 | 0.0090 | 2.3006 | 0.0329 | 0.5255 | 0.0091 | 1685 | 65 | | | | |
| PS | bt | 57 | 23.2204 | 131.8521 | 87.0852 | 17.6205 | 27.1786 | 63.4038 | 0.2187 | 0.0073 | 1.9723 | 0.0305 | 0.2987 | 0.0069 | 1558 | 74 | | | | |
| PS | bt | 59 | 32.4594 | 194.9389 | 167.8345 | 17.1971 | 28.4212 | 64.8507 | 0.6055 | 0.0123 | 3.1124 | 0.0381 | 1.2983 | 0.0143 | 1672 | 46 | | | | |
| PS | bt | 60 | 23.7329 | 156.2982 | 86.9727 | 16.8327 | 26.9946 | 64.5836 | 0.2710 | 0.0082 | 2.4315 | 0.0338 | 0.2826 | 0.0067 | 1693 | 73 | | | | |
| PS | bt | 62 | 34.0597 | 225.1019 | 184.5021 | 17.2786 | 26.7675 | 63.4038 | 0.6684 | 0.0129 | 3.7201 | 0.0418 | 1.5378 | 0.0156 | 1567 | 41 | | | | |
| PS | bt | 63 | 27.5335 | 222.6736 | 100.1051 | 16.6323 | 27.6920 | 64.6503 | 0.4341 | 0.0104 | 3.6748 | 0.0416 | 0.4518 | 0.0085 | 1757 | 60 | | | | |
| PS | bt | 65 | 21.7014 | 111.0120 | 76.6926 | 17.1454 | 28.4704 | 62.8028 | 0.1764 | 0.0065 | 1.5566 | 0.0271 | 0.1748 | 0.0052 | 1735 | 93 | | | | |
| PS | bt | 66 | 23.4517 | 114.4143 | 97.9037 | 17.7012 | 29.5479 | 66.1417 | 0.2249 | 0.0074 | 1.5989 | 0.0274 | 0.3996 | 0.0079 | 1603 | 74 | | | | |
| PS | bt | 67 | 28.7650 | 265.0105 | 106.7967 | 17.2012 | 27.6716 | 62.6247 | 0.4592 | 0.0107 | 4.4588 | 0.0458 | 0.5638 | 0.0095 | 1538 | 51 | | | | |
| PS | bt | 68 | 24.3268 | 167.2839 | 91.9629 | 17.2076 | 28.2643 | 65.0065 | 0.2822 | 0.0084 | 2.6329 | 0.0353 | 0.3430 | 0.0074 | 1582 | 67 | | | | |
| PS | bt | 70 | 33.9222 | 234.6901 | 180.1348 | 17.8114 | 29.4193 | 65.4517 | 0.6389 | 0.0126 | 3.8349 | 0.0423 | 1.4514 | 0.0152 | 1535 | 42 | | | | |
| PS | bt | 72 | 27.8023 | 207.0535 | 121.2691 | 16.6879 | 26.3563 | 62.6247 | 0.4422 | 0.0105 | 3.3962 | 0.0399 | 0.7438 | 0.0109 | 1579 | 53 | | | | |
| PS | bt | 74 | 39.7047 | 267.8651 | 237.9072 | 18.4572 | 28.8382 | 69.4808 | 0.8395 | 0.0144 | 4.4523 | 0.0455 | 2.1350 | 0.0184 | 1509 | 35 | | | | |
| PS | bt | 76 | 39.0608 | 250.7885 | 211.9221 | 17.9430 | 29.6766 | 66.8541 | 0.8343 | 0.0144 | 4.1205 | 0.0438 | 1.8371 | 0.0171 | 1671 | 39 | | | | |
| PS | bt | 78 | 38.7045 | 242.8268 | 208.8433 | 18.4857 | 27.7370 | 65.1623 | 0.8000 | 0.0141 | 4.0116 | 0.0432 | 1.8194 | 0.0170 | 1634 | 39 | | | | |
| PS | bt | 79 | 37.9418 | 253.5427 | 213.6869 | 17.4538 | 28.8706 | 66.1640 | 0.8072 | 0.0141 | 4.1706 | 0.0440 | 1.8606 | 0.0171 | 1607 | 38 | | | | |
| PS | bt | 81 | 36.6915 | 244.1036 | 219.8699 | 17.7144 | 28.0020 | 65.0287 | 0.7497 | 0.0136 | 4.0241 | 0.0433 | 1.9574 | 0.0176 | 1481 | 37 | | | | |
| PS | bt | 82 | 35.9476 | 245.0300 | 228.7944 | 16.6464 | 27.4509 | 63.7377 | 0.7596 | 0.0137 | 4.0375 | 0.0433 | 2.0803 | 0.0181 | 1446 | 35 | | | | |
| PS | bt | 83 | 34.6223 | 234.6400 | 209.8696 | 16.6498 | 28.6274 | 64.5836 | 0.7069 | 0.0132 | 3.8179 | 0.0421 | 1.8248 | 0.0169 | 1488 | 38 | | | | |
| PS | bt | 84 | 36.4102 | 241.8003 | 218.5682 | 17.9933 | 29.2645 | 66.6760 | 0.7258 | 0.0134 | 3.9481 | 0.0428 | 1.9142 | 0.0174 | 1467 | 37 | | | | |
| PS | bt | 85 | 37.1729 | 254.8697 | 193.3871 | 18.1415 | 29.2559 | 65.5630 | 0.7528 | 0.0136 | 4.2052 | 0.0443 | 1.6182 | 0.0160 | 1622 | 40 | | | | |
| PS | bt | 86 | 35.1225 | 257.5238 | 193.4122 | 17.3754 | 29.3649 | 64.4500 | 0.6981 | 0.0131 | 4.2317 | 0.0443 | 1.6252 | 0.0160 | 1510 | 39 | | | | |
| PS | bt | 1 | 37.8981 | 448.5027 | 121.2441 | 18.4750 | 32.5355 | 70.3489 | 0.6985 | 0.0125 | 7.0218 | 0.0544 | 0.5824 | 0.0091 | 1655 | 42 | | | | |
| PS | bt | 2 | 37.1791 | 408.8509 | 123.6959 | 19.5859 | 30.2503 | 71.1726 | 0.6332 | 0.0119 | 6.4000 | 0.0520 | 0.5995 | 0.0092 | 1602 | 43 | | | | |

| Sample | Occluding phase | Label | Peak Counts Pk(Pb) | Pk(Th) | Pk(U ) | Background counts Bg(Pb) | Bg(Th) | Bg(U ) | W%(Pb) | W%(Pb) 1σ | W%(Th) | W%(Th) 1σ | W%(U) | W%(U) 1σ | Chemical age (Ma) | 1σ | Early/peak meta. age (Ma) & error (2σ) | n = | Post peak meta. age (Ma) & error (2σ) | n = |
|---|---|---|---|---|---|---|---|---|---|---|---|---|---|---|---|---|---|---|---|---|
| PS | bt | 3 | 36.8291 | 414.1640 | 123.3331 | 17.5149 | 32.2341 | 69.7590 | 0.6945 | 0.0125 | 6.4430 | 0.0521 | 0.6106 | 0.0093 | 1729 | 45 | | | | |
| PS | bt | 4 | 36.6290 | 417.1714 | 123.0829 | 18.8380 | 31.5455 | 71.6623 | 0.6386 | 0.0120 | 6.4989 | 0.0523 | 0.5856 | 0.0091 | 1607 | 43 | | | | |
| PS | bt | 5 | 36.8353 | 421.1314 | 126.1352 | 19.7260 | 32.1028 | 70.6606 | 0.6165 | 0.0118 | 6.5830 | 0.0528 | 0.6344 | 0.0095 | 1513 | 41 | | | | |
| PS | bt | 6 | 36.0414 | 424.5651 | 124.8467 | 18.2563 | 31.3029 | 69.2804 | 0.6418 | 0.0120 | 6.6639 | 0.0531 | 0.6370 | 0.0096 | 1556 | 41 | | | | |
| PS | bt | 7 | 36.8603 | 438.2504 | 122.3824 | 18.5914 | 30.7482 | 69.3917 | 0.6604 | 0.0122 | 6.9173 | 0.0542 | 0.6093 | 0.0094 | 1572 | 41 | | | | |
| PS | bt | 8 | 37.5667 | 434.5407 | 120.3434 | 18.2904 | 31.7979 | 71.2505 | 0.6955 | 0.0125 | 6.8204 | 0.0537 | 0.5629 | 0.0090 | 1695 | 44 | | | | |
| PS | bt | 10 | 35.3788 | 426.3947 | 124.5715 | 18.2948 | 29.5979 | 69.9260 | 0.6144 | 0.0118 | 6.7054 | 0.0532 | 0.6249 | 0.0095 | 1494 | 40 | | | | |
| PS | bt | 11 | 37.3354 | 430.4301 | 123.8085 | 18.3723 | 31.5012 | 69.9594 | 0.6863 | 0.0125 | 6.7778 | 0.0537 | 0.6194 | 0.0094 | 1646 | 43 | | | | |
| PS | bt | 13 | 35.6476 | 416.9709 | 131.0515 | 18.8400 | 29.4883 | 69.3249 | 0.6092 | 0.0117 | 6.5996 | 0.0530 | 0.7110 | 0.0101 | 1452 | 39 | | | | |
| PS | bt | 14 | 34.2723 | 430.2045 | 112.9132 | 18.6931 | 31.9518 | 68.4234 | 0.5610 | 0.0112 | 6.7476 | 0.0535 | 0.5103 | 0.0086 | 1427 | 40 | | | | |
| PS | bt | 16 | 39.4734 | 380.0578 | 139.2707 | 19.4426 | 27.9248 | 68.6460 | 0.7285 | 0.0129 | 6.0083 | 0.0506 | 0.8125 | 0.0108 | 1750 | 44 | | | | |
| PS | bt | 17 | 35.4538 | 411.7079 | 123.8085 | 18.3398 | 29.9257 | 69.4140 | 0.6169 | 0.0118 | 6.4650 | 0.0523 | 0.6224 | 0.0094 | 1540 | 42 | | | | |
| PS | bt | 18 | 38.6420 | 444.5421 | 124.3589 | 18.7933 | 30.9867 | 72.9200 | 0.7170 | 0.0127 | 7.0135 | 0.0545 | 0.5915 | 0.0092 | 1691 | 43 | | | | |
| PS | bt | 19 | 37.0916 | 394.2658 | 136.1306 | 18.5068 | 29.3526 | 76.7045 | 0.6706 | 0.0123 | 6.1804 | 0.0512 | 0.6793 | 0.0099 | 1677 | 44 | | | | |
| PS | bt | 20 | 36.3915 | 405.0165 | 120.0182 | 18.8513 | 30.6544 | 69.2916 | 0.6298 | 0.0119 | 6.3139 | 0.0516 | 0.5778 | 0.0091 | 1623 | 44 | | | | |
| PS | bt | 21 | 37.5292 | 465.6997 | 128.5621 | 19.3625 | 32.1602 | 89.1046 | 0.6522 | 0.0121 | 7.3158 | 0.0556 | 0.4522 | 0.0080 | 1581 | 42 | | | | |
| PS | bt | 22 | 35.4475 | 409.1516 | 121.7695 | 19.1377 | 30.9170 | 70.8943 | 0.5848 | 0.0114 | 6.3767 | 0.0518 | 0.5794 | 0.0091 | 1504 | 42 | 1601 ± 18 | 90 | | |
| CB6 | qtz | a_5 | 34.1160 | 293.8087 | 121.5943 | 19.2835 | 30.2847 | 65.5964 | 0.5444 | 0.0112 | 4.7186 | 0.0460 | 0.6899 | 0.0103 | 1634 | 48 | | | | |
| CB6 | qtz | a_6 | 32.7157 | 288.4494 | 123.4332 | 19.2398 | 28.2196 | 65.0065 | 0.4942 | 0.0106 | 4.6622 | 0.0457 | 0.7200 | 0.0105 | 1486 | 45 | | | | |
| CB6 | qtz | a_7 | 32.5657 | 296.0878 | 121.1315 | 19.2536 | 29.8746 | 65.6409 | 0.4869 | 0.0106 | 4.7589 | 0.0461 | 0.6828 | 0.0102 | 1472 | 45 | | | | |
| CB6 | qtz | a_8 | 32.9032 | 287.8484 | 119.1050 | 18.7173 | 28.6840 | 63.1256 | 0.5214 | 0.0109 | 4.6477 | 0.0456 | 0.6905 | 0.0103 | 1584 | 47 | | | | |
| CB6 | qtz | a_9 | 34.4786 | 308.8359 | 122.6451 | 18.4930 | 28.9140 | 65.7856 | 0.5869 | 0.0116 | 5.0110 | 0.0474 | 0.7018 | 0.0104 | 1678 | 48 | | | | |
| CB6 | qtz | a_10 | 41.0300 | 513.5149 | 115.6276 | 19.2469 | 31.5839 | 67.4996 | 0.7966 | 0.0135 | 8.5896 | 0.0619 | 0.6036 | 0.0097 | 1603 | 39 | | | | |
| CB6 | qtz | a_11 | 39.6297 | 425.3671 | 145.6011 | 18.6885 | 31.2716 | 63.2814 | 0.7687 | 0.0133 | 7.0435 | 0.0561 | 1.0263 | 0.0126 | 1555 | 38 | | | | |
| CB6 | qtz | a_12 | 33.0220 | 320.4828 | 117.6040 | 18.5917 | 29.6574 | 66.1640 | 0.5296 | 0.0110 | 5.2100 | 0.0483 | 0.6358 | 0.0099 | 1535 | 46 | | | | |
| CB6 | qtz | a_13 | 33.1533 | 313.9955 | 118.0543 | 18.1609 | 30.0679 | 66.0304 | 0.5510 | 0.0113 | 5.0909 | 0.0478 | 0.6432 | 0.0100 | 1610 | 47 | | | | |
| CB6 | qtz | a_15 | 42.7617 | 471.9422 | 157.2366 | 19.2493 | 31.0640 | 66.0861 | 0.8624 | 0.0141 | 7.8736 | 0.0593 | 1.1412 | 0.0134 | 1562 | 36 | | | | |
| CB6 | qtz | a_16 | 42.8618 | 475.5775 | 156.2482 | 19.1742 | 31.3421 | 65.4851 | 0.8679 | 0.0141 | 7.9262 | 0.0595 | 1.1357 | 0.0133 | 1567 | 36 | | | | |
| CB6 | qtz | a_17 | 42.3616 | 473.4214 | 159.8016 | 18.9148 | 31.8209 | 65.1623 | 0.8592 | 0.0140 | 7.8764 | 0.0593 | 1.1831 | 0.0136 | 1539 | 36 | | | | |
| CB6 | qtz | a_18 | 43.0993 | 556.5527 | 131.4893 | 19.5907 | 31.2456 | 66.1863 | 0.8566 | 0.0140 | 9.3347 | 0.0644 | 0.8205 | 0.0114 | 1516 | 35 | | | | |
| CB6 | qtz | a_19 | 45.7813 | 701.4731 | 101.5434 | 19.6330 | 31.6036 | 67.8892 | 0.9465 | 0.0146 | 11.8371 | 0.0723 | 0.4264 | 0.0082 | 1537 | 34 | | | | |
| CB6 | qtz | a_20 | 34.0472 | 292.1308 | 143.8746 | 18.5195 | 30.3837 | 65.5741 | 0.5695 | 0.0114 | 4.6886 | 0.0458 | 0.9661 | 0.0122 | 1518 | 43 | | | | |
| CB6 | qtz | a_21 | 42.5992 | 652.6755 | 97.8912 | 18.8853 | 31.9054 | 67.3994 | 0.8598 | 0.0140 | 10.9795 | 0.0697 | 0.3846 | 0.0078 | 1511 | 35 | | | | |
| CB6 | qtz | a_22 | 42.4241 | 467.1538 | 158.3127 | 18.8102 | 30.6825 | 66.1417 | 0.8635 | 0.0140 | 7.7725 | 0.0588 | 1.1500 | 0.0134 | 1572 | 36 | | | | |
| CB6 | qtz | a_23 | 40.3111 | 458.8307 | 152.1569 | 18.6730 | 32.0781 | 65.7745 | 0.7912 | 0.0134 | 7.5986 | 0.0582 | 1.0764 | 0.0129 | 1502 | 36 | | | | |
| CB6 | qtz | a_24 | 41.8928 | 473.4465 | 161.6659 | 19.7742 | 29.8575 | 66.2308 | 0.8085 | 0.0136 | 7.8989 | 0.0593 | 1.1915 | 0.0136 | 1450 | 34 | | | | |
| CB6 | qtz | a_25 | 42.7492 | 472.4938 | 160.9527 | 18.4835 | 31.8479 | 66.3087 | 0.8890 | 0.0143 | 7.8599 | 0.0592 | 1.1834 | 0.0136 | 1589 | 36 | | | | |
| CB6 | qtz | a_26 | 42.1491 | 460.3850 | 156.3733 | 18.9162 | 31.2720 | 65.3626 | 0.8515 | 0.0140 | 7.6585 | 0.0585 | 1.1373 | 0.0133 | 1572 | 37 | | | | |
| CB6 | qtz | a_27 | 43.8308 | 611.3191 | 113.8013 | 18.8649 | 30.2221 | 65.1401 | 0.9087 | 0.0144 | 10.3145 | 0.0677 | 0.6139 | 0.0098 | 1574 | 36 | | | | |
| CB6 | qtz | a_28 | 41.4239 | 452.6639 | 154.3464 | 18.9277 | 29.8104 | 64.6058 | 0.8244 | 0.0137 | 7.5504 | 0.0581 | 1.1215 | 0.0132 | 1546 | 37 | | | | |
| CB6 | qtz | a_29 | 41.9803 | 497.2908 | 155.2222 | 19.3142 | 29.6209 | 64.8841 | 0.8290 | 0.0138 | 8.3333 | 0.0609 | 1.1314 | 0.0133 | 1459 | 34 | | | | |
| CB6 | qtz | a_34 | 32.9345 | 297.6656 | 121.2441 | 18.3509 | 30.9825 | 66.2976 | 0.5346 | 0.0111 | 4.7706 | 0.0462 | 0.6765 | 0.0102 | 1606 | 48 | | | | |
| CB6 | qtz | a_35 | 33.7534 | 316.6505 | 116.3906 | 18.0381 | 30.6403 | 65.8301 | 0.5767 | 0.0115 | 5.1154 | 0.0478 | 0.6235 | 0.0098 | 1688 | 48 | | | | |
| CB6 | qtz | a_36 | 33.1408 | 312.0919 | 117.6415 | 19.1729 | 28.8838 | 66.4534 | 0.5115 | 0.0108 | 5.0639 | 0.0476 | 0.6309 | 0.0099 | 1517 | 46 | | | | |
| CB6 | qtz | a_37 | 34.2910 | 307.7088 | 119.3427 | 18.6680 | 30.4246 | 65.4517 | 0.5727 | 0.0115 | 4.9567 | 0.0471 | 0.6638 | 0.0101 | 1680 | 48 | | | | |
| CB6 | qtz | a_39 | 34.1723 | 349.3908 | 115.3899 | 18.7831 | 30.6879 | 67.6109 | 0.5644 | 0.0114 | 5.7031 | 0.0505 | 0.5916 | 0.0096 | 1564 | 45 | | | | |
| CB6 | qtz | a_40 | 34.3098 | 330.8531 | 120.8688 | 18.3239 | 28.7954 | 65.7411 | 0.5866 | 0.0116 | 5.4044 | 0.0492 | 0.6814 | 0.0103 | 1615 | 46 | | | | |
| CB6 | qtz | a_41 | 32.9720 | 317.8027 | 114.3392 | 18.5719 | 30.8564 | 66.7205 | 0.5287 | 0.0110 | 5.1427 | 0.0480 | 0.5886 | 0.0095 | 1579 | 47 | | | | |
| CB6 | qtz | a_42 | 32.8907 | 313.0938 | 119.2802 | 18.7918 | 29.8533 | 66.7094 | 0.5168 | 0.0109 | 5.0704 | 0.0476 | 0.6488 | 0.0100 | 1518 | 46 | | | | |
| CB6 | qtz | a_43 | 45.1311 | 715.5076 | 98.2414 | 19.4451 | 31.1394 | 66.6871 | 0.9301 | 0.0145 | 12.1000 | 0.0731 | 0.4005 | 0.0080 | 1494 | 33 | | | | |
| CB6 | qtz | a_44 | 43.2556 | 621.8078 | 114.7645 | 19.0736 | 32.1219 | 67.7222 | 0.8788 | 0.0141 | 10.4557 | 0.0681 | 0.5933 | 0.0097 | 1517 | 35 | | | | |
| CB6 | qtz | a_45 | 42.3679 | 472.0175 | 158.6129 | 18.4481 | 31.0338 | 65.8746 | 0.8765 | 0.0142 | 7.8678 | 0.0592 | 1.1598 | 0.0135 | 1578 | 36 | | | | |
| CB6 | qtz | a_46 | 41.8678 | 462.9671 | 157.4243 | 18.4798 | 28.7699 | 66.3643 | 0.8563 | 0.0140 | 7.7389 | 0.0587 | 1.1368 | 0.0133 | 1570 | 37 | | | | |

| Sample | Occluding phase | Label | Peak Counts Pk(Pb) | Pk(Th) | Pk(U ) | Background counts Bg(Pb) | Bg(Th) | Bg(U ) | W%(Pb) | W%(Pb) 1σ | W%(Th) | W%(Th) 1σ | W%(U) | W%(U) 1σ | Chemical age (Ma) | 1σ | Early/peak meta. age (Ma) & error (2σ) | n = | Post peak meta. age (Ma) & error (2σ) | n = |
|---|---|---|---|---|---|---|---|---|---|---|---|---|---|---|---|---|---|---|---|---|
| CB6 | qtz | a_47 | 42.2304 | 470.7639 | 160.6274 | 19.3797 | 31.3053 | 66.5647 | 0.8370 | 0.0138 | 7.8389 | 0.0591 | 1.1758 | 0.0136 | 1510 | 35 | | | | |
| CB6 | qtz | a_48 | 41.6990 | 470.9645 | 163.3175 | 18.2787 | 32.0766 | 64.9286 | 0.8576 | 0.0140 | 7.8258 | 0.0591 | 1.2295 | 0.0139 | 1523 | 35 | | | | |
| CB6 | qtz | a_51 | 41.0926 | 474.3741 | 146.3267 | 19.0105 | 30.4890 | 65.6298 | 0.8076 | 0.0136 | 7.9075 | 0.0593 | 1.0077 | 0.0125 | 1523 | 37 | | | | |
| CB6 | qtz | a_53 | 43.5432 | 471.0648 | 158.9007 | 18.8888 | 29.8836 | 66.7539 | 0.9035 | 0.0144 | 7.8712 | 0.0593 | 1.1526 | 0.0134 | 1625 | 37 | | | | |
| CB6 | qtz | a_55 | 40.9488 | 462.9170 | 152.7074 | 19.1808 | 29.6344 | 66.2753 | 0.7965 | 0.0135 | 7.7301 | 0.0587 | 1.0807 | 0.0130 | 1494 | 36 | | | 1554 ± 18 | 41 |
| R899 | bt | 62 | 31.7468 | 354.6519 | 99.9049 | 17.8204 | 28.1748 | 67.0878 | 0.5255 | 0.0111 | 5.8545 | 0.0512 | 0.3951 | 0.0077 | 1567 | 47 | | | | |
| R899 | bt | 63 | 30.8966 | 357.6333 | 95.0896 | 17.8738 | 28.9292 | 65.9748 | 0.4911 | 0.0108 | 5.8937 | 0.0514 | 0.3505 | 0.0073 | 1494 | 46 | | | | |
| R899 | bt | 65 | 33.1158 | 346.7603 | 101.3558 | 18.0507 | 31.5554 | 64.7950 | 0.5684 | 0.0116 | 5.6417 | 0.0502 | 0.4387 | 0.0081 | 1697 | 50 | | | | |
| R899 | bt | 66 | 32.7032 | 354.2511 | 102.5190 | 18.4154 | 31.4397 | 68.1340 | 0.5389 | 0.0113 | 5.7816 | 0.0509 | 0.4131 | 0.0079 | 1606 | 48 | | | | |
| R899 | bt | 67 | 31.7968 | 343.1278 | 109.4359 | 17.7904 | 28.5912 | 65.7967 | 0.5280 | 0.0112 | 5.6374 | 0.0503 | 0.5248 | 0.0089 | 1525 | 46 | | | | |
| R899 | bt | 68 | 32.5344 | 385.5705 | 105.2332 | 18.7525 | 29.9648 | 66.1306 | 0.5211 | 0.0111 | 6.3921 | 0.0536 | 0.4732 | 0.0085 | 1407 | 42 | | | | |
| R899 | bt | 69 | 31.8655 | 337.7168 | 111.4372 | 18.0431 | 29.6417 | 67.0655 | 0.5211 | 0.0111 | 5.5160 | 0.0497 | 0.5321 | 0.0089 | 1525 | 46 | | | | |
| R899 | bt | 70 | 32.1156 | 348.1132 | 105.1582 | 18.9283 | 28.9742 | 65.3738 | 0.4960 | 0.0108 | 5.7079 | 0.0505 | 0.4772 | 0.0085 | 1457 | 45 | | | | |
| R899 | bt | 71 | 33.3283 | 369.3338 | 105.8836 | 19.6154 | 33.0831 | 69.2916 | 0.5160 | 0.0110 | 6.0299 | 0.0520 | 0.4415 | 0.0082 | 1475 | 45 | | | | |
| R899 | bt | 72 | 34.2098 | 277.8564 | 153.6083 | 17.3369 | 26.9785 | 63.3036 | 0.6436 | 0.0124 | 4.5297 | 0.0452 | 1.0870 | 0.0128 | 1645 | 44 | | | | |
| R899 | bt | 73 | 32.9908 | 254.4691 | 154.6467 | 17.7222 | 29.6312 | 65.6409 | 0.5807 | 0.0117 | 4.0477 | 0.0427 | 1.0642 | 0.0126 | 1596 | 45 | | | | |
| R899 | bt | 74 | 29.6526 | 261.9557 | 113.1134 | 17.6272 | 29.2843 | 65.5964 | 0.4548 | 0.0104 | 4.1809 | 0.0433 | 0.5674 | 0.0092 | 1584 | 51 | | | | |
| R899 | bt | 75 | 30.9466 | 307.2830 | 105.3958 | 17.4747 | 29.5741 | 66.3866 | 0.5085 | 0.0110 | 4.9720 | 0.0472 | 0.4662 | 0.0083 | 1652 | 51 | | | | |
| R899 | bt | 76 | 32.1156 | 346.7603 | 99.8674 | 18.2834 | 28.4873 | 63.8935 | 0.5225 | 0.0111 | 5.7059 | 0.0506 | 0.4324 | 0.0081 | 1561 | 47 | | | | |
| R899 | bt | 77 | 35.1225 | 306.0558 | 165.5697 | 17.9777 | 28.7841 | 64.2497 | 0.6543 | 0.0125 | 5.0072 | 0.0475 | 1.2223 | 0.0136 | 1515 | 40 | | | | |
| R899 | bt | 79 | 31.0216 | 310.1133 | 120.3810 | 18.3456 | 29.6137 | 65.4294 | 0.4807 | 0.0107 | 5.0538 | 0.0477 | 0.6615 | 0.0100 | 1415 | 44 | | | | |
| R899 | bt | 80 | 33.1033 | 355.3785 | 98.2164 | 17.9250 | 28.1074 | 64.5947 | 0.5735 | 0.0116 | 5.8656 | 0.0513 | 0.4046 | 0.0078 | 1690 | 49 | | | | |
| R899 | bt | 82 | 33.6096 | 358.8108 | 132.0273 | 16.9663 | 29.2311 | 65.0065 | 0.6283 | 0.0122 | 5.8986 | 0.0514 | 0.8059 | 0.0110 | 1551 | 43 | | | | |
| R899 | bt | 84 | 32.7532 | 315.4482 | 126.8483 | 18.3720 | 29.2236 | 67.4328 | 0.5395 | 0.0112 | 5.0888 | 0.0476 | 0.7056 | 0.0102 | 1537 | 45 | | | | |
| R899 | bt | 85 | 30.2652 | 320.0570 | 100.0425 | 18.0227 | 27.5066 | 65.6854 | 0.4553 | 0.0103 | 5.1738 | 0.0478 | 0.4061 | 0.0077 | 1494 | 48 | | | | |
| R899 | bt | 87 | 33.1846 | 312.5428 | 138.1322 | 17.3699 | 31.2696 | 65.8524 | 0.5971 | 0.0119 | 5.0252 | 0.0474 | 0.8622 | 0.0113 | 1591 | 45 | | | | |
| R899 | bt | 88 | 33.9222 | 296.1629 | 154.1212 | 17.3403 | 29.4359 | 66.0638 | 0.6266 | 0.0122 | 4.7579 | 0.0461 | 1.0465 | 0.0125 | 1592 | 43 | | | | |
| R899 | bt | 89 | 32.1531 | 338.7439 | 117.7916 | 17.5729 | 29.7836 | 67.0321 | 0.5480 | 0.0113 | 5.5050 | 0.0495 | 0.6057 | 0.0095 | 1549 | 46 | | | | |
| R899 | bt | 91 | 32.6094 | 331.3040 | 116.1905 | 18.0812 | 30.9880 | 65.8858 | 0.5458 | 0.0113 | 5.3535 | 0.0488 | 0.6002 | 0.0095 | 1575 | 46 | | | | |
| R899 | bt | 92 | 32.6219 | 285.4192 | 148.5662 | 17.8425 | 29.5336 | 66.3309 | 0.5596 | 0.0115 | 4.5832 | 0.0453 | 0.9807 | 0.0121 | 1503 | 43 | | | | |
| R899 | bt | 93 | 33.0845 | 301.3722 | 138.1197 | 18.3001 | 28.6453 | 65.9525 | 0.5583 | 0.0115 | 4.8772 | 0.0467 | 0.8610 | 0.0113 | 1523 | 44 | | | | |
| R899 | bt | 95 | 34.1222 | 317.7276 | 132.9905 | 17.8749 | 30.3338 | 65.9303 | 0.6110 | 0.0120 | 5.1140 | 0.0477 | 0.7972 | 0.0109 | 1652 | 46 | | | | |
| R899 | bt | 96 | 34.5223 | 299.7443 | 148.6663 | 17.6034 | 30.5647 | 67.3994 | 0.6364 | 0.0122 | 4.7848 | 0.0461 | 0.9631 | 0.0119 | 1663 | 45 | | | | |
| R899 | bt | 97 | 32.3281 | 298.5922 | 135.9930 | 18.3389 | 28.1338 | 65.6075 | 0.5238 | 0.0111 | 4.8010 | 0.0462 | 0.8333 | 0.0111 | 1467 | 44 | | | | |
| R899 | bt | 99 | 32.4219 | 318.8046 | 123.1830 | 17.6002 | 29.8120 | 65.8412 | 0.5558 | 0.0114 | 5.1351 | 0.0478 | 0.6808 | 0.0101 | 1588 | 46 | | | | |
| R899 | bt | 100 | 34.2223 | 330.7779 | 124.8092 | 18.9610 | 30.2485 | 65.4294 | 0.5740 | 0.0116 | 5.3621 | 0.0489 | 0.7092 | 0.0103 | 1573 | 45 | | | | |
| R899 | bt | 101 | 33.7597 | 370.5114 | 116.5532 | 18.0161 | 30.7652 | 66.2753 | 0.5875 | 0.0117 | 6.0137 | 0.0516 | 0.5981 | 0.0094 | 1561 | 44 | | | | |
| R899 | bt | 102 | 32.4282 | 325.0417 | 119.9431 | 18.1582 | 28.5080 | 62.4466 | 0.5324 | 0.0111 | 5.2550 | 0.0483 | 0.6819 | 0.0101 | 1504 | 45 | | | | |
| R899 | bt | 103 | 32.9032 | 318.5792 | 114.8020 | 18.4747 | 29.6854 | 65.9080 | 0.5403 | 0.0112 | 5.1358 | 0.0478 | 0.5811 | 0.0093 | 1617 | 48 | | | | |
| R899 | bt | 105 | 30.5465 | 295.0359 | 103.0443 | 17.5996 | 26.4424 | 61.4227 | 0.4838 | 0.0106 | 4.7722 | 0.0460 | 0.4936 | 0.0086 | 1600 | 50 | | | | |
| R899 | bt | 106 | 33.4784 | 375.7731 | 95.3148 | 18.5042 | 30.3528 | 67.8669 | 0.5599 | 0.0114 | 6.1318 | 0.0522 | 0.3276 | 0.0070 | 1655 | 48 | | | | |
| R899 | bt | 107 | 32.8782 | 326.0937 | 117.1537 | 18.5463 | 29.8622 | 67.0321 | 0.5339 | 0.0111 | 5.2408 | 0.0481 | 0.5933 | 0.0094 | 1570 | 47 | | | | |
| R899 | bt | 108 | 32.1844 | 308.9110 | 122.2698 | 17.9136 | 28.4953 | 66.1640 | 0.5318 | 0.0111 | 4.9608 | 0.0468 | 0.6629 | 0.0099 | 1570 | 47 | | | | |
| R899 | bt | 109 | 33.5909 | 337.0154 | 114.9396 | 18.0695 | 31.5765 | 66.9542 | 0.5787 | 0.0116 | 5.4017 | 0.0489 | 0.5683 | 0.0092 | 1676 | 48 | | | | |
| R899 | bt | 110 | 32.9470 | 343.6790 | 118.1043 | 18.3473 | 30.0927 | 66.1417 | 0.5437 | 0.0112 | 5.5458 | 0.0495 | 0.6160 | 0.0096 | 1523 | 45 | | | | |
| R899 | bt | 111 | 32.3031 | 316.5503 | 118.4171 | 18.1593 | 29.0454 | 66.8095 | 0.5270 | 0.0111 | 5.0845 | 0.0474 | 0.6098 | 0.0095 | 1570 | 47 | | | | |
| R899 | bt | 112 | 32.0156 | 364.3979 | 102.4690 | 18.2361 | 30.0439 | 67.0210 | 0.5141 | 0.0109 | 5.9296 | 0.0513 | 0.4222 | 0.0079 | 1502 | 45 | | | | |
| R899 | bt | 113 | 32.0781 | 327.7970 | 116.9785 | 17.6258 | 29.5169 | 65.3293 | 0.5384 | 0.0112 | 5.2761 | 0.0483 | 0.6113 | 0.0095 | 1563 | 46 | | | | |
| R899 | bt | 114 | 32.0593 | 330.7028 | 116.5908 | 17.6297 | 31.1224 | 67.4662 | 0.5356 | 0.0111 | 5.2791 | 0.0482 | 0.5792 | 0.0092 | 1577 | 47 | | | | |
| R899 | bt | 115 | 32.8970 | 334.2599 | 120.7312 | 18.7809 | 29.9599 | 67.6443 | 0.5248 | 0.0110 | 5.3745 | 0.0487 | 0.6278 | 0.0096 | 1497 | 45 | | | | |
| R899 | bt | 116 | 32.9658 | 345.6581 | 116.0279 | 18.2504 | 30.5583 | 68.6460 | 0.5478 | 0.0113 | 5.5695 | 0.0496 | 0.5614 | 0.0091 | 1566 | 46 | | | | |
| R899 | bt | 117 | 32.6970 | 349.5412 | 115.1523 | 18.2728 | 30.2075 | 67.5998 | 0.5360 | 0.0112 | 5.6362 | 0.0499 | 0.5628 | 0.0091 | 1521 | 45 | | | | |
| R899 | bt | 118 | 32.5094 | 342.9525 | 110.0113 | 18.4091 | 29.4741 | 67.2325 | 0.5256 | 0.0111 | 5.5494 | 0.0496 | 0.5075 | 0.0087 | 1547 | 46 | | | | |

| Sample | Occluding phase | Label | Peak Counts Pk(Pb) | Pk(Th) | Pk(U ) | Background counts Bg(Pb) | Bg(Th) | Bg(U ) | W%(Pb) | W%(Pb) 1σ | W%(Th) | W%(Th) 1σ | W%(U) | W%(U) 1σ | Chemical age (Ma) | 1σ | Early/peak meta. age (Ma) & error (2σ) | n = | Post peak meta. age (Ma) & error (2σ) | n = |
|---|---|---|---|---|---|---|---|---|---|---|---|---|---|---|---|---|---|---|---|---|
| R899 | bt | 119 | 32.5969 | 357.0821 | 104.8079 | 18.1572 | 31.3353 | 66.0082 | 0.5374 | 0.0112 | 5.7590 | 0.0505 | 0.4604 | 0.0083 | 1572 | 47 | | | | |
| R899 | bt | 120 | 33.6784 | 340.0215 | 121.8570 | 18.8120 | 29.7646 | 67.9448 | 0.5532 | 0.0113 | 5.4801 | 0.0492 | 0.6378 | 0.0097 | 1545 | 45 | | | | |
| R899 | bt | 121 | 31.2154 | 349.0401 | 101.0056 | 17.8788 | 29.2451 | 65.2736 | 0.4954 | 0.0107 | 5.6484 | 0.0499 | 0.4233 | 0.0079 | 1503 | 46 | | | | |
| R899 | bt | 122 | 31.4467 | 349.4409 | 102.1813 | 17.4152 | 31.6149 | 67.1991 | 0.5203 | 0.0110 | 5.6037 | 0.0497 | 0.4137 | 0.0078 | 1590 | 48 | | | | |
| R899 | bt | 123 | 33.7784 | 364.7236 | 107.1594 | 18.7618 | 31.5839 | 67.5330 | 0.5579 | 0.0114 | 5.8766 | 0.0509 | 0.4693 | 0.0083 | 1597 | 47 | | | | |
| R899 | bt | 124 | 32.5844 | 335.3120 | 119.8306 | 17.8382 | 30.0265 | 67.2214 | 0.5475 | 0.0113 | 5.3803 | 0.0487 | 0.6207 | 0.0096 | 1561 | 46 | | | | |
| R899 | bt | 125 | 32.1218 | 361.4666 | 104.2076 | 18.3708 | 31.0894 | 65.4517 | 0.5104 | 0.0109 | 5.8289 | 0.0507 | 0.4590 | 0.0082 | 1486 | 45 | | | | |
| R899 | bt | 126 | 32.6532 | 366.4023 | 104.3827 | 18.0195 | 29.5376 | 67.6554 | 0.5433 | 0.0112 | 5.9401 | 0.0512 | 0.4351 | 0.0080 | 1570 | 46 | | | | |
| R899 | bt | 127 | 31.4967 | 310.2635 | 113.3761 | 17.9994 | 29.1468 | 66.3198 | 0.5028 | 0.0108 | 4.9735 | 0.0469 | 0.5560 | 0.0091 | 1564 | 48 | | | | |
| R899 | bt | 128 | 31.8405 | 330.1016 | 116.9535 | 18.4258 | 28.5028 | 66.0638 | 0.4957 | 0.0107 | 5.2994 | 0.0482 | 0.5985 | 0.0094 | 1452 | 44 | | | | |
| R899 | bt | 129 | 31.8593 | 365.2498 | 105.7961 | 18.4976 | 29.7836 | 66.6426 | 0.4970 | 0.0107 | 5.9338 | 0.0512 | 0.4651 | 0.0083 | 1427 | 44 | | | | |
| R899 | bt | 130 | 33.2221 | 357.3076 | 104.0450 | 18.1411 | 30.1456 | 66.3309 | 0.5595 | 0.0114 | 5.7613 | 0.0504 | 0.4457 | 0.0081 | 1642 | 48 | | | | |
| R899 | bt | 131 | 32.8907 | 339.8211 | 119.9181 | 18.9254 | 31.1226 | 65.0955 | 0.5158 | 0.0109 | 5.4180 | 0.0488 | 0.6444 | 0.0097 | 1455 | 43 | | | | |
| R899 | bt | 132 | 32.9408 | 356.2553 | 123.0454 | 18.2014 | 29.3601 | 67.9003 | 0.5427 | 0.0112 | 5.7165 | 0.0500 | 0.6470 | 0.0097 | 1471 | 43 | | | 1554 ± 17 | 62 |
| R899 | pl | 46 | 32.4219 | 344.5057 | 103.5572 | 18.4554 | 29.1297 | 65.1289 | 0.5289 | 0.0112 | 5.6744 | 0.0505 | 0.4636 | 0.0084 | 1563 | 47 | | | | |
| R899 | pl | 49 | 35.8851 | 476.8813 | 103.6197 | 18.3488 | 29.6637 | 67.1101 | 0.6585 | 0.0124 | 7.9639 | 0.0595 | 0.4417 | 0.0082 | 1499 | 40 | | | | |
| R899 | pl | 50 | 31.7030 | 308.5103 | 123.9211 | 17.8194 | 30.2524 | 66.7650 | 0.5257 | 0.0112 | 4.9960 | 0.0474 | 0.6850 | 0.0101 | 1532 | 46 | | | | |
| R899 | pl | 51 | 34.0035 | 371.2631 | 121.8946 | 17.6473 | 29.8104 | 67.1657 | 0.6155 | 0.0120 | 6.0903 | 0.0521 | 0.6560 | 0.0099 | 1579 | 44 | | | | |
| R899 | pl | 52 | 34.1035 | 372.3906 | 99.1045 | 19.4635 | 31.1116 | 66.2642 | 0.5540 | 0.0114 | 6.1424 | 0.0526 | 0.3977 | 0.0078 | 1585 | 47 | | | | |
| R899 | pl | 53 | 31.1404 | 340.0966 | 102.0938 | 17.5774 | 28.6069 | 65.8635 | 0.5132 | 0.0110 | 5.5994 | 0.0502 | 0.4365 | 0.0081 | 1554 | 47 | | | | |
| R899 | pl | 54 | 35.1350 | 398.0498 | 115.0897 | 18.0267 | 29.6392 | 65.7967 | 0.6481 | 0.0124 | 6.6165 | 0.0545 | 0.5970 | 0.0095 | 1601 | 44 | | | | |
| R899 | pl | 55 | 32.6532 | 331.7047 | 123.9211 | 17.8399 | 30.5665 | 67.2325 | 0.5597 | 0.0115 | 5.3954 | 0.0492 | 0.6797 | 0.0101 | 1550 | 45 | | | | |
| R899 | pl | 56 | 32.0656 | 338.7439 | 107.0969 | 19.2067 | 29.5589 | 66.5090 | 0.4878 | 0.0108 | 5.5733 | 0.0501 | 0.4901 | 0.0086 | 1451 | 45 | | | | |
| R899 | pl | 58 | 32.1281 | 360.5897 | 102.8067 | 18.3305 | 30.8966 | 65.8858 | 0.5185 | 0.0110 | 5.8852 | 0.0512 | 0.4424 | 0.0081 | 1508 | 46 | | | | |
| R899 | pl | 59 | 32.7470 | 347.0610 | 117.4163 | 17.2038 | 29.9715 | 66.6537 | 0.5868 | 0.0118 | 5.6755 | 0.0504 | 0.6092 | 0.0096 | 1614 | 46 | | | | |
| R899 | pl | 61 | 31.0216 | 314.9974 | 98.3915 | 17.3512 | 28.0037 | 65.2625 | 0.5156 | 0.0110 | 5.1477 | 0.0480 | 0.3976 | 0.0077 | 1690 | 52 | | | 1560 ± 38 | 12 |
| R899 | gt | 6 | 32.3969 | 358.2346 | 101.5309 | 18.1792 | 30.1908 | 65.9971 | 0.5425 | 0.0114 | 5.9413 | 0.0519 | 0.4321 | 0.0081 | 1570 | 47 | | | | |
| R899 | gt | 7 | 32.0531 | 344.7813 | 101.1182 | 18.1483 | 30.4667 | 66.5536 | 0.5295 | 0.0112 | 5.6820 | 0.0507 | 0.4189 | 0.0080 | 1596 | 48 | | | | |
| R899 | gt | 14 | 31.7655 | 361.2661 | 103.0318 | 17.6143 | 29.3444 | 64.6949 | 0.5436 | 0.0114 | 6.0538 | 0.0525 | 0.4699 | 0.0085 | 1526 | 46 | | | | |
| R899 | gt | 15 | 32.6094 | 343.2782 | 105.9086 | 17.0483 | 28.0089 | 64.6281 | 0.6001 | 0.0120 | 5.7615 | 0.0513 | 0.5060 | 0.0088 | 1705 | 49 | | | | |
| R899 | gt | 16 | 30.6903 | 323.4886 | 110.8869 | 18.0173 | 28.4450 | 65.1289 | 0.4870 | 0.0108 | 5.3914 | 0.0496 | 0.5598 | 0.0093 | 1436 | 45 | | | | |
| R899 | gt | 17 | 28.5712 | 289.2508 | 108.5228 | 16.4475 | 29.0842 | 62.1461 | 0.4646 | 0.0105 | 4.7628 | 0.0467 | 0.5678 | 0.0093 | 1488 | 48 | | | | |
| R899 | gt | 18 | 31.4592 | 281.5125 | 133.1657 | 17.0551 | 29.0707 | 63.3593 | 0.5581 | 0.0116 | 4.6317 | 0.0461 | 0.8533 | 0.0114 | 1572 | 46 | | | | |
| R899 | gt | 19 | 31.5092 | 314.8221 | 98.7417 | 17.6910 | 27.7856 | 63.1589 | 0.5315 | 0.0113 | 5.2443 | 0.0489 | 0.4350 | 0.0082 | 1683 | 51 | | | | |
| R899 | gt | 21 | 31.1092 | 327.4965 | 108.8981 | 18.3184 | 29.0019 | 65.3181 | 0.4880 | 0.0108 | 5.4132 | 0.0495 | 0.5291 | 0.0090 | 1455 | 45 | | | | |
| R899 | gt | 22 | 29.5526 | 320.5079 | 98.4791 | 17.5245 | 28.6204 | 64.4055 | 0.4600 | 0.0105 | 5.3135 | 0.0492 | 0.4151 | 0.0080 | 1472 | 48 | | | | |
| R899 | gt | 23 | 29.7214 | 284.2422 | 97.0282 | 17.7988 | 27.0585 | 61.9569 | 0.4590 | 0.0105 | 4.7132 | 0.0465 | 0.4288 | 0.0081 | 1590 | 52 | | | | |
| R899 | gt | 25 | 32.1719 | 360.1387 | 105.2582 | 17.7276 | 30.3889 | 64.8618 | 0.5546 | 0.0115 | 6.0122 | 0.0523 | 0.4949 | 0.0087 | 1545 | 46 | | | | |
| R899 | gt | 26 | 32.6407 | 342.1258 | 117.2287 | 17.1722 | 28.1229 | 65.9971 | 0.5934 | 0.0119 | 5.7098 | 0.0509 | 0.6248 | 0.0098 | 1614 | 46 | | | | |
| R899 | gt | 27 | 29.3776 | 302.2739 | 131.5769 | 16.1254 | 29.2097 | 63.4706 | 0.5107 | 0.0111 | 4.9899 | 0.0477 | 0.8311 | 0.0113 | 1403 | 43 | | | | |
| R899 | gt | 30 | 31.9156 | 311.0400 | 123.1330 | 17.2751 | 28.8874 | 64.9174 | 0.5635 | 0.0116 | 5.1485 | 0.0485 | 0.7101 | 0.0104 | 1585 | 46 | | | | |
| R899 | gt | 31 | 30.4778 | 318.3287 | 100.8930 | 18.1195 | 29.3559 | 65.2402 | 0.4720 | 0.0106 | 5.2510 | 0.0488 | 0.4335 | 0.0081 | 1508 | 48 | | | | |
| R899 | gt | 32 | 30.0965 | 324.9665 | 100.1176 | 18.0177 | 26.5067 | 65.5741 | 0.4593 | 0.0104 | 5.4035 | 0.0495 | 0.4188 | 0.0080 | 1450 | 47 | | | | |
| R899 | gt | 33 | 31.5655 | 303.2005 | 115.9653 | 17.8087 | 29.7593 | 63.8935 | 0.5276 | 0.0112 | 4.9740 | 0.0476 | 0.6324 | 0.0098 | 1578 | 48 | | | | |
| R899 | gt | 34 | 31.1154 | 335.6627 | 100.7054 | 18.0164 | 27.7817 | 65.7411 | 0.4987 | 0.0109 | 5.5730 | 0.0502 | 0.4243 | 0.0080 | 1527 | 47 | | | | |
| R899 | gt | 35 | 32.7720 | 329.5255 | 102.9568 | 18.9203 | 29.3241 | 65.2180 | 0.5301 | 0.0113 | 5.4625 | 0.0498 | 0.4601 | 0.0084 | 1612 | 49 | | | | |
| R899 | gt | 37 | 31.2592 | 288.3743 | 133.2032 | 17.6416 | 29.5714 | 65.5852 | 0.5212 | 0.0112 | 4.6957 | 0.0462 | 0.8176 | 0.0111 | 1488 | 45 | | | | |
| R899 | gt | 38 | 31.2279 | 293.3579 | 119.8306 | 17.6344 | 28.2334 | 65.6186 | 0.5194 | 0.0111 | 4.8079 | 0.0467 | 0.6559 | 0.0100 | 1572 | 48 | | | | |
| R899 | gt | 39 | 30.8404 | 302.3741 | 105.9462 | 18.5979 | 29.4006 | 66.7650 | 0.4679 | 0.0106 | 4.9615 | 0.0475 | 0.4755 | 0.0085 | 1525 | 49 | | | | |
| R899 | gt | 40 | 30.4715 | 307.9843 | 106.8217 | 17.8620 | 28.9708 | 64.9954 | 0.4799 | 0.0107 | 5.0487 | 0.0478 | 0.5057 | 0.0087 | 1520 | 48 | | | | |
| R899 | gt | 41 | 29.1776 | 300.0198 | 104.7079 | 17.4250 | 29.3497 | 63.6820 | 0.4464 | 0.0103 | 4.8920 | 0.0470 | 0.4950 | 0.0086 | 1459 | 48 | | | | |
| R899 | gt | 42 | 32.6344 | 287.5228 | 133.5535 | 18.0031 | 28.5644 | 66.3087 | 0.5575 | 0.0115 | 4.6728 | 0.0459 | 0.8086 | 0.0110 | 1593 | 46 | | | | |
| R899 | gt | 43 | 31.6280 | 340.6227 | 107.4346 | 17.6835 | 28.4249 | 66.0304 | 0.5288 | 0.0112 | 5.6243 | 0.0503 | 0.5002 | 0.0087 | 1547 | 47 | | | | |

| Sample | Occluding phase | Label | Peak Counts Pk(Pb) | Pk(Th) | Pk(U ) | Background counts Bg(Pb) | Bg(Th) | Bg(U ) | W%(Pb) | W%(Pb) 1σ | W%(Th) | W%(Th) 1σ | W%(U) | W%(U) 1σ | Chemical age (Ma) | 1σ | Early/peak meta. age (Ma) & error (2σ) | n = | Post peak meta. age (Ma) & error (2σ) | n = |
|---|---|---|---|---|---|---|---|---|---|---|---|---|---|---|---|---|---|---|---|---|
| R899 | gt | 44 | 31.3842 | 346.9608 | 103.3695 | 17.6972 | 28.6004 | 67.2547 | 0.5177 | 0.0111 | 5.7226 | 0.0507 | 0.4355 | 0.0081 | 1542 | 47 | | | | |
| R899 | gt | 45 | 35.3913 | 360.5145 | 104.4702 | 20.6745 | 28.7435 | 67.3772 | 0.5598 | 0.0115 | 6.0035 | 0.0521 | 0.4511 | 0.0083 | 1590 | 47 | | | 1542 ± 27 | 29 |
| AH5C | gt | gt17 | 32.2281 | 64.9376 | 188.5691 | 19.1930 | 30.0896 | 65.4406 | 0.4741 | 0.0104 | 0.6262 | 0.0168 | 1.4443 | 0.0146 | 1733 | 48 | | | | |
| AH5C | gt | gt18 | 27.9523 | 63.1370 | 148.5036 | 18.6982 | 29.2660 | 66.3755 | 0.3343 | 0.0087 | 0.6090 | 0.0165 | 0.9634 | 0.0119 | 1744 | 59 | | | | |
| AH5C | gt | gt26 | 37.8418 | 291.4296 | 170.9376 | 18.9657 | 30.3361 | 66.6982 | 0.6849 | 0.0125 | 4.6721 | 0.0457 | 1.2470 | 0.0137 | 1616 | 41 | | | | |
| AH5C | gt | gt29 | 39.4609 | 286.6463 | 198.1677 | 18.5400 | 31.9900 | 67.9114 | 0.7606 | 0.0131 | 4.5605 | 0.0452 | 1.5584 | 0.0153 | 1617 | 39 | | | | |
| AH5C | gt | gt38 | 39.3234 | 333.5584 | 172.1764 | 18.8637 | 28.1626 | 66.6315 | 0.7427 | 0.0130 | 5.4731 | 0.0495 | 1.2713 | 0.0138 | 1600 | 39 | | | | |
| AH5C | gt | gt43 | 36.9353 | 247.2082 | 178.5581 | 18.7431 | 28.9213 | 65.7299 | 0.6630 | 0.0123 | 3.9227 | 0.0420 | 1.3493 | 0.0142 | 1630 | 42 | | | | |
| AH5C | gt | gt46 | 28.8713 | 53.7587 | 166.9336 | 18.5328 | 29.0339 | 68.3121 | 0.3749 | 0.0092 | 0.4444 | 0.0141 | 1.1549 | 0.0130 | 1734 | 54 | | | | |
| AH5C | gt | gt47 | 22.1952 | 65.1627 | 90.0868 | 19.4192 | 28.8331 | 65.1067 | 0.0936 | 0.0044 | 0.6538 | 0.0172 | 0.2932 | 0.0066 | 1224 | 81 | | | | |
| AH5C | gt | gt48 | 33.9972 | 218.4681 | 180.1974 | 18.3220 | 27.2657 | 65.6965 | 0.5696 | 0.0114 | 3.4291 | 0.0392 | 1.3624 | 0.0142 | 1493 | 41 | | | | |
| AH5C | gt | gt52 | 22.7203 | 43.0806 | 104.1075 | 18.3824 | 29.6795 | 64.9174 | 0.1522 | 0.0058 | 0.2414 | 0.0104 | 0.4591 | 0.0082 | 1715 | 85 | | | | |
| AH5C | gt | gt55 | 28.4837 | 73.0660 | 161.8911 | 19.0838 | 29.8581 | 65.2291 | 0.3401 | 0.0088 | 0.7771 | 0.0187 | 1.1350 | 0.0129 | 1526 | 52 | | | | |
| AH5C | gt | gt58 | 31.8530 | 206.7782 | 151.7190 | 18.9375 | 30.2985 | 65.5852 | 0.4683 | 0.0103 | 3.1668 | 0.0377 | 1.0238 | 0.0123 | 1492 | 46 | | | | |
| AH5C | gt | gt63 | 25.7895 | 87.7481 | 120.8313 | 18.7498 | 30.4465 | 65.4406 | 0.2526 | 0.0075 | 1.0316 | 0.0215 | 0.6519 | 0.0098 | 1616 | 66 | | | | |
| AH5C | gt | gt68 | 30.6216 | 138.9829 | 150.4929 | 18.7263 | 28.6464 | 65.1289 | 0.4320 | 0.0099 | 1.9835 | 0.0299 | 1.0092 | 0.0122 | 1656 | 52 | | | | |
| AH5C | gt | gt69 | 36.4790 | 251.5898 | 183.9515 | 18.6410 | 29.9396 | 64.3832 | 0.6477 | 0.0121 | 3.9707 | 0.0422 | 1.4263 | 0.0146 | 1547 | 40 | | | | |
| AH5C | gt | gt71 | 21.9264 | 50.6077 | 93.4637 | 18.5350 | 30.3694 | 67.1212 | 0.1168 | 0.0050 | 0.3646 | 0.0128 | 0.3089 | 0.0067 | 1695 | 99 | | | | |
| AH5C | gt | gt1 | 34.9099 | 305.1791 | 138.1447 | 18.6058 | 31.3168 | 64.4277 | 0.5921 | 0.0116 | 4.9092 | 0.0469 | 0.8842 | 0.0115 | 1586 | 44 | | | | |
| AH5C | gt | gt3 | 37.8731 | 264.7852 | 195.0516 | 18.5744 | 30.4314 | 65.9303 | 0.6994 | 0.0126 | 4.1873 | 0.0432 | 1.5384 | 0.0151 | 1562 | 39 | | | | |
| AH5C | gt | gt5 | 24.4080 | 74.4916 | 105.6460 | 18.9623 | 28.4572 | 66.1863 | 0.1923 | 0.0065 | 0.8250 | 0.0192 | 0.4618 | 0.0082 | 1663 | 78 | | | | |
| AH5C | gt | gt14 | 22.4140 | 59.6107 | 96.5405 | 19.0213 | 30.8838 | 66.7650 | 0.1165 | 0.0050 | 0.5163 | 0.0152 | 0.3487 | 0.0071 | 1445 | 85 | | | | |
| AH5C | gt | gt16 | 32.6595 | 121.8946 | 190.5338 | 18.4626 | 30.6298 | 65.4294 | 0.5168 | 0.0108 | 1.6392 | 0.0271 | 1.4751 | 0.0147 | 1608 | 45 | | | | |
| AH5C | gt | gt19 | 26.7146 | 106.9343 | 127.0609 | 18.8687 | 29.0767 | 65.5964 | 0.2813 | 0.0079 | 1.3987 | 0.0251 | 0.7242 | 0.0103 | 1530 | 59 | | | | |
| AH5C | gt | gt22 | 20.8263 | 38.7795 | 82.5830 | 18.5839 | 29.2502 | 65.8969 | 0.0739 | 0.0039 | 0.1715 | 0.0088 | 0.1951 | 0.0053 | 1791 | 128 | | | | |
| AH5C | gt | gt23 | 21.8202 | 66.0381 | 88.9988 | 18.4994 | 30.6743 | 66.5647 | 0.1142 | 0.0050 | 0.6381 | 0.0170 | 0.2640 | 0.0062 | 1561 | 95 | | | | |
| AH5C | gt | gt24 | 38.3044 | 294.2094 | 173.8531 | 19.3020 | 30.2082 | 66.6648 | 0.6903 | 0.0125 | 4.7307 | 0.0460 | 1.2848 | 0.0139 | 1598 | 41 | | | | |
| AH5C | gt | gt27 | 26.0145 | 107.1344 | 125.5598 | 18.7949 | 29.1659 | 66.0972 | 0.2584 | 0.0076 | 1.4001 | 0.0251 | 0.6996 | 0.0101 | 1447 | 58 | | | | |
| AH5C | gt | gt28 | 31.1904 | 117.7916 | 171.7509 | 18.6597 | 30.2889 | 66.1863 | 0.4554 | 0.0102 | 1.5720 | 0.0266 | 1.2442 | 0.0135 | 1624 | 49 | | | | |
| AH5C | gt | gt30 | 35.7101 | 307.6337 | 163.5427 | 18.1916 | 30.2210 | 64.1272 | 0.6341 | 0.0120 | 4.9666 | 0.0471 | 1.1936 | 0.0134 | 1494 | 40 | | | | |
| AH5C | gt | gt34 | 31.7280 | 152.1194 | 161.3656 | 18.9517 | 31.0351 | 66.6760 | 0.4636 | 0.0103 | 2.1728 | 0.0312 | 1.1188 | 0.0129 | 1616 | 49 | | | | |
| AH5C | gt | gt36 | 24.5456 | 45.1311 | 127.6739 | 18.5444 | 29.8004 | 66.7650 | 0.2141 | 0.0069 | 0.2761 | 0.0111 | 0.7139 | 0.0102 | 1623 | 67 | | | | |
| AH5C | gt | gt37 | 23.1016 | 62.1366 | 99.2671 | 18.5131 | 29.3208 | 66.4756 | 0.1613 | 0.0060 | 0.5909 | 0.0163 | 0.3849 | 0.0075 | 1741 | 88 | | | | |
| AH5C | gt | gt39 | 40.5924 | 303.4009 | 191.4474 | 19.9398 | 29.5276 | 65.4628 | 0.7509 | 0.0131 | 4.9082 | 0.0469 | 1.5115 | 0.0151 | 1574 | 38 | | | | |
| AH5C | gt | gt40 | 40.8175 | 325.1669 | 242.3761 | 19.2616 | 30.2308 | 65.9748 | 0.7826 | 0.0133 | 5.2848 | 0.0487 | 2.1231 | 0.0179 | 1339 | 31 | | | | |
| AH5C | gt | gt44 | 27.9523 | 61.6864 | 157.1616 | 18.3027 | 29.0200 | 67.0655 | 0.3498 | 0.0089 | 0.5881 | 0.0163 | 1.0577 | 0.0125 | 1701 | 56 | | | | |
| AH5C | gt | gt45 | 25.0519 | 62.1616 | 124.0962 | 18.5426 | 28.4334 | 66.2308 | 0.2328 | 0.0072 | 0.6070 | 0.0165 | 0.6790 | 0.0100 | 1643 | 68 | | | | |
| AH5C | gt | gt49 | 37.4917 | 255.0700 | 188.0060 | 18.9561 | 29.7838 | 65.4406 | 0.6744 | 0.0124 | 4.0423 | 0.0426 | 1.4649 | 0.0148 | 1571 | 40 | | | | |
| AH5C | gt | gt50 | 39.5672 | 319.7815 | 186.0538 | 18.1023 | 28.8189 | 65.0733 | 0.7808 | 0.0133 | 5.2156 | 0.0483 | 1.4543 | 0.0148 | 1615 | 39 | | | | |
| AH5C | gt | gt54 | 27.5148 | 101.5809 | 149.1917 | 17.8245 | 28.1778 | 64.4723 | 0.3507 | 0.0089 | 1.3235 | 0.0244 | 1.0018 | 0.0122 | 1548 | 53 | | | | |
| AH5C | gt | gt56 | 25.9458 | 56.9597 | 135.1923 | 18.3798 | 28.2473 | 66.6092 | 0.2722 | 0.0078 | 0.5168 | 0.0152 | 0.8044 | 0.0109 | 1705 | 64 | | | | |
| AH5C | gt | gt57 | 37.1041 | 251.3895 | 185.2154 | 18.5031 | 29.6843 | 66.4089 | 0.6758 | 0.0124 | 3.9717 | 0.0422 | 1.4172 | 0.0145 | 1611 | 41 | | | | |
| AH5C | gt | gt61 | 42.0428 | 302.7998 | 227.3174 | 18.3209 | 31.6036 | 66.2753 | 0.8627 | 0.0140 | 4.8617 | 0.0467 | 1.9338 | 0.0170 | 1582 | 36 | | | | |
| AH5C | gt | gt62 | 24.7018 | 97.2033 | 103.7948 | 18.9592 | 28.4873 | 65.9859 | 0.2041 | 0.0067 | 1.2369 | 0.0236 | 0.4455 | 0.0081 | 1560 | 72 | | | | |
| AH5C | gt | gt64 | 25.8645 | 59.0104 | 134.1665 | 18.4769 | 27.5162 | 65.9748 | 0.2657 | 0.0077 | 0.5672 | 0.0160 | 0.8007 | 0.0108 | 1656 | 63 | | | | |
| AH5C | gt | gt65 | 26.0083 | 80.7195 | 121.1065 | 18.1913 | 27.4036 | 65.1846 | 0.2809 | 0.0079 | 0.9581 | 0.0207 | 0.6567 | 0.0098 | 1794 | 69 | | | | |
| AH5C | gt | gt67 | 27.4835 | 59.4856 | 145.7137 | 18.9969 | 28.2703 | 66.9431 | 0.3066 | 0.0083 | 0.5621 | 0.0159 | 0.9248 | 0.0116 | 1687 | 60 | | | | |
| AH5C | gt | gt72 | 24.3455 | 59.7607 | 119.0175 | 18.1659 | 29.8209 | 65.7077 | 0.2205 | 0.0070 | 0.5387 | 0.0156 | 0.6252 | 0.0096 | 1693 | 71 | | | | |
| AH5C | gt | gt76 | 39.0358 | 257.7241 | 209.0185 | 18.6319 | 29.9122 | 64.9842 | 0.7421 | 0.0130 | 4.0831 | 0.0428 | 1.7205 | 0.0160 | 1567 | 38 | | | | |
| AH5C | gt | gt77 | 34.7536 | 68.2390 | 236.8432 | 18.7636 | 27.3867 | 64.9731 | 0.5834 | 0.0115 | 0.7344 | 0.0182 | 2.0185 | 0.0172 | 1581 | 40 | | | | |
| AH5C | gt | gt78 | 22.2640 | 47.8319 | 105.7961 | 18.8647 | 28.5659 | 64.8284 | 0.1172 | 0.0050 | 0.3472 | 0.0125 | 0.4805 | 0.0084 | 1266 | 72 | 1605 ± 30 | 49 | | |
| NWI3 | and-mu | 4 | 24.9769 | 151.8942 | 93.4887 | 19.0843 | 30.1194 | 72.1075 | 0.2045 | 0.0067 | 2.0446 | 0.0293 | 0.2373 | 0.0057 | 1533 | 71 | | | | |
| NWI3 | and-mu | 6 | 22.6265 | 108.9106 | 95.2522 | 18.1112 | 32.1028 | 69.6366 | 0.1548 | 0.0058 | 1.2928 | 0.0233 | 0.2838 | 0.0063 | 1462 | 77 | | | | |

| Sample | Occluding phase | Label | Peak Counts Pk(Pb) | Pk(Th) | Pk(U ) | Background counts Bg(Pb) | Bg(Th) | Bg(U ) | W%(Pb) | W%(Pb) 1σ | W%(Th) | W%(Th) 1σ | W%(U) | W%(U) 1σ | Chemical age (Ma) | 1σ | Early/peak meta. age (Ma) & error (2σ) n = | Post peak meta. age (Ma) & error (2σ) n = |
|---|---|---|---|---|---|---|---|---|---|---|---|---|---|---|---|---|---|---|
| NWI3 | and-mu | 9 | 21.5764 | 93.5763 | 89.7617 | 17.7068 | 31.0270 | 69.5253 | 0.1312 | 0.0053 | 1.0514 | 0.0210 | 0.2236 | 0.0056 | 1537 | 88 | | |
| NWI3 | and-mu | 10 | 24.4643 | 147.6404 | 93.1885 | 18.5756 | 30.9307 | 71.3061 | 0.2043 | 0.0067 | 1.9601 | 0.0287 | 0.2429 | 0.0058 | 1564 | 73 | | |
| NWI3 | and-mu | 16 | 24.7643 | 160.8526 | 77.3930 | 19.5096 | 28.7653 | 70.7051 | 0.1821 | 0.0063 | 2.2294 | 0.0307 | 0.0747 | 0.0032 | 1580 | 78 | | |
| NWI3 | and-mu | 19 | 25.4957 | 182.6750 | 80.9446 | 19.1315 | 30.2932 | 71.7513 | 0.2220 | 0.0070 | 2.5641 | 0.0328 | 0.1026 | 0.0038 | 1637 | 74 | | |
| NWI3 | and-mu | 21 | 26.0270 | 163.4801 | 96.8281 | 19.0592 | 30.8906 | 68.2676 | 0.2423 | 0.0073 | 2.2190 | 0.0305 | 0.3166 | 0.0066 | 1566 | 67 | | |
| NWI3 | and-mu | 22 | 23.9267 | 114.3892 | 89.2364 | 18.9556 | 30.5469 | 72.1743 | 0.1714 | 0.0061 | 1.4105 | 0.0244 | 0.1891 | 0.0051 | 1758 | 90 | | |
| NWI3 | and-mu | 24 | 47.2317 | 766.4332 | 115.9528 | 19.7228 | 33.8404 | 73.5322 | 0.9612 | 0.0145 | 12.1267 | 0.0708 | 0.4930 | 0.0085 | 1503 | 32 | | |
| NWI3 | and-mu | 27 | 28.7837 | 205.3014 | 103.9324 | 19.4940 | 29.1636 | 75.5357 | 0.3277 | 0.0085 | 2.9646 | 0.0353 | 0.3180 | 0.0067 | 1716 | 64 | | |
| NWI3 | and-mu | 33 | 26.7271 | 135.9054 | 114.0515 | 19.3698 | 29.6526 | 69.5142 | 0.2581 | 0.0075 | 1.7918 | 0.0275 | 0.4967 | 0.0083 | 1565 | 64 | | |
| NWI3 | and-mu | 35 | 25.1144 | 176.8187 | 80.7446 | 19.0650 | 29.8209 | 70.4825 | 0.2120 | 0.0068 | 2.4866 | 0.0324 | 0.1150 | 0.0040 | 1584 | 73 | | |
| NWI3 | and-mu | 36 | 26.8834 | 218.6183 | 86.0097 | 18.7658 | 30.0582 | 70.2487 | 0.2858 | 0.0079 | 3.1805 | 0.0366 | 0.1772 | 0.0050 | 1620 | 64 | | |
| NWI3 | and-mu | 37 | 29.4776 | 316.6505 | 86.5850 | 18.9002 | 31.9507 | 73.2762 | 0.3708 | 0.0090 | 4.7508 | 0.0445 | 0.1493 | 0.0046 | 1523 | 52 | | |
| NWI3 | and-mu | 38 | 29.7151 | 286.3958 | 88.2734 | 19.1371 | 31.2255 | 70.0707 | 0.3732 | 0.0091 | 4.2812 | 0.0424 | 0.2047 | 0.0054 | 1610 | 56 | | |
| NWI3 | and-mu | 39 | 25.7457 | 192.2108 | 79.7441 | 19.3649 | 31.6530 | 70.7719 | 0.2223 | 0.0070 | 2.6990 | 0.0337 | 0.1001 | 0.0037 | 1576 | 70 | | |
| NWI3 | and-mu | 41 | 25.2019 | 132.8029 | 97.6161 | 18.8111 | 31.3768 | 70.9834 | 0.2222 | 0.0069 | 1.7010 | 0.0267 | 0.2948 | 0.0064 | 1727 | 77 | | |
| NWI3 | and-mu | 43 | 25.9395 | 214.1375 | 83.7210 | 18.5873 | 32.5264 | 72.3746 | 0.2569 | 0.0075 | 3.0472 | 0.0358 | 0.1267 | 0.0042 | 1589 | 66 | | |
| NWI3 | and-mu | 44 | 33.9722 | 386.4475 | 103.2445 | 18.5302 | 30.3099 | 69.6477 | 0.5453 | 0.0110 | 5.9527 | 0.0499 | 0.3804 | 0.0073 | 1612 | 46 | | |
| NWI3 | and-mu | 45 | 28.6962 | 237.6944 | 95.4273 | 19.2242 | 30.8743 | 73.7771 | 0.3333 | 0.0086 | 3.4706 | 0.0382 | 0.2424 | 0.0058 | 1658 | 61 | | |
| NWI3 | and-mu | 48 | 26.8772 | 177.2442 | 102.7066 | 19.5370 | 30.6313 | 72.1632 | 0.2551 | 0.0074 | 2.4485 | 0.0320 | 0.3383 | 0.0068 | 1514 | 63 | | |
| NWI3 | and-mu | 49 | 25.8770 | 139.3332 | 95.1647 | 19.5029 | 31.0696 | 71.4063 | 0.2212 | 0.0069 | 1.8143 | 0.0276 | 0.2630 | 0.0060 | 1722 | 77 | | |
| NWI3 | and-mu | 50 | 32.5532 | 347.7625 | 92.9509 | 19.9998 | 30.5162 | 71.1392 | 0.4383 | 0.0098 | 5.2662 | 0.0467 | 0.2444 | 0.0059 | 1548 | 49 | | |
| NWI3 | and-mu | 51 | 26.4458 | 189.3325 | 94.9395 | 18.6146 | 32.5532 | 71.1837 | 0.2727 | 0.0077 | 2.6169 | 0.0330 | 0.2632 | 0.0060 | 1652 | 67 | | |
| NWI3 | and-mu | 52 | 27.2335 | 213.7119 | 95.2647 | 19.2801 | 28.8058 | 68.4568 | 0.2767 | 0.0078 | 3.0921 | 0.0360 | 0.2990 | 0.0065 | 1449 | 58 | | |
| NWI3 | and-mu | 53 | 27.3960 | 196.6159 | 93.8389 | 18.5007 | 30.2164 | 70.0262 | 0.3127 | 0.0083 | 2.7907 | 0.0342 | 0.2653 | 0.0061 | 1790 | 69 | | |
| NWI3 | and-mu | 54 | 28.7400 | 247.1832 | 97.8412 | 19.3200 | 32.1340 | 70.1820 | 0.3318 | 0.0085 | 3.6104 | 0.0389 | 0.3100 | 0.0066 | 1526 | 56 | | |
| NWI3 | and-mu | 55 | 25.5395 | 174.7916 | 87.5605 | 19.0651 | 31.5335 | 70.9277 | 0.2253 | 0.0070 | 2.4051 | 0.0318 | 0.1851 | 0.0051 | 1590 | 71 | | |
| NWI3 | and-mu | 56 | 29.7527 | 239.8725 | 112.7256 | 18.9756 | 30.7650 | 68.6126 | 0.3807 | 0.0092 | 3.5098 | 0.0384 | 0.4942 | 0.0083 | 1562 | 53 | | |
| NWI3 | and-mu | 59 | 26.2771 | 218.5933 | 80.5695 | 19.0870 | 29.1088 | 68.4568 | 0.2511 | 0.0074 | 3.1856 | 0.0366 | 0.1357 | 0.0044 | 1487 | 62 | | |
| NWI3 | and-mu | 60 | 25.2144 | 183.8263 | 78.9812 | 18.7380 | 29.9422 | 71.0947 | 0.2262 | 0.0070 | 2.5918 | 0.0330 | 0.0881 | 0.0035 | 1680 | 75 | | |
| NWI3 | and-mu | 61 | 24.7581 | 143.6369 | 83.6960 | 19.5888 | 30.8715 | 69.8592 | 0.1778 | 0.0062 | 1.8909 | 0.0282 | 0.1533 | 0.0046 | 1578 | 79 | | |
| NWI3 | and-mu | 62 | 24.6581 | 145.5135 | 85.6470 | 19.2254 | 29.8141 | 70.7941 | 0.1868 | 0.0063 | 1.9353 | 0.0284 | 0.1642 | 0.0048 | 1601 | 78 | | |
| NWI3 | and-mu | 63 | 28.6212 | 257.8493 | 95.7025 | 19.5198 | 29.9922 | 72.9980 | 0.3182 | 0.0083 | 3.8045 | 0.0399 | 0.2534 | 0.0059 | 1470 | 55 | | |
| NWI3 | and-mu | 64 | 28.5962 | 260.6286 | 92.3631 | 18.9691 | 30.8365 | 70.5827 | 0.3367 | 0.0086 | 3.8344 | 0.0400 | 0.2431 | 0.0058 | 1552 | 56 | | |
| NWI3 | and-mu | 65 | 26.3146 | 155.1722 | 97.2284 | 19.4189 | 31.7457 | 72.8978 | 0.2393 | 0.0072 | 2.0603 | 0.0293 | 0.2686 | 0.0061 | 1702 | 74 | | |
| NWI3 | and-mu | 66 | 31.0779 | 307.4333 | 102.2939 | 19.8730 | 30.3467 | 70.6383 | 0.3931 | 0.0093 | 4.6228 | 0.0439 | 0.3549 | 0.0071 | 1453 | 49 | | |
| NWI3 | and-mu | 67 | 31.3905 | 362.1681 | 103.9574 | 19.1948 | 32.5215 | 71.5065 | 0.4269 | 0.0097 | 5.4802 | 0.0477 | 0.3644 | 0.0072 | 1375 | 44 | | |
| NWI3 | and-mu | 68 | 33.5159 | 315.6987 | 112.2628 | 19.0112 | 32.2388 | 71.8181 | 0.5089 | 0.0106 | 4.7029 | 0.0442 | 0.4510 | 0.0079 | 1730 | 52 | | |
| NWI3 | and-mu | 69 | 25.2644 | 62.3617 | 126.6356 | 18.7431 | 30.9084 | 70.4936 | 0.2284 | 0.0071 | 0.5291 | 0.0149 | 0.6185 | 0.0092 | 1761 | 72 | | |
| NWI3 | and-mu | 70 | 27.3210 | 63.6622 | 157.5995 | 19.3394 | 32.1391 | 70.2376 | 0.2817 | 0.0079 | 0.5304 | 0.0149 | 0.9627 | 0.0115 | 1536 | 55 | | |
| NWI3 | and-mu | 71 | 26.4271 | 82.6455 | 135.0297 | 18.4338 | 30.1384 | 71.9406 | 0.2812 | 0.0079 | 0.8816 | 0.0192 | 0.6955 | 0.0098 | 1766 | 66 | | |
| NWI3 | and-mu | 72 | 24.8394 | 61.4363 | 125.7850 | 19.2508 | 29.8458 | 71.5733 | 0.1940 | 0.0065 | 0.5309 | 0.0149 | 0.5968 | 0.0091 | 1571 | 69 | | |
| NWI3 | and-mu | 73 | 26.8772 | 71.3903 | 146.3642 | 18.5208 | 30.7325 | 72.6084 | 0.2929 | 0.0080 | 0.6788 | 0.0168 | 0.8073 | 0.0105 | 1740 | 62 | | |
| NWI3 | and-mu | 75 | 25.6582 | 112.5130 | 125.0719 | 18.6119 | 30.9433 | 69.7479 | 0.2464 | 0.0073 | 1.3681 | 0.0240 | 0.6111 | 0.0092 | 1507 | 62 | | |
| NWI3 | and-mu | 77 | 27.3460 | 79.4939 | 140.7469 | 18.6830 | 30.0644 | 69.1914 | 0.3068 | 0.0082 | 0.8324 | 0.0187 | 0.7907 | 0.0105 | 1771 | 63 | | |
| NWI3 | and-mu | 78 | 28.4774 | 91.4501 | 155.9604 | 18.7181 | 31.0172 | 72.2411 | 0.3462 | 0.0088 | 1.0166 | 0.0207 | 0.9253 | 0.0113 | 1704 | 57 | | |
| NWI3 | and-mu | 79 | 26.4834 | 94.9520 | 142.2857 | 19.4688 | 30.8710 | 70.6161 | 0.2463 | 0.0074 | 1.0786 | 0.0213 | 0.7928 | 0.0105 | 1384 | 55 | | |
| NWI3 | and-mu | 81 | 29.8839 | 135.7052 | 140.0964 | 19.1271 | 31.6887 | 70.5827 | 0.3787 | 0.0091 | 1.7351 | 0.0269 | 0.7654 | 0.0103 | 1793 | 59 | | |
| NWI3 | and-mu | 82 | 39.6547 | 517.7028 | 112.1252 | 19.7641 | 34.1654 | 70.8164 | 0.6937 | 0.0123 | 7.9772 | 0.0574 | 0.4672 | 0.0081 | 1559 | 39 | | |
| NWI3 | and-mu | 83 | 38.8358 | 516.8502 | 113.1759 | 19.4307 | 32.5401 | 71.8404 | 0.6763 | 0.0121 | 7.9907 | 0.0574 | 0.4678 | 0.0081 | 1520 | 39 | | |
| NWI3 | and-mu | 84 | 27.4148 | 213.1863 | 103.6572 | 19.0265 | 31.4034 | 71.8626 | 0.2911 | 0.0079 | 3.0192 | 0.0354 | 0.3514 | 0.0070 | 1481 | 57 | | |
| NWI3 | and-mu | 86 | 27.1335 | 210.7582 | 100.1301 | 18.6007 | 30.3467 | 73.1204 | 0.2962 | 0.0080 | 2.9948 | 0.0353 | 0.2983 | 0.0064 | 1579 | 61 | | |
| NWI3 | and-mu | 87 | 27.6648 | 212.1349 | 111.3122 | 18.5095 | 30.2824 | 67.6109 | 0.3201 | 0.0084 | 3.0434 | 0.0357 | 0.4876 | 0.0082 | 1457 | 54 | | |
| NWI3 | and-mu | 88 | 24.9206 | 143.6869 | 95.5649 | 19.1622 | 30.4395 | 71.8626 | 0.1972 | 0.0065 | 1.8807 | 0.0279 | 0.2600 | 0.0060 | 1523 | 72 | | |

| Sample | Occluding phase | Label | Peak Counts Pk(Pb) | Pk(Th) | Pk(U ) | Background counts Bg(Pb) | Bg(Th) | Bg(U ) | W%(Pb) | W%(Pb) 1σ | W%(Th) | W%(Th) 1σ | W%(U) | W%(U) 1σ | Chemical age (Ma) | 1σ | Early/peak meta. age (Ma) & error (2σ) | n = | Post peak meta. age (Ma) & error (2σ) | n = |
|---|---|---|---|---|---|---|---|---|---|---|---|---|---|---|---|---|---|---|---|---|
| NWI3 | and-mu | 89 | 28.1774 | 209.8821 | 99.5422 | 18.7060 | 31.6910 | 68.7017 | 0.3310 | 0.0085 | 2.9731 | 0.0352 | 0.3426 | 0.0069 | 1695 | 62 | | | | |
| NWI3 | and-mu | 91 | 32.3844 | 361.5167 | 94.4518 | 19.2075 | 32.5952 | 71.5510 | 0.4611 | 0.0100 | 5.4627 | 0.0476 | 0.2569 | 0.0060 | 1566 | 48 | | | | |
| NWI3 | and-mu | 92 | 37.8043 | 543.2590 | 101.2933 | 19.4874 | 31.7357 | 72.5750 | 0.6355 | 0.0117 | 8.4153 | 0.0588 | 0.3249 | 0.0068 | 1445 | 37 | | | | |
| NWI3 | and-mu | 93 | 28.1086 | 198.4931 | 105.5584 | 19.2509 | 30.4039 | 69.5476 | 0.3100 | 0.0082 | 2.8082 | 0.0342 | 0.3998 | 0.0074 | 1582 | 60 | | | | |
| NWI3 | and-mu | 94 | 33.5159 | 376.0989 | 98.8043 | 19.2327 | 30.4259 | 70.4157 | 0.5016 | 0.0105 | 5.7550 | 0.0489 | 0.3199 | 0.0067 | 1575 | 47 | | | | |
| NWI3 | and-mu | 96 | 31.7530 | 324.8412 | 101.9687 | 18.8520 | 33.1729 | 70.4380 | 0.4535 | 0.0100 | 4.8630 | 0.0450 | 0.3538 | 0.0070 | 1601 | 50 | | | | |
| NWI3 | and-mu | 97 | 32.8032 | 367.0537 | 98.5291 | 19.2561 | 31.8650 | 70.1152 | 0.4758 | 0.0102 | 5.5818 | 0.0482 | 0.3198 | 0.0067 | 1535 | 47 | | | | |
| NWI3 | and-mu | 98 | 33.9910 | 368.4318 | 102.9443 | 19.1019 | 32.3402 | 70.0707 | 0.5232 | 0.0107 | 5.5916 | 0.0482 | 0.3697 | 0.0072 | 1635 | 48 | 1589 ± 26 | 63 | | |
| NWI5 | and | 7 | 23.9330 | 132.6528 | 84.8466 | 17.9422 | 30.6482 | 64.8507 | 0.2280 | 0.0074 | 1.8859 | 0.0295 | 0.2419 | 0.0060 | 1773 | 83 | | | | |
| NWI5 | and | 8 | 31.2717 | 389.9557 | 83.9461 | 17.6582 | 29.2582 | 66.0972 | 0.5230 | 0.0112 | 6.6139 | 0.0551 | 0.2202 | 0.0058 | 1534 | 46 | | | | |
| NWI5 | and | 9 | 22.3515 | 114.7145 | 84.8341 | 17.3715 | 26.6545 | 63.1812 | 0.1881 | 0.0067 | 1.6303 | 0.0275 | 0.2620 | 0.0063 | 1584 | 80 | | | | |
| NWI5 | and | 10 | 31.0341 | 363.9469 | 82.8581 | 17.4680 | 28.8454 | 65.6520 | 0.5205 | 0.0112 | 6.1332 | 0.0530 | 0.2113 | 0.0057 | 1634 | 50 | | | | |
| NWI5 | and | 12 | 24.5143 | 175.6926 | 84.8716 | 17.7165 | 28.7335 | 65.3404 | 0.2586 | 0.0078 | 2.7043 | 0.0353 | 0.2362 | 0.0060 | 1578 | 69 | | | | |
| NWI5 | and | 16 | 23.8392 | 156.7987 | 86.2098 | 17.2602 | 27.0427 | 63.2814 | 0.2512 | 0.0077 | 2.4000 | 0.0333 | 0.2784 | 0.0065 | 1599 | 71 | | | | |
| NWI5 | and | 20 | 24.1768 | 128.6246 | 87.2979 | 18.1565 | 27.3427 | 64.8062 | 0.2292 | 0.0074 | 1.8727 | 0.0294 | 0.2720 | 0.0064 | 1727 | 80 | | | | |
| NWI5 | and | 21 | 25.3519 | 132.3525 | 102.7692 | 17.7737 | 29.0491 | 65.2959 | 0.2918 | 0.0084 | 1.9163 | 0.0298 | 0.4550 | 0.0083 | 1757 | 71 | | | | |
| NWI5 | and | 23 | 23.7579 | 134.5793 | 87.2478 | 17.6713 | 27.7550 | 65.8078 | 0.2310 | 0.0074 | 1.9685 | 0.0301 | 0.2586 | 0.0062 | 1714 | 79 | | | | |
| NWI5 | and | 48 | 27.1210 | 207.6292 | 101.0556 | 18.6648 | 30.2787 | 67.3994 | 0.3125 | 0.0085 | 3.1497 | 0.0374 | 0.3938 | 0.0076 | 1491 | 57 | | | | |
| NWI5 | and | 52 | 23.7579 | 131.3768 | 87.0978 | 17.8527 | 28.2712 | 65.4962 | 0.2214 | 0.0072 | 1.8794 | 0.0293 | 0.2576 | 0.0062 | 1698 | 79 | | | | |
| NWI5 | and | 53 | 24.8581 | 160.6774 | 75.7547 | 18.2406 | 27.6391 | 62.4800 | 0.2502 | 0.0077 | 2.4399 | 0.0334 | 0.1599 | 0.0049 | 1782 | 80 | | | | |
| NWI5 | and | 55 | 23.4954 | 152.1194 | 81.2073 | 16.8311 | 26.6754 | 66.4534 | 0.2524 | 0.0077 | 2.3013 | 0.0325 | 0.1776 | 0.0052 | 1838 | 82 | | | | |
| NWI5 | and | 84 | 25.2644 | 192.9366 | 85.6345 | 17.2438 | 30.2430 | 64.5168 | 0.3074 | 0.0086 | 3.0037 | 0.0372 | 0.2569 | 0.0063 | 1687 | 68 | | | | |
| NWI5 | and | 85 | 25.2769 | 153.9210 | 100.4928 | 17.8583 | 27.5205 | 65.7188 | 0.2829 | 0.0082 | 2.3279 | 0.0327 | 0.4204 | 0.0080 | 1595 | 66 | | | | |
| NWI5 | and | 86 | 32.6907 | 398.8767 | 91.3876 | 18.1839 | 28.8400 | 64.3498 | 0.5570 | 0.0116 | 6.7854 | 0.0558 | 0.3341 | 0.0072 | 1516 | 45 | | | | |
| NWI5 | and | 87 | 28.0086 | 250.2127 | 91.6377 | 17.2765 | 29.1707 | 67.1101 | 0.4102 | 0.0099 | 4.0464 | 0.0430 | 0.2978 | 0.0067 | 1726 | 60 | | | | |
| NWI5 | and | 88 | 27.0772 | 133.3533 | 123.7209 | 17.4727 | 28.1286 | 64.8395 | 0.3718 | 0.0095 | 1.9489 | 0.0300 | 0.7140 | 0.0104 | 1757 | 62 | | | | |
| NWI5 | and | 89 | 28.1586 | 138.8578 | 133.9163 | 17.6432 | 28.3271 | 65.4628 | 0.4060 | 0.0099 | 2.0394 | 0.0307 | 0.8275 | 0.0112 | 1731 | 58 | | | | |
| NWI5 | and | 90 | 22.0765 | 71.3153 | 95.8400 | 17.9151 | 27.0745 | 64.2831 | 0.1557 | 0.0060 | 0.8193 | 0.0195 | 0.3800 | 0.0076 | 1548 | 83 | | | | |
| NWI5 | and | 91 | 25.9958 | 182.2246 | 104.4702 | 17.6118 | 28.1090 | 65.6743 | 0.3212 | 0.0088 | 2.8398 | 0.0362 | 0.4706 | 0.0084 | 1540 | 60 | | | | |
| NWI5 | and | 92 | 27.0772 | 189.9332 | 104.4452 | 17.1231 | 28.2774 | 65.0955 | 0.3827 | 0.0096 | 2.9774 | 0.0370 | 0.4776 | 0.0085 | 1748 | 63 | | | | |
| NWI5 | and | 93 | 29.6276 | 246.9078 | 112.3128 | 17.5434 | 29.9105 | 65.1512 | 0.4671 | 0.0106 | 4.0070 | 0.0430 | 0.5774 | 0.0094 | 1656 | 54 | | | | |
| NWI5 | and | 94 | 25.7145 | 138.7077 | 116.7659 | 17.4556 | 29.1753 | 65.0287 | 0.3155 | 0.0087 | 2.0116 | 0.0304 | 0.6224 | 0.0097 | 1606 | 62 | | | | |
| NWI5 | and | 106 | 25.2707 | 202.1725 | 82.8081 | 17.3629 | 27.9289 | 64.4500 | 0.3014 | 0.0085 | 3.1993 | 0.0383 | 0.2223 | 0.0058 | 1630 | 66 | | | | |
| NWI5 | and | 107 | 24.9144 | 153.8460 | 85.9847 | 17.6703 | 29.7026 | 64.7616 | 0.2762 | 0.0081 | 2.2842 | 0.0324 | 0.2561 | 0.0062 | 1841 | 78 | | | | |
| NWI5 | and | 108 | 30.0090 | 347.5620 | 81.7575 | 17.7870 | 28.9115 | 64.4389 | 0.4683 | 0.0106 | 5.8425 | 0.0518 | 0.2128 | 0.0057 | 1539 | 49 | | | | |
| NWI5 | and | 109 | 24.3205 | 220.9714 | 83.8336 | 16.6391 | 27.5406 | 63.4706 | 0.2923 | 0.0083 | 3.5567 | 0.0404 | 0.2476 | 0.0061 | 1434 | 58 | | | | |
| NWI5 | and | 110 | 22.3703 | 113.2134 | 85.5720 | 17.9931 | 28.6287 | 65.2291 | 0.1631 | 0.0062 | 1.5572 | 0.0268 | 0.2446 | 0.0061 | 1461 | 79 | | | | |
| NWI5 | and | 111 | 24.7768 | 100.4553 | 112.5755 | 17.8836 | 28.5453 | 65.1734 | 0.2642 | 0.0080 | 1.3301 | 0.0248 | 0.5716 | 0.0093 | 1676 | 70 | | | | |
| NWI5 | and | 112 | 24.8706 | 121.4192 | 98.0163 | 18.2460 | 28.3905 | 65.4072 | 0.2527 | 0.0078 | 1.7173 | 0.0282 | 0.3935 | 0.0077 | 1729 | 75 | | | | |
| NWI5 | and | 113 | 24.3143 | 141.8103 | 92.2880 | 18.1479 | 28.3024 | 65.2625 | 0.2344 | 0.0075 | 2.0944 | 0.0311 | 0.3267 | 0.0070 | 1556 | 71 | | | | |
| NWI5 | and | 114 | 23.0516 | 83.2208 | 102.0562 | 17.7016 | 28.0324 | 65.8078 | 0.2021 | 0.0069 | 1.0173 | 0.0217 | 0.4348 | 0.0081 | 1682 | 79 | | | | |
| NWI5 | and | 116 | 24.0017 | 136.5559 | 95.3273 | 17.1342 | 28.8588 | 64.9620 | 0.2613 | 0.0079 | 1.9811 | 0.0302 | 0.3657 | 0.0074 | 1704 | 73 | | | | |
| NWI5 | and | 118 | 29.2213 | 295.2363 | 94.8770 | 18.0908 | 30.6195 | 66.4311 | 0.4264 | 0.0101 | 4.8520 | 0.0472 | 0.3474 | 0.0073 | 1519 | 51 | | | | |
| NWI5 | and | 119 | 24.6206 | 63.7622 | 129.5003 | 18.0796 | 27.3576 | 64.2385 | 0.2503 | 0.0077 | 0.6728 | 0.0176 | 0.7832 | 0.0108 | 1558 | 63 | | | | |
| NWI5 | and | 120 | 24.8456 | 168.9856 | 93.9515 | 17.0285 | 30.0276 | 65.1846 | 0.2985 | 0.0084 | 2.5546 | 0.0343 | 0.3474 | 0.0072 | 1690 | 68 | | | | |
| NWI5 | and | 121 | 22.3953 | 89.0738 | 90.7372 | 17.6008 | 27.6999 | 66.6537 | 0.1789 | 0.0065 | 1.1239 | 0.0227 | 0.2872 | 0.0065 | 1771 | 91 | | | | |
| NWI5 | and | 122 | 29.8777 | 332.6065 | 96.6030 | 17.6078 | 28.8732 | 66.3421 | 0.4690 | 0.0106 | 5.5470 | 0.0503 | 0.3696 | 0.0075 | 1485 | 48 | | | | |
| NWI5 | and | 123 | 22.9016 | 96.1777 | 94.2266 | 17.2698 | 27.7928 | 65.4294 | 0.2129 | 0.0071 | 1.2589 | 0.0241 | 0.3455 | 0.0072 | 1811 | 85 | | | | |
| NWI5 | and | 124 | 26.2021 | 144.9630 | 114.7020 | 16.8957 | 28.5516 | 64.1161 | 0.3569 | 0.0092 | 2.1390 | 0.0313 | 0.6093 | 0.0096 | 1761 | 64 | | | | |
| NWI5 | and | 125 | 23.4079 | 108.0600 | 101.0556 | 17.7124 | 28.6557 | 64.1829 | 0.2157 | 0.0071 | 1.4622 | 0.0259 | 0.4429 | 0.0082 | 1535 | 71 | | | | |
| NWI5 | and | 128 | 21.8327 | 112.2878 | 85.8221 | 17.0040 | 27.0343 | 64.8618 | 0.1804 | 0.0065 | 1.5647 | 0.0268 | 0.2513 | 0.0061 | 1584 | 81 | | | | |
| NWI5 | and | 130 | 21.7889 | 89.0488 | 94.1141 | 16.9505 | 27.5632 | 64.0938 | 0.1804 | 0.0065 | 1.1288 | 0.0228 | 0.3595 | 0.0073 | 1610 | 81 | | | | |
| NWI5 | and | 132 | 26.0083 | 218.2678 | 92.5257 | 18.4183 | 27.8191 | 64.6281 | 0.2880 | 0.0083 | 3.4960 | 0.0401 | 0.3388 | 0.0072 | 1340 | 54 | | | | |

| Sample | Occluding phase | Label | Peak Counts Pk(Pb) | Pk(Th) | Pk(U ) | Background counts Bg(Pb) | Bg(Th) | Bg(U ) | W%(Pb) | W%(Pb) 1σ | W%(Th) | W%(Th) 1σ | W%(U) | W%(U) 1σ | Chemical age (Ma) | 1σ | Early/peak meta. age (Ma) & error (2σ) n = | Post peak meta. age (Ma) & error (2σ) n = |
|---|---|---|---|---|---|---|---|---|---|---|---|---|---|---|---|---|---|---|
| NWI5 | and | 134 | 22.8266 | 116.5658 | 86.5725 | 17.3237 | 28.9846 | 65.8524 | 0.2066 | 0.0070 | 1.6042 | 0.0271 | 0.2479 | 0.0061 | 1772 | 86 | | |
| NWI5 | and | 5 | 26.6584 | 222.0728 | 81.0572 | 17.3864 | 28.7335 | 64.4723 | 0.3564 | 0.0093 | 3.5447 | 0.0403 | 0.2013 | 0.0055 | 1793 | 67 | | |
| NWI5 | and | 6 | 23.8142 | 134.5293 | 103.1444 | 16.8702 | 28.0948 | 64.5056 | 0.2680 | 0.0080 | 1.9705 | 0.0302 | 0.4690 | 0.0084 | 1587 | 67 | | |
| NWI5 | and | 12 | 24.6956 | 161.1779 | 97.6786 | 17.5896 | 28.5108 | 64.3053 | 0.2726 | 0.0081 | 2.4434 | 0.0335 | 0.4043 | 0.0078 | 1522 | 64 | | |
| NWI5 | and | 13 | 26.4396 | 233.5385 | 91.5376 | 17.6994 | 28.0392 | 64.2719 | 0.3394 | 0.0091 | 3.8018 | 0.0419 | 0.3340 | 0.0072 | 1478 | 56 | | |
| NWI5 | and | 14 | 24.2830 | 126.4480 | 94.1016 | 17.9294 | 30.7306 | 66.7428 | 0.2324 | 0.0073 | 1.6886 | 0.0273 | 0.3159 | 0.0068 | 1761 | 79 | | |
| NWI5 | and | 15 | 31.8843 | 350.7938 | 91.1499 | 18.7999 | 30.7748 | 68.1229 | 0.4860 | 0.0106 | 5.6476 | 0.0499 | 0.2725 | 0.0063 | 1589 | 49 | | |
| NWI5 | and | 16 | 23.5454 | 145.8138 | 87.5605 | 17.5791 | 30.1480 | 67.2325 | 0.2200 | 0.0071 | 2.0651 | 0.0304 | 0.2382 | 0.0059 | 1628 | 76 | | |
| NWI5 | and | 17 | 21.2701 | 114.3392 | 82.2953 | 17.0292 | 28.0702 | 62.7583 | 0.1552 | 0.0060 | 1.5543 | 0.0265 | 0.2303 | 0.0058 | 1425 | 78 | | |
| NWI5 | and | 20 | 26.6709 | 241.8754 | 83.9336 | 17.7642 | 29.2294 | 65.7856 | 0.3371 | 0.0089 | 3.8451 | 0.0417 | 0.2177 | 0.0057 | 1579 | 60 | | |
| NWI5 | and | 21 | 21.4951 | 110.6617 | 80.8821 | 17.0856 | 30.1337 | 63.6375 | 0.1634 | 0.0062 | 1.4654 | 0.0258 | 0.2052 | 0.0055 | 1605 | 87 | | |
| NWI5 | and | 23 | 24.2018 | 159.3762 | 81.3198 | 17.5543 | 27.9423 | 64.2274 | 0.2513 | 0.0077 | 2.3914 | 0.0330 | 0.2044 | 0.0055 | 1729 | 77 | | |
| NWI5 | and | 24 | 30.2778 | 332.4813 | 87.1853 | 18.1066 | 29.4216 | 66.4534 | 0.4631 | 0.0105 | 5.4784 | 0.0498 | 0.2510 | 0.0062 | 1574 | 51 | | |
| NWI5 | and | 25 | 28.4649 | 311.8916 | 82.3453 | 17.2675 | 27.9072 | 65.0510 | 0.4275 | 0.0101 | 5.1694 | 0.0485 | 0.2107 | 0.0057 | 1565 | 53 | | |
| NWI5 | and | 28 | 20.6200 | 83.9962 | 82.2578 | 17.5590 | 27.0875 | 62.9697 | 0.1108 | 0.0050 | 1.0400 | 0.0218 | 0.2301 | 0.0059 | 1310 | 83 | | |
| NWI5 | and | 30 | 21.1388 | 95.5024 | 81.5449 | 17.1106 | 26.6362 | 64.9174 | 0.1488 | 0.0059 | 1.2555 | 0.0239 | 0.1980 | 0.0054 | 1634 | 92 | | |
| NWI5 | and | 31 | 20.1325 | 82.1452 | 83.8586 | 16.8408 | 26.8010 | 63.1033 | 0.1199 | 0.0052 | 1.0103 | 0.0215 | 0.2471 | 0.0061 | 1388 | 85 | | |
| NWI5 | and | 34 | 21.6889 | 134.8045 | 80.3569 | 16.4684 | 26.9420 | 61.5674 | 0.1958 | 0.0068 | 1.9706 | 0.0300 | 0.2253 | 0.0058 | 1530 | 76 | | |
| NWI5 | and | 35 | 23.9455 | 166.9336 | 80.5570 | 17.3461 | 29.0968 | 64.7171 | 0.2500 | 0.0077 | 2.5148 | 0.0339 | 0.1901 | 0.0053 | 1686 | 75 | | |
| NWI5 | and | 36 | 26.9897 | 266.9887 | 79.8691 | 17.3997 | 27.1149 | 63.9825 | 0.3662 | 0.0093 | 4.3644 | 0.0446 | 0.1922 | 0.0054 | 1571 | 57 | | |
| NWI5 | and | 38 | 22.7703 | 135.7052 | 78.6435 | 17.8521 | 29.5463 | 65.2402 | 0.1839 | 0.0066 | 1.9364 | 0.0297 | 0.1603 | 0.0049 | 1586 | 81 | | |
| NWI5 | and | 39 | 22.0452 | 126.0226 | 80.8571 | 17.6586 | 29.8741 | 65.6854 | 0.1630 | 0.0062 | 1.7538 | 0.0283 | 0.1812 | 0.0052 | 1477 | 80 | | |
| NWI5 | and | 40 | 21.6577 | 106.6591 | 81.5324 | 17.5504 | 28.4696 | 65.0399 | 0.1520 | 0.0059 | 1.4256 | 0.0255 | 0.1965 | 0.0054 | 1548 | 87 | | |
| NWI5 | and | 44 | 22.4515 | 172.2640 | 75.2670 | 15.8968 | 26.4831 | 59.6420 | 0.2485 | 0.0077 | 2.6703 | 0.0350 | 0.1888 | 0.0053 | 1606 | 71 | | |
| NWI5 | and | 45 | 29.3963 | 333.6587 | 80.2818 | 18.1382 | 29.6295 | 64.9286 | 0.4295 | 0.0101 | 5.5203 | 0.0501 | 0.1868 | 0.0053 | 1508 | 50 | | |
| NWI5 | and | 47 | 24.0705 | 146.4143 | 94.4142 | 17.7802 | 29.1335 | 64.8729 | 0.2388 | 0.0075 | 2.1459 | 0.0313 | 0.3548 | 0.0073 | 1518 | 68 | | |
| NWI5 | and | 48 | 21.9077 | 87.6730 | 95.8275 | 17.4134 | 28.6656 | 63.1923 | 0.1676 | 0.0063 | 1.0776 | 0.0222 | 0.3888 | 0.0076 | 1479 | 77 | | |
| NWI5 | and | 50 | 22.2077 | 72.0156 | 93.9640 | 18.6536 | 27.1605 | 62.9586 | 0.1311 | 0.0055 | 0.8219 | 0.0194 | 0.3699 | 0.0074 | 1347 | 78 | | |
| NWI5 | and | 54 | 22.5640 | 107.5597 | 87.6480 | 17.8411 | 29.5741 | 63.7822 | 0.1765 | 0.0064 | 1.4236 | 0.0255 | 0.2847 | 0.0065 | 1565 | 81 | | |
| NWI5 | and | 55 | 22.0265 | 103.2069 | 95.9776 | 17.3442 | 28.6461 | 64.0605 | 0.1755 | 0.0064 | 1.3658 | 0.0250 | 0.3820 | 0.0076 | 1407 | 72 | | |
| NWI5 | and | 56 | 22.0015 | 97.5035 | 83.4084 | 17.8383 | 28.3949 | 64.8507 | 0.1546 | 0.0060 | 1.2629 | 0.0240 | 0.2215 | 0.0057 | 1622 | 90 | | |
| NWI5 | and | 97 | 23.2516 | 158.5754 | 78.3309 | 17.3281 | 27.7238 | 65.2847 | 0.2242 | 0.0073 | 2.3941 | 0.0331 | 0.1569 | 0.0049 | 1638 | 77 | | |
| NWI5 | and | 98 | 26.4521 | 193.7876 | 82.1077 | 18.2012 | 28.1095 | 65.9859 | 0.3150 | 0.0087 | 3.0259 | 0.0372 | 0.1943 | 0.0054 | 1814 | 72 | | |
| NWI5 | and | 99 | 29.5839 | 328.9744 | 84.5464 | 18.0002 | 28.8207 | 65.5185 | 0.4419 | 0.0103 | 5.4473 | 0.0497 | 0.2313 | 0.0059 | 1529 | 50 | | |
| NWI5 | and | 100 | 24.0892 | 161.9036 | 76.2549 | 18.1061 | 29.8360 | 64.8173 | 0.2255 | 0.0073 | 2.4085 | 0.0331 | 0.1372 | 0.0045 | 1677 | 78 | | |
| NWI5 | and | 101 | 26.5896 | 242.7767 | 84.0712 | 17.3141 | 28.4134 | 63.3815 | 0.3534 | 0.0092 | 3.9004 | 0.0421 | 0.2499 | 0.0061 | 1595 | 59 | | |
| NWI5 | and | 104 | 26.6584 | 201.5968 | 78.6561 | 18.4204 | 28.0773 | 62.9475 | 0.3124 | 0.0086 | 3.1509 | 0.0378 | 0.1885 | 0.0053 | 1755 | 70 | | |
| NWI5 | and | 105 | 24.1455 | 170.9376 | 82.3328 | 18.1818 | 28.5887 | 65.7633 | 0.2250 | 0.0073 | 2.5966 | 0.0344 | 0.1989 | 0.0055 | 1480 | 68 | | |
| NWI5 | and | 106 | 22.6015 | 116.9910 | 79.4189 | 17.9156 | 26.9103 | 64.6726 | 0.1748 | 0.0064 | 1.6441 | 0.0274 | 0.1762 | 0.0051 | 1657 | 87 | | |
| NWI5 | and | 107 | 24.9394 | 176.5685 | 80.3819 | 17.7752 | 27.8317 | 66.8986 | 0.2722 | 0.0080 | 2.7139 | 0.0352 | 0.1621 | 0.0049 | 1774 | 76 | | |
| NWI5 | and | 108 | 25.8395 | 220.9964 | 86.0222 | 17.3041 | 28.4524 | 64.3943 | 0.3255 | 0.0088 | 3.5112 | 0.0400 | 0.2611 | 0.0063 | 1585 | 61 | | |
| NWI5 | and | 109 | 27.5648 | 271.3958 | 85.9221 | 18.1319 | 28.0789 | 65.1734 | 0.3589 | 0.0092 | 4.4207 | 0.0448 | 0.2510 | 0.0062 | 1468 | 54 | | |
| NWI5 | and | 110 | 22.9328 | 142.7111 | 88.7361 | 17.2160 | 27.3141 | 63.3704 | 0.2158 | 0.0071 | 2.1155 | 0.0311 | 0.3056 | 0.0068 | 1465 | 69 | | |
| NWI5 | and | 112 | 22.8578 | 142.6110 | 86.9602 | 17.5317 | 27.6469 | 64.5168 | 0.1996 | 0.0068 | 2.0935 | 0.0309 | 0.2682 | 0.0063 | 1427 | 69 | | |
| NWI5 | and | 113 | 26.0645 | 222.0979 | 82.0827 | 17.8385 | 28.1473 | 65.0176 | 0.3123 | 0.0086 | 3.5233 | 0.0400 | 0.2052 | 0.0056 | 1588 | 63 | | |
| NWI5 | and | 114 | 22.1202 | 104.8580 | 84.1587 | 17.5052 | 29.5523 | 64.5947 | 0.1714 | 0.0063 | 1.3696 | 0.0250 | 0.2325 | 0.0059 | 1674 | 88 | | |
| NWI5 | and | 16 | 25.6020 | 168.7604 | 83.2708 | 19.0389 | 30.7111 | 66.2864 | 0.2333 | 0.0072 | 2.4825 | 0.0334 | 0.2029 | 0.0055 | 1575 | 70 | | |
| NWI5 | and | 17 | 29.2838 | 273.9750 | 83.2583 | 18.5303 | 29.3997 | 65.5185 | 0.3867 | 0.0093 | 4.3875 | 0.0444 | 0.2138 | 0.0057 | 1623 | 56 | | |
| NWI5 | and | 18 | 27.5835 | 253.5928 | 83.4959 | 18.9370 | 29.0071 | 67.3215 | 0.3088 | 0.0083 | 4.0253 | 0.0425 | 0.1944 | 0.0054 | 1426 | 55 | | |
| NWI5 | and | 19 | 30.9341 | 295.5117 | 85.4469 | 19.1157 | 30.7350 | 66.5869 | 0.4244 | 0.0098 | 4.7372 | 0.0460 | 0.2273 | 0.0059 | 1652 | 55 | | |
| NWI5 | and | 20 | 25.4144 | 163.8055 | 83.4209 | 18.8569 | 30.0837 | 66.5981 | 0.2336 | 0.0072 | 2.4076 | 0.0329 | 0.2011 | 0.0055 | 1615 | 72 | | |
| NWI5 | and | 21 | 33.0283 | 370.3360 | 88.2108 | 18.5832 | 30.1144 | 66.4422 | 0.5210 | 0.0108 | 6.0995 | 0.0523 | 0.2650 | 0.0064 | 1600 | 48 | | |
| NWI5 | and | 22 | 25.1644 | 136.7561 | 87.0852 | 18.7211 | 28.0291 | 65.1512 | 0.2297 | 0.0072 | 1.9639 | 0.0298 | 0.2626 | 0.0063 | 1700 | 77 | | |

| Sample | Occluding phase | Label | Peak Counts Pk(Pb) | Pk(Th) | Pk(U ) | Background counts Bg(Pb) | Bg(Th) | Bg(U ) | W%(Pb) | W%(Pb) 1σ | W%(Th) | W%(Th) 1σ | W%(U) | W%(U) 1σ | Chemical age (Ma) | 1σ | Early/peak meta. age (Ma) & error (2σ) | n = | Post peak meta. age (Ma) & error (2σ) | n = |
|---|---|---|---|---|---|---|---|---|---|---|---|---|---|---|---|---|---|---|---|---|
| NWI5 | and | 23 | 27.5898 | 169.4611 | 100.6554 | 19.0346 | 27.6586 | 66.5202 | 0.3075 | 0.0083 | 2.5538 | 0.0339 | 0.4087 | 0.0078 | 1649 | 64 | | | | |
| NWI5 | and | 25 | 25.5457 | 167.6343 | 85.6845 | 18.4137 | 27.2810 | 66.4534 | 0.2543 | 0.0075 | 2.5242 | 0.0337 | 0.2299 | 0.0059 | 1640 | 70 | | | | |
| NWI5 | and | 26 | 26.1646 | 164.9316 | 94.6769 | 19.0871 | 30.7695 | 65.6854 | 0.2523 | 0.0075 | 2.4121 | 0.0329 | 0.3462 | 0.0072 | 1502 | 64 | | | | |
| NWI5 | and | 28 | 26.0833 | 163.5302 | 85.2468 | 18.7445 | 30.1646 | 67.5219 | 0.2624 | 0.0077 | 2.4009 | 0.0329 | 0.2119 | 0.0056 | 1780 | 76 | | | | |
| NWI5 | and | 32 | 24.3893 | 125.9726 | 81.6075 | 18.7011 | 29.3812 | 67.1991 | 0.2016 | 0.0067 | 1.7409 | 0.0280 | 0.1718 | 0.0051 | 1828 | 89 | | | | |
| NWI5 | and | 33 | 24.6643 | 149.9674 | 86.0472 | 18.7261 | 28.2805 | 67.0433 | 0.2106 | 0.0068 | 2.1923 | 0.0314 | 0.2271 | 0.0058 | 1522 | 71 | | | | |
| NWI5 | and | 35 | 24.5393 | 151.5689 | 86.2973 | 18.4380 | 28.7462 | 66.4422 | 0.2168 | 0.0069 | 2.2129 | 0.0316 | 0.2373 | 0.0060 | 1536 | 71 | | | | |
| NWI5 | and | 36 | 24.1142 | 155.2973 | 82.6205 | 18.1818 | 30.5957 | 65.1846 | 0.2106 | 0.0068 | 2.2480 | 0.0318 | 0.2085 | 0.0056 | 1527 | 72 | | | | |
| NWI5 | and | 37 | 27.5523 | 217.1914 | 86.9227 | 17.8034 | 28.2780 | 64.9731 | 0.3526 | 0.0089 | 3.4213 | 0.0394 | 0.2659 | 0.0063 | 1733 | 64 | | | | |
| NWI5 | and | 38 | 34.4536 | 410.3546 | 89.8117 | 18.9684 | 30.6338 | 66.8986 | 0.5592 | 0.0112 | 6.8136 | 0.0553 | 0.2804 | 0.0065 | 1551 | 45 | | | | |
| NWI5 | and | 39 | 28.1149 | 219.0438 | 87.4729 | 18.7846 | 28.7310 | 66.1974 | 0.3358 | 0.0087 | 3.4271 | 0.0393 | 0.2561 | 0.0062 | 1667 | 63 | | | | |
| NWI5 | and | 40 | 25.7332 | 150.4929 | 86.6225 | 18.7685 | 30.4361 | 65.0176 | 0.2490 | 0.0075 | 2.1644 | 0.0312 | 0.2583 | 0.0062 | 1730 | 75 | | | | |
| NWI5 | and | 42 | 27.7836 | 262.2812 | 83.8711 | 18.2350 | 30.6790 | 66.9320 | 0.3431 | 0.0088 | 4.1633 | 0.0433 | 0.2044 | 0.0056 | 1522 | 56 | | | | |
| NWI5 | and | 43 | 30.6153 | 321.4096 | 86.8726 | 18.9405 | 28.4307 | 64.7060 | 0.4209 | 0.0097 | 5.2789 | 0.0488 | 0.2702 | 0.0064 | 1467 | 48 | | | | |
| NWI5 | and | 44 | 27.5148 | 227.3550 | 85.3969 | 18.7169 | 30.0663 | 66.6315 | 0.3157 | 0.0084 | 3.5498 | 0.0400 | 0.2259 | 0.0058 | 1570 | 60 | | | | |
| NWI5 | and | 45 | 24.5018 | 157.5494 | 84.3463 | 18.2329 | 30.8457 | 64.4723 | 0.2229 | 0.0070 | 2.2829 | 0.0321 | 0.2376 | 0.0060 | 1543 | 70 | | | | |
| NWI5 | and | 46 | 32.5532 | 350.7437 | 84.0337 | 18.4599 | 31.1910 | 65.8412 | 0.5085 | 0.0107 | 5.7307 | 0.0507 | 0.2210 | 0.0058 | 1683 | 51 | | | | |
| NWI5 | and | 47 | 31.3217 | 331.7799 | 87.3604 | 18.7896 | 29.8642 | 65.4517 | 0.4520 | 0.0101 | 5.4205 | 0.0493 | 0.2660 | 0.0064 | 1539 | 49 | | | | |
| NWI5 | and | 49 | 31.4342 | 318.7295 | 85.5845 | 18.8243 | 30.2484 | 66.9542 | 0.4554 | 0.0101 | 5.1838 | 0.0483 | 0.2261 | 0.0059 | 1642 | 53 | | | | |
| NWI5 | and | 50 | 28.3837 | 224.8516 | 85.7596 | 19.1681 | 30.5009 | 66.2085 | 0.3313 | 0.0086 | 3.4972 | 0.0397 | 0.2352 | 0.0059 | 1648 | 62 | | | | |
| NWI5 | and | 52 | 26.1145 | 175.2921 | 87.4980 | 18.8541 | 28.9874 | 66.8875 | 0.2598 | 0.0076 | 2.6376 | 0.0345 | 0.2471 | 0.0061 | 1596 | 68 | | | | |
| NWI5 | and | 53 | 25.8020 | 162.5292 | 87.5855 | 18.6818 | 27.8747 | 66.7428 | 0.2546 | 0.0075 | 2.4272 | 0.0331 | 0.2496 | 0.0061 | 1653 | 71 | | | | |
| NWI5 | and | 54 | 26.3333 | 172.6394 | 87.4229 | 18.7774 | 29.3708 | 64.1718 | 0.2708 | 0.0078 | 2.5873 | 0.0342 | 0.2794 | 0.0065 | 1630 | 68 | | | | |
| NWI5 | and | 57 | 24.7331 | 130.0507 | 85.6970 | 18.3682 | 27.8598 | 65.2959 | 0.2270 | 0.0071 | 1.8432 | 0.0288 | 0.2435 | 0.0060 | 1787 | 82 | | | | |
| NWI5 | and | 58 | 23.4642 | 106.4090 | 81.0697 | 19.1625 | 29.6918 | 65.1734 | 0.1504 | 0.0057 | 1.3852 | 0.0250 | 0.1894 | 0.0053 | 1578 | 87 | | | | |
| NWI5 | and | 59 | 25.2894 | 180.6979 | 78.9062 | 18.6442 | 29.6002 | 65.6298 | 0.2367 | 0.0073 | 2.7200 | 0.0350 | 0.1590 | 0.0049 | 1560 | 69 | | | | |
| NWI5 | and | 60 | 27.6210 | 228.3313 | 83.6210 | 18.5089 | 27.4047 | 64.9174 | 0.3273 | 0.0086 | 3.6142 | 0.0403 | 0.2251 | 0.0058 | 1602 | 61 | | | | |
| NWI5 | and | 61 | 26.9334 | 197.4169 | 83.0707 | 18.5510 | 29.4498 | 64.4166 | 0.3008 | 0.0082 | 3.0250 | 0.0369 | 0.2240 | 0.0058 | 1693 | 67 | | | | |
| NWI5 | and | 62 | 25.2019 | 202.0975 | 72.6033 | 19.2499 | 29.7669 | 65.9637 | 0.2101 | 0.0068 | 3.0948 | 0.0373 | 0.0795 | 0.0034 | 1357 | 62 | | | | |
| NWI5 | and | 63 | 27.6460 | 231.4105 | 81.5449 | 18.8448 | 28.5333 | 65.8524 | 0.3163 | 0.0084 | 3.6534 | 0.0406 | 0.1891 | 0.0053 | 1582 | 61 | | | | |
| NWI5 | and | 65 | 27.1710 | 204.5755 | 86.2473 | 18.6068 | 27.5508 | 65.5741 | 0.3079 | 0.0083 | 3.1912 | 0.0379 | 0.2487 | 0.0061 | 1630 | 64 | | | | |
| NWI5 | and | 66 | 24.5768 | 186.6545 | 72.7659 | 18.7763 | 30.7076 | 66.5090 | 0.2049 | 0.0067 | 2.8040 | 0.0355 | 0.0749 | 0.0033 | 1452 | 68 | | | | |
| NWI5 | and | 67 | 25.4332 | 183.2507 | 70.7775 | 19.1544 | 28.7763 | 67.7111 | 0.2223 | 0.0070 | 2.7765 | 0.0353 | 0.0367 | 0.0023 | 1653 | 74 | | | | |
| NWI5 | and | 68 | 26.3833 | 184.4770 | 83.3834 | 18.4839 | 27.4188 | 64.3610 | 0.2834 | 0.0080 | 2.8307 | 0.0357 | 0.2283 | 0.0059 | 1675 | 68 | | | | |
| NWI5 | and | 70 | 22.6140 | 83.1958 | 82.1953 | 18.6476 | 29.8765 | 65.8635 | 0.1383 | 0.0055 | 0.9644 | 0.0209 | 0.1944 | 0.0054 | 1777 | 102 | | | | |
| NWI5 | and | 82 | 30.7028 | 301.1969 | 85.1342 | 18.8498 | 30.1529 | 67.7111 | 0.4273 | 0.0098 | 4.8709 | 0.0468 | 0.2111 | 0.0057 | 1641 | 54 | | | | |
| NWI5 | and | 83 | 28.1336 | 254.6945 | 92.5007 | 18.3986 | 28.5268 | 68.0672 | 0.3511 | 0.0089 | 4.0793 | 0.0429 | 0.2957 | 0.0067 | 1486 | 54 | | | | |
| NWI5 | and | 84 | 24.2205 | 110.9869 | 82.9456 | 18.9283 | 29.3883 | 64.9731 | 0.1873 | 0.0064 | 1.4733 | 0.0258 | 0.2143 | 0.0057 | 1786 | 89 | | | | |
| NWI5 | and | 85 | 29.7089 | 276.9799 | 85.9972 | 18.9996 | 30.0887 | 65.0065 | 0.3859 | 0.0093 | 4.4433 | 0.0447 | 0.2541 | 0.0062 | 1563 | 54 | | | | |
| NWI5 | and | 86 | 25.2707 | 148.5412 | 84.3839 | 18.7825 | 28.8489 | 65.7967 | 0.2316 | 0.0072 | 2.1604 | 0.0312 | 0.2225 | 0.0058 | 1686 | 76 | | | | |
| NWI5 | and | 87 | 25.9895 | 169.8865 | 82.9456 | 19.2931 | 29.1297 | 67.4440 | 0.2390 | 0.0073 | 2.5382 | 0.0338 | 0.1858 | 0.0053 | 1613 | 71 | | | | |
| NWI5 | and | 88 | 26.7396 | 198.8185 | 85.0967 | 18.9973 | 28.4727 | 66.4089 | 0.2777 | 0.0079 | 3.0723 | 0.0372 | 0.2247 | 0.0058 | 1553 | 64 | | | | |
| NWI5 | and | 89 | 23.4829 | 108.5353 | 86.9602 | 18.8573 | 29.6455 | 65.6298 | 0.1627 | 0.0060 | 1.4264 | 0.0254 | 0.2546 | 0.0062 | 1512 | 80 | | | | |
| NWI5 | and | 91 | 24.7706 | 120.3935 | 85.0092 | 18.8176 | 27.8361 | 66.5424 | 0.2121 | 0.0069 | 1.6722 | 0.0275 | 0.2205 | 0.0057 | 1836 | 87 | | | | |
| NWI5 | and | 92 | 21.7077 | 103.5572 | 78.0183 | 17.8692 | 29.0716 | 63.8713 | 0.1333 | 0.0054 | 1.3463 | 0.0247 | 0.1687 | 0.0050 | 1487 | 87 | | | | |
| NWI5 | and | 94 | 22.9953 | 104.5328 | 85.3844 | 18.4011 | 29.1935 | 65.7633 | 0.1614 | 0.0060 | 1.3618 | 0.0248 | 0.2341 | 0.0059 | 1587 | 84 | | | | |
| NWI5 | and | 95 | 25.8895 | 167.2589 | 92.3381 | 19.0023 | 30.7932 | 66.0972 | 0.2465 | 0.0074 | 2.4658 | 0.0334 | 0.3150 | 0.0069 | 1492 | 64 | | | | |
| NWI5 | and | 96 | 24.1643 | 110.8869 | 86.9352 | 18.9024 | 30.1377 | 65.9748 | 0.1863 | 0.0064 | 1.4591 | 0.0257 | 0.2501 | 0.0061 | 1699 | 85 | | | | |
| NWI5 | and | 97 | 27.2085 | 221.9477 | 86.9477 | 18.3364 | 29.3401 | 65.9971 | 0.3184 | 0.0085 | 3.4677 | 0.0395 | 0.2523 | 0.0062 | 1578 | 60 | | | | |
| NWI5 | and | 98 | 24.0392 | 115.7152 | 87.4855 | 18.7581 | 29.8051 | 66.4311 | 0.1870 | 0.0064 | 1.5527 | 0.0265 | 0.2514 | 0.0061 | 1643 | 82 | | | | |
| NWI5 | and | 99 | 23.9705 | 119.7680 | 88.2108 | 19.1168 | 30.4183 | 65.0733 | 0.1711 | 0.0061 | 1.6148 | 0.0270 | 0.2764 | 0.0064 | 1435 | 74 | | | | |
| NWI5 | and | 100 | 26.7459 | 191.2597 | 89.3740 | 18.6254 | 30.5849 | 66.5090 | 0.2923 | 0.0081 | 2.9052 | 0.0362 | 0.2755 | 0.0064 | 1623 | 65 | | | | |
| NWI5 | and | 103 | 23.8892 | 108.3602 | 84.6215 | 18.6040 | 29.9027 | 66.5758 | 0.1873 | 0.0064 | 1.4187 | 0.0253 | 0.2154 | 0.0057 | 1823 | 91 | | | | |

| Sample | Occluding phase | Label | Peak Counts Pk(Pb) | Pk(Th) | Pk(U ) | Background counts Bg(Pb) | Bg(Th) | Bg(U ) | W%(Pb) | W%(Pb) 1σ | W%(Th) | W%(Th) 1σ | W%(U) | W%(U) 1σ | Chemical age (Ma) | 1σ | Early/peak meta. age (Ma) & error (2σ) | n = | Post peak meta. age (Ma) & error (2σ) | n = |
|---|---|---|---|---|---|---|---|---|---|---|---|---|---|---|---|---|---|---|---|---|
| NWI5 | and | 104 | 29.5526 | 292.8070 | 91.2375 | 18.3066 | 28.9644 | 66.8429 | 0.4060 | 0.0096 | 4.7502 | 0.0462 | 0.2959 | 0.0067 | 1518 | 51 | | | | |
| NWI5 | and | 105 | 23.1766 | 81.1197 | 88.3234 | 18.9353 | 27.3880 | 65.7299 | 0.1487 | 0.0057 | 0.9732 | 0.0210 | 0.2694 | 0.0063 | 1650 | 90 | | | | |
| NWI5 | and | 106 | 27.5523 | 200.8960 | 91.6127 | 18.9937 | 30.3513 | 67.1657 | 0.3082 | 0.0083 | 3.0788 | 0.0373 | 0.2943 | 0.0067 | 1612 | 63 | | | | |
| NWI5 | and | 107 | 28.6150 | 260.7538 | 85.6845 | 18.5814 | 30.3927 | 65.9303 | 0.3615 | 0.0090 | 4.1497 | 0.0432 | 0.2389 | 0.0060 | 1565 | 56 | | | | |
| NWI5 | and | 108 | 25.3707 | 162.2039 | 83.1332 | 18.4332 | 28.6764 | 65.3404 | 0.2485 | 0.0075 | 2.4127 | 0.0330 | 0.2135 | 0.0057 | 1685 | 74 | | | | |
| NWI5 | and | 109 | 25.6082 | 168.0096 | 83.5709 | 19.2311 | 29.2901 | 66.8318 | 0.2278 | 0.0071 | 2.5077 | 0.0337 | 0.2011 | 0.0055 | 1532 | 69 | | | | |
| NWI5 | and | 110 | 25.2582 | 152.8450 | 82.5204 | 18.8766 | 28.6613 | 63.7600 | 0.2278 | 0.0071 | 2.2448 | 0.0319 | 0.2250 | 0.0058 | 1614 | 73 | | | | |
| NWI5 | and | 111 | 31.5717 | 339.8712 | 84.5339 | 18.6618 | 29.4029 | 66.0082 | 0.4662 | 0.0103 | 5.5819 | 0.0501 | 0.2255 | 0.0059 | 1581 | 50 | | | | |
| NWI5 | and | 112 | 26.9459 | 189.7580 | 81.4574 | 18.4530 | 29.7885 | 66.0638 | 0.3061 | 0.0083 | 2.8906 | 0.0361 | 0.1853 | 0.0053 | 1843 | 73 | | | | |
| NWI5 | and | 113 | 32.2094 | 368.9078 | 83.7585 | 19.0662 | 28.9109 | 66.1863 | 0.4746 | 0.0103 | 6.1129 | 0.0524 | 0.2146 | 0.0057 | 1499 | 46 | | | | |
| NWI5 | and | 114 | 29.1088 | 261.1294 | 82.6080 | 19.0094 | 29.7503 | 66.5647 | 0.3650 | 0.0091 | 4.1775 | 0.0434 | 0.1944 | 0.0054 | 1620 | 58 | | | | |
| NWI5 | and | 115 | 32.2531 | 352.6226 | 87.9982 | 19.2093 | 28.1732 | 66.8652 | 0.4719 | 0.0103 | 5.8414 | 0.0513 | 0.2579 | 0.0063 | 1515 | 47 | | | | |
| NWI5 | and | 116 | 30.3903 | 286.0202 | 84.4089 | 19.2267 | 28.5932 | 65.9414 | 0.4038 | 0.0096 | 4.6427 | 0.0458 | 0.2242 | 0.0058 | 1605 | 55 | | | | |
| NWI5 | and | 118 | 27.3710 | 246.0315 | 79.6315 | 18.5912 | 29.4755 | 65.5407 | 0.3157 | 0.0084 | 3.9052 | 0.0420 | 0.1703 | 0.0051 | 1519 | 58 | | | | |
| NWI5 | and | 119 | 26.2396 | 177.8699 | 84.3463 | 18.9188 | 29.6827 | 65.9303 | 0.2628 | 0.0077 | 2.6784 | 0.0348 | 0.2214 | 0.0058 | 1635 | 69 | | | | |
| NWI5 | and | 120 | 31.4967 | 337.2158 | 84.7090 | 18.4412 | 30.5195 | 65.5407 | 0.4726 | 0.0103 | 5.5267 | 0.0499 | 0.2338 | 0.0060 | 1607 | 51 | | | | |
| NWI5 | and | 121 | 33.8159 | 422.8106 | 86.5225 | 18.8482 | 29.9877 | 64.7394 | 0.5405 | 0.0110 | 7.0540 | 0.0563 | 0.2671 | 0.0064 | 1468 | 43 | | | | |
| NWI5 | and | 122 | 26.4333 | 212.6856 | 82.6080 | 18.4525 | 30.4647 | 63.6820 | 0.2870 | 0.0080 | 3.2956 | 0.0386 | 0.2286 | 0.0059 | 1515 | 61 | | | | |
| NWI5 | and | 123 | 27.0897 | 213.3615 | 80.7070 | 18.5701 | 30.1193 | 64.7282 | 0.3070 | 0.0083 | 3.3132 | 0.0387 | 0.1930 | 0.0054 | 1655 | 65 | | | | |
| NWI5 | and | 124 | 23.7392 | 126.9984 | 84.3463 | 18.4807 | 30.5338 | 66.7094 | 0.1865 | 0.0064 | 1.7466 | 0.0281 | 0.2112 | 0.0056 | 1610 | 80 | | | | |
| NWI5 | and | 125 | 28.2461 | 240.4483 | 83.5459 | 19.1734 | 29.2435 | 65.5741 | 0.3268 | 0.0086 | 3.8094 | 0.0414 | 0.2171 | 0.0057 | 1546 | 58 | 1607 ± 17 | 172 | | |
| OL3D | mx | 2 | 36.4852 | 305.4797 | 176.9063 | 17.0727 | 28.5932 | 64.7505 | 0.7411 | 0.0133 | 4.9606 | 0.0471 | 1.3495 | 0.0142 | 1630 | 41 | | | | |
| OL3D | mx | 3 | 37.0354 | 285.3691 | 197.5045 | 17.8885 | 28.5791 | 63.6153 | 0.7294 | 0.0132 | 4.5933 | 0.0453 | 1.6162 | 0.0156 | 1526 | 38 | | | | |
| OL3D | mx | 4 | 38.4169 | 291.7802 | 201.1213 | 18.4773 | 29.7892 | 65.9637 | 0.7606 | 0.0135 | 4.6922 | 0.0458 | 1.6384 | 0.0158 | 1560 | 38 | | | | |
| OL3D | mx | 5 | 31.6092 | 287.5729 | 147.8906 | 17.9069 | 28.8937 | 64.8284 | 0.5210 | 0.0111 | 4.6332 | 0.0455 | 0.9942 | 0.0122 | 1393 | 41 | | | | |
| OL3D | mx | 6 | 31.3717 | 299.6191 | 125.8225 | 17.6799 | 27.8365 | 63.4817 | 0.5213 | 0.0111 | 4.8816 | 0.0468 | 0.7419 | 0.0105 | 1504 | 45 | | | | |
| OL3D | mx | 7 | 36.1852 | 276.2538 | 179.5091 | 17.8880 | 29.2795 | 63.3370 | 0.6996 | 0.0129 | 4.4343 | 0.0446 | 1.3732 | 0.0142 | 1613 | 41 | | | | |
| OL3D | mx | 13 | 38.0231 | 294.1093 | 202.2852 | 17.7978 | 30.0561 | 65.1512 | 0.7711 | 0.0136 | 4.7251 | 0.0460 | 1.6615 | 0.0159 | 1564 | 38 | | | | |
| OL3D | mx | 15 | 33.5034 | 342.0757 | 104.5078 | 18.6056 | 30.2163 | 64.7950 | 0.5649 | 0.0116 | 5.5723 | 0.0499 | 0.4673 | 0.0083 | 1680 | 49 | | | | |
| OL3D | mx | 17 | 33.6221 | 308.1346 | 142.3983 | 17.9521 | 30.2932 | 66.2085 | 0.5975 | 0.0119 | 4.9842 | 0.0473 | 0.9333 | 0.0120 | 1555 | 44 | | | | |
| OL3D | mx | 18 | 36.1352 | 289.9019 | 188.3439 | 18.1295 | 29.9929 | 66.6982 | 0.6882 | 0.0128 | 4.6704 | 0.0458 | 1.4845 | 0.0150 | 1500 | 39 | | | | |
| OL3D | mx | 19 | 33.8972 | 382.2879 | 101.3058 | 17.8867 | 29.2559 | 65.9303 | 0.6092 | 0.0120 | 6.3251 | 0.0532 | 0.4303 | 0.0081 | 1670 | 47 | | | | |
| OL3D | mx | 22 | 28.0086 | 230.4592 | 110.2490 | 17.5107 | 30.4338 | 64.5613 | 0.3980 | 0.0097 | 3.5858 | 0.0401 | 0.5307 | 0.0088 | 1571 | 54 | | | | |
| OL3D | mx | 23 | 27.1022 | 228.0810 | 86.5725 | 17.5604 | 30.3562 | 68.0561 | 0.3604 | 0.0092 | 3.5379 | 0.0398 | 0.2364 | 0.0061 | 1765 | 66 | | | | |
| OL3D | mx | 24 | 26.0020 | 218.2678 | 90.1744 | 18.4008 | 26.8197 | 65.8524 | 0.2860 | 0.0082 | 3.4339 | 0.0392 | 0.2777 | 0.0063 | 1410 | 57 | | | | |
| OL3D | mx | 25 | 29.9714 | 297.7407 | 90.6747 | 18.8188 | 30.9351 | 65.4962 | 0.4230 | 0.0100 | 4.7863 | 0.0463 | 0.2876 | 0.0064 | 1576 | 53 | | | | |
| OL3D | mx | 26 | 26.2083 | 233.9641 | 85.8096 | 17.7808 | 28.9450 | 65.0955 | 0.3189 | 0.0087 | 3.6861 | 0.0407 | 0.2531 | 0.0062 | 1509 | 58 | | | | |
| OL3D | mx | 27 | 25.4207 | 218.6183 | 86.5225 | 18.0390 | 28.9287 | 65.1289 | 0.2779 | 0.0081 | 3.4070 | 0.0391 | 0.2505 | 0.0061 | 1409 | 58 | | | | |
| OL3D | mx | 28 | 30.6278 | 305.6550 | 110.5366 | 18.2023 | 27.9410 | 64.5613 | 0.4721 | 0.0106 | 4.9792 | 0.0472 | 0.5512 | 0.0091 | 1478 | 47 | | | | |
| OL3D | mx | 29 | 25.9083 | 238.6457 | 84.8466 | 17.4986 | 29.1636 | 65.7411 | 0.3177 | 0.0087 | 3.7603 | 0.0411 | 0.2279 | 0.0058 | 1508 | 58 | | | | |
| OL3D | mx | 30 | 34.5536 | 259.9526 | 177.1191 | 17.9741 | 28.9025 | 64.7616 | 0.6355 | 0.0123 | 4.1594 | 0.0433 | 1.3459 | 0.0142 | 1536 | 41 | | | | |
| OL3D | mx | 31 | 35.2975 | 260.0778 | 184.4270 | 17.3629 | 29.2815 | 61.0888 | 0.6865 | 0.0128 | 4.1446 | 0.0431 | 1.4515 | 0.0146 | 1588 | 41 | | | | |
| OL3D | mx | 32 | 35.3663 | 256.5222 | 173.6905 | 18.0177 | 30.0908 | 63.8713 | 0.6634 | 0.0126 | 4.0643 | 0.0427 | 1.3024 | 0.0139 | 1636 | 43 | | | | |
| OL3D | mx | 33 | 25.6832 | 184.4520 | 93.7389 | 18.0514 | 29.8925 | 66.3421 | 0.2872 | 0.0082 | 2.7709 | 0.0352 | 0.3131 | 0.0067 | 1596 | 65 | | | | |
| OL3D | mx | 34 | 33.0845 | 416.3945 | 86.8101 | 17.4000 | 28.1024 | 64.4055 | 0.5935 | 0.0118 | 6.9189 | 0.0555 | 0.2475 | 0.0058 | 1644 | 47 | | | | |
| OL3D | mx | 35 | 32.7720 | 259.1513 | 152.1069 | 18.1151 | 28.6336 | 66.7761 | 0.5588 | 0.0115 | 4.1337 | 0.0430 | 1.0460 | 0.0127 | 1539 | 44 | | | | |
| OL3D | mx | 36 | 29.2651 | 316.6756 | 86.5600 | 18.0680 | 28.5963 | 66.6203 | 0.4238 | 0.0100 | 5.1524 | 0.0480 | 0.2380 | 0.0060 | 1532 | 51 | | | | |
| OL3D | mx | 37 | 27.6710 | 278.9833 | 83.1958 | 17.8020 | 29.6527 | 65.4962 | 0.3725 | 0.0094 | 4.4590 | 0.0446 | 0.2085 | 0.0055 | 1552 | 55 | | | | |
| OL3D | mx | 38 | 29.9527 | 261.5801 | 112.8382 | 18.1264 | 27.6882 | 66.9876 | 0.4479 | 0.0103 | 4.1813 | 0.0432 | 0.5705 | 0.0094 | 1559 | 51 | | | | |
| OL3D | mx | 39 | 33.2658 | 395.8947 | 87.0227 | 17.7300 | 30.0289 | 65.7856 | 0.5893 | 0.0118 | 6.5360 | 0.0540 | 0.2466 | 0.0060 | 1712 | 49 | | | | |
| OL3D | mx | 40 | 28.3587 | 290.0522 | 83.3333 | 18.0170 | 28.5893 | 66.6426 | 0.3906 | 0.0096 | 4.6739 | 0.0457 | 0.1986 | 0.0054 | 1572 | 55 | | | | |
| OL3D | mx | 41 | 33.8659 | 261.3047 | 160.9402 | 17.9098 | 28.6191 | 64.1384 | 0.6108 | 0.0121 | 4.1856 | 0.0434 | 1.1619 | 0.0132 | 1582 | 44 | | | | |
| OL3D | mx | 42 | 37.9731 | 271.4709 | 175.9553 | 18.7908 | 28.0397 | 65.3070 | 0.7355 | 0.0133 | 4.3883 | 0.0445 | 1.3765 | 0.0146 | 1691 | 43 | | | | |

| Sample | Occluding phase | Label | Peak Counts Pk(Pb) | Pk(Th) | Pk(U ) | Background counts Bg(Pb) | Bg(Th) | Bg(U ) | W%(Pb) | W%(Pb) 1σ | W%(Th) | W%(Th) 1σ | W%(U) | W%(U) 1σ | Chemical age (Ma) | 1σ | Early/peak meta. age (Ma) & error (2σ) | n = | Post peak meta. age (Ma) & error (2σ) | n = |
|---|---|---|---|---|---|---|---|---|---|---|---|---|---|---|---|---|---|---|---|---|
| OL3D | mx | 43 | 29.0900 | 275.5776 | 104.2326 | 17.8033 | 29.0001 | 66.5424 | 0.4285 | 0.0101 | 4.4217 | 0.0445 | 0.4762 | 0.0087 | 1519 | 51 | | | | |
| OL3D | mx | 45 | 32.7657 | 290.2024 | 128.7747 | 17.6075 | 30.0346 | 67.2436 | 0.5773 | 0.0117 | 4.6619 | 0.0457 | 0.7576 | 0.0108 | 1683 | 49 | | | | |
| OL3D | mx | 46 | 39.1734 | 621.1804 | 89.3990 | 18.0312 | 30.4942 | 63.2925 | 0.7962 | 0.0137 | 10.4754 | 0.0681 | 0.2758 | 0.0060 | 1509 | 36 | | | | |
| OL3D | mx | 47 | 32.5907 | 404.4401 | 87.4104 | 18.2151 | 30.0484 | 65.8746 | 0.5438 | 0.0113 | 6.6785 | 0.0546 | 0.2645 | 0.0064 | 1547 | 46 | | | | |
| OL3D | mx | 48 | 33.0970 | 361.6169 | 106.8092 | 18.0708 | 28.4931 | 65.4628 | 0.5687 | 0.0116 | 5.9362 | 0.0514 | 0.4927 | 0.0086 | 1598 | 46 | | | | |
| OL3D | mx | 49 | 33.8472 | 435.8441 | 87.2478 | 18.6769 | 28.6976 | 65.6632 | 0.5724 | 0.0116 | 7.2420 | 0.0567 | 0.2776 | 0.0067 | 1510 | 43 | | | | |
| OL3D | mx | 50 | 35.5788 | 505.7662 | 82.2328 | 18.1291 | 29.8289 | 65.8190 | 0.6577 | 0.0124 | 8.4479 | 0.0612 | 0.1903 | 0.0053 | 1562 | 41 | | | | |
| OL3D | mx | 53 | 33.2221 | 263.4581 | 147.8781 | 17.6798 | 27.1890 | 65.9525 | 0.5945 | 0.0119 | 4.2617 | 0.0438 | 1.0748 | 0.0133 | 1585 | 45 | | | | |
| OL3D | mx | 54 | 37.8731 | 328.3732 | 187.8808 | 18.8393 | 28.1874 | 66.5313 | 0.7265 | 0.0132 | 5.3863 | 0.0492 | 1.4932 | 0.0152 | 1475 | 37 | | | | |
| OL3D | mx | 55 | 37.4917 | 334.3350 | 180.9732 | 18.0627 | 29.1821 | 65.8858 | 0.7393 | 0.0133 | 5.4561 | 0.0494 | 1.4144 | 0.0147 | 1526 | 38 | | | | |
| OL3D | mx | 56 | 31.7843 | 374.5955 | 86.3599 | 17.9344 | 30.6219 | 65.6520 | 0.5239 | 0.0111 | 6.1343 | 0.0523 | 0.2417 | 0.0059 | 1619 | 49 | | | | |
| OL3D | mx | 57 | 37.2542 | 334.4102 | 212.7232 | 17.7805 | 28.7988 | 66.2530 | 0.7387 | 0.0132 | 5.4503 | 0.0493 | 1.7806 | 0.0164 | 1373 | 34 | | | | |
| OL3D | mx | 58 | 34.2473 | 463.1927 | 92.3881 | 18.6247 | 28.5334 | 65.9525 | 0.5898 | 0.0118 | 7.7343 | 0.0587 | 0.3188 | 0.0069 | 1447 | 41 | | | | |
| OL3D | mx | 59 | 30.7466 | 293.7336 | 113.6888 | 17.8333 | 28.4750 | 65.3070 | 0.4897 | 0.0108 | 4.7474 | 0.0461 | 0.6126 | 0.0098 | 1531 | 48 | | | | |
| OL3D | mx | 60 | 34.0535 | 448.7283 | 90.8247 | 18.4208 | 28.7737 | 65.9637 | 0.5905 | 0.0118 | 7.4714 | 0.0576 | 0.2899 | 0.0065 | 1508 | 42 | | | | |
| OL3D | mx | 61 | 28.7837 | 300.7962 | 87.8982 | 17.8598 | 29.4743 | 65.0287 | 0.4136 | 0.0099 | 4.8561 | 0.0466 | 0.2616 | 0.0061 | 1549 | 53 | | | | |
| OL3D | mx | 62 | 28.7462 | 330.7028 | 85.0717 | 17.7032 | 30.7266 | 66.0416 | 0.4181 | 0.0099 | 5.3724 | 0.0490 | 0.2360 | 0.0060 | 1464 | 49 | | | | |
| OL3D | mx | 64 | 37.7855 | 282.4141 | 198.1427 | 17.6956 | 27.5654 | 66.7428 | 0.7651 | 0.0135 | 4.5548 | 0.0451 | 1.6000 | 0.0156 | 1605 | 39 | | | | |
| OL3D | mx | 65 | 36.5978 | 339.6958 | 162.0287 | 17.7913 | 28.8835 | 66.5202 | 0.7157 | 0.0130 | 5.5556 | 0.0498 | 1.1663 | 0.0133 | 1590 | 41 | | | | |
| OL3D | mx | 67 | 34.0285 | 357.9840 | 144.5126 | 17.9164 | 30.3837 | 64.7839 | 0.6128 | 0.0121 | 5.8681 | 0.0513 | 0.9505 | 0.0119 | 1443 | 40 | | | | |
| OL3D | mx | 68 | 36.0476 | 263.4581 | 183.3758 | 17.8040 | 28.8239 | 66.5647 | 0.6960 | 0.0129 | 4.2026 | 0.0434 | 1.4321 | 0.0148 | 1609 | 41 | | | | |
| OL3D | mx | 69 | 31.8655 | 305.4547 | 115.4149 | 18.5176 | 28.8888 | 64.9731 | 0.5049 | 0.0109 | 4.9327 | 0.0469 | 0.6005 | 0.0095 | 1546 | 47 | | | | |
| OL3D | mx | 70 | 26.4396 | 210.7331 | 96.5279 | 17.6256 | 28.6975 | 65.7522 | 0.3330 | 0.0089 | 3.2606 | 0.0382 | 0.3600 | 0.0073 | 1584 | 60 | | | | |
| OL3D | mx | 71 | 29.7214 | 248.1095 | 117.6415 | 17.7794 | 28.7189 | 67.6888 | 0.4510 | 0.0103 | 3.9094 | 0.0417 | 0.6270 | 0.0099 | 1585 | 52 | | | | |
| OL3D | mx | 72 | 28.3149 | 220.0201 | 92.1129 | 18.4146 | 27.1869 | 67.6666 | 0.3744 | 0.0094 | 3.4540 | 0.0393 | 0.3346 | 0.0076 | 1729 | 63 | | | | |
| OL3D | mx | 73 | 25.8958 | 190.7841 | 94.5143 | 17.9422 | 29.6574 | 64.3387 | 0.2976 | 0.0083 | 2.8693 | 0.0357 | 0.3252 | 0.0066 | 1596 | 63 | | | | |
| OL3D | mx | 74 | 23.5392 | 154.7468 | 80.3944 | 17.5312 | 29.6098 | 66.7205 | 0.2238 | 0.0072 | 2.2401 | 0.0317 | 0.1759 | 0.0053 | 1681 | 79 | | | | |
| OL3D | mx | 75 | 27.8023 | 285.9451 | 86.1848 | 17.6873 | 27.8361 | 62.8250 | 0.3817 | 0.0095 | 4.6154 | 0.0454 | 0.2592 | 0.0060 | 1497 | 53 | | | | |
| OL3D | mx | 76 | 23.8080 | 176.6936 | 77.2429 | 17.5284 | 30.1896 | 65.9637 | 0.2340 | 0.0074 | 2.6187 | 0.0342 | 0.1455 | 0.0048 | 1612 | 73 | | | | |
| OL3D | mx | 77 | 28.8713 | 292.8821 | 84.9466 | 18.2360 | 29.6961 | 65.0287 | 0.4015 | 0.0097 | 4.7007 | 0.0458 | 0.2255 | 0.0056 | 1579 | 54 | | | | |
| OL3D | mx | 78 | 31.4217 | 397.6739 | 94.4142 | 17.9247 | 29.4526 | 65.1512 | 0.5108 | 0.0110 | 6.5726 | 0.0542 | 0.3525 | 0.0073 | 1422 | 43 | | | | |
| OL3D | mx | 79 | 30.3403 | 332.1056 | 80.8321 | 17.2704 | 28.8021 | 65.7522 | 0.4955 | 0.0108 | 5.4201 | 0.0492 | 0.1864 | 0.0054 | 1753 | 55 | | | | |
| OL3D | mx | 80 | 25.6395 | 227.3550 | 82.2453 | 17.4096 | 29.9302 | 65.4739 | 0.3089 | 0.0085 | 3.5267 | 0.0397 | 0.2041 | 0.0056 | 1572 | 62 | | | | |
| OL3D | mx | 81 | 32.0781 | 413.4873 | 83.4084 | 18.4073 | 31.4940 | 69.8703 | 0.5156 | 0.0110 | 6.7948 | 0.0550 | 0.2020 | 0.0061 | 1491 | 45 | | | | |
| OL3D | mx | 82 | 36.8041 | 552.2635 | 84.2213 | 17.6300 | 31.1997 | 66.2864 | 0.7204 | 0.0130 | 9.2165 | 0.0638 | 0.2136 | 0.0056 | 1565 | 40 | | | | |
| OL3D | mx | 83 | 37.2542 | 572.3059 | 84.2463 | 18.0134 | 31.5268 | 65.3515 | 0.7259 | 0.0131 | 9.6040 | 0.0653 | 0.2423 | 0.0062 | 1506 | 38 | | | | |
| OL3D | mx | 84 | 34.5786 | 386.9737 | 135.1923 | 18.0934 | 28.0743 | 64.9842 | 0.6242 | 0.0122 | 6.3995 | 0.0534 | 0.8444 | 0.0113 | 1445 | 40 | | | | |
| OL3D | mx | 85 | 32.4344 | 456.6999 | 79.2313 | 17.6083 | 28.1869 | 64.6726 | 0.5580 | 0.0115 | 7.6254 | 0.0582 | 0.2335 | 0.0068 | 1436 | 42 | | | | |
| OL3D | mx | 87 | 31.7218 | 304.0270 | 124.2088 | 17.6956 | 28.1448 | 65.1401 | 0.5293 | 0.0112 | 4.9047 | 0.0467 | 0.6852 | 0.0100 | 1559 | 46 | | | | |
| OL3D | mx | 89 | 25.2519 | 201.8472 | 79.2188 | 17.6415 | 30.6454 | 65.0844 | 0.2850 | 0.0082 | 3.0556 | 0.0369 | 0.1436 | 0.0043 | 1720 | 70 | | | | |
| OL3D | mx | 90 | 34.7724 | 505.3901 | 84.4214 | 17.9090 | 29.6193 | 66.8207 | 0.6331 | 0.0122 | 8.4159 | 0.0610 | 0.2196 | 0.0059 | 1495 | 40 | | | | |
| OL3D | mx | 91 | 31.5530 | 345.9837 | 100.3677 | 17.5896 | 28.0227 | 66.1529 | 0.5262 | 0.0111 | 5.6482 | 0.0501 | 0.4204 | 0.0080 | 1592 | 48 | | | | |
| OL3D | mx | 92 | 25.1519 | 211.5592 | 81.1948 | 17.3754 | 28.4055 | 66.8541 | 0.2908 | 0.0082 | 3.2625 | 0.0381 | 0.1878 | 0.0055 | 1599 | 65 | | | | |
| OL3D | mx | 93 | 29.7464 | 297.3400 | 91.7127 | 17.3924 | 28.8667 | 65.9637 | 0.4669 | 0.0105 | 4.7870 | 0.0462 | 0.3078 | 0.0068 | 1707 | 55 | | | | |
| OL3D | mx | 94 | 32.8657 | 354.2761 | 119.6054 | 17.7983 | 29.8112 | 65.8969 | 0.5668 | 0.0115 | 5.7463 | 0.0504 | 0.6623 | 0.0101 | 1517 | 44 | | | | |
| OL3D | mx | 95 | 39.6047 | 611.8460 | 101.9187 | 19.8986 | 31.0793 | 65.6409 | 0.7376 | 0.0131 | 10.2528 | 0.0673 | 0.4303 | 0.0080 | 1366 | 34 | | | | |
| OL3D | mx | 96 | 30.9466 | 301.7729 | 110.6367 | 17.9945 | 29.0703 | 66.9097 | 0.4878 | 0.0107 | 4.8428 | 0.0464 | 0.5434 | 0.0092 | 1557 | 49 | | | | |
| OL3D | mx | 97 | 36.1352 | 294.5851 | 163.3550 | 18.3995 | 29.3072 | 65.1067 | 0.6708 | 0.0126 | 4.7114 | 0.0457 | 1.1798 | 0.0133 | 1619 | 42 | | | | |
| OL3D | mx | 99 | 25.8082 | 215.4141 | 82.6455 | 17.9836 | 29.4980 | 65.6854 | 0.2920 | 0.0083 | 3.3059 | 0.0383 | 0.1891 | 0.0051 | 1588 | 64 | | | | |
| OL3D | mx | 100 | 29.5901 | 244.5293 | 118.2169 | 17.9677 | 27.6288 | 68.4234 | 0.4384 | 0.0102 | 3.8618 | 0.0415 | 0.6078 | 0.0096 | 1572 | 52 | | | | |
| OL3D | mx | 101 | 32.9283 | 287.0720 | 137.3691 | 18.4787 | 28.7662 | 65.1734 | 0.5450 | 0.0113 | 4.5883 | 0.0451 | 0.8684 | 0.0114 | 1536 | 45 | | | | |
| OL3D | mx | 102 | 31.2279 | 370.6367 | 87.7231 | 18.0211 | 29.7955 | 66.2197 | 0.4969 | 0.0108 | 6.0565 | 0.0519 | 0.2750 | 0.0066 | 1532 | 47 | | | | |
| OL3D | mx | 103 | 34.3098 | 281.5376 | 167.5967 | 18.2975 | 29.6840 | 67.6999 | 0.6047 | 0.0119 | 4.4739 | 0.0446 | 1.2213 | 0.0137 | 1488 | 41 | | | | |

| Sample | Occluding phase | Label | Peak Counts Pk(Pb) | Pk(Th) | Pk(U ) | Background counts Bg(Pb) | Bg(Th) | Bg(U ) | W%(Pb) | W%(Pb) 1σ | W%(Th) | W%(Th) 1σ | W%(U) | W%(U) 1σ | Chemical age (Ma) | 1σ | Early/peak meta. age (Ma) & error (2σ) | n = | Post peak meta. age (Ma) & error (2σ) | n = |
|---|---|---|---|---|---|---|---|---|---|---|---|---|---|---|---|---|---|---|---|---|
| OL3D | mx | 104 | 34.3848 | 468.5327 | 83.8711 | 17.5880 | 29.6978 | 66.5313 | 0.6313 | 0.0122 | 7.7671 | 0.0586 | 0.2107 | 0.0057 | 1604 | 44 | | | | |
| OL3D | mx | 105 | 41.7802 | 702.6531 | 89.2364 | 18.8986 | 33.8273 | 66.5536 | 0.8541 | 0.0141 | 11.7618 | 0.0719 | 0.2619 | 0.0061 | 1463 | 34 | | | | |
| OL3D | mx | 106 | 29.7277 | 267.1139 | 110.8243 | 18.0126 | 28.9132 | 66.5313 | 0.4399 | 0.0102 | 4.2257 | 0.0433 | 0.5393 | 0.0091 | 1549 | 51 | | | | |
| OL3D | mx | 107 | 26.8147 | 236.5177 | 76.5176 | 18.0957 | 30.3759 | 65.8524 | 0.3253 | 0.0087 | 3.6515 | 0.0402 | 0.1063 | 0.0036 | 1739 | 66 | | | | |
| OL3D | mx | 110 | 34.8349 | 282.7146 | 163.1548 | 18.0452 | 30.1631 | 66.1306 | 0.6341 | 0.0122 | 4.4840 | 0.0446 | 1.1597 | 0.0132 | 1587 | 43 | | | | |
| OL3D | mx | 111 | 33.7847 | 251.2643 | 160.0143 | 17.8989 | 28.3706 | 67.0210 | 0.5989 | 0.0119 | 3.9504 | 0.0418 | 1.1221 | 0.0130 | 1620 | 45 | | | | |
| OL3D | mx | 112 | 35.7038 | 293.8338 | 172.5768 | 18.1794 | 30.2813 | 65.1846 | 0.6607 | 0.0125 | 4.6689 | 0.0455 | 1.2737 | 0.0137 | 1551 | 41 | | | | |
| OL3D | mx | 113 | 31.4467 | 255.3705 | 124.8467 | 18.2579 | 29.1040 | 65.4406 | 0.4965 | 0.0108 | 4.0141 | 0.0422 | 0.7083 | 0.0103 | 1634 | 50 | | | | |
| OL3D | mx | 114 | 35.3600 | 290.9287 | 178.1577 | 17.9335 | 28.8816 | 67.5886 | 0.6589 | 0.0125 | 4.6547 | 0.0455 | 1.3321 | 0.0142 | 1519 | 40 | | | | |
| OL3D | mx | 115 | 37.7605 | 300.9465 | 194.0003 | 17.9445 | 30.0396 | 63.5930 | 0.7496 | 0.0133 | 4.8092 | 0.0462 | 1.5567 | 0.0152 | 1563 | 38 | | | | |
| OL3D | mx | 116 | 32.4657 | 287.4977 | 137.8320 | 17.5814 | 27.7654 | 66.0750 | 0.5598 | 0.0115 | 4.5946 | 0.0451 | 0.8486 | 0.0112 | 1586 | 46 | | | | |
| OL3D | mx | 117 | 31.8718 | 282.2638 | 135.9930 | 17.9308 | 30.1590 | 65.8524 | 0.5241 | 0.0111 | 4.4624 | 0.0444 | 0.8353 | 0.0112 | 1527 | 45 | | | | |
| OL3D | mx | 118 | 30.5090 | 318.2285 | 103.3070 | 18.2985 | 29.9837 | 67.4662 | 0.4576 | 0.0104 | 5.0982 | 0.0475 | 0.4525 | 0.0085 | 1482 | 48 | | | | |
| OL3D | mx | 119 | 27.2272 | 270.5194 | 82.1077 | 17.3268 | 28.0239 | 65.1178 | 0.3690 | 0.0093 | 4.2819 | 0.0435 | 0.2129 | 0.0058 | 1584 | 57 | | | | |
| OL3D | mx | 120 | 41.9990 | 673.9097 | 87.4980 | 17.9977 | 31.4231 | 65.6075 | 0.8926 | 0.0144 | 11.2460 | 0.0702 | 0.2302 | 0.0055 | 1602 | 36 | | | | |
| OL3D | mx | 121 | 29.7839 | 310.6392 | 97.1908 | 18.0996 | 30.9373 | 65.9859 | 0.4382 | 0.0101 | 4.9545 | 0.0468 | 0.3848 | 0.0077 | 1504 | 49 | | | 1559 ± 16 | 101 |
| WW18 | mx | 1 | 25.2644 | 185.1528 | 100.2176 | 17.9495 | 28.8345 | 65.1178 | 0.2724 | 0.0080 | 2.8270 | 0.0358 | 0.4118 | 0.0078 | 1386 | 57 | | | | |
| WW18 | mx | 4 | 31.2592 | 350.5683 | 84.0212 | 17.9227 | 29.2478 | 65.5519 | 0.5048 | 0.0109 | 5.8377 | 0.0515 | 0.2134 | 0.0056 | 1652 | 51 | | | | |
| WW18 | mx | 5 | 26.5709 | 210.4828 | 87.7606 | 17.9699 | 28.4188 | 66.3309 | 0.3237 | 0.0087 | 3.3116 | 0.0388 | 0.2435 | 0.0059 | 1669 | 65 | | | | |
| WW18 | mx | 7 | 23.6767 | 136.9312 | 86.0597 | 17.5538 | 28.1667 | 66.1751 | 0.2303 | 0.0074 | 1.9969 | 0.0303 | 0.2578 | 0.0065 | 1696 | 78 | | | | |
| WW18 | mx | 8 | 27.5148 | 216.6157 | 91.7753 | 18.0846 | 28.0333 | 65.6854 | 0.3580 | 0.0092 | 3.4516 | 0.0397 | 0.3427 | 0.0075 | 1651 | 61 | | | | |
| WW18 | mx | 13 | 28.7712 | 271.9216 | 85.8096 | 17.8459 | 29.1610 | 66.2864 | 0.4148 | 0.0099 | 4.4342 | 0.0450 | 0.2425 | 0.0061 | 1687 | 58 | | | | |
| WW18 | mx | 14 | 32.5344 | 349.0902 | 87.1728 | 18.0846 | 29.9122 | 66.0638 | 0.5492 | 0.0114 | 5.8220 | 0.0515 | 0.2750 | 0.0067 | 1737 | 52 | | | | |
| WW18 | mx | 15 | 23.2204 | 125.7474 | 82.0952 | 17.7621 | 26.4464 | 64.9842 | 0.2034 | 0.0069 | 1.8170 | 0.0288 | 0.2242 | 0.0061 | 1672 | 82 | | | | |
| WW18 | mx | 17 | 24.4705 | 168.5852 | 84.8341 | 17.7603 | 29.3522 | 67.3549 | 0.2515 | 0.0077 | 2.5407 | 0.0340 | 0.2593 | 0.0069 | 1570 | 70 | | | | |
| WW18 | mx | 18 | 25.3957 | 197.3668 | 84.4464 | 18.1978 | 30.3210 | 66.1195 | 0.2705 | 0.0080 | 3.0527 | 0.0373 | 0.2339 | 0.0061 | 1511 | 64 | | | | |
| WW18 | mx | 20 | 29.8152 | 320.4828 | 85.6095 | 18.1458 | 28.2500 | 67.1546 | 0.4411 | 0.0102 | 5.3118 | 0.0491 | 0.2544 | 0.0066 | 1538 | 51 | | | | |
| WW18 | mx | 21 | 33.0220 | 421.0061 | 90.5496 | 17.5187 | 30.0707 | 64.5056 | 0.5884 | 0.0118 | 7.1150 | 0.0569 | 0.3011 | 0.0066 | 1557 | 44 | | | | |
| WW18 | mx | 22 | 31.3217 | 347.8376 | 86.2973 | 18.0428 | 29.1713 | 66.0750 | 0.5023 | 0.0109 | 5.7852 | 0.0512 | 0.2399 | 0.0060 | 1635 | 51 | | | | |
| WW18 | mx | 24 | 25.7582 | 187.5054 | 95.6149 | 17.3278 | 27.4426 | 65.9080 | 0.3194 | 0.0087 | 2.9305 | 0.0366 | 0.3601 | 0.0074 | 1633 | 64 | | | | |
| WW18 | mx | 25 | 33.3221 | 418.5499 | 90.7497 | 17.7033 | 29.8646 | 67.2770 | 0.5926 | 0.0119 | 7.0702 | 0.0567 | 0.3236 | 0.0075 | 1561 | 45 | | | | |
| WW18 | mx | 26 | 31.3842 | 247.3584 | 127.4612 | 17.9271 | 29.2208 | 66.1306 | 0.5141 | 0.0111 | 3.9939 | 0.0428 | 0.7259 | 0.0104 | 1676 | 51 | | | | |
| WW18 | mx | 27 | 38.9483 | 608.5089 | 95.1146 | 18.5223 | 31.2201 | 67.4996 | 0.7706 | 0.0135 | 10.4565 | 0.0688 | 0.3674 | 0.0078 | 1426 | 35 | | | | |
| WW18 | mx | 30 | 33.4033 | 325.7681 | 127.1360 | 17.7732 | 29.1571 | 66.7650 | 0.5965 | 0.0119 | 5.4181 | 0.0497 | 0.7576 | 0.0109 | 1587 | 45 | | | | |
| WW18 | mx | 31 | 23.0016 | 122.4950 | 84.3964 | 17.7206 | 28.1948 | 66.0193 | 0.1967 | 0.0068 | 1.7275 | 0.0281 | 0.2327 | 0.0061 | 1655 | 82 | | | | |
| WW18 | mx | 33 | 33.5284 | 411.1565 | 95.0521 | 18.0863 | 28.8358 | 66.8986 | 0.5857 | 0.0118 | 6.9545 | 0.0562 | 0.3696 | 0.0078 | 1536 | 44 | | | | |
| WW18 | mx | 35 | 31.5092 | 357.1322 | 87.5980 | 17.9247 | 30.4368 | 66.0527 | 0.5142 | 0.0110 | 5.9324 | 0.0519 | 0.2822 | 0.0068 | 1603 | 49 | | | | |
| WW18 | mx | 36 | 32.4657 | 406.3448 | 88.0983 | 17.9670 | 29.3289 | 63.7933 | 0.5480 | 0.0114 | 6.8406 | 0.0557 | 0.2753 | 0.0062 | 1521 | 45 | | | | |
| WW18 | mx | 38 | 30.1715 | 326.8702 | 85.5470 | 17.9951 | 29.1798 | 67.3660 | 0.4610 | 0.0104 | 5.4146 | 0.0496 | 0.2543 | 0.0067 | 1579 | 51 | | | | |
| WW18 | mx | 39 | 32.1719 | 204.7507 | 162.9296 | 17.2274 | 26.9379 | 64.1829 | 0.5725 | 0.0117 | 3.2580 | 0.0386 | 1.2407 | 0.0140 | 1604 | 45 | | | | |
| WW18 | mx | 41 | 31.3655 | 382.1626 | 94.0640 | 16.9484 | 31.3616 | 64.1161 | 0.5459 | 0.0114 | 6.3932 | 0.0540 | 0.3729 | 0.0076 | 1533 | 45 | | | | |
| WW18 | mx | 42 | 30.7716 | 350.0923 | 89.8367 | 17.5605 | 30.2248 | 66.9542 | 0.4994 | 0.0109 | 5.8053 | 0.0513 | 0.2875 | 0.0067 | 1583 | 49 | | | | |
| WW18 | mx | 44 | 29.0525 | 318.6794 | 88.3484 | 17.7521 | 28.6452 | 64.8173 | 0.4268 | 0.0100 | 5.2725 | 0.0490 | 0.2926 | 0.0067 | 1470 | 49 | | | | |
| WW18 | mx | 45 | 29.1025 | 346.4848 | 88.0357 | 17.9244 | 28.3930 | 66.2864 | 0.4215 | 0.0100 | 5.7759 | 0.0512 | 0.2603 | 0.0062 | 1372 | 46 | | | | |
| WW18 | mx | 46 | 33.7659 | 483.9767 | 90.6747 | 17.9587 | 29.1264 | 65.7633 | 0.5956 | 0.0118 | 8.2280 | 0.0610 | 0.2977 | 0.0067 | 1398 | 39 | | | | |
| WW18 | mx | 47 | 26.8772 | 235.9920 | 86.3474 | 17.7889 | 27.9512 | 67.8780 | 0.3429 | 0.0090 | 3.7887 | 0.0415 | 0.2529 | 0.0066 | 1582 | 60 | | | | |
| WW18 | mx | 50 | 30.8091 | 360.8903 | 88.7861 | 17.8734 | 32.0341 | 68.2231 | 0.4869 | 0.0107 | 5.9439 | 0.0518 | 0.2659 | 0.0066 | 1533 | 48 | | | | |
| WW18 | mx | 51 | 37.7855 | 530.0164 | 95.5899 | 17.8740 | 29.9162 | 67.8001 | 0.7508 | 0.0133 | 9.0315 | 0.0639 | 0.3698 | 0.0078 | 1571 | 40 | | | | |
| WW18 | mx | 52 | 31.9093 | 407.3973 | 86.0472 | 17.8495 | 29.8192 | 65.8190 | 0.5310 | 0.0112 | 6.8454 | 0.0557 | 0.2387 | 0.0059 | 1499 | 45 | | | | |
| WW18 | mx | 53 | 33.9410 | 458.9310 | 91.5126 | 17.6323 | 28.0650 | 66.0638 | 0.6163 | 0.0121 | 7.8108 | 0.0595 | 0.3387 | 0.0075 | 1485 | 41 | | | | |
| WW18 | mx | 54 | 25.2394 | 159.7515 | 83.9086 | 18.2753 | 27.9371 | 65.9414 | 0.2610 | 0.0078 | 2.4023 | 0.0331 | 0.2239 | 0.0059 | 1748 | 76 | | | | |
| WW18 | mx | 55 | 27.8961 | 247.3083 | 92.8634 | 17.7272 | 29.1525 | 66.9208 | 0.3841 | 0.0095 | 3.9709 | 0.0425 | 0.3196 | 0.0070 | 1623 | 58 | | | | |
| WW18 | mx | 56 | 25.0894 | 167.8595 | 85.7846 | 18.3570 | 29.9464 | 65.2514 | 0.2524 | 0.0077 | 2.5165 | 0.0339 | 0.2236 | 0.0055 | 1642 | 72 | | | | |

| Sample | Occluding phase | Label | Peak Counts Pk(Pb) | Pk(Th) | Pk(U ) | Background counts Bg(Pb) | Bg(Th) | Bg(U ) | W%(Pb) | W%(Pb) 1σ | W%(Th) | W%(Th) 1σ | W%(U) | W%(U) 1σ | Chemical age (Ma) | 1σ | Early/peak meta. age (Ma) & error (2σ) | n = | Post peak meta. age (Ma) & error (2σ) | n = |
|---|---|---|---|---|---|---|---|---|---|---|---|---|---|---|---|---|---|---|---|---|
| WW18 | mx | 60 | 32.4344 | 393.1131 | 87.3604 | 18.4158 | 30.4147 | 61.9347 | 0.5305 | 0.0112 | 6.5879 | 0.0547 | 0.2962 | 0.0066 | 1507 | 45 | | | | |
| WW18 | mx | 61 | 33.5409 | 399.8541 | 87.9982 | 18.2301 | 27.0286 | 63.5151 | 0.5798 | 0.0117 | 6.7721 | 0.0555 | 0.2726 | 0.0062 | 1619 | 46 | | | | |
| WW18 | mx | 67 | 32.4407 | 211.1086 | 164.0932 | 17.1872 | 28.5486 | 63.5930 | 0.5830 | 0.0118 | 3.3349 | 0.0390 | 1.1978 | 0.0134 | 1644 | 46 | | | | |
| WW18 | mx | 68 | 22.3015 | 121.1190 | 82.0702 | 18.3868 | 28.9158 | 63.7600 | 0.1431 | 0.0057 | 1.6857 | 0.0278 | 0.1972 | 0.0052 | 1314 | 74 | | | | |
| WW18 | mx | 69 | 29.6964 | 242.1758 | 118.9925 | 17.9521 | 29.4276 | 62.0015 | 0.4451 | 0.0103 | 3.8721 | 0.0420 | 0.6452 | 0.0096 | 1560 | 51 | | | | |
| WW18 | mx | 70 | 27.4585 | 172.5142 | 108.8355 | 17.7616 | 29.0588 | 62.8028 | 0.3678 | 0.0093 | 2.6208 | 0.0346 | 0.5184 | 0.0085 | 1756 | 63 | | | | |
| WW18 | mx | 71 | 28.5462 | 268.1906 | 84.7966 | 17.4854 | 28.2924 | 62.7694 | 0.4195 | 0.0100 | 4.3747 | 0.0447 | 0.2227 | 0.0053 | 1745 | 59 | | | | |
| WW18 | mx | 72 | 30.1777 | 352.1967 | 91.8503 | 17.9098 | 30.9898 | 63.3036 | 0.4648 | 0.0105 | 5.8485 | 0.0516 | 0.3188 | 0.0067 | 1448 | 46 | | | | |
| WW18 | mx | 73 | 28.2711 | 306.2311 | 90.2744 | 17.5962 | 28.7337 | 62.0460 | 0.4033 | 0.0098 | 5.0623 | 0.0480 | 0.3020 | 0.0064 | 1431 | 49 | | | | |
| WW18 | mx | 77 | 32.4907 | 385.2698 | 88.0107 | 18.7003 | 30.1480 | 61.8679 | 0.5226 | 0.0111 | 6.4707 | 0.0543 | 0.2686 | 0.0059 | 1527 | 46 | | | | |
| WW18 | mx | 78 | 23.5142 | 140.2840 | 86.0347 | 17.9323 | 28.4568 | 61.8679 | 0.2080 | 0.0070 | 2.0439 | 0.0306 | 0.2419 | 0.0055 | 1550 | 73 | | | | |
| WW18 | mx | 81 | 23.8080 | 120.6186 | 91.6502 | 17.7171 | 28.7549 | 62.8584 | 0.2283 | 0.0073 | 1.6815 | 0.0277 | 0.3172 | 0.0066 | 1735 | 79 | | | | |
| WW18 | mx | 83 | 23.5142 | 150.1176 | 82.2078 | 18.0352 | 27.8099 | 62.3576 | 0.2043 | 0.0069 | 2.2391 | 0.0320 | 0.1963 | 0.0049 | 1509 | 72 | | | | |
| WW18 | mx | 85 | 30.4465 | 347.0109 | 89.9368 | 18.2985 | 27.4881 | 62.1128 | 0.4593 | 0.0104 | 5.8095 | 0.0514 | 0.3054 | 0.0065 | 1449 | 46 | | | | |
| WW18 | mx | 86 | 33.1908 | 429.9539 | 88.1358 | 18.0579 | 28.3449 | 61.6676 | 0.5716 | 0.0116 | 7.2831 | 0.0575 | 0.2727 | 0.0059 | 1504 | 43 | | | | |
| WW18 | mx | 87 | 32.0968 | 387.9760 | 85.7220 | 18.2067 | 30.3781 | 62.7137 | 0.5260 | 0.0112 | 6.4991 | 0.0543 | 0.2335 | 0.0054 | 1555 | 46 | | | | |
| WW18 | mx | 88 | 33.6409 | 432.8112 | 95.4273 | 17.9003 | 29.8575 | 61.4895 | 0.5935 | 0.0118 | 7.2884 | 0.0574 | 0.3558 | 0.0068 | 1506 | 42 | | | | |
| WW18 | mx | 89 | 22.5328 | 119.4428 | 84.6590 | 17.1383 | 27.6943 | 61.6676 | 0.2003 | 0.0068 | 1.6737 | 0.0276 | 0.2385 | 0.0056 | 1702 | 83 | | | 1573 ± 29 | 55 |
| | | | | | | | | | | | | | | | **All analyses** | | **1597 ± 6** | **782** | **1560** ± 7 | **452** |

# Appendix 3
# MONAZITE COMPOSITIONAL DATA

**Table A3.1.** Compositions of all monazite analysed by EPMA technique.

| Sample | Phase | Label | W%(O) | W%(Al) | W%(Si) | W%(P) | W%(Ca) | W%(Y) | W%(La) | W%(Ce) | W%(Pr) | W%(Nd) | W%(Sm) | W%(Gd) | W%(Dy) | W%(Er) | W%(Pb) | W%(Th) | W%(U) | W%(SUM) |
|---|---|---|---|---|---|---|---|---|---|---|---|---|---|---|---|---|---|---|---|---|
| SC2 | matrix | 1 | 26.9153 | 0.0164 | 0.2313 | 12.8664 | 1.0807 | 0.3532 | 11.3661 | 24.3364 | 2.4860 | 9.7165 | 1.7044 | 1.1238 | 0.2534 | 0.0328 | 0.6542 | 5.5306 | 0.8901 | 99.5676 |
| SC2 | matrix | 2 | 26.9446 | 0.0074 | 0.2172 | 12.9006 | 1.0781 | 0.4505 | 11.7429 | 24.6777 | 2.4360 | 9.5833 | 1.5982 | 1.1550 | 0.2609 | 0.0415 | 0.5861 | 5.0527 | 0.8785 | 99.6212 |
| SC2 | matrix | 3 | 26.6303 | 0.0024 | 0.2140 | 12.6715 | 0.9833 | 0.3084 | 11.6085 | 25.0329 | 2.5253 | 9.7413 | 1.6394 | 1.0934 | 0.1963 | 0.0256 | 0.5491 | 4.9171 | 0.7627 | 98.9115 |
| SC2 | matrix | 4 | 25.3950 | 0.0103 | 0.2228 | 12.1179 | 0.9688 | 0.5600 | 10.7826 | 22.9127 | 2.5868 | 9.9832 | 1.6384 | 1.1913 | 0.2989 | 0.0853 | 0.5538 | 4.1546 | 0.6868 | 94.1592 |
| SC2 | matrix | 5 | 26.4393 | 0.0233 | 0.2741 | 12.6498 | 1.0099 | 0.2877 | 11.4664 | 23.9187 | 2.4179 | 9.6338 | 1.5708 | 1.1065 | 0.2511 | 0.0181 | 0.6054 | 4.8800 | 0.7161 | 97.2789 |
| SC2 | matrix | 6 | 26.6165 | 0.0144 | 0.2168 | 12.6551 | 1.0185 | 0.3471 | 11.5464 | 24.3873 | 2.5737 | 9.7674 | 1.7167 | 1.1748 | 0.2950 | 0.0552 | 0.5787 | 5.1587 | 0.8305 | 98.9628 |
| SC2 | matrix | 7 | 25.5863 | 0.0049 | 0.2346 | 12.0270 | 1.0356 | 0.4815 | 11.3369 | 23.8952 | 2.4100 | 9.2948 | 1.6795 | 1.1432 | 0.2965 | 0.0426 | 0.5813 | 5.2018 | 0.7959 | 96.0576 |
| SC2 | matrix | 8 | 26.8849 | 0.0006 | 0.2170 | 12.9115 | 1.0163 | 0.3812 | 11.5530 | 24.3559 | 2.5938 | 9.9599 | 1.6206 | 1.1204 | 0.2277 | 0.0260 | 0.5753 | 4.8935 | 0.7829 | 99.1305 |
| SC2 | matrix | 9 | 26.7858 | 0.0077 | 0.2163 | 12.8763 | 1.0812 | 0.2928 | 11.5167 | 24.0823 | 2.5684 | 9.5266 | 1.4964 | 1.0858 | 0.2365 | 0.0500 | 0.6036 | 5.2574 | 0.8751 | 98.5689 |
| SC2 | matrix | 11 | 26.5221 | 0.0118 | 0.2298 | 12.7025 | 0.9801 | 0.6555 | 11.6644 | 23.8375 | 2.5034 | 9.6190 | 1.6544 | 1.1817 | 0.3389 | 0.0774 | 0.5498 | 4.8576 | 0.8351 | 98.2310 |
| SC2 | matrix | 12 | 25.8658 | 0.0218 | 0.3484 | 12.2056 | 0.8896 | 0.8715 | 11.4529 | 23.7388 | 2.5284 | 9.3665 | 1.4577 | 1.0921 | 0.3484 | 0.1088 | 0.4703 | 5.2887 | 0.4971 | 96.5624 |
| SC2 | matrix | 13 | 26.6411 | 0.0156 | 0.2103 | 12.7708 | 1.0528 | 0.6595 | 11.3878 | 23.8216 | 2.6204 | 9.6441 | 1.6193 | 1.3064 | 0.3066 | 0.0774 | 0.6029 | 5.0092 | 0.9336 | 98.6894 |
| SC2 | matrix | 14 | 26.5795 | 0.0068 | 0.2296 | 12.7792 | 1.1993 | 0.9938 | 11.0254 | 22.9670 | 2.3692 | 9.3461 | 1.6413 | 1.2229 | 0.4405 | 0.1080 | 0.7529 | 5.5743 | 1.3201 | 98.5659 |
| SC2 | matrix | 15 | 26.7089 | 0.0150 | 0.2285 | 12.8999 | 1.1684 | 1.1259 | 11.0632 | 22.7664 | 2.4456 | 9.2333 | 1.6756 | 1.3819 | 0.4632 | 0.0661 | 0.7247 | 5.5207 | 1.2898 | 98.7871 |
| SC2 | matrix | 16 | 26.4656 | 0.0082 | 0.3120 | 12.5795 | 0.9144 | 0.9099 | 11.1370 | 23.9203 | 2.5261 | 9.6982 | 1.7102 | 1.2426 | 0.3878 | 0.0733 | 0.5213 | 5.9130 | 0.3133 | 98.6427 |
| SC2 | matrix | 17 | 26.3122 | 0.0720 | 1.5143 | 11.8214 | 0.9792 | 0.6846 | 10.2109 | 21.1892 | 2.2324 | 8.8154 | 1.5121 | 1.0399 | 0.4077 | 0.0350 | 0.6721 | 7.7966 | 0.2495 | 95.5545 |
| SC2 | matrix | 18 | 26.2292 | 0.0117 | 0.4367 | 12.3419 | 1.0555 | 0.8732 | 10.8311 | 21.9819 | 2.3620 | 9.8125 | 1.8310 | 1.3602 | 0.3584 | 0.0531 | 0.5948 | 7.6017 | 0.2693 | 98.0142 |
| SC2 | matrix | 19 | 26.7310 | 0.0219 | 0.3921 | 12.7867 | 0.8694 | 0.8921 | 11.0499 | 23.4346 | 2.4954 | 9.7440 | 1.7392 | 1.2717 | 0.3649 | 0.1364 | 0.5404 | 5.9095 | 0.2568 | 98.6460 |
| SC2 | matrix | 20 | 25.8578 | 0.0241 | 0.2180 | 12.3120 | 1.1127 | 1.1056 | 11.1900 | 23.0878 | 2.2860 | 8.9475 | 1.5918 | 1.4172 | 0.4854 | 0.0521 | 0.6830 | 5.1868 | 1.1996 | 96.7674 |
| SC2 | matrix | 21 | 26.3991 | 0.0068 | 0.3697 | 12.5240 | 0.8305 | 0.7947 | 11.1898 | 23.8766 | 2.5448 | 9.5303 | 1.6502 | 1.0186 | 0.4061 | 0.1108 | 0.5196 | 6.2178 | 0.2467 | 98.2461 |
| SC2 | matrix | 22 | 27.0488 | 0.0198 | 0.2232 | 13.2146 | 1.1382 | 1.1515 | 10.9965 | 22.9932 | 2.4060 | 9.2870 | 1.5923 | 1.3828 | 0.4847 | 0.0827 | 0.6832 | 5.0902 | 1.1995 | 99.0042 |
| SC2 | matrix | 23 | 26.3783 | 0.0152 | 0.2367 | 12.7681 | 1.1735 | 1.3757 | 10.8983 | 22.2792 | 2.3685 | 9.0251 | 1.5929 | 1.4781 | 0.5431 | 0.1065 | 0.7489 | 5.2520 | 1.3181 | 97.5682 |
| SC2 | matrix | 24 | 26.4342 | 0.0077 | 0.2617 | 12.7353 | 1.0094 | 1.3095 | 10.8589 | 23.1404 | 2.5042 | 9.5117 | 1.6993 | 1.1152 | 0.4518 | 0.0804 | 0.5040 | 5.8986 | 0.4446 | 97.9769 |
| SC2 | matrix | 25 | 26.3457 | 0.0164 | 0.2102 | 12.7397 | 1.1079 | 1.1599 | 11.0077 | 22.8339 | 2.3629 | 9.2821 | 1.5907 | 1.3031 | 0.4815 | 0.0638 | 0.6293 | 5.0775 | 1.1632 | 97.3855 |
| SC2 | matrix | 26 | 26.5871 | 0.0206 | 0.2233 | 12.7683 | 1.1121 | 0.5383 | 11.1177 | 23.4336 | 2.4516 | 9.6423 | 1.6508 | 1.2089 | 0.3192 | 0.0557 | 0.6349 | 5.3649 | 0.9940 | 98.1333 |
| SC2 | matrix | 27 | 26.3036 | 0.0294 | 0.3308 | 12.6009 | 0.8221 | 0.9529 | 10.9054 | 23.2815 | 2.5761 | 9.6151 | 1.7118 | 1.1536 | 0.4960 | 0.0530 | 0.4734 | 5.7298 | 0.2455 | 97.2909 |
| SC2 | matrix | 28 | 26.2299 | 0.0043 | 0.4034 | 12.5762 | 0.9525 | 0.9542 | 10.5550 | 22.0824 | 2.4081 | 9.4251 | 1.7351 | 1.2912 | 0.4844 | 0.0605 | 0.5498 | 6.7003 | 0.3052 | 96.7276 |
| SC2 | matrix | 29 | 26.3686 | 0.0141 | 0.3094 | 12.6484 | 0.7879 | 0.8236 | 11.2590 | 23.1295 | 2.4946 | 9.9664 | 1.8420 | 1.2705 | 0.3895 | 0.0606 | 0.4715 | 5.3344 | 0.2925 | 97.4725 |
| SC2 | matrix | 30 | 27.5746 | 0.0238 | 0.2150 | 13.7796 | 0.8126 | 1.0721 | 11.2277 | 23.5059 | 2.4621 | 9.5696 | 1.6750 | 1.1521 | 0.4574 | 0.0761 | 0.4534 | 4.3938 | 0.3695 | 98.8303 |
| SC2 | matrix | 31 | 26.1198 | 0.0064 | 0.4318 | 12.4080 | 1.0261 | 0.9319 | 10.4594 | 22.3163 | 2.3576 | 9.3915 | 1.6642 | 1.1334 | 0.5190 | 0.1136 | 0.6349 | 7.0476 | 0.3232 | 96.8947 |
| SC2 | matrix | 32 | 26.3170 | 0.0035 | 0.4098 | 12.5178 | 1.0591 | 0.8228 | 10.9742 | 21.5133 | 2.2644 | 9.7055 | 1.6966 | 1.2322 | 0.4475 | 0.0665 | 0.6678 | 7.5871 | 0.3390 | 97.6341 |
| SC2 | matrix | 33 | 26.0766 | 0.0147 | 0.3115 | 12.4634 | 0.9250 | 0.9414 | 10.7382 | 22.7801 | 2.5345 | 9.6172 | 1.7343 | 1.1962 | 0.3840 | 0.0940 | 0.5445 | 6.1174 | 0.3017 | 96.7847 |
| SC2 | matrix | 34 | 25.8180 | 0.0751 | 0.3137 | 12.4761 | 0.7208 | 1.1051 | 11.1342 | 22.8369 | 2.4193 | 9.6056 | 1.6929 | 1.2501 | 0.4973 | 0.1425 | 0.4203 | 3.7151 | 0.3711 | 94.6041 |
| SC2 | matrix | 35 | 26.2085 | 0.0439 | 0.3824 | 12.5260 | 0.9525 | 0.8280 | 10.5160 | 22.1384 | 2.5474 | 9.6777 | 1.8479 | 1.2866 | 0.4143 | 0.1094 | 0.5824 | 6.3240 | 0.2979 | 96.6933 |
| SC2 | matrix | 36 | 26.8191 | 0.0002 | 0.2027 | 12.9923 | 1.0440 | 0.4904 | 11.3213 | 23.7125 | 2.5583 | 9.6461 | 1.6364 | 1.1491 | 0.2529 | 0.0093 | 0.6172 | 5.0551 | 0.8581 | 98.3750 |
| SC2 | matrix | 37 | 26.4597 | 0.0198 | 0.2173 | 12.7990 | 0.9736 | 0.9447 | 11.0814 | 23.3971 | 2.4772 | 9.3365 | 1.6775 | 1.2229 | 0.4168 | 0.1261 | 0.5145 | 5.0995 | 0.7693 | 97.5429 |
| SC2 | matrix | 38 | 25.6702 | 0.0010 | 0.8216 | 11.8328 | 0.9479 | 0.8081 | 10.3912 | 22.0419 | 2.5036 | 9.5337 | 1.5395 | 1.1808 | 0.4364 | 0.1316 | 0.5697 | 6.5295 | 0.2787 | 95.2282 |
| SC2 | matrix | 39 | 26.0161 | 0.0224 | 0.4014 | 12.2783 | 0.8957 | 0.7641 | 11.0742 | 23.1229 | 2.3872 | 9.4084 | 1.6024 | 1.0651 | 0.3940 | 0.0862 | 0.5535 | 6.6239 | 0.2587 | 96.9645 |
| SC2 | matrix | 40 | 25.9441 | 0.0002 | 0.3875 | 12.2961 | 0.8381 | 0.6951 | 10.8409 | 23.1578 | 2.4385 | 9.3813 | 1.6084 | 1.1201 | 0.3943 | 0.0785 | 0.5540 | 6.5333 | 0.2417 | 96.5199 |
| SC2 | matrix | 41 | 25.8151 | 0.0042 | 0.2885 | 12.3976 | 0.9215 | 1.2693 | 10.7489 | 22.6464 | 2.4187 | 9.1602 | 1.5850 | 1.3045 | 0.5691 | 0.0714 | 0.5649 | 5.4702 | 0.6597 | 95.9052 |
| SC2 | matrix | 42 | 26.2411 | 0.0095 | 0.2245 | 12.6358 | 0.6899 | 0.9232 | 11.4861 | 24.3303 | 2.5654 | 9.7331 | 1.5841 | 1.1453 | 0.4821 | 0.0597 | 0.4026 | 4.3362 | 0.2941 | 97.1530 |
| SC2 | matrix | 43 | 26.1439 | 0.0156 | 0.2812 | 12.4885 | 0.9159 | 0.9210 | 10.8752 | 23.4354 | 2.5386 | 9.6095 | 1.6221 | 1.2068 | 0.4429 | 0.0796 | 0.5364 | 5.7119 | 0.3259 | 97.1604 |
| SC2 | matrix | 44 | 26.0929 | 0.0309 | 0.2842 | 12.4474 | 0.9073 | 0.9598 | 10.7473 | 23.4372 | 2.4270 | 9.7226 | 1.6065 | 1.1402 | 0.5103 | 0.1096 | 0.4912 | 5.7926 | 0.3348 | 97.0518 |
| SC2 | matrix | 45 | 26.2273 | 0.0203 | 0.1834 | 12.6132 | 0.5896 | 1.0295 | 11.8585 | 25.3237 | 2.6086 | 9.8157 | 1.6229 | 1.1498 | 0.4910 | 0.0499 | 0.3316 | 3.1052 | 0.3348 | 97.3650 |
| SC2 | matrix | 46 | 26.1984 | 0.0032 | 0.1972 | 12.7197 | 0.9174 | 1.4332 | 11.1606 | 23.3987 | 2.5375 | 9.0504 | 1.4653 | 1.1790 | 0.5573 | 0.2079 | 0.5581 | 4.6384 | 0.7162 | 96.9485 |
| SC2 | matrix | 47 | 26.4223 | 0.0136 | 0.2972 | 12.6196 | 0.9591 | 0.9925 | 10.9755 | 23.4751 | 2.4282 | 9.4404 | 1.7122 | 1.2283 | 0.5240 | 0.1162 | 0.5584 | 6.1236 | 0.3626 | 98.2588 |
| SC2 | matrix (bt) | 49 | 26.4471 | 0.0059 | 0.2130 | 12.7211 | 1.0468 | 0.9907 | 11.0500 | 23.6569 | 2.5010 | 9.5759 | 1.6224 | 1.1496 | 0.5137 | 0.1077 | 0.5582 | 4.9810 | 0.8772 | 98.0282 |
| SC2 | matrix (bt) | 50 | 26.1455 | 0.0027 | 0.2171 | 12.6043 | 1.1271 | 1.6480 | 10.4365 | 22.9610 | 2.4499 | 9.1031 | 1.6404 | 1.3718 | 0.6273 | 0.0676 | 0.7523 | 4.7739 | 1.5731 | 97.5116 |
| SC2 | matrix (bt) | 51 | 26.0519 | 0.0025 | 0.2044 | 12.6304 | 1.0835 | 1.8844 | 10.5670 | 22.5437 | 2.3950 | 9.1418 | 1.5674 | 1.4427 | 0.7161 | 0.1342 | 0.7210 | 4.3723 | 1.5180 | 96.9863 |
| SC2 | matrix (bt) | 52 | 26.3007 | 0.0078 | 0.2287 | 12.6467 | 0.9314 | 1.3581 | 11.0713 | 23.9025 | 2.5484 | 9.3331 | 1.6379 | 1.0916 | 0.5377 | 0.1462 | 0.5135 | 4.9637 | 0.6227 | 97.8520 |
| SC2 | matrix (bt) | 53 | 26.3338 | 0.0002 | 0.2008 | 12.7381 | 0.9959 | 1.6795 | 10.7666 | 23.7880 | 2.4940 | 9.3485 | 1.5382 | 1.1979 | 0.5542 | 0.1423 | 0.5342 | 4.8101 | 0.8029 | 97.9352 |
| SC2 | matrix (bt) | 54 | 26.1096 | 0.0055 | 0.2127 | 12.5580 | 1.1294 | 1.5610 | 10.4866 | 23.1792 | 2.3512 | 9.2383 | 1.5991 | 1.2113 | 0.5417 | 0.1608 | 0.6219 | 5.5229 | 0.9111 | 97.4103 |
| SC2 | matrix (bt) | 56 | 26.0855 | 0.1068 | 0.3028 | 12.5115 | 1.0119 | 1.7956 | 10.5891 | 23.0300 | 2.4363 | 9.1496 | 1.4905 | 1.2149 | 0.6641 | 0.2036 | 0.5777 | 4.7287 | 0.9388 | 96.8474 |
| SC2 | matrix (bt) | 57 | 25.9955 | 0.0002 | 0.1858 | 12.5289 | 0.9799 | 1.6244 | 10.8025 | 23.6975 | 2.4152 | 9.3039 | 1.4752 | 1.1679 | 0.6239 | 0.1282 | 0.5575 | 4.7372 | 0.8032 | 97.0369 |
| SC2 | matrix (bt) | 58 | 26.0945 | 0.0002 | 0.2372 | 12.4543 | 0.7066 | 0.8674 | 11.4890 | 24.4301 | 2.6034 | 9.8693 | 1.6620 | 1.0949 | 0.5306 | 0.0659 | 0.4078 | 4.4613 | 0.2776 | 97.2621 |
| SC2 | matrix (bt) | 59 | 25.1702 | 0.0271 | 0.4524 | 11.6734 | 0.5672 | 0.8214 | 11.3206 | 24.5164 | 2.5512 | 9.9855 | 1.7377 | 1.1626 | 0.4072 | 0.0810 | 0.3019 | 3.6252 | 0.2156 | 94.6266 |
| SC2 | matrix (bt) | 60 | 25.7282 | 0.0002 | 0.6051 | 11.9666 | 0.7282 | 0.7131 | 11.1649 | 24.3074 | 2.4552 | 9.0621 | 1.6061 | 1.0767 | 0.3513 | 0.0778 | 0.4338 | 5.2733 | 0.2381 | 95.7981 |
| SC2 | matrix (bt) | 61 | 26.3642 | 0.0103 | 1.0130 | 12.0352 | 0.7079 | 0.6544 | 11.2207 | 24.5744 | 2.5025 | 9.3399 | 1.5958 | 1.0674 | 0.3913 | 0.0741 | 0.4532 | 5.0579 | 0.2239 | 97.2961 |
| SC2 | matrix (bt) | 62 | 25.9031 | 0.0070 | 0.1998 | 12.4687 | 1.0468 | 1.6994 | 10.7088 | 23.5591 | 2.3727 | 9.1197 | 1.4870 | 1.0565 | 0.6298 | 0.2191 | 0.5919 | 4.8442 | 0.7907 | 96.7143 |

| Sample | Phase | Label | W%(O ) | W%(Al) | W%(Si) | W%(P) | W%(Ca) | W%(Y ) | W%(La) | W%(Ce) | W%(Pr) | W%(Nd) | W%(Sm) | W%(Gd) | W%(Dy) | W%(Er) | W%(Pb) | W%(Th) | W%(U ) | W%(SUM) |
|---|---|---|---|---|---|---|---|---|---|---|---|---|---|---|---|---|---|---|---|---|
| SC2 | matrix (bt) | 63 | 26.2156 | 0.0074 | 0.1941 | 12.6830 | 0.9986 | 1.6824 | 10.7742 | 23.5406 | 2.5085 | 9.2420 | 1.5215 | 1.3044 | 0.5274 | 0.1389 | 0.5325 | 4.8163 | 0.7996 | 97.4970 |
| SC2 | matrix (bt) | 64 | 27.0076 | 0.6877 | 0.9655 | 12.2756 | 1.0446 | 0.5281 | 10.8193 | 22.9102 | 2.5422 | 9.0378 | 1.4925 | 1.1032 | 0.2791 | 0.0414 | 0.5395 | 4.8533 | 0.9816 | 97.1192 |
| SC2 | matrix (bt) | 65 | 25.9501 | 0.0014 | 0.1866 | 12.4159 | 1.0144 | 1.5690 | 11.0748 | 23.9846 | 2.4500 | 9.0797 | 1.5731 | 1.1603 | 0.5630 | 0.2146 | 0.5858 | 4.7521 | 0.7872 | 97.3726 |
| SC2 | matrix (bt) | 66 | 26.1698 | 0.0033 | 0.2063 | 12.5618 | 1.0079 | 1.4629 | 11.0402 | 23.7892 | 2.4228 | 9.2981 | 1.5537 | 1.1543 | 0.5793 | 0.1119 | 0.5467 | 5.0884 | 0.7166 | 97.7232 |
| SC2 | matrix (bt) | 67 | 26.0570 | 0.0295 | 0.2855 | 12.2737 | 0.5756 | 0.7099 | 11.6927 | 25.8624 | 2.6726 | 9.8654 | 1.6509 | 1.0821 | 0.4031 | 0.0979 | 0.3715 | 3.7668 | 0.2170 | 97.6236 |
| SC2 | matrix (bt) | 68 | 26.4195 | 0.0113 | 0.2622 | 12.5213 | 0.6285 | 0.7923 | 11.8635 | 25.5236 | 2.6796 | 9.9851 | 1.7174 | 1.1353 | 0.4137 | 0.1018 | 0.3789 | 4.1252 | 0.2235 | 98.7927 |
| SC2 | matrix (bt) | 71 | 27.2679 | 0.0071 | 2.0064 | 12.0615 | 0.8711 | 0.8323 | 10.3376 | 22.6645 | 2.4284 | 9.4369 | 1.6890 | 1.2087 | 0.4382 | 0.0420 | 0.4938 | 5.7982 | 0.2814 | 97.8750 |
| SC2 | matrix (bt) | 72 | 26.2369 | 0.0034 | 0.2682 | 12.4247 | 0.6666 | 0.7336 | 11.4965 | 25.1322 | 2.5594 | 10.0008 | 1.7520 | 1.3037 | 0.3982 | 0.1173 | 0.3860 | 4.4347 | 0.2311 | 98.1553 |
| SC2 | matrix (bt) | 73 | 26.1982 | 0.0002 | 0.2343 | 12.5921 | 0.8809 | 1.3704 | 10.9980 | 24.2243 | 2.4269 | 9.2482 | 1.5938 | 1.1606 | 0.5687 | 0.2041 | 0.5196 | 4.6503 | 0.6761 | 97.5567 |
| SC2 | matrix (bt) | 74 | 25.9845 | 0.0064 | 0.2751 | 12.3407 | 0.7514 | 0.7626 | 11.2022 | 24.5506 | 2.6310 | 9.6442 | 1.6184 | 1.1277 | 0.4866 | 0.0786 | 0.3918 | 4.7955 | 0.2296 | 96.8869 |
| SC2 | matrix (bt) | 76 | 26.0975 | 0.0002 | 0.2636 | 12.4332 | 0.6479 | 0.8150 | 11.4351 | 24.7199 | 2.5829 | 9.8081 | 1.6556 | 1.1198 | 0.5212 | 0.1348 | 0.3848 | 4.4368 | 0.2091 | 97.2755 |
| SC2 | matrix (bt) | 77 | 26.0523 | 0.0547 | 0.4998 | 12.3515 | 0.7987 | 1.2964 | 11.0876 | 23.7207 | 2.4152 | 9.5196 | 1.5879 | 1.2187 | 0.5486 | 0.0877 | 0.5107 | 3.7294 | 0.7787 | 96.2682 |
| SC2 | matrix (bt) | 78 | 26.0312 | 0.0035 | 0.2012 | 12.5190 | 0.9790 | 1.2296 | 10.8961 | 23.8576 | 2.4905 | 9.3266 | 1.5227 | 1.1672 | 0.4640 | 0.1372 | 0.4800 | 4.8653 | 0.5908 | 96.7715 |
| SC2 | matrix (bt) | 92 | 26.5790 | 0.0023 | 0.1995 | 12.8003 | 1.0793 | 0.7702 | 11.2120 | 23.6176 | 2.5310 | 9.4149 | 1.6358 | 1.3263 | 0.3987 | 0.0420 | 0.6467 | 4.9944 | 1.0576 | 98.3176 |
| SC2 | matrix (bt) | 93 | 26.2909 | 0.0014 | 0.1829 | 12.6518 | 0.6436 | 1.1234 | 11.8926 | 24.9918 | 2.6495 | 9.7795 | 1.6006 | 1.2222 | 0.4971 | 0.0600 | 0.3650 | 3.3863 | 0.3983 | 97.7469 |
| SC2 | matrix (bt) | 94 | 26.3802 | 0.0115 | 0.2167 | 12.6670 | 0.7905 | 0.8986 | 11.3534 | 24.5112 | 2.5400 | 9.8211 | 1.6020 | 1.1790 | 0.3768 | 0.1082 | 0.4481 | 4.6667 | 0.2858 | 97.8668 |
| SC2 | matrix (bt) | 95 | 26.2360 | 0.0002 | 0.2040 | 12.6247 | 0.6480 | 0.9540 | 11.4356 | 24.2057 | 2.5808 | 9.9894 | 1.7957 | 1.3197 | 0.4650 | 0.0797 | 0.4153 | 4.1884 | 0.3018 | 97.4540 |
| SC2 | matrix (bt) | 96 | 26.2799 | 0.0666 | 0.3533 | 12.3878 | 0.8217 | 0.7475 | 11.3975 | 23.8795 | 2.4970 | 9.8414 | 1.7676 | 1.1932 | 0.4562 | 0.1140 | 0.5318 | 5.1972 | 0.4871 | 98.0293 |
| SC2 | matrix (bt) | 97 | 26.4804 | 0.0035 | 0.5505 | 12.4118 | 0.9348 | 0.8414 | 10.9711 | 22.8021 | 2.4112 | 9.5282 | 1.7301 | 1.1290 | 0.3981 | 0.0976 | 0.6032 | 7.5932 | 0.2738 | 98.7700 |
| SC2 | matrix (bt) | 99 | 26.2670 | 0.0026 | 0.2194 | 12.6028 | 0.5337 | 0.8166 | 11.8747 | 25.6519 | 2.6521 | 9.8252 | 1.6159 | 1.0973 | 0.3778 | 0.0727 | 0.3072 | 3.3011 | 0.1839 | 97.4119 |
| SC2 | matrix (bt) | 100 | 26.5454 | 0.0288 | 0.1978 | 12.7706 | 1.0835 | 0.8136 | 11.2521 | 23.7333 | 2.5115 | 9.2773 | 1.5833 | 1.2828 | 0.3989 | 0.0868 | 0.6759 | 4.8933 | 1.0653 | 98.2102 |
| SC2 | matrix (bt) | 101 | 26.3591 | 0.0171 | 0.2012 | 12.6991 | 1.0873 | 1.0465 | 10.9368 | 23.4717 | 2.3850 | 9.3047 | 1.6062 | 1.2484 | 0.5583 | 0.0829 | 0.6621 | 4.7770 | 1.2373 | 97.6907 |
| SC2 | matrix (bt) | 102 | 26.1664 | 0.0002 | 0.1873 | 12.5827 | 0.6582 | 1.0356 | 11.6475 | 25.1383 | 2.5763 | 9.4702 | 1.6611 | 1.1876 | 0.4638 | 0.1563 | 0.3427 | 3.6286 | 0.3320 | 97.2448 |
| RND | garnet | 1 | 26.4792 | 0.0206 | 0.1800 | 12.6170 | 0.8684 | 0.3340 | 11.9918 | 25.0905 | 2.4926 | 9.8551 | 1.7359 | 0.8758 | 0.2193 | 0.0869 | 0.4642 | 4.4967 | 0.5278 | 98.3458 |
| RND | garnet | 4 | 26.9023 | 0.0126 | 0.1670 | 12.9597 | 0.8550 | 0.3460 | 11.8380 | 25.1956 | 2.5763 | 9.8386 | 1.6854 | 0.9509 | 0.1894 | 0.0408 | 0.4872 | 4.5656 | 0.5376 | 99.1580 |
| RND | garnet | 5 | 26.4568 | 0.0323 | 0.1756 | 12.6214 | 0.8573 | 0.2949 | 12.0747 | 25.2720 | 2.5206 | 9.8682 | 1.6820 | 0.9690 | 0.1635 | 0.0046 | 0.4112 | 4.1156 | 0.4508 | 97.9805 |
| RND | garnet | 6 | 26.3230 | 0.0078 | 0.1696 | 12.5652 | 0.8355 | 0.3763 | 11.8246 | 25.1441 | 2.6277 | 9.9679 | 1.6220 | 0.9165 | 0.1731 | 0.0423 | 0.4152 | 4.1608 | 0.5302 | 97.7118 |
| RND | garnet | 7 | 26.6439 | 0.0002 | 0.1603 | 12.7620 | 0.8576 | 0.3700 | 11.7548 | 25.4671 | 2.6476 | 9.8312 | 1.6561 | 0.9180 | 0.2203 | 0.0001 | 0.4783 | 4.4499 | 0.5301 | 98.7575 |
| RND | garnet | 8 | 25.7977 | 0.0186 | 0.1752 | 12.1380 | 0.8328 | 0.3010 | 11.8708 | 25.0490 | 2.5492 | 9.9052 | 1.7096 | 0.9527 | 0.1830 | 0.0674 | 0.4587 | 4.2838 | 0.5200 | 96.8227 |
| RND | garnet | 9 | 26.2732 | 0.0143 | 0.1644 | 12.4957 | 0.8475 | 0.2904 | 12.0570 | 24.9836 | 2.5122 | 9.8548 | 1.6911 | 0.9271 | 0.2469 | 0.0671 | 0.4472 | 4.3944 | 0.5247 | 97.8016 |
| RND | garnet | 12 | 26.2887 | 0.0061 | 0.1789 | 12.5340 | 0.8480 | 0.3094 | 11.9117 | 24.8715 | 2.5698 | 9.8482 | 1.6336 | 1.0183 | 0.1824 | 0.0373 | 0.4242 | 4.4104 | 0.5311 | 97.6136 |
| RND | garnet | 14 | 26.1322 | 0.0043 | 0.1883 | 12.4573 | 0.8861 | 0.3033 | 11.7829 | 24.4788 | 2.6512 | 9.7641 | 1.6956 | 0.9627 | 0.2327 | 0.0457 | 0.4396 | 4.3848 | 0.5333 | 96.9529 |
| RND | garnet | 15 | 26.3574 | 0.0118 | 0.1691 | 12.5919 | 0.8845 | 0.3190 | 11.9519 | 24.6633 | 2.6347 | 9.8178 | 1.6022 | 0.9114 | 0.2041 | 0.0033 | 0.4523 | 4.6130 | 0.5383 | 97.7360 |
| RND | garnet | 48 | 26.0758 | 0.0067 | 0.1621 | 12.4635 | 0.8891 | 0.5472 | 11.5718 | 24.5749 | 2.5104 | 9.8052 | 1.5895 | 0.9741 | 0.2011 | 0.0803 | 0.4650 | 4.4907 | 0.5145 | 96.9319 |
| RND | garnet | 50 | 25.9019 | 0.0206 | 0.2150 | 12.2641 | 0.8804 | 0.3556 | 11.4370 | 24.5563 | 2.5181 | 9.8453 | 1.6370 | 0.9168 | 0.1615 | 0.0555 | 0.4605 | 4.8866 | 0.4345 | 96.5567 |
| RND | garnet | 51 | 25.9152 | 0.0290 | 0.1805 | 12.3442 | 0.9174 | 0.4835 | 11.5369 | 24.5298 | 2.3494 | 9.5451 | 1.5209 | 0.9068 | 0.2202 | 0.1222 | 0.4637 | 4.7053 | 0.5789 | 96.3590 |
| RND | garnet | 52 | 25.8667 | 0.0321 | 0.1880 | 12.3088 | 0.9712 | 0.5146 | 11.4060 | 23.9418 | 2.5104 | 9.6052 | 1.6193 | 0.9518 | 0.1989 | 0.0403 | 0.5189 | 5.0224 | 0.5406 | 96.2470 |
| RND | garnet | 53 | 26.0035 | 0.0141 | 0.1808 | 12.4067 | 0.9236 | 0.4430 | 11.5793 | 24.4092 | 2.5248 | 9.6477 | 1.4775 | 0.9465 | 0.2350 | 0.0247 | 0.4551 | 4.7492 | 0.5180 | 96.5487 |
| RND | garnet | 54 | 26.1477 | 0.0225 | 0.1786 | 12.4522 | 0.9579 | 0.4849 | 11.8327 | 24.6463 | 2.4557 | 9.5512 | 1.5144 | 0.8194 | 0.2256 | 0.0535 | 0.4877 | 4.8647 | 0.5366 | 97.2416 |
| RND | garnet | 55 | 26.1343 | 0.0087 | 0.1630 | 12.7916 | 0.9322 | 1.8429 | 10.9602 | 23.1525 | 2.3761 | 9.2205 | 1.4414 | 1.1130 | 0.5961 | 0.1019 | 0.4975 | 4.4912 | 0.6830 | 96.5161 |
| RND | garnet | 56 | 25.7569 | 0.0233 | 0.3306 | 12.2064 | 0.9807 | 0.8538 | 9.8506 | 22.1974 | 2.4321 | 10.2546 | 1.9827 | 1.3591 | 0.4192 | 0.1312 | 0.6006 | 6.4070 | 0.3446 | 96.1408 |
| RND | garnet | 57 | 25.9452 | 0.0066 | 0.1767 | 12.5949 | 0.9105 | 1.7426 | 11.2669 | 23.3874 | 2.4606 | 8.9338 | 1.4449 | 1.0829 | 0.5791 | 0.2126 | 0.5251 | 4.2848 | 0.8094 | 96.3740 |
| RND | garnet | 58 | 25.6630 | 0.0032 | 0.1593 | 12.5096 | 0.9128 | 2.2859 | 10.7510 | 22.4883 | 2.3258 | 9.1726 | 1.5342 | 1.2307 | 0.7132 | 0.2214 | 0.4990 | 4.5714 | 0.6673 | 95.7187 |
| RND | garnet | 59 | 26.1450 | 0.0102 | 0.1679 | 12.5434 | 0.9189 | 0.5013 | 11.6180 | 24.4545 | 2.4905 | 9.4912 | 1.5375 | 0.8657 | 0.1615 | 0.0778 | 0.4802 | 4.7492 | 0.5660 | 96.7888 |
| RND | garnet | 60 | 25.7894 | 0.0251 | 0.1839 | 12.2689 | 0.9173 | 0.4994 | 11.6647 | 24.3406 | 2.5088 | 9.2716 | 1.6117 | 0.8884 | 0.2484 | 0.0674 | 0.4897 | 4.7096 | 0.4984 | 95.9933 |
| RND | garnet | 90 | 24.8060 | 0.0839 | 0.2720 | 11.4801 | 0.9546 | 0.4707 | 11.4667 | 23.6443 | 2.4336 | 9.5238 | 1.5213 | 0.7953 | 0.1633 | 0.0738 | 0.4559 | 4.9652 | 0.4957 | 93.6162 |
| RND | garnet | 91 | 26.4203 | 0.0070 | 0.1850 | 12.6734 | 1.0145 | 0.5970 | 11.8452 | 24.1987 | 2.3888 | 9.5165 | 1.4274 | 0.8418 | 0.2326 | 0.0987 | 0.5469 | 5.2970 | 0.5465 | 97.8473 |
| RND | garnet | 92 | 25.9510 | 0.0002 | 0.1569 | 12.5994 | 1.1034 | 1.7089 | 10.8408 | 22.5572 | 2.2171 | 9.1571 | 1.3955 | 1.1065 | 0.5622 | 0.1540 | 0.6597 | 5.3602 | 1.0165 | 96.5566 |
| RND | garnet | 93 | 26.7665 | 0.0611 | 0.9563 | 12.4073 | 0.8927 | 0.8396 | 9.1239 | 21.6772 | 2.4164 | 11.3773 | 2.5272 | 1.6162 | 0.4950 | 0.0836 | 0.4985 | 6.1851 | 0.1763 | 98.1102 |
| RND | garnet | 94 | 25.4298 | 0.0386 | 0.2081 | 12.0387 | 0.9660 | 0.4768 | 11.4911 | 23.6794 | 2.4583 | 9.5484 | 1.4674 | 0.8384 | 0.1379 | 0.0001 | 0.4991 | 5.0561 | 0.4437 | 94.7879 |
| RND | garnet | 95 | 25.2926 | 0.0223 | 0.1730 | 12.0520 | 0.5962 | 0.9026 | 12.1187 | 24.6020 | 2.5116 | 9.5878 | 1.4397 | 0.9624 | 0.4328 | 0.0233 | 0.3284 | 3.0799 | 0.3684 | 94.5037 |
| RND | garnet | 96 | 25.3722 | 0.0256 | 0.1878 | 12.0418 | 0.6412 | 0.8468 | 11.7925 | 24.4158 | 2.5381 | 9.5875 | 1.6751 | 1.0151 | 0.3912 | 0.0792 | 0.3554 | 3.8155 | 0.2783 | 95.0691 |

| Sample | Phase | Label | W%(O ) | W%(Al) | W%(Si) | W%(P) | W%(Ca) | W%(Y ) | W%(La) | W%(Ce) | W%(Pr) | W%(Nd) | W%(Sm) | W%(Gd) | W%(Dy) | W%(Er) | W%(Pb) | W%(Th) | W%(U ) | W%(SUM) |
|---|---|---|---|---|---|---|---|---|---|---|---|---|---|---|---|---|---|---|---|---|
| RND | garnet | 97 | 26.0090 | 0.0004 | 0.1831 | 12.5558 | 0.8654 | 1.3930 | 11.4130 | 23.6937 | 2.3954 | 9.3295 | 1.4691 | 1.0805 | 0.5052 | 0.1548 | 0.4967 | 4.5880 | 0.6169 | 96.7595 |
| RND | garnet | 98 | 26.1014 | 0.7264 | 1.6174 | 11.3150 | 0.8803 | 0.4545 | 11.0390 | 22.4956 | 2.2290 | 8.5276 | 1.3540 | 0.7368 | 0.1881 | 0.1289 | 0.4274 | 4.5019 | 0.4612 | 93.1945 |
| RND | garnet | 99 | 26.1858 | 0.0695 | 0.2252 | 12.5588 | 1.0050 | 0.8030 | 11.4591 | 23.8034 | 2.4540 | 9.1389 | 1.4852 | 0.8854 | 0.2983 | 0.0426 | 0.5206 | 5.1329 | 0.6137 | 96.6914 |
| RND | garnet | 100 | 26.4110 | 0.0180 | 0.2650 | 12.5823 | 1.0616 | 0.2548 | 11.4597 | 23.9699 | 2.4446 | 9.5081 | 1.4522 | 0.7769 | 0.1425 | 0.0690 | 0.5892 | 6.1297 | 0.4855 | 97.6300 |
| RND | garnet | 101 | 26.1499 | 0.0002 | 0.1909 | 12.5915 | 0.9638 | 0.8473 | 11.5884 | 23.7212 | 2.3118 | 9.5544 | 1.5298 | 0.8300 | 0.2420 | 0.0817 | 0.5103 | 5.2066 | 0.4703 | 96.8001 |
| RND | garnet | 102 | 26.0662 | 0.0088 | 0.1706 | 12.6201 | 0.9521 | 1.3639 | 11.4966 | 23.4429 | 2.3859 | 9.3372 | 1.4382 | 0.9897 | 0.3597 | 0.1421 | 0.4953 | 4.8332 | 0.4958 | 96.6083 |
| RND | garnet | 103 | 26.1681 | 0.0215 | 0.3036 | 12.4501 | 0.9038 | 0.2148 | 11.3487 | 24.4522 | 2.4902 | 9.6847 | 1.5992 | 0.8663 | 0.1220 | 0.0798 | 0.4692 | 4.7666 | 0.5201 | 96.4709 |
| RND | garnet | 104 | 26.3667 | 0.0008 | 0.2230 | 12.6383 | 0.9425 | 0.3165 | 11.7584 | 24.0446 | 2.4923 | 9.6661 | 1.5033 | 0.9017 | 0.1501 | 0.0568 | 0.5226 | 5.2467 | 0.4521 | 97.2925 |
| RND | garnet | 105 | 25.8659 | 0.0030 | 0.1752 | 12.6477 | 0.8995 | 2.2021 | 10.8329 | 22.6096 | 2.3269 | 9.2550 | 1.4942 | 1.2471 | 0.5975 | 0.2353 | 0.4671 | 4.5500 | 0.5733 | 95.9923 |
| RND | garnet | 106 | 25.6815 | 0.0252 | 0.2460 | 12.1547 | 0.9906 | 0.2219 | 11.3443 | 23.6397 | 2.4084 | 9.6452 | 1.4999 | 0.8564 | 0.0135 | 0.0351 | 0.5276 | 5.6799 | 0.4626 | 95.4425 |
| RND | garnet | 108 | 26.1085 | 0.0002 | 0.2985 | 12.3911 | 0.9579 | 0.2372 | 11.6595 | 23.9662 | 2.5146 | 9.6213 | 1.5416 | 0.8164 | 0.1580 | 0.0294 | 0.4756 | 5.4118 | 0.4076 | 96.6054 |
| RND | garnet | 109 | 25.6811 | 0.0133 | 0.1945 | 12.4428 | 0.8752 | 1.5755 | 11.4040 | 23.1831 | 2.2790 | 9.0845 | 1.3557 | 1.0505 | 0.5037 | 0.1751 | 0.5292 | 4.1146 | 0.7811 | 95.2529 |
| RND | sillimanite | 18 | 26.6487 | 0.7072 | 0.7869 | 12.0881 | 0.9525 | 0.5214 | 11.4223 | 22.9352 | 2.4790 | 9.6704 | 1.4967 | 0.9418 | 0.1967 | 0.1164 | 0.4670 | 4.8485 | 0.4963 | 96.7851 |
| RND | sillimanite | 19 | 26.3158 | 0.0269 | 0.2187 | 12.7348 | 0.8746 | 0.8220 | 11.6405 | 23.4789 | 2.4820 | 9.3588 | 1.4327 | 0.9200 | 0.3816 | 0.1244 | 0.4952 | 5.1924 | 0.2856 | 96.7949 |
| RND | sillimanite | 20 | 26.6365 | 0.0883 | 0.2364 | 13.0942 | 0.9865 | 2.1111 | 11.0006 | 22.1466 | 2.4933 | 9.2044 | 1.5335 | 1.1221 | 0.6446 | 0.1741 | 0.5786 | 4.7062 | 0.7862 | 97.5532 |
| RND | sillimanite | 23 | 25.7104 | 0.0129 | 0.1296 | 12.3244 | 0.3657 | 0.8986 | 12.7032 | 25.3881 | 2.6659 | 10.2157 | 1.5656 | 0.9632 | 0.4872 | 0.1436 | 0.2120 | 1.8473 | 0.2430 | 95.8864 |
| RND | sillimanite | 24 | 25.8683 | 0.0157 | 0.1657 | 12.5474 | 1.0445 | 1.8346 | 11.0417 | 22.5759 | 2.4102 | 9.1463 | 1.3995 | 1.0756 | 0.5182 | 0.1650 | 0.6246 | 4.9312 | 0.9121 | 96.2865 |
| RND | sillimanite | 26 | 25.8642 | 0.0391 | 0.1730 | 12.5414 | 1.0153 | 1.7763 | 11.1253 | 22.4026 | 2.3285 | 9.2533 | 1.4433 | 1.1331 | 0.6343 | 0.2165 | 0.5631 | 4.7141 | 0.8521 | 96.0855 |
| RND | sillimanite | 28 | 26.3171 | 0.0468 | 0.1761 | 12.7391 | 0.5778 | 0.9156 | 12.3510 | 24.9536 | 2.5173 | 9.4652 | 1.6059 | 0.8465 | 0.3935 | 0.0998 | 0.3114 | 3.3080 | 0.3256 | 96.9603 |
| RND | sillimanite | 30 | 25.9578 | 0.0052 | 0.1539 | 12.6373 | 1.0917 | 1.9078 | 10.8895 | 22.4827 | 2.3458 | 9.0845 | 1.4253 | 1.0914 | 0.5492 | 0.2275 | 0.6474 | 5.0172 | 0.9650 | 96.4892 |
| RND | sillimanite | 31 | 26.4499 | 0.0152 | 0.1837 | 12.9651 | 1.0230 | 1.7924 | 11.1147 | 22.7558 | 2.4021 | 9.0712 | 1.4779 | 1.1310 | 0.5632 | 0.1644 | 0.5918 | 4.8503 | 0.8190 | 97.3807 |
| RND | sillimanite | 32 | 26.0534 | 0.0003 | 0.1541 | 12.6955 | 1.1059 | 1.7150 | 10.9290 | 22.5772 | 2.1919 | 9.0592 | 1.4585 | 1.0861 | 0.6206 | 0.1929 | 0.6405 | 5.0849 | 1.0216 | 96.5966 |
| RND | sillimanite | 33 | 26.2344 | 0.0002 | 0.1043 | 12.7162 | 0.3031 | 0.8895 | 12.8111 | 26.0255 | 2.5905 | 10.0827 | 1.6964 | 1.1826 | 0.4759 | 0.1024 | 0.1750 | 1.4894 | 0.2098 | 97.0990 |
| RND | sillimanite | 35 | 25.6437 | 0.0623 | 0.1878 | 12.4294 | 0.9991 | 1.8301 | 10.8680 | 22.3189 | 2.4006 | 9.0759 | 1.4091 | 1.1546 | 0.5980 | 0.1803 | 0.6105 | 4.5232 | 0.8855 | 95.1870 |
| RND | sillimanite | 36 | 26.2543 | 0.0183 | 0.1460 | 12.8254 | 0.8568 | 1.6022 | 11.5979 | 23.4661 | 2.5042 | 9.1196 | 1.4460 | 1.1000 | 0.5171 | 0.1662 | 0.5137 | 4.1234 | 0.6942 | 96.9614 |
| RND | sillimanite | 37 | 26.1135 | 0.0088 | 0.1783 | 12.6369 | 0.8345 | 0.9295 | 11.7361 | 23.8714 | 2.4854 | 9.2499 | 1.3457 | 0.9091 | 0.3805 | 0.1507 | 0.4454 | 4.7458 | 0.3847 | 96.4162 |
| RND | sillimanite | 38 | 25.7062 | 0.0078 | 0.1524 | 12.4232 | 0.9313 | 1.3541 | 11.4032 | 23.2266 | 2.5009 | 9.1122 | 1.4271 | 1.0012 | 0.5178 | 0.1940 | 0.5266 | 4.2742 | 0.7859 | 95.5547 |
| RND | sillimanite | 39 | 26.1062 | 0.0143 | 0.1606 | 12.8181 | 0.9286 | 2.2048 | 10.7939 | 22.5115 | 2.3484 | 9.1728 | 1.5186 | 1.2155 | 0.6963 | 0.2111 | 0.5128 | 4.7089 | 0.6719 | 96.6043 |
| RND | sillimanite | 41 | 26.3043 | 0.0253 | 0.1574 | 12.8697 | 0.9172 | 1.7363 | 10.9016 | 23.1439 | 2.4786 | 9.2452 | 1.5560 | 1.1843 | 0.5168 | 0.1688 | 0.4871 | 4.8104 | 0.5838 | 97.0967 |
| RND | sillimanite | 42 | 25.7973 | 0.0033 | 0.1617 | 12.5520 | 0.9342 | 1.7783 | 10.9270 | 22.8019 | 2.4766 | 9.2508 | 1.4685 | 1.0942 | 0.5209 | 0.1914 | 0.4917 | 4.7389 | 0.5681 | 95.7668 |
| RND | sillimanite | 43 | 26.0320 | 0.0370 | 0.1578 | 12.7077 | 0.9182 | 1.7619 | 10.8941 | 23.0643 | 2.3756 | 9.1162 | 1.5321 | 1.1940 | 0.4955 | 0.1550 | 0.4842 | 4.7411 | 0.5601 | 96.2368 |
| RND | sillimanite | 44 | 26.4479 | 0.0537 | 0.1748 | 12.8998 | 0.9709 | 1.7485 | 10.9572 | 23.1498 | 2.4913 | 9.3383 | 1.5985 | 1.0415 | 0.5237 | 0.2336 | 0.5217 | 4.9143 | 0.5660 | 97.6415 |
| RND | sillimanite | 45 | 25.9208 | 0.0108 | 0.1606 | 12.5947 | 0.9092 | 1.6249 | 11.0068 | 23.2438 | 2.3960 | 9.2876 | 1.5556 | 1.0943 | 0.4689 | 0.1937 | 0.4800 | 4.6676 | 0.5330 | 96.1583 |
| RND | sillimanite | 46 | 27.5610 | 0.0237 | 0.1558 | 13.8359 | 0.9783 | 1.9225 | 11.0781 | 23.3500 | 2.2696 | 9.0259 | 1.4712 | 1.0806 | 0.4766 | 0.1565 | 0.5408 | 5.0490 | 0.5406 | 99.5261 |
| RND | sillimanite | 47 | 25.7932 | 0.0125 | 0.1550 | 12.5047 | 0.9138 | 1.5882 | 10.8199 | 23.3150 | 2.4262 | 9.2560 | 1.5530 | 1.1169 | 0.5626 | 0.1186 | 0.4949 | 4.7179 | 0.5159 | 95.8743 |
| RND | sillimanite | 61 | 25.6829 | 0.0131 | 0.1616 | 12.4421 | 0.9417 | 1.9157 | 10.7660 | 22.9086 | 2.3534 | 9.1416 | 1.5126 | 1.1521 | 0.6800 | 0.2234 | 0.5289 | 4.6009 | 0.8429 | 95.8775 |
| RND | sillimanite | 62 | 26.0079 | 0.0240 | 0.1553 | 12.6677 | 0.9430 | 1.8718 | 11.0147 | 23.1395 | 2.3402 | 9.2038 | 1.4027 | 1.1327 | 0.5129 | 0.2305 | 0.5691 | 4.4891 | 0.8165 | 96.5314 |
| RND | sillimanite | 63 | 26.9288 | 0.3488 | 0.3612 | 12.9848 | 0.9573 | 1.6786 | 10.8843 | 23.1716 | 2.3602 | 9.0957 | 1.5984 | 0.9916 | 0.5114 | 0.1825 | 0.5530 | 4.7565 | 0.6349 | 98.0096 |
| RND | sillimanite | 64 | 26.0105 | 0.0123 | 0.1491 | 12.6596 | 0.9568 | 1.8888 | 10.8853 | 23.3983 | 2.3932 | 9.1024 | 1.4181 | 1.1242 | 0.5759 | 0.2011 | 0.5328 | 4.4417 | 0.9214 | 96.6815 |
| RND | sillimanite | 65 | 26.0130 | 0.0176 | 0.1545 | 12.6653 | 0.8567 | 2.0565 | 10.7684 | 23.5132 | 2.4024 | 9.3759 | 1.5888 | 1.2263 | 0.6035 | 0.1671 | 0.4611 | 4.3761 | 0.5510 | 96.8074 |
| RND | sillimanite | 66 | 26.0202 | 0.0634 | 0.1708 | 12.6590 | 0.8762 | 2.0444 | 10.7949 | 23.2720 | 2.3483 | 9.3239 | 1.5669 | 1.1436 | 0.5570 | 0.2580 | 0.4771 | 4.4529 | 0.5575 | 96.5961 |
| RND | sillimanite | 67 | 25.8671 | 0.0099 | 0.1537 | 12.5500 | 0.8997 | 1.9528 | 10.8671 | 23.5555 | 2.3303 | 9.1422 | 1.5721 | 1.1805 | 0.6136 | 0.1986 | 0.4724 | 4.5457 | 0.5499 | 96.4711 |
| RND | sillimanite | 68 | 26.1960 | 0.0162 | 0.1612 | 12.5619 | 0.3184 | 0.7229 | 10.1765 | 25.2264 | 2.6924 | 12.3109 | 2.7636 | 1.5898 | 0.4214 | 0.1371 | 0.1800 | 1.9443 | 0.1143 | 97.5433 |
| RND | sillimanite | 69 | 28.1944 | 1.9761 | 1.0710 | 12.5000 | 0.8434 | 1.4229 | 10.7345 | 22.5763 | 2.2553 | 8.8440 | 1.4699 | 1.0690 | 0.4429 | 0.1383 | 0.5100 | 3.9078 | 0.7417 | 98.7075 |
| RND | sillimanite | 70 | 26.1607 | 0.0002 | 0.6458 | 12.2912 | 0.4630 | 0.8084 | 9.5257 | 23.6395 | 2.5652 | 12.3095 | 2.6698 | 1.6047 | 0.3508 | 0.1560 | 0.2696 | 2.9319 | 0.1297 | 96.5317 |
| RND | sillimanite | 71 | 26.1729 | 0.0147 | 0.1493 | 12.6811 | 1.1600 | 1.6214 | 10.7978 | 23.1203 | 2.4026 | 8.9409 | 1.3694 | 1.1231 | 0.5385 | 0.1711 | 0.6657 | 5.5466 | 0.8784 | 97.3638 |
| RND | sillimanite | 72 | 26.0489 | 0.0221 | 0.1691 | 12.5242 | 0.9756 | 1.1468 | 11.2864 | 24.0207 | 2.4187 | 9.2572 | 1.4588 | 0.9381 | 0.3353 | 0.1006 | 0.5310 | 4.9678 | 0.6805 | 96.8918 |
| RND | sillimanite | 73 | 25.9150 | 0.0653 | 0.1979 | 12.4400 | 1.0005 | 1.5898 | 10.9974 | 23.1864 | 2.3972 | 9.2149 | 1.5069 | 1.1129 | 0.5817 | 0.1146 | 0.5994 | 4.9351 | 0.8560 | 96.7210 |
| RND | sillimanite | 74 | 26.0562 | 0.0189 | 0.1567 | 12.5400 | 0.5287 | 0.9226 | 10.1782 | 24.0346 | 2.5653 | 11.6026 | 2.6253 | 1.5240 | 0.4615 | 0.1071 | 0.2883 | 3.1462 | 0.1660 | 96.9322 |
| RND | sillimanite | 75 | 26.2989 | 0.0074 | 0.1420 | 12.7329 | 0.5326 | 0.7084 | 10.7573 | 24.5383 | 2.5821 | 11.3851 | 2.2438 | 1.2294 | 0.3432 | 0.1004 | 0.3003 | 2.9239 | 0.3160 | 97.1520 |
| RND | sillimanite | 76 | 26.1768 | 0.0119 | 0.1361 | 12.6449 | 0.3486 | 0.6974 | 10.7263 | 24.9959 | 2.6650 | 11.8777 | 2.4497 | 1.4175 | 0.3747 | 0.0848 | 0.1909 | 1.9487 | 0.1480 | 96.9049 |
| RND | sillimanite | 77 | 26.3355 | 0.0359 | 0.1709 | 12.7778 | 0.7665 | 1.2392 | 10.9618 | 23.7104 | 2.4581 | 10.2802 | 1.9289 | 1.2205 | 0.4245 | 0.1438 | 0.4285 | 3.8747 | 0.5448 | 97.3120 |
| RND | sillimanite | 78 | 26.6284 | 0.0062 | 0.1772 | 12.8667 | 0.9465 | 0.4553 | 11.6094 | 24.5527 | 2.5090 | 9.5959 | 1.5789 | 0.9105 | 0.1624 | 0.0576 | 0.4964 | 4.8288 | 0.4844 | 97.8763 |
| RND | sillimanite | 79 | 26.2375 | 0.0045 | 0.1620 | 12.6804 | 0.9745 | 1.0918 | 11.2223 | 23.8113 | 2.3690 | 9.4995 | 1.5696 | 1.0079 | 0.3295 | 0.1567 | 0.5478 | 4.9021 | 0.6692 | 97.2456 |
| RND | sillimanite | 81 | 26.1956 | 0.0246 | 0.1657 | 12.5167 | 0.9372 | 0.6190 | 11.3743 | 24.3927 | 2.4779 | 9.6802 | 1.6422 | 0.9794 | 0.2402 | 0.1217 | 0.5296 | 5.0517 | 0.5173 | 97.4760 |
| RND | sillimanite | 84 | 26.1878 | 0.0243 | 0.1611 | 12.5556 | 0.9512 | 0.7332 | 11.6805 | 24.4259 | 2.4928 | 9.4103 | 1.4298 | 0.8964 | 0.2309 | 0.1129 | 0.4871 | 4.9027 | 0.5075 | 97.2000 |

| Sample | Phase | Label | W%(O ) | W%(Al) | W%(Si) | W%(P) | W%(Ca) | W%(Y ) | W%(La) | W%(Ce) | W%(Pr) | W%(Nd) | W%(Sm) | W%(Gd) | W%(Dy) | W%(Er) | W%(Pb) | W%(Th) | W%(U ) | W%(SUM) |
|---|---|---|---|---|---|---|---|---|---|---|---|---|---|---|---|---|---|---|---|---|
| RND | sillimanite | 85 | 26.1041 | 0.0016 | 0.1676 | 12.5501 | 0.9440 | 0.6798 | 11.3882 | 23.9608 | 2.3980 | 9.7552 | 1.4493 | 0.8740 | 0.2471 | 0.1098 | 0.4912 | 5.0714 | 0.5280 | 96.7302 |
| RND | sillimanite | 86 | 26.2695 | 0.0082 | 0.1686 | 12.6079 | 0.9461 | 0.6273 | 11.5706 | 24.1634 | 2.4602 | 9.8065 | 1.4886 | 0.8726 | 0.2324 | 0.1271 | 0.4838 | 5.0407 | 0.4972 | 97.3807 |
| RND | sillimanite | 88 | 25.8659 | 0.0050 | 0.1778 | 12.4122 | 0.9615 | 0.6958 | 11.3293 | 23.7208 | 2.4375 | 9.5016 | 1.5479 | 0.8308 | 0.2367 | 0.0416 | 0.5196 | 5.1305 | 0.5032 | 95.9277 |
| RND | matrix | 110 | 26.4694 | 0.0095 | 0.1724 | 12.8216 | 0.8386 | 0.4044 | 11.6825 | 24.2698 | 2.4944 | 9.7688 | 1.6185 | 0.9738 | 0.2086 | 0.0640 | 0.4353 | 4.3693 | 0.4751 | 97.0860 |
| RND | matrix | 111 | 26.5268 | 0.0211 | 0.1695 | 12.8435 | 0.8152 | 0.4896 | 11.5983 | 24.5321 | 2.5889 | 9.8220 | 1.5773 | 0.9434 | 0.2123 | 0.0573 | 0.4807 | 4.2333 | 0.4985 | 97.4198 |
| RND | matrix | 113 | 26.5811 | 0.0057 | 0.1687 | 12.8366 | 0.8159 | 0.4411 | 11.6626 | 24.6175 | 2.5380 | 9.9803 | 1.6001 | 1.0604 | 0.2596 | 0.1103 | 0.4658 | 4.2268 | 0.4992 | 97.8797 |
| RND | matrix | 114 | 26.7796 | 0.0286 | 0.1874 | 12.9602 | 0.8217 | 0.4283 | 11.5794 | 24.7165 | 2.5679 | 9.8419 | 1.6244 | 0.9742 | 0.2515 | 0.0831 | 0.4837 | 4.3806 | 0.5130 | 98.2320 |
| RND | matrix | 115 | 25.8867 | 0.0102 | 0.1827 | 12.3322 | 0.7947 | 0.4322 | 11.3964 | 24.7891 | 2.6493 | 9.9097 | 1.6901 | 0.9106 | 0.2351 | 0.1110 | 0.4338 | 4.0170 | 0.4855 | 96.2763 |
| RND | matrix | 116 | 26.4468 | 0.0036 | 0.1661 | 12.7411 | 0.8561 | 0.4825 | 11.6026 | 24.5891 | 2.5453 | 9.7355 | 1.6249 | 1.0633 | 0.2766 | 0.0966 | 0.4466 | 4.3942 | 0.5427 | 97.6236 |
| RND | matrix | 117 | 26.1592 | 0.0096 | 0.1749 | 12.5571 | 0.8351 | 0.4420 | 11.4656 | 24.7975 | 2.3988 | 9.7189 | 1.5691 | 0.9673 | 0.2173 | 0.0513 | 0.4605 | 4.3811 | 0.5293 | 96.7446 |
| RND | matrix | 118 | 25.5369 | 0.0712 | 0.2571 | 12.0680 | 0.7961 | 0.4583 | 11.5553 | 24.2813 | 2.5215 | 9.6517 | 1.6055 | 0.9296 | 0.1736 | 0.0976 | 0.4428 | 3.9725 | 0.5086 | 94.9376 |
| RND | matrix | 119 | 25.8523 | 0.0099 | 0.1643 | 12.3977 | 0.9111 | 0.5992 | 11.2020 | 23.8165 | 2.5107 | 9.7130 | 1.6341 | 1.0099 | 0.3379 | 0.0544 | 0.4872 | 4.6577 | 0.5335 | 95.9014 |
| RND | matrix | 120 | 26.4325 | 0.0190 | 0.1835 | 12.8007 | 0.8920 | 0.5162 | 11.3302 | 24.1306 | 2.4460 | 9.7857 | 1.6279 | 0.9071 | 0.2106 | 0.0365 | 0.4918 | 4.6301 | 0.5486 | 96.9990 |
| RND | matrix | 121 | 25.3667 | 0.0243 | 0.1829 | 12.0253 | 0.8141 | 0.4120 | 11.5040 | 24.2333 | 2.5352 | 9.6062 | 1.5521 | 0.9530 | 0.2553 | 0.0481 | 0.4107 | 4.1863 | 0.5029 | 94.6224 |
| RND | matrix | 122 | 25.8016 | 0.0116 | 0.2159 | 12.3066 | 0.8513 | 0.3866 | 11.2894 | 23.9566 | 2.5315 | 9.7304 | 1.6317 | 0.9534 | 0.2046 | 0.0356 | 0.4790 | 4.8453 | 0.4682 | 95.7093 |
| RND | matrix | 123 | 26.0720 | 0.0365 | 0.2037 | 12.4969 | 0.9045 | 0.5532 | 11.5602 | 23.8016 | 2.4710 | 9.4830 | 1.5982 | 1.0482 | 0.2049 | 0.0390 | 0.4793 | 4.8675 | 0.5698 | 96.3995 |
| RRQ | garnet | 1 | 26.5400 | 0.0022 | 0.1653 | 12.8624 | 0.8756 | 1.7054 | 11.1946 | 23.8885 | 2.4461 | 9.5259 | 1.7799 | 1.4416 | 0.5854 | 0.1478 | 0.5182 | 4.4675 | 0.7073 | 98.8637 |
| RRQ | garnet | 2 | 26.4534 | 0.0243 | 0.1857 | 12.7583 | 0.8822 | 1.5872 | 11.1592 | 23.6800 | 2.3905 | 9.7632 | 1.8580 | 1.3600 | 0.5826 | 0.1774 | 0.5248 | 4.6269 | 0.6168 | 98.6405 |
| RRQ | garnet | 3 | 27.0480 | 0.0083 | 0.2162 | 13.0991 | 0.6210 | 1.2982 | 11.8546 | 24.9013 | 2.5441 | 10.6525 | 1.6468 | 1.1557 | 0.4210 | 0.0745 | 0.3161 | 4.0404 | 0.1355 | 100.0433 |
| RRQ | garnet | 4 | 26.6742 | 0.0062 | 0.2280 | 12.7667 | 0.6539 | 1.2787 | 12.1188 | 24.8353 | 2.4883 | 10.5443 | 1.5939 | 1.1097 | 0.3810 | 0.0625 | 0.3722 | 4.3510 | 0.1346 | 99.6093 |
| RRQ | garnet | 5 | 26.6504 | 0.0002 | 0.2255 | 12.8088 | 0.6828 | 1.3482 | 11.2189 | 24.3145 | 2.6841 | 10.2302 | 1.8026 | 1.3046 | 0.4699 | 0.1874 | 0.4176 | 4.8567 | 0.2435 | 99.4559 |
| RRQ | garnet | 6 | 26.6331 | 0.0140 | 0.1636 | 12.8631 | 0.8663 | 1.6091 | 11.2840 | 24.1910 | 2.4860 | 9.6480 | 1.7839 | 1.3731 | 0.6380 | 0.2006 | 0.4778 | 4.4329 | 0.6724 | 99.3469 |
| RRQ | garnet | 7 | 26.4737 | 0.0085 | 0.1916 | 12.7618 | 0.8472 | 1.5852 | 11.0220 | 24.0059 | 2.4831 | 9.7895 | 1.8229 | 1.3636 | 0.6186 | 0.1262 | 0.5473 | 4.5872 | 0.5843 | 98.8286 |
| RRQ | garnet | 8 | 26.2975 | 0.0027 | 0.1883 | 12.6902 | 0.9149 | 1.7159 | 10.7411 | 23.5914 | 2.4224 | 9.5420 | 1.8212 | 1.4993 | 0.6572 | 0.1547 | 0.5361 | 4.7489 | 0.7141 | 98.2479 |
| RRQ | garnet | 9 | 26.3511 | 0.0070 | 0.1816 | 12.7152 | 0.9752 | 1.7454 | 10.8178 | 23.4122 | 2.4420 | 9.6213 | 1.6397 | 1.5782 | 0.6222 | 0.1174 | 0.5740 | 4.8485 | 0.8098 | 98.4686 |
| RRQ | garnet | 10 | 26.2267 | 0.0108 | 0.1783 | 12.6213 | 0.9107 | 1.7531 | 10.9857 | 23.6119 | 2.4511 | 9.6435 | 1.7848 | 1.3529 | 0.6828 | 0.1699 | 0.5500 | 4.5862 | 0.7151 | 98.2448 |
| RRQ | garnet | 11 | 26.2019 | 0.0027 | 0.1839 | 12.6322 | 0.9546 | 1.7803 | 10.6063 | 23.1446 | 2.5330 | 9.5385 | 1.7617 | 1.4661 | 0.6975 | 0.1608 | 0.6014 | 5.0175 | 0.8310 | 98.1240 |
| RRQ | garnet | 12 | 26.1740 | 0.0056 | 0.2336 | 12.5450 | 0.7672 | 1.6507 | 10.6607 | 23.9095 | 2.5219 | 9.9334 | 1.8061 | 1.4707 | 0.6212 | 0.1974 | 0.3875 | 5.0106 | 0.1747 | 98.0798 |
| RRQ | garnet | 13 | 26.3530 | 0.0031 | 0.2140 | 12.5691 | 0.6163 | 1.3629 | 11.4499 | 24.9000 | 2.5523 | 10.6528 | 1.7553 | 1.2325 | 0.4735 | 0.1433 | 0.3265 | 4.1839 | 0.1350 | 98.9334 |
| RRQ | garnet | 14 | 26.3111 | 0.0078 | 0.2525 | 12.6169 | 0.6778 | 1.8771 | 10.9382 | 24.0734 | 2.5115 | 9.9863 | 1.7718 | 1.4393 | 0.5661 | 0.2078 | 0.4645 | 4.9045 | 0.1676 | 98.7842 |
| RRQ | garnet | 15 | 26.4942 | 0.0002 | 0.2299 | 12.6641 | 0.6204 | 1.2282 | 11.6396 | 25.0694 | 2.6195 | 10.4845 | 1.5426 | 1.2114 | 0.4302 | 0.1408 | 0.3624 | 4.1478 | 0.1514 | 99.0466 |
| RRQ | garnet | 16 | 26.2695 | 0.0027 | 0.1734 | 12.5792 | 0.8899 | 1.5293 | 10.7192 | 23.8794 | 2.6304 | 9.7710 | 1.8796 | 1.5287 | 0.6222 | 0.1717 | 0.5529 | 4.9587 | 0.5800 | 98.7478 |
| RRQ | garnet | 17 | 26.3197 | 0.0002 | 0.1756 | 12.6897 | 0.8496 | 1.6095 | 11.1065 | 24.1569 | 2.4273 | 9.4940 | 1.7933 | 1.3549 | 0.5805 | 0.1091 | 0.4700 | 4.5301 | 0.6579 | 98.3348 |
| RRQ | garnet | 18 | 26.2837 | 0.0002 | 0.1897 | 12.6169 | 0.8486 | 1.5608 | 10.7655 | 23.8913 | 2.5805 | 9.8410 | 1.9137 | 1.4613 | 0.6494 | 0.2000 | 0.5053 | 4.5936 | 0.6037 | 98.5152 |
| RRQ | garnet | 19 | 26.3543 | 0.0020 | 0.1779 | 12.6816 | 0.8349 | 1.5808 | 11.0125 | 24.2517 | 2.4849 | 9.6356 | 1.8453 | 1.4090 | 0.6036 | 0.1793 | 0.4583 | 4.4742 | 0.5973 | 98.5932 |
| RRQ | garnet | 20 | 26.3282 | 0.0157 | 0.1760 | 12.6799 | 0.9829 | 1.3948 | 10.7002 | 23.4385 | 2.3796 | 9.7365 | 1.8214 | 1.5132 | 0.5964 | 0.0879 | 0.6042 | 4.8860 | 0.8606 | 98.2120 |
| RRQ | garnet | 21 | 26.0778 | 0.0064 | 0.1700 | 12.4892 | 0.9537 | 1.5643 | 10.6823 | 23.5839 | 2.4132 | 9.5698 | 1.9369 | 1.5160 | 0.6237 | 0.1596 | 0.5494 | 4.8500 | 0.8521 | 98.0083 |
| RRQ | garnet | 22 | 26.2542 | 0.0008 | 0.1960 | 12.5715 | 0.8416 | 1.4341 | 10.8836 | 24.3535 | 2.5026 | 9.6554 | 1.7571 | 1.4270 | 0.5773 | 0.1640 | 0.4617 | 4.8823 | 0.4431 | 98.4158 |
| RRQ | garnet | 23 | 26.0849 | 0.0002 | 0.2228 | 12.4480 | 0.6524 | 1.5373 | 11.0076 | 24.2198 | 2.5855 | 10.6446 | 1.7832 | 1.4080 | 0.5582 | 0.1497 | 0.3807 | 4.2404 | 0.1219 | 98.0552 |
| RRQ | garnet | 24 | 26.2383 | 0.0130 | 0.2285 | 12.4521 | 0.5694 | 1.0233 | 11.8302 | 25.2509 | 2.5548 | 10.6494 | 1.4970 | 1.2117 | 0.4203 | 0.1588 | 0.3071 | 3.8785 | 0.1187 | 98.4120 |
| RRQ | garnet | 25 | 26.0800 | 0.0071 | 0.2200 | 12.3531 | 0.5576 | 1.0472 | 11.9830 | 25.2205 | 2.6895 | 10.6694 | 1.5534 | 0.9712 | 0.3429 | 0.0624 | 0.3037 | 3.8485 | 0.1122 | 98.0317 |
| RRQ | garnet | 26 | 26.0919 | 0.0058 | 0.2659 | 12.4048 | 0.8483 | 1.5813 | 10.2753 | 23.5558 | 2.5001 | 9.9294 | 2.0724 | 1.6457 | 0.6258 | 0.0766 | 0.4263 | 5.7132 | 0.2388 | 98.2674 |
| RRQ | garnet | 27 | 25.9048 | 0.0002 | 0.1837 | 12.3795 | 0.9078 | 1.4542 | 10.8537 | 23.8199 | 2.5826 | 9.3557 | 1.7693 | 1.3545 | 0.5331 | 0.1846 | 0.5179 | 4.9647 | 0.5661 | 97.3423 |
| RRQ | garnet | 28 | 26.2667 | 0.0198 | 0.1704 | 12.6747 | 0.8179 | 1.4351 | 10.8937 | 24.2629 | 2.4474 | 9.5094 | 1.7687 | 1.3527 | 0.5276 | 0.0773 | 0.5216 | 4.5158 | 0.6196 | 97.8913 |
| RRQ | garnet | 29 | 25.9156 | 0.0093 | 0.1766 | 12.4143 | 0.8995 | 1.6845 | 10.7185 | 23.6406 | 2.4085 | 9.7107 | 1.7943 | 1.4109 | 0.6457 | 0.1139 | 0.5186 | 4.6168 | 0.7346 | 97.4229 |
| RRQ | garnet | 30 | 26.4927 | 0.4079 | 0.8274 | 11.9861 | 2.0391 | 0.8923 | 10.0257 | 22.3385 | 2.2597 | 9.2408 | 1.7834 | 1.4681 | 0.3925 | 0.0800 | 0.4955 | 5.0099 | 0.7954 | 96.5450 |
| RRQ | garnet | 31 | 26.1132 | 0.0054 | 0.1737 | 12.5529 | 0.8731 | 1.6735 | 10.7912 | 23.9313 | 2.4221 | 9.6856 | 1.7687 | 1.3646 | 0.6079 | 0.1024 | 0.5294 | 4.5743 | 0.7253 | 97.9046 |
| RRQ | garnet | 32 | 26.0633 | 0.0002 | 0.1490 | 12.5333 | 0.8181 | 1.5455 | 11.0565 | 24.2374 | 2.5231 | 9.6475 | 1.6881 | 1.4275 | 0.5584 | 0.1083 | 0.4694 | 4.2541 | 0.5728 | 97.6625 |
| RRQ | garnet | 33 | 25.8547 | 0.0042 | 0.2423 | 12.2391 | 0.7481 | 1.5108 | 10.7979 | 24.5466 | 2.5741 | 9.6943 | 1.8928 | 1.3351 | 0.4828 | 0.1304 | 0.4120 | 5.0477 | 0.1940 | 97.7169 |
| RRQ | garnet | 34 | 26.2418 | 0.0062 | 0.2127 | 12.5218 | 0.6080 | 1.3652 | 11.6099 | 25.1364 | 2.5002 | 10.4045 | 1.5671 | 1.1689 | 0.4059 | 0.1785 | 0.3045 | 4.0424 | 0.1324 | 98.4164 |
| RRQ | garnet | 35 | 26.1355 | 0.0078 | 0.2227 | 12.4456 | 0.5977 | 1.2105 | 11.8016 | 25.0921 | 2.6114 | 10.2991 | 1.5068 | 1.1280 | 0.3723 | 0.1712 | 0.3673 | 3.8712 | 0.1118 | 97.9626 |
| RRQ | garnet | 36 | 25.9453 | 0.0150 | 0.2267 | 12.2890 | 0.6141 | 1.4168 | 11.4882 | 24.9114 | 2.5896 | 10.4136 | 1.6464 | 1.1901 | 0.4514 | 0.1105 | 0.3148 | 4.1086 | 0.1176 | 97.8591 |
| RRQ | garnet | 37 | 26.1104 | 0.0065 | 0.2219 | 12.4362 | 0.6828 | 1.3856 | 11.0057 | 24.5762 | 2.5130 | 10.4074 | 1.7658 | 1.2800 | 0.4802 | 0.1468 | 0.3749 | 4.5898 | 0.1348 | 98.1280 |
| RRQ | garnet | 38 | 25.9873 | 0.0002 | 0.1630 | 12.4366 | 0.8665 | 1.3236 | 11.2825 | 24.3377 | 2.3177 | 9.3439 | 1.7192 | 1.3811 | 0.4887 | 0.1274 | 0.4876 | 4.6287 | 0.5699 | 97.4716 |
| RRQ | garnet | 39 | 25.9882 | 0.0257 | 0.2078 | 12.3860 | 0.9599 | 1.6165 | 10.4970 | 23.3080 | 2.4884 | 9.7119 | 1.8218 | 1.6247 | 0.6706 | 0.2239 | 0.5415 | 4.9120 | 0.8632 | 97.8571 |
| RRQ | garnet | 41 | 25.9313 | 0.0830 | 0.2373 | 12.3483 | 0.8415 | 1.4722 | 11.0226 | 23.9650 | 2.4502 | 9.4704 | 1.7828 | 1.3867 | 0.5753 | 0.1615 | 0.4408 | 4.2384 | 0.5960 | 97.0133 |

| Sample | Phase | Label | W%(O ) | W%(Al) | W%(Si) | W%(P) | W%(Ca) | W%(Y ) | W%(La) | W%(Ce) | W%(Pr) | W%(Nd) | W%(Sm) | W%(Gd) | W%(Dy) | W%(Er) | W%(Pb) | W%(Th) | W%(U ) | W%(SUM) |
|---|---|---|---|---|---|---|---|---|---|---|---|---|---|---|---|---|---|---|---|---|
| RRQ | garnet | 42 | 25.6888 | 0.0179 | 0.1654 | 12.2557 | 0.8070 | 1.5652 | 10.9116 | 24.2017 | 2.5720 | 9.4950 | 1.7915 | 1.3723 | 0.6021 | 0.1239 | 0.4573 | 4.2266 | 0.4998 | 96.7638 |
| RRQ | garnet | 1 | 26.2752 | 0.0947 | 0.2710 | 12.1773 | 2.0118 | 1.4254 | 10.6197 | 24.3073 | 2.5465 | 9.7025 | 1.7267 | 1.2992 | 0.4983 | 0.1252 | 0.5005 | 4.5158 | 0.6014 | 98.7085 |
| RRQ | garnet | 8 | 26.4204 | 0.0125 | 0.1772 | 12.6449 | 0.8869 | 1.3843 | 11.6265 | 24.4587 | 2.4650 | 9.4659 | 1.7319 | 1.3306 | 0.5199 | 0.1297 | 0.5051 | 4.6303 | 0.5879 | 98.9877 |
| RRQ | garnet | 9 | 26.3778 | 0.0034 | 0.1880 | 12.5869 | 0.8820 | 1.3268 | 11.4662 | 24.4222 | 2.3979 | 9.6579 | 1.7735 | 1.4006 | 0.5006 | 0.1369 | 0.5063 | 4.9129 | 0.5059 | 99.0558 |
| RRQ | garnet | 10 | 26.5786 | 0.0153 | 0.1984 | 12.7904 | 0.9612 | 1.6509 | 10.7651 | 23.8774 | 2.4693 | 9.6718 | 1.7892 | 1.5480 | 0.6098 | 0.1359 | 0.6178 | 4.8675 | 0.8083 | 99.3649 |
| RRQ | garnet | 12 | 26.6797 | 0.0132 | 0.1782 | 12.8196 | 0.8513 | 1.3395 | 11.4943 | 24.4668 | 2.5769 | 9.5466 | 1.6903 | 1.3926 | 0.5638 | 0.1675 | 0.5111 | 4.8283 | 0.5338 | 99.6635 |
| RRQ | garnet | 13 | 26.7899 | 0.0184 | 0.1997 | 12.7778 | 0.8409 | 1.2160 | 11.6255 | 24.9192 | 2.5312 | 9.7865 | 1.8820 | 1.4391 | 0.4779 | 0.2064 | 0.4534 | 4.8804 | 0.3361 | 100.3904 |
| RRQ | garnet | 14 | 26.2518 | 0.0352 | 0.2792 | 12.4340 | 0.8827 | 1.5458 | 10.9766 | 24.3009 | 2.4392 | 9.8604 | 1.7879 | 1.4311 | 0.4760 | 0.1290 | 0.4495 | 5.1419 | 0.3134 | 98.7446 |
| RRQ | garnet | 16 | 26.4244 | 0.0179 | 0.2135 | 12.5536 | 0.9549 | 1.0939 | 11.2804 | 24.3341 | 2.3897 | 9.7005 | 1.7826 | 1.4617 | 0.4645 | 0.0993 | 0.5225 | 5.2177 | 0.6289 | 99.1501 |
| RRQ | garnet | 17 | 26.8811 | 0.0635 | 0.2939 | 12.8110 | 0.7074 | 1.3793 | 11.9288 | 25.1825 | 2.6502 | 10.3519 | 1.5768 | 1.1292 | 0.4641 | 0.1791 | 0.3547 | 3.9678 | 0.1711 | 100.1024 |
| RRQ | garnet | 18 | 26.7560 | 0.0143 | 0.2141 | 12.9069 | 0.6337 | 1.7469 | 11.5952 | 24.6688 | 2.4727 | 10.2168 | 1.7009 | 1.3690 | 0.5601 | 0.1892 | 0.3678 | 4.2886 | 0.1435 | 99.8545 |
| RRQ | garnet | 19 | 26.8132 | 0.0201 | 0.2636 | 12.8174 | 0.6399 | 1.2918 | 11.8839 | 25.2351 | 2.6058 | 10.4974 | 1.5016 | 1.1615 | 0.3519 | 0.1096 | 0.3179 | 4.2884 | 0.1584 | 99.9675 |
| RRQ | garnet | 21 | 26.6423 | 0.0204 | 0.2205 | 12.6937 | 1.0975 | 1.0469 | 11.1611 | 24.1109 | 2.4936 | 9.7341 | 1.8244 | 1.4397 | 0.4484 | 0.0975 | 0.4749 | 5.2834 | 0.6252 | 99.4245 |
| RRQ | garnet | 22 | 26.5863 | 0.0147 | 0.2579 | 12.6078 | 0.6520 | 1.2391 | 11.9364 | 25.2929 | 2.5863 | 10.8222 | 1.5775 | 1.0752 | 0.3767 | 0.1277 | 0.3293 | 4.1424 | 0.1175 | 99.7519 |
| RRQ | garnet | 23 | 26.5570 | 0.0108 | 0.2410 | 12.7228 | 0.6766 | 1.9181 | 11.2075 | 24.4958 | 2.6725 | 10.2503 | 1.7490 | 1.4450 | 0.6129 | 0.1715 | 0.3546 | 4.4748 | 0.1576 | 99.7278 |
| RRQ | garnet | 26 | 26.6815 | 0.1561 | 0.4365 | 12.5727 | 0.8859 | 1.1458 | 11.3958 | 24.0023 | 2.5158 | 10.2019 | 1.6692 | 1.3115 | 0.4243 | 0.1020 | 0.4206 | 4.5053 | 0.3894 | 98.8266 |
| RRQ | garnet | 27 | 26.3844 | 0.0204 | 0.2374 | 12.6533 | 0.6910 | 1.9162 | 11.0767 | 24.1321 | 2.5688 | 10.3173 | 1.8038 | 1.3399 | 0.5886 | 0.1597 | 0.3650 | 4.5562 | 0.1487 | 98.9695 |
| RRQ | garnet | 28 | 26.4574 | 0.0042 | 0.2301 | 12.6596 | 0.8114 | 1.6666 | 11.2714 | 24.2979 | 2.5282 | 9.7515 | 1.7845 | 1.3943 | 0.5676 | 0.1586 | 0.4215 | 4.9038 | 0.3301 | 99.2487 |
| RRQ | garnet | 29 | 26.6424 | 0.0179 | 0.2363 | 12.7517 | 0.6626 | 1.4360 | 11.5900 | 24.8541 | 2.5354 | 10.5267 | 1.6275 | 1.1693 | 0.5075 | 0.0998 | 0.3881 | 4.3203 | 0.2219 | 99.5975 |
| RRQ | garnet | 31 | 26.5347 | 0.0331 | 0.2692 | 12.7543 | 0.8805 | 1.5656 | 11.0875 | 23.8971 | 2.3915 | 9.4844 | 1.8908 | 1.2967 | 0.5753 | 0.2096 | 0.4585 | 4.6666 | 0.6624 | 98.6678 |
| RRQ | garnet | 36 | 26.3949 | 0.3396 | 0.7898 | 12.2888 | 1.3157 | 1.5700 | 10.2477 | 22.1540 | 2.3983 | 9.1178 | 1.6846 | 1.3385 | 0.5448 | 0.2011 | 0.5051 | 4.3433 | 0.6506 | 95.8946 |
| RRQ | garnet | 37 | 27.2047 | 0.7147 | 1.2256 | 12.3140 | 1.9127 | 1.4253 | 9.9722 | 21.4015 | 2.2680 | 8.8002 | 1.6645 | 1.2758 | 0.5146 | 0.1345 | 0.4536 | 4.3225 | 0.6066 | 96.2210 |
| RRQ | garnet | 40 | 26.3974 | 0.0147 | 0.2111 | 12.7894 | 1.1218 | 1.8330 | 10.7998 | 22.7804 | 2.4460 | 9.4033 | 1.7907 | 1.4364 | 0.5953 | 0.1762 | 0.5434 | 4.8657 | 0.7463 | 97.9609 |
| RRQ | garnet | 41 | 26.3736 | 0.0002 | 0.1577 | 12.7541 | 0.8969 | 1.6395 | 11.3017 | 23.8044 | 2.4372 | 9.5546 | 1.6827 | 1.3749 | 0.5720 | 0.1402 | 0.4937 | 4.4982 | 0.6661 | 98.3577 |
| RRQ | garnet | 42 | 26.5224 | 0.0082 | 0.1669 | 12.8452 | 0.8501 | 1.5832 | 11.5264 | 24.0666 | 2.4989 | 9.4482 | 1.7049 | 1.3177 | 0.5448 | 0.1531 | 0.4372 | 4.2963 | 0.6304 | 98.6105 |
| RRQ | garnet | 43 | 26.4717 | 0.0002 | 0.1423 | 12.8553 | 0.8053 | 1.5858 | 11.5908 | 24.2413 | 2.4726 | 9.5168 | 1.7500 | 1.2116 | 0.5556 | 0.1284 | 0.4401 | 4.1126 | 0.4623 | 98.3527 |
| RRQ | garnet | 44 | 26.3748 | 0.0002 | 0.1454 | 12.7418 | 0.7868 | 1.5378 | 11.6700 | 24.5268 | 2.4518 | 9.4013 | 1.6351 | 1.4128 | 0.5484 | 0.1227 | 0.4225 | 4.1465 | 0.4612 | 98.3959 |
| RRQ | garnet | 45 | 26.6695 | 0.0002 | 0.1589 | 12.8875 | 0.8715 | 1.6961 | 11.2694 | 24.0337 | 2.5344 | 9.8261 | 1.8056 | 1.4020 | 0.5545 | 0.1284 | 0.4834 | 4.7596 | 0.5340 | 99.6248 |
| RRQ | garnet | 46 | 26.2902 | 0.0002 | 0.1739 | 12.6997 | 0.8359 | 1.6389 | 11.1130 | 23.8074 | 2.4776 | 9.7383 | 1.7778 | 1.3317 | 0.6046 | 0.1721 | 0.4959 | 4.3022 | 0.6374 | 98.1068 |
| RRQ | garnet | 47 | 26.4842 | 0.0034 | 0.1664 | 12.8197 | 0.8567 | 1.6648 | 10.9911 | 23.8393 | 2.4704 | 9.9059 | 1.7870 | 1.4371 | 0.5875 | 0.1508 | 0.4485 | 4.4407 | 0.6245 | 98.6880 |
| RRQ | garnet | 48 | 26.5221 | 0.0166 | 0.1760 | 12.8686 | 0.9016 | 1.7002 | 10.9680 | 23.7414 | 2.4206 | 9.5905 | 1.7997 | 1.3847 | 0.5409 | 0.1325 | 0.5310 | 4.5770 | 0.6689 | 98.5503 |
| RRQ | garnet | 49 | 26.2711 | 0.0160 | 0.2441 | 12.4636 | 2.1783 | 1.5458 | 10.5080 | 22.3816 | 2.3753 | 9.3138 | 1.6968 | 1.3982 | 0.5694 | 0.1597 | 0.5308 | 5.0093 | 0.6556 | 97.3274 |
| RRQ | garnet | 50 | 26.3813 | 0.0075 | 0.1642 | 12.6934 | 0.9068 | 1.6776 | 11.1440 | 23.6970 | 2.5349 | 9.6593 | 1.7726 | 1.4169 | 0.6272 | 0.2085 | 0.5359 | 4.7467 | 0.6933 | 98.8771 |
| RRQ | garnet | 51 | 26.3608 | 0.0055 | 0.1835 | 12.7155 | 0.8236 | 1.5576 | 11.2061 | 23.8947 | 2.5296 | 9.7459 | 1.7278 | 1.2818 | 0.6195 | 0.1343 | 0.4778 | 4.5366 | 0.5354 | 98.3460 |
| RRQ | garnet | 52 | 26.4052 | 0.0083 | 0.2114 | 12.7467 | 0.7101 | 1.7023 | 11.4730 | 24.1146 | 2.5814 | 9.7247 | 1.7219 | 1.2668 | 0.4878 | 0.1621 | 0.4425 | 4.3783 | 0.3067 | 98.4538 |
| RRQ | garnet | 53 | 26.2506 | 0.0068 | 0.1802 | 12.6104 | 0.7215 | 1.5788 | 11.5566 | 24.3395 | 2.5122 | 9.9280 | 1.5770 | 1.3138 | 0.5818 | 0.1955 | 0.4284 | 4.1409 | 0.3803 | 98.3123 |
| RRQ | garnet | 54 | 26.4942 | 0.0002 | 0.1439 | 12.8231 | 0.7712 | 1.5902 | 11.4456 | 24.1896 | 2.5528 | 9.7091 | 1.7907 | 1.4112 | 0.5103 | 0.1948 | 0.4697 | 4.2875 | 0.4466 | 98.8407 |
| RRQ | garnet | 55 | 26.3861 | 0.0139 | 0.1472 | 12.7912 | 0.7995 | 1.6165 | 11.1077 | 23.9191 | 2.4278 | 9.7971 | 1.7963 | 1.4154 | 0.6329 | 0.1595 | 0.4463 | 4.2978 | 0.4700 | 98.2343 |
| RRQ | garnet | 56 | 26.3673 | 0.0059 | 0.1710 | 12.7118 | 0.8288 | 1.6698 | 11.0587 | 23.8498 | 2.4962 | 10.0089 | 1.7983 | 1.3465 | 0.5698 | 0.1667 | 0.4915 | 4.4320 | 0.6331 | 98.6161 |
| RRQ | garnet | 57 | 26.2463 | 0.0067 | 0.1763 | 12.6442 | 0.8914 | 1.6298 | 10.8539 | 23.7152 | 2.5402 | 9.4990 | 1.9009 | 1.4378 | 0.5683 | 0.1826 | 0.5459 | 4.6086 | 0.7036 | 98.1607 |
| RRQ | garnet | 58 | 26.3157 | 0.0203 | 0.1836 | 12.6979 | 0.8935 | 1.6176 | 11.0544 | 23.6564 | 2.4249 | 9.7236 | 1.7764 | 1.3434 | 0.5865 | 0.1636 | 0.4849 | 4.4976 | 0.6354 | 98.0857 |
| RRQ | garnet | 59 | 26.3414 | 0.0006 | 0.2043 | 12.7178 | 0.8512 | 1.8436 | 10.6997 | 23.2621 | 2.5132 | 9.8989 | 1.8756 | 1.5012 | 0.5726 | 0.2253 | 0.5157 | 4.8842 | 0.5840 | 98.5014 |
| RRQ | garnet | 60 | 26.4533 | 0.0002 | 0.2357 | 12.6899 | 0.5708 | 1.4667 | 11.6445 | 24.8235 | 2.6913 | 10.1634 | 1.6320 | 1.2596 | 0.4557 | 0.1435 | 0.3522 | 4.1422 | 0.1299 | 98.8644 |
| RRQ | garnet | 62 | 26.4038 | 0.0191 | 0.2299 | 12.6005 | 0.5826 | 1.2271 | 12.0054 | 25.0833 | 2.5410 | 10.6033 | 1.6079 | 1.0572 | 0.3263 | 0.1281 | 0.3285 | 3.8083 | 0.1343 | 98.6966 |
| RRQ | garnet | 63 | 26.4048 | 0.0103 | 0.1944 | 12.5832 | 0.8024 | 1.1868 | 11.7873 | 24.5455 | 2.4038 | 10.2167 | 1.6257 | 1.2027 | 0.4046 | 0.1043 | 0.4580 | 4.6260 | 0.4718 | 99.0383 |
| RRQ | garnet | 64 | 26.2883 | 0.0002 | 0.2730 | 12.6250 | 0.7441 | 2.0852 | 10.4453 | 23.6797 | 2.5482 | 10.1157 | 1.8467 | 1.5112 | 0.6133 | 0.1064 | 0.4344 | 5.1322 | 0.1980 | 98.6569 |
| RRQ | garnet | 65 | 26.3085 | 0.0084 | 0.1786 | 12.6196 | 0.8680 | 1.5662 | 10.9996 | 24.1473 | 2.5613 | 9.6078 | 1.8496 | 1.4040 | 0.6122 | 0.1527 | 0.5088 | 4.7365 | 0.5156 | 98.6547 |
| RRQ | garnet | 66 | 26.4627 | 0.0046 | 0.1610 | 12.8059 | 0.8423 | 1.7142 | 11.0331 | 23.9965 | 2.5118 | 9.7727 | 1.7191 | 1.4675 | 0.6021 | 0.1320 | 0.5008 | 4.3971 | 0.6004 | 98.7338 |
| RRQ | garnet | 67 | 26.2078 | 0.0079 | 0.1688 | 12.5882 | 0.8657 | 1.6811 | 11.0975 | 23.8540 | 2.4277 | 9.8734 | 1.6771 | 1.4360 | 0.6212 | 0.1348 | 0.4973 | 4.5126 | 0.6632 | 98.3243 |
| RRQ | garnet | 68 | 26.4482 | 0.0085 | 0.2404 | 12.6130 | 0.5847 | 1.5838 | 11.5817 | 25.1870 | 2.5205 | 10.2808 | 1.6179 | 1.3634 | 0.4550 | 0.1911 | 0.3820 | 4.2230 | 0.1336 | 99.4246 |
| RRQ | garnet | 69 | 26.4390 | 0.0107 | 0.1991 | 12.6502 | 0.5021 | 1.3916 | 11.9149 | 25.3578 | 2.6772 | 10.8711 | 1.5386 | 1.1965 | 0.4236 | 0.1303 | 0.2668 | 3.3102 | 0.0990 | 98.9887 |
| RRQ | garnet | 70 | 26.2011 | 0.0075 | 0.2680 | 12.5590 | 0.7908 | 2.1477 | 10.3050 | 23.3687 | 2.5420 | 9.9658 | 1.9413 | 1.5334 | 0.6708 | 0.1748 | 0.4424 | 5.4238 | 0.2303 | 98.5824 |
| RRQ | garnet | 71 | 26.3023 | 0.0086 | 0.2281 | 12.5293 | 0.5851 | 1.4132 | 11.7208 | 24.8215 | 2.5968 | 10.5729 | 1.6736 | 1.1574 | 0.4474 | 0.1517 | 0.3683 | 4.0952 | 0.1399 | 98.8221 |
| RRQ | garnet | 72 | 26.4409 | 0.0079 | 0.2034 | 12.6445 | 0.7753 | 1.1775 | 11.3025 | 24.2569 | 2.5611 | 10.3060 | 1.8006 | 1.3729 | 0.4088 | 0.1768 | 0.4041 | 4.7394 | 0.2843 | 98.8729 |
| RRQ | garnet | 73 | 26.1911 | 0.0133 | 0.2626 | 12.5486 | 0.7108 | 1.9599 | 10.8271 | 23.8993 | 2.4815 | 10.1134 | 1.7447 | 1.3964 | 0.5729 | 0.1634 | 0.4398 | 4.8384 | 0.1592 | 98.3324 |
| RRQ | garnet | 74 | 26.1241 | 0.0314 | 0.1631 | 12.5219 | 0.8500 | 1.5726 | 11.1799 | 23.8249 | 2.5599 | 9.5921 | 1.8044 | 1.4761 | 0.5769 | 0.2230 | 0.5005 | 4.3654 | 0.6365 | 98.0127 |

| Sample | Phase | Label | W%(O) | W%(Al) | W%(Si) | W%(P) | W%(Ca) | W%(Y) | W%(La) | W%(Ce) | W%(Pr) | W%(Nd) | W%(Sm) | W%(Gd) | W%(Dy) | W%(Er) | W%(Pb) | W%(Th) | W%(U) | W%(SUM) |
|---|---|---|---|---|---|---|---|---|---|---|---|---|---|---|---|---|---|---|---|---|
| RRQ | garnet | 75 | 26.4022 | 0.0099 | 0.1451 | 12.7460 | 0.8322 | 1.5705 | 11.2929 | 24.0912 | 2.6109 | 9.7671 | 1.8180 | 1.2930 | 0.5638 | 0.1609 | 0.4485 | 4.2738 | 0.5297 | 98.5657 |
| RRQ | garnet | 76 | 26.1159 | 0.0046 | 0.2561 | 12.5268 | 0.7214 | 1.9083 | 10.9030 | 23.6399 | 2.5199 | 10.1052 | 1.7135 | 1.3037 | 0.5516 | 0.1968 | 0.4091 | 4.9026 | 0.1671 | 97.9555 |
| RRQ | garnet | 77 | 26.4429 | 0.0019 | 0.2169 | 12.6586 | 0.5442 | 1.2135 | 12.0795 | 25.1227 | 2.6629 | 10.5287 | 1.5802 | 1.1242 | 0.4126 | 0.0968 | 0.2568 | 3.6371 | 0.1107 | 98.7002 |
| RRQ | garnet | 78 | 26.4097 | 0.0241 | 0.2479 | 12.6625 | 0.6033 | 1.5279 | 11.5829 | 24.6983 | 2.5383 | 10.2558 | 1.6033 | 1.1543 | 0.4223 | 0.1266 | 0.3396 | 4.2420 | 0.1426 | 98.5914 |
| RRQ | garnet | 79 | 26.4152 | 0.0045 | 0.1731 | 12.7608 | 0.9143 | 1.5934 | 11.1157 | 23.6265 | 2.5036 | 9.5769 | 1.7950 | 1.4434 | 0.6188 | 0.1070 | 0.5391 | 4.6264 | 0.6709 | 98.4946 |
| RR2 | plagioclase | 1 | 26.0500 | 0.0496 | 0.3051 | 12.5033 | 1.2113 | 2.8498 | 10.1755 | 22.4224 | 2.5590 | 9.3145 | 1.7348 | 1.6896 | 0.8375 | 0.3212 | 0.4405 | 4.7025 | 0.4266 | 97.6032 |
| RR2 | plagioclase | 2 | 26.1242 | 0.0289 | 0.2895 | 12.7023 | 0.9359 | 2.9983 | 9.9868 | 22.2373 | 2.4437 | 9.2628 | 1.8178 | 1.6192 | 0.8656 | 0.2731 | 0.4671 | 5.0441 | 0.4780 | 97.5846 |
| RR2 | plagioclase | 3 | 25.9411 | 0.0021 | 0.2376 | 12.6140 | 0.9613 | 2.8929 | 9.9627 | 22.1599 | 2.5110 | 9.4423 | 1.7223 | 1.5625 | 0.9553 | 0.2238 | 0.4782 | 4.9835 | 0.5161 | 97.1766 |
| RR2 | plagioclase | 4 | 26.1566 | 0.0234 | 0.2109 | 12.6107 | 0.9926 | 1.7725 | 10.8501 | 22.8053 | 2.5586 | 9.2650 | 1.8081 | 1.3657 | 0.7044 | 0.1994 | 0.5348 | 5.1161 | 0.5946 | 97.5788 |
| RR2 | plagioclase | 5 | 26.0781 | 0.0002 | 0.2034 | 12.6651 | 0.9085 | 2.2707 | 10.6574 | 22.6146 | 2.6146 | 9.4699 | 1.7340 | 1.4869 | 0.7164 | 0.2442 | 0.4932 | 4.6426 | 0.5200 | 97.3298 |
| RR2 | plagioclase | 6 | 26.8610 | 0.0103 | 0.2730 | 12.8930 | 2.7600 | 2.7009 | 9.8436 | 21.7457 | 2.4529 | 9.3008 | 1.6952 | 1.6708 | 0.9152 | 0.1952 | 0.4438 | 4.5283 | 0.3841 | 98.6838 |
| RR2 | plagioclase | 7 | 25.9056 | 0.0048 | 0.2339 | 12.5739 | 0.9688 | 2.9165 | 10.1924 | 21.8637 | 2.5691 | 9.5339 | 1.8334 | 1.5809 | 0.9195 | 0.3400 | 0.4562 | 4.7175 | 0.5713 | 97.1914 |
| RR2 | plagioclase | 8 | 26.0586 | 0.0002 | 0.2549 | 12.5831 | 0.5850 | 2.2072 | 10.9938 | 23.5937 | 2.6691 | 10.2693 | 1.6358 | 1.3764 | 0.6366 | 0.2145 | 0.3270 | 3.8919 | 0.1747 | 97.4818 |
| RR2 | plagioclase | 9 | 25.9566 | 0.0002 | 0.2783 | 12.5250 | 0.6338 | 2.5130 | 10.4665 | 23.2105 | 2.7814 | 10.1096 | 1.7047 | 1.5102 | 0.7962 | 0.2110 | 0.3704 | 4.1528 | 0.1543 | 97.3845 |
| RR2 | plagioclase | 10 | 26.2545 | 0.0013 | 0.2266 | 12.7985 | 0.9019 | 2.5915 | 10.2065 | 22.6328 | 2.6737 | 9.4329 | 1.7805 | 1.5362 | 0.8596 | 0.2546 | 0.5038 | 4.7512 | 0.4956 | 97.9117 |
| RR2 | plagioclase | 11 | 25.8655 | 0.0120 | 0.2956 | 12.5746 | 0.9150 | 3.1606 | 9.9082 | 21.6825 | 2.4140 | 9.1541 | 1.7330 | 1.6982 | 1.1119 | 0.2286 | 0.4816 | 5.1302 | 0.5746 | 96.9502 |
| RR2 | plagioclase | 12 | 25.7893 | 0.0083 | 0.2815 | 12.5181 | 0.9130 | 3.1559 | 9.8604 | 21.9164 | 2.4612 | 9.1453 | 1.7267 | 1.7854 | 1.0676 | 0.2016 | 0.5172 | 4.9395 | 0.5747 | 96.8721 |
| RR2 | plagioclase | 13 | 26.0805 | 0.0022 | 0.2613 | 12.6098 | 0.7128 | 2.4443 | 10.5700 | 23.2060 | 2.6881 | 9.9365 | 1.6871 | 1.4841 | 0.7548 | 0.2267 | 0.4155 | 4.3289 | 0.2353 | 97.6539 |
| RR2 | plagioclase | 14 | 26.2701 | 0.0144 | 0.2061 | 12.8093 | 0.8802 | 2.7939 | 10.4315 | 22.7453 | 2.5609 | 9.5216 | 1.7251 | 1.5438 | 0.8737 | 0.2758 | 0.4355 | 4.6162 | 0.4580 | 98.1714 |
| RR2 | plagioclase | 15 | 25.7597 | 0.0123 | 0.2408 | 12.5455 | 0.9038 | 3.3910 | 9.5796 | 21.9067 | 2.5769 | 9.5198 | 1.8753 | 1.6967 | 0.9849 | 0.3376 | 0.4704 | 4.6730 | 0.3712 | 96.8552 |
| RR2 | plagioclase | 16 | 26.1788 | 0.0025 | 0.2490 | 12.8121 | 0.9253 | 3.1254 | 9.8849 | 22.0552 | 2.5734 | 9.3164 | 1.6473 | 1.7456 | 0.9020 | 0.3531 | 0.4636 | 5.0464 | 0.4450 | 97.7360 |
| RR2 | plagioclase | 17 | 26.1785 | 0.0320 | 0.3227 | 12.6763 | 0.9700 | 3.0350 | 10.1989 | 22.4506 | 2.4917 | 9.2381 | 1.7988 | 1.6213 | 0.8727 | 0.2732 | 0.4291 | 4.8053 | 0.4337 | 97.8379 |
| RR2 | plagioclase | 18 | 26.7293 | 0.0002 | 0.2093 | 12.9956 | 1.1616 | 2.1941 | 10.4710 | 22.3526 | 2.5748 | 9.3868 | 1.7477 | 1.5347 | 0.7872 | 0.2517 | 0.6655 | 5.6257 | 0.8508 | 99.5486 |
| RR2 | plagioclase | 19 | 26.5314 | 0.0002 | 0.2409 | 13.0430 | 0.9334 | 2.8798 | 10.2668 | 22.2161 | 2.4048 | 9.3780 | 1.7276 | 1.6124 | 0.8918 | 0.2700 | 0.4449 | 5.0707 | 0.4923 | 98.4141 |
| RR2 | plagioclase | 20 | 26.3001 | 0.0048 | 0.2975 | 12.8105 | 0.9215 | 3.2600 | 10.0569 | 22.1514 | 2.5248 | 9.2499 | 1.7507 | 1.7675 | 1.0296 | 0.2807 | 0.5482 | 4.8929 | 0.6453 | 98.5023 |
| RR2 | plagioclase | 21 | 26.2203 | 0.0051 | 0.2595 | 12.7612 | 0.9337 | 3.1027 | 10.2526 | 22.1751 | 2.5865 | 9.3944 | 1.7194 | 1.7024 | 0.9328 | 0.3348 | 0.4844 | 4.9497 | 0.4092 | 98.2338 |
| RR2 | plagioclase | 22 | 26.1776 | 0.0002 | 0.2586 | 12.7361 | 0.9030 | 3.0233 | 10.3181 | 22.5743 | 2.5590 | 9.2225 | 1.7628 | 1.5822 | 0.8848 | 0.1750 | 0.4511 | 4.8889 | 0.5085 | 98.0360 |
| RR2 | plagioclase | 23 | 26.4358 | 0.0018 | 0.1821 | 12.7855 | 1.0060 | 1.7826 | 11.3554 | 23.3715 | 2.6585 | 9.1277 | 1.5547 | 1.3228 | 0.6581 | 0.1551 | 0.5380 | 4.8919 | 0.6876 | 98.5251 |
| RR2 | plagioclase | 24 | 26.6601 | 0.0091 | 0.1870 | 12.8874 | 1.0652 | 1.6714 | 11.0782 | 23.1308 | 2.6353 | 9.4707 | 1.7283 | 1.3776 | 0.6453 | 0.2251 | 0.5662 | 5.2136 | 0.7051 | 99.2664 |
| RR2 | plagioclase | 25 | 26.3689 | 0.0020 | 0.2095 | 12.9172 | 0.9930 | 2.9386 | 10.2644 | 22.4675 | 2.6671 | 9.2985 | 1.6406 | 1.5720 | 0.8952 | 0.3280 | 0.4522 | 4.8018 | 0.3726 | 98.1991 |
| RR2 | plagioclase | 26 | 26.3774 | 0.0184 | 0.2315 | 12.8511 | 0.9386 | 2.9142 | 10.3845 | 22.6691 | 2.6261 | 9.3455 | 1.8178 | 1.5456 | 0.8894 | 0.3050 | 0.4250 | 4.7743 | 0.4151 | 98.5386 |
| RR2 | plagioclase | 27 | 26.2715 | 0.0211 | 0.3878 | 12.4564 | 1.6654 | 1.4174 | 9.7509 | 20.4959 | 2.3458 | 8.3555 | 1.6667 | 1.2890 | 0.6012 | 0.1883 | 0.8730 | 9.8474 | 0.5322 | 98.1755 |
| RR2 | plagioclase | 28 | 26.5682 | 0.0131 | 0.2018 | 12.7241 | 1.0665 | 1.4697 | 11.3702 | 23.7217 | 2.6023 | 9.3001 | 1.7190 | 1.3036 | 0.6240 | 0.1536 | 0.5679 | 5.3258 | 0.6366 | 99.3782 |
| RR2 | plagioclase | 29 | 26.1329 | 0.0229 | 0.2311 | 12.4831 | 1.3223 | 1.7095 | 10.4760 | 22.6901 | 2.6586 | 9.2913 | 1.7963 | 1.3695 | 0.7386 | 0.1578 | 0.6114 | 5.3041 | 0.7450 | 97.7505 |
| RR2 | plagioclase | 30 | 26.2114 | 0.0026 | 0.2165 | 12.7957 | 0.9028 | 2.8369 | 10.3138 | 22.5535 | 2.5649 | 9.3614 | 1.7459 | 1.6473 | 0.8307 | 0.1861 | 0.4731 | 4.7666 | 0.4877 | 97.9069 |
| RR2 | plagioclase | 31 | 26.3558 | 0.0002 | 0.1847 | 12.7361 | 1.1175 | 1.8129 | 10.4565 | 22.8721 | 2.6285 | 9.4758 | 1.7315 | 1.4117 | 0.6661 | 0.1610 | 0.5617 | 5.3998 | 0.7623 | 98.3442 |
| RR2 | plagioclase | 32 | 26.3652 | 0.0117 | 0.2045 | 12.7534 | 1.1296 | 1.7363 | 10.2477 | 22.6120 | 2.5122 | 9.4271 | 1.8385 | 1.5025 | 0.7047 | 0.1439 | 0.6056 | 5.5057 | 0.8062 | 98.1168 |
| RR2 | plagioclase | 33 | 26.0650 | 0.0049 | 0.2877 | 12.7104 | 0.9336 | 3.1854 | 9.8044 | 21.6949 | 2.5368 | 9.0649 | 1.7731 | 1.8969 | 0.9571 | 0.2231 | 0.5032 | 5.3249 | 0.5749 | 97.5512 |
| RR2 | plagioclase | 34 | 26.0378 | 0.0096 | 0.3171 | 12.6308 | 1.0035 | 3.2186 | 9.6639 | 21.6325 | 2.4574 | 9.0927 | 1.6023 | 1.8427 | 0.9343 | 0.2047 | 0.5818 | 6.0119 | 0.5351 | 97.7867 |
| RR2 | K-feldspar | 35 | 26.0514 | 0.0043 | 0.2238 | 12.7368 | 0.8948 | 2.8228 | 10.0223 | 22.2616 | 2.5656 | 9.4244 | 1.7087 | 1.5115 | 0.8470 | 0.2818 | 0.4964 | 4.6643 | 0.6509 | 97.1784 |
| RR2 | K-feldspar | 36 | 26.1322 | 0.0086 | 0.1794 | 12.7646 | 0.8901 | 2.4323 | 10.4313 | 22.6558 | 2.6494 | 9.4414 | 1.7949 | 1.5219 | 0.7749 | 0.2551 | 0.5057 | 4.1644 | 0.6928 | 97.3048 |
| RR2 | K-feldspar | 37 | 25.8254 | 0.0044 | 0.2506 | 12.6301 | 0.8802 | 3.1314 | 9.8080 | 21.9915 | 2.3417 | 9.2344 | 1.8027 | 1.6412 | 0.9408 | 0.2666 | 0.4597 | 4.7131 | 0.5741 | 96.5059 |
| RR2 | K-feldspar | 38 | 26.0338 | 0.0002 | 0.3927 | 12.6812 | 0.8878 | 3.0178 | 9.7788 | 21.4906 | 2.5659 | 9.3124 | 1.8220 | 1.7006 | 0.9461 | 0.2229 | 0.5149 | 4.7514 | 0.6090 | 96.7381 |
| RR2 | K-feldspar | 39 | 26.3738 | 0.2104 | 0.9125 | 12.3179 | 0.7173 | 2.5860 | 10.1765 | 22.2712 | 2.5427 | 9.0947 | 1.7952 | 1.6097 | 0.8573 | 0.1994 | 0.4073 | 4.7103 | 0.4938 | 97.2860 |
| RR2 | K-feldspar | 40 | 26.2037 | 0.0002 | 0.1743 | 12.7916 | 0.9370 | 2.4659 | 10.2990 | 22.9210 | 2.6749 | 9.4045 | 1.7085 | 1.5742 | 0.8890 | 0.2547 | 0.5068 | 4.1055 | 0.7484 | 97.6692 |
| RR2 | K-feldspar | 41 | 25.9686 | 0.0002 | 0.2531 | 12.7106 | 0.8737 | 2.9891 | 9.6672 | 22.0760 | 2.5637 | 9.1245 | 1.8338 | 1.6919 | 0.9547 | 0.2734 | 0.4703 | 4.8201 | 0.5872 | 96.8681 |
| RR2 | K-feldspar | 42 | 26.0915 | 0.0002 | 0.2431 | 12.7522 | 0.8546 | 2.8416 | 10.0425 | 22.5957 | 2.6359 | 9.1704 | 1.6435 | 1.5968 | 0.8615 | 0.2256 | 0.4608 | 4.7380 | 0.5278 | 97.2917 |
| RR2 | K-feldspar | 43 | 26.0476 | 0.0002 | 0.1681 | 12.6771 | 0.8947 | 2.2910 | 10.4152 | 23.0733 | 2.5741 | 9.4873 | 1.7719 | 1.4412 | 0.7747 | 0.1572 | 0.5409 | 4.1178 | 0.8210 | 97.2633 |
| RR2 | K-feldspar | 44 | 26.2884 | 0.0002 | 0.1645 | 12.8235 | 0.8859 | 2.2978 | 10.4299 | 23.0634 | 2.6552 | 9.7819 | 1.8217 | 1.5347 | 0.7544 | 0.2587 | 0.4533 | 3.9820 | 0.7262 | 97.9317 |
| RR2 | K-feldspar | 46 | 26.1651 | 0.0002 | 0.2438 | 12.8495 | 0.8783 | 3.0372 | 9.8197 | 21.9532 | 2.5688 | 9.3110 | 1.7097 | 1.6617 | 0.9581 | 0.2607 | 0.4683 | 4.9237 | 0.5897 | 97.4087 |
| RR2 | K-feldspar | 47 | 26.0574 | 0.0172 | 0.2189 | 12.6951 | 0.8977 | 2.6136 | 9.9645 | 22.8122 | 2.6975 | 9.0176 | 1.6757 | 1.6794 | 0.8175 | 0.2118 | 0.4892 | 4.7897 | 0.5848 | 97.2498 |
| RR2 | K-feldspar | 48 | 25.9338 | 0.0078 | 0.2157 | 12.6126 | 0.8813 | 2.8545 | 9.9827 | 22.4819 | 2.6877 | 9.3413 | 1.8632 | 1.5789 | 0.8373 | 0.2489 | 0.4812 | 4.6664 | 0.5661 | 97.2513 |
| RR2 | K-feldspar | 49 | 25.7982 | 0.0021 | 0.1947 | 12.5039 | 0.8351 | 2.5997 | 10.1240 | 23.1772 | 2.5974 | 9.3717 | 1.7611 | 1.5849 | 0.7936 | 0.2014 | 0.4597 | 4.3391 | 0.5248 | 96.8786 |
| RR2 | K-feldspar | 50 | 26.1886 | 0.0103 | 0.2597 | 12.7679 | 0.9484 | 2.9896 | 9.7834 | 22.2006 | 2.5496 | 9.2076 | 1.7955 | 1.6095 | 0.8943 | 0.2240 | 0.5552 | 5.3588 | 0.5924 | 97.9454 |
| RR2 | K-feldspar | 51 | 26.1644 | 0.0002 | 0.2429 | 12.7597 | 0.9373 | 2.9853 | 9.7400 | 22.6050 | 2.5558 | 9.0628 | 1.7096 | 1.5344 | 0.8672 | 0.3117 | 0.5354 | 5.3424 | 0.5967 | 97.9608 |
| RR2 | K-feldspar | 52 | 26.0321 | 0.0080 | 0.2671 | 12.6653 | 0.9476 | 3.0351 | 9.6756 | 22.2391 | 2.6334 | 9.0037 | 1.7368 | 1.6228 | 0.9887 | 0.3082 | 0.5404 | 5.2088 | 0.6287 | 97.5514 |

| Sample | Phase | Label | W%(O) | W%(Al) | W%(Si) | W%(P) | W%(Ca) | W%(Y) | W%(La) | W%(Ce) | W%(Pr) | W%(Nd) | W%(Sm) | W%(Gd) | W%(Dy) | W%(Er) | W%(Pb) | W%(Th) | W%(U) | W%(SUM) |
|---|---|---|---|---|---|---|---|---|---|---|---|---|---|---|---|---|---|---|---|---|
| RR2 | K-feldspar | 53 | 26.0999 | 0.0002 | 0.2579 | 12.7591 | 0.9129 | 2.9572 | 9.5413 | 22.3826 | 2.5472 | 9.1743 | 1.8147 | 1.7069 | 0.8738 | 0.2491 | 0.5062 | 4.9979 | 0.5894 | 97.3806 |
| RR2 | K-feldspar | 54 | 26.0972 | 0.0002 | 0.2288 | 12.7319 | 0.9077 | 3.0214 | 9.7233 | 22.5471 | 2.5362 | 9.1475 | 1.7561 | 1.6386 | 0.9573 | 0.2602 | 0.4764 | 5.1752 | 0.5748 | 97.7899 |
| RR2 | K-feldspar | 55 | 26.1693 | 0.0131 | 0.2424 | 12.7525 | 0.8892 | 3.0298 | 9.5841 | 22.7535 | 2.6030 | 9.2748 | 1.6693 | 1.5961 | 0.9650 | 0.3080 | 0.5200 | 5.0873 | 0.5988 | 98.0662 |
| RR2 | K-feldspar | 56 | 26.0828 | 0.0018 | 0.2353 | 12.7180 | 0.9140 | 3.0423 | 9.6073 | 22.6154 | 2.5469 | 9.1736 | 1.6960 | 1.6957 | 0.9057 | 0.2877 | 0.4842 | 5.1553 | 0.5830 | 97.7550 |
| RR2 | K-feldspar | 57 | 26.2492 | 0.0046 | 0.2311 | 12.8195 | 0.9071 | 3.0280 | 9.7164 | 22.8413 | 2.6270 | 9.2921 | 1.6652 | 1.7267 | 0.8396 | 0.2797 | 0.5102 | 4.9539 | 0.4814 | 98.1830 |
| RR2 | K-feldspar | 58 | 26.1971 | 0.0002 | 0.2217 | 12.7792 | 0.8794 | 2.9391 | 9.6728 | 23.0059 | 2.6143 | 9.3496 | 1.8116 | 1.5884 | 0.9173 | 0.2647 | 0.4989 | 4.8527 | 0.4872 | 98.0901 |
| RR2 | K-feldspar | 59 | 25.9789 | 0.0002 | 0.2245 | 12.6600 | 0.8609 | 2.9923 | 9.6430 | 22.8401 | 2.4913 | 9.2745 | 1.7877 | 1.6335 | 0.9385 | 0.3266 | 0.4803 | 4.8286 | 0.4621 | 97.4330 |
| RR2 | K-feldspar | 60 | 26.3045 | 0.0018 | 0.2295 | 12.9051 | 0.8949 | 2.8594 | 9.7427 | 22.8824 | 2.5289 | 9.2015 | 1.7255 | 1.6041 | 0.8701 | 0.2028 | 0.4502 | 4.9033 | 0.4916 | 97.8083 |
| RR2 | K-feldspar | 62 | 26.0775 | 0.0423 | 0.3010 | 12.6937 | 0.8342 | 2.9880 | 9.5941 | 22.8023 | 2.5293 | 9.2738 | 1.6954 | 1.6184 | 0.8689 | 0.2406 | 0.4419 | 4.8122 | 0.4219 | 97.2455 |
| RR2 | K-feldspar | 63 | 26.2681 | 0.0057 | 0.2021 | 12.6569 | 1.0413 | 1.4974 | 10.6606 | 23.4432 | 2.6543 | 9.2225 | 1.6423 | 1.2938 | 0.5977 | 0.1351 | 0.5664 | 5.3428 | 0.6026 | 97.8428 |
| RR2 | K-feldspar | 64 | 25.9635 | 0.0002 | 0.2046 | 12.4937 | 0.9976 | 1.4779 | 10.6742 | 23.3284 | 2.5348 | 9.1554 | 1.6081 | 1.3146 | 0.6151 | 0.1840 | 0.4836 | 5.1439 | 0.6097 | 96.7993 |
| RR2 | K-feldspar | 65 | 25.8393 | 0.0055 | 0.2194 | 12.5436 | 0.9136 | 2.5358 | 9.9435 | 22.6283 | 2.6614 | 9.1479 | 1.7061 | 1.5451 | 0.8581 | 0.2421 | 0.4900 | 4.9342 | 0.4796 | 96.7035 |
| RR2 | K-feldspar | 66 | 26.1938 | 0.0061 | 0.2367 | 12.7983 | 0.8820 | 2.8513 | 9.6990 | 22.9863 | 2.5823 | 9.1372 | 1.7231 | 1.6489 | 0.9195 | 0.1991 | 0.4771 | 4.8941 | 0.4742 | 97.7190 |
| RR2 | K-feldspar | 67 | 25.8676 | 0.0051 | 0.2214 | 12.6018 | 0.8512 | 2.8057 | 9.7448 | 22.9768 | 2.4720 | 9.2191 | 1.6893 | 1.6487 | 0.9107 | 0.2161 | 0.4899 | 4.6493 | 0.4301 | 96.8096 |
| RR2 | K-feldspar | 68 | 25.9151 | 0.0002 | 0.2243 | 12.6011 | 0.8704 | 2.7658 | 9.7590 | 22.9125 | 2.5624 | 9.2569 | 1.8135 | 1.5854 | 0.8582 | 0.2439 | 0.4797 | 4.7822 | 0.4657 | 97.1063 |
| RR2 | K-feldspar | 69 | 25.9773 | 0.0147 | 0.1981 | 12.3991 | 1.2174 | 1.4511 | 10.6523 | 23.2212 | 2.5070 | 9.0338 | 1.7058 | 1.2914 | 0.6342 | 0.1433 | 0.5522 | 5.7007 | 0.6013 | 97.3109 |
| RR2 | K-feldspar | 70 | 25.8927 | 0.0002 | 0.2277 | 12.5909 | 0.8370 | 2.8971 | 9.6944 | 22.6639 | 2.7355 | 9.1970 | 1.8170 | 1.6475 | 0.9228 | 0.2663 | 0.4618 | 4.8212 | 0.5221 | 97.2051 |
| RR2 | K-feldspar | 71 | 26.1388 | 0.0030 | 0.2420 | 12.7331 | 0.8617 | 3.0247 | 9.5590 | 23.0025 | 2.5745 | 9.2372 | 1.7930 | 1.6536 | 0.9762 | 0.3489 | 0.5128 | 4.8508 | 0.4863 | 98.0081 |
| RR2 | K-feldspar | 72 | 26.3035 | 0.0069 | 0.1769 | 12.6773 | 1.0250 | 1.5202 | 10.5466 | 23.7885 | 2.5361 | 9.4805 | 1.7381 | 1.3096 | 0.5871 | 0.1744 | 0.5494 | 4.8347 | 0.8302 | 98.0950 |
| RR2 | K-feldspar | 73 | 25.8115 | 0.0002 | 0.2303 | 12.4724 | 0.9105 | 2.5211 | 9.8854 | 22.9461 | 2.6263 | 9.2729 | 1.8343 | 1.5045 | 0.7390 | 0.2422 | 0.4820 | 4.8324 | 0.6016 | 96.9227 |
| RR2 | K-feldspar | 74 | 25.9330 | 0.0025 | 0.2418 | 12.5859 | 0.8910 | 2.7132 | 9.9580 | 23.0805 | 2.5379 | 9.1826 | 1.7176 | 1.4887 | 0.7751 | 0.2441 | 0.4441 | 4.7786 | 0.5124 | 97.0970 |
| RR2 | K-feldspar | 75 | 25.9158 | 0.0019 | 0.2519 | 12.6122 | 0.8341 | 3.0503 | 9.5150 | 22.7472 | 2.6100 | 9.2156 | 1.7389 | 1.7028 | 0.9372 | 0.2912 | 0.4658 | 4.8531 | 0.4945 | 97.2475 |
| RR2 | K-feldspar | 76 | 25.8915 | 0.0164 | 0.1936 | 12.3965 | 0.9037 | 1.6158 | 10.6051 | 24.1281 | 2.4530 | 9.3646 | 1.7292 | 1.3136 | 0.5970 | 0.1163 | 0.4810 | 4.7252 | 0.5683 | 97.1089 |
| RR2 | K-feldspar | 77 | 26.0493 | 0.0136 | 0.1994 | 12.5325 | 0.9184 | 2.0817 | 10.2565 | 23.5983 | 2.7363 | 9.4576 | 1.7023 | 1.4513 | 0.7331 | 0.2202 | 0.5392 | 4.6970 | 0.6214 | 97.8181 |
| RR2 | K-feldspar | 79 | 25.5825 | 0.0005 | 0.2427 | 12.3696 | 0.8801 | 2.7723 | 9.7470 | 22.7179 | 2.4600 | 9.1185 | 1.7256 | 1.6579 | 0.9082 | 0.2103 | 0.4739 | 4.8447 | 0.5354 | 96.2571 |
| RR2 | K-feldspar | 80 | 25.6064 | 0.0002 | 0.2395 | 12.3123 | 0.8919 | 2.6911 | 9.8705 | 23.0924 | 2.5857 | 9.0914 | 1.7356 | 1.6458 | 0.8940 | 0.2139 | 0.4421 | 4.9096 | 0.4596 | 96.6920 |
| RR2 | K-feldspar | 81 | 25.6517 | 0.0002 | 0.2230 | 12.4178 | 0.8862 | 2.8992 | 9.6218 | 22.7885 | 2.5500 | 9.3068 | 1.6217 | 1.6447 | 0.8919 | 0.2256 | 0.4543 | 4.9487 | 0.5062 | 96.6483 |
| ALM | sillimanite | 6 | 26.0487 | 0.0304 | 0.3907 | 12.2124 | 0.9957 | 1.0018 | 9.7234 | 23.2701 | 2.5374 | 10.0437 | 1.9507 | 1.4020 | 0.4165 | 0.0843 | 0.6241 | 6.4648 | 0.7507 | 97.9574 |
| ALM | sillimanite | 7 | 26.0165 | 0.0242 | 0.4111 | 12.2167 | 1.0093 | 0.8972 | 9.6245 | 23.3046 | 2.5740 | 9.6787 | 1.9031 | 1.4008 | 0.4039 | 0.0771 | 0.6582 | 6.6490 | 0.6573 | 97.5162 |
| ALM | sillimanite | 8 | 26.0608 | 0.0317 | 0.4320 | 12.1541 | 1.0242 | 0.7692 | 9.3231 | 23.2297 | 2.5824 | 10.1662 | 2.0253 | 1.3170 | 0.3804 | 0.0449 | 0.6584 | 7.2942 | 0.5343 | 98.0379 |
| ALM | sillimanite | 9 | 26.1255 | 0.0300 | 0.4321 | 12.2317 | 0.9141 | 1.1987 | 9.4231 | 23.2792 | 2.8348 | 10.1979 | 1.9486 | 1.5011 | 0.4841 | 0.1196 | 0.6658 | 6.5181 | 0.5372 | 98.4516 |
| ALM | sillimanite | 10 | 26.1434 | 0.0473 | 0.4678 | 12.1369 | 1.0899 | 0.5603 | 9.2925 | 23.3247 | 2.5792 | 10.1661 | 1.9767 | 1.1900 | 0.3216 | 0.0863 | 0.6502 | 7.5688 | 0.5798 | 98.1915 |
| ALM | sillimanite | 11 | 25.8274 | 0.0311 | 0.4546 | 11.9756 | 1.0876 | 0.6386 | 9.1650 | 22.9482 | 2.5831 | 10.1448 | 1.9428 | 1.2968 | 0.2965 | 0.0017 | 0.6731 | 7.6976 | 0.5614 | 97.3359 |
| ALM | sillimanite | 12 | 26.0451 | 0.0110 | 0.3180 | 12.2337 | 1.1589 | 0.8063 | 9.7523 | 23.2555 | 2.6070 | 9.6902 | 1.9927 | 1.4554 | 0.3947 | 0.0912 | 0.7263 | 6.3934 | 1.0318 | 97.9735 |
| ALM | sillimanite | 13 | 26.0506 | 0.0298 | 0.4480 | 12.1022 | 1.1110 | 0.5881 | 9.1755 | 22.9435 | 2.7303 | 10.2968 | 2.0569 | 1.3083 | 0.2807 | 0.0744 | 0.6937 | 7.5612 | 0.5377 | 97.9987 |
| ALM | sillimanite | 16 | 26.1506 | 0.1149 | 0.5631 | 12.1720 | 0.8753 | 1.1651 | 9.3374 | 23.4469 | 2.5450 | 10.3402 | 2.0026 | 1.3778 | 0.5026 | 0.1611 | 0.5655 | 5.8766 | 0.5546 | 97.7613 |
| ALM | sillimanite | 17 | 26.1036 | 0.0189 | 0.5313 | 12.1318 | 0.9621 | 1.1658 | 8.9614 | 22.9170 | 2.5696 | 10.4382 | 1.9453 | 1.5547 | 0.4528 | 0.1091 | 0.6816 | 7.3882 | 0.6045 | 98.5459 |
| ALM | sillimanite | 18 | 26.2371 | 0.0235 | 0.4241 | 12.2856 | 1.0678 | 0.7843 | 9.4758 | 23.3328 | 2.6329 | 10.1138 | 1.9065 | 1.3643 | 0.2966 | 0.0365 | 0.6570 | 7.1371 | 0.5977 | 98.3834 |
| ALM | sillimanite | 21 | 26.2480 | 0.0234 | 0.4740 | 12.1960 | 1.0992 | 0.5953 | 9.2680 | 23.2858 | 2.7368 | 10.2233 | 1.9739 | 1.2785 | 0.2393 | 0.1115 | 0.6513 | 7.6168 | 0.5953 | 98.6264 |
| ALM | sillimanite | 22 | 26.1664 | 0.0288 | 0.3568 | 12.3142 | 0.9844 | 1.0379 | 9.8468 | 23.9362 | 2.6062 | 9.6916 | 1.8347 | 1.3682 | 0.4651 | 0.1179 | 0.6600 | 6.0947 | 0.7675 | 98.2874 |
| ALM | sillimanite | 23 | 26.3214 | 0.0429 | 0.4470 | 12.3425 | 1.0230 | 0.7548 | 9.6752 | 23.5048 | 2.6325 | 9.8915 | 1.8444 | 1.3174 | 0.3783 | 0.0486 | 0.6182 | 6.8176 | 0.6628 | 98.3329 |
| ALM | sillimanite | 25 | 26.3656 | 0.0228 | 0.4532 | 12.2680 | 1.0778 | 0.6000 | 9.3177 | 23.4041 | 2.7865 | 10.4187 | 1.9916 | 1.2349 | 0.3114 | 0.0729 | 0.6843 | 7.5203 | 0.5724 | 99.1122 |
| ALM | sillimanite | 26 | 26.5075 | 0.0134 | 0.3937 | 12.4984 | 1.0388 | 0.9579 | 9.7382 | 23.8347 | 2.5389 | 9.9297 | 1.8928 | 1.3213 | 0.4537 | 0.0987 | 0.7271 | 6.5087 | 0.7761 | 99.2396 |
| ALM | sillimanite | 27 | 26.2413 | 0.0281 | 0.6114 | 12.0891 | 1.0897 | 0.8257 | 9.0456 | 22.5092 | 2.6154 | 10.2920 | 1.8956 | 1.3573 | 0.3329 | 0.0714 | 0.7650 | 8.7401 | 0.4748 | 98.9946 |
| ALM | sillimanite | 28 | 26.0632 | 0.0282 | 0.7249 | 11.8631 | 1.1563 | 0.8849 | 8.5776 | 21.9423 | 2.5135 | 9.9726 | 1.8911 | 1.3708 | 0.3726 | 0.0521 | 0.8118 | 10.1010 | 0.5521 | 98.8881 |
| ALM | sillimanite | 29 | 26.1052 | 0.0253 | 0.6255 | 12.0402 | 1.0333 | 1.1007 | 8.6801 | 22.5441 | 2.5614 | 10.1575 | 1.9636 | 1.4081 | 0.4667 | 0.0888 | 0.7596 | 8.5326 | 0.5699 | 98.6726 |
| ALM | sillimanite | 30 | 26.4494 | 0.0267 | 0.4271 | 12.3561 | 1.0914 | 0.5860 | 9.5141 | 23.3997 | 2.6663 | 10.2944 | 1.8588 | 1.2957 | 0.2990 | 0.1126 | 0.7222 | 7.5487 | 0.5741 | 99.2323 |
| ALM | sillimanite | 31 | 26.5609 | 0.0184 | 0.3849 | 12.5285 | 1.0375 | 0.7580 | 9.7060 | 23.7311 | 2.6800 | 10.1334 | 2.0013 | 1.3079 | 0.3758 | 0.0926 | 0.6931 | 6.4811 | 0.6993 | 99.1998 |
| ALM | sillimanite | 32 | 26.4141 | 0.0299 | 0.5226 | 12.3135 | 0.9849 | 0.9947 | 9.1436 | 23.0580 | 2.6176 | 10.4109 | 1.9809 | 1.4585 | 0.5383 | 0.0568 | 0.7136 | 7.3929 | 0.6669 | 99.3077 |
| ALM | sillimanite | 33 | 26.3762 | 0.0364 | 0.3956 | 12.3809 | 1.1113 | 0.5775 | 9.6421 | 23.4285 | 2.5161 | 10.2002 | 1.9285 | 1.2753 | 0.2509 | 0.0001 | 0.6866 | 7.0623 | 0.6735 | 98.5520 |
| ALM | sillimanite | 34 | 26.4643 | 0.0258 | 0.3719 | 12.4688 | 1.0293 | 0.6444 | 9.8288 | 23.8415 | 2.6511 | 9.9991 | 2.0116 | 1.3155 | 0.3119 | 0.0597 | 0.6335 | 6.4451 | 0.6994 | 98.8117 |
| ALM | sillimanite | 35 | 26.5427 | 0.0174 | 0.3731 | 12.5124 | 0.9819 | 0.7502 | 9.8882 | 24.0330 | 2.6772 | 10.0522 | 2.0891 | 1.3477 | 0.3139 | 0.1137 | 0.6038 | 6.2609 | 0.6485 | 99.2159 |
| ALM | sillimanite | 36 | 26.3901 | 0.0319 | 0.3928 | 12.3548 | 1.0452 | 0.6425 | 9.5692 | 23.6211 | 2.6000 | 10.3916 | 2.1458 | 1.3509 | 0.3170 | 0.0086 | 0.6372 | 6.8121 | 0.6419 | 98.9627 |
| ALM | sillimanite | 37 | 26.2925 | 0.0493 | 0.3908 | 12.4184 | 0.9201 | 1.0619 | 9.5312 | 23.4783 | 2.5417 | 10.3687 | 2.0870 | 1.5491 | 0.4661 | 0.0351 | 0.6140 | 5.6374 | 0.7820 | 98.2336 |
| ALM | sillimanite | 38 | 26.4721 | 0.0212 | 0.2999 | 12.5228 | 1.0766 | 0.7587 | 9.7380 | 23.8506 | 2.6461 | 10.1129 | 2.0871 | 1.5416 | 0.3229 | 0.0250 | 0.6937 | 5.7835 | 1.0316 | 98.9943 |
| ALM | sillimanite | 39 | 26.3433 | 0.0218 | 0.3006 | 12.4632 | 1.0392 | 0.8179 | 9.5203 | 23.8049 | 2.6003 | 10.1533 | 2.1639 | 1.6412 | 0.4888 | 0.0823 | 0.7013 | 5.3153 | 1.1226 | 98.5902 |

| Sample | Phase | Label | W%(O ) | W%(Al) | W%(Si) | W%(P) | W%(Ca) | W%(Y ) | W%(La) | W%(Ce) | W%(Pr) | W%(Nd) | W%(Sm) | W%(Gd) | W%(Dy) | W%(Er) | W%(Pb) | W%(Th) | W%(U ) | W%(SUM) |
|---|---|---|---|---|---|---|---|---|---|---|---|---|---|---|---|---|---|---|---|---|
| ALM | sillimanite | 40 | 26.5467 | 0.0189 | 0.3403 | 12.6213 | 0.8941 | 0.9878 | 9.6365 | 23.7911 | 2.8253 | 10.2700 | 2.1878 | 1.5676 | 0.4278 | 0.0951 | 0.5916 | 5.4584 | 0.6936 | 98.9639 |
| ALM | sillimanite | 42 | 26.2055 | 0.0040 | 0.2356 | 12.6057 | 1.0165 | 2.1872 | 8.7627 | 22.3373 | 2.6300 | 10.3042 | 2.5330 | 2.2752 | 0.8655 | 0.1189 | 0.8402 | 3.6392 | 2.1121 | 98.6828 |
| ALM | sillimanite | 43 | 26.2964 | 0.0104 | 0.2543 | 12.6158 | 1.0129 | 1.9056 | 8.7664 | 22.5294 | 2.6986 | 10.3594 | 2.4772 | 2.2290 | 0.8305 | 0.2020 | 0.8183 | 3.7804 | 2.0322 | 98.8288 |
| ALM | sillimanite | 44 | 26.3051 | 0.0336 | 0.2919 | 12.3993 | 0.9763 | 0.7403 | 9.8166 | 24.2275 | 2.7357 | 10.1473 | 2.0450 | 1.5339 | 0.3784 | 0.0570 | 0.6471 | 5.3374 | 0.9695 | 98.6519 |
| ALM | plagioclase | 45 | 26.5330 | 0.0280 | 0.3678 | 12.5456 | 1.1577 | 0.6808 | 9.5939 | 23.2697 | 2.5438 | 9.8278 | 1.8855 | 1.3524 | 0.3622 | 0.1095 | 0.7155 | 7.0248 | 0.8467 | 98.8547 |
| ALM | plagioclase | 46 | 26.6700 | 0.0220 | 0.3572 | 12.6259 | 1.1547 | 0.6096 | 9.5401 | 23.2924 | 2.6388 | 10.0627 | 2.0455 | 1.3877 | 0.3357 | 0.0188 | 0.7532 | 6.9113 | 0.8533 | 99.2889 |
| ALM | plagioclase | 49 | 26.7148 | 0.0239 | 0.3277 | 12.6948 | 1.1833 | 0.8899 | 9.7974 | 23.3041 | 2.4476 | 9.7257 | 1.8796 | 1.5137 | 0.4306 | 0.0919 | 0.7870 | 6.6828 | 1.0780 | 99.5828 |
| ALM | plagioclase | 50 | 26.4618 | 0.0249 | 0.3178 | 12.5419 | 1.1645 | 0.8180 | 9.6578 | 23.0053 | 2.6708 | 9.7384 | 2.0312 | 1.4581 | 0.3859 | 0.1293 | 0.7652 | 6.5699 | 1.0797 | 98.8305 |
| ALM | plagioclase | 51 | 26.2411 | 0.0707 | 0.4718 | 12.2508 | 1.1142 | 0.6098 | 9.4273 | 23.2233 | 2.6833 | 10.1240 | 1.9547 | 1.3499 | 0.2660 | 0.0695 | 0.6990 | 6.5234 | 0.7961 | 97.8849 |
| ALM | plagioclase | 52 | 25.9836 | 0.0342 | 0.3452 | 12.2497 | 1.1619 | 0.9139 | 9.5903 | 22.8039 | 2.5388 | 9.6357 | 1.9468 | 1.5194 | 0.4603 | 0.1301 | 0.7715 | 6.1294 | 1.0773 | 97.3020 |
| ALM | plagioclase | 53 | 26.3520 | 0.0089 | 0.2942 | 12.5162 | 1.1784 | 0.8552 | 9.9167 | 23.1209 | 2.5873 | 9.6932 | 1.8567 | 1.4276 | 0.3400 | 0.0213 | 0.7788 | 6.3446 | 1.0873 | 98.3893 |
| ALM | plagioclase | 54 | 26.5990 | 0.0128 | 0.3051 | 12.6334 | 1.1932 | 0.9740 | 9.8609 | 23.1099 | 2.5660 | 9.7585 | 1.9469 | 1.5568 | 0.4072 | 0.0755 | 0.7784 | 6.4964 | 1.1271 | 99.4111 |
| ALM | plagioclase | 56 | 27.0583 | 0.0218 | 0.4776 | 12.8151 | 1.1301 | 0.7355 | 9.3198 | 23.0532 | 2.6097 | 10.1204 | 1.9757 | 1.3159 | 0.3032 | 0.1289 | 0.7241 | 7.8591 | 0.6598 | 100.3182 |
| ALM | plagioclase | 57 | 26.6421 | 0.0287 | 0.3245 | 12.6584 | 1.1802 | 0.8408 | 9.6283 | 23.2397 | 2.6268 | 9.8901 | 1.9959 | 1.4096 | 0.4966 | 0.0642 | 0.7413 | 6.3937 | 1.0197 | 99.1906 |
| ALM | plagioclase | 58 | 26.4544 | 0.0174 | 0.2995 | 12.6213 | 1.1934 | 1.4382 | 9.6533 | 22.7379 | 2.4969 | 9.4558 | 2.0047 | 1.6312 | 0.6287 | 0.1555 | 0.8552 | 6.1396 | 1.2268 | 99.0198 |
| ALM | plagioclase | 59 | 26.4641 | 0.0233 | 0.4121 | 12.4789 | 1.0264 | 1.1781 | 9.0701 | 23.1178 | 2.7579 | 10.3378 | 2.0855 | 1.4404 | 0.4775 | 0.1726 | 0.6699 | 6.9088 | 0.5991 | 99.2303 |
| ALM | plagioclase | 60 | 26.2452 | 0.0201 | 0.4192 | 12.2980 | 1.0334 | 1.1919 | 9.1442 | 23.3076 | 2.5609 | 10.2735 | 1.9829 | 1.4866 | 0.5386 | 0.0948 | 0.6770 | 7.0583 | 0.5688 | 98.9110 |
| ALM | plagioclase | 61 | 26.2089 | 0.0140 | 0.4278 | 12.3042 | 1.1041 | 0.9491 | 9.1233 | 22.8948 | 2.5814 | 10.2714 | 2.0129 | 1.3618 | 0.4438 | 0.1104 | 0.6637 | 7.5280 | 0.2453 | 98.2549 |
| ALM | plagioclase | 62 | 26.5320 | 0.0172 | 0.4264 | 12.4872 | 1.1532 | 1.0005 | 9.0355 | 22.8808 | 2.5967 | 10.3868 | 2.0530 | 1.3825 | 0.4154 | 0.0884 | 0.7203 | 7.6914 | 0.4877 | 99.3650 |
| ALM | plagioclase | 63 | 26.3665 | 0.0298 | 0.4493 | 12.4105 | 1.1465 | 0.9943 | 8.9960 | 22.5342 | 2.5747 | 10.1656 | 2.0093 | 1.3684 | 0.4530 | 0.1821 | 0.6909 | 7.6453 | 0.5210 | 98.5474 |
| ALM | plagioclase | 64 | 26.2444 | 0.0139 | 0.3931 | 12.3474 | 1.0897 | 1.0025 | 9.3538 | 22.9333 | 2.6943 | 10.1586 | 2.0092 | 1.3272 | 0.3966 | 0.1473 | 0.6860 | 7.1695 | 0.4941 | 98.4709 |
| ALM | plagioclase | 65 | 26.5937 | 0.0180 | 0.4192 | 12.5126 | 1.2051 | 1.0959 | 9.0489 | 22.8101 | 2.6062 | 10.1941 | 2.0353 | 1.4351 | 0.4247 | 0.1283 | 0.7252 | 7.9146 | 0.5805 | 99.7575 |
| ALM | plagioclase | 66 | 26.1565 | 0.0113 | 0.4024 | 12.2519 | 1.1794 | 0.9658 | 9.0650 | 22.6164 | 2.5684 | 10.1218 | 2.0271 | 1.5062 | 0.4519 | 0.0586 | 0.6957 | 7.8108 | 0.5562 | 98.4554 |
| ALM | plagioclase | 67 | 26.0779 | 0.0350 | 0.4493 | 12.1369 | 1.1508 | 0.7652 | 9.3769 | 22.7136 | 2.6260 | 10.1205 | 1.9869 | 1.3417 | 0.3817 | 0.0544 | 0.6141 | 7.7485 | 0.4379 | 98.0273 |
| ALM | plagioclase | 68 | 26.5285 | 0.0329 | 0.3742 | 12.5631 | 1.0899 | 0.8693 | 9.5409 | 23.0710 | 2.7020 | 9.8990 | 2.0100 | 1.3368 | 0.3721 | 0.0798 | 0.6657 | 7.2091 | 0.5238 | 98.8781 |
| ALM | plagioclase | 69 | 26.3335 | 0.0148 | 0.3786 | 12.4127 | 1.1766 | 0.9347 | 9.3513 | 22.5279 | 2.5646 | 10.0275 | 1.9281 | 1.4342 | 0.4295 | 0.0896 | 0.7267 | 7.7845 | 0.5816 | 98.7064 |
| ALM | plagioclase | 70 | 26.3850 | 0.0241 | 0.3625 | 12.4328 | 1.0898 | 0.9825 | 9.7209 | 23.3204 | 2.5698 | 10.0622 | 1.8875 | 1.3360 | 0.4356 | 0.1151 | 0.6615 | 6.9935 | 0.5443 | 98.9335 |
| ALM | plagioclase | 71 | 26.0607 | 0.0190 | 0.3999 | 12.1563 | 1.0893 | 0.9427 | 9.3164 | 23.1233 | 2.6152 | 10.2564 | 1.9940 | 1.4040 | 0.4204 | 0.0949 | 0.6518 | 7.2987 | 0.5052 | 98.3582 |
| ALM | plagioclase | 73 | 26.3113 | 0.0149 | 0.3965 | 12.3830 | 1.1118 | 0.9424 | 9.1621 | 22.9103 | 2.7458 | 10.1116 | 1.9447 | 1.4334 | 0.4633 | 0.0866 | 0.6723 | 7.4113 | 0.5240 | 98.63 53 |
| ALM | plagioclase | 74 | 26.2894 | 0.0116 | 0.3884 | 12.3507 | 1.1705 | 1.0960 | 9.1018 | 22.6696 | 2.7076 | 10.2134 | 2.0466 | 1.4548 | 0.4395 | 0.0663 | 0.6550 | 7.6413 | 0.5719 | 98.8844 |
| ALM | plagioclase | 75 | 26.3025 | 0.0161 | 0.4062 | 12.3527 | 1.1745 | 1.0376 | 9.0147 | 22.5934 | 2.5944 | 10.2446 | 2.0682 | 1.3628 | 0.4099 | 0.1913 | 0.7292 | 7.8081 | 0.5354 | 98.8516 |
| ALM | plagioclase | 76 | 26.4205 | 0.0069 | 0.4072 | 12.4584 | 1.0936 | 0.9795 | 9.0254 | 23.0490 | 2.6710 | 10.2267 | 2.0628 | 1.4247 | 0.4733 | 0.0341 | 0.6968 | 7.4010 | 0.4918 | 98.9327 |
| ALM | plagioclase | 77 | 26.1697 | 0.0237 | 0.3968 | 12.2789 | 1.1460 | 1.0989 | 9.0839 | 22.5894 | 2.5898 | 10.0382 | 2.0435 | 1.4589 | 0.4454 | 0.0954 | 0.7003 | 7.7959 | 0.5605 | 98.5252 |
| ALM | plagioclase | 78 | 26.2827 | 0.0223 | 0.4150 | 12.3559 | 1.1409 | 0.9555 | 9.1121 | 22.6631 | 2.7114 | 10.1448 | 1.9321 | 1.3951 | 0.4453 | 0.0298 | 0.7288 | 7.6585 | 0.5144 | 98.5177 |
| ALM | plagioclase | 79 | 26.2951 | 0.0115 | 0.4944 | 12.3014 | 1.1139 | 1.3051 | 8.4970 | 22.2450 | 2.6598 | 10.4971 | 1.9901 | 1.6091 | 0.5144 | 0.1296 | 0.7220 | 8.0549 | 0.6651 | 99.1155 |
| GTCD | garnet | 1 | 26.0981 | 0.0175 | 0.5875 | 12.1101 | 0.5189 | 0.9361 | 8.8103 | 23.1405 | 2.7898 | 12.2917 | 2.1755 | 1.4033 | 0.3752 | 0.0857 | 0.5616 | 5.9684 | 0.4924 | 98.3726 |
| GTCD | garnet | 2 | 26.0144 | 0.0327 | 0.5883 | 12.1244 | 0.4981 | 0.8174 | 8.6918 | 23.3878 | 2.6933 | 11.9264 | 2.1540 | 1.3437 | 0.3645 | 0.0656 | 0.5179 | 5.7669 | 0.4562 | 97.4534 |
| GTCD | garnet | 3 | 26.4649 | 0.0428 | 0.5670 | 12.4628 | 0.5072 | 0.7911 | 8.5974 | 23.5268 | 2.6525 | 12.0323 | 2.2456 | 1.3656 | 0.4148 | 0.1283 | 0.5649 | 5.5231 | 0.4753 | 98.3724 |
| GTCD | garnet | 4 | 25.9085 | 0.0179 | 0.5878 | 12.0712 | 0.5290 | 0.8577 | 8.7430 | 22.8873 | 2.7198 | 12.0313 | 2.1892 | 1.3149 | 0.3980 | 0.0001 | 0.5648 | 5.8712 | 0.4876 | 97.1893 |
| GTCD | garnet | 5 | 25.8845 | 0.0111 | 0.5661 | 12.1009 | 0.5275 | 0.8481 | 8.6685 | 22.6896 | 2.7675 | 12.0244 | 2.1542 | 1.3940 | 0.3576 | 0.0972 | 0.5662 | 5.8292 | 0.4874 | 96.9840 |
| GTCD | garnet | 6 | 26.0661 | 0.0365 | 0.5734 | 12.2029 | 0.5120 | 0.8821 | 8.6655 | 23.0016 | 2.6437 | 12.1207 | 2.1884 | 1.3185 | 0.4177 | 0.0638 | 0.4938 | 5.6890 | 0.5197 | 97.4054 |
| GTCD | garnet | 7 | 25.8599 | 0.0002 | 0.5580 | 12.0921 | 0.5346 | 0.8547 | 8.7579 | 22.6925 | 2.7012 | 12.0249 | 2.1737 | 1.4026 | 0.3660 | 0.0415 | 0.5732 | 5.8083 | 0.5083 | 96.9596 |
| GTCD | garnet | 8 | 25.9664 | 0.0166 | 0.5345 | 12.1265 | 0.5066 | 0.8507 | 8.7444 | 22.9892 | 2.7562 | 12.4648 | 2.1343 | 1.3610 | 0.4293 | 0.1447 | 0.5391 | 5.4427 | 0.4784 | 97.4954 |
| GTCD | garnet | 9 | 25.8834 | 0.0137 | 0.4476 | 12.3272 | 0.5983 | 1.9187 | 8.8534 | 22.4013 | 2.6029 | 11.3812 | 1.9835 | 1.3959 | 0.6377 | 0.2431 | 0.5394 | 5.2788 | 0.5338 | 97.0499 |
| GTCD | garnet | 10 | 25.6346 | 0.0192 | 0.4417 | 12.3375 | 0.6022 | 2.6947 | 8.6878 | 21.3601 | 2.5707 | 10.9273 | 1.8961 | 1.4427 | 0.8278 | 0.2722 | 0.5481 | 5.2981 | 0.5146 | 96.0854 |
| GTCD | garnet | 11 | 25.5574 | 0.0053 | 0.4113 | 12.3239 | 0.6377 | 2.2862 | 8.8763 | 21.5937 | 2.5305 | 10.7225 | 1.9040 | 1.4816 | 0.6159 | 0.2282 | 0.5245 | 5.0263 | 0.5975 | 95.3328 |
| GTCD | garnet | 12 | 25.7842 | 0.0215 | 0.5342 | 12.0791 | 0.4923 | 0.9090 | 8.7369 | 22.5628 | 2.7782 | 12.0205 | 2.2071 | 1.4333 | 0.3676 | 0.0687 | 0.5125 | 5.6365 | 0.4625 | 96.6169 |
| GTCD | garnet | 13 | 25.8800 | 0.0002 | 0.5154 | 12.1289 | 0.4740 | 0.8308 | 8.8769 | 22.8868 | 2.8360 | 12.1716 | 2.2318 | 1.3517 | 0.3864 | 0.0841 | 0.5138 | 5.4285 | 0.4379 | 97.0448 |
| GTCD | garnet | 14 | 26.0517 | 0.0002 | 0.5265 | 12.3021 | 0.4849 | 0.8207 | 8.8108 | 22.6729 | 2.7087 | 12.0761 | 2.2297 | 1.3926 | 0.3891 | 0.0678 | 0.5202 | 5.4480 | 0.5076 | 97.0196 |
| GTCD | garnet | 15 | 25.6033 | 0.3883 | 1.2660 | 11.3912 | 0.5253 | 0.7594 | 8.2222 | 21.2891 | 2.6614 | 11.4404 | 2.0303 | 1.2082 | 0.3285 | 0.0750 | 0.5336 | 5.7283 | 0.5451 | 94.0056 |
| GTCD | garnet | 16 | 26.3289 | 0.3700 | 1.0589 | 12.0040 | 0.5167 | 0.9958 | 8.7154 | 21.9304 | 2.6873 | 11.5125 | 2.1340 | 1.3784 | 0.4100 | 0.0944 | 0.4664 | 5.2654 | 0.4703 | 96.3488 |
| GTCD | garnet | 17 | 25.8750 | 0.0319 | 0.3285 | 12.6004 | 0.6467 | 2.1703 | 9.4035 | 21.8652 | 2.5339 | 10.5791 | 1.7231 | 1.3335 | 0.6956 | 0.2252 | 0.5274 | 4.6627 | 0.6234 | 95.8354 |
| GTCD | garnet | 29 | 25.6503 | 0.0122 | 0.5088 | 12.0985 | 0.4663 | 0.7361 | 8.6239 | 22.3765 | 2.7639 | 12.4229 | 2.2321 | 1.2843 | 0.3229 | 0.0422 | 0.4597 | 5.0705 | 0.3650 | 95.4461 |
| GTCD | garnet | 30 | 25.5100 | 0.0007 | 0.3195 | 12.4982 | 0.6679 | 2.7472 | 9.1346 | 21.0367 | 2.4652 | 10.4864 | 1.7542 | 1.3486 | 0.8109 | 0.2773 | 0.4491 | 4.5801 | 0.6055 | 94.7021 |
| GTCD | garnet | 31 | 25.6215 | 0.2288 | 0.8362 | 11.7198 | 0.4556 | 0.5798 | 8.8844 | 22.1047 | 2.8765 | 11.9446 | 2.0603 | 1.3284 | 0.3496 | 0.0527 | 0.4177 | 4.9265 | 0.3578 | 94.7549 |
| GTCD | garnet | 33 | 25.1592 | 0.0199 | 0.4738 | 11.7491 | 0.4592 | 0.5654 | 8.9191 | 22.5685 | 2.8092 | 12.1477 | 2.0815 | 1.2892 | 0.4253 | 0.0365 | 0.3966 | 4.8253 | 0.3474 | 94.2829 |

| Sample | Phase | Label | W%(O) | W%(Al) | W%(Si) | W%(P) | W%(Ca) | W%(Y) | W%(La) | W%(Ce) | W%(Pr) | W%(Nd) | W%(Sm) | W%(Gd) | W%(Dy) | W%(Er) | W%(Pb) | W%(Th) | W%(U) | W%(SUM) |
|---|---|---|---|---|---|---|---|---|---|---|---|---|---|---|---|---|---|---|---|---|
| GTCD | garnet | 34 | 25.5818 | 0.0160 | 0.3582 | 12.4823 | 0.6484 | 2.4638 | 8.9883 | 20.9799 | 2.4551 | 10.6723 | 1.8549 | 1.4077 | 0.7712 | 0.2423 | 0.4672 | 4.8170 | 0.6062 | 94.8226 |
| GTCD | garnet | 35 | 25.6130 | 0.0135 | 0.5974 | 11.9696 | 0.4648 | 0.5758 | 8.5585 | 22.3039 | 2.8398 | 12.1152 | 2.0855 | 1.3478 | 0.2865 | 0.1324 | 0.4981 | 5.6681 | 0.4430 | 95.5229 |
| GTCD | garnet | 36 | 25.3729 | 0.0192 | 0.4849 | 11.8814 | 0.4783 | 0.5801 | 9.0061 | 22.9668 | 2.7646 | 11.9499 | 2.0657 | 1.2237 | 0.2764 | 0.0675 | 0.4249 | 4.9043 | 0.3304 | 94.8071 |
| GTCD | garnet | 39 | 25.7057 | 0.0196 | 0.5280 | 12.0695 | 0.4853 | 0.7024 | 8.8665 | 22.5772 | 2.7739 | 12.1451 | 2.1011 | 1.2795 | 0.3252 | 0.0281 | 0.5207 | 5.3671 | 0.3854 | 95.8903 |
| GTCD | garnet | 40 | 25.4922 | 0.0117 | 0.5356 | 11.9372 | 0.4820 | 0.7149 | 8.6751 | 22.5468 | 2.6860 | 12.0319 | 2.0752 | 1.3159 | 0.3816 | 0.0899 | 0.5094 | 5.4251 | 0.4101 | 95.3306 |
| GTCD | garnet | 41 | 25.6397 | 0.0112 | 0.5370 | 12.0437 | 0.4660 | 0.6549 | 8.8454 | 22.5739 | 2.7587 | 11.9074 | 2.1994 | 1.3078 | 0.2815 | 0.0861 | 0.4743 | 5.3752 | 0.3789 | 95.5511 |
| GTCD | garnet | 42 | 25.6763 | 0.0357 | 0.5299 | 12.0657 | 0.4717 | 0.6560 | 8.8488 | 22.7384 | 2.7647 | 12.0675 | 2.0512 | 1.1877 | 0.2749 | 0.1152 | 0.5009 | 5.1694 | 0.3866 | 95.5506 |
| GTCD | garnet | 43 | 25.6625 | 0.0106 | 0.5197 | 12.0912 | 0.4774 | 0.7036 | 8.7442 | 22.4206 | 2.6596 | 12.0304 | 2.1161 | 1.3278 | 0.4015 | 0.0674 | 0.4846 | 5.4347 | 0.4055 | 95.5674 |
| GTCD | garnet | 44 | 25.6667 | 0.0183 | 0.5212 | 12.0829 | 0.4685 | 0.6795 | 8.8043 | 22.6092 | 2.7364 | 12.1178 | 2.0867 | 1.2387 | 0.3037 | 0.0825 | 0.4840 | 5.2387 | 0.3854 | 95.5345 |
| GTCD | garnet | 45 | 25.5454 | 0.0048 | 0.5345 | 11.9827 | 0.4656 | 0.6201 | 8.6750 | 22.5444 | 2.8293 | 12.0163 | 2.0346 | 1.3034 | 0.2848 | 0.1041 | 0.5051 | 5.5044 | 0.3879 | 95.3524 |
| GTCD | garnet | 46 | 25.6514 | 0.0043 | 0.5407 | 12.0464 | 0.4860 | 0.6880 | 8.8482 | 22.4426 | 2.8006 | 11.9827 | 2.1407 | 1.2363 | 0.3031 | 0.0364 | 0.4703 | 5.5723 | 0.3932 | 95.6532 |
| GTCD | garnet | 47 | 25.9323 | 0.3602 | 1.0333 | 11.8135 | 0.4567 | 0.6040 | 8.6126 | 21.9969 | 2.6900 | 11.7283 | 1.9828 | 1.1923 | 0.3367 | 0.0646 | 0.4265 | 5.0098 | 0.3761 | 94.6266 |
| GTCD | garnet | 48 | 25.6996 | 0.0088 | 0.5499 | 12.0740 | 0.4689 | 0.6391 | 8.6855 | 22.5876 | 2.8026 | 12.0495 | 2.0024 | 1.2883 | 0.3232 | 0.1461 | 0.4333 | 5.5572 | 0.3717 | 95.6977 |
| GTCD | garnet | 49 | 25.3310 | 0.0060 | 0.5368 | 11.8360 | 0.4743 | 0.5881 | 8.7035 | 22.4929 | 2.7929 | 11.8153 | 2.0583 | 1.2653 | 0.3212 | 0.1141 | 0.5105 | 5.5340 | 0.4045 | 94.7947 |
| GTCD | garnet | 50 | 25.8800 | 0.0107 | 0.5357 | 12.1690 | 0.4701 | 0.6246 | 8.7827 | 22.8228 | 2.7987 | 12.1255 | 2.1373 | 1.3536 | 0.3221 | 0.0544 | 0.4971 | 5.3752 | 0.4059 | 96.3754 |
| GTCD | garnet | 51 | 25.6595 | 0.0090 | 0.5449 | 12.0306 | 0.4837 | 0.7207 | 8.8419 | 22.7098 | 2.6311 | 11.8974 | 2.2106 | 1.2577 | 0.3201 | 0.0763 | 0.5085 | 5.5403 | 0.3758 | 95.8279 |
| GTCD | garnet | 52 | 25.5610 | 0.0034 | 0.5518 | 11.9615 | 0.4804 | 0.7005 | 8.5936 | 22.6065 | 2.8086 | 12.1112 | 2.0763 | 1.2540 | 0.3827 | 0.0718 | 0.4824 | 5.5049 | 0.4063 | 95.5669 |
| GTCD | garnet | 53 | 25.6190 | 0.0350 | 0.5435 | 11.9878 | 0.4387 | 0.6540 | 8.8509 | 22.9599 | 2.7884 | 12.0209 | 2.0457 | 1.2187 | 0.3551 | 0.0536 | 0.5096 | 5.1618 | 0.3891 | 95.6417 |
| GTCD | garnet | 54 | 25.6687 | 0.0156 | 0.5542 | 12.0285 | 0.4735 | 0.6854 | 8.7563 | 22.8050 | 2.8088 | 11.8151 | 2.0913 | 1.2417 | 0.3072 | 0.0951 | 0.4766 | 5.5443 | 0.4056 | 95.7829 |
| GTCD | garnet | gt_94 | 25.8784 | 0.0067 | 0.5217 | 12.0870 | 0.4584 | 0.8758 | 9.1192 | 23.8327 | 3.0582 | 11.1147 | 2.1766 | 1.4901 | 0.4013 | 0.1070 | 0.5159 | 5.1757 | 0.4135 | 97.2429 |
| GTCD | garnet | gt_95 | 26.0452 | 0.0092 | 0.2175 | 12.6608 | 0.7185 | 2.2916 | 10.5357 | 23.3005 | 2.6337 | 9.6305 | 1.6319 | 1.3475 | 0.5924 | 0.2112 | 0.5176 | 4.1762 | 0.6761 | 97.2061 |
| GTCD | garnet | gt_96 | 25.9304 | 0.0045 | 0.2809 | 12.4634 | 0.7134 | 2.0915 | 10.1663 | 23.2632 | 2.7539 | 9.7814 | 1.8476 | 1.4007 | 0.6623 | 0.2041 | 0.5500 | 4.5081 | 0.6657 | 97.2974 |
| GTCD | garnet | gt_97 | 26.0645 | 0.0202 | 0.5281 | 12.1855 | 0.4961 | 1.1658 | 9.0933 | 23.7471 | 2.8485 | 11.2806 | 2.2214 | 1.5582 | 0.4515 | 0.1487 | 0.5477 | 5.2029 | 0.5226 | 98.0927 |
| GTCD | garnet | gt_98 | 25.8338 | 0.0140 | 0.5429 | 12.0263 | 0.4845 | 0.8999 | 8.7388 | 23.4755 | 2.9852 | 11.5773 | 2.2945 | 1.5421 | 0.3551 | 0.1125 | 0.4718 | 5.4066 | 0.4580 | 97.2288 |
| GTCD | garnet | gt_99 | 26.1046 | 0.0033 | 0.1468 | 12.7091 | 0.7890 | 2.0975 | 11.1803 | 23.6064 | 2.6613 | 9.1632 | 1.6223 | 1.2303 | 0.6572 | 0.2137 | 0.5105 | 3.9388 | 0.7267 | 97.3710 |
| GTCD | garnet | gt_100 | 26.1683 | 0.0130 | 0.1550 | 12.7607 | 0.7995 | 2.2104 | 11.0701 | 23.3039 | 2.5716 | 9.4939 | 1.6678 | 1.2581 | 0.5536 | 0.2590 | 0.4782 | 3.9569 | 0.7512 | 97.4812 |
| GTCD | garnet | gt_101 | 26.0039 | 0.0002 | 0.2556 | 12.6798 | 0.6995 | 2.7156 | 10.0153 | 22.7812 | 2.6270 | 9.7355 | 1.7200 | 1.4251 | 0.7633 | 0.2335 | 0.4769 | 4.2906 | 0.6894 | 97.1224 |
| GTCD | garnet | gt_102 | 25.9466 | 0.0097 | 0.5256 | 12.0622 | 0.5132 | 1.0272 | 8.8486 | 23.7208 | 2.9170 | 11.7868 | 2.2035 | 1.5161 | 0.3536 | 0.0758 | 0.5367 | 5.5093 | 0.4510 | 98.0137 |
| GTCD | garnet | gt_103 | 26.2243 | 0.0067 | 0.1726 | 12.8507 | 0.7997 | 2.5419 | 10.7621 | 23.1563 | 2.5119 | 9.2997 | 1.6863 | 1.2883 | 0.6883 | 0.2125 | 0.5126 | 4.1388 | 0.7339 | 97.5966 |
| GTCD | garnet | gt_104 | 25.8937 | 0.0100 | 0.1378 | 12.5558 | 0.8105 | 1.9607 | 11.2196 | 23.3394 | 2.5069 | 9.2839 | 1.6457 | 1.2918 | 0.6203 | 0.1586 | 0.5673 | 4.0376 | 0.8015 | 96.8511 |
| GTCD | garnet | gt_105 | 25.8440 | 0.0026 | 0.3319 | 12.3475 | 0.6946 | 1.7473 | 9.8360 | 23.1229 | 2.7815 | 10.2859 | 1.8762 | 1.4148 | 0.5928 | 0.1594 | 0.5710 | 4.5673 | 0.7176 | 96.9033 |
| GTCD | garnet | gt_106 | 25.7054 | 0.0128 | 0.5378 | 11.9663 | 0.4805 | 1.0424 | 8.9734 | 23.4068 | 2.8250 | 11.5344 | 2.1549 | 1.5094 | 0.4324 | 0.1266 | 0.5127 | 5.2639 | 0.4101 | 96.9048 |
| GTCD | garnet | gt_107 | 25.8598 | 0.0002 | 0.2311 | 12.6102 | 0.7432 | 2.5582 | 10.1690 | 22.8437 | 2.5526 | 9.4276 | 1.6310 | 1.3383 | 0.7263 | 0.2362 | 0.4992 | 4.3748 | 0.7061 | 96.5175 |
| GTCD | garnet | gt_108 | 26.0330 | 0.0162 | 0.2762 | 12.5514 | 0.7193 | 2.2740 | 10.0049 | 23.0200 | 2.6752 | 10.0032 | 1.8730 | 1.4779 | 0.6540 | 0.2388 | 0.4943 | 4.6039 | 0.6586 | 97.5839 |
| GTCD | garnet | gt_109 | 25.9686 | 0.0013 | 0.5637 | 12.1432 | 0.5069 | 0.9400 | 8.7862 | 23.4835 | 2.8686 | 11.3554 | 2.2872 | 1.5179 | 0.3574 | 0.0495 | 0.5591 | 5.4889 | 0.4963 | 97.3837 |
| GTCD | garnet | gt_110 | 25.8514 | 0.0083 | 0.5461 | 12.0246 | 0.5136 | 0.9692 | 8.8356 | 23.3600 | 2.9819 | 11.4031 | 2.3396 | 1.5577 | 0.3998 | 0.0808 | 0.5180 | 5.5711 | 0.4904 | 97.4612 |
| GTCD | garnet | gt_112 | 25.8853 | 0.0155 | 0.5552 | 12.0875 | 0.4879 | 0.9370 | 8.7976 | 23.4803 | 2.8212 | 11.5506 | 2.2990 | 1.5249 | 0.3500 | 0.0737 | 0.4972 | 5.2689 | 0.4763 | 97.1181 |
| GTCD | garnet | gt_113 | 25.8733 | 0.0057 | 0.5190 | 12.0939 | 0.4997 | 1.1879 | 8.8772 | 23.4883 | 2.9544 | 11.3929 | 2.2592 | 1.5296 | 0.4436 | 0.0995 | 0.5291 | 5.2948 | 0.4419 | 97.5000 |
| GTCD | garnet | gt_114 | 25.8559 | 0.0138 | 0.5399 | 11.9794 | 0.5330 | 1.0371 | 8.9081 | 23.3711 | 2.9416 | 11.5589 | 2.2866 | 1.5675 | 0.4130 | 0.1120 | 0.5805 | 5.7020 | 0.5014 | 97.9118 |
| GTCD | garnet | gt_116 | 26.3240 | 0.0828 | 0.6272 | 12.2310 | 0.4903 | 0.9966 | 8.8627 | 23.6664 | 2.9461 | 11.5455 | 2.3692 | 1.5319 | 0.3811 | 0.0940 | 0.5288 | 5.4681 | 0.4557 | 98.6114 |
| GTCD | garnet | gt_117 | 26.0076 | 0.0027 | 0.5231 | 12.1924 | 0.5022 | 1.0198 | 8.9924 | 23.6185 | 2.9111 | 11.2790 | 2.2057 | 1.4299 | 0.4302 | 0.1160 | 0.5363 | 5.3223 | 0.4961 | 97.5953 |
| GTCD | garnet | gt_118 | 25.7919 | 0.0089 | 0.5614 | 11.9744 | 0.4786 | 0.9121 | 8.8041 | 23.5201 | 2.9765 | 11.5538 | 2.3552 | 1.5101 | 0.3388 | 0.1473 | 0.5304 | 5.2795 | 0.4801 | 97.2332 |
| GTCD | garnet | gt_119 | 25.9309 | 0.0199 | 0.5563 | 12.0776 | 0.5123 | 1.2240 | 8.7945 | 23.2477 | 3.0277 | 11.5947 | 2.2076 | 1.5443 | 0.5007 | 0.0976 | 0.5302 | 5.4673 | 0.4571 | 97.8004 |
| GTCD | garnet | gt_120 | 25.7582 | 0.0002 | 0.4193 | 12.2112 | 0.5803 | 1.7459 | 9.2414 | 23.1854 | 2.7704 | 10.6783 | 2.1377 | 1.4589 | 0.5860 | 0.1944 | 0.5305 | 4.8756 | 0.5324 | 96.9161 |
| GTCD | garnet | gt_121 | 25.8571 | 0.0043 | 0.5278 | 12.0464 | 0.5166 | 1.1539 | 8.8458 | 23.6080 | 2.8898 | 11.4848 | 2.2869 | 1.4537 | 0.4522 | 0.1538 | 0.5152 | 5.3060 | 0.5013 | 97.6136 |
| GTCD | garnet | gt_122 | 26.1063 | 0.0019 | 0.1429 | 12.6380 | 0.8022 | 1.7717 | 11.2688 | 23.8152 | 2.5845 | 9.4475 | 1.6047 | 1.3329 | 0.5978 | 0.2413 | 0.4814 | 3.9201 | 0.7674 | 97.5346 |
| GTCD | garnet | gt_124 | 25.9005 | 0.0085 | 0.5099 | 12.1306 | 0.5148 | 1.3533 | 8.8673 | 23.5939 | 2.8686 | 11.3548 | 2.2524 | 1.5105 | 0.4133 | 0.1307 | 0.4983 | 5.1945 | 0.4904 | 97.6023 |
| GTCD | garnet | gt_125 | 26.1217 | 0.0058 | 0.1218 | 12.6279 | 0.8822 | 1.5436 | 11.5550 | 24.0148 | 2.4055 | 9.2065 | 1.6376 | 1.1908 | 0.5347 | 0.1877 | 0.5709 | 3.9190 | 0.9955 | 97.5310 |
| GTCD | garnet | gt_126 | 26.2354 | 0.0002 | 0.1617 | 12.8100 | 0.7836 | 2.2628 | 10.9757 | 23.7277 | 2.5851 | 9.3836 | 1.6392 | 1.1913 | 0.6227 | 0.2029 | 0.4581 | 3.9161 | 0.6993 | 97.6654 |
| GTCD | garnet | gt_127 | 26.0262 | 0.0071 | 0.5132 | 12.2250 | 0.5382 | 1.8274 | 8.6701 | 23.2436 | 2.9241 | 11.3091 | 2.2365 | 1.5771 | 0.5929 | 0.1994 | 0.5598 | 5.4359 | 0.5064 | 98.4020 |
| GTCD | garnet | gt_128 | 26.1960 | 0.0002 | 0.1688 | 12.7729 | 0.7994 | 2.2729 | 10.9418 | 23.5004 | 2.5120 | 9.3804 | 1.7036 | 1.2572 | 0.6282 | 0.2753 | 0.5316 | 3.9903 | 0.7320 | 97.6730 |
| GTCD | garnet | gt_129 | 26.3883 | 0.0048 | 0.1571 | 12.8870 | 0.7665 | 2.4003 | 11.0211 | 23.7188 | 2.6121 | 9.5108 | 1.5504 | 1.3472 | 0.6724 | 0.2279 | 0.5060 | 3.9331 | 0.7200 | 98.4338 |
| GTCD | K-feldspar | 18 | 26.1550 | 0.0291 | 0.4897 | 12.4058 | 0.4623 | 0.8841 | 9.3134 | 23.2667 | 2.7847 | 11.5522 | 2.0623 | 1.3756 | 0.4721 | 0.1254 | 0.4704 | 4.7838 | 0.3940 | 97.0366 |
| GTCD | K-feldspar | 19 | 25.8618 | 0.0131 | 0.4666 | 12.2484 | 0.4867 | 1.0653 | 9.1722 | 23.0961 | 2.8992 | 11.4229 | 2.0596 | 1.2550 | 0.4699 | 0.0965 | 0.4643 | 4.9049 | 0.4196 | 96.4121 |
| GTCD | K-feldspar | 20 | 26.1808 | 0.1279 | 0.7759 | 12.1691 | 0.4921 | 1.0637 | 9.1351 | 22.6555 | 2.6516 | 11.5774 | 2.0607 | 1.2745 | 0.3828 | 0.1031 | 0.5033 | 5.2907 | 0.5354 | 96.9896 |
| GTCD | K-feldspar | 21 | 25.8150 | 0.0196 | 0.5599 | 12.1691 | 0.5004 | 1.1712 | 8.9555 | 22.2902 | 2.7231 | 11.5486 | 2.0595 | 1.3983 | 0.3941 | 0.0923 | 0.5656 | 5.4556 | 0.6338 | 96.3618 |

| Sample | Phase | Label | W%(O) | W%(Al) | W%(Si) | W%(P) | W%(Ca) | W%(Y) | W%(La) | W%(Ce) | W%(Pr) | W%(Nd) | W%(Sm) | W%(Gd) | W%(Dy) | W%(Er) | W%(Pb) | W%(Th) | W%(U) | W%(SUM) |
|---|---|---|---|---|---|---|---|---|---|---|---|---|---|---|---|---|---|---|---|---|
| GTCD | K-feldspar | 22 | 26.0599 | 0.0034 | 0.4519 | 12.3909 | 0.4767 | 0.9710 | 9.1849 | 23.0804 | 2.8026 | 11.8674 | 2.0489 | 1.3008 | 0.4100 | 0.0866 | 0.4631 | 4.8576 | 0.4058 | 96.8719 |
| GTCD | K-feldspar | 24 | 25.9580 | 0.0115 | 0.4622 | 12.2990 | 0.4632 | 0.9434 | 9.2950 | 23.1285 | 2.7860 | 11.7270 | 2.0678 | 1.3776 | 0.4300 | 0.0836 | 0.4468 | 4.7783 | 0.3842 | 96.6521 |
| GTCD | K-feldspar | 25 | 25.9084 | 0.0142 | 0.5176 | 12.2209 | 0.4512 | 0.7954 | 9.0622 | 22.9579 | 2.7628 | 12.0820 | 2.1628 | 1.3144 | 0.3717 | 0.0791 | 0.4467 | 4.8555 | 0.3682 | 96.3810 |
| GTCD | K-feldspar | 26 | 25.9117 | 0.0169 | 0.4736 | 12.3147 | 0.4507 | 0.8609 | 9.1880 | 22.9164 | 2.6855 | 11.9300 | 2.0291 | 1.2705 | 0.4036 | 0.0751 | 0.4453 | 4.7120 | 0.3513 | 96.0453 |
| GTCD | K-feldspar | 27 | 25.7224 | 0.0076 | 0.4842 | 12.1552 | 0.4847 | 0.9582 | 9.2007 | 22.8499 | 2.7853 | 11.5499 | 2.0071 | 1.3444 | 0.3695 | 0.0903 | 0.4497 | 5.0390 | 0.3845 | 95.8926 |
| GTCD | plagioclase | 57 | 25.7247 | 0.0266 | 0.3710 | 12.2017 | 0.5336 | 0.7059 | 8.7468 | 23.3135 | 2.7113 | 12.0961 | 2.3152 | 1.3503 | 0.3660 | 0.0825 | 0.5299 | 4.0909 | 0.6196 | 95.7956 |
| GTCD | plagioclase | 58 | 25.8373 | 0.0121 | 0.4610 | 12.1876 | 0.5326 | 0.6947 | 8.7978 | 23.0360 | 2.9277 | 11.9854 | 2.2092 | 1.3376 | 0.3572 | 0.0651 | 0.4849 | 4.7885 | 0.5591 | 96.2838 |
| GTCD | plagioclase | 59 | 25.8364 | 0.0321 | 0.5571 | 12.2008 | 0.4167 | 0.9447 | 9.0752 | 22.5974 | 2.7519 | 11.8201 | 1.9721 | 1.4146 | 0.4249 | 0.0952 | 0.4479 | 5.0749 | 0.2661 | 95.9381 |
| GTCD | plagioclase | 60 | 25.5527 | 0.0224 | 0.5260 | 11.9304 | 0.4606 | 0.6407 | 8.7967 | 22.9358 | 2.8771 | 11.9394 | 2.1263 | 1.3052 | 0.3553 | 0.0785 | 0.4805 | 5.2507 | 0.4085 | 95.6968 |
| GTCD | plagioclase | 60 | 25.5761 | 0.0198 | 0.5021 | 11.9380 | 0.5174 | 0.7575 | 8.7083 | 23.1767 | 2.7512 | 11.9888 | 2.1990 | 1.3537 | 0.3277 | 0.0323 | 0.5110 | 5.1067 | 0.5340 | 96.0103 |
| GTCD | plagioclase | 61 | 25.7054 | 0.0082 | 0.5501 | 12.0239 | 0.4513 | 0.7199 | 8.7354 | 22.9248 | 2.7891 | 12.0410 | 2.2235 | 1.3650 | 0.3316 | 0.0685 | 0.4819 | 5.3637 | 0.3791 | 96.1724 |
| GTCD | plagioclase | 61 | 25.6737 | 0.0027 | 0.3704 | 12.1521 | 0.5351 | 0.6893 | 8.8836 | 23.5283 | 2.7870 | 11.9987 | 2.2225 | 1.3852 | 0.3446 | 0.0399 | 0.4443 | 4.1098 | 0.6196 | 95.7968 |
| GTCD | plagioclase | 62 | 25.4402 | 0.1095 | 0.7059 | 11.7896 | 0.4912 | 0.7627 | 8.6185 | 22.5775 | 2.9331 | 11.7675 | 2.0882 | 1.2440 | 0.3589 | 0.0833 | 0.4698 | 4.6041 | 0.3345 | 94.3885 |
| GTCD | plagioclase | 63 | 25.7123 | 0.0160 | 0.5293 | 12.1054 | 0.5971 | 1.1545 | 8.3867 | 22.3422 | 2.7259 | 11.6642 | 2.1094 | 1.4511 | 0.3975 | 0.1682 | 0.5087 | 5.9044 | 0.3642 | 96.1471 |
| GTCD | plagioclase | 64 | 25.5485 | 0.0177 | 0.5762 | 11.9562 | 0.4588 | 0.6624 | 8.6083 | 22.5016 | 2.7136 | 12.0303 | 2.3013 | 1.2847 | 0.3223 | 0.0949 | 0.5063 | 5.3371 | 0.3621 | 95.2923 |
| GTCD | plagioclase | 64 | 25.6337 | 0.0168 | 0.5347 | 12.0456 | 0.3832 | 1.1824 | 8.7959 | 22.5732 | 2.7482 | 12.1596 | 2.1571 | 1.4427 | 0.5128 | 0.0987 | 0.4715 | 5.1146 | 0.2081 | 96.0888 |
| GTCD | plagioclase | 65 | 25.9467 | 0.0138 | 0.5411 | 12.2401 | 0.4720 | 0.7240 | 8.7399 | 22.7718 | 2.9228 | 12.0288 | 2.0682 | 1.3346 | 0.3585 | 0.1118 | 0.4554 | 5.2370 | 0.3980 | 96.3745 |
| GTCD | plagioclase | 65 | 25.7158 | 0.0252 | 0.5431 | 12.1346 | 0.3756 | 1.2072 | 8.6914 | 22.5321 | 2.7367 | 12.0641 | 2.1747 | 1.4554 | 0.5057 | 0.1384 | 0.4111 | 5.0369 | 0.2240 | 95.9820 |
| GTCD | plagioclase | 66 | 25.7808 | 0.0221 | 0.5479 | 12.1085 | 0.4585 | 0.6806 | 8.7164 | 22.8895 | 2.7702 | 12.1830 | 2.0870 | 1.2640 | 0.3143 | 0.0700 | 0.4725 | 5.2379 | 0.3775 | 95.9907 |
| GTCD | plagioclase | 66 | 25.7312 | 0.0204 | 0.4739 | 12.2396 | 0.6493 | 1.2002 | 8.2764 | 22.0187 | 2.6666 | 11.5872 | 2.1552 | 1.4796 | 0.5373 | 0.1002 | 0.5583 | 5.2628 | 0.6873 | 95.6542 |
| GTCD | cordierite | 67 | 25.7251 | 0.0375 | 0.2015 | 12.6670 | 0.8158 | 2.2827 | 10.4738 | 21.7731 | 2.3428 | 9.6024 | 1.4395 | 1.1341 | 0.7033 | 0.2401 | 0.5094 | 4.1621 | 0.6609 | 94.7811 |
| GTCD | cordierite | 68 | 25.4715 | 0.0279 | 0.1900 | 12.4403 | 0.8358 | 2.1070 | 10.6194 | 21.8555 | 2.3732 | 9.5653 | 1.4892 | 1.1273 | 0.6030 | 0.2069 | 0.5140 | 4.3067 | 0.7133 | 94.4563 |
| GTCD | cordierite | crd_67 | 26.3889 | 0.0279 | 1.0108 | 11.8217 | 0.4359 | 0.4832 | 8.2022 | 23.0248 | 2.9217 | 12.0768 | 2.1632 | 1.2704 | 0.2458 | 0.1226 | 0.7807 | 8.6735 | 0.4108 | 100.0709 |
| GTCD | cordierite | crd_68 | 26.1469 | 0.0109 | 0.9245 | 11.7300 | 0.4437 | 0.3319 | 8.5322 | 23.3493 | 2.9446 | 11.8656 | 2.2459 | 1.1584 | 0.2185 | 0.0929 | 0.7162 | 8.0026 | 0.5231 | 99.2472 |
| GTCD | cordierite | crd_69 | 26.2267 | 0.0342 | 0.8562 | 11.9366 | 0.4866 | 0.8968 | 8.5328 | 22.9815 | 2.8023 | 11.4090 | 2.1382 | 1.3835 | 0.3495 | 0.1829 | 0.7175 | 7.5221 | 0.7661 | 99.2325 |
| GTCD | cordierite | crd_71 | 25.9273 | 0.0262 | 0.9599 | 11.6178 | 0.4586 | 0.5538 | 8.1547 | 22.8489 | 2.9340 | 11.8177 | 2.1902 | 1.3075 | 0.2551 | 0.0633 | 0.7178 | 7.8714 | 0.7384 | 98.4526 |
| GTCD | cordierite | crd_72 | 26.1919 | 0.0204 | 0.4168 | 12.4986 | 0.7352 | 2.0002 | 9.9882 | 22.9925 | 2.6680 | 9.9738 | 1.6899 | 1.1925 | 0.6092 | 0.1686 | 0.5981 | 5.6273 | 0.7395 | 98.1207 |
| GTCD | cordierite | crd_73 | 26.3774 | 0.0126 | 0.1926 | 12.8914 | 0.8587 | 2.4170 | 11.0249 | 23.1162 | 2.5762 | 9.2168 | 1.4955 | 1.1555 | 0.6847 | 0.2324 | 0.4936 | 4.6309 | 0.6990 | 98.0854 |
| GTCD | cordierite | crd_74 | 26.3547 | 0.0127 | 0.2286 | 12.8725 | 0.8149 | 2.4562 | 10.6223 | 23.1923 | 2.5175 | 9.4514 | 1.6038 | 1.1428 | 0.6712 | 0.2217 | 0.5317 | 4.5699 | 0.6930 | 97.9672 |
| GTCD | cordierite | crd_75 | 26.3658 | 0.0103 | 0.7668 | 12.0713 | 0.4647 | 0.3133 | 9.0364 | 24.0669 | 2.9455 | 11.6827 | 2.0312 | 1.0524 | 0.1625 | 0.0991 | 0.6361 | 6.7631 | 0.5617 | 99.0398 |
| GTCD | cordierite | crd_76 | 26.1176 | 0.0303 | 0.8465 | 11.8357 | 0.4463 | 0.4229 | 8.4088 | 23.2300 | 2.9521 | 11.9144 | 2.3018 | 1.3055 | 0.2595 | 0.0956 | 0.6239 | 7.4025 | 0.4428 | 98.6462 |
| GTCD | cordierite | crd_77 | 26.1389 | 0.0292 | 0.8593 | 11.7698 | 0.4762 | 0.2664 | 8.8690 | 23.5116 | 2.9741 | 11.8030 | 2.1622 | 1.0936 | 0.1597 | 0.0398 | 0.7311 | 7.5436 | 0.5739 | 99.0114 |
| GTCD | cordierite | crd_78 | 26.3876 | 0.0319 | 0.7999 | 12.0311 | 0.4620 | 0.2550 | 8.9292 | 23.8869 | 2.9305 | 11.6026 | 2.1816 | 1.1627 | 0.1114 | 0.0336 | 0.6645 | 7.1815 | 0.5567 | 99.2187 |
| GTCD | cordierite | crd_79 | 26.2203 | 0.0333 | 0.7855 | 11.9058 | 0.4661 | 0.3153 | 8.9896 | 24.0690 | 2.9147 | 11.6950 | 2.1901 | 1.0524 | 0.1116 | 0.0086 | 0.6593 | 6.9985 | 0.5450 | 98.9701 |
| GTCD | cordierite | crd_80 | 26.4006 | 0.0273 | 0.1733 | 12.9195 | 0.8163 | 2.2671 | 11.0543 | 23.4592 | 2.4852 | 9.3463 | 1.4993 | 1.1997 | 0.6064 | 0.2178 | 0.5062 | 4.2214 | 0.7335 | 97.9434 |
| GTCD | cordierite | crd_81 | 26.1339 | 0.0164 | 0.1616 | 12.7343 | 0.8173 | 2.0682 | 11.2289 | 23.5752 | 2.4676 | 9.2543 | 1.5363 | 1.1618 | 0.5773 | 0.1821 | 0.5050 | 4.0680 | 0.6879 | 97.1861 |
| GTCD | cordierite | crd_82 | 26.8451 | 0.8921 | 0.9638 | 11.8557 | 0.4691 | 0.9025 | 8.3986 | 22.8677 | 2.7498 | 11.3398 | 2.1877 | 1.3796 | 0.3436 | 0.0932 | 0.6561 | 7.1544 | 0.5375 | 99.6463 |
| GTCD | cordierite | crd_84 | 26.0683 | 0.0494 | 0.6571 | 12.0462 | 0.3782 | 1.1351 | 8.6295 | 23.9069 | 3.0904 | 11.9231 | 2.0874 | 1.3239 | 0.5098 | 0.1796 | 0.5174 | 5.3687 | 0.4183 | 98.2993 |
| GTCD | cordierite | crd_85 | 26.0490 | 0.0072 | 0.6517 | 12.1743 | 0.5585 | 1.8108 | 8.8654 | 22.6046 | 2.7991 | 10.8777 | 1.9781 | 1.3749 | 0.5417 | 0.1538 | 0.6464 | 6.5056 | 0.6772 | 98.2860 |
| GTCD | cordierite | crd_86 | 26.4668 | 0.0117 | 0.1446 | 12.9508 | 0.8650 | 1.9808 | 11.6273 | 23.7183 | 2.5254 | 9.0519 | 1.4583 | 1.0151 | 0.5780 | 0.1865 | 0.5320 | 4.1126 | 0.7938 | 98.0289 |
| GTCD | cordierite | crd_87 | 26.2466 | 0.0146 | 0.1687 | 12.8454 | 0.8051 | 2.3092 | 11.0569 | 23.4990 | 2.5663 | 9.1122 | 1.5589 | 1.0763 | 0.6149 | 0.2199 | 0.5245 | 4.1423 | 0.7171 | 97.4879 |
| GTCD | cordierite | crd_88 | 26.5094 | 0.0298 | 0.5867 | 12.4784 | 0.5962 | 0.9574 | 9.7846 | 23.6038 | 2.8270 | 10.6708 | 1.9323 | 1.0762 | 0.3045 | 0.1449 | 0.6421 | 5.8474 | 0.5776 | 98.5791 |
| GTCD | cordierite | crd_89 | 26.1021 | 0.0236 | 0.7118 | 11.9519 | 0.4970 | 0.4552 | 9.0876 | 23.6554 | 2.8523 | 11.4213 | 2.0945 | 1.1679 | 0.2464 | 0.0583 | 0.6095 | 6.8998 | 0.5500 | 98.3946 |
| GTCD | cordierite | crd_90 | 26.1651 | 0.0201 | 0.2396 | 12.6826 | 0.7879 | 2.3063 | 10.7525 | 23.0292 | 2.5243 | 9.6522 | 1.6375 | 1.1861 | 0.6398 | 0.1924 | 0.5092 | 4.6768 | 0.7076 | 97.7192 |
| GTCD | cordierite | crd_91 | 26.6352 | 0.4564 | 0.6213 | 12.3789 | 0.6577 | 1.8528 | 9.5227 | 22.7122 | 2.7407 | 10.5982 | 1.9321 | 1.3806 | 0.5328 | 0.2402 | 0.5668 | 5.4296 | 0.6172 | 98.8854 |
| GTCD | cordierite | crd_92 | 26.1060 | 0.0161 | 0.2021 | 12.7567 | 0.8302 | 2.4236 | 10.7788 | 23.0547 | 2.4130 | 9.1418 | 1.5806 | 1.1612 | 0.6507 | 0.2183 | 0.5182 | 4.4569 | 0.7582 | 97.0771 |
| GTCD | cordierite | crd_93 | 25.9014 | 0.0242 | 0.7997 | 11.7856 | 0.4687 | 0.8127 | 8.4582 | 22.9900 | 2.9512 | 11.6025 | 2.2748 | 1.3484 | 0.3252 | 0.0956 | 0.6879 | 6.9891 | 0.6135 | 98.1387 |
| GTCD | cordierite | crd_95 | 26.3236 | 0.1450 | 0.7313 | 12.0555 | 0.4380 | 0.9671 | 8.8333 | 24.0212 | 2.9845 | 11.5973 | 2.1472 | 1.2936 | 0.3648 | 0.1254 | 0.5266 | 5.9638 | 0.4849 | 99.0131 |
| GTCD | cordierite | crd_96 | 26.0264 | 0.0189 | 0.7532 | 11.8359 | 0.4610 | 0.7208 | 8.7442 | 23.7234 | 2.9164 | 11.8543 | 2.1269 | 1.2439 | 0.2647 | 0.0743 | 0.6526 | 6.6861 | 0.6575 | 98.7705 |
| GTCD | cordierite | crd_97 | 26.4098 | 0.0153 | 0.7296 | 12.1595 | 0.4257 | 0.6722 | 8.6376 | 23.5861 | 2.9885 | 11.9834 | 2.2539 | 1.4959 | 0.3235 | 0.0869 | 0.6147 | 6.6402 | 0.3455 | 99.3783 |
| GTCD | cordierite | crd_98 | 26.2903 | 0.0138 | 0.7287 | 12.0883 | 0.4494 | 0.7904 | 8.7411 | 23.5295 | 3.0046 | 11.7183 | 2.2193 | 1.3875 | 0.3389 | 0.1164 | 0.5922 | 6.5870 | 0.5170 | 99.1227 |
| GTCD | cordierite | crd_99 | 26.2364 | 0.0248 | 0.6322 | 12.0948 | 0.4910 | 0.9573 | 9.0156 | 23.7839 | 2.9403 | 11.7553 | 2.2292 | 1.3173 | 0.3841 | 0.0820 | 0.5848 | 6.1596 | 0.5307 | 99.2293 |
| GTCD | cordierite | crd_100 | 26.2051 | 0.0068 | 0.7194 | 12.0211 | 0.4575 | 0.9251 | 8.8333 | 23.7170 | 2.9747 | 11.7159 | 2.1215 | 1.2805 | 0.2950 | 0.1396 | 0.6462 | 6.4653 | 0.6677 | 99.2017 |
| GTCD | cordierite | crd_101 | 26.3789 | 0.0164 | 0.6914 | 12.1278 | 0.4819 | 0.6807 | 9.0025 | 24.2086 | 3.0525 | 11.6009 | 2.1746 | 1.2351 | 0.2647 | 0.0826 | 0.6035 | 6.2317 | 0.5835 | 99.4273 |
| GTCD | sillimanite | als_1 | 26.6065 | 0.0381 | 0.5929 | 12.4061 | 0.4935 | 0.7064 | 9.0237 | 24.2724 | 3.0332 | 11.8220 | 2.1768 | 1.3339 | 0.3826 | 0.0306 | 0.5160 | 5.6110 | 0.4007 | 99.4564 |
| GTCD | sillimanite | als_2 | 26.7354 | 0.0101 | 0.5265 | 12.5760 | 0.5577 | 1.0355 | 9.2181 | 24.2870 | 2.8827 | 11.5295 | 2.1019 | 1.3494 | 0.3596 | 0.0943 | 0.5443 | 5.6885 | 0.5022 | 100.0087 |

| Sample | Phase | Label | W%(O ) | W%(Al) | W%(Si) | W%(P) | W%(Ca) | W%(Y ) | W%(La) | W%(Ce) | W%(Pr) | W%(Nd) | W%(Sm) | W%(Gd) | W%(Dy) | W%(Er) | W%(Pb) | W%(Th) | W%(U ) | W%(SUM) |
|---|---|---|---|---|---|---|---|---|---|---|---|---|---|---|---|---|---|---|---|---|
| GTCD | sillimanite | als_3 | 26.5888 | 0.0816 | 0.4599 | 12.9115 | 0.7020 | 3.1301 | 9.1445 | 22.6859 | 2.5642 | 10.0721 | 1.8795 | 1.4161 | 0.8297 | 0.3017 | 0.5042 | 4.7784 | 0.6007 | 98.6609 |
| GTCD | sillimanite | als_4 | 26.8300 | 0.0201 | 0.2315 | 13.1535 | 0.7802 | 2.4691 | 10.5539 | 23.6995 | 2.5596 | 9.5926 | 1.7080 | 1.2068 | 0.6710 | 0.1932 | 0.5246 | 4.4476 | 0.7366 | 99.3878 |
| GTCD | sillimanite | als_5 | 26.4968 | 0.0170 | 0.4189 | 12.8113 | 0.6110 | 3.0312 | 8.8744 | 22.8315 | 2.6154 | 10.6224 | 1.9724 | 1.5262 | 0.7825 | 0.3455 | 0.4840 | 5.3366 | 0.5486 | 99.3357 |
| GTCD | sillimanite | als_6 | 27.1735 | 0.4004 | 0.3934 | 13.0998 | 0.8103 | 2.6004 | 9.7941 | 22.8773 | 2.5369 | 10.0485 | 1.8279 | 1.2998 | 0.6444 | 0.1887 | 0.5961 | 4.6918 | 0.8134 | 99.8067 |
| GTCD | sillimanite | als_7 | 26.6938 | 0.0127 | 0.5856 | 12.4915 | 0.4781 | 0.9679 | 8.8010 | 24.2613 | 2.9156 | 11.7618 | 2.2438 | 1.3955 | 0.3651 | 0.0798 | 0.5486 | 5.9408 | 0.4897 | 100.0426 |
| GTCD | sillimanite | als_8 | 26.3944 | 0.0021 | 0.3879 | 12.8002 | 0.6403 | 3.0619 | 8.8269 | 22.7810 | 2.7638 | 10.5922 | 1.9244 | 1.4473 | 0.7691 | 0.2825 | 0.5209 | 5.1301 | 0.5623 | 98.8973 |
| GTCD | sillimanite | als_9 | 26.5793 | 0.0134 | 0.2708 | 12.9991 | 0.8670 | 3.1016 | 9.2088 | 22.6096 | 2.5396 | 10.3140 | 1.8516 | 1.4720 | 0.7290 | 0.2910 | 0.6044 | 4.9292 | 0.8784 | 99.2688 |
| GTCD | sillimanite | als_10 | 26.7541 | 0.0002 | 0.5722 | 12.6808 | 0.5207 | 1.5925 | 8.6559 | 23.1049 | 2.9029 | 11.7290 | 2.2303 | 1.5552 | 0.4566 | 0.0943 | 0.5804 | 6.0203 | 0.5258 | 99.9861 |
| GTCD | sillimanite | als_11 | 26.8352 | 0.0002 | 0.4312 | 12.9264 | 0.6016 | 2.5169 | 9.1399 | 23.2099 | 2.7270 | 11.1226 | 2.0325 | 1.4811 | 0.6518 | 0.2077 | 0.5381 | 5.3996 | 0.5850 | 100.4167 |
| GTCD | sillimanite | als_13 | 26.8810 | 0.0257 | 0.5713 | 12.5471 | 0.4783 | 0.6508 | 9.0286 | 24.4596 | 2.9302 | 12.2019 | 2.3166 | 1.3875 | 0.3093 | 0.0567 | 0.5585 | 5.7708 | 0.4509 | 100.6348 |
| PS | matrix | 1 | 26.5051 | 0.0040 | 0.2072 | 12.7574 | 1.0857 | 0.3594 | 11.9396 | 22.9113 | 2.5260 | 9.3976 | 1.5880 | 1.1439 | 0.2190 | 0.1484 | 0.8170 | 4.0220 | 2.0642 | 98.5228 |
| PS | matrix | 2 | 26.1250 | 0.0002 | 0.1922 | 12.5006 | 1.0386 | 0.3591 | 12.1903 | 22.9860 | 2.4566 | 9.4445 | 1.5934 | 0.9730 | 0.1809 | 0.0363 | 0.7977 | 4.0698 | 1.9184 | 96.8726 |
| PS | matrix | 3 | 27.2293 | 0.0022 | 0.1950 | 13.3590 | 0.9706 | 0.6285 | 12.0791 | 23.2006 | 2.5297 | 9.5498 | 1.5982 | 1.1074 | 0.3053 | 0.0484 | 0.7219 | 4.0112 | 1.4956 | 99.0418 |
| PS | matrix | 4 | 25.9545 | 0.0149 | 0.1906 | 12.7103 | 0.6921 | 2.3186 | 11.8541 | 22.3712 | 2.4931 | 9.1785 | 1.5376 | 1.3379 | 0.7066 | 0.1750 | 0.4787 | 3.2773 | 1.0024 | 96.3034 |
| PS | matrix | 5 | 26.1522 | 0.0002 | 0.1404 | 12.7105 | 0.3668 | 1.4554 | 12.7354 | 24.6039 | 2.6875 | 10.2205 | 1.7808 | 1.1885 | 0.4575 | 0.1078 | 0.2697 | 1.5377 | 0.5773 | 97.0021 |
| PS | matrix | 6 | 26.1416 | 0.0021 | 0.2117 | 12.6463 | 0.7463 | 1.5825 | 12.2330 | 23.1746 | 2.3599 | 9.3730 | 1.5901 | 1.0608 | 0.5510 | 0.1933 | 0.4759 | 4.3384 | 0.4879 | 97.1784 |
| PS | matrix | 7 | 26.7979 | 0.0051 | 0.1416 | 13.2809 | 0.4101 | 1.6383 | 12.3499 | 24.0887 | 2.6425 | 10.2525 | 1.8098 | 1.2470 | 0.5762 | 0.1548 | 0.2852 | 1.4931 | 0.6549 | 97.8385 |
| PS | matrix | 8 | 26.3819 | 0.0057 | 0.1806 | 12.8670 | 0.6611 | 1.7463 | 12.2708 | 23.5373 | 2.5093 | 9.5794 | 1.6720 | 1.2057 | 0.5159 | 0.2020 | 0.4093 | 3.3044 | 0.5599 | 97.6186 |
| PS | matrix | 10 | 26.2655 | 0.0066 | 0.1695 | 12.8011 | 0.5518 | 1.6113 | 12.4190 | 23.7753 | 2.5285 | 9.9364 | 1.5657 | 1.0712 | 0.4944 | 0.1476 | 0.3872 | 2.8640 | 0.6053 | 97.2104 |
| PS | matrix | 11 | 26.0220 | 0.0128 | 0.1560 | 12.7297 | 0.4523 | 1.6264 | 12.4612 | 23.5555 | 2.5785 | 10.0118 | 1.6797 | 1.2350 | 0.5706 | 0.1355 | 0.2812 | 1.7331 | 0.7451 | 95.9964 |
| PS | matrix | 12 | 25.9400 | 0.0102 | 0.1238 | 12.6592 | 0.2966 | 1.4905 | 12.6636 | 24.6590 | 2.6691 | 10.1056 | 1.8019 | 1.2402 | 0.4946 | 0.0834 | 0.2876 | 0.5539 | 0.8636 | 95.9528 |
| PS | matrix | 13 | 25.9133 | 0.0051 | 0.2091 | 12.3927 | 0.9414 | 0.5213 | 12.0000 | 22.8156 | 2.6202 | 9.5444 | 1.5333 | 1.0593 | 0.2986 | 0.0671 | 0.6678 | 4.0263 | 1.5547 | 96.1802 |
| PS | matrix | 14 | 26.3202 | 0.0219 | 0.2094 | 12.6852 | 1.0674 | 0.3599 | 11.8775 | 22.5432 | 2.5288 | 9.4853 | 1.6089 | 0.9784 | 0.2322 | 0.0796 | 0.8354 | 3.9158 | 2.0566 | 96.8157 |
| PS | matrix | 15 | 26.3792 | 0.0002 | 0.2078 | 12.7123 | 1.0163 | 0.3641 | 12.0658 | 22.7217 | 2.4500 | 9.5166 | 1.5369 | 1.0866 | 0.2429 | 0.0917 | 0.8341 | 3.9902 | 1.9973 | 97.2237 |
| PS | matrix | 16 | 26.5176 | 0.0124 | 0.1942 | 12.8328 | 0.9872 | 0.4059 | 11.8839 | 22.9421 | 2.5829 | 9.5947 | 1.5529 | 0.9925 | 0.2180 | 0.0826 | 0.7356 | 4.1740 | 1.6718 | 97.3911 |
| PS | matrix | 17 | 26.1938 | 0.0002 | 0.2055 | 12.6268 | 0.9340 | 0.5376 | 11.9858 | 22.6733 | 2.5324 | 9.6647 | 1.5740 | 1.1229 | 0.2780 | 0.0602 | 0.6888 | 4.0286 | 1.5342 | 96.6508 |
| PS | matrix | 18 | 26.9767 | 0.0056 | 0.1742 | 13.3770 | 0.7932 | 1.6359 | 12.0215 | 22.7286 | 2.5399 | 9.3809 | 1.5310 | 1.2089 | 0.5245 | 0.1480 | 0.5846 | 3.5534 | 1.1615 | 98.3554 |
| PS | matrix | 19 | 25.7233 | 0.0064 | 0.1930 | 12.4441 | 0.5851 | 1.7628 | 12.1865 | 22.9811 | 2.5545 | 9.6825 | 1.6704 | 1.2469 | 0.5573 | 0.1080 | 0.4070 | 3.1583 | 0.6326 | 95.9098 |
| PS | matrix | 20 | 25.8020 | 0.0002 | 0.1794 | 12.6022 | 0.6675 | 1.9348 | 12.0223 | 22.4820 | 2.5223 | 9.3458 | 1.5268 | 1.1511 | 0.5482 | 0.1416 | 0.4350 | 3.5530 | 0.7467 | 95.6709 |
| PS | matrix | 21 | 26.0214 | 0.0136 | 0.1757 | 12.7573 | 0.6644 | 1.9114 | 12.0209 | 22.3784 | 2.4690 | 9.5304 | 1.6195 | 1.2330 | 0.5903 | 0.2059 | 0.4700 | 3.2554 | 0.7818 | 96.1084 |
| PS | matrix | 22 | 25.7519 | 0.0105 | 0.1824 | 12.5731 | 0.7671 | 1.9455 | 11.7748 | 22.0446 | 2.4104 | 9.4558 | 1.4707 | 1.2233 | 0.6002 | 0.2281 | 0.4721 | 3.6165 | 0.8936 | 95.4306 |
| PS | matrix | 23 | 27.0332 | 0.0233 | 0.2272 | 13.2743 | 1.3533 | 0.8293 | 11.6482 | 21.6817 | 2.5187 | 9.6089 | 1.5814 | 1.1395 | 0.3563 | 0.0621 | 0.7495 | 4.0349 | 1.6032 | 97.7350 |
| PS | matrix | 24 | 28.0466 | 0.0263 | 0.2206 | 13.9497 | 1.7560 | 0.6745 | 12.0073 | 21.9767 | 2.4777 | 9.3814 | 1.5136 | 1.1553 | 0.3443 | 0.0798 | 0.6564 | 3.8319 | 1.3099 | 99.4180 |
| PS | matrix | 25 | 26.0169 | 0.0178 | 0.2283 | 12.5726 | 0.8138 | 0.6325 | 11.9939 | 22.4939 | 2.5520 | 9.5185 | 1.6961 | 1.0760 | 0.3218 | 0.0067 | 0.5993 | 3.8925 | 1.2687 | 95.7113 |
| PS | matrix | 26 | 25.7284 | 0.0117 | 0.2256 | 12.2903 | 0.8445 | 0.6928 | 12.1654 | 22.4723 | 2.5918 | 9.6367 | 1.6040 | 1.1728 | 0.3351 | 0.0930 | 0.6260 | 3.9335 | 1.2524 | 95.6863 |
| PS | matrix | 27 | 26.5600 | 0.0097 | 0.2183 | 12.8687 | 0.9670 | 0.7542 | 12.3345 | 22.5074 | 2.5656 | 9.7108 | 1.6094 | 1.1669 | 0.2678 | 0.1442 | 0.6307 | 3.9647 | 1.2578 | 97.5477 |
| PS | matrix | 29 | 26.4576 | 0.0130 | 0.1984 | 12.8746 | 0.9781 | 0.6867 | 12.0712 | 22.3727 | 2.6623 | 9.4640 | 1.5726 | 1.1648 | 0.3402 | 0.0790 | 0.5996 | 3.9045 | 1.3617 | 96.8110 |
| PS | matrix | 30 | 25.9205 | 0.0021 | 0.2101 | 12.4263 | 1.0862 | 0.5731 | 11.9944 | 22.1853 | 2.6110 | 9.5527 | 1.5634 | 1.0701 | 0.2738 | 0.0388 | 0.7635 | 3.8619 | 1.8019 | 95.9451 |
| PS | matrix | 31 | 26.1869 | 0.0002 | 0.2076 | 12.6935 | 0.9462 | 1.0756 | 12.2216 | 22.5350 | 2.5944 | 9.2935 | 1.5625 | 1.0847 | 0.3768 | 0.1391 | 0.5944 | 3.8201 | 1.1750 | 96.5171 |
| PS | matrix | 32 | 26.0495 | 0.0011 | 0.1770 | 12.6572 | 0.6708 | 1.2483 | 12.3657 | 23.1005 | 2.6696 | 9.6447 | 1.6279 | 1.1868 | 0.5241 | 0.0714 | 0.4764 | 2.9248 | 0.8403 | 96.2461 |
| PS | matrix | 33 | 26.1708 | 0.0061 | 0.1376 | 12.7420 | 0.3675 | 1.0563 | 13.2059 | 24.1047 | 2.7475 | 10.0556 | 1.7527 | 1.2290 | 0.3967 | 0.1522 | 0.2220 | 1.8816 | 0.2365 | 96.4747 |
| PS | matrix | 34 | 26.4004 | 0.0099 | 0.3054 | 12.6822 | 1.1483 | 0.8237 | 11.1762 | 21.1256 | 2.5278 | 9.9201 | 1.9633 | 1.5216 | 0.4308 | 0.0362 | 0.7005 | 5.3883 | 1.2357 | 97.4060 |
| PS | matrix | 35 | 28.5515 | 0.0246 | 0.2367 | 14.3807 | 2.1786 | 1.2562 | 12.1972 | 21.7569 | 2.3973 | 9.3381 | 1.6063 | 1.2340 | 0.4546 | 0.0861 | 0.3269 | 3.1733 | 0.2742 | 99.4832 |
| PS | matrix | 36 | 25.8927 | 0.0013 | 0.1564 | 12.5821 | 0.3605 | 1.1159 | 12.9187 | 23.7676 | 2.7092 | 10.2669 | 1.7378 | 1.2396 | 0.4709 | 0.0239 | 0.2310 | 1.8085 | 0.3125 | 95.6055 |
| PS | matrix | 37 | 25.8994 | 0.0140 | 0.1376 | 12.6066 | 0.3475 | 1.0695 | 13.1588 | 23.8717 | 2.8166 | 10.1933 | 1.6488 | 1.0896 | 0.4285 | 0.1502 | 0.1993 | 1.4223 | 0.3572 | 95.4209 |
| PS | matrix | 38 | 25.8799 | 0.0138 | 0.1976 | 12.6316 | 0.6886 | 1.6665 | 12.0501 | 22.0643 | 2.6254 | 9.5194 | 1.5853 | 1.1340 | 0.5240 | 0.1602 | 0.4412 | 3.8725 | 0.5137 | 95.5781 |
| PS | matrix | 39 | 26.0684 | 0.0002 | 0.1775 | 12.7114 | 0.4534 | 1.0193 | 12.8424 | 23.2825 | 2.5917 | 10.1090 | 1.6733 | 1.2415 | 0.3785 | 0.1446 | 0.2885 | 2.5713 | 0.2234 | 95.7869 |
| PS | matrix | 41 | 27.0711 | 0.0115 | 0.1855 | 13.3339 | 1.2623 | 0.4210 | 12.0917 | 22.0282 | 2.2910 | 9.5227 | 1.5142 | 1.0229 | 0.2150 | 0.0714 | 0.7728 | 4.1926 | 1.5808 | 97.5986 |
| PS | matrix | 42 | 26.0187 | 0.0050 | 0.2020 | 12.5395 | 1.0071 | 0.3742 | 12.3010 | 22.1640 | 2.6147 | 9.2998 | 1.5864 | 1.0182 | 0.1834 | 0.0662 | 0.6952 | 4.0391 | 1.6293 | 95.7538 |
| PS | matrix | 44 | 26.8287 | 0.0141 | 0.2013 | 13.0980 | 1.1780 | 0.4837 | 12.0989 | 21.9348 | 2.5670 | 9.5217 | 1.6085 | 1.0147 | 0.2002 | 0.0426 | 0.8543 | 4.0948 | 1.9022 | 97.6535 |
| PS | matrix | 45 | 25.7055 | 0.0002 | 0.1967 | 12.3273 | 1.0448 | 0.3731 | 12.2415 | 21.8856 | 2.5113 | 9.3697 | 1.5885 | 1.0119 | 0.2304 | 0.0530 | 0.7203 | 4.0853 | 1.6840 | 95.0391 |
| PS | matrix | 46 | 26.2568 | 0.0037 | 0.1939 | 12.7750 | 1.0823 | 0.6261 | 11.9634 | 21.7817 | 2.5623 | 9.6171 | 1.5781 | 1.1247 | 0.3018 | 0.0128 | 0.6677 | 3.9830 | 1.4765 | 96.0169 |
| PS | matrix | 47 | 25.2274 | 0.0172 | 0.2312 | 12.0585 | 0.9230 | 1.2242 | 11.7551 | 21.5014 | 2.5468 | 9.5600 | 1.5678 | 1.1976 | 0.5015 | 0.0792 | 0.6474 | 3.9709 | 1.1470 | 94.1662 |
| PS | matrix | 48 | 25.6695 | 0.0002 | 0.1888 | 12.4573 | 0.9007 | 1.5053 | 11.8661 | 21.5551 | 2.4743 | 9.3508 | 1.5891 | 1.2313 | 0.5089 | 0.1178 | 0.6207 | 3.9698 | 1.1869 | 95.2026 |
| PS | matrix | 49 | 27.0256 | 0.0113 | 0.2041 | 13.4522 | 1.2563 | 1.6881 | 11.6201 | 20.9683 | 2.5243 | 9.4177 | 1.6047 | 1.2491 | 0.5522 | 0.1583 | 0.6368 | 3.9875 | 1.2189 | 97.5855 |
| PS | matrix | 50 | 25.4873 | 0.0011 | 0.1962 | 12.4393 | 0.8667 | 2.0105 | 11.5733 | 20.8813 | 2.4326 | 9.2359 | 1.5918 | 1.3756 | 0.6522 | 0.1291 | 0.5822 | 3.8819 | 1.2428 | 94.5898 |

| Sample | Phase | Label | W%(O) | W%(Al) | W%(Si) | W%(P) | W%(Ca) | W%(Y) | W%(La) | W%(Ce) | W%(Pr) | W%(Nd) | W%(Sm) | W%(Gd) | W%(Dy) | W%(Er) | W%(Pb) | W%(Th) | W%(U) | W%(SUM) |
|---|---|---|---|---|---|---|---|---|---|---|---|---|---|---|---|---|---|---|---|---|
| PS | matrix | 51 | 25.9765 | 0.0002 | 0.1927 | 12.8163 | 0.8973 | 2.3219 | 11.6421 | 20.8129 | 2.4654 | 9.2965 | 1.5678 | 1.3226 | 0.7211 | 0.1197 | 0.5841 | 3.7904 | 1.2022 | 95.7397 |
| PS | matrix | 53 | 25.3180 | 0.0015 | 0.1956 | 12.4079 | 0.8245 | 2.5652 | 11.1293 | 20.6339 | 2.4442 | 9.3119 | 1.6043 | 1.4068 | 0.7459 | 0.1972 | 0.5576 | 3.7197 | 1.1433 | 94.2168 |
| PS | matrix | 54 | 25.9585 | 0.0109 | 0.1763 | 12.7913 | 0.9714 | 2.4761 | 11.5631 | 21.1198 | 2.5067 | 9.1293 | 1.6290 | 1.3114 | 0.7209 | 0.1301 | 0.5590 | 3.6687 | 1.0899 | 95.8224 |
| PS | matrix | 56 | 26.4044 | 0.0128 | 0.1322 | 12.8998 | 1.1226 | 1.4290 | 12.5749 | 22.4541 | 2.6490 | 9.9876 | 1.8496 | 1.3095 | 0.5732 | 0.0806 | 0.3284 | 2.3006 | 0.5255 | 96.6438 |
| PS | matrix | 57 | 26.4180 | 0.0662 | 0.2287 | 12.8382 | 0.6113 | 1.1604 | 13.0579 | 23.6275 | 2.7335 | 10.0326 | 1.6367 | 1.0748 | 0.4500 | 0.1209 | 0.2187 | 1.9723 | 0.2987 | 96.5564 |
| PS | matrix | 59 | 25.7654 | 0.0002 | 0.2020 | 12.3994 | 0.7058 | 0.8157 | 12.5551 | 22.4906 | 2.5366 | 9.8343 | 1.6291 | 1.0855 | 0.3518 | 0.1631 | 0.6055 | 3.1124 | 1.2983 | 95.5608 |
| PS | matrix | 60 | 26.2324 | 0.0002 | 0.1417 | 12.9054 | 0.5071 | 1.1092 | 13.2671 | 23.0212 | 2.6071 | 9.6382 | 1.6931 | 1.2234 | 0.4541 | 0.0124 | 0.2710 | 2.4315 | 0.2826 | 95.8077 |
| PS | matrix | 62 | 25.9063 | 0.0002 | 0.2080 | 12.5272 | 0.8630 | 1.0682 | 11.8882 | 22.2111 | 2.5052 | 9.4803 | 1.6980 | 1.1783 | 0.3786 | 0.0496 | 0.6684 | 3.7201 | 1.5378 | 95.8985 |
| PS | matrix | 63 | 26.3868 | 0.0051 | 0.1794 | 12.9835 | 0.7308 | 1.5288 | 12.3076 | 22.5770 | 2.4679 | 9.5584 | 1.5371 | 1.1281 | 0.5009 | 0.1617 | 0.4341 | 3.6748 | 0.4518 | 96.6238 |
| PS | matrix | 65 | 26.0348 | 0.0002 | 0.1376 | 12.6843 | 0.3328 | 0.9439 | 13.5368 | 24.2354 | 2.7979 | 9.8779 | 1.6084 | 1.1059 | 0.3974 | 0.1338 | 0.1764 | 1.5566 | 0.1748 | 95.7449 |
| PS | matrix | 66 | 27.0308 | 0.0177 | 0.1277 | 13.3975 | 0.5109 | 1.3617 | 13.0908 | 24.0344 | 2.7020 | 10.1446 | 1.7471 | 1.2184 | 0.4482 | 0.1090 | 0.2249 | 1.5989 | 0.3996 | 98.1742 |
| PS | matrix | 67 | 25.9615 | 0.0002 | 0.1874 | 12.6567 | 0.9070 | 1.6585 | 11.9344 | 21.8746 | 2.5263 | 9.3708 | 1.5216 | 1.1425 | 0.4986 | 0.1844 | 0.4592 | 4.4588 | 0.5638 | 95.9163 |
| PS | matrix | 68 | 26.4262 | 0.0031 | 0.2200 | 13.1169 | 0.8457 | 2.1544 | 12.0129 | 22.2750 | 2.5745 | 9.4537 | 1.6250 | 1.3024 | 0.5574 | 0.1602 | 0.2822 | 2.6329 | 0.3430 | 95.9955 |
| PS | matrix | 70 | 25.9640 | 0.0002 | 0.1923 | 12.6661 | 0.8779 | 1.3344 | 11.7476 | 21.8340 | 2.4268 | 9.4731 | 1.5285 | 1.1697 | 0.3769 | 0.1915 | 0.6389 | 3.8349 | 1.4514 | 95.7182 |
| PS | matrix | 72 | 25.6806 | 0.0129 | 0.1790 | 12.5156 | 0.6688 | 1.9995 | 11.9216 | 22.1440 | 2.6423 | 9.4801 | 1.6384 | 1.1307 | 0.5916 | 0.2253 | 0.4422 | 3.3962 | 0.7438 | 95.4226 |
| PS | matrix | 74 | 27.4850 | 0.0356 | 0.2016 | 13.4930 | 1.1246 | 0.5077 | 12.1974 | 22.9011 | 2.4131 | 9.0578 | 1.5106 | 1.0153 | 0.2523 | 0.0246 | 0.8395 | 4.4523 | 2.1350 | 99.6565 |
| PS | matrix | 76 | 27.6889 | 0.0166 | 0.1931 | 13.5630 | 1.7213 | 0.4973 | 11.8998 | 22.6533 | 2.5303 | 9.4263 | 1.4947 | 0.9606 | 0.2629 | 0.0939 | 0.8343 | 4.1205 | 1.8371 | 99.8039 |
| PS | matrix | 78 | 26.8361 | 0.0160 | 0.2023 | 13.1215 | 1.0711 | 0.3522 | 11.9518 | 22.3182 | 2.5221 | 9.5616 | 1.5799 | 1.0857 | 0.2294 | 0.0001 | 0.8000 | 4.0116 | 1.8194 | 97.4890 |
| PS | matrix | 79 | 26.2189 | 0.0233 | 0.2060 | 12.6119 | 1.0265 | 0.4037 | 11.9665 | 22.5764 | 2.5221 | 9.4018 | 1.5671 | 1.0707 | 0.1953 | 0.0634 | 0.8072 | 4.1706 | 1.8606 | 96.7020 |
| PS | matrix | 81 | 26.0402 | 0.0002 | 0.2046 | 12.4666 | 1.1860 | 0.5098 | 11.6645 | 22.6362 | 2.4684 | 9.5119 | 1.5695 | 1.0790 | 0.2609 | 0.0664 | 0.7497 | 4.0241 | 1.9574 | 96.4054 |
| PS | matrix | 82 | 25.5251 | 0.0068 | 0.2171 | 12.0073 | 1.3780 | 0.3537 | 11.6702 | 22.4394 | 2.4884 | 9.5317 | 1.5611 | 1.1165 | 0.2155 | 0.0001 | 0.7596 | 4.0375 | 2.0803 | 95.3983 |
| PS | matrix | 83 | 25.6774 | 0.0179 | 0.2247 | 12.1252 | 0.9574 | 0.4421 | 12.0050 | 23.1377 | 2.4818 | 9.8217 | 1.5262 | 1.0659 | 0.2084 | 0.0547 | 0.7069 | 3.8179 | 1.8248 | 96.1057 |
| PS | matrix | 84 | 26.2042 | 0.0081 | 0.1890 | 12.5846 | 1.0022 | 0.4170 | 11.8057 | 22.9330 | 2.5974 | 9.6810 | 1.5664 | 1.0985 | 0.2302 | 0.0001 | 0.7258 | 3.9481 | 1.9142 | 96.9155 |
| PS | matrix | 85 | 26.9552 | 0.0016 | 0.1901 | 13.0950 | 0.9588 | 0.4323 | 12.2042 | 23.1493 | 2.6201 | 9.6922 | 1.5882 | 1.0610 | 0.2126 | 0.0654 | 0.7528 | 4.2052 | 1.6182 | 98.8122 |
| PS | matrix | 86 | 26.0297 | 0.0163 | 0.1902 | 12.4233 | 0.9888 | 0.4472 | 12.1415 | 23.2543 | 2.5779 | 9.3780 | 1.4711 | 1.0326 | 0.2189 | 0.0011 | 0.6981 | 4.2317 | 1.6252 | 96.7359 |
| PS | matrix | 1 | 26.4103 | 0.0114 | 0.2930 | 12.2977 | 1.4056 | 0.5143 | 9.6062 | 24.4564 | 2.4720 | 9.9945 | 1.9406 | 1.4564 | 0.3398 | 0.0645 | 0.6985 | 7.0218 | 0.5824 | 99.5754 |
| PS | matrix | 2 | 27.6749 | 0.0154 | 0.2449 | 13.3486 | 1.2207 | 0.7271 | 9.9379 | 24.8032 | 2.5580 | 10.0325 | 1.9365 | 1.4299 | 0.2680 | 0.0561 | 0.6332 | 6.4000 | 0.5995 | 101.8964 |
| PS | matrix | 3 | 26.0684 | 0.0152 | 0.2170 | 12.1796 | 1.2104 | 0.5366 | 9.9783 | 24.3751 | 2.5649 | 9.9057 | 1.8204 | 1.5219 | 0.3222 | 0.1242 | 0.6945 | 6.4430 | 0.6106 | 98.5980 |
| PS | matrix | 4 | 26.4526 | 0.0067 | 0.2215 | 12.4177 | 1.1929 | 0.4475 | 9.8219 | 24.6862 | 2.5162 | 10.1278 | 2.1183 | 1.5212 | 0.3205 | 0.0115 | 0.6386 | 6.4989 | 0.5856 | 99.5956 |
| PS | matrix | 5 | 26.9754 | 0.0067 | 0.2350 | 12.7975 | 1.2048 | 0.6916 | 9.9518 | 24.6569 | 2.4403 | 10.0703 | 2.0228 | 1.5611 | 0.3380 | 0.0638 | 0.6165 | 6.5830 | 0.6344 | 100.8599 |
| PS | matrix | 6 | 25.9035 | 0.0058 | 0.2250 | 12.0660 | 1.2424 | 0.5439 | 9.7912 | 24.2188 | 2.5186 | 9.8138 | 2.0151 | 1.4719 | 0.3756 | 0.0480 | 0.6418 | 6.6639 | 0.6370 | 98.1923 |
| PS | matrix | 7 | 26.4402 | 0.0063 | 0.2443 | 12.4106 | 1.2568 | 0.5095 | 9.7369 | 24.2562 | 2.5554 | 9.9707 | 2.0656 | 1.4940 | 0.3151 | 0.0413 | 0.6604 | 6.9173 | 0.6093 | 99.4999 |
| PS | matrix | 8 | 26.8512 | 0.0002 | 0.2356 | 12.7255 | 1.2884 | 0.4796 | 9.8548 | 24.3567 | 2.5092 | 9.9454 | 1.9564 | 1.4781 | 0.4151 | 0.0660 | 0.6955 | 6.8204 | 0.5629 | 100.2510 |
| PS | matrix | 10 | 25.9130 | 0.0002 | 0.2197 | 12.1041 | 1.2352 | 0.5086 | 9.7606 | 24.0545 | 2.4846 | 9.7706 | 2.0493 | 1.5710 | 0.3178 | 0.0939 | 0.6144 | 6.7054 | 0.6249 | 98.0378 |
| PS | matrix | 11 | 26.3351 | 0.0047 | 0.2296 | 12.4117 | 1.2454 | 0.5257 | 9.7268 | 23.9569 | 2.5845 | 9.8848 | 1.9637 | 1.5291 | 0.2931 | 0.1005 | 0.6863 | 6.7778 | 0.6194 | 98.8851 |
| PS | matrix | 13 | 25.9701 | 0.0059 | 0.2092 | 12.1605 | 1.2481 | 0.6095 | 9.8364 | 23.7979 | 2.5603 | 9.8766 | 2.0344 | 1.4953 | 0.3822 | 0.0539 | 0.6092 | 6.5996 | 0.7110 | 98.1701 |
| PS | matrix | 14 | 25.4582 | 0.0141 | 0.2385 | 11.7644 | 1.2162 | 0.4498 | 9.6413 | 24.0472 | 2.6298 | 9.8023 | 1.9922 | 1.4285 | 0.3361 | 0.0349 | 0.5610 | 6.7476 | 0.5103 | 96.8824 |
| PS | matrix | 16 | 27.0398 | 0.0495 | 0.2459 | 13.1405 | 1.3059 | 0.8593 | 9.3303 | 22.9380 | 2.5081 | 9.7145 | 2.0099 | 1.6031 | 0.4853 | 0.0683 | 0.7285 | 6.0083 | 0.8125 | 98.8577 |
| PS | matrix | 17 | 25.9725 | 0.0058 | 0.2143 | 12.1823 | 1.2180 | 0.5411 | 9.5671 | 23.9332 | 2.5674 | 9.9695 | 2.1120 | 1.4982 | 0.4208 | 0.0435 | 0.6169 | 6.4650 | 0.6224 | 97.9600 |
| PS | matrix | 18 | 26.5911 | 0.0169 | 0.2622 | 12.5615 | 1.2528 | 0.3508 | 9.5832 | 24.1286 | 2.4366 | 10.0027 | 1.9865 | 1.3271 | 0.3426 | 0.1105 | 0.7170 | 7.0135 | 0.5915 | 99.2851 |
| PS | matrix | 19 | 25.4663 | 0.0010 | 0.1977 | 11.9499 | 1.2648 | 0.6992 | 9.4000 | 23.4461 | 2.4491 | 9.8985 | 1.9302 | 1.4942 | 0.4065 | 0.0568 | 0.6706 | 6.1804 | 0.6793 | 96.2006 |
| PS | matrix | 20 | 25.9230 | 0.0124 | 0.2132 | 12.1929 | 1.1985 | 0.5182 | 9.5851 | 24.0394 | 2.5246 | 9.9048 | 1.9457 | 1.4478 | 0.4089 | 0.0337 | 0.6298 | 6.3139 | 0.5778 | 97.4797 |
| PS | matrix | 21 | 26.6534 | 0.0002 | 0.2721 | 12.6016 | 1.2833 | 0.3872 | 9.4770 | 24.2241 | 2.5711 | 9.7633 | 1.9929 | 1.3938 | 0.2813 | 0.1160 | 0.6522 | 7.3158 | 0.4522 | 99.4475 |
| PS | matrix | 22 | 25.7392 | 0.0101 | 0.2127 | 12.0606 | 1.2076 | 0.5637 | 9.6052 | 24.1050 | 2.4912 | 9.7269 | 1.9907 | 1.4611 | 0.3457 | 0.0429 | 0.5848 | 6.3767 | 0.5794 | 97.1135 |
| CB6 | quartz | a_5 | 26.8281 | 0.0002 | 0.2141 | 12.9103 | 0.8800 | 0.3426 | 11.5763 | 24.8907 | 2.6319 | 9.8965 | 1.7263 | 0.8007 | 0.0900 | 0.0435 | 0.5444 | 4.7186 | 0.6899 | 98.7941 |
| CB6 | quartz | a_6 | 26.5977 | 0.0002 | 0.2272 | 12.7075 | 0.8632 | 0.2964 | 11.7513 | 24.8116 | 2.6999 | 9.9143 | 1.6609 | 0.8428 | 0.0995 | 0.0584 | 0.4942 | 4.6622 | 0.7200 | 98.4173 |
| CB6 | quartz | a_7 | 26.3984 | 0.0058 | 0.2025 | 12.6046 | 0.8834 | 0.2950 | 11.5970 | 24.7737 | 2.7656 | 9.6845 | 1.7303 | 0.7935 | 0.1408 | 0.0001 | 0.4869 | 4.7589 | 0.6828 | 97.8138 |
| CB6 | quartz | a_8 | 26.0355 | 0.0023 | 0.2869 | 12.4002 | 0.8494 | 0.5687 | 11.3071 | 23.9028 | 2.6621 | 9.8054 | 1.6827 | 0.9595 | 0.1962 | 0.0279 | 0.5214 | 4.6477 | 0.6905 | 96.5563 |
| CB6 | quartz | a_9 | 26.0355 | 0.0007 | 0.2864 | 12.6061 | 0.8872 | 0.2665 | 11.2185 | 24.3079 | 2.7002 | 9.8219 | 1.7375 | 0.8705 | 0.1015 | 0.0001 | 0.5869 | 5.0110 | 0.7018 | 97.5264 |
| CB6 | quartz | a_10 | 26.5158 | 0.0156 | 0.5273 | 12.3527 | 1.0772 | 0.2956 | 10.6510 | 22.9299 | 2.4518 | 9.7113 | 1.5507 | 0.8026 | 0.1292 | 0.0141 | 0.7966 | 8.5896 | 0.6036 | 99.0246 |
| CB6 | quartz | a_11 | 26.3837 | 0.0082 | 0.3539 | 12.4629 | 1.0972 | 0.5208 | 10.7560 | 23.2312 | 2.5523 | 9.2867 | 1.6170 | 1.0681 | 0.2167 | 0.0156 | 0.7687 | 7.0435 | 1.0263 | 98.4188 |
| CB6 | quartz | a_12 | 26.6979 | 0.0101 | 0.2317 | 12.7707 | 0.8962 | 0.3433 | 11.3019 | 24.5382 | 2.6472 | 10.2538 | 1.6977 | 0.8243 | 0.1316 | 0.0151 | 0.5296 | 5.2100 | 0.6358 | 98.7451 |
| CB6 | quartz | a_13 | 26.7615 | 0.0002 | 0.2219 | 12.8525 | 0.9041 | 0.3522 | 11.1840 | 24.6831 | 2.6872 | 9.9728 | 1.7895 | 0.8142 | 0.1449 | 0.0778 | 0.5510 | 5.0909 | 0.6432 | 98.7410 |
| CB6 | quartz | a_14 | 25.7637 | 0.0737 | 0.5242 | 11.8846 | 0.7821 | 0.3901 | 11.3707 | 24.3028 | 2.5672 | 9.6151 | 1.6706 | 1.0061 | 0.1936 | 0.0725 | 0.3831 | 5.1834 | 0.5486 | 96.3421 |
| CB6 | quartz | a_15 | 26.4365 | 0.0025 | 0.3977 | 12.4841 | 1.2718 | 0.5777 | 10.4806 | 22.3765 | 2.4865 | 9.1038 | 1.5511 | 1.1301 | 0.2373 | 0.0672 | 0.8624 | 7.8736 | 1.1412 | 98.4906 |
| CB6 | quartz | a_16 | 26.3460 | 0.0002 | 0.3897 | 12.4406 | 1.2415 | 0.5344 | 10.4941 | 22.4088 | 2.4801 | 8.9324 | 1.5622 | 1.1074 | 0.2708 | 0.0696 | 0.8679 | 7.9262 | 1.1357 | 98.2176 |

| Sample | Phase | Label | W%(O) | W%(Al) | W%(Si) | W%(P) | W%(Ca) | W%(Y) | W%(La) | W%(Ce) | W%(Pr) | W%(Nd) | W%(Sm) | W%(Gd) | W%(Dy) | W%(Er) | W%(Pb) | W%(Th) | W%(U) | W%(SUM) |
|---|---|---|---|---|---|---|---|---|---|---|---|---|---|---|---|---|---|---|---|---|
| CB6 | quartz | a_17 | 26.3456 | 0.0060 | 0.4004 | 12.3805 | 1.2318 | 0.6028 | 10.4856 | 22.4529 | 2.5174 | 9.1079 | 1.6716 | 1.1614 | 0.2965 | 0.0269 | 0.8592 | 7.8764 | 1.1831 | 98.6160 |
| CB6 | quartz | a_18 | 26.2951 | 0.0020 | 0.5174 | 12.2221 | 1.2791 | 0.3136 | 10.1959 | 22.5771 | 2.4328 | 8.9904 | 1.5361 | 0.8905 | 0.1348 | 0.0461 | 0.8566 | 9.3347 | 0.8205 | 98.4548 |
| CB6 | quartz | a_19 | 25.9878 | 0.0179 | 0.8800 | 11.6167 | 1.1169 | 0.1405 | 10.0210 | 21.9983 | 2.3228 | 9.1207 | 1.4120 | 0.6782 | 0.0917 | 0.0323 | 0.9465 | 11.8371 | 0.4264 | 98.6568 |
| CB6 | quartz | a_20 | 26.3175 | 0.3627 | 0.8799 | 12.0466 | 0.8788 | 0.3920 | 10.9869 | 23.5301 | 2.4603 | 9.1904 | 1.4959 | 0.8273 | 0.1389 | 0.0171 | 0.5695 | 4.6886 | 0.9661 | 95.7586 |
| CB6 | quartz | a_21 | 26.1914 | 0.0039 | 0.8100 | 11.8224 | 1.0422 | 0.2081 | 10.1840 | 22.2839 | 2.6234 | 9.3725 | 1.4633 | 0.7455 | 0.0888 | 0.0481 | 0.8598 | 10.9795 | 0.3846 | 99.1214 |
| CB6 | quartz | a_22 | 26.5915 | 0.0002 | 0.3811 | 12.6186 | 1.2683 | 0.4934 | 10.4781 | 22.5626 | 2.3353 | 9.0837 | 1.6658 | 1.0518 | 0.2731 | 0.0832 | 0.8635 | 7.7725 | 1.1500 | 98.6827 |
| CB6 | quartz | a_23 | 26.2556 | 0.0086 | 0.4107 | 12.3333 | 1.1801 | 0.5422 | 10.4663 | 22.8476 | 2.3328 | 9.1410 | 1.6952 | 1.1216 | 0.2537 | 0.0657 | 0.7912 | 7.5986 | 1.0764 | 98.1306 |
| CB6 | quartz | a_24 | 26.3086 | 0.0101 | 0.4001 | 12.3778 | 1.2780 | 0.5330 | 10.4102 | 22.2421 | 2.4112 | 9.1875 | 1.6392 | 1.2096 | 0.2506 | 0.0470 | 0.8085 | 7.8989 | 1.1915 | 98.2139 |
| CB6 | quartz | a_25 | 26.5765 | 0.0051 | 0.3928 | 12.5876 | 1.2678 | 0.5551 | 10.5467 | 22.3684 | 2.5722 | 8.9260 | 1.6305 | 1.1598 | 0.2246 | 0.0311 | 0.8890 | 7.8599 | 1.1834 | 98.7865 |
| CB6 | quartz | a_26 | 26.5305 | 0.0046 | 0.3660 | 12.5700 | 1.2580 | 0.4832 | 10.5330 | 22.5873 | 2.4527 | 9.1243 | 1.6321 | 1.1077 | 0.2593 | 0.0540 | 0.8515 | 7.6585 | 1.1373 | 98.6200 |
| CB6 | quartz | a_27 | 26.3782 | 0.0002 | 0.6522 | 12.1378 | 1.1968 | 0.2664 | 10.1751 | 22.2612 | 2.3746 | 9.1856 | 1.5524 | 0.8370 | 0.0913 | 0.1065 | 0.9087 | 10.3145 | 0.6139 | 99.0624 |
| CB6 | quartz | a_28 | 26.9415 | 0.2132 | 0.6591 | 12.5878 | 1.2400 | 0.5766 | 10.4342 | 22.3252 | 2.3143 | 8.9481 | 1.6997 | 1.1255 | 0.2739 | 0.0131 | 0.8244 | 7.5504 | 1.1215 | 98.8585 |
| CB6 | quartz | a_29 | 26.3196 | 0.0124 | 0.4714 | 12.3105 | 1.2678 | 0.5081 | 10.2997 | 22.3130 | 2.4585 | 8.9973 | 1.6630 | 1.1838 | 0.2574 | 0.0120 | 0.8290 | 8.3333 | 1.1314 | 98.3782 |
| CB6 | quartz | a_34 | 26.7244 | 0.0002 | 0.2142 | 12.7979 | 0.8770 | 0.3403 | 11.6231 | 25.0602 | 2.7178 | 9.8242 | 1.6981 | 0.8030 | 0.1404 | 0.0074 | 0.5346 | 4.7706 | 0.6765 | 98.8199 |
| CB6 | quartz | a_35 | 26.6793 | 0.0020 | 0.2179 | 12.7686 | 0.8933 | 0.3646 | 11.3070 | 24.5564 | 2.6966 | 10.0943 | 1.7424 | 0.9408 | 0.1438 | 0.0609 | 0.5767 | 5.1154 | 0.6235 | 98.7935 |
| CB6 | quartz | a_36 | 26.7638 | 0.0002 | 0.2230 | 12.7911 | 0.9089 | 0.2907 | 11.3243 | 24.6086 | 2.7868 | 10.1934 | 1.7946 | 0.9525 | 0.1522 | 0.0690 | 0.5115 | 5.0639 | 0.6309 | 99.0754 |
| CB6 | quartz | a_37 | 26.7427 | 0.0061 | 0.2209 | 12.8226 | 0.8858 | 0.2824 | 11.5614 | 24.7974 | 2.6334 | 9.9224 | 1.6416 | 0.8117 | 0.1533 | 0.0259 | 0.5727 | 4.9567 | 0.6638 | 98.7108 |
| CB6 | quartz | a_39 | 26.7298 | 0.0119 | 0.2703 | 12.7438 | 0.9382 | 0.2950 | 11.1823 | 24.3955 | 2.7266 | 10.0484 | 1.7068 | 0.8441 | 0.1016 | 0.0517 | 0.5644 | 5.7031 | 0.5916 | 98.9151 |
| CB6 | quartz | a_40 | 26.7061 | 0.0002 | 0.2661 | 12.7666 | 0.9379 | 0.3610 | 11.2525 | 24.3993 | 2.6197 | 9.9303 | 1.7129 | 0.8537 | 0.1606 | 0.0765 | 0.5866 | 5.4044 | 0.6814 | 98.7258 |
| CB6 | quartz | a_41 | 26.7123 | 0.0002 | 0.2152 | 12.8088 | 0.8783 | 0.3588 | 11.3016 | 24.8236 | 2.7190 | 9.9275 | 1.6967 | 0.8619 | 0.1218 | 0.0473 | 0.5287 | 5.1427 | 0.5886 | 98.7430 |
| CB6 | quartz | a_42 | 26.8260 | 0.0002 | 0.2318 | 12.8639 | 0.9233 | 0.3274 | 11.4171 | 24.7215 | 2.6144 | 10.0037 | 1.8010 | 0.8348 | 0.1457 | 0.0144 | 0.5168 | 5.0704 | 0.6488 | 98.9712 |
| CB6 | quartz | a_43 | 26.1168 | 0.0136 | 0.9199 | 11.6666 | 1.1088 | 0.1631 | 9.9709 | 22.0450 | 2.3588 | 9.2586 | 1.3311 | 0.5893 | 0.0169 | 0.0579 | 0.9301 | 12.1000 | 0.4005 | 99.0579 |
| CB6 | quartz | a_44 | 26.4435 | 0.0049 | 0.6221 | 12.1908 | 1.2574 | 0.2461 | 10.2378 | 22.2537 | 2.4112 | 9.0941 | 1.4913 | 0.8848 | 0.1185 | 0.0108 | 0.8788 | 10.4557 | 0.5933 | 99.2048 |
| CB6 | quartz | a_45 | 26.6972 | 0.0116 | 0.3989 | 12.6658 | 1.2381 | 0.5270 | 10.5142 | 22.6456 | 2.3418 | 9.0920 | 1.6053 | 1.1036 | 0.2269 | 0.0597 | 0.8765 | 7.8678 | 1.1598 | 99.0418 |
| CB6 | quartz | a_46 | 26.4478 | 0.0002 | 0.3924 | 12.4811 | 1.2360 | 0.5765 | 10.5416 | 22.7286 | 2.4629 | 9.0144 | 1.5382 | 1.1719 | 0.2681 | 0.0413 | 0.8563 | 7.7389 | 1.1368 | 98.6430 |
| CB6 | quartz | a_47 | 26.7417 | 0.0002 | 0.4008 | 12.6955 | 1.2710 | 0.5902 | 10.3628 | 22.7462 | 2.3388 | 9.1315 | 1.5996 | 1.1245 | 0.2540 | 0.0763 | 0.8370 | 7.8389 | 1.1758 | 99.1948 |
| CB6 | quartz | a_48 | 26.5542 | 0.0036 | 0.3786 | 12.5759 | 1.2724 | 0.5242 | 10.4390 | 22.6795 | 2.3580 | 8.9375 | 1.6597 | 1.1015 | 0.2732 | 0.0768 | 0.8576 | 7.8258 | 1.2295 | 98.7570 |
| CB6 | quartz | a_51 | 26.6508 | 0.0080 | 0.4515 | 12.5557 | 1.1973 | 0.5293 | 10.6392 | 22.9155 | 2.4194 | 9.1145 | 1.6443 | 1.0315 | 0.2358 | 0.0186 | 0.8076 | 7.9075 | 1.0077 | 99.1442 |
| CB6 | quartz | a_53 | 26.6039 | 0.0002 | 0.3856 | 12.6442 | 1.2826 | 0.5463 | 10.4010 | 22.3719 | 2.4060 | 8.9796 | 1.5673 | 1.1312 | 0.3044 | 0.0948 | 0.9035 | 7.8712 | 1.1526 | 98.6563 |
| CB6 | quartz | a_55 | 26.5324 | 0.2061 | 0.7049 | 12.2961 | 1.2598 | 0.5828 | 10.3293 | 22.1385 | 2.4106 | 8.6463 | 1.5852 | 1.0627 | 0.2559 | 0.0896 | 0.7965 | 7.7301 | 1.0807 | 97.7175 |
| AH5C | garnet | gt17 | 26.8847 | 0.0676 | 0.1778 | 13.1407 | 0.4767 | 1.1511 | 12.9908 | 24.4745 | 2.6783 | 10.3546 | 1.8277 | 1.0353 | 0.3847 | 0.1620 | 0.4741 | 0.6262 | 1.4443 | 98.3611 |
| AH5C | garnet | gt18 | 26.4812 | 0.0949 | 0.1651 | 12.8756 | 0.4500 | 1.1751 | 13.0430 | 24.4467 | 2.7045 | 10.4208 | 1.7612 | 1.0541 | 0.4756 | 0.1076 | 0.3343 | 0.6090 | 0.9634 | 97.1721 |
| AH5C | garnet | gt26 | 26.5075 | 0.0095 | 0.1239 | 12.9186 | 1.0484 | 1.6496 | 11.5882 | 22.9654 | 2.4143 | 9.2291 | 1.5081 | 1.1811 | 0.4778 | 0.1260 | 0.6849 | 4.6721 | 1.2470 | 98.3615 |
| AH5C | garnet | gt29 | 26.7256 | 0.0002 | 0.1078 | 13.0782 | 1.1147 | 1.8567 | 11.4158 | 22.9558 | 2.4032 | 9.3018 | 1.5079 | 1.1141 | 0.5381 | 0.1432 | 0.7606 | 4.5605 | 1.5584 | 99.1526 |
| AH5C | garnet | gt38 | 26.8831 | 0.1734 | 0.3038 | 13.0472 | 1.3692 | 1.6999 | 10.5939 | 22.0909 | 2.3591 | 8.8776 | 1.4554 | 1.1478 | 0.4625 | 0.2500 | 0.7427 | 5.4731 | 1.2713 | 98.2109 |
| AH5C | garnet | gt43 | 27.4235 | 0.0154 | 0.1091 | 13.5247 | 0.9588 | 1.5612 | 11.7929 | 23.9639 | 2.5979 | 9.4218 | 1.5099 | 1.1271 | 0.5082 | 0.1663 | 0.6630 | 3.9227 | 1.3493 | 100.6257 |
| AH5C | garnet | gt46 | 26.6794 | 0.0179 | 0.1068 | 12.9596 | 0.3292 | 1.3374 | 13.0380 | 25.0806 | 2.8672 | 10.8621 | 2.0781 | 1.1562 | 0.4176 | 0.1091 | 0.3749 | 0.4444 | 1.1549 | 99.0234 |
| AH5C | garnet | gt47 | 27.1341 | 0.0253 | 0.1462 | 13.2012 | 0.4487 | 1.0727 | 13.4788 | 24.8944 | 2.7854 | 11.3062 | 2.2823 | 1.1958 | 0.4091 | 0.1824 | 0.0936 | 0.6538 | 0.2932 | 99.6132 |
| AH5C | garnet | gt48 | 26.9923 | 0.0002 | 0.1116 | 13.2015 | 0.8910 | 1.5785 | 11.9746 | 23.8426 | 2.6476 | 9.7965 | 1.6282 | 1.0332 | 0.5351 | 0.2183 | 0.5696 | 3.4291 | 1.3624 | 99.8223 |
| AH5C | garnet | gt52 | 26.8700 | 0.0113 | 0.0938 | 13.0986 | 0.1695 | 1.1027 | 13.4508 | 25.3409 | 2.7869 | 11.3502 | 2.2907 | 1.1808 | 0.5001 | 0.1146 | 0.1522 | 0.2414 | 0.4591 | 99.2236 |
| AH5C | garnet | gt55 | 26.6910 | 0.0017 | 0.0879 | 13.0738 | 0.3770 | 1.4374 | 13.1147 | 24.7531 | 2.7014 | 10.5952 | 1.8056 | 1.1119 | 0.5021 | 0.0654 | 0.3401 | 0.7771 | 1.1350 | 98.5804 |
| AH5C | garnet | gt58 | 26.7886 | 0.0141 | 0.1186 | 13.1090 | 0.8166 | 1.5286 | 12.0715 | 23.3510 | 2.7004 | 10.0180 | 1.8616 | 1.0934 | 0.5168 | 0.1661 | 0.4683 | 3.1668 | 1.0238 | 98.8232 |
| AH5C | garnet | gt63 | 26.9547 | 0.0108 | 0.0998 | 13.2105 | 0.3444 | 1.2550 | 13.0355 | 24.7000 | 2.7858 | 11.1616 | 2.0157 | 1.1723 | 0.4218 | 0.0542 | 0.2526 | 1.0316 | 0.6519 | 99.1682 |
| AH5C | garnet | gt68 | 26.9573 | 0.0114 | 0.1111 | 13.1979 | 0.5900 | 1.3995 | 12.6913 | 24.1559 | 2.6705 | 10.5494 | 1.8435 | 1.0687 | 0.5093 | 0.1857 | 0.4320 | 1.9835 | 1.0092 | 99.3762 |
| AH5C | garnet | gt69 | 26.9630 | 0.0002 | 0.1197 | 13.2829 | 1.0213 | 1.6578 | 11.6178 | 23.0268 | 2.5315 | 9.5915 | 1.5244 | 1.0897 | 0.4909 | 0.1125 | 0.6477 | 3.9707 | 1.4263 | 99.0847 |
| AH5C | garnet | gt71 | 26.7967 | 0.0055 | 0.1114 | 13.1024 | 0.1591 | 1.0866 | 13.7512 | 24.4205 | 2.7772 | 11.3169 | 2.4677 | 1.2343 | 0.5140 | 0.0561 | 0.1168 | 0.3646 | 0.3089 | 98.5999 |
| AH5C | garnet | gt1 | 26.6209 | 0.0238 | 0.1427 | 13.0614 | 1.0316 | 1.9774 | 11.1671 | 22.3424 | 2.3920 | 9.4494 | 1.6118 | 1.3291 | 0.6503 | 0.1741 | 0.5921 | 4.9092 | 0.8842 | 98.3695 |
| AH5C | garnet | gt3 | 26.1333 | 0.0088 | 0.1173 | 12.6294 | 1.0946 | 1.5158 | 11.6141 | 22.8546 | 2.4721 | 9.3595 | 1.5297 | 1.0706 | 0.5446 | 0.1404 | 0.6994 | 4.1873 | 1.5384 | 97.5199 |
| AH5C | garnet | gt5 | 26.0957 | 0.0233 | 0.0972 | 12.6018 | 0.2587 | 0.9345 | 13.6619 | 25.5565 | 2.7400 | 10.1699 | 1.6643 | 1.0315 | 0.3998 | 0.1276 | 0.1923 | 0.8250 | 0.4618 | 96.8518 |
| AH5C | garnet | gt14 | 26.6988 | 0.0049 | 0.1217 | 12.9859 | 0.2677 | 1.0770 | 13.4839 | 25.6332 | 2.6985 | 10.9817 | 1.7742 | 1.0996 | 0.4510 | 0.1945 | 0.1165 | 0.5163 | 0.3487 | 98.4641 |
| AH5C | garnet | gt16 | 26.6216 | 0.0264 | 0.1164 | 13.0086 | 0.6146 | 1.5077 | 12.3521 | 23.9855 | 2.7354 | 10.2129 | 1.7498 | 1.0891 | 0.5396 | 0.1700 | 0.5168 | 1.6392 | 1.4751 | 98.3708 |
| AH5C | garnet | gt19 | 26.2085 | 0.3744 | 0.4931 | 12.3675 | 0.6211 | 1.0899 | 12.3401 | 23.4512 | 2.5977 | 10.0709 | 1.7978 | 0.9925 | 0.4100 | 0.1198 | 0.2813 | 1.3987 | 0.7242 | 95.3487 |
| AH5C | garnet | gt22 | 26.2478 | 0.0077 | 0.1169 | 12.6487 | 0.2007 | 1.1662 | 13.3781 | 24.9987 | 2.8890 | 11.5831 | 2.2480 | 1.1492 | 0.4765 | 0.1481 | 0.0739 | 0.1715 | 0.1951 | 97.7092 |
| AH5C | garnet | gt23 | 26.5191 | 0.1361 | 0.6690 | 12.5782 | 0.3257 | 1.2552 | 12.9169 | 24.0816 | 2.7229 | 10.4569 | 2.0014 | 1.0544 | 0.4645 | 0.1513 | 0.1142 | 0.6381 | 0.2640 | 96.3595 |
| AH5C | garnet | gt24 | 26.5576 | 0.0496 | 0.1463 | 12.9763 | 1.1185 | 1.6585 | 11.4031 | 22.3904 | 2.3252 | 9.1520 | 1.4811 | 1.2474 | 0.5946 | 0.1839 | 0.6903 | 4.7307 | 1.2848 | 98.0003 |
| AH5C | garnet | gt27 | 26.8096 | 0.0259 | 0.1222 | 13.0815 | 0.4458 | 1.3111 | 13.0029 | 25.0447 | 2.7103 | 10.4088 | 1.7994 | 1.1055 | 0.4215 | 0.1510 | 0.2584 | 1.4001 | 0.6996 | 98.8083 |

| Sample | Phase | Label | W%(O) | W%(Al) | W%(Si) | W%(P) | W%(Ca) | W%(Y) | W%(La) | W%(Ce) | W%(Pr) | W%(Nd) | W%(Sm) | W%(Gd) | W%(Dy) | W%(Er) | W%(Pb) | W%(Th) | W%(U) | W%(SUM) |
|---|---|---|---|---|---|---|---|---|---|---|---|---|---|---|---|---|---|---|---|---|
| AH5C | garnet | gt28 | 26.6497 | 0.0092 | 0.1132 | 13.0369 | 0.5036 | 1.4865 | 12.6536 | 24.3044 | 2.6184 | 10.2806 | 1.7463 | 1.1720 | 0.4990 | 0.1410 | 0.4554 | 1.5720 | 1.2442 | 98.4960 |
| AH5C | garnet | gt30 | 25.9881 | 0.2795 | 0.3465 | 12.4019 | 1.3888 | 1.5274 | 10.7400 | 21.6059 | 2.3328 | 8.5764 | 1.4131 | 1.1240 | 0.5249 | 0.1794 | 0.6341 | 4.9666 | 1.1936 | 95.2330 |
| AH5C | garnet | gt34 | 27.1449 | 0.0044 | 0.1093 | 13.3325 | 0.6302 | 1.4674 | 12.6455 | 24.5297 | 2.5733 | 10.1890 | 1.7341 | 1.0960 | 0.5111 | 0.1593 | 0.4636 | 2.1728 | 1.1188 | 99.8919 |
| AH5C | garnet | gt36 | 27.0823 | 0.0209 | 0.1093 | 13.2660 | 0.2556 | 1.2318 | 13.4187 | 25.2566 | 2.7178 | 11.0957 | 2.1175 | 1.1559 | 0.5070 | 0.0896 | 0.2141 | 0.2761 | 0.7139 | 99.5388 |
| AH5C | garnet | gt37 | 26.9110 | 0.1019 | 0.2012 | 13.0049 | 0.2656 | 1.1382 | 13.2037 | 25.5817 | 2.7642 | 10.9815 | 2.0655 | 1.1600 | 0.4156 | 0.1158 | 0.1613 | 0.5909 | 0.3849 | 99.0579 |
| AH5C | garnet | gt39 | 27.0976 | 0.0740 | 0.1751 | 13.2286 | 1.2409 | 1.8577 | 11.0547 | 22.8027 | 2.4018 | 9.3425 | 1.5602 | 1.2490 | 0.4938 | 0.1706 | 0.7509 | 4.9082 | 1.5115 | 99.9298 |
| AH5C | garnet | gt40 | 26.3359 | 0.1178 | 0.3911 | 12.7121 | 1.4033 | 1.9967 | 10.4179 | 21.0247 | 2.2376 | 8.5589 | 1.4123 | 1.2082 | 0.6649 | 0.1438 | 0.7826 | 5.2848 | 2.1231 | 96.8257 |
| AH5C | garnet | gt44 | 26.7936 | 0.0063 | 0.0878 | 13.1153 | 0.3512 | 1.4451 | 13.2291 | 25.2060 | 2.6545 | 10.5029 | 1.8265 | 1.1454 | 0.5036 | 0.1237 | 0.3498 | 0.5881 | 1.0577 | 98.9966 |
| AH5C | garnet | gt45 | 26.9221 | 0.0420 | 0.1484 | 13.0925 | 0.3087 | 1.2769 | 13.2440 | 25.3197 | 2.7886 | 10.9600 | 1.9825 | 1.1574 | 0.4336 | 0.0825 | 0.2328 | 0.6070 | 0.6790 | 99.2877 |
| AH5C | garnet | gt49 | 27.1738 | 0.0684 | 0.1722 | 13.3346 | 1.0254 | 1.6279 | 11.4670 | 23.2883 | 2.4360 | 9.4749 | 1.5967 | 1.1027 | 0.4668 | 0.1942 | 0.6744 | 4.0423 | 1.4649 | 99.6205 |
| AH5C | garnet | gt50 | 26.8110 | 0.0109 | 0.1296 | 13.1138 | 1.1820 | 1.7733 | 11.0149 | 22.5400 | 2.5105 | 9.3556 | 1.5663 | 1.1495 | 0.5034 | 0.1707 | 0.7808 | 5.2156 | 1.4543 | 99.2922 |
| AH5C | garnet | gt54 | 26.7057 | 0.6115 | 0.7556 | 12.4581 | 0.6333 | 1.2897 | 12.0690 | 23.2768 | 2.4033 | 9.7872 | 1.7474 | 0.9920 | 0.3571 | 0.1615 | 0.3507 | 1.3235 | 1.0018 | 95.9342 |
| AH5C | garnet | gt56 | 26.8209 | 0.0139 | 0.0962 | 13.1742 | 0.3069 | 1.3902 | 13.1524 | 24.6104 | 2.6990 | 10.9797 | 2.0610 | 1.1688 | 0.4560 | 0.1014 | 0.2722 | 0.5168 | 0.8044 | 98.6344 |
| AH5C | garnet | gt57 | 26.7691 | 0.0195 | 0.1192 | 13.1308 | 1.0402 | 1.6476 | 11.4240 | 22.9403 | 2.5337 | 9.6464 | 1.6205 | 1.0657 | 0.4919 | 0.1408 | 0.6758 | 3.9717 | 1.4172 | 98.6644 |
| AH5C | garnet | gt61 | 26.7002 | 0.0203 | 0.1203 | 13.1597 | 1.3407 | 1.6697 | 10.7111 | 21.6155 | 2.4731 | 9.0704 | 1.5438 | 1.1542 | 0.6008 | 0.1700 | 0.8627 | 4.8617 | 1.9338 | 98.0180 |
| AH5C | garnet | gt62 | 27.1737 | 0.0098 | 0.1260 | 13.3356 | 0.3737 | 1.1135 | 13.0663 | 25.0471 | 2.7437 | 11.0581 | 1.9521 | 1.0582 | 0.3825 | 0.1440 | 0.2041 | 1.2369 | 0.4455 | 99.4808 |
| AH5C | garnet | gt64 | 26.9428 | 0.0087 | 0.1053 | 13.1995 | 0.2949 | 1.2199 | 13.2106 | 24.9607 | 2.7835 | 11.1325 | 2.0230 | 1.0640 | 0.3825 | 0.1387 | 0.2657 | 0.5672 | 0.8007 | 99.1102 |
| AH5C | garnet | gt65 | 26.6378 | 0.0072 | 0.1115 | 12.9105 | 0.3158 | 0.9712 | 13.1863 | 25.3396 | 2.7912 | 10.9042 | 1.9538 | 1.0963 | 0.4239 | 0.1003 | 0.2809 | 0.9581 | 0.6567 | 98.6553 |
| AH5C | garnet | gt67 | 26.6754 | 0.0138 | 0.1063 | 12.9825 | 0.3616 | 1.1762 | 13.2335 | 24.8368 | 2.6399 | 10.9409 | 2.0831 | 1.1870 | 0.4682 | 0.0972 | 0.3066 | 0.5621 | 0.9248 | 98.6059 |
| AH5C | garnet | gt72 | 26.8974 | 0.0131 | 0.1030 | 13.2063 | 0.2973 | 1.1584 | 13.2779 | 24.6267 | 2.7865 | 11.0751 | 2.0590 | 1.0991 | 0.5157 | 0.1285 | 0.2205 | 0.5387 | 0.6252 | 98.6384 |
| AH5C | garnet | gt76 | 26.7516 | 0.0136 | 0.1066 | 13.1404 | 1.1090 | 1.6058 | 11.5289 | 22.3132 | 2.5764 | 9.3893 | 1.6095 | 1.1354 | 0.5915 | 0.1569 | 0.7421 | 4.0831 | 1.7205 | 98.5838 |
| AH5C | garnet | gt77 | 26.9420 | 0.0044 | 0.0949 | 13.2659 | 0.5686 | 1.2094 | 12.8726 | 23.8663 | 2.7010 | 10.3675 | 1.9531 | 1.0753 | 0.4279 | 0.1289 | 0.5834 | 0.7344 | 2.0185 | 98.8241 |
| AH5C | garnet | gt78 | 26.6746 | 0.0186 | 0.1173 | 13.0151 | 0.2503 | 1.1484 | 13.6083 | 24.3436 | 2.6892 | 11.1260 | 2.3985 | 1.2425 | 0.4546 | 0.1840 | 0.1172 | 0.3472 | 0.4805 | 98.2259 |
| NWI3 | anda-retro | 4 | 26.5538 | 0.0037 | 0.1369 | 12.9317 | 0.4488 | 1.5388 | 12.8974 | 25.1011 | 2.8645 | 9.9408 | 1.5344 | 1.1686 | 0.5310 | 0.1056 | 0.2045 | 2.0446 | 0.2373 | 98.2535 |
| NWI3 | anda-retro | 6 | 26.3529 | 0.0017 | 0.1239 | 12.7745 | 0.3075 | 0.9858 | 12.9156 | 25.8206 | 2.8725 | 10.1537 | 1.7457 | 1.0949 | 0.4755 | 0.0977 | 0.1548 | 1.2928 | 0.2838 | 97.4639 |
| NWI3 | anda-retro | 9 | 25.8744 | 0.0011 | 0.1354 | 12.4115 | 0.2786 | 0.9055 | 12.8419 | 25.7319 | 3.1107 | 10.4128 | 1.8018 | 1.0189 | 0.4039 | 0.0285 | 0.1312 | 1.0514 | 0.2236 | 96.3731 |
| NWI3 | anda-retro | 10 | 26.3660 | 0.0002 | 0.1319 | 12.7647 | 0.4107 | 1.0984 | 12.8880 | 25.4189 | 2.9086 | 9.8376 | 1.7527 | 1.1825 | 0.4471 | 0.0710 | 0.2043 | 1.9601 | 0.2429 | 97.6956 |
| NWI3 | anda-retro | 16 | 27.0402 | 0.2209 | 0.5598 | 13.1027 | 0.5705 | 1.8723 | 11.8890 | 23.3640 | 2.8492 | 9.9098 | 1.6307 | 1.1240 | 0.4879 | 0.2275 | 0.1821 | 2.2294 | 0.0747 | 97.3447 |
| NWI3 | anda-retro | 19 | 26.4725 | 0.0014 | 0.1612 | 12.9686 | 0.5826 | 1.6364 | 12.3806 | 24.4524 | 2.7976 | 9.6156 | 1.5726 | 1.0496 | 0.5685 | 0.1719 | 0.2220 | 2.5641 | 0.1026 | 97.3302 |
| NWI3 | anda-retro | 21 | 26.1034 | 0.0601 | 0.2080 | 12.5183 | 0.5260 | 0.6643 | 13.0696 | 24.7279 | 2.6843 | 9.7184 | 1.7193 | 1.1214 | 0.2935 | 0.0942 | 0.2423 | 2.2190 | 0.3166 | 96.2966 |
| NWI3 | anda-retro | 22 | 26.4552 | 0.0289 | 0.1370 | 12.8569 | 0.3990 | 1.1871 | 12.6894 | 25.2638 | 2.8951 | 10.1530 | 1.7373 | 1.2103 | 0.5960 | 0.1825 | 0.1714 | 1.4105 | 0.1891 | 97.5725 |
| NWI3 | anda-retro | 24 | 26.5358 | 0.0200 | 0.6955 | 12.3011 | 1.6233 | 0.8775 | 10.6658 | 20.0859 | 2.0982 | 7.7960 | 1.3767 | 0.9454 | 0.3846 | 0.1487 | 0.9612 | 12.1267 | 0.4930 | 99.1454 |
| NWI3 | anda-retro | 27 | 27.0995 | 0.1833 | 0.3034 | 13.1153 | 0.5269 | 0.8970 | 12.6650 | 24.4950 | 2.8128 | 9.8556 | 1.5833 | 0.9737 | 0.3501 | 0.0800 | 0.3277 | 2.9646 | 0.3180 | 98.5612 |
| NWI3 | anda-retro | 33 | 27.5171 | 0.1365 | 0.2041 | 13.4776 | 1.4760 | 1.3074 | 12.0784 | 23.9065 | 2.8686 | 9.6966 | 1.6812 | 1.2347 | 0.5551 | 0.0942 | 0.2581 | 1.7918 | 0.4967 | 98.7906 |
| NWI3 | anda-retro | 35 | 26.4030 | 0.0228 | 0.1704 | 13.1133 | 0.0001 | 1.5163 | 12.0679 | 23.6260 | 2.7765 | 9.7092 | 1.8230 | 1.2434 | 0.5635 | 0.6691 | 0.2120 | 2.4866 | 0.1150 | 96.5281 |
| NWI3 | anda-retro | 36 | 26.9474 | 0.0354 | 0.1714 | 13.1432 | 1.5637 | 1.5402 | 11.9500 | 23.1461 | 2.6751 | 9.4284 | 1.8431 | 1.1947 | 0.5920 | 0.1534 | 0.2858 | 3.1805 | 0.1772 | 98.0376 |
| NWI3 | anda-retro | 37 | 25.9951 | 0.0090 | 0.3909 | 12.2940 | 0.6346 | 0.8404 | 12.2558 | 23.6561 | 2.7423 | 9.7555 | 1.5478 | 0.9075 | 0.3362 | 0.0972 | 0.3708 | 4.7508 | 0.1493 | 96.7433 |
| NWI3 | anda-retro | 38 | 26.3033 | 0.0079 | 0.1897 | 12.7394 | 0.8109 | 1.2485 | 12.2207 | 23.3637 | 2.7109 | 9.2356 | 1.6618 | 1.2149 | 0.5043 | 0.1528 | 0.3732 | 4.2812 | 0.2047 | 97.2335 |
| NWI3 | anda-retro | 39 | 26.0662 | 0.0002 | 0.1674 | 12.6318 | 0.4939 | 1.2876 | 12.3852 | 24.1125 | 2.7753 | 9.8907 | 1.9026 | 1.1703 | 0.5065 | 0.1245 | 0.2223 | 2.6990 | 0.1001 | 96.5461 |
| NWI3 | anda-retro | 41 | 26.2127 | 0.0317 | 0.1571 | 12.6498 | 0.4045 | 1.0151 | 13.2941 | 25.2338 | 2.8271 | 9.5479 | 1.7530 | 1.1091 | 0.4828 | 0.0556 | 0.2222 | 1.7010 | 0.2948 | 97.0023 |
| NWI3 | anda-retro | 43 | 26.5239 | 0.0295 | 0.1964 | 12.8981 | 0.8570 | 1.5486 | 11.9345 | 23.8563 | 2.7317 | 9.9799 | 1.7190 | 1.0989 | 0.5520 | 0.1494 | 0.2569 | 3.0472 | 0.1267 | 97.5160 |
| NWI3 | anda-retro | 44 | 26.1899 | 0.1335 | 0.3665 | 12.4605 | 0.9324 | 1.1658 | 12.0107 | 22.4350 | 2.4982 | 8.7883 | 1.4087 | 1.0418 | 0.4827 | 0.1094 | 0.5453 | 5.9527 | 0.3804 | 96.9118 |
| NWI3 | anda-retro | 45 | 26.7130 | 0.0379 | 0.3235 | 12.9767 | 0.6339 | 1.3246 | 12.6285 | 24.3874 | 2.7019 | 9.1718 | 1.2916 | 0.8615 | 0.4505 | 0.0972 | 0.3333 | 3.4706 | 0.2424 | 97.6563 |
| NWI3 | anda-retro | 48 | 27.0589 | 0.0152 | 0.1602 | 13.2843 | 0.4689 | 0.9597 | 13.2893 | 25.0776 | 2.7259 | 9.5466 | 1.4959 | 1.0048 | 0.4066 | 0.1538 | 0.2551 | 2.4485 | 0.3383 | 98.6996 |
| NWI3 | anda-retro | 49 | 27.2042 | 0.0407 | 0.1952 | 13.3640 | 0.3586 | 0.9074 | 13.4474 | 25.4336 | 2.7617 | 9.7094 | 1.5980 | 1.0027 | 0.3759 | 0.0916 | 0.2212 | 1.8143 | 0.2630 | 98.7989 |
| NWI3 | anda-retro | 50 | 26.5370 | 0.0876 | 0.4273 | 12.5936 | 1.0467 | 0.4189 | 12.1490 | 23.0060 | 2.5183 | 9.3675 | 1.6439 | 1.1621 | 0.2072 | 0.0100 | 0.4383 | 5.2662 | 0.2444 | 97.1340 |
| NWI3 | anda-retro | 51 | 26.4043 | 0.2760 | 0.2632 | 12.5950 | 0.5086 | 0.9504 | 12.5593 | 24.7699 | 2.8057 | 9.6167 | 1.5910 | 1.0590 | 0.3523 | 0.1109 | 0.2727 | 2.6169 | 0.2632 | 97.0251 |
| NWI3 | anda-retro | 52 | 26.8192 | 0.0359 | 0.3346 | 12.8291 | 2.2682 | 1.2434 | 11.4292 | 23.0007 | 2.6568 | 9.2847 | 1.5923 | 1.1358 | 0.5708 | 0.1560 | 0.2767 | 3.0921 | 0.2990 | 97.0345 |
| NWI3 | anda-retro | 53 | 26.4261 | 0.0703 | 0.1981 | 12.7848 | 0.5333 | 1.1040 | 12.4265 | 24.4441 | 2.8257 | 9.7944 | 1.6573 | 1.1158 | 0.4350 | 0.1877 | 0.3127 | 2.7907 | 0.2653 | 97.3818 |
| NWI3 | anda-retro | 54 | 26.2097 | 0.0214 | 0.1934 | 12.7014 | 0.6926 | 1.3810 | 12.1148 | 23.6816 | 2.8086 | 9.4647 | 1.5662 | 1.1269 | 0.5921 | 0.1031 | 0.3318 | 3.6104 | 0.3100 | 96.9197 |
| NWI3 | anda-retro | 55 | 26.4740 | 0.0203 | 0.4004 | 12.6596 | 0.4905 | 1.1080 | 12.6523 | 24.9128 | 2.8879 | 9.8844 | 1.6182 | 1.0203 | 0.4314 | 0.1033 | 0.2253 | 2.4051 | 0.1851 | 97.4889 |
| NWI3 | anda-retro | 56 | 26.2040 | 0.2678 | 0.2613 | 12.5181 | 0.6964 | 1.4270 | 12.1994 | 23.4636 | 2.7048 | 9.3154 | 1.5323 | 1.0747 | 0.5413 | 0.1342 | 0.3807 | 3.5098 | 0.4942 | 96.7350 |
| NWI3 | anda-retro | 59 | 26.8442 | 1.1100 | 0.6118 | 12.3541 | 0.6318 | 1.4313 | 11.5387 | 23.0321 | 2.6884 | 9.3344 | 1.6797 | 1.0821 | 0.4537 | 0.1921 | 0.2511 | 3.1856 | 0.1357 | 96.5668 |
| NWI3 | anda-retro | 60 | 26.7736 | 0.2939 | 0.2619 | 12.9035 | 0.4999 | 1.5339 | 12.3002 | 24.7888 | 2.9749 | 9.7349 | 1.4109 | 0.9300 | 0.4979 | 0.1849 | 0.2262 | 2.5918 | 0.0881 | 98.0053 |
| NWI3 | anda-retro | 61 | 26.3902 | 0.0214 | 0.1759 | 12.8020 | 0.3357 | 1.0193 | 13.1194 | 25.5834 | 2.9099 | 9.8234 | 1.4314 | 0.8631 | 0.4039 | 0.0779 | 0.1778 | 1.8909 | 0.1533 | 97.1889 |
| NWI3 | anda-retro | 62 | 26.0367 | 0.0554 | 0.2055 | 12.5221 | 0.4262 | 0.9374 | 12.7537 | 25.2467 | 2.8106 | 9.8204 | 1.5526 | 0.9924 | 0.3743 | 0.1006 | 0.1868 | 1.9353 | 0.1642 | 96.1309 |

| Sample | Phase | Label | W%(O ) | W%(Al) | W%(Si) | W%(P) | W%(Ca) | W%(Y ) | W%(La) | W%(Ce) | W%(Pr) | W%(Nd) | W%(Sm) | W%(Gd) | W%(Dy) | W%(Er) | W%(Pb) | W%(Th) | W%(U ) | W%(SUM) |
|---|---|---|---|---|---|---|---|---|---|---|---|---|---|---|---|---|---|---|---|---|
| NWI3 | anda-retro | 63 | 26.4740 | 0.0074 | 0.2270 | 12.7902 | 0.6879 | 1.0340 | 12.2198 | 24.1284 | 2.8201 | 9.8081 | 1.5801 | 1.0839 | 0.3734 | 0.0375 | 0.3182 | 3.8045 | 0.2534 | 97.6579 |
| NWI3 | anda-retro | 64 | 26.0601 | 0.1828 | 0.3630 | 12.3544 | 0.7384 | 0.9769 | 11.9705 | 23.8495 | 2.8549 | 9.3474 | 1.4567 | 0.9925 | 0.3831 | 0.0885 | 0.3367 | 3.8344 | 0.2431 | 96.0429 |
| NWI3 | anda-retro | 65 | 26.3283 | 0.0042 | 0.1691 | 12.7520 | 0.4530 | 1.1038 | 12.8257 | 24.9807 | 2.8902 | 9.9076 | 1.6430 | 1.0523 | 0.5002 | 0.0905 | 0.2393 | 2.0603 | 0.2686 | 97.2788 |
| NWI3 | anda-retro | 66 | 26.5302 | 0.0801 | 0.2927 | 12.7718 | 0.9339 | 1.1181 | 11.8529 | 23.2525 | 2.7729 | 9.2080 | 1.5994 | 1.1240 | 0.4268 | 0.1357 | 0.3931 | 4.6228 | 0.3549 | 97.4798 |
| NWI3 | anda-retro | 67 | 25.9135 | 0.0239 | 0.4633 | 12.3096 | 0.9822 | 1.1150 | 10.6042 | 22.2921 | 2.5853 | 9.4955 | 1.7232 | 1.3860 | 0.4763 | 0.0773 | 0.4269 | 5.4802 | 0.3644 | 95.7289 |
| NWI3 | anda-retro | 68 | 26.3823 | 0.0085 | 0.3358 | 12.6997 | 0.8326 | 1.2636 | 10.4407 | 23.4393 | 2.7926 | 10.2233 | 1.6422 | 1.0891 | 0.4856 | 0.1130 | 0.5089 | 4.7029 | 0.4510 | 97.4211 |
| NWI3 | anda-retro | 69 | 26.4643 | 0.0002 | 0.1644 | 12.9934 | 0.3504 | 1.8598 | 10.9046 | 24.3691 | 3.1333 | 11.7786 | 2.0924 | 1.2276 | 0.6843 | 0.0714 | 0.2284 | 0.5291 | 0.6185 | 97.4798 |
| NWI3 | anda-retro | 70 | 26.4368 | 0.0002 | 0.1624 | 13.0102 | 0.3615 | 2.0154 | 10.8013 | 24.0704 | 3.0123 | 11.6249 | 2.1089 | 1.2581 | 0.6866 | 0.1117 | 0.2817 | 0.5304 | 0.9627 | 97.4455 |
| NWI3 | anda-retro | 71 | 26.4738 | 0.0025 | 0.1607 | 13.0173 | 0.4792 | 1.7523 | 11.0344 | 24.3468 | 3.0566 | 11.3121 | 1.8242 | 1.1034 | 0.5955 | 0.1652 | 0.2812 | 0.8816 | 0.6955 | 97.1923 |
| NWI3 | anda-retro | 72 | 26.3355 | 0.0054 | 0.1629 | 12.9030 | 0.2798 | 1.5606 | 11.4760 | 24.5204 | 3.1352 | 11.4263 | 1.9810 | 1.1477 | 0.4986 | 0.1392 | 0.1940 | 0.5309 | 0.5968 | 96.9033 |
| NWI3 | anda-retro | 73 | 26.2306 | 0.0043 | 0.1563 | 12.9185 | 0.3534 | 1.8862 | 10.9310 | 23.9061 | 2.8992 | 11.3923 | 2.0030 | 1.2048 | 0.6887 | 0.1583 | 0.2929 | 0.6788 | 0.8073 | 96.5217 |
| NWI3 | anda-retro | 75 | 25.8904 | 0.0262 | 0.2298 | 12.5853 | 0.5218 | 1.6311 | 10.9762 | 23.6289 | 2.9246 | 10.9242 | 1.9620 | 1.1055 | 0.6085 | 0.1677 | 0.2464 | 1.3681 | 0.6111 | 95.4178 |
| NWI3 | anda-retro | 77 | 26.2177 | 0.0002 | 0.1862 | 12.8069 | 0.4063 | 1.9149 | 11.0208 | 24.0047 | 3.0388 | 11.2545 | 2.0761 | 1.2585 | 0.6687 | 0.2241 | 0.3068 | 0.8324 | 0.7907 | 97.0183 |
| NWI3 | anda-retro | 78 | 26.1757 | 0.0002 | 0.1543 | 12.8305 | 0.4675 | 1.9436 | 10.8944 | 23.8878 | 3.0022 | 11.1569 | 2.0041 | 1.1631 | 0.6576 | 0.1196 | 0.3462 | 1.0166 | 0.9253 | 96.7556 |
| NWI3 | anda-retro | 79 | 26.1457 | 0.0002 | 0.1756 | 12.7394 | 0.4467 | 1.8145 | 11.1068 | 24.1937 | 2.9574 | 11.2362 | 1.9053 | 1.2143 | 0.6374 | 0.1534 | 0.2463 | 1.0786 | 0.7928 | 96.8543 |
| NWI3 | anda-retro | 81 | 26.5398 | 0.0155 | 0.2043 | 13.0321 | 0.6084 | 1.7932 | 10.8235 | 23.7541 | 2.8798 | 10.8674 | 1.9720 | 1.1924 | 0.6317 | 0.1580 | 0.3787 | 1.7351 | 0.7654 | 97.3614 |
| NWI3 | anda-retro | 82 | 26.3234 | 0.0257 | 0.3678 | 12.4746 | 1.2688 | 0.6657 | 11.1359 | 21.6577 | 2.5344 | 8.7109 | 1.7127 | 1.3117 | 0.3028 | 0.1158 | 0.6937 | 7.9772 | 0.4672 | 97.7560 |
| NWI3 | anda-retro | 83 | 26.4094 | 0.0258 | 0.3944 | 12.5554 | 1.3780 | 0.6865 | 11.2845 | 21.3796 | 2.3549 | 8.4838 | 1.5970 | 1.3700 | 0.3570 | 0.1090 | 0.6763 | 7.9907 | 0.4678 | 97.5301 |
| NWI3 | anda-retro | 84 | 26.2531 | 0.0357 | 0.1766 | 12.5899 | 0.6109 | 0.7265 | 12.7075 | 24.7170 | 2.8232 | 9.7783 | 1.5691 | 1.0859 | 0.4052 | 0.1352 | 0.2911 | 3.0192 | 0.3514 | 97.2858 |
| NWI3 | anda-retro | 86 | 26.1920 | 0.0384 | 0.1817 | 12.6625 | 0.9230 | 1.1646 | 11.8184 | 23.6129 | 2.8264 | 9.7283 | 1.7416 | 1.1534 | 0.5679 | 0.2117 | 0.2962 | 2.9948 | 0.2983 | 96.4221 |
| NWI3 | anda-retro | 87 | 27.5908 | 1.4448 | 1.7712 | 11.9633 | 0.5917 | 1.2512 | 11.6147 | 22.0775 | 2.3577 | 8.5786 | 1.3926 | 1.0529 | 0.4701 | 0.1632 | 0.3201 | 3.0434 | 0.4876 | 96.1814 |
| NWI3 | anda-retro | 88 | 26.0211 | 0.0342 | 0.1728 | 12.5452 | 0.3650 | 1.0674 | 12.7840 | 24.9798 | 2.9457 | 9.9747 | 1.6101 | 0.9577 | 0.4823 | 0.1065 | 0.1972 | 1.8807 | 0.2600 | 96.3944 |
| NWI3 | anda-retro | 89 | 27.1129 | 1.2641 | 0.6904 | 12.2567 | 0.5360 | 0.9733 | 12.1051 | 23.5692 | 2.7282 | 9.5769 | 1.6118 | 1.0004 | 0.4438 | 0.1169 | 0.3310 | 2.9731 | 0.3426 | 97.6424 |
| NWI3 | anda-retro | 91 | 26.2396 | 0.1108 | 0.3725 | 12.4082 | 0.8235 | 0.5393 | 11.9936 | 23.2851 | 2.6353 | 9.1770 | 1.6123 | 1.2555 | 0.2796 | 0.1016 | 0.4611 | 5.4627 | 0.2569 | 97.0246 |
| NWI3 | anda-retro | 92 | 26.0680 | 0.0356 | 0.4598 | 12.1762 | 1.1849 | 0.2075 | 11.4351 | 21.8373 | 2.4351 | 9.0080 | 1.5868 | 1.0590 | 0.0475 | 0.0765 | 0.6355 | 8.4153 | 0.3249 | 97.0030 |
| NWI3 | anda-retro | 93 | 26.5062 | 0.0170 | 0.1958 | 12.9373 | 0.5564 | 1.2856 | 12.3071 | 24.2151 | 2.9454 | 9.6855 | 1.5244 | 0.9851 | 0.5219 | 0.1152 | 0.3100 | 2.8082 | 0.3998 | 97.3260 |
| NWI3 | anda-retro | 94 | 25.8541 | 0.0088 | 0.2409 | 12.4393 | 1.0120 | 0.9888 | 11.4352 | 22.5522 | 2.5702 | 8.9332 | 1.5178 | 0.9663 | 0.4677 | 0.0532 | 0.5016 | 5.7550 | 0.3199 | 95.6262 |
| NWI3 | anda-retro | 96 | 26.1125 | 0.0129 | 0.2161 | 12.6209 | 0.8734 | 1.0375 | 11.6472 | 23.0566 | 2.6914 | 9.3108 | 1.5727 | 1.0446 | 0.4552 | 0.0581 | 0.4535 | 4.8630 | 0.3538 | 96.3902 |
| NWI3 | anda-retro | 97 | 25.8509 | 0.0059 | 0.2734 | 12.3069 | 0.9300 | 0.8721 | 12.1941 | 22.6895 | 2.4784 | 8.9440 | 1.5508 | 1.2480 | 0.4256 | 0.1168 | 0.4758 | 5.5818 | 0.3198 | 96.2738 |
| NWI3 | anda-retro | 98 | 25.9194 | 0.0178 | 0.3070 | 12.4370 | 0.9010 | 1.1391 | 11.7834 | 22.5626 | 2.5361 | 8.7155 | 1.4875 | 1.0872 | 0.4685 | 0.1208 | 0.5232 | 5.5916 | 0.3697 | 95.9774 |
| NWI5 | anda | 7 | 26.6605 | 0.0569 | 0.1419 | 12.8255 | 0.3361 | 0.9082 | 12.2017 | 26.6308 | 2.7948 | 10.5126 | 1.8035 | 1.2206 | 0.3960 | 0.1000 | 0.2280 | 1.8859 | 0.2419 | 98.9549 |
| NWI5 | anda | 8 | 26.3812 | 0.0552 | 0.3275 | 12.4439 | 0.8845 | 0.8319 | 10.8185 | 23.4970 | 2.5003 | 9.8011 | 1.8623 | 1.5457 | 0.4109 | 0.0713 | 0.5230 | 6.6139 | 0.2202 | 98.7984 |
| NWI5 | anda | 9 | 26.4766 | 0.1226 | 0.3109 | 12.6151 | 0.2851 | 0.7020 | 12.1927 | 26.4590 | 2.6767 | 10.3184 | 1.6613 | 1.2328 | 0.4280 | 0.0478 | 0.1881 | 1.6303 | 0.2620 | 97.6194 |
| NWI5 | anda | 10 | 26.0540 | 0.0350 | 0.3167 | 12.1983 | 0.8201 | 0.8075 | 11.0016 | 24.1112 | 2.5043 | 9.8622 | 1.7615 | 1.3368 | 0.4944 | 0.0821 | 0.5205 | 6.1332 | 0.2113 | 98.2607 |
| NWI5 | anda | 12 | 26.4297 | 0.0213 | 0.1418 | 12.5652 | 0.4196 | 0.8417 | 12.1332 | 26.5729 | 2.7256 | 10.5779 | 1.8201 | 1.1757 | 0.4722 | 0.1349 | 0.2586 | 2.7043 | 0.2362 | 99.2409 |
| NWI5 | anda | 16 | 26.2202 | 0.1817 | 0.2809 | 12.2706 | 0.4407 | 0.6639 | 12.0667 | 26.3039 | 2.7545 | 10.5961 | 1.6785 | 1.1331 | 0.3892 | 0.0599 | 0.2512 | 2.4000 | 0.2784 | 97.9795 |
| NWI5 | anda | 20 | 26.6147 | 0.0301 | 0.1216 | 12.8143 | 0.4020 | 0.8443 | 11.9194 | 26.3443 | 2.6813 | 10.8957 | 1.8203 | 1.4026 | 0.4725 | 0.0914 | 0.2292 | 1.8727 | 0.2720 | 98.8384 |
| NWI5 | anda | 21 | 27.2675 | 0.0670 | 0.1882 | 13.1396 | 0.7998 | 0.9563 | 11.7456 | 25.6763 | 2.6463 | 11.0225 | 2.0188 | 1.5276 | 0.5437 | 0.0759 | 0.2918 | 1.9163 | 0.4550 | 100.3482 |
| NWI5 | anda | 23 | 26.4268 | 0.0182 | 0.1109 | 12.6274 | 0.4378 | 0.8477 | 12.1438 | 26.4928 | 2.7232 | 10.8036 | 1.8771 | 1.3496 | 0.4739 | 0.0442 | 0.2310 | 1.9685 | 0.2586 | 98.8451 |
| NWI5 | anda | 48 | 26.4320 | 0.0051 | 0.1807 | 12.5622 | 0.5486 | 1.0400 | 11.4157 | 25.2490 | 2.8722 | 10.8337 | 2.1068 | 1.6692 | 0.5152 | 0.0910 | 0.3125 | 3.1497 | 0.3938 | 99.3874 |
| NWI5 | anda | 52 | 26.5732 | 0.1666 | 0.2107 | 12.5582 | 0.4826 | 0.9367 | 12.2445 | 26.0520 | 2.8081 | 10.7309 | 1.9645 | 1.4617 | 0.5154 | 0.0712 | 0.2214 | 1.8794 | 0.2576 | 99.1447 |
| NWI5 | anda | 53 | 27.5873 | 0.1787 | 0.2224 | 13.3565 | 0.9446 | 0.8498 | 11.7999 | 25.4565 | 2.6837 | 10.3940 | 1.8132 | 1.4486 | 0.4186 | 0.1041 | 0.2502 | 2.4399 | 0.1599 | 100.1179 |
| NWI5 | anda | 55 | 26.8187 | 0.1355 | 0.1938 | 12.8064 | 0.3739 | 0.6929 | 12.5705 | 26.7259 | 2.6761 | 10.3013 | 1.6725 | 1.1301 | 0.4018 | 0.0834 | 0.2524 | 2.3013 | 0.1776 | 99.3241 |
| NWI5 | anda | 84 | 26.4537 | 0.2844 | 0.3382 | 12.4900 | 0.5370 | 0.8838 | 12.1364 | 25.1001 | 2.6295 | 9.7869 | 1.7070 | 1.2252 | 0.4004 | 0.0614 | 0.3074 | 3.0037 | 0.2569 | 97.6120 |
| NWI5 | anda | 85 | 26.8789 | 0.3383 | 0.2372 | 12.6865 | 0.4054 | 0.5222 | 12.4382 | 26.5504 | 2.7629 | 10.4103 | 1.6201 | 1.0736 | 0.2596 | 0.0269 | 0.2829 | 2.3279 | 0.4204 | 99.2517 |
| NWI5 | anda | 86 | 26.8479 | 0.0505 | 0.3047 | 12.7969 | 0.9888 | 0.6160 | 11.2043 | 23.7457 | 2.5081 | 9.5963 | 1.5437 | 1.2631 | 0.2645 | 0.0493 | 0.5570 | 6.7854 | 0.3341 | 99.4663 |
| NWI5 | anda | 87 | 26.7671 | 0.0611 | 0.1969 | 12.7896 | 0.6864 | 0.4983 | 12.1257 | 25.6208 | 2.6856 | 9.8907 | 1.6065 | 1.1535 | 0.3382 | 0.0001 | 0.4102 | 4.0464 | 0.2978 | 99.1849 |
| NWI5 | anda | 88 | 26.8184 | 0.0546 | 0.1570 | 12.9235 | 0.4587 | 0.8338 | 11.7205 | 25.6260 | 2.8302 | 10.9871 | 1.9559 | 1.3510 | 0.4878 | 0.0763 | 0.3718 | 1.9489 | 0.7140 | 99.3255 |
| NWI5 | anda | 89 | 26.6203 | 0.0299 | 0.1471 | 12.8135 | 0.5099 | 0.7948 | 11.7513 | 25.6145 | 2.8385 | 10.8575 | 1.8892 | 1.1608 | 0.3820 | 0.0652 | 0.4060 | 2.0394 | 0.8275 | 98.7574 |
| NWI5 | anda | 90 | 26.7436 | 0.0437 | 0.1385 | 12.8313 | 0.3572 | 0.6734 | 12.5288 | 27.1453 | 2.8302 | 10.9837 | 1.8120 | 1.2032 | 0.3538 | 0.0678 | 0.1557 | 0.8193 | 0.3800 | 99.0775 |
| NWI5 | anda | 91 | 26.6800 | 0.0568 | 0.1721 | 12.7951 | 0.5989 | 0.7487 | 11.9561 | 25.7861 | 2.7368 | 10.3126 | 1.7176 | 1.1706 | 0.3893 | 0.1191 | 0.3212 | 2.8398 | 0.4706 | 98.8814 |
| NWI5 | anda | 92 | 26.7358 | 0.0863 | 0.2714 | 12.7232 | 0.6071 | 0.6720 | 12.2487 | 25.7745 | 2.7064 | 10.1220 | 1.6803 | 1.1288 | 0.3160 | 0.0690 | 0.3827 | 2.9774 | 0.4776 | 98.9892 |
| NWI5 | anda | 93 | 27.1329 | 0.3769 | 0.3621 | 12.7687 | 0.6925 | 0.7287 | 11.8258 | 25.0830 | 2.6195 | 9.9203 | 1.6731 | 1.2015 | 0.3725 | 0.0842 | 0.4671 | 4.0070 | 0.5774 | 99.9032 |
| NWI5 | anda | 94 | 26.3171 | 0.0654 | 0.1684 | 12.5364 | 0.5692 | 0.7909 | 12.1513 | 25.8724 | 2.7189 | 10.4643 | 1.7264 | 1.1576 | 0.4184 | 0.1151 | 0.3155 | 2.0116 | 0.6224 | 98.0313 |
| NWI5 | anda | 106 | 26.7194 | 0.0568 | 0.1715 | 12.7424 | 0.5215 | 0.7791 | 12.2853 | 26.2299 | 2.5468 | 10.3502 | 1.6910 | 1.3505 | 0.4491 | 0.0176 | 0.3014 | 3.1993 | 0.2223 | 99.6441 |
| NWI5 | anda | 107 | 26.4843 | 0.0270 | 0.1446 | 12.6651 | 0.4073 | 0.7960 | 12.4542 | 26.4598 | 2.7630 | 10.2047 | 1.8119 | 1.2079 | 0.4628 | 0.0901 | 0.2762 | 2.2842 | 0.2561 | 98.8052 |

| Sample | Phase | Label | W%(O) | W%(Al) | W%(Si) | W%(P) | W%(Ca) | W%(Y) | W%(La) | W%(Ce) | W%(Pr) | W%(Nd) | W%(Sm) | W%(Gd) | W%(Dy) | W%(Er) | W%(Pb) | W%(Th) | W%(U) | W%(SUM) |
|---|---|---|---|---|---|---|---|---|---|---|---|---|---|---|---|---|---|---|---|---|
| NWI5 | anda | 108 | 26.7847 | 0.5200 | 0.4972 | 12.3365 | 0.9193 | 0.7337 | 11.1491 | 24.2204 | 2.5313 | 9.3703 | 1.5460 | 1.3145 | 0.4168 | 0.0946 | 0.4683 | 5.8425 | 0.2128 | 98.9680 |
| NWI5 | anda | 109 | 26.6452 | 0.4785 | 0.5047 | 12.3381 | 0.5212 | 0.5684 | 11.9163 | 25.4246 | 2.5878 | 9.8003 | 1.5625 | 1.1242 | 0.3283 | 0.0211 | 0.2923 | 3.5567 | 0.2476 | 97.9278 |
| NWI5 | anda | 110 | 26.7877 | 0.1810 | 0.1940 | 12.7516 | 0.2780 | 0.6597 | 12.6886 | 27.3914 | 2.7233 | 10.4051 | 1.6851 | 1.0375 | 0.3508 | 0.0666 | 0.1631 | 1.5572 | 0.2446 | 99.1753 |
| NWI5 | anda | 111 | 26.8773 | 0.0603 | 0.1598 | 12.9984 | 0.4057 | 1.1549 | 11.2278 | 25.6163 | 2.8201 | 11.6009 | 2.2197 | 1.4519 | 0.5173 | 0.1612 | 0.2642 | 1.3301 | 0.5716 | 99.4475 |
| NWI5 | anda | 112 | 27.1912 | 0.1650 | 0.2568 | 13.0923 | 0.4253 | 1.0691 | 11.6005 | 26.0553 | 2.7387 | 11.0777 | 1.9670 | 1.2019 | 0.5174 | 0.1104 | 0.2527 | 1.7173 | 0.3935 | 99.8421 |
| NWI5 | anda | 113 | 26.9336 | 0.0601 | 0.1433 | 12.9730 | 0.4290 | 0.8327 | 12.1311 | 26.3889 | 2.7997 | 10.8241 | 1.7891 | 1.2183 | 0.4162 | 0.1090 | 0.2344 | 2.0944 | 0.3267 | 99.7136 |
| NWI5 | anda | 114 | 26.6824 | 0.0995 | 0.1724 | 12.7656 | 0.2752 | 0.9686 | 12.1654 | 26.8601 | 2.7873 | 11.1002 | 1.8173 | 1.2307 | 0.5202 | 0.0669 | 0.2021 | 1.0173 | 0.4348 | 99.1760 |
| NWI5 | anda | 116 | 26.0988 | 0.0570 | 0.1429 | 12.4352 | 0.4359 | 0.7419 | 11.8724 | 25.9061 | 2.7621 | 10.8470 | 1.9247 | 1.1176 | 0.3787 | 0.0917 | 0.2613 | 1.9811 | 0.3657 | 97.4301 |
| NWI5 | anda | 118 | 26.9713 | 0.0907 | 0.2805 | 12.9287 | 0.7621 | 0.7666 | 11.0800 | 24.5470 | 2.5398 | 10.3098 | 1.8741 | 1.2716 | 0.3641 | 0.0617 | 0.4264 | 4.8520 | 0.3474 | 99.4838 |
| NWI5 | anda | 119 | 26.1415 | 0.1161 | 0.2739 | 12.4277 | 0.3923 | 1.3213 | 10.9888 | 24.9683 | 2.7553 | 11.7964 | 2.4232 | 1.3996 | 0.5777 | 0.0755 | 0.2503 | 0.6728 | 0.7832 | 97.3739 |
| NWI5 | anda | 120 | 26.3754 | 0.0566 | 0.1474 | 12.5520 | 0.5130 | 0.8862 | 11.8391 | 26.0895 | 2.6478 | 10.8589 | 1.8812 | 1.1908 | 0.4224 | 0.0350 | 0.2985 | 2.5546 | 0.3474 | 98.7058 |
| NWI5 | anda | 121 | 26.4029 | 0.0315 | 0.1241 | 12.5829 | 0.2365 | 0.7585 | 12.4267 | 27.4074 | 2.8139 | 11.0154 | 1.7758 | 1.1129 | 0.4449 | 0.0720 | 0.1789 | 1.1239 | 0.2872 | 98.8054 |
| NWI5 | anda | 122 | 26.2117 | 0.0262 | 0.2705 | 12.3472 | 0.8467 | 0.7532 | 10.9004 | 24.3749 | 2.6009 | 10.0266 | 1.8569 | 1.2422 | 0.4820 | 0.1404 | 0.4690 | 5.5470 | 0.3696 | 98.4754 |
| NWI5 | anda | 123 | 26.3417 | 0.1513 | 0.2137 | 12.4681 | 0.3055 | 0.7618 | 11.8889 | 26.4544 | 2.9492 | 11.1146 | 2.0189 | 1.1644 | 0.3578 | 0.1039 | 0.2129 | 1.2589 | 0.3455 | 98.1215 |
| NWI5 | anda | 124 | 25.9804 | 0.3208 | 0.4261 | 12.0787 | 0.4565 | 0.8909 | 11.1418 | 24.8198 | 2.6872 | 10.7195 | 2.0626 | 1.3421 | 0.4451 | 0.0545 | 0.3569 | 2.1390 | 0.6093 | 96.5412 |
| NWI5 | anda | 125 | 26.4135 | 0.0012 | 0.1260 | 12.5831 | 0.4517 | 0.9981 | 11.5645 | 26.3271 | 2.8995 | 11.5187 | 2.1161 | 1.3442 | 0.5629 | 0.1241 | 0.2157 | 1.4622 | 0.4429 | 99.1615 |
| NWI5 | anda | 128 | 26.5254 | 0.4575 | 0.4703 | 12.1910 | 0.3882 | 0.8021 | 11.9930 | 26.4932 | 2.7535 | 10.8614 | 1.8505 | 1.0922 | 0.3895 | 0.1105 | 0.1804 | 1.5647 | 0.2513 | 98.3847 |
| NWI5 | anda | 130 | 28.2830 | 2.5296 | 1.3474 | 11.6719 | 0.3085 | 0.8282 | 11.2911 | 25.4259 | 2.5874 | 10.8005 | 1.9131 | 1.0519 | 0.4544 | 0.0553 | 0.1804 | 1.1288 | 0.3595 | 100.2269 |
| NWI5 | anda | 132 | 27.2767 | 0.4927 | 0.5463 | 13.0500 | 0.6919 | 0.8168 | 10.7310 | 23.7077 | 2.3898 | 10.0080 | 1.8826 | 1.1803 | 0.3785 | 0.1010 | 0.2880 | 3.4960 | 0.3388 | 97.3861 |
| NWI5 | anda | 134 | 26.4802 | 0.0856 | 0.1454 | 12.5595 | 0.2935 | 0.6873 | 12.6789 | 27.4174 | 2.8232 | 10.5983 | 1.7005 | 1.0917 | 0.3543 | 0.0753 | 0.2066 | 1.6042 | 0.2479 | 99.0598 |
| NWI5 | anda | 5 | 26.7907 | 0.0881 | 0.2710 | 12.8684 | 0.5380 | 0.8422 | 11.5255 | 25.3032 | 2.6179 | 10.1485 | 1.7109 | 1.3581 | 0.4694 | 0.1280 | 0.3564 | 3.5447 | 0.2013 | 98.7723 |
| NWI5 | anda | 6 | 26.3400 | 0.0412 | 0.2164 | 12.6613 | 0.4325 | 1.2558 | 11.3658 | 25.3324 | 2.7484 | 10.8435 | 1.9317 | 1.3482 | 0.5468 | 0.0610 | 0.2680 | 1.9705 | 0.4690 | 97.8425 |
| NWI5 | anda | 12 | 26.1074 | 0.0285 | 0.1500 | 12.5354 | 0.4922 | 0.8458 | 11.6455 | 25.5289 | 2.5757 | 10.4498 | 1.8291 | 1.1652 | 0.4746 | 0.0890 | 0.2726 | 2.4434 | 0.4043 | 97.0474 |
| NWI5 | anda | 13 | 26.1602 | 0.0652 | 0.2023 | 12.5613 | 0.0515 | 1.0125 | 11.1704 | 24.9631 | 2.6759 | 10.0904 | 1.8581 | 1.2054 | 0.3589 | 1.1219 | 0.3394 | 3.8018 | 0.3340 | 97.9823 |
| NWI5 | anda | 14 | 26.2763 | 0.1997 | 0.1494 | 12.5228 | 0.3632 | 1.0795 | 12.0031 | 26.3348 | 2.6467 | 10.4987 | 1.6923 | 1.1973 | 0.4690 | 0.1024 | 0.2324 | 1.6886 | 0.3159 | 97.7821 |
| NWI5 | anda | 15 | 26.8304 | 0.0860 | 0.2579 | 12.8621 | 0.8462 | 0.6729 | 11.0857 | 24.3792 | 2.5156 | 9.7512 | 1.6868 | 1.1933 | 0.3789 | 0.0749 | 0.4860 | 5.6476 | 0.2725 | 99.0372 |
| NWI5 | anda | 16 | 26.3833 | 0.0736 | 0.1407 | 12.6786 | 0.4358 | 0.6925 | 12.0385 | 26.4556 | 2.5845 | 10.4538 | 1.6696 | 1.0477 | 0.3777 | 0.0301 | 0.2200 | 2.0651 | 0.2382 | 97.5953 |
| NWI5 | anda | 17 | 25.9539 | 0.0791 | 1.1375 | 11.6305 | 0.3043 | 0.7803 | 11.7836 | 25.8353 | 2.7524 | 10.6086 | 1.7006 | 0.9907 | 0.3767 | 0.1154 | 0.1552 | 1.5543 | 0.2303 | 95.9987 |
| NWI5 | anda | 20 | 26.1891 | 0.0122 | 0.1551 | 12.5123 | 0.6689 | 0.7642 | 11.3732 | 25.2864 | 2.7468 | 10.3658 | 1.6720 | 1.1181 | 0.3765 | 0.0662 | 0.3371 | 3.8451 | 0.2177 | 97.7167 |
| NWI5 | anda | 21 | 26.2586 | 0.2359 | 0.5056 | 12.2708 | 0.3288 | 0.8039 | 11.8473 | 26.4926 | 2.6500 | 10.3992 | 1.6804 | 1.0000 | 0.3615 | 0.0897 | 0.1634 | 1.4654 | 0.2052 | 96.7683 |
| NWI5 | anda | 23 | 25.9857 | 0.0175 | 0.1240 | 12.3713 | 0.4130 | 0.7659 | 11.7798 | 26.3832 | 2.7372 | 10.6754 | 1.8123 | 1.0924 | 0.3717 | 0.0296 | 0.2513 | 2.3914 | 0.2044 | 97.4161 |
| NWI5 | anda | 24 | 26.1254 | 0.0267 | 0.2719 | 12.4134 | 0.7802 | 0.8445 | 10.8594 | 23.9992 | 2.5502 | 9.9980 | 1.7213 | 1.2097 | 0.4945 | 0.0572 | 0.4631 | 5.4784 | 0.2510 | 97.5541 |
| NWI5 | anda | 25 | 27.5881 | 0.8993 | 1.8499 | 11.7296 | 0.8627 | 0.7815 | 10.5383 | 23.3829 | 2.4318 | 9.7497 | 1.7709 | 1.2878 | 0.4516 | 0.0481 | 0.4275 | 5.1694 | 0.2107 | 99.1898 |
| NWI5 | anda | 28 | 27.7469 | 1.0688 | 1.0634 | 12.4310 | 0.3183 | 0.6748 | 12.0362 | 26.2924 | 2.5318 | 10.4182 | 1.6202 | 1.0230 | 0.3420 | 0.0652 | 0.1108 | 1.0400 | 0.2301 | 99.0231 |
| NWI5 | anda | 30 | 25.9940 | 0.5567 | 0.3437 | 11.9446 | 0.3472 | 0.6281 | 12.1662 | 26.5465 | 2.6564 | 10.5297 | 1.6825 | 0.9613 | 0.3751 | 0.0602 | 0.1488 | 1.2555 | 0.1980 | 96.4045 |
| NWI5 | anda | 31 | 26.4650 | 0.0764 | 0.9095 | 12.1534 | 0.2170 | 0.6628 | 11.9902 | 27.0289 | 2.6363 | 10.5542 | 1.6828 | 1.0621 | 0.3731 | 0.0426 | 0.1199 | 1.0103 | 0.2471 | 97.2416 |
| NWI5 | anda | 34 | 26.2229 | 0.9455 | 0.8791 | 11.4879 | 0.4068 | 0.6542 | 11.5622 | 25.5269 | 2.6792 | 10.4972 | 1.6896 | 1.0920 | 0.3785 | 0.0060 | 0.1958 | 1.9706 | 0.2253 | 96.4297 |
| NWI5 | anda | 35 | 26.5985 | 0.0971 | 0.2339 | 12.6574 | 0.4475 | 0.7941 | 11.9987 | 26.5364 | 2.7333 | 10.3934 | 1.7266 | 1.1428 | 0.4346 | 0.0202 | 0.2500 | 2.5148 | 0.1901 | 98.7794 |
| NWI5 | anda | 36 | 26.4432 | 0.0323 | 0.2355 | 12.5770 | 0.6744 | 0.8385 | 10.8439 | 24.8666 | 2.5934 | 10.5886 | 1.9322 | 1.6184 | 0.4670 | 0.1335 | 0.3662 | 4.3644 | 0.1922 | 98.7773 |
| NWI5 | anda | 38 | 26.4325 | 0.0261 | 0.1449 | 12.6256 | 0.3557 | 0.7468 | 12.1538 | 27.2099 | 2.6469 | 10.6693 | 1.6824 | 1.0813 | 0.4096 | 0.1043 | 0.1839 | 1.9364 | 0.1603 | 98.5797 |
| NWI5 | anda | 39 | 26.4109 | 0.0076 | 0.1385 | 12.6475 | 0.3464 | 0.7501 | 12.1417 | 27.0168 | 2.7357 | 10.7109 | 1.7233 | 1.1375 | 0.4131 | 0.0972 | 0.1630 | 1.7538 | 0.1812 | 98.3852 |
| NWI5 | anda | 40 | 26.4212 | 0.0293 | 0.1845 | 12.6350 | 0.2801 | 0.8801 | 12.2528 | 27.1319 | 2.6378 | 10.6274 | 1.8544 | 1.1596 | 0.3990 | 0.0606 | 0.1520 | 1.4256 | 0.1965 | 98.3378 |
| NWI5 | anda | 44 | 26.9329 | 1.7895 | 1.5734 | 11.0819 | 0.4557 | 0.6858 | 10.7184 | 23.8470 | 2.5334 | 10.3811 | 1.8664 | 1.2215 | 0.4021 | 0.0313 | 0.2485 | 2.6703 | 0.1888 | 96.6380 |
| NWI5 | anda | 45 | 26.3056 | 0.0400 | 0.2370 | 12.4849 | 0.8434 | 0.6022 | 10.9753 | 24.5536 | 2.4182 | 10.0975 | 1.7215 | 1.2269 | 0.3584 | 0.0884 | 0.4295 | 5.5203 | 0.1868 | 98.0995 |
| NWI5 | anda | 47 | 26.3221 | 0.0185 | 0.2068 | 12.6205 | 0.5205 | 1.0555 | 11.0368 | 25.1992 | 2.7920 | 11.4933 | 2.0138 | 1.2668 | 0.4414 | 0.0833 | 0.2388 | 2.1459 | 0.3548 | 97.8200 |
| NWI5 | anda | 48 | 26.6853 | 0.3211 | 0.5106 | 12.4678 | 0.3110 | 0.8653 | 11.2891 | 25.9138 | 2.8460 | 11.5862 | 2.0745 | 1.1152 | 0.4280 | 0.0956 | 0.1676 | 1.0776 | 0.3888 | 98.1535 |
| NWI5 | anda | 50 | 26.8162 | 0.0276 | 0.1168 | 13.1755 | 0.3158 | 1.1880 | 11.1183 | 25.4547 | 2.8415 | 11.7212 | 2.1692 | 1.2976 | 0.4668 | 0.1183 | 0.1311 | 0.8219 | 0.3699 | 98.1604 |
| NWI5 | anda | 54 | 26.3955 | 0.0255 | 0.1565 | 12.7161 | 0.3643 | 0.9497 | 11.7253 | 26.2436 | 2.7476 | 10.9495 | 1.8789 | 1.1933 | 0.4584 | 0.1360 | 0.1765 | 1.4236 | 0.2847 | 97.8350 |
| NWI5 | anda | 55 | 26.1668 | 0.2257 | 0.3722 | 12.3121 | 0.4375 | 1.0042 | 11.3078 | 25.4669 | 2.6801 | 11.1499 | 1.9244 | 1.2752 | 0.4696 | 0.1139 | 0.1755 | 1.3658 | 0.3820 | 96.8396 |
| NWI5 | anda | 56 | 26.2721 | 0.0713 | 0.1620 | 12.5869 | 0.4411 | 0.8110 | 11.9185 | 26.0187 | 2.7390 | 11.0761 | 1.8536 | 1.1633 | 0.4884 | 0.0520 | 0.1546 | 1.2629 | 0.2215 | 97.3030 |
| NWI5 | anda | 97 | 26.7623 | 0.0174 | 0.1394 | 12.8798 | 0.4475 | 0.8069 | 11.6936 | 26.2953 | 2.7438 | 10.9791 | 1.9519 | 1.3810 | 0.3986 | 0.0628 | 0.2242 | 2.3941 | 0.1569 | 99.3446 |
| NWI5 | anda | 98 | 27.2734 | 0.0274 | 0.1307 | 13.2963 | 0.5824 | 0.8042 | 11.6932 | 26.1785 | 2.5063 | 10.5971 | 1.7285 | 1.2336 | 0.3794 | 0.1074 | 0.3150 | 3.0259 | 0.1943 | 100.0836 |
| NWI5 | anda | 99 | 26.4356 | 0.0096 | 0.2366 | 12.5919 | 0.8558 | 0.6053 | 11.1724 | 24.7794 | 2.5040 | 9.6952 | 1.6757 | 1.2473 | 0.3704 | 0.0851 | 0.4419 | 5.4473 | 0.2313 | 98.3948 |
| NWI5 | anda | 100 | 26.6903 | 0.0488 | 0.1871 | 13.0093 | 0.4689 | 0.7015 | 11.4586 | 26.1193 | 2.4273 | 10.1141 | 1.7339 | 1.2500 | 0.3351 | 0.0850 | 0.2255 | 2.4085 | 0.1372 | 97.4104 |
| NWI5 | anda | 101 | 26.5092 | 0.2342 | 0.3394 | 12.5264 | 0.7614 | 0.7176 | 11.0689 | 24.7648 | 2.4878 | 10.4505 | 1.6983 | 1.2435 | 0.3623 | 0.0316 | 0.3534 | 3.9004 | 0.2499 | 97.7096 |
| NWI5 | anda | 104 | 26.5697 | 0.0321 | 0.2287 | 12.8893 | 0.5277 | 0.7923 | 11.3671 | 25.7910 | 2.5826 | 9.8388 | 1.5039 | 1.0977 | 0.4539 | 0.0587 | 0.3124 | 3.1509 | 0.1885 | 97.3953 |

| Sample | Phase | Label | W%(O ) | W%(Al) | W%(Si) | W%(P) | W%(Ca) | W%(Y ) | W%(La) | W%(Ce) | W%(Pr) | W%(Nd) | W%(Sm) | W%(Gd) | W%(Dy) | W%(Er) | W%(Pb) | W%(Th) | W%(U ) | W%(SUM) |
|---|---|---|---|---|---|---|---|---|---|---|---|---|---|---|---|---|---|---|---|---|
| NWI5 | anda | 105 | 26.4276 | 0.0296 | 0.1473 | 12.6902 | 0.4992 | 0.8800 | 11.6189 | 26.2861 | 2.7541 | 10.2992 | 1.7149 | 1.2378 | 0.4652 | 0.1455 | 0.2250 | 2.5966 | 0.1989 | 98.2261 |
| NWI5 | anda | 106 | 26.6328 | 0.0142 | 0.1240 | 12.8720 | 0.3255 | 0.7219 | 12.1794 | 27.6886 | 2.6291 | 10.3038 | 1.5385 | 0.9463 | 0.4111 | 0.0217 | 0.1748 | 1.6441 | 0.1762 | 98.4140 |
| NWI5 | anda | 107 | 26.9020 | 0.0337 | 0.1806 | 12.9425 | 0.4790 | 0.7881 | 11.9513 | 26.7684 | 2.6849 | 10.3194 | 1.6267 | 1.1462 | 0.4592 | 0.1272 | 0.2722 | 2.7139 | 0.1621 | 99.5674 |
| NWI5 | anda | 108 | 26.3054 | 0.0682 | 0.1865 | 12.5866 | 0.5687 | 0.7855 | 11.5741 | 25.7328 | 2.6082 | 9.9194 | 1.6848 | 1.1412 | 0.3760 | 0.0465 | 0.3255 | 3.5112 | 0.2611 | 97.6917 |
| NWI5 | anda | 109 | 26.8586 | 0.0149 | 0.1471 | 12.9994 | 0.9250 | 0.8002 | 10.9856 | 25.1954 | 2.5570 | 10.0851 | 1.6969 | 1.2095 | 0.4274 | 0.0354 | 0.3589 | 4.4207 | 0.2510 | 98.9781 |
| NWI5 | anda | 110 | 27.8456 | 1.3787 | 1.1257 | 12.2306 | 0.4484 | 0.7745 | 11.4488 | 26.0491 | 2.5401 | 10.1621 | 1.4429 | 0.9394 | 0.4692 | 0.0560 | 0.2158 | 2.1155 | 0.3056 | 99.5580 |
| NWI5 | anda | 112 | 26.1348 | 0.0249 | 0.1313 | 12.5170 | 0.4210 | 0.8370 | 11.7448 | 26.9807 | 2.6392 | 10.3142 | 1.5717 | 1.0460 | 0.4028 | 0.0341 | 0.1996 | 2.0935 | 0.2682 | 97.3708 |
| NWI5 | anda | 113 | 26.0221 | 0.0543 | 0.2158 | 12.3244 | 0.5484 | 0.7575 | 11.4080 | 25.7507 | 2.5928 | 10.3733 | 1.6905 | 1.0678 | 0.4804 | 0.0245 | 0.3123 | 3.5233 | 0.2052 | 97.3613 |
| NWI5 | anda | 114 | 26.1248 | 0.0500 | 0.1575 | 12.5122 | 0.2948 | 0.7359 | 12.2857 | 27.5471 | 2.6793 | 9.9127 | 1.5650 | 0.8761 | 0.3274 | 0.0958 | 0.1714 | 1.3696 | 0.2325 | 96.9478 |
| NWI5 | als1 | 16 | 26.8432 | 0.0519 | 0.1864 | 13.0051 | 0.3859 | 0.7689 | 12.9455 | 25.4452 | 2.6802 | 9.9855 | 1.8668 | 1.1637 | 0.3682 | 0.0425 | 0.2333 | 2.4825 | 0.2029 | 98.6677 |
| NWI5 | als2 | 17 | 26.5607 | 0.0330 | 0.2170 | 12.7377 | 0.6932 | 0.7348 | 12.1071 | 24.1616 | 2.6128 | 9.8046 | 1.9352 | 1.3333 | 0.4611 | 0.0545 | 0.3867 | 4.3875 | 0.2138 | 98.4446 |
| NWI5 | als3 | 18 | 26.5753 | 0.0367 | 0.2134 | 12.7270 | 0.8944 | 0.7817 | 12.1975 | 24.2071 | 2.6811 | 9.7972 | 1.7881 | 1.3174 | 0.4497 | 0.0637 | 0.3088 | 4.0253 | 0.1944 | 98.2688 |
| NWI5 | als4 | 19 | 26.2604 | 0.0425 | 0.2309 | 12.4791 | 0.7293 | 0.7118 | 12.4522 | 24.3013 | 2.5024 | 9.5654 | 1.6535 | 1.1756 | 0.3727 | 0.0490 | 0.4244 | 4.7372 | 0.2273 | 97.9250 |
| NWI5 | als5 | 20 | 26.5073 | 0.0431 | 0.1532 | 12.7986 | 0.4096 | 0.9025 | 12.7532 | 25.2840 | 2.6973 | 9.9459 | 1.9495 | 1.2672 | 0.4794 | 0.0189 | 0.2336 | 2.4076 | 0.2011 | 98.0620 |
| NWI5 | als6 | 21 | 26.9141 | 0.2068 | 0.9371 | 12.3699 | 0.8557 | 0.9037 | 11.3177 | 22.7125 | 2.4396 | 9.5264 | 1.8097 | 1.4270 | 0.4707 | 0.0547 | 0.5210 | 6.0995 | 0.2650 | 98.8411 |
| NWI5 | als7 | 22 | 27.4147 | 0.0277 | 1.1403 | 12.8152 | 0.3360 | 0.7613 | 12.7828 | 25.1796 | 2.6036 | 9.7681 | 1.6918 | 1.0979 | 0.3209 | 0.0633 | 0.2297 | 1.9639 | 0.2626 | 98.4694 |
| NWI5 | als8 | 23 | 26.7140 | 0.0516 | 0.1573 | 12.9904 | 0.4703 | 0.9109 | 12.4658 | 24.9977 | 2.7547 | 10.0050 | 1.7221 | 1.2067 | 0.4060 | 0.0483 | 0.3075 | 2.5538 | 0.4087 | 98.1808 |
| NWI5 | als10 | 25 | 26.6856 | 0.1518 | 0.2231 | 12.7921 | 0.4238 | 0.6161 | 12.9168 | 25.4234 | 2.7291 | 10.0278 | 1.7148 | 1.1060 | 0.3217 | 0.0001 | 0.2543 | 2.5242 | 0.2299 | 98.1506 |
| NWI5 | als11 | 26 | 26.5281 | 0.0192 | 0.1483 | 12.8315 | 0.4595 | 0.7386 | 12.9298 | 25.5189 | 2.6426 | 9.7530 | 1.7039 | 1.2000 | 0.3225 | 0.0669 | 0.2523 | 2.4121 | 0.3462 | 97.8834 |
| NWI5 | als13 | 28 | 26.6135 | 0.0236 | 0.1560 | 12.8782 | 0.4431 | 0.8325 | 12.7820 | 25.5744 | 2.7478 | 9.8722 | 1.7177 | 1.1780 | 0.4198 | 0.0869 | 0.2624 | 2.4009 | 0.2119 | 98.2109 |
| NWI5 | als17 | 32 | 26.4840 | 0.0355 | 0.1782 | 12.8279 | 0.4192 | 0.8505 | 12.7913 | 25.4461 | 2.6071 | 10.0659 | 1.8629 | 1.1976 | 0.4646 | 0.0137 | 0.2016 | 1.7409 | 0.1718 | 97.3688 |
| NWI5 | als18 | 33 | 26.7319 | 0.2177 | 0.3261 | 12.8101 | 0.3780 | 0.9044 | 12.7986 | 25.1909 | 2.6446 | 9.8883 | 1.7003 | 1.0829 | 0.4282 | 0.0199 | 0.2106 | 2.1923 | 0.2271 | 97.7619 |
| NWI5 | als20 | 35 | 26.5119 | 0.0205 | 0.2327 | 12.7768 | 0.3832 | 0.8735 | 12.6622 | 25.3557 | 2.6285 | 10.2146 | 1.8305 | 1.1594 | 0.4529 | 0.0606 | 0.2168 | 2.2129 | 0.2373 | 97.8400 |
| NWI5 | als21 | 36 | 26.5808 | 0.1797 | 0.2762 | 12.7591 | 0.3715 | 0.7978 | 12.4923 | 24.8687 | 2.7287 | 10.2002 | 1.7904 | 1.1753 | 0.4490 | 0.1116 | 0.2106 | 2.2480 | 0.2085 | 97.4584 |
| NWI5 | als22 | 37 | 27.8898 | 1.3318 | 1.3671 | 12.2769 | 0.5971 | 0.8846 | 11.5088 | 23.0522 | 2.5240 | 9.4984 | 1.7848 | 1.2723 | 0.5013 | 0.1429 | 0.3526 | 3.4213 | 0.2659 | 98.6818 |
| NWI5 | als23 | 38 | 26.1345 | 0.0532 | 0.3156 | 12.5337 | 0.9695 | 0.9931 | 10.8455 | 21.8574 | 2.4693 | 9.0214 | 1.9400 | 1.3562 | 0.5121 | 0.0228 | 0.5592 | 6.8136 | 0.2804 | 96.6875 |
| NWI5 | als24 | 39 | 26.4668 | 0.1306 | 0.2980 | 12.7431 | 0.5511 | 0.8693 | 11.8861 | 24.0380 | 2.5841 | 9.6880 | 1.9003 | 1.2917 | 0.4221 | 0.1161 | 0.3358 | 3.4271 | 0.2561 | 97.0143 |
| NWI5 | als25 | 40 | 26.4596 | 0.0255 | 0.1476 | 12.8973 | 0.3650 | 0.9213 | 12.6449 | 24.9936 | 2.7052 | 9.9032 | 1.7561 | 1.2580 | 0.4070 | 0.0639 | 0.2490 | 2.1644 | 0.2583 | 97.2299 |
| NWI5 | als27 | 42 | 26.8241 | 0.0465 | 0.2221 | 12.9923 | 0.6340 | 0.8981 | 12.3219 | 24.0788 | 2.6138 | 9.7749 | 1.8190 | 1.1757 | 0.4306 | 0.0894 | 0.3431 | 4.1633 | 0.2044 | 98.6420 |
| NWI5 | als28 | 43 | 28.0548 | 1.1308 | 1.2670 | 12.5167 | 0.7790 | 0.7349 | 11.3623 | 22.7417 | 2.4290 | 9.3000 | 1.7244 | 1.0834 | 0.4172 | 0.0895 | 0.4209 | 5.2789 | 0.2702 | 99.6107 |
| NWI5 | als29 | 44 | 26.5215 | 0.0746 | 0.5782 | 12.5441 | 0.5542 | 0.8603 | 12.4602 | 24.0639 | 2.5022 | 9.6710 | 1.7985 | 1.1091 | 0.4152 | 0.0326 | 0.3157 | 3.5498 | 0.2259 | 97.2870 |
| NWI5 | als30 | 45 | 26.5262 | 0.1448 | 0.2510 | 12.7336 | 0.3838 | 0.7748 | 12.5609 | 25.0431 | 2.8376 | 9.9613 | 1.9003 | 1.1603 | 0.3791 | 0.0980 | 0.2229 | 2.2829 | 0.2376 | 97.5082 |
| NWI5 | als31 | 46 | 26.5280 | 0.0592 | 0.2913 | 12.7103 | 0.8249 | 0.8553 | 11.6105 | 23.1173 | 2.5683 | 9.5848 | 1.8378 | 1.2275 | 0.3907 | 0.0370 | 0.5085 | 5.7307 | 0.2210 | 98.1131 |
| NWI5 | als32 | 47 | 26.6118 | 0.0507 | 0.2790 | 12.7978 | 0.7917 | 0.9135 | 11.6549 | 23.0770 | 2.4959 | 9.5508 | 2.0040 | 1.4199 | 0.4401 | 0.0427 | 0.4520 | 5.4205 | 0.2660 | 98.2783 |
| NWI5 | als34 | 49 | 26.5540 | 0.0977 | 0.3163 | 12.6968 | 0.7683 | 0.8928 | 11.6481 | 23.2197 | 2.6805 | 9.6912 | 1.9172 | 1.1432 | 0.4671 | 0.1085 | 0.4554 | 5.1838 | 0.2261 | 98.0767 |
| NWI5 | als35 | 50 | 26.4744 | 0.0418 | 0.2030 | 12.7793 | 0.5609 | 0.9285 | 12.3710 | 24.4475 | 2.6965 | 9.8360 | 1.8007 | 1.1088 | 0.4218 | 0.0040 | 0.3313 | 3.4972 | 0.2352 | 97.7479 |
| NWI5 | als37 | 52 | 26.5672 | 0.0451 | 0.1831 | 12.8759 | 0.4601 | 0.8903 | 12.4463 | 24.7910 | 2.7312 | 10.1090 | 1.8236 | 1.2050 | 0.4254 | 0.0633 | 0.2598 | 2.6376 | 0.2471 | 97.7710 |
| NWI5 | als38 | 53 | 26.5383 | 0.0427 | 0.1647 | 12.8892 | 0.4114 | 0.8206 | 12.7044 | 24.9192 | 2.6930 | 10.0223 | 1.8217 | 1.1033 | 0.3602 | 0.0994 | 0.2546 | 2.4272 | 0.2496 | 97.5318 |
| NWI5 | als39 | 54 | 26.4206 | 0.2866 | 0.3483 | 12.6284 | 0.8221 | 0.8444 | 12.0226 | 23.7343 | 2.6592 | 9.4902 | 1.8422 | 1.2290 | 0.4180 | 0.0001 | 0.2708 | 2.5873 | 0.2794 | 95.8935 |
| NWI5 | als42 | 57 | 26.4507 | 0.0283 | 0.1389 | 12.8166 | 0.3258 | 0.8677 | 12.7711 | 25.2259 | 2.7943 | 10.2186 | 1.9461 | 1.2671 | 0.4359 | 0.0721 | 0.2270 | 1.8432 | 0.2435 | 97.6828 |
| NWI5 | als43 | 58 | 26.3744 | 0.0261 | 0.1378 | 12.8287 | 0.2641 | 0.8832 | 12.9711 | 25.4108 | 2.7066 | 10.2292 | 1.7390 | 1.1980 | 0.4613 | 0.0661 | 0.1504 | 1.3852 | 0.1894 | 97.0314 |
| NWI5 | als44 | 59 | 26.4768 | 0.0347 | 0.1964 | 12.7558 | 0.4250 | 0.7607 | 12.5087 | 24.9130 | 2.7344 | 10.2548 | 1.8859 | 1.2236 | 0.4259 | 0.1017 | 0.2367 | 2.7200 | 0.1590 | 97.8231 |
| NWI5 | als45 | 60 | 26.4580 | 0.0323 | 0.1447 | 12.7913 | 0.6641 | 0.8501 | 12.1491 | 24.3098 | 2.6460 | 10.1031 | 1.8048 | 1.2328 | 0.3405 | 0.0441 | 0.3273 | 3.6142 | 0.2251 | 97.7473 |
| NWI5 | als46 | 61 | 26.4035 | 0.0778 | 0.3297 | 12.6634 | 0.6181 | 0.8615 | 12.2692 | 24.4105 | 2.5499 | 9.7607 | 1.7559 | 1.1863 | 0.3716 | 0.0926 | 0.3008 | 3.0250 | 0.2240 | 96.9105 |
| NWI5 | als47 | 62 | 26.6439 | 0.0340 | 0.2006 | 12.8212 | 0.4453 | 0.3176 | 12.8439 | 25.6259 | 2.7447 | 9.9891 | 1.7851 | 0.8824 | 0.2221 | 0.0481 | 0.2101 | 3.0948 | 0.0795 | 97.9983 |
| NWI5 | als48 | 63 | 26.5114 | 0.0412 | 0.1847 | 12.7972 | 0.5964 | 0.8982 | 12.2877 | 24.5599 | 2.5319 | 9.7452 | 1.8567 | 1.2781 | 0.4691 | 0.0277 | 0.3163 | 3.6534 | 0.1891 | 97.9542 |
| NWI5 | als50 | 65 | 26.7384 | 0.0242 | 0.1325 | 13.0296 | 0.6031 | 0.8721 | 12.4895 | 24.7133 | 2.5917 | 9.7921 | 1.8702 | 1.2039 | 0.3701 | 0.0257 | 0.3079 | 3.1912 | 0.2487 | 98.2142 |
| NWI5 | als51 | 66 | 26.5129 | 0.0251 | 0.1818 | 12.7053 | 0.4308 | 0.4159 | 12.9664 | 25.7052 | 2.7562 | 10.1774 | 1.7678 | 0.9616 | 0.2542 | 0.1376 | 0.2049 | 2.8040 | 0.0749 | 98.0920 |
| NWI5 | als52 | 67 | 26.8352 | 0.0422 | 0.2000 | 12.9369 | 0.4069 | 0.2761 | 13.7153 | 25.7680 | 2.7309 | 9.7654 | 1.5429 | 0.9090 | 0.2466 | 0.0126 | 0.2223 | 2.7765 | 0.0367 | 98.4335 |
| NWI5 | als53 | 68 | 26.5459 | 0.0408 | 0.1399 | 12.8647 | 0.5291 | 0.8664 | 12.6373 | 24.9043 | 2.6522 | 9.7760 | 1.8487 | 1.2400 | 0.3898 | 0.0973 | 0.2834 | 2.8307 | 0.2283 | 97.8848 |
| NWI5 | als55 | 70 | 26.6897 | 0.0520 | 0.1219 | 12.9964 | 0.2037 | 0.8804 | 13.1533 | 26.1720 | 2.7017 | 10.3140 | 1.7611 | 1.1815 | 0.4327 | 0.0955 | 0.1383 | 0.9644 | 0.1944 | 98.0630 |
| NWI5 | als58 | 82 | 26.5645 | 0.0367 | 0.2421 | 12.7345 | 0.8413 | 0.6218 | 12.1084 | 24.2654 | 2.5808 | 9.4145 | 1.6506 | 1.1226 | 0.2880 | 0.0759 | 0.4273 | 4.8709 | 0.2111 | 98.0664 |
| NWI5 | als59 | 83 | 26.1383 | 0.0992 | 0.2520 | 12.5443 | 0.8064 | 0.9318 | 11.6856 | 23.1737 | 2.4999 | 9.6686 | 1.8158 | 1.4024 | 0.4579 | 0.1288 | 0.3511 | 4.0793 | 0.2957 | 96.3408 |
| NWI5 | als60 | 84 | 26.4873 | 0.0186 | 0.1303 | 12.8425 | 0.2843 | 0.7709 | 13.2949 | 25.8512 | 2.5839 | 10.0924 | 1.8672 | 1.0775 | 0.4122 | 0.0752 | 0.1873 | 1.4733 | 0.2143 | 97.6733 |
| NWI5 | als61 | 85 | 27.0366 | 0.0924 | 0.2387 | 13.0918 | 0.7552 | 0.6561 | 12.4458 | 23.9467 | 2.4603 | 9.5837 | 1.7774 | 1.1710 | 0.3485 | 0.1304 | 0.3859 | 4.4433 | 0.2541 | 98.8279 |
| NWI5 | als62 | 86 | 26.5289 | 0.0206 | 0.1385 | 12.9124 | 0.3529 | 0.8202 | 12.7981 | 25.0574 | 2.7836 | 10.0240 | 1.8362 | 1.2044 | 0.3905 | 0.0859 | 0.2316 | 2.1604 | 0.2225 | 97.5781 |

| Sample | Phase | Label | W%(O ) | W%(Al) | W%(Si) | W%(P) | W%(Ca) | W%(Y ) | W%(La) | W%(Ce) | W%(Pr) | W%(Nd) | W%(Sm) | W%(Gd) | W%(Dy) | W%(Er) | W%(Pb) | W%(Th) | W%(U ) | W%(SUM) |
|---|---|---|---|---|---|---|---|---|---|---|---|---|---|---|---|---|---|---|---|---|
| NWI5 | als63 | 87 | 26.6340 | 0.0289 | 0.1693 | 12.9451 | 0.4103 | 0.8468 | 12.7454 | 25.0066 | 2.6148 | 10.0034 | 1.8211 | 1.2373 | 0.3965 | 0.0589 | 0.2390 | 2.5382 | 0.1858 | 97.8914 |
| NWI5 | als64 | 88 | 26.6308 | 0.0334 | 0.1583 | 12.9455 | 0.4905 | 0.8414 | 12.4021 | 24.6815 | 2.6610 | 9.9375 | 1.9086 | 1.1965 | 0.3878 | 0.0764 | 0.2777 | 3.0723 | 0.2247 | 97.9360 |
| NWI5 | als65 | 89 | 26.7872 | 0.0297 | 0.1181 | 13.0569 | 0.2966 | 0.9319 | 13.0976 | 25.6643 | 2.8784 | 10.3184 | 1.8586 | 1.1494 | 0.3990 | 0.0457 | 0.1627 | 1.4264 | 0.2546 | 98.4855 |
| NWI5 | als67 | 91 | 26.6268 | 0.0178 | 0.1312 | 12.9272 | 0.2873 | 0.9172 | 13.1001 | 25.7110 | 2.7578 | 10.1334 | 1.8352 | 1.1754 | 0.4355 | 0.1198 | 0.2121 | 1.6722 | 0.2205 | 98.2905 |
| NWI5 | als68 | 92 | 25.7154 | 0.2239 | 0.4204 | 12.0458 | 0.2952 | 0.8410 | 12.6215 | 25.1116 | 2.6442 | 10.0218 | 1.7516 | 1.2475 | 0.4522 | 0.0633 | 0.1333 | 1.3463 | 0.1687 | 95.1137 |
| NWI5 | als70 | 94 | 26.5678 | 0.1746 | 0.2940 | 12.7544 | 0.2892 | 0.8075 | 13.2071 | 25.3870 | 2.6349 | 9.9608 | 1.8138 | 1.0556 | 0.4114 | 0.0864 | 0.1614 | 1.3618 | 0.2341 | 97.2118 |
| NWI5 | als71 | 95 | 26.8330 | 0.0552 | 0.1721 | 13.0809 | 0.4868 | 0.8868 | 12.8539 | 24.7391 | 2.6687 | 9.8000 | 1.7704 | 1.2304 | 0.4153 | 0.1757 | 0.2465 | 2.4658 | 0.3150 | 98.2056 |
| NWI5 | als72 | 96 | 26.7726 | 0.0077 | 0.1135 | 13.0861 | 0.2833 | 0.8423 | 13.2594 | 25.8597 | 2.7261 | 10.0910 | 1.7755 | 1.0631 | 0.4030 | 0.0479 | 0.1863 | 1.4591 | 0.2501 | 98.2367 |
| NWI5 | als73 | 97 | 25.9969 | 0.0305 | 0.2401 | 12.4210 | 1.1203 | 0.7874 | 12.1943 | 23.6575 | 2.5587 | 9.3192 | 1.7790 | 1.0902 | 0.4173 | 0.1053 | 0.3184 | 3.4677 | 0.2523 | 95.7661 |
| NWI5 | als74 | 98 | 26.6425 | 0.0483 | 0.1348 | 12.9629 | 0.2803 | 0.8243 | 13.0114 | 25.6623 | 2.7200 | 10.1657 | 1.8238 | 1.1222 | 0.4239 | 0.0623 | 0.1870 | 1.5527 | 0.2514 | 97.8858 |
| NWI5 | als75 | 99 | 26.3274 | 0.0256 | 0.1258 | 12.7668 | 0.3033 | 0.7685 | 13.0991 | 25.4518 | 2.6734 | 10.0946 | 1.7499 | 1.0942 | 0.3866 | 0.1382 | 0.1711 | 1.6148 | 0.2764 | 97.0775 |
| NWI5 | als76 | 100 | 26.4416 | 0.2179 | 0.3496 | 12.6986 | 0.4951 | 0.9025 | 12.0819 | 24.0737 | 2.6673 | 9.4331 | 1.8199 | 1.2368 | 0.4458 | 0.0950 | 0.2923 | 2.9052 | 0.2755 | 96.4418 |
| NWI5 | als79 | 103 | 26.7011 | 0.0335 | 0.1328 | 12.9858 | 0.2829 | 0.7975 | 13.0517 | 25.9577 | 2.7733 | 10.2254 | 1.8105 | 1.0756 | 0.4197 | 0.0624 | 0.1873 | 1.4187 | 0.2154 | 98.1413 |
| NWI5 | als80 | 104 | 26.5931 | 0.0192 | 0.2461 | 12.8811 | 0.7039 | 0.8827 | 11.9400 | 23.4078 | 2.6799 | 9.6014 | 1.6521 | 1.2660 | 0.4301 | 0.0540 | 0.4060 | 4.7502 | 0.2959 | 97.8195 |
| NWI5 | als81 | 105 | 26.8742 | 0.0270 | 0.1551 | 13.1974 | 0.2166 | 0.8738 | 13.1100 | 25.6266 | 2.6842 | 10.2617 | 1.8550 | 1.1557 | 0.4315 | 0.0529 | 0.1487 | 0.9732 | 0.2694 | 97.9230 |
| NWI5 | als82 | 106 | 26.5675 | 0.0771 | 0.1942 | 12.8517 | 0.5441 | 0.9019 | 12.6219 | 24.2402 | 2.5608 | 9.9760 | 1.8001 | 1.2394 | 0.4022 | 0.0843 | 0.3082 | 3.0788 | 0.2943 | 97.7527 |
| NWI5 | als83 | 107 | 26.5619 | 0.0930 | 0.2717 | 12.8041 | 0.6388 | 0.7269 | 12.2409 | 23.7905 | 2.4891 | 9.6023 | 1.7153 | 1.1656 | 0.4395 | 0.1379 | 0.3615 | 4.1497 | 0.2389 | 97.4376 |
| NWI5 | als84 | 108 | 26.6223 | 0.0237 | 0.1567 | 12.9539 | 0.4057 | 0.8541 | 12.6629 | 24.8775 | 2.6424 | 10.1201 | 1.9444 | 1.2091 | 0.4418 | 0.0638 | 0.2485 | 2.4127 | 0.2135 | 97.8631 |
| NWI5 | als85 | 109 | 26.5088 | 0.0147 | 0.1614 | 12.8551 | 0.4381 | 0.8205 | 12.5912 | 24.8292 | 2.6423 | 10.0106 | 2.0184 | 1.3379 | 0.4491 | 0.0669 | 0.2278 | 2.5077 | 0.2011 | 97.6908 |
| NWI5 | als86 | 110 | 26.6729 | 0.0246 | 0.2763 | 12.8846 | 0.4009 | 0.7374 | 12.8267 | 25.1945 | 2.7830 | 9.9503 | 1.8182 | 1.1325 | 0.3360 | 0.0450 | 0.2278 | 2.2448 | 0.2250 | 97.7905 |
| NWI5 | als87 | 111 | 26.4989 | 0.0319 | 0.2250 | 12.7578 | 0.9371 | 0.6881 | 11.5713 | 22.8960 | 2.5151 | 9.7108 | 1.9337 | 1.2477 | 0.4132 | 0.0290 | 0.4662 | 5.5819 | 0.2255 | 97.7392 |
| NWI5 | als88 | 112 | 26.6440 | 0.0294 | 0.3321 | 12.8732 | 0.4568 | 0.8299 | 12.5189 | 24.3230 | 2.6184 | 9.9478 | 1.8861 | 1.2075 | 0.3902 | 0.0908 | 0.3061 | 2.8906 | 0.1853 | 97.5401 |
| NWI5 | als89 | 113 | 26.4505 | 0.0309 | 0.3079 | 12.7509 | 0.8705 | 0.8277 | 11.3606 | 22.4226 | 2.4132 | 9.3770 | 1.8750 | 1.3665 | 0.4557 | 0.0036 | 0.4746 | 6.1129 | 0.2146 | 97.3247 |
| NWI5 | als90 | 114 | 26.7245 | 0.0689 | 0.2471 | 12.9680 | 0.6537 | 0.8577 | 11.8787 | 23.7133 | 2.5372 | 9.6297 | 1.9632 | 1.3575 | 0.4132 | 0.0991 | 0.3650 | 4.1775 | 0.1944 | 97.8587 |
| NWI5 | als91 | 115 | 26.5585 | 0.0366 | 0.2970 | 12.7774 | 0.8522 | 0.8717 | 11.5846 | 22.7044 | 2.4390 | 9.3994 | 1.8911 | 1.4544 | 0.4263 | 0.0985 | 0.4719 | 5.8414 | 0.2579 | 97.9723 |
| NWI5 | als92 | 116 | 26.6760 | 0.0383 | 0.2392 | 12.9027 | 0.6775 | 0.8762 | 11.9874 | 23.4111 | 2.5550 | 9.9543 | 1.8810 | 1.3325 | 0.3491 | 0.0559 | 0.4038 | 4.6427 | 0.2242 | 98.2169 |
| NWI5 | als94 | 118 | 25.8109 | 0.1516 | 0.3302 | 12.2198 | 0.5861 | 0.6844 | 11.8737 | 23.5171 | 2.6487 | 9.8704 | 1.7250 | 1.2281 | 0.3288 | 0.1099 | 0.3157 | 3.9052 | 0.1703 | 95.4859 |
| NWI5 | als95 | 119 | 26.4042 | 0.0394 | 0.1792 | 12.7248 | 0.4272 | 0.8146 | 12.6828 | 24.9007 | 2.6968 | 10.1073 | 1.7882 | 1.2389 | 0.4064 | 0.0769 | 0.2628 | 2.6784 | 0.2214 | 97.6600 |
| NWI5 | als96 | 120 | 26.4368 | 0.0448 | 0.6978 | 12.4986 | 0.7963 | 0.9569 | 11.3945 | 22.4326 | 2.4221 | 9.2323 | 1.7351 | 1.3116 | 0.4598 | 0.0649 | 0.4726 | 5.5267 | 0.2338 | 96.7272 |
| NWI5 | als97 | 121 | 26.3632 | 0.0151 | 0.3009 | 12.6453 | 1.0438 | 0.7709 | 10.8216 | 22.0194 | 2.4525 | 9.3603 | 1.8964 | 1.4430 | 0.4129 | 0.0707 | 0.5405 | 7.0540 | 0.2671 | 97.4876 |
| NWI5 | als98 | 122 | 27.1748 | 0.1119 | 0.8224 | 12.8721 | 0.5637 | 0.9103 | 12.3283 | 23.4042 | 2.6082 | 9.8398 | 1.8723 | 1.2418 | 0.4632 | 0.0464 | 0.2870 | 3.2956 | 0.2286 | 98.0806 |
| NWI5 | als99 | 123 | 26.9307 | 0.0680 | 1.1844 | 12.3843 | 0.5227 | 0.8799 | 11.9769 | 23.9029 | 2.5577 | 9.8479 | 1.8956 | 1.1993 | 0.4928 | 0.1203 | 0.3070 | 3.3132 | 0.1930 | 97.7866 |
| NWI5 | als100 | 124 | 26.6088 | 0.3996 | 0.4378 | 12.5004 | 0.3470 | 0.9285 | 12.6755 | 24.9204 | 2.7627 | 10.1864 | 1.9140 | 1.2035 | 0.4478 | 0.0764 | 0.1865 | 1.7466 | 0.2112 | 97.5631 |
| NWI5 | als101 | 125 | 26.4712 | 0.0291 | 0.1931 | 12.7690 | 0.5967 | 0.8091 | 12.4170 | 24.1650 | 2.7049 | 9.7349 | 1.8434 | 1.2273 | 0.3830 | 0.1061 | 0.3268 | 3.8094 | 0.2171 | 97.8131 |
| R899 | gt | 6 | 26.4163 | 0.0095 | 0.2718 | 12.4643 | 0.9870 | 0.2713 | 11.0512 | 24.2638 | 2.6672 | 10.2687 | 1.8252 | 0.9575 | 0.1141 | 0.0461 | 0.5425 | 5.9413 | 0.4321 | 98.5399 |
| R899 | gt | 7 | 26.2469 | 0.0054 | 0.2512 | 12.4102 | 0.9107 | 0.2119 | 11.0122 | 24.3636 | 2.6058 | 10.2757 | 1.7874 | 0.9527 | 0.0952 | 0.0818 | 0.5295 | 5.6820 | 0.4189 | 97.8511 |
| R899 | gt | 14 | 26.2908 | 0.0129 | 0.2604 | 12.4564 | 0.9994 | 0.2694 | 10.9685 | 23.8244 | 2.6791 | 9.9696 | 1.7965 | 1.0058 | 0.1602 | 0.0243 | 0.5436 | 6.0538 | 0.4699 | 97.7950 |
| R899 | gt | 15 | 26.5254 | 0.0203 | 0.2616 | 12.5919 | 0.9503 | 0.2299 | 10.7165 | 23.9669 | 2.6995 | 10.4405 | 1.8939 | 1.0745 | 0.1813 | 0.0968 | 0.6001 | 5.7615 | 0.5060 | 98.5269 |
| R899 | gt | 16 | 26.2787 | 0.0163 | 0.2541 | 12.4954 | 1.0958 | 0.2204 | 10.4650 | 23.8370 | 2.5396 | 10.1800 | 2.0263 | 1.1741 | 0.1243 | 0.0472 | 0.4870 | 5.3914 | 0.5598 | 97.2024 |
| R899 | gt | 17 | 27.3343 | 0.0114 | 1.2014 | 12.3258 | 3.0817 | 0.4165 | 9.7411 | 22.1381 | 2.3344 | 9.5850 | 2.0911 | 1.2984 | 0.2368 | 0.0371 | 0.4646 | 4.7628 | 0.5678 | 97.6383 |
| R899 | gt | 18 | 25.7845 | 0.0110 | 0.2367 | 12.2875 | 0.9138 | 0.6894 | 10.4080 | 23.0629 | 2.5480 | 9.9684 | 2.1182 | 1.4884 | 0.3504 | 0.1270 | 0.5581 | 4.6317 | 0.8533 | 96.0473 |
| R899 | gt | 19 | 26.6295 | 0.0267 | 0.2588 | 12.7966 | 0.9778 | 0.2600 | 11.1785 | 24.1395 | 2.6375 | 9.7646 | 1.7362 | 0.9044 | 0.0644 | 0.0584 | 0.5315 | 5.2443 | 0.4350 | 97.6537 |
| R899 | gt | 21 | 26.2087 | 0.0073 | 0.2332 | 12.4410 | 0.9233 | 0.2481 | 10.9861 | 24.2171 | 2.5436 | 10.0783 | 2.0102 | 0.9682 | 0.1026 | 0.0493 | 0.4880 | 5.4132 | 0.5291 | 97.4573 |
| R899 | gt | 22 | 25.8751 | 0.0081 | 0.2675 | 12.2735 | 0.8983 | 0.2003 | 11.2501 | 23.7323 | 2.6171 | 9.6774 | 1.7356 | 1.0031 | 0.1580 | 0.0914 | 0.4600 | 5.3135 | 0.4151 | 95.9864 |
| R899 | gt | 23 | 26.3898 | 0.0276 | 0.4830 | 12.6099 | 0.8962 | 0.2365 | 10.4567 | 23.3754 | 2.5626 | 10.2249 | 1.9517 | 0.9190 | 0.1374 | 0.0706 | 0.4590 | 4.7132 | 0.4288 | 95.9523 |
| R899 | gt | 25 | 26.4994 | 0.0279 | 0.4066 | 12.5406 | 0.9723 | 0.2328 | 10.7784 | 23.7420 | 2.5524 | 9.9343 | 1.8393 | 1.0091 | 0.0763 | 0.1064 | 0.5546 | 6.0122 | 0.4949 | 97.7895 |
| R899 | gt | 26 | 26.1608 | 0.0042 | 0.2714 | 12.3626 | 0.9713 | 0.2188 | 10.6205 | 23.5875 | 2.7253 | 10.3514 | 2.0421 | 1.0803 | 0.1593 | 0.0178 | 0.5934 | 5.7098 | 0.6248 | 97.5113 |
| R899 | gt | 27 | 24.4950 | 0.0513 | 0.2965 | 11.2571 | 0.8849 | 0.5564 | 10.1746 | 22.8228 | 2.6344 | 9.8619 | 2.1396 | 1.4743 | 0.2909 | 0.1123 | 0.5107 | 4.9899 | 0.8311 | 93.3937 |
| R899 | gt | 30 | 26.0499 | 0.0002 | 0.2445 | 12.4100 | 0.9177 | 0.2886 | 10.5814 | 23.2681 | 2.5428 | 10.2803 | 2.2590 | 1.2000 | 0.1152 | 0.0855 | 0.5635 | 5.1485 | 0.7101 | 96.6753 |
| R899 | gt | 31 | 26.0044 | 0.0075 | 0.2246 | 12.3982 | 0.8978 | 0.2337 | 11.3062 | 23.9335 | 2.5504 | 9.6582 | 1.8576 | 0.9209 | 0.1207 | 0.0359 | 0.4720 | 5.2510 | 0.4335 | 96.3161 |
| R899 | gt | 32 | 26.1146 | 0.0252 | 0.2245 | 12.4772 | 0.9001 | 0.2296 | 11.0408 | 23.7958 | 2.6483 | 9.8713 | 1.7399 | 0.9472 | 0.1645 | 0.0299 | 0.4593 | 5.4035 | 0.4188 | 96.5005 |
| R899 | gt | 33 | 25.9677 | 0.0024 | 0.2222 | 12.3960 | 0.9110 | 0.4736 | 10.7764 | 23.1793 | 2.5906 | 10.0817 | 2.0531 | 1.3055 | 0.3084 | 0.0437 | 0.5276 | 4.9740 | 0.6324 | 96.4556 |
| R899 | gt | 34 | 25.7485 | 0.0100 | 0.2379 | 12.2069 | 0.9324 | 0.2460 | 10.9780 | 23.6456 | 2.5250 | 9.8664 | 1.8302 | 0.9092 | 0.1327 | 0.0001 | 0.4987 | 5.5730 | 0.4243 | 95.7749 |
| R899 | gt | 35 | 28.4132 | 0.0223 | 0.5900 | 13.9426 | 0.9424 | 0.2435 | 10.7527 | 23.7448 | 2.6128 | 9.9204 | 1.7812 | 1.0232 | 0.1539 | 0.0035 | 0.5301 | 5.4625 | 0.4601 | 100.6092 |
| R899 | gt | 37 | 26.0876 | 0.0002 | 0.2379 | 12.4715 | 0.8902 | 0.5578 | 10.4177 | 23.0174 | 2.5836 | 10.2542 | 2.3181 | 1.5827 | 0.3332 | 0.0618 | 0.5212 | 4.6957 | 0.8176 | 96.8584 |
| R899 | gt | 38 | 26.0139 | 0.0055 | 0.2391 | 12.3806 | 0.8653 | 0.2644 | 10.7905 | 23.7911 | 2.6764 | 10.1643 | 2.0180 | 1.0955 | 0.1527 | 0.0977 | 0.5194 | 4.8079 | 0.6559 | 96.5482 |

| Sample | Phase | Label | W%(O ) | W%(Al) | W%(Si) | W%(P) | W%(Ca) | W%(Y ) | W%(La) | W%(Ce) | W%(Pr) | W%(Nd) | W%(Sm) | W%(Gd) | W%(Dy) | W%(Er) | W%(Pb) | W%(Th) | W%(U ) | W%(SUM) |
|---|---|---|---|---|---|---|---|---|---|---|---|---|---|---|---|---|---|---|---|---|
| R899 | gt | 39 | 26.8062 | 0.0029 | 0.2185 | 12.9718 | 0.8622 | 0.3599 | 11.0330 | 24.2876 | 2.5748 | 9.9852 | 1.9471 | 1.0863 | 0.1648 | 0.0558 | 0.4679 | 4.9615 | 0.4755 | 98.2710 |
| R899 | gt | 40 | 25.9614 | 0.0117 | 0.2247 | 12.3413 | 0.8763 | 0.2468 | 10.9553 | 24.2473 | 2.5697 | 9.8383 | 1.9386 | 1.0435 | 0.0937 | 0.0276 | 0.4799 | 5.0487 | 0.5057 | 96.4205 |
| R899 | gt | 41 | 25.5047 | 0.0065 | 0.2369 | 12.0227 | 0.8489 | 0.2023 | 10.8247 | 23.8357 | 2.6738 | 10.0860 | 1.9327 | 1.0693 | 0.1567 | 0.0541 | 0.4464 | 4.8920 | 0.4950 | 95.2984 |
| R899 | gt | 42 | 26.0463 | 0.0002 | 0.2207 | 12.4519 | 0.8980 | 0.6868 | 10.4694 | 23.5894 | 2.5667 | 9.9577 | 2.1091 | 1.5016 | 0.3247 | 0.0231 | 0.5575 | 4.6728 | 0.8086 | 96.8945 |
| R899 | gt | 43 | 25.8307 | 0.0117 | 0.2245 | 12.2349 | 0.9750 | 0.2586 | 10.9766 | 24.3200 | 2.4216 | 9.5062 | 1.6979 | 0.9095 | 0.0795 | 0.1003 | 0.5288 | 5.6243 | 0.5002 | 96.2103 |
| R899 | gt | 44 | 26.1013 | 0.0058 | 0.2666 | 12.3521 | 0.9653 | 0.2280 | 11.0813 | 24.4627 | 2.5326 | 9.5761 | 1.8235 | 0.8732 | 0.0940 | 0.0071 | 0.5177 | 5.7226 | 0.4355 | 97.0554 |
| R899 | gt | 45 | 30.2961 | 0.0755 | 1.3675 | 14.6117 | 1.0299 | 0.3131 | 10.7065 | 24.4341 | 2.3971 | 9.5037 | 1.7343 | 0.8985 | 0.1185 | 0.0236 | 0.5598 | 6.0035 | 0.4511 | 104.5345 |
| R899 | pl | 46 | 26.9382 | 0.0307 | 0.2978 | 12.9498 | 0.9640 | 0.2255 | 10.8489 | 23.9762 | 2.5677 | 10.1230 | 1.9163 | 0.9653 | 0.0987 | 0.0546 | 0.5289 | 5.6744 | 0.4636 | 98.6336 |
| R899 | pl | 49 | 26.0715 | 0.0061 | 0.5526 | 12.0205 | 0.8778 | 0.1344 | 10.0857 | 23.5224 | 2.5010 | 10.2946 | 1.8498 | 0.8864 | 0.0628 | 0.0344 | 0.6585 | 7.9639 | 0.4417 | 97.9741 |
| R899 | pl | 50 | 26.2502 | 0.0015 | 0.2408 | 12.5327 | 0.8701 | 0.5134 | 10.5901 | 23.7948 | 2.4546 | 10.2243 | 2.0030 | 1.4290 | 0.2869 | 0.1168 | 0.5257 | 4.9960 | 0.6850 | 97.5249 |
| R899 | pl | 51 | 26.4651 | 0.0139 | 0.2842 | 12.4945 | 0.9790 | 0.1574 | 10.6654 | 24.2577 | 2.5334 | 10.2365 | 2.0015 | 1.0178 | 0.0984 | 0.0432 | 0.6155 | 6.0903 | 0.6560 | 98.6198 |
| R899 | pl | 52 | 28.2394 | 0.1441 | 0.5555 | 13.7842 | 1.0375 | 0.2537 | 10.4671 | 23.8439 | 2.4353 | 9.5628 | 1.6786 | 0.8791 | 0.1233 | 0.0148 | 0.5540 | 6.1424 | 0.3977 | 100.1234 |
| R899 | pl | 53 | 26.3720 | 0.0002 | 0.2405 | 12.4984 | 0.9550 | 0.2153 | 11.2486 | 24.6987 | 2.6676 | 9.7085 | 1.8243 | 0.9954 | 0.1005 | 0.0332 | 0.5132 | 5.5994 | 0.4365 | 98.1173 |
| R899 | pl | 54 | 26.3397 | 0.0002 | 0.3306 | 12.4303 | 1.0154 | 0.1169 | 10.3937 | 23.7787 | 2.5499 | 10.1334 | 2.0582 | 0.9246 | 0.0186 | 0.0107 | 0.6481 | 6.6165 | 0.5970 | 97.9725 |
| R899 | pl | 55 | 26.3170 | 0.0030 | 0.2610 | 12.4391 | 0.9086 | 0.1888 | 10.7641 | 24.4217 | 2.6127 | 10.1675 | 2.0893 | 1.0868 | 0.0846 | 0.1475 | 0.5597 | 5.3954 | 0.6797 | 98.1365 |
| R899 | pl | 56 | 26.5427 | 0.0002 | 0.2794 | 12.5726 | 0.9412 | 0.2517 | 10.6395 | 24.5794 | 2.6143 | 10.3416 | 2.0110 | 1.0881 | 0.2014 | 0.0679 | 0.4878 | 5.5733 | 0.4901 | 98.6922 |
| R899 | pl | 58 | 26.3893 | 0.0051 | 0.2769 | 12.4427 | 0.9560 | 0.2248 | 11.0854 | 24.8428 | 2.5634 | 9.9041 | 1.7790 | 0.9456 | 0.1741 | 0.0001 | 0.5185 | 5.8852 | 0.4424 | 98.4454 |
| R899 | pl | 59 | 26.3837 | 0.0193 | 0.2719 | 12.4987 | 0.9557 | 0.2398 | 10.6399 | 24.3466 | 2.5100 | 10.0859 | 2.0131 | 1.0620 | 0.1615 | 0.0273 | 0.5868 | 5.6755 | 0.6092 | 98.0969 |
| R899 | pl | 61 | 25.6517 | 0.1072 | 0.3906 | 12.1189 | 0.9754 | 0.2659 | 10.7014 | 23.6982 | 2.3684 | 9.2182 | 1.6548 | 0.8964 | 0.1525 | 0.0035 | 0.5156 | 5.1477 | 0.3976 | 94.2740 |
| R899 | mx | 62 | 26.8008 | 0.0108 | 0.2476 | 12.9267 | 0.9875 | 0.2020 | 10.3976 | 24.1424 | 2.5909 | 10.1748 | 1.8505 | 0.9047 | 0.1475 | 0.0001 | 0.5255 | 5.8545 | 0.3951 | 98.1690 |
| R899 | mx | 63 | 25.8207 | 0.0155 | 0.2746 | 12.1238 | 0.9501 | 0.1725 | 10.1913 | 24.4221 | 2.5718 | 10.3808 | 1.8809 | 0.8715 | 0.1227 | 0.0038 | 0.4911 | 5.8937 | 0.3505 | 96.5474 |
| R899 | mx | 65 | 26.5753 | 0.0002 | 0.2604 | 12.6593 | 0.9305 | 0.1814 | 10.4505 | 24.6601 | 2.7868 | 10.4390 | 1.8214 | 0.8174 | 0.0955 | 0.0569 | 0.5684 | 5.6417 | 0.4387 | 98.3935 |
| R899 | mx | 66 | 27.2733 | 0.0093 | 0.2265 | 13.2015 | 0.9792 | 0.2109 | 10.5120 | 24.9093 | 2.5113 | 10.1719 | 1.8761 | 0.9241 | 0.1345 | 0.0753 | 0.5389 | 5.7816 | 0.4131 | 99.7588 |
| R899 | mx | 67 | 25.8312 | 0.0394 | 0.2618 | 12.3515 | 0.9348 | 0.2561 | 10.5422 | 24.0768 | 2.3752 | 9.1922 | 1.6382 | 0.7926 | 0.1098 | 0.0553 | 0.5280 | 5.6374 | 0.5248 | 95.1573 |
| R899 | mx | 68 | 26.9650 | 0.0105 | 0.2509 | 12.9521 | 1.0210 | 0.2851 | 10.3973 | 24.5892 | 2.5780 | 10.0057 | 1.7864 | 0.8581 | 0.1325 | 0.0252 | 0.5211 | 6.3921 | 0.4732 | 99.2534 |
| R899 | mx | 69 | 26.7107 | 0.0002 | 0.2225 | 12.7446 | 0.9475 | 0.2443 | 11.0521 | 25.0066 | 2.6771 | 9.8110 | 1.8178 | 0.9789 | 0.1345 | 0.0568 | 0.5211 | 5.5160 | 0.5321 | 98.9838 |
| R899 | mx | 70 | 26.6759 | 0.0013 | 0.2342 | 12.7532 | 0.9450 | 0.1726 | 10.6993 | 24.7948 | 2.7220 | 10.1085 | 1.8235 | 0.7955 | 0.0700 | 0.0592 | 0.4960 | 5.7079 | 0.4772 | 98.5461 |
| R899 | mx | 71 | 27.5771 | 0.0207 | 0.2020 | 13.7365 | 1.0318 | 0.2407 | 11.3011 | 25.3305 | 1.9283 | 7.7840 | 1.4243 | 0.6367 | 0.0543 | 0.0001 | 0.5160 | 6.0299 | 0.4415 | 98.2655 |
| R899 | mx | 72 | 25.7010 | 0.1865 | 0.4637 | 12.3825 | 1.1440 | 1.6274 | 10.1298 | 21.3161 | 2.2249 | 8.5893 | 1.6258 | 1.1347 | 0.5379 | 0.1264 | 0.6436 | 4.5297 | 1.0870 | 93.4603 |
| R899 | mx | 73 | 26.2696 | 0.0137 | 0.1297 | 12.8560 | 0.9938 | 1.5026 | 11.3993 | 23.9597 | 2.3716 | 8.4862 | 1.4843 | 0.9963 | 0.4206 | 0.1735 | 0.5807 | 4.0477 | 1.0642 | 96.7595 |
| R899 | mx | 74 | 25.7554 | 0.0119 | 0.1520 | 12.3988 | 0.8187 | 1.1343 | 11.7331 | 24.3944 | 2.4152 | 9.0251 | 1.3854 | 0.9737 | 0.3330 | 0.0575 | 0.4548 | 4.1809 | 0.5674 | 95.8016 |
| R899 | mx | 75 | 25.6428 | 0.0002 | 0.2847 | 12.1950 | 0.7276 | 0.9884 | 11.3994 | 24.1840 | 2.5342 | 8.8779 | 1.5215 | 1.0141 | 0.3607 | 0.1450 | 0.5085 | 4.9720 | 0.4662 | 95.8322 |
| R899 | mx | 76 | 25.8055 | 0.0063 | 0.2570 | 12.3076 | 0.9368 | 1.0054 | 11.2318 | 23.6214 | 2.3622 | 8.9531 | 1.5642 | 1.0146 | 0.3794 | 0.1074 | 0.5225 | 5.7059 | 0.4324 | 96.2235 |
| R899 | mx | 77 | 26.1736 | 0.0184 | 0.1634 | 12.6172 | 1.1379 | 0.9717 | 10.7729 | 23.1269 | 2.3853 | 9.2414 | 1.7918 | 1.3104 | 0.3787 | 0.0691 | 0.6543 | 5.0072 | 1.2223 | 97.0525 |
| R899 | mx | 79 | 25.9059 | 0.0278 | 0.2301 | 12.4922 | 0.9691 | 1.1621 | 11.1517 | 23.4125 | 2.3660 | 8.6736 | 1.5742 | 0.9675 | 0.4787 | 0.1728 | 0.4807 | 5.0538 | 0.6615 | 95.7902 |
| R899 | mx | 80 | 26.1891 | 0.0220 | 0.2680 | 12.6394 | 0.9911 | 0.9489 | 11.0888 | 23.5187 | 2.3704 | 8.6151 | 1.4973 | 0.9089 | 0.4117 | 0.1345 | 0.5735 | 5.8656 | 0.4046 | 96.4576 |
| R899 | mx | 82 | 25.8298 | 0.0002 | 0.1463 | 12.5299 | 1.2324 | 1.2020 | 10.9236 | 22.8866 | 2.3135 | 8.3095 | 1.3699 | 0.9922 | 0.4198 | 0.0284 | 0.6283 | 5.8986 | 0.8059 | 95.5269 |
| R899 | mx | 84 | 25.8971 | 0.0068 | 0.2632 | 12.3150 | 0.8516 | 0.4918 | 10.1638 | 23.1646 | 2.6180 | 10.2382 | 2.2357 | 1.4354 | 0.3367 | 0.0774 | 0.5395 | 5.0888 | 0.7056 | 96.4392 |
| R899 | mx | 85 | 25.8082 | 0.0047 | 0.2831 | 12.1518 | 0.8156 | 0.2765 | 10.4849 | 24.2156 | 2.6802 | 10.3682 | 2.1716 | 0.9788 | 0.1044 | 0.0569 | 0.4553 | 5.1738 | 0.4061 | 96.4457 |
| R899 | mx | 87 | 26.0992 | 0.0016 | 0.2557 | 12.4274 | 0.9366 | 0.6044 | 10.2059 | 23.1296 | 2.5966 | 10.2113 | 2.2582 | 1.5373 | 0.3585 | 0.1056 | 0.5971 | 5.0252 | 0.8622 | 97.2224 |
| R899 | mx | 88 | 25.8090 | 0.0081 | 0.2228 | 12.4063 | 0.9348 | 1.4569 | 9.7597 | 22.0787 | 2.5120 | 9.8780 | 2.3169 | 1.8843 | 0.6260 | 0.1369 | 0.6266 | 4.7579 | 1.0465 | 96.4714 |
| R899 | mx | 89 | 25.6253 | 0.0021 | 0.3044 | 12.0298 | 0.8830 | 0.3544 | 10.3372 | 23.1967 | 2.5724 | 10.2688 | 2.0930 | 1.4420 | 0.2287 | 0.0892 | 0.5480 | 5.5050 | 0.6057 | 96.0957 |
| R899 | mx | 91 | 26.2738 | 0.0109 | 0.2525 | 12.5799 | 0.9103 | 0.3299 | 10.3710 | 23.9365 | 2.5558 | 9.9732 | 1.9926 | 1.1402 | 0.1922 | 0.0001 | 0.5458 | 5.3535 | 0.6002 | 97.0284 |
| R899 | mx | 92 | 25.7491 | 0.0002 | 0.2120 | 12.3508 | 0.9285 | 1.1250 | 10.0822 | 22.5421 | 2.5814 | 9.7056 | 2.2399 | 1.8781 | 0.4515 | 0.0844 | 0.5596 | 4.5832 | 0.9807 | 96.0643 |
| R899 | mx | 93 | 25.9229 | 0.0062 | 0.2389 | 12.3647 | 0.8986 | 0.6206 | 10.2202 | 22.9598 | 2.4988 | 10.1066 | 2.2586 | 1.7763 | 0.3438 | 0.0001 | 0.5583 | 4.8772 | 0.8610 | 96.5226 |
| R899 | mx | 95 | 26.2093 | 0.0002 | 0.2334 | 12.5834 | 0.9087 | 0.7682 | 10.4048 | 23.1363 | 2.5456 | 10.0782 | 2.0040 | 1.3875 | 0.3424 | 0.1266 | 0.6110 | 5.1140 | 0.7972 | 97.2608 |
| R899 | mx | 96 | 25.7411 | 0.0002 | 0.2300 | 12.2730 | 0.9617 | 0.8306 | 10.0683 | 22.5776 | 2.5133 | 9.8407 | 2.3265 | 1.8826 | 0.4419 | 0.0820 | 0.6364 | 4.7848 | 0.9631 | 96.1638 |
| R899 | mx | 97 | 25.6624 | 0.0068 | 0.2649 | 12.2043 | 0.9047 | 0.7657 | 10.1994 | 23.0345 | 2.5428 | 10.0275 | 2.1287 | 1.3919 | 0.3318 | 0.0595 | 0.5238 | 4.8010 | 0.8333 | 95.6930 |
| R899 | mx | 99 | 25.9652 | 0.0055 | 0.2854 | 12.3071 | 0.8398 | 0.5395 | 10.6456 | 23.5162 | 2.5836 | 10.1941 | 2.1119 | 1.2155 | 0.2504 | 0.0122 | 0.5558 | 5.1351 | 0.6808 | 96.8537 |
| R899 | mx | 100 | 26.9142 | 0.0169 | 0.2965 | 13.0477 | 0.9109 | 0.3136 | 10.4348 | 23.3015 | 2.5531 | 10.1993 | 2.1404 | 1.1538 | 0.1476 | 0.0281 | 0.5740 | 5.3621 | 0.7092 | 98.1137 |
| R899 | mx | 101 | 25.8756 | 0.0002 | 0.4557 | 12.1374 | 0.9763 | 0.2844 | 10.3135 | 22.8194 | 2.4296 | 10.1249 | 2.0628 | 1.1646 | 0.1714 | 0.1154 | 0.5875 | 6.0137 | 0.5981 | 96.1405 |
| R899 | mx | 102 | 26.0416 | 0.0064 | 0.2150 | 12.4288 | 0.9930 | 0.2247 | 10.8918 | 23.6640 | 2.5617 | 9.9464 | 1.9324 | 0.8884 | 0.1126 | 0.0019 | 0.5324 | 5.2550 | 0.6819 | 96.3880 |
| R899 | mx | 103 | 26.9846 | 0.0003 | 0.2054 | 13.0850 | 0.9756 | 0.2388 | 11.1779 | 24.0733 | 2.6086 | 10.0004 | 1.8706 | 0.9381 | 0.1160 | 0.0969 | 0.5403 | 5.1358 | 0.5811 | 98.6387 |
| R899 | mx | 105 | 25.0719 | 0.0226 | 0.2655 | 11.8325 | 0.9209 | 0.2011 | 10.4749 | 22.7694 | 2.6717 | 10.0739 | 1.9908 | 1.0404 | 0.0828 | 0.0712 | 0.4838 | 4.7722 | 0.4936 | 93.2492 |
| R899 | mx | 106 | 26.5253 | 0.0153 | 0.2774 | 12.6689 | 0.9632 | 0.2016 | 10.4870 | 23.9395 | 2.5785 | 10.2731 | 1.9261 | 0.8237 | 0.1272 | 0.0394 | 0.5599 | 6.1318 | 0.3276 | 97.8755 |
| R899 | mx | 107 | 25.9714 | 0.0002 | 0.2026 | 12.3922 | 0.9867 | 0.2674 | 10.7776 | 23.7728 | 2.6428 | 9.9888 | 1.9468 | 0.9024 | 0.0275 | 0.0114 | 0.5339 | 5.2408 | 0.5933 | 96.2686 |

| Sample | Phase | Label | W%(O) | W%(Al) | W%(Si) | W%(P) | W%(Ca) | W%(Y) | W%(La) | W%(Ce) | W%(Pr) | W%(Nd) | W%(Sm) | W%(Gd) | W%(Dy) | W%(Er) | W%(Pb) | W%(Th) | W%(U) | W%(SUM) |
|---|---|---|---|---|---|---|---|---|---|---|---|---|---|---|---|---|---|---|---|---|
| R899 | mx | 108 | 26.2517 | 0.0002 | 0.1899 | 12.5625 | 0.9519 | 0.2320 | 11.1272 | 24.0846 | 2.5759 | 9.9747 | 1.8847 | 0.9265 | 0.1660 | 0.0386 | 0.5318 | 4.9608 | 0.6629 | 97.1319 |
| R899 | mx | 109 | 26.2799 | 0.0002 | 0.2358 | 12.5689 | 0.9522 | 0.2378 | 10.8175 | 23.8740 | 2.6417 | 9.8749 | 1.9695 | 0.9403 | 0.1209 | 0.0502 | 0.5787 | 5.4017 | 0.5683 | 97.1225 |
| R899 | mx | 110 | 25.9578 | 0.0015 | 0.2335 | 12.3487 | 0.9549 | 0.1681 | 10.9041 | 23.5466 | 2.5764 | 9.8828 | 1.8772 | 0.9900 | 0.1306 | 0.0212 | 0.5437 | 5.5458 | 0.6160 | 96.3089 |
| R899 | mx | 111 | 26.2951 | 0.0156 | 0.2204 | 12.5111 | 0.9040 | 0.2417 | 11.1721 | 24.2215 | 2.6086 | 10.0412 | 1.9306 | 0.9559 | 0.1899 | 0.0920 | 0.5270 | 5.0845 | 0.6098 | 97.6310 |
| R899 | mx | 112 | 26.5911 | 0.0350 | 0.2773 | 12.7066 | 0.9968 | 0.1882 | 10.4784 | 23.9057 | 2.6065 | 10.1552 | 1.9288 | 1.0033 | 0.1240 | 0.0384 | 0.5141 | 5.9296 | 0.4222 | 97.9112 |
| R899 | mx | 113 | 26.0233 | 0.0002 | 0.2027 | 12.4091 | 0.9449 | 0.2408 | 10.9528 | 23.8444 | 2.6335 | 9.9184 | 1.8957 | 0.9246 | 0.1010 | 0.0369 | 0.5384 | 5.2761 | 0.6113 | 96.5641 |
| R899 | mx | 114 | 26.0319 | 0.0002 | 0.2229 | 12.3841 | 0.9270 | 0.1896 | 11.0447 | 23.7095 | 2.6069 | 10.0938 | 1.8819 | 0.9303 | 0.1389 | 0.0888 | 0.5356 | 5.2791 | 0.5792 | 96.6544 |
| R899 | mx | 115 | 26.0506 | 0.0002 | 0.2180 | 12.4204 | 0.9428 | 0.1924 | 10.9342 | 23.6804 | 2.6372 | 10.0473 | 1.9110 | 0.9033 | 0.0771 | 0.0013 | 0.5248 | 5.3745 | 0.6278 | 96.5533 |
| R899 | mx | 116 | 25.9358 | 0.0002 | 0.2368 | 12.3268 | 0.9583 | 0.1759 | 10.7958 | 23.6466 | 2.6330 | 10.0062 | 1.8273 | 0.9238 | 0.0790 | 0.0426 | 0.5478 | 5.5695 | 0.5614 | 96.2768 |
| R899 | mx | 117 | 26.1104 | 0.0113 | 0.2474 | 12.4188 | 0.9852 | 0.1868 | 10.8191 | 23.6210 | 2.5406 | 10.0171 | 1.9570 | 0.9715 | 0.0835 | 0.0444 | 0.5360 | 5.6362 | 0.5628 | 96.7591 |
| R899 | mx | 118 | 26.2208 | 0.0176 | 0.2321 | 12.4885 | 0.9628 | 0.2075 | 10.6060 | 23.8529 | 2.6696 | 10.2102 | 1.9671 | 0.9694 | 0.1077 | 0.0415 | 0.5256 | 5.5494 | 0.5075 | 97.1462 |
| R899 | mx | 119 | 25.7851 | 0.0079 | 0.2275 | 12.2307 | 1.0155 | 0.2238 | 10.5813 | 23.6307 | 2.6359 | 9.9593 | 1.8695 | 0.8271 | 0.0780 | 0.0278 | 0.5374 | 5.7590 | 0.4604 | 95.8669 |
| R899 | mx | 120 | 26.9649 | 0.0106 | 0.2169 | 13.0407 | 0.9569 | 0.2396 | 10.9421 | 24.0112 | 2.6078 | 10.0089 | 1.9501 | 1.0079 | 0.1497 | 0.0161 | 0.5532 | 5.4801 | 0.6378 | 98.8045 |
| R899 | mx | 121 | 25.3453 | 0.0071 | 0.2291 | 11.8803 | 0.9809 | 0.1569 | 10.5418 | 23.7321 | 2.6758 | 10.0753 | 1.8763 | 0.8967 | 0.0969 | 0.0111 | 0.4954 | 5.6484 | 0.4233 | 95.0827 |
| R899 | mx | 122 | 25.9762 | 0.1155 | 0.5208 | 12.0843 | 1.1057 | 0.2137 | 10.5804 | 23.3447 | 2.5834 | 9.9429 | 1.8043 | 0.8873 | 0.1347 | 0.0063 | 0.5203 | 5.6037 | 0.4137 | 95.8479 |
| R899 | mx | 123 | 26.8381 | 0.0002 | 0.2185 | 12.9760 | 1.0110 | 0.1889 | 10.4366 | 24.0018 | 2.5622 | 10.1344 | 1.9058 | 0.9150 | 0.1632 | 0.0519 | 0.5579 | 5.8766 | 0.4693 | 98.3174 |
| R899 | mx | 124 | 26.4371 | 0.0139 | 0.2326 | 12.6444 | 0.9439 | 0.2011 | 10.9774 | 24.1426 | 2.5344 | 9.9025 | 1.8816 | 0.9232 | 0.1598 | 0.0769 | 0.5475 | 5.3803 | 0.6207 | 97.6299 |
| R899 | mx | 125 | 26.2727 | 0.0002 | 0.2347 | 12.5224 | 0.9858 | 0.1742 | 10.6679 | 23.8584 | 2.5699 | 10.1864 | 1.9187 | 0.8706 | 0.1125 | 0.1249 | 0.5104 | 5.8289 | 0.4590 | 97.3076 |
| R899 | mx | 126 | 26.0988 | 0.0058 | 0.2354 | 12.4200 | 1.0105 | 0.2016 | 10.4780 | 23.8498 | 2.5765 | 10.0594 | 1.8813 | 0.8401 | 0.1417 | 0.0456 | 0.5433 | 5.9401 | 0.4351 | 96.7730 |
| R899 | mx | 127 | 25.8495 | 0.0074 | 0.2321 | 12.2541 | 0.8822 | 0.1940 | 10.8291 | 24.0228 | 2.5525 | 10.1349 | 1.9333 | 0.9772 | 0.1418 | 0.1194 | 0.5028 | 4.9735 | 0.5560 | 96.1726 |
| R899 | mx | 128 | 26.1169 | 0.0142 | 0.2510 | 12.4623 | 0.9163 | 0.2345 | 10.9361 | 23.7479 | 2.4932 | 10.0541 | 1.8561 | 0.8800 | 0.1667 | 0.0001 | 0.4957 | 5.2994 | 0.5985 | 96.5330 |
| R899 | mx | 129 | 26.2692 | 0.0059 | 0.2337 | 12.4987 | 1.0099 | 0.1728 | 10.5216 | 23.9822 | 2.5985 | 10.2124 | 1.9045 | 0.9543 | 0.0519 | 0.0734 | 0.4970 | 5.9338 | 0.4651 | 97.3949 |
| R899 | mx | 130 | 26.1641 | 0.0215 | 0.2475 | 12.4559 | 0.9993 | 0.2513 | 10.3310 | 23.6799 | 2.6973 | 10.3739 | 1.9089 | 0.8666 | 0.1086 | 0.0157 | 0.5595 | 5.7613 | 0.4457 | 96.8980 |
| R899 | mx | 131 | 26.0533 | 0.0090 | 0.2156 | 12.4221 | 0.9749 | 0.1970 | 10.5456 | 23.9724 | 2.5790 | 9.9171 | 1.8970 | 0.9264 | 0.1930 | 0.0383 | 0.5158 | 5.4180 | 0.6444 | 96.5289 |
| R899 | mx | 132 | 26.2940 | 0.0579 | 0.3367 | 12.4441 | 1.0008 | 0.2448 | 10.6160 | 23.9753 | 2.4942 | 9.8458 | 1.9024 | 0.9248 | 0.1517 | 0.0122 | 0.5427 | 5.7165 | 0.6470 | 97.2169 |
| OL3D | retro | 2 | 26.1766 | 0.0002 | 0.1315 | 12.6178 | 1.3622 | 1.6261 | 10.4128 | 23.4976 | 2.3820 | 9.1011 | 1.5292 | 1.1417 | 0.5355 | 0.1746 | 0.7411 | 4.9606 | 1.3495 | 97.7501 |
| OL3D | retro | 3 | 26.0369 | 0.0039 | 0.1386 | 12.5838 | 1.3298 | 1.5324 | 10.2464 | 23.4011 | 2.3270 | 9.0912 | 1.5170 | 1.0849 | 0.5131 | 0.1160 | 0.7294 | 4.5933 | 1.6162 | 96.8710 |
| OL3D | retro | 4 | 26.3127 | 0.0045 | 0.1301 | 12.7917 | 1.3402 | 1.5264 | 10.4262 | 23.5251 | 2.3461 | 8.8556 | 1.4414 | 1.0900 | 0.4629 | 0.0856 | 0.7606 | 4.6922 | 1.6384 | 97.4397 |
| OL3D | retro | 5 | 26.5061 | 0.0223 | 0.2000 | 12.7037 | 1.2322 | 1.4347 | 10.6833 | 24.6642 | 2.4296 | 9.3495 | 1.5554 | 1.1142 | 0.5017 | 0.1169 | 0.5210 | 4.6332 | 0.9942 | 98.6722 |
| OL3D | retro | 6 | 26.9469 | 0.5763 | 0.6758 | 12.4168 | 1.0355 | 1.1051 | 10.6576 | 23.9371 | 2.4577 | 9.2441 | 1.6263 | 1.0997 | 0.4187 | 0.1124 | 0.5213 | 4.8816 | 0.7419 | 98.4648 |
| OL3D | retro | 7 | 26.1576 | 0.0103 | 0.1368 | 12.5869 | 1.1571 | 1.2725 | 10.8697 | 24.2856 | 2.4206 | 9.0036 | 1.5194 | 1.0015 | 0.4630 | 0.1025 | 0.6996 | 4.4343 | 1.3732 | 97.5042 |
| OL3D | retro | 13 | 25.9514 | 0.0002 | 0.1189 | 12.5508 | 1.3110 | 1.4691 | 10.3005 | 22.9650 | 2.4416 | 9.0725 | 1.5765 | 1.0780 | 0.5051 | 0.1477 | 0.7711 | 4.7251 | 1.6615 | 96.6560 |
| OL3D | retro | 15 | 27.2252 | 0.0093 | 0.3088 | 13.2671 | 1.0341 | 1.0525 | 10.7969 | 24.2180 | 2.4476 | 9.2874 | 1.4630 | 1.0132 | 0.4118 | 0.1423 | 0.5649 | 5.5723 | 0.4673 | 99.2917 |
| OL3D | retro | 17 | 26.2811 | 0.0077 | 0.1289 | 12.6996 | 1.1171 | 1.2144 | 10.6566 | 24.2254 | 2.3582 | 9.2468 | 1.4966 | 1.1733 | 0.4133 | 0.0928 | 0.5975 | 4.9842 | 0.9333 | 97.6368 |
| OL3D | retro | 18 | 26.3620 | 0.0210 | 0.1643 | 12.8090 | 1.4945 | 1.4548 | 10.3341 | 23.0335 | 2.3373 | 8.9268 | 1.5004 | 1.1869 | 0.4288 | 0.1665 | 0.6882 | 4.6704 | 1.4845 | 97.0730 |
| OL3D | retro | 19 | 26.1730 | 0.0144 | 0.2842 | 12.4702 | 1.0554 | 0.9723 | 10.6156 | 23.7692 | 2.3372 | 9.2466 | 1.5839 | 1.0879 | 0.3914 | 0.1119 | 0.6092 | 6.3251 | 0.4303 | 97.4878 |
| OL3D | retro | 22 | 26.2332 | 0.0081 | 0.3241 | 12.4577 | 0.7972 | 1.0181 | 11.1511 | 25.5155 | 2.5623 | 9.7711 | 1.5617 | 1.0537 | 0.4733 | 0.1092 | 0.3980 | 3.5858 | 0.5307 | 97.5608 |
| OL3D | retro | 23 | 26.7236 | 0.0156 | 0.2182 | 12.8879 | 0.5729 | 1.0055 | 11.6118 | 26.3283 | 2.5089 | 9.4848 | 1.6654 | 1.1482 | 0.4715 | 0.0724 | 0.3604 | 3.5379 | 0.2364 | 98.8597 |
| OL3D | retro | 24 | 26.3547 | 0.0164 | 0.2238 | 12.5427 | 0.5762 | 0.9321 | 11.6582 | 26.3207 | 2.6343 | 9.8581 | 1.6445 | 1.1616 | 0.4070 | 0.0966 | 0.2860 | 3.4339 | 0.2777 | 98.4345 |
| OL3D | retro | 25 | 27.2180 | 0.0388 | 0.2603 | 13.2500 | 0.8357 | 1.0902 | 11.3076 | 25.2201 | 2.4036 | 9.2316 | 1.5264 | 1.0573 | 0.4160 | 0.1847 | 0.4230 | 4.7863 | 0.2876 | 99.5472 |
| OL3D | retro | 26 | 26.1470 | 0.0002 | 0.2186 | 12.4282 | 0.5817 | 1.0062 | 11.6656 | 26.1587 | 2.7049 | 9.5775 | 1.6103 | 1.0567 | 0.4476 | 0.1029 | 0.3189 | 3.6861 | 0.2531 | 97.9742 |
| OL3D | retro | 27 | 26.3491 | 0.0005 | 0.2073 | 12.6142 | 0.5409 | 0.9397 | 11.7407 | 26.0438 | 2.6596 | 9.7401 | 1.6104 | 1.1846 | 0.4412 | 0.1143 | 0.2779 | 3.4070 | 0.2505 | 98.1318 |
| OL3D | retro | 28 | 26.2254 | 0.0291 | 0.2016 | 12.4646 | 0.9576 | 1.0840 | 11.0598 | 25.0296 | 2.5724 | 9.4265 | 1.5986 | 1.1317 | 0.3226 | 0.0996 | 0.4721 | 4.9792 | 0.5512 | 98.2156 |
| OL3D | retro | 29 | 26.0786 | 0.0103 | 0.2804 | 12.2786 | 0.5726 | 0.9341 | 11.2565 | 26.2748 | 2.6790 | 10.0962 | 1.6344 | 1.1022 | 0.4485 | 0.1049 | 0.3177 | 3.7603 | 0.2279 | 98.0670 |
| OL3D | retro | 30 | 26.1043 | 0.0134 | 0.1818 | 12.5254 | 1.2245 | 1.5498 | 10.6216 | 23.9891 | 2.3529 | 9.2760 | 1.4815 | 1.2405 | 0.5262 | 0.1850 | 0.6355 | 4.1594 | 1.3459 | 97.4228 |
| OL3D | retro | 31 | 26.0798 | 0.0002 | 0.1054 | 12.5378 | 1.2403 | 1.6073 | 10.7416 | 23.9976 | 2.3432 | 9.3767 | 1.5042 | 1.1886 | 0.5436 | 0.1872 | 0.6865 | 4.1446 | 1.4515 | 97.7461 |
| OL3D | retro | 32 | 26.5660 | 0.0190 | 0.1051 | 12.8747 | 1.1804 | 1.4798 | 10.8322 | 24.5107 | 2.3927 | 9.2777 | 1.5070 | 1.2285 | 0.4899 | 0.1694 | 0.6634 | 4.0643 | 1.3024 | 98.6732 |
| OL3D | retro | 33 | 26.5845 | 0.0079 | 0.1403 | 12.7532 | 0.5985 | 1.0029 | 11.8135 | 26.9929 | 2.7298 | 9.7985 | 1.5767 | 1.1326 | 0.4362 | 0.1036 | 0.2872 | 2.7709 | 0.3131 | 99.0523 |
| OL3D | retro | 34 | 26.3165 | 0.0184 | 0.3630 | 12.4164 | 0.9295 | 0.9759 | 10.9952 | 24.0940 | 2.2465 | 9.2280 | 1.5615 | 1.1504 | 0.3861 | 0.1535 | 0.5935 | 6.9189 | 0.2475 | 98.6048 |
| OL3D | retro | 35 | 26.2048 | 0.0301 | 0.1863 | 12.5913 | 1.0695 | 1.4020 | 10.6712 | 24.3332 | 2.4981 | 9.4082 | 1.6147 | 1.1684 | 0.4648 | 0.1273 | 0.5588 | 4.1337 | 1.0460 | 97.5184 |
| OL3D | retro | 36 | 26.1393 | 0.0161 | 0.2660 | 12.3648 | 0.7248 | 0.9967 | 11.0930 | 25.3916 | 2.5482 | 9.5760 | 1.5361 | 1.1305 | 0.4569 | 0.0834 | 0.4238 | 5.1524 | 0.2380 | 98.1476 |
| OL3D | retro | 37 | 26.3613 | 0.0134 | 0.2384 | 12.5163 | 0.6651 | 0.8824 | 11.7936 | 26.1097 | 2.4466 | 9.3838 | 1.5978 | 1.0429 | 0.4671 | 0.0472 | 0.3725 | 4.4590 | 0.2085 | 98.6156 |
| OL3D | retro | 38 | 26.1319 | 0.0457 | 0.1994 | 12.5141 | 0.8319 | 1.0491 | 10.8519 | 25.0142 | 2.5344 | 9.6148 | 1.5968 | 1.0675 | 0.4056 | 0.1076 | 0.4479 | 4.1813 | 0.5705 | 97.1746 |
| OL3D | retro | 39 | 26.1129 | 0.0154 | 0.4329 | 12.2784 | 0.8633 | 0.9037 | 10.6871 | 24.2771 | 2.4217 | 9.1643 | 1.5523 | 1.0405 | 0.4683 | 0.0559 | 0.5893 | 6.5360 | 0.2466 | 97.6557 |
| OL3D | retro | 40 | 25.7022 | 0.0171 | 0.2876 | 12.0965 | 0.7666 | 0.9604 | 11.4077 | 24.9201 | 2.4160 | 9.3830 | 1.6634 | 1.1448 | 0.4590 | 0.0775 | 0.3906 | 4.6739 | 0.1986 | 96.5750 |
| OL3D | retro | 41 | 26.6032 | 0.0295 | 0.1561 | 12.8793 | 1.1260 | 1.4189 | 10.8890 | 24.3831 | 2.4902 | 9.1237 | 1.6109 | 1.2009 | 0.5429 | 0.1181 | 0.6108 | 4.1856 | 1.1619 | 98.5401 |

| Sample | Phase | Label | W%(O ) | W%(Al) | W%(Si) | W%(P) | W%(Ca) | W%(Y ) | W%(La) | W%(Ce) | W%(Pr) | W%(Nd) | W%(Sm) | W%(Gd) | W%(Dy) | W%(Er) | W%(Pb) | W%(Th) | W%(U ) | W%(SUM) |
|---|---|---|---|---|---|---|---|---|---|---|---|---|---|---|---|---|---|---|---|---|
| OL3D | retro | 42 | 28.5281 | 0.0497 | 0.9806 | 13.8142 | 1.2939 | 1.5415 | 10.4650 | 23.2763 | 2.3783 | 8.8979 | 1.4778 | 1.0427 | 0.4613 | 0.1445 | 0.7355 | 4.3883 | 1.3765 | 100.8621 |
| OL3D | retro | 43 | 26.1832 | 0.0036 | 0.2059 | 12.4488 | 0.7953 | 0.9719 | 11.1442 | 25.7032 | 2.3982 | 9.6458 | 1.6341 | 1.0693 | 0.4028 | 0.1438 | 0.4285 | 4.4217 | 0.4762 | 98.0865 |
| OL3D | retro | 45 | 26.2041 | 0.0221 | 0.1807 | 12.5651 | 1.0206 | 1.1668 | 10.8177 | 24.9308 | 2.3101 | 9.2799 | 1.5279 | 1.0408 | 0.4127 | 0.1086 | 0.5773 | 4.6619 | 0.7576 | 97.5947 |
| OL3D | retro | 46 | 25.5874 | 0.0077 | 0.6687 | 11.6771 | 1.1763 | 0.9866 | 9.4188 | 21.2459 | 2.2842 | 9.2757 | 1.6845 | 1.1569 | 0.4117 | 0.1520 | 0.7962 | 10.4754 | 0.2758 | 97.2909 |
| OL3D | retro | 47 | 26.0154 | 0.0410 | 0.3124 | 12.2725 | 1.0303 | 0.9024 | 10.5758 | 23.7381 | 2.3661 | 9.4052 | 1.5697 | 1.1333 | 0.4203 | 0.1299 | 0.5438 | 6.6785 | 0.2645 | 97.4092 |
| OL3D | retro | 48 | 26.0476 | 0.0238 | 0.4110 | 12.2568 | 0.9028 | 1.0495 | 10.5397 | 24.2957 | 2.4984 | 9.1474 | 1.5940 | 1.0898 | 0.4858 | 0.1317 | 0.5687 | 5.9362 | 0.4927 | 97.4816 |
| OL3D | retro | 49 | 25.9652 | 0.0128 | 0.4512 | 12.1118 | 1.0781 | 0.9100 | 10.2148 | 23.3717 | 2.4162 | 9.5903 | 1.6835 | 1.1677 | 0.4096 | 0.0419 | 0.5724 | 7.2420 | 0.2776 | 97.5268 |
| OL3D | retro | 50 | 25.9577 | 0.0133 | 0.5300 | 12.0532 | 1.1624 | 0.9578 | 9.9047 | 22.0561 | 2.2715 | 9.8265 | 1.8695 | 1.2129 | 0.3797 | 0.1478 | 0.6577 | 8.4479 | 0.1903 | 97.6490 |
| OL3D | retro | 53 | 26.7955 | 0.3891 | 0.9669 | 12.5299 | 1.4503 | 1.3921 | 9.7508 | 22.1338 | 2.2588 | 8.7908 | 1.4644 | 1.1138 | 0.4414 | 0.1267 | 0.5945 | 4.2617 | 1.0748 | 95.5453 |
| OL3D | retro | 54 | 26.7403 | 0.0119 | 0.1576 | 12.9412 | 1.5098 | 1.3404 | 10.6631 | 23.7627 | 2.3596 | 8.6855 | 1.4220 | 1.0500 | 0.4876 | 0.1226 | 0.7265 | 5.3863 | 1.4932 | 98.8703 |
| OL3D | retro | 55 | 26.5755 | 0.0040 | 0.1779 | 12.8065 | 1.3511 | 1.3622 | 10.7503 | 23.9741 | 2.3520 | 8.8053 | 1.4237 | 1.0025 | 0.4202 | 0.1450 | 0.7393 | 5.4561 | 1.4144 | 98.7701 |
| OL3D | retro | 56 | 26.5267 | 0.1359 | 0.5209 | 12.3896 | 0.8720 | 0.9359 | 10.9205 | 24.0936 | 2.4144 | 9.5486 | 1.7149 | 1.2338 | 0.3807 | 0.1002 | 0.5239 | 6.1343 | 0.2417 | 98.6976 |
| OL3D | retro | 57 | 26.5542 | 0.0002 | 0.1971 | 12.6969 | 1.7336 | 1.3378 | 10.4067 | 23.3898 | 2.2915 | 9.0474 | 1.3939 | 1.1481 | 0.4586 | 0.1955 | 0.7387 | 5.4503 | 1.7806 | 98.8309 |
| OL3D | retro | 58 | 26.2302 | 0.0305 | 0.4369 | 12.3124 | 1.0505 | 1.0516 | 10.4274 | 23.3047 | 2.2719 | 9.2513 | 1.6095 | 1.0963 | 0.4855 | 0.1108 | 0.5898 | 7.7343 | 0.3188 | 98.3224 |
| OL3D | retro | 59 | 25.8808 | 0.0919 | 0.4093 | 12.2166 | 1.0565 | 1.1067 | 10.6240 | 23.9002 | 2.4806 | 9.1208 | 1.5758 | 1.0230 | 0.4248 | 0.1439 | 0.4897 | 4.7474 | 0.6126 | 95.9146 |
| OL3D | retro | 60 | 26.4341 | 0.0157 | 0.6728 | 12.1911 | 0.9995 | 0.9929 | 10.6148 | 23.7377 | 2.3900 | 9.3760 | 1.6658 | 1.1560 | 0.4707 | 0.1253 | 0.5905 | 7.4714 | 0.2899 | 99.2042 |
| OL3D | retro | 61 | 26.2771 | 0.0095 | 0.2928 | 12.4121 | 0.7020 | 0.9454 | 11.3007 | 25.6526 | 2.5034 | 9.6838 | 1.5817 | 1.2024 | 0.3887 | 0.0865 | 0.4136 | 4.8561 | 0.2616 | 98.5800 |
| OL3D | retro | 62 | 26.0791 | 0.0600 | 0.3674 | 12.2584 | 0.7824 | 0.9570 | 11.2905 | 24.8373 | 2.4365 | 9.3240 | 1.5262 | 1.1131 | 0.4076 | 0.1057 | 0.4181 | 5.3724 | 0.2360 | 97.5817 |
| OL3D | retro | 64 | 26.3611 | 0.0217 | 0.1124 | 12.7465 | 1.3761 | 1.5095 | 10.6099 | 23.6705 | 2.3968 | 9.0150 | 1.5247 | 1.0871 | 0.5725 | 0.0868 | 0.7651 | 4.5548 | 1.6000 | 98.0205 |
| OL3D | retro | 65 | 26.0810 | 0.0013 | 0.2202 | 12.4658 | 1.1513 | 1.2827 | 10.3761 | 23.8135 | 2.2408 | 9.2306 | 1.4969 | 1.1714 | 0.4472 | 0.1445 | 0.7157 | 5.5556 | 1.1663 | 97.5709 |
| OL3D | retro | 67 | 26.5482 | 0.1438 | 0.3866 | 12.5969 | 1.1260 | 1.1919 | 10.7503 | 24.1985 | 2.2007 | 8.7114 | 1.3988 | 0.9864 | 0.4590 | 0.0769 | 0.6128 | 5.8681 | 0.9505 | 98.2168 |
| OL3D | retro | 68 | 26.4302 | 0.0441 | 0.1572 | 12.8344 | 1.2823 | 1.5767 | 10.4337 | 23.8009 | 2.3027 | 9.0475 | 1.5622 | 1.1056 | 0.5234 | 0.1971 | 0.6960 | 4.2026 | 1.4321 | 97.6387 |
| OL3D | retro | 69 | 26.3152 | 0.0301 | 0.1658 | 12.5964 | 1.0123 | 1.0850 | 11.1839 | 25.0345 | 2.4989 | 9.1867 | 1.4618 | 0.9068 | 0.4517 | 0.1141 | 0.5049 | 4.9327 | 0.6005 | 98.0913 |
| OL3D | retro | 70 | 26.1078 | 0.0352 | 0.1651 | 12.5186 | 0.6835 | 1.3860 | 10.9271 | 25.3632 | 2.6415 | 9.9750 | 1.7810 | 1.3866 | 0.5198 | 0.0803 | 0.3330 | 3.2606 | 0.3600 | 97.5343 |
| OL3D | retro | 71 | 26.3112 | 0.0425 | 0.1622 | 12.5889 | 0.8465 | 1.1203 | 11.3318 | 25.6792 | 2.4689 | 9.5108 | 1.4961 | 1.0236 | 0.4278 | 0.1287 | 0.4510 | 3.9094 | 0.6270 | 98.1359 |
| OL3D | retro | 72 | 27.0382 | 0.1012 | 0.2925 | 13.1678 | 0.7613 | 1.2133 | 11.2896 | 25.4228 | 2.3608 | 9.2111 | 1.5680 | 1.1797 | 0.4868 | 0.1032 | 0.3744 | 3.4540 | 0.3346 | 98.3693 |
| OL3D | retro | 73 | 26.3937 | 0.0064 | 0.1331 | 12.7202 | 0.6103 | 1.0525 | 11.6187 | 26.3528 | 2.5528 | 9.7824 | 1.6556 | 1.1177 | 0.4319 | 0.1530 | 0.2976 | 2.8693 | 0.3252 | 98.0832 |
| OL3D | retro | 74 | 25.7785 | 0.0410 | 0.3488 | 12.1878 | 0.3987 | 0.9097 | 11.5630 | 26.4863 | 2.6983 | 9.7555 | 1.5450 | 1.0488 | 0.3977 | 0.1008 | 0.2238 | 2.2401 | 0.1759 | 95.9097 |
| OL3D | retro | 75 | 26.4997 | 0.4882 | 0.7136 | 12.0581 | 0.6716 | 0.9717 | 11.0563 | 24.9854 | 2.4703 | 9.6459 | 1.5510 | 1.1551 | 0.4034 | 0.0933 | 0.3817 | 4.6154 | 0.2592 | 98.0299 |
| OL3D | retro | 76 | 25.0498 | 0.0358 | 0.2274 | 11.7620 | 0.4244 | 0.9767 | 11.4945 | 26.0340 | 2.6046 | 9.6820 | 1.6667 | 1.1285 | 0.4183 | 0.0156 | 0.2340 | 2.6187 | 0.1455 | 94.5285 |
| OL3D | retro | 77 | 26.0023 | 0.0087 | 0.2539 | 12.3451 | 0.6818 | 0.9349 | 11.6897 | 25.2983 | 2.3709 | 9.2553 | 1.5574 | 1.0890 | 0.3920 | 0.0880 | 0.4015 | 4.7007 | 0.2255 | 97.3050 |
| OL3D | retro | 78 | 25.7432 | 0.0239 | 0.3628 | 12.0369 | 0.9319 | 1.0226 | 10.5022 | 23.8366 | 2.4106 | 9.3255 | 1.6948 | 1.2439 | 0.4440 | 0.0991 | 0.5108 | 6.5726 | 0.3525 | 97.1239 |
| OL3D | retro | 79 | 26.1411 | 0.0040 | 0.2619 | 12.4600 | 0.7631 | 1.0342 | 10.8819 | 24.2317 | 2.5115 | 9.7556 | 1.8502 | 1.2661 | 0.4095 | 0.0204 | 0.4955 | 5.4201 | 0.1864 | 97.7032 |
| OL3D | retro | 80 | 26.1070 | 0.0205 | 0.4182 | 12.3398 | 0.6576 | 0.9327 | 11.5284 | 25.7584 | 2.5139 | 9.4037 | 1.5378 | 1.0343 | 0.4443 | 0.0812 | 0.3089 | 3.5267 | 0.2041 | 96.8275 |
| OL3D | retro | 81 | 25.7780 | 0.0215 | 0.3635 | 12.0588 | 0.8809 | 1.0239 | 10.8092 | 23.7893 | 2.3353 | 9.2569 | 1.7702 | 1.1480 | 0.4133 | 0.1253 | 0.5156 | 6.7948 | 0.2020 | 97.2965 |
| OL3D | retro | 82 | 25.6830 | 0.0100 | 0.6236 | 11.7915 | 1.0160 | 0.9923 | 9.8876 | 22.0742 | 2.2679 | 9.5246 | 1.7938 | 1.1382 | 0.3227 | 0.0547 | 0.7204 | 9.2165 | 0.2136 | 97.3406 |
| OL3D | retro | 83 | 25.8613 | 0.0002 | 0.6150 | 11.8948 | 1.0776 | 0.9475 | 9.6135 | 21.8331 | 2.2938 | 9.7759 | 1.8094 | 1.1376 | 0.3597 | 0.1632 | 0.7259 | 9.6040 | 0.2423 | 97.9648 |
| OL3D | retro | 84 | 25.8521 | 0.0689 | 0.5266 | 12.1512 | 1.1803 | 1.2641 | 9.8316 | 22.3555 | 2.3045 | 9.3148 | 1.6654 | 1.0434 | 0.4456 | 0.1609 | 0.6242 | 6.3995 | 0.8444 | 96.0430 |
| OL3D | retro | 85 | 26.0814 | 0.4239 | 1.6231 | 11.3431 | 1.0325 | 0.9201 | 9.3733 | 21.1537 | 2.1669 | 9.2965 | 1.7111 | 1.1429 | 0.4053 | 0.0208 | 0.5580 | 7.6254 | 0.2335 | 95.1215 |
| OL3D | retro | 87 | 26.0990 | 0.0135 | 0.1527 | 12.4997 | 1.0660 | 1.1438 | 10.8627 | 24.5483 | 2.4761 | 9.3286 | 1.5846 | 1.0580 | 0.3863 | 0.0690 | 0.5293 | 4.9047 | 0.6852 | 97.4175 |
| OL3D | retro | 89 | 26.1524 | 0.0002 | 0.2009 | 12.4945 | 0.4771 | 0.8544 | 11.7973 | 26.4555 | 2.6127 | 9.6610 | 1.6800 | 1.0856 | 0.4190 | 0.1239 | 0.2850 | 3.0556 | 0.1436 | 97.5087 |
| OL3D | retro | 90 | 25.6884 | 0.0143 | 0.4678 | 11.9776 | 1.0662 | 1.0086 | 9.8925 | 21.8480 | 2.3793 | 9.7254 | 1.7088 | 1.2503 | 0.3628 | 0.1320 | 0.6331 | 8.4159 | 0.2196 | 96.8006 |
| OL3D | retro | 91 | 26.0450 | 0.0165 | 0.2263 | 12.3808 | 0.9306 | 0.9237 | 10.9536 | 24.5986 | 2.4064 | 9.2357 | 1.5066 | 1.1084 | 0.4293 | 0.0809 | 0.5262 | 5.6482 | 0.4204 | 97.4472 |
| OL3D | retro | 92 | 26.2395 | 0.0241 | 0.2306 | 12.4373 | 0.5043 | 0.8571 | 11.7538 | 26.6581 | 2.7490 | 9.8560 | 1.5834 | 1.1045 | 0.4011 | 0.0700 | 0.2908 | 3.2625 | 0.1878 | 98.2199 |
| OL3D | retro | 93 | 25.9584 | 0.0301 | 0.2653 | 12.3452 | 0.7207 | 1.0198 | 10.9835 | 25.0229 | 2.5639 | 9.4005 | 1.5185 | 1.0242 | 0.4694 | 0.0676 | 0.4669 | 4.7870 | 0.3078 | 96.9617 |
| OL3D | retro | 94 | 26.1730 | 0.0179 | 0.2792 | 12.4334 | 0.9725 | 1.0759 | 10.6976 | 23.9550 | 2.4824 | 9.5286 | 1.6345 | 1.1252 | 0.4086 | 0.1200 | 0.5668 | 5.7463 | 0.6623 | 97.8892 |
| OL3D | retro | 95 | 26.9591 | 0.1409 | 0.7759 | 12.6595 | 1.2096 | 1.0474 | 9.2275 | 21.2823 | 2.1248 | 8.8807 | 1.6597 | 1.1510 | 0.3765 | 0.1051 | 0.7376 | 10.2528 | 0.4303 | 99.0307 |
| OL3D | retro | 96 | 26.1567 | 0.0121 | 0.1606 | 12.5039 | 0.9378 | 0.9824 | 11.0638 | 24.8060 | 2.4490 | 9.4368 | 1.6665 | 1.0936 | 0.4228 | 0.1405 | 0.4878 | 4.8428 | 0.5434 | 97.7165 |
| OL3D | retro | 97 | 25.7142 | 0.0037 | 0.1413 | 12.3023 | 1.1652 | 1.4417 | 10.5466 | 23.9538 | 2.3420 | 8.9870 | 1.5709 | 1.1006 | 0.5430 | 0.1395 | 0.6708 | 4.7114 | 1.1798 | 96.5238 |
| OL3D | retro | 99 | 26.1051 | 0.0121 | 0.1841 | 12.4138 | 0.5527 | 0.8130 | 11.6932 | 26.4967 | 2.6659 | 9.8545 | 1.5710 | 0.9964 | 0.4023 | 0.1045 | 0.2920 | 3.3059 | 0.1891 | 97.6623 |
| OL3D | retro | 100 | 25.9657 | 0.0123 | 0.1528 | 12.4620 | 0.8063 | 1.1430 | 11.0280 | 24.9901 | 2.5185 | 9.5515 | 1.6087 | 1.1420 | 0.4451 | 0.1202 | 0.4384 | 3.8618 | 0.6078 | 96.8642 |
| OL3D | retro | 101 | 26.1985 | 0.0067 | 0.1434 | 12.6234 | 1.0225 | 1.0960 | 11.0800 | 24.4321 | 2.4789 | 9.1480 | 1.4767 | 1.1096 | 0.4118 | 0.1324 | 0.5450 | 4.5883 | 0.8684 | 97.3717 |
| OL3D | retro | 102 | 26.4128 | 0.0067 | 0.9608 | 12.1732 | 0.8057 | 0.9197 | 10.6892 | 23.7165 | 2.5000 | 9.3249 | 1.5057 | 1.0947 | 0.4150 | 0.0360 | 0.4969 | 6.0565 | 0.2750 | 97.3993 |
| OL3D | retro | 103 | 26.0121 | 0.0164 | 0.1233 | 12.5483 | 1.1218 | 1.2606 | 10.7881 | 23.9481 | 2.3844 | 9.1989 | 1.4479 | 1.0709 | 0.4780 | 0.0669 | 0.6047 | 4.4739 | 1.2213 | 96.7756 |
| OL3D | retro | 104 | 26.4215 | 0.0564 | 0.3927 | 12.4989 | 1.0775 | 1.0450 | 10.4629 | 22.5554 | 2.3098 | 9.6317 | 1.7609 | 1.1582 | 0.4341 | 0.1134 | 0.6313 | 7.7671 | 0.2107 | 98.5375 |
| OL3D | retro | 105 | 25.4842 | 0.0276 | 0.8163 | 11.4296 | 1.1691 | 0.9123 | 9.0898 | 20.5676 | 2.2623 | 9.5034 | 1.7644 | 1.0782 | 0.4030 | 0.1013 | 0.8541 | 11.7618 | 0.2619 | 97.4969 |

| Sample | Phase | Label | W%(O) | W%(Al) | W%(Si) | W%(P) | W%(Ca) | W%(Y) | W%(La) | W%(Ce) | W%(Pr) | W%(Nd) | W%(Sm) | W%(Gd) | W%(Dy) | W%(Er) | W%(Pb) | W%(Th) | W%(U) | W%(SUM) |
|---|---|---|---|---|---|---|---|---|---|---|---|---|---|---|---|---|---|---|---|---|
| OL3D | retro | 106 | 26.0324 | 0.0041 | 0.1521 | 12.4547 | 0.8333 | 0.9093 | 11.7175 | 25.3307 | 2.4125 | 9.1025 | 1.4121 | 1.0717 | 0.4269 | 0.0671 | 0.4399 | 4.2257 | 0.5393 | 97.1418 |
| OL3D | retro | 107 | 26.0901 | 0.0273 | 0.2196 | 12.3661 | 0.5674 | 0.8824 | 11.6351 | 25.1566 | 2.5554 | 10.5414 | 1.9271 | 1.2243 | 0.4079 | 0.1002 | 0.3253 | 3.6515 | 0.1063 | 97.7940 |
| OL3D | retro | 110 | 26.4084 | 0.0422 | 0.2441 | 12.6624 | 1.1392 | 1.2399 | 10.7486 | 24.3959 | 2.4550 | 9.1445 | 1.5027 | 1.0759 | 0.4839 | 0.0868 | 0.6341 | 4.4840 | 1.1597 | 97.9173 |
| OL3D | retro | 111 | 26.1172 | 0.0167 | 0.1085 | 12.5884 | 0.9948 | 1.1094 | 11.1483 | 24.8942 | 2.3282 | 9.1715 | 1.4009 | 1.0210 | 0.4539 | 0.1719 | 0.5989 | 3.9504 | 1.1221 | 97.2063 |
| OL3D | retro | 112 | 26.0097 | 0.0216 | 0.1574 | 12.5125 | 1.2153 | 1.4659 | 10.5041 | 23.8691 | 2.3668 | 9.0648 | 1.5413 | 0.9709 | 0.5109 | 0.1238 | 0.6607 | 4.6689 | 1.2737 | 96.9474 |
| OL3D | retro | 113 | 26.3196 | 0.0271 | 0.1780 | 12.6287 | 0.9245 | 1.0479 | 11.4405 | 25.1549 | 2.5087 | 9.1840 | 1.4598 | 1.0988 | 0.4221 | 0.1739 | 0.4965 | 4.0141 | 0.7083 | 97.7974 |
| OL3D | retro | 114 | 26.0340 | 0.0199 | 0.1192 | 12.5410 | 1.2573 | 1.5527 | 10.4087 | 23.7842 | 2.4099 | 9.1387 | 1.5390 | 1.1682 | 0.4981 | 0.0793 | 0.6589 | 4.6547 | 1.3321 | 97.2059 |
| OL3D | retro | 115 | 26.2651 | 0.0076 | 0.1130 | 12.7110 | 1.3846 | 1.5717 | 10.1059 | 23.4893 | 2.3287 | 9.1905 | 1.5388 | 1.1739 | 0.6147 | 0.1502 | 0.7496 | 4.8092 | 1.5567 | 97.7705 |
| OL3D | retro | 116 | 26.1322 | 0.0179 | 0.1447 | 12.4204 | 0.9827 | 1.2075 | 11.1280 | 25.3278 | 2.4412 | 9.2834 | 1.5830 | 1.1100 | 0.4295 | 0.1561 | 0.5598 | 4.5946 | 0.8486 | 98.3774 |
| OL3D | retro | 117 | 26.1282 | 0.0054 | 0.1238 | 12.5165 | 1.0284 | 1.2138 | 10.8275 | 24.8137 | 2.4388 | 9.5328 | 1.5887 | 1.1774 | 0.4807 | 0.0979 | 0.5241 | 4.4624 | 0.8353 | 97.8054 |
| OL3D | retro | 118 | 26.2298 | 0.0229 | 0.2052 | 12.4567 | 0.8944 | 1.0489 | 10.9775 | 25.1715 | 2.5960 | 9.4614 | 1.4966 | 1.1856 | 0.4845 | 0.1236 | 0.4576 | 5.0982 | 0.4525 | 98.3729 |
| OL3D | retro | 119 | 25.2320 | 0.0737 | 0.3655 | 11.6509 | 0.6518 | 0.8718 | 11.0662 | 25.6151 | 2.5052 | 9.4866 | 1.5656 | 1.1159 | 0.3754 | 0.1162 | 0.3690 | 4.2819 | 0.2129 | 95.5657 |
| OL3D | retro | 120 | 25.9979 | 0.0348 | 0.7474 | 11.8038 | 1.1697 | 0.8925 | 9.2938 | 21.6434 | 2.1668 | 9.2839 | 1.6961 | 1.2009 | 0.4151 | 0.0903 | 0.8926 | 11.2460 | 0.2302 | 98.8152 |
| OL3D | retro | 121 | 26.1116 | 0.0045 | 0.2065 | 12.3489 | 0.8609 | 0.9861 | 10.9415 | 25.6585 | 2.4894 | 9.7189 | 1.5861 | 1.0764 | 0.3843 | 0.0877 | 0.4382 | 4.9545 | 0.3848 | 98.2488 |
| WW18 | mica (mx) | 1 | 26.3172 | 0.0235 | 0.2132 | 12.5498 | 0.5169 | 0.6270 | 12.8294 | 25.6909 | 2.7838 | 9.7023 | 1.6227 | 0.9262 | 0.4070 | 0.0616 | 0.2724 | 2.8270 | 0.4118 | 97.7927 |
| WW18 | mica (mx) | 4 | 26.4646 | 0.0108 | 0.3675 | 12.4812 | 0.8437 | 0.2473 | 11.4766 | 23.9525 | 2.4609 | 10.1634 | 1.9493 | 1.1532 | 0.1310 | 0.0490 | 0.5048 | 5.8377 | 0.2134 | 98.3169 |
| WW18 | mica (mx) | 5 | 26.2468 | 0.0085 | 0.1550 | 12.5865 | 0.5584 | 0.5876 | 12.5906 | 25.0910 | 2.7245 | 10.0338 | 1.5899 | 1.0109 | 0.3243 | 0.0657 | 0.3237 | 3.3116 | 0.2435 | 97.4623 |
| WW18 | mica (mx) | 7 | 26.2316 | 0.0092 | 0.1829 | 12.6083 | 0.3520 | 0.6970 | 13.1311 | 26.0842 | 2.7233 | 9.7340 | 1.5553 | 0.8492 | 0.3849 | 0.0729 | 0.2303 | 1.9969 | 0.2578 | 97.1109 |
| WW18 | mica (mx) | 8 | 25.9868 | 0.0086 | 0.1786 | 12.4905 | 0.5811 | 0.7310 | 12.4879 | 24.6089 | 2.6011 | 9.6372 | 1.4300 | 0.9757 | 0.3937 | 0.0686 | 0.3580 | 3.4516 | 0.3427 | 96.3420 |
| WW18 | mica (mx) | 13 | 26.2278 | 0.0094 | 0.2307 | 12.6360 | 0.7071 | 0.6034 | 12.1717 | 23.7606 | 2.5200 | 9.6760 | 1.5431 | 1.0697 | 0.3102 | 0.0945 | 0.4148 | 4.4342 | 0.2425 | 96.6617 |
| WW18 | mica (mx) | 14 | 26.7198 | 0.3853 | 0.9107 | 12.1715 | 0.9949 | 0.5619 | 11.6281 | 22.7196 | 2.5311 | 9.1715 | 1.5546 | 1.1469 | 0.3581 | 0.0621 | 0.5492 | 5.8220 | 0.2750 | 97.5723 |
| WW18 | mica (mx) | 15 | 25.9920 | 0.1289 | 0.2779 | 12.4518 | 0.3393 | 0.6099 | 12.8955 | 25.0006 | 2.7426 | 9.7721 | 1.5014 | 0.9090 | 0.4280 | 0.0309 | 0.2034 | 1.8170 | 0.2242 | 95.3345 |
| WW18 | mica (mx) | 17 | 26.0173 | 0.0059 | 0.1662 | 12.5369 | 0.4324 | 0.6735 | 12.8860 | 25.0592 | 2.5985 | 9.8495 | 1.5515 | 0.9773 | 0.3538 | 0.0481 | 0.2515 | 2.5407 | 0.2593 | 96.2176 |
| WW18 | mica (mx) | 18 | 26.6138 | 0.4293 | 0.5348 | 12.4410 | 0.4616 | 0.6426 | 12.6703 | 24.5265 | 2.5483 | 9.6400 | 1.5860 | 1.0617 | 0.3423 | 0.0402 | 0.2705 | 3.0527 | 0.2339 | 97.1055 |
| WW18 | mica (mx) | 20 | 26.0080 | 0.0244 | 0.2615 | 12.3268 | 0.7997 | 0.5549 | 12.2848 | 23.9793 | 2.4256 | 9.3477 | 1.5355 | 1.0097 | 0.2948 | 0.0651 | 0.4411 | 5.3118 | 0.2544 | 96.9351 |
| WW18 | mica (mx) | 21 | 26.0370 | 0.0187 | 0.4078 | 12.2928 | 1.0474 | 0.6196 | 11.0467 | 22.2600 | 2.4546 | 9.3103 | 1.7206 | 1.1973 | 0.3142 | 0.0280 | 0.5884 | 7.1150 | 0.3011 | 96.7695 |
| WW18 | mica (mx) | 22 | 25.9235 | 0.0063 | 0.2805 | 12.2964 | 0.8566 | 0.5345 | 11.6434 | 23.3548 | 2.5185 | 9.4293 | 1.6791 | 1.1812 | 0.2525 | 0.0926 | 0.5023 | 5.7852 | 0.2399 | 96.5866 |
| WW18 | mica (mx) | 24 | 26.2835 | 0.0075 | 0.1618 | 12.6800 | 0.5267 | 0.7590 | 12.5409 | 24.8722 | 2.7272 | 9.9080 | 1.5876 | 1.0472 | 0.4069 | 0.1223 | 0.3194 | 2.9305 | 0.3601 | 97.2508 |
| WW18 | mica (mx) | 25 | 26.2236 | 0.0002 | 0.3480 | 12.4176 | 1.0477 | 0.4279 | 11.0001 | 22.3603 | 2.4655 | 9.7189 | 1.8488 | 1.3443 | 0.2121 | 0.0698 | 0.5926 | 7.0702 | 0.3236 | 97.4812 |
| WW18 | mica (mx) | 26 | 26.4722 | 0.0627 | 0.2815 | 12.8133 | 0.8660 | 0.9900 | 12.0013 | 23.4455 | 2.4809 | 9.2633 | 1.4469 | 0.9878 | 0.4286 | 0.1217 | 0.5141 | 3.9939 | 0.7259 | 96.9056 |
| WW18 | mica (mx) | 27 | 26.1449 | 0.0191 | 0.5765 | 12.0757 | 1.3413 | 0.0962 | 10.5509 | 21.0341 | 2.2907 | 9.2254 | 1.7474 | 0.8877 | 0.1280 | 0.0468 | 0.7706 | 10.4565 | 0.3674 | 97.7692 |
| WW18 | mica (mx) | 30 | 26.1358 | 0.0209 | 0.2586 | 12.5173 | 0.9730 | 0.9201 | 11.4745 | 22.9046 | 2.4923 | 9.3417 | 1.6124 | 1.0558 | 0.3970 | 0.0920 | 0.5965 | 5.4181 | 0.7576 | 96.9782 |
| WW18 | mica (mx) | 31 | 26.1951 | 0.1716 | 0.4193 | 12.4272 | 0.3433 | 0.6058 | 12.8927 | 25.2567 | 2.7701 | 9.8828 | 1.4442 | 0.9149 | 0.3627 | 0.0123 | 0.1967 | 1.7275 | 0.2327 | 95.8656 |
| WW18 | mica (mx) | 33 | 25.9906 | 0.0052 | 0.3136 | 12.3632 | 1.0289 | 0.6570 | 11.4079 | 22.2398 | 2.4796 | 9.0882 | 1.5639 | 1.1028 | 0.4107 | 0.0386 | 0.5857 | 6.9545 | 0.3696 | 96.6098 |
| WW18 | mica (mx) | 35 | 26.2407 | 0.0081 | 0.2800 | 12.5127 | 0.8959 | 0.6375 | 11.6850 | 23.1320 | 2.5149 | 9.4467 | 1.7578 | 1.2265 | 0.3582 | 0.0080 | 0.5142 | 5.9324 | 0.2822 | 97.4428 |
| WW18 | mica (mx) | 36 | 25.8855 | 0.0152 | 0.3190 | 12.2268 | 1.0043 | 0.3189 | 11.4465 | 22.0109 | 2.5759 | 9.6208 | 1.8567 | 1.1569 | 0.1916 | 0.0525 | 0.5480 | 6.8406 | 0.2753 | 96.3554 |
| WW18 | mica (mx) | 38 | 25.5237 | 0.0216 | 0.2592 | 12.0411 | 0.8178 | 0.5836 | 11.7067 | 23.1067 | 2.5713 | 9.5796 | 1.6717 | 1.1857 | 0.3505 | 0.0365 | 0.4610 | 5.4146 | 0.2543 | 95.5956 |
| WW18 | mica (mx) | 39 | 24.9113 | 0.0615 | 0.1620 | 12.1014 | 0.8496 | 1.3199 | 11.2839 | 21.8915 | 2.4707 | 8.8629 | 1.3276 | 0.8926 | 0.5727 | 0.1262 | 0.5725 | 3.2580 | 1.2407 | 91.9150 |
| WW18 | mica (mx) | 41 | 28.0440 | 1.8872 | 1.9488 | 11.5583 | 0.9447 | 0.4953 | 10.7654 | 21.0505 | 2.3354 | 8.9556 | 1.7364 | 1.1810 | 0.3302 | 0.0619 | 0.5459 | 6.3932 | 0.3729 | 98.6167 |
| WW18 | mica (mx) | 42 | 25.8366 | 0.0210 | 0.2905 | 12.1409 | 0.8706 | 0.2767 | 11.4876 | 23.2007 | 2.7241 | 10.0815 | 1.8587 | 0.9906 | 0.1407 | 0.1039 | 0.4994 | 5.8053 | 0.2875 | 96.6263 |
| WW18 | mica (mx) | 44 | 25.9136 | 0.0025 | 0.2384 | 12.3314 | 0.7859 | 0.4625 | 12.2310 | 23.6528 | 2.5517 | 9.1819 | 1.5762 | 1.0312 | 0.3899 | 0.0637 | 0.4268 | 5.2725 | 0.2926 | 96.4146 |
| WW18 | mica (mx) | 45 | 25.8185 | 0.0002 | 0.2553 | 12.2543 | 0.8934 | 0.5525 | 11.8796 | 23.0531 | 2.4701 | 9.3942 | 1.6978 | 1.1406 | 0.3533 | 0.0001 | 0.4215 | 5.7759 | 0.2603 | 96.2307 |
| WW18 | mica (mx) | 46 | 25.9014 | 0.0003 | 0.3715 | 12.1217 | 1.1449 | 0.1961 | 10.6111 | 22.1048 | 2.4451 | 9.5225 | 1.9509 | 1.0963 | 0.2377 | 0.0889 | 0.5956 | 8.2280 | 0.2977 | 96.9245 |
| WW18 | mica (mx) | 47 | 25.7460 | 0.0135 | 0.2038 | 12.2730 | 0.5689 | 0.6326 | 12.3886 | 24.3461 | 2.6085 | 9.6761 | 1.5899 | 1.0621 | 0.3851 | 0.0385 | 0.3429 | 3.7887 | 0.2529 | 95.9272 |
| WW18 | mica (mx) | 50 | 26.0323 | 0.0134 | 0.2632 | 12.3502 | 0.8856 | 0.4607 | 11.6743 | 23.2350 | 2.4465 | 9.5105 | 1.7785 | 1.2678 | 0.3023 | 0.0531 | 0.4869 | 5.9439 | 0.2659 | 96.9801 |
| WW18 | mica (mx) | 51 | 26.1294 | 0.0244 | 0.3811 | 12.2833 | 1.2825 | 0.6301 | 10.5820 | 21.2755 | 2.3664 | 9.1698 | 1.7863 | 1.2204 | 0.3670 | 0.1366 | 0.7508 | 9.0315 | 0.3698 | 97.7969 |
| WW18 | mica (mx) | 52 | 26.1414 | 0.0055 | 0.3371 | 12.3224 | 0.9654 | 0.2579 | 10.9640 | 23.1185 | 2.4308 | 9.8669 | 1.9011 | 1.2183 | 0.2588 | 0.0001 | 0.5310 | 6.8454 | 0.2387 | 97.4133 |
| WW18 | mica (mx) | 53 | 26.1959 | 0.0131 | 0.3437 | 12.4532 | 1.1041 | 0.5904 | 11.0083 | 22.2814 | 2.3921 | 9.0561 | 1.5699 | 1.0741 | 0.3591 | 0.0001 | 0.6163 | 7.8108 | 0.3387 | 97.2173 |
| WW18 | mica (mx) | 54 | 26.0824 | 0.0002 | 0.1347 | 12.4632 | 0.4200 | 0.4940 | 13.1260 | 26.1619 | 2.7463 | 10.0150 | 1.5112 | 0.8253 | 0.1873 | 0.0521 | 0.2610 | 2.4023 | 0.2239 | 97.1168 |
| WW18 | mica (mx) | 55 | 26.3486 | 0.1804 | 0.3190 | 12.5183 | 0.7325 | 0.6580 | 12.0711 | 24.4481 | 2.4758 | 9.5947 | 1.5584 | 1.0432 | 0.2922 | 0.0299 | 0.3841 | 3.9709 | 0.3196 | 96.9548 |
| WW18 | mica (mx) | 56 | 26.2932 | 0.0162 | 0.1437 | 12.6105 | 0.4595 | 0.5923 | 12.8262 | 25.7253 | 2.7537 | 10.0823 | 1.6193 | 1.0089 | 0.3777 | 0.0936 | 0.2524 | 2.5165 | 0.2236 | 97.6049 |
| WW18 | mica (mx) | 60 | 25.7583 | 0.0341 | 0.3943 | 12.0595 | 0.9030 | 0.4062 | 11.2665 | 22.8267 | 2.4319 | 9.4896 | 1.7027 | 1.1721 | 0.2879 | 0.0933 | 0.5305 | 6.5879 | 0.2962 | 96.2507 |
| WW18 | mica (mx) | 61 | 26.5816 | 0.0496 | 0.3854 | 12.7143 | 0.9643 | 0.6006 | 11.4277 | 22.7905 | 2.4508 | 9.2200 | 1.5101 | 0.9857 | 0.3379 | 0.0600 | 0.5798 | 6.7721 | 0.2726 | 97.7130 |
| WW18 | mica (mx) | 67 | 25.7290 | 0.0002 | 0.1553 | 12.4471 | 0.8426 | 1.2286 | 11.7931 | 23.6249 | 2.4797 | 9.1225 | 1.3111 | 0.9669 | 0.5359 | 0.1097 | 0.5830 | 3.3349 | 1.1978 | 95.4723 |
| WW18 | mica (mx) | 68 | 25.8937 | 0.0002 | 0.1354 | 12.4147 | 0.2964 | 0.6630 | 13.2795 | 25.9831 | 2.7235 | 10.0522 | 1.5390 | 0.9127 | 0.3590 | 0.0001 | 0.1431 | 1.6857 | 0.1972 | 96.2885 |
| WW18 | mica (mx) | 69 | 26.0684 | 0.0031 | 0.1754 | 12.5220 | 0.7704 | 0.7535 | 12.1129 | 24.1756 | 2.6527 | 9.7709 | 1.4229 | 0.9201 | 0.2828 | 0.0875 | 0.4451 | 3.8721 | 0.6452 | 96.6906 |

| Sample | Phase | Label | W%(O ) | W%(Al) | W%(Si) | W%(P) | W%(Ca) | W%(Y ) | W%(La) | W%(Ce) | W%(Pr) | W%(Nd) | W%(Sm) | W%(Gd) | W%(Dy) | W%(Er) | W%(Pb) | W%(Th) | W%(U ) | W%(SUM) |
|---|---|---|---|---|---|---|---|---|---|---|---|---|---|---|---|---|---|---|---|---|
| WW18 | mica (mx) | 70 | 26.8460 | 0.0244 | 0.2931 | 13.0701 | 0.5597 | 0.8700 | 12.5588 | 24.6547 | 2.5964 | 9.7204 | 1.5640 | 1.0123 | 0.3577 | 0.1406 | 0.3678 | 2.6208 | 0.5184 | 97.7852 |
| WW18 | mica (mx) | 71 | 26.0751 | 0.0043 | 0.2496 | 12.4388 | 0.6907 | 0.5548 | 12.0814 | 24.1230 | 2.6772 | 9.7305 | 1.6133 | 1.1116 | 0.3523 | 0.0655 | 0.4195 | 4.3747 | 0.2227 | 96.7950 |
| WW18 | mica (mx) | 72 | 25.9578 | 0.0002 | 0.2754 | 12.3579 | 0.8651 | 0.5413 | 11.4324 | 23.0564 | 2.4363 | 9.4978 | 1.7618 | 1.2416 | 0.3170 | 0.1231 | 0.4648 | 5.8485 | 0.3188 | 96.5062 |
| WW18 | mica (mx) | 73 | 26.4318 | 0.0123 | 0.2552 | 12.5493 | 1.9887 | 0.5848 | 11.4283 | 23.1319 | 2.4356 | 9.2647 | 1.5931 | 1.0812 | 0.2752 | 0.0564 | 0.4033 | 5.0623 | 0.3020 | 96.8661 |
| WW18 | mica (mx) | 77 | 27.2087 | 0.0219 | 1.7840 | 12.1300 | 0.9661 | 0.5371 | 11.1238 | 22.1668 | 2.3948 | 9.1636 | 1.6853 | 1.1286 | 0.3005 | 0.0095 | 0.5226 | 6.4707 | 0.2686 | 97.8926 |
| WW18 | mica (mx) | 78 | 26.2768 | 0.0048 | 0.1515 | 12.7037 | 0.3518 | 0.7151 | 13.0140 | 25.9011 | 2.7330 | 9.8158 | 1.4838 | 0.9681 | 0.3534 | 0.0273 | 0.2080 | 2.0439 | 0.2419 | 97.0040 |
| WW18 | mica (mx) | 81 | 26.2420 | 0.0080 | 0.1280 | 12.7440 | 0.3540 | 0.6627 | 13.0124 | 25.6769 | 2.7794 | 9.7592 | 1.5759 | 0.9100 | 0.3835 | 0.0582 | 0.2283 | 1.6815 | 0.3172 | 96.5312 |
| WW18 | mica (mx) | 83 | 26.3694 | 0.0196 | 0.1730 | 12.7898 | 0.3869 | 0.6523 | 12.7628 | 25.3845 | 2.7290 | 10.0352 | 1.6386 | 0.8781 | 0.3032 | 0.0384 | 0.2043 | 2.2391 | 0.1963 | 96.8105 |
| WW18 | mica (mx) | 85 | 26.2089 | 0.0086 | 0.2985 | 12.5575 | 0.8415 | 0.5870 | 11.6052 | 23.2665 | 2.5010 | 9.2536 | 1.6879 | 1.0115 | 0.2999 | 0.0526 | 0.4593 | 5.8095 | 0.3054 | 96.7644 |
| WW18 | mica (mx) | 86 | 25.7488 | 0.0041 | 0.4120 | 12.1211 | 1.0394 | 0.2971 | 10.7207 | 21.9926 | 2.3424 | 9.6028 | 1.8729 | 1.1433 | 0.2289 | 0.0001 | 0.5716 | 7.2831 | 0.2727 | 95.6636 |
| WW18 | mica (mx) | 87 | 26.1417 | 0.0055 | 0.3237 | 12.4364 | 0.9016 | 0.4732 | 11.1722 | 22.7683 | 2.5290 | 9.4372 | 1.8176 | 1.3172 | 0.2991 | 0.0959 | 0.5260 | 6.4991 | 0.2335 | 96.9872 |
| WW18 | mica (mx) | 88 | 25.8865 | 0.0165 | 0.3309 | 12.2506 | 1.1415 | 0.6481 | 11.1057 | 22.0753 | 2.4729 | 9.1697 | 1.5674 | 1.0394 | 0.3614 | 0.0809 | 0.5935 | 7.2884 | 0.3558 | 96.3945 |
| WW18 | mica (mx) | 89 | 26.0252 | 0.0002 | 0.2321 | 12.5334 | 0.3172 | 0.6946 | 13.3338 | 25.6413 | 2.6814 | 9.6066 | 1.4610 | 0.8236 | 0.3373 | 0.0791 | 0.2003 | 1.6737 | 0.2385 | 95.8893 |
| MU | mica (mx) | 18 | 26.5852 | 0.0064 | 0.1367 | 12.8744 | 0.1656 | 0.9222 | 12.9555 | 26.6800 | 2.9318 | 10.6359 | 1.6894 | 0.9688 | 0.3970 | 0.0903 | 0.0341 | 0.9508 | 0.2403 | 98.2744 |
| MU | mica (mx) | 19 | 26.5925 | 0.0002 | 0.1202 | 12.9420 | 0.1583 | 0.8938 | 13.1174 | 26.6327 | 2.7036 | 10.5101 | 1.6627 | 0.9683 | 0.4067 | 0.0925 | 0.0425 | 0.8643 | 0.2476 | 97.9654 |
| MU | mica (mx) | 20 | 26.4447 | 0.0036 | 0.1717 | 12.8051 | 0.4609 | 1.1304 | 12.2671 | 25.1288 | 2.6615 | 9.8312 | 1.6060 | 1.1229 | 0.4544 | 0.0996 | 0.0975 | 3.3102 | 0.3002 | 97.9058 |
| MU | mica (mx) | 21 | 26.5396 | 0.0002 | 0.2064 | 12.8514 | 0.6320 | 1.0317 | 12.0045 | 24.2602 | 2.5494 | 9.8139 | 1.5016 | 1.0243 | 0.4482 | 0.0778 | 0.1264 | 4.5962 | 0.3188 | 97.9926 |
| MU | mica (mx) | 22 | 26.8270 | 0.0259 | 0.1436 | 13.0454 | 0.1585 | 0.9906 | 12.5157 | 26.7956 | 2.8882 | 11.0655 | 1.7342 | 1.0623 | 0.3472 | 0.0746 | 0.0461 | 0.8163 | 0.2150 | 98.7617 |
| MU | mica (mx) | 23 | 26.5384 | 0.0058 | 0.1693 | 12.8435 | 0.4674 | 1.2017 | 12.1512 | 25.0682 | 2.7151 | 10.1954 | 1.6551 | 1.0566 | 0.4623 | 0.0820 | 0.0947 | 3.3165 | 0.3450 | 98.3782 |
| MU | mica (mx) | 24 | 26.5444 | 0.0002 | 0.1553 | 12.8473 | 0.4240 | 1.0735 | 12.4280 | 25.3373 | 2.8026 | 10.1732 | 1.5846 | 1.0803 | 0.4320 | 0.1786 | 0.0690 | 2.9077 | 0.2760 | 98.3240 |
| MU | mica (mx) | 27 | 26.8852 | 0.0002 | 0.1362 | 13.1423 | 0.2293 | 0.9713 | 12.6325 | 26.5434 | 2.8179 | 10.5268 | 1.5932 | 1.0573 | 0.3965 | 0.1121 | 0.0422 | 1.3316 | 0.2186 | 98.6466 |
| MU | mica (mx) | 28 | 26.3074 | 0.6605 | 0.6550 | 12.0632 | 0.2701 | 0.9185 | 11.7678 | 25.4207 | 2.7078 | 10.0938 | 1.5501 | 0.9474 | 0.3426 | 0.1504 | 0.0534 | 1.7616 | 0.3638 | 96.0441 |
| MU | mica (mx) | 29 | 26.9570 | 0.3218 | 0.5383 | 12.7283 | 0.5225 | 0.9847 | 11.8612 | 24.4513 | 2.7260 | 9.9107 | 1.4532 | 1.0690 | 0.4083 | 0.0926 | 0.1304 | 3.9376 | 0.2969 | 98.3998 |
| MU | mica (mx) | 30 | 26.5558 | 0.0054 | 0.2293 | 12.8424 | 0.7003 | 0.9789 | 11.9211 | 23.9460 | 2.4545 | 9.4132 | 1.5275 | 0.9799 | 0.3753 | 0.1138 | 0.1358 | 5.6015 | 0.2429 | 98.0336 |
| MU | mica (mx) | 31 | 26.3776 | 0.0096 | 0.2295 | 12.6840 | 0.6765 | 1.0872 | 12.1570 | 23.7164 | 2.5385 | 9.6903 | 1.5832 | 1.0520 | 0.3530 | 0.0736 | 0.1235 | 5.2817 | 0.2752 | 97.9188 |
| MU | mica (mx) | 33 | 26.3782 | 0.0210 | 0.4139 | 12.4950 | 1.0400 | 1.0561 | 11.2836 | 21.3275 | 2.1957 | 9.0957 | 1.4722 | 1.0213 | 0.4724 | 0.1902 | 0.2317 | 9.3586 | 0.3795 | 98.4426 |
| MU | mica (mx) | 34 | 26.3826 | 0.0188 | 0.4177 | 12.5011 | 1.0655 | 1.1218 | 11.2899 | 21.3012 | 2.1858 | 8.9521 | 1.5094 | 1.1120 | 0.4538 | 0.1225 | 0.2399 | 9.4598 | 0.3140 | 98.4579 |
| MU | mica (mx) | 35 | 26.6107 | 0.0223 | 0.3030 | 12.8032 | 0.8469 | 1.0427 | 11.6476 | 23.0923 | 2.3565 | 9.3138 | 1.4670 | 0.9802 | 0.3430 | 0.1666 | 0.1497 | 6.8681 | 0.2859 | 98.3095 |
| MU | mica (mx) | 36 | 26.3969 | 0.0071 | 0.2026 | 12.7519 | 0.5985 | 1.0955 | 11.8071 | 24.4633 | 2.5857 | 9.7127 | 1.5906 | 1.1161 | 0.4174 | 0.0177 | 0.1389 | 4.5721 | 0.2799 | 97.7640 |
| MU | mica (mx) | 38 | 26.8383 | 0.0012 | 0.1338 | 13.0155 | 0.2867 | 0.9830 | 12.6665 | 26.7418 | 2.8089 | 10.6413 | 1.6072 | 0.9695 | 0.3868 | 0.1042 | 0.0680 | 1.7032 | 0.2113 | 99.1772 |
| MU | mica (mx) | 39 | 26.6433 | 0.0004 | 0.2038 | 12.9138 | 0.4851 | 1.0699 | 12.0475 | 25.2547 | 2.7885 | 9.9522 | 1.5338 | 1.1032 | 0.3996 | 0.0659 | 0.1144 | 3.4381 | 0.2839 | 98.3081 |
| MU | mica (mx) | 40 | 26.3890 | 0.0099 | 0.2601 | 12.6386 | 0.7334 | 1.1078 | 11.5289 | 23.8296 | 2.5279 | 9.7206 | 1.5518 | 1.0889 | 0.4057 | 0.1201 | 0.1751 | 5.8042 | 0.3270 | 98.2286 |
| MU | mica (mx) | 41 | 26.3656 | 0.0066 | 0.3095 | 12.5343 | 0.8575 | 1.0420 | 11.7331 | 23.0546 | 2.4290 | 9.3389 | 1.5800 | 0.9904 | 0.5025 | 0.0507 | 0.1975 | 7.2062 | 0.3063 | 98.5147 |
| MU | mica (mx) | 42 | 28.4066 | 0.7853 | 0.8638 | 13.2413 | 0.1011 | 0.9182 | 12.5273 | 26.8190 | 2.8652 | 10.4833 | 1.6507 | 1.1080 | 0.4143 | 0.0605 | 0.0301 | 0.4781 | 0.1751 | 100.9379 |
| MU | mica (mx) | 43 | 26.6670 | 0.0005 | 0.1238 | 12.9319 | 0.1689 | 0.9660 | 12.5530 | 27.2501 | 2.7853 | 10.8019 | 1.6548 | 0.9698 | 0.3431 | 0.1161 | 0.0422 | 0.9833 | 0.2407 | 98.6084 |
| MU | mica (mx) | 44 | 26.5693 | 0.0111 | 0.1548 | 12.8811 | 0.3663 | 1.1131 | 12.2328 | 26.0168 | 2.7869 | 10.1549 | 1.5798 | 1.0294 | 0.4382 | 0.0822 | 0.0818 | 2.4429 | 0.2966 | 98.2480 |
| MU | mica (mx) | 45 | 26.6046 | 0.0096 | 0.1227 | 12.9105 | 0.1851 | 1.0698 | 12.4680 | 26.8414 | 2.8340 | 10.6824 | 1.7248 | 1.0544 | 0.4464 | 0.0989 | 0.0508 | 1.0954 | 0.2044 | 98.4132 |
| MU | mica (mx) | 46 | 26.7128 | 0.0115 | 0.2377 | 12.8462 | 0.7051 | 1.0200 | 12.1868 | 24.6462 | 2.5550 | 9.3864 | 1.4456 | 0.9376 | 0.4338 | 0.1106 | 0.1554 | 5.3207 | 0.2827 | 99.0041 |
| MU | mica (mx) | 47 | 26.4353 | 0.0002 | 0.2055 | 12.7389 | 0.5932 | 1.0445 | 12.4111 | 24.7725 | 2.5976 | 9.3331 | 1.5290 | 1.0243 | 0.3859 | 0.1186 | 0.1086 | 4.4490 | 0.2599 | 98.0172 |
| MU | mica (mx) | 49 | 26.3344 | 0.0142 | 0.1588 | 12.7059 | 0.2430 | 0.9666 | 12.0552 | 26.5282 | 2.8991 | 10.6974 | 1.6316 | 0.9628 | 0.3768 | 0.0788 | 0.0713 | 1.6620 | 0.1998 | 97.5959 |
| MU | mica (mx) | 51 | 26.4751 | 0.0066 | 0.1378 | 12.8538 | 0.3129 | 0.9717 | 12.0533 | 26.1107 | 2.8221 | 10.4168 | 1.6505 | 1.0197 | 0.3394 | 0.1316 | 0.0824 | 2.1505 | 0.2158 | 97.7607 |
| MU | mica (mx) | 52 | 27.3446 | 0.5824 | 0.6548 | 12.7852 | 0.2998 | 0.9385 | 11.7284 | 25.7885 | 2.7648 | 10.3342 | 1.6723 | 0.9776 | 0.3857 | 0.1626 | 0.0751 | 2.0415 | 0.2479 | 98.7939 |
| MU | mica (mx) | 54 | 26.5678 | 0.0002 | 0.1460 | 12.8809 | 0.3036 | 1.0046 | 12.2028 | 26.2783 | 2.8232 | 10.4519 | 1.7165 | 0.9900 | 0.4191 | 0.1236 | 0.0562 | 2.0219 | 0.2176 | 98.2142 |
| MU | mica (mx) | 55 | 26.4852 | 0.0052 | 0.2047 | 12.7601 | 0.5821 | 1.0693 | 11.7696 | 24.9992 | 2.6698 | 9.9385 | 1.7229 | 0.9492 | 0.3865 | 0.0887 | 0.1095 | 4.2080 | 0.2622 | 98.2207 |
| MU | mica (mx) | 56 | 26.1616 | 0.0053 | 0.2576 | 12.4989 | 0.7160 | 1.0492 | 11.4307 | 24.0419 | 2.5178 | 9.6032 | 1.6192 | 1.0066 | 0.2968 | 0.0876 | 0.1427 | 5.7812 | 0.3047 | 97.5310 |
| MU | mica (mx) | 57 | 26.5165 | 0.0428 | 0.1848 | 12.7825 | 0.2783 | 0.9800 | 12.3238 | 26.4632 | 2.7612 | 10.5009 | 1.5997 | 1.1151 | 0.4151 | 0.0671 | 0.0496 | 1.7291 | 0.2389 | 98.0586 |
| MU | mica (mx) | 58 | 26.1144 | 0.0086 | 0.2915 | 12.4592 | 0.7772 | 1.0485 | 11.2109 | 23.6172 | 2.4771 | 9.4208 | 1.5774 | 0.9548 | 0.4604 | 0.0541 | 0.1974 | 6.3204 | 0.3250 | 97.3249 |
| MU | mica (mx) | 59 | 26.2837 | 0.0175 | 0.3697 | 12.4863 | 0.9057 | 0.9715 | 10.9337 | 22.9069 | 2.3675 | 9.1856 | 1.5291 | 1.0031 | 0.3505 | 0.1035 | 0.1730 | 7.9209 | 0.3534 | 97.8716 |
| MU | mica (mx) | 60 | 26.4449 | 0.0161 | 0.2471 | 12.7428 | 0.6860 | 1.1016 | 11.2671 | 24.1735 | 2.5839 | 9.6248 | 1.5139 | 1.0389 | 0.3744 | 0.1068 | 0.1259 | 5.5429 | 0.3439 | 97.9445 |
| MU | mica (mx) | 61 | 26.6271 | 0.0228 | 0.1698 | 12.9166 | 0.3936 | 1.1063 | 11.8326 | 25.6685 | 2.7705 | 10.2480 | 1.6485 | 1.1830 | 0.5083 | 0.1090 | 0.0737 | 2.7409 | 0.3012 | 98.3304 |
| MU | mica (mx) | 62 | 26.4381 | 0.0227 | 0.1668 | 12.7491 | 0.3208 | 1.0162 | 11.9109 | 26.2472 | 2.8419 | 10.6422 | 1.7368 | 1.1394 | 0.3498 | 0.0752 | 0.0623 | 2.0120 | 0.2396 | 97.9810 |
| MU | mica (mx) | 63 | 26.4467 | 0.0093 | 0.1747 | 12.7344 | 0.4031 | 1.0193 | 11.9481 | 26.0678 | 2.7410 | 10.2945 | 1.6644 | 1.0443 | 0.4050 | 0.1187 | 0.0685 | 2.8091 | 0.2271 | 98.1860 |
| MU | mica (mx) | 65 | 26.3511 | 0.0027 | 0.2415 | 12.6344 | 0.6852 | 1.0316 | 11.5174 | 24.2770 | 2.6348 | 9.8561 | 1.5769 | 0.9396 | 0.3670 | 0.0300 | 0.1469 | 5.4013 | 0.2819 | 97.9854 |
| MU | mica (mx) | 66 | 26.5967 | 0.0079 | 0.1851 | 12.8794 | 0.5284 | 0.9832 | 11.6463 | 25.2002 | 2.6275 | 10.2259 | 1.6008 | 1.0221 | 0.4034 | 0.1256 | 0.0913 | 3.8258 | 0.2594 | 98.2190 |
| MU | mica (mx) | 67 | 26.7032 | 0.0130 | 0.1983 | 12.9665 | 0.5256 | 1.1628 | 11.5590 | 24.8048 | 2.6957 | 10.1683 | 1.7460 | 1.0747 | 0.5123 | 0.1225 | 0.0947 | 3.8878 | 0.2644 | 98.5096 |
| MU | mica (mx) | 68 | 26.5022 | 0.0002 | 0.2485 | 12.8199 | 0.7395 | 1.0825 | 11.3470 | 23.9369 | 2.5780 | 9.3426 | 1.5359 | 0.9343 | 0.4306 | 0.1063 | 0.1161 | 5.7886 | 0.3046 | 97.8237 |

| Sample | Phase | Label | W%(O) | W%(Al) | W%(Si) | W%(P) | W%(Ca) | W%(Y) | W%(La) | W%(Ce) | W%(Pr) | W%(Nd) | W%(Sm) | W%(Gd) | W%(Dy) | W%(Er) | W%(Pb) | W%(Th) | W%(U) | W%(SUM) |
|---|---|---|---|---|---|---|---|---|---|---|---|---|---|---|---|---|---|---|---|---|
| MU | mica (mx) | 69 | 26.5823 | 0.0319 | 0.2584 | 12.8348 | 0.6277 | 0.9974 | 11.5350 | 24.3560 | 2.5600 | 9.7098 | 1.5886 | 1.0443 | 0.3574 | 0.1458 | 0.1428 | 4.9238 | 0.3114 | 98.0174 |
| MU | mica (mx) | 70 | 26.5748 | 0.0227 | 0.2047 | 12.8611 | 0.5889 | 1.0968 | 11.7071 | 24.6629 | 2.6145 | 9.7336 | 1.6381 | 1.0653 | 0.3558 | 0.1340 | 0.1322 | 4.4944 | 0.3014 | 98.1983 |
| MU | mica (mx) | 71 | 26.6678 | 0.0085 | 0.3223 | 12.7968 | 0.8272 | 1.0580 | 11.3287 | 23.1509 | 2.4823 | 9.5399 | 1.6409 | 0.9765 | 0.3788 | 0.1230 | 0.1387 | 7.0229 | 0.3067 | 98.7799 |
| MU | mica (mx) | 72 | 26.7090 | 0.0130 | 0.2294 | 12.9034 | 0.6794 | 1.0773 | 11.6309 | 24.3564 | 2.5939 | 9.7349 | 1.5487 | 1.0156 | 0.4248 | 0.1485 | 0.1517 | 5.2661 | 0.2602 | 98.7532 |
| MU | mica (mx) | 73 | 26.0394 | 0.0241 | 0.2092 | 12.6233 | 0.4268 | 1.0224 | 11.7218 | 24.7683 | 2.7139 | 9.8873 | 1.5955 | 1.0281 | 0.3521 | 0.1400 | 0.0822 | 2.9983 | 0.2209 | 95.8636 |
| MU | mica (mx) | 74 | 26.4797 | 0.0002 | 0.2392 | 12.7049 | 0.6431 | 1.1060 | 11.8253 | 24.2749 | 2.5475 | 9.9964 | 1.6477 | 1.0600 | 0.4260 | 0.0876 | 0.1433 | 5.0799 | 0.2525 | 98.5242 |
| MU | mica (mx) | 76 | 26.4429 | 0.0249 | 0.1601 | 12.7736 | 0.3381 | 0.9829 | 12.2272 | 26.0968 | 2.7626 | 10.3646 | 1.5969 | 1.0428 | 0.3409 | 0.1656 | 0.0577 | 2.2684 | 0.1877 | 97.8437 |
| MU | mica (mx) | 77 | 26.6682 | 0.0051 | 0.1693 | 12.8947 | 0.4089 | 0.9753 | 12.1342 | 25.7653 | 2.7616 | 10.3493 | 1.6167 | 1.1052 | 0.4530 | 0.1215 | 0.0951 | 2.9420 | 0.2232 | 98.6986 |
| MU | mica (mx) | 78 | 26.5898 | 0.0193 | 0.1930 | 12.8943 | 0.5141 | 0.9929 | 11.8178 | 25.0157 | 2.6996 | 9.9679 | 1.6308 | 1.0132 | 0.3870 | 0.0780 | 0.1257 | 3.7883 | 0.2702 | 98.0076 |
| MU | mica (mx) | 79 | 26.4793 | 0.0065 | 0.2331 | 12.7622 | 0.6747 | 1.0741 | 11.6031 | 24.3451 | 2.6075 | 9.7414 | 1.5286 | 0.9135 | 0.3687 | 0.1551 | 0.1230 | 5.1328 | 0.3061 | 98.0648 |
| MU | mica (mx) | 80 | 26.4141 | 0.0439 | 0.1965 | 12.7489 | 0.4375 | 1.0131 | 11.8825 | 25.4895 | 2.7252 | 10.1347 | 1.6485 | 0.9811 | 0.4413 | 0.0851 | 0.0593 | 2.9783 | 0.2858 | 97.5753 |
| MU | mica (mx) | 81 | 26.0429 | 0.0002 | 0.3281 | 12.3750 | 0.8396 | 1.0797 | 11.1686 | 23.1862 | 2.4790 | 9.3680 | 1.5150 | 0.9112 | 0.4189 | 0.1561 | 0.1856 | 6.8822 | 0.3185 | 97.2648 |
| MU | mica (mx) | 84 | 26.1489 | 0.0192 | 0.2567 | 12.5465 | 0.6376 | 1.0043 | 11.4238 | 24.1411 | 2.5217 | 9.8378 | 1.5802 | 0.9761 | 0.3180 | 0.1747 | 0.1208 | 5.0040 | 0.2624 | 96.9838 |
| MU | mica (mx) | 85 | 26.3238 | 0.0002 | 0.2646 | 12.6956 | 0.7123 | 1.0480 | 11.1026 | 23.7578 | 2.5715 | 9.6337 | 1.5803 | 0.9897 | 0.3432 | 0.1043 | 0.1601 | 5.7662 | 0.2862 | 97.3501 |
| MU | mica (mx) | 86 | 26.3772 | 0.0260 | 0.1744 | 12.6651 | 0.4054 | 0.9837 | 12.2096 | 25.5718 | 2.6953 | 10.4630 | 1.6826 | 1.0135 | 0.3957 | 0.1651 | 0.0966 | 2.9304 | 0.2390 | 98.1044 |
| MU | mica (mx) | 87 | 26.5433 | 0.0067 | 0.1687 | 12.9079 | 0.4033 | 0.9370 | 11.8957 | 25.6404 | 2.6808 | 10.3407 | 1.6721 | 0.9581 | 0.3166 | 0.0442 | 0.0705 | 2.8201 | 0.2303 | 97.6464 |
| MU | mica (mx) | 88 | 26.5840 | 0.0228 | 0.1666 | 12.9043 | 0.3069 | 0.9122 | 12.2846 | 26.2299 | 2.8114 | 10.2539 | 1.6636 | 0.9826 | 0.3611 | 0.0806 | 0.0443 | 2.0481 | 0.1572 | 97.8241 |
| MU | mica (mx) | 89 | 26.6580 | 0.0034 | 0.1736 | 12.9396 | 0.3101 | 0.9186 | 12.0394 | 26.0607 | 2.8438 | 10.4807 | 1.7594 | 1.0687 | 0.4379 | 0.1551 | 0.0566 | 2.0742 | 0.2271 | 98.2169 |
| MU | mica (mx) | 91 | 26.4764 | 0.0242 | 0.1870 | 12.8020 | 0.4327 | 0.9725 | 11.7222 | 25.3614 | 2.7535 | 10.2969 | 1.6374 | 0.9871 | 0.3997 | 0.1328 | 0.0959 | 3.2987 | 0.2489 | 97.8393 |
| MU | mica (mx) | 92 | 26.6166 | 0.0118 | 0.1522 | 12.9368 | 0.2774 | 0.9482 | 12.3230 | 26.1382 | 2.8275 | 10.6186 | 1.6190 | 1.0367 | 0.3684 | 0.0863 | 0.0649 | 1.8314 | 0.1543 | 98.0213 |
| MU | mica (mx) | 93 | 26.9660 | 0.0158 | 0.1666 | 13.1460 | 0.3963 | 1.0219 | 12.4860 | 25.8014 | 2.6633 | 10.1653 | 1.5697 | 1.0249 | 0.4077 | 0.0853 | 0.1090 | 2.7909 | 0.2511 | 99.0772 |
| MU | mica (mx) | 94 | 26.5351 | 0.0097 | 0.1543 | 12.8779 | 0.3661 | 1.0569 | 12.2603 | 25.6951 | 2.7466 | 10.1819 | 1.6543 | 1.1113 | 0.4414 | 0.1295 | 0.0690 | 2.4591 | 0.2348 | 97.9933 |
| MU | mica (mx) | 95 | 26.6225 | 0.0070 | 0.1452 | 12.9629 | 0.3755 | 1.0026 | 12.5778 | 25.9331 | 2.6872 | 10.0105 | 1.5454 | 0.8909 | 0.3325 | 0.1370 | 0.0800 | 2.4526 | 0.2031 | 97.9758 |
| MU | mica (mx) | 96 | 26.4787 | 0.0132 | 0.2809 | 12.7493 | 0.7214 | 1.1283 | 11.4324 | 23.8553 | 2.6004 | 9.5597 | 1.5173 | 1.0983 | 0.3508 | 0.1321 | 0.1149 | 5.5333 | 0.3560 | 97.9323 |
| MU | mica (mx) | 97 | 26.6124 | 0.0002 | 0.2736 | 12.8331 | 0.8054 | 1.1764 | 11.4551 | 23.3341 | 2.4693 | 9.5374 | 1.5198 | 1.0188 | 0.4539 | 0.1443 | 0.1742 | 6.3664 | 0.3448 | 98.5292 |
| MU | mica (mx) | 98 | 26.5332 | 0.0002 | 0.2264 | 12.8279 | 0.6152 | 1.0338 | 11.6753 | 24.5069 | 2.6515 | 9.6820 | 1.5914 | 1.0004 | 0.3918 | 0.0935 | 0.1381 | 4.7969 | 0.2728 | 98.0473 |
| MU | mica (mx) | 99 | 26.5674 | 0.0084 | 0.1430 | 12.9308 | 0.2955 | 0.9586 | 12.3662 | 25.9397 | 2.8223 | 10.5124 | 1.6600 | 0.9301 | 0.3185 | 0.0777 | 0.0681 | 2.0215 | 0.1670 | 97.7972 |
| MU | mica (mx) | 100 | 26.5945 | 0.0013 | 0.1601 | 12.9441 | 0.3619 | 0.9708 | 12.0601 | 25.6994 | 2.8369 | 10.3038 | 1.6093 | 1.0383 | 0.3447 | 0.1165 | 0.0880 | 2.5272 | 0.2219 | 97.8888 |
| MU | mica (mx) | 101 | 26.2804 | 0.0027 | 0.2100 | 12.6740 | 0.5923 | 1.1083 | 11.6101 | 24.4429 | 2.5863 | 9.8567 | 1.5799 | 1.0465 | 0.3914 | 0.1428 | 0.1042 | 4.5443 | 0.2815 | 97.4643 |
| MU | mica (mx) | 102 | 26.5101 | 0.0195 | 0.1644 | 12.8749 | 0.3308 | 0.8738 | 12.0245 | 25.8442 | 2.7079 | 10.4399 | 1.6126 | 1.0805 | 0.3799 | 0.0670 | 0.0842 | 2.3385 | 0.2079 | 97.5706 |
| MU | mica (mx) | 103 | 26.2021 | 0.0026 | 0.2836 | 12.5612 | 0.7605 | 1.0110 | 11.2817 | 23.4268 | 2.5460 | 9.5016 | 1.5824 | 1.0032 | 0.3419 | 0.1582 | 0.1504 | 6.1399 | 0.2872 | 97.2503 |
| MU | mica (mx) | 104 | 26.2450 | 0.0002 | 0.1938 | 12.5994 | 0.5463 | 1.0143 | 11.7143 | 24.7937 | 2.8229 | 10.0296 | 1.5760 | 1.0537 | 0.4512 | 0.1808 | 0.0905 | 4.1404 | 0.2426 | 97.7047 |
| MU | mica (mx) | 105 | 26.2896 | 0.0142 | 0.2148 | 12.6467 | 0.5815 | 1.0324 | 11.7577 | 24.6394 | 2.6449 | 9.8838 | 1.5872 | 0.9815 | 0.3927 | 0.0923 | 0.1189 | 4.3743 | 0.2633 | 97.5252 |
| MU | mica (mx) | 106 | 26.4877 | 0.0002 | 0.3220 | 12.6614 | 0.8763 | 1.0313 | 11.1236 | 23.0459 | 2.5169 | 9.3747 | 1.5745 | 1.0381 | 0.4460 | 0.1268 | 0.1885 | 7.3606 | 0.2932 | 98.4777 |
| MU | mica (mx) | 107 | 25.9296 | 0.0055 | 0.2063 | 12.3748 | 0.5587 | 0.9900 | 11.4717 | 24.7633 | 2.7300 | 10.1662 | 1.5685 | 1.0830 | 0.4048 | 0.1178 | 0.0870 | 4.1654 | 0.2460 | 96.8786 |
| MU | mica (mx) | 108 | 26.1889 | 0.0109 | 0.2732 | 12.5038 | 0.7489 | 1.0030 | 11.3540 | 23.8097 | 2.5730 | 9.5208 | 1.5402 | 1.0136 | 0.3942 | 0.0843 | 0.1654 | 6.0526 | 0.3099 | 97.5564 |
| MU | mica (mx) | 109 | 26.1934 | 0.0060 | 0.2235 | 12.5726 | 0.6543 | 0.9726 | 12.1921 | 24.2808 | 2.5034 | 9.3598 | 1.4327 | 0.9371 | 0.3682 | 0.1050 | 0.1365 | 5.0488 | 0.2955 | 97.2923 |
| MU | mica (mx) | 110 | 26.7029 | 0.0673 | 0.3064 | 12.8372 | 0.6843 | 0.9886 | 11.8888 | 24.0175 | 2.4785 | 9.5034 | 1.4910 | 1.0084 | 0.3958 | 0.0705 | 0.1280 | 5.4824 | 0.3416 | 98.4026 |
| MU | mica (mx) | 111 | 26.3870 | 0.0203 | 0.2159 | 12.6130 | 0.5306 | 1.0173 | 11.7869 | 25.2646 | 2.7766 | 10.3447 | 1.5844 | 1.0318 | 0.3809 | 0.0771 | 0.1129 | 3.9538 | 0.2519 | 98.3597 |
| MU | mica (mx) | 112 | 26.2788 | 0.0209 | 0.2294 | 12.5740 | 0.6763 | 1.0109 | 11.8612 | 24.4864 | 2.6444 | 9.6648 | 1.5243 | 0.9261 | 0.3153 | 0.0859 | 0.1382 | 5.0772 | 0.2632 | 97.7873 |
| MU | mica (mx) | 113 | 26.0914 | 0.0132 | 0.3281 | 12.3928 | 0.8822 | 1.0250 | 11.0973 | 22.7927 | 2.5411 | 9.3422 | 1.4548 | 0.9918 | 0.4335 | 0.2134 | 0.1846 | 7.3055 | 0.3111 | 97.4107 |
| MU | mica (mx) | 114 | 25.6383 | 0.0327 | 0.2128 | 12.2159 | 0.5382 | 0.9618 | 11.6406 | 24.7317 | 2.6663 | 9.8550 | 1.5227 | 0.9369 | 0.3746 | 0.0933 | 0.0895 | 3.9063 | 0.2640 | 95.6906 |
| MU | mica (mx) | 115 | 26.1974 | 0.0122 | 0.1961 | 12.6087 | 0.5369 | 0.9915 | 11.4271 | 24.8596 | 2.7854 | 9.9876 | 1.6231 | 1.0614 | 0.4246 | 0.0796 | 0.1394 | 4.0605 | 0.2397 | 97.2408 |
| TH | bt | 1 | 26.4996 | 0.0002 | 0.2168 | 12.6808 | 0.7893 | 1.5446 | 11.8060 | 24.7590 | 2.4293 | 9.4500 | 1.5326 | 1.1561 | 0.4897 | 0.0956 | 0.1350 | 5.0287 | 0.6281 | 99.2514 |
| TH | bt | 2 | 26.5637 | 0.0055 | 0.1714 | 12.8095 | 0.5894 | 1.4920 | 12.0144 | 25.4784 | 2.6084 | 9.6616 | 1.5898 | 1.1399 | 0.5056 | 0.1278 | 0.1306 | 3.6223 | 0.4825 | 99.0028 |
| TH | bt | 4 | 26.8452 | 0.0154 | 0.1815 | 12.9653 | 0.6155 | 1.5869 | 11.9498 | 25.4990 | 2.6270 | 9.6436 | 1.7347 | 1.1942 | 0.4728 | 0.0854 | 0.1404 | 3.8710 | 0.4940 | 99.9317 |
| TH | bt | 5 | 26.8721 | 0.0165 | 0.2378 | 12.9900 | 0.7913 | 1.7252 | 11.5672 | 24.3098 | 2.4486 | 9.3869 | 1.5449 | 1.2112 | 0.4822 | 0.1683 | 0.2034 | 5.2414 | 0.6656 | 99.8724 |
| TH | bt | 8 | 26.8089 | 0.0015 | 0.1994 | 12.9833 | 0.6990 | 1.7178 | 11.9033 | 24.7669 | 2.5203 | 9.5085 | 1.6009 | 1.1156 | 0.5447 | 0.1752 | 0.1682 | 4.2786 | 0.6770 | 99.6791 |
| TH | bt | 9 | 26.5947 | 0.0002 | 0.2137 | 12.8767 | 0.7058 | 1.5954 | 11.6183 | 24.5002 | 2.3911 | 9.3826 | 1.4699 | 1.2935 | 0.4906 | 0.1197 | 0.1673 | 4.7492 | 0.5900 | 98.7689 |
| TH | bt | 10 | 26.4994 | 0.0002 | 0.1700 | 12.7879 | 0.5750 | 1.6163 | 11.8897 | 25.3792 | 2.4868 | 9.7654 | 1.6257 | 1.2095 | 0.4701 | 0.1263 | 0.1487 | 3.6545 | 0.4878 | 98.9025 |
| TH | bt | 11 | 26.5030 | 0.0139 | 0.1762 | 12.7570 | 0.5724 | 1.4141 | 11.7762 | 25.3806 | 2.6702 | 9.7660 | 1.7120 | 1.1822 | 0.5527 | 0.1840 | 0.1062 | 3.5604 | 0.4847 | 98.8218 |
| TH | bt | 12 | 26.2671 | 0.0003 | 0.1902 | 12.6533 | 0.6441 | 1.5657 | 11.6827 | 24.7031 | 2.4280 | 9.6843 | 1.6860 | 1.1804 | 0.5069 | 0.0691 | 0.1434 | 4.0170 | 0.5927 | 98.0243 |
| TH | bt | 13 | 26.2385 | 0.0054 | 0.1669 | 12.6795 | 0.5239 | 1.5482 | 11.8613 | 25.1201 | 2.5494 | 9.6261 | 1.6194 | 1.1544 | 0.5192 | 0.1357 | 0.0861 | 3.3634 | 0.5337 | 97.7412 |
| TH | bt | 14 | 26.5593 | 0.0142 | 0.1980 | 12.8448 | 0.6420 | 1.4764 | 11.6980 | 24.6681 | 2.6529 | 9.5686 | 1.5919 | 1.2040 | 0.4467 | 0.1245 | 0.1319 | 4.2810 | 0.4849 | 98.5972 |
| TH | bt | 16 | 26.9174 | 0.0448 | 0.2435 | 13.0665 | 0.6000 | 1.5389 | 11.9080 | 25.0730 | 2.6143 | 9.5500 | 1.5772 | 1.1528 | 0.4733 | 0.1344 | 0.1279 | 3.6321 | 0.5463 | 99.2104 |
| TH | bt | 17 | 26.2812 | 0.0153 | 0.1664 | 12.6506 | 0.5371 | 1.5318 | 11.8120 | 25.3219 | 2.6634 | 9.7906 | 1.7288 | 1.1527 | 0.4450 | 0.1293 | 0.0869 | 3.2888 | 0.5229 | 98.1347 |

| Sample | Phase | Label | W%(O) | W%(Al) | W%(Si) | W%(P) | W%(Ca) | W%(Y) | W%(La) | W%(Ce) | W%(Pr) | W%(Nd) | W%(Sm) | W%(Gd) | W%(Dy) | W%(Er) | W%(Pb) | W%(Th) | W%(U) | W%(SUM) |
|---|---|---|---|---|---|---|---|---|---|---|---|---|---|---|---|---|---|---|---|---|
| TH | bt | 18 | 26.4044 | 0.0002 | 0.1808 | 12.7388 | 0.5782 | 1.5719 | 11.9369 | 25.1959 | 2.5142 | 9.6565 | 1.6012 | 1.1169 | 0.5338 | 0.1296 | 0.1471 | 3.5685 | 0.5762 | 98.4611 |
| TH | bt | 19 | 26.8449 | 0.0085 | 0.1751 | 13.1039 | 0.5573 | 1.6882 | 12.0124 | 25.1523 | 2.5204 | 9.4593 | 1.6900 | 1.2716 | 0.5182 | 0.0560 | 0.1462 | 3.3714 | 0.6122 | 99.1979 |
| TH | bt | 20 | 26.5769 | 0.0038 | 0.1890 | 12.9118 | 0.6003 | 1.6841 | 11.7897 | 24.8134 | 2.4273 | 9.5828 | 1.6001 | 1.1892 | 0.4914 | 0.1616 | 0.1449 | 3.8079 | 0.6030 | 98.5872 |
| TH | bt | 22 | 26.6005 | 0.0461 | 0.2371 | 12.8811 | 0.7530 | 1.6563 | 11.4323 | 23.9153 | 2.5107 | 9.2323 | 1.6033 | 1.1282 | 0.5738 | 0.1619 | 0.1868 | 4.8605 | 0.7350 | 98.5242 |
| TH | bt | 24 | 26.6675 | 0.0056 | 0.1866 | 12.9573 | 0.6434 | 1.6759 | 11.5807 | 24.7377 | 2.4849 | 9.4839 | 1.6526 | 1.2547 | 0.4677 | 0.1772 | 0.1781 | 4.1453 | 0.6427 | 98.9518 |
| TH | bt | 26 | 26.6203 | 0.1352 | 0.4602 | 12.7002 | 0.7750 | 1.6461 | 11.4029 | 23.7310 | 2.4194 | 9.4296 | 1.6313 | 1.1842 | 0.4554 | 0.1489 | 0.1719 | 4.4434 | 0.7018 | 98.0668 |
| TH | bt | 27 | 26.4090 | 0.0050 | 0.1865 | 12.7477 | 0.6803 | 1.6103 | 11.6996 | 24.6411 | 2.5674 | 9.5189 | 1.5957 | 1.2567 | 0.4838 | 0.1363 | 0.1427 | 4.0644 | 0.6452 | 98.4006 |
| TH | bt | 28 | 26.2825 | 0.0173 | 0.1858 | 12.6428 | 0.5581 | 1.5480 | 11.8380 | 24.8010 | 2.6566 | 9.8352 | 1.6621 | 1.2003 | 0.5042 | 0.1700 | 0.1319 | 3.5961 | 0.5262 | 98.1661 |
| TH | bt | 29 | 26.6258 | 0.0090 | 0.2031 | 12.8972 | 0.6885 | 1.4462 | 11.7445 | 24.5495 | 2.6058 | 9.4699 | 1.5564 | 1.1756 | 0.4667 | 0.1587 | 0.1532 | 4.3616 | 0.5238 | 98.6455 |
| TH | bt | 30 | 26.2434 | 0.0074 | 0.2012 | 12.6395 | 0.6643 | 1.6841 | 11.6033 | 24.2970 | 2.5453 | 9.5836 | 1.5840 | 1.2132 | 0.5227 | 0.1071 | 0.1182 | 4.3233 | 0.6703 | 98.0179 |
| TH | bt | 31 | 26.0187 | 0.0143 | 0.1918 | 12.5008 | 0.6720 | 1.4800 | 12.0073 | 24.2598 | 2.4619 | 9.0694 | 1.5605 | 1.1319 | 0.5021 | 0.1900 | 0.1179 | 4.3633 | 0.6256 | 97.1773 |
| TH | bt | 32 | 26.0929 | 0.0548 | 0.2825 | 12.4349 | 0.7010 | 1.6363 | 11.7649 | 24.1084 | 2.5627 | 9.5142 | 1.6718 | 1.2070 | 0.4778 | 0.1515 | 0.1514 | 4.0671 | 0.6501 | 97.5393 |
| TH | bt | 34 | 26.4300 | 0.0024 | 0.2256 | 12.7460 | 0.7476 | 1.6713 | 11.6787 | 23.9507 | 2.5398 | 9.4650 | 1.5992 | 1.1810 | 0.4455 | 0.1716 | 0.1672 | 4.7268 | 0.7045 | 98.4629 |
| TH | bt | 35 | 26.1382 | 0.0002 | 0.2014 | 12.5773 | 0.7709 | 1.7037 | 11.5072 | 23.9608 | 2.4979 | 8.9887 | 1.6426 | 1.2244 | 0.4811 | 0.1129 | 0.1769 | 5.0574 | 0.7332 | 97.7848 |
| TH | bt | 36 | 26.2168 | 0.0002 | 0.2220 | 12.6005 | 0.7461 | 1.6464 | 11.5806 | 24.0592 | 2.4820 | 9.2421 | 1.5787 | 1.1889 | 0.4873 | 0.1319 | 0.1443 | 4.9355 | 0.7142 | 97.9867 |
| TH | bt | 37 | 26.1876 | 0.0036 | 0.1921 | 12.5614 | 0.6657 | 1.4322 | 12.3358 | 24.5894 | 2.5224 | 9.1554 | 1.5271 | 1.1317 | 0.4066 | 0.0547 | 0.1542 | 4.4169 | 0.5752 | 97.9220 |
| TH | bt-fsp | 1 | 26.4550 | 0.0002 | 0.2130 | 12.6414 | 0.7532 | 1.4088 | 11.8067 | 24.6725 | 2.5586 | 9.6280 | 1.6723 | 1.1544 | 0.4857 | 0.1770 | 0.1222 | 4.8303 | 0.5038 | 99.0931 |
| TH | bt-fsp | 2 | 26.3932 | 0.0047 | 0.2121 | 12.6103 | 0.7110 | 1.5107 | 12.1399 | 24.7469 | 2.5389 | 9.5215 | 1.5332 | 1.1365 | 0.5010 | 0.0651 | 0.1525 | 4.6956 | 0.4878 | 98.9709 |
| TH | bt-fsp | 3 | 26.1948 | 0.1343 | 0.5801 | 12.2007 | 0.9228 | 1.2892 | 11.8046 | 23.7059 | 2.5409 | 9.1829 | 1.4768 | 1.1576 | 0.4447 | 0.1374 | 0.1601 | 4.7136 | 0.5208 | 97.1772 |
| TH | bt-fsp | 4 | 25.7781 | 0.0163 | 0.3093 | 12.2252 | 0.8117 | 1.5456 | 11.5235 | 23.8584 | 2.5435 | 9.4246 | 1.5577 | 1.1673 | 0.4790 | 0.1633 | 0.1447 | 4.4877 | 0.5237 | 96.5696 |
| TH | bt-fsp | 5 | 26.0789 | 0.0236 | 0.2781 | 12.4176 | 0.7508 | 1.4929 | 11.7825 | 24.3226 | 2.4390 | 9.5222 | 1.5739 | 1.1799 | 0.4691 | 0.1264 | 0.1701 | 4.3515 | 0.5397 | 97.5288 |
| TH | bt-fsp | 6 | 26.6288 | 0.0012 | 0.2050 | 12.8241 | 0.7069 | 1.5677 | 12.0265 | 24.5025 | 2.5155 | 9.5292 | 1.5956 | 1.1931 | 0.5417 | 0.1866 | 0.1563 | 4.6232 | 0.5190 | 99.3329 |
| TH | bt-fsp | 7 | 26.4403 | 0.0291 | 0.2215 | 12.6794 | 0.7261 | 1.5546 | 12.1569 | 24.5471 | 2.4968 | 9.4942 | 1.4801 | 1.1113 | 0.5046 | 0.1921 | 0.1088 | 4.3610 | 0.5293 | 98.6432 |
| TH | bt-fsp | 8 | 26.2004 | 0.0138 | 0.3305 | 12.4057 | 0.8936 | 1.5349 | 11.6415 | 23.5568 | 2.5613 | 9.1318 | 1.4618 | 1.1955 | 0.4816 | 0.1778 | 0.1887 | 5.9615 | 0.6245 | 98.3717 |
| TH | bt-fsp | 9 | 25.9704 | 0.0156 | 0.2712 | 12.3027 | 0.7552 | 1.5414 | 11.6148 | 24.2009 | 2.5428 | 9.4697 | 1.5620 | 1.2243 | 0.4471 | 0.1243 | 0.1582 | 5.0128 | 0.5577 | 97.7811 |
| TH | bt-fsp | 10 | 26.2722 | 0.0018 | 0.1897 | 12.5897 | 0.6928 | 1.4259 | 11.7579 | 24.8647 | 2.4920 | 9.6782 | 1.5932 | 1.1862 | 0.4301 | 0.1194 | 0.1300 | 4.3790 | 0.4844 | 98.2972 |
| TH | bt-fsp | 11 | 26.2470 | 0.0032 | 0.2199 | 12.5134 | 0.7694 | 1.5665 | 11.6964 | 24.5325 | 2.5684 | 9.5726 | 1.6186 | 1.1151 | 0.5391 | 0.1534 | 0.1413 | 4.8114 | 0.5199 | 98.5981 |
| TH | bt-fsp | 12 | 26.3359 | 0.0107 | 0.2113 | 12.5990 | 0.6533 | 1.5179 | 12.1965 | 25.0639 | 2.4316 | 9.4498 | 1.4581 | 1.1336 | 0.5052 | 0.1217 | 0.1247 | 4.2538 | 0.5538 | 98.6308 |
| TH | bt-fsp | 13 | 26.7235 | 0.2043 | 0.5493 | 12.5702 | 0.6715 | 1.5188 | 12.0517 | 24.4997 | 2.4749 | 9.1941 | 1.4722 | 1.1056 | 0.5075 | 0.1743 | 0.1144 | 4.3708 | 0.5227 | 98.7355 |
| TH | bt-fsp | 14 | 26.3296 | 0.0369 | 0.2696 | 12.5360 | 0.7536 | 1.4767 | 11.7199 | 24.6618 | 2.4420 | 9.3773 | 1.6455 | 1.1850 | 0.4814 | 0.1655 | 0.1288 | 4.7556 | 0.5302 | 98.5054 |
| TH | bt-fsp | 15 | 26.3957 | 0.0189 | 0.3000 | 12.6118 | 0.7757 | 1.5378 | 11.9980 | 24.3426 | 2.3998 | 9.1708 | 1.5548 | 1.0851 | 0.4839 | 0.0768 | 0.1427 | 4.9764 | 0.5262 | 98.4070 |
| TH | bt-fsp | 16 | 26.3427 | 0.0002 | 0.2014 | 12.5675 | 0.6356 | 1.5434 | 12.0139 | 25.2286 | 2.6104 | 9.6072 | 1.6490 | 1.1518 | 0.4352 | 0.1716 | 0.1507 | 4.1992 | 0.5340 | 99.0524 |
| TH | bt-fsp | 17 | 27.2111 | 0.8621 | 1.9756 | 11.5337 | 0.9300 | 1.3095 | 11.8493 | 22.7513 | 2.2541 | 8.3545 | 1.2987 | 1.0153 | 0.4173 | 0.0856 | 0.1615 | 4.9342 | 0.6031 | 97.5569 |
| TH | bt-fsp | 18 | 26.9170 | 0.4847 | 0.9400 | 12.3815 | 0.6651 | 1.4201 | 11.4950 | 23.9647 | 2.3769 | 9.4143 | 1.4881 | 1.1213 | 0.4409 | 0.1403 | 0.0911 | 3.8769 | 0.4693 | 97.6972 |
| TH | bt-fsp | 20 | 26.6490 | 0.0231 | 0.2354 | 12.7773 | 0.7213 | 1.6597 | 11.7244 | 24.8593 | 2.4625 | 9.7063 | 1.6447 | 1.1604 | 0.4697 | 0.2074 | 0.1680 | 4.5925 | 0.5152 | 99.5862 |
| TH | bt-fsp | 21 | 25.9247 | 0.2457 | 1.0836 | 11.7139 | 1.1642 | 1.6231 | 11.3399 | 21.8069 | 2.3566 | 8.8751 | 1.4186 | 1.2068 | 0.4408 | 0.2170 | 0.1695 | 5.0641 | 0.6650 | 95.3255 |
| TH | bt-fsp | 23 | 26.7994 | 0.1152 | 0.5274 | 12.6884 | 0.7166 | 1.4567 | 12.4790 | 24.6750 | 2.5219 | 9.5287 | 1.5481 | 1.0129 | 0.4009 | 0.0911 | 0.1194 | 3.4778 | 0.4822 | 98.6507 |
| TH | bt-fsp | 24 | 26.6688 | 0.0552 | 0.3445 | 12.6604 | 0.7227 | 1.6166 | 11.8980 | 24.8657 | 2.4765 | 9.6913 | 1.5716 | 1.2510 | 0.5311 | 0.1431 | 0.1631 | 4.4526 | 0.5461 | 99.6683 |
| TH | bt-fsp | 25 | 26.3449 | 0.0042 | 0.2316 | 12.6091 | 0.7840 | 1.6887 | 11.4601 | 24.3907 | 2.4769 | 9.5312 | 1.6552 | 1.2156 | 0.5289 | 0.1191 | 0.1359 | 4.9455 | 0.5867 | 98.7183 |
| TH | bt-fsp | 26 | 26.4845 | 0.0101 | 0.2142 | 12.7153 | 0.7112 | 1.5151 | 11.9573 | 24.8024 | 2.5564 | 9.3917 | 1.5646 | 1.1427 | 0.4614 | 0.1621 | 0.1731 | 4.5131 | 0.4779 | 98.8631 |
| TH | bt-fsp | 27 | 26.5315 | 0.0094 | 0.1948 | 12.7334 | 0.6789 | 1.4943 | 11.8795 | 25.1606 | 2.4961 | 9.6680 | 1.7139 | 1.2141 | 0.5110 | 0.0869 | 0.1277 | 4.1828 | 0.4300 | 99.1229 |
| TH | bt-fsp | 28 | 26.6955 | 0.0002 | 0.1870 | 12.8654 | 0.6111 | 1.5632 | 11.9846 | 25.0640 | 2.5610 | 9.8932 | 1.6886 | 1.3233 | 0.5159 | 0.1080 | 0.1211 | 3.8885 | 0.5209 | 99.6015 |
| TH | bt-fsp | 29 | 26.4853 | 0.0002 | 0.1834 | 12.7611 | 0.6443 | 1.6454 | 12.0143 | 24.9611 | 2.5437 | 9.5302 | 1.5888 | 1.2037 | 0.5186 | 0.1124 | 0.1256 | 4.0398 | 0.5432 | 98.9111 |
| TH | bt-fsp | 30 | 26.4884 | 0.1813 | 0.5218 | 12.5936 | 0.6313 | 1.4130 | 11.9232 | 24.3266 | 2.4735 | 9.1143 | 1.4423 | 1.1099 | 0.4352 | 0.1352 | 0.0887 | 3.5721 | 0.5258 | 96.9862 |
| TH | bt-fsp | 31 | 26.6915 | 0.0204 | 0.1732 | 12.8876 | 0.5946 | 1.4680 | 12.8791 | 25.5476 | 2.5557 | 9.0512 | 1.5010 | 1.0814 | 0.5167 | 0.1501 | 0.1345 | 3.4106 | 0.5274 | 99.2006 |
| TH | bt-fsp | 32 | 26.6801 | 0.0200 | 0.1702 | 12.8940 | 0.6339 | 1.4795 | 12.6972 | 25.2181 | 2.4704 | 9.3015 | 1.4845 | 1.0807 | 0.4849 | 0.1311 | 0.1084 | 3.6846 | 0.5524 | 99.1015 |
| TH | bt-fsp | 33 | 26.2853 | 0.0098 | 0.1849 | 12.6040 | 0.6139 | 1.4996 | 11.9338 | 25.1170 | 2.5823 | 9.7767 | 1.6177 | 1.1558 | 0.4508 | 0.1063 | 0.1370 | 3.7823 | 0.4886 | 98.3558 |
| TH | bt-fsp | 34 | 26.5269 | 0.0018 | 0.2076 | 12.6968 | 0.6930 | 1.5494 | 11.9838 | 24.9808 | 2.4878 | 9.8569 | 1.6181 | 1.2207 | 0.5058 | 0.1060 | 0.1516 | 4.3000 | 0.4765 | 99.3735 |
| TH | bt-fsp | 35 | 26.7584 | 0.0002 | 0.1897 | 12.8900 | 0.7014 | 1.5167 | 12.7053 | 25.3495 | 2.4188 | 9.1504 | 1.5094 | 1.1218 | 0.4876 | 0.1209 | 0.1375 | 4.0367 | 0.5676 | 99.6719 |
| TH | bt-fsp | 36 | 26.5688 | 0.0705 | 0.3064 | 12.7134 | 0.6255 | 1.4879 | 12.6409 | 25.2818 | 2.5236 | 9.0734 | 1.3512 | 0.9918 | 0.4149 | 0.2028 | 0.1129 | 3.5658 | 0.5810 | 98.5226 |
| TH | bt-fsp | 37 | 26.7066 | 0.0809 | 0.4303 | 12.7814 | 0.9998 | 1.8819 | 10.8576 | 22.8475 | 2.3495 | 9.0686 | 1.5246 | 1.2709 | 0.5089 | 0.1333 | 0.1984 | 6.4596 | 0.7742 | 98.8840 |
| TH | bt-fsp | 38 | 26.2762 | 0.0694 | 0.6722 | 12.3532 | 0.9816 | 1.5804 | 11.3232 | 22.6092 | 2.4251 | 9.1667 | 1.5974 | 1.1747 | 0.4961 | 0.1307 | 0.1796 | 5.1430 | 0.6543 | 96.8430 |
| TH | bt-fsp | 39 | 26.3358 | 0.0326 | 0.3013 | 12.5472 | 0.8279 | 1.6600 | 11.4324 | 24.0080 | 2.4549 | 9.5114 | 1.5346 | 1.1373 | 0.5252 | 0.1512 | 0.1991 | 5.2277 | 0.6558 | 98.5524 |
| TH | bt-fsp | 40 | 26.4811 | 0.0952 | 0.4085 | 12.5364 | 0.7580 | 1.4409 | 11.5991 | 24.2934 | 2.4609 | 9.7933 | 1.5857 | 1.0774 | 0.5119 | 0.1567 | 0.1474 | 4.6337 | 0.4458 | 98.4354 |
| TH | bt-fsp | 41 | 26.7108 | 0.0217 | 0.3791 | 12.8456 | 0.8688 | 1.6249 | 11.4877 | 23.6944 | 2.5015 | 9.2346 | 1.6122 | 1.1408 | 0.4059 | 0.1341 | 0.1455 | 5.2044 | 0.5900 | 98.6120 |
| TH | bt-fsp | 43 | 26.7669 | 0.0295 | 0.2544 | 12.9147 | 0.7657 | 1.5849 | 11.6097 | 24.4257 | 2.6130 | 9.5929 | 1.5785 | 1.1490 | 0.5213 | 0.1462 | 0.1279 | 4.6003 | 0.5028 | 99.1934 |

| Sample | Phase | Label | W%(O) | W%(Al) | W%(Si) | W%(P) | W%(Ca) | W%(Y) | W%(La) | W%(Ce) | W%(Pr) | W%(Nd) | W%(Sm) | W%(Gd) | W%(Dy) | W%(Er) | W%(Pb) | W%(Th) | W%(U) | W%(SUM) |
|---|---|---|---|---|---|---|---|---|---|---|---|---|---|---|---|---|---|---|---|---|
| TH | bt-fsp | 44 | 26.6079 | 0.0002 | 0.2028 | 12.8510 | 0.7257 | 1.4468 | 11.7405 | 24.6029 | 2.5988 | 9.5154 | 1.6435 | 1.1409 | 0.5058 | 0.1125 | 0.1075 | 4.5304 | 0.4706 | 98.8132 |
| TH | bt-fsp | 45 | 26.3693 | 0.0016 | 0.4125 | 12.5898 | 1.0788 | 1.8092 | 10.6399 | 22.3901 | 2.4049 | 9.0568 | 1.4951 | 1.2569 | 0.5073 | 0.1510 | 0.2292 | 6.9635 | 0.8525 | 98.2184 |
| TH | bt-fsp | 46 | 26.2359 | 0.0563 | 0.6253 | 12.4036 | 1.0123 | 1.6132 | 11.1736 | 22.5987 | 2.3729 | 8.9059 | 1.4994 | 1.1378 | 0.4417 | 0.1413 | 0.1928 | 5.5279 | 0.6622 | 96.6108 |
| TH | bt-fsp | 47 | 26.4893 | 0.0194 | 0.2719 | 12.7878 | 0.6793 | 1.6149 | 11.4579 | 24.6368 | 2.5853 | 9.5348 | 1.6140 | 1.1428 | 0.5270 | 0.1336 | 0.1141 | 3.9539 | 0.5079 | 98.0807 |
| TH | bt-fsp | 48 | 26.4809 | 0.0232 | 0.2738 | 12.6855 | 0.6639 | 1.4385 | 11.7903 | 24.6925 | 2.6316 | 9.7213 | 1.6325 | 1.2166 | 0.4712 | 0.1590 | 0.1373 | 4.0253 | 0.4876 | 98.5410 |
| TH | bt-fsp | 49 | 26.5990 | 0.0027 | 0.2044 | 12.8942 | 0.6935 | 1.4045 | 11.7998 | 24.6210 | 2.4753 | 9.5819 | 1.6857 | 1.0596 | 0.4431 | 0.0882 | 0.1010 | 4.2250 | 0.4839 | 98.3728 |
| TH | bt-fsp | 50 | 26.6079 | 0.0030 | 0.2388 | 12.8727 | 0.7496 | 1.3971 | 11.7117 | 24.3136 | 2.5236 | 9.6182 | 1.5249 | 1.1122 | 0.5421 | 0.0846 | 0.1140 | 4.4363 | 0.4965 | 98.3568 |
| TH | bt-fsp | 51 | 26.7327 | 0.1071 | 0.4223 | 12.9142 | 0.7119 | 1.3215 | 11.4061 | 23.8298 | 2.5535 | 9.3574 | 1.4991 | 1.0061 | 0.4715 | 0.1061 | 0.1588 | 4.3941 | 0.4123 | 97.4145 |
| TH | Kfsp | 52 | 26.7035 | 0.0093 | 0.2301 | 12.9587 | 0.8537 | 1.8257 | 11.3362 | 23.6418 | 2.5201 | 9.1862 | 1.6081 | 1.1687 | 0.5234 | 0.1596 | 0.1981 | 5.4506 | 0.6708 | 99.0546 |
| TH | Kfsp | 53 | 26.7081 | 0.0002 | 0.2281 | 12.9486 | 0.8832 | 1.7639 | 11.3019 | 23.7592 | 2.4073 | 9.2696 | 1.5537 | 1.2693 | 0.5573 | 0.1839 | 0.1963 | 5.3959 | 0.6696 | 99.1061 |
| TH | Kfsp | 54 | 26.8818 | 0.0065 | 0.1988 | 13.1219 | 0.6928 | 1.6191 | 11.8118 | 24.3494 | 2.4686 | 9.5824 | 1.5261 | 1.2032 | 0.4692 | 0.1744 | 0.1108 | 4.3394 | 0.5466 | 99.1128 |
| TH | Kfsp | 55 | 26.7187 | 0.0241 | 0.2075 | 12.9572 | 0.7444 | 1.5658 | 11.6565 | 24.1260 | 2.4319 | 9.5845 | 1.6671 | 1.2383 | 0.5292 | 0.0864 | 0.1905 | 4.6599 | 0.5458 | 98.9438 |
| TH | Kfsp | 56 | 26.8599 | 0.0193 | 0.2719 | 13.0580 | 0.6866 | 1.4710 | 11.8779 | 24.4563 | 2.6184 | 9.4857 | 1.5506 | 1.1279 | 0.4362 | 0.1711 | 0.1196 | 3.9817 | 0.4777 | 98.6798 |
| TH | Kfsp | 57 | 26.8645 | 0.0075 | 0.2185 | 13.0516 | 0.7523 | 1.4602 | 11.7413 | 24.3383 | 2.4992 | 9.5942 | 1.5586 | 1.0581 | 0.4383 | 0.1402 | 0.1829 | 4.7643 | 0.5123 | 99.1923 |
| TH | Kfsp | 58 | 26.5951 | 0.0154 | 0.2385 | 12.8475 | 0.8197 | 1.4558 | 11.4316 | 23.7374 | 2.5194 | 9.4949 | 1.5524 | 1.0792 | 0.4795 | 0.1871 | 0.1744 | 5.3672 | 0.5835 | 98.5886 |
| TH | Kfsp | 59 | 26.9718 | 0.0116 | 0.1839 | 13.1409 | 0.6716 | 1.5794 | 11.7893 | 24.8482 | 2.6203 | 9.6328 | 1.5500 | 1.1896 | 0.5250 | 0.1007 | 0.1401 | 4.1511 | 0.5075 | 99.6238 |
| TH | Kfsp | 60 | 26.6940 | 0.0043 | 0.2083 | 12.9567 | 0.7421 | 1.6688 | 11.5795 | 24.1208 | 2.5268 | 9.5201 | 1.6380 | 1.2007 | 0.4943 | 0.1220 | 0.1447 | 4.7641 | 0.5603 | 98.9555 |
| TH | Kfsp | 62 | 26.3939 | 0.0045 | 0.2783 | 12.6793 | 1.0033 | 1.8228 | 10.8360 | 22.4395 | 2.5003 | 9.2694 | 1.6332 | 1.2277 | 0.5842 | 0.1714 | 0.2198 | 6.8008 | 0.7539 | 98.6283 |
| TH | Kfsp | 63 | 26.5834 | 0.0092 | 0.2934 | 12.8641 | 1.1012 | 1.8549 | 10.6928 | 21.8992 | 2.2662 | 8.9698 | 1.6174 | 1.2436 | 0.5852 | 0.1719 | 0.2325 | 7.3595 | 0.8974 | 98.6517 |
| TH | Kfsp | 64 | 26.5795 | 0.0002 | 0.2708 | 12.8557 | 1.0191 | 1.7942 | 10.8298 | 22.6098 | 2.3648 | 9.1183 | 1.6061 | 1.1714 | 0.6113 | 0.1526 | 0.2332 | 6.6869 | 0.8304 | 98.7441 |
| TH | Kfsp | 65 | 26.7233 | 0.0035 | 0.2107 | 12.9543 | 0.7918 | 1.4990 | 11.6064 | 24.1887 | 2.5674 | 9.7371 | 1.5410 | 1.1409 | 0.4601 | 0.1644 | 0.1514 | 4.6190 | 0.5177 | 98.8867 |
| TH | Kfsp | 66 | 26.5769 | 0.0053 | 0.2648 | 12.7965 | 0.9779 | 1.7367 | 11.0171 | 23.1025 | 2.3908 | 9.2035 | 1.6374 | 1.2382 | 0.5038 | 0.1472 | 0.1964 | 6.5102 | 0.7261 | 99.0413 |
| TH | Kfsp | 67 | 26.4887 | 0.0172 | 0.3237 | 12.7405 | 1.1420 | 1.8883 | 10.5086 | 22.0493 | 2.2513 | 9.0066 | 1.4604 | 1.2496 | 0.4817 | 0.1802 | 0.2763 | 7.6915 | 0.8859 | 98.6518 |
| TH | Kfsp | 68 | 26.4749 | 0.0083 | 0.3178 | 12.7159 | 1.2030 | 1.7580 | 10.4949 | 21.9005 | 2.2373 | 8.7497 | 1.5238 | 1.1447 | 0.5465 | 0.1913 | 0.2951 | 8.1713 | 0.9488 | 98.6918 |
| TH | Kfsp | 69 | 26.5103 | 0.0007 | 0.2209 | 12.7909 | 0.8028 | 1.5973 | 11.4656 | 24.0489 | 2.5208 | 9.3596 | 1.5310 | 1.1531 | 0.4700 | 0.1845 | 0.1748 | 5.2278 | 0.6132 | 98.6822 |
| TH | Kfsp | 70 | 26.7442 | 0.0086 | 0.2285 | 12.9480 | 0.7397 | 1.5567 | 11.5275 | 24.2335 | 2.5182 | 9.6701 | 1.5823 | 1.1468 | 0.4888 | 0.1545 | 0.1585 | 4.8830 | 0.5415 | 99.1404 |
| TH | Kfsp | 71 | 26.7888 | 0.0243 | 0.2753 | 12.9243 | 0.9864 | 1.6515 | 11.1692 | 23.1542 | 2.3396 | 9.1000 | 1.6034 | 1.2387 | 0.5268 | 0.1789 | 0.1796 | 6.4867 | 0.7814 | 99.4191 |
| TH | Kfsp | 73 | 26.4850 | 0.0020 | 0.2492 | 12.7615 | 0.9094 | 1.8075 | 11.1217 | 23.0918 | 2.4878 | 9.4090 | 1.5844 | 1.1914 | 0.5406 | 0.2020 | 0.1809 | 6.0652 | 0.7198 | 98.8192 |
| TH | Kfsp | 74 | 26.3007 | 0.0019 | 0.2658 | 12.6895 | 0.9724 | 1.6098 | 10.9366 | 22.8305 | 2.4326 | 9.0422 | 1.5291 | 1.1536 | 0.5390 | 0.1032 | 0.2107 | 6.3458 | 0.7196 | 97.6930 |
| TH | Kfsp | 75 | 26.4319 | 0.0002 | 0.2484 | 12.7021 | 0.8794 | 1.6484 | 11.2966 | 23.6233 | 2.4238 | 9.3523 | 1.6197 | 1.1573 | 0.4718 | 0.1588 | 0.1880 | 5.7804 | 0.6593 | 98.6517 |
| TH | Kfsp | 76 | 26.5097 | 0.0002 | 0.2357 | 12.7926 | 0.7858 | 1.5729 | 11.4845 | 23.7983 | 2.5331 | 9.4674 | 1.6251 | 1.1842 | 0.5141 | 0.1991 | 0.1673 | 5.1142 | 0.5783 | 98.5725 |
| TH | Kfsp | 77 | 26.5990 | 0.0036 | 0.2454 | 12.8153 | 0.8303 | 1.5443 | 11.4634 | 23.9429 | 2.4948 | 9.4557 | 1.6318 | 1.1575 | 0.5177 | 0.1454 | 0.1912 | 5.2576 | 0.6083 | 98.9142 |
| TH | Kfsp | 78 | 26.5122 | 0.0002 | 0.2014 | 12.8309 | 0.7077 | 1.4426 | 11.6797 | 24.4788 | 2.4712 | 9.6492 | 1.5409 | 1.2143 | 0.5153 | 0.1302 | 0.1227 | 4.3156 | 0.4687 | 98.2916 |
| TH | Kfsp | 79 | 26.4987 | 0.0157 | 0.2936 | 12.7146 | 0.9111 | 1.5707 | 11.2842 | 23.4863 | 2.4355 | 9.0886 | 1.5977 | 1.2601 | 0.4370 | 0.2005 | 0.1832 | 5.9713 | 0.6688 | 98.6276 |
| TH | Kfsp | 80 | 26.5208 | 0.0002 | 0.2184 | 12.8382 | 0.7168 | 1.5359 | 11.5049 | 24.2769 | 2.5266 | 9.6128 | 1.5363 | 1.2265 | 0.4955 | 0.1485 | 0.1572 | 4.5039 | 0.5295 | 98.3589 |
| TH | Kfsp | 81 | 26.3627 | 0.0062 | 0.2044 | 12.6779 | 0.6645 | 1.4929 | 11.7842 | 24.7692 | 2.5486 | 9.6795 | 1.6231 | 1.1000 | 0.4070 | 0.1402 | 0.1563 | 4.2065 | 0.4831 | 98.3163 |
| TH | Kfsp | 82 | 26.5038 | 0.0103 | 0.2047 | 12.7771 | 0.6994 | 1.3312 | 11.8446 | 24.5793 | 2.5161 | 9.3549 | 1.6766 | 1.1988 | 0.4143 | 0.1597 | 0.1673 | 4.5419 | 0.5001 | 98.4901 |
| TH | Kfsp | 83 | 26.2796 | 0.0043 | 0.2603 | 12.5983 | 0.9243 | 1.7311 | 10.9263 | 23.3164 | 2.4108 | 9.3042 | 1.5745 | 1.2059 | 0.5619 | 0.1872 | 0.1892 | 6.1608 | 0.6831 | 98.3282 |
| TH | Kfsp | 84 | 26.3095 | 0.0002 | 0.2220 | 12.6792 | 0.6888 | 1.6101 | 11.4013 | 24.2097 | 2.5641 | 9.7305 | 1.6842 | 1.1883 | 0.4714 | 0.1319 | 0.1668 | 4.4640 | 0.5104 | 98.0424 |
| TH | Kfsp | 85 | 26.5062 | 0.0473 | 0.4554 | 12.6293 | 1.1189 | 1.4409 | 11.2508 | 23.0249 | 2.4486 | 8.8741 | 1.5367 | 1.0848 | 0.4972 | 0.1631 | 0.2104 | 5.7874 | 0.6442 | 97.7302 |
| TH | Kfsp | 86 | 26.1968 | 0.0099 | 0.2296 | 12.5888 | 0.7457 | 1.5369 | 11.4626 | 24.4205 | 2.4332 | 9.4458 | 1.5497 | 1.1803 | 0.5164 | 0.1501 | 0.1645 | 4.4376 | 0.5428 | 97.6212 |
| TH | Kfsp | 87 | 26.1131 | 0.0123 | 0.2261 | 12.4622 | 0.7508 | 1.6536 | 11.6051 | 24.5418 | 2.5400 | 9.7130 | 1.5256 | 1.1552 | 0.4534 | 0.1500 | 0.1643 | 4.3609 | 0.5363 | 97.9737 |
| TH | Kfsp | 88 | 26.1043 | 0.0061 | 0.1910 | 12.4612 | 0.6965 | 1.4687 | 11.9260 | 24.8222 | 2.4825 | 9.6536 | 1.5932 | 1.1490 | 0.4709 | 0.1992 | 0.1275 | 4.0765 | 0.5257 | 97.9641 |
| TH | Kfsp | 89 | 26.4134 | 0.0035 | 0.1908 | 12.7129 | 0.6376 | 1.4730 | 11.9458 | 25.2940 | 2.4594 | 9.5820 | 1.5563 | 1.1091 | 0.4261 | 0.1668 | 0.1455 | 3.8320 | 0.5053 | 98.4635 |
| TH | Kfsp | 90 | 26.4363 | 0.0002 | 0.3003 | 12.6166 | 0.9263 | 1.5775 | 11.1643 | 23.5323 | 2.3729 | 9.2581 | 1.5204 | 1.1979 | 0.4519 | 0.1565 | 0.1939 | 6.5422 | 0.7122 | 98.9698 |
| TH | Kfsp | 91 | 26.3312 | 0.0002 | 0.2409 | 12.6413 | 0.7679 | 1.6132 | 11.2961 | 24.2684 | 2.3989 | 9.4987 | 1.5624 | 1.2205 | 0.4575 | 0.1255 | 0.1494 | 5.0791 | 0.7077 | 98.3689 |
| TH | Kfsp | 92 | 26.3015 | 0.0002 | 0.2182 | 12.5843 | 0.7125 | 1.6479 | 11.4443 | 24.7017 | 2.5158 | 9.6187 | 1.6793 | 1.2495 | 0.4987 | 0.1719 | 0.1686 | 4.5720 | 0.5945 | 98.6896 |
| TH | Kfsp | 93 | 26.3938 | 0.0002 | 0.2213 | 12.6388 | 0.6457 | 1.4792 | 11.6606 | 25.2302 | 2.5257 | 9.8109 | 1.6116 | 1.1088 | 0.5083 | 0.1250 | 0.1121 | 4.1280 | 0.4958 | 98.7060 |
| TH | Kfsp | 95 | 26.2342 | 0.0058 | 0.2242 | 12.5283 | 0.7466 | 1.5811 | 11.3957 | 24.3794 | 2.4623 | 9.7305 | 1.6274 | 1.2556 | 0.5627 | 0.1864 | 0.1902 | 4.7919 | 0.5765 | 98.4888 |
| TH | Kfsp | 96 | 26.2627 | 0.0063 | 0.2267 | 12.5945 | 0.7404 | 1.6498 | 11.1769 | 24.4312 | 2.4651 | 9.4857 | 1.6097 | 1.2854 | 0.4733 | 0.1862 | 0.1470 | 4.9436 | 0.6151 | 98.3096 |
| TH | Kfsp | 97 | 26.3924 | 0.0089 | 0.2045 | 12.7238 | 0.6621 | 1.4897 | 11.5473 | 24.9004 | 2.4328 | 9.6914 | 1.5654 | 1.2281 | 0.4464 | 0.1496 | 0.1562 | 4.0923 | 0.5082 | 98.2095 |
| TH | Kfsp | 98 | 26.3150 | 0.0019 | 0.1889 | 12.6368 | 0.7168 | 1.4953 | 11.6636 | 24.7252 | 2.5190 | 9.7241 | 1.5518 | 1.0699 | 0.5417 | 0.1264 | 0.1221 | 4.4690 | 0.4579 | 98.3354 |
| TH | Kfsp | 99 | 26.1737 | 0.0133 | 0.2129 | 12.5352 | 0.7625 | 1.3600 | 11.5331 | 24.5695 | 2.5833 | 9.5753 | 1.6019 | 1.1029 | 0.5140 | 0.1157 | 0.1565 | 4.3638 | 0.4702 | 97.6538 |
| KY2 | kyanite | 16 | 25.9007 | 0.0906 | 0.3237 | 12.2741 | 0.6546 | 1.1176 | 12.6740 | 24.2138 | 2.4928 | 9.6153 | 1.5342 | 1.0313 | 0.4224 | 0.0651 | 0.0756 | 3.3253 | 0.2976 | 96.1187 |
| KY2 | kyanite | 17 | 27.2925 | 0.0002 | 0.1871 | 13.5153 | 0.5861 | 1.2218 | 12.7383 | 24.4483 | 2.5413 | 9.8182 | 1.4559 | 1.0992 | 0.4817 | 0.0625 | 0.1318 | 2.9616 | 0.2868 | 98.8386 |
| KY2 | kyanite | 18 | 26.6600 | 0.0134 | 0.1875 | 13.0739 | 0.6631 | 1.1809 | 12.4478 | 23.5843 | 2.5292 | 9.8229 | 1.6020 | 1.1725 | 0.4842 | 0.1251 | 0.1075 | 3.3282 | 0.2976 | 97.2901 |

| Sample | Phase | Label | W%(O) | W%(Al) | W%(Si) | W%(P) | W%(Ca) | W%(Y) | W%(La) | W%(Ce) | W%(Pr) | W%(Nd) | W%(Sm) | W%(Gd) | W%(Dy) | W%(Er) | W%(Pb) | W%(Th) | W%(U) | W%(SUM) |
|---|---|---|---|---|---|---|---|---|---|---|---|---|---|---|---|---|---|---|---|---|
| KY2 | kyanite | 19 | 27.8594 | 0.0539 | 0.2052 | 14.0329 | 0.6671 | 1.2337 | 12.4549 | 23.4501 | 2.4924 | 9.8490 | 1.4695 | 1.0699 | 0.4707 | 0.0479 | 0.1126 | 3.1117 | 0.3447 | 98.9356 |
| KY2 | kyanite | 20 | 26.6708 | 0.0043 | 0.1223 | 13.1822 | 0.6294 | 1.3673 | 12.8771 | 24.5010 | 2.5875 | 9.6009 | 1.4073 | 1.0704 | 0.4679 | 0.1462 | 0.0864 | 1.9424 | 0.3078 | 96.9812 |
| KY2 | kyanite | 21 | 26.6038 | 0.0182 | 0.1501 | 13.0628 | 0.7129 | 1.1019 | 13.3695 | 24.2569 | 2.4808 | 9.4805 | 1.3898 | 0.9797 | 0.4009 | 0.1106 | 0.0827 | 2.2396 | 0.2761 | 96.7268 |
| KY2 | kyanite | 22 | 26.0967 | 0.0842 | 0.1931 | 12.7110 | 0.6542 | 1.2945 | 12.7479 | 23.6137 | 2.6119 | 9.7109 | 1.4820 | 1.0437 | 0.4613 | 0.0964 | 0.0626 | 2.1255 | 0.3192 | 95.3188 |
| KY2 | kyanite | 23 | 27.1193 | 0.0506 | 0.1738 | 13.4814 | 0.6378 | 1.2841 | 13.0279 | 24.2171 | 2.6151 | 9.5836 | 1.5238 | 1.0448 | 0.4411 | 0.1154 | 0.0779 | 1.7711 | 0.2913 | 97.4661 |
| KY2 | kyanite | 24 | 28.0802 | 0.0549 | 0.2066 | 14.1810 | 0.6370 | 1.5624 | 12.7151 | 24.4036 | 2.4526 | 9.8263 | 1.4846 | 1.0396 | 0.4316 | 0.1355 | 0.1018 | 1.8825 | 0.3974 | 99.6027 |
| KY2 | kyanite | 28 | 26.3374 | 0.0225 | 0.1846 | 12.8636 | 0.6400 | 1.0663 | 12.6384 | 23.6116 | 2.5320 | 9.5442 | 1.4755 | 1.0991 | 0.4744 | 0.1147 | 0.1364 | 3.1973 | 0.3865 | 96.3345 |
| KY2 | kyanite | 29 | 25.7884 | 0.0124 | 0.1579 | 12.4724 | 0.6717 | 1.1178 | 13.0094 | 24.1331 | 2.6181 | 9.4950 | 1.4442 | 0.9466 | 0.4639 | 0.1333 | 0.0778 | 2.2895 | 0.2371 | 95.0786 |
| KY2 | kyanite | 31 | 26.4766 | 0.0014 | 0.2416 | 12.8242 | 0.7326 | 1.4321 | 12.1266 | 25.0073 | 2.4728 | 9.3859 | 1.5652 | 1.0017 | 0.5388 | 0.1427 | 0.0881 | 3.1101 | 0.3524 | 97.5101 |
| KY2 | kyanite | 31 | 27.1692 | 0.0338 | 0.1851 | 13.6257 | 0.6294 | 1.3642 | 12.5823 | 24.1968 | 2.5253 | 10.0412 | 1.4979 | 0.9396 | 0.4304 | 0.1648 | 0.0490 | 1.0947 | 0.2811 | 96.8205 |
| KY2 | kyanite | 32 | 26.6037 | 0.0002 | 0.2188 | 12.9040 | 0.9160 | 1.2964 | 12.3328 | 24.9568 | 2.5151 | 8.8274 | 1.5717 | 0.9792 | 0.4902 | 0.0769 | 0.0690 | 3.5321 | 0.3449 | 97.6452 |
| KY2 | kyanite | 32 | 27.3630 | 0.0220 | 0.1315 | 13.6794 | 0.5023 | 1.2404 | 13.1768 | 25.0484 | 2.6524 | 9.8856 | 1.4011 | 0.9247 | 0.5021 | 0.1459 | 0.0476 | 1.1288 | 0.3394 | 98.2014 |
| KY2 | kyanite | 33 | 26.2826 | 0.0002 | 0.2222 | 12.6997 | 1.3947 | 1.6504 | 11.8268 | 23.7371 | 2.2604 | 8.5411 | 1.3476 | 1.0041 | 0.5190 | 0.1374 | 0.1300 | 4.6060 | 0.3537 | 96.7230 |
| KY2 | kyanite | 33 | 27.3743 | 0.1724 | 0.2559 | 13.4562 | 0.6006 | 1.2726 | 13.5644 | 24.8259 | 2.5105 | 9.6430 | 1.4168 | 0.9741 | 0.4583 | 0.0958 | 0.0598 | 1.3429 | 0.2916 | 98.3251 |
| KY2 | kyanite | 34 | 26.4868 | 0.0013 | 0.3271 | 12.7814 | 0.7355 | 1.2670 | 11.5082 | 24.5726 | 2.5646 | 9.4153 | 1.7568 | 1.0838 | 0.4717 | 0.0087 | 0.0997 | 3.9298 | 0.3516 | 97.3719 |
| KY2 | kyanite | 34 | 27.3295 | 0.0634 | 0.1107 | 13.5742 | 0.6759 | 1.0732 | 14.5248 | 25.4206 | 2.4409 | 9.1863 | 1.2204 | 0.8069 | 0.3234 | 0.0836 | 0.0335 | 0.9463 | 0.2206 | 98.0442 |
| KY2 | kyanite | 35 | 26.5415 | 0.2338 | 0.1564 | 12.7834 | 0.8024 | 1.0463 | 14.4916 | 25.6606 | 2.4370 | 8.8664 | 1.2028 | 0.7885 | 0.3375 | 0.0884 | 0.0283 | 0.9985 | 0.1733 | 96.6467 |
| KY2 | kyanite | 35 | 26.3796 | 0.0002 | 0.2629 | 12.7093 | 0.7794 | 1.2477 | 11.4096 | 24.5896 | 2.6509 | 9.4772 | 1.6486 | 1.0982 | 0.4609 | 0.0718 | 0.1310 | 4.1927 | 0.3557 | 97.4753 |
| KY2 | kyanite | 36 | 26.3948 | 0.0002 | 0.1770 | 12.7872 | 0.8841 | 1.3535 | 11.7602 | 24.6509 | 2.5231 | 9.2776 | 1.6780 | 1.0929 | 0.4890 | 0.1527 | 0.0894 | 3.7479 | 0.3517 | 97.4202 |
| KY2 | kyanite | 37 | 26.3715 | 0.0035 | 0.1591 | 12.8313 | 0.7105 | 1.4548 | 11.4819 | 24.9476 | 2.5325 | 9.7935 | 1.6948 | 1.0785 | 0.5691 | 0.1101 | 0.0737 | 3.0581 | 0.4003 | 97.2808 |
| KY2 | kyanite | 37 | 27.9736 | 0.5150 | 1.1126 | 13.3777 | 0.7927 | 1.1930 | 12.4530 | 23.4327 | 2.4383 | 8.6742 | 1.3139 | 0.9159 | 0.3866 | 0.0929 | 0.0508 | 1.3193 | 0.1993 | 96.2515 |
| KY2 | kyanite | 38 | 25.9288 | 0.0002 | 0.2098 | 12.5299 | 1.6610 | 2.0313 | 9.7821 | 21.1645 | 2.2320 | 8.5941 | 1.7393 | 1.2215 | 0.7006 | 0.1953 | 0.2000 | 7.4839 | 0.5778 | 96.2621 |
| KY2 | kyanite | 39 | 26.2780 | 0.0132 | 0.1619 | 12.6724 | 1.4870 | 1.5340 | 12.1277 | 23.7968 | 2.3664 | 8.6302 | 1.4716 | 1.0048 | 0.5385 | 0.0830 | 0.1220 | 4.2057 | 0.3293 | 96.8325 |
| KY2 | kyanite | 40 | 26.4883 | 0.0111 | 0.1978 | 12.7259 | 1.2931 | 1.2840 | 12.6679 | 24.8282 | 2.4080 | 8.6318 | 1.3860 | 0.9034 | 0.4412 | 0.0959 | 0.1098 | 3.8423 | 0.2927 | 97.6174 |
| KY2 | kyanite | 41 | 26.2848 | 0.0225 | 0.1805 | 12.6267 | 1.1265 | 1.2397 | 13.0991 | 25.5868 | 2.3328 | 8.3563 | 1.2817 | 0.9668 | 0.4414 | 0.1309 | 0.0930 | 2.8383 | 0.2676 | 96.8854 |
| KY2 | kyanite | 42 | 26.5369 | 0.2706 | 0.1717 | 12.7835 | 0.7081 | 1.0863 | 14.3178 | 25.1627 | 2.5611 | 9.4043 | 1.1745 | 0.7700 | 0.3199 | 0.1055 | 0.0371 | 0.9154 | 0.2161 | 96.5515 |
| KY2 | kyanite | 44 | 26.1593 | 0.0125 | 0.1853 | 12.6620 | 1.5787 | 2.0334 | 9.9236 | 22.0544 | 2.2200 | 8.8804 | 1.6321 | 1.2653 | 0.6829 | 0.0949 | 0.2048 | 6.8367 | 0.6061 | 97.0424 |
| KY2 | kyanite | 45 | 26.1832 | 0.0077 | 0.1866 | 12.7035 | 1.3708 | 1.5980 | 11.1384 | 23.0567 | 2.3683 | 8.7231 | 1.6479 | 1.0866 | 0.5508 | 0.0600 | 0.1700 | 5.0449 | 0.4164 | 96.3229 |
| KY2 | kyanite | 45 | 27.5651 | 0.0375 | 0.1756 | 13.6585 | 0.8708 | 1.1139 | 14.3825 | 25.6732 | 2.3419 | 9.0070 | 1.2351 | 0.8521 | 0.3122 | 0.1133 | 0.0545 | 1.0144 | 0.2440 | 98.6616 |
| KY2 | kyanite | 46 | 25.8883 | 0.3607 | 0.7455 | 11.9741 | 0.7973 | 1.1721 | 13.0084 | 24.9761 | 2.1705 | 8.4966 | 1.1665 | 0.8005 | 0.4104 | 0.0887 | 0.0577 | 1.4461 | 0.3174 | 93.8869 |
| KY2 | kyanite | 46 | 30.3961 | 0.0676 | 5.9643 | 11.3596 | 0.7393 | 1.1753 | 10.3652 | 22.3077 | 2.4548 | 9.4002 | 1.5841 | 1.0127 | 0.4332 | 0.0597 | 0.1104 | 3.2340 | 0.3592 | 101.0334 |
| KY2 | kyanite | 47 | 26.4867 | 0.0002 | 0.2435 | 12.8064 | 1.2048 | 1.3354 | 12.3231 | 24.3608 | 2.3687 | 8.5417 | 1.4118 | 0.9791 | 0.4612 | 0.1276 | 0.1112 | 4.0389 | 0.2796 | 97.0907 |
| KY2 | kyanite | 49 | 27.9547 | 0.0795 | 0.2555 | 13.8951 | 0.8643 | 1.5286 | 12.8719 | 24.5169 | 2.5750 | 9.7229 | 1.4543 | 1.0315 | 0.4371 | 0.1298 | 0.0622 | 2.0880 | 0.4428 | 99.9201 |
| KY2 | kyanite | 50 | 26.1632 | 0.0262 | 0.1645 | 12.5825 | 1.6337 | 1.5795 | 11.5165 | 23.3456 | 2.2549 | 8.4497 | 1.5130 | 1.0152 | 0.5541 | 0.1299 | 0.1894 | 5.1533 | 0.3822 | 96.6634 |
| KY2 | kyanite | 51 | 26.4254 | 0.0372 | 0.1883 | 12.8051 | 1.1160 | 1.5952 | 11.8634 | 24.3077 | 2.4210 | 8.9545 | 1.6746 | 1.0377 | 0.5376 | 0.0745 | 0.0990 | 3.5999 | 0.4552 | 97.2023 |
| KY2 | kyanite | 51 | 26.7726 | 0.0101 | 0.1455 | 13.1518 | 1.0949 | 1.5061 | 12.2620 | 23.2802 | 2.4286 | 9.3615 | 1.3926 | 1.0871 | 0.4142 | 0.1334 | 0.1261 | 4.0719 | 0.4475 | 97.6961 |
| KY2 | kyanite | 52 | 26.7761 | 0.4074 | 0.4595 | 12.7189 | 0.8582 | 1.5067 | 12.2452 | 23.2445 | 2.5037 | 9.5133 | 1.4079 | 1.1041 | 0.5249 | 0.1020 | 0.0740 | 3.3780 | 0.4455 | 97.2799 |
| KY2 | kyanite | 52 | 26.4088 | 0.0342 | 0.2078 | 12.8456 | 0.8291 | 1.6234 | 11.4102 | 24.5902 | 2.4570 | 9.4857 | 1.6440 | 1.1823 | 0.5781 | 0.1427 | 0.1152 | 3.0600 | 0.4687 | 97.0930 |
| KY2 | kyanite | 53 | 26.8726 | 0.0002 | 0.1170 | 13.2680 | 0.7021 | 1.4500 | 13.2770 | 24.9356 | 2.5019 | 9.5875 | 1.4858 | 0.9927 | 0.3760 | 0.1082 | 0.0430 | 1.6100 | 0.4013 | 97.7389 |
| KY2 | kyanite | 53 | 26.3889 | 0.0128 | 0.1691 | 12.7743 | 0.5412 | 1.3428 | 12.1645 | 25.9287 | 2.6306 | 9.7776 | 1.6775 | 1.1043 | 0.5026 | 0.0882 | 0.0599 | 2.0438 | 0.3378 | 97.5546 |
| KY2 | kyanite | 54 | 26.7907 | 0.0229 | 0.1386 | 13.1327 | 0.7206 | 1.3644 | 13.2210 | 24.8432 | 2.5753 | 9.9673 | 1.4518 | 1.0418 | 0.4204 | 0.1230 | 0.0539 | 1.4822 | 0.3745 | 97.7343 |
| KY2 | kyanite | 54 | 26.4539 | 0.0028 | 0.2223 | 12.8308 | 0.6743 | 1.3356 | 11.4607 | 25.0664 | 2.5685 | 9.7195 | 1.6564 | 1.0556 | 0.4659 | 0.1248 | 0.1091 | 3.3773 | 0.3379 | 98.7985 |
| KY2 | kyanite | 55 | 27.7763 | 0.2229 | 0.4799 | 13.5380 | 0.5298 | 1.1093 | 13.7615 | 25.0975 | 2.4671 | 9.5829 | 1.3302 | 0.9452 | 0.3694 | 0.0615 | 0.0615 | 1.3118 | 0.3044 | 98.9592 |
| KY2 | kyanite | 59 | 26.4514 | 0.0228 | 0.1064 | 12.9033 | 0.9105 | 1.0862 | 13.8729 | 24.5669 | 2.5339 | 9.3765 | 1.3111 | 0.9639 | 0.3636 | 0.0979 | 0.0670 | 1.6505 | 0.2267 | 96.5215 |
| KY2 | kyanite | 60 | 26.3323 | 0.0116 | 0.0927 | 12.8576 | 0.9783 | 1.1944 | 13.8200 | 24.4198 | 2.4753 | 9.1672 | 1.3191 | 1.0127 | 0.3896 | 0.0919 | 0.0665 | 1.6840 | 0.2358 | 96.1588 |
| KY2 | kyanite | 61 | 26.4754 | 0.0242 | 0.1032 | 12.9834 | 0.7617 | 1.4416 | 12.8600 | 24.2874 | 2.4867 | 9.9726 | 1.6291 | 1.0818 | 0.4646 | 0.0897 | 0.0664 | 1.7420 | 0.3685 | 96.8483 |
| KY2 | kyanite | 62 | 26.5272 | 0.0164 | 0.1040 | 13.0549 | 0.5718 | 1.2623 | 13.4244 | 25.0552 | 2.5136 | 9.7916 | 1.4004 | 1.0147 | 0.4215 | 0.1429 | 0.0370 | 0.9824 | 0.2972 | 96.6275 |
| KY2 | kyanite | 63 | 26.5330 | 0.0167 | 0.1073 | 12.9971 | 0.7327 | 1.2808 | 13.6862 | 24.6460 | 2.6146 | 9.5611 | 1.3759 | 1.0327 | 0.4366 | 0.2041 | 0.0489 | 1.3342 | 0.2876 | 96.9055 |
| KY2 | kyanite | 64 | 26.4493 | 0.0258 | 0.1186 | 12.9995 | 0.5732 | 1.3647 | 12.7537 | 24.2501 | 2.5432 | 9.7706 | 1.5516 | 1.1501 | 0.5222 | 0.0256 | 0.0906 | 2.2195 | 0.3168 | 96.7351 |
| KY2 | kyanite | 65 | 26.3847 | 0.0394 | 0.1172 | 12.9353 | 0.9432 | 1.6846 | 12.3196 | 23.6918 | 2.4638 | 10.0251 | 1.4925 | 1.2204 | 0.5837 | 0.1144 | 0.0567 | 1.7989 | 0.6096 | 96.4909 |
| KY2 | kyanite | 66 | 26.3779 | 0.0253 | 0.1066 | 12.9533 | 0.9740 | 1.6584 | 12.0426 | 23.4689 | 2.5100 | 10.0779 | 1.6024 | 1.0895 | 0.5942 | 0.1115 | 0.0711 | 2.2160 | 0.5674 | 96.4570 |
| KY2 | kyanite | 68 | 26.4339 | 0.0127 | 0.0961 | 12.9795 | 0.7164 | 1.4016 | 13.4965 | 24.6843 | 2.5267 | 9.6281 | 1.3117 | 1.0568 | 0.4649 | 0.0853 | 0.0505 | 1.2924 | 0.2998 | 96.5472 |
| KY2 | kyanite | 70 | 26.4886 | 0.0056 | 0.0914 | 13.0035 | 0.9124 | 1.2319 | 13.6345 | 24.3955 | 2.5021 | 9.3905 | 1.4148 | 0.8936 | 0.4299 | 0.0880 | 0.0428 | 1.6771 | 0.2050 | 96.4172 |
| KY2 | kyanite | 71 | 26.3269 | 0.0205 | 0.0872 | 12.8580 | 0.9131 | 1.1533 | 13.8987 | 24.3348 | 2.4536 | 9.2297 | 1.3178 | 0.9198 | 0.4191 | 0.1653 | 0.0448 | 1.7923 | 0.2291 | 96.1740 |
| KY2 | kyanite | 72 | 26.1870 | 0.0197 | 0.1007 | 12.7379 | 0.9095 | 1.1465 | 13.6208 | 24.2708 | 2.4554 | 9.2407 | 1.3290 | 0.9859 | 0.4113 | 0.0600 | 0.0864 | 2.2140 | 0.2407 | 96.0263 |
| KY2 | kyanite | 73 | 26.2275 | 0.0016 | 0.0908 | 12.8068 | 0.8890 | 1.1326 | 13.7264 | 24.4320 | 2.4239 | 9.3171 | 1.2557 | 1.0516 | 0.3863 | 0.1335 | 0.0393 | 1.7500 | 0.2139 | 95.8880 |

| Sample | Phase | Label | W%(O) | W%(Al) | W%(Si) | W%(P) | W%(Ca) | W%(Y) | W%(La) | W%(Ce) | W%(Pr) | W%(Nd) | W%(Sm) | W%(Gd) | W%(Dy) | W%(Er) | W%(Pb) | W%(Th) | W%(U) | W%(SUM) |
|---|---|---|---|---|---|---|---|---|---|---|---|---|---|---|---|---|---|---|---|---|
| KY2 | kyanite | 74 | 26.4091 | 0.0063 | 0.0882 | 12.9439 | 0.7855 | 1.1541 | 13.7656 | 24.9023 | 2.5052 | 9.4322 | 1.2628 | 0.9092 | 0.3723 | 0.1662 | 0.0401 | 1.2883 | 0.2599 | 96.3012 |
| KY2 | kyanite | 76 | 26.2826 | 0.0232 | 0.1246 | 12.9331 | 0.5933 | 1.2034 | 13.2788 | 24.4130 | 2.5211 | 9.5653 | 1.4738 | 0.9642 | 0.5218 | 0.0822 | 0.0553 | 1.2356 | 0.2939 | 95.5752 |
| KY2 | kyanite | 77 | 26.1170 | 0.0253 | 0.1083 | 12.7673 | 0.9533 | 1.4357 | 12.8785 | 23.7631 | 2.5225 | 9.6007 | 1.5182 | 1.1318 | 0.4784 | 0.1362 | 0.0532 | 1.4812 | 0.5022 | 95.4829 |
| KY2 | kyanite | 78 | 26.3102 | 0.0224 | 0.1205 | 12.9318 | 0.9069 | 1.5721 | 12.5931 | 23.7406 | 2.5535 | 9.7776 | 1.3760 | 0.9785 | 0.4909 | 0.1530 | 0.0747 | 1.8144 | 0.5085 | 95.9347 |
| KY2 | kyanite | 79 | 26.5713 | 0.2741 | 0.3047 | 12.8261 | 0.7947 | 1.5819 | 13.0451 | 23.5800 | 2.4767 | 9.5341 | 1.4681 | 1.0898 | 0.5148 | 0.1146 | 0.0562 | 1.7674 | 0.4333 | 96.4429 |
| KY2 | kyanite | 80 | 26.2810 | 0.0363 | 0.1177 | 12.8866 | 0.8079 | 1.6158 | 12.8850 | 23.7293 | 2.3867 | 9.6073 | 1.4610 | 1.0886 | 0.5024 | 0.0772 | 0.0774 | 2.2367 | 0.4199 | 96.2268 |
| KY2 | kyanite | 81 | 26.0752 | 0.0153 | 0.1132 | 12.8261 | 0.9766 | 1.8152 | 11.9143 | 22.9020 | 2.4125 | 9.7266 | 1.5809 | 1.1691 | 0.5897 | 0.0729 | 0.1207 | 2.5620 | 0.5846 | 95.4669 |
| KY2 | kyanite | 82 | 26.1036 | 0.0178 | 0.1054 | 12.8110 | 0.9330 | 1.6684 | 11.8766 | 23.4255 | 2.5115 | 9.9181 | 1.5603 | 1.1811 | 0.5496 | 0.1317 | 0.1162 | 2.1839 | 0.5199 | 95.6236 |
| KY2 | kyanite | 85 | 26.3400 | 0.0080 | 0.0894 | 12.9124 | 0.8966 | 1.1220 | 13.5483 | 24.4691 | 2.4823 | 9.2939 | 1.3171 | 0.9566 | 0.4252 | 0.1219 | 0.0558 | 1.6213 | 0.2464 | 95.9163 |
| KY2 | kyanite | 86 | 26.2310 | 0.0201 | 0.1058 | 12.7938 | 0.8766 | 1.1279 | 13.7870 | 24.3179 | 2.4512 | 9.2961 | 1.3489 | 0.9759 | 0.4799 | 0.0934 | 0.0782 | 1.6347 | 0.2233 | 95.8517 |
| KY2 | kyanite | 87 | 26.0186 | 0.0200 | 0.0924 | 12.6805 | 0.8860 | 1.0045 | 14.0695 | 24.4074 | 2.4256 | 8.9195 | 1.3542 | 0.8341 | 0.3590 | 0.0823 | 0.0496 | 1.5841 | 0.2074 | 95.0047 |
| KY2 | kyanite | 88 | 26.7515 | 0.0221 | 0.1277 | 13.1985 | 0.8962 | 1.3294 | 13.0835 | 24.0202 | 2.4405 | 9.7078 | 1.4390 | 1.0470 | 0.4197 | 0.1166 | 0.0649 | 1.9654 | 0.2596 | 96.8996 |
| KY2 | kyanite | 89 | 26.2172 | 0.0345 | 0.1524 | 12.8130 | 0.4698 | 1.2887 | 13.2043 | 24.2134 | 2.5051 | 9.8775 | 1.4325 | 1.1239 | 0.5201 | 0.1032 | 0.0893 | 1.7555 | 0.2962 | 96.1066 |
| KY2 | kyanite | 90 | 25.8315 | 0.0063 | 0.1237 | 12.6532 | 0.9935 | 1.8826 | 11.9556 | 22.5305 | 2.4599 | 9.5966 | 1.4569 | 1.2224 | 0.6101 | 0.1622 | 0.0812 | 2.9162 | 0.5012 | 94.9936 |
| KY2 | kyanite | 91 | 26.0467 | 0.0134 | 0.1087 | 12.7933 | 0.8918 | 1.4676 | 12.8123 | 23.6286 | 2.4708 | 9.2610 | 1.4141 | 1.0209 | 0.4414 | 0.1483 | 0.0613 | 2.0376 | 0.4323 | 95.0601 |
| KY2 | kyanite | 92 | 26.0107 | 0.0234 | 0.1243 | 12.6934 | 0.8686 | 1.4977 | 12.5352 | 23.3266 | 2.5173 | 9.7600 | 1.5172 | 1.0178 | 0.4764 | 0.1676 | 0.0913 | 2.3985 | 0.4939 | 95.5299 |
| KY2 | kyanite | 93 | 26.0434 | 0.0304 | 0.1126 | 12.7409 | 0.5451 | 1.3141 | 13.2014 | 24.5633 | 2.5716 | 9.7061 | 1.3151 | 1.0691 | 0.4818 | 0.1056 | 0.0683 | 1.2091 | 0.3351 | 95.4230 |
| KY2 | kyanite | 94 | 26.2621 | 0.0210 | 0.1218 | 12.8846 | 0.6739 | 1.5076 | 12.7589 | 23.9425 | 2.4940 | 9.9024 | 1.4261 | 1.1129 | 0.4778 | 0.1144 | 0.0661 | 1.9987 | 0.4034 | 96.1782 |
| KY2 | kyanite | 95 | 25.8374 | 0.0029 | 0.1128 | 12.6081 | 0.8600 | 1.5306 | 12.8640 | 23.5586 | 2.5260 | 9.5081 | 1.4008 | 1.0370 | 0.5335 | 0.1463 | 0.0511 | 1.9650 | 0.4091 | 94.9613 |
| KY2 | kyanite | 96 | 26.2461 | 0.0108 | 0.1052 | 12.8464 | 0.8788 | 1.3266 | 13.0690 | 23.6363 | 2.4706 | 9.8726 | 1.3928 | 1.0151 | 0.4932 | 0.1906 | 0.0961 | 1.9815 | 0.3623 | 96.0040 |
| KY2 | kyanite | 97 | 25.9926 | 0.0077 | 0.1052 | 12.6736 | 0.9819 | 1.1458 | 13.2063 | 23.6866 | 2.4428 | 9.2577 | 1.3380 | 1.0196 | 0.4809 | 0.1624 | 0.1034 | 2.2369 | 0.2435 | 95.0949 |
| KY2 | kyanite | 98 | 26.0659 | 0.0238 | 0.0921 | 12.7119 | 0.8993 | 0.9689 | 14.3154 | 24.1289 | 2.4838 | 9.1242 | 1.1643 | 0.8351 | 0.4284 | 0.0603 | 0.0714 | 1.4652 | 0.1884 | 95.0373 |
| KY2 | kyanite | 99 | 26.0942 | 0.0993 | 0.2000 | 12.6637 | 0.7710 | 1.3049 | 12.8490 | 22.9197 | 2.4682 | 9.6823 | 1.4219 | 1.1511 | 0.5080 | 0.0800 | 0.1061 | 2.9216 | 0.2953 | 95.5463 |
| KY2 | kyanite | 100 | 25.8759 | 0.0382 | 0.1785 | 12.5241 | 0.8266 | 1.1114 | 13.0365 | 23.6553 | 2.5373 | 9.7120 | 1.3834 | 1.0524 | 0.4249 | 0.0211 | 0.0624 | 2.1556 | 0.2538 | 94.8594 |
| KY2 | kyanite | 101 | 26.1863 | 0.0154 | 0.1214 | 12.7814 | 0.8437 | 0.9201 | 13.5002 | 24.0194 | 2.4811 | 9.4922 | 1.2840 | 0.9379 | 0.3857 | 0.1148 | 0.0992 | 2.0292 | 0.2582 | 95.4802 |
| KY2 | kyanite | 102 | 26.1377 | 0.0191 | 0.1336 | 12.7235 | 0.8089 | 1.0772 | 13.7267 | 24.0781 | 2.4308 | 9.1345 | 1.3616 | 0.8963 | 0.4339 | 0.1202 | 0.0449 | 2.2870 | 0.2320 | 95.6560 |
| KY2 | kyanite | 103 | 27.1314 | 0.9283 | 0.7550 | 12.4557 | 0.7831 | 0.9303 | 13.3568 | 23.6481 | 2.2994 | 9.0279 | 1.1913 | 0.9178 | 0.4251 | 0.1095 | 0.0852 | 2.4795 | 0.2918 | 96.8262 |
| GST | staurolite | a12 | 26.0615 | 0.0002 | 0.3860 | 12.3993 | 0.8745 | 0.8761 | 11.5436 | 21.8871 | 2.3778 | 9.0921 | 1.5304 | 1.0623 | 0.4230 | 0.1259 | 0.1646 | 7.6690 | 0.3147 | 96.7981 |
| GST | staurolite | b11 | 26.0478 | 1.0621 | 1.0675 | 11.8251 | 0.9402 | 1.4236 | 10.4066 | 19.7510 | 2.1500 | 7.7839 | 1.3694 | 1.1553 | 0.5263 | 0.1225 | 0.1474 | 6.0485 | 0.4702 | 92.3074 |
| GST | staurolite | b16 | 25.8110 | 0.0121 | 0.1620 | 12.6615 | 0.7192 | 1.6216 | 11.6495 | 21.8921 | 2.5418 | 9.0799 | 1.7145 | 1.3712 | 0.6529 | 0.1181 | 0.1268 | 4.2213 | 0.6239 | 94.9894 |
| GST | staurolite | a51 | 25.5013 | 0.0160 | 0.3060 | 12.1922 | 0.4190 | 0.7142 | 11.9129 | 22.9832 | 2.6404 | 9.6868 | 1.7999 | 1.2631 | 0.4715 | 0.0183 | 0.0980 | 4.3290 | 0.1011 | 94.4629 |
| GST | staurolite | b9 | 25.2977 | 0.0185 | 0.1745 | 12.2866 | 0.7643 | 1.3601 | 11.6847 | 21.7821 | 2.5316 | 9.0104 | 1.5859 | 1.3081 | 0.5995 | 0.1189 | 0.1240 | 4.3472 | 0.4722 | 93.4763 |
| GST | staurolite | b27 | 25.5824 | 0.0104 | 0.2049 | 12.3819 | 0.7924 | 1.3286 | 11.7194 | 21.9574 | 2.4457 | 8.8804 | 1.4857 | 1.3177 | 0.5415 | 0.1306 | 0.1444 | 5.4160 | 0.4406 | 94.7900 |
| GST | staurolite | a4 | 26.3750 | 0.0298 | 0.3938 | 12.7885 | 1.1701 | 2.8690 | 10.3750 | 20.3316 | 2.2240 | 8.5682 | 1.3626 | 1.2299 | 0.7425 | 0.2642 | 0.2157 | 8.7893 | 0.4282 | 98.1674 |
| GST | staurolite | b8 | 25.9473 | 0.0067 | 0.2564 | 12.6425 | 1.0599 | 1.5303 | 10.7058 | 20.8366 | 2.3130 | 8.6956 | 1.5887 | 1.2547 | 0.5129 | 0.1326 | 0.1929 | 7.3801 | 0.5085 | 95.5745 |
| GST | staurolite | b14 | 25.4613 | 0.0507 | 0.5535 | 11.9256 | 1.7078 | 1.4818 | 9.1720 | 17.5356 | 1.9911 | 7.2719 | 1.3331 | 1.2620 | 0.5284 | 0.1219 | 0.3464 | 14.2499 | 0.5484 | 95.5514 |
| GST | staurolite | a36 | 26.1352 | 0.0002 | 0.1475 | 12.7266 | 0.7742 | 0.6051 | 11.9104 | 23.0694 | 2.5886 | 9.4217 | 1.7402 | 1.1662 | 0.3832 | 0.0439 | 0.1124 | 4.8000 | 0.1232 | 95.7580 |
| GST | staurolite | b33 | 25.7777 | 0.0377 | 0.2014 | 12.5320 | 0.7663 | 1.3821 | 11.2966 | 21.9892 | 2.4349 | 9.2349 | 1.7400 | 1.3701 | 0.5993 | 0.1602 | 0.1376 | 5.0393 | 0.3900 | 95.0993 |
| GST | staurolite | b13 | 25.5184 | 0.0281 | 0.4427 | 12.0972 | 1.7363 | 1.6429 | 8.9807 | 17.6358 | 1.9619 | 7.8296 | 1.3923 | 1.2510 | 0.5993 | 0.2160 | 0.3382 | 13.1730 | 0.6655 | 95.5189 |
| GST | staurolite | b28 | 25.7286 | 0.2198 | 0.3333 | 12.3379 | 0.7521 | 1.3683 | 11.6064 | 21.9753 | 2.4200 | 8.9186 | 1.5594 | 1.2271 | 0.4993 | 0.1527 | 0.1331 | 4.8013 | 0.3787 | 94.4219 |
| GST | staurolite | b25 | 25.3241 | 0.0282 | 0.4747 | 11.9555 | 1.6287 | 1.4439 | 9.6447 | 18.0027 | 2.0170 | 7.4675 | 1.2424 | 1.2242 | 0.5291 | 0.1660 | 0.3175 | 12.7431 | 0.4796 | 94.6989 |
| GST | staurolite | a7 | 26.1891 | 0.0221 | 0.5110 | 12.3627 | 1.3778 | 1.1476 | 10.6082 | 19.5933 | 2.0795 | 8.3433 | 1.3356 | 1.3201 | 0.4278 | 0.0820 | 0.2853 | 11.3843 | 0.4463 | 97.5260 |
| GST | staurolite | b10 | 25.7075 | 0.0167 | 0.1806 | 12.5094 | 0.7994 | 1.5099 | 11.6678 | 21.9361 | 2.3931 | 9.0553 | 1.5257 | 1.3527 | 0.5495 | 0.1556 | 0.1604 | 4.8247 | 0.7073 | 95.0617 |
| GST | staurolite | b30 | 25.5653 | 0.0183 | 0.2941 | 12.3034 | 1.1732 | 1.4279 | 10.6651 | 20.0974 | 2.2463 | 8.4251 | 1.4454 | 1.2915 | 0.6678 | 0.1293 | 0.2259 | 8.4265 | 0.4747 | 94.8872 |
| GST | staurolite | a9 | 26.1754 | 0.0170 | 0.4805 | 12.3846 | 1.2438 | 0.9567 | 11.3590 | 19.9141 | 2.0776 | 8.1260 | 1.4446 | 1.2590 | 0.4117 | 0.1303 | 0.2704 | 10.6772 | 0.3615 | 97.2994 |
| GST | staurolite | b26 | 25.6628 | 0.0104 | 0.3156 | 12.2976 | 1.2407 | 1.4236 | 10.7453 | 20.0999 | 2.1941 | 8.1281 | 1.5189 | 1.1916 | 0.5919 | 0.1305 | 0.2449 | 9.3398 | 0.4124 | 95.5581 |
| GST | staurolite | b6 | 25.9480 | 0.0106 | 0.1783 | 12.6724 | 0.8018 | 1.5767 | 11.4946 | 21.9091 | 2.5153 | 9.1890 | 1.6221 | 1.4122 | 0.6120 | 0.1322 | 0.1626 | 4.9046 | 0.6124 | 95.7639 |
| GST | staurolite | b20 | 25.4477 | 0.0247 | 0.5088 | 11.9916 | 1.5485 | 1.7110 | 9.2716 | 18.1804 | 2.1274 | 7.8335 | 1.6077 | 1.3679 | 0.5828 | 0.1815 | 0.3296 | 12.2335 | 0.5276 | 95.4858 |
| GST | staurolite | a1 | 26.1393 | 0.0002 | 0.3905 | 12.4446 | 0.3093 | 0.6012 | 12.1789 | 23.8677 | 2.6374 | 10.1237 | 1.8072 | 1.2235 | 0.3448 | 0.0963 | 0.1168 | 4.3981 | 0.1413 | 96.8308 |
| GST | staurolite | b7 | 25.8332 | 0.0126 | 0.1596 | 12.6287 | 0.6493 | 1.3394 | 11.6113 | 22.4838 | 2.5358 | 9.3888 | 1.7454 | 1.3336 | 0.5499 | 0.1229 | 0.1307 | 4.2086 | 0.3731 | 95.1167 |
| GST | staurolite | b17 | 25.4819 | 0.0239 | 0.4709 | 12.0366 | 1.7704 | 1.4841 | 9.1399 | 17.7009 | 2.0550 | 7.5162 | 1.3328 | 1.2425 | 0.6146 | 0.1559 | 0.3682 | 13.3433 | 0.5823 | 95.3294 |
| GST | staurolite | b2 | 26.1185 | 0.0143 | 0.1488 | 12.8034 | 0.5557 | 1.2595 | 12.3283 | 22.9969 | 2.5989 | 9.5252 | 1.7553 | 1.2121 | 0.5532 | 0.0773 | 0.1102 | 3.4279 | 0.3363 | 95.8318 |
| GST | staurolite | a21 | 26.1172 | 0.0133 | 0.3482 | 12.5858 | 1.2895 | 1.2317 | 10.2413 | 20.0320 | 2.2835 | 8.7169 | 1.5488 | 1.1809 | 0.4971 | 0.1220 | 0.2673 | 9.4349 | 0.4561 | 96.3765 |
| GST | staurolite | a8 | 26.2398 | 0.0118 | 0.4629 | 12.4613 | 1.3669 | 1.1918 | 10.4611 | 19.6944 | 2.2140 | 8.3438 | 1.5245 | 1.2655 | 0.5172 | 0.0846 | 0.3021 | 10.9901 | 0.4053 | 97.5471 |
| GST | staurolite | a49 | 25.7156 | 0.0099 | 0.2651 | 12.3325 | 0.4381 | 0.6082 | 12.0621 | 23.2587 | 2.7370 | 9.9095 | 1.7898 | 1.1969 | 0.3936 | 0.1235 | 0.1078 | 4.0194 | 0.1097 | 95.0874 |
| GST | staurolite | b31 | 25.7905 | 0.0129 | 0.3381 | 12.3698 | 1.3211 | 1.4792 | 10.5693 | 19.9934 | 2.1835 | 8.0084 | 1.4568 | 1.2497 | 0.5234 | 0.1253 | 0.2794 | 9.6347 | 0.5128 | 95.8583 |

| Sample | Phase | Label | W%(O ) | W%(Al) | W%(Si) | W%(P) | W%(Ca) | W%(Y ) | W%(La) | W%(Ce) | W%(Pr) | W%(Nd) | W%(Sm) | W%(Gd) | W%(Dy) | W%(Er) | W%(Pb) | W%(Th) | W%(U ) | W%(SUM) |
|---|---|---|---|---|---|---|---|---|---|---|---|---|---|---|---|---|---|---|---|---|
| GST | staurolite | a31 | 26.0775 | 0.0039 | 0.2851 | 12.5163 | 0.4536 | 0.6543 | 12.0394 | 23.5886 | 2.6518 | 10.0569 | 1.8404 | 1.2267 | 0.3154 | 0.0398 | 0.1188 | 4.3493 | 0.1316 | 96.3594 |
| GST | staurolite | b1 | 25.4882 | 0.1955 | 0.2856 | 12.4055 | 0.4681 | 1.5613 | 11.6689 | 22.2969 | 2.5294 | 9.1809 | 1.6814 | 1.3312 | 0.6006 | 0.0773 | 0.1069 | 2.4043 | 0.5771 | 92.8691 |
| GST | staurolite | b4 | 25.6873 | 0.0212 | 0.1647 | 12.5252 | 0.6435 | 1.4191 | 12.0591 | 22.5044 | 2.4617 | 9.2506 | 1.5924 | 1.2447 | 0.4642 | 0.0883 | 0.1365 | 4.0662 | 0.4184 | 94.7575 |
| GST | staurolite | b5 | 25.9282 | 0.0082 | 0.1849 | 12.7050 | 0.7887 | 1.5646 | 11.3535 | 21.8302 | 2.5257 | 9.1654 | 1.6116 | 1.3544 | 0.7027 | 0.0852 | 0.1725 | 4.7892 | 0.5898 | 95.3698 |
| GST | staurolite | b29 | 27.9754 | 3.1904 | 1.7279 | 11.3415 | 0.6061 | 1.1789 | 10.7079 | 20.6056 | 2.4007 | 8.6118 | 1.6084 | 1.1414 | 0.5122 | 0.1146 | 0.1197 | 3.5133 | 0.3227 | 95.6885 |
| GST | staurolite | a42 | 25.2433 | 0.2446 | 0.4361 | 12.1027 | 1.0547 | 1.3720 | 9.9514 | 19.8265 | 2.1264 | 8.5796 | 1.6427 | 1.2158 | 0.5528 | 0.1213 | 0.2154 | 6.9630 | 0.3745 | 92.0328 |
| GST | staurolite | a3 | 26.5107 | 0.0035 | 0.3206 | 12.7176 | 0.3364 | 0.5253 | 12.1486 | 24.4581 | 2.7350 | 10.1855 | 1.7862 | 1.1813 | 0.4320 | 0.0542 | 0.1224 | 4.1797 | 0.1018 | 97.8089 |
| GST | staurolite | a2 | 26.3596 | 0.0006 | 0.3397 | 12.6076 | 0.3536 | 0.7109 | 12.0214 | 24.1268 | 2.6553 | 10.2757 | 1.8106 | 1.3834 | 0.4133 | 0.0647 | 0.1313 | 4.1587 | 0.1835 | 97.6067 |
| GST | staurolite | b3 | 25.5515 | 0.3111 | 0.3988 | 12.2388 | 0.5917 | 1.6146 | 11.5868 | 21.9746 | 2.3821 | 9.0469 | 1.6444 | 1.3825 | 0.5934 | 0.0620 | 0.1567 | 3.2185 | 0.5729 | 93.3373 |
| GST | staurolite | a41 | 25.9695 | 0.0016 | 0.3145 | 12.4943 | 0.9781 | 1.0789 | 11.1682 | 21.7424 | 2.3791 | 8.9181 | 1.4665 | 0.9688 | 0.4166 | 0.0988 | 0.2651 | 7.3432 | 0.3822 | 95.9959 |
| GST | staurolite | a45 | 25.9095 | 0.0105 | 0.1377 | 12.6248 | 0.8327 | 0.7161 | 11.7344 | 22.2739 | 2.6348 | 9.2449 | 1.6844 | 1.2081 | 0.4206 | 0.0932 | 0.1928 | 5.0766 | 0.2581 | 95.0631 |
| GST | staurolite | a35 | 26.2951 | 0.0173 | 0.2196 | 12.7572 | 0.7980 | 0.7542 | 11.6578 | 22.6295 | 2.6102 | 9.4248 | 1.7635 | 1.1876 | 0.3844 | 0.1008 | 0.3781 | 5.1661 | 0.4348 | 96.5890 |
| GST | staurolite | a23 | 26.4113 | 0.0136 | 0.2632 | 12.7833 | 0.8063 | 0.6916 | 11.7672 | 22.6936 | 2.5197 | 9.5905 | 1.5760 | 1.1010 | 0.2735 | 0.0723 | 0.4295 | 5.4847 | 0.4834 | 96.9707 |
| GST | staurolite | a50 | 25.6112 | 0.0070 | 0.2240 | 12.3703 | 0.7107 | 0.7216 | 11.6051 | 22.4597 | 2.4503 | 9.3936 | 1.5611 | 1.2842 | 0.3085 | 0.0860 | 0.3743 | 4.9413 | 0.3420 | 94.4609 |
| GST | staurolite | a20 | 26.3072 | 0.0227 | 0.2580 | 12.6826 | 0.8584 | 0.6606 | 11.5440 | 22.7518 | 2.4338 | 9.5421 | 1.7439 | 1.1336 | 0.2720 | 0.1051 | 0.4580 | 5.6191 | 0.4623 | 96.8652 |
| GST | staurolite | a33 | 25.9693 | 0.0055 | 0.2724 | 12.4617 | 0.8338 | 0.6066 | 11.5703 | 22.4571 | 2.5582 | 9.3779 | 1.7670 | 1.1564 | 0.2846 | 0.0450 | 0.4635 | 5.6608 | 0.4751 | 95.9752 |
| GST | staurolite | a28 | 26.0285 | 0.0178 | 0.2302 | 12.5224 | 0.8739 | 0.6767 | 11.4973 | 22.5907 | 2.4786 | 9.5643 | 1.7186 | 1.1362 | 0.3222 | 0.0272 | 0.4711 | 5.4940 | 0.5072 | 96.1669 |
| GST | staurolite | a10 | 26.4604 | 0.0054 | 0.2291 | 12.8431 | 0.8709 | 0.9770 | 11.5652 | 22.3333 | 2.5023 | 9.5435 | 1.7660 | 1.1617 | 0.3921 | 0.1494 | 0.5184 | 5.5690 | 0.5800 | 97.4768 |
| GST | staurolite | a54 | 25.7000 | 0.0030 | 0.2307 | 12.3807 | 0.8566 | 0.7270 | 11.4397 | 21.8559 | 2.4995 | 9.4918 | 1.7082 | 1.1744 | 0.3194 | 0.1436 | 0.5006 | 5.4292 | 0.5410 | 95.0113 |
| GST | staurolite | a44 | 26.0591 | 0.0155 | 0.2355 | 12.5844 | 0.8672 | 0.7511 | 11.2916 | 22.1383 | 2.4422 | 9.5951 | 1.8650 | 1.2850 | 0.3598 | 0.0364 | 0.5140 | 5.5154 | 0.5380 | 96.1036 |
| GST | staurolite | a39 | 26.0185 | 0.0202 | 0.2334 | 12.5429 | 0.8477 | 0.7561 | 11.3395 | 22.4140 | 2.5707 | 9.5687 | 1.7339 | 1.2026 | 0.3323 | 0.0318 | 0.5133 | 5.4068 | 0.5328 | 96.0752 |
| GST | staurolite | a24 | 26.4919 | 0.0158 | 0.2299 | 12.8732 | 0.8434 | 0.5704 | 11.8153 | 22.8218 | 2.5747 | 9.3614 | 1.7250 | 1.1479 | 0.2030 | 0.0316 | 0.4901 | 5.2309 | 0.4829 | 96.9192 |
| GST | staurolite | a17 | 26.5318 | 0.0038 | 0.2424 | 12.8387 | 0.8977 | 0.6061 | 11.5317 | 22.6800 | 2.4954 | 9.7065 | 1.7577 | 1.1300 | 0.2779 | 0.1138 | 0.5356 | 5.5932 | 0.5552 | 97.5075 |
| GST | staurolite | a40 | 25.8900 | 0.0013 | 0.2269 | 12.4470 | 0.8460 | 0.6866 | 11.5115 | 22.6660 | 2.5787 | 9.3934 | 1.7133 | 1.2052 | 0.3392 | 0.0949 | 0.4934 | 5.2289 | 0.4877 | 95.8200 |
| GST | staurolite | a53 | 25.5738 | 0.0053 | 0.2403 | 12.3029 | 0.8499 | 0.7225 | 11.2360 | 21.8197 | 2.4938 | 9.2272 | 1.8638 | 1.2663 | 0.3310 | 0.0827 | 0.5320 | 5.5325 | 0.5549 | 94.6446 |
| GST | staurolite | a18 | 26.5673 | 0.0059 | 0.2340 | 12.9014 | 0.8937 | 0.8165 | 11.2255 | 22.5516 | 2.5503 | 9.6349 | 1.9730 | 1.2439 | 0.3392 | 0.0529 | 0.5293 | 5.5360 | 0.5361 | 97.6015 |
| GST | staurolite | a37 | 25.8820 | 0.0048 | 0.1773 | 12.6337 | 0.9698 | 1.6203 | 11.3427 | 21.6082 | 2.4760 | 8.9749 | 1.6554 | 1.1761 | 0.5451 | 0.1496 | 0.5468 | 5.1998 | 0.6943 | 95.6668 |
| GST | staurolite | a14 | 26.3550 | 0.0031 | 0.1371 | 13.0842 | 1.0144 | 2.2144 | 11.0674 | 21.5637 | 2.2934 | 9.0533 | 1.5522 | 1.1369 | 0.6910 | 0.1830 | 0.5592 | 5.0264 | 0.7907 | 96.7354 |
| GST | staurolite | a30 | 26.2981 | 0.0040 | 0.2307 | 12.7026 | 0.8483 | 0.5817 | 11.6674 | 22.5858 | 2.5929 | 9.5531 | 1.7813 | 1.1805 | 0.3277 | 0.0737 | 0.5170 | 5.3764 | 0.5166 | 96.8478 |
| GST | staurolite | a19 | 26.2540 | 0.0058 | 0.2241 | 12.7037 | 0.8422 | 0.6384 | 11.6402 | 22.6616 | 2.5566 | 9.6444 | 1.6663 | 1.1674 | 0.3189 | 0.0851 | 0.5008 | 5.1439 | 0.5081 | 96.5715 |
| GST | staurolite | a38 | 26.2607 | 0.0053 | 0.2237 | 12.7876 | 0.8744 | 0.8928 | 11.3372 | 22.2825 | 2.5202 | 9.3357 | 1.7836 | 1.2014 | 0.3369 | 0.1054 | 0.5322 | 5.2855 | 0.5801 | 96.3552 |
| GST | staurolite | a13 | 26.3663 | 0.0036 | 0.2396 | 12.7167 | 0.8759 | 0.5737 | 11.6956 | 22.6724 | 2.5600 | 9.6596 | 1.6656 | 1.2046 | 0.2870 | 0.0902 | 0.5252 | 5.5123 | 0.4897 | 97.1480 |
| GST | staurolite | a34 | 26.3290 | 0.0037 | 0.2415 | 12.7418 | 0.8424 | 0.5694 | 11.5065 | 22.5782 | 2.5799 | 9.6761 | 1.7040 | 1.1677 | 0.2500 | 0.0331 | 0.5298 | 5.4852 | 0.4939 | 96.7422 |
| GST | staurolite | a26 | 26.5084 | 0.0112 | 0.2059 | 12.9498 | 0.9296 | 1.0540 | 11.3514 | 22.5651 | 2.4968 | 9.2636 | 1.6343 | 1.2415 | 0.4356 | 0.0984 | 0.5515 | 5.2420 | 0.6168 | 97.1659 |
| GST | staurolite | a29 | 26.3267 | 0.0043 | 0.2050 | 12.8061 | 0.9197 | 1.0734 | 11.5300 | 22.2870 | 2.5562 | 9.3598 | 1.7009 | 1.2135 | 0.3874 | 0.0856 | 0.5600 | 5.3320 | 0.5813 | 96.9389 |
| GST | staurolite | a25 | 26.2762 | 0.0021 | 0.2374 | 12.7208 | 0.8482 | 0.7091 | 11.6126 | 22.6932 | 2.4278 | 9.3832 | 1.7812 | 1.1871 | 0.2762 | 0.1129 | 0.5470 | 5.3481 | 0.5066 | 96.6797 |
| GST | staurolite | a27 | 26.5403 | 0.0031 | 0.2307 | 12.8805 | 0.9112 | 0.9251 | 11.5165 | 22.5456 | 2.5915 | 9.5327 | 1.7703 | 1.1666 | 0.3968 | 0.0506 | 0.5863 | 5.4113 | 0.6015 | 97.6706 |
| G&G | mx | d_31 | 25.9719 | 0.0148 | 0.1343 | 12.5722 | 0.3327 | 0.1226 | 12.5019 | 25.026 | 2.6398 | 9.8471 | 2.2235 | 1.4282 | 0.1253 | 0.0745 | 0.0518 | 1.9474 | 0.2147 | 95.2387 |
| G&G | mx | e_5 | 27.0922 | 0.0814 | 0.2056 | 13.4302 | 0.4548 | 0.0621 | 12.4781 | 24.4036 | 2.5947 | 9.4372 | 2.0834 | 1.2286 | 0.1446 | 0.0142 | 0.0631 | 2.2842 | 0.3701 | 96.4381 |
| G&G | mx | c_3 | 26.1717 | 0.0047 | 0.1167 | 12.7079 | 0.4556 | 0.0697 | 12.602 | 24.6866 | 2.6442 | 9.7229 | 2.1605 | 1.2474 | 0.136 | 0.0405 | 0.0891 | 2.6744 | 0.2369 | 95.7768 |
| G&G | mx | i_3 | 26.1114 | 0.0021 | 0.1067 | 12.6991 | 0.2836 | 0.1168 | 12.3918 | 25.1499 | 2.8421 | 10.2108 | 2.2491 | 1.3702 | 0.1416 | 0.0526 | 0.0462 | 1.4609 | 0.3172 | 95.5621 |
| G&G | mx | a_8 | 25.9514 | 0.0002 | 0.123 | 12.5784 | 0.1798 | 0.1513 | 12.4842 | 25.4459 | 2.7771 | 10.378 | 2.3122 | 1.4936 | 0.1735 | 0.0446 | 0.0281 | 0.8503 | 0.2432 | 95.2248 |
| G&G | mx | h_8 | 25.9612 | 0.0131 | 0.1084 | 12.5651 | 0.3421 | 0.035 | 12.5624 | 25.2462 | 2.7313 | 10.0302 | 2.245 | 1.1164 | 0.0991 | 0.0922 | 0.0656 | 1.653 | 0.3368 | 95.2131 |
| G&G | mx | e_2 | 25.9396 | 0.0054 | 0.1162 | 12.5698 | 0.4716 | 0.0794 | 12.3083 | 24.6739 | 2.598 | 9.6324 | 2.204 | 1.3191 | 0.077 | 0.0826 | 0.0661 | 2.6796 | 0.2474 | 95.0804 |
| G&G | mx | a_2 | 26.2459 | 0.0049 | 0.1178 | 12.7284 | 0.5332 | 0.0714 | 12.5837 | 24.4771 | 2.6541 | 9.8479 | 2.1109 | 1.215 | 0.0824 | 0.0679 | 0.0916 | 2.8302 | 0.4381 | 96.1105 |
| G&G | mx | i_12 | 26.097 | 0.0131 | 0.1135 | 12.6949 | 0.4319 | 0.0094 | 12.7083 | 24.8406 | 2.6543 | 9.8453 | 2.0543 | 0.9428 | 0.0001 | 0.0373 | 0.089 | 2.2592 | 0.4011 | 95.2021 |
| G&G | mx | a_6 | 25.8923 | 0.0002 | 0.1386 | 12.5433 | 0.2326 | 0.1857 | 12.5215 | 24.9948 | 2.6673 | 10.0048 | 2.3388 | 1.6631 | 0.2466 | 0.0815 | 0.0539 | 1.2424 | 0.2179 | 95.0353 |
| G&G | mx | g_2 | 26.0242 | 0.0089 | 0.1567 | 12.6495 | 0.1782 | 0.1725 | 12.5273 | 25.3944 | 2.7329 | 10.0231 | 2.2335 | 1.5665 | 0.1444 | 0.052 | 0.0459 | 0.8797 | 0.2626 | 95.0623 |
| G&G | mx | a_10 | 26.1004 | 0.0002 | 0.1233 | 12.6612 | 0.2076 | 0.0831 | 12.5624 | 25.9041 | 2.808 | 10.1132 | 2.2385 | 1.3539 | 0.0872 | 0.013 | 0.0286 | 1.0566 | 0.2381 | 95.5894 |
| G&G | mx | a_1 | 26.0497 | 0.0002 | 0.1286 | 12.632 | 0.2384 | 0.0994 | 12.3087 | 25.303 | 2.8549 | 10.2777 | 2.3006 | 1.3661 | 0.1517 | 0.1017 | 0.0604 | 1.3402 | 0.2711 | 95.4944 |
| G&G | mx | d_7 | 26.1051 | 0.0193 | 0.1491 | 12.5909 | 0.5438 | 0.0421 | 12.6037 | 24.9155 | 2.6685 | 9.5828 | 2.0032 | 0.7482 | 0.0451 | 0.0001 | 0.1153 | 3.3194 | 0.301 | 95.7631 |
| G&G | mx | f_3 | 25.9847 | 0.0002 | 0.1356 | 12.6038 | 0.2583 | 0.0694 | 12.4845 | 25.2567 | 2.7144 | 9.9155 | 2.2324 | 1.4007 | 0.148 | 0.0524 | 0.0481 | 1.5685 | 0.2704 | 95.1536 |
| G&G | mx | h_12 | 26.0221 | 0.0002 | 0.1193 | 12.6465 | 0.1689 | 0.1534 | 12.6074 | 25.6897 | 2.6449 | 10.363 | 2.1807 | 1.446 | 0.1246 | 0.0274 | 0.0513 | 0.7252 | 0.2928 | 95.2734 |
| G&G | mx | h_10 | 25.9084 | 0.0059 | 0.1572 | 12.4632 | 0.4433 | 0.1366 | 12.2215 | 24.6508 | 2.6653 | 9.7317 | 2.1728 | 1.6368 | 0.1937 | 0.0234 | 0.0939 | 2.7068 | 0.2736 | 95.4949 |
| G&G | mx | i_8 | 26.2237 | 0.0013 | 0.232 | 12.5863 | 0.6163 | 0.1897 | 11.7904 | 23.7871 | 2.5834 | 9.6562 | 2.2407 | 1.5748 | 0.2031 | 0.1007 | 0.1098 | 4.4505 | 0.269 | 96.625 |
| G&G | mx | h_7 | 27.1369 | 0.0276 | 1.6856 | 12.2295 | 0.2766 | 0.0706 | 12.1613 | 24.7651 | 2.6688 | 9.8706 | 2.2297 | 1.3689 | 0.1114 | 0.0001 | 0.0678 | 1.6799 | 0.2303 | 96.5907 |

| Sample | Phase | Label | W%(O) | W%(Al) | W%(Si) | W%(P) | W%(Ca) | W%(Y) | W%(La) | W%(Ce) | W%(Pr) | W%(Nd) | W%(Sm) | W%(Gd) | W%(Dy) | W%(Er) | W%(Pb) | W%(Th) | W%(U) | W%(SUM) |
|---|---|---|---|---|---|---|---|---|---|---|---|---|---|---|---|---|---|---|---|---|
| G&G | mx | d_19 | 26.8086 | 0.0702 | 0.9875 | 12.4175 | 0.5155 | 0.1195 | 11.9594 | 24.0772 | 2.6107 | 9.9066 | 2.2234 | 1.5735 | 0.132 | 0.0638 | 0.1026 | 3.1501 | 0.2291 | 96.9572 |
| G&G | mx | d_12 | 26.3398 | 0.0018 | 0.1217 | 12.8226 | 0.3139 | 0.1146 | 12.7026 | 25.1254 | 2.7632 | 9.9275 | 2.0898 | 1.5297 | 0.2205 | 0.0421 | 0.0671 | 1.8125 | 0.2558 | 96.2606 |
| G&G | mx | d_24 | 26.0781 | 0.0004 | 0.2058 | 12.5481 | 0.615 | 0.1561 | 11.9889 | 23.4822 | 2.5244 | 9.5374 | 2.1423 | 1.6328 | 0.1909 | 0.1036 | 0.1057 | 4.4119 | 0.2441 | 95.9777 |
| G&G | mx | i_4 | 27.1178 | 0.0626 | 1.3818 | 12.4634 | 0.498 | 0.1339 | 12.0285 | 23.7227 | 2.4977 | 9.3767 | 2.1906 | 1.493 | 0.2053 | 0.0001 | 0.1157 | 3.0231 | 0.2502 | 96.5711 |
| G&G | mx | g_3 | 26.1973 | 0.0002 | 0.1425 | 12.7167 | 0.391 | 0.131 | 12.2864 | 24.7437 | 2.6045 | 9.7805 | 2.2479 | 1.5982 | 0.1861 | 0.1098 | 0.0817 | 2.4794 | 0.2304 | 95.9373 |
| G&G | mx | i_16 | 26.2702 | 0.0219 | 0.1777 | 12.7153 | 0.4559 | 0.1195 | 12.2509 | 24.3974 | 2.6264 | 9.6484 | 2.221 | 1.6782 | 0.1386 | 0.0521 | 0.0794 | 3.0516 | 0.2434 | 96.1579 |
| G&G | mx | f_10 | 26.2695 | 0.0057 | 0.159 | 12.7201 | 0.4496 | 0.149 | 12.1918 | 24.5817 | 2.6901 | 9.7812 | 2.3361 | 1.5851 | 0.1566 | 0.0001 | 0.0849 | 2.8759 | 0.2544 | 96.3008 |
| G&G | mx | e_1 | 26.1263 | 0.015 | 0.1416 | 12.5674 | 0.3137 | 0.128 | 12.4612 | 25.4082 | 2.749 | 10.2667 | 2.2257 | 1.5935 | 0.129 | 0.0571 | 0.068 | 1.7958 | 0.2796 | 96.3358 |
| G&G | mx | h_11 | 26.1055 | 0.0078 | 0.1413 | 12.6328 | 0.3433 | 0.1704 | 12.3784 | 25.0011 | 2.7119 | 9.9025 | 2.2404 | 1.5619 | 0.1904 | 0.033 | 0.0693 | 2.0812 | 0.2647 | 95.8459 |
| G&G | mx | i_13 | 26.1943 | 0.0133 | 0.1254 | 12.6853 | 0.2889 | 0.1639 | 12.3932 | 25.4648 | 2.7344 | 10.0267 | 2.2579 | 1.5551 | 0.1503 | 0.012 | 0.0739 | 1.7582 | 0.2707 | 96.1783 |
| G&G | mx | f_9 | 26.3656 | 0.1714 | 0.3003 | 12.5968 | 0.2008 | 0.0893 | 12.7235 | 25.732 | 2.8125 | 10.0217 | 2.2339 | 1.4194 | 0.1495 | 0.0369 | 0.0287 | 0.9264 | 0.3074 | 96.1261 |
| G&G | mx | a_11 | 26.3197 | 0.0198 | 0.1225 | 12.9035 | 0.4526 | 1.0417 | 11.7308 | 24.8317 | 2.6337 | 10.2032 | 2.204 | 1.4461 | 0.5136 | 0.0841 | 0.0443 | 1.4806 | 0.1843 | 96.2262 |
| G&G | mx | f_7 | 26.379 | 0.0002 | 0.1066 | 12.8598 | 0.3215 | 0.565 | 12.7439 | 26.3981 | 2.7744 | 9.5879 | 2.0539 | 1.146 | 0.2983 | 0.0649 | 0.0277 | 1.138 | 0.1212 | 96.5964 |
| G&G | mx | f_8 | 26.0105 | 0.0035 | 0.1347 | 12.8299 | 0.3408 | 2.2197 | 10.559 | 24.1605 | 2.7514 | 10.3218 | 2.1812 | 1.5927 | 0.7111 | 0.1953 | 0.0399 | 1.7053 | 0.2895 | 96.0568 |
| G&G | mx | i_15 | 26.4361 | 0.0055 | 0.1283 | 12.8418 | 0.1786 | 0.0848 | 12.5514 | 26.268 | 2.8944 | 10.5201 | 2.1657 | 1.3351 | 0.1367 | 0.0274 | 0.0428 | 0.7984 | 0.242 | 96.6671 |
| G&G | mx | h_13 | 26.2336 | 0.0015 | 0.2065 | 12.5645 | 0.5203 | 0.1027 | 12.0485 | 24.7118 | 2.5737 | 9.9139 | 2.2571 | 1.4313 | 0.1189 | 0.0001 | 0.0921 | 3.7843 | 0.2727 | 96.8435 |
| G&G | mx | d_25 | 26.2298 | 0.004 | 0.1824 | 12.6288 | 0.4409 | 0.1063 | 12.4312 | 25.0454 | 2.6289 | 9.675 | 2.1387 | 1.3835 | 0.0776 | 0.0377 | 0.1072 | 3.1139 | 0.2388 | 96.4801 |
| G&G | mx | h_14 | 26.2672 | 0.0086 | 0.3486 | 12.482 | 0.9043 | 0.0723 | 11.4491 | 22.6898 | 2.5409 | 9.1237 | 2.0953 | 1.2389 | 0.0239 | 0.0001 | 0.1736 | 7.206 | 0.2484 | 96.8827 |
| G&G | mx | d_28 | 25.9959 | 0.0309 | 0.3693 | 12.3135 | 0.8339 | 0.0799 | 11.4582 | 22.5444 | 2.4866 | 9.2244 | 2.109 | 1.3134 | 0.0984 | 0.0779 | 0.1619 | 6.5311 | 0.285 | 95.9237 |
| G&G | mx | h_16 | 26.1719 | 0.0105 | 0.4685 | 12.2831 | 0.9457 | 0.0826 | 11.0457 | 21.9155 | 2.5537 | 8.9127 | 2.0496 | 1.323 | 0.1016 | 0.1048 | 0.2077 | 8.6483 | 0.311 | 97.1459 |
| G&G | mx | h_9 | 25.9323 | 0.0174 | 0.2004 | 12.5384 | 0.42 | 0.836 | 11.8043 | 24.0014 | 2.6144 | 9.7757 | 2.0924 | 1.5399 | 0.4046 | 0.1202 | 0.0799 | 3.1 | 0.2046 | 95.6919 |
| G&G | mx | a_9 | 27.8656 | 2.2528 | 3.0345 | 10.8724 | 0.5221 | 0.0389 | 10.3746 | 21.2126 | 2.416 | 8.4914 | 1.9436 | 1.1957 | 0.0505 | 0.0369 | 0.0636 | 2.6609 | 0.2132 | 93.2553 |
| G&G | mx | i_19 | 26.2983 | 0.0002 | 0.232 | 12.6958 | 0.6556 | 0.1082 | 11.5812 | 23.6748 | 2.5919 | 9.6726 | 2.221 | 1.3718 | 0.0735 | 0.037 | 0.1164 | 4.6714 | 0.2776 | 96.2893 |
| G&G | mx | a_12 | 26.3137 | 0.0002 | 0.1369 | 12.7827 | 0.4579 | 0.1595 | 12.3546 | 24.3346 | 2.6957 | 9.8595 | 2.2546 | 1.5358 | 0.1957 | 0.0456 | 0.0954 | 2.9242 | 0.188 | 96.3446 |
| G&G | mx | h_4 | 26.4099 | 0.0918 | 0.2405 | 12.7424 | 0.324 | 0.1366 | 12.2086 | 25.1947 | 2.7535 | 10.0855 | 2.321 | 1.2832 | 0.0799 | 0.0602 | 0.0891 | 1.9599 | 0.2561 | 96.2469 |
| G&G | mx | d_26 | 26.1873 | 0.0206 | 0.1892 | 12.5785 | 0.4951 | 0.1095 | 12.0652 | 24.3914 | 2.6415 | 9.8971 | 2.2495 | 1.5482 | 0.1785 | 0.0481 | 0.1071 | 3.5253 | 0.228 | 96.4701 |
| G&G | mx | d_23 | 26.2017 | 0.0337 | 0.2153 | 12.6743 | 0.4263 | 0.1489 | 12.0846 | 24.1313 | 2.7829 | 9.8029 | 2.1991 | 1.5235 | 0.1466 | 0.0555 | 0.1002 | 3.0053 | 0.2065 | 95.7486 |
| G&G | mx | d_17 | 26.2385 | 0.0002 | 0.211 | 12.652 | 0.5886 | 0.1076 | 11.889 | 23.7408 | 2.6284 | 9.6117 | 2.1762 | 1.5324 | 0.1253 | 0.1073 | 0.1013 | 4.3931 | 0.2132 | 96.3266 |
| G&G | mx | a_4 | 26.2931 | 0.0002 | 0.2251 | 12.7011 | 0.6141 | 0.105 | 12.1928 | 23.7912 | 2.4923 | 9.2825 | 2.1485 | 1.2522 | 0.0936 | 0.013 | 0.0921 | 4.7834 | 0.1689 | 96.2591 |
| G&G | mx | h_17 | 26.0457 | 0.0002 | 0.2341 | 12.4996 | 0.6388 | 0.1305 | 11.8924 | 23.6246 | 2.4106 | 9.3399 | 2.2095 | 1.5604 | 0.1217 | 0.0699 | 0.1324 | 4.7418 | 0.2513 | 95.9134 |
| G&G | mx | d_11 | 26.3352 | 0.0165 | 0.2252 | 12.7669 | 0.5421 | 0.1508 | 11.7684 | 23.8729 | 2.4723 | 9.7149 | 2.1951 | 1.5482 | 0.1143 | 0.023 | 0.0937 | 4.057 | 0.2064 | 96.1129 |
| G&G | mx | d_14 | 26.1723 | 0.0273 | 0.2859 | 12.5441 | 0.7013 | 0.1269 | 11.5669 | 23.0388 | 2.5481 | 9.3282 | 2.301 | 1.5875 | 0.1766 | 0.056 | 0.1302 | 5.2452 | 0.2668 | 96.1131 |
| G&G | mx | b_9 | 26.3418 | 0.0002 | 0.2139 | 12.7448 | 0.5969 | 0.1137 | 12.0889 | 23.763 | 2.4991 | 9.4669 | 2.2067 | 1.4254 | 0.1216 | 0.0879 | 0.0999 | 4.4053 | 0.1968 | 96.3828 |
| G&G | mx | c_5 | 25.9426 | 0.0002 | 0.3125 | 12.3801 | 0.728 | 0.1076 | 11.9269 | 22.7732 | 2.5074 | 9.1779 | 2.0364 | 1.1322 | 0.105 | 0.0794 | 0.1531 | 6.0068 | 0.2107 | 95.59 |
| G&G | mx | f_2 | 25.8357 | 0.0002 | 0.2105 | 12.4116 | 0.6205 | 0.1098 | 11.7443 | 23.3804 | 2.5707 | 9.4937 | 2.2486 | 1.6623 | 0.1562 | 0.047 | 0.1154 | 4.2806 | 0.2033 | 95.1008 |
| G&G | mx | g_4 | 25.9585 | 0.0002 | 0.1134 | 12.5846 | 0.3002 | 0.0666 | 12.2263 | 25.4345 | 2.8604 | 10.3235 | 2.1658 | 1.3248 | 0.1529 | 0.0776 | 0.0571 | 1.2255 | 0.219 | 95.1009 |
| G&G | mx | c_4 | 26.0487 | 0.0002 | 0.2374 | 12.454 | 0.6786 | 0.1209 | 11.6775 | 23.4964 | 2.4982 | 9.5806 | 2.3356 | 1.6643 | 0.1608 | 0.0001 | 0.1326 | 4.8791 | 0.2184 | 96.1934 |
| G&G | mx | h_5 | 26.2513 | 0.007 | 0.1353 | 12.7168 | 0.4503 | 0.0668 | 12.2837 | 25.1388 | 2.7237 | 9.8637 | 2.2459 | 1.2829 | 0.057 | 0.0667 | 0.0912 | 2.3996 | 0.3409 | 96.1316 |
| G&G | mx | i_7 | 26.0598 | 0.0002 | 0.1114 | 12.6493 | 0.1322 | 0.1129 | 13.1223 | 25.5602 | 2.8067 | 10.2999 | 2.3102 | 1.4023 | 0.0907 | 0.0063 | 0.0419 | 0.4775 | 0.3145 | 95.5083 |
| G&G | mx | f_4 | 26.0835 | 0.0002 | 0.1158 | 12.6547 | 0.5239 | 0.0976 | 12.1934 | 24.3545 | 2.6166 | 9.7809 | 2.2733 | 1.2991 | 0.0869 | 0.0881 | 0.0733 | 2.8216 | 0.5052 | 95.5786 |
| G&G | mx | b_8 | 26.16 | 0.0002 | 0.1191 | 12.6472 | 0.4249 | 0.0827 | 12.691 | 24.8409 | 2.7046 | 9.8285 | 2.3495 | 1.3125 | 0.1203 | 0.0631 | 0.0741 | 2.3213 | 0.3802 | 96.1301 |
| G&G | mx | i_2 | 26.1437 | 0.0002 | 0.1132 | 12.7446 | 0.1036 | 0.1387 | 12.9698 | 25.5477 | 2.7407 | 10.3523 | 2.3511 | 1.404 | 0.1298 | 0.1002 | 0.0362 | 0.3607 | 0.2522 | 95.4987 |
| G&G | mx | d_13 | 26.1478 | 0.0002 | 0.1204 | 12.6425 | 0.4611 | 0.1007 | 12.5858 | 24.9155 | 2.6254 | 9.9456 | 2.1672 | 1.2387 | 0.0877 | 0.0569 | 0.1014 | 2.4851 | 0.3711 | 96.0631 |
| G&G | mx | d_29 | 25.966 | 0.0042 | 0.1692 | 12.5129 | 0.523 | 0.0984 | 12.4869 | 24.3551 | 2.5489 | 9.6848 | 2.1606 | 1.2807 | 0.1368 | 0.0691 | 0.0874 | 2.784 | 0.495 | 95.373 |
| G&G | mx | i_14 | 25.7965 | 0.0002 | 0.1271 | 12.4431 | 0.2517 | 0.0879 | 12.7295 | 25.1495 | 2.6792 | 10.0047 | 2.3809 | 1.419 | 0.1314 | 0.0665 | 0.0458 | 1.2742 | 0.371 | 94.9682 |
| G&G | mx | h_15 | 26.0224 | 0.0467 | 0.1775 | 12.5686 | 0.1459 | 0.1543 | 12.7427 | 25.5006 | 2.8306 | 10.3018 | 2.2929 | 1.4477 | 0.1414 | 0.0001 | 0.0356 | 0.4706 | 0.3639 | 95.2533 |
| G&G | mx | d_20 | 26.1874 | 0.0002 | 0.113 | 12.7228 | 0.4227 | 0.1018 | 12.6347 | 24.5835 | 2.6701 | 9.8175 | 2.1987 | 1.376 | 0.1556 | 0.0767 | 0.1026 | 2.3242 | 0.4078 | 95.9053 |
| G&G | mx | d_10 | 25.9729 | 0.0002 | 0.1173 | 12.6204 | 0.1569 | 0.1675 | 12.4523 | 25.5463 | 2.7382 | 10.2008 | 2.5027 | 1.5635 | 0.1888 | 0.129 | 0.0407 | 0.2773 | 0.4652 | 95.15 |
| G&G | mx | i_5 | 26.0073 | 0.0002 | 0.1159 | 12.5923 | 0.4219 | 0.0438 | 12.6181 | 24.8042 | 2.692 | 9.9904 | 2.1757 | 1.1074 | 0.0788 | 0.0301 | 0.0745 | 2.201 | 0.4067 | 95.3703 |
| G&G | mx | h_1 | 26.3807 | 0.2371 | 0.5058 | 12.4924 | 0.3948 | 0.0676 | 12.6895 | 24.4817 | 2.6255 | 9.7757 | 2.1019 | 1.1243 | 0.0622 | 0.0295 | 0.0777 | 1.9144 | 0.402 | 95.3728 |

# Appendix 4
# TEXTURAL CONSTRAINTS ON MONAZITE CHEMICAL AGES

## A4.1 Introduction

A total of eighteen samples were selected from the southern Curnamona Province (SCP) and petrographically analysed for their metamorphic history and the textural relationship of monazite with major silicate phases. Following are descriptions on the textural siting of monazite grains in all samples analysed using the EPMA chemical monazite age technique. Sample localities of monazite that records Mesoproterozoic metamorphism are listed in Table 3.1. Sample localities of monazite that records Delamerian reworking are listed in Table 7.1. From a combination of monazite textural position, mean chemical age and composition, four major monazite groups were identified. Following is a description of the petrography, textural position and chemical ages of monazites in each group. Where possible, the metamorphic assemblage and dominant fabric in each sample is related to the regional metamorphism and structure as defined for the terrain (Clarke et al., 1986; 1987; 1995; Laing et al., 1996b; Laing et al. 1978; Stuwe & Ehlers, 1997; Wilson & Powell, 2001).

## A4.2 Group 1: early $M_1$, intermediate- to high-yttrium

The oldest chemical ages are recorded from metapelitic lithologies in both the Broken Hill and Olary Domains. Early growth of monazite is recorded as inclusions within porphyroblastic silicate phases such as andalusite and garnet. A garnet-sillimanite-cordierite-mica metapelitic gneiss from near Round Hill (***RND***) has leucocratic stringers of quartz, garnet and feldspar separated by sillimanite and biotite layers. This layering is axial planar to the $F_2$ Broken Hill Antiform, but may alternatively developed during $D_1$ partial melting (Laing et al., 1978). Monazite grains included by coarse-grained sillimanite (*1612 ± 18 Ma*) have relatively high concentration of Y (~1.371 wt%) potentially reflecting the absence of garnet forming reactions at this time. Monazites included within matrix biotite (*1601 ± 42 Ma*) have relatively low Y (~0.4 wt%) indicating garnet crystallisation occurred prior to monazite growth. growth began prior to this. These ages are interpreted to reflect $D_1$ and/or $D_2$ ages.

Syn-kinematic garnet porphyroblasts (~1 cm) in the Southern Cross mine region (***SC2***) are enveloped by sillimanite-fibrolite-biotite fabric elements with a muscovite-quartz matrix. Micas with monazite included in them record a chemical age of *1594 ± 17 Ma*. They have relatively high-Y content (~0.96 wt%), potentially reflecting partial breakdown of garnet by the time of fabric development ($S_2$; Wilson & Powell, 2001). A garnet-sillimanite-biotite-muscovite metapelitic unit (***PS***) forms rare interbedded units within the Hores Gneiss, which is interpreted as metamorphosed rhyodacitic crystal lithic ashflow tuff (Willis et al., 1983). The interbedded metapelitic units are strongly foliated, defined by sillimanite and bands of fine- to very fine-grained matrix of predominantly muscovite ( quartz). The fabric is interpreted to be axial planar to the $F_2$ Broken Hill Antiform (Laing et al., 1978). Some muscovite forms oval shaped aggregates, possibly after cordierite. Garnet porphyroblasts are flattened along foliation plane, with some containing fibrolite inclusions that are orientated at an angle to the pervasive sillimanite-mica fabric. All analysed are included within the mica matrix (*1601 ± 18 Ma*), which is interpreted to represent the maximum age of development of the $S_2$ at this locality. Monazites have relatively high Y contents (~0.99 wt%) indicating they crystallised either prior to garnet growth, or after partial garnet breakdown.

Metapelitic lithologies in the upper-greenschist to amphibolite Olary Domain also record the early Olarian Orogeny ages. Pristine andalusite-garnet-staurolite-mica metapelites (***NWI5***) contain large andalusite porphyroblasts (<5 cm) with multiple monazite inclusions *1607 ± 17 Ma*. Monazite Y composition reflects growth either prior to, or at the onset of garnet growth as indicated by relatively high-Y (0.8 wt%). Garnet-fibrolite-biotite-muscovite-chloritoid metapeltic units from Ameroo Hill (***AH5C***) are interpreted to record near post-peak metamorphic conditions. Garnet porphyroblasts (<1 cm) within this lithology have distinctive poly-metamorphic garnet growth. Monazite aggregates have developed within fractures. Such textural settings are highly susceptible to fluid induced crystallisation (Gibson et al., 2004b). Monazites have a mean chemical age of *1605 ± 30 Ma*, with relatively high-Y contents (~1.4 wt%), indicating partial garnet breakdown prior to monazite recrystallisation. High Ca, low Mg Delamerian garnet rims overgrow the dominant penetrative fabric in this sample, interpreted to be $S_2$ of Laing (1996b). Static growth of post-kinematic chloritoid dominates this sample. Chloritoid growth is likely related to the growth of garnet rims.

Granitic gneiss lithologies including the Rasp Ridge Gneiss (***RRQ***) and Alma Gneiss (***ALM***) have SHRIMP U-Pb isotopic igneous crystallisation ages of 1704 ± 3 Ma and 1683 ± 3 Ma, respectively (Page et al., 2000; 2003). ***RRQ*** is a plagioclase-quartz-biotite-garnet gneissic lithology with leucosomes and melanosomes defining the fabric. Garnet stringers are flattened within the fabric and pervasively fractured. Monazites (50 – 150 m) included within the fractured garnet porphyroblasts have a mean chemical age of *1591 ± 17 Ma*. Relatively high Y contents (~1.53 wt%) of the monazites indicate that monazite growth likely occurred after partial breakdown and fracturing of the garnet porphyroblasts. The Alma Gneiss (***ALM***) lithology analysed is located in the core of the Broken Hill Synform (Laing et al., 1978). A sillimanite-quartz-feldspar-garnet-biotite granitic gneiss has a foliation defined by biotite and coarse-grained sillimanite ($S_2$; Laing et al., 1978). At least one high-grade fabric predates the biotite fabric, preserved as oriented fibrolite inclusions within plagioclase. The biotite foliation overgrows or replaces garnet, often forming coronas. Monazites analysed (25 – 100 m) in this sample which are occluded by plagioclase have a mean chemical age of *1596 ± 22 Ma*. Relatively high Y content in these monazites (~0.96 wt%) implies they crystallised prior to the growth of garnet. It is unclear when plagioclase crystallised in relation to fabric development, but is tentatively correlated with $S_2$. Monazites occluded by coarse-grained sillimanite are distinctly different in mean age than those occluded by plagioclase, and have been assigned to *Group 3*. The zircon crystallisation age of 1704 ± 3 Ma and 1682 ± 3 Ma for the Alma Gneiss and Rasp Ridge Gneiss (Page et al., 2000), was

not preserved by monazite in this study.

**A4.3 Group 2: peak $M_1$, low- to intermediate-yttrium**

A garnet-cordierite-sillimanite-feldspar-biotite gneissic metapelitic lithology (***CUES***) from the Cues Formation, lower Thackaringa Group, contains monazite included within all major silicate phases. Prominent gneissic layering in this sample interpreted to be axial planar to the Broken Hill Synform ($F_2$; Laing et al., 1978). Although this layering may represent an anisotropy associated with an $F_1$ structure, it is interpreted to represent $S_2$ (Laing et al., 1978). Cordierite ubiquitously replaces and/or forms embayment into pervasively fractured garnet porphyroblasts, forming classic decompression textures (Swapp & Frost, 2003). Analysed monazites (50 – 100 m) are occluded by plagioclase, cordierite, garnet and sillimanite, have mean chemical ages of *1591 ± 50 Ma*, *1587 ± 23 Ma*, *1586 ± 20 Ma and 1585 ± 31 Ma*, respectively. High Y contents in monazite occluded by garnet, cordierite and sillimanite (~1.2 – 2.0 wt%) suggest monazite growth occurred prior to the crystallisation of garnet. Monazites occluded by K-feldspar have a mean age of *1575 ± 30 Ma*. These monazite also have relatively high Y contents (~0.97 wt%), although there are too few analyses to make any major inferences.

Another andalusite-garnet-staurolite-mica metapelitic unit (***NWI3***) from the northern Weekeroo region is partly retrogressed, characterised by replacement of andalusite by muscovite and sericite. Euhedral garnet and staurolite inclusions are observed within the andalusite porphyroblasts. All monazites that were analysed were included within the partly retrogressed andalusite porphyroblasts. They have a mean chemical age of *1589 ± 26 Ma*. Y contents in the monazites from both samples are relatively high (~1.2 wt%), indicating monazite crystallised prior to garnet growth, or after partial garnet breakdown. A strong chlorite-muscovite–biotite-quartz fabric wraps around, and overprints the andalusite porphyroblasts ($S_3$; Grady et al., 1989). Static growth of staurolite and garnet overgrows this foliation, and therefore represent another generation of staurolite and garnet growth.

**A4.4 Group 3: post-peak $M_1$, intermediate- to high-yttrium**

A garnet-sillimanite-mica metapelitic unit from Round Hill (***RND***) has garnet porphyroblasts (~1.5 cm) that are attenuated and fractured within a pervasive fabric, indicating that the pervasive fabric post-dates garnet growth. Garnet porphyroblasts may also be partially retrogressed to a sillimanite-fibrolite-mica-quartz assemblage. Multiple monazites (50 – 150 m) analysed from within the fractured garnet, have a mean chemical age of *1570 ± 18 Ma*. The relatively high Y content of the monazites (~0.72 wt%) is interpreted to be due to the partial breakdown of garnet, and therefore the chemical age likely represents the timing of hydrous retrogression. A garnet-sillimanite-biotite-feldspar-quartz metapelitic granulite (***R899***) from the Mingary region, in the western Broken Hill Domain, is interbedded with a NNE trending two-pyroxene granulite. The unit is moderately foliated, defined by biotite and aggregates of felsic minerals. Garnet porphyroblasts are pervasively fractured, often infilled or entirely replaced by biotite and chlorite. The relationship between garnet porphyroblasts and the fabric is inconclusive, as the foliation both wraps around garnet, and is overprinted by garnet. The mean chemical age of matrix monazites (40 – 150 m) included within biotite is *1554 ± 17 Ma*. Monazite included within plagioclase have a mean chemical age of *1560 ± 38 Ma*. Monazite included within the fractured garnet porphyroblasts have a mean chemical age of *1542 ± 27 Ma*. All the monazites analysed in this sample have relatively low Y contents (~0.2 – 0.4 wt%). This is interpreted to be reflect that earlier garnet growth consumed most of the available Y budget.

An altered and strongly foliated and mineralised mica-magnetite-quartz lithology (***CB6***) from adjacent to the Copper Blow Cu-Au prospect was analysed. Relic clinopyroxene in this mineralised sample indicates that a mafic protolith is also part of the sequence. Strong Fe-alteration preceded or accompanied fabric formation, presumably associated with shear zone movement ($S_3$; Corbett & Phillips, 1981). Only one monazite was analysed (~80 m), located at a quartz triple point. This monazite has compositional zoning evident from BSE image, related to differences in Th content (~4 – 12 wt%). When data is grouped together relative to their position in relation to the compositional zoning on the BSE image, there is no correlation between compositional zones and age domain. The monazite has a mean chemical age of *1554 ± 18 Ma*. Y contents in this lithology is relatively low (~0.4 wt%), likely as a result of the growth of garnet in adjacent lithologies.

Two foliated retrogressed metapelitic schist from the northern Weekeroo region (***WW18*** and ***OL3D***), north of the Walter-Outalpa shear zone, have euhedral garnet and staurolite crystals contained within sericite-muscovite pseudomorphs after andalusite. Sample ***WW18*** located 600 m north of the shear zone, contains flattened euhedral garnets within the pseudomorphs defining a trend at a high angle to the pervasive fabric that is defined by matrix minerals (biotite-muscovite-quartz; $S_3$ of Grady et al., 1989). Garnet porphyroblasts typically are polymetamorphic, with distinctive post-kinematic rims. However, in other sample from the same area as ***WW18***, the garnet overgrowths are interpreted to be syn-kinematic. Static growth of post-kinematic staurolite is pervasive in this sample, and indicates that there is two generations of staurolite growth. All monazite analysed in sample ***WW18*** were from the mica matrix, and are relatively low in Y contents (~0.6 wt%) suggesting crystallisation after garnet growth. The mean chemical age for monazite in sample ***WW18*** is *1573 ± 29 Ma*. Sample ***OL3D*** is located ~1 km northeast of ***WW18***, from the same metapelitic lithology. Ellipsoidal phengite-sericite-muscovite pseudomorphs are preserved within a chlorite-muscovite-biotite-quartz matrix. The pseudomorphs have a core composed of very fine- to fine-grained phengite, sericite and quartz, which are surrounded by a rim of fine- to medium-grained quartz, muscovite, biotite and chlorite. Garnet occurs as inclusions preserved in the pseudomorphs, although they overgrow the internal foliation preserved within the pseudomorphs. This suggests they grew after retrogression. All monazite analysed were from the strongly foliated matrix, and have a mean chemical age of *1559 ± 16 Ma*. These monazites have relatively high Y contents (~1.1 wt%), indicating that that grew after partial breakdown of pre-existing garnet.

Monazite occluded by coarse-grained sillimanite in the felsic Alma Gneiss (***ALM***) have younger mean chemical age ages than those occluded by plagioclase in the same sample. The Mean chemical age of monazite included within sillimanite is *1565 ± 22 Ma*. Y contents

of these monazites is relatively high (~0.9 wt%), potentially reflecting partial breakdown of garnet in the sample. Another sample of the Rasp Ridge Gneiss (***RR2***) from the Broken Hill town (Block 10 locality) with monazite inclusions (50 – 100 m) in feldspars were analysed. The lithology at this locality is a quartz-feldspar-biotite felsic gneiss that contains a weak foliation defined by biotite (axial planar to the Hanging Wall Synform; $S_2$ of Laing et al., 1978). Mean chemical ages from monazite occluded by plagioclase are *1571 ± 29 Ma*, whereas those occluded by K-feldspar are *1547 ± 24 Ma* (n=44). The relatively high Y contents of monazites in sample ***RR2*** (~2.5 wt%) likely due to the absence of garnet at this locality, or due to the complete breakdown of garnet.

### A4.5 Group 4: early $M_2$, intermediate- to high-yttrium

Metapelitic samples from the western Broken Hill Domain are represented by foliated garnet-biotite-muscovite-feldspar-quartz lithologies. Fabrics are primarily defined by biotite and muscovite, in addition to felsic mineral aggregate stringers (quartz + feldspar). Sample ***TH*** from the Thackaringa Hills region has pervasively fractured garnet porphyroblasts (<2 mm), some of which have biotite coronas. Other garnet porphyroblasts postdate fabric formation and are less fractured. Monazites included (50 – 150 m) within matrix biotite and feldspar were analysed. Monazite occluded by biotite have a mean chemical age of *529 ± 28 Ma*, whereas monazites growth along the grain boundary between biotite and plagioclase have a mean age of *503 ± 21 Ma*. Monazite occluded by only plagioclase have a mean age of *539 ± 19 Ma*. All analysed monazite have relatively high Y contents (~1.6 wt%), indicating they recrystallised after breakdown of residual Mesoproterozoic garnet.

Another garnet-chlorite-biotite-muscovite-feldspar-quartz metapelite (***MU***) from the Mingary region in the western Broken Hill Domain is intensely retrogressed, with a very fine-grained matrix composed primarily of muscovite (+ sericite?). Monazites analysed from this sample are from entirely within the matrix. The morphology of these monazites is highly irregular, suggesting they grew or recrytallised during a high fluid/rock ratio regime (Gibson et al., 2004). The mean chemical age for these monazites is *506 ± 17 Ma*. Monazite grains have relatively high Y contents (~1 wt%), reflecting partial garnet breakdown prior to monazite crystallisation.

A foliated garnet–staurolite–biotite metapelitic schist (***GST***) contains small post-kinematic garnets (<2 mm) overgrowing the foliation. Syn- and post-kinematic staurolite (<5 mm) have inclusions of anhedral monazite (100 **m**m). Two separate monazites from these late-stage staurolites were analysed. They have complex compositional patterns as detected by the BSE images, due to variations between 4-10 wt% Th. One of the monazites has a bimodal age distribution with mean ages at *545 ± 42 Ma* and *1511 ± 42 Ma*. The other monazite had a single mean age of *513 ± 19 Ma*. The Cambrian age component of this sample reduced to a mean age of *525 ± 19 Ma*. A coarse-grained kyanite-biotite schist (***KY2***) from near the same locality as sample ***GST*** has large post-kinematic kyanite blade (<3 cm). Monazites (~70 **m**m) included within these kyanite blades have complicated compositional zoning when viewed by BSE imaging. This variation is due to differences in Th content (~1 – 4 wt%). No relationship was observed between compositional domains and apparent age. The mean chemical age of monazite included within kyanite is *517 ± 25 Ma*. Relatively high Y contents (~1.3 wt%) of the monazites in ***KY2*** are interpreted to be due to the absence of garnet in this sample, possibly through its consumption during retrograde metamorphism.

# Appendix 5
# ALKALINE MAGAMATIC ROCK SUMMARY

**A5.1.** Sample localities of alkaline magmatic phases from the Billeroo alkaline magmatic complex.

| Sample # | RN# | Northing | Easting | Lithology |
|---|---|---|---|---|
| **BN1** | 493975 | 6475861 | 397095 | ijolite |
| **BN2** | 493991 | 6476152 | 396880 | syenite |
| **BN3** | 493976 | 6476169 | 396885 | ijolite |
| **BN4** | 493977 | 6475877 | 397125 | ijolite |
| **BN5** | 493978 | 6475877 | 397125 | ijolite |
| **BN6** | 493985 | 6475867 | 397139 | dyke |
| **BN7** | 493986 | 6475867 | 397139 | dyke |
| **BN8** | 493979 | 6475875 | 397122 | ijolite |
| **BN9** | 493980 | 6475895 | 397142 | ijolite |
| **BN10** | 493981 | 6475897 | 397144 | ijolite |
| **BN11** | 493987 | 6475865 | 397093 | dyke |
| **BN12** | 493982 | 6475882 | 397105 | ijolite |
| **BN13** | 493983 | 6475887 | 397107 | ijolite |
| **BN14** | 493984 | 6475882 | 397114 | ijolite |
| **BN15** | 493988 | 6475975 | 396867 | syenite |
| **BN16** | 493989 | 6475975 | 396867 | syenite |
| **BN17** | 493990 | 6476107 | 396786 | syenite |
| **PIRSA*** | 474884 | ? | ? | ijolite? |
| **PIRSA*** | 474885 | ? | ? | syenite |
| **PIRSA*** | 474886 | ? | ? | syenite |
| **PIRSA*** | 474887 | ? | ? | ijolite |
| **PIRSA*** | 474888 | ? | ? | porph syen |

* Sample collected by PIRSA before this study, GPS locations unknown

**A5.2.** Detailed petrographic descriptions of samples discussed in *Chapter 5*.

***Petrological description in order of increasing silica:***

**R493982 (BN12): *Feldspathic porphyritic ijolite***
Hand specimen: dark grey-green colour. Visible dark-purple garnet (<2mm). Light-green speckly mineral – probably pyroxene appears altered. Larger lighter grey mineral probably feldspar (<3mm). One of the coarser-grained varieties.
Thin section: alb, pyx, canc, ne, gt, phl, sph, mag, soda, apa.

Medium-grained porphyritic feldspathic ijolite. Albite phenocrysts and cumulophyric pyroxenes often pseudomorphed by garnet phlogopite symplectites. Pseudomorphs often rimmed by magnetite. Sphene-magnetiteilmenite also apparently pseudomorph presumably pyroxene (or amphibole?). Garnet grows as fine-grained euhedral to sub-euhedral aggregates. Relict pyroxene preserved in some pseudomorphs, often with visible zoning (dark green and brown varieties). Fabric defined by coarse dark and light coloured stringers of magnetite-sphene, garnet-phlogopite and albite-nepheline. Albite phenocrysts rimmed by fine-grained albite-nepheline-sodalite (mantled porphyroclast?). Matrix composed of albite-nepheline-cancrinite-sodalite aggregates possibly recrystallised. Some albite phenocrysts fractured and infilled by matrix minerals. Definite textures affiliated with dynamic metamorphism.

| | |
|---|---|
| alb | 35% |
| phl | 15% |
| pyx | 10% |
| gt | 10% |
| ne+canc | 10% |
| sph | 8% |
| mag | 7% |
| soda | 3% |
| apa | 2% |

**R474887: *Ijolite augen gneiss (see RS474884)***
Hand specimen: Foliated rock similar to RS474884 with phl-gt aggregates.
Thin section: alb, pyx, canc, ne, gt, phl, sph, mag, haem, soda, apa, anal?

Partly recrystallised augen of nepheline? (3mm) with triangular hexagonal microlites of haematite or ferrian ilmenite. Large sphene enclosing oxides, with separate aggregates of oxide (3mm). Sphene also without inclusions. Both haematite and magnetite within in sphene and nepheline-cancrinite aggregates. All fine-grained and recrystallised. Phlogopite and fine-grained garnet aggregates possibly after pyroxene. Massive garnet aggregates (6mm). Recrystallised nepheline, cancrinite and possibly analcime and sodalite in a micromosaic texture. Apatite needles (2mm). Less deformed sample than RS474884 with more euhedral crystals replaced by phlogopite-garnet, but has been altered, recrystallised and veined. (*Pontifex & Associates Report 8111, 24/7/01*)

**R493978 (BN5): *Feldspathic ijolite***
Hand specimen: Dark-grey colour, greenish speckly tinge. Finer-grained variety. Visible light-grey almost clear mineral (<1mm). Speckly green mineral probably pyroxene. Ruby purple garnets not visible as in last sample.
Thin section: alb, ne, gt, phl, sph, canc, mag, soda, apa.

Fine-grained feldspathic ijolite. Schistose character with alternating light and dark thin bands. Light bands composed of albite, nepheline, cancrinite and abundant sodalite. Dark bands composed of garnet-phlogopite and sphene-magnetite stringers. Pyroxenes apparently entirely replaced by garnet-phlogopite pseudomorphs. Microphenocrysts of albite wrapped by foliation occasionally. Other microphenocrysts composed of mosaic aggregate of albite. Epidote appears late in crystallisation history. Garnet is anhedral to subanhedral aggregates. Dynamic recrystallisation interpreted to by dominant in this sample.

| | |
|---|---|
| alb | 35% |
| neph | 15% |
| gt | 10% |
| phl | 10% |
| sph | 8% |
| mag | 7% |
| soda | 10% |
| canc | 5% |

**R493983 (BN13): *Feldspathic ijolite***
Hand specimen: Dark-grey colour; green, ruby red, and bluish tinges. Coarser-grained variety similar in appearance and mineralogy to BN12. Pervasive fabric defined by green and red mineral bands. Garnet sizes <2mm.
Thin section: alb-pyx-canc-ne-phl-sph-gt-mt-soda.

Alternating dark (mt-sph-pyx-phl-gt) and light (ne-canc-alb-soda) bands. Light bands commonly have microphenocrystic albite, wrapped around by f-g matrix of alb-neph-canc. Canc frequently coarser and rims alb, replacement-type texture. Pyx-rich clots common in dark bands. Pyx has zoned appearance. Mottley brown Mg-rich cores often rimmed by bright green pleochroic Na-variety. Both types strongly birefringent. Sodic variety not always bright green. Symplectic replacement of pyx by phl-epi or more frequently

pseudomorphed by gt-phl. Pyx rimmed by mt(-ilm?)-sph.

| | |
|---|---|
| alb | 35% |
| pyx | 15% |
| canc | 10% |
| phl | 10% |
| ne | 7% |
| sph | 7% |
| gt | 7% |
| epi | 3% |
| mt | 3% |
| others | 3% |

**R493977 (BN4):** ***Feldspathic ijolite***
Hand specimen: Dark grey fine-grained (<1mm) variety similar to BN5. Greenish tinge, probably phlogopite. Pervasive fabric with stringers of sphene-magnetite and phlogopite. Has a grimy green sericitised appearance?
Thin section: gt-phl-apa-sph-rut-ilm-epi-Kspar-canc-ne-alb-pyx-mag-calc.

Fine-grained feldspathic ijolite. Schistose character with alternating light and dark thin bands. Light bands composed of albite, nepheline, cancrinite, and sodalite. Dark bands composed of garnet-phlogopite and sphene-magnetite stringers. Sphene nearly always rimmed by magnetite. Pyroxenes apparently entirely replaced by garnet-phlogopite pseudomorphs. Microphenocrysts of albite composed of mosaic aggregate of albite. Epidote appears late in crystallisation history. Garnet is anhedral to subanhedral aggregates. Cancrinite appears primary, although could form from reaction between other phases. Several generations of sphene growth interpreted based on colour and shape.

| | |
|---|---|
| alb | 30% |
| neph | 15% |
| canc | 10% |
| gt | 10% |
| phl | 10% |
| sph | 8% |
| pyx | 5% |
| K-spar | 5% |
| mag | 5% |
| ilm+rut | tr |
| apa | tr |

**R493979 (BN8):** ***Feldspathic-muscovite ijolite***
Hand specimen: Dark-grey with light-grey/white bands of coarse-grained variety unlike any other. Whitish bands probably feldspar-nepheline-cancrinite aggregate. Pervasive fabric in this sample. Green-tinge probably phlogopite.
Thin section: alb-mu-phl-canc-sph-apa-epi-calc-ilm-mag-?calc.

Pervasive schistose character to this sample, dominated by colourless minerals. Unlike any samples described previously. Thin green-black stringers of phlogopite and magnetite define foliation in thin sections. White bands of albite, cancrinite, and fine-grained muscovite also form bands. Microphenocrysts of sphene and albite often wrapped by foliation. Some albite phenocrysts composed of micromosaic albite aggregates. Relationship of muscovite to crystallisation order unknown, it forms intergrowths with cancrinite and albite in matrix, but coarser-grained muscovite appears to be late in other areas of this section. Manky sphene not as abundant in this sample – euhedral prismatic forms dominate and appear to be late in crystallisation order. Some albite microphenorysts appear to have undergone brittle deformation forming domino boudins with dextral shear in this sample.

| | |
|---|---|
| alb | 40% |
| canc | 15% |
| mu | 10% |
| phl | 10% |
| mag | 8% |
| sph | 6% |
| epi | 5% |
| apa | 3% |
| K-spar | 3% |
| calc? | tr |

**R493976 (BN3):** ***Feldspathic epidotised ijolite***
Hand specimen: Lighter-grey colour. Coarse-grained, highly ?altered variety. Strong ruby purple mineral (<3mm), and greeny-yellow tinge. Greenish-yellow and grey bands define pervasive foliation in this sample.
Thin section: alb-phl-pyx-gt-epi-ne-sph-soda-mag-(Sr-Na-Ba)-silicates.

Alternating layers of clear minerals and darker layers of garnet-phlogopite with or without sphene. Lighter bands composed of aggregates of nepheline and albite. Albite porphyroclasts often mantled by fine-grained albite indicative of recrystallisation. Abundant fine-grained epidote in lighter-bands. Garnet-phlogopite symplectites after pyroxene. Garnet grows as euhedral to subeuhedral aggregates. Highly altered ijolite. Na-Ca-Fe alteration dominate. Effects of metamorphism more pronounced in this rocks, possibly related to adjacent syenite intrusion and/or pegmatite.

| | |
|---|---|
| alb | 35% |
| ne | 15% |
| gt | 15% |
| phl | 10% |
| epi | 10% |
| sph | 5% |
| mag | 5% |
| pyx | 3% |
| other | 2% |

**R474884:** ***Ijolite?***
Hand specimen: Strongly foliated rock with grey and yellow components. K-spar staining picked out phlogopite-garnet aggregates.
Thin section: neph-canc-phl-gt-pyx-sph-opaq-anal-soda-apa.

Almost mylonitic augen gneiss (2mm diameter) composed of nepheline but apparently free of K. Augen within layered coloured and uncoloured matrix. Colourless include nepheline-cancrinite, analcime-sodalite. Some lenses almost certainly recrystallised analcime. Pale-yellow phlogopite and fine-grained granular garnet aggregates derived from pre-existing pyroxene. Aggregates also contain blue, green or yellow prismatic minerals (aegirine or acmite, and/or Zr-Ti silicates such as lavenite and neptunite?) Rare large blocky bright-green grains with high birefringence are aegirine. Large aggregates of sphene also disseminated, with inclusions of oxides. Prisms of apatite (0.6mm). Oxide also disseminated as very small grains and larger masses, locally with narrow rims of sphene. Former ijolite is probable. (*Pontifex & Associates Report 8111, 24/7/01*)

**R493984 (BN14):** ***Ijolite***
Hand specimen: Dark-grey very coarse-grained variety with large (up to 1cm) clots of whitish mineral with a pink tinge. Light-grey mineral (<2mm) and greenish yellow stringy mineral define foliation. Almost porphyritic like texture to this sample.

Thin section: alb-canc-phl-gt-ne?-mt-sph-epi-mu-Ksp-cal?

Alternating dark/light bands. Coarser variety. Light bands contain large alb phenocrysts with multiple twinning. Pyx commonly pseudomorphed by phl, others replaced by mt-sph. Epidote orientated with matrix fsbric – either reorientated or syn-kinematic. Epi not involved with replacement textures. Phl-mt stringers define foliation. Light-bands canc-rich, with alb and minor K-spar. Abundant canc – often coarser then alb-ne? aggregates. Canc xtals flattened in foliation – pre-kinematic.

| | |
|---|---|
| alb | 40% |
| canc | 20% |
| phl | 15% |
| mt | 6% |
| sph | 6% |
| epi | 5% |
| K-spar | 3% |
| mu | 3% |
| calc? | 2% |

**R493987 (BN11):** ***Lamprophyre dyke***
Hand specimen: Dark-grey fine-grained dyke phase with a speckly green-yellow mineral. Coarse light-browny white aggregate (<5mm) occurs within matrix.
Thin section: alb-canc-ne?-mag-epi-soda-apa-sph-gt-phl-calc.

Very fine-grained rock with bands of fine-grained clear minerals composed of aggregates of cancrinite, sodalite and albite. Thin section dominated by Fe-oxides, which are rarer or absent in the lighter bands. Very fine-grained nature of the majority of this rock makes visual identification difficult. However, its mineralogy is typical to that of the ijolites, with abundant apatite.

**R493975 (BN1):** ***Feldspathic porphyritic ijolite***
Hand specimen: Alternating bands of white-brown clotty minerals and light-grey and greeny-yellow stringers. Very coarse-grained in places similar to BN8 and BN14. Strongly foliated appearance. Whitish clots probably feldspar or nepheline-cancrinite-albite aggregate.
Thin section: alb-pyx-gt-epi-ne-phl-mu-canc-sph-mag-Kspar-apa-(Sr-Na) silicates.

Coarser-grained porphyritic variety containing large albite phenocrysts. Strong schistose character. Foliation defined by dark and light bands. Dark bands composed of sphene and magnetite, with the later often rimming the former. Other coarser phases include garnet-phlogopite and relict primary pyroxene. Garnet-phlogopite aggregates have pyroxene inclusions in them. Prismatic shapes to some albite phenocrysts probably represent altered pyroxenes. Some albite phenocrysts appear attenuated and boudinaged, others are domino boudinaged. Lighter bands composed dominantly of micromosaic albite, muscovite but nepheline also common. Phlogopite defines foliation, often wrapping around porphyroclasts and porphyroblasts. Epidote appears late-stage in crystallisation history.

| | |
|---|---|
| alb | 25% |
| ne | 20% |
| phl | 10% |
| gt | 10% |
| canc | 5% |
| pyx | 5% |
| mu | 5% |
| sph | 5% |
| epi | 5% |
| K-spar | 3% |
| Other | 5% |

**R493981 (BN10):** ***Feldspathic porphyritic ijolite***
Hand specimen: Dark-grey porphyritic texture with fine-grained dark-grey matrix with coarse (<5mm) white-brown clots similar to BN14. White clots probably K-feldspar phenocrysts. Slight green-tinge to matrix. Small thin yellow stringers (<0.5mmx2mm).
Thin section: alb-ne-canc-Kspar-phl-epi-gt-sph-apa-soda-calc-mag.

Strongly schistose character to this sample. Foliation defined by phlogopite and fine- to medium-grained bands composed of cancrinite or albite. These wrap the albite and K-feldspar porphyroclasts, some of which have been pulverised with interstitial recrystallised material. Albite phenocrysts have both undulose extinction and tarten twinning in K-feldspars. Magnetite abundant in the matrix, and also is weakly aligned in places parallel top the foliation. Majority of matrix composed of albite, nepheline and phlogopite. Epidote appears late-stage in crystallisation order, and/or grew contemporaneously with cancrinite in lighter bands. Calcite veins crosscut fabric in places. Dynamic recrystallisation dominant in this sample, as are the effects of regional deformation.

| | |
|---|---|
| alb | 35% |
| K-spar | 10% |
| canc | 10% |
| ne | 8% |
| phl | 7% |
| epi | 7% |
| gt | 5% |
| calc | 5% |
| sph | 3% |
| epi | 7% |
| Other | 3% |

**R493988 (BN15):** ***Porphyritic syenite***
Hand specimen: Dark grey-pink potassic syenite. Phenocrysts appear fractured or attenuated with indistinct boundaries (<5x2mm).
Thin section: K-spar-alb-calc-bt-mu-phl-oxides-opaques.

Feldspar-rich rocks with large K-spar phenocrysts, often perthitic within a fine- to medium-grained matrix of feldspar, micas and calcite. The later is a dominant phase in this rock, present as both cross-cutting veins and as part of the matrix. Biotite is iron-rich based on its dark brown-red colour. Sulphides may or may not be present in this sample

| | | |
|---|---|---|
| K-spar | 60% | |
| alb | 15% | overall mineralogy including phenocrysts |
| mica | 10% | |
| calc | 10% | |
| opaq | 5% | |

**R474888:** ***Porphyritic syenite***
Hand specimen: Similar to RS474885&6, but more abundant in other minerals than K-spar.
Thin section: orth-alb-carb-oxide-rutile-mu.

Perthitic orthoclase (25x10mm). Small mass of carbonate in this, with albite, opaque oxide and rutile pseudomorphs after sphene. Rest of rock is inequigranular orthoclase (4mm), abundant patches of fine-grained albite and patches of carbonate enclosing muscovite, rutile or opaque oxide. Euhedral magnetite (0.5mm) aggregates and fluffy leucoxene masses (3mm

long), apparently derived from sphene, are abundant but no biotite. Narrow carbonate veins crosscut all phases. Fine-grained rock is altered. (*Pontifex & Associates Report 8111, 24/7/01*)

| | | |
|---|---|---|
| orth | 70% | mineralogy of f-g part to syenite |
| alb | 15% | |
| carb | 7-8% | |
| oxide | 5% | |
| rutile | 2-3% | |
| mu | 1% | |

**R474886:** ***seri-bt-opaq ox syenite with carb veins***
Hand specimen: Similar syenite to RS474885, with seams of muscovite set between abundant K-spar.
Thin section: Finer-grained but less inequigranular compared with RS474885. Perthitic orthoclase laths (<5mm), commonly fractured and veined by carbonate. Fine-grained orthoclase areas, accompanied by decussate biotite, inequigranular magnetite (0.5mm) and minor albite, are less abundant than RS474885. More abundant, larger masses of schistose sericite (2mm wide), between larger orthoclase crystals, and carbonate more abundant. Orthoclase has abundant fluid inclusions and small inclusions of opaque oxide and biotite. (*Pontifex & Associates Report 8111, 24/7/01*)

| | |
|---|---|
| orth | 75% |
| bt | 7-8% |
| oxide | 4% |
| mu | 7-8% |
| carb | 4% |
| alb | 2% |

**R493991 (BN2):** ***Porphyritic potassic syenite***
Hand specimen: Randomly orientated large K-spar phenocrysts, some apparently fractured. Some are very coarse-grained, up to 10x5mm. Matrix is grey brown, fine-grained and of indistinguishable mineralogy.
Thin section: K-spar-alb-calc-bt-phl-oxides-ilm-apa-opaques.

Feldspar-rich rocks with large K-spar phenocrysts, often perthitic. Very little other mineralogy to this sample apart from feldspar. A little biotite present. Calcite again is a dominant phase. Unclear whether matrix is really just pulverised K-spar and albite. Biotite is iron-rich based on its dark brown-red colour. Sulphides may or may not be present in this sample

| | | |
|---|---|---|
| K-spar | 75% | overall mineralogy including phenocrysts% |
| alb | 10% | |
| calc | 7% | |
| opaq | 5% | |
| mica | 3% | |

**R474885: bt-mu** ***syenite with alb-carb***
Hand specimen: Grey rock with seams of mica (mu?), between abundant K-spar.
Thin section: ortho-bt-mu-oxide-carb-alb.

Abundant perthitic orthoclase as equant to elongate crystals (<10mm). Between orthoclase grains are fine-grained orthoclase with decussate biotite and aggregates of inequigranular opaques (<2mm diameter). Flakes of muscovite and albite disseminated, and irregular seams of muscovite-biotite. Inequigranular carbonate present as elongate grains (<1.5mm). Some carbonate stained by limonite, suggesting Fe-rich. Some biotite altered to chlorite, most fresh. (*Pontifex & Associates Report 8111, 24/7/01*)

| | |
|---|---|
| ortho | 75-80% |
| bt | 7-8% |
| mu | 5% |
| oxide | 3% |
| carb | 2% |
| Alb | 5% |

**R493990 (BN17):** ***Porphyritic potassic syenite***
Hand specimen: Randomly orientated K-spar phenocrysts, some apparently fractured. Range in size from 0.5x2mm to 2x6mm. Matrix grey, very fine-grained matrix of indistinguishable mineralogy.
Thin section: K-spar-alb-bt-phl-sph-ilm-calc-cpy-py-ga?-ba?

Similar to BN2. Mineralogy relatively simple, dominated by perthitic feldspar. Biotite is iron-rich based on colour. Calcite occurs interstitially and as veins.

| | |
|---|---|
| K-spar | 60% |
| alb | 10% |
| mica | 10% |
| oxide | 5% |
| sph | 5% |
| calc | 5% |
| other | 5% |

**R493989 (BN16):** ***Porphyritic potassic syenite***
Hand specimen: Dark grey colour, less dominated by K-spar phenocrysts that appear heavily fractured. Very dark coloured matrix with visible sulphides. This sample is matrix dominated whereas the other syenites are phenocryst dominated.
Thin section: K-spar-alb-bt-mu-calc-mag-apa-ilm-cpy
Same as BN17 & BN2 although more dominated by opaques (sulphides?). Calcite far less dominant in this sample.

| | |
|---|---|
| K-spar | 65% |
| alb | 15% |
| mica | 10% |
| opaq | 8% |
| calc | 2% |

**R493985 (BN6):** ***Porphyritic dyke***
Hand specimen: Dark-grey very fine-grained dyke phase. Coarse yellow euhedral crystal within darker matrix (<8x4mm).
Thin section: alb-epi-mag-phl-bt-gt-canc-flu-sph-apa.

Very fine-grained matrix composed predominantly of albite and opaques. Grainsize makes visual identification difficult. Coarser subeuhedral phenocrysts are apparently replacement textures composed of garnet with cancrinite inclusions. A weak foliation wraps around these phenocrysts. Very-fine grain fluorite occurs in the pressure shadows of the phenocryst. It is interpreted that the phenocryst was originally nepheline that was pseudomorphed by cancrinite then garnet.

**R493986 (BN7):** ***dyke***
Hand specimen: Dark-grey very fine-grained dyke phase
Thin section: alb-epi-mag-phl-bt-mu.

Very similar to BN6 although without garnet-cancrinite phenocrysts. Albite is the dominant phase although epidote and muscovite appear more common than previous description.

# Appendix 6
# ALKALINE MAGMATIC ROCK MINERAL CHEMISTRIES

This appendix contains mineral chemistries from samples used in petrogenetic interpretations on the Billeroo alkaline magmatic complex. Analyses were performed on the Cameca SX51 Electron Microprobe. Operating conditions were accelerating voltage 15kV, bream current 20nA. Standards used were a combination of natural and synthetic materials. End-member calculations followed procedures outline in Deer et al. (1992).

### A6.1 Clinopyroxene

| | *Ijolite* | | | | | | *Ijolite* | | | | *Ijolite* |
|---|---|---|---|---|---|---|---|---|---|---|---|
| | **BN1_1** | | | **BN1_3** | | **BN1_5** | **BN3_1** | | **BN3_2** | | **BN4_2** |
| | *aeg1* | *aeg2* | *aeg3* | *pyx?* | *aeg1* | *pyx1* | *???* | *??<>* | *pyx?* | *??* | *aeg1* |
| **$SiO_2$** | 52.3025 | 51.7832 | 52.1247 | 48.6921 | 51.2824 | 47.0298 | 48.5142 | 50.7910 | 42.0538 | 51.7180 | 52.3893 |
| **$TiO_2$** | 3.4942 | 3.4916 | 0.6566 | 4.4903 | 4.2256 | 2.2055 | 0.2490 | 2.1836 | 1.0616 | 0.3318 | 0.0795 |
| **$Al_2O_3$** | 0.7495 | 0.6138 | 1.7285 | 0.6581 | 0.7859 | 1.5879 | 5.7863 | 0.9226 | 1.3803 | 1.6410 | 1.0107 |
| **$Fe_2O_3$** | 21.5000 | 24.4900 | 24.1100 | 12.1800 | 18.0300 | 19.1000 | 16.8700 | 18.0000 | 28.0100 | 26.0600 | 26.3600 |
| **FeO** | 5.0400 | 3.7900 | 1.3000 | 9.8400 | 8.1200 | 1.5600 | 0.0000 | 6.2800 | 0.0000 | 1.6700 | 2.0700 |
| **CaO** | 1.0361 | 0.6912 | 5.3085 | 8.9256 | 3.4979 | 16.4365 | 6.0506 | 6.1954 | 16.5701 | 2.2503 | 3.9714 |
| **MnO** | 0.5575 | 0.5341 | 0.3917 | 0.4252 | 0.2713 | 0.8105 | 0.3262 | 0.4130 | 0.7159 | 0.4269 | 0.3893 |
| **MgO** | 1.2413 | 1.0028 | 3.3274 | 2.4991 | 1.4603 | 4.4562 | 9.3953 | 2.3668 | 0.2572 | 1.2737 | 2.0490 |
| **$Na_2O$** | 12.1950 | 12.5228 | 10.4398 | 7.7864 | 10.7065 | 5.7885 | 5.3689 | 9.4398 | 6.3428 | 11.8370 | 11.1083 |
| **$K_2O$** | 0.0001 | 0.0001 | 0.0281 | 0.0001 | 0.0001 | 0.0001 | 4.0699 | 0.0249 | 0.0001 | 0.0001 | 0.0050 |
| **Total** | 98.1162 | 98.9196 | 99.4153 | 95.4969 | 98.3800 | 98.9750 | 96.6304 | 96.6171 | 96.3918 | 97.2088 | 99.4325 |
| | | | | | | | | | | | |
| **Si*** | 2.026 | 1.998 | 1.983 | 1.968 | 1.998 | 1.837 | 1.875 | 2.008 | 1.744 | 2.018 | 2.008 |
| **Ti** | 0.102 | 0.101 | 0.019 | 0.136 | 0.124 | 0.065 | 0.007 | 0.065 | 0.033 | 0.010 | 0.002 |
| **$Al^{iv}$** | 0.000 | 0.002 | 0.017 | 0.032 | 0.002 | 0.073 | 0.125 | 0.000 | 0.000 | 0.000 | 0.000 |
| **$Al^{vi}$** | 0.034 | 0.025 | 0.061 | 0.000 | 0.034 | 0.000 | 0.139 | 0.043 | 0.067 | 0.075 | 0.046 |
| **$Fe^{3+}$** | 0.627 | 0.711 | 0.690 | 0.370 | 0.529 | 0.561 | 0.491 | 0.536 | 0.874 | 0.765 | 0.760 |
| **$Fe^{2+}$** | 0.163 | 0.122 | 0.041 | 0.333 | 0.265 | 0.051 | 0.000 | 0.208 | 0.000 | 0.054 | 0.066 |
| **Ca** | 0.043 | 0.029 | 0.216 | 0.386 | 0.146 | 0.688 | 0.251 | 0.262 | 0.736 | 0.094 | 0.163 |
| **Mn** | 0.018 | 0.017 | 0.013 | 0.015 | 0.009 | 0.027 | 0.011 | 0.014 | 0.025 | 0.014 | 0.013 |
| **Mg** | 0.072 | 0.058 | 0.189 | 0.151 | 0.085 | 0.260 | 0.541 | 0.140 | 0.016 | 0.074 | 0.117 |
| **Na** | 0.916 | 0.937 | 0.770 | 0.610 | 0.809 | 0.438 | 0.402 | 0.724 | 0.510 | 0.895 | 0.825 |
| **K** | 0.000 | 0.000 | 0.001 | 0.000 | 0.000 | 0.000 | 0.201 | 0.001 | 0.000 | 0.000 | 0.000 |
| | 4.000 | 4.000 | 4.000 | 4.001 | 4.000 | 4.000 | 4.042 | 4.000 | 4.007 | 4.000 | 4.000 |
| | | | | | | | | | | | |
| **Mg#** | 0.31 | 0.32 | 0.82 | 0.31 | 0.24 | 0.84 | 1.00 | 0.40 | 1.00 | 0.58 | 0.64 |
| | | | | | | | | | | | |
| **Na** | 0.783 | 0.826 | 0.760 | 0.551 | 0.693 | 0.565 | 0.422 | 0.667 | 0.926 | 0.863 | 0.808 |
| **Mg** | 0.061 | 0.051 | 0.186 | 0.136 | 0.073 | 0.335 | 0.567 | 0.129 | 0.029 | 0.071 | 0.115 |
| **$Fe^{2+}$+Mn** | 0.155 | 0.123 | 0.053 | 0.313 | 0.234 | 0.100 | 0.011 | 0.204 | 0.046 | 0.066 | 0.077 |

*** Based on 6 oxygens**

**Bold analyses were not included in text figures**

| | | *Ijolite* | | | | *Ijolite* | | | | | |
|---|---|---|---|---|---|---|---|---|---|---|---|
| | **BN4_2** | **BN12_2** | | | | **BN13_1** | | | | | |
| | *aeg2* | *pyx1?* | *pyx3* | *pyx4* | *pyx5* | *pyx1* | *pyx2* | *pyx3* | *pyx4* | *pyx5* | *pyx6* |
| **$SiO_2$** | 52.4025 | 49.7810 | 50.1456 | 50.2826 | 50.6196 | 52.4939 | 52.4442 | 52.5543 | 52.1807 | 54.1093 | 52.2251 |
| **$TiO_2$** | 0.8205 | 6.0737 | 1.0490 | 4.8187 | 0.2694 | 5.2961 | 4.9192 | 5.8434 | 5.1147 | 0.0717 | 0.78 |
| **$Al_2O_3$** | 1.4803 | 0.7691 | 1.1195 | 0.6815 | 2.2974 | 0.7996 | 1.0969 | 0.7221 | 0.7414 | 1.4094 | 2.2567 |
| **$Fe_2O_3$** | 23.4200 | 18.9100 | 23.3200 | 19.5700 | 26.3700 | 19.36 | 17.86 | 21.63 | 21.48 | 19.23 | 26.07 |
| **FeO** | 2.9600 | 5.1200 | 4.1400 | 5.7200 | 0.1200 | 6.98 | 8.16 | 4.86 | 5.7 | 1.11 | 0.48 |
| **CaO** | 5.2206 | 2.3594 | 3.7183 | 1.7748 | 3.8651 | 1.4057 | 1.1927 | 1.1018 | 1.3913 | 9.8753 | 4.2955 |
| **MnO** | 0.3017 | 0.5121 | 0.2095 | 0.3002 | 0.0550 | 0.3068 | 0.3464 | 0.2871 | 0.2705 | 0.2284 | 0.1829 |
| **MgO** | 2.8253 | 0.9349 | 1.6435 | 1.0227 | 2.2757 | 0.5531 | 0.6805 | 0.7357 | 0.6741 | 6.8881 | 2.4036 |
| **$Na_2O$** | 10.4391 | 11.7770 | 10.5276 | 11.7198 | 11.1144 | 12.3791 | 12.0446 | 12.9821 | 12.5168 | 8.2834 | 11.3477 |
| **$K_2O$** | 0.0025 | 0.0182 | 0.0157 | 0.0001 | 0.0183 | 0.0205 | 0.0123 | 0.0123 | 0.0001 | 0.0298 | 0.0277 |
| **Total** | 99.8725 | **96.2554** | **95.8887** | **95.8904** | 97.0049 | 99.5948 | 98.7568 | 100.7288 | 100.0696 | 101.2354 | 100.0692 |
| | | | | | | | | | | | |
| **Si*** | 1.993 | 1.972 | 2.000 | 1.999 | 1.973 | 2.011 | 2.024 | 1.986 | 1.991 | 1.997 | 1.973 |
| **Ti** | 0.023 | 0.181 | 0.031 | 0.144 | 0.008 | 0.153 | 0.143 | 0.166 | 0.147 | 0.002 | 0.022 |
| **$Al^{iv}$** | 0.007 | 0.000 | 0.000 | 0.000 | 0.000 | 0.000 | 0.000 | 0.014 | 0.009 | 0.003 | 0.027 |
| **$Al^{vi}$** | 0.060 | 0.036 | 0.053 | 0.032 | 0.106 | 0.036 | 0.050 | 0.018 | 0.025 | 0.059 | 0.074 |
| **$Fe^{3+}$** | 0.670 | 0.564 | 0.700 | 0.585 | 0.773 | 0.558 | 0.519 | 0.615 | 0.617 | 0.534 | 0.741 |
| **$Fe^{2+}$** | 0.094 | 0.170 | 0.138 | 0.190 | 0.004 | 0.224 | 0.263 | 0.154 | 0.182 | 0.034 | 0.015 |
| **Ca** | 0.213 | 0.100 | 0.159 | 0.076 | 0.161 | 0.058 | 0.049 | 0.045 | 0.057 | 0.391 | 0.174 |
| **Mn** | 0.010 | 0.017 | 0.007 | 0.010 | 0.002 | 0.010 | 0.011 | 0.009 | 0.009 | 0.007 | 0.006 |
| **Mg** | 0.160 | 0.055 | 0.098 | 0.061 | 0.132 | 0.032 | 0.039 | 0.041 | 0.038 | 0.379 | 0.135 |
| **Na** | 0.770 | 0.904 | 0.814 | 0.903 | 0.840 | 0.919 | 0.901 | 0.951 | 0.926 | 0.593 | 0.831 |
| **K** | 0.000 | 0.001 | 0.001 | 0.000 | 0.001 | 0.001 | 0.001 | 0.001 | 0.000 | 0.001 | 0.001 |
| | 4.000 | 4.000 | 4.000 | 4.000 | 4.000 | 4.000 | 4.000 | 4.000 | 4.000 | 4.000 | 4.000 |
| | | | | | | | | | | | |
| **Mg#** | 0.63 | 0.25 | 0.41 | 0.24 | 0.97 | 0.12 | 0.13 | 0.21 | 0.17 | 0.92 | 0.90 |
| | | | | | | | | | | | |
| **Na** | 0.745 | **0.789** | **0.770** | **0.776** | 0.859 | 0.776 | 0.742 | 0.823 | 0.802 | 0.585 | 0.842 |
| **Mg** | 0.155 | **0.048** | **0.092** | **0.052** | 0.135 | 0.027 | 0.032 | 0.036 | 0.033 | 0.374 | 0.137 |
| **$Fe^{2+}$+Mn** | 0.100 | **0.163** | **0.137** | **0.172** | 0.006 | 0.197 | 0.226 | 0.141 | 0.165 | 0.041 | 0.021 |

| | **BN13_1** | **BN13_2** | **BN13_2** | | | | | | | | **BN13_3** |
|---|---|---|---|---|---|---|---|---|---|---|---|
| | *pyx7* | *pyx1* | *pyx2* | *pyx3* | *pyx4* | *pyx5* | *pyx6* | *pyx7* | *pyx9* | *pyx10* | *pyx1* |
| **$SiO_2$** | 52.5845 | 51.601 | 51.2502 | 52.7567 | 52.8822 | 51.4752 | 51.3318 | 51.3671 | 52.0755 | 52.5038 | 52.195 |
| **$TiO_2$** | 2.1918 | 1.1809 | 1.2548 | 0.0528 | 0.1999 | 0.4371 | 1.8985 | 1.6808 | 1.7999 | 1.5473 | 2.1835 |
| **$Al_2O_3$** | 1.0455 | 0.5933 | 0.7242 | 0.6067 | 0.6399 | 0.7082 | 0.6857 | 0.6239 | 0.6399 | 0.7221 | 0.6237 |
| **$Fe_2O_3$** | 24.73 | 13.04 | 24 | 27.46 | 22.37 | 23.97 | 19.85 | 20.88 | 20.4 | 18.5 | 20.75 |
| **FeO** | 3.22 | 11.63 | 4.63 | 1.84 | 2.38 | 4.01 | 8.38 | 7.94 | 7.79 | 5.76 | 6.78 |
| **CaO** | 3.0502 | 12.3725 | 6.166 | 4.5043 | 7.0827 | 7.2374 | 7.7064 | 6.6947 | 6.0115 | 8.0261 | 5.4488 |
| **MnO** | 0.4337 | 0.4793 | 0.3934 | 0.4458 | 0.3712 | 0.501 | 0.376 | 0.3189 | 0.1939 | 0.5183 | 0.2261 |
| **MgO** | 1.5055 | 3.5461 | 1.6857 | 2.5661 | 4.2586 | 2.5904 | 1.3766 | 1.1947 | 1.5385 | 3.6836 | 1.7102 |
| **$Na_2O$** | 11.7601 | 6.1391 | 9.997 | 10.8922 | 9.4884 | 9.3577 | 9.0592 | 9.4838 | 9.805 | 8.8511 | 10.2014 |
| **$K_2O$** | 0.0257 | 0.0053 | 0.0411 | 0.0001 | 0.0001 | 0.0508 | 0.0001 | 0.0001 | 0.0001 | 0.0001 | 0.0144 |
| **Total** | 100.547 | 100.5875 | 100.1424 | 101.1247 | 99.673 | 100.3378 | 100.6643 | 100.184 | 100.2543 | 100.1124 | 100.1331 |
| | | | | | | | | | | | |
| **Si*** | 1.994 | 1.993 | 1.974 | 1.994 | 2.010 | 1.975 | 1.980 | 1.989 | 2.004 | 2.001 | 2.003 |
| **Ti** | 0.063 | 0.034 | 0.036 | 0.002 | 0.006 | 0.013 | 0.055 | 0.049 | 0.052 | 0.044 | 0.063 |
| **$Al^{iv}$** | 0.006 | 0.007 | 0.026 | 0.006 | 0.000 | 0.025 | 0.020 | 0.011 | 0.000 | 0.000 | 0.000 |
| **$Al^{vi}$** | 0.041 | 0.020 | 0.007 | 0.021 | 0.029 | 0.007 | 0.011 | 0.017 | 0.029 | 0.032 | 0.028 |
| **$Fe^{3+}$** | 0.706 | 0.379 | 0.695 | 0.781 | 0.640 | 0.692 | 0.576 | 0.608 | 0.591 | 0.531 | 0.599 |
| **$Fe^{2+}$** | 0.102 | 0.376 | 0.149 | 0.058 | 0.076 | 0.129 | 0.270 | 0.257 | 0.251 | 0.184 | 0.218 |
| **Ca** | 0.124 | 0.512 | 0.254 | 0.182 | 0.288 | 0.297 | 0.318 | 0.278 | 0.248 | 0.328 | 0.224 |
| **Mn** | 0.014 | 0.016 | 0.013 | 0.014 | 0.012 | 0.016 | 0.012 | 0.010 | 0.006 | 0.017 | 0.007 |
| **Mg** | 0.085 | 0.204 | 0.097 | 0.145 | 0.241 | 0.148 | 0.079 | 0.069 | 0.088 | 0.209 | 0.098 |
| **Na** | 0.865 | 0.460 | 0.746 | 0.798 | 0.699 | 0.696 | 0.677 | 0.712 | 0.731 | 0.654 | 0.759 |
| **K** | 0.001 | 0.000 | 0.002 | 0.000 | 0.000 | 0.002 | 0.000 | 0.000 | 0.000 | 0.000 | 0.001 |
| | 4.000 | 4.000 | 4.000 | 4.000 | 4.000 | 4.000 | 4.000 | 4.000 | 4.000 | 4.000 | 4.000 |
| | | | | | | | | | | | |
| **Mg#** | 0.45 | 0.35 | 0.39 | 0.71 | 0.76 | 0.54 | 0.23 | 0.21 | 0.26 | 0.53 | 0.31 |
| | | | | | | | | | | | |
| **Na** | 0.811 | 0.436 | 0.743 | 0.786 | 0.680 | 0.704 | 0.652 | 0.679 | 0.679 | 0.615 | 0.702 |
| **Mg** | 0.080 | 0.194 | 0.096 | 0.142 | 0.235 | 0.150 | 0.076 | 0.066 | 0.082 | 0.197 | 0.090 |

| | | | | | | | | | | | |
|---|---|---|---|---|---|---|---|---|---|---|---|
| **$Fe^{2+}$+Mn** | 0.109 | 0.371 | 0.161 | 0.071 | 0.085 | 0.147 | 0.272 | 0.255 | 0.239 | 0.188 | 0.208 |

| | **BN13_3** | | | **BN13_3** | |
|---|---|---|---|---|---|
| | *pyx2* | *pyx3* | *pyx4* | *pyx5* | *pyx6* |
| **$SiO_2$** | 51.2824 | 52.2533 | 52.3618 | 52.6514 | 52.4237 |
| **$TiO_2$** | 3.0513 | 2.074 | 0.3965 | 1.2789 | 2.1588 |
| **$Al_2O_3$** | 1.3447 | 0.8313 | 1.7182 | 2.0913 | 0.6744 |
| **$Fe_2O_3$** | 26.1 | 20.72 | 26.62 | 25.69 | 24.75 |
| **FeO** | 1.73 | 5.87 | 0.69 | 1.46 | 4.16 |
| **CaO** | 3.9128 | 6.4995 | 5.4713 | 3.081 | 3.8577 |
| **MnO** | 0.1896 | 0.1703 | 0.2325 | 0.2197 | 0.1598 |
| **MgO** | 1.1637 | 2.2407 | 2.776 | 1.9234 | 1.3856 |
| **$Na_2O$** | 11.8677 | 9.9189 | 10.7991 | 11.8506 | 11.4078 |
| **$K_2O$** | 0.0103 | 0.0001 | 0.0062 | 0.0341 | 0.0001 |
| **Total** | 100.6525 | 100.5781 | 101.0716 | 100.2804 | 100.9779 |
| | | | | | |
| **Si*** | 1.947 | 1.991 | 1.968 | 1.987 | 1.990 |
| **Ti** | 0.087 | 0.059 | 0.011 | 0.036 | 0.062 |
| **$Al^{iv}$** | 0.053 | 0.009 | 0.032 | 0.013 | 0.010 |
| **$Al^{vi}$** | 0.007 | 0.029 | 0.044 | 0.080 | 0.020 |
| **$Fe^{3+}$** | 0.746 | 0.594 | 0.753 | 0.729 | 0.707 |
| **$Fe^{2+}$** | 0.055 | 0.187 | 0.022 | 0.046 | 0.132 |
| **Ca** | 0.159 | 0.265 | 0.220 | 0.125 | 0.157 |
| **Mn** | 0.006 | 0.005 | 0.007 | 0.007 | 0.005 |
| **Mg** | 0.066 | 0.127 | 0.156 | 0.108 | 0.078 |
| **Na** | 0.874 | 0.733 | 0.787 | 0.867 | 0.839 |
| **K** | 0.000 | 0.000 | 0.000 | 0.002 | 0.000 |
| | 4.000 | 4.000 | 4.000 | 4.000 | 4.000 |
| | | | | | |
| **Mg#** | 0.55 | 0.40 | 0.88 | 0.70 | 0.37 |
| | | | | | |
| **Na** | 0.873 | 0.696 | 0.810 | 0.843 | 0.796 |
| **Mg** | 0.066 | 0.121 | 0.160 | 0.105 | 0.074 |
| **$Fe^{2+}$+Mn** | 0.061 | 0.183 | 0.030 | 0.052 | 0.130 |

## A6.2 Nepheline

| | *Ijolite* | | | | | | | | | |
|---|---|---|---|---|---|---|---|---|---|---|
| | **BN1_1** | | **BN1_3** | **BN1_4** | | **BN1_5** | | | | **BN1_6** |
| | *ne1* | *ne2* | *ne1* | *ne1* | *ne2* | *ne1* | *ne2* | *ne3* | *ne4* | *ne3* |
| **$SiO_2$** | 44.0608 | 45.8516 | 41.5381 | 44.1108 | 45.1143 | 41.9531 | 41.6802 | 42.1494 | 42.0094 | 41.5646 |
| **$Al_2O_3$** | 35.7429 | 35.9236 | 33.7086 | 35.1583 | 35.8177 | 33.5092 | 33.643 | 33.4852 | 33.3685 | 33.8404 |
| **$TiO_2$** | 0.0516 | 0.0002 | 0.0366 | 0.0002 | 0.0002 | 0.0108 | 0.0002 | 0.0002 | 0.004 | 0.0269 |
| **$Fe_2O_3$** | 0.09 | 0.3 | 0.01 | 0.09 | 0.14 | 0.06 | 0.09 | 0.18 | 0.02 | 0.15 |
| **CaO** | 1.2227 | 0.8789 | 0.1674 | 1.2775 | 0.8032 | 0.2293 | 0.2052 | 0.1733 | 0.1941 | 0.1683 |
| **$Na_2O$** | 12.3761 | 5.1854 | 15.2142 | 10.5518 | 13.311 | 15.4731 | 15.5633 | 15.6303 | 15.4941 | 15.5134 |
| **$K_2O$** | 1.4924 | 0.8937 | 7.1306 | 3.0935 | 2.9974 | 7.0048 | 6.9619 | 6.6029 | 6.8972 | 7.1376 |
| **BaO** | 0.0002 | 0.0081 | 0.0002 | 0.0919 | 0.0485 | 0.0134 | 0.0002 | 0.1231 | 0.0002 | 0.0348 |
| **SrO** | 0.0002 | 0.0002 | 0.0002 | 0.0002 | 0.0002 | 0.0002 | 0.0002 | 0.0002 | 0.0002 | 0.0002 |
| **Total** | **95.0369** | 89.0417 | 97.8059 | **94.3742** | 98.2325 | 98.2539 | 98.1442 | 98.3446 | 97.9877 | 98.4362 |
| | | | | | | | | | | |
| **Si*** | 8.507 | 9.052 | 8.195 | 8.603 | 8.522 | 8.239 | 8.199 | 8.260 | 8.264 | 8.163 |
| **Al** | 8.133 | 8.358 | 7.837 | 8.081 | 7.974 | 7.755 | 7.799 | 7.733 | 7.736 | 7.832 |
| **Ti** | 0.007 | 0.000 | 0.005 | 0.000 | 0.000 | 0.002 | 0.000 | 0.000 | 0.001 | 0.004 |
| **$Fe^{3+}$** | 0.013 | 0.045 | 0.001 | 0.013 | 0.020 | 0.009 | 0.013 | 0.027 | 0.003 | 0.022 |
| **Ca** | 0.253 | 0.186 | 0.035 | 0.267 | 0.163 | 0.048 | 0.043 | 0.036 | 0.041 | 0.035 |
| **Na** | 4.632 | 1.985 | 5.819 | 3.990 | 4.875 | 5.891 | 5.935 | 5.938 | 5.909 | 5.906 |
| **K** | 0.368 | 0.225 | 1.794 | 0.770 | 0.722 | 1.755 | 1.747 | 1.651 | 1.731 | 1.788 |
| **Ba** | 0.000 | 0.001 | 0.000 | 0.007 | 0.004 | 0.001 | 0.000 | 0.009 | 0.000 | 0.003 |
| **Sr** | 0.000 | 0.000 | 0.000 | 0.000 | 0.000 | 0.000 | 0.000 | 0.000 | 0.000 | 0.000 |
| | 21.913 | 19.851 | 23.687 | 21.730 | 22.279 | 23.700 | 23.736 | 23.655 | 23.685 | 23.753 |
| | | | | | | | | | | |
| **Ne** | **59.80** | 25.40 | 73.06 | **51.59** | 62.20 | 74.09 | 74.59 | 74.57 | 74.25 | 74.16 |
| **Ks** | **4.74** | 2.88 | 22.53 | **9.95** | 9.22 | 22.07 | 21.95 | 20.73 | 21.75 | 22.45 |
| **Q** | **35.46** | 71.72 | 4.41 | **38.46** | 28.59 | 3.85 | 3.46 | 4.71 | 4.01 | 3.39 |

*** Based on 32O**

**Bold indicates those analyses not included in text discussion**

| | | *Ijolite* | | | | | | | | |
|---|---|---|---|---|---|---|---|---|---|---|
| | **BN1_6** | **BN3_3** | | | | | **BN3_5** | | **BN3_6** | |
| | *ne4* | *ne1* | *ne2* | *ne3* | *ne4* | *ne5* | *ne1* | *ne2* | *ne1* | *ne2* |
| **$SiO_2$** | 41.3317 | 42.8283 | 41.8168 | 43.1818 | 41.5022 | 42.1888 | 43.0627 | 42.0785 | 41.0250 | 43.4278 |
| **$Al_2O_3$** | 38.8039 | 34.2210 | 33.7241 | 35.4311 | 33.7330 | 33.9756 | 33.4498 | 33.8248 | 33.3177 | 34.7399 |
| **$TiO_2$** | 0.0406 | 0.0107 | 0.0161 | 0.0107 | 0.0228 | 0.0002 | 0.0002 | 0.0002 | 0.0276 | 0.0192 |
| **$Fe_2O_3$** | 0.16 | 0.0040 | 0.0900 | 0.0002 | 0.0200 | 0.0400 | 0.1900 | 0.0900 | 0.0500 | 0.0400 |
| **CaO** | 0.2084 | 0.2251 | 0.1861 | 0.0866 | 0.2071 | 0.2036 | 0.1995 | 0.1684 | 0.2169 | 0.2612 |
| **$Na_2O$** | 15.8464 | 15.9217 | 15.8755 | 15.7306 | 15.3969 | 15.7610 | 15.4706 | 15.7373 | 15.8462 | 15.6930 |
| **$K_2O$** | 7.1088 | 6.1489 | 6.1553 | 6.1747 | 6.2824 | 6.3363 | 5.3808 | 6.1578 | 6.2475 | 6.1848 |
| **BaO** | 0.0271 | 0.0268 | 0.0053 | 0.0080 | 0.0383 | 0.0264 | 0.0479 | 0.0287 | 0.0527 | 0.0002 |
| **SrO** | 0 | 0.0002 | 0.0002 | 0.0002 | 0.0002 | 0.0002 | 0.0002 | 0.0002 | 0.0002 | 0.0002 |
| **Total** | **103.5269** | 99.3867 | 97.8694 | 100.6239 | 97.2029 | 98.5321 | 97.8017 | 98.0859 | **96.7838** | 100.3663 |
| | | | | | | | | | | |
| **Si*** | 7.706 | 8.267 | 8.215 | 8.211 | 8.205 | 8.230 | 8.396 | 8.239 | 8.172 | 8.283 |
| **Al** | 8.526 | 7.785 | 7.808 | 7.939 | 7.859 | 7.811 | 7.686 | 7.805 | 7.822 | 7.809 |
| **Ti** | 0.006 | 0.002 | 0.002 | 0.002 | 0.003 | 0.000 | 0.000 | 0.000 | 0.004 | 0.003 |
| **$Fe^{3+}$** | 0.022 | 0.001 | 0.013 | 0.000 | 0.003 | 0.006 | 0.028 | 0.013 | 0.007 | 0.006 |
| **Ca** | 0.042 | 0.047 | 0.039 | 0.018 | 0.044 | 0.043 | 0.042 | 0.035 | 0.046 | 0.053 |
| **Na** | 5.728 | 5.958 | 6.046 | 5.799 | 5.901 | 5.961 | 5.848 | 5.974 | 6.120 | 5.803 |
| **K** | 1.691 | 1.514 | 1.542 | 1.498 | 1.584 | 1.577 | 1.338 | 1.538 | 1.587 | 1.505 |
| **Ba** | 0.002 | 0.002 | 0.000 | 0.001 | 0.003 | 0.002 | 0.004 | 0.002 | 0.004 | 0.000 |
| **Sr** | 0.000 | 0.000 | 0.000 | 0.000 | 0.000 | 0.000 | 0.000 | 0.000 | 0.000 | 0.000 |
| | 23.723 | 23.575 | 23.667 | 23.466 | 23.603 | 23.630 | 23.340 | 23.607 | 23.763 | 23.461 |
| | | | | | | | | | | |
| **Ne** | **71.97** | 74.91 | 75.95 | 72.64 | 74.17 | 74.91 | 73.48 | 75.01 | **76.94** | 73.02 |
| **Ks** | **21.24** | 19.04 | 19.38 | 18.76 | 19.91 | 19.82 | 16.81 | 19.31 | **19.96** | 18.94 |
| **Q** | **6.78** | 6.05 | 4.67 | 8.59 | 5.91 | 5.27 | 9.71 | 5.68 | **3.10** | 8.04 |

| | *Ijolite* | | | | | | *Ijolite* | | |
|---|---|---|---|---|---|---|---|---|---|
| | **BN4_1** | | | **BN4_4** | | | **BN12_1** | | |
| | *neph1* | *neph2* | *neph3* | *ne1* | *ne2* | *ne3* | *ne1* | *ne2* | *ne3* |
| **$SiO_2$** | 41.9248 | 43.4718 | 42.1863 | 41.3270 | 41.6228 | 41.5942 | 40.381 | 42.0307 | 40.6926 |
| **$Al_2O_3$** | 34.1597 | 35.4180 | 34.4732 | 33.5287 | 33.5799 | 33.2824 | 32.1343 | 31.8986 | 32.7079 |
| **$TiO_2$** | 0.0256 | 0.0002 | 0.0002 | 0.0002 | 0.0308 | 0.0002 | 0.018 | 0.0002 | 0.0168 |
| **$Fe_2O_3$** | 0.2700 | 0.1000 | 0.1200 | 0.1017 | 0.1380 | 0.0756 | 0.07 | 0.08 | 0.05 |
| **CaO** | 0.0796 | 0.0953 | 0.0374 | 0.0910 | 0.0921 | 0.1242 | 0.0504 | 0.0503 | 0.0329 |
| **$Na_2O$** | 16.0411 | 15.8207 | 16.1257 | 15.6527 | 15.3491 | 15.5355 | 15.54 | 15.7187 | 15.57 |
| **$K_2O$** | 7.0395 | 6.9964 | 7.1214 | 7.1805 | 7.2652 | 6.9763 | 6.5226 | 5.8003 | 6.3386 |
| **BaO** | 0.0002 | 0.0097 | 0.0364 | 0.0128 | 0.0204 | 0.0002 | 0.0002 | 0.0239 | 0.0002 |
| **SrO** | - | - | - | - | - | - | - | - | - |
| **Total** | 99.5405 | 101.9121 | 100.1006 | 97.8946 | 98.0983 | 97.5886 | **94.7165** | **95.6027** | **95.409** |
| | | | | | | | | | |
| **Si*** | 8.146 | 8.204 | 8.148 | 8.169 | 8.200 | 8.229 | 8.233 | 8.430 | 8.218 |
| **Al** | 7.822 | 7.877 | 7.847 | 7.810 | 7.797 | 7.760 | 7.721 | 7.540 | 7.784 |
| **Ti** | 0.004 | 0.000 | 0.000 | 0.000 | 0.005 | 0.000 | 0.003 | 0.000 | 0.003 |
| **$Fe^{3+}$** | 0.039 | 0.014 | 0.017 | 0.015 | 0.020 | 0.011 | 0.011 | 0.012 | 0.008 |
| **Ca** | 0.017 | 0.019 | 0.008 | 0.019 | 0.019 | 0.026 | 0.011 | 0.011 | 0.007 |
| **Na** | 6.042 | 5.788 | 6.038 | 5.998 | 5.862 | 5.958 | 6.142 | 6.112 | 6.096 |
| **K** | 1.745 | 1.684 | 1.755 | 1.810 | 1.826 | 1.761 | 1.696 | 1.484 | 1.633 |
| **Ba** | 0.000 | 0.001 | 0.003 | 0.001 | 0.002 | 0.000 | 0.000 | 0.002 | 0.000 |
| **Sr** | - | - | - | - | - | - | - | - | - |
| | 23.814 | 23.587 | 23.816 | 23.823 | 23.731 | 23.745 | 23.818 | 23.592 | 23.748 |
| | | | | | | | | | |
| **Ne** | 75.68 | 72.53 | 75.55 | 75.16 | 73.46 | 74.73 | **76.89** | **76.51** | **76.27** |
| **Ks** | 21.85 | 21.10 | 21.95 | 22.69 | 22.88 | 22.08 | **21.23** | **18.58** | **20.43** |
| **Q** | 2.46 | 6.37 | 2.49 | 2.16 | 3.66 | 3.19 | **1.88** | **4.92** | **3.31** |

## A6.3 Cancrinite

| | *Dyke* | | | | | | | | | |
|---|---|---|---|---|---|---|---|---|---|---|
| | **BN6_1** | | | | **BN6_2** | | | | | |
| | **canc1** | **canc2** | **canc3** | **canc4** | **canc1** | **canc2** | **canc3** | **canc4** | **canc5** | **canc6** |
| **$SiO_2$** | 39.4611 | 40.3648 | 41.8006 | 40.5632 | 42.4143 | 41.5207 | 40.9849 | 43.2819 | 41.6313 | 42.2437 |
| **$Al_2O_3$** | 33.1081 | 33.8127 | 35.438 | 32.231 | 34.2492 | 34.3033 | 33.6386 | 35.4646 | 34.157 | 34.5782 |
| **FeO** | 0.2639 | 0.1197 | 0.0957 | 0.3174 | 0.0637 | 0.0722 | 0.3104 | 0.0193 | 0.167 | 0.0837 |
| **CaO** | 5.5047 | 4.9678 | 4.8289 | 5.7346 | 5.6895 | 5.8104 | 7.0187 | 5.6177 | 5.643 | 5.8914 |
| **MnO** | 0.0544 | 0.0739 | 0.0128 | 0.0287 | 0.0002 | 0.0383 | 0.0256 | 0.0002 | 0.0071 | 0.025 |
| **MgO** | 0.0003 | 0.0063 | 0.0106 | 0.0003 | 0.0118 | 0.0003 | 0.0158 | 0.0067 | 0.0003 | 0.0003 |
| **$Na_2O$** | 15.2264 | 12.2698 | 15.3057 | 11.6739 | 2.9096 | 11.1081 | 5.8371 | 13.2881 | 8.3071 | 9.6296 |
| **$K_2O$** | 1.4631 | 1.3268 | 0.7285 | 1.0844 | 0.6432 | 0.7649 | 0.3632 | 0.6815 | 1.187 | 0.582 |
| **BaO** | 0.0028 | 0.036 | 0.0002 | 0.0002 | 0.0002 | 0.0002 | 0.0002 | 0.0002 | 0.0127 | 0.0152 |
| **SrO** | - | - | - | - | - | - | - | 0.0002 | 0.0002 | 0.0002 |
| **$SO_3$** | 2.9246 | 4.6584 | 4.9497 | 3.7766 | 4.0166 | 3.9356 | 2.8173 | 2.1364 | 2.2333 | 2.1842 |
| **Cl** | 0.0182 | 0.0122 | 0.0218 | 0.0166 | 0.0067 | 0.0017 | 0.01 | 0.012 | 0.0072 | 0.012 |
| **F** | 0.1594 | 0.1621 | 0.022 | 0.0006 | 0.0006 | 0.0006 | 0.0006 | 0.0006 | 0.0503 | 0.3249 |
| **Total** | 98.187 | 97.8105 | 103.2145 | 95.4275 | 90.0056 | 97.5563 | 91.0224 | 100.5094 | 93.4035 | 95.5704 |
| | | | | | | | | | | |
| **Si*** | 6.034 | 6.039 | 6.003 | 6.197 | 6.149 | 6.080 | 6.100 | 6.105 | 6.101 | 6.108 |
| **Al** | 5.966 | 5.961 | 5.997 | 5.803 | 5.851 | 5.920 | 5.900 | 5.895 | 5.899 | 5.892 |
| **$Fe^{2+}$** | 0.034 | 0.015 | 0.011 | 0.041 | 0.008 | 0.009 | 0.039 | 0.002 | 0.020 | 0.010 |
| **Ca** | 0.902 | 0.796 | 0.743 | 0.939 | 0.884 | 0.912 | 1.119 | 0.849 | 0.886 | 0.913 |
| **Mn** | 0.007 | 0.009 | 0.002 | 0.004 | 0.000 | 0.005 | 0.003 | 0.000 | 0.001 | 0.003 |
| **Mg** | 0.000 | 0.001 | 0.002 | 0.000 | 0.003 | 0.000 | 0.004 | 0.001 | 0.000 | 0.000 |
| **Na** | 4.514 | 3.559 | 4.261 | 3.458 | 0.818 | 3.154 | 1.684 | 3.634 | 2.360 | 2.699 |
| **K** | 0.285 | 0.253 | 0.133 | 0.211 | 0.119 | 0.143 | 0.069 | 0.123 | 0.222 | 0.107 |
| **Ba** | 0.000 | 0.002 | 0.000 | 0.000 | 0.000 | 0.000 | 0.000 | 0.000 | 0.001 | 0.001 |
| **Sr** | - | - | - | - | - | - | - | 0.000 | 0.000 | 0.000 |
| **S** | 0.838 | 1.306 | 1.332 | 1.081 | 1.091 | 1.080 | 0.786 | 0.565 | 0.613 | 0.592 |
| **Cl** | 0.005 | 0.003 | 0.005 | 0.004 | 0.002 | 0.000 | 0.003 | 0.003 | 0.002 | 0.003 |
| **F** | 0.077 | 0.077 | 0.010 | 0.000 | 0.000 | 0.000 | 0.000 | 0.000 | 0.023 | 0.149 |
| **Total** | 18.662 | 18.022 | 18.500 | 17.738 | 14.924 | 17.302 | 15.706 | 17.177 | 16.129 | 16.477 |

*** Number of ions on basis of 12(Si,Al)**

| | **BN6_2** | **BN6_4** | | | | | *Ijolite* **BN4_1** | | *Ijolite* **BN4_3** | |
|---|---|---|---|---|---|---|---|---|---|---|
| | **canc7** | **canc1** | **canc2** | **canc3** | **canc4** | **canc5** | **canc1?** | **canc(-?-)** | **canc1** | **canc2** |
| **$SiO_2$** | 42.9543 | 42.3031 | 41.5046 | 42.2783 | 41.6647 | 42.3518 | 41.1520 | 42.0826 | 43.1886 | 42.4692 |
| **$Al_2O_3$** | 35.2712 | 34.4258 | 33.0879 | 33.7275 | 33.5497 | 34.0167 | 33.9967 | 34.5072 | 33.865 | 33.7192 |
| **FeO** | 0.0064 | 0.0482 | 0.0002 | 0.0546 | 0.0546 | 0.0289 | 0.7083 | 0.0217 | 0.0002 | 0.0957 |
| **CaO** | 5.9317 | 5.8927 | 5.869 | 5.8046 | 5.4472 | 5.7634 | 5.5350 | 5.4563 | 6.7575 | 6.6055 |
| **MnO** | 0.0002 | 0.0819 | 0.0002 | 0.0002 | 0.0002 | 0.0002 | 0.0137 | 0.0171 | 0.0002 | 0.0144 |
| **MgO** | 0.0003 | 0.0003 | 0.0002 | 0.0002 | 0.0016 | 0.0103 | 0.0054 | 0.0002 | 0.0002 | 0.0003 |
| **$Na_2O$** | 10.8689 | 9.4597 | 5.3115 | 5.2344 | 6.372 | 5.7486 | 6.5368 | 4.8172 | 3.0592 | 6.958 |
| **$K_2O$** | 0.4243 | 1.0537 | 1.0767 | 0.6268 | 0.7849 | 0.8503 | 0.0391 | 0.03442 | 0.2083 | 0.3769 |
| **BaO** | 0.0002 | 0.0002 | 0.0002 | 0.0002 | 0.0989 | 0.0002 | 0.0002 | 0.0269 | 0.0026 | 0.0026 |
| **SrO** | 0.0002 | 0.0002 | 0.0002 | 0.0002 | 0.0002 | 0.0002 | - | - | 0.0002 | 0.0002 |
| **$SO_3$** | 2.3069 | 2.0435 | 2.0435 | 2.1381 | 2.2281 | 2.2132 | 3.8002 | 3.7433 | 1.4875 | 1.5691 |
| **Cl** | 0.0191 | 0.0335 | 0.0072 | 0.012 | 0.0048 | 0.0168 | 0.0072 | 0.0126 | 0.0002 | 0.0002 |
| **F** | 0.0006 | 0.0006 | 0.179 | 0.1277 | 0.0006 | 0.0764 | 0.0974 | 0.0006 | 0.1829 | 0.2051 |
| **Total** | 97.7843 | 95.3434 | 89.0804 | 90.0048 | 90.2075 | 91.077 | 91.8920 | 90.72012 | 88.7526 | 92.0164 |
| | | | | | | | | | | |
| **Si*** | 6.098 | 6.125 | 6.187 | 6.185 | 6.157 | 6.165 | 6.080 | 6.103 | 6.237 | 6.199 |
| **Al** | 5.902 | 5.875 | 5.813 | 5.815 | 5.843 | 5.835 | 5.920 | 5.897 | 5.763 | 5.801 |
| **$Fe^{2+}$** | 0.001 | 0.006 | 0.000 | 0.007 | 0.007 | 0.004 | 0.088 | 0.003 | 0.000 | 0.012 |
| **Ca** | 0.902 | 0.914 | 0.937 | 0.910 | 0.862 | 0.899 | 0.876 | 0.848 | 1.045 | 1.033 |
| **Mn** | 0.000 | 0.010 | 0.000 | 0.000 | 0.000 | 0.000 | 0.002 | 0.002 | 0.000 | 0.002 |
| **Mg** | 0.000 | 0.000 | 0.000 | 0.000 | 0.000 | 0.002 | 0.001 | 0.000 | 0.000 | 0.000 |
| **Na** | 2.992 | 2.656 | 1.535 | 1.485 | 1.826 | 1.622 | 1.872 | 1.354 | 0.856 | 1.969 |
| **K** | 0.077 | 0.195 | 0.205 | 0.117 | 0.148 | 0.158 | 0.007 | 0.006 | 0.038 | 0.070 |
| **Ba** | 0.000 | 0.000 | 0.000 | 0.000 | 0.006 | 0.000 | 0.000 | 0.002 | 0.000 | 0.000 |
| **Sr** | 0.000 | 0.000 | 0.000 | 0.000 | 0.000 | 0.000 | - | - | 0.000 | 0.000 |
| **S** | 0.614 | 0.555 | 0.571 | 0.586 | 0.617 | 0.604 | 1.052 | 1.017 | 0.403 | 0.429 |
| **Cl** | 0.005 | 0.008 | 0.002 | 0.003 | 0.001 | 0.004 | 0.002 | 0.003 | 0.000 | 0.000 |
| **F** | 0.000 | 0.000 | 0.084 | 0.059 | 0.000 | 0.035 | 0.046 | 0.000 | 0.084 | 0.095 |
| **Total** | 16.590 | 16.343 | 15.334 | 15.166 | 15.467 | 15.328 | 15.946 | 15.235 | 14.427 | 15.610 |

| | | *Ijolite* | | *Ijolite* | |
|---|---|---|---|---|---|
| | **BN4_4** | **BN8_3** | **BN8_3** | **BN12_1** | |
| | **canc1** | **canc1** | **canc2** | **cac1** | **cac2** |
| **$SiO_2$** | 42.6629 | 37.9071 | 39.7225 | 42.4104 | 40.7370 |
| **$Al_2O_3$** | 35.299 | 32.3415 | 32.1324 | 34.3420 | 32.8368 |
| **FeO** | 0.138 | 0.1435 | 0.1016 | 0.0429 | 0.0547 |
| **CaO** | 5.331 | 6.0312 | 5.9262 | 4.9198 | 5.1364 |
| **MnO** | 0.0646 | 0.0202 | 0.0002 | 0.0170 | 0.0002 |
| **MgO** | 0.0003 | 0.0003 | 0.0089 | 0.0016 | 0.0003 |
| **$Na_2O$** | 16.0242 | 15.4397 | 15.2093 | 10.7094 | 9.7417 |
| **$K_2O$** | 0.8541 | 0.5609 | 0.6273 | 0.4951 | 0.5518 |
| **BaO** | 0.0051 | 0.0002 | 0.046 | 0.0002 | 0.0168 |
| **SrO** | 0.0002 | - | - | 0.0002 | 0.0002 |
| **$SO_3$** | 2.1949 | 4.4875 | 3.9741 | 1.2902 | 1.2927 |
| **Cl** | 0.0241 | 0.0053 | 0.0002 | 0.0023 | 0.0002 |
| **F** | 0.1224 | 0.0006 | 0.0467 | 0.0006 | 0.0006 |
| **Total** | 102.7208 | 96.938 | 97.7954 | 94.2317 | 90.3694 |
| | | | | | |
| **Si*** | 6.076 | 5.984 | 6.143 | 6.140 | 6.154 |
| **Al** | 5.924 | 6.016 | 5.857 | 5.860 | 5.846 |
| **$Fe^{2+}$** | 0.016 | 0.019 | 0.013 | 0.005 | 0.007 |
| **Ca** | 0.813 | 1.020 | 0.982 | 0.763 | 0.831 |
| **Mn** | 0.008 | 0.003 | 0.000 | 0.002 | 0.000 |
| **Mg** | 0.000 | 0.000 | 0.002 | 0.000 | 0.000 |
| **Na** | 4.424 | 4.725 | 4.560 | 3.006 | 2.853 |
| **K** | 0.155 | 0.113 | 0.124 | 0.091 | 0.106 |
| **Ba** | 0.000 | 0.000 | 0.003 | 0.000 | 0.001 |
| **Sr** | 0.000 | - | - | 0.000 | 0.000 |
| **S** | 0.586 | 1.327 | 1.152 | 0.350 | 0.366 |
| **Cl** | 0.006 | 0.001 | 0.000 | 0.001 | 0.000 |
| **F** | 0.055 | 0.000 | 0.023 | 0.000 | 0.000 |
| **Total** | 18.064 | 19.209 | 18.859 | 16.219 | 16.165 |

| | *Ijolite* | | |
|---|---|---|---|
| | **BN1_6** | | |
| | **ne1?** | **ne2** | **??** |
| **$SiO_2$** | 38.352 | 38.387 | 38.564 |
| **$Al_2O_3$** | 32.003 | 31.985 | 32.230 |
| **$TiO_2$** | 0.042 | 0.050 | 0.046 |
| **FeO** | 0.103 | 0.213 | 0.196 |
| **CaO** | 0.603 | 0.612 | 0.530 |
| **MnO** | 0.004 | 0.069 | 0.000 |
| **MgO** | 0.007 | 0.218 | 0.000 |
| **$Na_2O$** | 9.766 | 9.628 | 9.814 |
| **$K_2O$** | 0.047 | 0.149 | 0.033 |
| **BaO** | 1.592 | 1.621 | 2.710 |
| **SrO** | 12.402 | 11.806 | 11.477 |
| **$SO_3$** | 0.000 | 0.000 | 0.000 |
| **Cl** | 0.000 | 0.000 | 0.000 |
| **F** | 0.000 | 0.000 | 0.000 |
| **Total** | 94.921 | 94.736 | 95.600 |
| | | | |
| **Si** | 6.050 | 6.055 | 6.046 |
| **Al** | 5.950 | 5.945 | 5.954 |
| **Ti** | 0.005 | 0.006 | 0.005 |
| **$Fe^{2+}$** | 0.014 | 0.028 | 0.026 |
| **Ca** | 0.102 | 0.103 | 0.089 |
| **Mn** | 0.000 | 0.009 | 0.000 |
| **Mg** | 0.002 | 0.051 | 0.000 |
| **Na** | 2.987 | 2.944 | 2.983 |
| **K** | 0.009 | 0.030 | 0.006 |
| **Ba** | 0.098 | 0.100 | 0.166 |
| **Sr** | 1.134 | 1.080 | 1.043 |
| **S** | 0.000 | 0.000 | 0.000 |
| **Cl** | 0.000 | 0.000 | 0.000 |
| **F** | 0.000 | 0.000 | 0.000 |
| **Total** | 16.352 | 16.352 | 16.319 |

**A6.4 Garnet**

| | *Ijolite* | | | | | | | *Ijolite* | | | |
|---|---|---|---|---|---|---|---|---|---|---|---|
| | **BN1_3** | **BN1_5** | | | **BN1_55** | | | **BN3_1** | | **BN3_2** | |
| | *gt1* | *gt1* | *gt2* | *gt3* | *gt1* | *gt2* | *gt3* | *gt1* | *gt2* | *gt1* | *gt2* |
| **$SiO_2$** | 34.3755 | 34.7168 | 34.4206 | 34.9139 | 34.2366 | 34.3192 | 34.2058 | 34.6403 | 36.0544 | 34.4797 | 35.2650 |
| **$TiO_2$** | 0.5592 | 1.0796 | 1.1597 | 0.5977 | 1.2533 | 1.9777 | 1.1600 | 1.2970 | 2.4765 | 1.4213 | 0.7423 |
| **$Al_2O_3$** | 1.9812 | 2.2685 | 2.4818 | 2.5126 | 2.4791 | 3.3093 | 2.5002 | 2.1380 | 1.8908 | 2.3731 | 4.2269 |
| **$Cr_2O_3$** | 0.0664 | 0.0000 | 0.0000 | 0.0000 | 0.0001 | 0.0001 | 0.0026 | 0.0573 | 0.0143 | 0.0001 | 0.0086 |
| **$Fe_2O_3$** | 27.7900 | 25.8400 | 25.6600 | 26.7800 | 25.7700 | 23.5100 | 25.6500 | 25.5600 | 18.3900 | 24.7900 | 22.3000 |
| **FeO** | 0.0000 | 0.4600 | 0.9700 | 0.1400 | 0.0000 | 0.5300 | 0.0900 | 0.1200 | 5.7800 | 0.3200 | 0.8400 |
| **CaO** | 31.8781 | 31.5585 | 30.8148 | 31.7467 | 31.4583 | 31.6668 | 31.2777 | 32.0756 | 29.7142 | 32.0411 | 31.5610 |
| **MnO** | 1.1057 | 1.5765 | 1.7368 | 1.4598 | 1.7586 | 1.6739 | 1.7665 | 1.3523 | 0.9326 | 1.0631 | 1.5434 |
| **MgO** | 0.0003 | 0.0003 | 0.0003 | 0.0003 | 0.0003 | 0.0133 | 0.0003 | 0.0040 | 0.3084 | 0.0326 | 0.0003 |
| **$Na_2O$** | 0.0984 | 0.0269 | 0.0364 | 0.0414 | 0.0772 | 0.0592 | 0.0347 | 0.0665 | 0.2300 | 0.0749 | 0.0376 |
| **$K_2O$** | 0.0175 | 0.0001 | 0.0225 | 0.0147 | 0.0287 | 0.0132 | 0.0001 | 0.0130 | 0.0147 | 0.0043 | 0.0069 |
| **Total** | 97.8723 | 97.5272 | 97.3029 | 98.2071 | 97.0622 | 97.0727 | 96.6879 | 97.3240 | 95.8059 | 96.6002 | 96.5320 |
| | | | | | | | | | | | |
| **Si** | 5.904 | 5.960 | 5.931 | 5.951 | 5.907 | 5.889 | 5.921 | 5.9547 | 6.2658 | 5.9580 | 6.0385 |
| **$Al^{iv}$** | 0.000 | 0.000 | 0.000 | 0.000 | 0.000 | 0.000 | 0.000 | 0.000 | 0.000 | 0.000 | 0.000 |
| | 5.904 | 5.960 | 5.931 | 5.951 | 5.907 | 5.889 | 5.921 | 5.955 | 6.266 | 5.958 | 6.038 |
| **$Al^{vi}$** | 0.401 | 0.459 | 0.504 | 0.505 | 0.504 | 0.669 | 0.510 | 0.433 | 0.387 | 0.483 | 0.853 |
| **Cr** | 0.000 | 0.000 | 0.000 | 0.000 | 0.000 | 0.000 | 0.000 | 0.000 | 0.000 | 0.000 | 0.000 |
| **$Fe^{3+}$** | 3.592 | 3.338 | 3.327 | 3.435 | 3.345 | 3.035 | 3.341 | 3.306 | 2.405 | 3.223 | 2.873 |
| **Ti** | 0.072 | 0.139 | 0.150 | 0.077 | 0.163 | 0.255 | 0.151 | 0.168 | 0.324 | 0.185 | 0.096 |
| | 4.065 | 3.937 | 3.981 | 4.016 | 4.012 | 3.960 | 4.002 | 3.907 | 3.116 | 3.891 | 3.822 |
| **Mg** | 0.000 | 0.000 | 0.000 | 0.000 | 0.000 | 0.003 | 0.000 | 0.001 | 0.080 | 0.008 | 0.000 |
| **$Fe^{2+}$** | 0.000 | 0.066 | 0.140 | 0.020 | 0.000 | 0.076 | 0.013 | 0.017 | 0.840 | 0.046 | 0.120 |
| **Mn** | 0.161 | 0.229 | 0.253 | 0.211 | 0.257 | 0.243 | 0.259 | 0.197 | 0.137 | 0.156 | 0.224 |
| **Ca** | 5.866 | 5.805 | 5.689 | 5.797 | 5.814 | 5.821 | 5.801 | 5.907 | 5.532 | 5.932 | 5.790 |
| | 6.027 | 6.100 | 6.082 | 6.028 | 6.071 | 6.144 | 6.073 | 6.122 | 6.589 | 6.142 | 6.134 |
| **Na** | 0.033 | 0.009 | 0.012 | 0.014 | 0.026 | 0.020 | 0.012 | 0.022 | 0.077 | 0.025 | 0.012 |
| **K** | 0.004 | 0.000 | 0.005 | 0.003 | 0.006 | 0.003 | 0.000 | 0.003 | 0.003 | 0.001 | 0.002 |
| **Total** | 16.032 | 16.006 | 16.012 | 16.011 | 16.022 | 16.015 | 16.008 | 16.009 | 16.052 | 16.017 | 16.008 |
| | | | | | | | | | | | |
| **pyr** | 0.001 | 0.001 | 0.001 | 0.001 | 0.001 | 0.055 | 0.001 | 0.017 | 1.213 | 0.137 | 0.001 |
| **alm** | 0.000 | 1.083 | 2.298 | 0.331 | 0.000 | 1.238 | 0.215 | 0.282 | 12.747 | 0.753 | 1.961 |
| **spe** | 2.669 | 3.758 | 4.167 | 3.496 | 4.232 | 3.959 | 4.265 | 3.216 | 2.083 | 2.533 | 3.649 |
| **and** | 88.355 | 84.799 | 83.566 | 85.524 | 83.383 | 76.655 | 83.482 | 84.620 | 77.182 | 82.834 | 75.180 |
| **uv** | 0.002 | 0.000 | 0.000 | 0.000 | 0.000 | 0.000 | 0.000 | 0.002 | 0.001 | 0.000 | 0.000 |
| **gro** | 8.973 | 10.359 | 9.967 | 10.647 | 12.383 | 18.093 | 12.038 | 11.864 | 6.775 | 13.744 | 19.209 |

*** Based on 24O**

| | *Ijolite* | | | | | *Ijolite* | | | | *Dyke* | |
|---|---|---|---|---|---|---|---|---|---|---|---|
| | **BN3_3** | **BN3_5** | **BN3_6** | **BN3_8** | | **BN4_1** | **BN4_2** | | **BN4_3** | **BN6_1** | |
| | *gt1* | *gt1* | *gt1* | *gt1* | *gt2* | *gt1* | *gt1* | *gt2* | *gt1* | *gt1* | *gt2* |
| **$SiO_2$** | 36.0586 | 34.3499 | 34.2846 | 34.6612 | 34.1880 | 35.2591 | 35.4697 | 35.3486 | 37.9488 | 35.4039 | 35.1648 |
| **$TiO_2$** | 1.2609 | 1.4951 | 1.1790 | 1.5964 | 1.1998 | 0.6851 | 0.9804 | 0.7046 | 1.0905 | 1.8846 | 1.1064 |
| **$Al_2O_3$** | 2.5643 | 2.4831 | 2.1150 | 4.3298 | 1.7249 | 2.9293 | 3.0031 | 3.0103 | 2.9084 | 7.0505 | 6.8223 |
| **$Cr_2O_3$** | 0.0172 | 0.0001 | 0.0001 | 0.0001 | 0.0179 | 0.0300 | 0.0001 | 0.0494 | 0.0000 | 0.0001 | 0.0149 |
| **$Fe_2O_3$** | 21.7300 | 25.2100 | 25.5800 | 23.1100 | 26.4800 | 23.3300 | 22.2200 | 23.7900 | 16.7100 | 16.6500 | 17.6300 |
| **FeO** | 2.5800 | 0.3500 | 0.1700 | 0.1400 | 0.5800 | 2.5400 | 3.3800 | 2.3900 | 7.6100 | 2.9600 | 1.9600 |
| **CaO** | 30.8261 | 31.8292 | 31.9249 | 32.4196 | 31.4453 | 30.2687 | 30.4145 | 31.0030 | 28.8343 | 30.5408 | 30.4422 |
| **MnO** | 1.3041 | 1.2721 | 0.9534 | 1.1905 | 1.0804 | 1.4399 | 0.9351 | 0.7447 | 0.5739 | 1.8774 | 2.0222 |
| **MgO** | 0.4799 | 0.0027 | 0.0142 | 0.0026 | 0.0003 | 0.0003 | 0.0003 | 0.0251 | 0.6911 | 0.0229 | 0.0214 |
| **$Na_2O$** | 0.0705 | 0.0857 | 0.0703 | 0.0428 | 0.0448 | 0.0521 | 0.0526 | 0.0136 | 1.6218 | 0.0513 | 0.0094 |
| **$K_2O$** | 0.0304 | 0.0062 | 0.0271 | 0.0094 | 0.0001 | 0.0129 | 0.0024 | 0.0362 | 0.0117 | 0.0001 | 0.0456 |
| **Total** | 96.9220 | 97.0841 | 96.3186 | 97.5024 | 96.7615 | 96.5474 | 96.4582 | 97.1155 | 98.0005 | 96.4416 | 95.2392 |
| | | | | | | | | | | | |
| **Si** | 6.1734 | 5.9159 | 5.9534 | 5.8843 | 5.9341 | 6.091 | 6.122 | 6.064 | 6.419 | 5.994 | 6.028 |
| **$Al^{iv}$** | 0.000 | 0.000 | 0.000 | 0.000 | 0.000 | 0.000 | 0.000 | 0.000 | 0.000 | 0.000 | 0.000 |
| | 6.173 | 5.916 | 5.953 | 5.884 | 5.934 | 6.091 | 6.122 | 6.064 | 6.419 | 5.994 | 6.028 |
| **$Al^{vi}$** | 0.517 | 0.504 | 0.433 | 0.866 | 0.353 | 0.596 | 0.611 | 0.609 | 0.580 | 1.407 | 1.378 |
| **Cr** | 0.000 | 0.000 | 0.000 | 0.000 | 0.000 | 0.000 | 0.000 | 0.000 | 0.000 | 0.000 | 0.000 |
| **$Fe^{3+}$** | 2.799 | 3.267 | 3.342 | 2.952 | 3.458 | 3.033 | 2.886 | 3.071 | 2.127 | 2.121 | 2.274 |
| **Ti** | 0.162 | 0.194 | 0.154 | 0.204 | 0.157 | 0.089 | 0.127 | 0.091 | 0.139 | 0.240 | 0.143 |
| | 3.479 | 3.965 | 3.929 | 4.022 | 3.968 | 3.718 | 3.624 | 3.770 | 2.845 | 3.768 | 3.795 |
| **Mg** | 0.122 | 0.001 | 0.004 | 0.001 | 0.000 | 0.000 | 0.000 | 0.006 | 0.174 | 0.006 | 0.005 |
| **$Fe^{2+}$** | 0.369 | 0.050 | 0.025 | 0.020 | 0.084 | 0.367 | 0.488 | 0.343 | 1.076 | 0.419 | 0.281 |
| **Mn** | 0.189 | 0.186 | 0.140 | 0.171 | 0.159 | 0.211 | 0.137 | 0.108 | 0.082 | 0.269 | 0.294 |
| **Ca** | 5.654 | 5.873 | 5.939 | 5.896 | 5.847 | 5.602 | 5.624 | 5.698 | 5.225 | 5.539 | 5.591 |
| | 6.335 | 6.109 | 6.108 | 6.088 | 6.090 | 6.180 | 6.248 | 6.155 | 6.558 | 6.233 | 6.171 |
| **Na** | 0.023 | 0.029 | 0.024 | 0.014 | 0.015 | 0.017 | 0.018 | 0.005 | 0.532 | 0.017 | 0.003 |
| **K** | 0.007 | 0.001 | 0.006 | 0.002 | 0.000 | 0.003 | 0.001 | 0.008 | 0.003 | 0.000 | 0.010 |
| **Total** | 16.017 | 16.020 | 16.020 | 16.011 | 16.008 | 16.009 | 16.012 | 16.002 | 16.356 | 16.011 | 16.007 |
| | | | | | | | | | | | |
| **pyr** | 1.934 | 0.011 | 0.060 | 0.011 | 0.001 | 0.001 | 0.001 | 0.104 | 2.657 | 0.093 | 0.089 |
| **alm** | 5.830 | 0.825 | 0.404 | 0.326 | 1.382 | 5.937 | 7.807 | 5.570 | 16.413 | 6.722 | 4.553 |
| **spe** | 2.985 | 3.037 | 2.296 | 2.812 | 2.608 | 3.409 | 2.188 | 1.758 | 1.254 | 4.318 | 4.758 |
| **and** | 80.461 | 82.403 | 85.065 | 73.395 | 87.160 | 81.565 | 79.632 | 81.446 | 74.748 | 56.295 | 59.923 |
| **uv** | 0.001 | 0.000 | 0.000 | 0.000 | 0.001 | 0.001 | 0.000 | 0.002 | 0.000 | 0.000 | 0.001 |
| **gro** | 8.789 | 13.723 | 12.175 | 23.456 | 8.849 | 9.086 | 10.373 | 11.120 | 4.928 | 32.571 | 30.677 |

| | *Dyke* | | | | | | *Dyke* | | *Ijolite* |
|---|---|---|---|---|---|---|---|---|---|
| | **BN6_1** | **BN6_2** | **BN6_3** | **BN6_4** | | | **BN7_1** | | **BN12_2** |
| | *gt3* | *gt1* | *gt1* | *gt1* | *gt2* | *gt3* | *gt1* | *gt2* | *gt1* |
| **$SiO_2$** | 35.2028 | 34.3425 | 35.4034 | 35.0066 | 34.7468 | 35.0086 | 35.5724 | 36.2056 | 35.1625 |
| **$TiO_2$** | 0.9605 | 8.7491 | 1.0161 | 1.3882 | 1.8417 | 1.3978 | 1.0777 | 1.0929 | 0.9419 |
| **$Al_2O_3$** | 5.5296 | 3.8555 | 4.3517 | 5.4266 | 4.6849 | 6.1979 | 5.4571 | 9.4386 | 7.6469 |
| **$Cr_2O_3$** | 0.0001 | 0.0247 | 0.0001 | 0.0082 | 0.0001 | 0.0001 | 0.0258 | 0.0338 | 0.0262 |
| **$Fe_2O_3$** | 18.9300 | 7.3800 | 20.7700 | 20.5900 | 21.6700 | 20.1800 | 18.3400 | 13.2800 | 17.6600 |
| **FeO** | 2.2500 | 9.8900 | 2.4000 | 0.0000 | 0.1800 | 0.0000 | 2.9400 | 2.7100 | 0.3600 |
| **CaO** | 30.1971 | 29.2257 | 30.5921 | 32.6236 | 32.3364 | 32.4470 | 30.0635 | 30.9254 | 32.1691 |
| **MnO** | 1.9525 | 1.5826 | 1.6388 | 1.3006 | 1.5691 | 1.6904 | 2.0216 | 1.9221 | 1.3059 |
| **MgO** | 0.0279 | 0.0003 | 0.0003 | 0.0003 | 0.0028 | 0.0003 | 0.0003 | 0.0003 | 0.0003 |
| **$Na_2O$** | 0.0222 | 0.4812 | 0.0023 | 0.0196 | 0.0229 | 0.0528 | 0.0385 | 0.0446 | 0.0388 |
| **$K_2O$** | 0.0066 | 0.0024 | 0.0022 | 0.0066 | 0.0001 | 0.0001 | 0.0055 | 0.0171 | 0.0165 |
| **Total** | 95.0793 | 95.5340 | 96.1770 | 96.3703 | 97.0548 | 96.9750 | 95.5424 | 95.6704 | 95.3281 |
| | | | | | | | | | |
| **Si** | 6.081 | 5.955 | 6.085 | 5.958 | 5.908 | 5.913 | 6.117 | 6.083 | 5.979 |
| **$Al^{iv}$** | 0.000 | 0.000 | 0.000 | 0.000 | 0.000 | 0.000 | 0.000 | 0.000 | 0.000 |
| | 6.081 | 5.955 | 6.085 | 5.958 | 5.908 | 5.913 | 6.117 | 6.083 | 5.979 |
| **$Al^{vi}$** | 1.126 | 0.788 | 0.881 | 1.088 | 0.939 | 1.234 | 1.106 | 1.869 | 1.532 |
| **Cr** | 0.000 | 0.000 | 0.000 | 0.000 | 0.000 | 0.000 | 0.000 | 0.000 | 0.000 |
| **$Fe^{3+}$** | 2.460 | 0.963 | 2.686 | 2.637 | 2.772 | 2.565 | 2.373 | 1.679 | 2.260 |
| **Ti** | 0.125 | 1.141 | 0.131 | 0.178 | 0.236 | 0.178 | 0.139 | 0.138 | 0.120 |
| | 3.711 | 2.892 | 3.699 | 3.903 | 3.947 | 3.976 | 3.618 | 3.686 | 3.912 |
| **Mg** | 0.007 | 0.000 | 0.000 | 0.000 | 0.001 | 0.000 | 0.000 | 0.000 | 0.000 |
| **$Fe^{2+}$** | 0.325 | 1.434 | 0.345 | 0.000 | 0.026 | 0.000 | 0.423 | 0.381 | 0.051 |
| **Mn** | 0.286 | 0.232 | 0.239 | 0.187 | 0.226 | 0.242 | 0.294 | 0.273 | 0.188 |
| **Ca** | 5.588 | 5.429 | 5.633 | 5.948 | 5.890 | 5.871 | 5.539 | 5.566 | 5.860 |
| | 6.206 | 7.096 | 6.216 | 6.136 | 6.143 | 6.113 | 6.256 | 6.221 | 6.100 |
| **Na** | 0.007 | 0.162 | 0.001 | 0.006 | 0.008 | 0.017 | 0.013 | 0.015 | 0.013 |
| **K** | 0.001 | 0.001 | 0.000 | 0.001 | 0.000 | 0.000 | 0.001 | 0.004 | 0.004 |
| **Total** | 16.006 | 16.105 | 16.001 | 16.004 | 16.005 | 16.019 | 16.006 | 16.008 | 16.007 |
| | | | | | | | | | |
| **pyr** | 0.116 | 0.001 | 0.001 | 0.001 | 0.012 | 0.001 | 0.001 | 0.001 | 0.001 |
| **alm** | 5.237 | 20.209 | 5.548 | 0.000 | 0.417 | 0.000 | 6.758 | 6.120 | 0.839 |
| **spe** | 4.603 | 3.275 | 3.837 | 3.055 | 3.678 | 3.955 | 4.706 | 4.397 | 3.083 |
| **and** | 66.303 | 33.297 | 72.619 | 67.560 | 70.247 | 64.505 | 65.583 | 45.549 | 57.753 |
| **uv** | 0.000 | 0.001 | 0.000 | 0.000 | 0.000 | 0.000 | 0.001 | 0.001 | 0.001 |
| **gro** | 23.741 | 43.216 | 17.994 | 29.384 | 25.647 | 31.538 | 22.950 | 43.932 | 38.322 |

**A6.5 Epidote**

| | *Ijolite* | | | | | | *Ijolite* | *Ijolite* | | | *Dyke* |
|---|---|---|---|---|---|---|---|---|---|---|---|
| | **BN1_1** | | **BN1_4** | **BN1_5** | | | **BN3_3** | **BN4_1** | | **BN4_3** | **BN6_1** |
| | *epi1* | *epi2* | *epi1* | *epi1* | *epi2* | *epi3* | *epi1* | *epi1* | *epi2* | *epi1* | *epi3* |
| **$SiO_2$** | 37.1458 | 36.8597 | 36.4306 | 36.7641 | 36.8474 | 37.0795 | 36.8320 | 37.0775 | 37.3998 | 36.5787 | 36.3110 |
| **$TiO_2$** | 0.0977 | 0.0040 | 0.0002 | 0.0373 | 0.0386 | 0.0305 | 0.0264 | 0.0672 | 0.0072 | 0.0304 | 0.6487 |
| **$Al_2O_3$** | 22.2814 | 22.0178 | 22.0364 | 22.0403 | 22.9587 | 22.1535 | 21.7509 | 21.5747 | 21.5836 | 21.1844 | 11.3503 |
| **$Fe_2O_3$** | 13.5900 | 13.9900 | 14.3000 | 13.7900 | 12.9500 | 13.6000 | 13.4400 | 15.6900 | 15.0500 | 13.3666 | 15.0800 |
| **CaO** | 22.3894 | 22.2886 | 21.7734 | 21.6943 | 21.0243 | 21.9785 | 22.1277 | 21.5894 | 21.4272 | 22.7284 | 32.1118 |
| **MnO** | 0.1639 | 0.1042 | 0.1597 | 0.1410 | 0.1334 | 0.0849 | 0.3308 | 0.1305 | 0.1170 | 0.0810 | 1.4690 |
| **MgO** | 0.0164 | 0.0036 | 0.0003 | 0.0003 | 0.0003 | 0.0003 | 0.0003 | 0.0003 | 0.0025 | 0.0026 | 0.0003 |
| **$Na_2O$** | 0.0157 | 0.0130 | 0.0003 | 0.0437 | 1.2154 | 0.0031 | 0.0045 | 0.0288 | 0.0226 | 0.0065 | 0.0183 |
| **$K_2O$** | 0.0201 | 0.0192 | 0.0091 | 0.0027 | 0.0437 | 0.0308 | 0.0072 | 0.0362 | 0.0386 | 0.0001 | 0.0248 |
| **Total** | 95.7204 | 95.3001 | 94.7100 | 94.5137 | 95.2118 | 94.9611 | 94.5198 | 96.1946 | 95.6485 | 93.9787 | 97.0142 |
| | | | | | | | | | | | |
| **Si*** | 3.028 | 3.023 | 3.007 | 3.033 | 3.014 | 3.042 | 1.507 | 3.021 | 3.054 | 3.045 | 3.101 |
| **Ti** | 0.006 | 0.000 | 0.000 | 0.002 | 0.002 | 0.002 | 0.001 | 0.004 | 0.000 | 0.002 | 0.042 |
| **$Al^{iv}$** | 0.000 | 0.000 | 0.000 | 0.000 | 0.000 | 0.000 | 0.000 | 0.000 | 0.000 | 0.000 | 0.000 |
| **$Al^{vi}$** | 2.141 | 2.128 | 2.144 | 2.143 | 2.213 | 2.142 | 0.000 | 2.072 | 2.077 | 2.078 | 1.142 |
| **$Fe^{3+}$** | 0.834 | 0.863 | 0.888 | 0.856 | 0.797 | 0.840 | 1.476 | 0.962 | 0.925 | 0.837 | 0.969 |
| **Ca** | 1.955 | 1.958 | 1.926 | 1.917 | 1.843 | 1.932 | 0.797 | 1.885 | 1.875 | 2.027 | 2.938 |
| **Mn** | 0.011 | 0.007 | 0.011 | 0.010 | 0.009 | 0.006 | 1.843 | 0.009 | 0.008 | 0.006 | 0.106 |
| **Mg** | 0.002 | 0.000 | 0.000 | 0.000 | 0.000 | 0.000 | 0.009 | 0.000 | 0.000 | 0.000 | 0.000 |
| **Na** | 0.002 | 0.002 | 0.000 | 0.007 | 0.193 | 0.000 | 0.000 | 0.005 | 0.004 | 0.001 | 0.003 |
| **K** | 0.002 | 0.002 | 0.001 | 0.000 | 0.005 | 0.003 | 0.386 | 0.004 | 0.004 | 0.000 | 0.003 |
| | 7.981 | 7.984 | 7.977 | 7.969 | 8.077 | 7.967 | 6.019 | 7.962 | 7.948 | 7.996 | 8.304 |

*** Based on 12.5O**

| | *Dyke* | | | | | | | *Ijolite* | | | |
|---|---|---|---|---|---|---|---|---|---|---|---|
| | **BN7_1** | | **BN7_2** | | **BN7_3** | | | **BN8_2** | **BN8_3** | **BN8_3** | |
| | *epi1* | *epi2* | *epi1* | *epi2* | *epi1* | *epi2* | *epi3* | *epi1* | *epi1* | *epi2* | *epi3* |
| **$SiO_2$** | 37.4978 | 37.3558 | 37.5288 | 37.7778 | 37.4809 | 37.7588 | 37.2462 | 36.6599 | 37.1998 | 37.1308 | 37.1896 |
| **$TiO_2$** | 0.0716 | 0.0070 | 0.0353 | 0.0164 | 0.0198 | 0.0002 | 0.0467 | 0.0365 | 0.0404 | 0.0178 | 0.0191 |
| **$Al_2O_3$** | 22.2750 | 22.5497 | 23.5793 | 22.8828 | 22.0668 | 22.8435 | 22.4057 | 21.6521 | 22.1151 | 22.4458 | 22.0675 |
| **$Fe_2O_3$** | 14.3800 | 14.9600 | 13.7200 | 13.7200 | 14.3300 | 13.8800 | 13.8700 | 13.8700 | 13.7700 | 13.7600 | 14.0400 |
| **CaO** | 20.4391 | 21.4511 | 20.6912 | 20.5088 | 21.1375 | 21.2698 | 20.5275 | 19.7417 | 19.5017 | 20.3196 | 21.0916 |
| **MnO** | 0.1797 | 0.3451 | 0.2392 | 0.1205 | 0.1722 | 0.1704 | 0.2216 | 0.1545 | 0.1127 | 0.0596 | 0.0002 |
| **MgO** | 0.0073 | 0.0168 | 0.0003 | 0.0206 | 0.0088 | 0.0168 | 0.0003 | 0.0314 | 0.0003 | 0.0040 | 0.0003 |
| **$Na_2O$** | 0.0196 | 0.0392 | 0.0003 | 0.0082 | 0.0003 | 0.0003 | 0.0023 | 0.0011 | 0.0003 | 0.0003 | 0.0128 |
| **$K_2O$** | 0.0001 | 0.0144 | 0.0001 | 0.0001 | 0.0048 | 0.0097 | 0.0209 | 0.0065 | 0.0646 | 0.0171 | 0.0001 |
| **Total** | 94.8702 | 96.7391 | 95.7945 | 95.0552 | 95.2211 | 95.9495 | 94.3412 | 92.1537 | 92.8049 | 93.7550 | 94.4212 |
| | | | | | | | | | | | |
| **Si*** | 3.068 | 3.016 | 3.033 | 3.074 | 3.063 | 3.054 | 3.063 | 3.083 | 3.097 | 3.067 | 3.061 |
| **Ti** | 0.004 | 0.000 | 0.002 | 0.001 | 0.001 | 0.000 | 0.003 | 0.002 | 0.003 | 0.001 | 0.001 |
| **$Al^{iv}$** | 0.000 | 0.000 | 0.000 | 0.000 | 0.000 | 0.000 | 0.000 | 0.000 | 0.000 | 0.000 | 0.000 |
| **$Al^{vi}$** | 2.148 | 2.146 | 2.246 | 2.194 | 2.125 | 2.178 | 2.171 | 2.146 | 2.170 | 2.185 | 2.140 |
| **$Fe^{3+}$** | 0.885 | 0.909 | 0.834 | 0.840 | 0.881 | 0.845 | 0.858 | 0.878 | 0.863 | 0.855 | 0.870 |
| **Ca** | 1.791 | 1.856 | 1.792 | 1.788 | 1.850 | 1.843 | 1.808 | 1.779 | 1.740 | 1.798 | 1.860 |
| **Mn** | 0.012 | 0.024 | 0.016 | 0.008 | 0.012 | 0.012 | 0.015 | 0.011 | 0.008 | 0.004 | 0.000 |
| **Mg** | 0.001 | 0.002 | 0.000 | 0.002 | 0.001 | 0.002 | 0.000 | 0.004 | 0.000 | 0.000 | 0.000 |
| **Na** | 0.003 | 0.006 | 0.000 | 0.001 | 0.000 | 0.000 | 0.000 | 0.000 | 0.000 | 0.000 | 0.002 |
| **K** | 0.000 | 0.001 | 0.000 | 0.000 | 0.001 | 0.001 | 0.002 | 0.001 | 0.007 | 0.002 | 0.000 |
| | 7.913 | 7.960 | 7.924 | 7.909 | 7.934 | 7.935 | 7.921 | 7.903 | 7.887 | 7.913 | 7.934 |

**A6.6 Titanite**

| | *Ijolite* | | *Ijolite* | | | *Dyke* | | *Ijolite* | | | |
|---|---|---|---|---|---|---|---|---|---|---|---|
| | **BN1_1** | **BN1_4** | **BN4_1** | | | **BN6_1** | **BN6_3** | **BN8_2** | | **BN8_3** | **BN8_4** |
| | tit1 | tit1 | tit1 | tit2 | tit3 | tit1 | tit1 | tit1 | tit2 | tit1 | tit1 |
| **$SiO_2$** | 30.3452 | 29.9900 | 30.1675 | 29.9540 | 30.2604 | 30.3225 | 30.1619 | 30.4313 | 30.4257 | 30.0668 | 30.3054 |
| **$TiO_2$** | 30.8302 | 30.5318 | 37.0132 | 38.2827 | 38.5822 | 34.4503 | 34.7551 | 37.8077 | 35.1151 | 37.6063 | 37.3555 |
| **$Al_2O_3$** | 1.2883 | 2.0343 | 0.7377 | 0.0149 | 0.0043 | 1.5523 | 1.7855 | 0.1106 | 1.8530 | 0.0987 | 0.1125 |
| **FeO** | 1.6911 | 0.8644 | 0.7138 | 1.2678 | 0.7674 | 1.8067 | 1.0059 | 0.7527 | 0.9297 | 0.5931 | 0.5833 |
| **CaO** | 27.9004 | 28.1575 | 26.6496 | 25.0981 | 24.4544 | 26.2516 | 26.4496 | 25.1504 | 26.2665 | 24.2687 | 24.7612 |
| **MnO** | 0.0002 | 0.1014 | 0.0002 | 0.0002 | 0.0677 | 0.0002 | 0.0819 | 0.0002 | 0.0002 | 0.0433 | 0.0736 |
| **MgO** | 0.0003 | 0.0003 | 0.0003 | 0.0003 | 0.0003 | 0.0003 | 0.0003 | 0.0003 | 0.0003 | 0.0003 | 0.0003 |
| **$Na_2O$** | 0.0847 | 0.0194 | 0.0925 | 0.9736 | 0.9980 | 0.1704 | 0.0481 | 0.6104 | 0.0524 | 0.7225 | 0.6387 |
| **$K_2O$** | 0.0017 | 0.0224 | 0.0001 | 0.0124 | 0.0124 | 0.0180 | 0.0679 | 0.0001 | 0.0001 | 0.0001 | 0.0001 |
| **F** | 0.6719 | 1.1356 | 0.1312 | 0.1306 | 0.0008 | 0.7421 | 0.9905 | 0.6080 | 1.1072 | 0.6424 | 0.4517 |
| **Total** | 92.8140 | 92.8571 | 95.5061 | 95.7346 | 95.1479 | 95.3144 | 95.3467 | 95.4717 | 95.7502 | 94.0422 | 94.2823 |
| | | | | | | | | | | | |
| **Si*** | 4.000 | 4.000 | 4.000 | 4.000 | 4.000 | 4.000 | 4.000 | 4.000 | 4.000 | 4.000 | 4.000 |
| **Al** | 0.200 | 0.320 | 0.115 | 0.002 | 0.001 | 0.241 | 0.279 | 0.017 | 0.287 | 0.015 | 0.017 |
| **Ti** | 3.057 | 3.063 | 3.691 | 3.845 | 3.836 | 3.418 | 3.467 | 3.738 | 3.472 | 3.763 | 3.708 |
| **$Fe^{2+}$** | 0.000 | 0.000 | 0.000 | 0.000 | 0.000 | 0.000 | 0.000 | 0.000 | 0.000 | 0.000 | 0.000 |
| **$Fe^{3+}$** | 0.186 | 0.096 | 0.079 | 0.085 | 0.063 | 0.200 | 0.112 | 0.083 | 0.102 | 0.066 | 0.065 |
| **Mn** | 0.000 | 0.011 | 0.000 | 0.000 | 0.008 | 0.000 | 0.009 | 0.000 | 0.000 | 0.005 | 0.008 |
| **Mg** | 0.000 | 0.000 | 0.000 | 0.000 | 0.000 | 0.000 | 0.000 | 0.000 | 0.000 | 0.000 | 0.000 |
| **Ca** | 3.940 | 4.023 | 3.786 | 3.591 | 3.463 | 3.710 | 3.758 | 3.542 | 3.700 | 3.459 | 3.501 |
| **Na** | 0.022 | 0.005 | 0.024 | 0.252 | 0.256 | 0.044 | 0.012 | 0.156 | 0.013 | 0.186 | 0.163 |
| **K** | 0.000 | 0.004 | 0.000 | 0.002 | 0.002 | 0.003 | 0.011 | 0.000 | 0.000 | 0.000 | 0.000 |
| **F** | 0.280 | 0.479 | 0.055 | 0.055 | 0.000 | 0.310 | 0.415 | 0.253 | 0.460 | 0.270 | 0.189 |
| **Total** | 11.685 | 12.002 | 11.750 | 11.833 | 11.628 | 11.925 | 12.064 | 11.788 | 12.034 | 11.765 | 11.652 |

*** Number of ions on basis of 4Si**

| | *Ijolite* | | *Syenite* | |
|---|---|---|---|---|
| | **BN12_1** | **BN12_2** | **BN17_1** | **BN17_3** |
| | tit1 | ??? | sph1 | tit1 |
| **$SiO_2$** | 28.8538 | 34.2548 | 30.6028 | 29.8308 |
| **$TiO_2$** | 33.4679 | 27.9968 | 35.0914 | 35.4602 |
| **$Al_2O_3$** | 0.4911 | 0.2161 | 2.1935 | 1.5334 |
| **FeO** | 0.9554 | 6.1689 | 1.3057 | 0.8085 |
| **CaO** | 26.1108 | 20.6081 | 25.6145 | 25.6601 |
| **MnO** | 0.0166 | 0.1556 | 0.1090 | 0.2226 |
| **MgO** | 0.0003 | 0.2470 | 0.3556 | 0.0003 |
| **$Na_2O$** | 0.0624 | 5.5874 | 0.0361 | 0.0003 |
| **$K_2O$** | 0.0053 | 0.0117 | 0.5294 | 0.0194 |
| **F** | 0.3200 | 0.0575 | 0.1340 | 0.6442 |
| **Total** | 90.2836 | 95.3039 | 95.9720 | 94.1798 |
| | | | | |
| **Si*** | 4.000 | 4.000 | 4.000 | 4.000 |
| **Al** | 0.080 | 0.030 | 0.338 | 0.242 |
| **Ti** | 3.490 | 2.459 | 3.450 | 3.576 |
| **$Fe^{2+}$** | 0.000 | 0.602 | 0.000 | 0.000 |
| **$Fe^{3+}$** | 0.111 | 0.000 | 0.143 | 0.091 |
| **Mn** | 0.002 | 0.015 | 0.012 | 0.025 |
| **Mg** | 0.000 | 0.043 | 0.069 | 0.000 |
| **Ca** | 3.878 | 2.578 | 3.587 | 3.686 |
| **Na** | 0.017 | 1.265 | 0.009 | 0.000 |
| **K** | 0.001 | 0.002 | 0.088 | 0.003 |
| **F** | 0.140 | 0.021 | 0.055 | 0.273 |
| **Total** | 11.718 | 11.015 | 11.751 | 11.897 |

**A6.7 Mica**

| | *Ijolite* | | | | | | | | | *Ijolite* | |
|---|---|---|---|---|---|---|---|---|---|---|---|
| | **BN1_1** | **BN1_3** | **BN1_4** | | **BN1_5** | | | | **BN1_6** | **BN3_1** | |
| | *mi1* | *mi1?* | *bt1* | *bt2* | *mi1* | *mi2* | *mi3* | *mi4* | *mi1* | *mi1* | *mi2* |
| **$SiO_2$** | 38.3631 | 44.6597 | 36.4902 | 40.5748 | 39.2308 | 44.4838 | 45.5115 | 43.7486 | 43.7710 | 39.9285 | 40.0403 |
| **$TiO_2$** | 0.2817 | 0.0761 | 0.3900 | 0.1102 | 0.5105 | 0.0654 | 0.0002 | 0.1609 | 0.0002 | 0.6888 | 0.8014 |
| **$Al_2O_3$** | 19.1246 | 32.0270 | 17.8041 | 17.5308 | 16.9865 | 30.7416 | 37.8754 | 30.3745 | 39.9968 | 16.1967 | 16.2831 |
| **FeO** | 5.4500 | 5.3206 | 5.6572 | 3.5853 | 5.7105 | 6.0937 | 0.2482 | 6.3488 | 1.9190 | 3.8498 | 4.2140 |
| **CaO** | 0.0002 | 0.0315 | 0.0261 | 0.0262 | 0.0002 | 0.0002 | 0.0186 | 0.0002 | 0.0002 | 0.0184 | 0.0032 |
| **MnO** | 1.3628 | 0.0560 | 1.5636 | 1.4363 | 1.3354 | 0.0935 | 0.0641 | 0.0447 | 0.0693 | 0.7519 | 0.6332 |
| **MgO** | 20.1602 | 0.8028 | 18.5355 | 20.2724 | 18.6742 | 0.7577 | 0.7365 | 0.7889 | 0.3330 | 20.8050 | 20.5427 |
| **$Na_2O$** | 0.0784 | 0.2240 | 0.4316 | 0.2155 | 0.1011 | 0.2853 | 0.2313 | 0.2491 | 0.2031 | 0.1903 | 0.1490 |
| **$K_2O$** | 10.1163 | 10.7272 | 10.1422 | 9.6699 | 10.2831 | 10.3529 | 10.3971 | 10.3243 | 10.3069 | 10.4864 | 10.1756 |
| **F** | - | - | - | - | - | - | - | - | - | 1.2621 | 0.4106 |
| **Total** | 94.9373 | 93.9249 | 91.0405 | 93.4214 | 92.8323 | 92.8741 | 95.0829 | 92.0400 | 96.5995 | 94.1779 | 93.2531 |
| | | | | | | | | | | | |
| **Si*** | 5.507 | 6.186 | 5.512 | 5.829 | 5.767 | 6.250 | 6.024 | 6.218 | 5.760 | 5.657 | 5.769 |
| **$Al^{iv}$** | 2.493 | 1.814 | 2.488 | 2.171 | 2.233 | 1.750 | 1.976 | 1.782 | 2.240 | 2.343 | 2.231 |
| | 8.000 | 8.000 | 8.000 | 8.000 | 8.000 | 8.000 | 8.000 | 8.000 | 8.000 | 8.000 | 8.000 |
| **$Al^{vi}$** | 0.743 | 3.414 | 0.681 | 0.797 | 0.710 | 3.339 | 3.932 | 3.306 | 3.963 | 0.361 | 0.534 |
| **Ti** | 0.030 | 0.008 | 0.044 | 0.012 | 0.056 | 0.007 | 0.000 | 0.017 | 0.000 | 0.073 | 0.087 |
| **$Fe^{2+}$** | 0.654 | 0.616 | 0.715 | 0.431 | 0.702 | 0.716 | 0.027 | 0.755 | 0.211 | 0.456 | 0.508 |
| **Mn** | 0.166 | 0.007 | 0.200 | 0.175 | 0.166 | 0.011 | 0.007 | 0.005 | 0.008 | 0.090 | 0.077 |
| **Mg** | 4.315 | 0.166 | 4.174 | 4.342 | 4.092 | 0.159 | 0.145 | 0.167 | 0.065 | 4.394 | 4.413 |
| | 5.908 | 4.210 | 5.814 | 5.755 | 5.727 | 4.232 | 4.112 | 4.250 | 4.247 | 5.375 | 5.618 |
| **Ca** | 0.000 | 0.005 | 0.004 | 0.004 | 0.000 | 0.000 | 0.003 | 0.000 | 0.000 | 0.003 | 0.000 |
| **Na** | 0.022 | 0.060 | 0.126 | 0.060 | 0.029 | 0.078 | 0.059 | 0.069 | 0.052 | 0.052 | 0.042 |
| **K** | 1.852 | 1.895 | 1.954 | 1.772 | 1.928 | 1.855 | 1.755 | 1.872 | 1.730 | 1.895 | 1.870 |
| **F** | - | - | - | - | - | - | - | - | - | 0.565 | 0.187 |
| | 1.874 | 1.960 | 2.085 | 1.836 | 1.957 | 1.933 | 1.817 | 1.941 | 1.782 | 2.516 | 2.099 |
| **Total** | 15.782 | 14.170 | 15.899 | 15.591 | 15.684 | 14.165 | 13.929 | 14.191 | 14.029 | 15.891 | 15.718 |

*** Based on 22O**

| | *Ijolite* | | | | | | | | *Ijolite* | | |
|---|---|---|---|---|---|---|---|---|---|---|---|
| | **BN3_2** | | **BN3_5** | | **BN3_6** | **BN3_8** | | | **BN4_1** | | |
| | *mi1* | *mi2* | *phl1* | *phl2* | *phl1* | *phl1* | *phl2* | *phl3* | *phlog1* | *phlog2* | *phlog3* |
| **$SiO_2$** | 39.8639 | 38.8102 | 40.2908 | 39.7057 | 39.3775 | 40.5674 | 38.4543 | 38.2692 | 39.4987 | 37.4998 | 35.0988 |
| **$TiO_2$** | 0.6548 | 2.6614 | 0.7196 | 0.7147 | 0.7004 | 0.6943 | 0.3727 | 0.3698 | 0.4389 | 0.544 | 0.4932 |
| **$Al_2O_3$** | 16.3092 | 15.2995 | 16.0751 | 16.2852 | 17.4899 | 16.8690 | 21.3059 | 21.2630 | 16.3465 | 18.0786 | 18.7525 |
| **FeO** | 4.2998 | 3.6855 | 3.9989 | 4.3616 | 3.8914 | 3.8189 | 3.8646 | 3.7635 | 7.7091 | 8.5101 | 9.3117 |
| **CaO** | 0.0097 | 1.7188 | 0.0126 | 0.0135 | 0.0002 | 0.0002 | 0.0378 | 0.0029 | 0.1289 | 0.0196 | 0.0416 |
| **MnO** | 0.6400 | 0.6374 | 0.6939 | 0.7426 | 0.5681 | 0.5981 | 0.7736 | 0.7217 | 0.9386 | 1.1110 | 1.1513 |
| **MgO** | 20.9172 | 19.8289 | 20.7013 | 20.8178 | 19.6869 | 20.0190 | 17.9503 | 18.1160 | 20.4934 | 19.0503 | 17.5780 |
| **$Na_2O$** | 0.1350 | 0.1507 | 0.1969 | 0.1578 | 0.1195 | 0.1104 | 0.2605 | 0.2677 | 0.0401 | 0.1128 | 0.0875 |
| **$K_2O$** | 10.3211 | 10.2291 | 10.0375 | 10.0271 | 10.3488 | 10.1687 | 9.5146 | 10.1875 | 9.3539 | 9.5152 | 9.3690 |
| **F** | 0.7421 | 0.7626 | 0.8286 | 0.8944 | 0.8997 | 0.7641 | 0.4385 | 0.0006 | - | - | - |
| **Total** | 93.8928 | 93.7841 | 93.5552 | 93.7204 | 93.0824 | 93.6101 | 92.9728 | 92.9619 | 94.9481 | 94.4414 | 91.8836 |
| | | | | | | | | | | | |
| **Si*** | 5.697 | 5.589 | 5.752 | 5.673 | 5.648 | 5.775 | 5.510 | 5.531 | 5.699 | 5.484 | 5.319 |
| **$Al^{iv}$** | 2.303 | 2.411 | 2.248 | 2.327 | 2.352 | 2.225 | 2.490 | 2.469 | 2.301 | 2.516 | 2.681 |
| | 8.000 | 8.000 | 8.000 | 8.000 | 8.000 | 8.000 | 8.000 | 8.000 | 8.000 | 8.000 | 8.000 |
| **$Al^{vi}$** | 0.444 | 0.185 | 0.457 | 0.415 | 0.605 | 0.604 | 1.108 | 1.153 | 0.478 | 0.600 | 0.669 |
| **Ti** | 0.070 | 0.288 | 0.077 | 0.077 | 0.076 | 0.074 | 0.040 | 0.040 | 0.048 | 0.060 | 0.056 |
| **$Fe^{2+}$** | 0.514 | 0.444 | 0.477 | 0.521 | 0.467 | 0.455 | 0.463 | 0.455 | 0.930 | 1.041 | 1.180 |
| **Mn** | 0.077 | 0.078 | 0.084 | 0.090 | 0.069 | 0.072 | 0.094 | 0.088 | 0.115 | 0.138 | 0.148 |
| **Mg** | 4.457 | 4.257 | 4.406 | 4.434 | 4.210 | 4.248 | 3.835 | 3.904 | 4.408 | 4.153 | 3.972 |
| | 5.563 | 5.252 | 5.501 | 5.537 | 5.426 | 5.454 | 5.540 | 5.640 | 5.978 | 5.992 | 6.024 |
| **Ca** | 0.001 | 0.265 | 0.002 | 0.002 | 0.000 | 0.000 | 0.006 | 0.000 | 0.020 | 0.003 | 0.007 |
| **Na** | 0.037 | 0.042 | 0.054 | 0.044 | 0.033 | 0.030 | 0.072 | 0.075 | 0.011 | 0.032 | 0.026 |
| **K** | 1.882 | 1.879 | 1.828 | 1.827 | 1.894 | 1.846 | 1.739 | 1.878 | 1.721 | 1.775 | 1.811 |
| **F** | 0.335 | 0.347 | 0.374 | 0.404 | 0.408 | 0.344 | 0.199 | 0.000 | - | - | - |
| | 2.256 | 2.533 | 2.258 | 2.277 | 2.335 | 2.221 | 2.016 | 1.954 | 1.753 | 1.810 | 1.844 |
| **Total** | 15.818 | 15.785 | 15.760 | 15.815 | 15.761 | 15.675 | 15.556 | 15.594 | 15.730 | 15.802 | 15.868 |

| | *Ijolite* | | | | | | | | | *Dyke* | |
|---|---|---|---|---|---|---|---|---|---|---|---|
| | **BN4_1** | | | | **BN4_2** | | | **BN4_3** | **BN4_4** | **BN6_1** | |
| | *phlog4* | *phlog5* | *phlog6* | *phlog7* | *phlog1* | *phlog2* | *phlog3* | *bt1* | *bt1* | *phl1* | *phl2* |
| **$SiO_2$** | 37.4680 | 37.6746 | 37.2403 | 37.2246 | 37.8568 | 37.2178 | 38.4395 | 36.8639 | 37.0457 | 36.8156 | 37.0977 |
| **$TiO_2$** | 0.5226 | 0.5353 | 0.6133 | 0.474 | 0.3857 | 0.3744 | 0.4618 | 0.5159 | 0.5469 | 0.4656 | 0.595 |
| **$Al_2O_3$** | 18.6539 | 18.2862 | 17.7578 | 18.3901 | 18.2113 | 18.5408 | 18.6424 | 17.6656 | 17.8367 | 17.8891 | 18.1584 |
| **FeO** | 8.3896 | 8.5600 | 8.6762 | 8.5421 | 7.8070 | 8.1591 | 8.1183 | 8.7468 | 8.3974 | 8.9569 | 9.1008 |
| **CaO** | 0.0130 | 0.0407 | 0.0184 | 0.0305 | 0.0037 | 0.0222 | 0.0351 | 0.0317 | 0.0164 | 0.0086 | 0.0002 |
| **MnO** | 1.2157 | 1.1271 | 1.0325 | 1.1502 | 0.8711 | 0.8330 | 0.9772 | 0.7067 | 1.1648 | 1.8071 | 1.6233 |
| **MgO** | 18.8909 | 19.2423 | 19.0047 | 19.0129 | 19.8474 | 19.1141 | 19.4758 | 19.0945 | 18.3454 | 17.0258 | 16.9827 |
| **$Na_2O$** | 0.0621 | 0.1275 | 0.1196 | 0.0504 | 0.0945 | 0.0718 | 0.0640 | 0.1348 | 0.1268 | 0.1194 | 0.0944 |
| **$K_2O$** | 9.8941 | 10.0483 | 10.1426 | 10.1292 | 10.0939 | 10.1924 | 10.1167 | 9.9527 | 9.9020 | 9.8970 | 9.9494 |
| **F** | - | - | - | - | - | - | - | - | - | - | - |
| **Total** | 95.1099 | 95.6420 | 94.6054 | 95.0040 | 95.1714 | 94.5256 | 96.3308 | 93.7126 | 93.3821 | 92.9851 | 93.6019 |
| | | | | | | | | | | | |
| **Si*** | 5.448 | 5.458 | 5.467 | 5.435 | 5.484 | 5.444 | 5.501 | 5.457 | 5.497 | 5.518 | 5.517 |
| **$Al^{iv}$** | 2.552 | 2.542 | 2.533 | 2.565 | 2.516 | 2.556 | 2.499 | 2.543 | 2.503 | 2.482 | 2.483 |
| | 8.000 | 8.000 | 8.000 | 8.000 | 8.000 | 8.000 | 8.000 | 8.000 | 8.000 | 8.000 | 8.000 |
| **$Al^{vi}$** | 0.645 | 0.580 | 0.539 | 0.600 | 0.593 | 0.641 | 0.645 | 0.539 | 0.616 | 0.677 | 0.700 |
| **Ti** | 0.057 | 0.058 | 0.068 | 0.052 | 0.042 | 0.041 | 0.050 | 0.057 | 0.061 | 0.052 | 0.067 |
| **$Fe^{2+}$** | 1.020 | 1.037 | 1.065 | 1.043 | 0.946 | 0.998 | 0.971 | 1.083 | 1.042 | 1.122 | 1.132 |
| **Mn** | 0.150 | 0.138 | 0.128 | 0.142 | 0.107 | 0.103 | 0.118 | 0.089 | 0.146 | 0.229 | 0.204 |
| **Mg** | 4.095 | 4.156 | 4.159 | 4.139 | 4.286 | 4.168 | 4.155 | 4.214 | 4.058 | 3.804 | 3.765 |
| | 5.968 | 5.970 | 5.960 | 5.975 | 5.973 | 5.952 | 5.940 | 5.981 | 5.924 | 5.885 | 5.868 |
| **Ca** | 0.002 | 0.006 | 0.003 | 0.005 | 0.001 | 0.003 | 0.005 | 0.005 | 0.003 | 0.001 | 0.000 |
| **Na** | 0.018 | 0.036 | 0.034 | 0.014 | 0.027 | 0.020 | 0.018 | 0.039 | 0.036 | 0.035 | 0.027 |
| **K** | 1.835 | 1.857 | 1.899 | 1.887 | 1.865 | 1.902 | 1.847 | 1.879 | 1.874 | 1.892 | 1.887 |
| **F** | - | - | - | - | - | - | - | - | - | - | - |
| | 1.855 | 1.899 | 1.936 | 1.906 | 1.892 | 1.926 | 1.870 | 1.923 | 1.913 | 1.928 | 1.915 |
| **Total** | 15.822 | 15.869 | 15.896 | 15.881 | 15.866 | 15.877 | 15.810 | 15.904 | 15.838 | 15.814 | 15.782 |

| | *Dyke* | | | | | | *Dyke* | | | | |
|---|---|---|---|---|---|---|---|---|---|---|---|
| | **BN6_1** | **BN6_2** | | | **BN6_3** | **BN6_4** | **BN7_1** | | **BN7_2** | | |
| | *bio1* | *phl1* | *mica2* | *mica3* | *phl1* | *mi1* | *bio1* | *bio2* | *bio1* | *bio2* | *bio3* |
| **$SiO_2$** | 36.3601 | 39.5861 | 35.6705 | 36.7158 | 36.4438 | 36.5278 | 36.4885 | 36.6432 | 36.6219 | 35.8449 | 36.3979 |
| **$TiO_2$** | 0.5766 | 0.4912 | 0.3652 | 0.4767 | 0.565 | 0.4323 | 0.41 | 0.4344 | 0.5383 | 0.5653 | 0.6252 |
| **$Al_2O_3$** | 18.1040 | 19.0404 | 18.1646 | 18.2012 | 18.4151 | 17.8573 | 19.2196 | 19.2015 | 19.1878 | 18.7679 | 18.6772 |
| **FeO** | 9.7535 | 8.2965 | 9.2738 | 9.2154 | 9.4916 | 9.4301 | 8.8449 | 9.3034 | 9.6824 | 10.6673 | 9.9266 |
| **CaO** | 0.0002 | 0.0565 | 0.0002 | 0.0002 | 0.0002 | 0.0040 | 0.0002 | 0.0557 | 0.0596 | 0.0002 | 0.0002 |
| **MnO** | 1.7774 | 1.5529 | 1.6818 | 1.7700 | 1.6457 | 1.6160 | 2.2932 | 2.0325 | 2.2275 | 2.2148 | 2.2451 |
| **MgO** | 17.0761 | 15.0452 | 16.6071 | 16.9860 | 16.5475 | 16.9808 | 16.2209 | 16.2276 | 15.1244 | 15.3171 | 15.4491 |
| **$Na_2O$** | 0.1228 | 1.4244 | 0.1098 | 0.1122 | 0.1501 | 0.0888 | 0.1194 | 0.0826 | 0.2592 | 0.1951 | 0.1161 |
| **$K_2O$** | 9.8438 | 8.4752 | 10.0200 | 10.0389 | 9.8012 | 10.0769 | 9.9549 | 9.9148 | 9.7432 | 9.6746 | 9.8362 |
| **F** | - | - | - | - | - | - | - | - | - | - | - |
| **Total** | 93.6145 | 93.9684 | 91.8930 | 93.5164 | 93.0602 | 93.0140 | 93.5516 | 93.8957 | 93.4443 | 93.2472 | 93.2736 |
| | | | | | | | | | | | |
| **Si*** | 5.438 | 5.764 | 5.433 | 5.481 | 5.466 | 5.491 | 5.440 | 5.445 | 5.480 | 5.412 | 5.471 |
| **$Al^{iv}$** | 2.562 | 2.236 | 2.567 | 2.519 | 2.534 | 2.509 | 2.560 | 2.555 | 2.520 | 2.588 | 2.529 |
| | 8.000 | 8.000 | 8.000 | 8.000 | 8.000 | 8.000 | 8.000 | 8.000 | 8.000 | 8.000 | 8.000 |
| **$Al^{vi}$** | 0.628 | 1.031 | 0.694 | 0.684 | 0.721 | 0.654 | 0.817 | 0.808 | 0.863 | 0.752 | 0.779 |
| **Ti** | 0.065 | 0.054 | 0.042 | 0.054 | 0.064 | 0.049 | 0.046 | 0.049 | 0.061 | 0.064 | 0.071 |
| **$Fe^{2+}$** | 1.220 | 1.010 | 1.181 | 1.150 | 1.190 | 1.185 | 1.103 | 1.156 | 1.211 | 1.347 | 1.248 |
| **Mn** | 0.225 | 0.191 | 0.217 | 0.224 | 0.209 | 0.206 | 0.290 | 0.256 | 0.282 | 0.283 | 0.286 |
| **Mg** | 3.807 | 3.266 | 3.771 | 3.780 | 3.700 | 3.805 | 3.606 | 3.595 | 3.374 | 3.448 | 3.462 |
| | 5.945 | 5.552 | 5.905 | 5.892 | 5.884 | 5.899 | 5.861 | 5.864 | 5.791 | 5.894 | 5.845 |
| **Ca** | 0.000 | 0.009 | 0.000 | 0.000 | 0.000 | 0.001 | 0.000 | 0.009 | 0.010 | 0.000 | 0.000 |
| **Na** | 0.036 | 0.402 | 0.032 | 0.032 | 0.044 | 0.026 | 0.035 | 0.024 | 0.075 | 0.057 | 0.034 |
| **K** | 1.878 | 1.574 | 1.947 | 1.912 | 1.875 | 1.932 | 1.893 | 1.879 | 1.860 | 1.863 | 1.886 |
| **F** | - | - | - | - | - | - | - | - | - | - | - |
| | 1.913 | 1.985 | 1.979 | 1.944 | 1.919 | 1.959 | 1.928 | 1.912 | 1.944 | 1.920 | 1.920 |
| **Total** | 15.859 | 15.537 | 15.884 | 15.836 | 15.802 | 15.858 | 15.789 | 15.776 | 15.735 | 15.814 | 15.764 |

| | | | *Ijolite* | | | | | | | | *Ijolite* |
|---|---|---|---|---|---|---|---|---|---|---|---|
| | **BN7_3** | | **BN8_1** | | | **BN8_2** | | **BN8_3** | | **BN8_4** | **BN12_1** |
| | *bio1* | *bio2* | *mica1* | *mu1?* | *mica2* | *phl1* | *mica1* | *phlo1* | *phlo2* | *mica1* | *phl2* |
| **$SiO_2$** | 36.5226 | 35.8727 | 43.3986 | 44.4793 | 43.8903 | 35.5064 | 35.3028 | 34.9890 | 34.9864 | 42.0223 | 37.264 |
| **$TiO_2$** | 0.6291 | 0.5752 | 0.1509 | 0.0263 | 0.1628 | 0.7115 | 0.8185 | 0.6081 | 0.9413 | 0.2113 | 0.5044 |
| **$Al_2O_3$** | 19.1756 | 18.5591 | 32.2046 | 35.4747 | 32.7166 | 19.0252 | 19.1537 | 19.0419 | 19.0370 | 29.8901 | 14.3943 |
| **FeO** | 10.4700 | 9.8300 | 4.9225 | 2.6604 | 4.6047 | 14.2961 | 15.4575 | 14.1508 | 14.3485 | 7.6871 | 4.5881 |
| **CaO** | 0.0054 | 0.0002 | 0.0197 | 0.0002 | 0.0002 | 0.0279 | 0.0135 | 0.0243 | 0.4428 | 0.0332 | 0.0068 |
| **MnO** | 2.2408 | 2.1966 | 0.0341 | 0.0301 | 0.0765 | 0.9333 | 1.0243 | 1.0875 | 1.0435 | 0.3281 | 0.5519 |
| **MgO** | 15.5500 | 15.3023 | 0.5413 | 0.1885 | 0.6209 | 13.1755 | 12.5629 | 13.5123 | 12.6739 | 3.0703 | 21.979 |
| **$Na_2O$** | 0.2060 | 0.0760 | 0.4047 | 0.4109 | 0.3296 | 0.1454 | 0.1176 | 0.1090 | 0.1068 | 0.2226 | 0.0917 |
| **$K_2O$** | 9.5125 | 9.7238 | 9.9848 | 10.2634 | 9.9803 | 9.4758 | 9.5842 | 9.4209 | 9.2364 | 10.0309 | 9.2658 |
| **F** | - | - | 0.2612 | 0.0718 | 0.0467 | 0.4081 | 1.2380 | 1.0071 | 0.6476 | 0.1155 | 1.7423 |
| **Total** | 94.3120 | 92.1359 | 91.9224 | 93.6056 | 92.4286 | 93.7052 | 95.2730 | 93.9509 | 93.4642 | 93.6114 | 90.3883 |
| | | | | | | | | | | | |
| **Si*** | 5.429 | 5.458 | 6.100 | 6.062 | 6.129 | 5.365 | 5.235 | 5.244 | 5.296 | 5.945 | 5.490 |
| **$Al^{iv}$** | 2.571 | 2.542 | 1.900 | 1.938 | 1.871 | 2.635 | 2.765 | 2.756 | 2.704 | 2.055 | 2.510 |
| | 8.000 | 8.000 | 8.000 | 8.000 | 8.000 | 8.000 | 8.000 | 8.000 | 8.000 | 8.000 | 8.000 |
| **$Al^{vi}$** | 0.788 | 0.786 | 3.435 | 3.761 | 3.514 | 0.752 | 0.581 | 0.608 | 0.692 | 2.929 | -0.010 |
| **Ti** | 0.070 | 0.066 | 0.016 | 0.003 | 0.017 | 0.081 | 0.091 | 0.069 | 0.107 | 0.022 | 0.056 |
| **$Fe^{2+}$** | 1.301 | 1.251 | 0.579 | 0.303 | 0.538 | 1.806 | 1.916 | 1.774 | 1.816 | 0.909 | 0.565 |
| **Mn** | 0.282 | 0.283 | 0.004 | 0.003 | 0.009 | 0.119 | 0.129 | 0.138 | 0.134 | 0.039 | 0.069 |
| **Mg** | 3.446 | 3.471 | 0.113 | 0.038 | 0.129 | 2.968 | 2.777 | 3.019 | 2.860 | 0.648 | 4.828 |
| | 5.888 | 5.857 | 4.147 | 4.108 | 4.207 | 5.727 | 5.495 | 5.608 | 5.609 | 4.548 | 5.507 |
| **Ca** | 0.001 | 0.000 | 0.003 | 0.000 | 0.000 | 0.005 | 0.002 | 0.004 | 0.072 | 0.005 | 0.001 |
| **Na** | 0.059 | 0.022 | 0.110 | 0.109 | 0.089 | 0.043 | 0.034 | 0.032 | 0.031 | 0.061 | 0.026 |
| **K** | 1.804 | 1.887 | 1.790 | 1.784 | 1.778 | 1.826 | 1.813 | 1.801 | 1.783 | 1.810 | 1.741 |
| **F** | - | - | 0.116 | 0.031 | 0.021 | 0.195 | 0.580 | 0.477 | 0.310 | 0.052 | 0.812 |
| | 1.864 | 1.910 | 2.020 | 1.924 | 1.888 | 2.068 | 2.429 | 2.314 | 2.197 | 1.928 | 2.580 |
| **Total** | 15.752 | 15.767 | 14.167 | 14.032 | 14.095 | 15.795 | 15.924 | 15.922 | 15.806 | 14.476 | 16.088 |

| | *Ijolite* | *Syenite* | *Syenite* | | | | | | | | |
|---|---|---|---|---|---|---|---|---|---|---|---|
| | **BN12_2** | **BN15_1** | **BN16_1** | **BN16_2** | | | | **BN16_4** | | | |
| | *phl1* | *mu1* | *mi1* | *mi1* | *mi2* | *mi3* | *mi4* | *mi2* | *mi3* | *mi4* | *mi5* |
| **$SiO_2$** | 38.2289 | 47.6582 | 36.2518 | 36.6797 | 35.9266 | 46.7611 | 35.4964 | 46.6065 | 36.2597 | 36.6462 | 36.6528 |
| **$TiO_2$** | 0.3935 | 0.9458 | 2.4386 | 2.4893 | 2.3537 | 1.3984 | 2.4847 | 0.0787 | 1.0995 | 1.0713 | 1.0526 |
| **$Al_2O_3$** | 15.8080 | 30.0305 | 18.2626 | 18.6306 | 18.7025 | 33.5629 | 17.8089 | 33.6215 | 18.6935 | 18.3577 | 17.9459 |
| **FeO** | 5.2050 | 4.8780 | 18.1991 | 17.0903 | 17.9509 | 5.2819 | 18.0753 | 5.0579 | 17.7273 | 17.1419 | 16.2041 |
| **CaO** | 0.0097 | 0.0002 | 0.0752 | 0.0299 | 0.0002 | 0.0158 | 0.0195 | 0.0064 | 0.0372 | 0.0002 | 0.0145 |
| **MnO** | 0.6185 | 0.0447 | 0.3501 | 0.4560 | 0.4068 | 0.0852 | 0.4628 | 0.1032 | 0.4118 | 0.4521 | 0.5470 |
| **MgO** | 21.8910 | 1.4748 | 11.0222 | 11.3009 | 11.0637 | 1.6232 | 11.4168 | 1.7347 | 12.1316 | 12.3112 | 12.2968 |
| **$Na_2O$** | 0.1125 | 0.2032 | 0.0715 | 0.0944 | 0.0668 | 0.1871 | 0.0249 | 0.2681 | 0.2114 | 0.1371 | 1.0008 |
| **$K_2O$** | 10.0568 | 10.4170 | 9.2109 | 9.2539 | 9.4904 | 10.5531 | 8.7221 | 10.2301 | 9.4267 | 9.4395 | 8.9535 |
| **F** | 1.2005 | 0.3447 | - | - | - | - | - | - | - | - | - |
| **Total** | 93.5244 | 95.9971 | 95.8820 | 96.0250 | 95.9616 | 99.4687 | 94.5114 | 97.7071 | 95.9987 | 95.5572 | 94.6680 |
| | | | | | | | | | | | |
| **Si*** | 5.503 | 6.390 | 5.447 | 5.468 | 5.398 | 6.095 | 5.410 | 6.160 | 5.436 | 5.500 | 5.536 |
| **$Al^{iv}$** | 2.497 | 1.610 | 2.553 | 2.532 | 2.602 | 1.905 | 2.590 | 1.840 | 2.564 | 2.500 | 2.464 |
| | 8.000 | 8.000 | 8.000 | 8.000 | 8.000 | 8.000 | 8.000 | 8.000 | 8.000 | 8.000 | 8.000 |
| **$Al^{vi}$** | 0.185 | 3.136 | 0.680 | 0.740 | 0.710 | 3.250 | 0.609 | 3.396 | 0.739 | 0.747 | 0.731 |
| **Ti** | 0.043 | 0.095 | 0.276 | 0.279 | 0.266 | 0.137 | 0.285 | 0.008 | 0.124 | 0.121 | 0.120 |
| **$Fe^{2+}$** | 0.627 | 0.547 | 2.286 | 2.130 | 2.255 | 0.576 | 2.304 | 0.559 | 2.222 | 2.151 | 2.047 |
| **Mn** | 0.075 | 0.005 | 0.045 | 0.058 | 0.052 | 0.009 | 0.060 | 0.012 | 0.052 | 0.057 | 0.070 |
| **Mg** | 4.698 | 0.295 | 2.469 | 2.511 | 2.478 | 0.315 | 2.594 | 0.342 | 2.712 | 2.755 | 2.769 |
| | 5.627 | 4.078 | 5.756 | 5.719 | 5.761 | 4.288 | 5.851 | 4.317 | 5.850 | 5.832 | 5.736 |
| **Ca** | 0.001 | 0.000 | 0.012 | 0.005 | 0.000 | 0.002 | 0.003 | 0.001 | 0.006 | 0.000 | 0.002 |
| **Na** | 0.031 | 0.053 | 0.021 | 0.027 | 0.019 | 0.047 | 0.007 | 0.069 | 0.061 | 0.040 | 0.293 |
| **K** | 1.847 | 1.782 | 1.765 | 1.760 | 1.819 | 1.755 | 1.696 | 1.725 | 1.803 | 1.807 | 1.725 |
| **F** | 0.546 | 0.146 | - | - | - | - | - | - | - | - | - |
| | 2.426 | 1.981 | 1.798 | 1.792 | 1.838 | 1.804 | 1.706 | 1.794 | 1.870 | 1.847 | 2.020 |
| **Total** | 16.053 | 14.059 | 15.554 | 15.510 | 15.599 | 14.091 | 15.557 | 14.111 | 15.720 | 15.679 | 15.756 |

| | **BN16_4** | | | | **BN16_5** | **BN17_1** | | | **BN17_2** | | |
|---|---|---|---|---|---|---|---|---|---|---|---|
| | *mi6* | *mi7* | *mi8* | *mi9* | *mi1* | *bio2* | *bio (???)* | *phlog1* | *bio1* | *bio2* | *bio3* |
| **$SiO_2$** | 45.8968 | 46.1883 | 36.2057 | 45.8388 | 35.2567 | 36.7878 | 37.555 | 37.1067 | 37.7294 | 37.9361 | 36.7584 |
| **$TiO_2$** | 0.1500 | 0.0002 | 1.5691 | 0.0474 | 2.3660 | 2.4125 | 2.4267 | 2.5049 | 2.4422 | 2.471 | 2.4792 |
| **$Al_2O_3$** | 34.5306 | 34.3066 | 18.8170 | 34.5129 | 15.4257 | 15.4763 | 15.8418 | 15.5703 | 14.6544 | 15.2825 | 15.3292 |
| **FeO** | 4.6438 | 4.8110 | 17.8644 | 4.5989 | 18.0113 | 15.5689 | 14.4171 | 15.7354 | 14.6146 | 14.9503 | 15.4408 |
| **CaO** | 0.0181 | 0.0032 | 0.0155 | 0.0245 | 0.0049 | 0.0333 | 0.0669 | 0.0123 | 0.0002 | 0.0211 | 0.0002 |
| **MnO** | 0.0405 | 0.0002 | 0.3997 | 0.0002 | 0.5359 | 0.6803 | 0.6026 | 0.7629 | 0.6696 | 0.5754 | 0.6375 |
| **MgO** | 1.3561 | 1.5518 | 12.1377 | 1.4267 | 10.3555 | 12.4245 | 13.0294 | 12.7786 | 13.2953 | 13.1749 | 13.1798 |
| **$Na_2O$** | 0.3002 | 0.2384 | 0.1087 | 0.2867 | 0.0998 | 0.116 | 0.1031 | 0.134 | 0.0833 | 0.1022 | 0.0974 |
| **$K_2O$** | 10.4483 | 10.3686 | 9.5562 | 10.2100 | 9.4480 | 9.7766 | 9.344 | 9.606 | 9.8211 | 9.676 | 9.8576 |
| **F** | - | - | - | - | 0.3119 | 1.4337 | 1.6737 | 1.4553 | 1.3351 | 1.6089 | 1.215 |
| **Total** | 97.3844 | 97.4683 | 96.6740 | 96.9461 | 91.8157 | 94.7099 | 95.0603 | 95.6664 | 94.6452 | 95.7984 | 94.9951 |
| | | | | | | | | | | | |
| **Si*** | 6.084 | 6.114 | 5.396 | 6.092 | 5.564 | 5.483 | 5.502 | 5.470 | 5.600 | 5.541 | 5.476 |
| **$Al^{iv}$** | 1.916 | 1.886 | 2.604 | 1.908 | 2.436 | 2.517 | 2.498 | 2.530 | 2.400 | 2.459 | 2.524 |
| | 8.000 | 8.000 | 8.000 | 8.000 | 8.000 | 8.000 | 8.000 | 8.000 | 8.000 | 8.000 | 8.000 |
| **$Al^{vi}$** | 3.478 | 3.465 | 0.700 | 3.497 | 0.433 | 0.202 | 0.236 | 0.175 | 0.164 | 0.172 | 0.168 |
| **Ti** | 0.015 | 0.000 | 0.176 | 0.005 | 0.281 | 0.270 | 0.267 | 0.278 | 0.273 | 0.271 | 0.278 |
| **$Fe^{2+}$** | 0.515 | 0.532 | 2.226 | 0.511 | 2.377 | 1.940 | 1.766 | 1.940 | 1.814 | 1.826 | 1.924 |
| **Mn** | 0.005 | 0.000 | 0.050 | 0.000 | 0.072 | 0.086 | 0.075 | 0.095 | 0.084 | 0.071 | 0.080 |
| **Mg** | 0.268 | 0.306 | 2.697 | 0.283 | 2.436 | 2.761 | 2.846 | 2.808 | 2.942 | 2.869 | 2.927 |
| | 4.280 | 4.304 | 5.850 | 4.295 | 5.598 | 5.260 | 5.190 | 5.297 | 5.277 | 5.210 | 5.377 |
| **Ca** | 0.003 | 0.000 | 0.002 | 0.003 | 0.001 | 0.005 | 0.010 | 0.002 | 0.000 | 0.003 | 0.000 |
| **Na** | 0.077 | 0.061 | 0.031 | 0.074 | 0.031 | 0.034 | 0.029 | 0.038 | 0.024 | 0.029 | 0.028 |
| **K** | 1.767 | 1.751 | 1.817 | 1.731 | 1.902 | 1.859 | 1.746 | 1.806 | 1.860 | 1.803 | 1.873 |
| **F** | - | - | - | - | 0.156 | 0.676 | 0.775 | 0.678 | 0.627 | 0.743 | 0.572 |
| | 1.846 | 1.812 | 1.850 | 1.808 | 2.089 | 2.573 | 2.561 | 2.525 | 2.510 | 2.578 | 2.474 |
| **Total** | 14.126 | 14.116 | 15.700 | 14.103 | 15.687 | 15.833 | 15.751 | 15.822 | 15.787 | 15.788 | 15.851 |

| | **BN17_3** | | | |
|---|---|---|---|---|
| | *bt1* | *bt2* | *bt3* | *bt4* |
| **$SiO_2$** | 36.9758 | 36.745 | 36.6409 | 36.9172 |
| **$TiO_2$** | 2.5434 | 2.393 | 2.2505 | 2.4896 |
| **$Al_2O_3$** | 15.6573 | 15.5424 | 15.7664 | 15.8859 |
| **FeO** | 15.6038 | 15.9987 | 16.124 | 16.228 |
| **CaO** | 0.0152 | 0.0002 | 0.0143 | 0.0076 |
| **MnO** | 0.7435 | 0.6934 | 0.6654 | 0.7312 |
| **MgO** | 12.0473 | 12.3043 | 12.4148 | 11.9519 |
| **$Na_2O$** | 0.0664 | 0.0775 | 0.1189 | 0.1003 |
| **$K_2O$** | 8.9033 | 9.2482 | 9.0179 | 9.1842 |
| **F** | 0.9838 | 1.4096 | 0.7946 | 1.4551 |
| **Total** | 93.5398 | 94.4123 | 93.8077 | 94.951 |
| | | | | |
| **Si*** | 5.573 | 5.488 | 5.541 | 5.479 |
| **$Al^{iv}$** | 2.427 | 2.512 | 2.459 | 2.521 |
| | 8.000 | 8.000 | 8.000 | 8.000 |
| **$Al^{vi}$** | 0.354 | 0.223 | 0.350 | 0.258 |
| **Ti** | 0.288 | 0.269 | 0.256 | 0.278 |
| **$Fe^{2+}$** | 1.967 | 1.998 | 2.039 | 2.014 |
| **Mn** | 0.095 | 0.088 | 0.085 | 0.092 |
| **Mg** | 2.707 | 2.740 | 2.799 | 2.644 |
| | 5.411 | 5.318 | 5.529 | 5.286 |
| **Ca** | 0.002 | 0.000 | 0.002 | 0.001 |
| **Na** | 0.019 | 0.022 | 0.035 | 0.029 |
| **K** | 1.712 | 1.762 | 1.739 | 1.739 |
| **F** | 0.469 | 0.666 | 0.380 | 0.683 |
| | 2.202 | 2.450 | 2.157 | 2.452 |
| **Total** | 15.614 | 15.768 | 15.686 | 15.738 |

**A6.8 Feldspar**

| | *Ijolite* | | | | | | | | *Syenite* |
|---|---|---|---|---|---|---|---|---|---|
| | **BN1_1** | | | **BN1_4** | | **BN1_5** | | **BN1_6** | **BN2_1** |
| | *or1* | *pl1* | *pl2* | *or1* | *pl1* | *or1* | *pl1* | *pl1* | *or1* |
| **$SiO_2$** | 62.7124 | 71.0259 | 70.5872 | 63.2272 | 72.7800 | 61.7134 | 68.7171 | 69.0481 | 65.5281 |
| **$Al_2O_3$** | 17.5797 | 19.9865 | 20.1530 | 18.2536 | 20.0673 | 18.4415 | 19.3052 | 22.7549 | 21.4088 |
| **FeO** | 0.0278 | 0.2172 | 0.1438 | 0.0139 | 0.0908 | 0.0824 | 0.0797 | 0.0581 | 0.2600 |
| **CaO** | 0.1647 | 0.1696 | 0.2245 | 0.0002 | 0.0567 | 0.0002 | 0.1787 | 0.2776 | 0.0250 |
| **MnO** | 0.0038 | 0.0002 | 0.0002 | 0.0002 | 0.0381 | 0.0002 | 0.0606 | 0.0280 | 0.0002 |
| **MgO** | 0.0098 | 0.0003 | 0.0003 | 0.0058 | 0.0003 | 0.0041 | 0.0003 | 0.0097 | 0.0047 |
| **$Na_2O$** | 0.2195 | 11.5391 | 10.9492 | 0.8601 | 11.4145 | 0.5400 | 11.4421 | 11.5382 | 0.1352 |
| **$K_2O$** | 15.6195 | 0.1005 | 0.1135 | 14.4128 | 0.1711 | 14.8368 | 0.1181 | 0.0833 | 14.1132 |
| **BaO** | 0.2481 | 0.0002 | 0.0002 | 0.9444 | 0.0135 | 1.7936 | 0.0054 | 0.0002 | 0.7968 |
| **SrO** | 0.0001 | 0.0001 | 0.0001 | 0.1914 | 0.0001 | 0.3439 | 0.0001 | 0.0001 | - |
| **Total** | 96.5854 | 103.0396 | 102.1720 | 97.9096 | 104.6324 | 97.7561 | 99.9073 | 103.7982 | 102.2720 |
| | | | | | | | | | |
| **Si*** | 12.017 | 12.026 | 12.025 | 11.954 | 12.106 | 11.826 | 12.013 | 11.633 | 11.741 |
| **Al** | 3.970 | 3.988 | 4.046 | 4.067 | 3.934 | 4.165 | 3.977 | 4.518 | 4.521 |
| **$Fe^{2+}$** | 0.004 | 0.031 | 0.020 | 0.002 | 0.013 | 0.013 | 0.012 | 0.008 | 0.039 |
| **Ca** | 0.034 | 0.031 | 0.041 | 0.000 | 0.010 | 0.000 | 0.033 | 0.050 | 0.005 |
| **Mn** | 0.001 | 0.000 | 0.000 | 0.000 | 0.005 | 0.000 | 0.009 | 0.004 | 0.000 |
| **Mg** | 0.003 | 0.000 | 0.000 | 0.002 | 0.000 | 0.001 | 0.000 | 0.002 | 0.001 |
| **Na** | 0.082 | 3.788 | 3.616 | 0.315 | 3.681 | 0.201 | 3.878 | 3.769 | 0.047 |
| **K** | 3.818 | 0.022 | 0.025 | 3.476 | 0.036 | 3.627 | 0.026 | 0.018 | 3.226 |
| **Ba** | 0.019 | 0.000 | 0.000 | 0.070 | 0.001 | 0.135 | 0.000 | 0.000 | 0.056 |
| **Sr** | 0.000 | 0.000 | 0.000 | 0.021 | 0.000 | 0.038 | 0.000 | 0.000 | - |
| | 19.947 | 19.885 | 19.773 | 19.908 | 19.786 | 20.005 | 19.950 | 20.002 | 19.635 |
| | | | | | | | | | |
| **Or** | 97.07 | 0.57 | 0.66 | 91.68 | 0.97 | 94.76 | 0.67 | 0.47 | 98.42 |
| **Ab** | 2.07 | 98.63 | 97.14 | 8.32 | 98.75 | 5.24 | 98.48 | 98.23 | 1.43 |
| **An** | 0.86 | 0.80 | 2.20 | 0.00 | 0.27 | 0.00 | 0.85 | 1.31 | 0.15 |

* Based on 32O
- not analysed

| | *Syenite* | | | | | | | | |
|---|---|---|---|---|---|---|---|---|---|
| | **BN2_1** | | **BN2_2** | | | | **BN2_3** | | **BN2_4** |
| | *or2* | *or3* | *or1* | *pl1* | *pl2* | *or2* | *or1* | *or2* | *or1* |
| **$SiO_2$** | 63.5458 | 64.6022 | 63.6415 | 69.4784 | 67.9813 | 63.8435 | 64.1534 | 64.9354 | 62.0145 |
| **$Al_2O_3$** | 20.6204 | 20.7703 | 20.7320 | 22.7589 | 22.2253 | 20.5246 | 20.7026 | 20.6726 | 20.3798 |
| **FeO** | 0.0321 | 0.0995 | 0.0002 | 0.1781 | 0.1424 | 0.0547 | 0.0612 | 0.2119 | 0.0322 |
| **CaO** | 0.0700 | 0.0002 | 0.0002 | 0.4185 | 0.0855 | 0.0002 | 0.0052 | 0.0002 | 0.0147 |
| **MnO** | 0.0002 | 0.0044 | 0.0002 | 0.0002 | 0.0398 | 0.0002 | 0.0002 | 0.0528 | 0.0088 |
| **MgO** | 0.0002 | 0.0002 | 0.0218 | 0.0003 | 0.0266 | 0.0241 | 0.0002 | 0.0002 | 0.0125 |
| **$Na_2O$** | 0.2244 | 0.1232 | 0.3584 | 10.9469 | 11.1466 | 0.1242 | 0.1716 | 0.1971 | 0.2444 |
| **$K_2O$** | 15.9989 | 15.4691 | 15.6136 | 0.1113 | 0.1420 | 16.3930 | 15.9449 | 15.5924 | 15.2535 |
| **BaO** | 0.5269 | 0.5331 | 0.3118 | 0.0345 | 0.0002 | 0.0491 | 0.1908 | 0.9709 | 0.4907 |
| **SrO** | - | - | - | - | - | - | - | - | - |
| **Total** | 101.0189 | 101.6022 | 100.6797 | 103.9271 | 101.7897 | 101.0136 | 101.2301 | 102.6335 | 98.4511 |
| | | | | | | | | | |
| **Si*** | 11.668 | 11.732 | 11.678 | 11.672 | 11.669 | 11.698 | 11.706 | 11.730 | 11.654 |
| **Al** | 4.462 | 4.445 | 4.483 | 4.506 | 4.496 | 4.432 | 4.452 | 4.401 | 4.513 |
| **$Fe^{2+}$** | 0.005 | 0.015 | 0.000 | 0.025 | 0.020 | 0.008 | 0.009 | 0.032 | 0.005 |
| **Ca** | 0.014 | 0.000 | 0.000 | 0.075 | 0.016 | 0.000 | 0.001 | 0.000 | 0.003 |
| **Mn** | 0.000 | 0.001 | 0.000 | 0.000 | 0.006 | 0.000 | 0.000 | 0.008 | 0.001 |
| **Mg** | 0.000 | 0.000 | 0.006 | 0.000 | 0.007 | 0.007 | 0.000 | 0.000 | 0.004 |
| **Na** | 0.080 | 0.043 | 0.127 | 3.565 | 3.709 | 0.044 | 0.061 | 0.069 | 0.089 |
| **K** | 3.747 | 3.584 | 3.655 | 0.024 | 0.031 | 3.831 | 3.711 | 3.593 | 3.656 |
| **Ba** | 0.038 | 0.038 | 0.022 | 0.002 | 0.000 | 0.004 | 0.014 | 0.069 | 0.036 |
| **Sr** | - | - | - | - | - | - | - | - | - |
| | 20.014 | 19.858 | 19.972 | 19.870 | 19.954 | 20.024 | 19.954 | 19.901 | 19.962 |
| | | | | | | | | | |
| **Or** | 97.56 | 98.80 | 96.63 | 0.65 | 0.83 | 98.86 | 98.36 | 98.11 | 97.55 |
| **Ab** | 2.08 | 1.20 | 3.37 | 97.29 | 98.75 | 1.14 | 1.61 | 1.88 | 2.38 |
| **An** | 0.36 | 0.00 | 0.00 | 2.06 | 0.42 | 0.00 | 0.03 | 0.00 | 0.08 |

| | | | | | | | *Ijolite* | | |
|---|---|---|---|---|---|---|---|---|---|
| | **BN2_4** | **BN2_5** | | | **BN2_6** | | **BN3_1** | | **BN3_2** |
| | *or2* | *pl1* | *pl2* | *or1* | *pl1* | *or1* | *pl1* | *pl2* | *pl1* |
| **$SiO_2$** | 63.5121 | 70.7204 | 70.7204 | 64.1627 | 71.3971 | 64.1388 | 70.8123 | 68.5728 | 73.0394 |
| **$Al_2O_3$** | 20.3805 | 20.3473 | 20.3473 | 17.6948 | 19.8519 | 17.7890 | 20.4191 | 19.6497 | 20.9684 |
| **FeO** | 0.1321 | 0.0837 | 0.0837 | 0.0609 | 0.0548 | 0.0352 | 0.0682 | 0.1807 | 0.1741 |
| **CaO** | 0.0819 | 0.2417 | 0.2417 | 0.0002 | 0.0583 | 0.0002 | 0.4186 | 0.0767 | 0.1342 |
| **MnO** | 0.0662 | 0.0002 | 0.0002 | 0.0534 | 0.0322 | 0.0107 | 0.0038 | 0.0002 | 0.0002 |
| **MgO** | 0.0618 | 0.0195 | 0.0195 | 0.0002 | 0.0003 | 0.0002 | 0.0003 | 0.0345 | 0.0003 |
| **$Na_2O$** | 0.2690 | 10.8247 | 10.8247 | 0.1604 | 11.1906 | 0.1726 | 11.0629 | 10.7762 | 11.1277 |
| **$K_2O$** | 15.7365 | 0.1250 | 0.1250 | 16.2017 | 0.1373 | 16.0740 | 0.0448 | 0.0789 | 0.0790 |
| **BaO** | 0.4078 | 0.0202 | 0.0202 | 0.1070 | 0.0685 | 0.0002 | 0.0002 | 0.0054 | 0.0002 |
| **SrO** | - | 0.0001 | 0.0001 | 0.0001 | 0.0001 | 0.0001 | 0.0001 | 0.0001 | 0.0001 |
| **Total** | 100.6479 | 102.3828 | 102.3828 | 98.4414 | 102.7911 | 98.2210 | 102.8303 | 99.3752 | 105.5236 |
| | | | | | | | | | |
| **Si*** | 11.690 | 12.015 | 12.015 | 12.061 | 12.089 | 12.060 | 11.991 | 12.013 | 12.031 |
| **Al** | 4.421 | 4.074 | 4.074 | 3.920 | 3.961 | 3.942 | 4.075 | 4.057 | 4.070 |
| **$Fe^{2+}$** | 0.020 | 0.012 | 0.012 | 0.010 | 0.008 | 0.006 | 0.010 | 0.026 | 0.024 |
| **Ca** | 0.016 | 0.044 | 0.044 | 0.000 | 0.011 | 0.000 | 0.076 | 0.014 | 0.024 |
| **Mn** | 0.010 | 0.000 | 0.000 | 0.009 | 0.005 | 0.002 | 0.001 | 0.000 | 0.000 |
| **Mg** | 0.017 | 0.005 | 0.005 | 0.000 | 0.000 | 0.000 | 0.000 | 0.009 | 0.000 |
| **Na** | 0.096 | 3.565 | 3.565 | 0.058 | 3.674 | 0.063 | 3.632 | 3.660 | 3.553 |
| **K** | 3.695 | 0.027 | 0.027 | 3.885 | 0.030 | 3.855 | 0.010 | 0.018 | 0.017 |
| **Ba** | 0.029 | 0.001 | 0.001 | 0.008 | 0.005 | 0.000 | 0.000 | 0.000 | 0.000 |
| **Sr** | - | 0.000 | 0.000 | 0.000 | 0.000 | 0.000 | 0.000 | 0.000 | 0.000 |
| | 19.995 | 19.744 | 19.744 | 19.951 | 19.782 | 19.928 | 19.793 | 19.797 | 19.719 |
| | | | | | | | | | |
| **Or** | 97.05 | 0.74 | 0.74 | 98.52 | 0.80 | 98.39 | 0.26 | 0.48 | 0.46 |
| **Ab** | 2.52 | 98.05 | 98.05 | 1.48 | 98.92 | 1.61 | 97.70 | 99.13 | 98.88 |
| **An** | 0.42 | 1.21 | 1.21 | 0.00 | 0.28 | 0.00 | 2.04 | 0.39 | 0.66 |

| | | | | | | *Ijolite* | | | |
|---|---|---|---|---|---|---|---|---|---|
| | **BN3_2** | **BN3_3** | **BN3_5** | | **BN3_8** | **BN4_1** | | | |
| | *pl2* | *pl2* | *pl1* | *pl2* | *pl1* | *ortho1* | *plag* | *plag2* | *plag3* |
| **$SiO_2$** | 71.1128 | 68.9476 | 69.7329 | 71.0069 | 69.6087 | 63.0693 | 70.7758 | 69.7142 | 69.7319 |
| **$Al_2O_3$** | 20.1236 | 19.6098 | 20.1950 | 20.1982 | 20.1612 | 18.9706 | 20.8578 | 20.7656 | 20.5759 |
| **FeO** | 0.1737 | 0.0920 | 0.2355 | 0.0612 | 0.0858 | 0.4505 | 0.1808 | 0.1586 | 0.0809 |
| **CaO** | 0.1944 | 0.2302 | 0.1735 | 0.0456 | 0.0913 | 0.0002 | 0.4003 | 0.4665 | 0.2129 |
| **MnO** | 0.0189 | 0.0002 | 0.0474 | 0.0002 | 0.0509 | 0.0002 | 0.0379 | 0.0515 | 0.0378 |
| **MgO** | 0.0138 | 0.0182 | 0.0163 | 0.0155 | 0.0249 | 0.0112 | 0.0003 | 0.0166 | 0.0276 |
| **$Na_2O$** | 11.3253 | 11.1122 | 11.0277 | 11.1882 | 11.2009 | 0.4322 | 11.3702 | 11.6252 | 11.2806 |
| **$K_2O$** | 0.0584 | 0.0526 | 0.0777 | 0.0358 | 0.1120 | 14.2806 | 0.0833 | 0.0866 | 0.0876 |
| **BaO** | 0.0002 | 0.0563 | 0.0002 | 0.0409 | 0.0361 | 1.7883 | 0.0195 | 0.0049 | 0.0002 |
| **SrO** | 0.0001 | 0.0001 | 0.0001 | 0.0001 | 0.0001 | - | - | - | - |
| **Total** | 103.0212 | 100.1192 | 101.5063 | 102.5926 | 101.3719 | 99.0031 | 103.7259 | 102.8897 | 102.0354 |
| | | | | | | | | | |
| **Si*** | 12.027 | 12.008 | 11.974 | 12.040 | 11.972 | 11.851 | 11.913 | 11.856 | 11.920 |
| **Al** | 4.011 | 4.025 | 4.087 | 4.036 | 4.087 | 4.201 | 4.137 | 4.162 | 4.145 |
| **$Fe^{2+}$** | 0.025 | 0.013 | 0.034 | 0.009 | 0.012 | 0.071 | 0.025 | 0.023 | 0.012 |
| **Ca** | 0.035 | 0.043 | 0.032 | 0.008 | 0.017 | 0.000 | 0.072 | 0.085 | 0.039 |
| **Mn** | 0.003 | 0.000 | 0.007 | 0.000 | 0.007 | 0.000 | 0.005 | 0.007 | 0.005 |
| **Mg** | 0.003 | 0.005 | 0.004 | 0.004 | 0.006 | 0.003 | 0.000 | 0.004 | 0.007 |
| **Na** | 3.713 | 3.752 | 3.671 | 3.678 | 3.735 | 0.157 | 3.710 | 3.833 | 3.738 |
| **K** | 0.013 | 0.012 | 0.017 | 0.008 | 0.025 | 3.423 | 0.018 | 0.019 | 0.019 |
| **Ba** | 0.000 | 0.004 | 0.000 | 0.003 | 0.002 | 0.132 | 0.001 | 0.000 | 0.000 |
| **Sr** | 0.000 | 0.000 | 0.000 | 0.000 | 0.000 | - | - | - | - |
| | 19.830 | 19.861 | 19.826 | 19.785 | 19.864 | 19.838 | 19.883 | 19.989 | 19.886 |
| | | | | | | | | | |
| **Or** | 0.33 | 0.31 | 0.46 | 0.21 | 0.65 | 95.60 | 0.47 | 0.48 | 0.50 |
| **Ab** | 98.73 | 98.56 | 98.68 | 99.57 | 98.90 | 4.40 | 97.63 | 97.36 | 98.47 |
| **An** | 0.94 | 1.13 | 0.86 | 0.22 | 0.45 | 0.00 | 1.90 | 2.16 | 1.03 |

| | | | | | | *Dyke* | | | |
|---|---|---|---|---|---|---|---|---|---|
| | **BN4_2** | | | **BN4_3** | | **BN6_1** | | | **BN6_2** |
| | *plag1* | *plag2* | *plag3* | *plag1* | *plag2* | *plag1* | *plag2* | *plag3* | *plag2* |
| **$SiO_2$** | 71.3066 | 72.2813 | 69.3735 | 70.1100 | 69.5853 | 68.9556 | 70.6358 | 69.3543 | 70.0989 |
| **$Al_2O_3$** | 21.1333 | 21.2087 | 20.0220 | 19.8490 | 19.6803 | 20.3309 | 20.7891 | 20.4902 | 19.9829 |
| **FeO** | 0.2585 | 0.4511 | 0.1989 | 0.3864 | 0.2316 | 0.1195 | 0.0842 | 0.1391 | 0.2766 |
| **CaO** | 0.3385 | 0.3342 | 0.4449 | 0.1784 | 0.3441 | 0.3209 | 0.1499 | 0.353 | 0.0157 |
| **MnO** | 0.0002 | 0.0549 | 0.0377 | 0.0541 | 0.0002 | 0.0002 | 0.0128 | 0.016 | 0.0354 |
| **MgO** | 0.0003 | 0.0110 | 0.0003 | 0.0003 | 0.0041 | 0.0003 | 0.0003 | 0.0003 | 0.0169 |
| **$Na_2O$** | 11.4254 | 11.4944 | 11.4096 | 10.9535 | 10.9343 | 10.995 | 11.1213 | 11.2041 | 11.3089 |
| **$K_2O$** | 0.0822 | 0.1389 | 0.1087 | 0.0938 | 0.0782 | 0.0796 | 0.0776 | 0.0997 | 0.0605 |
| **BaO** | 0.1169 | 0.0487 | 0.0073 | 0.0002 | 0.0410 | 0.0002 | 0.0002 | 0.0002 | 0.0002 |
| **SrO** | - | - | 0.0000 | 0.0001 | 0.0001 | - | - | - | - |
| **Total** | 104.6619 | 106.0232 | 101.6029 | 101.6258 | 100.8992 | 100.8022 | 102.8712 | 101.6569 | 101.796 |
| | | | | | | | | | |
| **Si*** | 11.902 | 11.916 | 11.939 | 12.027 | 12.024 | 11.927 | 11.954 | 11.909 | 12.007 |
| **Al** | 4.157 | 4.121 | 4.061 | 4.013 | 4.008 | 4.144 | 4.146 | 4.146 | 4.034 |
| **$Fe^{2+}$** | 0.036 | 0.062 | 0.029 | 0.055 | 0.033 | 0.017 | 0.012 | 0.020 | 0.040 |
| **Ca** | 0.061 | 0.059 | 0.082 | 0.033 | 0.064 | 0.059 | 0.027 | 0.065 | 0.003 |
| **Mn** | 0.000 | 0.008 | 0.005 | 0.008 | 0.000 | 0.000 | 0.002 | 0.002 | 0.005 |
| **Mg** | 0.000 | 0.003 | 0.000 | 0.000 | 0.001 | 0.000 | 0.000 | 0.000 | 0.004 |
| **Na** | 3.697 | 3.674 | 3.807 | 3.643 | 3.663 | 3.687 | 3.649 | 3.730 | 3.755 |
| **K** | 0.018 | 0.029 | 0.024 | 0.021 | 0.017 | 0.018 | 0.017 | 0.022 | 0.013 |
| **Ba** | 0.008 | 0.003 | 0.000 | 0.000 | 0.003 | 0.000 | 0.000 | 0.000 | 0.000 |
| **Sr** | - | - | 0.000 | 0.000 | 0.000 | - | - | - | - |
| | 19.877 | 19.875 | 19.946 | 19.799 | 19.812 | 19.853 | 19.806 | 19.894 | 19.861 |
| | | | | | | | | | |
| **Or** | 0.46 | 0.78 | 0.61 | 0.56 | 0.46 | 0.47 | 0.45 | 0.57 | 0.35 |
| **Ab** | 97.93 | 97.65 | 97.29 | 98.56 | 97.84 | 97.95 | 98.81 | 97.73 | 99.57 |
| **An** | 1.60 | 1.57 | 2.10 | 0.89 | 1.70 | 1.58 | 0.74 | 1.70 | 0.08 |

| | | | | | | *Dyke* | | | |
|---|---|---|---|---|---|---|---|---|---|
| | **BN6_2** | **BN6_3** | **BN6_4** | | | **BN7_1** | | **BN7_2** | |
| | *plag4* | *plag1* | *pl1* | *pl2* | *pl3* | *plag1* | *plag2* | *plag1* | *plag2* |
| **$SiO_2$** | 70.1683 | 71.5675 | 72.0695 | 69.5674 | 71.3209 | 68.9688 | 69.1532 | 68.5977 | 68.2871 |
| **$Al_2O_3$** | 20.4267 | 20.9794 | 20.6954 | 20.5746 | 20.4336 | 19.3779 | 19.3379 | 19.4269 | 19.2871 |
| **FeO** | 0.0319 | 0.0727 | 0.0968 | 0.0515 | 0.2226 | 0.1168 | 0.1186 | 0.282 | 0.2326 |
| **CaO** | 0.1351 | 0.0995 | 0.1728 | 0.1655 | 0.1657 | 0.0258 | 0.1615 | 0.182 | 0.4112 |
| **MnO** | 0.0002 | 0.0289 | 0.0322 | 0.0002 | 0.0002 | 0.0102 | 0.0302 | 0.0002 | 0.01 |
| **MgO** | 0.0003 | 0.0003 | 0.0003 | 0.0003 | 0.0003 | 0.0003 | 0.0154 | 0.0062 | 0.0176 |
| **$Na_2O$** | 11.1958 | 9.9764 | 9.9463 | 10.9392 | 11.2726 | 11.3311 | 11.5795 | 11.5812 | 11.4425 |
| **$K_2O$** | 0.0719 | 0.125 | 0.117 | 0.1307 | 0.1023 | 0.1006 | 0.1505 | 0.0854 | 0.0489 |
| **BaO** | 0.0182 | 0.0002 | 0.0507 | 0.0177 | 0.0355 | 0.0144 | 0.0167 | 0.0427 | 0.0118 |
| **SrO** | - | - | 0.0001 | 0.0001 | 0.0001 | - | - | - | - |
| **Total** | 102.0484 | 102.8499 | 103.1811 | 101.4472 | 103.5538 | 99.9459 | 100.5635 | 100.2043 | 99.7488 |
| | | | | | | | | | |
| **Si*** | 11.974 | 12.043 | 12.090 | 11.942 | 12.003 | 12.035 | 12.018 | 11.977 | 11.976 |
| **Al** | 4.108 | 4.160 | 4.091 | 4.162 | 4.053 | 3.985 | 3.960 | 3.997 | 3.986 |
| **$Fe^{2+}$** | 0.005 | 0.010 | 0.014 | 0.007 | 0.031 | 0.017 | 0.017 | 0.041 | 0.034 |
| **Ca** | 0.025 | 0.018 | 0.031 | 0.030 | 0.030 | 0.005 | 0.030 | 0.034 | 0.077 |
| **Mn** | 0.000 | 0.004 | 0.005 | 0.000 | 0.000 | 0.002 | 0.004 | 0.000 | 0.001 |
| **Mg** | 0.000 | 0.000 | 0.000 | 0.000 | 0.000 | 0.000 | 0.004 | 0.002 | 0.005 |
| **Na** | 3.704 | 3.255 | 3.235 | 3.640 | 3.678 | 3.833 | 3.901 | 3.920 | 3.890 |
| **K** | 0.016 | 0.027 | 0.025 | 0.029 | 0.022 | 0.022 | 0.033 | 0.019 | 0.011 |
| **Ba** | 0.001 | 0.000 | 0.003 | 0.001 | 0.002 | 0.001 | 0.001 | 0.003 | 0.001 |
| **Sr** | - | - | 0.000 | 0.000 | 0.000 | - | - | - | - |
| | 19.832 | 19.517 | 19.494 | 19.812 | 19.820 | 19.900 | 19.970 | 19.994 | 19.982 |
| | | | | | | | | | |
| **Or** | 0.42 | 0.81 | 0.76 | 0.77 | 0.59 | 0.58 | 0.84 | 0.48 | 0.27 |
| **Ab** | 98.92 | 98.64 | 98.30 | 98.40 | 98.61 | 99.30 | 98.40 | 98.66 | 97.78 |
| **An** | 0.66 | 0.54 | 0.94 | 0.82 | 0.80 | 0.12 | 0.76 | 0.86 | 1.94 |

| | | *Ijolite* | | *Syenite* | | | | | |
|---|---|---|---|---|---|---|---|---|---|
| | **BN7_2** | **BN12_2** | | **BN15_1** | | | **BN15_2** | | |
| | *plag3* | *pl1* | *pl2* | *pl1* | *or1* | *pl2* | *pl1* | *or1* | *pl2* |
| **$SiO_2$** | 68.9185 | 68.6759 | 69.2765 | 72.6757 | 63.1491 | 71.6106 | 71.2626 | 63.4019 | 70.5786 |
| **$Al_2O_3$** | 19.5346 | 19.7892 | 19.4259 | 20.4595 | 18.2434 | 20.2452 | 20.3324 | 18.4502 | 19.9562 |
| **FeO** | 0.7782 | 0.3848 | 0.0336 | 0.0989 | 0.0541 | 0.0715 | 0.0579 | 0.3918 | 0.2153 |
| **CaO** | 0.1135 | 0.0407 | 0.2094 | 0.0616 | 0.0002 | 0.2590 | 0.2658 | 0.0002 | 0.1332 |
| **MnO** | 0.0201 | 0.0575 | 0.0002 | 0.0002 | 0.0338 | 0.0189 | 0.0002 | 0.0002 | 0.0002 |
| **MgO** | 0.0301 | 0.0003 | 0.0039 | 0.0198 | 0.0002 | 0.0121 | 0.0026 | 0.0139 | 0.0364 |
| **$Na_2O$** | 11.6535 | 11.3069 | 11.2521 | 11.1258 | 0.2755 | 10.9458 | 10.2787 | 0.4199 | 11.2192 |
| **$K_2O$** | 0.1163 | 0.0393 | 0.0839 | 0.0526 | 15.5000 | 0.0554 | 0.0604 | 15.0790 | 0.0752 |
| **BaO** | 0.1019 | 0.0504 | 0.0002 | 0.0002 | 1.2255 | 0.0002 | 0.0456 | 1.5857 | 0.0002 |
| **SrO** | - | 0.0001 | 0.0001 | 0.0001 | 0.0001 | 0.0001 | 0.0001 | 0.0791 | 0.0001 |
| **Total** | 101.2667 | 100.3451 | 100.2858 | 104.4944 | 98.4819 | 103.2188 | 102.3063 | 99.4219 | 102.2146 |
| | | | | | | | | | |
| **Si*** | 11.946 | 11.960 | 12.041 | 12.080 | 11.939 | 12.059 | 12.077 | 11.902 | 12.030 |
| **Al** | 3.990 | 4.061 | 3.979 | 4.008 | 4.065 | 4.018 | 4.061 | 4.082 | 4.009 |
| **$Fe^{2+}$** | 0.113 | 0.056 | 0.005 | 0.014 | 0.009 | 0.010 | 0.008 | 0.062 | 0.031 |
| **Ca** | 0.021 | 0.008 | 0.039 | 0.011 | 0.000 | 0.047 | 0.048 | 0.000 | 0.024 |
| **Mn** | 0.003 | 0.008 | 0.000 | 0.000 | 0.005 | 0.003 | 0.000 | 0.000 | 0.000 |
| **Mg** | 0.008 | 0.000 | 0.001 | 0.005 | 0.000 | 0.003 | 0.001 | 0.004 | 0.009 |
| **Na** | 3.916 | 3.817 | 3.791 | 3.585 | 0.101 | 3.573 | 3.377 | 0.153 | 3.707 |
| **K** | 0.026 | 0.009 | 0.019 | 0.011 | 3.738 | 0.012 | 0.013 | 3.611 | 0.016 |
| **Ba** | 0.007 | 0.003 | 0.000 | 0.000 | 0.091 | 0.000 | 0.003 | 0.117 | 0.000 |
| **Sr** | - | 0.000 | 0.000 | 0.000 | 0.000 | 0.000 | 0.000 | 0.009 | 0.000 |
| | 20.030 | 19.923 | 19.875 | 19.714 | 19.948 | 19.725 | 19.588 | 19.939 | 19.827 |
| | | | | | | | | | |
| **Or** | 0.65 | 0.23 | 0.48 | 0.31 | 97.37 | 0.33 | 0.38 | 95.94 | 0.44 |
| **Ab** | 98.82 | 99.57 | 98.50 | 99.39 | 2.63 | 98.39 | 98.22 | 4.06 | 98.91 |
| **An** | 0.53 | 0.20 | 1.01 | 0.30 | 0.00 | 1.29 | 1.40 | 0.00 | 0.65 |

| | | *Syenite* | | | | | | | |
|---|---|---|---|---|---|---|---|---|---|
| | **BN15_2** | **BN16_1** | | | | | **BN16_3** | | |
| | *or2* | *pl1* | *or1* | *pl2* | *or2* | *pl3* | *or1* | *pl1* | *pl2* |
| **$SiO_2$** | 64.4059 | 68.1382 | 64.2927 | 71.3888 | 63.7212 | 68.0554 | 62.7924 | 70.9901 | 71.1260 |
| **$Al_2O_3$** | 18.0869 | 22.4258 | 21.1993 | 23.1799 | 20.7581 | 23.3470 | 20.9361 | 23.1431 | 23.5570 |
| **FeO** | 0.0475 | 0.1571 | 0.1091 | 0.0601 | 0.0133 | 0.0433 | 0.0198 | 0.0732 | 0.0701 |
| **CaO** | 0.0002 | 0.1892 | 0.0032 | 0.1605 | 0.0097 | 0.7025 | 0.0002 | 0.0551 | 0.2784 |
| **MnO** | 0.0002 | 0.1050 | 0.0498 | 0.0002 | 0.2768 | 0.0182 | 0.0498 | 0.0002 | 0.0137 |
| **MgO** | 0.0236 | 0.0003 | 0.0177 | 0.0003 | 0.0002 | 0.0003 | 0.0008 | 0.0003 | 0.0003 |
| **$Na_2O$** | 0.2702 | 11.4791 | 0.5808 | 11.2847 | 0.2410 | 11.1099 | 0.3171 | 11.2942 | 11.0552 |
| **$K_2O$** | 15.7565 | 0.1321 | 15.6572 | 0.0957 | 15.8226 | 0.1154 | 15.6965 | 0.0649 | 0.0717 |
| **BaO** | 0.3103 | 0.0267 | 0.3354 | 0.0178 | 0.3361 | 0.0002 | 0.7718 | 0.0236 | 0.0002 |
| **SrO** | 0.0001 | - | - | - | - | - | - | - | - |
| **Total** | 98.9014 | 102.6535 | 102.2452 | 106.1880 | 101.1790 | 103.3922 | 100.5845 | 105.6447 | 106.1726 |
| | | | | | | | | | |
| **Si*** | 12.032 | 11.625 | 11.630 | 11.716 | 11.662 | 11.521 | 11.596 | 11.709 | 11.670 |
| **Al** | 3.982 | 4.509 | 4.519 | 4.483 | 4.477 | 4.658 | 4.557 | 4.499 | 4.555 |
| **$Fe^{2+}$** | 0.007 | 0.022 | 0.017 | 0.008 | 0.002 | 0.006 | 0.003 | 0.010 | 0.010 |
| **Ca** | 0.000 | 0.035 | 0.001 | 0.028 | 0.002 | 0.127 | 0.000 | 0.010 | 0.049 |
| **Mn** | 0.000 | 0.015 | 0.008 | 0.000 | 0.043 | 0.003 | 0.008 | 0.000 | 0.002 |
| **Mg** | 0.007 | 0.000 | 0.005 | 0.000 | 0.000 | 0.000 | 0.000 | 0.000 | 0.000 |
| **Na** | 0.098 | 3.797 | 0.204 | 3.590 | 0.086 | 3.646 | 0.114 | 3.611 | 3.517 |
| **K** | 3.755 | 0.029 | 3.613 | 0.020 | 3.694 | 0.025 | 3.698 | 0.014 | 0.015 |
| **Ba** | 0.023 | 0.002 | 0.024 | 0.001 | 0.024 | 0.000 | 0.056 | 0.002 | 0.000 |
| **Sr** | 0.000 | - | - | - | - | - | - | - | - |
| | 19.903 | 20.033 | 20.019 | 19.848 | 19.989 | 19.986 | 20.031 | 19.854 | 19.818 |
| | | | | | | | | | |
| **Or** | 97.46 | 0.74 | 94.65 | 0.55 | 97.69 | 0.66 | 97.02 | 0.38 | 0.42 |
| **Ab** | 2.54 | 98.36 | 5.34 | 98.67 | 2.26 | 95.99 | 2.98 | 99.36 | 98.21 |
| **An** | 0.00 | 0.90 | 0.02 | 0.78 | 0.05 | 3.35 | 0.00 | 0.27 | 1.37 |

| | **BN16_3** | **BN16_5** | | **BN16_6** | | | **BN17_1** | | |
|---|---|---|---|---|---|---|---|---|---|
| | *or2* | *pl1* | *or1* | *or1* | *pl1* | *pl2* | *plag2* | *kfeld1* | *plag1?* |
| **$SiO_2$** | 62.6962 | 72.5904 | 62.2634 | 63.7386 | 71.7913 | 70.6329 | 70.8785 | 69.7412 | 71.2409 |
| **$Al_2O_3$** | 20.6085 | 20.7854 | 17.5662 | 17.8865 | 20.3756 | 20.0442 | 19.8930 | 19.6999 | 20.9023 |
| **FeO** | 0.0265 | 0.2703 | 0.1214 | 0.0832 | 0.0450 | 0.2155 | 0.0520 | 0.0680 | 0.0002 |
| **CaO** | 0.0313 | 0.0510 | 0.0002 | 0.0083 | 0.1806 | 0.2347 | 0.1376 | 0.0069 | 0.0362 |
| **MnO** | 0.0002 | 0.0143 | 0.0002 | 0.0002 | 0.0002 | 0.0002 | 0.0179 | 0.0002 | 0.0431 |
| **MgO** | 0.0137 | 0.0003 | 0.0084 | 0.0038 | 0.0003 | 0.0003 | 0.0364 | 0.0015 | 0.0189 |
| **$Na_2O$** | 0.4112 | 11.4661 | 0.3102 | 0.2774 | 11.3674 | 10.9664 | 8.8147 | 0.2357 | 11.5296 |
| **$K_2O$** | 15.3686 | 0.0818 | 14.8578 | 15.8182 | 0.0579 | 0.0846 | 0.1175 | 11.0350 | 0.0732 |
| **BaO** | 0.6892 | 0.0002 | 0.3507 | 0.4174 | 0.0002 | 0.0202 | 0.0002 | 0.0614 | 0.0867 |
| **SrO** | - | 0.0001 | 0.0001 | 0.0001 | 0.0001 | 0.0001 | - | - | - |
| **Total** | 99.8454 | 105.2599 | 95.4786 | 98.2337 | 103.8186 | 102.1991 | 99.9478 | 100.8498 | 103.9311 |
| | | | | | | | | | |
| **Si*** | 11.639 | 12.012 | 12.031 | 12.019 | 12.035 | 12.034 | 12.207 | 12.285 | 11.949 |
| **Al** | 4.509 | 4.053 | 4.000 | 3.975 | 4.025 | 4.025 | 4.038 | 4.090 | 4.132 |
| **$Fe^{2+}$** | 0.004 | 0.037 | 0.020 | 0.013 | 0.006 | 0.031 | 0.007 | 0.010 | 0.000 |
| **Ca** | 0.006 | 0.009 | 0.000 | 0.002 | 0.032 | 0.043 | 0.025 | 0.001 | 0.007 |
| **Mn** | 0.000 | 0.002 | 0.000 | 0.000 | 0.000 | 0.000 | 0.003 | 0.000 | 0.006 |
| **Mg** | 0.004 | 0.000 | 0.002 | 0.001 | 0.000 | 0.000 | 0.009 | 0.000 | 0.005 |
| **Na** | 0.148 | 3.678 | 0.116 | 0.101 | 3.694 | 3.622 | 2.943 | 0.080 | 3.749 |
| **K** | 3.639 | 0.017 | 3.662 | 3.805 | 0.012 | 0.018 | 0.026 | 2.479 | 0.016 |
| **Ba** | 0.050 | 0.000 | 0.027 | 0.031 | 0.000 | 0.001 | 0.000 | 0.004 | 0.006 |
| **Sr** | - | 0.000 | 0.000 | 0.000 | 0.000 | 0.000 | - | - | - |
| | 20.000 | 19.809 | 19.858 | 19.947 | 19.806 | 19.774 | 19.259 | 18.950 | 19.868 |
| | | | | | | | | | |
| **Or** | 95.93 | 0.47 | 96.92 | 97.36 | 0.33 | 0.50 | 0.86 | 96.81 | 0.42 |
| **Ab** | 3.90 | 99.29 | 3.08 | 2.60 | 98.80 | 98.34 | 98.29 | 3.14 | 99.41 |
| **An** | 0.16 | 0.24 | 0.00 | 0.04 | 0.87 | 1.16 | 0.85 | 0.05 | 0.17 |

| | **BN17_1** | | | **BN17_2** | | | | |
|---|---|---|---|---|---|---|---|---|
| | *kspar2* | *kspar3* | *kspar4* | *plag1* | *kspar1* | *kspar2* | *kspar3* | *kspar4* |
| **$SiO_2$** | 64.7665 | 65.3175 | 65.2039 | 69.2595 | 64.3648 | 63.8042 | 59.7356 | 63.3901 |
| **$Al_2O_3$** | 18.6392 | 19.1149 | 18.8574 | 21.2047 | 19.0259 | 18.4366 | 17.1971 | 18.2487 |
| **FeO** | 0.0939 | 0.1783 | 0.0260 | 0.1207 | 0.0681 | 0.2728 | 2.3905 | 0.5003 |
| **CaO** | 0.0169 | 0.0002 | 0.0002 | 0.1009 | 0.0010 | 0.0002 | 0.1253 | 0.0669 |
| **MnO** | 0.0466 | 0.0072 | 0.0002 | 0.0324 | 0.0287 | 0.0002 | 0.0609 | 0.0002 |
| **MgO** | 0.0002 | 0.0140 | 0.0002 | 0.0003 | 0.0002 | 0.0002 | 0.0300 | 0.0093 |
| **$Na_2O$** | 0.2457 | 0.3992 | 0.3479 | 11.3106 | 0.2025 | 0.3226 | 0.3375 | 0.2751 |
| **$K_2O$** | 16.4162 | 16.0213 | 16.4018 | 0.0752 | 16.3585 | 16.3490 | 15.6161 | 16.0026 |
| **BaO** | 0.2438 | 0.5520 | 0.0875 | 0.0002 | 0.0951 | 0.0412 | 0.2152 | 0.1905 |
| **SrO** | - | - | - | - | - | - | - | - |
| **Total** | 100.4690 | 101.6046 | 100.9251 | 102.1045 | 100.1448 | 99.2270 | 95.7082 | 98.6837 |
| | | | | | | | | |
| **Si*** | 11.951 | 11.915 | 11.950 | 11.836 | 11.898 | 11.927 | 11.765 | 11.926 |
| **Al** | 4.053 | 4.109 | 4.073 | 4.271 | 4.145 | 4.062 | 3.992 | 4.046 |
| **$Fe^{2+}$** | 0.014 | 0.027 | 0.004 | 0.017 | 0.011 | 0.043 | 0.394 | 0.079 |
| **Ca** | 0.003 | 0.000 | 0.000 | 0.018 | 0.000 | 0.000 | 0.026 | 0.013 |
| **Mn** | 0.007 | 0.001 | 0.000 | 0.005 | 0.004 | 0.000 | 0.010 | 0.000 |
| **Mg** | 0.000 | 0.004 | 0.000 | 0.000 | 0.000 | 0.000 | 0.009 | 0.003 |
| **Na** | 0.088 | 0.141 | 0.124 | 3.747 | 0.073 | 0.117 | 0.129 | 0.100 |
| **K** | 3.864 | 3.728 | 3.835 | 0.016 | 3.857 | 3.898 | 3.923 | 3.840 |
| **Ba** | 0.018 | 0.039 | 0.006 | 0.000 | 0.007 | 0.003 | 0.017 | 0.014 |
| **Sr** | - | - | - | - | - | - | - | - |
| | 19.999 | 19.965 | 19.992 | 19.911 | 19.995 | 20.050 | 20.265 | 20.021 |
| | | | | | | | | |
| **Or** | 97.69 | 96.35 | 96.88 | 0.43 | 98.15 | 97.09 | 96.19 | 97.12 |
| **Ab** | 2.22 | 3.65 | 3.12 | 99.08 | 1.85 | 2.91 | 3.16 | 2.54 |
| **An** | 0.08 | 0.00 | 0.00 | 0.49 | 0.01 | 0.00 | 0.65 | 0.34 |

| | **BN17_3** | | |
|---|---|---|---|
| | *fsp1* | *pl1* | *pl2* |
| **$SiO_2$** | 65.0940 | 70.4260 | 69.2059 |
| **$Al_2O_3$** | 18.5985 | 20.4661 | 19.8816 |
| **FeO** | 0.0579 | 0.1904 | 0.1613 |
| **CaO** | 0.0002 | 0.0706 | 0.0323 |
| **MnO** | 0.0002 | 0.0108 | 0.0002 |
| **MgO** | 0.0002 | 0.0361 | 0.0148 |
| **$Na_2O$** | 0.2485 | 10.1115 | 11.1875 |
| **$K_2O$** | 14.6445 | 1.5929 | 0.1001 |
| **BaO** | 0.0720 | 0.0920 | 0.0002 |
| **SrO** | - | - | - |
| **Total** | 98.7160 | 102.9964 | 100.5839 |
| | | | |
| **Si*** | 12.060 | 11.976 | 11.993 |
| **Al** | 4.061 | 4.101 | 4.060 |
| **$Fe^{2+}$** | 0.009 | 0.027 | 0.023 |
| **Ca** | 0.000 | 0.013 | 0.006 |
| **Mn** | 0.000 | 0.002 | 0.000 |
| **Mg** | 0.000 | 0.009 | 0.004 |
| **Na** | 0.089 | 3.333 | 3.759 |
| **K** | 3.461 | 0.346 | 0.022 |
| **Ba** | 0.005 | 0.006 | 0.000 |
| **Sr** | - | - | - |
| | 19.685 | 19.813 | 19.867 |
| | | | |
| **Or** | 97.48 | 9.36 | 0.58 |
| **Ab** | 2.51 | 90.29 | 99.26 |
| **An** | 0.00 | 0.35 | 0.16 |

# Appendix 7
# CIPW NORM CALCULATIONS OF ALKALINE MAGMATIC PHASES

**Table A7.1.** CIPW norm calculations for different phases of the Billeroo alkaline magmatic complex.

| Sample | R no. | Phase | Or | Ab | An | Ne | Ac | Di | Wo | Hy | Ol | Il | Hm | Tn | Pf | Ru | Ap | Sum |
|---|---|---|---|---|---|---|---|---|---|---|---|---|---|---|---|---|---|---|
| BN7 | R493986 | Lampro | 2.955 | 77.002 | 5.153 | 0 | 0 | 0.13 | 0 | 0 | 1.18 | 0.278 | 10.3 | 0.174 | 1.809 | 0 | 0.237 | 99.217 |
| BN6 | R493985 | Lampro | 3.9 | 72.208 | 4.766 | 2.23 | 0 | 0.992 | 0 | 0 | 1.371 | 0.342 | 10.2 | 0 | 2.026 | 0 | 0.426 | 98.462 |
| BN2 | R493991 | Syen | 72.689 | 2.028 | 4.501 | 1.789 | 0 | 1.666 | 1.944 | 0 | 0 | 0.406 | 10.1 | 0 | 2.071 | 0 | 0.142 | 97.336 |
| BN17 | R493990 | Syen | 65.598 | 6.384 | 4.126 | 2.317 | 0 | 5.802 | 0 | 0 | 1.048 | 0.984 | 8.95 | 0 | 1.417 | 0 | 0.237 | 96.862 |
| 886 | R474886 | Syen | 63.234 | 9.283 | 4.824 | 2.076 | 0 | 4.591 | 0 | 0 | 0.603 | 0.599 | 9.7 | 0 | 1.506 | 0 | 0.355 | 96.772 |
| BN16 | R493989 | Syen | 24.348 | 46.921 | 4.604 | 2.315 | 0 | 4.621 | 0.089 | 0 | 0 | 0.749 | 10.8 | 0 | 2.087 | 0 | 0.758 | 97.292 |
| BN15 | R493988 | Syen | 22.811 | 37.226 | 5.096 | 7.292 | 0 | 6.609 | 4.804 | 0 | 0 | 0.813 | 8.12 | 0 | 1.383 | 0 | 0.687 | 94.84 |
| 888 | R474888 | Syen | 44.973 | 23.358 | 2.12 | 4.582 | 0 | 1.182 | 6.59 | 0 | 0 | 0.792 | 10.5 | 0 | 1.794 | 0 | 0.64 | 96.529 |
| 885 | R474885 | Syen | 63.825 | 11.677 | 5.292 | 0 | 0 | 0 | 0 | 0.301 | 2.215 | 0.898 | 11.6 | 1.393 | 0 | 0.25 | 0.261 | 97.712 |
| BN14 | R493984 | Ijo | 17.493 | 35.705 | 7.442 | 15.679 | 0 | 2.175 | 0 | 0 | 2.749 | 0.556 | 10.7 | 0 | 2.907 | 0 | 1.255 | 96.662 |
| BN1 | R493975 | Ijo | 23.816 | 29.536 | 5.283 | 19.113 | 0 | 3.883 | 0 | 0 | 2.229 | 0.471 | 9.7 | 0 | 2.847 | 0 | 1.161 | 98.039 |
| BN3 | R493976 | Ijo | 17.67 | 19.492 | 6.758 | 31.201 | 0 | 7.939 | 0 | 0 | 1.959 | 0.449 | 8.76 | 0 | 2.339 | 0 | 1.776 | 98.342 |
| BN13 | R493983 | Ijo | 16.843 | 14.294 | 0 | 33.817 | 2.562 | 15.178 | 0 | 0 | 0.253 | 0.492 | 9.314 | 0 | 2.743 | 0 | 2.155 | 97.651 |
| 884 | R474884 | Ijo | 13.829 | 21.214 | 0 | 34.392 | 0.672 | 14.991 | 0.476 | 0 | 0 | 0.428 | 8.167 | 0 | 2.085 | 0 | 1.705 | 97.96 |
| BN12 | R493982 | Ijo | 17.434 | 12.814 | 0.444 | 33.306 | 0 | 17.084 | 0 | 0 | 0.332 | 0.471 | 9.89 | 0 | 2.796 | 0 | 2.416 | 96.986 |
| BN4 | R493977 | Ijo | 18.616 | 16.561 | 8.1 | 25.362 | 0 | 11.844 | 0 | 0 | 2.017 | 0.428 | 9.42 | 0 | 2.647 | 0 | 2.605 | 97.6 |
| BN10 | R493981 | Ijo | 14.833 | 46.298 | 7.023 | 8.382 | 0 | 2.302 | 0 | 0 | 2.603 | 0.449 | 11.2 | 0 | 2.986 | 0 | 1.397 | 97.474 |
| BN5 | R493978 | Ijo | 19.443 | 15.039 | 7.649 | 26.783 | 0 | 11.704 | 0 | 0 | 1.975 | 0.406 | 9.74 | 0 | 2.581 | 0 | 2.937 | 98.257 |
| BN8 | R493979 | Ijo | 20.743 | 19.927 | 17.388 | 22.163 | 0 | 0 | 0 | 0 | 3.473 | 0.342 | 8.7 | 0 | 0.189 | 2.1 | 0.876 | 95.902 |
| BN11 | R493987 | Lampro | 7.801 | 43.096 | 4.506 | 18.506 | 0 | 5.695 | 0 | 0 | 1.85 | 0.471 | 10.8 | 0 | 2.83 | 0 | 1.942 | 97.496 |
| 887 | R474887 | Ijo | 16.252 | 13.692 | 0 | 33.051 | 4.039 | 15.367 | 0.494 | 0 | 0 | 0.62 | 9.304 | 0 | 3.054 | 0 | 1.966 | 97.838 |
| BN9 | R493980 | Ijo | 13.888 | 46.491 | 10.027 | 7.086 | 0 | 0.006 | 0 | 0 | 3.786 | 0.428 | 11.1 | 0 | 2.869 | 0 | 1.753 | 97.432 |

*Abbreviations:* Or - orthoclase; Ab - albite; An - anorthite; Ne - nepheline; Ac - acmite; Di - diopside; Wo - wollastonite; Hy - hypersthene; Ol - olivine; Il - ilmenite; Hm - hematite; Tn - titanite; Pf - perovskite; Ru - rutile; Ap - apatite.

# Appendix 8
# IOCG PROSPECT SUMMARIES

## A8.1 Introduction

This appendix list details about the seven Fe-oxide Cu-Au (IOCG) prospects that are geochemically and isotopically studied in *Chapter 6*. Information relating the different IOCG systems to the regional and local geology is summarised. The different mineralisation styles from each of the systems are listed along with detailed petrographical observations.

## A8.2 North Portia

The North Portia prospect occurs along the closure of a large-scale, north-south-trending, north-plunging anticline (Fig. A8.1a). Primary mineralisation occurs within an easterly dipping metasedimentary sequence on the eastern flank of the fold closure. The North Portia prospect is situated within a broad region known as the Benagerie Ridge Magnetic Complex, a geophysically defined area with anomolous base metal concentrations (Cu, Au, Pb, U; Fig. A8.1b, c). Evaporitic units, carbonate units and porphyroblastic metapelite (magnetite-hematite rich) comprise the footwall, whereas highly reduced albitic metapelite make up the hangingwall to the main mineralised sequence (Fig. A8.2; Teale & Fanning, 2000a).

Primary mineralisation in carbonate-rich units contains replacement and bedding parallel mineralisation that emanates from crosscutting veins. Secondary mineralisation occurs in veins and fractures in the hangingwall albitic pelite (Fig. A8.2; Teale & Fanning, 2000a). Although the hangingwall mineralisation is likely of the same generation as the primary mineralisation, it is referred to as secondary mineralisation so that the two can easily be distinguished from one other. A zone of supergene enrichment also occurs in the saprolitic overburden (Teale & Fanning, 2000a).

Multiple samples were taken from diamond drill holes at the North Portia prospect, from both primary mineralisation and secondary hangingwall mineralisation. Sulphide mineralogy in all samples is dominated by chalcopyrite with subordinate pyrite and molybdenite. Massive or replacement primary chalcopyrite-pyrite mineralisation can be siliceous (*BN4*; Fig. A8.3a, A8.4a), or associated with albite – biotite (*BN600*; Fig. A8.3b, A8.4b). Accessory phases include ankerite – calcite ± magnetite ± apatite (Fig. A8.4a, b). Primary mineralisation also occurs in vein networks that have a complicated multi-stage crystallisation history. Early chalcopyrite mineralisation (± pyrite) is rimmed by quartz-calcite-barite-hematite (*BN1*; Fig. A8.3c, A8.4c). Replacement-style primary mineralisation can also have complicated contact with the invasively altered host (*BN600*: Fig. A8.3b, A8.4b). Host rock associated with mineralisation is often K ± Na altered (biotite ± albite), with calcite and barite being the dominant accessory phases.

Mineralisation in the hangingwall sequence occurs as both vein-style and replacement-style. Chalcopyrite – pyrite – quartz – ankerite veins crosscut invasively Na-altered (albite) host rock (*BN5*; Fig. A8.3d, A8.4d). Invasively albitised host rock preserves bedding, and possibly diagenetic mineralisation (*BN6*; Fig. A8.3d). Replacement-style mineralisation (chalcopyrite – pyrite) in the hangingwall also contains significant proportions

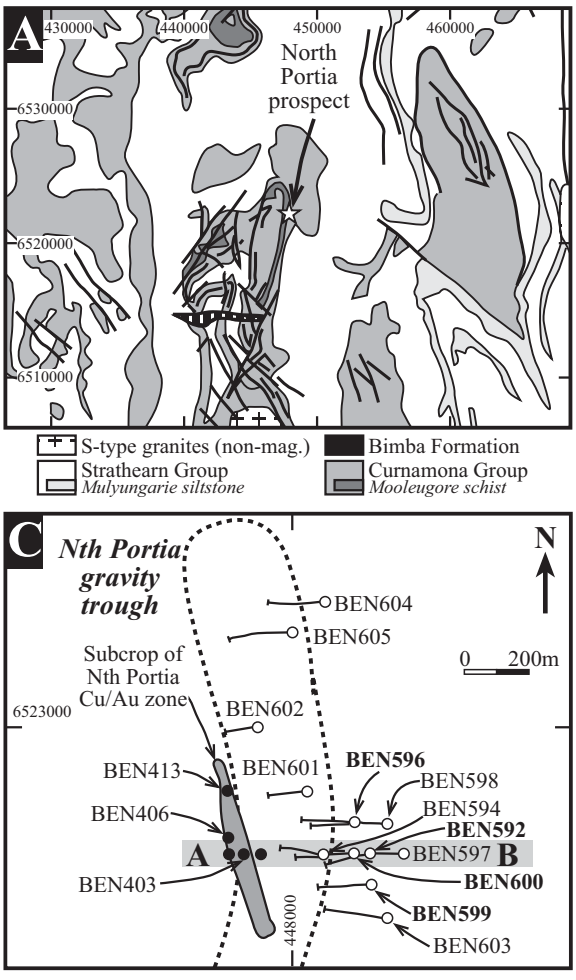


**Figure A8.1.** (a) Interpreted solid geology of North Portia region (Jenkins & Burtt, 2003); (b) Plan view of Benagerie Ridge Magnetic Complex mineralisation showing significant Cu-Au and U-Pb intersections in drill holes (C Giles *pers. comm.* 2004); (c) Plan view of North Portia Cu-Au prospect with diamond drill hole localities and notable mineralised intersections. Those in italic are drill holes in this study (C Giles *pers. comm.* 2004).

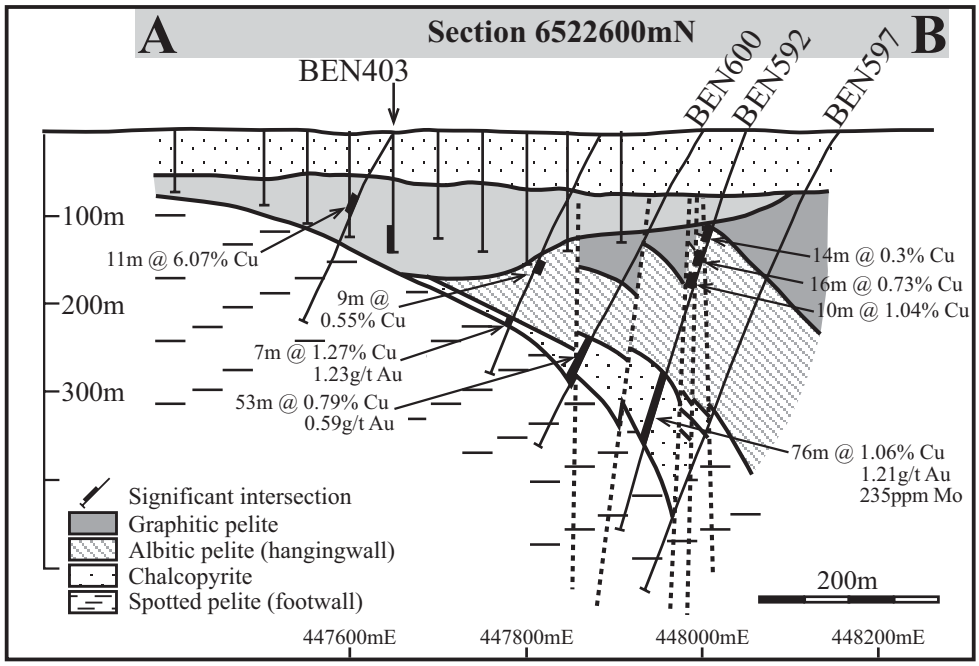


**Figure A8.2.** Cross section of North Portia Cu-Au system showing major mineralised intersections in the primary mineralisation zone, hangingwall (referred to herein as secondary mineralisation) and in the supergene enrichment zone (Teale & Fanning, 2000a).

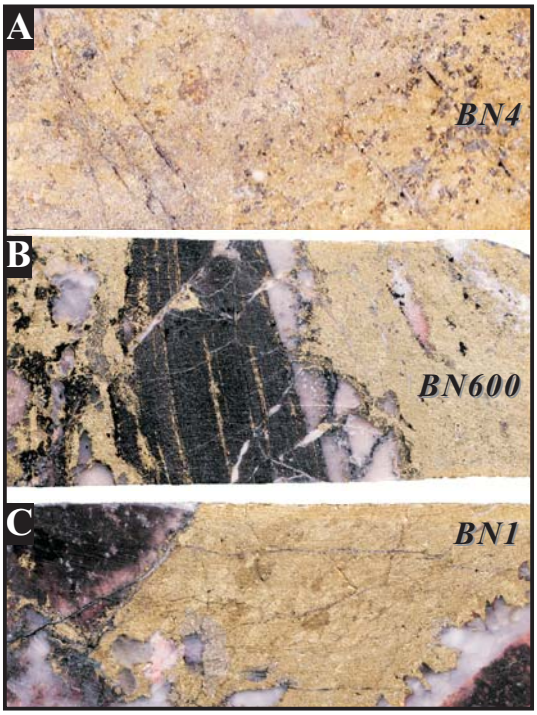


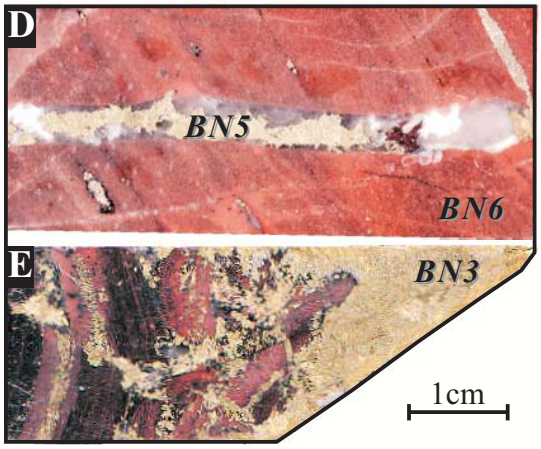


**Figure A8.3.** Representative samples from North Portia prospect. Sample numbers in italics. Diamond drill hole number prefixed with 'BEN'. Primary mineralisation: (a) *BN4*: BEN592 - 348m; (b) *BN600*: BEN600 - 320.8m; (c) *BN1*: BEN599 - 356.65m. Secondary mineralisation: (d) *BN5*: BEN592 - 243.8m; (e) *BN3*: BEN596 - 263.65m. A sample of the invasively albitised host rock (*BN6*) adjacent to vein mineralisation from BEN592 - 243.8m was also included. Scale same for each sample block.

of barite – calcite – quartz ± apatite within strongly K – Na altered host rock (*BN3*; Fig. A8.3e, A8.4e).

The main vein mineralisation has zoning from early Ca-rich veins (tremolite – actinolite – calcite – quartz – titanite ± biotite), to Ca-Fe-rich veins (biotite – K-feldspar – quartz – calcite – chalcopyrite – pyrite – monazite), which become more hematite-rich (Teale & Fanning, 2000a). Monazite and REE fluocarbonates are the dominant REE-bearing phases in the hydrothermal systems, that are interpreted to have reacted with earlier formed titanite and allanite (Teale & Fanning, 2000a). Replacement of biotite – actinolite – hematite by chlorite – talc – calcite – sericite further enriched copper mineralisation forming intense phyllic alteration zones (muscovite – calcite – talc; Teale & Fanning, 2000a).

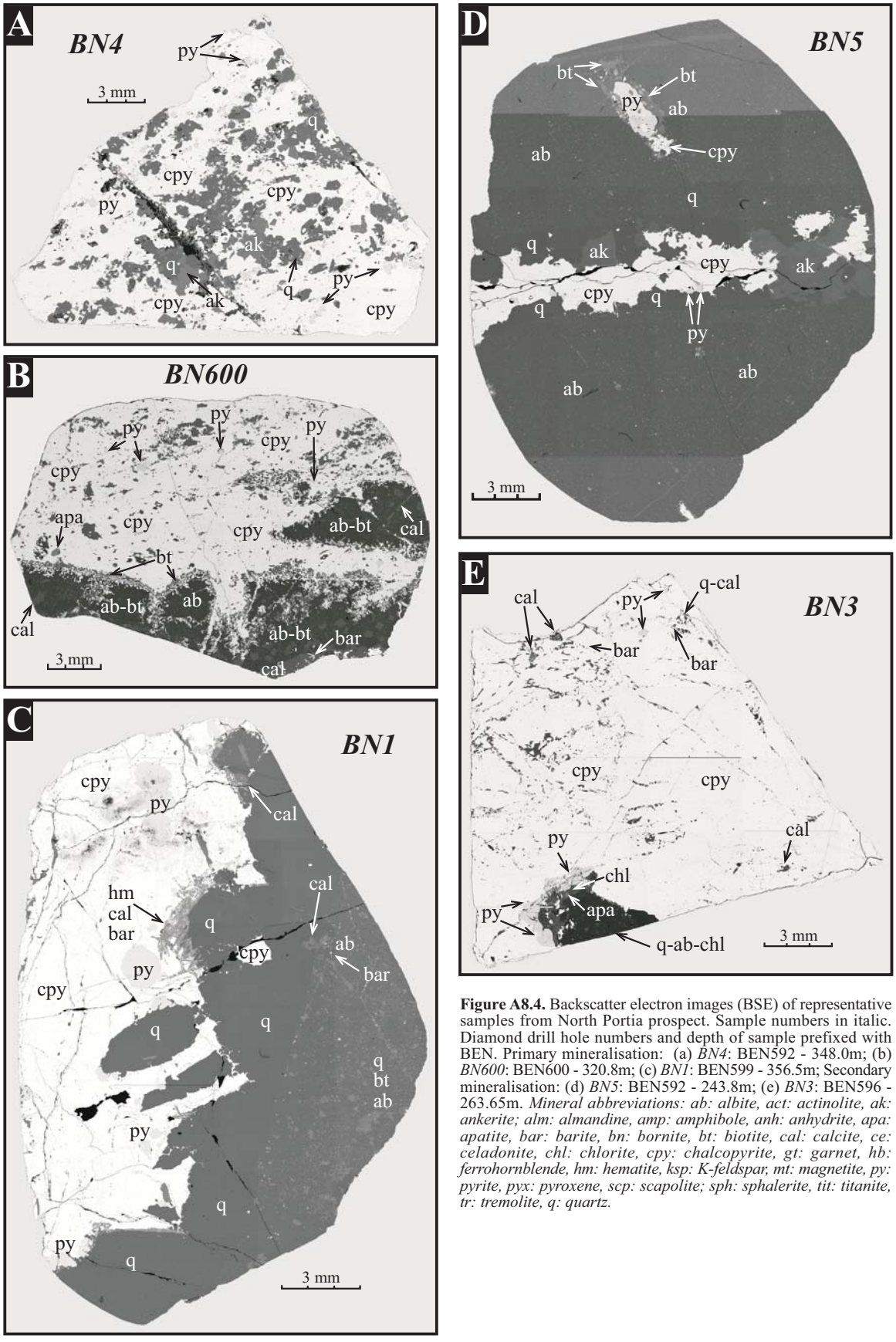


**Figure A8.4.** Backscatter electron images (BSE) of representative samples from North Portia prospect. Sample numbers in italic. Diamond drill hole numbers and depth of sample prefixed with BEN. Primary mineralisation: (a) *BN4*: BEN592 - 348.0m; (b) *BN600*: BEN600 - 320.8m; (c) *BN1*: BEN599 - 356.5m; Secondary mineralisation: (d) *BN5*: BEN592 - 243.8m; (e) *BN3*: BEN596 - 263.65m. *Mineral abbreviations: ab: albite, act: actinolite, ak: ankerite; alm: almandine, amp: amphibole, anh: anhydrite, apa: apatite, bar: barite, bn: bornite, bt: biotite, cal: calcite, ce: celadonite, chl: chlorite, cpy: chalcopyrite, gt: garnet, hb: ferrohornblende, hm: hematite, ksp: K-feldspar, mt: magnetite, py: pyrite, pyx: pyroxene, scp: scapolite; sph: sphalerite, tit: titanite, tr: tremolite, q: quartz.*

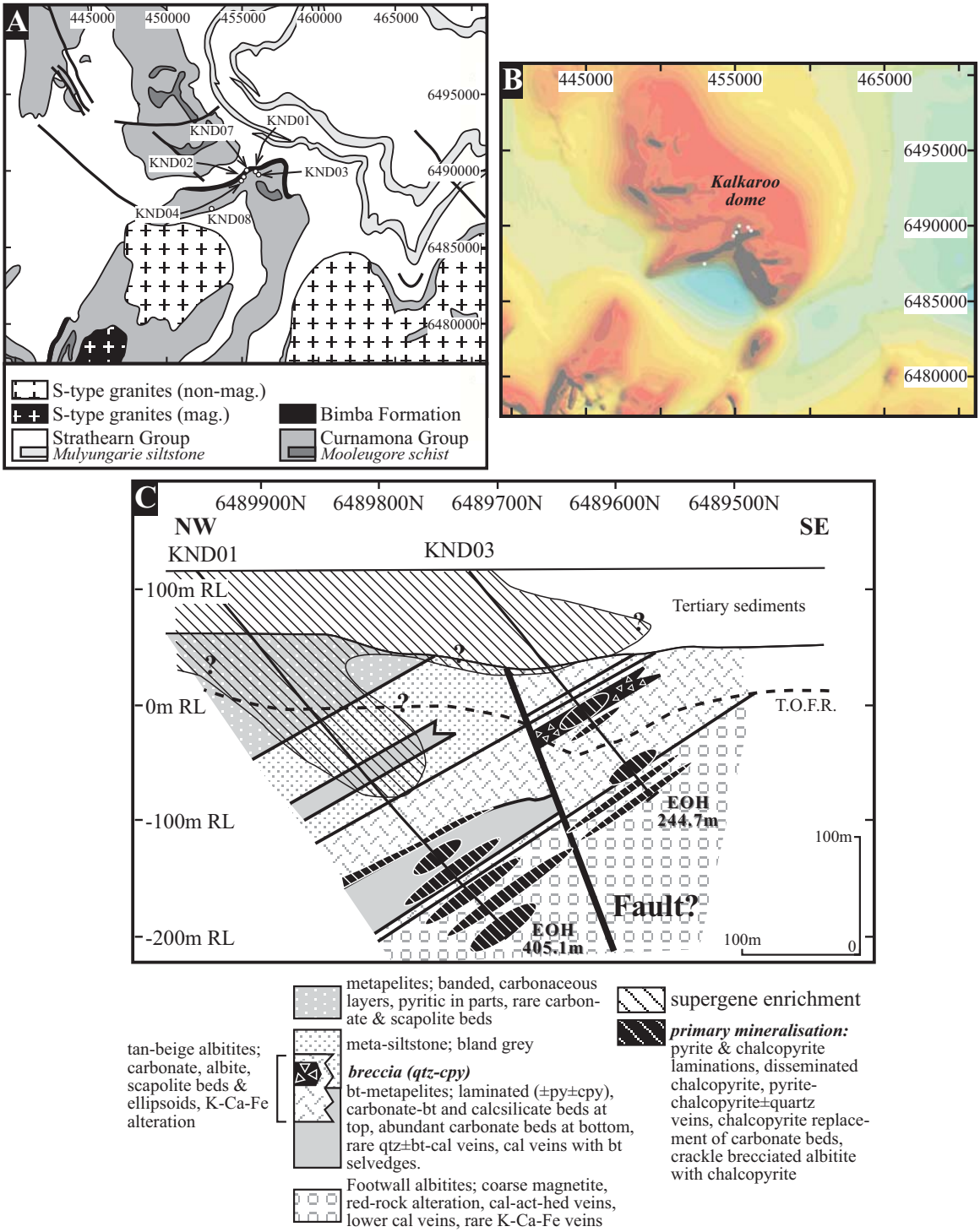


**Figure A8.5.** (a) Regional-scale solid geology interpretation of Kalkaroo prospect and surrounding area (Jenkinf & Burtt, 2003). Location of diamond drill holes highlighted (C. Giles *pers. comm.*, 2004); (b) Regional-scale total magnetic intensity image of Kalkaroo prospect region (Jenkins & Burtt, 2003); (c) Schematic interpreted cross-section of Kalkaroo prospect in vicinity of DDH KND001 and KND003 (based on logs from G. Teale *pers. comm.*, 2005).

## A8.3 Kalkaroo

The Kalkaroo prospect is very similar to the North Portia system being situated along the same regional anticline as the North Portia system, but nearer to the northern margin of the Willyama Inliers. Significant Cu-Au mineralisation occurs over a strike length of >1.5 km (C. Giles *pers. comm.*, 2004). Mineralisation is associated with a prominent magnetic high, situated north of a linear ENE-trending anomaly (Fig. A8.5). At least three other E-W-trending linear magnetic features interpreted as shear zones or faults are within <4 km of the prospect. A large circular low magnetic anomaly is situated ~3 km to the southeast of the prospect. These magnetic anomalies are common in the Benagerie Ridge and Mulyungarie region, and are correlated with leucocratic, unaltered, undeformed, muscovite-bearing felsic intrusives related to ~1585 Ma anatexis (Hayward, 1998; Teale & Fanning, 2000a; Williams & Skirrow, 2000).

Similar to the primary mineralisation at North Portia, Kalkaroo primary mineralisation also occurs along the contact between the strongly magnetic Fe-K-Ca altered albitite-magnetite footwall sequence (Curnamona Group) and carbonaceous pelite hangingwall sequence

(Strathearn Group). The majority of mineralisation occurs within a north dipping weakly magnetic biotite-albitite unit (Williams & Skirrow, 2000). Initial pyrite mineralisation and albitisation occurred during diagenesis (Hayward, 1998; Williams & Skirrow, 2000). Disseminated magnetite may also have formed at this time or prior to the main mineralisation and alteration event. Main-stage primary mineralisation occurs as veins, replacments and disseminations (Fig. A8.6).

Chalcopyrite and pyrite are dominant sulphides in replacement-style mineralisation occurring as blebs and lenses within bedding planes and fractures, which are crosscut by chalcopyrite ± molybdenite veins (*K7* and *K9*; Fig. A8.6a, b; A8.7a, b; Hayward, 1998). Primary mineralisation at depth occurs as vein networks with associated Fe-Ca-K alteration, some of which form breccia bodies. Assemblages include magnetite – actinolite – K-feldspar – titanite – chalcopyrite – pyrite ± albite ± quartz (*K8*: Fig. A8.6c, A8.7c; Skirrow et al., 2000). Major deposition of Cu, Au and Mo occurred in association with K-feldspar – biotite – albite (K±Na) that may have occurred at the same time as the Fe-Ca metasomatism. Biotite-quartz-molybdenite-carbonate veins, and carbonate – albite – biotite veins are also associated with primary mineralisation, and associated with K±Na alteration (Fig. A8.6b). Oxygen isotope geothermometry on quartz – amphibole – magnetite yielded temperatures of ~420 – 450°C, and fluid inclusions indicate hypersaline Na-Ca-K and $CO_2$ ± $N_2$ rich fluids (Skirrow et al., 2000).

All previous mineralisation and alteration is overprinted by chlorite – carbonate – rutile ± hematite ± fluorite ± sericite alteration, which when intense, is similar to phyllitic alteration styles. Remobilisation and upgrading of Cu-Au-Mo is associated with this alteration. Oxygen isotope geothermometry on quartz – chlorite yield assemblages of ~300 – 420°C (Skirrow et al., 2000). Supergene enrichment also occurred at Kalkaroo, with the formation of native copper and chalcocite. The supergene enrichment zone occurs above primary mineralisation, with heterogeneous enrichment of Cu, Au and Mo (Hayward, 1998).

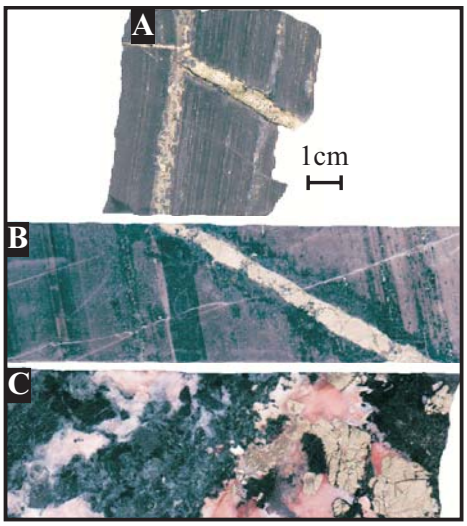


**Fig. A8.6.** Representative samples from Kalkaroo prospect. Sample numbers in italic. Diamond drill hole number prefixed with 'KND'. (a) *K7*: KND1 - 298.16m; (b) *K9:* KND8 - 246.0m; (c) *K8*: KND3 - 239.4m. Scale same for each sample block.

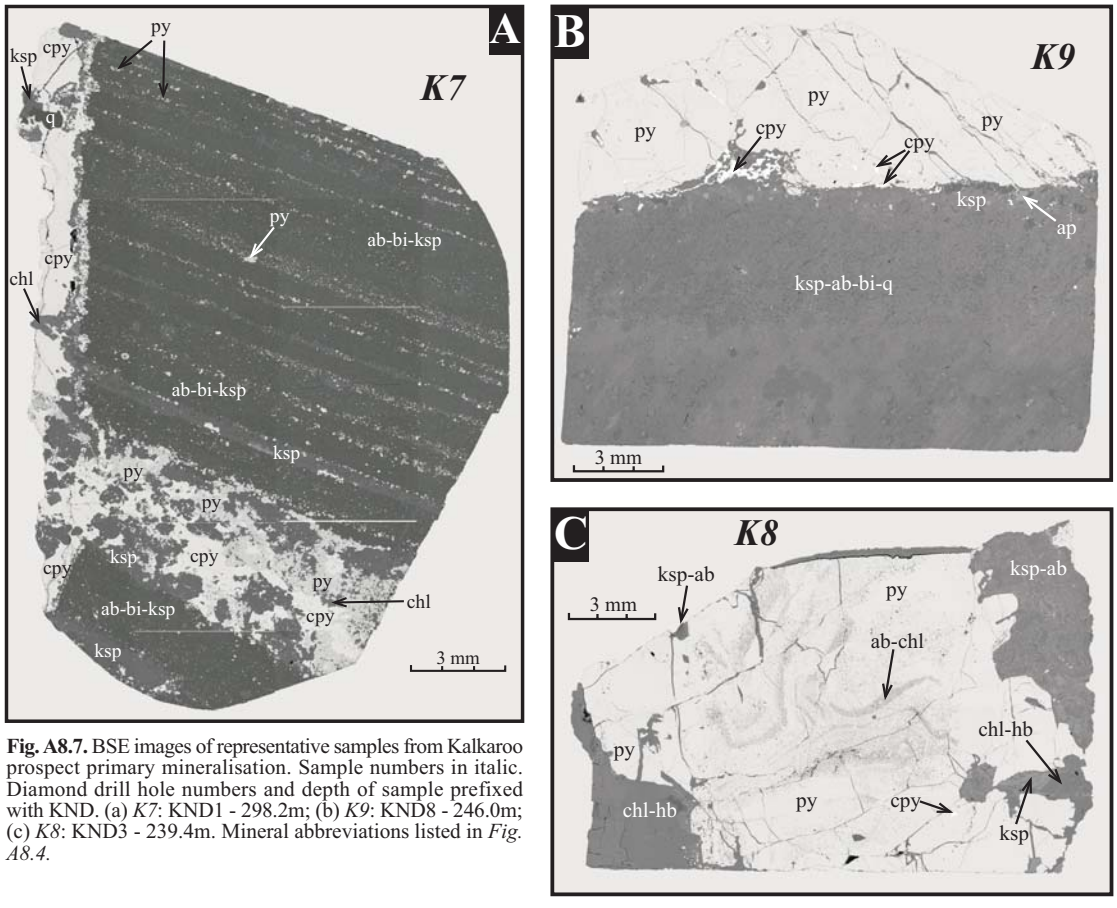


**Fig. A8.7.** BSE images of representative samples from Kalkaroo prospect primary mineralisation. Sample numbers in italic. Diamond drill hole numbers and depth of sample prefixed with KND. (a) *K7*: KND1 - 298.2m; (b) *K9*: KND8 - 246.0m; (c) *K8*: KND3 - 239.4m. Mineral abbreviations listed in *Fig. A8.4.*

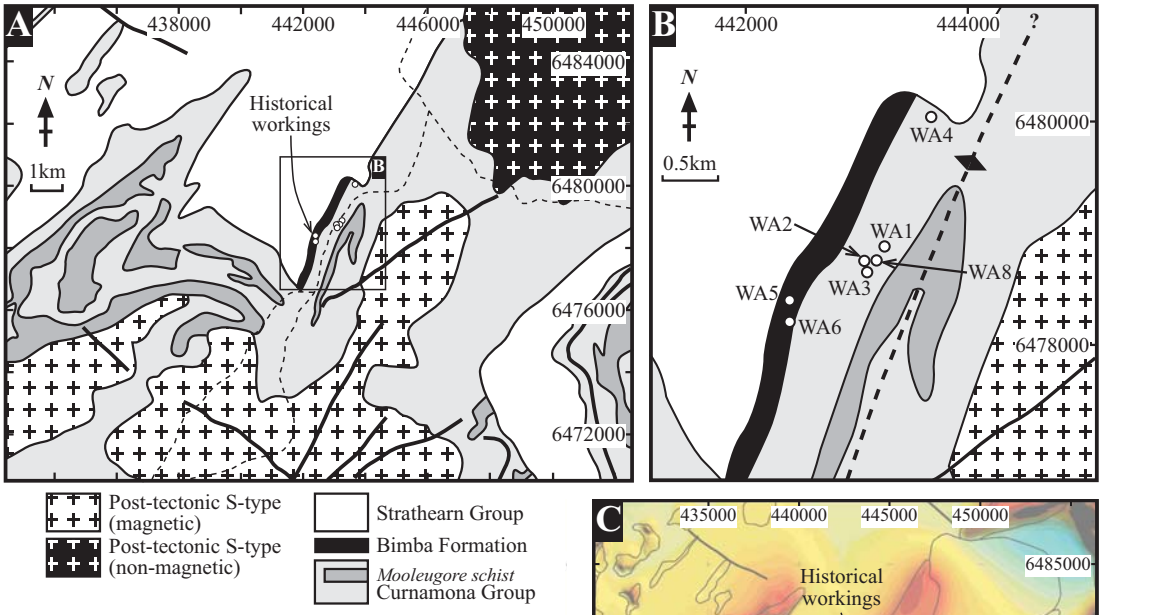


**Figure A8.8.** (a) Regional-scale interpreted solid geology of Waukaloo prospect region (Jenkins & Burtt, 2003); (b) Close-up of Waukaloo prospect showing interpreted solid geology and location of drill holes (*G. Teale pers. comm.*); (c) Total magnetic intensity image of Waukaloo prospect and surrounding area. Note that the prospect is situated along the regional magnetic gradient between the Curnamona and Strathearn Group's that coincides with Bimba Formation/redox boundary.

## A8.4 Waukaloo

The Waukaloo Cu-Au-Mo prospect is situated in the northern Olary Domain, near the northernmost outcrop of the Willyama Inliers. Subeconomic stratabound mineralisation occurs within predominantly psammopelitic units, which are part of a more extensive calcsilicate, psammopelite-psammite sequence. Similar to mineralisation at North Portia and Kalkaroo, mineralisation at Waukaloo occurs at approximately the level of the redox boundary (Fig. A8.8). However, mineralisation occurs at a slightly deeper stratigraphic level within psammopelite and calcsilicate rocks correlated with the Ethiudna Subgroup. Mineralisation is stratigraphically overlain by carbonaceous metapelites correlated with the Strathearn Group metasediments (Jenkins & Burtt, 2003).

Primary sulphide mineralisation is dominated by chalcopyrite and pyrite, with subordinate molybdenite, bornite and covellite. Mineralisation occurs as veins and patchy replacements locally within brecciated albitite (Skirrow et al., 2000). Mineralisation is associated with magnetite – actinolite – albite – titanite – quartz – calcite – chlorite (Fig. A8.9, A8.10). The majority of chalcopyrite is associated with chlorite-quartz stringer crackle breccia (G. Teale *pers. comm.*, 2004). Magnetite abundances are greatest in the footwall, although some does occur associated with mineralisation. Mineralisation at Waukaloo is predominantly associated with Fe-Ca assemblages, similar to primary mineralisation associated with Fe-Ca-K assemblages in the deeper parts of Kalkaroo. However, albite is the dominant feldspar in the Waukaloo mineralisation, suggesting a Fe-Ca-Na association. Oxygen isotope geothermometry for quartz – amphibole – magnetite at Waukaloo yielded temperatures of ~300 – 450°C (Skirrow et al., 2000; Williams & Skirrow, 2000).


**Figure A8.9.** Representative sample from Waukaloo prospect. Sample from DDH WA8 (sample *WA17*: 143.7m).

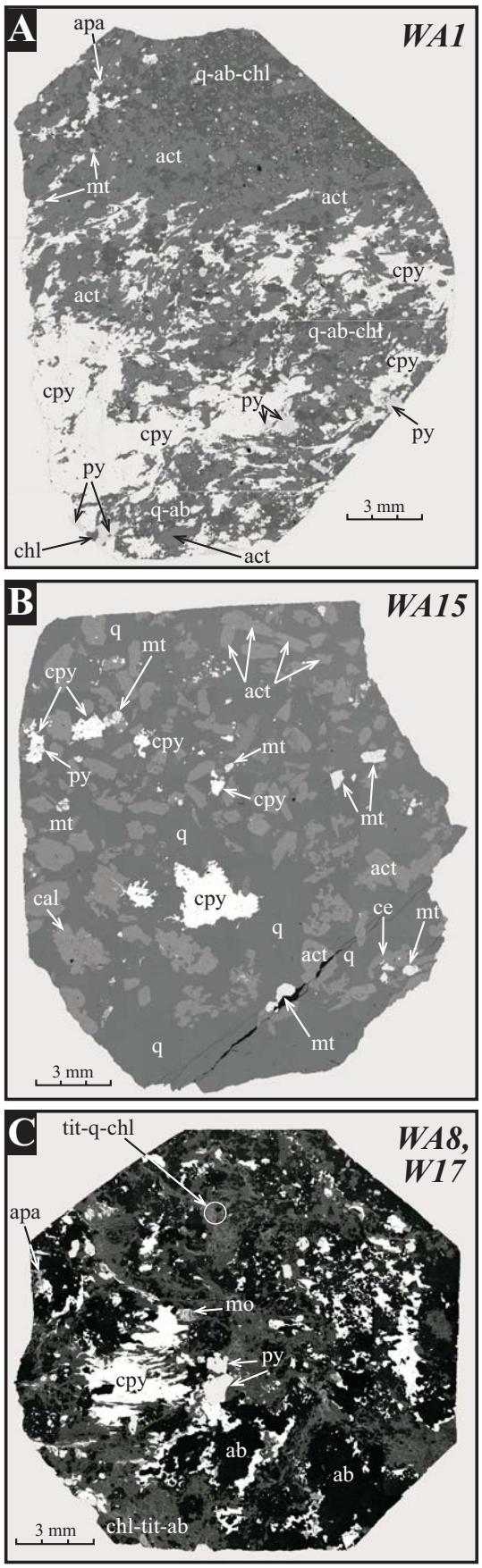


**Figure A8.10.** BSE images of representative samples from Waukaloo prospect mineralisation. Sample numbers in italic. Diamond drill hole numbers and depth of sample prefixed with 'WA'. (a) *WA1*: WA1 - 101.2m; (b) *WA15*: WA8 - 101.9m; (c) *WA8 & WA17*: WA8 - 143.8m. Mineral abbreviations listed in *Fig. A8.4*.

### A8.5 Polygonum

The Polygonum Cu-Au prospect is in the Mundi Mundi Plains region, west of the Mulyungarie dome. Polygonum is part of a larger mineralised region termed the Woolshed Area (Grid 4; Leyh & Conor, 2000). Drilling has intersected a stratigraphic package that includes facets from what is known about the stratigraphy in both the Broken Hill and Olary Domain's (Leyh & Conor, 2000; Leyh, 1995). Polygonum occurs along the same regional redox boundary as Portia, Kalkaroo and Waukaloo, although the magnetic gradient is not as intense across the Bimba Formation as is at the other prospects, primarily due to a greater abundance of magnetite in the hangingwall relative to the other stratabound prospects (Fig. A8.11).

Cu-Au(-Mo) mineralisation at Polygonum occurs within a stratigraphic package composed of quartz albitite, siltstone, iron formations with minor calcsilicate and pelite (Leyh, 1995). These units have been correlated with the Thackaringa Group (Himalaya Formation) and Ethiudna Subgroup of the Broken Hill Domain and Olary Domain, respectively (Leyh & Conor, 2000). Mineralisation occurs as stratiform to stratabound packages that dip ~45 NE, bounded at the footwall by strongly magnetic lithologies, including quartz-magnetite rock, magnetite-rich metasediments, metasiltstone and albitic metapsammites (Fig. A8.12; Leyh, 1995). These lithological units are stratigraphically overlain by units correlated with the Bimba Formation, Plumbago Formation and Broken Hill Group.

Primary mineralisation occurs within quartz-albitite and magnetite-rich siltstone/shale grading to iron formation (~70m package; Leyh, 1995). High-grade Cu-Au mineralisation occurs as stratabound veins associated with brecciated, Fe-Si altered (magnetite – quartz) siltstone (*SR1A* – DDH SR1 338m; Fig. A8.13a). Mineralisation occurred late-stage in the brecciation process, forming ~20 cm long veins containing blebs and patches of massive chalcopyrite – pyrite – pyrrhotite – magnetite – quartz. Altered host rock is composed of magnetite – K-feldspar – quartz – biotite ± muscovite ± apatite (Fig. A8.14a). Mineralisation over the interval 337.6m – 338.1m in DDH SR1 grades at 12.5% Cu, 4ppm Au and 285ppm Mo (Leyh, 1995). The mineralised and altered sequence is overprinted by low-temperature chlorite – calcite alteration forming veins and replacement of earlier formed silicates (biotite).

Medium-grade mineralisation occurs deeper in the stratigraphic package, within quartzite and quartz albitites that is locally brecciated. The host rock is also Fe-Si altered, resulting in silicification and hematite formation. Mineralisation is dominated by chalcopyrite, with minor pyrite that forms massive, patchy anastomosing veins (*SR1C* – DDH SR1 504.8m; Fig. A8.13b). Altered host rock is composed of K-feldspar – quartz – biotite ± apatite (Fig. A8.14b). Mineralisation over the interval 504.5m – 504.9m in DDH SR1 grades at 3.5% Cu, 6.6ppm Au and 128ppm Mo (Leyh, 1995). Patchy chlorite alteration also overprints the mineralisation and alteration at depth.

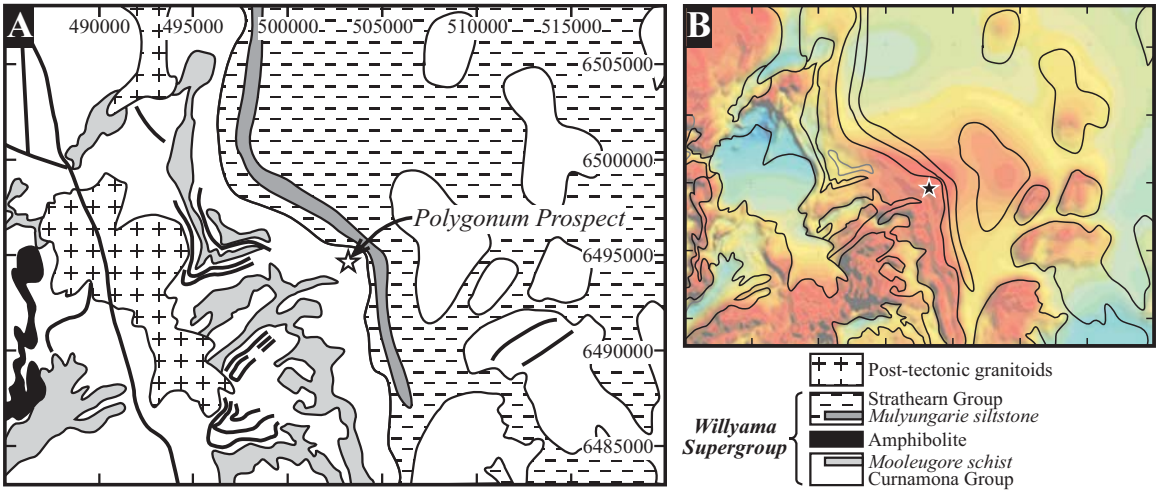


**Figure A8.11.** (a) Regional-scale interpreted solid geology of Polygonum prospect region, Mundi Mundi Plains (Jenkins & Burtt, 2003); (b) Regional-scale total magnetic intensity image of Polygonum prospect and surrounding area (Jenkins & Burtt, 2003).

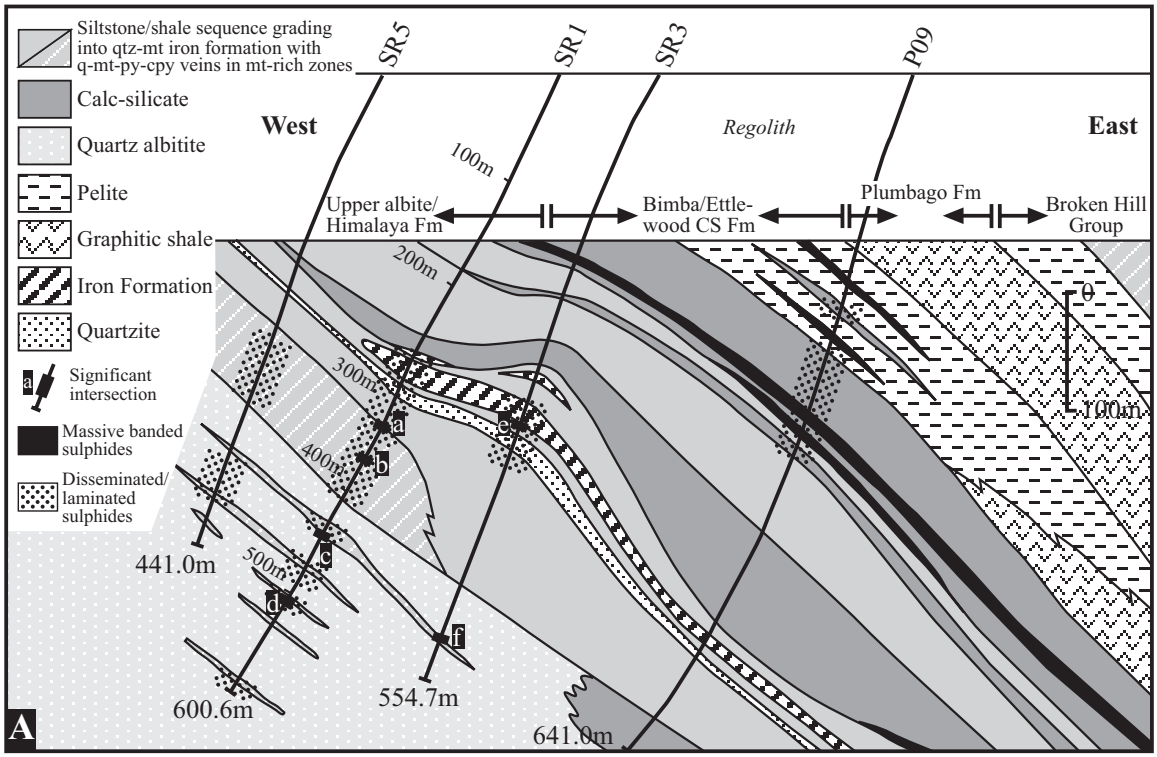


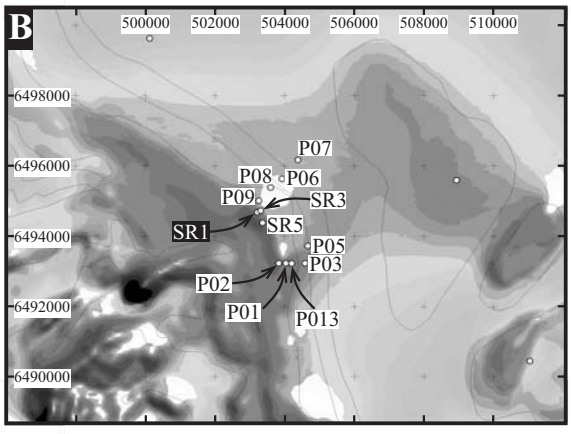


**Significant intersections:**

a. SR1: 1.8m @ 7.4% Cu from 338m
b. SR1: 0.1m @ 1.8% Cu, 0.5g/t Au from 368.6m
c. SR1: 0.7m @ 0.7% Cu, 0.3g/t Au from 442.8m
d. SR1: 0.4m @ 3.5% Cu, 6.6g/t Au from 504.8m
e. SR3: 0.6m @ 0.1g/t Au from 325.8m
f. SR3: 0.3m @ 0.3% Cu, 0.4g/t Au from 517.4m

**Figure A8.12.** (a) Cross section of interprted geology through Polygonum prospect along ~503000mE (W. Leyh *pers. comm.*, 2004); (b) Location of major drill holes in Polygonum prospect region, draped over TMI image (W. Leyh *pers. comm.*, 2004).

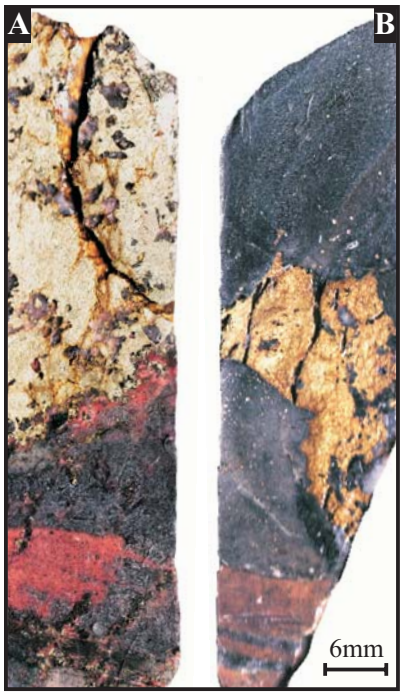


**Figure A8.13.** Representative samples from Polygonum prospect. Sample taken from diamond drillhole SR1. Sample numbers in italic. (a) *SR1A* - 338m; (b) *SR1C* - 504.8m. Scale same for each sample block.

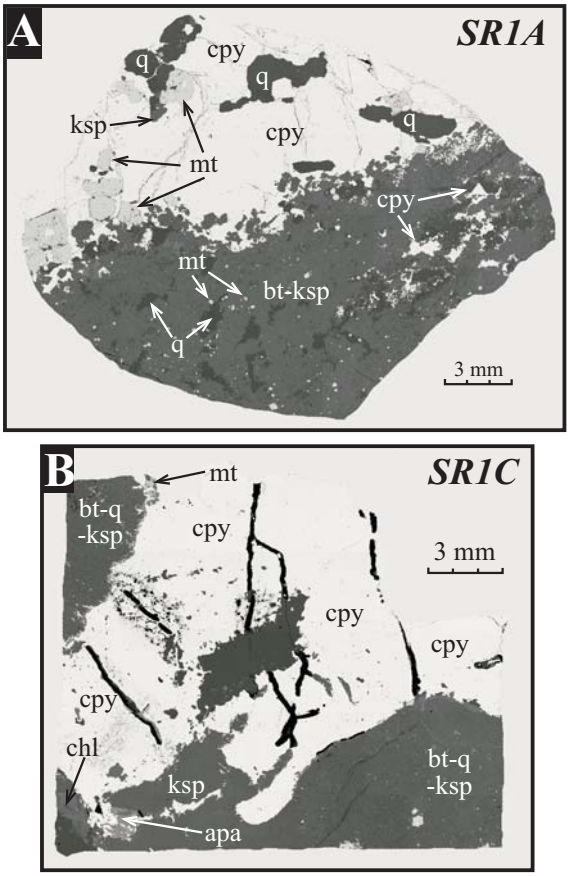


**Figure A8.14.** BSE images of representative samples from Polygonum prospect primary mineralisation. Sample numbers in italic. Samples taken from diamond drill hole SR1. (a) *SR1A* - 338.0m; (b) *SR1C* - 504.8m. Mineral abbreviations listed in *Fig. A8.4.*

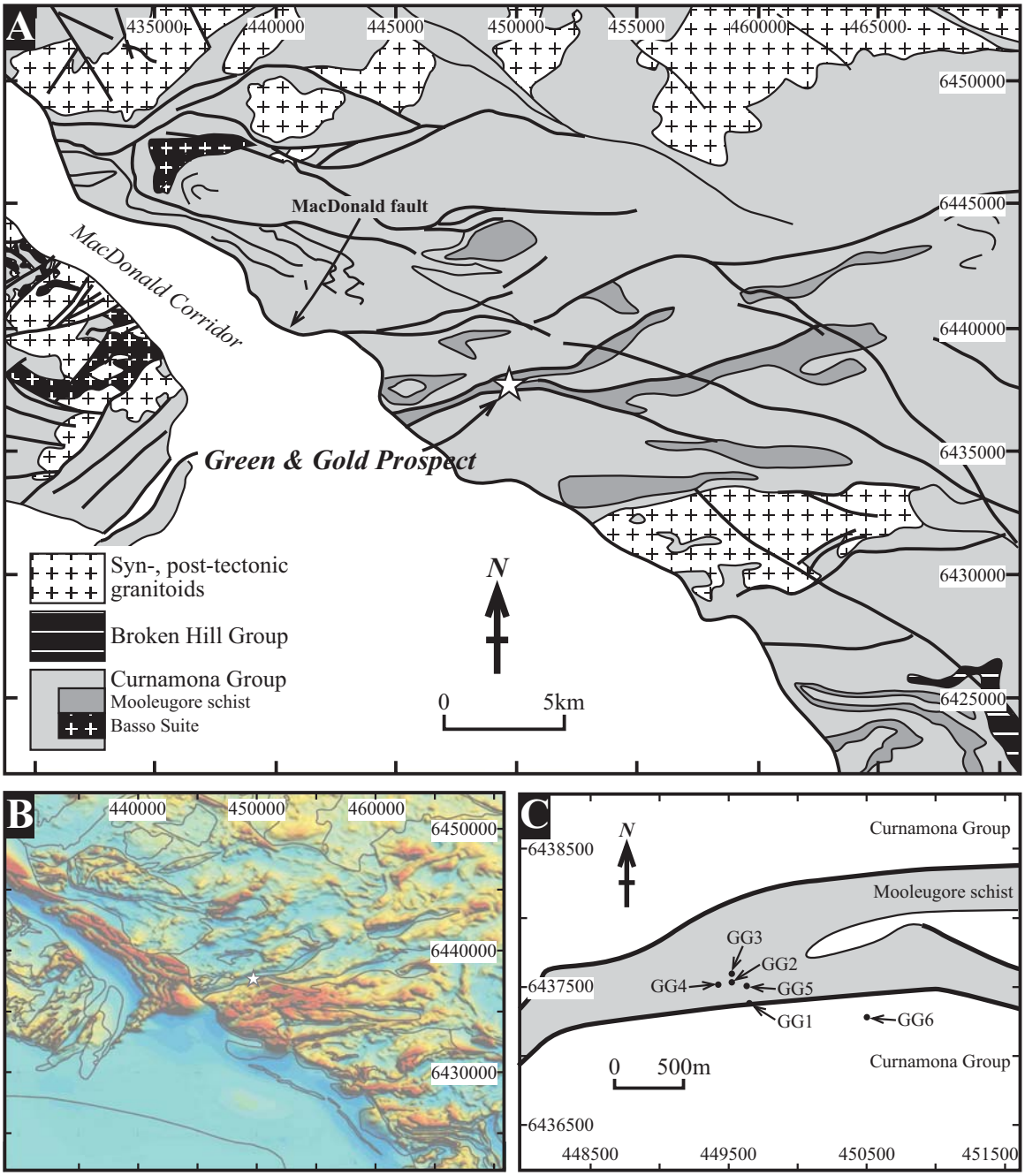


**Figure A8.15.** (a) Regional interpreted solid geology of the Green & Gold prospect (Jenkins & Burtt, 2003); (b) Total magnetic intensity image of surrounding area to Green & Gold prospect (Jenkins & Burtt, 2003); (c) Drill hole locations at Green & Gold prospect (Jenkins & Burtt, 2003).

## A8.6 Green and Gold

The Green and Gold prospect is located in the medium- to high-metamorphic grade southern Olary Domain, <10 km from the major SE-trending, half-graben MacDonald Corridor that bounds the southwestern Kalabity Inlier (Fig A8.15a; Preiss; 2001). It is bounded to the north and south by ENE-trending shear zones that form a conjugate set to the MacDonald Fault (Fig. A8.15a). The last major movement on many of the major shear zone systems in the SCP was during the ~505 Ma Delamerian Orogeny (Dutch et al., 2005). The Green and Gold prospect is a Cu-poor, Au-rich type of IOCG mineralisation (e.g. 27m @ 1.79 g/t Au; Green, 1996). Alteration and mineralisation forms in zones as replacements of near vertical, cigar-shaped boudins, flattened parallel to the penetrative ENE-trending fabric (Green, 1996).

The host rock to the mineralisation is the weakly magnetic Mooleugore Schist of the lower Curnamona Group (Fig. A8.15; Jenkins & Burtt, 2003). Sheared and dynamically recrystallised biotite – plagioclase – sillimanite layered gneiss is the dominant host rock. Mineralisation is associated with Fe-Si(-Mn) alteration that forms layered biotite – magnetite – amphibole – garnet – mica – chlorite – quartz schists (Fig. A8.16). Mineralisation is predominantly hosted within felsic layers occurring in the form of disseminated magnetite – arsenopyrite – pyrite ± chalcopyrite (Fig. A8.16, A8.17). Patches of abundant arsenopyrite and magnetite also occur, with accessory phase including apatite and anhydrite (Fig. A8.17). Late-stage replacement of mica by chlorite also occurred. Aspects of the mineralogy associated with the shear zone that hosts the Green & Gold prospect, such as late-chlorite replacement, are similar to those described by Dutch et al. (2005) for shear zones reactivated during the Delamerian Orogeny

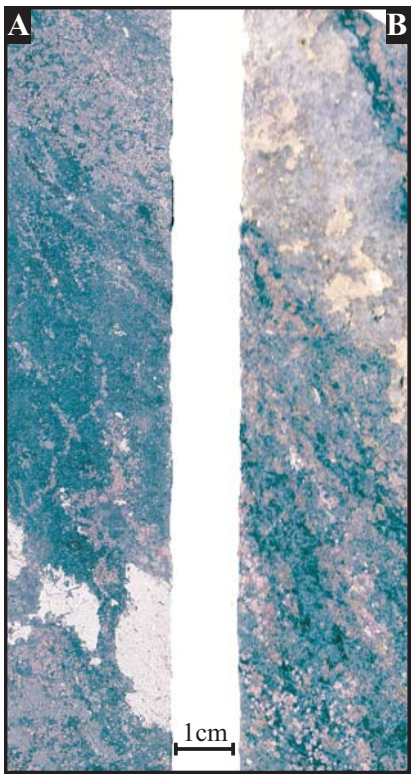


**Figure A8.16.** Representative samples of primary mineralisation from Green and Gold prospect. Samples from DDH GG2. Sample number in italic. (a) *GG2* - 85.25m; (b) *GG19* - 87.2m. Scale same for each sample block.

elsewhere in the SCP. Monazite EPMA chemical age constraints from the Green & Gold shear zone also record Delamerian reactivation (*Chapter 7*).

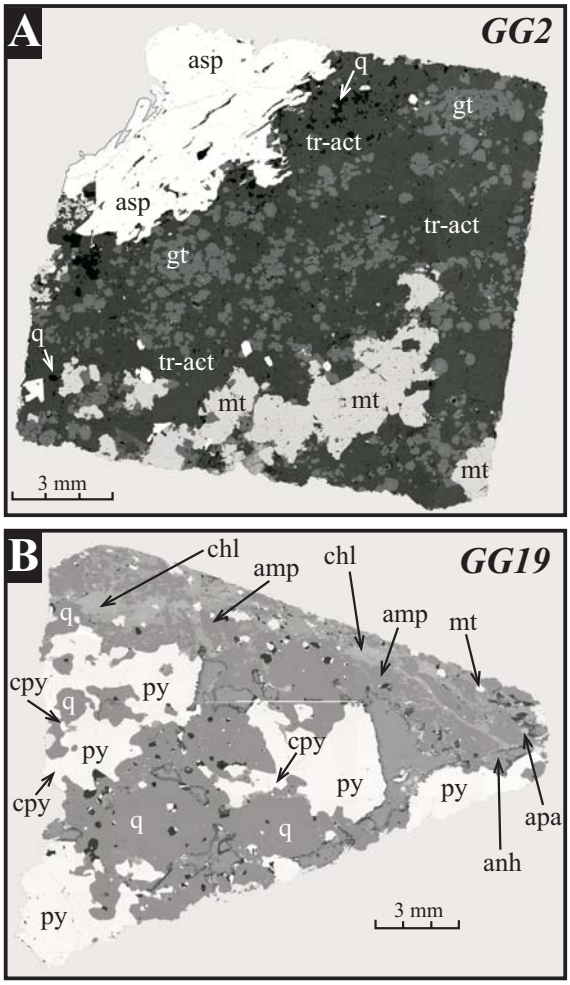


**Figure A8.17.** BSE images of representative sample from Green and Gold propsect. Samples from DDH GG2. Sample numbers in italic. (a) GG2 - 85.25m; (b) GG19 - 87.2m. Mineral abbreviations listed in *Fig. A8.4*.

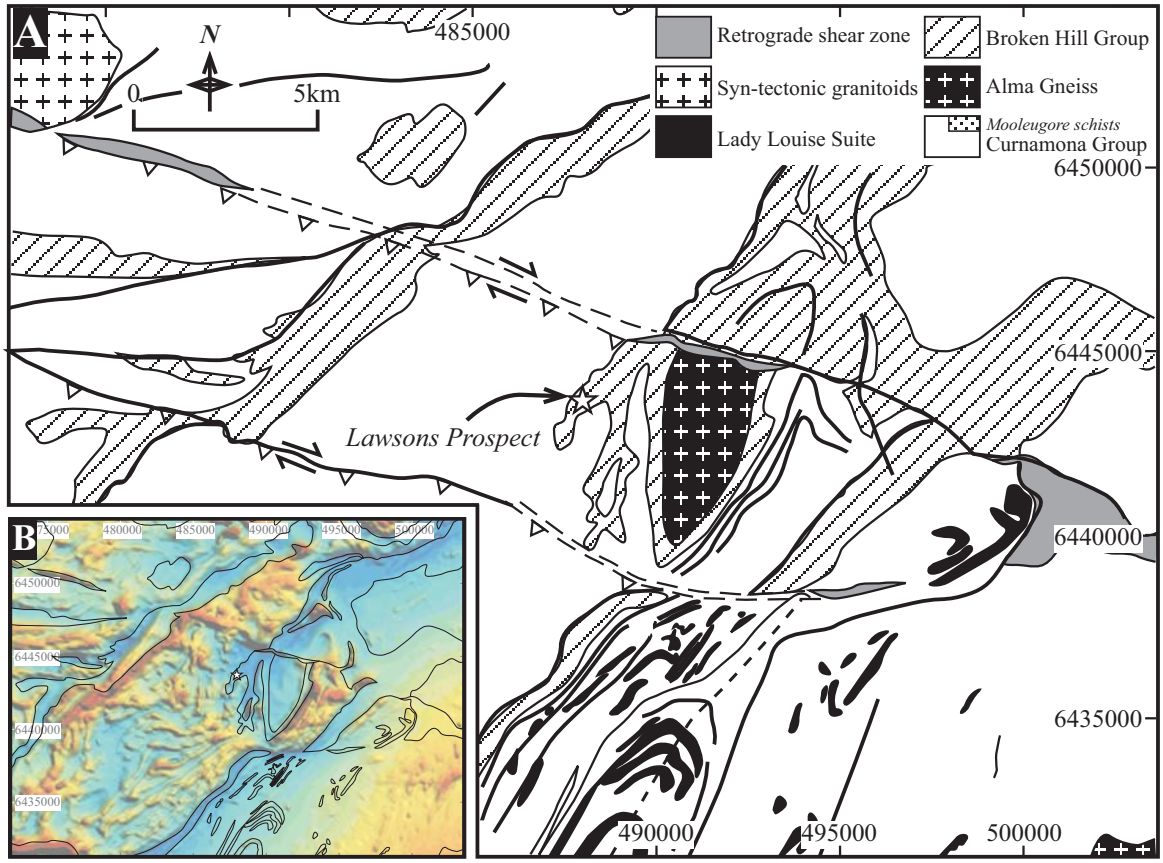


**Figure A8.18.** (a) Regional-scale geology of the Lawsons Prospect region, Mingary (Jenkins & Burtt, 2003); (b) Regional-scale total magnetic intensity image of the Lawsons prospect region, Mingary (Jenkins & Burtt, 2003).

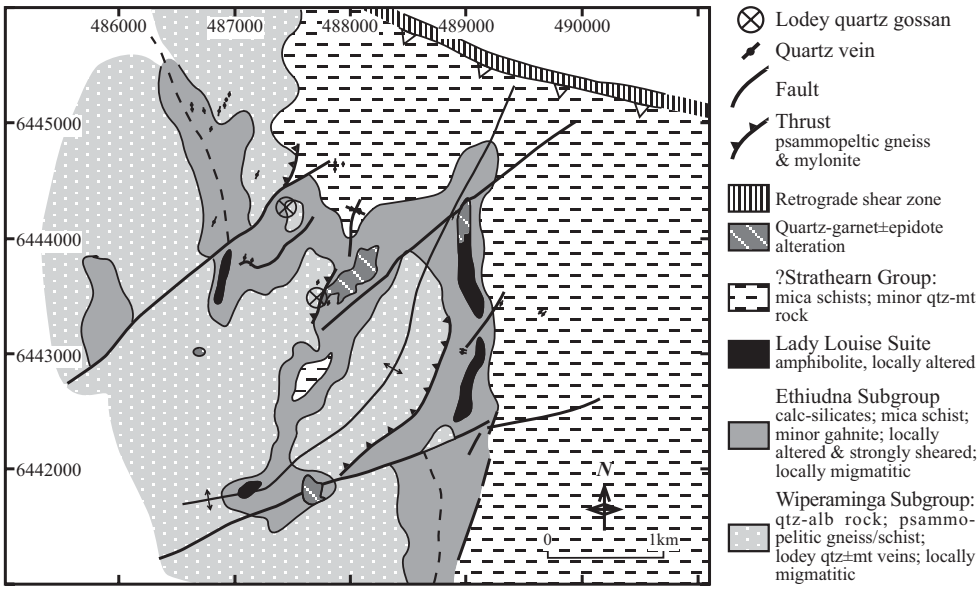


**Figure A8.19.** Prospect-scale interpreted solid geology of Lawsons prospect region showing location of 'lodey' quartz veins adjacent to northeast-trending shear zones (CRA Exploration, 1995).

## A8.7 Lawsons

Lawson prospect is located in the southern Curnamona Province, southwestern Broken Hill Domain. It is a low-grade, low-volume mineralised area that is located within the highly deformed and amphibolite- to granulite-facies Mingary region. The Mingary region is dominated by felsic and mafic gneisses with minor S-type intrusives (Alma Gneiss) and is dissected by a series of ESE- to SE-trending retrograde shear zones. The shear zones were last active during the Delamerian Orogeny (e.g. Kings Dam and Mutooroo shear zones; Dutch et al., 2005). The Mingary region was pervasively reworked during the Delamerian Orogeny (*Chapter 7*), resulting in garnet-staurolite and staurolite-kyanite assemblages (amphibolite facies). The Lawsons prospect is situated ~1 km south of a major ESE-trending retrograde shear zone (Fig. A8.18). Mineralisation occurs at the contact between highly deformed Ethiudna Subgroup (Broken Hill Group equivalent) and Wiperaminga Subgroup metasediments (Fig. A8.19).

Mineralisation is anomolous in lodey quartz gossans adjacent to NE-trending faults and thrusts that form in an orientation that is conjugate to the ESE-trending

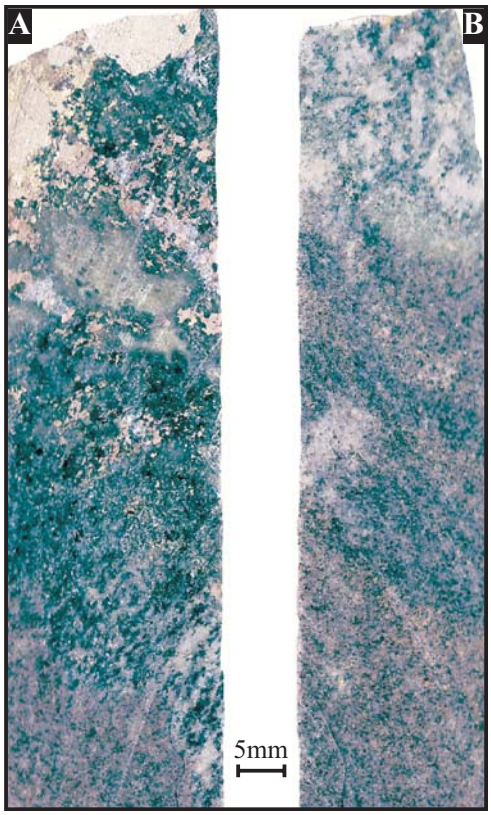


**Figure A8.20.** Representative samples from Lawsons prospect mineralisation (a) and host rock (b). Samples taken from DD96 MN33. Sample number in italic. (a) *DD96*: 108.50 - 108.57m; (b) 108.58 - 108.65m. Scale same for each sample block.

retrograde shear zone (Fig. A8.19; CRA Exploration, 1995). Quartz veins also dominate the outcrop geology, some of which eminate from faults/shears. At depth the mineralisation is hosted by metamorphic magnetite – amphibole – quartz – biotite – garnet rock tentatively correlated with the Ethiudna Subgroup (Fig. A8.20). Pyrite – chalcopyrite ± pyrrhotite mineralisation is associated with almandine – actinolite-tremolite – quartz alteration with accessory pyroxene, K-feldspar and scapolite (Fig. A8.21).

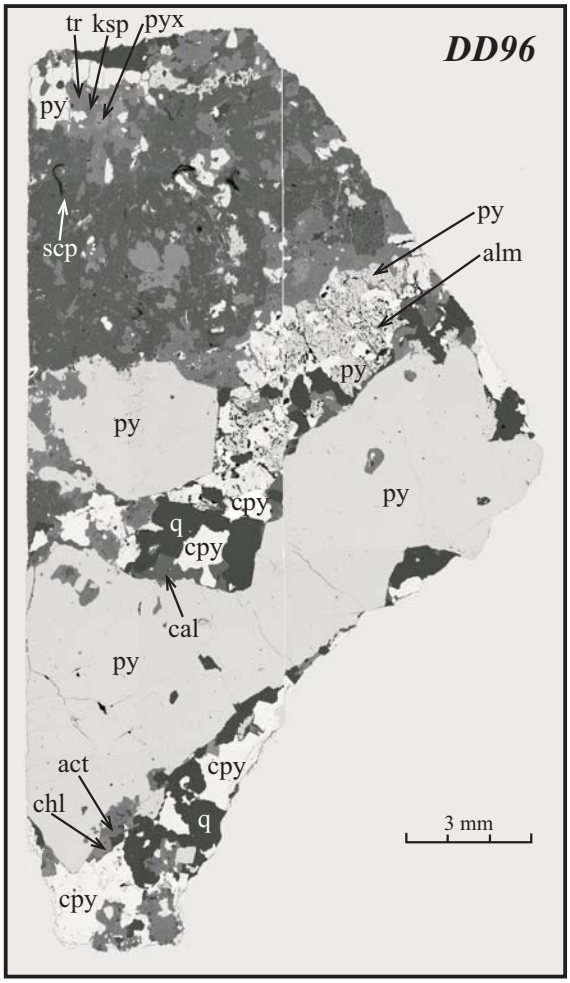


**Figure A8.21.** BSE image of representative sample of primary mineralisation from Lawsons prospect. Sample number *DD96*. Sample taken from drill hole DD96MN33 - 108.5m. Mineral abbreviations listed in *Fig. A8.4*.

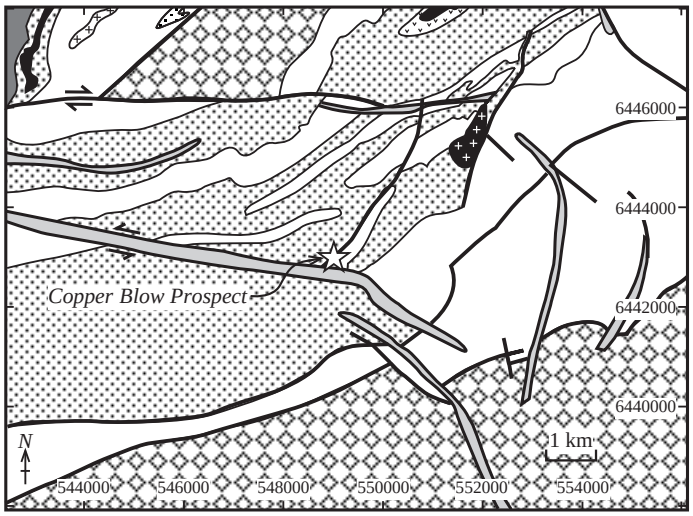


**Figure A8.22.** Regional-scale interpreted solid geology of Copper Blow prospect and surrounding region, south of Broken Hill, N.S.W. Prospect is adjacent to ESE-trending Thackaringa-Pinnacles retrograde shear zone (Jenkins & Burtt, 2003).

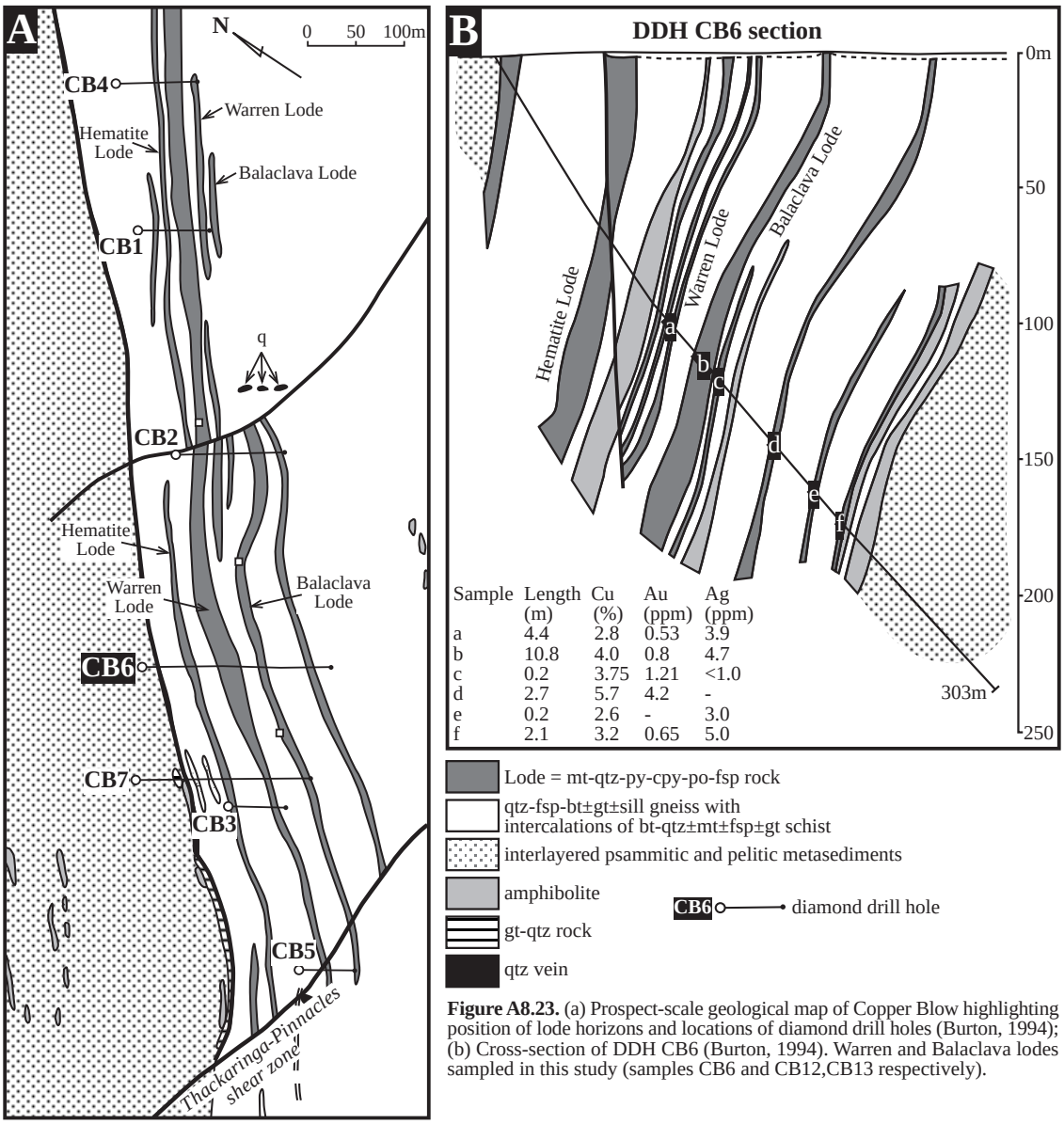


**Figure A8.23.** (a) Prospect-scale geological map of Copper Blow highlighting position of lode horizons and locations of diamond drill holes (Burton, 1994); (b) Cross-section of DDH CB6 (Burton, 1994). Warren and Balaclava lodes sampled in this study (samples CB6 and CB12,CB13 respectively).

### A8.8 Copper Blow

Copper Blow prospect is located south of Broken Hill township. The Copper Blow lode is ~4km long, extending in a northeast direction from the ESE-trending Thackaringa-Pinnacles shear zone (Fig. A8.22). Geological mapping has interpreted a NE-trending conjugate shear that bounds the highly magnetic Thackaringa Group host rocks to the west (Burton, 1996). The last timing of movement on the Thackaringa-Pinnacles shear zone is constrained at its western extension to have occurred during the Delamerian Orogeny (Dutch et al., 2005). It is highly probable that the conjugate shear system was also active at this time.

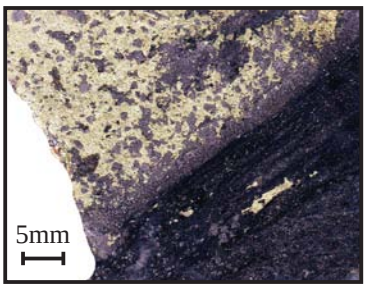


**Figure A8.24.** Representative sample from Copper Blow mineralisation. Sample number *CB6*. Sample taken from DDH CB6 - 188.2m.

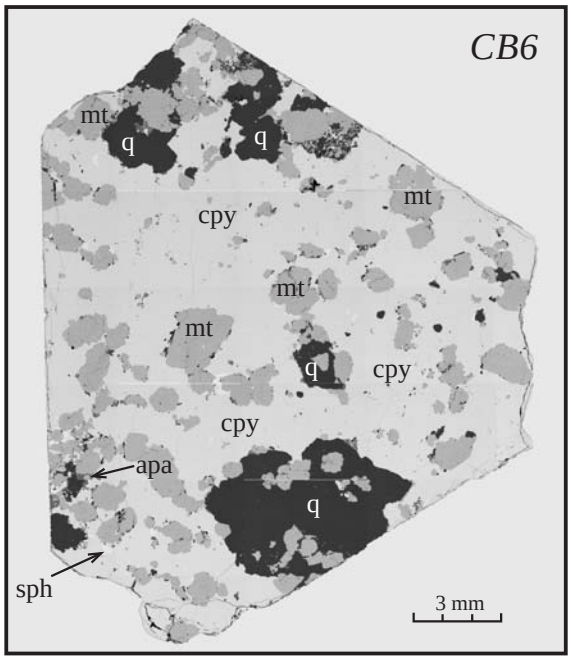


**Fig. A8.25.** Representative sample of Copper Blow prospect primary mineralisation. Sample number *CB6*. Sample taken from DDH CB6 - 118.2m. Mineral abbreviations listed in *Fig. A8.4*.

Host rocks to the Copper Blow lodes were metamorphosed at amphibolite- to granulite-facies between ~1610 – 1550 Ma (*Chapter 3*).

Mineralisation occurs in a series of lodes that are either magnetite- and/or hematite-rich, some of which contain anomalous Cu-Au(-U). Differing interpretations surrounding the relationship between the lode horizons and the surrounding metasediments have lead to the mineralisation being interpreted to be both syngenetic (Corbett & Willis, 1989; Bradley & Brown, 1988) and epigenetic (Dashlooty & Elliot, 1985; 1986). Given the known timing of movement along the Thackaringa-Pinnacles shear zone and the known metamorphic grade of the SCP during the Delamerian Orogeny (~530 – 600°C, ~5 kbars; Dutch et al., 2005), any stratabound mineralisation is likely to have been locally remobilised given the solubility of chalcopyrite and pyrite in oxidised, chlorine-rich fluids (Davidson & Large, 1994). Subsequently, the mineralisation at Copper Blow is interpreted to be epigenetic in form. However, it can be speculated that the anomolous metal content of this region is likely to be initially related to depositional characteristics (e.g. hot spring, exhalative/inhalative hydrothermal activity).

The lode horizons at Copper Blow are all NE-trending, steeply NW-dipping, and truncated at the south by the Thackaringa-Pinnacles shear zone (Fig. A8.23). Quartz – feldspar – biotite ± garnet ± sillimanite gneisses with intercalated biotite – quartz ± magnetite ± feldspar ± garnet schists host the lode horizons (Fig. A8.24). These lithologies are correlated with the Thackaringa Group (Cues Formation; Burton, 1994). Interlayered metapsammitic and metapelitic metasediments of the Broken Hill Group immediately overlie the mineralised sequence to the west. Three of the main lode horizons (Hematite, Warren and Balaklava) are composed of fine- to medium-grained magnetite – quartz ± pyrite ± pyrrhotite ± feldspar rock, forming anastomosing layers (Burton, 1994). Individual layers are intercalated with gneiss and biotite chlorite schist with sharp, concordant contacts (Fig. A8.24). Within the magnetite – quartz rock, chalcopyrite occurs as disseminated, stringer and patchy mineralisation (Fig. A8.25), and rare breccias mixtures with the country rock (Burton, 1994). Accessory minerals include apatite and sphalerite. The lode horizons at Copper Blow are different from the stratiform quartz-magnetite bodies that are associated with Broken Hill-type mineralisation, having features more in common with the Cu-Au prospects in the Olary Domain or the Starra deposit near Mt Isa (Burton, 1994).

# Appendix 9
# LA-ICPMS TRACE ELEMENT DATA

The following appendix lists trace element concentrations (ppm) of sulphides and Fe-oxides collected using the LA-ICPMS technique. Analytical procedures are listed in *Chapter 6.* Analytical precision (%) of each element for each analysis stated after each concentration.

**Table A9.1.** Chalcopyrite

| SAMPLE | SR1A 03 cpy | | SR1A 04 cpy | | SR1A 07 cpy | | SR1A 08 cpy | | SR1A 09 cpy | | SR1C 01 cpy | | SR1C 02 cpy | | SR1C 03 cpy | | SR1C 04 cpy | | SR1C 05 cpy | |
|---|---|---|---|---|---|---|---|---|---|---|---|---|---|---|---|---|---|---|---|---|
| **Ti49** | 11.514 | 6 | 11.427 | 6 | 11.705 | 6 | 12.748 | 6 | 10.575 | 7 | 6.976 | 6 | 6.084 | 7 | 7.412 | 7 | 6.782 | 7 | 6.740 | 7 |
| **Cr53** | <0.436 | | 0.136 | 97 | <0.487 | | <0.511 | | <0.394 | | <0.4 | | <0.457 | | 0.432 | 31 | 0.365 | 37 | <0.451 | |
| **Mn55** | 0.406 | 30 | <0.395 | | 1.595 | 12 | 0.473 | 31 | 0.506 | 27 | <0.408 | | <0.392 | | 0.500 | 34 | <0.405 | | 0.860 | 21 |
| **Fe57** | 304300 | | 304300 | | 304300 | | 304300 | | 304300 | | 304300 | | 304300 | | 304300 | | 304300 | | 304300 | |
| **Co59** | 3.557 | 4 | 3.892 | 4 | 3.655 | 5 | 3.657 | 4 | 4.365 | 6 | 2.350 | 4 | 2.648 | 5 | 3.196 | 5 | 2.847 | 7 | 3.475 | 4 |
| **Ni60** | <0.104 | | <0.107 | | 0.207 | 24 | <0.108 | | 0.089 | 31 | <0.101 | | 0.104 | 36 | <0.123 | | 0.096 | 81 | 1.077 | 18 |
| **Cu65** | 349782 | 4 | 355433 | 4 | 355681 | 5 | 377809 | 5 | 321187 | 6 | 350872 | 4 | 350032 | 4 | 362010 | 4 | 359457 | 4 | 354613 | 3 |
| **Zn66** | 72.115 | 4 | 54.658 | 3 | 63.178 | 6 | 48.090 | 4 | 68.838 | 6 | 46.992 | 4 | 41.765 | 4 | 36.897 | 4 | 40.202 | 4 | 39.942 | 4 |
| **As75** | 2.416 | 9 | 2.254 | 12 | 2.510 | 10 | 2.079 | 13 | 2.277 | 11 | 1.803 | 12 | 1.811 | 14 | 2.464 | 10 | 2.625 | 9 | 2.626 | 9 |
| **Se77** | 20.398 | 5 | 21.923 | 5 | 21.914 | 6 | 25.516 | 5 | 21.976 | 7 | 94.981 | 4 | 90.932 | 4 | 99.289 | 4 | 106.137 | 4 | 99.417 | 4 |
| **Zr90** | <0.012 | | <0.014 | | 0.090 | 18 | <0.006 | | <0.011 | | <0.015 | | <0.016 | | 155.147 | 10 | 1.081 | 53 | 0.029 | 62 |
| **Mo95** | <0.294 | | <0.293 | | <0.273 | | <0.306 | | <0.236 | | <0.339 | | <0.351 | | <0.419 | | <0.298 | | <0.415 | |
| **Ag107** | 2.268 | 5 | 1.669 | 5 | 209.155 | 14 | 1.236 | 6 | 1.405 | 7 | 2.052 | 6 | 0.708 | 7 | 2.153 | 12 | 3.814 | 29 | 1.470 | 5 |
| **Cd111** | <0.901 | | <1.281 | | 0.093 | 235 | <1.369 | | <1.279 | | <1.64 | | <1.72 | | <1.807 | | <1.779 | | <1.993 | |
| **Sn118** | 25.881 | 4 | 22.381 | 4 | 25.211 | 6 | 20.826 | 4 | 28.294 | 6 | 6.230 | 4 | 11.584 | 4 | 8.027 | 4 | 7.013 | 5 | 7.036 | 4 |
| **Sb121** | <0.064 | | <0.078 | | 0.232 | 17 | <0.095 | | <0.08 | | 0.076 | 38 | 0.096 | 36 | <0.088 | | 0.096 | 26 | 0.152 | 21 |
| **Te125** | 0.471 | 39 | 0.680 | 26 | <0.526 | | <0.525 | | <0.348 | | 0.753 | 34 | 0.164 | 173 | <0.709 | | 0.973 | 30 | <0.716 | |
| **Ba137** | <0.06 | | <0.077 | | 0.232 | 40 | <0.048 | | <0.041 | | <0.088 | | <0.075 | | <0.07 | | <0.062 | | <0.079 | |
| **La139** | <0.005 | | <0.005 | | 0.024 | 24 | 0.006 | 44 | <0.006 | | <0.005 | | <0.008 | | <0.007 | | <0.005 | | 0.077 | 44 |
| **W182** | <0.024 | | <0.031 | | <0.025 | | <0.035 | | <0.018 | | <0.043 | | <0.04 | | <0.055 | | <0.049 | | <0.043 | |
| **Au197** | 0.017 | 36 | 0.083 | 17 | <0.029 | | <0.023 | | 0.027 | 29 | 0.090 | 17 | 0.044 | 20 | 0.034 | 35 | 0.058 | 23 | 0.032 | 44 |
| **Tl205** | <0.008 | | 0.296 | 13 | <0.007 | | <0.009 | | 0.036 | 29 | 0.131 | 14 | 0.022 | 41 | <0.015 | | <0.011 | | | |
| **Pb208** | 0.359 | 6 | 0.108 | 12 | 4.305 | 10 | 0.148 | 9 | 0.410 | 7 | 3.215 | 5 | 0.998 | 5 | 5.851 | 9 | 3.756 | 5 | 3.803 | 4 |
| **Bi209** | 4.457 | 4 | 1.315 | 4 | 10.736 | 5 | 1.621 | 4 | 3.662 | 6 | 21.150 | 5 | 7.903 | 4 | 19.661 | 8 | 23.181 | 8 | 21.956 | 4 |
| **Th232** | <0.005 | | 0.015 | 26 | 0.089 | 44 | <0.006 | | <0.007 | | <0.006 | | <0.011 | | 0.183 | 13 | 0.015 | 41 | 0.010 | 52 |
| **U238** | <0.007 | | <0.008 | | 0.016 | 28 | <0.007 | | <0.003 | | 0.007 | 38 | <0.01 | | 1.345 | 11 | <0.01 | | 0.006 | 37 |

| SAMPLE | SR1C 06 cpy | | CB6 06 cpy | | CB6 07 cpy | | CB6 08 cpy | | CB6 09 cpy | | CB6 10 cpy | | DD96 07 cpy | | DD96 08 cpy | | DD96 09 cpy | | DD96 10 cpy | |
|---|---|---|---|---|---|---|---|---|---|---|---|---|---|---|---|---|---|---|---|---|
| **Ti49** | 7.661 | 7 | 9.351 | 6 | 11.351 | 6 | 9.326 | 7 | 10.290 | 6 | 10.251 | 6 | 9.532 | 8 | 9.611 | 8 | 9.509 | 6 | 10.258 | 6 |
| **Cr53** | 0.374 | 38 | <0.607 | 40 | 0.403 | 40 | <0.588 | | 0.516 | 29 | <0.671 | | <0.597 | | <0.457 | | <0.493 | | <0.62 | |
| **Mn55** | <0.458 | | 0.461 | 38 | 1.798 | 11 | 0.402 | 39 | 2.257 | 8 | 1.511 | 13 | 0.628 | 22 | 2.845 | 20 | 0.568 | 21 | <0.386 | |
| **Fe57** | 304300 | | 304300 | | 304300 | | 304300 | | 304300 | | 304300 | | 304300 | | 304300 | | 304300 | | 304300 | |
| **Co59** | 3.987 | 4 | 14.423 | 10 | 4.677 | 14 | 7.503 | 17 | 4.193 | 4 | 3.578 | 13 | 2.591 | 7 | 6.497 | 6 | 4.331 | 4 | 4.136 | 6 |
| **Ni60** | <0.142 | | 29.743 | 15 | 85.227 | 15 | 13.697 | 18 | 2.493 | 6 | 11.621 | 8 | 12.517 | 6 | 40.306 | 30 | 4.660 | 5 | 5.252 | 5 |
| **Cu65** | 367803 | 4 | 364705 | 4 | 356128 | 4 | 357420 | 4 | 384580 | 4 | 355114 | 4 | 355623 | 6 | 371033 | 5 | 366326 | 4 | 378453 | 4 |
| **Zn66** | 64.460 | 6 | 1259.615 | 17 | 884.558 | 5 | 435.351 | 3 | 456.766 | 3 | 460.249 | 3 | 568.936 | 6 | 7125.344 | 18 | 589.875 | 5 | 524.546 | 4 |
| **As75** | 3.126 | 9 | 2.397 | 11 | 2.274 | 12 | 1.766 | 15 | 2.212 | 10 | 2.173 | 13 | 2.685 | 11 | 2.428 | 11 | 2.188 | 12 | 2.696 | 10 |
| **Se77** | 119.179 | 4 | 168.945 | 4 | 171.074 | 3 | 173.079 | 4 | 169.288 | 4 | 186.308 | 4 | 58.079 | 4 | 81.499 | 7 | 80.648 | 4 | 89.578 | 4 |
| **Zr90** | <0.018 | | <0.016 | | <0.009 | | <0.01 | | <0.016 | | <0.014 | | <0.014 | | <0.013 | | <0.01 | | <0.013 | |
| **Mo95** | <0.395 | | <0.349 | | <0.289 | | <0.28 | | <0.299 | | <0.301 | | <0.411 | | <0.298 | | <0.245 | | <0.314 | |
| **Ag107** | 2.807 | 7 | 65.911 | 3 | 75.144 | 3 | 52.581 | 3 | 41.377 | 3 | 54.033 | 4 | 75.080 | 6 | 140.663 | 9 | 83.101 | 4 | 87.377 | 4 |
| **Cd111** | <2.184 | | 4.371 | 13 | 3.179 | 9 | 1.748 | 16 | 1.901 | 16 | 2.082 | 13 | 4.668 | 9 | 31.536 | 17 | 4.307 | 8 | 4.739 | 8 |
| **Sn118** | 9.053 | 4 | 15.962 | 4 | 17.996 | 4 | 13.906 | 4 | 13.683 | 4 | 13.300 | 4 | 2.026 | 7 | 2.439 | 5 | 2.125 | 5 | 2.505 | 5 |
| **Sb121** | <0.11 | | 0.216 | 15 | <0.092 | | <0.126 | | 0.058 | 42 | <0.085 | | <0.148 | | <0.116 | | <0.114 | | <0.131 | |
| **Te125** | 0.983 | 38 | 7.751 | 8 | 9.392 | 7 | 6.226 | 8 | 10.226 | 6 | 9.588 | 7 | 2.429 | 15 | 5.724 | 17 | 5.878 | 9 | 4.274 | 11 |
| **Ba137** | <0.094 | | <0.09 | | <0.056 | | <0.078 | | <0.05 | | <0.059 | | <0.056 | | 0.062 | 39 | 0.024 | 54 | <0.052 | |
| **La139** | <0.006 | | <0.007 | | <0.009 | | <0.004 | | <0.007 | | 0.011 | 41 | 0.011 | 84 | <0.007 | | <0.007 | | <0.007 | |
| **W182** | <0.053 | | <0.042 | | <0.031 | | <0.035 | | <0.026 | | <0.013 | | <0.04 | | <0.033 | | <0.033 | | <0.022 | |
| **Au197** | 0.034 | 36 | 0.041 | 26 | 0.028 | 35 | 0.017 | 42 | <0.039 | | 0.025 | 33 | <0.054 | | <0.044 | | <0.026 | | <0.032 | |
| **Tl205** | <0.015 | | 4.295 | 4 | <0.008 | | <0.01 | | <0.01 | | 0.391 | 8 | <0.008 | | 0.425 | 15 | 0.033 | 28 | 0.036 | 32 |
| **Pb208** | 4.137 | 4 | 33.832 | 4 | 9.217 | 4 | 3.755 | 4 | 12.764 | 3 | 16.610 | 3 | 0.668 | 7 | 5.192 | 27 | 3.216 | 6 | 2.481 | 5 |
| **Bi209** | 26.813 | 4 | 2.366 | 4 | 0.739 | 4 | 0.508 | 4 | 0.914 | 4 | 0.980 | 4 | 0.077 | 11 | 0.218 | 10 | 0.148 | 7 | 0.202 | 6 |
| **Th232** | 0.237 | 31 | 0.152 | 43 | <0.009 | | 0.007 | 63 | <0.008 | | <0.008 | | <0.006 | | 0.016 | 44 | 0.007 | 38 | 0.012 | 28 |
| **U238** | <0.013 | | <0.007 | | <0.005 | | 0.014 | 50 | <0.008 | | <0.004 | | <0.006 | | <0.006 | | <0.006 | | <0.009 | |

**Table A9.1.** *Continued.*

| SAMPLE | DD96 11 cpy | | GG19 09 cpy | | GG19 10 cpy | | GG19 11 cpy | | K7 08 cpy | | K7 09 cpy | | K7 10 cpy | | K7 11 cpy | | K7 12 cpy | | K7 13 cpy | |
|---|---|---|---|---|---|---|---|---|---|---|---|---|---|---|---|---|---|---|---|---|
| **Ti49** | 8.706 | 7 | 8.412 | 10 | 13.880 | 8 | 9.299 | 6 | 10.388 | 6 | 8.968 | 6 | 10.324 | 6 | 8.871 | 7 | 16.302 | 15 | 8.695 | 6 |
| **Cr53** | <0.44 | | 0.576 | 34 | <0.499 | | <0.542 | | 0.452 | 26 | <0.449 | | <0.547 | | <0.428 | | <0.538 | | 0.343 | 33 |
| **Mn55** | 0.866 | 15 | 0.710 | 23 | 0.863 | 17 | 0.550 | 27 | 3.085 | 23 | 0.453 | 31 | 0.919 | 16 | 1.408 | 22 | 2.631 | 12 | <0.369 | |
| **Fe57** | 304300 | | 304300 | | 304300 | | 304300 | | 304300 | | 304300 | | 304300 | | 304300 | | 304300 | | 304300 | |
| **Co59** | 2.242 | 4 | 4.086 | 5 | 3.562 | 4 | 3.597 | 4 | 1.243 | 8 | 0.648 | 13 | 0.218 | 11 | 0.274 | 11 | 0.268 | 9 | 0.030 | 32 |
| **Ni60** | 7.913 | 5 | <0.099 | | 0.163 | 73 | <0.133 | | <0.091 | | <0.065 | | <0.113 | | <0.113 | | 0.162 | 36 | 0.076 | 45 |
| **Cu65** | 342243 | 4 | 379561 | 5 | 362597 | 4 | 356687 | 4 | 357299 | 4 | 351639 | 4 | 360604 | 4 | 358689 | 5 | 362409 | 4 | 347214 | 4 |
| **Zn66** | 575.027 | 6 | 165.525 | 4 | 165.097 | 4 | 153.947 | 3 | 190.326 | 6 | 161.680 | 4 | 184.020 | 4 | 167.391 | 6 | 150.599 | 5 | 150.590 | 6 |
| **As75** | 2.187 | 10 | 2.531 | 12 | 2.480 | 10 | 2.270 | 11 | 2.653 | 9 | 2.866 | 9 | 3.016 | 9 | 2.446 | 10 | 2.665 | 9 | 2.722 | 9 |
| **Se77** | 64.508 | 5 | 36.564 | 9 | 36.025 | 5 | 38.932 | 5 | 117.979 | 4 | 111.704 | 4 | 125.355 | 4 | 105.092 | 4 | 104.923 | 4 | 86.699 | 4 |
| **Zr90** | <0.011 | | <0.017 | | <0.009 | | <0.011 | | 0.015 | 43 | <0.014 | | <0.013 | | <0.012 | | 0.203 | 27 | <0.01 | |
| **Mo95** | <0.322 | | <0.359 | | 0.375 | 49 | <0.353 | | <0.329 | | <0.34 | | <0.283 | | <0.375 | | <0.413 | | <0.321 | |
| **Ag107** | 75.072 | 4 | 11.064 | 5 | 7.851 | 4 | 4.383 | 4 | 0.102 | 25 | 0.178 | 14 | 0.176 | 21 | 0.301 | 12 | 0.474 | 10 | 0.147 | 14 |
| **Cd111** | 4.252 | 9 | 2.024 | 17 | 1.525 | 18 | 1.759 | 15 | 6.983 | 8 | 5.323 | 8 | 5.157 | 10 | 4.580 | 9 | 5.199 | 9 | 4.372 | 9 |
| **Sn118** | 1.885 | 5 | 8.210 | 5 | 10.217 | 4 | 5.123 | 4 | 7.213 | 5 | 8.275 | 4 | 5.122 | 4 | 4.808 | 5 | 5.375 | 5 | 4.019 | 5 |
| **Sb121** | <0.1 | | <0.14 | | 0.090 | 38 | <0.096 | | 0.771 | 8 | 0.336 | 9 | 0.853 | 7 | 1.158 | 7 | 2.200 | 5 | 0.918 | 6 |
| **Te125** | 6.118 | 8 | <0.785 | | 0.737 | 26 | <0.486 | | 1.463 | 32 | 4.810 | 12 | 0.968 | 26 | 0.744 | 31 | 1.017 | 26 | <0.462 | |
| **Ba137** | <0.038 | | <0.083 | | 1.187 | 18 | 0.060 | 34 | 0.222 | 20 | <0.081 | | <0.071 | | 0.506 | 32 | 4.773 | 11 | 0.111 | 42 |
| **La139** | <0.005 | | 0.045 | 16 | 0.553 | 95 | <0.007 | | <0.006 | | <0.004 | | <0.007 | | <0.009 | | <0.008 | | <0.005 | |
| **W182** | <0.031 | | <0.032 | | <0.032 | | <0.034 | | <0.039 | | <0.032 | | <0.058 | | 0.021 | 38 | 0.062 | 86 | <0.039 | |
| **Au197** | <0.025 | | 0.109 | 18 | <0.029 | | 0.019 | 39 | <0.028 | | 0.054 | 21 | <0.031 | | <0.026 | | 0.027 | 41 | <0.039 | |
| **Tl205** | 1.024 | 7 | 0.080 | 24 | 0.102 | 13 | 0.210 | 13 | <0.014 | | <0.012 | | 0.196 | 11 | 0.203 | 12 | 1.125 | 6 | 0.043 | 36 |
| **Pb208** | 6.154 | 4 | 3.032 | 5 | 6.402 | 5 | 1.304 | 4 | 5.233 | 6 | 1.483 | 5 | 2.821 | 4 | 4.953 | 5 | 10.498 | 5 | 3.975 | 4 |
| **Bi209** | 0.264 | 6 | 1.670 | 5 | 2.878 | 5 | 0.445 | 5 | 5.252 | 14 | 6.980 | 7 | 2.478 | 4 | 4.493 | 6 | 7.442 | 4 | 2.646 | 4 |
| **Th232** | <0.005 | | <0.006 | | <0.007 | | <0.008 | | <0.007 | | 0.033 | 61 | <0.008 | | <0.008 | | 0.036 | 34 | <0.007 | |
| **U238** | <0.007 | | 0.017 | 26 | <0.009 | | <0.007 | | <0.009 | | <0.008 | | <0.008 | | <0.009 | | 0.011 | 44 | <0.004 | |

| SAMPLE | K9 07 cpy | | K9 08 cpy | | K9 09 cpy | | K9 10 cpy | | K9 11 cpy | | BN1 06 cpy | | BN1 07 cpy | | BN1 08 cpy | | BN1 09 cpy | | BN5 07 cpy | |
|---|---|---|---|---|---|---|---|---|---|---|---|---|---|---|---|---|---|---|---|---|
| **Ti49** | 8.031 | 7 | 8.030 | 7 | 6.247 | 18 | 7.564 | 13 | 5.904 | 16 | 10.110 | 6 | 9.992 | 6 | 9.419 | 7 | 8.416 | 7 | 40.462 | 14 |
| **Cr53** | <0.411 | | <0.389 | | <1.74 | | <1.6 | | <1.709 | | <0.468 | | <0.442 | | <0.474 | | <0.417 | | 2.076 | 17 |
| **Mn55** | 53.770 | 18 | 1.060 | 14 | 2.185 | 24 | <1.268 | | <1.226 | | 0.902 | 18 | 57.283 | 15 | <0.33 | | 1.111 | 11 | 1.158 | 16 |
| **Fe57** | 304300 | | 304300 | | 304300 | | 304300 | | 304300 | | 304300 | | 304300 | | 304300 | | 304300 | | 304300 | |
| **Co59** | 0.393 | 16 | 1.071 | 25 | 0.424 | 19 | 781.109 | 15 | 0.755 | 52 | 1.510 | 19 | 0.062 | 22 | 0.035 | 24 | 0.024 | 34 | 2.662 | 44 |
| **Ni60** | 8.424 | 13 | 3.093 | 16 | 1.699 | 23 | 26.705 | 16 | 0.531 | 31 | 5.905 | 19 | <0.123 | | <0.126 | | <0.102 | | 1.215 | 14 |
| **Cu65** | 357892 | 4 | 345885 | 4 | 352802 | 4 | 327268 | 4 | 357118 | 4 | 343607 | 4 | 349860 | 4 | 352293 | 4 | 347473 | 4 | 370825 | 4 |
| **Zn66** | 264.699 | 5 | 285.822 | 4 | 198.931 | 3 | 515.409 | 10 | 182.638 | 3 | 65.682 | 7 | 58.791 | 5 | 57.650 | 4 | 64.296 | 4 | 25.599 | 4 |
| **As75** | 5.085 | 19 | 4.147 | 20 | 3.081 | 22 | 80.600 | 12 | 3.774 | 30 | 4.331 | 7 | 3.572 | 8 | 2.675 | 10 | 2.730 | 9 | 4.392 | 11 |
| **Se77** | 51.587 | 4 | 48.473 | 4 | 53.720 | 5 | 68.042 | 5 | 41.376 | 7 | 87.412 | 6 | 152.268 | 4 | 244.733 | 4 | 121.590 | 4 | 113.139 | 4 |
| **Zr90** | <0.018 | | <0.014 | | <0.043 | | <0.056 | | <0.041 | | <0.011 | | <0.016 | | <0.017 | | <0.011 | | 16.780 | 33 |
| **Mo95** | <0.416 | | <0.358 | | <1.511 | | 0.645 | 73 | <1.407 | | <0.377 | | <0.346 | | <0.48 | | <0.337 | | <0.416 | |
| **Ag107** | 14.231 | 4 | 13.195 | 4 | 20.282 | 3 | 9.071 | 4 | 21.258 | 3 | 6.349 | 17 | 2.303 | 5 | 1.090 | 6 | 1.059 | 7 | 0.659 | 9 |
| **Cd111** | 4.213 | 10 | 4.160 | 10 | <6.088 | | 4.854 | 23 | 4.677 | 25 | 5.433 | 8 | 5.089 | 9 | 4.556 | 11 | 3.230 | 12 | 2.192 | 19 |
| **Sn118** | 8.423 | 4 | 7.052 | 4 | 8.326 | 4 | 8.707 | 5 | 24.265 | 3 | 48.032 | 17 | 24.562 | 18 | 24.280 | 16 | 35.090 | 20 | 2.700 | 9 |
| **Sb121** | 1.087 | 7 | 1.310 | 8 | 1.823 | 8 | 3.333 | 7 | 1.479 | 11 | 1.566 | 7 | 1.113 | 7 | 0.168 | 28 | 0.149 | 29 | 2.363 | 16 |
| **Te125** | <0.651 | | <0.698 | | <2.201 | | <2.195 | | <2.255 | | 14.275 | 31 | 2.139 | 15 | <0.674 | | <0.688 | | <0.591 | |
| **Ba137** | 1.001 | 23 | <0.074 | | 0.213 | 46 | <0.188 | | <0.221 | | 0.805 | 11 | 0.085 | 34 | <0.083 | | 0.048 | 42 | 5.117 | 13 |
| **La139** | 0.105 | 20 | 1.132 | 28 | <0.019 | | <0.023 | | <0.028 | | <0.006 | | 0.075 | 28 | <0.009 | | <0.01 | | 0.019 | 74 |
| **W182** | <0.051 | | <0.031 | | <0.148 | | <0.117 | | <0.143 | | <0.023 | | <0.05 | | <0.028 | | <0.044 | | <0.04 | |
| **Au197** | <0.033 | | <0.029 | | <0.103 | | <0.082 | | <0.124 | | 0.041 | 34 | <0.04 | | <0.046 | | <0.039 | | <0.03 | |
| **Tl205** | 0.055 | 23 | 0.788 | 11 | 0.223 | 21 | 0.358 | 17 | 1.059 | 8 | 0.256 | 10 | 0.137 | 13 | <0.009 | | <0.009 | | 0.104 | 18 |
| **Pb208** | 2.679 | 4 | 6.339 | 8 | 5.213 | 5 | 58.219 | 33 | 13.445 | 12 | 205.912 | 28 | 90.699 | 13 | 44.753 | 13 | 2.722 | 5 | 2.693 | 13 |
| **Bi209** | 0.412 | 5 | 0.808 | 8 | 0.371 | 9 | 1.776 | 13 | 0.426 | 8 | 25.579 | 15 | 11.995 | 4 | 1.864 | 7 | 1.969 | 5 | 1.091 | 9 |
| **Th232** | <0.014 | | <0.007 | | 0.097 | 25 | 0.076 | 35 | <0.023 | | <0.009 | | <0.011 | | 0.117 | 25 | 0.005 | 38 | 0.023 | 33 |
| **U238** | <0.008 | | <0.006 | | <0.015 | | <0.015 | | 0.026 | 36 | <0.01 | | <0.008 | | <0.006 | | <0.008 | | 0.214 | 32 |

**Table A9.1.** *Continued.*

| SAMPLE | BN5 08 cpy | | BN5 09 cpy | | BN5 10 cpy | | BN5 11 cpy | | BN600 06 cpy | | BN600 07 cpy | | BN600 08 cpy | | BN600 09 cpy | | BN600 10 cpy | | WA1 01 cpy | |
|---|---|---|---|---|---|---|---|---|---|---|---|---|---|---|---|---|---|---|---|---|
| **Ti49** | 7.436 | 7 | 6.815 | 7 | 6.519 | 7 | 6.061 | 8 | 9.565 | 8 | 9.985 | 7 | 9.468 | 7 | 8.474 | 7 | 10.170 | 6 | 9.291 | 6 |
| **Cr53** | 0.356 | 37 | <0.381 | | 0.334 | 39 | <0.387 | | <0.529 | | <0.493 | | <0.396 | | <0.472 | | 0.362 | 37 | <0.65 | |
| **Mn55** | 0.521 | 30 | <0.384 | | 4.153 | 8 | 0.529 | 28 | 0.671 | 26 | 3.198 | 24 | 131.949 | 16 | <0.354 | | 11.495 | 28 | <0.408 | |
| **Fe57** | 304300 | | 304300 | | 304300 | | 304300 | | 304300 | | 304300 | | 304300 | | 304300 | | 304300 | | 304300 | |
| **Co59** | 1.246 | 19 | 0.036 | 23 | 0.432 | 15 | 0.261 | 28 | 20.838 | 23 | 0.071 | 90 | 0.039 | 74 | <0.016 | | <0.023 | | 1.755 | 4 |
| **Ni60** | 0.158 | 47 | <0.1 | | 0.123 | 78 | <0.11 | | 0.262 | 23 | <0.107 | | <0.13 | | <0.114 | | <0.116 | | <0.06 | |
| **Cu65** | 345008 | 5 | 357369 | 4 | 354618 | 4 | 343520 | 4 | 370475 | 4 | 379673 | 5 | 366152 | 4 | 347914 | 4 | 357394 | 4 | 408957 | 5 |
| **Zn66** | 27.031 | 5 | 24.870 | 4 | 29.695 | 4 | 25.690 | 4 | 55.642 | 5 | 69.585 | 11 | 46.540 | 4 | 52.745 | 4 | 51.532 | 4 | 114.017 | 8 |
| **As75** | 2.927 | 9 | 2.220 | 11 | 2.184 | 10 | 2.178 | 10 | 7.415 | 10 | 3.353 | 9 | 3.080 | 9 | 3.233 | 9 | 3.364 | 8 | 2.485 | 10 |
| **Se77** | 116.756 | 5 | 109.271 | 4 | 97.777 | 4 | 122.959 | 4 | 71.117 | 5 | 68.775 | 5 | 70.318 | 4 | 72.160 | 4 | 75.827 | 4 | 98.023 | 4 |
| **Zr90** | 0.014 | 34 | <0.012 | | <0.009 | | <0.015 | | <0.014 | | <0.016 | | <0.01 | | 0.001 | 751 | <0.017 | | <0.009 | |
| **Mo95** | <0.43 | | <0.339 | | <0.385 | | <0.387 | | <0.359 | | <0.324 | | <0.328 | | <0.29 | | <0.281 | | <0.246 | |
| **Ag107** | 7.202 | 5 | 6.391 | 4 | 6.837 | 4 | 5.578 | 4 | 37.417 | 16 | 14.885 | 4 | 50.676 | 4 | 8.602 | 5 | 237.366 | 25 | 3.679 | 5 |
| **Cd111** | 2.211 | 17 | 1.263 | 28 | 2.032 | 17 | 2.367 | 14 | 1.642 | 17 | 1.352 | 23 | 0.936 | 28 | 1.346 | 18 | 1.368 | 17 | 3.060 | 10 |
| **Sn118** | 4.041 | 5 | 9.039 | 4 | 4.820 | 5 | 4.264 | 4 | 5.854 | 5 | 5.467 | 7 | 8.663 | 4 | 8.691 | 4 | 5.616 | 5 | 9.211 | 4 |
| **Sb121** | 0.381 | 11 | 0.107 | 30 | 0.292 | 14 | 0.138 | 23 | 6.962 | 4 | 1.939 | 5 | 1.390 | 5 | 1.215 | 6 | 1.888 | 6 | 0.757 | 7 |
| **Te125** | 1.131 | 29 | 0.844 | 31 | 1.006 | 30 | 0.716 | 37 | 2.886 | 15 | 2.713 | 13 | 1.221 | 24 | 1.655 | 18 | 142.193 | 26 | 1.487 | 17 |
| **Ba137** | 0.061 | 39 | <0.069 | | 0.644 | 12 | <0.055 | | 0.078 | 37 | 0.656 | 16 | 0.136 | 29 | <0.056 | | 0.693 | 13 | <0.062 | |
| **La139** | 0.034 | 86 | <0.009 | | <0.005 | | <0.005 | | <0.009 | | <0.004 | | <0.006 | | <0.008 | | <0.005 | | <0.005 | |
| **W182** | <0.03 | | <0.033 | | <0.04 | | <0.036 | | <0.055 | | <0.037 | | <0.017 | | <0.027 | | <0.029 | | <0.024 | |
| **Au197** | <0.023 | | <0.028 | | 0.068 | 17 | <0.027 | | 12.743 | 41 | 0.099 | 17 | 0.051 | 21 | 0.058 | 16 | 0.277 | 9 | 0.044 | 24 |
| **Tl205** | <0.009 | | <0.011 | | 0.062 | 21 | <0.008 | | 0.620 | 6 | 0.280 | 8 | 0.137 | 11 | 0.045 | 28 | 0.218 | 9 | 0.536 | 7 |
| **Pb208** | 4.847 | 6 | 1.236 | 4 | 15.904 | 8 | 3.091 | 14 | 62.704 | 5 | 42.435 | 4 | 15.072 | 4 | 11.343 | 5 | 9.703 | 6 | 9.091 | 5 |
| **Bi209** | 4.163 | 5 | 1.348 | 6 | 3.267 | 5 | 1.175 | 4 | 35.084 | 4 | 20.209 | 4 | 10.451 | 4 | 7.274 | 5 | 6.033 | 5 | 2.769 | 4 |
| **Th232** | 0.149 | 31 | <0.008 | | 0.204 | 21 | <0.008 | | 0.035 | 46 | 0.038 | 49 | <0.005 | | 0.117 | 22 | 0.041 | 56 | 0.248 | 26 |
| **U238** | <0.008 | | <0.009 | | <0.008 | | <0.006 | | 0.235 | 56 | <0.009 | | <0.006 | | <0.006 | | 0.007 | 24 | 0.037 | 13 |

| SAMPLE | WA9 09 cpy | | WA9 10 cpy | | WA9 11 cpy | | WA9 12 cpy | | WA1 02 cpy | | WA1 06 cpy | | WA1 07 cpy | | WA1 08 cpy | | WA8 07 cpy | | WA8 08 cpy | |
|---|---|---|---|---|---|---|---|---|---|---|---|---|---|---|---|---|---|---|---|---|
| **Ti49** | 6.103 | 8 | 6.634 | 8 | 6.213 | 7 | 6.315 | 8 | 9.473 | 6 | 10.353 | 6 | 10.031 | 6 | 10.843 | 6 | 8.209 | 6 | 8.162 | 6 |
| **Cr53** | <0.438 | | <0.441 | | <0.385 | | <0.396 | | <0.507 | | <0.419 | | 0.358 | 41 | <0.475 | | <0.399 | | <0.518 | |
| **Mn55** | 0.418 | 38 | <0.454 | | <0.38 | | <0.372 | | <0.417 | | 0.518 | 25 | 0.822 | 40 | <0.348 | | <0.4 | | 0.653 | 24 |
| **Fe57** | 304300 | | 304300 | | 304300 | | 304300 | | 304300 | | 304300 | | 304300 | | 304300 | | 304300 | | 304300 | |
| **Co59** | 0.552 | 5 | 17.829 | 21 | 0.621 | 5 | 0.542 | 8 | 2.415 | 4 | 41.560 | 12 | 1.407 | 5 | 0.797 | 5 | 0.268 | 7 | 0.262 | 7 |
| **Ni60** | <0.127 | | <0.13 | | <0.125 | | <0.116 | | <0.088 | | 0.146 | 23 | 0.723 | 16 | 0.136 | 70 | <0.095 | | <0.092 | |
| **Cu65** | 379021 | 5 | 363125 | 5 | 345462 | 4 | 367646 | 7 | 373699 | 4 | 348734 | 4 | 334026 | 5 | 345876 | 4 | 352512 | 4 | 355978 | 4 |
| **Zn66** | 42.920 | 6 | 32.116 | 4 | 47.963 | 7 | 27.471 | 4 | 97.901 | 4 | 72.137 | 5 | 89.525 | 7 | 64.305 | 9 | 68.357 | 4 | 96.030 | 5 |
| **As75** | 2.032 | 12 | 3.811 | 37 | 1.907 | 13 | 2.263 | 11 | 2.276 | 11 | 5.931 | 11 | 2.166 | 11 | 1.787 | 14 | 3.128 | 8 | 3.029 | 9 |
| **Se77** | 73.239 | 4 | 72.171 | 4 | 68.905 | 4 | 56.720 | 5 | 110.982 | 4 | 115.171 | 4 | 111.137 | 5 | 132.264 | 4 | 120.273 | 4 | 131.278 | 4 |
| **Zr90** | <0.019 | | 0.010 | 50 | <0.018 | | 0.067 | 42 | <0.013 | | 0.018 | 43 | <0.015 | | <0.012 | | <0.01 | | <0.013 | |
| **Mo95** | <0.338 | | <0.418 | | <0.534 | | 6542.749 | 27 | <0.359 | | <0.263 | | <0.357 | | <0.308 | | <0.29 | | <0.383 | |
| **Ag107** | 10.306 | 4 | 10.625 | 4 | 9.199 | 4 | 13.944 | 5 | 2.252 | 5 | 2.206 | 5 | 3.399 | 5 | 4.200 | 4 | 6.314 | 4 | 7.435 | 4 |
| **Cd111** | 2.554 | 18 | 1.969 | 21 | 3.233 | 11 | 4.242 | 16 | 1.512 | 17 | 1.521 | 15 | 1.520 | 18 | 1.511 | 16 | 2.779 | 13 | 2.762 | 15 |
| **Sn118** | 7.281 | 4 | 5.391 | 5 | 5.835 | 4 | 2.211 | 6 | 9.758 | 4 | 7.520 | 4 | 8.119 | 5 | 7.036 | 4 | 17.610 | 4 | 19.112 | 4 |
| **Sb121** | 0.516 | 9 | 0.619 | 8 | 0.327 | 14 | 0.620 | 10 | 0.270 | 13 | 0.438 | 9 | 0.654 | 8 | 0.685 | 8 | 0.183 | 21 | 0.149 | 24 |
| **Te125** | 0.850 | 35 | 2.106 | 20 | <0.911 | | 3.973 | 23 | 1.864 | 15 | 1.164 | 17 | 1.237 | 21 | 1.249 | 24 | <0.702 | | 2.774 | 13 |
| **Ba137** | <0.058 | | <0.064 | | <0.043 | | 0.112 | 30 | <0.044 | | <0.044 | | <0.06 | | <0.049 | | <0.062 | | 0.128 | 26 |
| **La139** | <0.01 | | <0.008 | | <0.006 | | <0.009 | | <0.008 | | <0.006 | | <0.006 | | 0.174 | 8 | <0.008 | | <0.007 | |
| **W182** | <0.031 | | <0.042 | | <0.041 | | 0.123 | 31 | <0.029 | | 0.065 | 106 | <0.023 | | <0.045 | | <0.027 | | <0.049 | |
| **Au197** | <0.025 | | 0.196 | 10 | <0.029 | | <0.027 | | 0.022 | 39 | 0.047 | 25 | 0.022 | 27 | 0.077 | 17 | 0.020 | 43 | <0.028 | |
| **Tl205** | 0.391 | 8 | 0.061 | 25 | 0.063 | 22 | 0.338 | 19 | <0.009 | | 0.366 | 9 | 0.166 | 12 | 0.878 | 7 | 0.045 | 40 | <0.015 | |
| **Pb208** | 4.196 | 4 | 2.299 | 5 | 2.780 | 11 | 8.509 | 15 | 3.212 | 4 | 4.158 | 5 | 6.235 | 5 | 7.600 | 4 | 0.674 | 11 | 0.948 | 9 |
| **Bi209** | 2.712 | 4 | 3.778 | 4 | 2.699 | 8 | 9.839 | 9 | 1.383 | 4 | 1.549 | 4 | 2.847 | 6 | 2.681 | 4 | 0.632 | 5 | 1.267 | 9 |
| **Th232** | 0.577 | 17 | <0.008 | | 0.035 | 24 | <0.008 | | <0.007 | | 0.019 | 34 | 0.014 | 31 | 0.519 | 27 | <0.007 | | 0.189 | 23 |
| **U238** | <0.009 | | <0.009 | | <0.007 | | <0.008 | | <0.008 | | 0.092 | 21 | <0.007 | | 1.472 | 49 | <0.008 | | <0.01 | |

**Table A9.1.** *Continued.*

| SAMPLE | WA8 09 cpy | | WA8 10 cpy | | WA8 11 cpy | | WA9 07 cpy | | WA9 08 cpy | |
|---|---|---|---|---|---|---|---|---|---|---|
| **Ti49** | 7.564 | 9 | 9.158 | 6 | 8.680 | 8 | 6.414 | 8 | 6.454 | 7 |
| **Cr53** | <0.485 | | 0.438 | 65 | 0.348 | 40 | <0.408 | | <0.316 | |
| **Mn55** | 0.411 | 38 | 0.745 | 22 | <0.526 | | <0.408 | | <0.351 | |
| **Fe57** | 304300 | | 304300 | | 304300 | | 304300 | | 304300 | |
| **Co59** | 0.247 | 10 | 1.779 | 18 | 0.361 | 10 | 0.733 | 7 | 0.651 | 5 |
| **Ni60** | <0.103 | | 0.522 | 19 | <0.11 | | <0.104 | | <0.118 | |
| **Cu65** | 334472 | 5 | 345806 | 4 | 371403 | 5 | 343158 | 5 | 346510 | 4 |
| **Zn66** | 41.678 | 8 | 37.328 | 5 | 34.973 | 6 | 40.564 | 5 | 38.443 | 4 |
| **As75** | 2.607 | 10 | 3.286 | 8 | 2.924 | 12 | 1.517 | 14 | 2.326 | 22 |
| **Se77** | 110.596 | 5 | 109.816 | 4 | 125.929 | 5 | 63.867 | 5 | 65.537 | 4 |
| **Zr90** | <0.014 | | 0.058 | 32 | 0.110 | 49 | <0.018 | | <0.011 | |
| **Mo95** | <0.341 | | <0.429 | | <0.35 | | <0.402 | | <0.377 | |
| **Ag107** | 8.752 | 5 | 6.243 | 4 | 8.495 | 5 | 7.437 | 4 | 7.587 | 4 |
| **Cd111** | 2.602 | 15 | 1.892 | 20 | 3.453 | 13 | 1.797 | 20 | 2.402 | 17 |
| **Sn118** | 15.403 | 6 | 15.475 | 5 | 16.070 | 5 | 5.408 | 5 | 5.425 | 4 |
| **Sb121** | 0.199 | 19 | 0.870 | 13 | 0.366 | 14 | 0.538 | 8 | 0.237 | 13 |
| **Te125** | 0.789 | 39 | 0.605 | 45 | 1.211 | 28 | 0.995 | 28 | 1.388 | 20 |
| **Ba137** | 0.364 | 24 | 0.735 | 18 | <0.052 | | <0.068 | | <0.059 | |
| **La139** | <0.008 | | <0.006 | | 0.425 | 42 | <0.006 | | <0.004 | |
| **W182** | <0.029 | | <0.033 | | <0.042 | | <0.026 | | <0.025 | |
| **Au197** | 0.036 | 38 | <0.037 | | <0.043 | | <0.032 | | <0.023 | |
| **Tl205** | 0.039 | 33 | <0.013 | | 0.086 | 26 | 0.534 | 9 | <0.008 | |
| **Pb208** | 1.394 | 11 | 1.925 | 11 | 5.137 | 11 | 1.135 | 5 | 1.284 | 4 |
| **Bi209** | 1.125 | 7 | 0.870 | 7 | 2.740 | 6 | 1.059 | 5 | 1.171 | 4 |
| **Th232** | <0.009 | | <0.009 | | 0.010 | 51 | 0.006 | 32 | <0.007 | |
| **U238** | <0.006 | | <0.011 | | 0.024 | 27 | <0.007 | | <0.007 | |

**Table A9.2.** Pyrite.

| SAMPLE | DD96 01 py | | DD96 02 py | | DD96 03 py | | DD96 04 py | | DD96 05 py | | DD96 06 py | | GG19 01 py | | GG19 02 py | | GG19 03 py | | GG19 04 py | |
|---|---|---|---|---|---|---|---|---|---|---|---|---|---|---|---|---|---|---|---|---|
| **Ti49** | 8.532 | 7 | 10.628 | 6 | 11.863 | 6 | 12.017 | 5 | 12.018 | 6 | 11.839 | 5 | 9.794 | 4 | 9.747 | 4 | 8.936 | 5 | 10.086 | 6 |
| **Cr53** | 2.657 | 32 | <0.277 | | 0.272 | 27 | 0.254 | 53 | 0.178 | 29 | 0.245 | 31 | 0.218 | 31 | 0.236 | 20 | 0.210 | 27 | 0.398 | 37 |
| **Mn55** | 0.855 | 23 | 0.346 | 16 | 0.363 | 18 | 1.285 | 22 | 2.623 | 15 | 0.296 | 24 | 0.543 | 11 | 0.538 | 9 | 0.402 | 13 | 0.388 | 18 |
| **Fe57** | 465500 | | 465500 | | 465500 | | 465500 | | 465500 | | 465500 | | 465500 | | 465500 | | 465500 | | 465500 | |
| **Co59** | 6957.432 | 6 | 9113.476 | 7 | 13529.170 | 6 | 6305.188 | 5 | 7020.240 | 6 | 4430.781 | 8 | 1473.554 | 3 | 557.339 | 4 | 667.143 | 4 | 398.184 | 5 |
| **Ni60** | 5.745 | 9 | 9.955 | 6 | 24.251 | 5 | 3.920 | 5 | 5.028 | 6 | 30.913 | 4 | 1033.552 | 3 | 623.558 | 4 | 705.705 | 4 | 346.659 | 5 |
| **Cu65** | <0.184 | | <0.236 | | 4.654 | 97 | 0.331 | 28 | 0.457 | 21 | 0.291 | 43 | <0.226 | | 3.970 | 5 | 3.155 | 9 | 0.406 | 22 |
| **Zn66** | 0.622 | 11 | 0.728 | 9 | 1.039 | 9 | 1.332 | 11 | 1.713 | 8 | 2.142 | 22 | 1.102 | 6 | 1.056 | 9 | 0.861 | 7 | 1.072 | 10 |
| **As75** | 24.974 | 7 | 56.596 | 10 | 169.665 | 6 | 17.476 | 5 | 33.061 | 5 | 11.784 | 5 | 11.069 | 4 | 11.462 | 4 | 1.351 | 8 | 2.141 | 7 |
| **Se77** | 20.401 | 8 | 27.107 | 6 | 27.543 | 6 | 32.487 | 5 | 25.579 | 6 | 30.951 | 5 | 64.258 | 4 | 40.991 | 4 | 53.199 | 4 | 56.279 | 6 |
| **Zr90** | <0.004 | | <0.005 | | <0.006 | | <0.006 | | <0.003 | | <0.007 | | <0.004 | | <0.003 | | <0.005 | | <0.005 | |
| **Mo95** | 0.383 | 64 | <0.126 | | 0.113 | 64 | <0.153 | | <0.11 | | 0.172 | 34 | 0.522 | 13 | 0.573 | 11 | 0.681 | 8 | 0.862 | 9 |
| **Ag107** | <0.018 | | <0.024 | | <0.024 | | 0.037 | 35 | 0.129 | 35 | <0.021 | | 0.055 | 18 | 0.160 | 9 | 0.107 | 11 | 0.276 | 9 |
| **Cd111** | <0.47 | | <0.453 | | <0.497 | | <0.511 | | <0.408 | | <0.551 | | <0.526 | | <0.353 | | <0.409 | | <0.523 | |
| **Sn118** | 0.165 | 13 | 0.185 | 10 | 0.286 | 9 | 0.264 | 12 | 0.254 | 9 | 0.303 | 12 | 0.213 | 8 | 0.385 | 8 | 0.184 | 9 | 0.237 | 9 |
| **Sb121** | 0.080 | 22 | <0.058 | | <0.065 | | 0.076 | 29 | 0.045 | 32 | <0.054 | | 0.060 | 26 | <0.037 | | <0.04 | | 0.040 | 39 |
| **Te125** | <0.243 | | <0.215 | | <0.262 | | 2.660 | 23 | 0.420 | 22 | <0.289 | | <0.144 | | <0.136 | | <0.168 | | <0.214 | |
| **Ba137** | <0.02 | | <0.021 | | <0.021 | | 0.360 | 26 | 1.910 | 23 | <0.027 | | <0.028 | | 0.017 | 45 | <0.016 | | <0.02 | |
| **La139** | <0.002 | | <0.002 | | <0.003 | | <0.003 | | <0.002 | | <0.002 | | 0.035 | 9 | 0.026 | 9 | 0.013 | 14 | 0.004 | 32 |
| **W182** | <0.01 | | <0.014 | | <0.015 | | 0.010 | 108 | <0.008 | | <0.012 | | 6.589 | 4 | 2.895 | 5 | 1.345 | 4 | 0.676 | 6 |
| **Au197** | <0.015 | | <0.014 | | <0.01 | | 0.008 | 33 | <0.008 | | <0.011 | | 0.010 | 35 | <0.009 | | <0.011 | | <0.018 | |
| **Tl205** | <0.005 | | 0.005 | 39 | <0.003 | | 0.019 | 26 | 0.018 | 25 | <0.006 | | 0.072 | 9 | 0.224 | 6 | 0.020 | 17 | 0.014 | 33 |
| **Pb208** | 0.177 | 27 | 0.017 | 24 | 0.094 | 15 | 6.209 | 21 | 3.654 | 13 | 0.160 | 23 | 4.538 | 3 | 2.882 | 4 | 0.281 | 5 | 0.627 | 10 |
| **Bi209** | 0.048 | 28 | <0.006 | | <0.004 | | 0.260 | 19 | 0.905 | 14 | 0.006 | 36 | 0.046 | 8 | 0.102 | 6 | 0.197 | 10 | 0.414 | 16 |
| **Th232** | 0.002 | 57 | <0.003 | | 0.010 | 33 | 0.021 | 23 | 0.004 | 36 | 0.183 | 32 | 0.061 | 7 | 0.099 | 5 | 0.033 | 9 | 0.044 | 21 |
| **U238** | 0.001 | 51 | <0.004 | | 0.005 | 110 | 0.015 | 97 | 0.026 | 102 | 0.018 | 92 | 0.021 | 9 | 0.042 | 7 | 0.067 | 7 | 0.031 | 10 |

| SAMPLE | BN1 01 py | | BN1 02 py | | BN1 03 py | | BN1 04 py | | BN1 05 py | | BN5 01 py | | BN5 02 py | | BN5 03 py | | BN5 04 py | | BN5 05 py | |
|---|---|---|---|---|---|---|---|---|---|---|---|---|---|---|---|---|---|---|---|---|
| **Ti49** | 9.431 | 6 | 9.979 | 6 | 10.411 | 6 | 8.985 | 6 | 9.315 | 6 | 9.260 | 8 | 5.038 | 18 | 6.613 | 15 | 7.142 | 9 | 8.089 | 5 |
| **Cr53** | <0.282 | | 0.162 | 41 | 0.174 | 29 | <0.209 | | 0.194 | 38 | <0.698 | | <0.626 | | <0.541 | | <0.722 | | <0.245 | |
| **Mn55** | 0.463 | 12 | 0.226 | 29 | 0.360 | 16 | 0.582 | 12 | 0.502 | 17 | 0.576 | 29 | 0.520 | 57 | 0.910 | 24 | 0.625 | 34 | 0.261 | 25 |
| **Fe57** | 465500 | | 465500 | | 465500 | | 465500 | | 465500 | | 465500 | | 465500 | | 465500 | | 465500 | | 465500 | |
| **Co59** | 1628.504 | 5 | 579.494 | 6 | 2797.029 | 8 | 429.604 | 11 | 323.745 | 5 | 4743.285 | 5 | 3782.317 | 12 | 4180.965 | 13 | 0.321 | 38 | 11212.599 | 6 |
| **Ni60** | 230.641 | 5 | 1139.563 | 5 | 672.781 | 5 | 761.284 | 5 | 1193.494 | 6 | 663.953 | 5 | 733.892 | 12 | 533.051 | 14 | 0.686 | 18 | 71.120 | 4 |
| **Cu65** | 698.333 | 9 | <0.234 | | 0.834 | 15 | 3726.206 | 19 | 9.457 | 25 | 43.471 | 24 | 6.914 | 37 | 95.155 | 25 | 887.736 | 6 | 0.265 | 37 |
| **Zn66** | 0.744 | 8 | 0.966 | 8 | 0.672 | 10 | 1.255 | 19 | 0.449 | 14 | 1.597 | 21 | 2.607 | 58 | 0.710 | 31 | 11.082 | 7 | 0.506 | 9 |
| **As75** | 26.620 | 5 | 9.564 | 7 | 46.782 | 6 | 28.146 | 6 | 4.929 | 7 | 211.792 | 5 | 92.421 | 12 | 81.319 | 13 | 1.209 | 28 | 1329.218 | 6 |
| **Se77** | 81.336 | 6 | 111.468 | 5 | 121.829 | 6 | 53.178 | 6 | 92.923 | 6 | 192.799 | 5 | 71.373 | 12 | 60.120 | 13 | 124.732 | 6 | 20.254 | 5 |
| **Zr90** | <0.005 | | <0.005 | | <0.003 | | <0.005 | | <0.006 | | <0.027 | | <0.013 | | 0.010 | 50 | <0.023 | | <0.007 | |
| **Mo95** | 0.164 | 24 | <0.1 | | <0.118 | | <0.153 | | <0.179 | | <0.701 | | <0.626 | | <0.486 | | <0.462 | | <0.15 | |
| **Ag107** | 1.290 | 11 | 0.031 | 35 | <0.023 | | 2.960 | 15 | 0.158 | 23 | <0.079 | | 0.406 | 23 | <0.073 | | 4.394 | 7 | <0.03 | |
| **Cd111** | 0.668 | 19 | <0.64 | | 0.430 | 31 | <0.659 | | <0.889 | | <2.374 | | <2.614 | | <2.307 | | <2.185 | | <0.828 | |
| **Sn118** | 0.203 | 9 | 11.141 | 35 | 0.191 | 10 | 0.608 | 39 | 0.226 | 11 | 0.285 | 25 | 0.277 | 28 | 0.312 | 21 | 3.037 | 7 | 0.224 | 10 |
| **Sb121** | 0.245 | 10 | 0.108 | 28 | <0.068 | | 0.249 | 18 | <0.064 | | <0.187 | | 0.134 | 70 | <0.136 | | 0.323 | 21 | 0.043 | 31 |
| **Te125** | 4.828 | 13 | 0.295 | 37 | <0.161 | | 9.299 | 12 | 0.788 | 26 | <0.819 | | 4.517 | 21 | <0.77 | | <0.715 | | <0.215 | |
| **Ba137** | 0.017 | 45 | 0.015 | 46 | 1.006 | 39 | <0.024 | | <0.037 | | 0.067 | 43 | <0.071 | | <0.099 | | <0.088 | | <0.026 | |
| **La139** | <0.002 | | <0.003 | | <0.004 | | <0.003 | | <0.004 | | <0.01 | | <0.015 | | <0.007 | | <0.009 | | 0.003 | 33 |
| **W182** | 0.014 | 63 | 0.015 | 103 | 0.014 | 67 | <0.013 | | <0.022 | | <0.062 | | <0.052 | | <0.048 | | <0.052 | | <0.021 | |
| **Au197** | 0.016 | 27 | <0.011 | | <0.011 | | 0.056 | 18 | 0.043 | 28 | <0.051 | | 0.336 | 24 | <0.046 | | <0.047 | | 0.008 | 45 |
| **Tl205** | <0.006 | | <0.004 | | <0.005 | | 0.038 | 16 | 0.025 | 49 | <0.012 | | <0.016 | | <0.013 | | 0.045 | 31 | 0.008 | 70 |
| **Pb208** | 3.884 | 10 | 0.122 | 9 | 0.068 | 12 | 9.886 | 13 | 6.436 | 16 | 0.158 | 18 | 1.301 | 13 | 0.124 | 51 | 203.591 | 7 | 0.018 | 31 |
| **Bi209** | 4.730 | 13 | 0.072 | 18 | 0.021 | 23 | 6.922 | 14 | 0.790 | 16 | 0.018 | 42 | 5.042 | 12 | 0.313 | 22 | 1.095 | 7 | <0.005 | |
| **Th232** | 0.007 | 32 | <0.004 | | 0.010 | 24 | <0.005 | | <0.005 | | 0.409 | 27 | 0.837 | 43 | 0.204 | 73 | <0.016 | | 0.003 | 53 |
| **U238** | 0.005 | 117 | 0.008 | 112 | <0.003 | | <0.003 | | 0.329 | 101 | <0.013 | | <0.015 | | <0.007 | | <0.014 | | 0.007 | 131 |

**Table A9.2.** *Continued.*

| SAMPLE | BN5 06 py | | BN600 01 py | | BN600 02 py | | BN600 03 py | | BN600 04 py | | BN600 05 py | | WA1 03 py | | WA1 04 py | | WA1 05 py | | WA8 02 py | |
|---|---|---|---|---|---|---|---|---|---|---|---|---|---|---|---|---|---|---|---|---|
| **Ti49** | 14.015 | 14 | 10.470 | 6 | 16.167 | 17 | 11.852 | 6 | 10.766 | 7 | 16.254 | 9 | 10.186 | 6 | 11.050 | 5 | 17.651 | 25 | 20.152 | 11 |
| **Cr53** | 0.334 | 21 | <0.402 | | 0.154 | 40 | <0.267 | | 0.211 | 36 | 0.620 | 22 | 0.328 | 24 | 0.285 | 31 | 0.278 | 23 | 1.055 | 23 |
| **Mn55** | 0.389 | 16 | 11.075 | 20 | 0.398 | 18 | 0.341 | 21 | 0.301 | 23 | 0.608 | 15 | 0.338 | 24 | 0.378 | 19 | 2.817 | 13 | 55.768 | 15 |
| **Fe57** | 465500 | | 465500 | | 465500 | | 465500 | | 465500 | | 465500 | | 465500 | | 465500 | | 465500 | | 465500 | |
| **Co59** | 10392.808 | 7 | 1048.271 | 12 | 10664.937 | 6 | 15688.169 | 6 | 11458.583 | 8 | 24834.982 | 7 | 2053.208 | 8 | 82.724 | 5 | 18867.680 | 7 | 3889.915 | 9 |
| **Ni60** | 91.871 | 5 | 96.509 | 9 | 63.785 | 6 | 90.102 | 6 | 71.374 | 6 | 377.329 | 6 | 338.299 | 6 | 1293.095 | 7 | 32.826 | 9 | 1542.811 | 10 |
| **Cu65** | 0.346 | 24 | 787.611 | 5 | 0.555 | 25 | 24.069 | 32 | 1.479 | 36 | 6.530 | 18 | 0.528 | 41 | 0.294 | 33 | 1621.705 | 31 | 198.728 | 22 |
| **Zn66** | 0.421 | 12 | 42.773 | 11 | 0.583 | 11 | 0.737 | 9 | 1.852 | 22 | 0.499 | 12 | 0.605 | 10 | 0.782 | 9 | 1.610 | 34 | 3.570 | 15 |
| **As75** | 340.281 | 5 | 67.191 | 9 | 656.025 | 6 | 1436.176 | 7 | 657.683 | 6 | 3917.348 | 9 | 1.622 | 10 | 9.347 | 8 | 2110.125 | 23 | 740.123 | 9 |
| **Se77** | 18.962 | 5 | 96.585 | 5 | 24.312 | 6 | 29.843 | 6 | 25.196 | 7 | 51.858 | 6 | 106.188 | 6 | 132.801 | 5 | 91.271 | 8 | 102.014 | 10 |
| **Zr90** | 0.168 | 27 | <0.011 | | 0.260 | 34 | 143.107 | 34 | 0.006 | 40 | 0.013 | 51 | <0.006 | | 0.044 | 96 | 18.701 | 15 | 0.240 | 15 |
| **Mo95** | 0.491 | 64 | <0.255 | | <0.131 | | 3479.654 | 20 | 3.350 | 21 | 175.720 | 18 | <0.141 | | <0.18 | | 0.121 | 41 | <0.435 | |
| **Ag107** | <0.017 | | 33.817 | 8 | 1.524 | 23 | 57.146 | 23 | <0.021 | | 0.447 | 18 | <0.016 | | <0.022 | | 0.178 | 18 | 1.488 | 14 |
| **Cd111** | <0.601 | | 2.008 | 15 | 0.301 | 34 | 1.212 | 21 | <0.563 | | <0.537 | | <0.711 | | <0.501 | | <0.582 | | <2.058 | |
| **Sn118** | 0.162 | 10 | 3.385 | 6 | 0.207 | 20 | 0.200 | 10 | 0.210 | 12 | 0.172 | 12 | 0.217 | 10 | 0.213 | 10 | 0.292 | 22 | 0.223 | 21 |
| **Sb121** | <0.034 | | 10.567 | 5 | 0.030 | 36 | 0.034 | 42 | 0.035 | 35 | <0.035 | | <0.040 | | <0.047 | | 0.244 | 19 | 0.314 | 18 |
| **Te125** | <0.264 | | 5.333 | 21 | 3.455 | 12 | 36.580 | 24 | 0.425 | 29 | 1.759 | 13 | 113.719 | 55 | <0.208 | | 15.302 | 21 | 141.329 | 26 |
| **Ba137** | 0.194 | 19 | <0.036 | | <0.025 | | <0.022 | | <0.019 | | 0.129 | 33 | <0.032 | | <0.018 | | 0.052 | 25 | 0.195 | 35 |
| **La139** | <0.002 | | | | 0.018 | 42 | 0.010 | 30 | <0.003 | | <0.003 | 0 | <0.003 | | <0.004 | | 0.133 | 27 | 0.750 | 25 |
| **W182** | <0.014 | | <0.023 | | 0.008 | 77 | 0.206 | 20 | <0.013 | | 0.021 | 41 | <0.013 | | <0.015 | | 0.060 | 20 | 0.096 | 22 |
| **Au197** | <0.012 | | 0.186 | 11 | 0.042 | 16 | 0.275 | 68 | 0.029 | 22 | 0.036 | 27 | 0.066 | 46 | <0.017 | | 0.379 | 13 | 0.718 | 23 |
| **Tl205** | <0.003 | 0 | 1.369 | 7 | 0.013 | 79 | 0.038 | 46 | 0.010 | 36 | 0.010 | 38 | <0.005 | | <0.005 | | 0.078 | 20 | 0.093 | 32 |
| **Pb208** | 0.070 | 11 | 121.087 | 5 | 11.130 | 15 | 115.271 | 19 | 0.126 | 12 | 0.750 | 16 | 0.164 | 9 | 0.047 | 17 | 18.983 | 16 | 5.520 | 9 |
| **Bi209** | 0.056 | 18 | 28.181 | 5 | 0.625 | 12 | 3.709 | 19 | 0.076 | 13 | 0.461 | 11 | 0.034 | 21 | 0.020 | 14 | 1.484 | 12 | 167.545 | 27 |
| **Th232** | 0.003 | 44 | <0.005 | | 10.808 | 38 | 0.711 | 26 | 0.017 | 46 | 0.021 | 36 | <0.002 | | 0.035 | 42 | 19.404 | 14 | 0.040 | 20 |
| **U238** | 0.009 | 24 | <0.006 | | 17.533 | 30 | 9.306 | 25 | 0.010 | 28 | 0.122 | 65 | 0.019 | 85 | <0.003 | | 41.014 | 13 | 0.153 | 15 |

| SAMPLE | WA9 01 py | | WA9 02 py | | WA9 03 py | | WA9 04 py | | K9 04 py | | K9 05 py | | K9 06 py | | WA9 05 py | | WA9 06 py | | K7 01 py | |
|---|---|---|---|---|---|---|---|---|---|---|---|---|---|---|---|---|---|---|---|---|
| **Ti49** | 7.864 | 7 | 7.749 | 7 | 8.864 | 6 | 7.805 | 6 | 9.143 | 7 | 9.563 | 6 | 8.079 | 6 | 6.605 | 7 | 7.442 | 6 | 33.600 | 10 |
| **Cr53** | 0.132 | 53 | 0.206 | 29 | 0.233 | 34 | 0.184 | 28 | 0.217 | 49 | 0.251 | 34 | <0.202 | | 0.149 | 42 | <0.196 | | 2.488 | 9 |
| **Mn55** | 0.438 | 20 | 0.261 | 25 | 0.599 | 12 | <0.167 | | 0.276 | 19 | 0.234 | 23 | 0.987 | 16 | 0.283 | 24 | 0.164 | 37 | 28.773 | 8 |
| **Fe57** | 465500 | | 465500 | | 465500 | | 465500 | | 465500 | | 465500 | | 465500 | | 465500 | | 465500 | | 465500 | |
| **Co59** | 14639.183 | 8 | 12074.863 | 7 | 11589.615 | 6 | 11256.603 | 6 | 22643.585 | 7 | 1390.568 | 5 | 641.685 | 5 | 13559.422 | 7 | 14723.997 | 6 | 2543.535 | 6 |
| **Ni60** | 116.974 | 7 | 156.028 | 7 | 94.622 | 5 | 94.125 | 5 | 60.361 | 6 | 6339.950 | 5 | 1313.068 | 5 | 126.022 | 6 | 124.797 | 5 | 207.666 | 5 |
| **Cu65** | 263.220 | 13 | 43.993 | 25 | 4.995 | 8 | 0.329 | 25 | 23.019 | 31 | 0.652 | 16 | 0.314 | 33 | 0.481 | 34 | 0.386 | 23 | 309.547 | 21 |
| **Zn66** | 0.652 | 12 | 0.444 | 12 | 1.950 | 27 | 0.798 | 11 | 0.885 | 13 | 1.822 | 10 | 0.448 | 13 | 0.509 | 16 | 0.484 | 11 | 2.867 | 7 |
| **As75** | 614.188 | 18 | 640.930 | 7 | 167.147 | 5 | 140.603 | 5 | 264.139 | 6 | 4077.360 | 6 | 874.453 | 5 | 137.132 | 6 | 167.123 | 5 | 1279.753 | 6 |
| **Se77** | 78.817 | 8 | 41.175 | 7 | 29.513 | 5 | 33.574 | 5 | 14.813 | 6 | 19.380 | 5 | 26.768 | 5 | 28.302 | 6 | 32.730 | 5 | 12.711 | 6 |
| **Zr90** | <0.006 | | <0.004 | | 0.020 | 24 | <0.005 | | <0.003 | | 0.004 | 43 | <0.005 | | <0.009 | | <0.006 | | 2.633 | 16 |
| **Mo95** | <0.217 | | <0.182 | | <0.211 | | <0.21 | | 0.503 | 15 | <0.143 | | <0.159 | | <0.169 | | <0.18 | | 5.144 | 9 |
| **Ag107** | 1.874 | 11 | <0.026 | | 2.186 | 7 | <0.026 | | <0.019 | | 0.053 | 19 | <0.028 | | <0.026 | | <0.026 | | 7.706 | 9 |
| **Cd111** | <0.746 | | <0.797 | | <0.924 | | <0.809 | | 0.397 | 35 | <0.63 | | <0.918 | | <0.715 | | <0.754 | | 0.562 | 36 |
| **Sn118** | 0.270 | 11 | 0.212 | 11 | 0.429 | 10 | 0.308 | 9 | 0.166 | 10 | 0.385 | 10 | 0.221 | 13 | 0.333 | 12 | 0.265 | 9 | 1.796 | 75 |
| **Sb121** | 0.104 | 19 | <0.049 | | 0.157 | 14 | 0.054 | 26 | <0.03 | | 0.038 | 44 | 0.038 | 39 | 0.067 | 20 | <0.032 | | 1.430 | 7 |
| **Te125** | 371.542 | 12 | 2.790 | 20 | 2.874 | 10 | <0.332 | | <0.243 | | 1.189 | 15 | 1.434 | 13 | 0.258 | 41 | <0.278 | | 9.841 | 8 |
| **Ba137** | 0.050 | 46 | <0.025 | | 0.033 | 41 | <0.025 | | <0.021 | | <0.013 | | 0.236 | 20 | <0.028 | | <0.024 | | 387.057 | 10 |
| **La139** | <0.002 | | <0.003 | | 0.023 | 16 | <0.002 | | 0.002 | 35 | <0.002 | | <0.004 | | <0.003 | | <0.004 | | 0.174 | 7 |
| **W182** | <0.027 | | 0.012 | 98 | <0.019 | | <0.017 | | <0.014 | | 0.017 | 94 | <0.021 | | <0.016 | | 0.011 | 125 | 0.054 | 77 |
| **Au197** | 0.315 | 14 | 0.024 | 26 | 0.031 | 22 | <0.011 | | <0.011 | | <0.011 | | 0.012 | 29 | <0.014 | | <0.012 | | 0.091 | 14 |
| **Tl205** | 0.035 | 21 | <0.004 | | <0.004 | | <0.003 | | <0.003 | | 0.012 | 27 | <0.004 | | <0.005 | | <0.006 | | 1.598 | 8 |
| **Pb208** | 626.508 | 12 | 0.260 | 17 | 2.793 | 7 | 0.084 | 13 | 0.138 | 12 | 0.280 | 9 | 0.043 | 22 | 0.084 | 24 | 0.061 | 16 | 37.701 | 8 |
| **Bi209** | 560.348 | 11 | 2.235 | 18 | 6.861 | 5 | <0.054 | | 0.259 | 11 | 0.156 | 17 | 0.096 | 16 | <0.006 | | 0.006 | 28 | 45.905 | 7 |
| **Th232** | <0.003 | | <0.005 | | 0.112 | 20 | 0.126 | 19 | 0.068 | 58 | 0.157 | 16 | <0.005 | | 0.113 | 19 | | | 0.088 | 19 |
| **U238** | 0.034 | 104 | 0.015 | 95 | <0.004 | | <0.004 | | 0.002 | 42 | <0.002 | | <0.003 | | <0.003 | | 0.011 | 84 | 0.086 | 19 |

**Table A9.2.** *Continued.*

| SAMPLE | K7 02 py | | K7 03 py | | K7 04 py | | K7 05 py | | K7 06 py | | K8 01 py | | K8 02 py | | K8 03 py | | K8 04 py | | K8 05 py | |
|---|---|---|---|---|---|---|---|---|---|---|---|---|---|---|---|---|---|---|---|---|
| **Ti49** | 925.697 | 23 | 12.710 | 6 | 42.828 | 16 | 1107.906 | 16 | 419.952 | 14 | 10.931 | 5 | 12.383 | 5 | 12.544 | 5 | 10.715 | 6 | 11.606 | 7 |
| **Cr53** | 0.362 | 55 | 0.575 | 31 | <0.562 | | 3.610 | 17 | <0.393 | | 0.276 | 29 | 0.295 | 21 | 0.215 | 37 | 0.205 | 29 | <0.319 | |
| **Mn55** | 1.256 | 18 | 10.947 | 9 | <0.524 | | 18.683 | 17 | 3.748 | 18 | 0.693 | 20 | 0.373 | 15 | 0.487 | 14 | 0.230 | 25 | 0.495 | 22 |
| **Fe57** | 465500 | | 465500 | | 465500 | | 465500 | | 465500 | | 465500 | | 465500 | | 465500 | | 465500 | | 465500 | |
| **Co59** | 1672.229 | 11 | 1462.672 | 5 | 396.480 | 7 | 792.658 | 6 | 343.968 | 5 | 581.966 | 5 | 700.556 | 5 | 130.319 | 5 | 508.261 | 6 | 2214.989 | 6 |
| **Ni60** | 177.230 | 9 | 183.560 | 5 | 183.073 | 6 | 234.451 | 6 | 115.123 | 5 | 67.817 | 5 | 136.392 | 5 | 29.639 | 5 | 109.246 | 5 | 233.775 | 6 |
| **Cu65** | 1.891 | 18 | 1175.222 | 12 | 0.901 | 38 | 9974.109 | 7 | 18.862 | 32 | 1.183 | 12 | 0.436 | 18 | 0.436 | 22 | 0.383 | 21 | 0.205 | 41 |
| **Zn66** | 0.825 | 15 | 1.756 | 10 | 0.575 | 19 | 5.259 | 15 | 0.666 | 12 | 3.819 | 80 | 1.167 | 14 | 0.673 | 9 | 0.520 | 10 | 0.551 | 12 |
| **As75** | 1163.674 | 9 | 1099.792 | 5 | 1155.026 | 6 | 1475.037 | 6 | 955.970 | 5 | 24.904 | 5 | 32.817 | 5 | 25.283 | 5 | 25.024 | 6 | 21.788 | 6 |
| **Se77** | 8.801 | 24 | 14.162 | 9 | 7.289 | 13 | 15.225 | 9 | 6.171 | 10 | 53.627 | 5 | 87.203 | 4 | 71.720 | 5 | 79.873 | 5 | 27.281 | 6 |
| **Zr90** | 0.307 | 51 | 2.261 | 30 | 12.392 | 36 | 83.875 | 19 | 490.712 | 22 | 0.008 | 37 | <0.007 | | 0.010 | 31 | 0.009 | 54 | <0.006 | |
| **Mo95** | 0.973 | 23 | 3.951 | 11 | <0.404 | | 4.596 | 38 | <0.293 | | <0.116 | | <0.091 | | <0.122 | | <0.131 | | <0.173 | |
| **Ag107** | <0.061 | | 1.897 | 6 | <0.069 | | 4.114 | 9 | 0.445 | 11 | 0.017 | 40 | <0.02 | | <0.022 | | <0.014 | | <0.016 | |
| **Cd111** | <1.59 | | <1.826 | | <2.401 | | <1.975 | | <1.329 | | <0.511 | | <0.426 | | <0.575 | | <0.447 | | <0.566 | |
| **Sn118** | 0.148 | 23 | 0.163 | 27 | 0.214 | 24 | 0.619 | 10 | 0.385 | 10 | 0.190 | 9 | 0.179 | 9 | 0.313 | 42 | 0.176 | 10 | 0.174 | 13 |
| **Sb121** | 0.241 | 27 | 1.010 | 9 | <0.156 | | 3.354 | 7 | 0.710 | 8 | 0.050 | 25 | <0.025 | | <0.051 | | 0.034 | 31 | <0.035 | |
| **Te125** | 1.709 | 21 | 5.335 | 12 | <0.897 | | 10.733 | 14 | 0.982 | 22 | 5.084 | 23 | 1.071 | 11 | 0.576 | 21 | 0.424 | 19 | <0.212 | |
| **Ba137** | 0.389 | 44 | 0.490 | 31 | 5.101 | 19 | 0.267 | 24 | 9.679 | 15 | 0.136 | 26 | <0.02 | | 0.054 | 30 | <0.024 | | <0.028 | |
| **La139** | 0.007 | 54 | 0.244 | 31 | <0.008 | | 0.033 | 19 | 0.027 | 38 | 0.009 | 47 | <0.002 | | <0.003 | 0 | <0.002 | | <0.003 | |
| **W182** | 0.028 | 64 | 0.024 | 42 | 0.057 | 31 | 2.364 | 16 | 0.346 | 14 | <0.011 | | <0.009 | | 0.026 | 94 | <0.011 | | <0.011 | |
| **Au197** | 0.030 | 41 | 0.059 | 29 | <0.047 | | 0.137 | 20 | 0.042 | 25 | 0.010 | 56 | <0.008 | | <0.012 | | <0.006 | | <0.019 | |
| **Tl205** | 0.141 | 30 | 2.803 | 10 | 0.044 | 33 | 1.532 | 12 | 0.046 | 26 | 0.009 | 33 | 0.016 | 46 | 0.013 | 31 | <0.003 | | <0.004 | |
| **Pb208** | 3.252 | 30 | 29.806 | 10 | 0.244 | 13 | 21.885 | 9 | 8.738 | 7 | 0.133 | 12 | 0.213 | 13 | 0.034 | 16 | 0.042 | 15 | 0.014 | 32 |
| **Bi209** | 4.659 | 12 | 21.523 | 6 | 0.548 | 12 | 48.296 | 8 | 19.240 | 5 | 9.454 | 18 | 0.357 | 10 | 0.590 | 25 | 0.057 | 8 | <0.006 | |
| **Th232** | 0.010 | 35 | 0.064 | 29 | 0.018 | 45 | 0.548 | 14 | 5.761 | 28 | 0.004 | 47 | 0.019 | 18 | 0.003 | 38 | 0.003 | 52 | <0.003 | |
| **U238** | 0.027 | 98 | 0.067 | 33 | 0.146 | 40 | 1.098 | 15 | 3.535 | 19 | 0.053 | 83 | 0.001 | 31 | <0.003 | | 0.017 | 99 | <0.003 | |

| SAMPLE | K8 06 py | | K8 07 py | | K9 01 py | | K9 02 py | | K9 03 py | |
|---|---|---|---|---|---|---|---|---|---|---|
| **Ti49** | 12.241 | 6 | 11.834 | 6 | 8.567 | 6 | 9.701 | 6 | 9.949 | 5 |
| **Cr53** | 0.517 | 53 | 0.165 | 38 | <0.467 | | <0.216 | | 0.186 | 36 |
| **Mn55** | 0.217 | 30 | 0.341 | 16 | 0.380 | 21 | 0.358 | 18 | 0.620 | 12 |
| **Fe57** | 465500 | | 465500 | | 465500 | | 465500 | | 465500 | |
| **Co59** | 932.233 | 6 | 3612.099 | 6 | 206.169 | 6 | 10596.293 | 7 | 3910.413 | 5 |
| **Ni60** | 54.276 | 6 | 133.244 | 6 | 505.753 | 5 | 3229.162 | 7 | 237.042 | 5 |
| **Cu65** | 0.405 | 31 | 0.426 | 24 | 0.295 | 29 | 0.455 | 32 | 0.416 | 25 |
| **Zn66** | 0.659 | 10 | 0.625 | 11 | 0.596 | 9 | 0.532 | 11 | 1.688 | 26 |
| **As75** | 27.507 | 5 | 26.138 | 6 | 254.953 | 5 | 3010.089 | 6 | 515.344 | 5 |
| **Se77** | 93.128 | 6 | 31.361 | 6 | 20.828 | 6 | 18.538 | 6 | 34.309 | 5 |
| **Zr90** | 22.639 | 39 | <0.004 | | <0.006 | | <0.006 | | 0.006 | 36 |
| **Mo95** | <0.15 | | <0.101 | | 0.188 | 25 | <0.199 | | <0.13 | |
| **Ag107** | <0.017 | | <0.018 | | <0.023 | | <0.026 | | <0.03 | |
| **Cd111** | <0.474 | | <0.523 | | 0.810 | 22 | <0.784 | | <0.816 | |
| **Sn118** | 0.235 | 11 | 0.236 | 11 | 0.204 | 10 | 0.171 | 12 | 0.368 | 10 |
| **Sb121** | 0.042 | 31 | <0.037 | | 0.031 | 0 | 0.046 | 32 | 0.145 | 15 |
| **Te125** | 2.398 | 11 | 0.436 | 20 | 4.561 | 8 | 0.514 | 32 | 7.146 | 8 |
| **Ba137** | <0.013 | | 0.109 | 23 | <0.02 | | | | <0.024 | |
| **La139** | <0.003 | | 0.002 | 54 | 0.003 | 33 | <0.004 | | <0.003 | |
| **W182** | <0.012 | | 0.008 | 95 | <0.011 | | <0.019 | | <0.011 | |
| **Au197** | <0.011 | | <0.01 | | <0.011 | | <0.013 | | <0.011 | |
| **Tl205** | <0.004 | | <0.003 | | 0.017 | 82 | 0.009 | 89 | 0.012 | 31 |
| **Pb208** | 0.066 | 12 | 0.097 | 16 | 0.030 | 20 | 0.023 | 28 | 0.509 | 12 |
| **Bi209** | 0.410 | 11 | 0.531 | 13 | 0.017 | 28 | 0.215 | 6 | 0.372 | 13 |
| **Th232** | 0.100 | 22 | 0.022 | 26 | <0.003 | | <0.004 | | 0.051 | 68 |
| **U238** | 0.132 | 37 | 0.001 | 48 | <0.003 | | 0.005 | 134 | <0.004 | |

**Table A9.3.** Fe-oxides.

| SAMPLE | SR1A 01 mt | | SR1A 02 mt | | SR1A 05 mt | | SR1A 06 mt | | SR1A 10 mt | | CB6 01 mt | | CB6 02 mt | | CB6 03 mt | | CB6 04 mt | | CB6 05 mt | |
|---|---|---|---|---|---|---|---|---|---|---|---|---|---|---|---|---|---|---|---|---|
| **Ti49** | 504.674 | 5 | 528.799 | 6 | 701.460 | 4 | 506.780 | 5 | 534.669 | 4 | 898.395 | 6 | 1032.818 | 4 | 1353.426 | 4 | 1113.964 | 4 | 1006.094 | 7 |
| **Cr53** | 80.570 | 7 | 18.653 | 7 | 101.996 | 6 | 136.453 | 6 | 153.900 | 7 | <0.918 | | 1.223 | 29 | 1.423 | 21 | 0.997 | 34 | <0.821 | |
| **Mn55** | 513.252 | 4 | 537.949 | 4 | 569.265 | 4 | 550.472 | 4 | 530.876 | 4 | 507.899 | 5 | 596.041 | 4 | 850.004 | 4 | 733.133 | 4 | 636.041 | 6 |
| **Fe57** | 723600 | | 723600 | | 723600 | | 723600 | | 723600 | | 723600 | | 723600 | | 723600 | | 723600 | | 723600 | |
| **Co59** | 530.264 | 4 | 522.463 | 4 | 550.071 | 4 | 547.098 | 4 | 532.697 | 4 | 6.359 | 6 | 7.567 | 4 | 11.844 | 4 | 12.612 | 4 | 6.449 | 7 |
| **Ni60** | 114.746 | 4 | 91.157 | 4 | 92.554 | 4 | 100.074 | 4 | 111.159 | 4 | 46.433 | 6 | 48.094 | 4 | 53.706 | 4 | 55.180 | 4 | 43.375 | 7 |
| **Cu65** | <0.647 | | 0.832 | 37 | <0.695 | | <0.586 | | <0.929 | | 12.845 | 23 | <0.675 | | <0.511 | | <0.947 | | 8.394 | 44 |
| **Zn66** | 9.321 | 5 | 9.661 | 5 | 11.777 | 4 | 12.534 | 6 | 10.318 | 5 | 74.017 | 6 | 82.461 | 4 | 133.297 | 4 | 111.357 | 4 | 81.642 | 7 |
| **As75** | 1.953 | 18 | 2.061 | 17 | 1.480 | 26 | 2.110 | 17 | 2.223 | 18 | 2.197 | 15 | 2.716 | 14 | 1.783 | 20 | 2.281 | 18 | 1.789 | 27 |
| **Se77** | <1.289 | | 1.955 | 31 | <1.097 | | <1.25 | | 1.752 | 36 | 1.739 | 29 | 2.132 | 34 | <1.118 | | 2.613 | 32 | <1.578 | |
| **Zr90** | <0.019 | | <0.022 | | <0.019 | | 0.019 | 40 | <0.022 | | <0.023 | | 0.030 | 40 | 0.104 | 14 | <0.031 | | 0.081 | 24 |
| **Mo95** | <0.445 | | <0.466 | | 0.487 | 35 | <0.399 | | <0.622 | | <0.474 | | <0.549 | | <0.503 | | <0.61 | | <0.497 | |
| **Ag107** | <0.061 | | <0.053 | | <0.069 | | <0.08 | | <0.073 | | 0.134 | 114 | <0.103 | | <0.092 | | <0.072 | | <0.074 | |
| **Cd111** | 1.018 | 111 | <1.419 | | <1.784 | | <2.27 | | <1.835 | | <1.61 | | <1.709 | | <2.163 | | <2.208 | | <1.99 | |
| **Sn118** | 0.598 | 10 | 0.639 | 12 | 0.663 | 9 | 1.057 | 33 | 0.747 | 9 | 0.527 | 14 | 0.669 | 10 | 1.163 | 7 | 0.837 | 8 | 0.815 | 15 |
| **Sb121** | <0.12 | | <0.135 | | <0.126 | | 0.334 | 15 | 0.113 | 41 | <0.103 | | <0.134 | | <0.144 | | <0.152 | | <0.15 | |
| **Te125** | <0.61 | | <0.558 | | <0.631 | | <0.781 | | <1.041 | | <0.604 | | <0.65 | | <0.894 | | <0.664 | | <0.59 | |
| **Ba137** | 0.152 | 33 | 0.192 | 29 | <0.08 | | <0.094 | | <0.074 | | 1.468 | 11 | 3.414 | 7 | 22.186 | 7 | 6.906 | 7 | 14.747 | 10 |
| **La139** | <0.01 | | <0.011 | | <0.007 | | 0.013 | 21 | 0.008 | 47 | 0.008 | 57 | 0.015 | 31 | 0.082 | 11 | 0.031 | 23 | 0.024 | 27 |
| **W182** | 0.018 | 37 | <0.069 | | <0.057 | | <0.049 | | <0.059 | | <0.047 | | 0.104 | 18 | 0.461 | 7 | 0.119 | 19 | 0.110 | 37 |
| **Au197** | <0.0462 | | <0.052 | | <0.041 | | 0.041 | 26 | 0.028 | 40 | <0.038 | | <0.072 | | <0.029 | | <0.054 | | <0.07 | |
| **Tl205** | <0.011 | | <0.013 | | <0.012 | | <0.013 | | <0.015 | | 0.023 | 41 | <0.012 | | 0.051 | 23 | <0.013 | | <0.017 | |
| **Pb208** | <0.028 | | <0.034 | | <0.028 | | 0.160 | 26 | 0.869 | 100 | 1.508 | 12 | 0.181 | 16 | 3.576 | 8 | 0.122 | 16 | 9.260 | 14 |
| **Bi209** | <0.011 | | <0.014 | | <0.019 | | 0.340 | 6 | <0.014 | | <0.013 | | 0.027 | 22 | 0.091 | 14 | 0.020 | 35 | 0.071 | 22 |
| **Th232** | 0.008 | 82 | <0.01 | | <0.010 | | 0.030 | 29 | <0.01 | | 0.007 | 48 | <0.009 | | <0.012 | | 0.055 | 31 | <0.011 | |
| **U238** | <0.008 | | <0.009 | | <0.009 | | 0.309 | 6 | <0.007 | | 0.042 | 16 | 0.024 | 24 | 0.105 | 9 | 0.046 | 16 | 0.099 | 12 |

| SAMPLE | BN1 12 hm | | GG2 01 mt | | GG2 02 mt | | GG2 03 mt | | GG2 04 mt | | GG2 05 mt | | GG19 05 mt | | GG19 06 mt | | GG19 07 mt | | WA1 09 mt | |
|---|---|---|---|---|---|---|---|---|---|---|---|---|---|---|---|---|---|---|---|---|
| **Ti49** | 10769.092 | 5 | 1425.384 | 6 | 1153.977 | 5 | 1070.699 | 5 | 1618.308 | 5 | 1135.775 | 4 | 1705.517 | 4 | 1482.694 | 5 | 1610.291 | 5 | 996.487 | 6 |
| **Cr53** | 1141.427 | 6 | 113.763 | 6 | 96.360 | 6 | 69.314 | 7 | 36.055 | 6 | 84.238 | 6 | 332.168 | 7 | 576.311 | 7 | 907.597 | 7 | 9.723 | 8 |
| **Mn55** | 17637.468 | 5 | 1304.268 | 4 | 1332.098 | 4 | 1158.652 | 4 | 1375.648 | 4 | 1508.894 | 4 | 80.895 | 5 | 59.208 | 4 | 63.941 | 5 | 451.271 | 5 |
| **Fe57** | 699400 | | 723600 | | 723600 | | 723600 | | 723600 | | 723600 | | 723600 | | 723600 | | 723600 | | 723600 | |
| **Co59** | 38.344 | 7 | 2.244 | 4 | 2.709 | 4 | 3.475 | 5 | 3.773 | 4 | 1.050 | 5 | 9.977 | 5 | 7.217 | 5 | 12.805 | 5 | 374.681 | 5 |
| **Ni60** | 36.032 | 6 | 4.409 | 4 | 4.210 | 5 | 4.134 | 6 | 3.906 | 5 | 4.014 | 5 | 5.248 | 6 | 5.325 | 6 | 5.937 | 6 | 42.528 | 5 |
| **Cu65** | 8819.921 | 7 | 0.626 | 28 | <0.544 | | <0.433 | | <0.477 | | <0.546 | | 105.858 | 8 | <0.918 | | <0.821 | | 135.534 | 19 |
| **Zn66** | 75.270 | 7 | 188.258 | 5 | 81.644 | 5 | 153.012 | 7 | 122.772 | 9 | 82.222 | 4 | 6.228 | 7 | 3.313 | 8 | 4.307 | 7 | 19.374 | 5 |
| **As75** | 12.821 | 8 | 175.321 | 9 | 4.743 | 7 | 53.156 | 9 | 1.884 | 11 | 4.378 | 15 | 1.895 | 23 | 1.931 | 21 | 2.118 | 19 | 2.657 | 15 |
| **Se77** | 9.531 | 21 | 0.861 | 37 | <0.926 | | 1.340 | 26 | <0.706 | | 0.868 | 41 | 3.277 | 26 | <3.025 | | 2.143 | 40 | <1.927 | |
| **Zr90** | 5.222 | 5 | 0.013 | 44 | 0.184 | 9 | <0.011 | | <0.016 | | <0.013 | | 0.165 | 12 | 0.036 | 29 | 2.398 | 56 | 0.034 | 34 |
| **Mo95** | <1.812 | | 1.194 | 23 | <0.401 | | <0.32 | | <0.375 | | <0.337 | | <0.44 | | <0.576 | | <0.481 | | <0.504 | |
| **Ag107** | <0.265 | | <0.049 | | <0.061 | | <0.052 | | <0.053 | | <0.062 | | <0.094 | | 0.058 | 44 | <0.099 | | <0.09 | |
| **Cd111** | <9.227 | | <1.666 | | <1.845 | | <1.778 | | 1.120 | 30 | <1.983 | | <1.917 | | <1.9 | | <1.632 | | <2.069 | |
| **Sn118** | 254.047 | 5 | 0.623 | 8 | 0.547 | 7 | 0.539 | 8 | 0.576 | 8 | 0.600 | 8 | 1.084 | 8 | 0.955 | 9 | 0.852 | 10 | 0.738 | 9 |
| **Sb121** | 2.988 | 8 | <0.076 | | <0.074 | | <0.085 | | <0.066 | | <0.072 | | <0.172 | | <0.179 | | 0.147 | 57 | <0.137 | |
| **Te125** | <3.035 | | <0.537 | | <0.6 | | <0.578 | | <0.736 | | <0.693 | | <0.814 | | <0.85 | | <1.115 | | 0.587 | 43 |
| **Ba137** | 151.556 | 10 | 0.938 | 9 | 0.153 | 19 | 0.826 | 10 | <0.051 | | <0.076 | | <0.117 | | <0.062 | | <0.069 | | <0.092 | |
| **La139** | 177.090 | 4 | 0.010 | 29 | 0.101 | 8 | 0.024 | 56 | <0.005 | | <0.006 | | 0.163 | 9 | 0.042 | 25 | 0.012 | 44 | 0.012 | 41 |
| **W182** | 281.116 | 4 | 0.260 | 10 | 0.069 | 22 | 0.114 | 14 | <0.04 | | <0.043 | | <0.053 | | <0.055 | | <0.063 | | <0.046 | |
| **Au197** | <0.169 | | <0.028 | | <0.044 | | <0.022 | | <0.024 | | <0.03 | | <0.05 | | <0.056 | | <0.037 | | <0.034 | |
| **Tl205** | 0.279 | 16 | 0.015 | 46 | <0.008 | | 0.030 | 31 | <0.007 | | <0.01 | | <0.017 | | <0.015 | | <0.018 | | <0.015 | |
| **Pb208** | 47.164 | 4 | 26.132 | 9 | 0.323 | 11 | 2.913 | 8 | 0.044 | 44 | 0.066 | 31 | 1.794 | 8 | 0.214 | 17 | 0.074 | 25 | <0.029 | |
| **Bi209** | 1.149 | 9 | 0.583 | 10 | <0.014 | | 0.147 | 11 | <0.015 | | <0.013 | | 0.921 | 8 | 0.383 | 15 | 0.033 | 30 | <0.017 | |
| **Th232** | 0.520 | 9 | 0.006 | 44 | <0.008 | | <0.006 | | <0.007 | | <0.012 | | <0.011 | | <0.012 | | <0.01 | | <0.008 | |
| **U238** | 40.439 | 6 | 0.041 | 13 | 0.340 | 7 | 0.018 | 22 | 0.005 | 41 | 0.023 | 22 | 0.242 | 9 | 0.098 | 15 | 0.042 | 14 | <0.009 | |

**Table A9.3.** Fe-oxides.

| SAMPLE | WA1 10 mt | | WA1 11 mt | | WA1 12 mt | | WA8 03 mt | | WA8 04 mt | | WA8 05 mt | | WA8 06 mt | | BN1 10 hm | | BN1 11 hm | |
|---|---|---|---|---|---|---|---|---|---|---|---|---|---|---|---|---|---|---|
| **Ti49** | 103.088 | 5 | 244.188 | 6 | 258.484 | 6 | 329.360 | 5 | 189.253 | 7 | 595.079 | 8 | 164.447 | 5 | 14276.985 | 8 | 204757.955 | 6 |
| **Cr53** | <0.717 | | 212.608 | 6 | 219.835 | 6 | 4.488 | 9 | 5.710 | 9 | 2.435 | 13 | 27.035 | 20 | 761.695 | 9 | 8049.223 | 7 |
| **Mn55** | 434.358 | 5 | 436.622 | 4 | 439.827 | 4 | 520.747 | 5 | 514.139 | 6 | 683.965 | 4 | 404.296 | 4 | 40610.518 | 8 | 96529.726 | 4 |
| **Fe57** | 723600 | | 723600 | | 723600 | | 723600 | | 723600 | | 723600 | | 723600 | | 699400 | | 699400 | |
| **Co59** | 412.197 | 5 | 429.249 | 4 | 423.566 | 4 | 41.248 | 5 | 40.030 | 6 | 53.750 | 4 | 45.828 | 5 | 14.399 | 19 | 6.045 | 15 |
| **Ni60** | 31.372 | 5 | 29.555 | 4 | 30.583 | 4 | 33.367 | 5 | 31.801 | 6 | 55.646 | 4 | 44.470 | 4 | 22.081 | 9 | 17.128 | 9 |
| **Cu65** | 70.866 | 26 | <0.67 | | <0.89 | | <0.74 | | 1.641 | 18 | 3.161 | 17 | 4.455 | 12 | 8.740 | 25 | 24.062 | 24 |
| **Zn66** | 18.545 | 5 | 18.421 | 4 | 19.606 | 5 | 12.205 | 6 | 12.269 | 6 | 18.540 | 5 | 11.560 | 6 | 20.792 | 10 | 78.309 | 9 |
| **As75** | 1.796 | 25 | 2.380 | 16 | 2.096 | 21 | 3.325 | 12 | 3.137 | 12 | 2.912 | 13 | 3.025 | 15 | 27.227 | 10 | 63.199 | 8 |
| **Se77** | <1.719 | | <1.771 | | <1.986 | | <1.482 | | <1.605 | | <1.385 | | <1.759 | | 13.929 | 27 | 25.840 | 22 |
| **Zr90** | 0.016 | 38 | 0.470 | 41 | <0.024 | | <0.033 | | 6.782 | 10 | 1.957 | 17 | 0.397 | 11 | 13.357 | 8 | 127.337 | 8 |
| **Mo95** | <0.462 | | <0.54 | | <0.477 | | <0.479 | | <0.583 | | <0.582 | | <0.503 | | <3.304 | | 5.755 | 37 |
| **Ag107** | <0.074 | | <0.076 | | <0.087 | | <0.076 | | <0.086 | | <0.096 | | 0.083 | 39 | <0.431 | | <0.896 | |
| **Cd111** | <1.743 | | <2.074 | | <2.225 | | <2.531 | | <2.799 | | <2.273 | | <2.762 | | <15.141 | | <30.119 | |
| **Sn118** | 0.536 | 11 | 0.574 | 11 | 0.586 | 11 | 0.729 | 9 | 0.707 | 11 | 1.398 | 8 | 0.677 | 12 | 707.614 | 8 | 974.630 | 4 |
| **Sb121** | <0.134 | | <0.142 | | <0.124 | | <0.106 | | 0.115 | 39 | 0.447 | 12 | <0.126 | | 7.501 | 9 | 20.364 | 7 |
| **Te125** | <0.803 | | <0.73 | | <0.749 | | <1.055 | | <0.958 | | <1.047 | | <1.1 | | <5.911 | | <12.395 | |
| **Ba137** | <0.103 | | 0.664 | 25 | <0.099 | | <0.118 | | 0.171 | 27 | 4.789 | 7 | 0.317 | 34 | 11292.359 | 13 | 373580 | 13 |
| **La139** | <0.008 | | <0.013 | | <0.008 | | <0.011 | | 7.524 | 15 | 0.938 | 6 | 0.051 | 19 | 303.420 | 7 | 702.712 | 4 |
| **W182** | <0.039 | | <0.064 | | <0.045 | | <0.069 | | <0.066 | | 0.745 | 10 | <0.055 | | 572.806 | 8 | 2031.980 | 6 |
| **Au197** | <0.047 | | <0.074 | | <0.044 | | <0.06 | | <0.046 | | <0.059 | | <0.051 | | <0.367 | | <0.554 | |
| **Tl205** | <0.017 | | <0.012 | | <0.009 | | <0.018 | | <0.016 | | <0.024 | | <0.013 | | 0.211 | 38 | <0.228 | |
| **Pb208** | 0.090 | 44 | 0.115 | 42 | 0.188 | 23 | 0.056 | 45 | 2.518 | 6 | 0.201 | 31 | 2.263 | 14 | 80.058 | 8 | 441.586 | 6 |
| **Bi209** | <0.018 | | <0.018 | | <0.018 | | <0.027 | | <0.021 | | 0.030 | 29 | <0.017 | | <0.104 | | 0.471 | 36 |
| **Th232** | 0.100 | 101 | 0.021 | 46 | 0.089 | 26 | <0.011 | | 4.649 | 10 | 0.525 | 14 | 0.064 | 22 | 0.839 | 11 | 2.311 | 7 |
| **U238** | <0.008 | | 0.017 | 35 | <0.013 | | <0.017 | | 14.479 | 7 | 7.237 | 14 | 0.117 | 12 | 114.436 | 8 | 1087.635 | 6 |

**Table A9.4.** Arsenopyrite.

| SAMPLE | GG206 asp | | GG207 asp | | GG208 asp | | GG209 asp | | GG210 asp | | GG211 asp | |
|---|---|---|---|---|---|---|---|---|---|---|---|---|
| **Ti49** | 4.387 | 7 | 3.245 | 7 | 3.383 | 8 | 3.709 | 8 | 3.824 | 7 | 3.321 | 8 |
| **Cr53** | 0.217 | 31 | <0.322 | | <0.268 | | <0.3 | | <0.194 | | <0.22 | |
| **Mn55** | 10.456 | 8 | <0.26 | | 0.563 | 16 | 2.854 | 30 | 0.487 | 17 | 0.720 | 15 |
| **Fe57** | 343000 | | 343000 | | 343000 | | 343000 | | 343000 | | 343000 | |
| **Co59** | 13664.286 | 6 | 13712.271 | 5 | 13589.166 | 6 | 10740.466 | 6 | 3545.532 | 7 | 4548.149 | 6 |
| **Ni60** | 1024.421 | 5 | 1333.005 | 5 | 1355.170 | 5 | 586.253 | 5 | 49.919 | 5 | 58.503 | 5 |
| **Cu65** | 0.362 | 32 | <0.363 | | 0.564 | 24 | <0.414 | | <0.261 | | <0.427 | |
| **Zn66** | 0.865 | 10 | 0.216 | 26 | 0.168 | 27 | 1.682 | 21 | 0.195 | 20 | 0.313 | 18 |
| **As75** | 381097.019 | 5 | 440351.120 | 5 | 416391.458 | 6 | 458383.261 | 5 | 344727.984 | 5 | 385569.427 | 6 |
| **Se77** | 13.831 | 6 | 16.286 | 6 | 16.710 | 7 | 16.083 | 7 | 12.521 | 7 | 14.372 | 7 |
| **Zr90** | 0.027 | 19 | 0.019 | 30 | 0.025 | 23 | 0.025 | 26 | 0.022 | 25 | 0.025 | 21 |
| **Mo95** | 0.495 | 16 | 0.339 | 32 | 0.342 | 30 | <0.356 | | <0.249 | | <0.269 | |
| **Ag107** | <0.04 | | <0.041 | | <0.031 | | <0.045 | | 0.030 | 41 | <0.041 | |
| **Cd111** | <0.962 | | <1.395 | | <1.169 | | <1.091 | | <1.1 | | <1.022 | |
| **Sn118** | 0.196 | 12 | 0.187 | 13 | 0.158 | 17 | 0.373 | 12 | 0.235 | 11 | 0.275 | 11 |
| **Sb121** | 12.726 | 5 | 14.184 | 4 | 14.599 | 5 | 15.804 | 5 | 0.155 | 14 | 426.028 | 5 |
| **Te125** | 10.143 | 7 | 12.143 | 8 | 14.143 | 9 | 16.143 | 11 | 18.143 | 7 | 20.143 | 10 |
| **Ba137** | 0.620 | 13 | <0.045 | | <0.034 | | 3.110 | 38 | <0.022 | | 0.336 | 14 |
| **La139** | <0.004 | | <0.004 | | <0.004 | | <0.007 | | <0.004 | | <0.004 | |
| **W182** | <0.032 | | <0.016 | | <0.031 | | <0.038 | | <0.019 | | <0.02 | |
| **Au197** | 1.912 | 6 | 1.402 | 6 | 1.308 | 7 | 0.671 | 8 | 0.123 | 11 | 0.298 | 9 |
| **Tl205** | <0.008 | | <0.006 | | <0.009 | | <0.007 | | <0.004 | | <0.007 | |
| **Pb208** | 1.588 | 6 | 0.411 | 7 | 0.163 | 8 | 4.876 | 28 | 0.057 | 14 | 0.331 | 8 |
| **Bi209** | 9.943 | 5 | 3.098 | 5 | 2.728 | 6 | 2.474 | 7 | 0.733 | 7 | 1.609 | 6 |
| **Th232** | <0.006 | | <0.006 | | <0.006 | | 0.017 | 33 | <0.004 | | <0.004 | |
| **U238** | <0.004 | | <0.004 | | <0.005 | | <0.006 | | <0.004 | | <0.006 | |

# Appendix 10
# DELAMERIAN MONAZITE CHEMICAL AGE DATA

**Table A10.1.** EPMA chemical age data of monazite that records Delamerian ages.

| Sample | Occluding phase | Label | Peak counts | | | Background counts | | | W%(Pb) | W%(Pb) | W%(Th) | W%(Th) | W%(U) | W%(U) | Chemical age (Ma) | | M2 age (Ma & error (2σ) | n = |
|---|---|---|---|---|---|---|---|---|---|---|---|---|---|---|---|---|---|---|
| | | | Pk(Pb) | Pk(Th) | Pk(U) | Bg(Pb) | Bg(Th) | Bg(U) | | 1σ | | 1σ | | 1σ | | 1σ | | |
| MU | mica (mx) | 18 | 19.8324 | 83.0207 | 84.8466 | 18.6515 | 29.6455 | 62.0015 | 0.0341 | 24.81 | 0.9508 | 205.77 | 0.2403 | 56.21 | 439 | 42 | | |
| MU | mica (mx) | 19 | 20.1700 | 77.6181 | 86.9477 | 18.7635 | 29.0656 | 61.5563 | 0.0425 | 28.33 | 0.8643 | 196.12 | 0.2476 | 54.94 | 564 | 49 | | |
| MU | mica (mx) | 20 | 21.6452 | 214.8884 | 90.7997 | 18.7485 | 28.3524 | 61.4784 | 0.0975 | 45.29 | 3.3102 | 383.22 | 0.3002 | 61.98 | 506 | 30 | | |
| MU | mica (mx) | 21 | 22.2640 | 288.9753 | 91.7753 | 18.5739 | 29.4875 | 62.0237 | 0.1264 | 52.02 | 4.5962 | 451.14 | 0.3188 | 65.35 | 499 | 26 | | |
| MU | mica (mx) | 22 | 19.9762 | 76.7177 | 85.0092 | 18.4724 | 30.8508 | 63.2702 | 0.0461 | 29.72 | 0.8163 | 190.58 | 0.2150 | 51.56 | 669 | 58 | | |
| MU | mica (mx) | 23 | 21.4076 | 216.1401 | 95.2147 | 18.5835 | 29.1571 | 61.4450 | 0.0947 | 44.55 | 3.3165 | 383.49 | 0.3450 | 66.38 | 475 | 29 | | |
| MU | mica (mx) | 24 | 21.5264 | 193.8376 | 89.7116 | 19.3998 | 30.0247 | 61.8679 | 0.0690 | 37.41 | 2.9077 | 359.21 | 0.2760 | 58.48 | 405 | 28 | | |
| MU | mica (mx) | 27 | 20.2387 | 104.4327 | 86.7601 | 18.8387 | 29.5788 | 60.6103 | 0.0422 | 28.20 | 1.3316 | 243.35 | 0.2186 | 47.79 | 460 | 40 | | |
| MU | mica (mx) | 28 | 19.7449 | 126.6481 | 93.2261 | 18.0410 | 27.6904 | 63.4594 | 0.0534 | 32.34 | 1.7616 | 280.00 | 0.3638 | 74.55 | 405 | 32 | | |
| MU | mica (mx) | 29 | 22.2202 | 250.6634 | 88.7486 | 18.4275 | 28.7792 | 63.1478 | 0.1304 | 52.94 | 3.9376 | 417.96 | 0.2969 | 65.61 | 590 | 31 | | |
| MU | mica (mx) | 30 | 23.2204 | 344.9316 | 86.1848 | 19.2672 | 28.3293 | 61.5006 | 0.1358 | 54.00 | 5.6015 | 497.76 | 0.2429 | 54.66 | 473 | 24 | | |
| MU | mica (mx) | 31 | 22.9391 | 329.0495 | 89.5240 | 19.3207 | 30.5078 | 61.7566 | 0.1235 | 51.33 | 5.2817 | 483.33 | 0.2752 | 58.39 | 446 | 23 | | |
| MU | mica (mx) | 33 | 25.9520 | 563.3505 | 96.5655 | 19.3322 | 31.0831 | 61.1890 | 0.2317 | 71.19 | 9.3586 | 641.38 | 0.3795 | 71.34 | 487 | 19 | | |
| MU | mica (mx) | 34 | 26.1395 | 569.2204 | 92.8634 | 19.2936 | 31.1547 | 63.1033 | 0.2399 | 72.49 | 9.4598 | 644.81 | 0.3140 | 64.35 | 509 | 19 | | |
| MU | mica (mx) | 35 | 23.3391 | 420.8557 | 93.2511 | 18.9935 | 31.8012 | 62.1573 | 0.1497 | 56.77 | 6.8681 | 550.56 | 0.2859 | 57.32 | 428 | 20 | | |
| MU | mica (mx) | 36 | 22.7641 | 286.7465 | 90.3870 | 18.7380 | 28.8238 | 62.9363 | 0.1389 | 54.73 | 4.5721 | 450.13 | 0.2799 | 59.73 | 563 | 28 | | |
| MU | mica (mx) | 38 | 21.4639 | 125.1470 | 85.5720 | 19.3691 | 29.3407 | 62.0794 | 0.0680 | 37.14 | 1.7032 | 275.13 | 0.2113 | 48.74 | 629 | 45 | | |
| MU | mica (mx) | 39 | 21.7327 | 223.3996 | 89.6366 | 18.3773 | 29.5661 | 60.9998 | 0.1144 | 49.37 | 3.4381 | 390.46 | 0.2839 | 59.31 | 582 | 33 | | |
| MU | mica (mx) | 40 | 23.6954 | 357.7586 | 94.4017 | 18.6688 | 29.1441 | 63.2369 | 0.1751 | 61.74 | 5.8042 | 506.25 | 0.3270 | 65.49 | 566 | 26 | | |
| MU | mica (mx) | 41 | 24.3705 | 437.3230 | 92.4006 | 18.7127 | 28.4195 | 60.9775 | 0.1975 | 65.64 | 7.2062 | 563.46 | 0.3063 | 61.09 | 535 | 23 | | |
| MU | mica (mx) | 42 | 19.7387 | 56.3595 | 82.8831 | 18.6680 | 29.6550 | 61.9013 | 0.0301 | 23.00 | 0.4781 | 146.28 | 0.1751 | 42.74 | 633 | 64 | | |
| MU | mica (mx) | 43 | 20.3012 | 84.3213 | 85.9096 | 18.9024 | 29.0751 | 59.5418 | 0.0422 | 28.21 | 0.9833 | 209.17 | 0.2407 | 52.41 | 530 | 46 | | |
| MU | mica (mx) | 44 | 21.3389 | 166.9586 | 90.8122 | 18.8702 | 29.4621 | 60.7772 | 0.0818 | 41.16 | 2.4429 | 329.40 | 0.2966 | 60.51 | 533 | 35 | | |
| MU | mica (mx) | 45 | 20.1450 | 91.5751 | 84.9466 | 18.5184 | 30.1003 | 61.9124 | 0.0508 | 31.49 | 1.0954 | 220.90 | 0.2044 | 47.62 | 637 | 52 | | |
| MU | mica (mx) | 46 | 23.4329 | 330.6777 | 89.1989 | 18.9465 | 29.7902 | 61.5451 | 0.1554 | 58.00 | 5.3207 | 484.99 | 0.2827 | 60.10 | 553 | 26 | | |
| MU | mica (mx) | 47 | 22.9453 | 281.0367 | 88.3859 | 19.7375 | 29.9678 | 61.1667 | 0.1086 | 47.94 | 4.4490 | 443.95 | 0.2599 | 55.70 | 457 | 25 | | |
| MU | mica (mx) | 49 | 20.5450 | 120.8438 | 81.9702 | 18.3650 | 27.4926 | 63.6487 | 0.0713 | 38.18 | 1.6620 | 271.98 | 0.1998 | 52.19 | 680 | 49 | | |
| MU | mica (mx) | 51 | 21.1388 | 149.8173 | 84.0837 | 18.6576 | 28.9133 | 61.6119 | 0.0824 | 41.36 | 2.1505 | 309.24 | 0.2158 | 50.90 | 639 | 42 | | |
| MU | mica (mx) | 52 | 20.9888 | 143.0113 | 84.4339 | 18.7079 | 28.5755 | 61.4784 | 0.0751 | 39.31 | 2.0415 | 301.74 | 0.2479 | 57.85 | 584 | 40 | | |
| MU | mica (mx) | 54 | 20.1887 | 140.9346 | 83.2583 | 18.4134 | 27.4328 | 61.2780 | 0.0562 | 33.35 | 2.0219 | 300.07 | 0.2176 | 51.89 | 459 | 35 | | |
| MU | mica (mx) | 55 | 22.1265 | 267.3643 | 88.2233 | 18.8974 | 30.0024 | 62.9920 | 0.1095 | 48.17 | 4.2080 | 431.86 | 0.2622 | 58.36 | 482 | 27 | | |
| MU | mica (mx) | 56 | 23.2891 | 356.6061 | 90.2369 | 19.1421 | 29.2708 | 59.0299 | 0.1427 | 55.40 | 5.7812 | 505.23 | 0.3047 | 60.98 | 470 | 23 | | |
| MU | mica (mx) | 57 | 20.3950 | 126.7982 | 85.0717 | 18.7956 | 29.6312 | 61.2446 | 0.0496 | 31.01 | 1.7291 | 277.35 | 0.2389 | 54.72 | 442 | 35 | | |
| MU | mica (mx) | 58 | 24.1205 | 387.8257 | 90.7622 | 18.4804 | 29.9785 | 63.5040 | 0.1974 | 65.71 | 6.3204 | 528.28 | 0.3250 | 69.60 | 594 | 26 | | |
| MU | mica (mx) | 59 | 24.4018 | 478.5109 | 94.5268 | 19.4069 | 29.0024 | 62.4021 | 0.1730 | 61.20 | 7.9209 | 590.71 | 0.3534 | 69.71 | 426 | 19 | | |
| MU | mica (mx) | 60 | 22.8703 | 342.4014 | 93.4137 | 19.1898 | 29.3693 | 63.0922 | 0.1259 | 51.88 | 5.5429 | 495.35 | 0.3439 | 69.83 | 422 | 22 | | |
| MU | mica (mx) | 61 | 21.2889 | 182.9003 | 91.8753 | 19.0392 | 28.8454 | 62.4133 | 0.0737 | 38.85 | 2.7409 | 349.16 | 0.3012 | 62.04 | 442 | 30 | | |
| MU | mica (mx) | 62 | 20.4575 | 142.0105 | 85.1718 | 18.5195 | 29.0940 | 62.2908 | 0.0623 | 35.38 | 2.0120 | 299.38 | 0.2396 | 56.00 | 497 | 37 | | |
| MU | mica (mx) | 63 | 21.1013 | 187.7056 | 85.1718 | 18.9913 | 29.7801 | 61.7232 | 0.0685 | 37.28 | 2.8091 | 353.44 | 0.2271 | 52.43 | 431 | 30 | | |
| MU | mica (mx) | 65 | 23.1016 | 334.4352 | 88.2859 | 18.8549 | 29.6550 | 61.1779 | 0.1469 | 56.36 | 5.4013 | 489.19 | 0.2819 | 60.53 | 517 | 25 | | |
| MU | mica (mx) | 66 | 21.6202 | 244.1287 | 86.4349 | 18.8918 | 28.9005 | 61.4005 | 0.0913 | 43.70 | 3.8258 | 412.33 | 0.2594 | 57.96 | 436 | 26 | | |
| MU | mica (mx) | 67 | 21.8889 | 249.9122 | 88.0107 | 19.0726 | 31.2767 | 62.4133 | 0.0947 | 44.61 | 3.8878 | 415.73 | 0.2644 | 58.43 | 445 | 26 | | |
| MU | mica (mx) | 68 | 22.7641 | 354.8022 | 89.9368 | 19.3509 | 28.2075 | 63.0031 | 0.1161 | 49.68 | 5.7886 | 506.45 | 0.3046 | 65.62 | 383 | 20 | | |
| MU | mica (mx) | 69 | 22.8141 | 306.5066 | 90.6371 | 18.6804 | 28.7274 | 62.3799 | 0.1428 | 55.53 | 4.9238 | 467.11 | 0.3114 | 65.50 | 535 | 27 | | |
| MU | mica (mx) | 70 | 22.2890 | 284.8181 | 90.9873 | 18.4497 | 31.5295 | 60.5546 | 0.1322 | 53.34 | 4.4944 | 446.51 | 0.3014 | 61.08 | 537 | 28 | | |
| MU | mica (mx) | 71 | 23.7954 | 429.5528 | 92.7258 | 19.7540 | 32.1328 | 61.2780 | 0.1387 | 54.54 | 7.0229 | 557.01 | 0.3067 | 61.15 | 386 | 19 | | |
| MU | mica (mx) | 72 | 23.2516 | 326.3943 | 87.4729 | 18.8753 | 29.2561 | 62.0126 | 0.1517 | 57.33 | 5.2661 | 483.04 | 0.2602 | 57.65 | 551 | 27 | | |
| MU | mica (mx) | 73 | 21.4514 | 198.4431 | 84.4589 | 18.9730 | 29.9646 | 62.2018 | 0.0822 | 41.28 | 2.9983 | 365.24 | 0.2209 | 52.35 | 492 | 32 | | |
| MU | mica (mx) | 74 | 23.1391 | 315.0475 | 87.9482 | 18.9944 | 28.4400 | 61.7677 | 0.1433 | 55.65 | 5.0799 | 474.44 | 0.2525 | 55.17 | 540 | 27 | | |
| MU | mica (mx) | 76 | 20.3825 | 155.8228 | 81.6075 | 18.5662 | 28.4200 | 61.2335 | 0.0577 | 33.85 | 2.2684 | 317.76 | 0.1877 | 46.49 | 447 | 33 | | |
| MU | mica (mx) | 77 | 21.7014 | 195.1892 | 84.5714 | 18.8746 | 29.7385 | 62.1461 | 0.0951 | 44.72 | 2.9420 | 361.64 | 0.2232 | 52.70 | 575 | 35 | | |
| MU | mica (mx) | 78 | 22.4828 | 243.4026 | 89.2989 | 18.8259 | 30.2797 | 62.4244 | 0.1257 | 51.97 | 3.7883 | 410.30 | 0.2702 | 58.27 | 597 | 32 | | |
| MU | mica (mx) | 79 | 22.7516 | 319.3807 | 91.0624 | 19.1572 | 30.0526 | 61.7677 | 0.1230 | 51.29 | 5.1328 | 477.12 | 0.3061 | 63.23 | 448 | 24 | | |

| Sample | Occluding phase | Label | Peak counts Pk(Pb) | Pk(Th) | Pk(U ) | Background counts Bg(Pb) | Bg(Th) | Bg(U ) | W%(Pb) | W%(Pb) 1σ | W%(Th) | W%(Th) 1σ | W%(U ) | W%(U ) 1σ | Chemical age (Ma) | 1σ | M2 age (Ma & error (2σ) | n = |
|---|---|---|---|---|---|---|---|---|---|---|---|---|---|---|---|---|---|---|
| MU | mica (mx) | 80 | 21.0326 | 197.9174 | 90.2869 | 19.1714 | 30.5827 | 62.2908 | 0.0593 | 34.36 | 2.9783 | 364.04 | 0.2858 | 60.39 | 340 | 25 | | |
| MU | mica (mx) | 81 | 24.3893 | 419.3770 | 92.3256 | 19.0770 | 30.2138 | 60.9108 | 0.1856 | 63.66 | 6.8822 | 551.61 | 0.3185 | 63.53 | 521 | 23 | | |
| MU | mica (mx) | 84 | 22.6515 | 311.1652 | 87.2728 | 19.1153 | 29.0516 | 58.9742 | 0.1208 | 50.79 | 5.0040 | 471.06 | 0.2624 | 55.15 | 460 | 24 | | |
| MU | mica (mx) | 85 | 23.3641 | 355.3284 | 89.7366 | 18.7598 | 30.1481 | 62.3465 | 0.1601 | 58.99 | 5.7662 | 505.59 | 0.2862 | 61.14 | 532 | 25 | | |
| MU | mica (mx) | 86 | 21.2201 | 194.0629 | 86.7476 | 18.3556 | 29.4022 | 63.2369 | 0.0966 | 45.12 | 2.9304 | 361.08 | 0.2390 | 55.11 | 578 | 35 | | |
| MU | mica (mx) | 87 | 20.6575 | 187.1300 | 84.2713 | 18.4941 | 28.6665 | 63.1701 | 0.0705 | 37.89 | 2.8201 | 354.22 | 0.2303 | 56.05 | 441 | 30 | | |
| MU | mica (mx) | 88 | 20.1075 | 146.0139 | 80.7696 | 18.6509 | 31.1315 | 63.1144 | 0.0443 | 29.02 | 2.0481 | 302.13 | 0.1572 | 41.83 | 387 | 32 | | |
| MU | mica (mx) | 89 | 20.5638 | 146.5394 | 84.5589 | 18.7806 | 30.2614 | 61.1000 | 0.0566 | 33.51 | 2.0742 | 304.14 | 0.2271 | 52.42 | 449 | 34 | | |
| MU | mica (mx) | 91 | 21.9952 | 214.4629 | 85.7471 | 19.1478 | 29.1002 | 62.7694 | 0.0959 | 44.93 | 3.2987 | 383.09 | 0.2489 | 58.05 | 519 | 31 | | |
| MU | mica (mx) | 92 | 20.7950 | 131.4268 | 79.1563 | 18.7896 | 28.7359 | 62.4800 | 0.0649 | 36.23 | 1.8314 | 285.75 | 0.1543 | 42.24 | 616 | 45 | | |
| MU | mica (mx) | 93 | 22.2327 | 187.7557 | 86.7851 | 19.0377 | 31.1398 | 62.6025 | 0.1090 | 48.21 | 2.7909 | 352.61 | 0.2511 | 57.09 | 667 | 39 | | |
| MU | mica (mx) | 94 | 20.8075 | 166.5081 | 86.0722 | 18.6904 | 28.5905 | 61.9458 | 0.0690 | 37.49 | 2.4591 | 331.08 | 0.2348 | 53.44 | 477 | 33 | | |
| MU | mica (mx) | 95 | 21.2013 | 167.8845 | 83.6460 | 18.7873 | 30.3161 | 61.4005 | 0.0800 | 40.71 | 2.4526 | 330.63 | 0.2031 | 48.14 | 570 | 38 | | |
| MU | mica (mx) | 96 | 22.6703 | 341.2991 | 94.9145 | 19.2967 | 29.7756 | 63.9380 | 0.1149 | 49.46 | 5.5333 | 495.69 | 0.3560 | 71.51 | 384 | 21 | | |
| MU | mica (mx) | 97 | 23.9830 | 388.1264 | 93.7764 | 18.9931 | 28.9331 | 61.8902 | 0.1742 | 61.65 | 6.3664 | 531.13 | 0.3448 | 68.27 | 518 | 23 | | |
| MU | mica (mx) | 98 | 22.6015 | 299.8445 | 86.9477 | 18.6044 | 29.8393 | 63.1812 | 0.1381 | 54.61 | 4.7969 | 461.58 | 0.2728 | 62.56 | 540 | 27 | | |
| MU | mica (mx) | 99 | 21.3764 | 142.8112 | 81.2823 | 19.2848 | 29.4618 | 61.5117 | 0.0681 | 37.23 | 2.0215 | 300.22 | 0.1670 | 41.99 | 589 | 42 | | |
| MU | mica (mx) | 100 | 21.7639 | 171.2379 | 83.2583 | 19.1366 | 29.4960 | 61.9235 | 0.0880 | 42.92 | 2.5272 | 335.63 | 0.2219 | 53.71 | 600 | 38 | | |
| MU | mica (mx) | 101 | 22.3077 | 283.9417 | 88.6736 | 19.2279 | 28.1045 | 63.3593 | 0.1042 | 46.94 | 4.5443 | 449.22 | 0.2815 | 62.55 | 426 | 24 | | |
| MU | mica (mx) | 102 | 21.0951 | 162.1288 | 83.0457 | 18.5700 | 31.0574 | 61.1779 | 0.0842 | 41.89 | 2.3385 | 322.96 | 0.2079 | 49.71 | 618 | 40 | | |
| MU | mica (mx) | 103 | 23.2266 | 376.1740 | 91.2125 | 18.8780 | 29.4764 | 62.6358 | 0.1504 | 57.02 | 6.1399 | 521.38 | 0.2872 | 60.07 | 474 | 23 | | |
| MU | mica (mx) | 104 | 21.2201 | 262.7820 | 85.9847 | 18.5153 | 29.9785 | 64.2831 | 0.0905 | 43.50 | 4.1404 | 429.06 | 0.2426 | 58.22 | 410 | 25 | | |
| MU | mica (mx) | 105 | 22.3703 | 273.8498 | 87.7731 | 18.8979 | 27.8071 | 63.7043 | 0.1189 | 50.44 | 4.3743 | 440.93 | 0.2633 | 60.00 | 506 | 27 | | |
| MU | mica (mx) | 106 | 23.9142 | 446.9485 | 91.4376 | 18.5250 | 31.1267 | 62.2797 | 0.1885 | 64.19 | 7.3606 | 570.73 | 0.2932 | 60.71 | 505 | 22 | | |
| MU | mica (mx) | 107 | 21.5514 | 264.6099 | 84.6590 | 18.9368 | 30.0711 | 62.6581 | 0.0870 | 42.54 | 4.1654 | 430.05 | 0.2460 | 58.64 | 392 | 24 | | |
| MU | mica (mx) | 108 | 23.3266 | 370.6617 | 90.9123 | 18.5765 | 29.2390 | 61.3448 | 0.1654 | 60.00 | 6.0526 | 517.92 | 0.3099 | 63.72 | 521 | 24 | | |
| MU | mica (mx) | 109 | 22.6328 | 315.0224 | 87.8982 | 18.6720 | 30.3614 | 62.9030 | 0.1365 | 54.22 | 5.0488 | 473.14 | 0.2955 | 66.08 | 505 | 26 | | |
| MU | mica (mx) | 110 | 22.8953 | 340.0465 | 93.3762 | 19.1628 | 31.0331 | 61.6787 | 0.1280 | 52.38 | 5.4824 | 493.12 | 0.3416 | 67.84 | 433 | 22 | | |
| MU | mica (mx) | 111 | 22.1515 | 252.8917 | 87.0102 | 18.8406 | 30.2715 | 61.5229 | 0.1129 | 49.05 | 3.9538 | 418.99 | 0.2519 | 55.79 | 526 | 29 | | |
| MU | mica (mx) | 112 | 22.9453 | 316.4251 | 87.6355 | 18.9386 | 30.1408 | 63.4261 | 0.1382 | 54.58 | 5.0772 | 474.46 | 0.2632 | 59.81 | 518 | 26 | | |
| MU | mica (mx) | 113 | 24.0767 | 446.3970 | 92.4882 | 18.7607 | 31.0584 | 62.3353 | 0.1846 | 63.30 | 7.3055 | 566.79 | 0.3111 | 63.34 | 494 | 21 | | |
| MU | mica (mx) | 114 | 21.0826 | 247.8091 | 86.8851 | 18.3981 | 27.6469 | 61.6119 | 0.0895 | 43.18 | 3.9063 | 416.26 | 0.2640 | 58.71 | 419 | 25 | | |
| MU | mica (mx) | 115 | 22.1765 | 257.7491 | 85.6220 | 18.1510 | 29.2660 | 62.5023 | 0.1394 | 54.93 | 4.0605 | 424.74 | 0.2397 | 55.74 | 638 | 33 | 506 ± 17 | 86 |
| TH | bt | 1 | 21.4951 | 290.4779 | 111.0620 | 17.9545 | 26.6563 | 63.7043 | 0.1350 | 56.72 | 5.0287 | 489.52 | 0.6281 | 102.04 | 426 | 23 | | |
| TH | bt | 2 | 20.3887 | 216.5406 | 101.5684 | 16.9590 | 26.5227 | 61.3782 | 0.1306 | 55.75 | 3.6223 | 415.49 | 0.4825 | 85.09 | 558 | 31 | | |
| TH | bt | 4 | 20.2637 | 228.7569 | 102.2689 | 16.6162 | 26.9015 | 62.9141 | 0.1404 | 58.12 | 3.8710 | 430.80 | 0.4940 | 88.04 | 568 | 30 | | |
| TH | bt | 5 | 22.6703 | 303.0002 | 115.7152 | 17.4595 | 28.2572 | 62.7137 | 0.2034 | 70.44 | 5.2414 | 499.98 | 0.6656 | 102.22 | 608 | 27 | | |
| TH | bt | 8 | 21.7202 | 251.3644 | 114.8145 | 17.4008 | 28.4834 | 60.4767 | 0.1682 | 63.98 | 4.2786 | 453.14 | 0.6770 | 102.68 | 575 | 28 | | |
| TH | bt | 9 | 21.8702 | 275.6778 | 108.5854 | 17.5792 | 28.8615 | 62.7137 | 0.1673 | 63.85 | 4.7492 | 477.97 | 0.5900 | 97.39 | 557 | 27 | | |
| TH | bt | 10 | 20.6638 | 217.7672 | 100.7179 | 16.8470 | 28.6310 | 62.1684 | 0.1487 | 60.17 | 3.6545 | 420.16 | 0.4878 | 87.84 | 627 | 33 | | |
| TH | bt | 11 | 19.6887 | 210.5079 | 101.0181 | 16.8957 | 26.3038 | 62.0905 | 0.1062 | 50.24 | 3.5604 | 414.78 | 0.4847 | 86.86 | 461 | 28 | | |
| TH | bt | 12 | 20.3200 | 236.6429 | 108.3477 | 16.6037 | 27.3890 | 62.8139 | 0.1434 | 58.81 | 4.0170 | 439.07 | 0.5927 | 98.20 | 536 | 28 | | |
| TH | bt | 13 | 19.3011 | 201.8472 | 103.5572 | 16.9852 | 27.3335 | 63.3704 | 0.0861 | 44.73 | 3.3634 | 402.56 | 0.5337 | 94.13 | 378 | 25 | | |
| TH | bt | 14 | 20.0137 | 247.2583 | 99.4046 | 16.6010 | 25.9330 | 61.6119 | 0.1319 | 56.45 | 4.2810 | 454.99 | 0.4849 | 88.19 | 501 | 27 | | |
| TH | bt | 16 | 20.7638 | 216.4404 | 105.2832 | 17.4504 | 28.7549 | 62.5468 | 0.1279 | 55.55 | 3.6321 | 419.19 | 0.5463 | 93.43 | 525 | 29 | | |
| TH | bt | 17 | 19.3261 | 197.9925 | 103.1444 | 16.9961 | 27.7054 | 62.0571 | 0.0869 | 45.01 | 3.2888 | 398.49 | 0.5229 | 91.21 | 390 | 25 | | |
| TH | bt | 18 | 20.3762 | 213.2363 | 106.9968 | 16.5929 | 28.3699 | 63.5040 | 0.1471 | 59.79 | 3.5685 | 414.98 | 0.5762 | 97.68 | 598 | 32 | | |
| TH | bt | 19 | 20.5075 | 202.3478 | 109.4609 | 16.7428 | 27.5107 | 62.0126 | 0.1462 | 59.57 | 3.3714 | 403.15 | 0.6122 | 99.37 | 603 | 32 | | |
| TH | bt | 20 | 20.2637 | 226.3786 | 109.7736 | 16.5206 | 28.4808 | 62.8918 | 0.1449 | 59.21 | 3.8079 | 427.99 | 0.6030 | 98.46 | 557 | 29 | | |
| TH | bt | 22 | 21.6264 | 280.1603 | 118.3420 | 16.8741 | 28.1810 | 63.3593 | 0.1868 | 67.74 | 4.8605 | 484.14 | 0.7350 | 110.82 | 571 | 27 | | |
| TH | bt | 24 | 21.4389 | 240.1479 | 111.3247 | 16.9277 | 26.4420 | 62.9586 | 0.1781 | 66.29 | 4.1453 | 448.35 | 0.6427 | 103.32 | 631 | 31 | | |
| TH | bt | 26 | 20.9826 | 257.1983 | 116.6158 | 16.5970 | 27.1561 | 65.8301 | 0.1719 | 64.89 | 4.4434 | 463.21 | 0.7018 | 110.10 | 566 | 28 | | |
| TH | bt | 27 | 20.5513 | 237.8947 | 113.0633 | 16.8762 | 27.5380 | 61.8345 | 0.1427 | 58.85 | 4.0644 | 443.09 | 0.6452 | 100.78 | 515 | 27 | | |

| Sample | Occluding phase | Label | Peak counts Pk(Pb) | Pk(Th) | Pk(U ) | Background counts Bg(Pb) | Bg(Th) | Bg(U ) | W%(Pb) | W%(Pb) 1σ | W%(Th) | W%(Th) 1σ | W%(U ) | W%(U ) 1σ | Chemical age (Ma) | 1σ | M2 age (Ma & error (2σ) | n = |
|---|---|---|---|---|---|---|---|---|---|---|---|---|---|---|---|---|---|---|
| TH | bt | 28 | 20.1825 | 212.9359 | 104.9580 | 16.7628 | 26.5074 | 61.3114 | 0.1319 | 56.39 | 3.5961 | 416.43 | 0.5262 | 89.05 | 551 | 30 | | |
| TH | bt | 29 | 20.7075 | 254.7195 | 101.8436 | 16.7748 | 28.9739 | 64.7505 | 0.1532 | 61.07 | 4.3616 | 458.99 | 0.5238 | 96.16 | 560 | 29 | | |
| TH | bt | 30 | 20.2637 | 251.2893 | 115.1147 | 17.1737 | 27.2501 | 63.5485 | 0.1182 | 53.16 | 4.3233 | 456.69 | 0.6703 | 104.36 | 406 | 23 | | |
| TH | bt | 31 | 20.0512 | 255.4206 | 111.2997 | 16.9579 | 28.6929 | 63.1144 | 0.1179 | 53.00 | 4.3633 | 458.18 | 0.6256 | 100.76 | 412 | 23 | | |
| TH | bt | 32 | 20.6450 | 238.8210 | 112.3003 | 16.7585 | 28.3430 | 63.6820 | 0.1514 | 60.71 | 4.0671 | 443.25 | 0.6501 | 104.24 | 544 | 28 | | |
| TH | bt | 34 | 21.2576 | 272.9233 | 117.9042 | 16.9870 | 28.3020 | 65.9191 | 0.1672 | 63.96 | 4.7268 | 477.85 | 0.7045 | 109.24 | 529 | 26 | | |
| TH | bt | 35 | 20.7888 | 288.9002 | 120.7312 | 16.2930 | 27.6380 | 59.6976 | 0.1769 | 65.96 | 5.0574 | 494.72 | 0.7332 | 104.93 | 528 | 25 | | |
| TH | bt | 36 | 20.2450 | 283.3156 | 116.6783 | 16.5310 | 28.1660 | 62.7360 | 0.1443 | 59.20 | 4.9355 | 488.54 | 0.7142 | 108.72 | 443 | 23 | | |
| TH | bt | 37 | 20.8326 | 257.0981 | 107.6848 | 16.8700 | 28.1833 | 62.5246 | 0.1542 | 61.24 | 4.4169 | 461.58 | 0.5752 | 95.70 | 544 | 28 | 529 ± 28 | 29 |
| TH | bt-fsp | 1 | 19.7949 | 274.8765 | 101.2307 | 16.6199 | 25.5135 | 62.2797 | 0.1222 | 54.22 | 4.8303 | 483.65 | 0.5038 | 90.25 | 422 | 24 | | |
| TH | bt-fsp | 2 | 20.8763 | 270.6946 | 101.0431 | 16.9653 | 27.9002 | 60.2652 | 0.1525 | 60.96 | 4.6956 | 476.48 | 0.4878 | 85.41 | 539 | 28 | | |
| TH | bt-fsp | 3 | 20.2512 | 273.0986 | 102.4565 | 16.1413 | 28.6953 | 63.1033 | 0.1601 | 62.43 | 4.7136 | 476.73 | 0.5208 | 92.82 | 555 | 28 | | |
| TH | bt-fsp | 4 | 19.9262 | 261.1795 | 102.3314 | 16.1917 | 28.4587 | 65.3960 | 0.1447 | 59.20 | 4.4877 | 465.13 | 0.5237 | 96.34 | 520 | 27 | | |
| TH | bt-fsp | 5 | 20.6700 | 252.5412 | 103.5071 | 16.3281 | 27.1645 | 63.9492 | 0.1701 | 64.54 | 4.3515 | 458.30 | 0.5397 | 95.94 | 616 | 31 | | |
| TH | bt-fsp | 6 | 20.4888 | 266.6131 | 101.5559 | 16.4842 | 27.3106 | 65.7856 | 0.1563 | 61.75 | 4.6232 | 472.54 | 0.5190 | 97.02 | 550 | 28 | | |
| TH | bt-fsp | 7 | 19.9262 | 254.3439 | 102.9318 | 17.0703 | 29.0200 | 67.5107 | 0.1088 | 50.90 | 4.3610 | 459.36 | 0.5293 | 99.43 | 400 | 24 | | |
| TH | bt-fsp | 8 | 21.1763 | 336.5895 | 111.0245 | 16.3903 | 28.4482 | 56.1474 | 0.1887 | 68.19 | 5.9615 | 536.97 | 0.6245 | 94.25 | 525 | 24 | | |
| TH | bt-fsp | 9 | 20.3825 | 286.1955 | 104.3076 | 16.3284 | 26.5889 | 65.5741 | 0.1582 | 62.12 | 5.0128 | 491.92 | 0.5577 | 100.19 | 515 | 26 | | |
| TH | bt-fsp | 10 | 19.8824 | 255.2954 | 99.8799 | 16.5169 | 28.9977 | 65.9748 | 0.1300 | 56.02 | 4.3790 | 460.26 | 0.4844 | 93.01 | 486 | 27 | | |
| TH | bt-fsp | 11 | 20.3200 | 275.1770 | 102.5941 | 16.6762 | 26.1233 | 74.5451 | 0.1413 | 58.52 | 4.8114 | 482.05 | 0.5199 | 109.75 | 484 | 26 | | |
| TH | bt-fsp | 12 | 19.7574 | 246.7575 | 104.4952 | 16.5293 | 27.5921 | 65.1957 | 0.1247 | 54.87 | 4.2538 | 454.32 | 0.5538 | 98.77 | 459 | 26 | | |
| TH | bt-fsp | 13 | 19.6574 | 251.4646 | 101.5059 | 16.6751 | 26.3830 | 64.4611 | 0.1144 | 52.37 | 4.3708 | 460.64 | 0.5227 | 96.02 | 421 | 24 | | |
| TH | bt-fsp | 14 | 20.0450 | 274.7262 | 102.9318 | 16.6861 | 27.4700 | 62.8473 | 0.1288 | 55.56 | 4.7556 | 478.19 | 0.5302 | 93.63 | 443 | 24 | | |
| TH | bt-fsp | 15 | 20.9451 | 286.1204 | 101.8186 | 17.2545 | 27.8689 | 64.9286 | 0.1427 | 58.72 | 4.9764 | 489.63 | 0.5262 | 96.86 | 475 | 25 | | |
| TH | bt-fsp | 16 | 20.3512 | 246.0815 | 102.6191 | 16.4812 | 28.5644 | 65.3404 | 0.1507 | 60.56 | 4.1992 | 450.18 | 0.5340 | 97.78 | 563 | 29 | | |
| TH | bt-fsp | 17 | 19.5386 | 279.4591 | 107.4596 | 15.4161 | 25.6484 | 66.2530 | 0.1615 | 62.88 | 4.9342 | 489.70 | 0.6031 | 105.04 | 521 | 26 | | |
| TH | bt-fsp | 18 | 18.7823 | 226.6540 | 95.2522 | 16.3544 | 26.7998 | 63.3259 | 0.0911 | 46.22 | 3.8769 | 433.61 | 0.4693 | 92.86 | 377 | 24 | | |
| TH | bt-fsp | 20 | 20.9451 | 264.1341 | 100.4428 | 16.6626 | 26.6551 | 63.8379 | 0.1680 | 64.18 | 4.5925 | 471.20 | 0.5152 | 95.21 | 594 | 30 | | |
| TH | bt-fsp | 21 | 20.2200 | 287.6981 | 110.1364 | 15.8941 | 26.1965 | 64.1161 | 0.1695 | 64.43 | 5.0641 | 495.15 | 0.6650 | 109.60 | 521 | 26 | | |
| TH | bt-fsp | 23 | 19.2511 | 205.8521 | 98.8543 | 16.1489 | 26.7003 | 64.0159 | 0.1194 | 53.59 | 3.4778 | 410.83 | 0.4822 | 91.34 | 526 | 31 | | |
| TH | bt-fsp | 24 | 20.6138 | 256.1967 | 104.7329 | 16.4644 | 26.7999 | 63.3481 | 0.1631 | 63.30 | 4.4526 | 464.83 | 0.5461 | 94.91 | 580 | 29 | | |
| TH | bt-fsp | 25 | 20.5450 | 282.9650 | 106.6841 | 17.0366 | 27.3459 | 63.3481 | 0.1359 | 57.36 | 4.9455 | 489.08 | 0.5867 | 99.64 | 442 | 24 | | |
| TH | bt-fsp | 26 | 20.7263 | 260.9291 | 98.8793 | 16.3222 | 27.7086 | 63.0588 | 0.1731 | 65.21 | 4.5131 | 467.26 | 0.4779 | 89.27 | 631 | 31 | | |
| TH | bt-fsp | 27 | 20.3700 | 244.6294 | 96.3403 | 17.0577 | 28.1923 | 63.8601 | 0.1277 | 55.47 | 4.1828 | 449.54 | 0.4300 | 84.36 | 509 | 28 | | |
| TH | bt-fsp | 28 | 20.3450 | 227.8056 | 101.5434 | 17.2000 | 27.1581 | 64.0493 | 0.1211 | 53.99 | 3.8885 | 434.05 | 0.5209 | 95.11 | 483 | 28 | | |
| TH | bt-fsp | 29 | 20.0575 | 236.4676 | 104.2326 | 16.8040 | 28.0405 | 65.3849 | 0.1256 | 55.05 | 4.0398 | 442.44 | 0.5432 | 97.44 | 482 | 27 | | |
| TH | bt-fsp | 30 | 19.3324 | 210.6831 | 102.9568 | 16.9694 | 27.0022 | 63.5262 | 0.0887 | 45.62 | 3.5721 | 416.74 | 0.5258 | 93.62 | 376 | 24 | | |
| TH | bt-fsp | 31 | 20.3325 | 203.6243 | 103.1944 | 16.8706 | 27.8586 | 61.9903 | 0.1345 | 57.15 | 3.4106 | 406.76 | 0.5274 | 91.86 | 581 | 32 | | |
| TH | bt-fsp | 32 | 20.2012 | 215.6394 | 104.6453 | 17.3736 | 26.4388 | 64.0605 | 0.1084 | 50.96 | 3.6846 | 423.54 | 0.5524 | 96.95 | 441 | 26 | | |
| TH | bt-fsp | 33 | 20.2950 | 222.1229 | 100.1051 | 16.7727 | 27.1786 | 62.3576 | 0.1370 | 57.71 | 3.7823 | 428.32 | 0.4886 | 88.91 | 566 | 31 | | |
| TH | bt-fsp | 34 | 20.3512 | 248.9107 | 99.6923 | 16.4771 | 27.2650 | 62.6358 | 0.1516 | 60.89 | 4.3000 | 456.68 | 0.4765 | 87.52 | 575 | 30 | | |
| TH | bt-fsp | 35 | 19.8074 | 235.4913 | 107.4221 | 16.2837 | 28.1619 | 64.2051 | 0.1375 | 57.91 | 4.0367 | 443.27 | 0.5676 | 96.53 | 519 | 28 | | |
| TH | bt-fsp | 36 | 19.8949 | 212.0849 | 106.4590 | 16.9506 | 28.4522 | 63.4817 | 0.1129 | 52.02 | 3.5658 | 416.06 | 0.5810 | 99.09 | 461 | 27 | | |
| TH | bt-fsp | 37 | 22.1952 | 360.8903 | 122.1948 | 17.1750 | 27.3467 | 63.0810 | 0.1984 | 70.00 | 6.4596 | 559.24 | 0.7742 | 112.58 | 492 | 22 | | |
| TH | bt-fsp | 38 | 21.0826 | 293.0825 | 111.5999 | 16.5049 | 26.8144 | 63.6153 | 0.1796 | 66.36 | 5.1430 | 498.34 | 0.6543 | 105.60 | 548 | 26 | | |
| TH | bt-fsp | 39 | 21.3951 | 296.2631 | 112.3504 | 16.3641 | 26.1419 | 64.6837 | 0.1991 | 70.18 | 5.2277 | 502.92 | 0.6558 | 106.20 | 599 | 28 | | |
| TH | bt-fsp | 40 | 20.2200 | 265.2359 | 97.8287 | 16.4350 | 25.9181 | 62.8028 | 0.1474 | 59.90 | 4.6337 | 473.60 | 0.4458 | 84.22 | 538 | 28 | | |
| TH | bt-fsp | 41 | 21.5451 | 295.2363 | 108.0975 | 17.8064 | 26.6878 | 65.0733 | 0.1455 | 59.49 | 5.2044 | 502.15 | 0.5900 | 100.57 | 455 | 24 | | |
| TH | bt-fsp | 43 | 19.8949 | 265.9620 | 100.1176 | 16.5848 | 28.6191 | 63.7933 | 0.1279 | 55.58 | 4.6003 | 472.14 | 0.5028 | 93.27 | 457 | 25 | | |
| TH | bt-fsp | 44 | 20.8326 | 261.6302 | 97.2784 | 18.0060 | 27.4547 | 63.9269 | 0.1075 | 50.55 | 4.5304 | 468.10 | 0.4706 | 91.11 | 396 | 24 | | |
| TH | bt-fsp | 45 | 22.3015 | 389.0285 | 126.7232 | 16.5059 | 27.6049 | 62.3465 | 0.2292 | 75.27 | 6.9635 | 579.15 | 0.8525 | 118.79 | 523 | 22 | | |
| TH | bt-fsp | 46 | 21.3139 | 310.5891 | 110.1989 | 16.4400 | 25.8102 | 63.6932 | 0.1928 | 69.04 | 5.5279 | 517.94 | 0.6622 | 108.57 | 557 | 26 | | |
| TH | bt-fsp | 47 | 19.5136 | 230.9099 | 101.5935 | 16.5418 | 27.2286 | 64.7171 | 0.1141 | 52.33 | 3.9539 | 438.05 | 0.5079 | 93.51 | 454 | 27 | | |

| Sample | Occluding phase | Label | Peak counts Pk(Pb) | Pk(Th) | Pk(U ) | Background counts Bg(Pb) | Bg(Th) | Bg(U ) | W%(Pb) | W%(Pb) 1σ | W%(Th) | W%(Th) 1σ | W%(U ) | W%(U ) 1σ | Chemical age (Ma) | 1σ | M2 age (Ma & error (2σ) | n = |
|---|---|---|---|---|---|---|---|---|---|---|---|---|---|---|---|---|---|---|
| TH | bt-fsp | 48 | 19.7387 | 237.2187 | 98.6792 | 16.1876 | 28.5882 | 64.3164 | 0.1373 | 57.60 | 4.0253 | 440.64 | 0.4876 | 93.00 | 543 | 30 | | |
| TH | bt-fsp | 49 | 19.6574 | 243.8282 | 99.7048 | 16.9968 | 26.2168 | 63.8601 | 0.1010 | 48.95 | 4.2250 | 452.85 | 0.4839 | 90.36 | 389 | 24 | | |
| TH | bt-fsp | 50 | 20.4763 | 257.2734 | 99.3171 | 17.4960 | 28.2191 | 62.3799 | 0.1140 | 52.21 | 4.4363 | 463.47 | 0.4965 | 91.34 | 421 | 24 | | |
| TH | bt-fsp | 51 | 20.5263 | 252.6664 | 92.2630 | 16.4792 | 26.6574 | 64.5836 | 0.1588 | 62.40 | 4.3941 | 462.14 | 0.4123 | 87.62 | 613 | 32 | 503 ± 21 | 48 |
| TH | Kfsp | 52 | 21.8452 | 307.5836 | 113.1009 | 16.8557 | 27.1149 | 64.5613 | 0.1981 | 70.11 | 5.4506 | 514.60 | 0.6708 | 107.65 | 575 | 26 | | |
| TH | Kfsp | 53 | 21.5576 | 306.6318 | 114.5894 | 16.5988 | 28.1687 | 64.0716 | 0.1963 | 69.69 | 5.3959 | 511.27 | 0.6696 | 105.33 | 575 | 26 | | |
| TH | Kfsp | 54 | 20.3762 | 251.7400 | 104.2576 | 17.4735 | 27.6646 | 62.9475 | 0.1108 | 51.41 | 4.3394 | 458.36 | 0.5466 | 95.08 | 405 | 24 | | |
| TH | Kfsp | 55 | 21.2013 | 268.4660 | 103.6447 | 16.3820 | 27.8687 | 64.4166 | 0.1905 | 68.60 | 4.6599 | 475.01 | 0.5458 | 97.43 | 654 | 31 | | |
| TH | Kfsp | 56 | 20.3075 | 232.4370 | 100.0050 | 17.1869 | 26.4259 | 63.0254 | 0.1196 | 53.52 | 3.9817 | 438.62 | 0.4777 | 87.83 | 481 | 28 | | |
| TH | Kfsp | 57 | 21.1451 | 273.0234 | 101.2683 | 16.4784 | 25.6277 | 63.2591 | 0.1829 | 66.93 | 4.7643 | 478.93 | 0.5123 | 92.90 | 629 | 30 | | |
| TH | Kfsp | 58 | 21.4639 | 305.0289 | 108.2476 | 17.0085 | 26.7183 | 63.4928 | 0.1744 | 65.32 | 5.3672 | 508.69 | 0.5835 | 97.52 | 533 | 26 | | |
| TH | Kfsp | 59 | 20.7825 | 240.9741 | 100.6429 | 17.1799 | 26.8103 | 62.8584 | 0.1401 | 58.35 | 4.1511 | 448.50 | 0.5075 | 92.31 | 536 | 29 | | |
| TH | Kfsp | 60 | 20.7638 | 273.7747 | 105.2332 | 17.0552 | 28.4453 | 65.1401 | 0.1447 | 59.40 | 4.7641 | 480.92 | 0.5603 | 98.93 | 489 | 26 | | |
| TH | Kfsp | 62 | 22.4703 | 381.1353 | 121.0564 | 16.8985 | 27.6518 | 63.3481 | 0.2198 | 73.62 | 6.8008 | 571.93 | 0.7539 | 110.96 | 528 | 23 | | |
| TH | Kfsp | 63 | 22.6703 | 409.4022 | 129.4628 | 16.7963 | 27.5406 | 59.7199 | 0.2325 | 75.84 | 7.3595 | 595.48 | 0.8974 | 120.14 | 503 | 21 | | |
| TH | Kfsp | 64 | 22.7766 | 373.9941 | 125.1345 | 16.8840 | 26.7569 | 60.2652 | 0.2332 | 75.95 | 6.6869 | 567.39 | 0.8304 | 115.27 | 551 | 23 | | |
| TH | Kfsp | 65 | 20.4513 | 267.8400 | 101.5434 | 16.5637 | 28.8021 | 57.7389 | 0.1514 | 60.71 | 4.6190 | 472.37 | 0.5177 | 87.45 | 534 | 27 | | |
| TH | Kfsp | 66 | 21.6514 | 365.2498 | 118.9424 | 16.6482 | 26.7832 | 59.8423 | 0.1964 | 69.42 | 6.5102 | 559.51 | 0.7261 | 105.60 | 493 | 22 | | |
| TH | Kfsp | 67 | 24.2455 | 429.7283 | 131.2767 | 17.2736 | 28.7751 | 60.6993 | 0.2763 | 82.73 | 7.6915 | 607.34 | 0.8859 | 117.90 | 579 | 22 | | |
| TH | Kfsp | 68 | 24.1580 | 453.7418 | 134.7920 | 16.7229 | 27.7761 | 59.9759 | 0.2951 | 85.56 | 8.1713 | 626.00 | 0.9488 | 122.64 | 581 | 22 | | |
| TH | Kfsp | 69 | 20.9951 | 298.7926 | 109.2108 | 16.5387 | 28.0552 | 58.8963 | 0.1748 | 65.46 | 5.2278 | 502.36 | 0.6132 | 96.65 | 538 | 26 | | |
| TH | Kfsp | 70 | 21.0076 | 281.5626 | 104.4577 | 16.9326 | 27.8891 | 59.2079 | 0.1585 | 62.07 | 4.8830 | 484.75 | 0.5415 | 90.00 | 530 | 27 | | |
| TH | Kfsp | 71 | 21.8827 | 364.1724 | 121.0564 | 17.2984 | 27.8809 | 59.1412 | 0.1796 | 66.31 | 6.4867 | 559.29 | 0.7814 | 111.03 | 444 | 21 | | |
| TH | Kfsp | 73 | 21.9890 | 343.5788 | 117.8041 | 17.3425 | 26.7626 | 59.3192 | 0.1809 | 66.35 | 6.0652 | 538.78 | 0.7198 | 105.23 | 479 | 22 | | |
| TH | Kfsp | 74 | 22.0577 | 358.5603 | 117.2537 | 16.7004 | 28.4341 | 59.1300 | 0.2107 | 71.97 | 6.3458 | 552.23 | 0.7196 | 105.53 | 539 | 24 | | |
| TH | Kfsp | 75 | 22.1890 | 326.2440 | 112.5880 | 17.4102 | 26.8958 | 63.3370 | 0.1880 | 67.99 | 5.7804 | 528.25 | 0.6593 | 105.03 | 527 | 25 | | |
| TH | Kfsp | 76 | 21.5264 | 293.3579 | 107.1594 | 17.2469 | 28.3263 | 60.9887 | 0.1673 | 63.94 | 5.1142 | 496.71 | 0.5783 | 95.15 | 531 | 26 | | |
| TH | Kfsp | 77 | 21.4639 | 301.8731 | 108.6104 | 16.5988 | 29.0121 | 59.5196 | 0.1912 | 68.53 | 5.2576 | 503.25 | 0.6083 | 97.07 | 586 | 27 | | |
| TH | Kfsp | 78 | 20.1387 | 250.0875 | 99.0794 | 16.9283 | 25.7390 | 60.7549 | 0.1227 | 54.14 | 4.3156 | 455.56 | 0.4687 | 84.65 | 468 | 26 | | |
| TH | Kfsp | 79 | 21.4701 | 338.5685 | 114.8396 | 16.7866 | 27.9763 | 52.8977 | 0.1832 | 66.92 | 5.9713 | 535.73 | 0.6688 | 95.01 | 500 | 23 | | |
| TH | Kfsp | 80 | 20.8763 | 263.0074 | 104.8830 | 16.8228 | 28.4555 | 59.5641 | 0.1572 | 61.73 | 4.5039 | 464.99 | 0.5295 | 87.94 | 560 | 28 | | |
| TH | Kfsp | 81 | 21.0513 | 246.8577 | 101.3933 | 17.0213 | 27.8023 | 59.3304 | 0.1563 | 61.55 | 4.2065 | 449.38 | 0.4831 | 83.28 | 599 | 31 | | |
| TH | Kfsp | 82 | 21.0451 | 264.5598 | 100.3927 | 16.7383 | 27.5451 | 61.0777 | 0.1673 | 63.73 | 4.5419 | 466.47 | 0.5001 | 89.17 | 601 | 30 | | |
| TH | Kfsp | 83 | 21.6139 | 351.5453 | 115.9653 | 16.7472 | 28.5057 | 60.1985 | 0.1892 | 67.80 | 6.1608 | 541.97 | 0.6831 | 102.27 | 502 | 23 | | |
| TH | Kfsp | 84 | 21.0326 | 259.8774 | 102.4440 | 16.7519 | 27.5793 | 60.6770 | 0.1668 | 63.74 | 4.4640 | 463.10 | 0.5104 | 88.30 | 603 | 30 | | |
| TH | Kfsp | 85 | 22.6890 | 330.7028 | 110.3865 | 17.3137 | 28.3195 | 64.2831 | 0.2104 | 71.74 | 5.7874 | 526.23 | 0.6442 | 106.07 | 591 | 26 | | |
| TH | Kfsp | 86 | 21.0638 | 257.7491 | 104.9831 | 16.8342 | 26.6967 | 68.0561 | 0.1645 | 63.23 | 4.4376 | 461.60 | 0.5428 | 99.87 | 588 | 30 | | |
| TH | Kfsp | 87 | 20.9201 | 254.9198 | 103.9574 | 16.6997 | 27.9023 | 65.8301 | 0.1643 | 63.23 | 4.3609 | 457.63 | 0.5363 | 97.11 | 596 | 30 | | |
| TH | Kfsp | 88 | 20.2387 | 239.9476 | 103.1694 | 16.9064 | 27.5048 | 65.3849 | 0.1275 | 55.22 | 4.0765 | 442.22 | 0.5257 | 95.62 | 490 | 27 | | |
| TH | Kfsp | 89 | 20.8451 | 227.5302 | 102.3314 | 17.0783 | 27.9309 | 70.7941 | 0.1455 | 59.27 | 3.8320 | 428.86 | 0.5053 | 100.60 | 589 | 32 | | |
| TH | Kfsp | 90 | 22.0577 | 369.3087 | 118.5171 | 17.0754 | 26.4945 | 64.8729 | 0.1939 | 68.68 | 6.5422 | 558.68 | 0.7122 | 108.72 | 487 | 22 | | |
| TH | Kfsp | 91 | 21.1701 | 294.0842 | 116.8034 | 17.2870 | 28.2949 | 66.3977 | 0.1494 | 59.94 | 5.0791 | 492.59 | 0.7077 | 111.45 | 451 | 23 | | |
| TH | Kfsp | 92 | 21.3951 | 264.8102 | 108.7730 | 17.0744 | 27.0617 | 65.7967 | 0.1686 | 64.12 | 4.5720 | 468.83 | 0.5945 | 101.39 | 574 | 28 | | |
| TH | Kfsp | 93 | 19.9887 | 242.1007 | 100.7930 | 17.0304 | 26.9707 | 66.2085 | 0.1121 | 51.53 | 4.1280 | 445.00 | 0.4958 | 94.26 | 436 | 26 | | |
| TH | Kfsp | 95 | 21.6514 | 279.6594 | 108.6229 | 16.7702 | 28.5134 | 66.0527 | 0.1902 | 68.06 | 4.7919 | 478.10 | 0.5765 | 98.79 | 631 | 30 | | |
| TH | Kfsp | 96 | 20.5763 | 286.6212 | 110.1864 | 16.7415 | 27.0759 | 64.8952 | 0.1470 | 59.35 | 4.9436 | 485.18 | 0.6151 | 102.19 | 472 | 24 | | |
| TH | Kfsp | 97 | 20.6700 | 240.9491 | 102.6066 | 16.6399 | 27.6018 | 65.0176 | 0.1562 | 61.51 | 4.0923 | 442.99 | 0.5082 | 92.67 | 602 | 31 | | |
| TH | Kfsp | 98 | 20.7825 | 260.2030 | 99.2420 | 17.5636 | 26.0592 | 65.7299 | 0.1221 | 53.80 | 4.4690 | 461.78 | 0.4579 | 88.44 | 457 | 26 | | |
| TH | Kfsp | 99 | 21.0076 | 257.7491 | 99.9299 | 16.9349 | 28.4521 | 65.8524 | 0.1565 | 61.31 | 4.3638 | 455.65 | 0.4702 | 90.05 | 588 | 30 | 539 ± 19 | 45 |
| KY2 | kyanite | 16 | 19.6574 | 208.7807 | 89.8367 | 17.4242 | 27.6421 | 65.8301 | 0.0756 | 39.99 | 3.3253 | 390.66 | 0.2976 | 67.91 | 394 | 26 | | |
| KY2 | kyanite | 17 | 22.2765 | 189.8831 | 87.1978 | 18.5898 | 29.1957 | 64.1050 | 0.1318 | 54.27 | 2.9616 | 369.41 | 0.2868 | 66.73 | 745 | 41 | | |
| KY2 | kyanite | 18 | 21.4389 | 206.9034 | 85.7721 | 18.3802 | 26.1460 | 61.8345 | 0.1075 | 48.59 | 3.3282 | 391.41 | 0.2976 | 68.01 | 555 | 33 | | |
| KY2 | kyanite | 19 | 22.3515 | 196.2655 | 88.9737 | 19.1669 | 27.8023 | 61.3114 | 0.1126 | 49.88 | 3.1117 | 379.07 | 0.3447 | 73.27 | 589 | 34 | | |

| Sample | Occluding phase | Label | Peak counts Pk(Pb) | Pk(Th) | Pk(U ) | Background counts Bg(Pb) | Bg(Th) | Bg(U ) | W%(Pb) | W%(Pb) 1σ | W%(Th) | W%(Th) 1σ | W%(U ) | W%(U ) 1σ | Chemical age (Ma) | 1σ | M2 age (Ma & error (2σ) | n = |
|---|---|---|---|---|---|---|---|---|---|---|---|---|---|---|---|---|---|---|
| KY2 | kyanite | 20 | 20.7763 | 134.8796 | 89.6991 | 18.2713 | 29.4463 | 64.7505 | 0.0864 | 43.16 | 1.9424 | 299.10 | 0.3078 | 68.90 | 648 | 43 | | |
| KY2 | kyanite | 21 | 20.4575 | 150.0675 | 85.8971 | 18.0440 | 28.3985 | 63.5485 | 0.0827 | 42.08 | 2.2396 | 321.03 | 0.2761 | 65.30 | 584 | 39 | | |
| KY2 | kyanite | 22 | 19.8387 | 141.4100 | 88.9487 | 17.9519 | 26.0605 | 63.1144 | 0.0626 | 36.03 | 2.1255 | 312.91 | 0.3192 | 70.21 | 441 | 33 | | |
| KY2 | kyanite | 23 | 20.6950 | 124.2713 | 87.2478 | 18.4161 | 28.3740 | 63.6820 | 0.0779 | 40.80 | 1.7711 | 285.96 | 0.2913 | 67.09 | 633 | 44 | | |
| KY2 | kyanite | 24 | 22.0827 | 131.7020 | 97.9913 | 19.1900 | 29.9694 | 65.9191 | 0.1018 | 47.32 | 1.8825 | 295.10 | 0.3974 | 78.45 | 705 | 44 | | |
| KY2 | kyanite | 28 | 21.5951 | 200.8459 | 93.6888 | 17.7775 | 26.8603 | 62.5246 | 0.1364 | 55.19 | 3.1973 | 383.26 | 0.3865 | 77.41 | 676 | 36 | | |
| KY2 | kyanite | 29 | 19.6262 | 151.9943 | 81.4949 | 17.3414 | 27.4689 | 62.2797 | 0.0778 | 40.69 | 2.2895 | 324.40 | 0.2371 | 60.47 | 564 | 39 | | |
| KY2 | kyanite | 31 | 19.7137 | 186.6044 | 86.3349 | 17.3050 | 27.0531 | 59.7199 | 0.0881 | 44.88 | 3.1101 | 389.31 | 0.3524 | 76.37 | 461 | 30 | | |
| KY2 | kyanite | 31 | 20.0762 | 87.2478 | 85.8721 | 18.5530 | 28.1452 | 63.1033 | 0.0490 | 31.39 | 1.0947 | 225.14 | 0.2811 | 65.86 | 541 | 46 | | |
| KY2 | kyanite | 32 | 19.4949 | 208.1799 | 86.2723 | 17.5522 | 26.7402 | 60.2652 | 0.0690 | 39.14 | 3.5321 | 414.61 | 0.3449 | 75.61 | 332 | 24 | | |
| KY2 | kyanite | 32 | 20.6388 | 88.2984 | 92.9509 | 19.1472 | 27.2135 | 65.3960 | 0.0476 | 30.81 | 1.1288 | 228.36 | 0.3394 | 72.29 | 475 | 40 | | |
| KY2 | kyanite | 33 | 21.3514 | 262.8571 | 84.1963 | 17.9044 | 26.5734 | 57.7389 | 0.1300 | 55.36 | 4.6060 | 473.78 | 0.3537 | 76.88 | 503 | 27 | | |
| KY2 | kyanite | 33 | 20.9263 | 102.3564 | 87.6105 | 19.1168 | 29.6244 | 63.9492 | 0.0598 | 35.14 | 1.3429 | 248.97 | 0.2916 | 67.02 | 578 | 45 | | |
| KY2 | kyanite | 34 | 20.0887 | 227.5302 | 86.2848 | 17.3907 | 25.7865 | 59.8423 | 0.0997 | 47.99 | 3.9298 | 437.46 | 0.3516 | 76.45 | 438 | 27 | | |
| KY2 | kyanite | 34 | 19.8012 | 80.7696 | 83.7460 | 18.6723 | 29.4348 | 65.7856 | 0.0335 | 24.93 | 0.9463 | 208.83 | 0.2206 | 58.20 | 449 | 44 | | |
| KY2 | kyanite | 35 | 19.4574 | 81.9952 | 81.6450 | 18.4602 | 27.7296 | 67.5107 | 0.0283 | 22.40 | 0.9985 | 214.32 | 0.1733 | 51.54 | 405 | 42 | | |
| KY2 | kyanite | 35 | 20.4513 | 243.3525 | 87.4354 | 16.9812 | 27.9263 | 60.6993 | 0.1310 | 55.60 | 4.1927 | 451.66 | 0.3557 | 76.91 | 544 | 30 | | |
| KY2 | kyanite | 36 | 19.8324 | 218.1427 | 86.4099 | 17.3924 | 26.0598 | 59.9759 | 0.0894 | 45.25 | 3.7479 | 427.58 | 0.3517 | 76.48 | 408 | 26 | | |
| KY2 | kyanite | 37 | 19.6637 | 184.3519 | 89.1113 | 17.6129 | 27.6380 | 58.8963 | 0.0737 | 40.69 | 3.0581 | 386.25 | 0.4003 | 81.42 | 378 | 26 | | |
| KY2 | kyanite | 37 | 20.6013 | 95.9776 | 72.2156 | 19.0280 | 24.8676 | 56.1474 | 0.0508 | 32.02 | 1.3193 | 247.37 | 0.1993 | 55.59 | 572 | 48 | | |
| KY2 | kyanite | 38 | 22.3015 | 411.5074 | 101.9061 | 17.0977 | 25.8638 | 59.2079 | 0.2000 | 69.31 | 7.4839 | 602.57 | 0.5778 | 98.86 | 476 | 21 | | |
| KY2 | kyanite | 39 | 20.8138 | 243.3025 | 83.9086 | 17.5538 | 26.8613 | 59.1412 | 0.1220 | 53.42 | 4.2057 | 452.00 | 0.3293 | 73.98 | 514 | 29 | | |
| KY2 | kyanite | 40 | 20.2450 | 224.6012 | 81.3949 | 17.2862 | 26.7278 | 59.3192 | 0.1098 | 50.46 | 3.8423 | 431.88 | 0.2927 | 69.65 | 509 | 30 | | |
| KY2 | kyanite | 41 | 19.6887 | 171.2630 | 79.4189 | 17.1480 | 25.1902 | 59.1300 | 0.0930 | 46.13 | 2.8383 | 371.32 | 0.2676 | 66.42 | 557 | 36 | | |
| KY2 | kyanite | 42 | 19.8387 | 78.1933 | 83.1833 | 18.6144 | 28.5093 | 65.5741 | 0.0371 | 26.51 | 0.9154 | 205.34 | 0.2161 | 57.58 | 509 | 48 | | |
| KY2 | kyanite | 44 | 22.4328 | 380.5590 | 105.9462 | 17.1161 | 28.3556 | 60.9887 | 0.2048 | 70.22 | 6.8367 | 576.00 | 0.6061 | 101.06 | 517 | 23 | | |
| KY2 | kyanite | 45 | 21.5951 | 286.7214 | 90.7247 | 17.1425 | 26.7474 | 59.5196 | 0.1700 | 63.69 | 5.0449 | 494.72 | 0.4164 | 83.34 | 589 | 29 | | |
| KY2 | kyanite | 45 | 20.8075 | 84.1462 | 85.8346 | 19.1310 | 29.1149 | 65.9748 | 0.0545 | 33.28 | 1.0144 | 216.21 | 0.2440 | 61.21 | 664 | 55 | | |
| KY2 | kyanite | 46 | 19.1073 | 107.1344 | 100.3427 | 17.3449 | 28.5810 | 74.5451 | 0.0577 | 34.36 | 1.4461 | 257.98 | 0.3174 | 69.87 | 517 | 40 | | |
| KY2 | kyanite | 46 | 19.1011 | 188.5065 | 82.6705 | 16.1611 | 24.3865 | 55.9248 | 0.1104 | 50.90 | 3.2340 | 399.14 | 0.3592 | 77.65 | 557 | 34 | | |
| KY2 | kyanite | 47 | 20.4888 | 233.5385 | 81.8201 | 17.4952 | 25.5395 | 60.7549 | 0.1112 | 50.81 | 4.0389 | 442.79 | 0.2796 | 68.11 | 500 | 29 | | |
| KY2 | kyanite | 49 | 21.1013 | 142.7861 | 100.9431 | 19.2298 | 29.7419 | 65.1957 | 0.0622 | 35.94 | 2.0880 | 310.51 | 0.4428 | 82.80 | 394 | 29 | | |
| KY2 | kyanite | 50 | 22.0452 | 293.2578 | 88.3234 | 17.0849 | 26.4075 | 59.5641 | 0.1894 | 67.23 | 5.1533 | 498.79 | 0.3822 | 79.68 | 655 | 31 | | |
| KY2 | kyanite | 51 | 20.3262 | 211.7094 | 93.8389 | 17.6286 | 25.7105 | 59.3304 | 0.0990 | 47.65 | 3.5999 | 417.35 | 0.4552 | 86.64 | 435 | 27 | | |
| KY2 | kyanite | 51 | 22.2702 | 249.6368 | 100.3677 | 18.7164 | 27.9833 | 64.4611 | 0.1261 | 52.88 | 4.0719 | 432.44 | 0.4475 | 83.50 | 507 | 27 | | |
| KY2 | kyanite | 52 | 20.4825 | 212.3602 | 98.6542 | 18.2963 | 28.9097 | 62.8473 | 0.0740 | 39.57 | 3.3780 | 394.34 | 0.4455 | 83.24 | 344 | 23 | | |
| KY2 | kyanite | 52 | 20.6325 | 184.8775 | 96.6780 | 17.5422 | 27.0498 | 61.0777 | 0.1152 | 51.81 | 3.0600 | 385.12 | 0.4687 | 87.83 | 557 | 33 | | |
| KY2 | kyanite | 53 | 20.0887 | 115.9403 | 97.5035 | 18.7132 | 28.5750 | 64.9286 | 0.0430 | 28.99 | 1.6100 | 272.35 | 0.4013 | 78.61 | 331 | 28 | | |
| KY2 | kyanite | 53 | 19.1699 | 132.4526 | 86.0472 | 17.4450 | 26.9382 | 60.1985 | 0.0599 | 36.06 | 2.0438 | 314.60 | 0.3378 | 74.28 | 426 | 33 | | |
| KY2 | kyanite | 54 | 20.0387 | 111.4873 | 95.7775 | 18.3802 | 31.0362 | 65.3404 | 0.0539 | 33.09 | 1.4822 | 261.28 | 0.3745 | 75.89 | 445 | 35 | | |
| KY2 | kyanite | 54 | 20.4012 | 201.4467 | 86.3349 | 17.4557 | 26.9792 | 60.6770 | 0.1091 | 50.26 | 3.3773 | 404.28 | 0.3379 | 74.58 | 541 | 32 | | |
| KY2 | kyanite | 55 | 20.8826 | 99.6298 | 90.9748 | 19.0249 | 28.5056 | 66.2530 | 0.0615 | 35.67 | 1.3118 | 245.94 | 0.3044 | 68.45 | 591 | 46 | | |
| KY2 | kyanite | 59 | 20.2512 | 116.8409 | 81.7575 | 18.2469 | 27.0641 | 63.3259 | 0.0670 | 37.41 | 1.6505 | 275.43 | 0.2267 | 59.04 | 620 | 46 | | |
| KY2 | kyanite | 60 | 20.2262 | 120.5686 | 83.0332 | 18.2322 | 28.8609 | 63.8379 | 0.0665 | 37.23 | 1.6840 | 278.04 | 0.2358 | 60.17 | 601 | 45 | | |
| KY2 | kyanite | 61 | 20.0075 | 122.4950 | 94.0140 | 18.0231 | 27.9512 | 64.1161 | 0.0664 | 37.26 | 1.7420 | 283.27 | 0.3685 | 75.35 | 502 | 37 | | |
| KY2 | kyanite | 62 | 20.0012 | 81.6200 | 88.2108 | 18.7826 | 28.3633 | 64.0159 | 0.0370 | 26.50 | 0.9824 | 212.85 | 0.2972 | 67.55 | 424 | 40 | | |
| KY2 | kyanite | 63 | 19.8887 | 99.3046 | 86.7351 | 18.3592 | 26.9114 | 63.3481 | 0.0489 | 31.26 | 1.3342 | 247.94 | 0.2876 | 66.49 | 480 | 40 | | |
| KY2 | kyanite | 64 | 20.7638 | 148.3910 | 88.9863 | 18.1518 | 27.9012 | 63.3481 | 0.0906 | 44.32 | 2.2195 | 319.71 | 0.3168 | 69.95 | 616 | 40 | | |
| KY2 | kyanite | 65 | 20.3950 | 128.1242 | 112.4004 | 18.6673 | 30.6885 | 63.0588 | 0.0567 | 34.10 | 1.7989 | 288.15 | 0.6096 | 97.03 | 337 | 25 | | |
| KY2 | kyanite | 66 | 20.6825 | 147.5153 | 109.7111 | 18.5789 | 27.3699 | 63.8601 | 0.0711 | 38.76 | 2.2160 | 319.66 | 0.5674 | 93.68 | 392 | 27 | | |
| KY2 | kyanite | 68 | 20.1012 | 97.8537 | 88.4234 | 18.5317 | 27.7427 | 64.0493 | 0.0505 | 31.87 | 1.2924 | 244.05 | 0.2998 | 67.89 | 495 | 41 | | |
| KY2 | kyanite | 70 | 19.8074 | 118.4171 | 82.0202 | 18.4356 | 27.3769 | 65.3849 | 0.0428 | 28.89 | 1.6771 | 277.92 | 0.2050 | 56.19 | 408 | 36 | | |
| KY2 | kyanite | 71 | 20.1825 | 125.7975 | 82.1327 | 18.7554 | 28.3605 | 63.5262 | 0.0448 | 29.65 | 1.7923 | 287.09 | 0.2291 | 59.38 | 395 | 34 | | |

| Sample | Occluding phase | Label | Peak counts Pk(Pb) | Pk(Th) | Pk(U ) | Background counts Bg(Pb) | Bg(Th) | Bg(U ) | W%(Pb) | W%(Pb) 1σ | W%(Th) | W%(Th) 1σ | W%(U ) | W%(U ) 1σ | Chemical age (Ma) | 1σ | M2 age (Ma & error (2σ) | n = |
|---|---|---|---|---|---|---|---|---|---|---|---|---|---|---|---|---|---|---|
| KY2 | kyanite | 72 | 20.7450 | 148.8414 | 81.5074 | 18.2332 | 28.3619 | 61.9903 | 0.0864 | 43.10 | 2.2140 | 318.93 | 0.2407 | 60.91 | 637 | 42 | | |
| KY2 | kyanite | 73 | 19.8074 | 122.2198 | 81.4324 | 18.5258 | 27.1017 | 64.0605 | 0.0393 | 27.44 | 1.7500 | 283.71 | 0.2139 | 57.38 | 360 | 32 | | |
| KY2 | kyanite | 74 | 19.6012 | 98.5291 | 83.4959 | 18.3005 | 28.5933 | 62.3576 | 0.0401 | 27.80 | 1.2883 | 243.58 | 0.2599 | 63.20 | 420 | 38 | | |
| KY2 | kyanite | 76 | 20.0450 | 95.6274 | 88.0733 | 18.3544 | 28.7057 | 64.2051 | 0.0553 | 33.62 | 1.2356 | 238.82 | 0.2939 | 67.26 | 559 | 45 | | |
| KY2 | kyanite | 77 | 19.8512 | 109.2108 | 104.2201 | 18.2128 | 28.9296 | 63.4817 | 0.0532 | 32.86 | 1.4812 | 261.38 | 0.5022 | 87.97 | 383 | 30 | | |
| KY2 | kyanite | 78 | 20.4763 | 127.0734 | 104.2326 | 18.2818 | 28.7907 | 63.0810 | 0.0747 | 39.87 | 1.8144 | 289.38 | 0.5085 | 88.62 | 479 | 33 | | |
| KY2 | kyanite | 79 | 20.3075 | 124.5465 | 98.6667 | 18.5933 | 28.8763 | 63.6153 | 0.0562 | 33.93 | 1.7674 | 285.70 | 0.4333 | 81.83 | 396 | 31 | | |
| KY2 | kyanite | 80 | 20.6325 | 148.8915 | 98.6042 | 18.3661 | 27.6509 | 64.6837 | 0.0774 | 40.65 | 2.2367 | 321.18 | 0.4199 | 80.61 | 478 | 33 | | |
| KY2 | kyanite | 81 | 21.1951 | 166.5081 | 109.9362 | 17.8034 | 27.6262 | 62.8028 | 0.1207 | 51.81 | 2.5620 | 343.74 | 0.5846 | 95.20 | 598 | 34 | | |
| KY2 | kyanite | 82 | 21.1388 | 144.9630 | 107.0469 | 17.8677 | 26.6929 | 65.0733 | 0.1162 | 50.79 | 2.1839 | 317.52 | 0.5199 | 89.72 | 660 | 38 | | |
| KY2 | kyanite | 85 | 20.3762 | 115.7152 | 83.7836 | 18.6663 | 27.7331 | 63.7933 | 0.0558 | 33.74 | 1.6213 | 273.30 | 0.2464 | 61.61 | 512 | 41 | | |
| KY2 | kyanite | 86 | 20.2325 | 116.3656 | 82.0327 | 17.9431 | 27.7087 | 63.9269 | 0.0782 | 40.86 | 1.6347 | 274.51 | 0.2233 | 58.67 | 728 | 51 | | |
| KY2 | kyanite | 87 | 19.5949 | 114.1141 | 79.2063 | 18.0439 | 27.9872 | 62.3465 | 0.0496 | 31.49 | 1.5841 | 269.89 | 0.2074 | 56.47 | 489 | 41 | | |
| KY2 | kyanite | 88 | 20.1700 | 134.9296 | 84.6840 | 18.2274 | 28.4431 | 63.6932 | 0.0649 | 36.81 | 1.9654 | 301.14 | 0.2596 | 63.35 | 513 | 38 | | |
| KY2 | kyanite | 89 | 20.1825 | 123.6959 | 88.7236 | 17.6087 | 28.5432 | 64.7171 | 0.0893 | 44.01 | 1.7555 | 284.55 | 0.2962 | 67.59 | 722 | 48 | | |
| KY2 | kyanite | 90 | 21.0388 | 185.9537 | 104.6453 | 18.6731 | 27.8952 | 64.3164 | 0.0812 | 41.74 | 2.9162 | 366.76 | 0.5012 | 88.24 | 399 | 26 | | |
| KY2 | kyanite | 91 | 20.3950 | 138.2323 | 98.8168 | 18.5444 | 27.7789 | 63.8601 | 0.0613 | 35.62 | 2.0376 | 306.55 | 0.4323 | 81.75 | 398 | 30 | | |
| KY2 | kyanite | 92 | 21.3451 | 157.8998 | 102.2564 | 18.7149 | 27.8238 | 62.3799 | 0.0913 | 44.51 | 2.3985 | 332.51 | 0.4939 | 87.45 | 507 | 32 | | |
| KY2 | kyanite | 93 | 20.1637 | 93.8514 | 91.8003 | 18.1371 | 28.3786 | 64.5836 | 0.0683 | 37.93 | 1.2091 | 236.27 | 0.3351 | 71.81 | 654 | 49 | | |
| KY2 | kyanite | 94 | 19.9887 | 137.0813 | 97.1908 | 18.0168 | 28.7917 | 64.5613 | 0.0661 | 37.21 | 1.9987 | 303.69 | 0.4034 | 78.96 | 445 | 32 | | |
| KY2 | kyanite | 95 | 20.1262 | 134.8796 | 97.1783 | 18.5428 | 28.3548 | 64.0716 | 0.0511 | 32.10 | 1.9650 | 301.03 | 0.4091 | 79.49 | 348 | 28 | | |
| KY2 | kyanite | 96 | 21.2576 | 135.4550 | 92.2505 | 18.5061 | 28.0702 | 62.9475 | 0.0961 | 45.80 | 1.9815 | 302.34 | 0.3623 | 74.83 | 670 | 43 | | |
| KY2 | kyanite | 97 | 20.9763 | 150.5430 | 84.1087 | 18.0279 | 29.0954 | 64.4166 | 0.1034 | 47.61 | 2.2369 | 320.94 | 0.2435 | 61.35 | 751 | 47 | | |
| KY2 | kyanite | 98 | 19.9949 | 106.4590 | 78.3309 | 17.8779 | 26.9043 | 63.0254 | 0.0714 | 38.80 | 1.4652 | 259.74 | 0.1884 | 53.84 | 755 | 56 | | |
| KY2 | kyanite | 99 | 21.3951 | 187.2802 | 87.0477 | 18.3754 | 28.7166 | 63.2591 | 0.1061 | 48.27 | 2.9216 | 366.85 | 0.2953 | 67.69 | 605 | 36 | | |
| KY2 | kyanite | 100 | 20.1700 | 144.0872 | 84.0462 | 18.2864 | 26.9688 | 63.4928 | 0.0624 | 35.94 | 2.1556 | 314.94 | 0.2538 | 62.59 | 466 | 35 | | |
| KY2 | kyanite | 101 | 20.1450 | 138.0822 | 83.7836 | 17.3019 | 27.8071 | 62.8584 | 0.0992 | 46.51 | 2.0292 | 305.53 | 0.2582 | 63.11 | 760 | 48 | | |
| KY2 | kyanite | 102 | 20.1137 | 152.6449 | 83.9336 | 18.6847 | 28.2430 | 65.1401 | 0.0449 | 29.69 | 2.2870 | 324.21 | 0.2320 | 59.83 | 331 | 28 | | |
| KY2 | kyanite | 103 | 20.9013 | 163.6553 | 86.8851 | 18.4223 | 29.1005 | 63.3481 | 0.0852 | 42.78 | 2.4795 | 337.97 | 0.2918 | 67.25 | 552 | 36 | 517 ± 25 | 86 |
| GST | staurolite | a12 | 23.1704 | 453.4410 | 89.1989 | 18.5325 | 28.9742 | 64.2831 | 0.1646 | 60.42 | 7.6690 | 588.55 | 0.3147 | 70.49 | 423 | 19 | | |
| GST | staurolite | b11 | 22.8703 | 359.6125 | 105.1206 | 18.7310 | 28.6786 | 68.0561 | 0.1474 | 57.28 | 6.0485 | 525.71 | 0.4702 | 86.35 | 434 | 21 | | |
| GST | staurolite | b16 | 22.0515 | 262.5316 | 115.7026 | 18.4722 | 31.3934 | 65.8301 | 0.1268 | 52.99 | 4.2213 | 439.02 | 0.6239 | 98.77 | 452 | 24 | | |
| GST | staurolite | a51 | 22.0140 | 266.8635 | 73.5037 | 19.1710 | 28.5048 | 65.3849 | 0.0980 | 45.95 | 4.3290 | 443.35 | 0.1011 | 39.67 | 469 | 28 | | |
| GST | staurolite | b9 | 21.9389 | 267.1640 | 108.6354 | 18.4171 | 28.2792 | 70.7941 | 0.1240 | 52.24 | 4.3472 | 444.72 | 0.4722 | 85.82 | 470 | 25 | | |
| GST | staurolite | b27 | 22.2015 | 328.8241 | 99.9675 | 18.1391 | 31.1696 | 64.8729 | 0.1444 | 56.64 | 5.4160 | 496.36 | 0.4406 | 83.15 | 470 | 23 | | |
| GST | staurolite | a4 | 24.4080 | 513.1136 | 99.9049 | 18.4601 | 29.8837 | 66.3977 | 0.2157 | 69.92 | 8.7893 | 632.19 | 0.4282 | 82.71 | 472 | 19 | | |
| GST | staurolite | b8 | 23.8392 | 434.3904 | 105.9212 | 18.4733 | 27.8123 | 65.7967 | 0.1929 | 65.83 | 7.3801 | 578.71 | 0.5085 | 89.75 | 476 | 21 | | |
| GST | staurolite | b14 | 28.6587 | 825.9917 | 108.2601 | 19.0447 | 31.6750 | 66.2085 | 0.3464 | 88.32 | 14.2499 | 799.44 | 0.5484 | 94.55 | 481 | 15 | | |
| GST | staurolite | a36 | 21.9639 | 294.3347 | 75.9173 | 18.7380 | 30.1067 | 66.0527 | 0.1124 | 49.47 | 4.8000 | 466.90 | 0.1232 | 43.86 | 481 | 27 | | |
| GST | staurolite | b33 | 21.8202 | 306.4314 | 95.9651 | 17.9490 | 30.1246 | 64.8952 | 0.1376 | 55.29 | 5.0393 | 479.34 | 0.3900 | 78.23 | 486 | 25 | | |
| GST | staurolite | b13 | 28.1774 | 762.8920 | 116.1655 | 18.8376 | 31.6258 | 65.0176 | 0.3382 | 87.49 | 13.1730 | 770.22 | 0.6655 | 104.04 | 491 | 16 | | |
| GST | staurolite | b28 | 22.2015 | 292.0306 | 95.9776 | 18.4390 | 28.3188 | 65.7299 | 0.1331 | 54.25 | 4.8013 | 467.48 | 0.3787 | 76.98 | 491 | 26 | | |
| GST | staurolite | b25 | 27.6273 | 737.8296 | 102.7942 | 18.8364 | 30.1747 | 65.8524 | 0.3175 | 84.66 | 12.7431 | 757.42 | 0.4796 | 88.22 | 494 | 17 | | |
| GST | staurolite | a7 | 26.2458 | 663.5684 | 99.3171 | 18.3313 | 30.7943 | 64.5947 | 0.2853 | 80.17 | 11.3843 | 715.57 | 0.4463 | 84.68 | 495 | 18 | | |
| GST | staurolite | b10 | 23.0703 | 293.8588 | 121.0189 | 18.5941 | 28.9263 | 64.5279 | 0.1604 | 59.94 | 4.8247 | 468.68 | 0.7073 | 105.21 | 501 | 24 | | |
| GST | staurolite | b30 | 25.4394 | 498.1433 | 104.3702 | 19.1711 | 32.1643 | 67.0099 | 0.2259 | 71.33 | 8.4265 | 617.21 | 0.4747 | 86.83 | 504 | 20 | | |
| GST | staurolite | a9 | 26.1583 | 624.6434 | 93.0135 | 18.6536 | 31.6078 | 64.7950 | 0.2704 | 78.03 | 10.6772 | 693.25 | 0.3615 | 76.08 | 508 | 19 | | |
| GST | staurolite | b26 | 24.9831 | 545.7672 | 98.8918 | 18.2129 | 29.9893 | 66.6426 | 0.2449 | 74.41 | 9.3398 | 650.24 | 0.4124 | 81.19 | 510 | 20 | | |
| GST | staurolite | b6 | 22.7203 | 299.3436 | 114.2516 | 18.1840 | 29.8932 | 65.3293 | 0.1626 | 60.35 | 4.9046 | 472.43 | 0.6124 | 97.89 | 524 | 25 | | |
| GST | staurolite | b20 | 27.6023 | 710.0342 | 104.9831 | 18.5104 | 31.1902 | 64.2163 | 0.3296 | 86.42 | 12.2335 | 742.40 | 0.5276 | 92.39 | 526 | 18 | | |
| GST | staurolite | a1 | 21.9890 | 271.7714 | 74.9168 | 18.6507 | 29.4781 | 63.5596 | 0.1168 | 50.54 | 4.3981 | 446.75 | 0.1413 | 46.88 | 535 | 30 | | |
| GST | staurolite | b7 | 22.4390 | 259.2765 | 95.1146 | 18.7466 | 28.2143 | 65.2068 | 0.1307 | 53.77 | 4.2086 | 437.77 | 0.3731 | 76.28 | 536 | 28 | | |
| GST | staurolite | b17 | 28.7900 | 773.2144 | 111.1746 | 18.6104 | 30.5240 | 66.3643 | 0.3682 | 91.23 | 13.3433 | 774.16 | 0.5823 | 97.26 | 537 | 17 | | |

| Sample | Occluding phase | Label | Peak counts Pk(Pb) | Pk(Th) | Pk(U ) | Background counts Bg(Pb) | Bg(Th) | Bg(U ) | W%(Pb) | W%(Pb) 1σ | W%(Th) | W%(Th) 1σ | W%(U ) | W%(U ) 1σ | Chemical age (Ma) | 1σ | M2 age (Ma & error (2σ) | n = |
|---|---|---|---|---|---|---|---|---|---|---|---|---|---|---|---|---|---|---|
| GST | staurolite | b2 | 21.9139 | 217.5669 | 93.0260 | 18.7643 | 29.5463 | 65.9637 | 0.1102 | 49.09 | 3.4279 | 395.27 | 0.3363 | 72.28 | 541 | 31 | | |
| GST | staurolite | a21 | 25.3144 | 551.9875 | 99.4422 | 17.9305 | 30.0561 | 63.7377 | 0.2673 | 77.77 | 9.4349 | 652.98 | 0.4561 | 85.34 | 544 | 20 | | |
| GST | staurolite | a8 | 26.6396 | 640.4783 | 97.5911 | 18.2962 | 30.7919 | 66.0416 | 0.3021 | 82.68 | 10.9901 | 703.75 | 0.4053 | 80.67 | 546 | 19 | | |
| GST | staurolite | a49 | 21.9014 | 251.2643 | 73.4412 | 18.8017 | 30.0277 | 64.6169 | 0.1078 | 48.41 | 4.0194 | 427.27 | 0.1097 | 41.29 | 548 | 31 | | |
| GST | staurolite | b31 | 26.0708 | 564.8807 | 106.1838 | 18.3574 | 31.4353 | 66.0527 | 0.2794 | 79.53 | 9.6347 | 659.57 | 0.5128 | 90.50 | 549 | 20 | | |
| GST | staurolite | a31 | 21.8389 | 269.1171 | 75.6547 | 18.4468 | 29.6244 | 65.0844 | 0.1188 | 50.99 | 4.3493 | 444.37 | 0.1316 | 45.26 | 553 | 30 | | |
| GST | staurolite | b1 | 21.2076 | 159.8516 | 110.7993 | 18.1614 | 28.5834 | 64.3053 | 0.1069 | 48.42 | 2.4043 | 331.80 | 0.5771 | 94.63 | 553 | 33 | | |
| GST | staurolite | b4 | 22.2952 | 254.3940 | 100.4678 | 18.4480 | 31.0315 | 66.8875 | 0.1365 | 55.02 | 4.0662 | 430.18 | 0.4184 | 80.72 | 558 | 29 | | |
| GST | staurolite | b5 | 22.8703 | 292.9072 | 112.4129 | 18.0755 | 29.9269 | 65.2959 | 0.1725 | 62.28 | 4.7892 | 466.95 | 0.5898 | 96.07 | 570 | 27 | | |
| GST | staurolite | b29 | 20.1762 | 218.2929 | 84.4964 | 16.7909 | 27.3618 | 58.8518 | 0.1197 | 51.43 | 3.5133 | 402.02 | 0.3227 | 71.25 | 582 | 33 | | |
| GST | staurolite | a42 | 24.0205 | 413.8381 | 91.8503 | 18.0681 | 31.2196 | 62.3353 | 0.2154 | 69.80 | 6.9630 | 562.84 | 0.3745 | 77.07 | 584 | 24 | | |
| GST | staurolite | a3 | 21.7514 | 259.7272 | 74.1290 | 18.2652 | 29.5209 | 65.9414 | 0.1224 | 51.83 | 4.1797 | 435.57 | 0.1018 | 39.78 | 602 | 33 | | |
| GST | staurolite | a2 | 21.8827 | 258.2249 | 79.1188 | 18.1653 | 29.3254 | 64.3610 | 0.1313 | 53.84 | 4.1587 | 434.62 | 0.1835 | 53.40 | 612 | 33 | | |
| GST | staurolite | b3 | 22.0390 | 204.8008 | 110.0989 | 17.6806 | 28.7157 | 64.0827 | 0.1567 | 59.34 | 3.2185 | 383.50 | 0.5729 | 94.42 | 679 | 34 | | |
| GST | staurolite | a41 | 26.3083 | 435.0922 | 96.1027 | 19.0049 | 29.3256 | 65.8524 | 0.2651 | 77.55 | 7.3432 | 576.39 | 0.3822 | 77.69 | 683 | 26 | | |
| GST | staurolite | a45 | 24.1267 | 307.3832 | 85.0592 | 18.7746 | 27.8186 | 64.4277 | 0.1928 | 65.88 | 5.0766 | 480.07 | 0.2581 | 63.53 | 720 | 32 | 525 ± 19 | 40 |
| GST | staurolite | a35 | 28.4899 | 313.6198 | 99.6673 | 18.2445 | 29.3411 | 64.9508 | 0.3781 | 93.39 | 5.1661 | 484.46 | 0.4348 | 82.50 | 1238 | 43 | | |
| GST | staurolite | a23 | 30.0965 | 331.1787 | 103.5822 | 18.4681 | 29.0071 | 65.0176 | 0.4295 | 99.57 | 5.4847 | 498.88 | 0.4834 | 87.03 | 1306 | 43 | | |
| GST | staurolite | a50 | 28.7837 | 302.5243 | 92.3256 | 18.6208 | 30.1346 | 64.9397 | 0.3743 | 92.82 | 4.9413 | 473.39 | 0.3420 | 73.07 | 1330 | 47 | | |
| GST | staurolite | a20 | 30.8904 | 338.1427 | 102.2939 | 18.5039 | 28.4951 | 65.4294 | 0.4580 | 102.88 | 5.6191 | 504.90 | 0.4623 | 85.13 | 1377 | 44 | | |
| GST | staurolite | a33 | 31.3780 | 343.0026 | 100.3802 | 18.8520 | 31.2614 | 62.5357 | 0.4635 | 103.53 | 5.6608 | 506.93 | 0.4751 | 86.35 | 1377 | 44 | | |
| GST | staurolite | a28 | 31.7093 | 332.8320 | 103.4821 | 18.9562 | 29.6650 | 62.9586 | 0.4711 | 104.29 | 5.4940 | 498.90 | 0.5072 | 89.08 | 1408 | 44 | | |
| GST | staurolite | a10 | 32.7532 | 335.7128 | 109.5985 | 18.7986 | 29.4445 | 63.4149 | 0.5184 | 109.71 | 5.5690 | 503.15 | 0.5800 | 95.42 | 1476 | 45 | | |
| GST | staurolite | a54 | 32.4407 | 331.3541 | 108.4353 | 18.9288 | 32.2677 | 65.2736 | 0.5006 | 107.66 | 5.4292 | 496.37 | 0.5410 | 92.07 | 1479 | 45 | | |
| GST | staurolite | a44 | 32.6532 | 332.6566 | 106.5340 | 18.7965 | 29.0294 | 63.6598 | 0.5140 | 109.16 | 5.5154 | 500.47 | 0.5380 | 91.86 | 1502 | 46 | | |
| GST | staurolite | a39 | 32.2531 | 326.2189 | 108.2977 | 18.3849 | 27.9423 | 65.7188 | 0.5133 | 108.97 | 5.4068 | 494.99 | 0.5328 | 91.29 | 1524 | 46 | | |
| GST | staurolite | a24 | 32.3969 | 316.7006 | 103.9074 | 19.1581 | 28.5486 | 65.3404 | 0.4901 | 106.49 | 5.2309 | 487.23 | 0.4829 | 86.94 | 1529 | 48 | | |
| GST | staurolite | a17 | 32.9032 | 337.3911 | 110.2865 | 18.4441 | 28.9775 | 65.9859 | 0.5356 | 111.36 | 5.5932 | 503.57 | 0.5552 | 93.26 | 1533 | 46 | | |
| GST | staurolite | a40 | 32.3906 | 318.1784 | 104.6829 | 19.0544 | 29.6822 | 65.6632 | 0.4934 | 106.81 | 5.2289 | 486.75 | 0.4877 | 87.29 | 1535 | 48 | | |
| GST | staurolite | a53 | 33.3096 | 335.9382 | 108.9481 | 18.9655 | 31.2077 | 64.7171 | 0.5320 | 111.05 | 5.5325 | 501.11 | 0.5549 | 93.28 | 1535 | 46 | | |
| GST | staurolite | a18 | 32.8220 | 335.5875 | 107.8849 | 18.5671 | 30.9100 | 65.1623 | 0.5293 | 110.83 | 5.5360 | 501.47 | 0.5361 | 91.70 | 1540 | 46 | | |
| GST | staurolite | a37 | 33.1721 | 315.9993 | 120.3309 | 18.5030 | 30.5668 | 65.0399 | 0.5468 | 112.87 | 5.1998 | 486.64 | 0.6943 | 104.39 | 1543 | 45 | | |
| GST | staurolite | a14 | 33.0845 | 305.6550 | 127.2986 | 18.1444 | 30.5430 | 64.4277 | 0.5592 | 114.37 | 5.0264 | 479.15 | 0.7907 | 111.49 | 1544 | 45 | | |
| GST | staurolite | a30 | 32.8907 | 325.0166 | 106.6091 | 18.9309 | 28.5856 | 65.3404 | 0.5170 | 109.39 | 5.3764 | 493.74 | 0.5166 | 89.91 | 1551 | 47 | | |
| GST | staurolite | a19 | 31.9468 | 313.3443 | 106.4715 | 18.4336 | 30.0408 | 65.8746 | 0.5008 | 107.70 | 5.1439 | 483.21 | 0.5081 | 89.16 | 1559 | 48 | | |
| GST | staurolite | a38 | 33.1533 | 322.7372 | 111.6499 | 18.8172 | 31.7887 | 65.3626 | 0.5322 | 111.12 | 5.2855 | 489.95 | 0.5801 | 95.33 | 1566 | 47 | | |
| GST | staurolite | a13 | 32.6094 | 334.0594 | 104.4952 | 18.4230 | 29.9664 | 65.3849 | 0.5252 | 110.24 | 5.5123 | 499.80 | 0.4897 | 87.55 | 1566 | 47 | | |
| GST | staurolite | a34 | 33.0033 | 331.0535 | 104.1825 | 18.7167 | 28.9964 | 64.8062 | 0.5298 | 110.81 | 5.4852 | 499.02 | 0.4939 | 88.00 | 1581 | 47 | | |
| GST | staurolite | a26 | 33.7472 | 316.7256 | 115.3774 | 18.9071 | 28.2706 | 66.1529 | 0.5515 | 113.18 | 5.2420 | 488.01 | 0.6168 | 98.29 | 1601 | 47 | | |
| GST | staurolite | a29 | 33.7909 | 322.1360 | 110.7243 | 18.7192 | 28.6144 | 64.3387 | 0.5600 | 114.04 | 5.3320 | 492.08 | 0.5813 | 95.43 | 1631 | 48 | | |
| GST | staurolite | a25 | 33.4033 | 324.3904 | 106.8592 | 18.6595 | 29.7668 | 66.4200 | 0.5470 | 112.62 | 5.3481 | 492.65 | 0.5066 | 89.07 | 1648 | 49 | | |
| GST | staurolite | a27 | 34.0660 | 328.6487 | 113.1009 | 18.2905 | 30.6693 | 65.1067 | 0.5863 | 116.70 | 5.4113 | 495.65 | 0.6015 | 97.07 | 1670 | 48 | 1511 ± 42 | 26 |
| G&G | mx | d_31 | 21.6452 | 139.1581 | 85.9847 | 19.9774 | 30.0567 | 68.0116 | 0.0518 | 31.71 | 1.9474 | 294.79 | 0.2147 | 80.07 | 437 | 36 | | |
| G&G | mx | e_5 | 21.5951 | 157.0239 | 97.3159 | 19.6194 | 29.2049 | 66.4645 | 0.0631 | 35.49 | 2.2842 | 319.45 | 0.3701 | 105.35 | 404 | 30 | | |
| G&G | mx | c_3 | 21.7389 | 180.3976 | 85.9972 | 19.0553 | 30.3325 | 66.2308 | 0.0891 | 43.00 | 2.6744 | 345.19 | 0.2369 | 84.25 | 574 | 38 | | |
| G&G | mx | i_3 | 20.6513 | 112.2628 | 95.2022 | 19.1375 | 30.5891 | 68.6237 | 0.0462 | 29.69 | 1.4609 | 255.59 | 0.3172 | 97.28 | 414 | 36 | | |
| G&G | mx | a_8 | 20.4388 | 78.5185 | 87.6981 | 19.4150 | 31.0026 | 67.2547 | 0.0281 | 21.96 | 0.8503 | 195.04 | 0.2432 | 85.05 | 383 | 41 | | |
| G&G | mx | h_8 | 21.2264 | 122.5200 | 96.7156 | 19.1827 | 29.8670 | 68.4679 | 0.0656 | 36.28 | 1.6530 | 271.53 | 0.3368 | 100.20 | 530 | 40 | | |
| G&G | mx | e_2 | 21.4951 | 180.9732 | 87.8732 | 19.4340 | 30.5599 | 67.2214 | 0.0661 | 36.40 | 2.6796 | 345.46 | 0.2474 | 86.08 | 424 | 31 | | |
| G&G | mx | a_2 | 22.3015 | 189.4326 | 102.8192 | 19.5452 | 30.5105 | 66.2753 | 0.0916 | 43.62 | 2.8302 | 354.97 | 0.4381 | 114.59 | 479 | 31 | | |
| G&G | mx | i_12 | 21.5576 | 158.5504 | 101.9562 | 18.8745 | 31.7382 | 68.4011 | 0.0890 | 42.95 | 2.2592 | 317.21 | 0.4011 | 109.48 | 554 | 37 | | |
| G&G | mx | a_6 | 20.6825 | 101.6060 | 87.0727 | 18.9621 | 32.0803 | 68.7684 | 0.0539 | 32.49 | 1.2424 | 235.59 | 0.2179 | 80.53 | 611 | 52 | | |
| G&G | mx | g_2 | 20.0387 | 80.0942 | 89.6741 | 18.5329 | 30.8616 | 67.5664 | 0.0459 | 29.57 | 0.8797 | 198.23 | 0.2626 | 88.31 | 585 | 53 | | |

| Sample | Occluding phase | Label | Peak counts Pk(Pb) | Pk(Th) | Pk(U ) | Background counts Bg(Pb) | Bg(Th) | Bg(U ) | W%(Pb) | W%(Pb) 1σ | W%(Th) | W%(Th) 1σ | W%(U ) | W%(U ) 1σ | Chemical age (Ma) | 1σ | M2 age (Ma & error (2σ) | n = |
|---|---|---|---|---|---|---|---|---|---|---|---|---|---|---|---|---|---|---|
| G&G | mx | a_10 | 20.6888 | 88.8737 | 88.0983 | 19.6446 | 29.5023 | 68.0005 | 0.0286 | 22.13 | 1.0566 | 216.82 | 0.2381 | 83.98 | 350 | 37 | | |
| G&G | mx | a_1 | 20.8201 | 106.6591 | 90.5621 | 18.9150 | 31.2982 | 67.6999 | 0.0604 | 34.60 | 1.3402 | 244.10 | 0.2711 | 89.65 | 601 | 48 | | |
| G&G | mx | d_7 | 21.9639 | 217.0663 | 93.6763 | 18.5359 | 29.2600 | 68.4568 | 0.1153 | 49.23 | 3.3194 | 382.98 | 0.3010 | 94.77 | 594 | 35 | | |
| G&G | mx | f_3 | 20.9763 | 116.7659 | 90.7872 | 19.4023 | 28.6309 | 68.0339 | 0.0481 | 30.31 | 1.5685 | 264.17 | 0.2704 | 89.63 | 438 | 38 | | |
| G&G | mx | h_12 | 20.7825 | 70.5899 | 91.2500 | 19.1276 | 29.9067 | 66.5202 | 0.0513 | 31.53 | 0.7252 | 179.77 | 0.2928 | 93.10 | 671 | 59 | | |
| G&G | mx | h_10 | 21.9639 | 184.4520 | 90.4620 | 19.1395 | 31.8584 | 67.5219 | 0.0939 | 44.17 | 2.7068 | 346.46 | 0.2736 | 90.32 | 579 | 37 | | |
| G&G | mx | i_8 | 22.4953 | 282.0885 | 90.1494 | 19.2275 | 30.8525 | 67.8001 | 0.1098 | 48.02 | 4.4505 | 443.95 | 0.2690 | 89.97 | 460 | 26 | | |
| G&G | mx | h_7 | 20.7325 | 120.5936 | 85.7220 | 18.6259 | 26.3708 | 66.4089 | 0.0678 | 36.93 | 1.6799 | 273.64 | 0.2303 | 82.86 | 617 | 47 | | |
| G&G | mx | d_19 | 21.8452 | 207.7294 | 87.5980 | 18.7817 | 30.3766 | 68.4679 | 0.1026 | 46.34 | 3.1501 | 374.00 | 0.2291 | 82.82 | 584 | 36 | | |
| G&G | mx | d_12 | 21.3576 | 132.8779 | 89.5240 | 19.2630 | 30.7432 | 67.9671 | 0.0671 | 36.65 | 1.8125 | 283.57 | 0.2558 | 87.11 | 563 | 42 | | |
| G&G | mx | d_24 | 22.9953 | 280.3857 | 88.8237 | 19.8305 | 30.7111 | 68.4902 | 0.1057 | 46.97 | 4.4119 | 441.48 | 0.2441 | 85.59 | 453 | 26 | | |
| G&G | mx | i_4 | 22.6453 | 201.1213 | 88.0858 | 19.2250 | 30.9648 | 67.1991 | 0.1157 | 49.46 | 3.0231 | 366.44 | 0.2502 | 86.56 | 666 | 39 | | |
| G&G | mx | g_3 | 21.6327 | 170.7124 | 88.2358 | 19.1361 | 30.6842 | 68.8575 | 0.0817 | 40.88 | 2.4794 | 331.29 | 0.2304 | 82.76 | 562 | 38 | | |
| G&G | mx | i_16 | 21.8389 | 202.1475 | 88.5110 | 19.4009 | 29.7060 | 68.1006 | 0.0794 | 40.20 | 3.0516 | 367.43 | 0.2434 | 85.19 | 461 | 31 | | |
| G&G | mx | f_10 | 22.1202 | 193.2620 | 89.0613 | 19.5301 | 30.5841 | 67.6777 | 0.0849 | 41.71 | 2.8759 | 356.52 | 0.2544 | 86.99 | 510 | 34 | | |
| G&G | mx | e_1 | 21.3889 | 130.6512 | 91.0624 | 19.2645 | 29.1412 | 67.4217 | 0.0680 | 36.88 | 1.7958 | 281.82 | 0.2796 | 90.92 | 557 | 42 | | |
| G&G | mx | h_11 | 21.5826 | 149.6422 | 90.1119 | 19.4271 | 32.2540 | 67.8224 | 0.0693 | 37.32 | 2.0812 | 303.72 | 0.2647 | 88.65 | 523 | 38 | | |
| G&G | mx | i_13 | 20.8075 | 129.4503 | 90.3495 | 18.5268 | 30.3003 | 67.5107 | 0.0739 | 38.69 | 1.7582 | 279.18 | 0.2707 | 89.56 | 619 | 45 | | |
| G&G | mx | f_9 | 20.3012 | 80.2443 | 94.5768 | 19.2499 | 28.0372 | 68.5347 | 0.0287 | 22.13 | 0.9264 | 202.72 | 0.3074 | 95.24 | 335 | 35 | | |
| G&G | mx | a_11 | 20.8451 | 112.8382 | 82.7205 | 19.3776 | 29.7193 | 67.2102 | 0.0443 | 28.91 | 1.4806 | 256.78 | 0.1843 | 73.99 | 474 | 42 | | |
| G&G | mx | f_7 | 20.1325 | 92.8759 | 76.8927 | 19.1101 | 28.8378 | 66.6537 | 0.0277 | 21.66 | 1.1380 | 224.85 | 0.1212 | 59.89 | 404 | 43 | | |
| G&G | mx | f_8 | 20.6263 | 124.2213 | 92.3756 | 19.2868 | 28.8990 | 68.1229 | 0.0399 | 27.25 | 1.7053 | 276.17 | 0.2895 | 92.95 | 338 | 31 | | |
| G&G | mx | i_15 | 21.0138 | 76.2925 | 89.5741 | 19.5802 | 31.2553 | 69.0356 | 0.0428 | 28.26 | 0.7984 | 188.11 | 0.2420 | 84.43 | 596 | 56 | | |
| G&G | mx | h_13 | 22.1952 | 245.8312 | 90.6246 | 19.3978 | 31.0886 | 67.7556 | 0.0921 | 43.53 | 3.7843 | 408.32 | 0.2727 | 90.16 | 440 | 27 | | |
| G&G | mx | d_25 | 22.3703 | 205.9772 | 88.4485 | 19.1664 | 29.6795 | 68.3900 | 0.1072 | 47.35 | 3.1139 | 370.81 | 0.2388 | 84.31 | 610 | 37 | | |
| G&G | mx | h_14 | 24.9519 | 443.5143 | 89.1864 | 19.8677 | 32.1913 | 68.6683 | 0.1736 | 60.87 | 7.2060 | 561.79 | 0.2484 | 86.71 | 483 | 22 | | |
| G&G | mx | d_28 | 24.1392 | 405.3173 | 91.5877 | 19.3811 | 32.4270 | 67.9448 | 0.1619 | 58.68 | 6.5311 | 534.77 | 0.2850 | 92.68 | 484 | 23 | | |
| G&G | mx | h_16 | 25.8895 | 527.9348 | 93.6013 | 19.8395 | 33.1771 | 68.0561 | 0.2077 | 66.76 | 8.6483 | 614.76 | 0.3110 | 97.29 | 479 | 20 | | |
| G&G | mx | h_9 | 21.9827 | 205.3014 | 84.8716 | 19.5361 | 30.1384 | 67.7111 | 0.0799 | 40.38 | 3.1000 | 370.35 | 0.2046 | 78.09 | 473 | 32 | | |
| G&G | mx | a_9 | 20.4575 | 176.5685 | 79.9442 | 18.4597 | 27.8333 | 62.2797 | 0.0636 | 35.57 | 2.6609 | 344.98 | 0.2132 | 80.21 | 423 | 31 | | |
| G&G | mx | i_19 | 23.2141 | 295.7372 | 90.7497 | 19.7472 | 30.8879 | 67.6220 | 0.1164 | 49.42 | 4.6714 | 453.86 | 0.2776 | 91.27 | 465 | 26 | | |
| G&G | mx | a_12 | 21.5576 | 195.8650 | 82.7205 | 18.6789 | 30.4183 | 66.9208 | 0.0954 | 44.45 | 2.9242 | 359.46 | 0.1880 | 74.78 | 598 | 38 | | |
| G&G | mx | h_4 | 21.5451 | 140.0338 | 88.9112 | 18.8448 | 29.2588 | 67.2881 | 0.0891 | 42.87 | 1.9599 | 294.43 | 0.2561 | 87.08 | 703 | 48 | | |
| G&G | mx | d_26 | 22.4265 | 232.2868 | 86.9602 | 19.2154 | 32.1354 | 67.8001 | 0.1071 | 47.25 | 3.5253 | 393.99 | 0.2280 | 82.36 | 557 | 33 | | |
| G&G | mx | d_23 | 22.3515 | 200.2953 | 86.7601 | 19.3382 | 29.9813 | 69.3917 | 0.1002 | 45.63 | 3.0053 | 364.11 | 0.2065 | 78.34 | 604 | 37 | | |
| G&G | mx | d_17 | 22.5828 | 280.5609 | 85.8971 | 19.5256 | 30.9723 | 68.0672 | 0.1013 | 45.80 | 4.3931 | 439.67 | 0.2132 | 79.83 | 444 | 26 | | |
| G&G | mx | a_4 | 22.5328 | 303.6514 | 83.3458 | 19.7214 | 31.2667 | 69.2248 | 0.0921 | 43.42 | 4.7834 | 458.26 | 0.1689 | 71.07 | 386 | 23 | | |
| G&G | mx | h_17 | 23.6892 | 301.4474 | 86.6850 | 19.7707 | 31.5802 | 65.6743 | 0.1324 | 52.88 | 4.7418 | 456.39 | 0.2513 | 86.68 | 530 | 28 | | |
| G&G | mx | d_11 | 22.4515 | 260.6787 | 85.2968 | 19.6061 | 30.3582 | 68.0116 | 0.0937 | 43.91 | 4.0570 | 422.68 | 0.2064 | 78.50 | 442 | 27 | | |
| G&G | mx | d_14 | 23.8017 | 327.6968 | 89.2364 | 19.9437 | 29.3002 | 67.0099 | 0.1302 | 52.40 | 5.2452 | 480.10 | 0.2668 | 89.48 | 475 | 25 | | |
| G&G | mx | b_9 | 22.4640 | 280.6110 | 85.0967 | 19.4374 | 29.7653 | 68.6015 | 0.0999 | 45.40 | 4.4053 | 439.79 | 0.1968 | 76.62 | 442 | 26 | | |
| G&G | mx | c_5 | 23.7767 | 375.0465 | 87.1353 | 19.2586 | 31.6503 | 69.5809 | 0.1531 | 56.94 | 6.0068 | 512.53 | 0.2107 | 79.51 | 509 | 25 | | |
| G&G | mx | f_2 | 22.7453 | 275.5276 | 87.7856 | 19.2917 | 31.6978 | 70.7274 | 0.1154 | 49.09 | 4.2806 | 433.44 | 0.2033 | 77.83 | 519 | 29 | | |
| G&G | mx | g_4 | 20.6263 | 98.7793 | 87.0227 | 18.7949 | 29.3526 | 68.4011 | 0.0571 | 33.36 | 1.2255 | 232.55 | 0.2190 | 80.24 | 650 | 54 | | |
| G&G | mx | c_4 | 23.4141 | 308.5604 | 85.9472 | 19.4961 | 31.3749 | 67.7333 | 0.1326 | 52.96 | 4.8791 | 463.37 | 0.2184 | 80.91 | 528 | 28 | | |
| G&G | mx | h_5 | 22.0452 | 164.8315 | 97.6411 | 19.2814 | 28.9765 | 68.8909 | 0.0912 | 43.37 | 2.3996 | 325.52 | 0.3409 | 100.53 | 576 | 38 | | |
| G&G | mx | i_7 | 20.2262 | 56.6846 | 96.2653 | 18.8153 | 29.7024 | 69.4696 | 0.0419 | 27.89 | 0.4775 | 145.35 | 0.3145 | 96.06 | 615 | 58 | | |
| G&G | mx | f_4 | 21.9014 | 189.5327 | 109.6861 | 19.6194 | 29.3841 | 67.0878 | 0.0733 | 38.36 | 2.8216 | 352.54 | 0.5052 | 122.39 | 368 | 25 | | |
| G&G | mx | b_8 | 21.6577 | 164.4061 | 99.3171 | 19.3563 | 32.6770 | 67.1546 | 0.0741 | 38.62 | 2.3213 | 319.79 | 0.3802 | 106.00 | 464 | 33 | | |
| G&G | mx | i_2 | 20.3200 | 50.4076 | 90.6246 | 19.0635 | 30.0290 | 69.1246 | 0.0362 | 25.53 | 0.3607 | 126.34 | 0.2522 | 86.00 | 671 | 69 | | |
| G&G | mx | d_13 | 21.8202 | 170.6123 | 100.6304 | 18.7631 | 29.3526 | 69.2248 | 0.1014 | 45.85 | 2.4851 | 330.60 | 0.3711 | 104.70 | 608 | 38 | | |
| G&G | mx | d_29 | 21.4701 | 190.2335 | 109.6611 | 18.7938 | 31.7695 | 67.7890 | 0.0874 | 42.24 | 2.7840 | 349.68 | 0.4950 | 120.95 | 444 | 29 | | |
| G&G | mx | i_14 | 20.6763 | 102.4315 | 99.3171 | 19.1520 | 30.1789 | 67.7556 | 0.0458 | 29.33 | 1.2742 | 237.02 | 0.3710 | 104.42 | 413 | 36 | | |

| Sample | Occluding phase | Label | Peak counts Pk(Pb) | Pk(Th) | Pk(U ) | Background counts Bg(Pb) | Bg(Th) | Bg(U ) | W%(Pb) | W%(Pb) 1σ | W%(Th) | W%(Th) 1σ | W%(U ) | W%(U ) 1σ | Chemical age (Ma) | 1σ | M2 age (Ma & error (2σ) | n = |
|---|---|---|---|---|---|---|---|---|---|---|---|---|---|---|---|---|---|---|
| G&G | mx | h_15 | 20.5450 | 58.4853 | 99.6048 | 19.3026 | 31.8084 | 68.5013 | 0.0356 | 25.25 | 0.4706 | 144.06 | 0.3639 | 103.17 | 479 | 47 | | |
| G&G | mx | d_20 | 22.4515 | 161.8035 | 101.9937 | 19.3649 | 29.6895 | 67.4440 | 0.1026 | 46.17 | 2.3242 | 319.72 | 0.4078 | 109.70 | 621 | 39 | | |
| G&G | mx | d_10 | 20.5075 | 45.5312 | 106.2338 | 19.1312 | 29.8693 | 66.5647 | 0.0407 | 27.43 | 0.2773 | 110.79 | 0.4652 | 116.78 | 504 | 47 | | |
| G&G | mx | i_5 | 21.9890 | 155.3223 | 103.3695 | 19.6777 | 30.4814 | 68.9688 | 0.0745 | 38.74 | 2.2010 | 311.47 | 0.4067 | 109.64 | 471 | 33 | | |
| G&G | mx | h_1 | 22.0327 | 139.7836 | 102.0562 | 19.6330 | 31.2672 | 68.0339 | 0.0777 | 39.65 | 1.9144 | 290.57 | 0.4020 | 108.97 | 535 | 38 | 512 ± 23 | 69 |